ISSN 0289-0003

An International Journal

ZOOLOGICAL SCIENCE

Vol. 11 No.4

August 1994

PHYSIOLOGY
CELL and MOLECULAR BIOLOGY
GENETICS
IMMUNOLOGY
BIOCHEMISTRY
DEVELOPMENTAL BIOLOGY
REPRODUCTIVE BIOLOGY
ENDOCRINOLOGY
BEHAVIOR BIOLOGY
ENVIRONMENTAL BIOLOGY and ECOLOGY
SYSTEMATICS and TAXONOMY

published by Zoological Society of Japan
distributed by Business Center for Academic Societies Japan
VSP, Zeist, The Netherlands

ZOOLOGICAL SCIENCE

The Official Journal of the Zoological Society of Japan

The Zoological Society of Japan:
Toshin-building, Hongo 2–27–2, Bunkyo-ku,
Tokyo 113, Japan. Phone 03-3814–5461
Fax 03-3814-5352

ZOOLOGICAL SCIENCE is devoted to publication of original articles, reviews and rapid communications in the broad field of Zoology. The journal was founded in 1984 as a result of unification of Zoological Magazine (1888–1983) and Annotationes Zoologicae Japonenses (1897–1983), the former official journals of the Zoological Soceity of Japan. An annual volume consists of six regular numbers and one supplement (abstracts of papers presented at the annual meeting of the Zoological Society of Japan) of more than 850 pages. The regular numbers appear bimonthly.

MANUSCRIPTS OFFERED FOR CONSIDERATION AND CORRESPONDENCE CONCERNING EDITORIAL MATTERS should be sent to:

Dr. Tsuneo Yamaguchi, Editor-in-Chief, Zoological Science, Department of Biology, Faculty of Science, Okayama University, Okayama 700, Japan, in accordance with the instructions to authors which appear in the first issue of each volume. Copies of instructions to authors will be sent upon request.

SUBSCRIPTIONS. ZOOLOGICAL SCIENCE is distributed free of charge to the members, both domestic and foreign, of the Zoological Society of Japan.To non-member subscribers within Japan, it is distributed by Business Center for Academic Societies Japan, 5–16–9 Honkomagome, Bunkyo-ku, Tokyo 113. Subscriptions outside Japan should be ordered from the sole agent, VSP, Godfried van Seystlaan 47, 3703 BR Zeist (postal address: P. O. Box 346, 3700 AH Zeist), The Netherlands. Subscription rates will be provided on request to these agents. New subscriptions and renewals begin with the first issue of the current volume.

[Publication of Zoological Science has been supported in part by a Grant-in-Aid for Publication of Scientific Research Results from the Ministry of Education, Science and Culture, Japan.]

ZOOLOGICAL SCIENCE 11: 495–506 (1994)

REVIEW

The Vomeronasal System and Its Connections with Sexually Dimorphic Neural Structures

JORGE LARRIVA-SAHD and AKIRA MATSUMOTO[1]

Laboratory of Experimental Pathology, Instituto Nacional de la Nutrición SZ, Mexico City, Mexico and [1]Department of Anatomy, Juntendo University School of Medicine, Hongo, Tokyo 113, Japan

INTRODUCTION

The vomeronasal system in rodents plays an important role in modulating the sexual neuroendocrine and behavioral responses elicited by pheromones. This influence largely depends on the ability of the vomeronasal organ (VNO) to transduce chemical signals (i.e. pheromones) released from individuals of the same colony into receptor potentials which ultimately modulate the neural substrates controlling gonadotropin secretion. Since most if not all sexual endocrine and behavioral responses modulated by the vomeronasal system are sexually dimorphic and so are most of its central relay nuclei, this unit constitutes a model system in which morphological and functional sex differences are evident. Furthermore, this system has provided a better understanding of the mechanisms by which exteroceptive stimuli may influence mammalian reproductive functions. The present review concerns with the structure and function of the rodents VNO and emphasizes on the central pathways and sex differences of the vomeronasal system.

STRUCTURE AND EFFERENT CONNECTIONS OF THE VNO

(i) *Macroscopic anatomy*

The vomeronasal organ (VNO) (Organ of Jacobson) [53] is a paired, fusiform chemoreceptor. In the rat, it is approximately from 5 to 7 mm in length and 1.5 mm in diameter. Bilaterally located in the most ventral part of the nasal septum, the VNO contains a blind sac lined by two types of epithelia [32, 45, 112] (Fig. 1). In most mammals, the organ housed in an osseous chamber opens anteriorly by way of a narrow duct. The epithelial tube in some species opens ventrally to the mouth through the nasopalatine duct. The VNO in rodents and higher terrestrial mammals opens directly into the nasal cavity, just behind the nostrils [32]. The epithelium lies on highly vascularized loose connective tissue containing numerous serous glands and nerves (Fig. 2). The osseus shell of the VNO is pierced in its posterior third by branches of the vomeronasal nerves, which reach the accessory olfactory bulb (AOB) as they pass through the cribriform plate of the ethmoid bone. It is noteworthy that as the branches of the vomeronasal nerves leave the VNO, they become intimately associated with branches and ganglia of the terminal nerve. This association makes the terminal nerve prone to damage in experiments designed to study the effects of the removal of the VNO [94]. This should not be underestimated since like the VNO, the terminal nerve has also been implicated in the sexual responses elicited by olfactory signals [140, 141]. In addition to the vomeronasal nerves, the VNO receives autonomic and sensory innervation from the sphenopalatine and trigeminal ganglia [66, 73, 74, 119].

(ii) *Microscopic structure*

Although marked histological differences of the VNO have been documented in several species [32, 45, 112], three elements remain constant: a neurosensory epithelium, exocrine glands, and large venous sinuses [45, 112] (Figs. 1 and 2). In rodents, the vomeronasal epithelium lies medial to a large confluent venous sinus, the vomeronasal vein [130], for which the epithelial sac adopts a crescent moon shape. As mentioned, the lumen is lined by two different types of epithelium. In the concave (i.e. lateral) portion, there is a pseudostratified columnar epithelium with short microvilli and occasional cilia. The convex (i.e. medial) one is covered by a sensory neuroepithelium (Fig. 2). The former has been properly termed as receptor-free epithelium, instead of respiratory or ciliated, since its morphology is markedly different from that of these other epithelia [12]. Unlike most epithelia, the VNO neuroepithelium is devoid of basal lamina and possesses a capillary network (Fig 3), displaying distinct ultrastructural and probably functional characteristics [13, 88].

The VNO neuroepithelium is composed of three cell types: bipolar, supporting, and basal cells. Bipolar cells are chemoreceptors with a dendrite that runs apically and reaches the lumen and with an axon which leaves the neuroepithelium as it reaches the lamina propria. Cell nuclei of bipolars are round and located within the middle and basal third of the neuroepithelium [86]. Supporting cells also extend from the

Received May 11, 1994

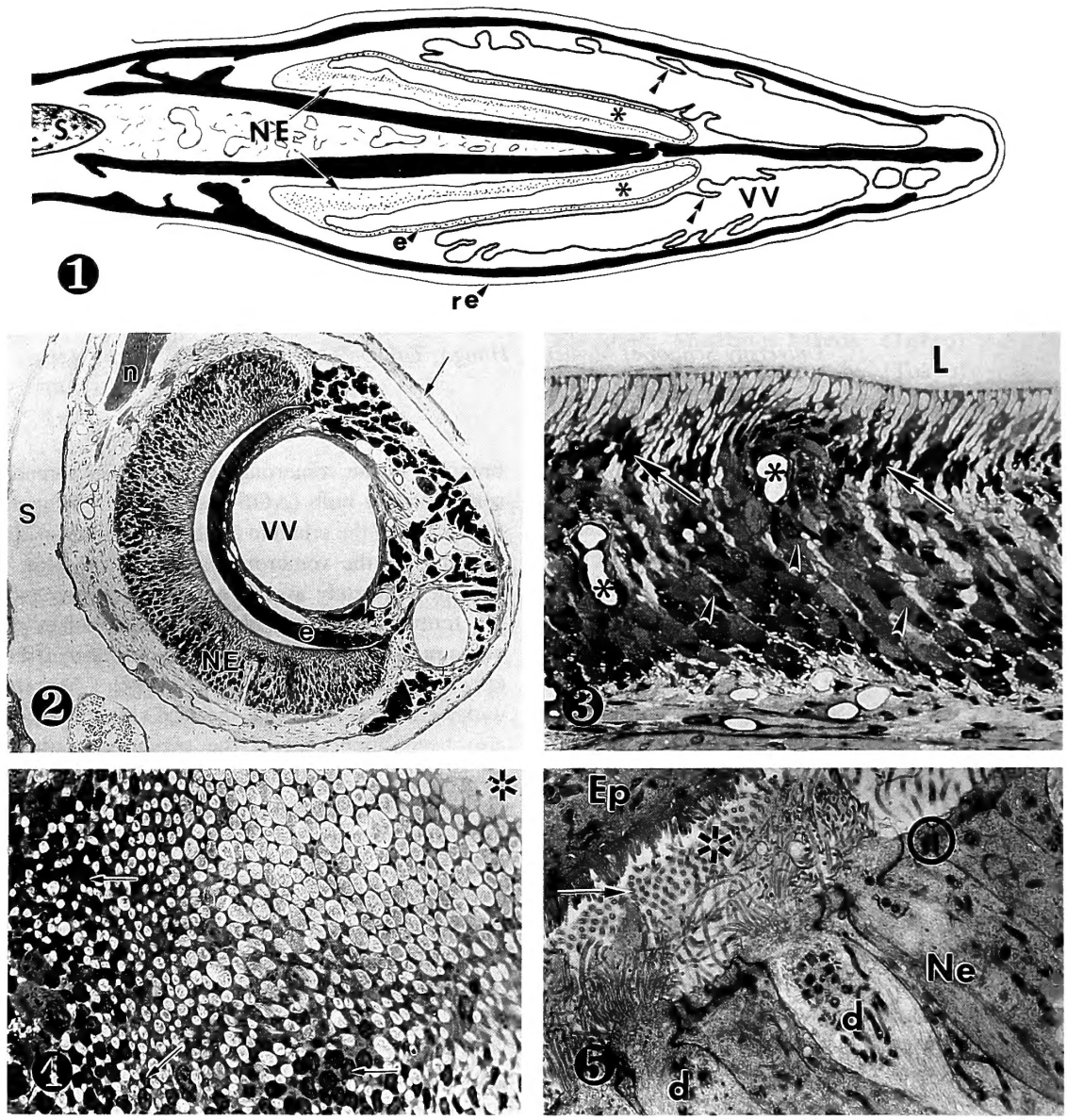

FIG. 1. Camera lucida drawing of an horizontal section of the rat vomeronasal organ. In the anterior part is identified by the cartilaginous nasal septum (S). On each side of the septum, the neuroepithelium (NE) is seen separated from the receptor-free epithelium (e) by the lumen (asters), more laterally the vomeronasal vein (VV) is also illustrated. The valves (arrowheads) project to the lumen of the vein. The organ is sequestered by bone (black), which is covered by the respiratory epithelium (re). Notice the association of the vascular and epithelial laminae which lie parallel to each other. 45×. Toluidine blue staining.

FIG. 2. Coronal section through the right vomeronasal organ. The organ is seen surrounded by bone, medially by the septum (S) and laterally by a thin bonny shell (arrow). The neuroepithelium (NE) shows its characteristic crescent-shape being separated from the receptor-free epithelium (e) by the lumen (no labeled), the vomeronasal vein (VV) lies laterally, in association with numerous serous acini (arrowheads). A non-myelinated nerve is seen in the lamina propria (n). 40×. Toluidine blue staining.

FIG. 3. Light micrograph of the rat vomeronasal neuroepithelium. Nuclei of supporting cells are oval and aligned in the inner part of the apical third whereas bipolar cell nuclei are evenly distributed within the basal area (arrowheads). The neuroepithelium contains blood capillaries (asters). Dendrites of bipolars project apically alternating with the basophilic processes from supporting cells (L=lumen). 300×. Toluidine blue staining.

FIG. 4. Micrograph from an horizontal section of the vomeronasal neuroepithelium. Most nuclei belong to supporting cells, whose basophilic cytoplasm surround dendrites which are somewhat paler. Notice that each dendrite is surrounded by supporting cells given a honeycomb appearance. 320×. Toluidine blue staining.

FIG. 5. Electron micrograph showing the apices of the receptor-free epithelium (Ep) and the neurosensory epithelium (Ne). Cells of the former send short microvilli to the lumen. 7000×.

lumen to the base of the epithelium, however these cells have smaller oval-shaped nuclei and remain within the luminal third [45]. Supporting cells show darker cytoplasm than that seen in bipolars (Fig. 3). Horizontal sections through the apical portion of the sensory epithelium reveal that supporting cells surround each dendrite of the receptor cell. Thus,

supporting cells provide a high degree of independence to each receptor dendrite (Fig. 4).

The apical part of the neuroepithelium has a number of membrane specializations [14]. Electron microscope shows that supporting cells alternate with dendrites of bipolar cells (Fig. 5). Dendrites of receptor cells send numerous thin and thick microvilli and occasionally cilia to the lumen, while supporting cells send only microvilli [86, 112]. Both cell types are united apically by tight junctions and desmosomes. Unlike the primary olfactory epithelium in which gap junctions occur between receptor cells, gap junctions in the VNO epithelium are only found between supporting cells [97, 98]. This may again reflect a high degree of functional individuality in the receptor cell.

Basal cells are confined to the base of the epithelium. These cells are devoid of processes and show occasional mitoses [134]. Contrary to earlier suppositions [102, 103], it is now accepted that basal cells actually represent the stem cell of the neuroepithelium which gives rise to supporting and receptor cells [4, 5]. This has been documented in experiments performed on adult mice, which show that following axotomy or removal of the AOB, basal cells incorporate thymidine and undergo mitosis. Thus, basal cells give rise to precursors which migrate and differentiate into mature bipolar and supporting cells [5, 6]. It is interesting to note that young receptor cells must have the potential of originating new axons, which by reaching the central nervous system achieve functional maturity. Furthermore, it has estimated that in the adult mouse, each new axon must travel at least 7 mm from the VNO to the first relay: the AOB [6]. This plasticity of VNO receptor cells has become even more interesting with the recent demonstration that VNO axons reach the medial preoptic area (MPOA) and hypothalamus [64]. These direct connections bring up the question of whether the newly-formed axons travel within the central nervous system to reach the diencephalon. In this case, the distance estimated by Barber [6] is at least twice long. Resolution of this issue is required to enhance our understanding of the plasticity of sensory cells.

(iii) *Sex differences in the VNO*

The existence of possible structural sex differences in the VNO is still matter of controversy. While several authors have reported a lack of sex differences in VNO size [32] or the neuroepithelium [14, 34], others have reported sex differences in neuroepithelial volume and nuclear size in bipolar and supporting cells [116, 117]. These results deserve to be taken into account, since if sex differences are present in the VNO neuroepithelium, it implies that perinatal titers of sex steroids could induce perinatally permanent changes on the cells of which (i.e. basal cells) undergo a process of cell division and differentiation [3] beyond the so-called critical period of development.

INTERACTION OF PHEROMONES WITH THE VNO

(i) *Extrinsic mechanisms of transport of odors*

Transduction of odors into receptor potentials is the main task of the VNO neuroepithelium [100]. The VNO is isolated from the nasal and oral cavities and its opening is exceedingly narrow [45]. Therefore, the process of transduction largely depends on the transport of a potential stimulus to the domain of the receptor cell [91]. Consequently, the VNO possesses an associated group of structures facilitating the transport of minute quantities of non-volatile material from the habitat to the lumen of the organ. On this premise, the transport could be divided into two systems: an extrinsic one located outside the VNO, and an intrinsic one within the VNO itself. Among the most illustrative extrinsic mechanisms is that used by garter snakes to internalize airborne stimuli. These reptiles capture environmental molecules by fast tongue flicking followed by a retraction of the tongue transferring airborne molecules to the opening of the VNO [17, 36, 44, 45]. In mammals, especially in ungulates and carnivores, the so-called "Flehmen" seems to be the counterpart [83]. This consists of coordinated movements of the neck, facial, and tongue muscles, which, in conjunction with the inspiratory flow of gases through the nasal cavity, displace particles attached to mucous and serous secretions from nostrils to vestibulum, thereby facilitating the entry of substances into the VNO. In laboratory animals, especially in guinea pigs, transport of low-volatility substances is achieved by the so-called "head-bobbing". This is preceeded by an investigative behavior leading to reach the urine of conspecifics, followed by fast, backward and forward head movements, varying from one to four cycles per second [7]. The head-bobbing culminates with the entry of non-volatile substances into the VNO lumen [143].

(ii) *Intrinsic mechanism of transport of odors*

According to Broman's early postulation, the VNO itself acts as a pump, taking up or ejecting fluids to or from the lumen [16]. In fact, once a potential stimulus has been brought to the VNO opening, the VNO promotes further transport towards the neurosensory epithelium on its own. Wysocki *et al.* [143] demonstrated that when hamster's urine is mixed with rhodamine, the fluorescent tracer eventually reaches the lumen of the VNO. More recently, autoradiographic studies have given additional evidence to the uptake of odors by the VNO [107]. Studies in cats [31] demonstrated that electrical stimulation of the cervical sympathetic nerve produced suction of fluid into the VNO lumen, whereas parasympathetic stimulation produced ejection of fluid from the VNO. This "pumping" seems to be due to the caliber of the VNO, which in turn is determined by the vasomotor activity of the autonomous nervous system [91, 92]. In fact, this displacement results from the amount of blood passing through the vomeronasal vein. Since the VNO epithelial tube lies in parallel to the vomeronasal vein [130] (Figs. 1 and 2), the volume of the VNO lumen is inversely related to the diameter of the vomeronasal vein. In summary, the auto-

nomic nervous system controls the access of non-volatile material to the VNO by influencing the rate of blood supplied to the vomeronasal vein [91].

Ciliary activity and secretions from the associated glands represent additional means of promoting transport and distribution of non-volatiles along the VNO lumen. In fact, ciliated cells of the receptor-free epithelium [13, 104], may contribute to the transport of substances along the epithelial surface. In addition, the serous glands lying in the lamina propria may also play a role in the process of transport of potential stimuli. Mendoza [87] has found that acini of the vomeronasal glands and surrounding smooth muscle fibers receive autonomic nerve endings. Therefore, it is likely that upon autonomic stimulation, serous secretory products are released to the lumen. These secretions are capable of distributing and rendering odors water soluble, which is a prerequisite for interaction with the receptor's plasma membrane [93].

Immunohistochemical studies have demonstrated the presence of some peptides in the lamina propria, blood vessels and receptor-free epithelium. These substances include galanin [73, 74], substance P [66], and calcitonin gene-related protein (CGRP) [119]. However, their possible functional implications remain to be elucidated. Recently, it has been proposed that because of its association with the sphenopalatine ganglion and nervous plexuses of the VNO, galanin may be involved in controlling the vasomotor activity of the VNO venous plexuses [74].

(iii) *Transduction of olfactory stimuli*

Once pheromones have reached their targets (i.e. receptor cells), the process of transduction from chemical stimulation to receptor potentials takes places. Most of the available information about the cellular events involved in the transduction of odors into action potentials derives from the main olfactory system. Hence, even though there are cytological and immunocytochemical differences between bipolar cells from the main and accessory olfactory system [23, 54, 85], there seems to be no reason to suppose that the transduction process in the VNO would be different [94]. On this premise, the microvilli of bipolar cells of the VNO are the counterpart of the cilia which comprise most of the transduction apparatus of primary olfactory receptor cells [70, 84]. In this place olfactory stimuli bind to the receptor cell membrane inducing an intracellular increment of cAMP or IP_3 via G-protein binding receptor molecules [10, 11]. Receptor potentials seem to be mediated by activation of non-specific cation channels [37] via cAMP-activated or IP_3-activated Ca^{++} channels [55].

EFFERENT CONNECTIONS OF THE VNO

(i) *The polysynaptic pathway*

Santiago Ramón y Cajal [19] demonstrated that the vomeronasal nerves project to dendrites of mitral cells of the AOB. These original observations have been confirmed by other researchers so it is accepted that the AOB is the first relay of the vomeronasal system. Apart from this direct projection, a short path from mitral cells to the granule cell layer has been proposed on the basis of quantitative autoradiography [3] and anterograde transsynaptic transport of horseradish peroxidase [51]. From the AOB fibers project centrally in the accessory olfactory tract to the bed nucleus of the accessory olfactory tract (BNAOT), medial amygdaloid nucleus (MAN) and posteromedial cortical amygdala (PMCAN), as well as to the posterodorsal part of the bed nucleus of the stria terminalis (BNST) [15, 114]. Since it was found that the MAN and PMCAN receive mostly, but not exclusively [69], direct projections from the AOB [51], these nuclei have been joined by the term "vomeronasal amygdala" [57]. Electrophysiological studies have typified the excitatory and inhibitory nature of these connections. Furthermore, this technique has also shown that the vomeronasal amygdala has reciprocal inhibitory and excitatory connections with both the AOB and hypothalamic ventromedial nucleus (VMN) [142]. Because of the implications of the amygdala in reproductive functions [82, 113], this circuitry may represent a substratum of the process of integration of olfactory inputs prior to reaching the diencephalic nuclei involved in sex behavior and gonadotropin secretion [142]. The vomeronasal amygdala has different outputs. While the MAN sends efferents to the medial preoptic-anterior hypothalamic area and ventromedial and ventral premammillary hypothalamic nuclei, the PMCAN projects to the retrocommissural BNST as well as to the contralateral MAN.

(ii) *The direct pathway*

Recently a monosynaptic link between the VNO and the MPOA, VMN, and hypothalamic arcuate nucleus (ARCN) has been found [64]. Thus, selective transection of the vomeronasal nerves inside the bonny capsule (Figs. 6 and 7) produces orthograde degeneration in the neuropil of these nuclei, demonstrating that axons of bipolar cells do end up in the neuropil of these nuclei. Although this approach precluded proving whether vomeronasal efferents project on luteinizing hormone-releasing hormone (LHRH) producing neurons, it is conclusive that bipolar cells from the VNO can have direct access to the nuclei in which LHRH neurons have been encountered [21, 33, 60, 118]. Therefore, it is likely that through this direct pathway the excitatory and inhibitory receptor potentials generated in bipolar cells may reach the MPOA and medial basal hypothalamus, influencing sex behavior and gonadotropin secretion in a monosynaptic fashion (Figs. 8 to 12).

SEXUALLY DIMORPHIC NUCLEI RECEIVING INPUTS FROM THE VNO

The VNO projects to some of the brain areas involved in the control of gonadotropin secretion and sex behavior displaying structural sex differences [40, 45, 71, 117]. These nuclei will be reviewed next.

(i) *Sex differences in the neuroendocrine brain at light microscopic level*

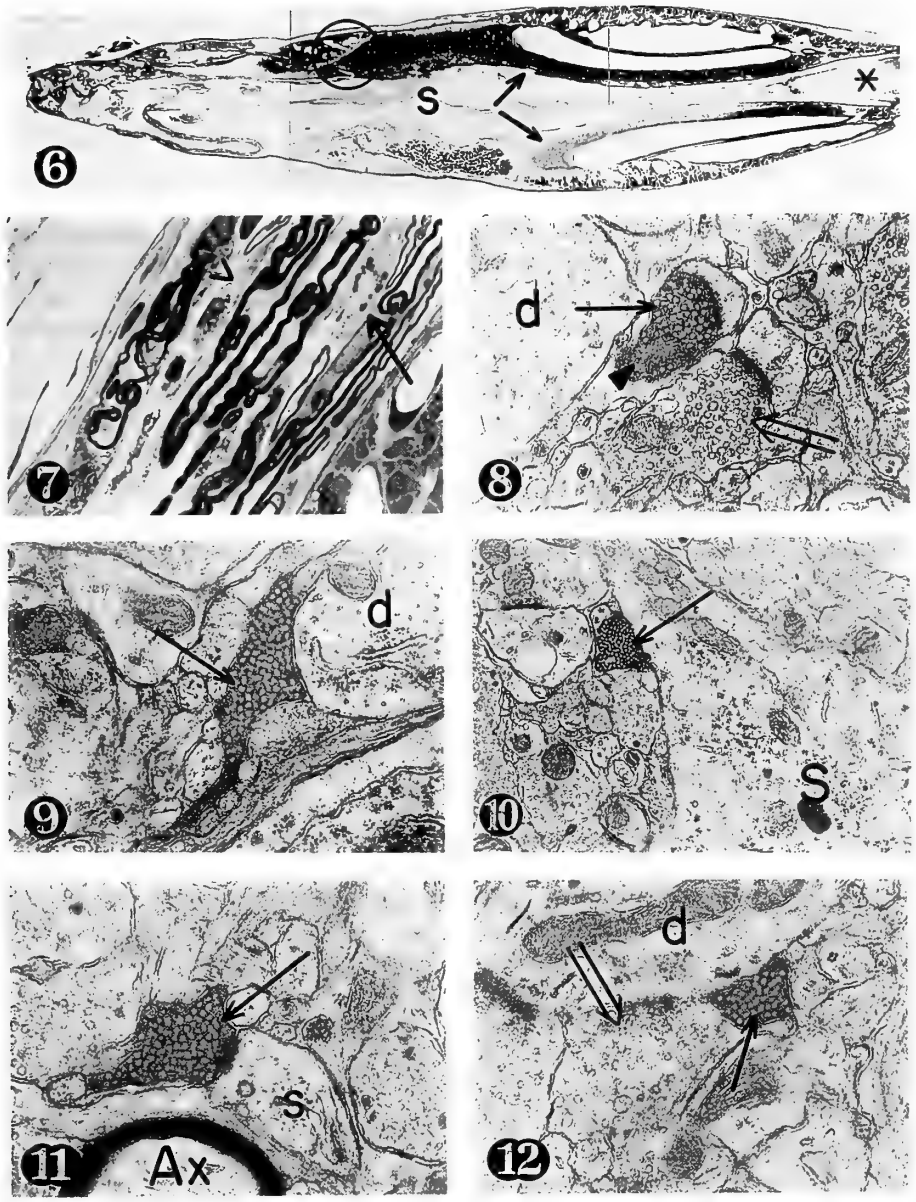

FIG. 6. Horizontal section of the vomeronasal organ. The cartilage of the nasal septum can be seen in the anterior part (aster). The neuroepithelium (arrows) is seen on both sides of the septal bone (S). As shown the lesion (circle) is circumscribed to the lumen, which is encased by the bonny shell. 40×. Toluidine blue staining. (Reproduced with permission from Ref. [64]).

FIG. 7. Light micrograph of a branch of the vomeronasal nerve caudal to the cut. The myelinated nerves have a waving contour and some Schwann cells display vacuolated cytoplasm (arrow head). A mitotic spindle of a Schwann cell is seen (arrow). 480×. Toluidine blue staining. (Reproduced with permission from Ref. [64]).

FIG. 8. Electron micrograph of the neuropil of the central part of the MPOA of a rat with transection of the vomeronasal nerves. Two axodendritic spine synapses are seen, a degenerating one (single arrow) whose matrix is very electron-dense, containing numerous round-shaped vesicles and a mitochondrion (arrow head). Another bouton of normal appearance is seen (double-tailed arrow). In the upper left a dendritic shaft (d) is observed. 15,000×. (Reproduced with permission from Ref. [64]).

FIG. 9. Electron micrograph showing a degenerating terminal (arrow) contacting with a dendritic shaft (d) in the neuropil of the central part of the MPOA. 15,200× (Reproduced with permission from Ref. [64]).

FIG. 10. Micrograph of the central part of the MPOA in which a degenerating bouton makes an axosomatic contact (S=neuronal soma). 7,000 × (Reproduced with permission from Ref. [64]).

FIG. 11. Neuropil of the VMN showing orthograde degeneration (arrow). The bouton is synapsing a dendritic spine (s). At the bottom a myelinated axon (Ax) is seen. 15,200× (Reproduced with permission from Ref. [64]).

FIG. 12. Electron micrograph of the neuropil of the ARCN. A degenerating terminal (single arrow) is seen in contact with a dendritic shaft (d). A normal appearance synaptic bouton (double arrow) is also seen forming an axodendritic synapse. 15,000× (Reproduced with permission from Ref. [64]).

In 1978, Gorski *et al.* [39] reported a marked sex difference in the MPOA of the rat brain. The volume of this intensely stained neuron group, which was termed as sexually dimorphic nucleus of the POA (SDN-POA), is markedly larger in the male than in the female. Sex difference in nuclear volume is also found in the AOB of rats [24, 110, 116], in the BNST of rats and guinea pigs [49, 50] in the BNAOT [24, 25], VMN [77], in the MAN of rats [50, 99]. According to Del Abril *et al.* [28], no sex difference exists in the total nuclear volume of the BNST, but a sexual difference is found in the posterior region of the medial BNST. In general, it is assumed that the volume of these nuclei is larger in males than in females, and that neonatal castration of the male reduces the volume of these nuclei to the size of the female's. Conversely, the volume of the anteroventral periventricular nucleus (AVPV) of the POA is larger in female rats and guinea pigs than that in males [8]. Furthermore, in female rats [52] and guinea pigs [18] the volume of the AVPV decreases with perinatal exposure to androgen. In addition, it has been demonstrated that the nuclear volume of the anterior region of the medial BNST is greater in female rats than that in males, and is likewise modified by perinatal exposure to androgens [28]. These findings strongly suggest underlying sex differences in the number of neurons, afferent fibers and synapses as well as in the dendritic morphology, which ultimately account for the difference in nuclear volume. This postulated is supported by two facts. There is a difference in neuron density in the AOB [132], BNAOT [24, 25], BNST [42], AVPV [124], and MPOA [39] between sexes, and the difference in neuron density is determined by sex steroids in the perinatal period. As far as neuron processes are concerned, differences have been documented in dendritic morphology of AOB neurons in rats [20], and POA neurons in hamsters [41], monkeys [2], rats [46] and ferrets [22, 131]. Since studies of Weisz and Ward [138] indicate that plasma titers of androgen are much higher in males than in females, the observed sex differences in neuron density cannot be attributed only to genomic sex differences. This is further supported by the fact that suppression of endogenous gonadal sex steroid (i.e. testosterone) by perinatal castration of the male produces a feminine phenotype in terms of nuclear volume, neuronal density and dendritic morphology.

In 1985, Swaab and Fiers [129] reported a sexual dimorphism in the POA, in an area that appears to be the human counterpart of the SDN-POA [39]. Soon afterward, Allen *et al.* examined the human POA and subdivided the interstitial nucleus of the anterior hypothalamus (INAH) into four neuron groups: INAH 1–4 [1]. They found that the volume of both INAH-2 and INAH-3 is larger in men than in women, and argued that Swaab and Fliers's SDN-POA is the equivalent of their INAH-1 but did not detect significant sex difference in the INAH-1 volume. LeVay [68] reported that the INAH-3 was the only nucleus displaying sexual dimorphism. Although further studies are necessary to reconcile these results, it is worthwhile to note that sexual dimorphism is found in neuronal structures which are thought to be responsible for sexual functions [127]. It has now been demonstrated that during the early stages of development of the central nervous system, plasma levels of androgen are much higher in male than in female fetuses [139]. Therefore, it is conceivable that the male's higher plasma titers of perinatal androgen may in fact induce the difference in the nuclear volume of the POA in humans.

(ii) *Ultrastructural sex differences in the VNO pathways and neuroendocrine brain*

Quantitative electron microscopic studies have disclosed numerous sex differences in the synaptic organization of the mammalian brain [29, 78, 81]. Most efferent nuclei of the vomeronasal system are sexually dimorphic in terms of synaptic inputs. The number of axodendritic shaft synapses in the MAN of male rats is significantly greater than that of females [105]. In the ARCN, the number of axodendritic spine synapses in female rats is approximately two-fold greater than that in males, whereas the number of axosomatic synapses in females is approximately half of that in males (Table 1) [75, 76]. However, no sex difference was detected in the number of shaft synapses. This sexually dimorphic pattern of synaptic distribution is similar to that found in the strial part of the POA [108, 109]. More recently it was determined that in the

TABLE 1. Number of axodendritic and axosomatic synapscs in the arcuate nucleus (ARCN) of normal and neonatally androgenized or castrated rats

Group	Number of rats	Axodendritic synapses[a]		Axosomatic synapses[b]
		Shaft synapses	Spine synapses	
Normal females	8	1655±94*	242±30	2.11±0.15 (166)[c]
Androgenized females	7	1507±79	174±31	3.84±0.26 (130)
Normal males	7	1607±138	144±24	3.86±0.20 (160)
Castrated males	7	1462±62	257±24	1.97±0.25 (150)

Reproduced with permission from Ref. [75]

* Mean±SEM.

[a] Axodendritic synapses were counted per 18,000 μm^2 in the ARCN.

[b] Number of axosomatic synapes per cell body. For counting synapes, only cell bodies whose profiles could be seen were randomly selected.

[c] Number of neurons in parenthesis.

MPOA the number of shaft synapses was higher in males than in females, while no sex difference was found in the number of spine synapses [63]. In the suprachiasmatic nucleus, the incidence of spine synapses is higher in males than in females [43, 65]. As previously proposed, the sexual dimorphism in neural connectivity [30, 111] may be due to a sexually differentiated synaptic population under the influence of perinatal sex steroid environment. All of these nuclei except the suprachiasmatic nucleus contain a number of sex steroid-accumulating neurons. Given the fact that with exception of the suprachiasmatic nucleus, all of these sexually dimorphic nuclei contain sex steroid-accumulating neurons [106, 128], these sex differences strongly support the idea that synaptic organization may vary according to the genomic responses of each individual nucleus to organizational action of sex steroids.

Although quantitative studies are required to determine whether the observed light microscopic sex differences in the AOB and BNAOT (vide supra) are underlain by ultrastructural difference(s), it is predictable that AOB and BNAOT may have quantitative sex differences in their synaptic organization. However, this hypothesis needs to be investigated.

According to Stumpf [128], Pfaff and Keiner [106] and Simerly *et al.* [126], there is a regional difference in the distribution pattern of sex steroid-accumulating neurons in the VMN. This correlates with a regional difference in the synaptic pattern in the VMN [78, 79, 80]. As shown in Figure 13, the number of shaft and spine synapses in the ventrolateral part of the VMN (VL-VMN), which contains abundant sex steroid-accumulating neurons, is significantly greater than that in the dorsomedial VMN (DM-VMN), which only contains a few. The number of shaft and spine synapses in the male VL-VMN is significantly greater than in the female VL-VMN, but no sex difference is found in the DM-VMN. These findings indicate that the presence of sexually dimorphic synaptic organization is only restricted to the VL-VMN which contains a number of sex steroid-accumulating neurons. Neonatal castration of the male reduces the number of shaft and spine synapses in the VL-VMN to a level comparable to the normal female. The number of shaft and spine synapses in the female VL-VMN is increased to the level comparable to that of normal males by neonatal exposure of androgen. These findings reinforce the significance of the sex steroid environment at neonatal period for the development of sexually dimorphic synaptic organization in the neuroendocrine brain.

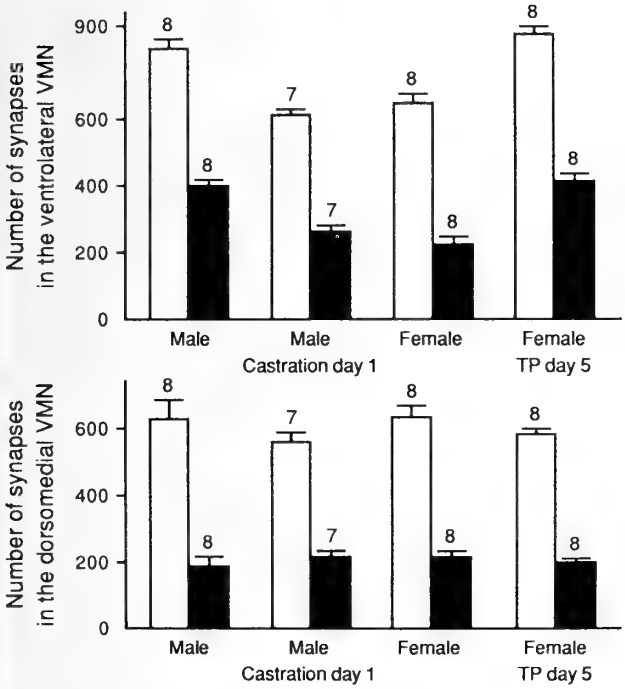

FIG. 13. Number of axodendritic shaft and spine synapses in the ventrolateral and dorsomedial parts per 10,000 μm^2 in the VMN of normal males (Male) and females (Female), males castrated on day 1 (Male Castrated day 1) and females treated with 1.25 mg testosteróne propionate (TP) on day 5 (Female TP day 5). Open bars=shaft synapses; solid bars=spine synapses. Vertical lines indicate SEM. Number of vertical lines refer to the number of rats examined. (Reproduced with permission from Ref. [79]).

(iii) *Immunohistochemical analysis of the sexual differences in the neuroendocrine brain*

Recent immunohistochemical studies have shown that there is sexual dimorphism in the distribution pattern of neuronal cell bodies and fibers containing several types of neurotransmitters and neuromodulators. These include vasopressin in the BNST and POA [26, 133, 135], substance P in the BNST and MAN [26, 27, 72], cholecystokinin in the POA, BNST and MAN [62, 95, 96, 125], opioid peptides in the periventricular POA and MPOA [35, 124, 125, 137], galanin in the MPOA [9, 89, 90], calcitonin gene-related peptide (CGRP) in the MPOA [47, 48] LHRH in the POA [58, 59, 60], serotonin in the MPOA [120, 121], and tyrosine hydroxylase (TH) in the AVPV [122, 123].

The distribution pattern of vasopressin-immunoreactive fibers in the BNST [135], enkephalin-immunoreactive fibers in the periventricular POA [136, 137], and serotonin-immunoreactive fibers in the MPOA [120, 121] is also sexually dimorphic, and the distribution of these neurotransmitters depends on perinatal exposure to sex steroids. Similarly, some neuronal groups of the neuroendocrine brain bear immunohistochemical characteristics which are determined by the perinatal influence of gonadal sex steroids. Thus, the number of CGRP-immunoreactive neurons in the MPOA is significantly larger in male rats than that in females [47, 48]. Furthermore, neonatal castration of the male rat reduces the number of these neurons to that observed in the female. Conversely, neonatal exposure of the female rat to androgen induces a masculine pattern in the density of CGRP-immunoreactive neurons. On the other hand, the number of TH-immunoreactive neurons in the AVPV is larger in the female rat than in the masculine homologue [122, 123]. Furthermore, recent in situ hybridization histochemistry revealed that there is a larger number of TH mRNA expressing

neurons in the AVPV of the female or neonatally castrated male than in the intact male or neonatally androgenized female [126]. According to Merchenthaler *et al.* [90], the number of LHRH-immunoreactive neurons coexpressing galanin in the MPOA/diagonal band of Broca is 4 to 5 times higher in female rats than that in males. Moreover, neonatal castration of the male reduces the incidence of galanin-LHRH co-localization to that found in the female. These sex differences in the number of CGRP- and TH-immunoreactive neurons represent a unique aspect of sexual differentiation in the sense that only certain phenotypic characteristics of particular neuron lineage are dimorphic.

The LHRH neurons of the POA represent the final common pathway regulating gonadotropin secretion by the anterior pituitary. The activity of LHRH neurons is considered to be regulated by intra- and extrahypothalamic neuronal elements as well as the steroidal environment [33]. Since LHRH neurons do not accumulate estrogen [118], it seems plausible that other estrogen-sensitive interneurons in the POA may integrate steroidal signals which in turn modify the activity of LHRH neurons. Immunohistochemical studies have suggested that other neurochemicals may also modulate estrogen receptor (ER)-immunoreactive neurons in the POA [56]. This is supported by immuno-electron microscopic studies indicating that neuropeptide Y-[56], LHRH-[60], and enkephalin-immunoreactive terminals [61] make synaptic connections with ER-immunoreactive neurons. Langub and Watson [61] have pointed out that in female rats more enkephalin-immunoreactive terminals (synaptic and non-synaptic) contact the cell body of ER-immunoreactive neurons than those in males. Neurons located in the POA may be influenced by both estrogen and neurotransmitters/neuromodulators via, respectively, nuclear receptors and synaptic inputs. With respect to the LHRH neuronal system, a sexual dimorphism exists in the synaptic inputs to LHRH neurons in the rat POA [21]. Thus, LHRH neurons in females have approximately twice the number of synapses as do those of males. β-Endorphin-immunoreactive terminals contribute to this dimorphism. Because a subset of β-endorphin-immunoreactive neurons has been reported to accumulate estrogen [101] and to contain immunoreactive ER [67], it is possible that physiological differences in the regulation of gonadotropin secretion may also be reflected in a sexually dimorphic connectivity of the LHRH system in which this neuronal subset may be involved.

CONCLUDING REMARKS

While it is well established that in mammals the interaction of gonadal sex steroids with the central nervous system and pituitary represents the main regulatory stimulus of gonadotropin secretion [38, 82], studies carried out during the past few decades support the assumption that certain olfactory stimuli are capable of exerting a modulatory effect upon the neural structures which control gonadotropin secretion. Furthermore, it has been shown that in rodents pheromones modify gonadotropin secretion via the vomeronasal system. In fact, certain pheromones released in excretory and secretory products influence in the endocrine and behavioral aspects of reproductive function. The interaction of pheromones with the vomeronasal neurosensorial epithelium modifies gonadotropin secretion influencing onset of puberty, estrous cycle, gestation, feminine and masculine sexual behaviors, and maternal behavior. It is interesting to highlight that regardless of the pathway that nerve impulses follow from the VNO to reach the brain, terminations in the vomeronasal amygdala and medial preoptic-hypothalamic nuclei are the neuronal structures whereby pheromones may modify the sex-steroidal responses governed by the brain. Moreover, since most of these brain areas contain neurons with sex steroid receptors and display quantitative structural and biochemical sex differences, it is plausible that these characteristics may represent the inherent ability of individuals from each sex to respond differently to pheromonal stimuli. This postulate is made on the assumption that the same stimulus placed in the VNO should produce a receptor potential of equal magnitude regardless of sex, as it has been demonstrated by stimulation with some putative pheromones [100].

ACKNOWLEDGMENTS

Our studies were partially supported by grants from Consejo Nacional de Ciencia y Tecnología (CONACYT), México. Grant No. 2171–M9104 to JLS and Ministry of Education, Culture and Science of Japan to AM.

REFERENCES

1 Allen LS, Hines M, Shryne JE, Gorski RA (1989) Two sexually dimorphic cell groups in the human brain. J Neurosci 9: 497–506

2 Ayoub DM, Greenough WT, Juraska JM (1983) Sex differences in dendritic structure in the preoptic area of the juvenile macaque monkey brain. Science 219: 197–198

3 Barber PC, Parry DM, Field PM, Raisman G (1978) Electron microscope autoradiographic evidence for specific transneuronal transport in the mouse accessory olfactory bulb. Brain Res 152: 283–302

4 Barber PC, Raisman G (1978) Cell division in the vomeronasal organ of the adult mouse. Brain Res 141: 57–76

5 Barber PC, Raisman G (1978) Replacement of receptor neurones after section of the vomeronasal nerves in the adult mouse. Brain Res 147: 297–313

6 Barber PC (1981) Axonal growth by newly-formed vomeronasal neurosensory cells in the normal adult mouse. Brain Res 216: 229–237

7 Beauchamp GK, Martin IG, Wysocki CJ, Wellington JL (1980) Chemoinvestigatory and sexual behavior in the guinea pig: Urinary components of low volatility and their access to the vomeronasal organ. In "Chemical Signals Vertebrates and Aquatic Invertebrates" Ed by D Müller-Schwarze and RM Silverstein, Plenum Press, New York, pp 327–329

8 Bleier R, Byne W, Siggelkow I (1982) Cytoarchitectonic sexual dimorphisms of the medial preoptic area and anterior hypothalamic areas in guinea pig, rat, hamster, and mouse. J

Comp Neurol 212: 118–130

9 Bloch GJ, Eckersell C, Millis R (1993) Distribution of galanin-immunoreactive cells within sexually dimorphic components of the medial preoptic area of the male and female rat. Brain Res 620: 259–268

10 Boekhoff I, Breer H (1990) Differential stimulation of second messenger pathways by distinct classes of ordorants. Neurochem Intern 17: 553–557

11 Breer H, Boekhoff I, Tareilus E (1990) Rapid kinetics of second messenger formation in olfactory transduction. Nature 344: 65–68

12 Breipohl W, Bhatnagar KP, Mendoza A (1979) Fine structure of the receptor-free epithelium in the vomeronasal organ of the rat. Cell Tissue Res 200: 383–395

13 Breipohl W, Bhatnagar KP, Mendoza A (1981) Intraepithelial blood vessels in the vomeronasal neuroepithelium of the rat. Cell Tissue Res 215: 465–473

14 Breipohl W, Mendoza A, Miragall F (1982) Freeze-fracturing studies on the main and vomeronasal olfactory sensory epithelia in NMRI-mice. In "Olfaction and Endocrine Regulation" Ed by W Breipohl, IRL Press Ltd., London, pp 309–322

15 Broadwell RD (1975) Olfactory relationships of the telencephalon and diencephalon in the rabbit. I. An autoradiographic study of the efferent connections of the main and accessory olfactory bulbs. J Comp Neurol 81: 21–30

16 Broman I (1919) Das organon vomero-nasale Jacobsoni ein Wassergeruchsorgan. Anat Hefte 58: 143–191

17 Burghardt GM (1977) The ontogeny, evolution, and stimulus control of feeding in humans and reptiles. In "The Chemical Senses and Nutrition" Ed by MR Kare and O Maller, Academic Press, New York, pp 253–275

18 Byne W, Bleier R (1987) Medial preoptic sexual dimorphism in the guinea pig. I. An investigation of their hormonal dependence. J Neurosci 7: 2688–2696

19 Cajal SR (1909) Appareil olfactif muqueuse et bulbe olfactif ou centre olfactif de primer orde. In "Histologie du Système Nerveux de L'homme & des Vertébre´s Vol 2" Ed by L Azoulay, Consejo Superior de Investigaciones Científicas Instituto Ramón y Cajal, Madrid, pp 647–674

20 Caminero AA, Segovia S, Guillamón A (1991) Sexual dimorphism in accessory olfactory bulb mitral cells: a quantitative Golgi study. Neuroscience 45: 663–670

21 Chen W-P, Witkin JW, Silverman AW (1990) Sexual dimorphism in the synaptic input to gonadotropin releasing hormone. Endocrinology 126: 695–702

22 Cherry JA, Tobet SA, DeVoogd TJ, Baum MJ (1992) Effects of sex steroids and androgen treatment on dendritic dimensions of neurons in the sexually dimorphic preoptic/anterior hypothalamic area of male and female ferrets. J Comp Neurol 323: 577–585

23 Cigues M, Labella T, Gayoso M, Sánchez G (1977) Ultrastructure of the organ of Jacobson and comparative study with olfactory mucosa. Acta Otolaryngol 83: 47–58

24 Collado P, Guillamón A, Valencia A, Segovia S (1990) Sexual dimorphism in the bed nucleus of the accessory olfactory tract in the rat. Dev Brain Res 56: 263–268

25 Collado P, Valencia A, Del Abril A, Rodríguez-Zafra M, Péez-Laso C, Segovia S, Guillamón A (1993) Effects of estradiol on the development of sexual dimorphism in the bed nucleus of the accessory olfactory tract. Dev Brain Res 75: 285–287

26 Crenshaw BJ, De Vries GJ, Yahr P (1992) Vasopressin innervation of sexually dimorphic structures of the gerbil forebrain under various hormonal conditions. J Comp Neurol 322: 589–598

27 Dees WL, Kolowski GP (1984) Effects of castration and ethanol on amygdaloid substance P immunoreactivity. Neuroendocrinology 39: 231–235

28 Del Abril A, Segovia S, Guillamón A (1987) The bed nucleus of the stria terminalis in the rat: Regional sex differences controlled by gonadal sex steroids early after birth. Dev Brain Res 32: 295–300

29 De Vries GJ, DeBruin JPC, Uylings HBM, Corner MA (1984) Sex Differences in the Brain. Elsevier/North-Holland, Amsterdam

30 Dyer RG, MacLeod NK, Ellendorff F (1976) Electrophysiological evidence for sexual dimorphism and synaptic convergence in the preoptic and anterior hypothalamic areas of the rat. Proc R Soc Lond B 193: 421–440

31 Eccles R (1982) Autonomic innervation of the vomeronasal organ of the cat. Physiol Behav 28: 1011–1015

32 Estes RD (1972) The role of the vomeronasal organ in mammalian reproduction. Mammalia 36:315–341

33 Fink G (1988) Gonadotropin secretion and its control. In "The Physiology of Reproduction" Ed by E Knobil, JD Neill, LL Ewing, GS Greenwald, CL Markert and DW Pfaff, Raven Press, New York, pp 1349–1377

34 Garrosa M, Coca S, Mora OA (1986) Histological development of the vomeronasal complex in the pre- and postnatal rat. Acta Otolaryngol 102: 291–301

35 Ge F, Hammer Jr RP, Tobet SA (1993) Ontogeny of leuenkephalin and β-endorphin innervation of the preoptic area in male and female rats. Dev Brain Res 73: 273–281

36 Gillinham JC, Clark DL (1981) Snake tongue-flicking: Transfer mechanics to Jacobson organ. Can J Zool 59: 1651–1657

37 Gold GH, Nakamura T (1987) Cyclic nucleotide-gated conductances: a new class of ion channels mediates visual and olfactory transduction. Trend Neurosci 8: 312–316

38 Gorski RA (1972) Physiology of menstruation: Hypothalamo-hypophyseo-ovarian axis. In "Gynecology and Obstetrics Vol I" Ed by Davis, Harper & Row Publishers Inc., Agerstown, pp 1–26

39 Gorski RA, Gordon JH, Shryne JE, Southam AM (1978) Evidence for a morphological sex difference within the medial preoptic area of the rat brain. Brain Res 148: 333–346

40 Goy E, McEwen BS (1980) Sexual Differentiation of the Brain. MIT Press, Cambridge

41 Greenough WT, Carter CS, Steerman C, DeVoogd TJ (1977) Sex differences in dendritic patterns in the hamster preoptic area. Brain Res 126: 63–72

42 Guillamón A, Segovia S, Del Abril A (1988) Early effects of gonadal steroids on the neuron number in the medial posterior region and lateral division of the bed nucleus of the stria terminalis in the rat. Dev Brain Res 44: 281–290

43 Güldner FH (1982) Sexual dimorphism of axo-spine synapses and postsynaptic density material in the suprachiasmatic nucleus of the rat. Neurosci Lett 28: 145–150

44 Halpern M, Kubie JL (1983) Snake tongue flicking behavior: Clues to vomeronasal system functions. In "Chemical Signals in Vertebrates" Ed by D Müller-Schwartze and RM Silverstein, Plenum Press, New York, pp 45–72

45 Halpern M (1987) The organization and function of the vomeronasal system. Annu Rev Neurosci 10: 1–114

46 Hammer RP, Jacobson CD (1984) Sex difference in dendritic development of the sexually dimorphic nucleus of the preoptic area in the rat. Intern J Dev Neurosci 2: 77–85

47 Herbison AE (1992) Identification of a sexually dimorphic neural population immunoreactive for calcitonin gene-related peptide (CGRP) in the rat medial preoptic area. Brain Res 591: 289–295

48 Herbison AE, Dye S (1993) Perinatal and adult factors responsible for the sexual dimorphic calcitonin gene-related peptide-containing cell population in the rat preoptic area. Neuroscience 54: 991–999

49 Hines M, Davis F, Coquelin A, Goy RW, Gorski RA (1985) Sexually dimorphic regions in the medial preoptic area and the bed nucleus of the stria terminalis of the guinea pig brain: A description and an investigation of their relationship to gonadal steroids in adulthood. J Neurosci 5: 40–47

50 Hines M, Allen LS, Gorski RA (1992) Sex differences in subregions of the medial nucleus of the amygdala and the bed nucleus of the stria terminalis of the rat. Brain Res 579: 321–326

51 Itaka SK (1987) Anterograde transport of WGA-HRP in rat olfactory pathways. Brain Res 123: 205–214

52 Ito S, Murakami S, Yamanouchi K, Arai Y (1986) Perinatal androgen decreases the size of the sexually dimorphic medial preoptic nucleus in the rat. Proc Jpn Acad Ser B 62: 408–411

53 Jacobson L (1811) Description anatomique d'un organe observé dans les mammifères. Ann Mus d'Hist Nat Paris 18: 412–424

54 Johnston EW, Eller PM, Jafek BW (1993) An immunoelectron microscopic comparison of olfactory marker protein localization in the supranuclear regions of the rat olfactory epithelium, and vomeronasal neuroepithelium. Acta Otolaryngol 113: 766–771

55 Kalinoski L, Aldinger S, Boyle A, Huque T, Restrepo D (1991) Characterization of an inositol-1,4,5-trisphosphate (IP_3) receptor in isolated olfactory cilia. Chem Senses 16: 183–192

56 Kallo I, Liposits ZS, Flerco B, Coen CW (1992) Immunocytochemical characterization of afferents to estrogen receptor-containing neurons in the medial preoptic area of the rat. Neuroscience 50: 299–308

57 Kevetter GA, Winans SS (1981) Connections of the corticomedial amygdala in the golden hamster. I. Efferents of the "vomeronasal amygdala". J Comp Neurol 197: 81–98

58 King J, Elkind KE, Gerall AA, Millar RP (1978) Investigation of the LH-RH system in the normal and neonatally steroid-treated male and female rat. In "Brain Endocrine Interaction III" Ed by DE Scott, GP Kozlowski and A Weindl, Karger, Basel, pp 97–107

59 King J, Kugel G, Zahniser D, Wooledge K, Damassa D, Alexsavich G (1987) Changes in population of LH-RH immunoreactive cell bodies following gonadectomy. Peptides 8: 721–735

60 Langub Jr MC, Maley BE, Watson Jr RE (1991) Ultrastructural evidence for luteinizing hormone-releasing hormone neural control of estrogen responsive neurons in the preoptic area. Endocrinology 128: 27–36

61 Langub Jr MC, Watson Jr RE (1992) Estrogen receptor neurons in the preoptic area of the rat are postsynaptic targets of a sexually dimorphic enkephalinergic fiber plexus. Brain Res 573: 61–69

62 Larriva-Sahd J, Gorski RA, Micevych PE (1986) Cholecystokinin synapses in the sexually dimorphic central part of the medial preoptic nucleus. Exp Neurol 92: 639–650

63 Larriva-Sahd J (1991) Ultrastructural evidence of a sexual dimorphism in the neuropil of the medial preoptic nucleus of the rat: a quantitative study. Neuroendocrinology 54: 416–419

64 Larriva-Sahd J, Rondán A, Orozco-Estévez H, Sánchez-Robles MR (1993) Evidence of a direct projection of the vomeronasal organ to the medial preoptic nucleus and hypothalamus. Neurosci Lett 163: 45–49

65 LeBlond CB, Morris S, Karakiulakis G, Powell R, Thomas PJ (1982) Development of sexual dimorphism in the suprachiasmatic nucleus of the rat. J Endocrinol 95: 137–145

66 Lee Y, Takami K, Kawai Y, Girgis S, Hillyard CJ, MacIntyre I, Emson PC, Tohyama M (1985) Distribution of calcitonin gene-related peptide in the rat peripheral nervous system with reference to its coexistence with substance P. Neuroscience 15: 1227–1237

67 Lehman MN, Karsch FJ (1993) Do gonadotropin-releasing hormone, tyrosine hydroxylase-, and β-endorphin-immunoreactive neurons contain estrogen receptors? A double-label immunocytochemical study in the Stuffolk ewe. Endocrinology 133: 887–895

68 LeVay S (1991) A difference in hypothalamic structure between heterosexual and homosexual men. Science 253: 1034–1037

69 Licht G, Meredith M (1987) Convergence of main and accessory olfactory pathways onto single neurons in the hamster amygdala. Exp Brain Res 69: 7–18

70 Lowe G, Gold GH (1991) Localization of transduction to olfactory receptor cilia. Chem Senses 16: 122–129

71 MacLusky NJ, Naftolin F (1981) Sexual differentiation of the central nervous system. Science 211: 1294–1303

72 Malsbury CW, McKay K (1987) A sex difference in the pattern of substance P-like immunoreactivity in the bed nucleus of the stria terminalis. Brain Res 420: 365–370

73 Matsuda H, Inagaki S, Kakai Y, Takagi H (1990) Distribution of galanin immunoreactive nerve fibers in the rat nasal mucosa. Brain Res 536: 344–346

74 Matsuda H, Nagahara T, Tsukuda M, Kadota T, Kusunori T, Kishida R (1993) Distribution of galanin immunoreactive fibers in the vomeronasal organ. Biomed Res 14: 177–181

75 Matsumoto A, Arai Y (1980) Sexual dimorphism in 'wiring pattern' in the hypothalamic arcuate nucleus and its modification by neonatal hormone environment. Brain Res 190: 238–242

76 Matsumoto A, Arai Y (1981) Effect of androgen on sexual differentiation of synaptic organization in the hypothalamic arcuate nucleus: an ontogenic study. Neuroendocrionology 33: 116–169

77 Matsumoto A, Arai Y (1983) Sex difference in volume of the ventromedial nucleus of the hypothalamus in the rat. Endocrinol Jpn 30: 277–280

78 Matsumoto A, Arai Y (1986) Morphological evidence for sexual dimorphism in wiring pattern in the neuroendocrine brain. In "Pars Distalis of the Pituitary Gland-Structure, Function and Regulation" Ed by F Yoshimura and A Gorbman, Elsevier, Amsterdam pp 239–245

79 Matsumoto A, Arai Y (1986) Male-female difference in synaptic organization of the ventromedial nucleus of the hypothalamus in the rat. Neuroendocrinology 42: 232–236

80 Matsumoto A, Arai Y (1986) Development of sexual dimorphism in synaptic organization in the ventromedial nucleus of the hypothalamus in rats. Neurosci Lett 68: 165–168

81 Matsumoto A (1991) Synaptogenic action of sex steroids in developing and adult neuroendocrine brain. Psychoneuroendocrinology 16: 25–40

82 McEwen BS (1994) Endocrine effects on the brain and their relationships to behavior. In "Basic Neurochemistry: Molecular, Cellular, and Medical Aspects" Ed by GJ Siegel, Raven Press, New York, pp 1003–1023

83 Melese-d'Hospital PY, Hart BL (1985) Vomeronasal organ cannulation in male goats: Evidence for transport of fluid from oral cavity to vomeronasal organ during flehmen. Physiol Behav 35: 941–944

84 Menco BPM (1991) Ultrastructural localization of the trans-

duction apparatus in the rat's olfactory epithelium. Chem Senses 16: 511–525

85 Mendoza AS, Breipohl W (1983) The cell coat of the olfactory epithelium proper and vomeronasal neuroepithelium of the rat as revealed by means of the ruthenium-red reaction. Cell Tissue Res 230: 139–146

86 Mendoza AS (1986) Morphologische Aspekte der Rezeptorzellen des vomeronasalen Organ von Mais und Ratte. Verh Anat Ges 80: 807–809

87 Mendoza AS (1986) The mouse vomeronasal glands: a light and electron microscopical study. Chem Senses 11: 541–555

88 Mendoza AS, Szabó K (1988) Developmental studies on the rat vomeronasal organ: vascular pattern and neuroepithelial differentiation. II. Electron Microscopy. Dev Brain Res 39: 259–268

89 Merchenthaler I, Lopez FJ, Lennard DE, Negro-Vilar A (1991) Sexual differences in the distribution of neurons coexpressing galanin and luteinizing hormone-releasing hormone in the rat brain. Endocrinology 129: 1977–1986

90 Merchenthaler I, Lopez FJ, Lennard DE, Negro-Vilar A (1993) Neonatal imprinting predetermines the sexually dimorphic estrogen-dependent expression of galanin in luteinizing hormone-releasing hormone neurons. Proc Natl Acad Sci USA 90: 10479–10483

91 Meredith M, O'Connell RJ (1979) Efferent control of stimulus access to the hamster vomeronasal organ. J Physiol 286: 301–316

92 Meredith M, Marquez DM, O'Connell RJ, Stern FL (1980) Vomeronasal pump: Significance for male sexual behavior. Science 207: 1224–1226

93 Meredith M, O'Connell RJ (1988) HRP uptake by olfactory and vomeronasal receptor neurons: use as an indicator of incomplete lesions and relevance for non-volatile chemoreception. Chem Senses 13: 487–515

94 Meredith M (1991) Sensory processing in the main and accessory olfactory systems: Comparisons and contrasts. J Steroid Biochem Mol Biol 39: 601–614

95 Micevych PE, Park SS, Akesson TR, Elde R (1987) Distribution of cholecystokinin-immunoreactive cell bodies in the male and female rat. I. Hypothalamus. J Comp Neurol 255: 124–136

96 Micevych PE, Akesson TR, Elde R (1988) Distribution of cholecystokinin-immunoreactive cell bodies in the male and female rat. II. Bed nucleus of the stria terminalis and amygdala. J Comp Neurol 269: 381–391

97 Mirgall F, Mendoza AS (1982) Intercellular junctions in the rat vomeronasal neuroepithelium. A freeze-fracture study. J Submicroscop Cytol 14: 597–605

98 Mirgall F, Mendoza AS, Breipohl W (1983) Intercellular junctions of the main and vomeronasal olfactory sensory epithelia in rodents. A freeze-fracture study. Verh Anat Ges 77: 745–746

99 Mizukami S, Nishizuka M, Arai Y (1983) Sexual difference in nuclear volume and its ontogeny in the rat amygdala. Exp Neurol 79: 569–575

100 Monti-Bloch L, Grosser BI (1991) Effect of putative pheromones on the electrical activity of the human vomeronasal organ and olfactory epithelium. J Steroid Biochem Mol Biol 39: 573–582

101 Morrell JI, McGinty JF, Pfaff DW (1985) A subset of beta-endorphin- or dynorphin-containing neurons in the medial basal hypothalamus accumulates estradiol. Neuroendocrinology 41: 417–426

102 Moulton DG, Celebi G, Fink RP (1970) Olfaction in mammals-two aspects: Proliferation of cells in the olfactory epithelium and sensitivity to ordours. In "Taste and Smell in Vertebrates" Ed by GEW Wostenholme and J Kinght, Churchill, London, pp 227–250

103 Moulton DG, Fink RP (1972) Cell proliferation and migration in the olfactory epithelium. In "Olfaction and Taste Vol 4" Ed by D Schneider, Wissensch Verlag, Stutgard, pp 20–26

104 Naguro T, Breipohl W (1982) The vomeronasal organ of NMRI mouse. A scanning electron-microscopic study. Cell Tissue Res 227: 519–534

105 Nishizuka M, Arai Y (1981) Sexual dimorphism in synaptic organization in the amygdala and its dependence on neonatal hormone environment. Brain Res 212: 31–38

106 Pfaff DW, Keiner M (1973) Atlas of estradiol-concentrating cells in the central nervous system of the female rat. J Comp Neurol 151: 121–158

107 Poran NS, Vandoros A, Halpern M (1993) Nuzzling in the gray short-tailed opossum. Delivery to ordours to the vomeronasal organ. Physiol Behav 53: 959–967

108 Raisman G, Field PM (1971) Sexual dimorphism in the preoptic area of the rat. Science 173: 731–733

109 Raisman G, Field PM (1973) Sexual dimorphism in the neuropil of the preoptic area of the rat and its dependence on neonatal androgen. Brain Res 54: 1–29

110 Roos J, Roos M, Schaefer C, Aron C (1988) Sexual differences in the development of accessory olfactory bulbs in the rat. J Comp Neurol 270: 121–131

111 Sakuma Y, Pfaff DW (1981) Electrophysiological determination of projections from ventromedial hypothalamus to midbrain central gray: differences between female and male rats. Brain Res 225: 184–188

112 Sánchez-Criado JE, Mora OA, Gallego A (1989) Structure and function of the vomeronasal system. The vomeronasal organ as a priming pheromone receptor in mammals. In "Progress in Sensory Physiology 9" Ed by GN Akoev, GN Adrianov, RD Foreman, A Gallego, OA Mora, Y Oomura, JE Sánchez-Criado and J Syka, Springer-Verlag, Berlin, pp 193–222

113 Sawyer CH (1971) Functions of the amygdala related to feedback actions of gonadal steroid hormones. In "The Neurobiology of the Amygdala" Ed by BE Eleftheriou, Plenum Press, New York, pp 745–762

114 Scalia F, Winans SS (1975) The differential projections of the olfactory bulb and accessory olfactory bulb in mammals. J Comp Neurol 161: 31–56

115 Segovia S, Guillamón A (1982) Effects of sex steroids on the development of the vomeronasal organ in the rat. Dev Brain Res 5: 209–212

116 Segovia S, Orensanz LM, Valencia A, Guillamón A (1984) Effects of sex steroids on the development of the accessory olfactory bulb in the rat: a volumetric study. Dev Brain Res 16: 312–314

117 Segovia S, Guillamón A (1993) Sexual dimorphism in the vomeronasal pathway and sex differences in reproductive behaviors. Brain Res Rev 18: 51–74

118 Shivers BD, Harlan RE, Morrell JI, Pfaff DW (1983) Absence of oestradiol concentration in cell nuclei of LHRH immunoreactive neurons. Nature 304: 345–347

119 Silverman JD, Kruger L (1989) Calcitonin-gene-related-peptide-immunoreactive innervation of the rat head with emphasis in specialized sensory structures. J Comp Neurol 280: 303–330

120 Simerly RB, Swanson LW, Gorski RA (1984) Demonstration of a sexual dimorphism in the distribution of serotonin-immunoreactive fibers in the medial preoptic nucleus of the rat. J Comp Neurol 225: 151–166

121 Simerly RB, Swanson LW, Gorski RA (1985) Reversal of the sexually dimorphic distribution of serotonin-immunoreactive fibers in the medial preoptic nucleus by treatment with perinatal androgen. Brain Res 340: 91–98

122 Simerly RB, Swanson LW, Gorski RA (1985) The distribution of monoaminergic cell and fibers in a periventricular preoptic nucleus involved in the control of gonadotropin release: Immunohistochemical evidence for a dopaminergic sexual dimorphism. Brain Res 330: 55–64

123 Simerly RB, Swanson LW, Handa RJ, Gorski RA (1985) Influence of perinatal androgen on the sexually dimorphic of tyrosine hydroxylase-immunoreactive cell and fibers in the anteroventral periventricular nucleus of the rat. Neuroendocrinology 40: 501–510

124 Simerly RB, McCall LD, Watson SJ (1988) Distribution of opioid peptides in the preoptic region: Immunohistochemical evidence for a steroid-sensitive enkephalin sexual dimorphism. J Comp Neurol 276: 442–459

125 Simerly RB, Young BJ, Capozza MA, Swanson LW (1989) Estrogen differentially regulates neuropeptide gene expression in a sexually dimorphic olfactory pathway. Proc Natl Acad Sci USA 86: 4766–4770

126 Simerly RB, Chang C, Muramatsu M, Swanson LW (1991) Distribution of androgen and estrogen receptor mRNA-containing cells in the rat brain: An in situ hybridization study. J Comp Neurol 294: 76–95

127 Slimp JC, Hart BL, Goy RW (1975) Heterosexual, autosexual and social behavior of adult male monkeys with medial preoptic-anterior hypothalamic lesions. Brain Res 142: 105–122

128 Stumpf WE (1970) Estrogen-neurons and estrogen-neuron system in the periventricular brain. Am J Anat 129: 207–218

129 Swaab DF, Fliers E (1985) A sexually dimorphic nucleus in the human brain. Science 228: 1112–1115

130 Szabó K, Mendoza AS (1988) Developmental studies on the rat vomeronasal organ: vascular pattern and neuroepithelial differentiation. Dev Brain Res 39: 253–258

131 Tobet SA, Zahniser DJ, Baum MJ (1986) Sexual dimorphism in the preoptic/anterior hypothalamic area of ferrets: Effects of adult exposure to sex steroids. Brain Res 364: 249–257

132 Valencia S, Segovia A, Guillamón A (1986) Effects of sex steroids on the development of the accessory olfactory bulb mitral cells in the rat. Dev Brain Res 24: 287–290

133 Van Leeuwen FW, Caffe AR, De Vries GJ (1985) Vasopressin cells in the bed nucleus of the stria terminalis of the rat: Sex differences and the influence of androgens. Brain Res 325: 391–394

134 Wang RT, Halpern M (1980) Light and electron microscopic observations on the normal structure of the vomeronasal organ of garter snakes. J Morphol 164: 47–67

135 Wang Z, Bullock N, De Vries GJ (1993) Sexual differentiation of vasopressin projections of the bed nucleus of the stria terminalis and medial amygdaloid nucleus in rats. Endocrinology 132: 2299–2306

136 Watson, RE, Hoffman GE, Wiegand SJ (1986) Sexually dimorphic opioid distribution in the preoptic area: Manipulation by gonadal steroids. Brain Res 398: 157–163

137 Watson, RE, Wiegand SJ, Hoffman GE (1988) Ontogeny of a sexually dimorphic opioid system in the preoptic area of the rat. Dev Brain Res 44: 49–58

138 Weisz J, Ward IL (1980) Plasma testosterone and progesterone titers of pregnant rats, their male and female fetuses and neonatal offspring. Endocrinology 106: 306–316

139 Winter JSD, Faiman C, Reyes F (1981) Sexual endocrinology of fetal and perinatal life. In " Mechanisms of Sex Determination in Animals and Man" Ed by CR Austin and RG Edwards, Academic Press, London, pp 205–253

140 Wirsig CR, Leonard CM (1986) The terminal nerve projects centrally in the hamster. Neuroscience 19: 709–717

141 Wirsig CR, Leonard CM (1987) Terminal nerve damage impairs the mating behavior of the male hamster. Brain Res 417: 293–303

142 Wong MY, Chen Y, Moss RL (1993) Excitatory and inhibitory synaptic processing in the accessory olfactory system in the female rat. Neuroscience 56: 355–365

143 Wysocki CJ, Wellington JL, Beauchamp GK (1980) Access of urinary nonvolatiles to the mammalian vomeronasal organ. Science 207: 781–783

ZOOLOGICAL SCIENCE 11: 507–510 (1994)

REVIEW

Cell-cycle-dependent Regulation of Myosin Light Chain Kinase

HIROSHI HOSOYA

Department of Biological Science, Faculty of Science, Hiroshima University, Higashi-Hiroshima 724, Japan

INTRODUCTION

In cell division of animal cells, the microfilament cytoskeleton undergoes dynamic reorganization [38, 41]. Microfilament bundles or stress fibers of cultured cells are disassembled during prophase concomitant with cell rounding. After chromosome segregation, the contractile ring is transiently formed perpendicular to the mitotic apparatus and is activated to separate the cytoplasm into two daughter cells. Then, as cells start to spread, microfilaments are reconstructed as stress fibers. However, the molecular mechanisms underlying these changes in microfilament organization are still unknown [for review see references 20, 28, 36, 37]. In particular, what controls the formation and activation of the contractile rings has been a primary objective for investigation.

Myosin light chain kinase (MLCK) has long been suspected to be a signal for the induction of cytokinesis. Although there is a lack of direct evidence, three factors argue for their important roles in activating the contraction of cleavage furrows. First, the regulatory light chain of cytoplasmic myosin II is the same as that of smooth muscle myosin II, which is substrate of MLCK. Second, in smooth muscle, strong physiological evidence has established that phosphorylation of Thr 18 and Ser 19 of the regulatory light chain is linked with the initiation of its actomyosin contraction [42]. Third, the MLCK which catalyzes this reaction is activated by calcium-calmodulin. Because there is growing evidence that Ca^{2+} acts as a second messenger in cytokinesis [14], it would provide a biochemical signal to activate MLCK.

In this short review, I will discuss roles of MLCK to understand mechanisms regulating cytokinesis.

A. FUNCTION OF MLCK

MLCK is activated in the presence of Ca^{+} -calmodulin and phosphorylates the regulatory light chain of myosin II. MLCK is widely present not only in various skeletal, cardiac and smooth muscle cells [1, 5, 9, 23, 35, 48–50, 52] but also in non-muscle cells such as those in the spleen [4], brain [10, 18], Myxomycetes [45], aorta [47], platelets [11, 17], and sea urchin eggs [7].

MLCK shows phosphorylation activity after binding to calmodulin at a ratio of 1 : 1 in the presence of Ca^{2+} (Kd=0.3 nM). However, MLCK detected in Myxomycetes lacks the calmodulin-binding site and shows calmodulin-independent phosphorylation activity [45]. The molecular weight of MLCK purified from smooth muscle, brain, and aorta is generally between 100 kD and 150 kD, but that of MLCK from Myxomycetes is about 35 kD due to the above reason.

MLCK is readily purified, and thus, there are many studies on the enzymatic properties of MLCK purified from the rabbit skeletal muscle or the smooth muscle of the chicken gizzard. The substrate specificity of MLCK is very high. No substrates other than the regulatory light chain (20 kD) of myosin II in muscle and non-muscle cells have been reported.

Previous studies using antibodies raised against smooth muscle MLCK found that MLCK was localized in the stress fibers of non-muscle cultured cells [6, 12], in the mitotic apparatus and midbody of mitotic cells and in the nucleolus of interphase cells [16]. It was also shown that MLCK was localized in the I bands of skeletal and cardiac muscle [6]. Several *in vitro* studies have shown binding of MLCK to actin filaments or myosin [6, 16]. The I-band location for MLCK, however, raises the possibility that MLCK is associated with actin filaments rather than its substrate, myosin, *in vivo*. Interestingly, there is no report showing MLCK localization in the contractile ring in dividing cells. The MLCK localization in this phase remains to be clarified.

MLCK is phosphorylated *in vitro* by several kinases such as cAMP-dependent protein kinase (A kinase) [8], cGMP-dependent protein kinase (G kinase) [31], Ca^{2+}-calmodulin-dependent protein kinase II (CaM kinase II) [22], and phospholipid-dependent protein kinase (C kinase) [23, 33]. Although the *in vitro* phosphorylation of MLCK by these kinases reduces the affinity for calmodulin, the possible role of the phosphorylation of MLCK *in situ* requires further study.

B. MECHANISM OF EXPRESSION OF MLCK ACTIVITY

Recently, the entire amino acid sequence of smooth

Received August 5, 1994

muscle MLCK has been clarified, and the relationship between the structure and function of this enzyme has been studied in detail [34]. Comparison with kinases other than MLCK and ATP-binding proteins has suggested that the glycine-rich region in about middle of the MLCK molecule functions as the catalytic site of this enzyme. In addition, the peptides containing the site phosphorylated by A kinase has been shown to strongly bind to calmodulin. This suggests that the calmodulin binding site is present near the site phosphorylated by A kinase. This area corresponds to Ala 796-Leu 813 near the C terminal in MLCK (Fig. 1). Bagchi *et al.* [2] produced various point mutants using the *E. coli* expression system and suggested the importance of Gly811 and Arg812 at the calmodulin binding site for binding to calmodulin.

On the other hand, Kemp *et al.* [25] reported that a sequence resembling the sequence at the site of myosin 20 kD light chain phosphorylation by MLCK is present near the N terminal of the calmodulin binding site. The synthetic peptide containing the sequence of this region (Ala783-Gly804) inhibited MLCK activity and was termed a pseudo-substrate inhibitor since its structure resembles that of the 20 kD light chain. Ikebe *et al.* [24] partially degraded MLCK with trypsin and evaluated in detail the relationship between the amino acid sequence of each fragment and activity. They confirmed the presence of a site inhibiting calmodulin-dependent kinase activity of MLCK near the N terminal of the calmodulin binding site and showed the primary importance of Arg797-Lys799 at this site for inhibiting activity.

These findings suggest the following mechanism of the expression of MLCK activity. When MLCK is not bound with calmodulin, the pseudo-substrate inhibitor site is bound with or close to the catalytic site of MLCK. Therefore, the catalytic site cannot come into contact with the myosin light chain, and MLCK cannot phosphorylates the myosin light chain. On the other hand, when MLCK is bound with calmodulin, the pseudo-substrate inhibitor site dissociates from the catalytic site, and MLCK phosphorylates the myosin light chain.

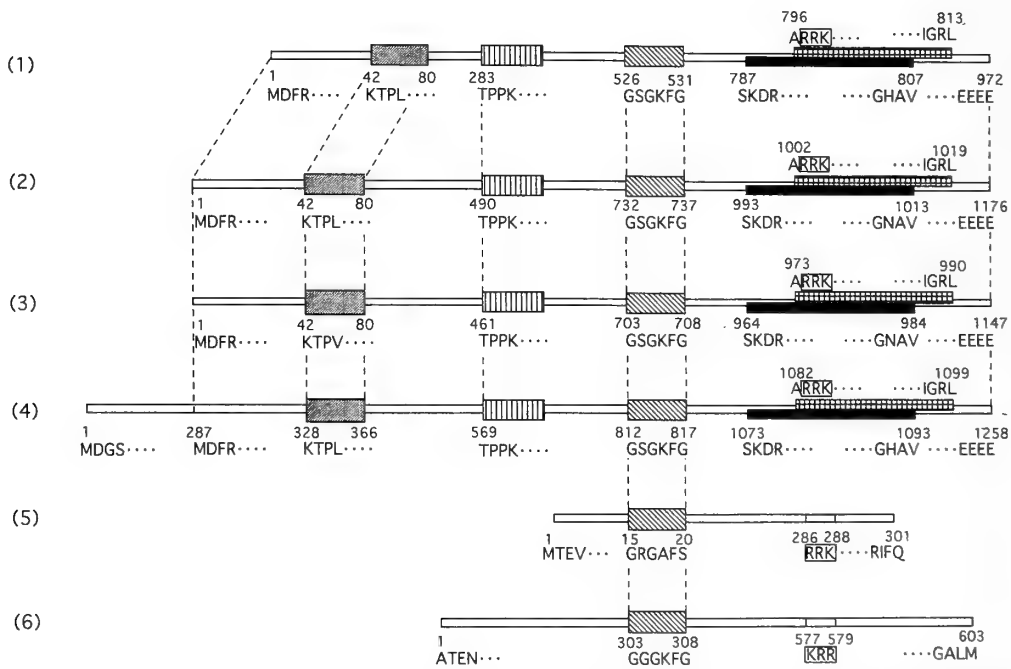

FIG. 1. Schematic representation of regulatory and putative structural domains of MLCKs. (1), chicken gizzard smooth muscle MLCK [34]; (2), bovine stomach smooth muscle MLCK [26]; (3), rabbit uterine smooth muscle MLCK [15]; (4), chick embryo fibroblast MLCK [43]; (5), *Dictyostelium* MLCK [46]; (6), rabbit skeletal muscle MLCK [44]. The amino-terminal sequence of about 80 residues is a highly conserved region among smooth muscle MLCKs. A significant similarity between a sequence from Lys42 to Ala80 (fine lattice) in amino-terminal portion of these four smooth muscle MLCKs and that from Lys695 to Ala731 in the carboxyl-terminal portion of chicken gizzard caldesmon was found [27]. The corresponding sequence in caldesmon is characterized as the actin- and CaM-binding domain [19]. This similarity confirms the assumption that the amino-terminal sequence in the smooth muscle MLCKs plays an important role in the regulation of actin-myosin interaction. Comparison with the ATP binding site in ATP binding proteins suggests that the catalytic site of chicken gizzard MLCK is present in the glycine-rich region starting Gly526 (diagonal stripes). The sequence of the region from Ser787 to Val807 is called substrate inhibitory domain (black box). The pseudosubstrate hypotheis for the regulation of the smooth muscle MLCK was based on the observation that this region bore a remarkable similarity to the phosphorylation site sequence in the regulatory light chain of myosin II [25]. This region is considered to be bound with the catalytic site when not bound with calmodulin. The calmodulin binding site is present on its right side (C terminal side) (cross stripes). Ikebe *et al.* [24] showed the primary importance of three basic residues (Arg797 to Lys799; clear box) at this site for inhibiting NLCK activity. When this site is bound with calmodulin, the pseudosubstrate inhibitor site on the N terminal is impaired, making binding to the catalytic site impossible. This results in expression of MLCK activity. Vertical stripes represent the putative phosphorylation site by cdc2 kinase (Hosoya, unpublished data).

C. CELL CYCLE AND MLCK

As described above, the function and structure of MLCK in the smooth muscle have been extensively studied. In addition, analysis of amino acid sequences has shown that the structure of MLCK in non-muscle cells is similar to that in smooth muscle (Fig. 1). This section outlines the role of MLCK in non-muscle cells in each phase of the cell cycle based on results of previous studies.

Shoemaker *et al.* [43] introduced antisense DNA of MLCK into cultured chick embryo fibroblasts or 3T3 cells and observed a marked morphological changes in the cells. Both cells exhibited a more rounded morphology, reminiscent of the morphological changes seen in V-src-transformed cells. In addition to the effect on morphology, there appears to be an effect of antisense DNA on cell proliferation. These findings indicate that MLCK is indispensable to the progression of the cell cycle (cell division). The marked morphological changes also suggest an important role of MLCK in the maintenance and control of the cytoskeleton such as stress fibers.

Fishkind *et al.* [13] degraded MLCK by trypsin and obtained a fragment without calmodulin sensitivity. They microinjected this fragment into cultured cells during mitosis under a microscope and evaluated its effects on cell division. If MLCK regulates contraction of cleavage furrows, microinjection of this fragment would affect the kinetics of cytokinesis and the formation of cleavage furrows. However, the microinjection neither changed the rate of contraction of cleavage furrows nor affected the formation of cleavage furrows. After microinjection of this fragment, many projections formed near the cell surface, and they repeated protrusion and retraction during and after metaphase. Interestingly, there was a significant delay in the transit time from nuclear envelope breakdown to anaphase onset. These results suggest the involvement of MLCK in the function of the mitotic apparatus but not in the contraction of cleavage furrows.

Pharmacological approaches using MLCK inhibitor have shown interesting results. Mabuchi and Takano-Ohmuro [29] evaluated the action of ML-7 and ML-9 known as MLCK inhibitors on sea urchin eggs and observed inhibition of cytokinesis. We analyzed in detail the time point of action of MLCK using Wortmannin (WM), a MLCK inhibitor recently reported [30]. Cytokinesis was inhibited by addition of 2 to 5 μM of WM at any point of time before mitotic apparatus formation, but not after the mitotic apparatus formation (Hosoya, unpublished data). In the presence of WM below 1 μM, no effect was observed. These results suggest that the site of action of MLCK is present at the time of mitotic apparatus formation but not during contraction of the cleavage furrows (Fig. 2). In other words, MLCK may be involved in the mitotic apparatus formation itself.

Then, how does MLCK activity change during each process of the cell cycle?

Our study using Hela cells showed that MLCK is phosphorylated in mitotic cells (metaphase), and the activity of MLCK phosphorylation is high in metaphase cells but low in interphase cells [21]. After phosphorylation, the affinity of MLCK for calmodulin slightly decreases. As described above, MLCK is a substrate for many kinases (A kinase, G kinase, CaM kinase II and C kinase). However, studies have clarified that kinase that phosphorylates MLCK in metaphase is not these kinases but is cdc2 kinase (Hosoya, unpublished data). When MLCK is phosphorylated by cdc2 kinase in metaphase, MLCK activity may be decreased compared with that in interphase.

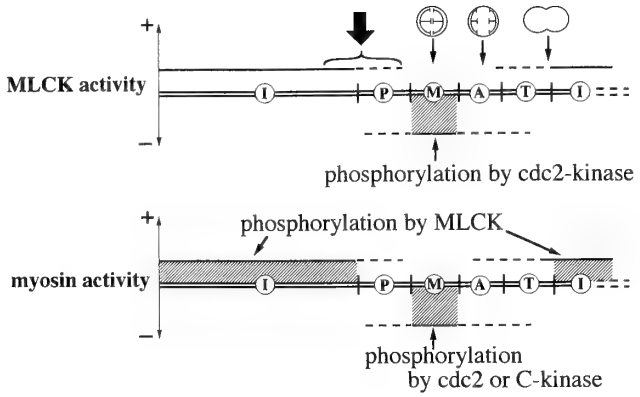

FIG. 2. MLCK activity and presence or absence of phosphorylation of myosin light chain as the substrate in each phase of the cell cycle. I, P, M, A, and T indicate the interphase, prophase, metaphase, anaphase, and telophase, respectively. In the upper figure, the areas above and below the two lines indicate high and low MLCK activity, respectively. In the lower figure, the areas above and below the two lines indicate that myosin is activated and not activated, respectively. In both figures, the shaded area represents that MLCK or myosin light chain is phosphorylated. In the upper figure, the thick arrow indicates the time at which first cell division is not inhibited by WM. At present, changes in phosphorylation and activity of MLCK and myosin in the borderline of the prophase, anaphase, and telophase are unclear, and therefore, the time of phosphorylation is indicated by dotted lines.

Satterwhite *et al.* [39] compared the phosphorylation state of myosin regulatory light chain in *Xenopus* oocyte extracts between metaphase and interphase. In both metaphase and interphase extracts, the light chain was phosphorylated. The sites of phosphorylation in interphase corresponded to those of phosphorylation by MLCK. In metaphase, the site of phosphorylation corresponded to a part of the phosphorylation site (Ser1 and/or Ser2 and Thr9) by C kinase or cdc2 kinase but not to that by MLCK. This result suggests that MLCK is transiently inactive in metaphase, because phosphorylation of these residues by C kinase inhibits the actin-activated ATPase of smooth muscle myosin previously phosphorylated on Ser19 [3, 32]. The inactivation of myosin in metaphase is consistent with our result.

Since phosphorylation of regulatory light chain at the sites (Ser1 and/or Ser2 and Thr9) in metaphase results in reduction of actin-activated myosin ATPase activity, they considered that dephosphorylation at the inhibition sites

should occur at metaphase/anaphase transition to activate the myosin ATPase activity necessary for cytokinesis [40]. Recently, Yamakita et al [51] reported the level of phosphorylation of MLCK sites (Ser19) is increased as cells undergo cell division.

CONCLUSIONS

In interphase, MLCK is active and phosphorylates the light chain of myosin II, and ATPase activity of phosphorylated myosin II is high. In metaphase, however, MLCK is inactive and C kinase and/or cdc2 kinase phosphorylate the light chain. Phosphorylated myosin II is inactive (Fig. 2).

The switching of sites of phosphorylation from Ser1 and/or Ser2 to Ser 19 is likely to be a signal to activate contractile rings during cell division. Which kinase is responsible for the phosphorylation of the MLCK sites at metaphase/anaphase transition? A natural candidate is MLCK. However, how is MLCK reactivated at metaphase/anaphase transition? How is MLCK involved in mitotic apparatus formation and expression of its function? Further studies are needed to elucidate these questions.

REFERENCES

1 Adelstein RS, Conti MA, Hathaway DR, Klee CB (1978) J Biol Chem 253: 8347–8350
2 Bagchi IC, Kemp BE, Means AR (1989) J Biol Chem 264: 15843–15849
3 Bengur AR, Robinson EE, Appella E, Sellers JR (1987) J Biol Chem 262: 7613–7617
4 Bissonnette MD, Kuhn D, de Lanerolle P (1989) Biochem J 258: 739–747
5 Blumenthal DK, Stull JT (1980) Biochemistry 19: 5608–5614
6 Cavadore JC, Molla A, Harricane MC, Gabrion J, BenyaminY, Demaille JG (1982) Proc Natl Acad Sci USA 79: 3475–3479
7 Chow YH, Rebhun LI (1986) J Biol Chem 261: 5389–5395
8 Conti MA, Adelstein RS (1981) J Biol Chem 256: 3178–3181
9 Dabrowska R, Aromatorio D, Sherry JM (1977) Biochem Biophys Res Commun 78: 1263–1272
10 Dabrowska R, Hartshorne DJ (1978) Biochem Biophys Res Commun 85: 1352–1359
11 Daniel JL, Adelstein RS (1976) Biochemistry 15: 2370–2377
12 deLanerolle P, Adelstein RS, Feramisco JR, Burridge K (1981) Proc Natl Acad Sci USA 78: 4738–4742
13 Fishkind DJ, Cao LG, Wang YL (1991) J Cell Biol 114: 967–975
14 Fluck RA, Miller AL, Jaffe LF (1991) J Cell Biol 115: 1259–1265
15 Gallagher PJ, Herring BP, Griffin SA, Stull JT (1991) J Biol Chem 266: 23936–23944
16 Guerriero VJr, Rowley DR, Means AR (1981) Cell 27: 449–458
17 Hathaway DR, Adelstein RS (1979) Proc Natl Acad Sci USA 76: 1653–1657
18 Hathaway DR, Adelstein RS, Klee CB (1981) J Biol Chem 256: 8183–8189
19 Hayashi K, Fujio Y, Kato I, Sobue K (1991) J Biol Chem 266: 355–361
20 Hepler PK (1989) J Cell Biol 109: 2657–2573
21 Hosoya H, Yamashiro S, Matsumura F (1991) J Biol Chem 266: 22173–22178
22 Ikebe M, Reardon S (1990) J Biol Chem 265: 8975–8978
23 Ikebe M, Inagaki M, Kanamaru K (1985) J Biol Chem 260: 4547–4550
24 Ikebe M, Maruta S, Reardon S (1989) J Biol Chem 264: 6967–6971
25 Kemp BE, Pearson RB, Guerriero IC (1987) 262: 2542–2548
26 Kobayashi H, Inoue A, Mikawa T, Kuwayama H, Hotta Y, Masaki T, Ebashi S (1992) J Biochm 112: 786–791
27 Kohama K, Okagaki T, Hayakawa K, Lin Y, Ishikawa R, Shimmen T, Inoue A (1992) Biochem Biophys Res Commun 184: 1204–1211
28 Mabuchi I (1986) Int Rev Cytol 101: 175–213
29 Mabuchi I, Takano-Ohmuro H (1990) Dev Growth Differ 32: 549–556
30 Nakanishi S, Kakita S, Takahashi I, Kawahara K, Tsukuda E, Sano T, Yamada K, Yoshida M, Kase H, Matsuda Y, Hashimoto Y, Nonomura Y (1992) J Biol Chem 267: 2157–2163
31 Nishikawa M, de Lanerolle P, Lincoln TM (1984) J Biol Chem 259: 8429–8436
32 Nishikawa M, Sellers JR, Adelstein RS, Hidaka H (1984) J Biol Chem 259: 8808–8814
33 Nishikawa M, Shirakawa S, Adelstein RS (1985) J Biol Chem 260: 8978–8983
34 Olson NJ, Perrson RB, Needleman DS, Hurwitz MY, Kemp BE, Means AR (1990) Proc Natl Acad Sci USA 87: 2284–2288
35 Pires EMV, Perry SV (1977) Biochem J 167: 137–146
36 Rappaport R (1986) Int Rev Cytol 101: 245–281
37 Salmon ED (1989) Curr Opin Cell Biol 1: 541–547
38 Sanger JW, Sanger JM (1976) In "Cell Motility" Ed by R Goldman, T Pollard, J Rosenbaum. Cold Spring Harbor Laboratory Press, Cold Spring Harbor, NY, pp 1295–1316
39 Satterwhite LL, Lohka MJ, Wilson KL, Scherson TY, Cisek LJ, Pollard TD (1992) J Cell Biol 118: 595–605
40 Satterwhite LL, Pollara TD (1992) Curr Opin Cell Biol 4: 43–52
41 Schroeder TE (1976) In "Cell Motility" Ed by R Goldman, T Pollard, J Rosenbaum. Cold Spring Harbor Laboratory Press, Cold Spring Harbor, NY, pp 265–278
42 Sellers JM (1990) Curr Opin Cell Biol 3: 98–104
43 Shoemaker MO, Lau W, Shattuck RL, Kwiatkowski AP, Matrisian PE, Guerra-Santos L, Wilson E, Lukas TJ, Van Eldik LJ, Watterson DM (1990) J Cell Biol 111: 1107–1125
44 Takio K, Blumenthal DK, Walsh KA, Titani K, Krebs EG (1986) Biochemistry 25: 8049–8057
45 Tan JL, Spudich JA (1990) J Biol Chem 265: 13818–13824
46 Tan JL, Spudich JA (1991) J Biol Chem 266: 16044–16049
47 Vallet B, Molla A, Demaille JG (1981) Biochim Biophys Acta 674: 256–264
48 Walsh MP, Vallet B, Autric F, Demaille JG (1979) J Biol Chem 254: 12136–12144
49 Walsh MP, Guilleux JC (1981) Adv Cyclic Nucleotide Res 14: 375–390
50 Wolf H, Hofman F (1980) Proc Natl Aca Sci USA 77: 5852–5855
51 Yamakita Y, Yamashiro S, Matsumura F (1994) J Cell Biol 124: 129–137
52 Yazawa M, Yagi K (1978) J Biochem 84: 1259–1265

ZOOLOGICAL SCIENCE 11: 511–515 (1994)

Stiffness Changes of Holothurian Dermis Induced by Mechanical Vibration

Rie Shibayama, Takakazu Kobayashi, Hiroaki Wada, Hiroko Ushitani, Jun Inoue, Toshimitsu Kawakami and Haruo Sugi[1]

Department of Physiology, School of Medicine, Teikyo University, Itabashi-ku, Tokyo 173, Japan

ABSTRACT—The effect of mechanical vibration on the stiffness of catch connective tissue in the dermis of a sea cucumber *Stichopus japonicus* was studied using the dermis strip preparation, held between a force transducer and a vibrator. During the application of vibration (peak-to-peak amplitude, 2–10%; 2–20 Hz), the stiffness of fresh, stiffened preparations increased by 40–200%, and then stayed constant or slowly decreased. After the stiffness reached a maximum, pause of vibration (5–20 min) had no effect on the steady level of stiffness, except that the stiffness initially showed a higher value on reapplication of vibration. The stiffness of non-fresh, softened preparations showed a much more marked transient increase during the period of vibration. Electrical stimulation either increased or decreased the stiffness by 10–20% in some preparations examined. The vibration-induced stiffness changes were not affected appreciably by Ca^{2+}-free, high-Ca^{2+} (100 mM) and high-K^+ (100 mM) solutions, acetylcholine (10^{-3} M), and low temperatures (1–2°C). These results are discussed in connection with nervous control of the dermis stiffness.

INTRODUCTION

Holothurians (sea cucumbers) are known to stiffen their body wall in response to mechanical stimuli [14, 15, 18]. The stiffening of the body wall results from an increase in stiffness of the dermis, which constitutes most of the thickness of the body wall. The dermis is mainly composed of extracellular materials containing a network of collagen fibres, no muscle cells being present [6]. The dermis of sea cucumbers is therefore called a catch connective tissue, since its stiffened state can be maintained for a long period of time [12]. Motokawa has shown that the stiffness of the dermis can be varied by a number of factors such as acetylcholine, changes in ionic composition of the medium, coelomic fluid, and mechanical and electrical stimulation [3–5, 7–11]. In the above studies, however, the effects of these factors were examined mainly by recording the rate of extension of the preparation under a constant load. As the preparation is being elongated during the course of experiments, it is difficult to study systematically the effect of mechanical stimulation, which is regarded as being a more natural stimulation to the animal.

The present work was undertaken to study the effect of mechanical vibration on the stiffness of the sea cucumber dermis strip preparations, which were held between a force transducer and a vibrator. It was found that mechanical vibrations are effective in changing the stiffness of the preparation.

Accepted June 17, 1994
Received April 4, 1994

[1] To whom correspondence should be addressed.

MATERIALS AND METHODS

Preparation

Sea cucumbers *Stichopus japonicus* were collected at the Misaki Marine Biological Station and kept in aerated sea water. The dermis, containing no muscular layers, was cut from the animal, and trimmed to obtain a dermis strip (0.5–1 cm long) with a square cross-section (ca. 1.5×1.5 mm). The dermis strip preparation was mounted horizontally in an experimental chamber (3 ml) between a force transducer (UT-100, Shinko: compliance 1 μm/g, resonant frequency 330 Hz) and a vibrator (model-201, Ling). Both ends of the preparation were firmly glued to the extensions of the force transducer and the vibrator.

The experimental chamber was filled with the standard experimental solution (artificial sea water) which had the following composition (mM): NaCl, 497; KCl, 10; $CaCl_2$, 20; $MgCl_2$, 52 (pH 7.2 by $NaHCO_3$). When the concentrations of K^+ and Ca^{2+} were changed, osmotically equivalent amounts of Na^+ were added or removed. Solutions in the chamber were exchanged from time to time using a water-vacuum suction tube. Experiments were made at room temperature (19–22°C), unless otherwise stated.

Stiffness measurement

The preparation was held at its slack length (L_o), i.e. the length at which the resting force was just barely detectable, and was subjected to continuous sinusoidal vibrations (peak-to-peak amplitude, 2–10% of Lo; 2–20 Hz) with the vibrator driven by a power amplifier to which sinusoidal voltages from a waveform generator (model 164, Wavetek) were fed. The length changes of the preparation were recorded with a light source-photodiode system attached to the shaft of the vibrator. In each experiment, the amplitude of vibration was kept constant, so that the amplitude of the vibration-induced force changes was taken as a measure of the stiffness of the dermis strip preparation. The length and force changes of the preparation were simultaneously recorded with an ink-writing oscillograph, or with a digital oscilloscope (model 310, Niolet) on a fast time

base.

Electrical stimulation

In some experiments, the preparation was placed in contact with 10–18 Pt wire electrodes, which were fixed to the bottom of the experimental chamber and connected as alternate anodes and cathodes, and was stimulated electrically with sinusoidal a.c. currents (20–30 V, 20–50 Hz) from an electronic stimulator (SEN-3301, Nihon Kohden).

Electron microscopy

The dermis strip preparation was fixed with a 2.5% glutaraldehyde solution containing 0.6 M sucrose and 2 mM $CaCl_2$ (pH 7.2 by 0.1 M cacodylate buffer). The tissue was then cut into small pieces, postfixed in 2% OsO_4, dehydrated with a graded series of ethanol, and embedded in Quetol 812. Ultrathin sections were cut on a Porter-Blum MT-2 ultramicrotome with a diamond knife, double stained with uranyl acetate and lead citrate, and examined with a JEOL JEM 1200EX electron microscope.

RESULTS

Force changes in response to vibrations

Fig. 1A shows typical force changes of the dermis strip preparation in response to externally applied sinusoidal vibration on a fast time base. Since the preparation was initially kept at its slack length L_o, only the upstroke phase of the applied vibration was effective in stretching the preparation to produce the resulting force changes. It was not possible to produce the force changes taking place symmetrically around a constant level of resting force, because the resting force in the stretched preparation decayed rapidly with time, reflecting the highly extensible nature of the dermis. The force-length loop in response to vibration was narrow and nonsymmetrical in shape with clockwise rotation (Fig. 1B).

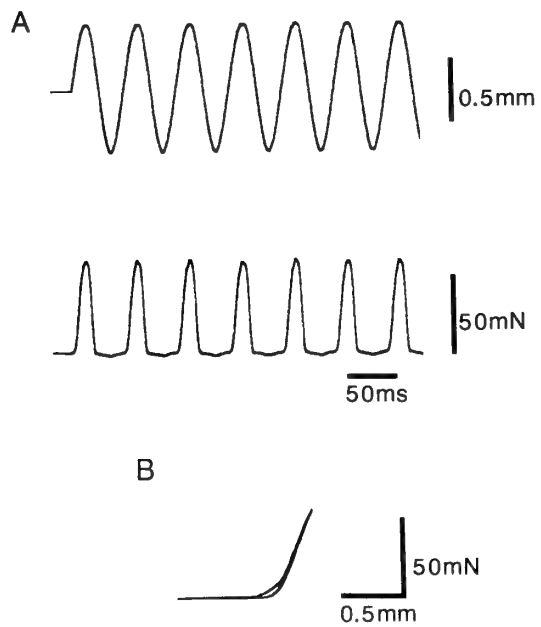

FIG. 1. Force changes of the dermis strip preparation in response to sinusoidal vibrations (5% of L_o, 20 Hz). (A) Length (upper trace) and force (lower trace) changes of the preparation. Note that the preparation is stretched during the upstroke phase of each sinusoidal wave to develop a force. (B) Force-length loop of the preparation.

In the present study, we focused attention on the magnitude of force developed during the stretch phase of vibration of constant amplitude as a measure of the stiffness of the preparation. The time course of the force changes did not change appreciably when the stiffness of the preparation changed markedly with the applied vibrations; in other words, the force changes were scaled according to their amplitude. The above features of the force changes indicate that the amplitude of the vibration-induced force changes serve as a valid measure of the stiffness of the preparation.

Vibration-induced stiffness changes

The sinusoidal vibrations were found to be effective in producing the stiffness changes of the dermis preparations, which were variable depending on the initial state of the preparation. When the dermis preparations were cut from the animal, it always stiffened its body wall. As a result, freshly dissected dermis preparations were obviously much stiffer than the dermis in freely moving animals. On application of vibration, the stiffness of fifteen fresh dermis preparation obtained from ten different animals increased by 40–200% for the first 2–10 min after the beginning of vibration, and then stayed at a constant level (Fig. 2A) or decreased slowly with time (Fig. 2B). The magnitude of the force response at the beginning of vibration (5% of L_o, 20 Hz) ranged from 5 to 20 mN, while the magnitude of force response when the stiffness reached a maximum ranged from 20 to 50 mN.

Fig. 3 shows the effect of pause (5–20 min) of vibration on the stiffness, which had reached a maximum by the

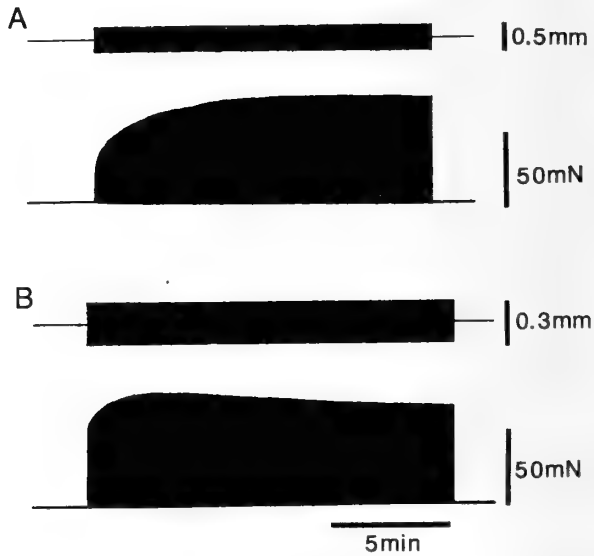

FIG. 2. Records showing the stiffness increase in fresh, stiffened preparations induced by vibration (5%, 20 Hz). The stiffness increased to a maximum value, and then stayed constant (A), or decreased slowly (B).

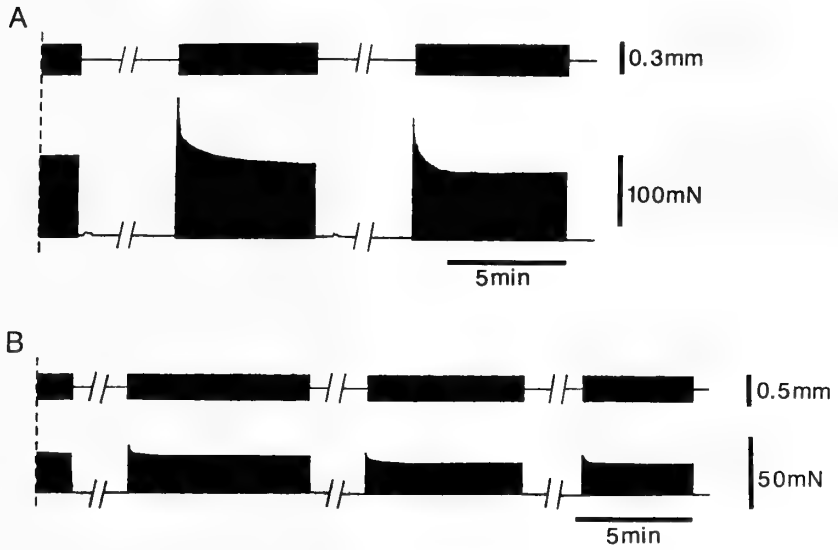

FIG. 3. Records showing the stiffness increase taking place during the period of pause in the preparations, in which the stiffness has reached a maximum by preceding vibration. The degree of the stiffness increase after each pause (10–20 min) of vibration (5%, 20 Hz) is much larger in A than in B. In both A and B, the increased stiffness decreases rapidly to the level equal to that at the end of preceding vibraton.

FIG. 4. Marked transient stiffness increase induced by vibration (2%, 10 Hz) in a nonfresh, softened preparation.

preceding vibration. At the beginning of reapplication of vibration, the stiffness was larger than the value at the end of preceding vibration, but decreased rapidly (in 1 min) to a value nearly as large as that at the end of preceding vibration; then the stiffness stayed at a constant level or decreased slowly with time. The degree of the transient stiffness increase observed after a pause of vibration was variable. In five out of seven preparations examined, the stiffness increased by 70–80% of the steady value at the end of preceding vibration (Fig. 3A), while in the rest two preparations the corresponding stiffness increase was less than 10%.

If, on the other hand, the dermis preparations were kept in the standard experimental solution for more than 10 hr, they tended to become much softer compared with the fresh preparations. Consequently, the length of L_o in the softened preparation was not accurately defined based on the just detectable resting force; instead, L_o was defined as the length at which the preparation became just taut. In such nonfresh, softened preparations, the stiffness exhibited much more marked changes in response to vibrations compared to fresh preparations. As shown in Fig. 4, the stiffness was very small at the beginning of vibration, but increased gradually during the application of vibration to reach a peak, and then decreased slowly with time. In seven softened preparations obtained from five different animals, the magnitude of the force changes when the stiffness was maximum during the application of vibration (5% of L_o, 20 Hz) was 20–30 mN. In three preparations, the above marked transient stiffness increase could be repeated two to three times when vibrations were repeatedly applied after pauses of 20–30 min, though the maximum stiffness value attained during vibration decreased each time of application of vibration.

The above marked effect of vibration on the softened preparations, however, could not be studied in more detail because the softened preparations tended to break with prolonged application of vibration.

Effect of electrical stimulation

To examine the effect of electrical stimulation on the stiffness of the dermis preparation, the fresh preparations were subjected to continuous vibration, and electrical stimulation was applied when the stiffness reached a constant value. In seven out of eleven preparations examined, electrical stimulation had no appreciable effect on the steady level of stiffness. In the rest four preparations, however, the stiffness increased by 10–20% (Fig. 5A) or decreased by 10–20% (Fig. 5B) during the application of electrical stimulation. After the cessation of electrical stimulation, the stiffness

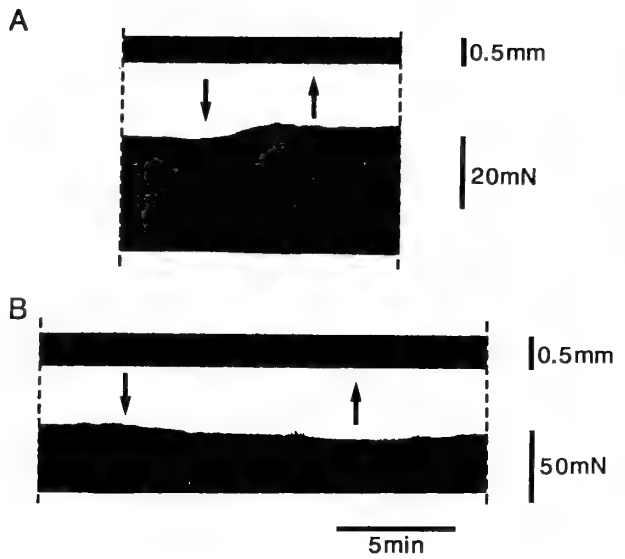

FIG. 5. Effect of electrical stimulation on fresh preparations. Downward and upward arrows indicate onset and cessation of electrical stimulation respectively. In A, the stiffness increased to a higher steady level, while in B the stiffness decreased to a lower value with subsequent slow recovery towards the initial value.

either stayed nearly constant (Fig. 5A) or returned slowly towards the level before stimulation (Fig. 5B)

Effect of ions, acetylcoline and low temperature

Since the rate of extension of the dermis strip preparation is known to be influenced by various ions and drugs such as acetylcholine, we examined the effect of Ca^{2+}-free, high·Ca^{2+} (100 mM), high·K^{+} (100 mM) and acetylcholine (10^{-3} M) solutions on the stiffness of eight fresh preparations, by applying these solutions either during the period of vibration or during the period of pause of 10–30 min. No appreciable effect of these solutions was observed on the subsequent time course of vibration-induced stiffness changes.

As nerve impulse propagation can be blocked by low temperatures (Parker, 1941), we also examined the effect of lowering temperature of the experimental solution to 1–2°C by circulating precooled water around the experimental chamber. In four preparations examined, the time course of vibration-induced stiffness changes was not appreciably affected by low temperatures.

Ultrastructure of the dermis

As shown in Fig. 6, the dermis of *Stichopus japonicus* contained cellular elements consisting of cells with large vacuoles ("vacuole cells") [6], cells without vacuoles ("morula cells") [2], and nerve cells containing clear and cored vesicles. These features are similar to those of the dermis of other species of sea cucumbers, *Thyone bareus* [2] and *Stichopus chloronotus* [6].

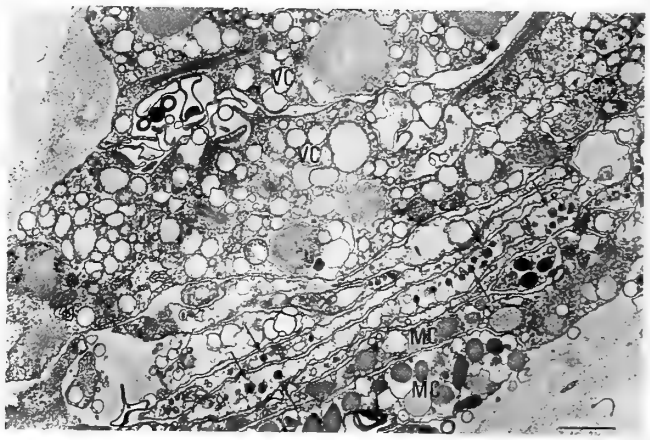

FIG. 6. Electron micrograph of cellular elements in the dermis tissue. Nerve cells containing vesicles (arrows) are closely apposed to vacuole cells (VC) and morula cells (MC). Scale bar, 1 μm.

DISCUSSION

The present experiments have shown that externally applied vibration is effective in changing the stiffness of the dermis preparation, as measured by the amplitude of the vibration-induced force changes. Evidence has been accumulating that the dermis stiffness is controlled by two different types of nerve, one stiffening and the other softening the dermis [12]. Concerning the stiffening of the dermis, Matsuno & Motokawa [1] recently demonstrated that the stiffening of the dermis is associated with release of calcium ions from the lumen of the vacuole cell into the dermis connective tissue, using the pyroantimonate method that is effective in studying calcium translocation associated with the contraction-relaxation cycle of various muscle cells [16, 17]. The present results will be discussed below on the above basis.

In the present study, vibration was used both to induce the stiffness changes and to measure the stiffness (Fig. 1). In fresh, stiffened preparations, the stiffness increased to a maximum for the first 2–10 min after the beginning of vibration (Fig. 2). The applied vibration may first mechanically stimulate the nervous elements in the dermis, which in turn causes release of "dermis-stiffening" substance (possibly calcium ions) from the vacuole cells closely apposed to the nervous elements (Fig. 6) to increase the dermis stiffness. On this basis, the wide range of the extent of vibration-induced stiffness increase (40–200%) depends on the variation in the degree of stiffening of the dermis before the application of vibration, as the nerves in the dermis are mechanically stimulated when the dermis preparation is being prepared. Once the stiffness reached a maximum by the applied vibration, it stayed constant or decreased only very slowly, indicating that vibration was no longer effective in changing the stiffness. This view is supported by the result that pauses of vibration had no appreciable effect on the stiffness; after each pause the stiffness first showed a higher value than that during the preceding vibration, but then

decreased rapidly to a value as large as that during the preceding vibration (Fig. 3). This indicates that the apparent stiffness increase taking place during the period of pause is rapidly eliminated by the subsequent vibration. Our impression at present is that the above rapid stiffness decrease at the beginning of reapplication of vibration might result from a thixotropic nature of the stiffened dermis rather than the action of "softening" nerve; it may be that cross-linkages between the molecules constituting the dermis tissue are partly broken by vibration to result in the initial rapid stiffness decrease. The slow stiffness decrease might also be explained in terms of slow breaking of the cross-linkages. Of course, the possibility is not excluded that the stiffness decrease is due to the action of "softening" nerves.

On the other hand, nonfresh, softened preparations exhibited a marked transient stiffness increase in response to vibration (Fig. 4). In such preparations, "dermis-softening" substance would be expected to be released from the vacuole cells into the dermis tissue as the preparation is kept standing over many hours, while "dermis-stiffening" substance might be taken up into the vacuole cells. The application of vibration might then release "dermis-stiffening" substance, which may overcome the existing effect of "dermis-softening" substance to cause a marked stiffness increase. The transient nature of the above stiffness increase might at least in part, be because the effect of "dermis-stiffening" substance is not long-lasting in the presence of "dermis-softening" substance.

In the present experiments, the initial application of vibration caused only an increase of the dermis stiffness (Figs. 2 and 4). This may be related to the fact that the dermis of living animals can be readily stiffened even by a brief weak mechanical stimulation, while its softening requires intense repeated mechanical stimulation [12]; the applied vibrations were probably insufficient in intensity to cause softening of the preparation. The result that electrical stimulation was effective in changing the stiffness only in some preparations (Fig. 5) may be because externally applied current can not effectively stimulate the nervous elements that are only sparsely distributed in the dermis tissue.

Concerning the mechanism of vibration-induced release of "stiffening" and "softening" substances, the only information obtained in the present study is that propagation of action potential may not be involved, since the vibration-induced stiffness changes were not appreciably influenced by low temperatures that block nerve impulse condition. Though the rate of extension of the dermis strip preparation is affected by Ca^{2+}-free, high-Ca^{2+} and high-K^{+}-solutions and acetylcholine [12], these factors had no appreciable effect on the vibration-induced stiffness changes. It seems possible that diffusion of substances in the dermis tissue occurs much more readily if the preparations is extended many times the initial length. Another possibility may be that these factors affect the "viscosity" of the preparation as measured by its rate of extension with a constant load, but not "stiffness" as measured by the amplitude of vibration-induced force changes in the preparation held at L_o.

REFERENCES

1 Matsuno A, Motokawa T (1992) Evidence for calcium translocation in catch connective tissue of the sea cucumber *Stichopus chloronotus*. Cell Tissue Res 267: 307–312

2 Menton DN, Eisen AZ (1970) The structure of the integument of the sea cucumber, *Thyone briareus*. J Morphol 131: 17–36

3 Motokawa T (1981) The stiffness change of the holothurian dermis caused by chemical and electrical stimulation. Comp Biochem Physiol 70C: 41–48

4 Motokawa T (1982*a*) Factors regulating the mechanical properties of holothurian dermis. J exp Biol 99: 29–41

5 Motokawa T (1982*b*) Rapid change in mechanical properties of echinoderm connective tissues caused by coelomic fluid. Comp Biochem Physiol 73C:223–229.

6 Motokawa T (1982*c*) Fine structure of the dermis of the body wall of the sea cucumber, *Stichopus chloronotus*, a connective tissue which changes its mechanical properties. Galaxea 1: 55–64

7 Motokawa T (1984*a*) The viscosity change of the body-wall dermis of the sea cucumber *Stichopus japonicus* caused by mechanical and cheical stimulation. Comp Biochem Physiol 77A: 419–423

8 Motokawa T (1984*b*) Viscosity increase of holothurian body wall in response to photic stimulation. Comp Biochem Physiol 79A: 501–503

9 Motokawa T (1986) Effects of ionic environment on viscosity of catch connective tissue in holothurian body wall. J exp Biol 125: 71–84

10 Motokawa T (1987*a*) Cholinergic control of the mechanical properties of the catch connective tissue in the holothurian body wall. Comp Biochem Physiol 86C: 333–337

11 Motokawa T (1987*b*) Calcium dependence of viscosity change caused by cations in holothurian catch connective tissue. Comp Biochem Physiol 87A: 579–582

12 Motokawa T (1987*c*) Catch connective tissue: A key character for echinoderms' success. In "Echinoderm Biology" Ed by RD Burke, PV Mladenov, P Lambert , RL Parsley, AA Balkema, Lotterdam, pp 39–54

13 Parker GH (1941) Melanophore bands and areas due to nerve cutting, in relation to the protracted activity of nerves. J gen Physiol 24: 483–504

14 Scott RSH, Hepburn HR, Joffe I, Heffron JJA (1974) Mechanical defensive mechanism of a sea cucumber. S Afr J Sci 70: 46–48

15 Serra-von Buddenbrock E (1963) Études physiologique et histologique sur le tégument des holothuries (*Holothuria tubulosa*). Vie Milieu 14: 55–70

16 Sugi H, Suzuki S, Daimon T (1982) Intracellular calcium translocation during contraction in vertebrate and invertebrate smooth muscles by the pyroantimonate method. Canad J Physiol Pharmacol 60: 576–587

17 Suzuki S, Sugi H (1989) Evaluation of the pyroantimonate method for detecting intracelular calcium translocation in smooth msucle fibers by the X-ray microanalysis of cryosections. Histochemistry 92: 95–101

18 Uexküll J von (1926) Die Sperrmuskulatur der Holothurien. Pflüg Arch ges Physiol 212: 1–14

ZOOLOGICAL SCIENCE 11: 517–526 (1994)

Life Cycle of *Paramecium bursaria* Syngen 1 in a Natural Pond

TOSHIKAZU KOSAKA

Department of Biological Science, Faculty of Science, Hiroshima University, Higashi-Hiroshima 724, Japan

ABSTRACT—Studies were made on the natural population density of *Paramecium bursaria* syngen 1, on the life cycle stages to which the individuals belonged, and on the length of the immature and adolescent periods. Green paramecia were collected from a natural pond once every 20 days for two years: 3176 individuals on 37 collection dates. Individuals in nature did not maintain a steady density, but a regular annual change in the population density was not found. Mating tests were conducted on 2955 of 3176 individuals. Of the total, 23 (1%) were adolescent, 21 (1%) were mature, while the others showed no mating reaction. 73 of 315 individuals from two other collections died within two weeks after undergoing 0 to 9 cell divisions. 178 of the other 242 stocks showed fission rates under 1.00. Only 2 stocks showed a rate of over 1.51. Further, 121 of 242 stocks died without expressing mating ability within 4 months after collection. The other stocks lowered their fission rates gradually and often produced abnormal or colorless individuals within stocks instead of expressing mating reactivity. Immature clones from a cross between two stocks originating from the same pond showed fission rates of 1.51 to 2.25. The clones grew to maturity after 38 to 59 cell divisions from clone initiation following an immature period of 36 to 58 cell divisions and an adolescent period of 0 to 17 cell divisions, during which no individuals with abnormal morphology appeared. These results indicate that the natural population in this pond consisted primarily of senile individuals.

INTRODUCTION

The clonal life cycle in ciliates has been analyzed based on the capacity for sexual reproduction, vitality, production of progeny with abnormal micro- and macronuclei or cell shape, and viable progeny following sexual reproduction. Such studies have included *Paramecium bursaria* [21], the *P. aurelia* complex [21, 23], *P. caudatum* [21], *Tetrahymena thermophila* [5, 22], *Euplotes patella* [8], and *E. woodruffi* [9]. In *P. bursaria, T. thermophila, E. patella*, and *E. woodruffi*, immaturity, adolescence, maturity, and senility have been described within the life cycle.

Almost all studies on the life cycle, however, have been done in the laboratory. Only one report of the life cycle in free-living ciliates was made in *Paramecium bursaria* syngen 1: natural populations in streams consisted of immature, adolescent, and mature individuals, but not senile ones. More than one half the individuals of the populations were immature; the appearance of individuals with mating ability appeared to be related closely to increasing population densities. The frequencies of the recessive genes for mating types (*a* and *b*) were higher than for dominant genes (*A* and *B*) [10].

The results obtained from the studies on *Paramecium bursaria* were carried out in two streams where the quality of water was beta-mesosaprobic to oligosaprobic [1, 10]. Would the same results observed in such streams be obtained from different habitats? In other words, does the same species (or syngen more strictly in this case) take the same strategy for survival regardless of its habitat?

Accepted June 24, 1994
Received October 21, 1993

This paper reports mainly field studies, using the holotrichous ciliate *Paramecium bursaria* syngen 1, carried out for two years in a natural pond where the quality of water was alpha-mesosaprobic [1], as well as laboratory work to clarify the following issues: Are there seasonal changes in densities within a natural population? How do frequencies of the four periods in the life cycle change in a natural population? Do individuals with mating capacity appear in certain months or all year? How long in fissions are the periods of immaturity or adolescence?

MATERIALS AND METHODS

Stocks and mating tests on newly-collected stocks

As testers, four mature stocks including stock SJ-2 (mating type I), SH-2 (II), KZ-1 (III), and FD-9 (IV) of *Paramecium bursaria* syngen 1 were used. Two stocks, which were collected in 1991 from Okuda-oike pond in Hiroshima Prefecture, Japan, OK-312 (I) and OK-223 (IV) were used to measure fission rates and the lengths of the immature and adolescent periods. *Paramecium bursaria* (a green *paramecium*) was grown in lettuce infusion containing *Klebsiella pneumoniae* as a food organism at 22–23°C. To avoid aging of paramecia, individuals were isolated and then were allowed to divide only four or five times before making mating tests on each stocks. For green paramecia cultures, we used natural window sunlight rather than artificial lighting. To prevent differences in the peak of mating reaction between tester stocks and newly-collected stocks from nature, we kept both cultures of tester stocks and newly-collected stocks in the same light/dark schedule. Illumination intensity from natural sunlight in the incubator was 1000–1300 lux in the day time. Mating tests were performed during the peak agglutination reactions from 11:30 a.m. to 2:00 p.m. Whenever mating tests were done, high reactivity of mating between the four tester stocks was confirmed. Four to eight cells of a given stock were mixed with 0.3 ml of culture, which included 400–500 individuals of

one tester stock. Based on mating reaction, stocks that did not mate with any of the four testers were considered immature; stocks that mated with one or two testers were adolescent; stocks that mated with three testers were considered mature; stocks that did not mate with any of the four testers, but showed low fission rates, or produced colorless (zoochlorellae-free) or abnormal individuals, were termed senile.

Field study site and a method for collecting green paramecia

After almost three years of preliminary investigation to select the field study site, we chose Okuda-oike pond, located in Hiroshima Prefecture, Japan. This pond has an abundance of water plants and is alpha-mesosaprobic without the possibility of drying up and without artificial pollutants from homes and industries. Six stations were established (Fig. 1). The studies took place once every 20 days from October, 1987 to October, 1989. Field samples of green paramecia were collected and isolated by the method which we have already reported [10].

FIG. 1. Sampling stations in Okuda-oike pond that is about 3 m at the deepest and has an area of 0.03 km^2 Water depth is 30 cm in station A; 15–20 cm in B, C, D, and E; 35–40 cm in F. Many leaves of water plants such as *Brasenia schreberi* and *Nymphaea tetragona* which cover the surface of the water are seen. White scale bar (arrow) is 1 m in length.

Fission rates and length of immature and adolescent periods

To measure fission rates, newly-collected green paramecia from nature, which were established from two times of collection in April, 1991, were used. The paramecia were washed three times with an exhausted medium of *P. caudatum* on the same day that water samples were gathered. Each green paramecium was cultured for two days in a medium which consisted of 1 part of the exhausted medium and 1 part of bacterized culture medium. Afterwards, one of the paramecia proliferated was transplanted to a fresh bacterized culture medium. The transplantation of the paramecium was made every 2 days. Fission rates were obtained by calculating the total number of fissions of a clone in two weeks divided by 14. Fission rates and the length of the immature and adolescent periods of descendant clones were also measured by 2 day period isolation culture. Stocks OK-312 and OK-223 were used as parental ones. All the newly-isolated stocks, descendant clones, and tester stocks were maintained and the experiments were made under the 10L/14D artificial lighting condition (4000–5000 lux).

Fixation and staining

Materials were fixed with a fixative solution consisting of 5 parts of saturated mercury chloride, 1 part of glacial acetic acid, 1 part of formalin, and 5 parts of t-butanol [2]. The nuclei were stained with Delamater's basic fuchsin for permanent staining [14]. Hydrolysis was done in 4N Hcl for 30 min at room temperature.

RESULTS

Population variations

Thirty-seven collections were done from October 13, 1987 to October 18, 1989. The results for population fluctuation of green paramecia are shown in Table 1 and Fig. 2. The 3176 green paramecia in samples collected from 6 stations in Okuda-oike pond were isolated. Because the population size did not vary among stations (e.g. 497 individuals from station C at the least to 572 from station A at the most), there may not be differences in the microhabitats that green paramecia prefer. Or they may prefer some, but this pond has a relatively uniform habitat.

Figures 2 and 3 show how the population density of green paramecia varied throughout the year. No periodic changes were seen. The population size did not decrease when water temperatures exceeded 20°C or even 30°C.

Frequency of immature, adolescent, mature, and senile stocks in a natural population

In the total of 37 collections, 3176 green paramecia were found and 2955 of them grew to stocks. These were examined by careful mating tests to determine to which period in the life cycle they belonged (Table 1), including mating types for mature stocks. Of 2955 stocks examined in detail, only 44 stocks showed mating capacity: 23 stocks (1%) were adolescent, and 21 stocks (1%) were mature. The others did not mate with the testers. It was not determined clearly whether the non-mating stocks belonged to the immature or to the senile life cycle stages. However, since most of them showed low fission rates (under 0.5), these stocks seemed to be senile. Also 567 of 3176 individuals which died before mating test or showed fission rates of about 0.1 might be senile individuals. The natural population seemed to consist mostly of senile individuals; Only 1% of individuals collected had mating capacity. Four mating types (I to IV) appeared at about the same rate among mature stocks.

From twelve collections, 23 adolescent stocks were isolated (Table 2). The adolescent stocks that did not mate with two or three testers could be divided into 10 subtypes. Fourteen of 23 stocks did not mate with two testers; the other 9 stocks did not conjugate with three testers.

Fission rates, short-lived stocks, and appearance of individuals with abnormality

Many individuals which seemed to be senile were found in the collections all through the two-year study. To examine in detail whether these individuals were truly senile, two more collections were done on April 3rd and 21st, 1991.

TABLE 1. Number of non-mating and mating individuals

Date			No. of paramecia tested					No. of paramecia not tested		
			Non-mating	Mating				Slow growing*	dead**	
				Adolescence	Maturity Mating types					
					I	II	III	IV			Total
1987	Oct.	13	72	0	0	0	0	0	11	5	77
	Nov.	4	22	0	0	0	1	0	5	0	23
	Nov.	22	26	0	0	0	0	0	2	3	29
	Dec.	15	45	0	0	0	0	0	6	5	50
1988	Jan.	6	61	0	0	0	0	0	4	7	68
	Jan.	26	211	0	0	0	0	0	15	12	223
	Feb.	16	59	0	0	0	0	0	1	0	59
	Mar.	6	14	0	0	0	0	0	1	2	16
	Mar.	25	29	1	0	0	0	0	5	2	32
	Apr.	14	77	3	1	0	0	2	9	6	89
	May	6	74	0	0	0	0	0	2	3	77
	May	26	64	0	0	0	0	0	9	3	67
	Jun.	15	80	0	0	0	0	0	13	11	91
	Jul.	6	163	0	0	0	0	0	17	18	181
	Jul.	26	174	0	0	0	0	0	5	11	185
	Aug.	15	94	0	1	0	0	0	10	5	100
	Sep.	4	107	0	0	0	0	0	18	4	111
	Sep.	25	123	3	0	0	1	0	19	10	137
	Oct.	17	77	0	0	0	0	0	14	11	88
	Nov.	7	30	0	0	0	0	0	5	11	41
	Nov.	25	66	3	0	1	0	0	13	9	79
	Dec.	15	86	0	1	3	1	0	7	5	96
1989	Jan.	4	110	3	1	2	0	2	2	4	122
	Jan.	25	160	3	0	0	1	0	17	8	172
	Feb.	16	60	1	0	0	0	0	11	8	69
	Mar.	7	98	2	0	0	1	0	19	4	105
	Mar.	28	105	0	0	0	0	0	24	5	110
	Apr.	18	86	0	0	0	0	0	6	5	91
	May	9	101	1	0	0	0	0	15	1	103
	May	28	33	0	0	0	0	0	4	1	34
	Jun.	17	139	1	0	0	0	0	6	1	141
	Jul.	6	28	0	0	0	0	0	10	14	42
	Jul.	27	55	0	0	0	0	0	23	22	77
	Aug.	17	48	0	0	0	0	0	3	1	49
	Sep.	6	57	1	0	0	0	1	5	0	59
	Sep.	27	43	1	0	0	1	0	4	1	46
	Oct.	18	34	0	0	0	0	0	6	3	37
Total			2911	23	4	6	6	5	346	221	3176

* Slow growing individuals which underwent only one or two cell divisions over ten days.
** Individuals died within ten days after isolation.

From these collections, 315 individuals were isolated.

The individuals collected were cultured by 2-day period isolation for two weeks. Seventy-three of 315 individuals died after undergoing 0 to 9 cell divisions within the term (Table 3). Fifty-four (74%) of 73 individuals died without cell division or after only one cell division. The other 242 individuals grew to stocks. They were transfered to fresh culture medium once every ten days and were cultured in Petri dishes 3.5 cm in diameter for four months and were examined about features of the life cycle.

Table 4 shows the stocks which died within four months. Although mating tests were done several times, 194 (80%) of

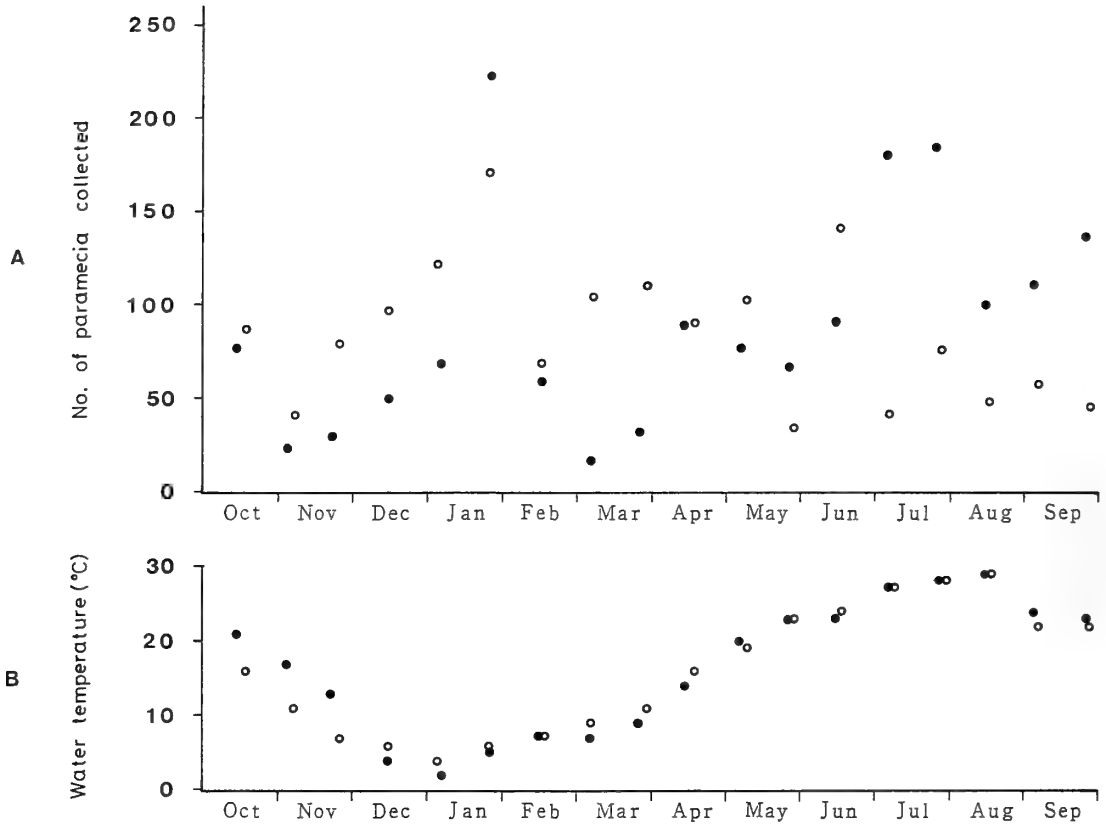

FIG. 2. Number of individuals collected in a Okuda-oike population (A). Water temperature (B). ●—●, 1987–1988; ○—○, 1988–1989.

the 242 stocks died without showing any mating reactivity with the testers. The other 48 stocks lived for over four months, but they showed no symptom of mating during the 4-month culture period except one stock.

Table 5 shows fission rates of the stocks which survived for over two weeks. 178 (74%) of 242 stocks showed fission rates under 1.00. Two stocks with the fission rate over 1.51 were mature, and belonged to mating type I or IV.

Of the stocks which did not react with the testers just after collection, only one stock began to express mating capacity during the 4-month culture period. Many of the other stocks died one by one instead of expressing mating capacity. Further, individuals with various abnormalities such as small individuals (Fig. 4, b, c), an amicronucleate (Fig. 4, d), a bi-micronucleate (Fig. 4, e), colorless individuals (Fig. 4, f, g), individuals with unusual shapes and nuclei (Fig. 4, h, i, j, k), and connected individuals (Fig. 4, l, m) appeared in the stocks. In 84 (35%) of 242 stocks which lived for over two weeks, individuals with some abnormality appeared. The various stocks might exhibit only one type of abnormality, or two or more types of abnormalities.

Fission rates and the length of immaturity and adolescence

The results obtained indicated that there might be many senile individuals in a natural population. To ascertain this possibility more clearly, it is necessary to provide further evidence that the individuals likely to be senile show quite different features from young individuals. Two remaining main issues to be re-solved are the following: How many times do young individuals divide per day?; How long is the immaturity period of the individuals?

Two stocks, OK-312 (I) and OK-223 (IV), were used as parental stocks. Using descendant clones from a cross between the parental stocks, fission rates and the lengths of immaturity and the adolescence were studied.

The viability of exconjugants was 99% when 100 exconjugants from 50 pairs were examined. 16 clones (8 syn-clones) of the exconjugant clones were randomly chosen, and were maintained by 2-day period isolation culture. Fission rates of the clones are shown in Table 6. All clones, which were in the immature period, showed fission rates over 1.50.

These clones were kept in 2-day period isolation culture, and were examined to determine the lengths of the immature and the adolescent periods. The results are shown in Figure 5. The shortest immature period was 35 fissions, while the longest was 57 fissions. Adolescence, which was 4 to 17 fissions in length, was observed in 9 of 16 clones, but not in the others. All the clones became mature immediately after the immature (or adolescent) period. When they became mature, each clone yielded steady aggultination reactions with three of four testers when mixed together. However, clones that had just become mature often did not produce conjugating pairs with the testers following the aggultination reaction. All four mating types (I to IV) arose in the

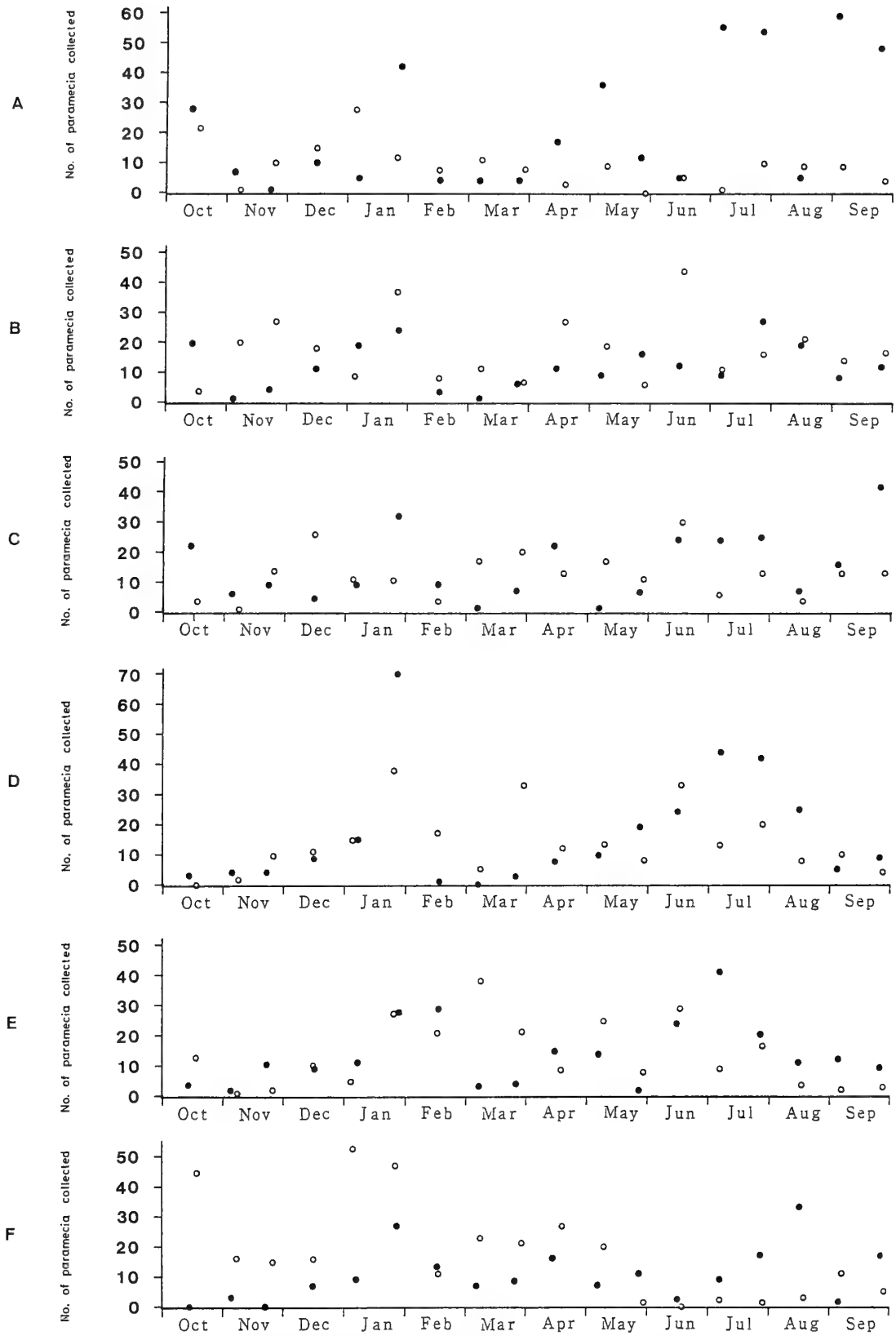

FIG. 3. Number of individuals collected in station A to F. ●—●, 1987–1988; ○—○, 1988–1989.

TABLE 2. Number of adolescent stocks classified into ten different types

Date		No. of adolescent paramecia: No mating reaction with: I II	I III	I IV	II III	II IV	III IV	I II III	I II IV	I III IV	II III IV	Total
1988	Mar. 25						1					1
	Apr. 14	1				2						3
	Sep. 25	2		1								3
	Nov. 25	1						1		1		3
1989	Jan. 4						1		1		1	3
	Jan. 25			1				1			1	3
	Feb. 16	1										1
	Mar. 7				1		1					2
	May 9		1									1
	Jun. 17							1				1
	Sep. 6								1			1
	Sep. 27							1				1
Total		5	1	2	1	2	3	4	2	1	2	23

TABLE 3. Length of life of the short-lived stocks

No. of cell divisions	No. of paramecia: Days 0–2	3–4	5–6	7–8	9–10	11–12	13–14	Total
0	1	27	2	1			1	32
1		11	6	4	1			22
2				3				3
3				3				3
4				1	2	1	1	5
5						2		2
6							1	1
7					1	1		2
8								0
9						1	2	3
Total	1	38	8	12	4	5	5	73

descendant clones. The mating types were determined synclonally. Individuals with abnormal morphology never were observed in the clones during 100 or more fissions after clone initiation.

DISCUSSION

Individuals of *Paramecium bursaria* appear through the entire year and seasonal changes in their population densities are not observed in Okuda-oike pond where the quality of water is alpha-mesosaprobic. It is unclear whether individuals with mating ability appear only in certain months of a year. By contrast, *P. bursaria* living in streams, where the quality of water is oligosaprobic to beta-mesosaprobic, show seasonal changes in population density and a close relationship between the increasing of population density and the appearance of individuals with mating ability [10]. The density of individuals contained in 600 ml of water samples,

TABLE 4. Number of the stocks which died within 4 months after isolation

	Length of life: 1 day-14 days	15 days-1 month	1 month-2 months	2 months-3 months	3 months-4 months	Total
No. of stocks	73	41	30	24	26	194

TABLE 5. Fission rates of the stocks isolated from nature

	Fission rates: 0–0.25	0.26–0.50	0.51–0.75	0.76–1.00	1.01–1.25	1.26–1.50	1.51–1.75	Total
No. of Stocks	3	4	43	128	58	4	2	242

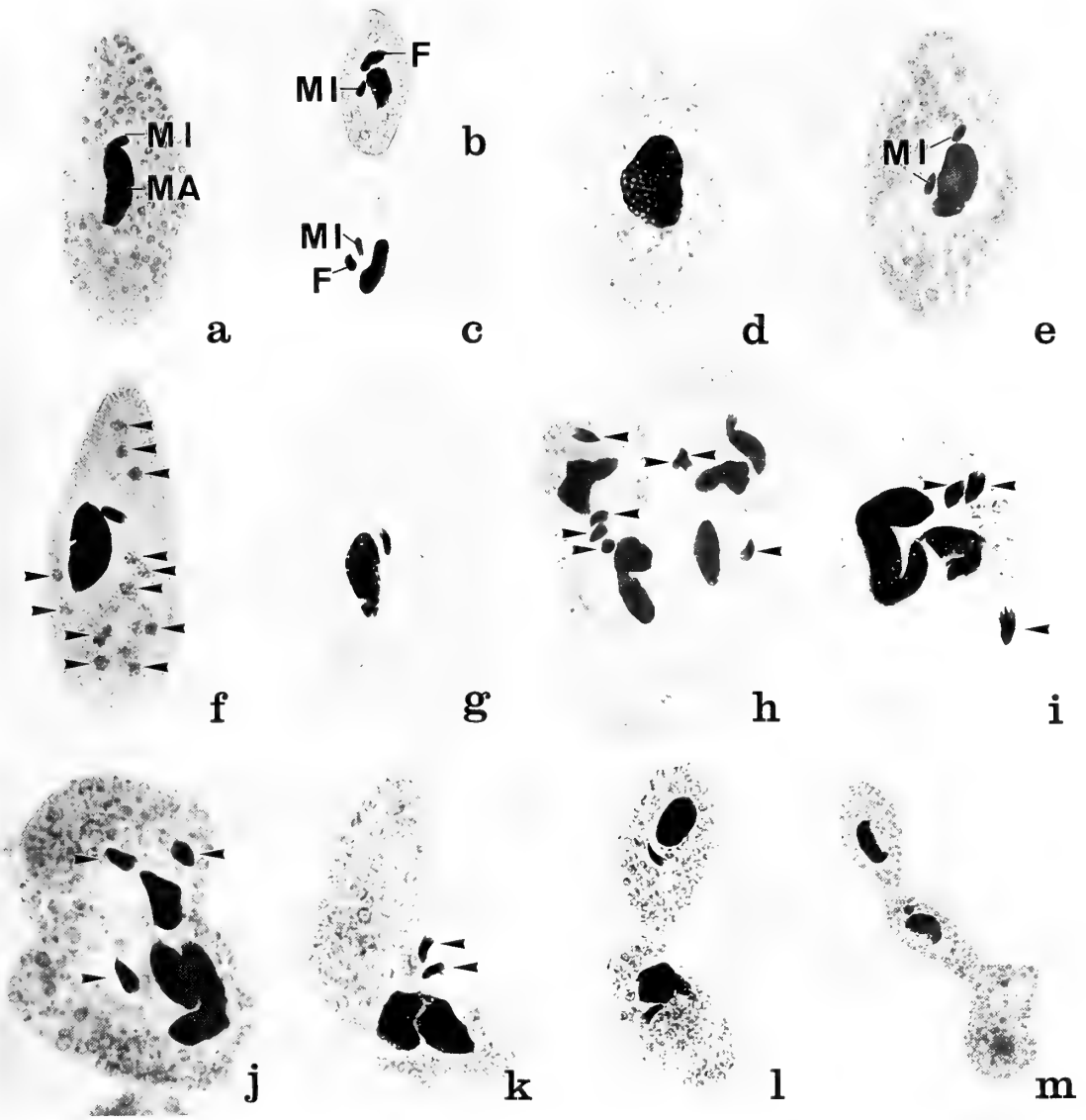

FIG. 4. A normal individual with one micronucleus(MI) and one macronucleus (MA) in which many zoochlorellae are uniformly distributed, × 270 (a). Small individuals with extra macronuclear fragments (F), ×270 (b, c). An amicronuclear individual, ×410 (d). A bimicronuclear individual, ×330 (e). A colorless individual. Several zoochlorellae (arrowhead) are still seen, ×330 (f). A colorless individual without zoochrorellae, ×360 (g). Abnormal and irregular-shaped individuals in which two to five macronuclei and two to seven micronuclei(arrowhead) are seen (h-k): ×360 (h); ×570 (i); ×430 (j); ×410 (k). Connected individuals (l, m): ×290 (l); ×170 (m).

TABLE 6. Fission rates of the immature clones from a cross between stock OK-312 and stock OK-223

	Fission rates				
	0–1.50	1.51–1.75	1.76–2.00	2.01–2.25	Total
No. of clones	0	5	8	3	16

which is obtained by calculating the total number of individuals divided by the total number of collections, is 15.9 in Mikumarikyo stream and 3.6 in Momijidanigawa stream [10], while 85.8 in Okuda-oike pond. Thus, many more individuals are contained in the same volumes of water samples in a pond than those in a stream. The results show that even the same species (syngen) might take different survival strategies in different habitats.

A period of adolescence has been reported in *Paramecium bursaria* [6, 16], *Tetrahymena thermophila* [17], *Euplotes patella* [8], *E. woodruffi* [9], and *E. octocarinatus* [12] which are regarded as outbreeding species. Clones with or without a period of adolescence were observed in the descendant clones of *P. bursaria* in Okuda-oike pond. The duration of adolescence was only 17 fissions at the most. The appearance of clones without adolescence is the first case so described in *P. bursaria*. Because the adolescent period is short or lacking, and the immature period short, it can be

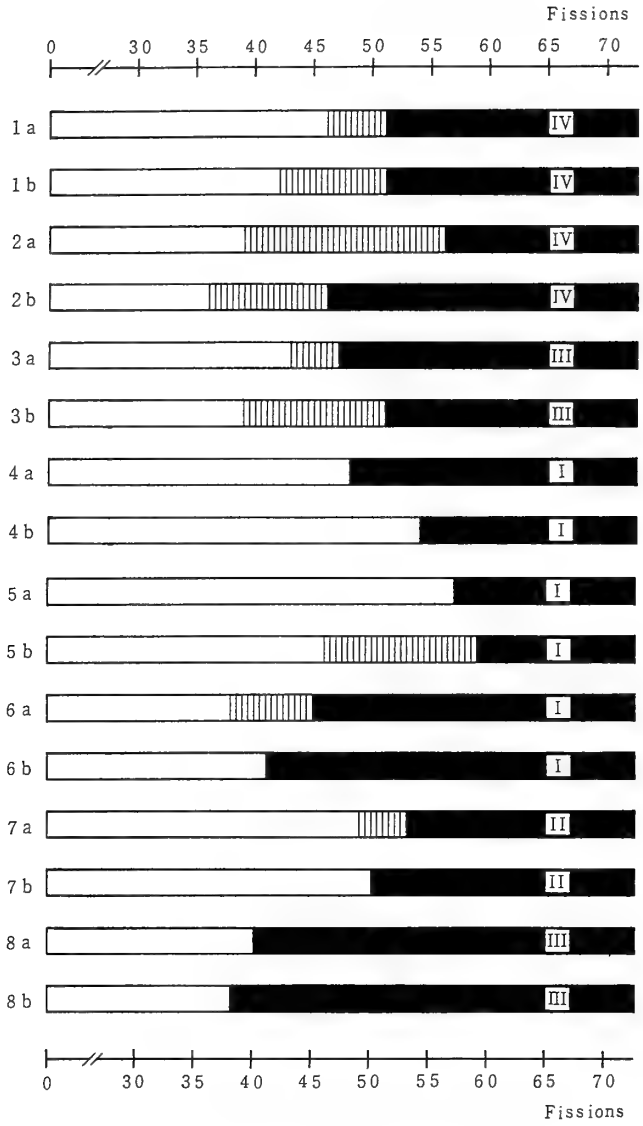

FIG. 5. Length of the immature and the adolescent periods. □ immature period; ▥ adolescent period; ■ mature period. Roman numerals in the figure mean the mating types to which F1 clones were differentiated. Each pair of clones (1a and 1b, for example) derived from a single synclone.

suggested that green paramecia take an inbreeding strategy in Okuda-oike pond.

The field studies on the life cycle for two years in Okuda-oike pond reveal that individuals with mating ability, which are adolescent individuals plus mature ones, were only 1% of the total individuals collected. The rate is very much lower than that found in a Mikumarikyo population (25%) and a Momijidanigawa population (47%) [10]. Furthermore, collections from Mikumarikyo and Momijidani-gawa populations revealed no senile individuals, whereas the Okuda-oike population consisted of many individuals with very low fission rates (under 0.5) and short-lived individuals. The data indicate that at least the 346 (11%) with low fission rates and 221 (7%) short-lived individuals of 3176 individuals probably belong to the senile period. Several features of senility have been reported: decline in fission rates is known in *Paramecium aurelia* [20], *P. caudatum* [24], and *E. woodruffi* [9]; cytological abnormality is in *P. aurelia* [4, 15, 21], *P. caudatum* [24], and *E. woodruffi* [9]; macronuclear abnormality is in *P. aurelia* [4], *P. caudatum* [3, 24], *E. patella* [8], and *E. woodruffi* [9]; micronuclear aberration or loss is in *Tetrahymena pyriformis* [25], and *P. aurelia* [4, 15, 21].

Again, the results from the later two times of collection show that the same population consists of many senile individuals. Of 315 individuals collected, 194 (62%) died within four months. Because more than half of the individuals died without expressing mating ability with advancing age, they must be considered to be senile. Of 242 stocks which lived for over two weeks, 178 (74%) showed fission rates under 1.0. Because all immature clones showed fission rates over 1.5, those individuals with fission rates under 1.0 would appear to be senile. Further, in 84 (35%) of 242 stocks, various abnormalities such as small-sized or colorless individuals, or cytological abnormalies in body shape and micro- and macronuclus, were observed. The appearance of individuals with abnormalities in the stocks indicates that those stocks also were senile.

It was reported that the life span of *Paramecium bursaria* was 2585 days [7]. If a green paramecium divides once a day, the length of life calculated in terms of cell divisions is about 2600 cell divisions; if it divides 0.5 a day, it is 1300 cell divisions. If we assume that the length of maturity of green paramecia is one half on the life-span, it would last from 650 to 1300 cell divisions. On the other hand, many senile individuals were most probably included in the Okuda-oike population. If members of the population have the same life span as the former report, they could naturally encounter and mate with mature individuals of complementary mating types during this long period. However, in reality this seems not to occur in Okuda-oike pond. Actually, the length of immaturity which was reported to last over one year [21] is only 36 to 57 cell divisions. A short immaturity period for *P. bursaria*, about 50 fissions, was briefly reported by Siegel [18]. Further, adolescence is short or even absent, and the life span is 151 to 281 cell divisions (171 to 260 days) in the Okuda-oike population (Kosaka, unpublished). These facts present the likelihood that the members of the Okuda-oike population are destined to reach the period of senility even more quickly. Because of three factors: (1) appearance of individuals with mating ability appear throughout the year, not concentrated in certain months, (2) only a few individuals show mating ability at a given time in a population, and (3) mature individuals show a short period of maturity, cells in this pond might have aged by missing chances to encounter and mate with individuals of complementary mating types.

The question arises why so many senile individuals which are already dead genetically continue to live in the pond population? The first answer to the question is that water flow might play an important role in removing senile individuals from the population, because senile individuals that

lower their physiological activities have never been observed in streams [10]. Since senile individuals are found in a pond where water current is very slow but not in streams, they might be carried away more easily than young individuals. The second answer is that green paramecia have symbiotic zoochlorellae in the cytoplasm [11, 26, 27]. The presence of zoochlorellae allows green paramecia to live even with depressed physiological activity, because nutrient is supplied to green paramecia from their zoochlorellae. The third answer is that the quality of water of the pond chosen for the present study is alpha-mesosaprobic. As expected, more bacteria as food organisms must be contained in the water of alpha-mesosaprobic than that of oligosaprobic and beta-mesosaprobic, because the former contains more organic substance. For these three reasons, even senile individuals of *P. bursaria* might be capable of living in a natural pond.

All four mating types (I-IV) were collected in Okuda-oike pond from the two-year collection (21 stocks) and the additional two times of collection (2 stocks): 5 stocks belonged to mating type I; 6 stocks, II; 6 stocks, III; 6 stocks, IV. The mating types of *Paramecium bursaria* syngen 1 are determined by the combination of dominant (*A* or *B*) or ressessive (*a* or *b*) alleles of two nonlinked loci [19]. Genotypes of mating type I are *AABB, AABb, AaBB,* and *AaBb*. The genotype of mating type III is the double recessive homozygote *aabb* while genotypes of mating types II and IV are recessive homozygote for one of two alleles (*aaBB* or *aaBb* and *AAbb* or *Aabb*, respectively). Frequencies of *a* and *A* or *b* and *B* can be calculated as follows: 12 of 23 mature stocks collected from Okuda-oike pond that belong to mating type II and III have recessive genes *aa*. The frequency of *aa* is obtained by dividing 12 by 23: therefore, the frequency of gene *a* is $\sqrt{12/23}=0.72$. Thus, the frequency of the *a* allele is 72% and the *A* allele is 28%. On the other hand, 12 of 23 mature stocks, which belong to mating type III and IV, have recessive genes *bb*. The frequency of *bb* is obtained by dividing 12 by 23: therefore the frequency of *b* is $\sqrt{12/23}=0.72$. The frequency of the *b* allele is 72%, and the *B* allele is 28%. The finding that the frequencies of the recessive alleles for mating types are higher than for dominant alleles in a pond population is very similar to the results obtained from stream populations [10]. This indicates that members of both populations increase their mating chances by decreasing in the frequencies of the dominant mating type alleles [10].

Mating type determination was synclonal in the descendants from a cross between two stocks from Okuda-oike pond. The results agree with those of Jennings [7]. According to Sonneborn, the usual synclonal uniformity in mating type serves to reduce the probability of mating between close relatives [21]. However, our results do not lead to the same conclusion. The first reason is that four mating types, which are determined synclonally, appeared in the decendant clones from the same cross. The results present the possibility that matings occur between close relatives. The second reason is that the frequencies of recessive alleles are three times higher than those of dominant ones in this pond. This means that the same cross can more easily yield more than one mating type. For example, let us consider the case when mating occurs between different stocks of mating type I and III. Mating between genotypes *AABB* (mating type I) and *aabb* (III) yields only genotype *AaBb* (corresponding to mating type I). However, mating between genotypes *AaBb* (I) and *aabb* (III), produces all four mating types at the same rate: genotypes produced will be *AaBb* (mating type I), *aaBb* (II), *aabb* (III), and *Aabb* (IV). For these two reasons, it is probable that sib-cross as well as out-crosses might occur in places where the frequencies of recessive alleles are higher than those of dominant ones. Further, the data indicate that *Paramecium bursaria* syngen 1, which has been considered one of the typical outbreeders [13, 21], adopts an inbreeding strategy when found in a pond environment.

ACKNOWLEDGMENTS

The author thanks Dr. J. A. Kloetzel of the University of Maryland Baltimore County for reviewing the manuscript and making valuable comments, and Dr. I. Miwa of Ibaraki University for identifying mating types of *Paramecium bursaria* syngen 1.

REFERENCES

1 Bick H (1972) Ciliated protozoa. WHO, Geneva
2 Borror AC (1968) Nigrosin-$HgCl_2$-Formalin; A stain-fixative for ciliates (Protozoa, Ciliophora). Stain Technology 43: 293–294
3 Bovee EC (1960) Morphological abnormalies in a population of large *Paramecium caudatum*. J Protozool 7: (suppl) 16
4 Dippell RV (1955) Some cytological aspects of aging in variety 4 of *Paramecium aurelia*. J Protozool 2: (suppl) 7
5 Elliott AM (1973) Life cycle and distribution of *Tetrahymena*. In "Biology of *Tetrahymena*" Ed by AM Elliott, Dowden, Hutchinson & Ross, Stroudsburg, Pennsylvania, pp 259–286
6 Grell KG (1973) Protozoology. Springer-Verlag, New York
7 Jennings HS (1942) Genetics of *Paramecium bursaria*. III. Inheritance of mating type in crosses and in clonal selffertilizations. Genetics 27: 193–211
8 Katashima R (1971) Several features of aged cells in *Euplotes patella* syngen 1. J Sci Hiroshima Univ (B-1) 23:59–93
9 Kosaka T (1974) Age-dependent monsters or macronuclear abnormalities, the length of life, and a change in the fission rate with clonal aging in marine *Euplotes woodruffi*. J Sci Hiroshima Univ (B-1) 25: 173–189
10 Kosaka T (1991) Life cycle of *Paramecium bursaria* syngen 1 in nature. J Protozool 38: 140–148
11 Kudo RR (1966) Protozoology, 5th ed. Charles C Thomas, Springfield, Illinois
12 Kuhlmann H-W, Heckmann K (1989) Adolescence in *Euplotes octocarinatus*. J Exp Zool 251: 316–328
13 Landis WG (1986) The interplay among ecology, breeding systems, and genetics in the *Paramecium aurelia* and *Paramecium bursaria* complexes. Prog Ptotistol 1: 287–307
14 Mackinnon DL, Hawes RSJ (1961) An introduction to the study of Protozoa. Clarendon Press, Oxford
15 Mitchison NA (1955) Evidence against micronuclear mutations as the sole basis for death at fertilization in aged, and in the

progeny of ultra-violet irradiated, *Paramecium aurelia*. Genetics 40: 61–75

16 Preer JR Jr (1969) Genetics of the Protozoa. In "Research in Protozoology Vol 3" Ed by TT Chen, Pergamon Press, Oxford, pp 129–278

17 Rogers M, Karrer KM (1985) Adolescence in *Tetrahymena thermophila*. Proc Nat Acad Sci 82: 436–439

18 Siegel RW (1960) Hereditary endosymbiosis in *Paramecium bursaria*. Exp Cell Res 19: 239–252

19 Siegel RW, Larison LL (1960) The genic control of mating types in *Paramecium bursaria*. Proc Nat Acad Sci 46: 344–349

20 Sonneborn TM (1954) The relation of autogamy to senescence and rejuvenescence in *Paramecium aurelia*. J Protozool 1: 38–53

21 Sonneborn TM (1957) Breeding systems, reproductive methods, and species problems in Protozoa. In "The Species Problem" Ed by E. Mayr, A A A S, Washington D C, pp. 155–324

22 Sonneborn TM (1974) *Tetrahymena pyriformis*. In "Handbook of Genetics Vol 2" Ed by RC King, Plenum Press, New York, pp. 433–467

23 Sonneborn TM (1974) *Paramecium aurelia*. In "Handbook of Genetics Vol 2" Ed by RC King, Plenum Press, New York, pp. 496–594

24 Takagi Y, Yoshida M (1980) Clonal death associated with the number of fissions in *Paramecium caudatum*. J Cell Sci 41: 177–191

25 Wells C (1965) Age associated nuclear anomalies in *Tetrahymena*. J Protozool 12: 561–563

26 Wichterman R (1953) The biology of *Paramecium*. Blakiston and McGraw-Hill, New York

27 Wichterman R (1986) The biology of *Paramecium*, 2nd ed, Plenum Press, New York and London

ZOOLOGICAL SCIENCE 11: 527–535 (1994)

The Blue Coloration of the Common Surgeonfish, *Paracanthurus hepatus*——I. Morphological Features of Chromatophores

Makoto Goda, Jun Toyohara, Maria A. Visconti[1], Noriko Oshima and Ryozo Fujii[2]

Department of Biomolecular Science, Faculty of Science, Toho University, Miyama, Funabashi, Chiba 274, Japan

ABSTRACT—In order to elucidate the mechanism by which the characteristic blue hues of the common surgeonfish, *Paracanthurus hepatus* (Acanthuridae), are generated, a histological and fine-structural examination was made on the integument. Under the epidermis of the sky blue portions of the skin, round iridophores without dendritic processes were compactly arranged in a double layer, which was lined by a single layer of melanophores. The configuration of each iridophore was very similar to that of the iridophores in the dermis of brilliantly blue-colored damselfish (Pomacentridae). In the cytoplasm, stacks of very thin light-reflecting platelets were arranged with their axes disposed radially from the apical part of the cell. In the dark blue region, by contrast, iridophores were found only rarely. These results indicate that the characteristic sky blue of the species may be dependent on the organized and double-layered arrangement of such light-reflecting cells. It seems likely that a multilayered thin-film interference phenomenon of the non-ideal type, occurring in the stacks of reflecting platelets, is primarily responsible for the generation of the blue hues. Iridophores of this type in the surgeonfish are the first to be found in a species that belongs to a family other than Pomacentridae.

INTRODUCTION

Many tropical fishes display beautiful colors and patterns, and the brilliantly bluish tints of some coral-reef fishes have attracted our particular attention. During the past decade, we have tried to understand the mechanism of the bluish colorations of some damselfish, including the blue damselfish, *Chrysiptera cyanea* [8, 15], and the blue-green damselfish, *Chromis viridis* [5]. To date, a fair amount of information has accumulated on the physics as well as the biology of the iridophores of these pomacentrids. Just under the epidermis of these fish, small, round or somewhat ellipsoidal iridophores can be found to be densely arranged in a single layer that resembles a brick pavement. Each cell contains a nucleus located in its apical part, from which a number of piles of light-reflecting platelets are disposed radially in the cytoplasm. Fine-structural observations have revealed that the reflecting platelets are not more than 5 nm thick. Some of these cells are motile, while some others are the immotile. The motile cells are believed to be responsible for the remarkable color changes in color that are characteristic of these fishes.

Among the beautiful fish found around coral reefs, the common surgeonfish or the regal tang, *Paracanthurus hepatus*, is also well known for its beautiful two-tone bluish colors, brighter and deeper, distributed over its trunk. We recognized, however, that, although the hues can be described as blue in a broad sense, they are rather different from the fluorescent-like blue displayed by many damselfishes. Having rather low purity, the lighter hue of the surgeonfish may appropriately be called "sky blue" or "cerulean blue", while the dark part appears "dark blue" or "midnight blue". In the present work, therefore, investigations were made to identify the morphological basis for the characteristic bluish hues displayed by this acanthurid fish.

Accepted June 24, 1994
Received May 23, 1994

[1] Present address: Departamento de Fisiologia Geral, Instituto de Biociências, Universidade de São Paulo, CP11176, São Paulo, Brazil.

[2] To whom reprint requests should be addressed.

MATERIALS AND METHODS

Material

The material used was the common surgeonfish, *Paracanthurus hepatus*, which belongs to the Acanthuridae (suborder Acanthuroidei, order Perciformes). They are described as being rather common around coral reefs in Indo-Pacific waters. Young adult forms with body lengths between 40 and 60 mm were purchased from local dealers in Tokyo and in Chiba Prefecture, and they were maintained in a seawater aquarium at our facility prior to sacrifice.

Light and electron microscopic observations

First, the general morphology of the skin was studied under the light microscope. Decapitation of a fish was rapidly followed by immersion of the trunk in physiological saline solution which had the following composition (mM): NaCl (128), KCl (2.7), $CaCl_2$ (1.8), (*R*)-(+)-glucose (5.6), and Tris-HCl buffer (10.0; pH 7.2). Then the body was fixed in a solution of 2% glutaraldehyde and 2% paraformaldehyde in 0.1 M phosphate buffer (pH 7.2). During the fixation for 2 hr at room temperature, the sky blue and/or dark blue region of the skin was carefully excised and cut into small pieces for better penetration of the fixative. After rinsing with 0.1 M phosphate buffer (pH 7.2), these pieces were dehydrated in a graded ethanol series. The samples were embedded in 2-hydroxyethyl methacrylate (Quetol 523M; Nisshin EM, Tokyo). One-μm sections were cut on a Porter-Blum MT-1 ultramicrotome (Ivan Sorvall,

Newtown, CT) with glass knives. After they had been spread on glass slides, the sections were stained with toluidine blue for general histological examination of the skin, or they were treated with van Gieson's stain that is specific for collagenous components.

For fine-structural observations, a fixative composed of 2.5% glutaraldehyde and 1% paraformaldehyde in 0.1M phosphate buffer (pH 7.2) was employed. While it was immersed in the fixative for a total of 2 hr at room temperature, the trunk was first filleted along the vertebral column. Then, the sky blue or dark blue region of the skin was carefully excised and cut into small squares of about 1 mm^2. Pieces from the yellow part of the tail fin were sometimes fixed for fine-structural observations of the integument. After a 30-min wash with 0.1M phosphate buffer, the specimens were postfixed in a solution of 1% osmium tetroxide in 0.1 M phosphate buffer (pH 7.2) for 30 min at 4°C. These samples were then dehydrated in a graded ethanol series, treated with methyl glycidyl ether, and embedded in Epoxy resin (Quetol 812; Nisshin EM).

Ultrathin sections were cut on the MT-1 ultramicrotome with a diamond knife and then mounted on Formvar™-coated grids. Specimens of the trunk skin were cut vertically to the plane of the skin. When a piece of tail-fin was used, the inter-ray membrane between adjacent fin-rays was cut perpendicularly to the direction of the rays. All the sections were stained with 3% uranyl acetate for 15 min and then with Reynolds' lead citrate for 7 min, and they were viewed with an electron microscope (JEM-1210, JEOL, Tokyo) operated at 80 kV.

RESULTS

Preliminary observations

Figure 1 shows a photograph of a live young specimen of the present material, namely, the common surgeonfish, *Paracanthurus hepatus*, hovering in a small aquarium that contained seawater. The sky blue background coloration that extended over the greater part of the trunk is characteristic of this species, and the region near the middle part of the trunk, namely, the area between the two "handles" of the dark scissors pattern, was used for most of our observations (SB in Fig. 1). The dark blue scissors-like pattern is also a prominent feature of this species, and pieces of skin from this region (DB in Fig. 1) were also used for comparisons. The characteristic pattern on the skin was still clearly visible in the fixative after decapitation. Thus, it was rather easy to prepare specimens from the designated portions of the skin for morphological examination.

The composition of chromatophores in the skin of the yellow portion of the caudal fin (Y in Fig. 1) was also examined for further comparisons.

Histological observations

The photomicrographs in panels A and B of Figure 2 show parts of 1-μm sections that were cut vertically across the integument of the sky blue part of a common surgeonfish which had a body length of about 50 mm. The section displayed in panel A was stained with toluidine blue to show the general construction of the skin, whereas that in panel B was treated with van Gieson's stain to demonstrate collagenous components in the tissue. The epidermis of a fish with a body length of about 50 mm was about 100 μm thick or slightly more. Near the surface of the epidermis, a number of mucous and serous cells were visible. No epidermal chromatophores were found at any level. Just under the epidermis, but above the thick collagenous layer, there were layers of chromatophores: a rather homogeneous lucent zone was lined with a very dense or black sheet underneath. The lucent zone was composed of polyhedral iridophores without dendritic processes, while the latter was a sheet of melanophores. Closer investigations indicated that the iridophores were densely packed in a double layer. The melanophores of the present material assumed a configuration that resembled the configuration found in amphibians [1, 2] or bluish damselfish [5, 8, 15]: the melanophores extended their dendritic processes upwards into the spaces among the iridophores, frequently reaching the boundary between the dermis and the epidermis.

Under the layer of chromatophores, a thick, homogeneous layer of uniform thickness was visible. When the histological sections were treated with van Gieson's stain, this layer stained red (Fig. 2B), a result that suggests the collagenous nature of this material.

In the present material, the main bodies of scales or scutes were buried in the dermis, just beneath the layer of chromatophores (Fig. 2B). They were also heavily stained with van Gieson's stain. Although not included in the present photomicrographs, a few denticles were normally found to protrude from these scales beyond the epidermis. Both the scales and the thick collagenous layer should contribute to the robustness of the integument, a characteristic feature of fish in the Acanthuridae.

Fine-structural observations

Figure 3 shows an electron micrograph, taken at low magnification, in which, just under the epidermis, a double layer of iridophores is clearly visible. Thus, the iridophores can be categorized into two groups, namely, those located in the upper layer and those located in the lower layer. The double layer of iridophores was lined with a monolayered network of dermal melanophores. Being classified as loose connective tissue, the tissue that included the melanophores contained various dermal components, such as bundles of collagen fibrils, blood capillaries and nerve fibers. Processes of melanophores were frequently observed to invade the double layer of iridophores (Fig. 4). Sometimes, these processes were accompanied by bundles of collagen fibrils that ran parallel to the processes (Fig. 4). Occasionally, the processes of melanophores were found to reach the basal lamina that lined the epidermis. However, the perikarya of the melanophores were always found below the double layer of iridophores.

The general morphology of the iridophores was fundamentally similar to that of the iridophores of the damselfish species studied to date [5, 8, 15], with stacks of very thin light-reflecting platelets in the cytoplasm. The stacks were arranged so that their axes radiated from the apical pole of

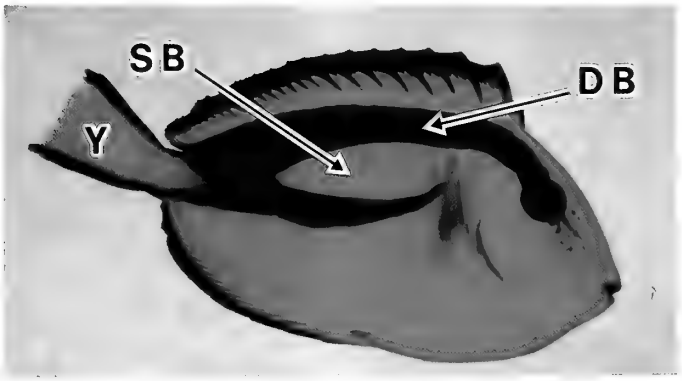

FIG. 1. Photograph of a young surgeonfish, *Paracanthurus hepatus*. The body length of this individual was about 45 mm. The sky blue region in the middle part of the trunk (SB), the dark blue region dorsal to the former (DB) and the yellow portion of the tail fin (Y) were examined.

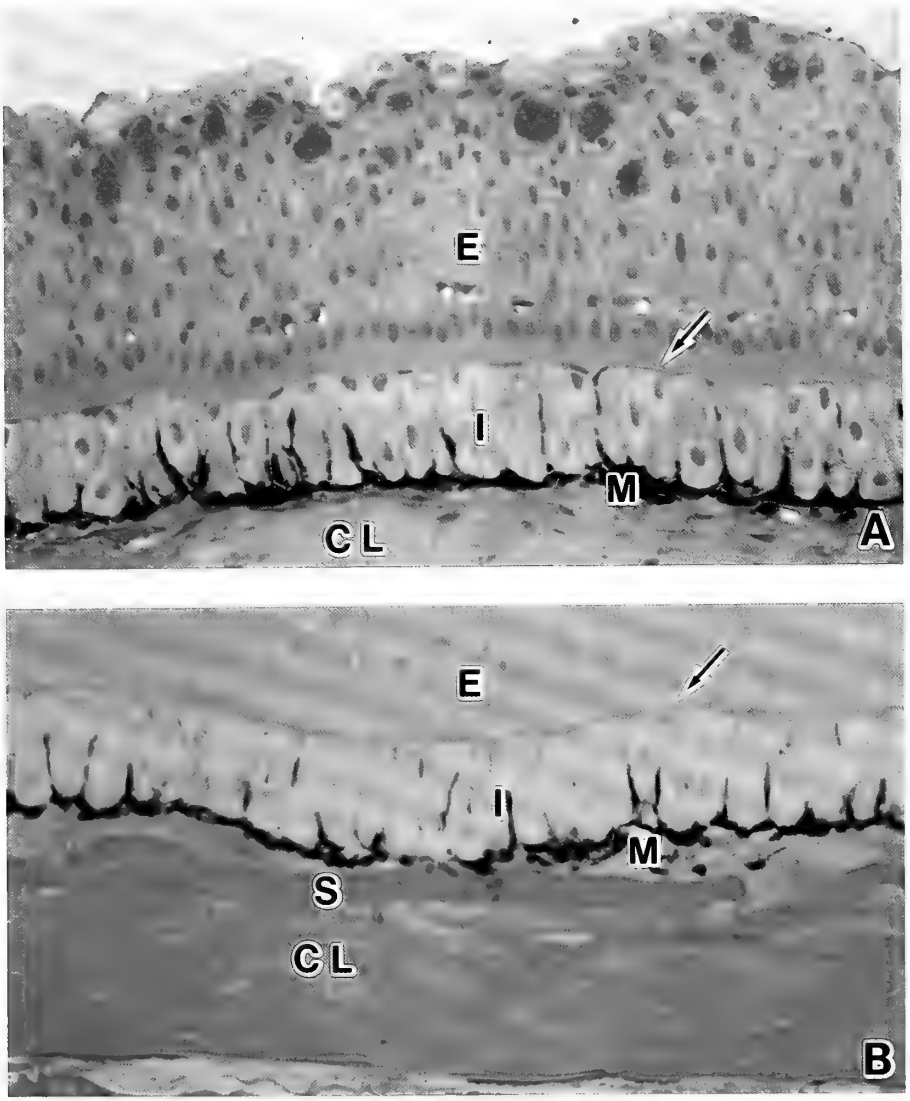

FIG. 2. Photomicrographs of 1-μm sections cut vertically across the integument of the sky blue part (SB in Fig. 1) of a surgeonfish with a body length of about 50 mm. **A**: Stained with toluidine blue. **B**: Stained with van Gieson's solution. Arrows indicate dermo-epidermal junction. CL, collagenous layer; E, epidermis; I, iridophore; M, melanophore; S, scale. $\times$360.

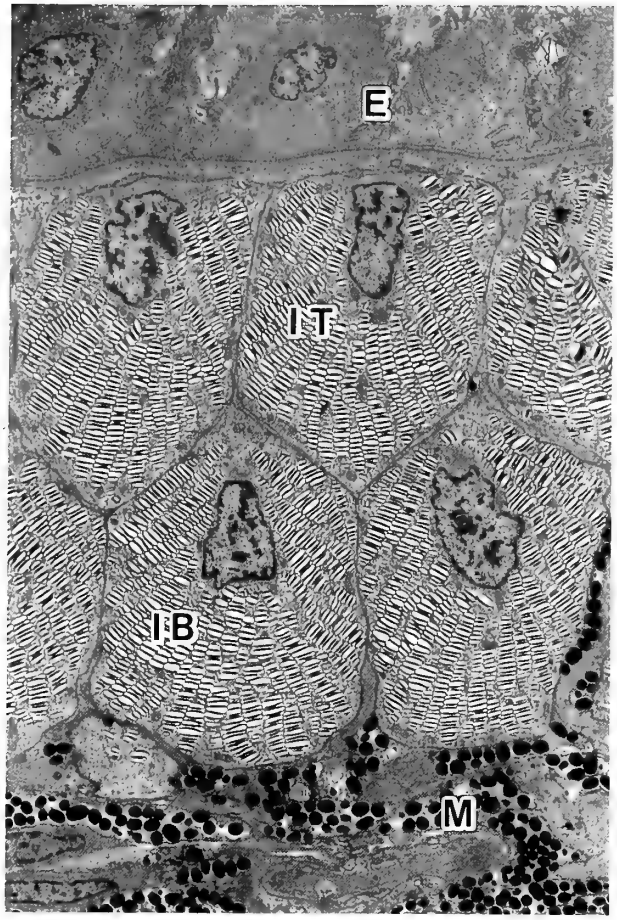

FIG. 3. Low-power electron micrograph of a vertical section across the sky blue part of the dermis of a surgeonfish. Iridophores constitute a double layer, which is lined by a sheet of melanophores. In the iridophores in the upper layer, nuclei are present in the topmost regions, while in iridophores in the bottom layer, nuclei are located more centrally. E, epidermis; IB, iridophore of the bottom layer; IT, iridophore of the top stratum; M, melanophore. ×3,700.

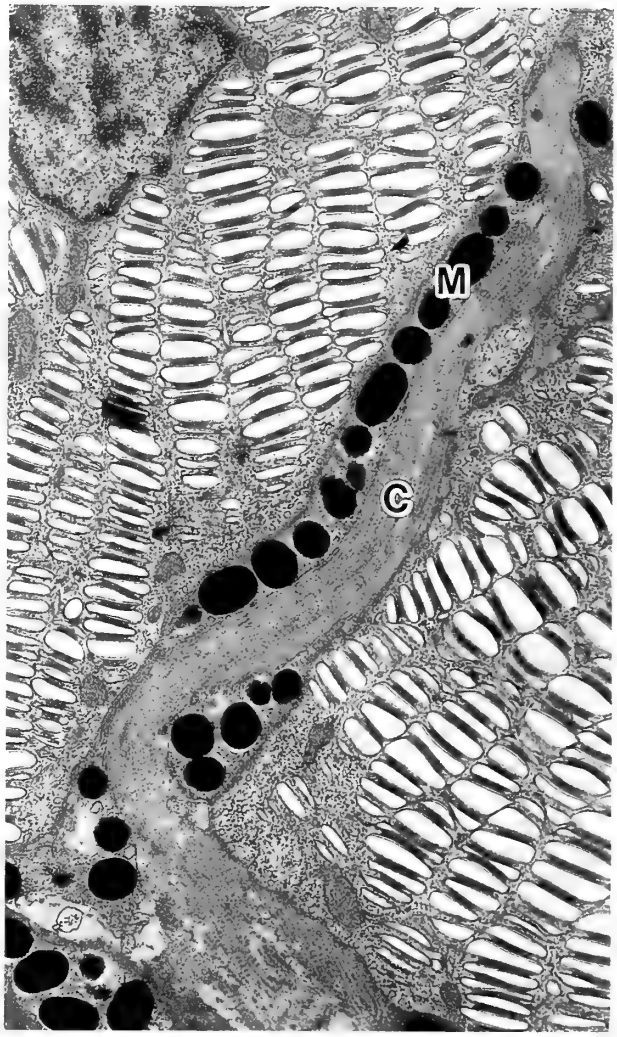

FIG. 4. Electron micrograph of part of the double layer of iridophores, showing that a process of a melanophore is invading the space between two iridophores. A bundle of collagen fibrils is seen to run parallel to the process. C, bundle of collagen fibrils; M, process of a melanophore. ×10,600.

the cell.

We noted a clear difference in the location of the nucleus between the two types of iridophore of the surgeonfish. In the iridophores in the top layer of the double layer, the nucleus was always found in an extremely apical region of the cytoplasm (Figs. 3 and 5A). By contrast, nuclei in the iridophores in the lower layer were more or less in the center of the cells (Figs. 3and5B). In each case, the arrangement of the stacks of reflecting platelets was analogous, as described above.

Each reflecting platelet was found to be enveloped by a smooth membrane, which may possibly have been the cisternal membrane of the smooth-surfaced endoplasmic reticulum (Fig. 6). The platelets seemed to be very uniform in thickness. However, it was not so easy to estimate their thickness exactly on electron micrographs, because of their extreme thinness. It may safely be said, however, that platelets were not more than 8 nm thick.

Electron-dense material was normally detectable between the adjacent cisternae that contained platelets. Careful observations indicated that such material was aggregated around the central region of the platelets, suggesting that the material might serve as a spacer to keep the distance between contiguous platelets both uniform and constant.

We also often observed that the reflecting platelets in pairs of adjacent piles were regularly interdigitated (Fig. 6). Presumably, such architecture is also useful for maintaining similar spacing between contiguous platelets in a particular pile as well as in adjacent piles. Such an interdigitated arrangement has not been observed in iridophores of the other fish species studied to date.

Figure 7 shows part of the cytoplasm of an iridophore, in which the plane of the reflecting platelets was almost parallel to the plane of the section. Some reflecting platelets clearly show a hexagonal crystalline pattern.

The very dark bluish portions of the skin, indicated as

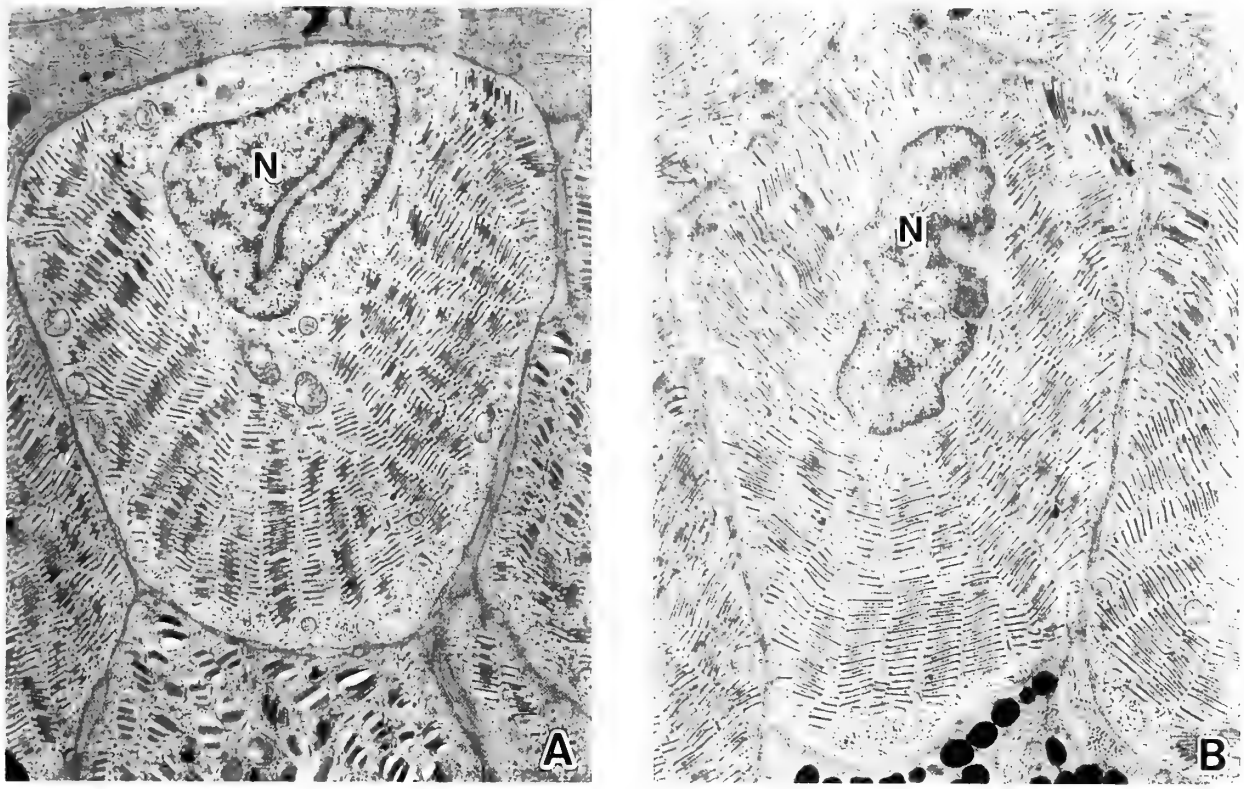

FIG. 5. Electron micrographs of iridophores that form a double layer in the dermis. **A**: An iridophore from the upper layer. The nucleus is located in the apical part of the cell. Stacks of reflecting platelets are arranged radially from the region of the nucleus. There are no stacks of platelets between the nucleus and the apical part of the cell membrane. Invagination of the nuclear envelope is seen as a long streak. **B**: An iridophore from the bottom layer of iridophores. The nucleus is located more centrally than in the cell in A (cf. Figs. 3 and 4). Stacks of reflecting platelets are visible in the apical cytoplasm. N, nucleus. ×7,800.

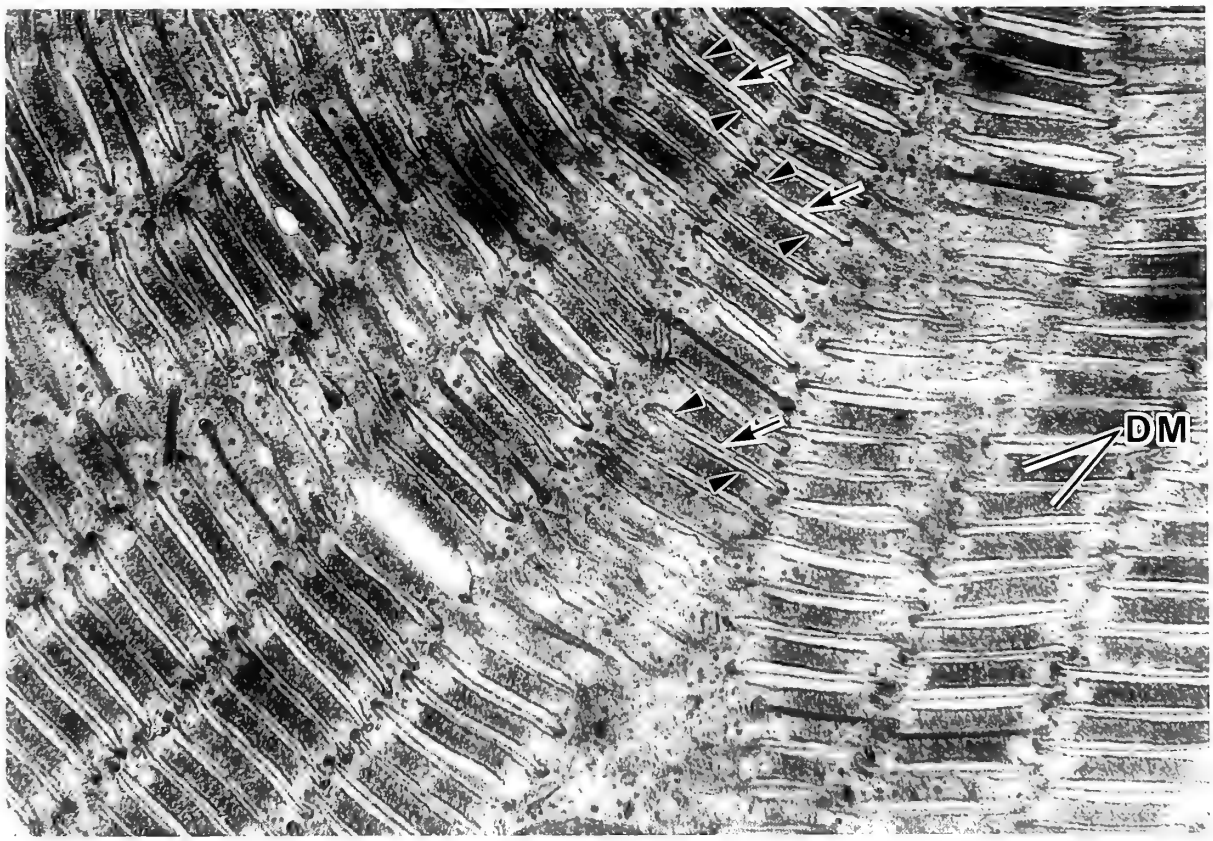

FIG. 6. Electron micrograph of part of the cytoplasm of an iridophore, showing details of the arrangement of the stacks of platelets. Arrows indicate reflecting platelets, while arrowheads indicate cisternal membranes that enclose the platelets. The reflecting platelets in adjacent stacks are frequently interdigitated in a very regular manner. DM, dense material. ×43,000.

FIG. 7. Electron micrograph of part of the cytoplasm of an iridophore. The section was cut, by chance, almost parallel to the plane of the reflecting platelets. In some reflecting platelets, a hexagonal crystalline pattern is visible. ×40,000.

FIG. 9. Electron micrograph of part of the skin between two fin-rays of the caudal fin. The section was cut vertically with respect to the plane of the skin and also to the fin-rays. Under the epidermis, part of the cytoplasm of a xanthophore containing a number of yellow pigment granules, the xanthosomes, is seen. E, epidermis; X, xanthophore. ×7,500.

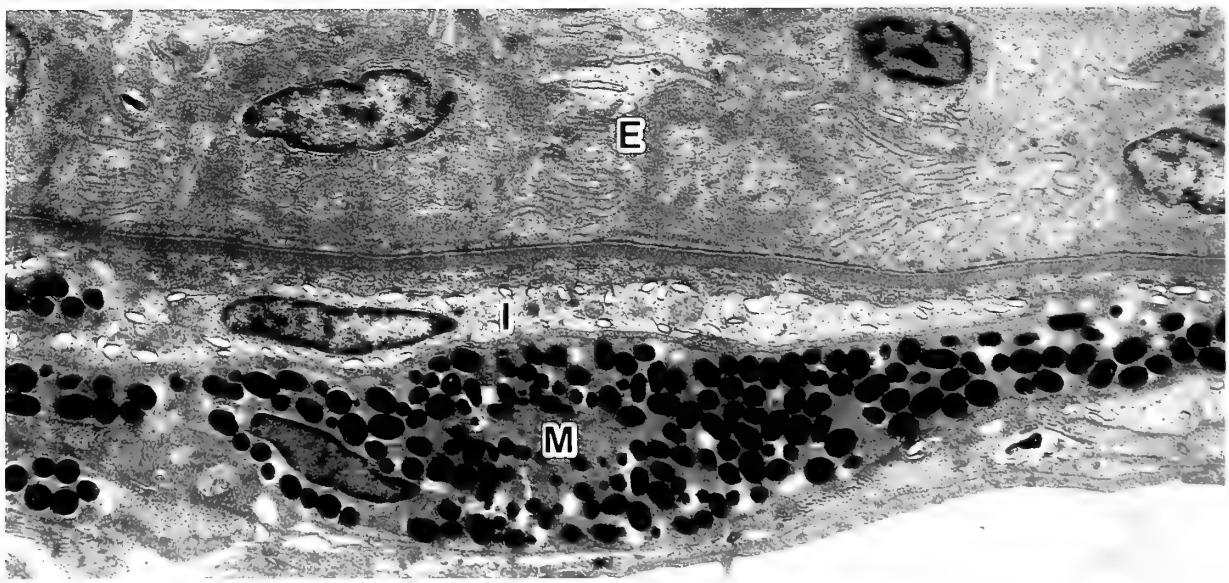

FIG. 8. Electron micrograph of a vertical section through skin taken from the dark blue region, indicated as DB in Fig. 1. A thin layer of cytoplasm of an iridophore in monolayer is seen just above the layer of melanophores. Being variously oriented, small light-reflecting platelets are found scattered in the cytoplasm. A monolayer of the cytoplasm of a melanophore lines the iridophore. E, epidermis; I, iridophore; M, melanophore. ×7,500.

DB in Figure 1, were also examined mainly with regard to the composition of chromatophores. Under the epidermis, we were always able to find a well defined sheet of melanophores (Fig. 8). By contrast, iridophores were only sparsely scattered, and in no case did they form a double layer of the type observed in the sky blue part of the skin. The iridophores themselves were also very thin. The disposition of the reflecting platelets in the cells seemed to be rather irregular, as compared with that in the iridophores in the sky blue region. Stacks of platelets were much smaller, and many of the platelets were rather randomly distributed.

The bright yellowish skin of the caudal fin was examined last of all. Xanthophores in the dermis, containing a number of yellow pigment granules (xanthosomes), were the only chromatophores found (Fig. 9). Such xanthophores can be considered to be responsible for the bright yellow coloration of this region of the skin.

DISCUSSION

The structural organization of the integumentary tissues of the present species, the common surgeonfish, was fundamentally similar to that described in teleosts, which are phylogenetically not very distant from the present material [16, 17]. In the present material, the scales were not recognizable from the outside. However, buried in the dermis, numerous small scales or scutes were found from which denticles or spines protruded through the surface of the skin *via* the layer of dermal chromatophores and the epidermis. These denticles are responsible for the rough feel of the surface of the skin. The dermal collagenous layer below the double layer chromatophores was very well developed. Apparently, both the sheet of scutes and the collagenous layer contribute to the robustness of the skin of this species. The epidermis was also found to be fairly thick, as compared to that of other fishes of similar size.

The nature of the chromatophores and their disposition in the skin are primarily responsible for the coloration of an animal. Such a statement should also apply to the present species, which, with its beautiful colors, is very popular among aquarists. Indeed, such bright blue hues are found only infrequently, even in teleosts. However, since vertebrates do not have blue chromatophores or blue pigment in the tissues, we have to seek the origin of bluish tints in other structures in the skin.

In the surgeonfish, no chromatophores were found in the epidermis. Thus, the characteristic hues of the skin must be dependent primarily on the chromatophores in the dermis. In the present study, we found a very particular combination of chromatophores in the dermis, with a rather similar organization to that found in the dermis of blue-colored damselfish [5, 8, 15]. Thus, it is not unreasonable to suppose that similar optical phenomena may be involved in the generation of bluish coloration in the surgeonfish and the damselfish.

In amphibians and reptiles, dermal chromatophore units have been shown to be responsible for the production of a characteristic greenish tone [1, 2]. The organized, layered arrangement of chromatophores, namely, the xanthophores, iridophores and melanophores, from top to bottom in the dermis, is the architectural requirement for such greenish coloration. Nishioka and Ueda [14] further showed that the dermal chromatophore units of blue mutant frogs (*Rhacophorus schlegelii*) lacked the xanthophores that are normally present at the top of these units. Namely, simpler units consisting of the light-scattering iridophores and the dark sheet of melanophores that underlies the iridophores are responsible for the production of the bluish tone of such mutants. In normal green frogs, the overlying xanthophores function as a yellow filter to shift the spectral reflectance peak towards a region of longer wavelengths, namely, green, by eliminating light of shorter wavelengths. In these cases, the scattering of light in the iridophores has been explained as the Tyndall phenomenon, associated with Rayleigh scattering, by which light of shorter wavelengths is more effectively scattered [1, 2].

During the evolution of teleosts, the three-layered chromatophore units of the type found in greenish amphibians and reptiles failed to develop [4]. As mentioned above, simpler bilayered units composed of iridophores and melanophores are found in the dermis of bluish damselfish [5, 8, 15]. The construction resembles that in the blue mutants of amphibians. However, in the iridophores of these pomacentrids, the light-reflecting platelets are arranged in a strikingly organized manner in the cytoplasm, and light has been shown to be reflected by a multilayered interference phenomenon of the non-ideal type, rather than by Tyndall scattering [4, 10].

Although included in the same very large order, Perciformes, fish of the family Acanthuridae (suborder Acanthuroidei), to which the present material belongs, and those of Pomacentridae (suborder Percoidei), of which all damselfish are members, are phylogenetically rather distant from each other. We were, therefore, surprised to find that the morphology of the iridophores of the present material so closely resembled that of iridophores of bluish damselfish [4, 5, 8, 15]. Both surgeonfish and the damselfish possess iridophores of a very similar that cause their bluish tints.

The currently available information about iridophores indicates that those of teleosts can be divided into several classes [4]. Containing few stacks of thick reflecting platelets, iridophores of the first type are known to function in the generation of the silvery glitter, or very strong whiteness of lateral or belly skin, acting *via* a multi-layered thin-film interference phenomenon of the ideal type [3, 4, 9, 10]. These cells are believed to be immotile. Also containing only a few stacks of large, very thin platelets, iridophores of the lateral blue-green stripe of neon tetras reflect light within a limited region of the spectrum by thin-film interference of the non-ideal type [11, 13]. These platelets are categorized as a type of motile iridophore, and the spacing between the platelets varies in response to various environ-

mental cues, leading to changes in spectral reflectance. The iridophores of bluish damselfishes have already been described above. In many cases, they are motile, and, as a result, the skin that contains these iridophores can vary its hue [5, 8, 15]. Iridophores of the last type are dendritic cells in which tiny platelets can move centripetally and centrifugally, resembling other common dendritic chromatophores such as melanophores, erythrophores and xanthophores [6, 7]. The iridophores of the present material are clearly of the damselfish type, although cellular motility is not significant, if it existed at all (Goda *et al.*, in preparation).

From our observations and experiments, we had previously reached the conclusion that, in bluish damselfishes, the iridophores have a definite role in the generation of the characteristic hue. It is, therefore, quite plausible to assume that the iridophores described in this study play the same role in the surgeonfish. In the surgeonfish also, a multiple layered thin-film interference phenomenon should be primarily responsible for the reflection of shorter-wavelength light. The light-absorbing black sheet containing large amounts of melanin functions to absorb light that has passed through the layer of iridophores, being responsible for the purer bluish tint of the skin.

It should be noted, however, that the mode of disposition of the iridophores in the dermis is not entirely the same in the two types of fish. In the dermis of damselfish, the iridophores were found without exception in a monolayer, but those in the surgeonfish were arranged as a double layer. This difference may be the principal cause of the difference in coloration between the surgeonfish and the damselfish.

In the iridophore of both the surgeonfish and damselfish, a number of piles of very thin light-reflecting platelets are arranged radially from the apical part of each cell. Thus, the axes of piles are oriented at various angles to the surface of the skin. Incident light is maximally reflected along the axis as a result of a multilayered thin-film interference phenomenon, as mentioned above. In the bluish damselfish, the light-reflecting platelets constituting a pile are extremely thin, each one being not more than 5 nm thick. Such architecture favors the reflection of light with a sharp spectral peak and, indeed, a fluorescent-like hue of very high purity is produced [4]. In the surgeonfish, by contrast, the platelets seemed to be a little thicker than those of the damselfish, each being 7–8 nm thick. It is known that, in multilayered interference systems, the spectral reflectance peak becomes sharper when the individual platelets in a stack are thinner. As if mixed with a larger amount of white paint, the sky blue of the surgeonfish is less pure or has lower "chroma", in terms of the Munsell color notation system, than the brilliant cobalt blue of the blue damselfish.

The iridophores are present in a double layer in the surgeonfish. Such a feature should also be related to the production of sky blue coloration rather than the very pure cobalt blue expressed by the reef damselfishes. When iridophores are in a single layer, the interference due to light reflected from a pile of platelets is not disturbed. However, it seems plausible that the light reflected from the iridophores in the bottom layer is complicatedly scattered by the reflecting platelets in the iridophores in the upper layer. If the iridophores of the surgeonfish were present in a monolayer, the bluish tint would be purer or more fluorescent-like, resembling that of the damselfishes.

In the iridophores on the epidermal side, a nucleus was found in an extremely apical part of the cytoplasm, while in the iridophores in the bottom layer, each nucleus of was in the center of the cell. We cannot explain this difference at present, because, in both cases, the arrangement of the piles of reflecting platelets in the cells was practically the same.

The fact that the epidermis is rather thick, as compared with that of other fish of comparable size, may also be related to the lower purity of the integumentary coloration of the present species. Light-scattering components in the epidermis may also contribute to widening of the spectral peak and elevation of the base line of the spectrum. However, the epidermis of fish is usually more transparent than that of terrestrial tetrapods.

In many fish with relatively thick epidermis, epidermal melanophores can be found [4, 12], but we failed to find such cells in the present material. The absence of pigmentary material in the epidermis should be advantageous for the more effective displaying of a bright hue because, if such cells were present in overlying structures, the light reflected from the iridophores in the dermis would be disturbed and weakened.

In the present analysis, we found for the first time iridophores, with a configuration very similar to that of iridophores of coral-reef bluish damselfish in a species that belongs to a family other than Pomacentridae. A more extensive survey of acanthurid species may result in the finding of such iridophores among species that are closely related to the present species. It is also possible that such iridophores will be found in other families or orders of teleosts. Such surveys would surely provide useful clues as to whether such iridophores have a common origin or have evolved sporadically in various groups of fish in more recent evolutionary time. Thus, the present results may provide some initial clues to the taxonomy of fishes within the order Perciformes.

A more detailed discussion of the optical mechanisms involved in the generation of the characteristic sky-blue and dark-blue portions of the strikingly beautiful surgeonfish will be presented in a separate paper (Goda *et al.*, in preparation).

ACKNOWLEDGMENTS

This work was supported in part by grant-in-aids from the Ministry of Education, Science and Culture of Japan. During the initial stages of the work, when M.A.V. was visiting Toho University on leave of absence from Departamento de Fisiologia Geral, Instituto de Biociências, Universidade de São Paulo, Brazil, the project was also supported by a grant from the Fund for the Advancement of Science in Commemoration of Toho University's 60th Anniversary.

REFERENCES

1 Bagnara JT, Hadley ME (1973) Chromatophores and Color Change. Prentice-Hall, Englewood-Cliffs, NJ

2 Bagnara JT, Taylor JD, Hadley ME (1968) The dermal chromatophore unit. J Cell Biol 38: 67–79

3 Denton EJ, Land MF (1971) Mechanism of reflexion in silvery layers of fish and cephalopods. Proc R Soc London, Ser B 178: 43–61

4 Fujii R (1993) Cytophysiology of fish chromatophores. Int Rev
Cytol 143: 191–255

5 Fujii R, Kasukawa H, Miyaji K, Oshima N (1989) Mechanism of skin coloration and its changes in the blue-green damselfish, *Chromis viridis*. Zool Sci 6: 477–486

6 Fujii R, Hayashi H, Toyohara J, Nishi H (1991) Analysis of the reflection of light from motile iridophores of the dark sleeper, *Odontobutis obscura obscura*. Zool Sci 8: 461–470

7 Iga T, Matsuno A (1986) Motile iridophores of a freshwater goby, *Odontobutis obscura*. Cell Tissue Res 244: 165–171

8 Kasukawa H, Oshima N, Fujii R (1987) Mechanism of light reflection in blue damselfish motile iridophores. Zool Sci 4: 243–257

9 Kawaguti S, Kamishima Y (1966) Electron microscopy on the blue back of a clupeoid fish, *Harengula zunasi*. Proc Jpn Acad 42: 389–393

10 Land MF (1972) The physics and biology of animal reflectors. Prog Biophys Mol Biol 24: 75–106

11 Lythgoe JN, Shand J (1982) Changes in spectral reflexions from the iridophores of the neon tetra. J Physiol 325: 23–34

12 Miyashita Y, Fujii R. (1980) Observations of the fine structure of catfish epidermal melanophores with due consideration to their functions. Annot Zool Japon 53: 174–181

13 Nagaishi H, Oshima N (1989) Neural control of motile activity of light-sensitive iridophores in the neon tetra. Pigment Cell Res 2: 485–492

14 Nishioka M, Ueda H (1985) Electron-microscopic observation on the dermal chromatophores of normal frogs and three kinds of color variants in *Rhacophorus schlegelii*. Sci Rep Lab Amphibian Biol, Hiroshima Univ 7: 123–155

15 Oshima N, Sato M, Kumazawa T, Okeda N, Kasukawa H, Fujii R (1985) Motile iridophores play the leading role in damselfish coloration. In "Pigment Cell 1985: Biological, Molecular and Clinical Aspects of Pigmentation" Ed by JT Bagnara, SN Klaus, E Paul, M Schartl, Univ Tokyo Press, Tokyo, pp 241–246

16 Whitear M (1986a) Epidermis. In "Biology of the Integument Vol 2 Vertebrates" Ed by J Bereiter-Hahn, AG Matoltsy, KS Richards, Springer-Verlag, Berlin, pp 8–38

17 Whitear M (1986b) Dermis. In "Biology of the Integument Vol 2 Vertebrates" Ed by J Bereiter-Hahn, AG Matoltsy, KS Richards, Springer-Verlag, Berlin, pp 39–64

ZOOLOGICAL SCIENCE 11: 537–545 (1994)

Structural and Functional Studies on Biliverdin-associated Cyanoprotein from the Bean Bug, *Riptortus clavatus*

KEN MIURA[1], MASANORI NAKAGAWA[1], YASUO CHINZEI[1], TETSURO SHINODA[2], ERIKO NAGAO[3] and HIDEHARU NUMATA[4]

[1]*Department of Medical Zoology, School of Medicine, Mie University, Edobashi 2-174, Tsu 514,* [2]*National Research Institute of Vegetables, Ornamental Plants and Tea, Kusawa 360, Ano-cho, Age-gun 514-23,* [3]*Biochemical Laboratory, Institute of Low-temperature Science, Hokkaido University, Kita, Sapporo 060, and* [4]*Department of Biology, Faculty of Science, Osaka City University, Sumiyoshi, Osaka 558, Japan*

ABSTRACT—Structural and functional analysis were performed on biliverdin-associated cyanoprotein (CP) from the hemolymph (CP-1 to CP-4) and eggs (CPegg, identical to CP-1) of the bean bug, *Riptortus clavatus*. Isoelectric focusing analysis of purified CPegg and CP-4 revealed that they are composed of a single α subunit and a more acidic β subunit respectively. N-terminal amino acid sequencing revealed that there are six different amino acid residues between the two subunits up to the 29 cycles determined, indicating that they are encoded by different genes. Appreciable sequence similarities in N-terminal region are found between the CP subunits and several insect hexamers. By chemical cross-linking analysis these CPs were demonstrated to have hexameric structures. Two dimensional peptide mapping revealed that α and β subunits share common structures in part and that CP-2 and CP-3 are hybrid molecules bearing both α and β subunits. From these results the molecular structure of CPs was established as follows: CP-1 (CPegg)$=\alpha_6$; CP-2 $=\alpha_4\beta_2$; CP-3$=\alpha_2\beta_4$; CP-4$=\beta_6$. In addition, using ^{125}I-labeled CPegg and CP-4, *in vivo* incorporation into several tissues was examined during the nymphal-adult development. During the late phase of the 5th instar, CP-4 was sequestered preferentially over CPegg by the fat body, while after emergence both proteins were suggested to be incorporated into the newly-formed cuticle. CPegg was sequestered massively by the developing ovaries whereas no appreciable incorporation of CP-4 was observed.

INTRODUCTION

The green coloration of many plant-feeding insects, which presumably provides a protective camouflage, results from a combination of a yellow carotenoid pigment with a blue pigment, biliverdin IXγ. In most cases, biliverdin occurs as a chromophore of specic blue proteins in epidermis and/or hemolymph.

Using the eggs of a hemipteran species, the bean bug, *Riptortus clavatus* as the experimental material, we recently have purified and partially characterized a biliverdin-binding protein and designated it as cyanoprotein (CPegg) [4]. CPegg is composed of a glycosylated 76 kDa subunit rich in aromatic amino acids like arylphorin-type storage hexamers [36, 37]. This cyanoprotein is different from the biliverdin-associated proteins of Lepidoptera. These proteins either have subunit molecular masses of about 20 kDa (*Manduca sexta* [16, 33] and *Pieris brassicae* [18, 19, 35]) and are thought to be tetramers, or are members of a class of very high density lipoproteins with either dimeric (*Trichoplusia ni* [20]) or tetrameric structures (*Heriothis zea* [15]). As for the number of subunits constituting insecticyanin, some authors reported the subunit structure to be trimer [2, 13, 32]). The cyanoprotein of *R. clavatus* appears to be similar to the cyanoprotein of *Locusta migratoria* [3, 9] which has similar molecular weight, physicochemical properties, and covalently bound mannose-rich oligosaccharide chains.

The hemolymph of *R. clavatus* contains four distinct CPs (CP-1 to CP-4) which are all immunologically related to CPegg [4, 5]. In the nymphal stages these fluctuate cyclically with each molt just as has been found with the lepidopteran arylphorins [6]. In nondiapause adults, CP-1 is the predominant form and is found only in the female where it accumulates in the developing oocytes [6, 23]. From these observations, it has been suggested that CPs may function both as a storage protein and an egg yolk protein. In addition to such unique functional multiplicity, *Riptortus* cyanoprotein offers a good system to study gene regulation. Under short day conditions the adult bugs enter reproductive diapause, which is readily terminated by transferring them to long day conditions or by treatment with the juvenile hormone analog (JHA), methoprene [29, 30]. We examined this phenomenon of diapause termination at the level of CP synthesis using fluorographic analysis of female hemolymph proteins [7, 23]. Diapause female adults synthesize CP (mainly CP-4) at a low level. After diapause is terminated by JHA treatment, CP-4 synthesis is suppressed within 2 days and in turn, CP-1 synthesis is remarkably activated. These results indicate that JHA switches over the synthesis of closely

Accepted July 3, 1994
Received May 20, 1994

related proteins, from CP-4 to CP-1. Assuming that CP-1 and CP-4 are the products of different genes, therefore, we can recognize this system as a suitable model for studying gene regulation by insect hormones. However, information on the relationship among these CPs is still insufficient. In the present study, experiments were conducted in order to clarify the structural and functional properties of each CP molecular species more closely and to position them in relation to other insect hemolymph proteins. In this paper we purify the hemolymph and egg CPs and show that they are all homo- or heterohexamers consisting of two distinct subunits. In addition, we report that the two subunits are considered to be encoded by different genes and that both subunits show homologies with other insect hexameric proteins. By using ^{125}I-labeled CPegg and CP-4, the functional features of the two are also examined.

MATERIALS AND METHODS

Animals

The bean bug, *Riptortus clavatus* Thunberg (Heteroptera : Alydidae) was reared at 25±1°C under long day (16L : 8D) or short day conditions (10L : 14D) through the nymphal and adult stages. The bugs enter diapause in the adult stage under the short day conditions and the females develop ovaries under the long day conditions [29, 30]. As for the nymphs, the hemolymph protein profile shows no discernible difference between nondiapause and diapause-destined animals.

Hemolymph was collected with glass capillaries from a cut in the legs or a pin-hole made in the neck membrane and diluted in phosphate-buffered saline containing several protease inhibitors as described previously [25]. Hemolymph samples were kept at −80°C until use.

Purification of CPs

CPegg was purified from newly laid eggs by gel filtration followed by ion-exchange chromatography as described previously [4]. CP-1 and CP-4 were also purified from the hemolymph of nymphs and diapause adults. Hemolymph CPs were fractionated by gel filtration using a Hiload Sephacryl-300 HR column (16×600 mm, Pharmacia). Fractions containing CPs were collected and chromatographed on an ion-exchange column (Mono-Q HR, 5×50 mm, Pharmacia). Fractions containing CP-1 and CP-4 were pooled separately and again subjected to the same ion-exchange chromatography. The CP-1 preparation obtained still showed extraneous minor protein bands, whereas CP-4 was electrophoretically homogeneous on native PAGE.

Preparation of antisera

A mixture of CP-1 to 4 was obtained as described above. A New Zealand white rabbit was immunized with the CP mixture in a manner described previously [4], and antiserum reacting to all hemolymph CPs separated. This antiserum was absorbed completely by addition of puried CPegg (α subunit) and the supernatant was used as antiserum to β subunit-specific epitopes (anti-β-specific).

Polyacrylamide gel electrophoresis (PAGE)

PAGE under non-denaturing conditions (native PAGE) and in the presence of sodium dodecyl sulfate (SDS-PAGE) were carried out as described previously [4].

Isoelectric focusing (IEF)

IEF under denaturing conditions was carried out on a 5% polyacrylamide gel slab containing 8M urea, 0.5% (w/v) Nonidet P-40 and 2.5% (w/v) Ampholine (pH 3.5–9.5, LKB) according to Görg *et al.* [14]. After focusing (4000 V×hr) at 7.5°C, the gel was stained with Serva Violet 17 (Serva) according to the method of Patestos *et al.* [31].

Immunoblotting

Immunoblotting was performed as described in a previous paper [24] except that peroxidase conjugated-goat IgG fraction against rabbit IgG (heavy and light chains specific; Cappel) was used as a secondary antibody.

Chemical cross-linking analysis

Chemical cross-linking analysis using dimethylsuberimidate (DMS) as a cross-linker was carried out according to Davies and Stark [8]. Purified CPegg, CP-4 and partially purified CP-1 were dialyzed against 0.2 M triethanolamine-HCl buffer, pH 8.5, and the protein concentration of each sample adjusted to 1 mg/ml with the same buffer. A series of 50 μl of protein samples was incubated with various amount of DMS (final conc.; 0 to 6.0 μg/μl) at 28°C for 2 hr. After incubation the reaction was stopped by addition of sample buffer (0.1 M Tris-HCl, pH 8.0 containing 20% (w/v) glycerol, 3% (w/v) SDS, and 1% (w/v) 2-mercaptoethanol) followed by boiling for 2 min. The reaction products were then analyzed by SDS-PAGE on 2.5 to 10% acrylamide gel slabs.

Analysis of amino acid composition

Amino acid composition of purified CP-4 was analyzed by an automatic amino acid analysis system (model 420H, Applied Biosystems). Tryptophan was not determined.

N-terminal amino acid sequencing

Sequences of N-terminal amino acids of CP-1 and CP-4 were determined as described by Nokihara *et al.* [27]. Nymphal hemolymph proteins were separated by native PAGE and electroblotted onto polyvinylidene difluoride membranes (Millipore) in 10 mM CAPS (3-cyclohexylaminopropanesulfonic acid), pH 11 containing 10% (v/v) methanol at a constant voltage of 70 V for 6 hr [28], and the membrane stained with Coomassie brilliant blue. The bands of CP-1 and CP-4 on the membrane were cut out. Amino acid sequencing of these CPs was carried out using a gas-phase sequencer (Applied Biosystems, Model 470A) with an on-line PTH-analyzer (Applied Biosystems, Model 120A) by direct insertion of the membrane strips into the sequencer.

Two dimensional peptide mapping (2D peptide mapping)

Radioiodinated CPs in gel slices were analyzed by 2D peptide mapping by the method of Ueno and Natori [38]. This method was first described by Elder *et al.* [11]. Hemolymph from 5th instar nymphs or crude egg extract was separated by 2.5 to 15% native PAGE and stained with Coomassie brilliant blue. Bands of CPs were cut out from the gel with a razor blade. Each gel slice (5×1×1 mm) containing about 0.5 μg of protein was dried under a heat lamp. Then proteins in the gel slices were radioiodinated in 1.5 ml Eppendorf tubes by sequential addition of 20 μl of 0.5 M Na-phosphate buffer, pH 7.5 , 300 μCi of ^{125}I (ICN, specific activity: 17 Ci/mg) in 5 μl and 5 μl of chloramine T solution (mg/ml). The tubes were kept

at 27°C for 1 hr followed by addition of 1 ml of sodium bisulfate solution (mg/ml) to stop the reaction. After 15 min the sodium bisulfate solution was removed and the gel slices were washed five times with 1 ml of 10% (v/v) methanol for 15 min for each wash. The gel slices were wrapped in nylon mesh and washed in one liter of 10% methanol for 48 hr with several changes of 10% methanol. After washing the gel slices were dried and put into 1.5 ml Eppendorf tubes containing 0.5 ml of L-1-tosylamido-2-phenylethyl chloromethyl ketone-treated trypsin (Sigma) solution (50 μg/ml in 0.05 M ammonium carbonate, pH 8.0) and allowed to absorb the solution, then homogenized thoroughly. After incubation at 37°C for 24 hr the supernatant was collected after centrifugation, lyophilized, then dissolved in 10 μl of a mixture of formic acid/acetic acid/water (25 : 87 : 887 v/v/v). Samples of up to 0.5 μl (1.5×10^5 cpm) were spotted onto cellulose-coated thin layer chromatography (TLC) plates (20×20 cm, Merk) and electrophoresed for 30 min at a constant voltage of 1000 V in the same solution used to dissolve samples, overlaid by a coolant, Solvent E (Nacalai Chemicals, Japan). After electrophoresis the TLC plates were dried and the peptides were chromatographed in a second dimension with a developing solvent system of n-butanol/pyridine/acetic acid/water (32.5 : 25 : 5 : 20 v/v/v/v). The plates were dried again and exposed to Fuji Super HR-S films with intensifying screens at −70°C for several hours. For densitometric scanning, spots on developed films were scanned and quantitized by an image analysis system (ACI Japan, Model TIAS-1000).

Electron microscopic observation

Purified CPegg, CP-4 and partially purified CP-1 were dissolved in 0.02 M phosphate buffer, pH 7.2 containing 0.15 M NaCl, stained negatively with uranium acetate and were observed with an electron microscope (Hitachi Model 11B).

Incorporation experiments

Radioiodination of CPs was done by Chloramine T method [17]. The reaction mixture in a total volume of 210 μl contained 120 μg protein/50 μl of phosphate buffered saline (PBS, 0.02 M sodium phosphate, pH 7.2, 0.15 M NaCl), 100 μl of 0.5 M Na-phosphate buffer pH 7.5, 0.5 mCi of $Na^{125}I$ (ICN), and 50 μl of 2 mg/ml Chloramine T in 0.05 M Na-phosphate buffer, pH 7.5. After incubation for 1 min at room temperature, 200 μl of 2 mg/ml $Na_2S_2O_5$ in H_2O was added to the reaction mixture. After 15 minutes, the reaction mixture was applied to a PD-10 column (Pharmacia) which had been equilibrated with PBS. The fractions containing excluded radioactivity were combined and stored at −80°C until use.

^{125}I-labeled CPs (c.a. 3×10^5 cpm in 1 μl) were injected into the nondiapause unsexed 5th instar nymphs and female adults. After incubation at 25°C for 6 hr, ovaries, abdominal fat body and abdominal integument (mainly cuticle and epidermis) were dissected in cold PBS, and were washed three times in PBS. The radioactivity incorporated into each tissue was counted by a γ-counter (Aloka, ARC-600).

RESULTS AND DISCUSSION

Separation of CP subunit by IEF

Hemolymph CPs (CP-1 to CP-4) are separable on native PAGE. When CP bands are cut from a stained native gel and subjected to SDS-PAGE, all CPs become indistinguishable from each other and are found to be composed of a subunit with a single apparent molecular mass of 76 kD [4]. However, the native pI of CP-1 (CPegg) (7.85) is higher than that of CP-4 (7.25) and CP-2 and 3 have pIs intermediate to CP-1 and 4. Furthermore, when bands of CP-1 and CP-4 on native PAGE are excised and subjected to rocket im-

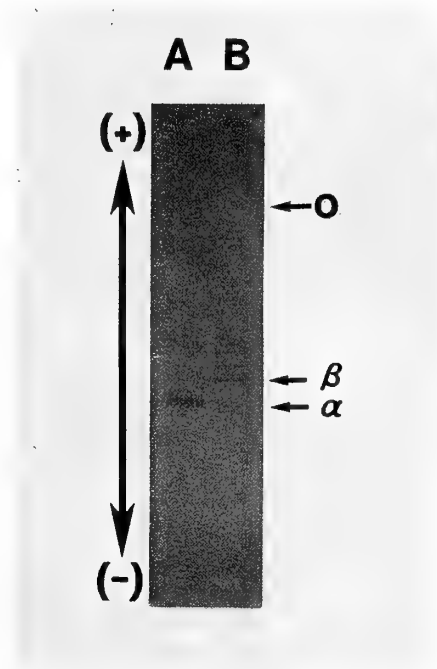

FIG. 1. Denaturing IEF of puried CPegg (A) and CP-4 (B). Samples were focused for 4000 V×hr on a 5% polyacrylamide gel slab containing 8 M urea, 0.5% (w/v) Nonidet P-40 and 2.5% (w/v) Ampholine (pH 3.5–9.5). After electrophoresis the gel was stained with Serva Violet 17. α, α subunit; β, β subunit. o: point of sample application.

TABLE 1. Amino acid composition of cyanoproteins. Data for CPegg is from [4]. Tryptophan not determined

Amino Acid	mol %	
	CPegg (α_6)	CP-4 (β_6)
Ala	6.47	7.65
Val	6.28	6.72
Leu	6.56	8.31
Ile	4.16	3.09
Pro	5.12	5.44
Met	1.48	0.54
Phe	8.96	6.89
Gly	6.16	6.93
Ser	6.65	5.78
Thr	3.99	5.04
Cys	0.00	0.00
Tyr	7.90	7.63
Asp+Asn	13.30	15.00
Glu+Gln	8.11	8.59
Lys	6.50	1.23
Arg	5.96	6.94
His	2.62	4.24

munoelectrophoresis with antiserum against CPegg, CP-1 and CP-4 form distinct precipitin lines . These facts suggest that CP-1 and CP-4 are composed of closely related subunits of the same size but different pI [5]. Separation of purified CPegg and CP-4 (see the Materials and Methods) by IEF under denaturing conditions showed that purified CPegg (identical to CP-1, see Fig. 4) was composed of a single subunit and that CP-4 was composed of a different subunit with a different pI (Fig. 1). In the previous papers we termed the putative subunits of CP-1 and CP-4 as *a* and *b*, respectively [4, 5]. Since they can be easily confused with CP-A (CP-1, 2 and 3) and CP-B (CP-4) which are separated as different precipitin lines by rocket immunoelectrophoresis [5], we therefore now name the CPegg (CP-1) subunit α and the CP-4 subunit β. The α subunit is more basic than the β subunit (subunit pIs under the denaturing conditions not determined), as is the native CPegg (CP-1) than CP-4. Some minor acidic bands other than the main band are visible for CP-4. This may be due to the uneven distribution of sialic acids in carbohydrate moiety of the β subunit.

Amino acid composition

The amino acid compositions of purified CPegg and CP-4 are presented in Table 1. The data for CPegg from [4] is also presented for comparison. Both show high aromatic amino acid (Tyr and Phe) content, 16.86% for CPegg and 14.52% for CP-4 while the Met content is low for both proteins. The content of Lys is much higher in CPegg, which may be the reason for the higher pI of CPegg.

Sequencing of N-terminal amino acids

Possible explanations for the different pIs of the two subunits are that α and β have different amino acid sequences which are encoded by different genes or that one of them is the processing product of the other. To distinguish between these alternatives, we determined the N-terminal amino acid sequences of CP-1 (α subunit) and CP-4 (β subunit) (Fig. 2). Six amino acid differences between the two subunits (indicated by dots) were seen. The amino acid sequences of the N-terminus of CP-1 and CP-4 are respectively identical to the sequences deduced from the cDNA for α and β subunits (our unpublished data). These results together with the amino

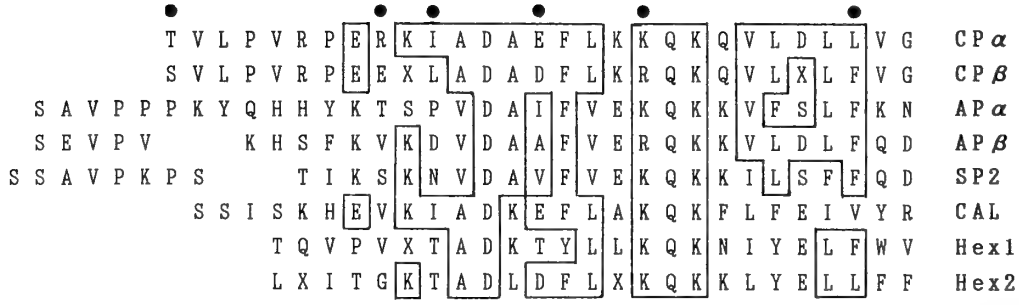

FIG. 2. Alignment of the N-terminal amino acid sequences of CPα (CP-1), CPβ (CP-4) and insect storage hexamers. Details are given under Materials and Methods. Amino acid differences between the two *R. clavatus* cyanoprotein subunits are marked with dots. Identical residues between the CP subunits and other hexamers are boxed. CPα and β: *R. clavatus* cyanoprotein α and β subunits. APα and β: *M. sexta* arylphorin α and β subunits. SP2: *B. mori* arylphorin subunit. CAL: *C. vicina* arylphorin subunit. Hex 1 and 2: subunits of *C. festinatus* storage hexamer 1 and 2. X: not identied amino acid.

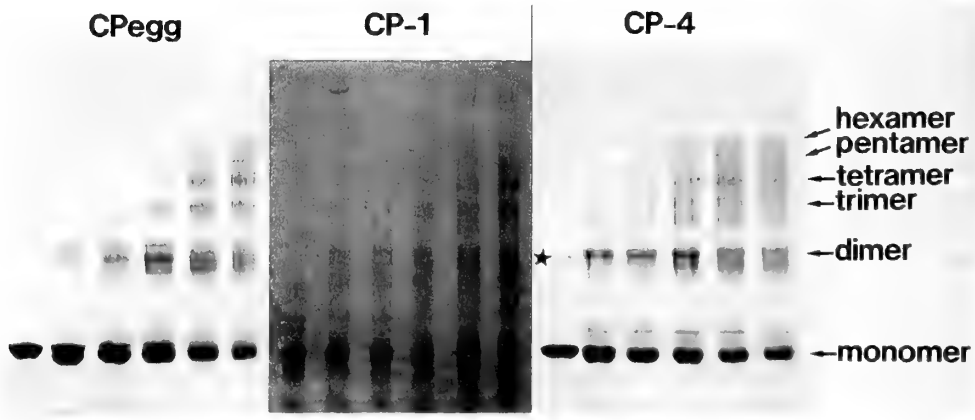

FIG. 3. SDS-PAGE analysis of chemically cross-linked products of CPegg, CP-1 and CP-4 with DMS. One microgram per one microliter of protein sample were incubated with increasing amounts of DMS. Final concentrations of the crosslinker in the incubation mixtures were 0, 0.2, 0.5, 1.0, 3.0, and 6.0 μg/μl from left to right for each protein sample. Resultant cross-linked products were analyzed by 2.5–10% SDS-PAGE. Asterisk indicates the position of the natural dimer of the β subunit which was not dissociated by SDS and 2-mercaptoethanol.

acid composition analysis confirm that the α subunit and the β subunit are products of different genes.

The two N-terminal sequences were aligned with those of several insect storage hexamers using a commercial program (Genetyx Ver. 8.0, SDC Software Development Co., Japan) (Fig. 2). As is evident here, appreciable sequence similarities in the N-terminus were found in CP subunits against storage hexamers of Lepidoptera (arylphorins of *Manduca sexta* [39], SP-2 of *Bombyx mori* [12]), Diptera (calliphorin of *Calliphora vicina* [26]) and Hymenoptera (Hex 1 and Hex 2 of *Camponotus festinatus* [22]). The results suggest that the cyanoproteins of *R. clavatus* fall in the category of insect storage hexamers.

Chemical cross-linking analysis of CPs

The CPs have a high aromatic amino acid content like arylphorin-type hexamers and show some sequence similarities to insect hexamers in the N-terminal region (Table 1 and Fig. 2). So, we examined the numbers of subunits composing native CPs by chemical cross-linking analysis. This was already announced in a footnote in the previous paper [4]. Here, we present the data. Figure 3 shows SDS-PAGE analysis of the cross-linked products of purified CPegg, CP-1 and CP-4 after incubation with increasing amounts of a cross-linker, DMS. As the concentration of DMS increased from left (0 μg/μl) to right (6 μg/μl), the cross-linked products increased in size up to the appearance of hexameric cross-linked products. Even after incubation with high concentrations of the crosslinker a large amount of the monomer

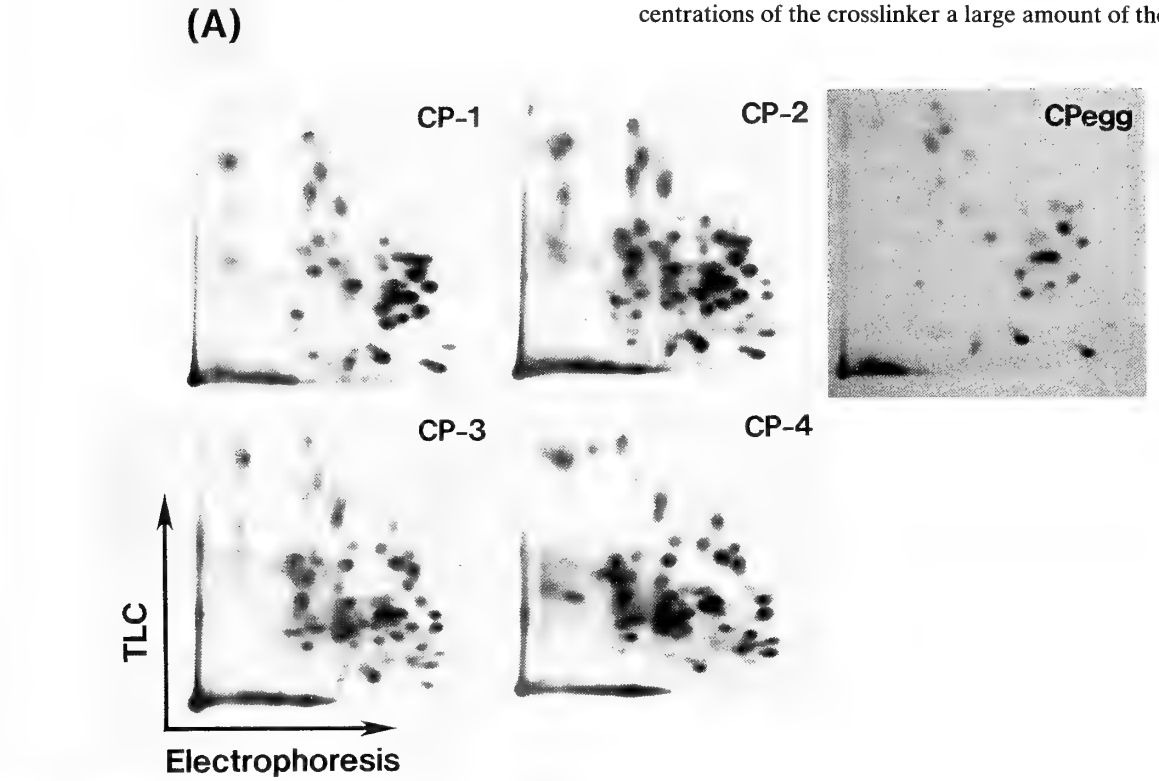

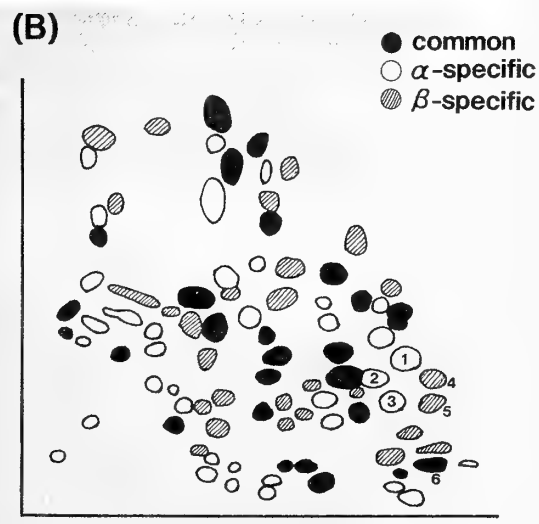

FIG. 4. Comparison of 2-dimensional tryptic peptide maps of radioiodinated CPs. CPs were separated by 2.5–15% native PAGE, and protein bands cut out from stained gels. Protein bands containing about 0.5 μg of each CPs were radioiodinated, digested with trypsin in the gel slices, and the resultant peptides extracted. Peptides were developed on cellulose plates by electrophoresis in the first dimension followed by thin layer chromatography in the second dimension, then autoradiographed. A, Maps of CP-1 to 4 and CPegg. B, A diagrammatic representation of the tryptic peptides of CPs. The spots on X-ray films were categorized into three groups as follows: spots common to both α and β subunits (solid); α subunit-specific spots (open); β subunit-specific spots (shadowed). The numbered spots were used for densitometric scanning.

still remained. This may be due to the spontaneous dissociation of the native molecules under the conditions employed for the crosslinking as discussed by Levenbook [21]. Thus, CPegg, CP-1 and CP-4 all have hexameric structures. Pore-limiting gradient PAGE analysis demonstrated that CP-2 and CP-3 have the same native molecular mass as the other CPs (not shown). Therefore, it is reasonable to consider that CP- 2 and CP-3 are also constructed by the assembly of six molecules of 76 kDa subunits.

Tryptic peptide analysis by 2D peptide mapping

In the previous paper we reported one-dimensional peptide mapping using V8 protease (without data) and discussed the subunit structures of CPs [4]. In this paper, we have employed an advanced method of 2D peptide mapping and clearly show the relationship among CP-1 to CP-4 and CPegg. CPs separated on native PAGE were radioiodinated in gel slices and digested with trypsin. The radioiodinated tryptic peptides were separated on cellulose-coated TLC plates, by electrophoresis for the first dimension and by TLC for the second dimension, then autoradiographed. The results are shown in Figure 4. As expected from the immunological relationship between CP-1 and CP-4, spots on maps of CP-1 (α subunit) and CP-4 (β subunit) could be categorized into three groups: common spots (solid); α subunit-specific spots (open); β subunit-specific spots (shadowed) (Fig. 4B). Therefore, α and β subunits have common regions as well as subunit-specific regions. The map of CPegg was identical to CP-1.

The peptide maps of CP-2 and CP-3 contained spots of all three groups. Thus, they were like superimpositions of CP-1 and CP-4. Therefore, both CP-2 and CP-3 appear to be hybrid molecules of α and β subunits. To determine the numbers of α and β subunits composing CP-2 and CP-3, the intensities of ve typical spots (1–3: α subunit-specific; 4 and 5: β subunit-specific, indicated in Fig. 4B as numbered spots) relative to one common spot (6 in Fig. 4B) were measured with an image analysis system. The relative intensities of α subunit-specific spots (1–3) in the maps decreased from CP-1 to 4 (6:4:2:0) while those of β subunit-specific spots (4 and 5) in the maps increased from CP-1 to 4 (0:2:4:6). Since CP-2 and CP-3 are also hexameric, the subunit structures of CP-2 and CP-3 were deduced to be $\alpha_4\beta_2$ and $\alpha_2\beta_4$, respectively.

According to these molecular structures, all the CP molecules are composed of even numbers of α and β subunits. As seen in Figure 3 (asterisk), small fractions of the β subunit were SDS- and 2-mercaptoethanol-nondissociable dimers in the CP-4 preparation. This natural dimer was also present in the other β subunit-bearing CPs, CP-2 and 3 (not shown). Since there is no CP molecule which has an odd number of either α or β subunits, we propose that the β subunit behaves as a dimeric form during the process of assembly of mature CP molecules.

Immunoblot analysis

CP-2, CP-3 and CP-4 were demonstrated to bear a β subunit, which is further supported here in another manner. The polyclonal antiserum obtained from a rabbit which was immunized with a mixture of CP-1 to 4 appears to be composed of three subpopulations of antibodies: antibodies recognizing epitopes common to both the α and β subunit; antibodies to α subunit-specific epitopes; antibodies to β subunit-specific epitopes. When the four CPs were analyzed by native PAGE followed by immunoblotting with this antiserum, all CP bands were visible (Fig. 5A). Then, this antiserum was absorbed completely with puried CPegg (α subunit). The absorbed antiserum (anti-β-specific) should contain solely antibodies to β subunit-specific epitopes. When a similar blot was probed with the anti-β-specific, only the bands of β subunit-bearing CPs (CP-2, 3 and 4) were detected (Fig. 5B). These results support the molecular structure, i.e. subunit composition of CP-1 to 4 mentioned above.

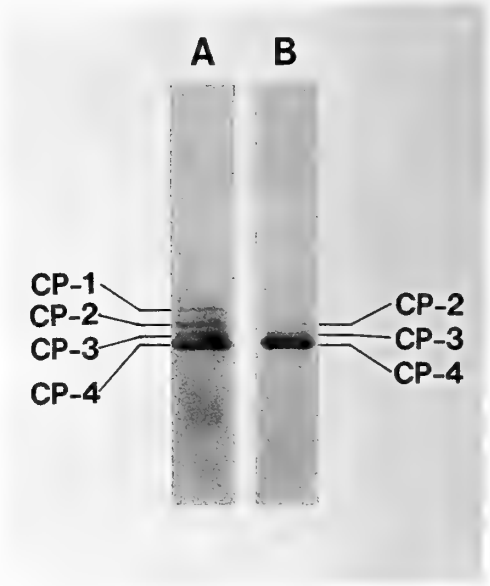

FIG. 5. Immunoblot analysis of CPs. Hemolymph protein of diapause adults was separated by 2.5–15% native PAGE, and electroblotted onto nitrocellulose. The blots were probed with (A) antiserum raised against hemolymph CPs (CP-1 to 4), or (B) absorbed antiserum to β subunit-specific epitopes (see Materials and Methods). This was followed by reaction with secondary antibodies conjugated with peroxidase.

Electron microscopy

When viewed with the electron microscope, all CPs showed hexagonal shapes touching internally to form a circle of about 130 Å in diameter (Fig. 6). Moreover, these CP molecules appear to be composed of six identical substructures, which agrees with the hexameric structures of CPs demonstrated by chemical cross-linking analysis. Some rectangular images were also observed (not shown). From these results we propose that CPs have a shape like a

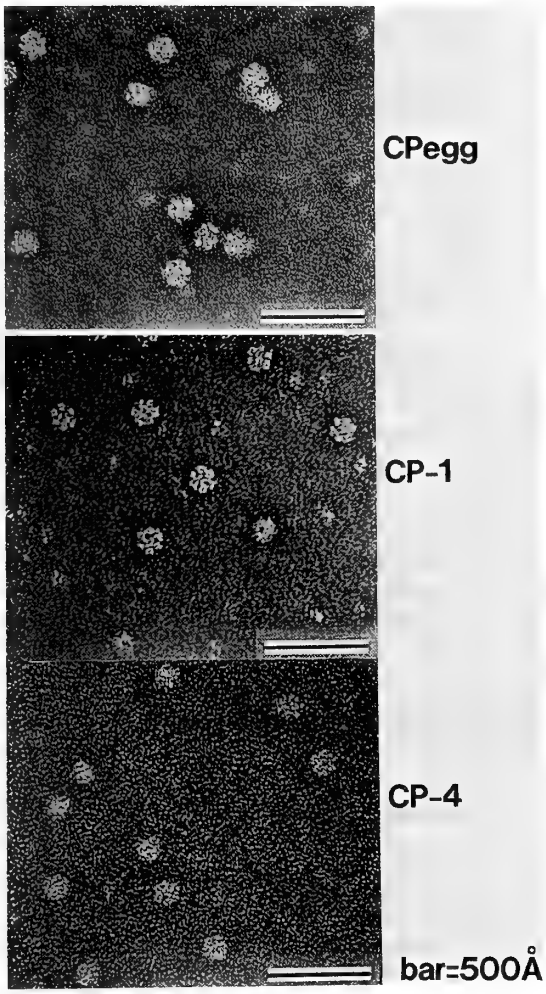

FIG. 6. Electron micrographs of CPegg, CP-1 and CP-4 stained negatively with uranium acetate. Each bar represents 500 Å.

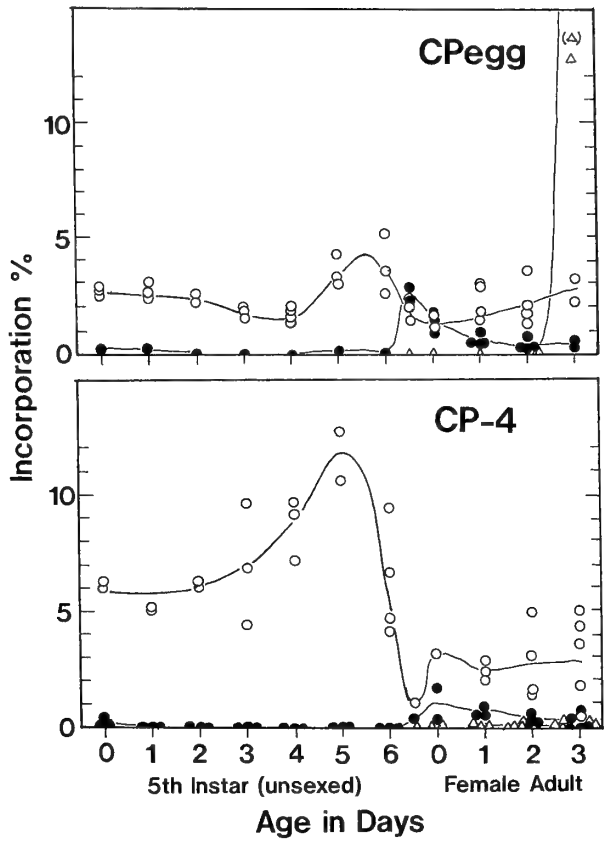

FIG. 7. Changes of CP incorporation into fat body, ovary and integument. Radioiodinated CPs were injected into unsexed 5th instar nymphs and female adults, dissected after 6 hr, and radioactivity incorporated into the tissues measured. In each experiment radioactivity of c.a. 3×10^5 cpm in a volume of 1 μl was injected per animal. Upper panel, incorporation of CPegg; lower panel, incorporation of CP-4. ○—○, fat body; △—△, ovary; ●—●, integument.

flattened hexagonal cylinder.

Incorporation of ^{125}I-labeled CPegg and CP-4 into several tissues during nymphal-adult development

Using purified CPegg (identical to hemolymph CP-1) and CP-4, we examined *in vivo* incorporation into several tissues. The purified CPs were radioiodinated by chloramine T method. The specic activities in CPegg and CP-4 preparations are 5.0×10^6 cpm/μg and 3.5×10^6 cpm/μg, respectively. The integrity of labeled CPs was checked by native PAGE and autoradiography. Electrophoretic behavior of the labeled CPs was same as unlabeled ones, and the bands showed no sign of degradation (data not shown). This confirmed that the labeled CPs still maintain their native structure.

The ^{125}I-CPegg and ^{125}I-CP-4 (3.0×10^5 cpm in 1 μl) were injected into the 5th instar nymphs (unsexed) and non-diapause female adults. After 6 hr incubation radioactivity distributing in the ovary, abdominal fat body and abdominal integument were counted following washing the tissues three times. The strength of washing (presence or absence of a detergent, Triton X-100) did not affect the radioactivity recovered. This indicates that CPs are internalized during the incubation. Results are illustrated in Figure 7. The incorporation rate is expressed as % incorporation. Through the 5th instar appreciable incorporation into the fat body was observed. The maximal rate of incorporation was demonstrated for both proteins at the final phase of the 5th instar, where the incorporation rate of CP-4 was 2.5-fold greater than that of CPegg. The rapid incorporation decreased dramatically just after adult emergence, and in turn, the incorporation into the integument was observed. The peak occurred for both proteins between day-0 and day-1 after emergence, and then declined. Thereafter, as the ovaries developed, solely CPegg was incorporated into the ovaries.

At the ultimate phase of *R. clavatus* nymphal development CP content in the hemolymph drops rapidly with a concomitant rise in the fat body content, which suggests the active sequestration of hemolymph CP molecules by fat body cells [6]. The present experiments have confirmed this hypothesis. CPegg and CP-4 were incorporated into the nymphal fat body and the maximal incorporation rate, which was about twice that at mid- instar, was observed at the final

phase of the 5th instar for both proteins. The hemolymph CP content at the final phase of the 5th instar is almost twice that of mid-instar [6]. Therefore, the specific activities of CPs injected in the late nymphs should be about one half those in the mid-instar nymphs, assuming that the labeled molecules behave in a similar manner to cold ones. Based on these values, the numbers of CP molecules incorporated at the last phase will be about 4-fold higher than those in mid-instar. Similarly, when the incorporation rate is expressed as the moles of sequestered protein, the maximal incorporation rate of CP-4 by the fat body of the last nymphal day would be 7-fold higher than that of CPegg. The question arises here whether this sequestration is driven by a nonselective or selective mechanism. We consider that some selective mechanisms at least for CP-4 sequestration other than a size barrier discussed by Duhamel and Kunkel [10] may be involved since CP-4 is shown to be incorporated at a much higher rate than CPegg. A specic receptor-mediated process found in *Sarcophaga peregrina* [38] might occur in *R. clavatus* as well. The CPs captured by the fat body are thought to be degraded without a storage process and to be utilized for constructing adult proteins because the CPs have been shown to almost disappear in the whole insect extract just after adult emergence [6]. By contrast to the fat body, the ovary sequestered exclusively CPegg (identical to CP-1) whereas no appreciable incorporation of CP-4 occurred. Moreover, hybrid molecules bearing both α and β subunits, CP-2 and CP-3 were not incorporated in the similar experiment using ^{125}I- labeled whole hemolymph proteins when examined by native PAGE and autoradiography of ovary extract after 6 hr incubation (data not shown). From these observations, the occurrence of a sorting system with high selectivity in the ovary is suggested. High pI nature and/or some structural features of protein and carbohydrate moiety of the CP-1 molecule may be involved in the ligand specificity. It was also demonstrated that CPs are incorporated into the abdominal integument of the newly emerged adults. This suggests the involvement of CPs in cuticle formation and sclerotizaition as discussed by Scheller *et al.* [34].

Conclusion

The present study confirmed that all CPs (CP-1, CP-2, CP-3, CP-4, and CPegg which is shown to be identical to CP-1) have hexameric structures composed of two types of distinct 76 kDa subunit, an α subunit and an β subunit which has a more acidic pI. Therefore, as the numbers of β subunits constituting CP molecules increase, the native pIs become more acidic. These hexamers are shaped like flattened hexagonal cylinders. There are six amino acid differences in the N-terminal amino acid sequences of the two subunits, four of which are conservative changes. Since these changes are not in a block, together with their amino acid compositions, it is reasonable to conclude that they are independent products of different genes. Moreover, the two subunits have both common and specific immunological and structural properties. The subunit structures of CPs were determined: CP-1 (CPegg)=α_6; CP-2=$\alpha_4\beta_2$; CP-3=$\alpha_2\beta_4$; CP-4=β_6. In addition, sequencing of N-terminal regions have revealed that both subunits show appreciable sequence similarities to other insect hexamers. Therefore, we conclude that CP of *R. clavatus* is a member of hexamerin superfamily [37].

In the previous studies we obtained data suggesting its function, which, in part, has been confirmed in this study. That is, at the last phase of nymphal development, hemolymph CPs (mainly CP-4) are sequestered by the fat body and are suggested to be utilized for constructing adult proteins. Possible involvement in cuticle formation is also suggested. CP-1 in the hemolymph of the reproductive females is sequestered selectively by the ovaries and accumulates as CPegg. Among insect hexamers, CP of *R. clavatus* is more similar to arylphorin in its function during nymphal-adult development as well as in its molecular structure and high aromatic nature. These physicochemical and functional properties satisfy some of the generally accepted definitions of arylphorin type storage hexamers [21, 37]. Therefore, it is reasonable to consider that the *R. clavatus* CP is a hemipteran counterpart of arylphorin of Holometabola. Emphasis should be placed on the function of CPegg as an egg yolk protein. CPegg occupies about one third of the total egg yolk protein [4]. Although the synthesis and accumulation of storage hexamers in adults insects have been shown in orthopteran *L. migratoria* [1] and hymenopteran *C. festinatus* [22], the accumulation of storage hexamers in the egg yolk in *R. clavatus* is the only example. In this connection, we have surveyed storage hexamers in the eggs of 19 heteropteran species other than *R. clavatus* from six families, and have failed to detect them (Kamiya *et al.*, unpublished). The changes in CPs of *R. clavatus* show complicated profiles depending on stages, sex and diapause [7]. The present study has also ascertained that the various expression of CPs can be ascribed to the expression of only two genes of the CP subunits.

ACKNOWLEDGMENTS

We thank Dr. Lynn M. Riddiford, University of Washington, and Dr. DeMar Taylor, Texas A & M University, for reading the manuscript. This work was supported in part by Grant-in-Aid for Scientic Research to KM (No. 04660047) and to YC (No. 04454060) from the Ministry of Education, Science and Culture, Japan.

REFERENCES

1 Ancsin JB, Wyatt GR (1990) Purification and characterization of two hemolymph proteins from *Locusta migratoria*. In "Molecular Insect Science" Ed by Hagedorn HH, Hildebrand JG, Kidwell MG, Law JH, Plenum Press, New York, pp 275

2 Cherbas P (1973) Biochemical Studies on Insecticyanin. Ph. D. thesis, Harvard University

3 Chino H, Abe U, Takahashi K (1983) Purification and characterization of a biliverdin-binding cyanoprotein from the locust hemolymph. Biochim Biophys Acta 48: 109–115

4 Chinzei Y, Haruna T, Miura K, Numata H, Nakayama S (1990) Purification and characterization of biliverdin-associated cyanoprotein from eggs and hemolymph of the bean bug, *Riptortus clavatus* (Heteroptera: Alydidae). Insect Biochem 20: 545–555

5 Chinzei Y, Nishi A, Miura K, Shinoda T, Numata H (1991a) Cyanoprotein: immunological properties and content changes during the development of non-diapause female bean bug, *Riptortus clavatus*. Insect Biochem 21: 223–231

6 Chinzei Y, Shinoda T, Miura K, Numata H (1991b) Quantitative changes and synthesis of cyanoprotein in whole body and tissues during development of the bean bug, *Riptortus clavatus*. Insect Biochem 21: 313–320

7 Chinzei Y, Miura K, Kobayashi L, Shinoda T, Numata H (1992) Cyanoprotein: developmental stage, sex and diapause-dependent expression, and synthesis regulation by juvenile hormone in the bean bug, *Riptortus clavatus*. Arch Insect Biochem Physiol 20: 61–73

8 Davies GE, Stark GR (1970) Use of dimethylsuberimidate, a cross-linking reagent, in studying the subunit structure of oligomeric proteins. Proc Natl Acad Sci USA 66: 651–656

9 deBruyn SM, Koopmanshap AB, deKort CAD (1986) High-molecular-weight serum proteins from *Locust migratoria*: identification of a protein specifically binding juvenile hormone-III. Physiol Entomol 11: 7–16

10 Duhamel R, Kunkel JG (1983) Cockroach larval-specific protein, a tyrosine-rich serum protein. J Biol Chem 258: 14461–14465

11 Elder JH, Pichett II RA, Hampton J, Learner RA (1977) Radioiodination of Proteins in single polyacrylamide gel slices. J Biol Chem 252: 6510–6515

12 Fujii T, Sakurai H, Izumi S, Tomino S (1989) Structure of the gene for the arylphorin-type storage protein SP-2 of *Bombyx mori*. J Biol Chem 264: 11020–11025

13 Goodman WG, Adams B, Carlson RO (1982) Purification and characterization of an epidermal and hemolymph protein from *Manduca sexta*. Am Zool 22: 977.

14 Görg A, Postel W, Gunter S (1988) The current state of two-dimensional electrophoresis with immobilized pH gradients. Electrophoresis 9: 531–546

15 Haunerland NH, Bowers WS (1986) A larval specific lipoprotein: purification and characterization of a blue chromoprotein from *Heliothis zea*. Biochem Biophys Res Commun 134: 580–586

16 Holden HM, Rypniewski WR, Law JH, Rayment I (1987) The molecular structure of insecticyanin from the tobacco hornworm, *Manduca sexta* L. at 2.6 Å resolution. EMBO J 6: 1565–1570

17 Hunter WM, Greenwood FC (1962) Preparation of iodine-131 labelled human growth hormones of high specific activity. Nature 194: 495–496

18 Huber R, Schneider M, Epp O, Mayr I, Messerschmidt A and Kayser H (1987a) Crystallization, crystal structure analysis and preliminary molecular model of the bilin binding protein from the insect. J Mol Biol 195: 423–434

19 Huber R, Schneider M, Mayr I, Mueller R, Deutzmann R, Suter F, Zuber H, Falk H, Kayser H (1987b) Molecular structure of the bilin binding protein (BBP) from *Pieris brassicae* after refinement at 2.0 Å resolution. J Mol Biol 198: 499–513

20 Jones G, Ryan RO, Haunerland NH, Law JH (1988) Purification and characterization of a very high density chromoprotein from the hemolymph of *Trichoplusia ni* (Hubner). Arch Insect Biochem Physiol 7:1–11

21 Levenbook L (1985) Insect storage proteins. In "Comprehensive Insect Physiology, Biochemistry and Pharmacology" Ed by Kerkut GA, Gilbert LI, Pergamon Press, New York, vol. 10, pp 307–346

22 Martinez T, Wheeler D (1993) Identification of two storage hexamers in the ant, *Camponotus festinatus*: accumulation in adult queenless workers. Insect Biochem Molec Biol 23: 309–317

23 Miura K, Chinzei Y, Shinoda T, Numata H (1991) Cyanoprotein: quantitative changes and synthesis in diapause and juvenile hormone analog treated bean bug, *Riptortus clavatus*. Insect Biochem 21: 553–561

24 Miura K, Shimizu I (1988) Identification and properties of lipophorin of the silkworm, *Bombyx mori*. Comp Biochem Physiol 89B: 95–103

25 Miura K, Shimizu I (1989) Changes of properties in lipophorin of the silkworm, *Bombyx mori* with ontogeny. Comp Biochem Physiol 92B: 197–204

26 Naumann U, Scheller K (1991) Complete cDNA and gene sequence of the developmentally regulated arylphorin of *Calliphora vicina* and its homology to insect hemolymph proteins and arthropod hemocyanins. Biochem Biophys Res Commun 177: 963–972

27 Nokihara K, Beck R, Herbst F (1988) Improved primary structure determination for peptides and proteins by electroblotting in combination with sequencing. Anal Lett 21: 1371–1382

28 Nokihara K, Herbst F (1990) Rapid isolation and characterization of coupling factor 6 from porcine atria. In "Peptide Chemistry 1989" Ed by Yanaihara N, Protein Research Foundation, Osaka, pp 69–74

29 Numata H, Hidaka T (1982) Photoperiodic control of adult diapause in the bean bug, *Riptortus clavatus* Thunberg (Heteroptera: Coreidae) I. Reversible induction and termination of diapause. Appl Ent Zool 17: 530–538

30 Numata H, Hidaka T (1984) Termination of adult diapause by a juvenile hormone analogue in the bean bug, *Riptortus clavatus*. Zool Sci 1: 751–754

31 Patestos NP, Fauth M, Radola BJ (1988) Fast and sensitive protein staining with colloidal Acid Violet 17 following isoelectric focusing in carrier ampholyte generated and immobilized pH gradients. Electrophoresis 9: 488–496

32 Petratos K, Tsernoglou D, Cherbas P (1986) Preliminary characterization of crystals of the protein insecticyanin from the tobacco hornworm *Manduca sexta* L. J Mol Biol 189: 727

33 Riley CT, Barbeau BK, Keim PS, Kezdy FJ, Heinrikson RL, Law JH (1984) The covalent protein structure of insecticyanin, a blue biliprotein from the hemolymph of the tobacco hornworm, *Manduca secta* L. J Biol Chem 259: 13159–13165

34 Scheller K, Zimmerman H-P, Sekeris CE (1980) Calliphorin, a protein involved in the cuticle formation of the blowfly, *Calliphora vicina*. Z Naturforsh 35c: 387–389

35 Suter F, Kayser H, Zuben H (1988) The complete amino-acid sequence of the bilin binding protein form *Pieris brassicae* and its similarity to a family of serum transport proteins like the retinol-binding proteins. Biol Chem Hoppe-Seyler 369: 497–505

36 Telfer WH, Keim PS, Law JH (1983) Arylphorin, a new protein from *Hyalophora* cecropia: Comparisons with calliphorin and manducin. Insect Biochme 13: 601–613

37 Telfer WH, Kunkel JG (1991) The function and evolution of insect storage hexamers. Ann Rev Ent 36: 205–228

38 Ueno K, Natori S (1984) Identification of storage protein receptor and its precursor in the fat body membrane of *Sarcophaga peregrina*. J Biol Chem 259: 12107–12111

39 Willot E, Wang X-Y, Wells MA (1989) cDNA and gene sequence of *Manduca sexta* arylphorin, an aromatic amino acid-rich larval serum protein. J Biol Chem 264: 19052–19059

ZOOLOGICAL SCIENCE 11: 547–553 (1994)

An Open Cephalic Neural Tube Reproducibly Induced by Cytochalasin D in Rat Embryos *in vitro*

MOTOKO MATSUDA[1] and HIROOMI KEINO[2]

Departments of Embryology[1] and Perinatology[2], Institute for Developmental Research, Kasugai, Aichi 480-03, Japan

ABSTRACT—Rat embryos at the head-fold stage (Slc : SD strain; 9.5 days of gestation) were cultured in rat serum in the presence of a relatively low concentration of cytochalasin D (2×10^{-8} M). Embryos developed into C-shaped structures (with the open part of the C directed ventrally) with an open cephalic neural tube. Elevation and apposition of the neural folds and eversion of the neural plates at the procencephalon, mesencephalon and some parts of rhombencephalon were observed during the course of development of the treated embryos. In control embryos, staining with rhodamine-conjugated phalloidin was observed at the basal region of the lateral margin of the fusing neural folds and at the luminal surface of the roof plates of the procencephalic neural tube. The latter diminished as embryos developed. However, the staining was confined to the edges of the apposed neural folds in the treated embryos and became intense at the luminal surface of the everted neural plates. By contrast, some parts of the rhombencephalon of the treated embryos showed fusion of the neural folds. The staining was observed in roof plates of the rhombencephalon in these embryos as like as control embryos. The area of the staining at the luminal surface of the roof plates spread as the fourth ventricle expanded. These results suggest that microfilaments do not play an essential role in the elevation of the neural plates but do play an important role in fusion of the neural folds and the moulding of the cephalic neural tube. Delicate changes in the distribution of microfilaments may result in changes in cell shape that cause the fusion of the neural folds and the moulding of the cephalic neural tube.

INTRODUCTION

Microfilaments are intimately associated with neurulation in amphibian, avian and mammalian embryos [5, 6, 9, 16, 19, 20, 23]. The growth of microfilaments in inhibited and preformed microfilaments are fragmented by treatment with cytochalasins [24]. Among the cytochalasins, cytochalasin D has a particularly high affinity for contractility-related binding sites but it has no effect on hexose transport [3, 11, 26–27]. Therefore, not unexpectedly, treatment of mammalian embryos with cytochalasin D induces abnormal neurulation.

Cytochalasins frequently induce exencephaly in fetuses when administrated to pregnant dams [1, 22, 30–31]. The concentrations of cytochalasin D, injected intraperitoneally, that induce exencephaly at high frequency range from 0.7 to 1.5 mg/kg. Some embryos from mothers treated with cytochalasins have an open neural tube, in which the everted cranial neuroepithelium can be seen [1, 22]. However, many other embryos from treated dams have other major malformations, such as spina bifida, tail defects, eye defects, and ear defects. Therefore, it is difficult to investigate the correlation between microfilaments and abnormal neurulation in such a system *in vivo*.

In experiments *in vitro*, Morriss-Kay and Tuckett [13] found that, in cytochalasin D-treated rat embryos, the neural folds lost their apical constriction, the elevated neural folds were flattened, and the neural folds collapsed. These embryos had been exposed to a relatively high concentration of cytochalasin D (3×10^{-7} M). Similar doses have been used in other systems [3, 11, 25, 29, 32–33]. However, when exposed to cytochalasin D at this rather high concentration (3×10^{-7} M), embryos of C57BL/6 mice die within 24 hr [17]. It is not clear that a culture system in which embryos have collapsed neural folds is useful as a model system for investigations of neurulation. Therefore, a system is needed in which embryos all show the same type of neural malformation, such as an open neural tube. We have cultured rat embryos in a medium that contains a relatively low concentration of cytochalasin D (2×10^{-8} M) and, under our conditions all the embryos develop an open cephalic neural tube.

In this report, we describe the morphological features of the open cephalic neural tube in cytochalasin-treated rat embryos, as well as the pattern of distribution of microfilaments during failure of closure of the cephalic neural tube. Possible causes of the anomaly are discussed.

MATERIALS AND METHODS

Embryo culture

Female Sprague-Dawley (SD) rats (Slc : SD strain; Japan SLC., Shizuoka, Japan) were caged overnight with males in breeding rooms with a 12-hr light cycle, constant temperature (24 ± 2°C) and constant humidity (55 ± 10%). Noon of the day on which a vaginal plug was observed was designated as day 0.5 of gestation. Embryos were cultured according to the methods of New et al. [15]. Embryos at the head-fold stage (9.5 days of gestation, 1.6–1.8 mm in egg cylinder length) were disssected from the uterus in Hanks' solution. After removal of the decidua and rupture of Reichert's membrane, four embryos at a time were put into a culture bottle that contained 4 ml

Accepted July 3, 1994
Received January 24, 1994

of rat serum. Serum was obtained by immediate centrifugation of blood after its withdrawal from SD rats; it was inactivated by heating at 56°C for 30 min. Streptomycin sulfate and benzyl penicillin, sodium salt (Meiji Seika Kaisha, Tokyo, Japan) were added to final concentrations of 1.4×10^{-4} M and 1.8×10^{-4} M, respectively. The culture bottles were gassed initially with 5% O_2, 5% CO_2, and 90% N_2, which was replaced with 20% O_2, 5% CO_2, and 75% N_2 after 22 hr of culture. Finally, the gas was replaced with 40% O_2, 5% CO_2, and 55% N_2 after 24 hr. The bottles were incubated at 37°C on a rotator (40 rev/min) throughout the culture period. Cytochalasin D (Sigma, St Louis, MO, USA), dissolved in dimethylsulfoxide (DMSO; Katayama Chemical Co., Osaka, Japan), was added to the culture medium to a final concentration of 2×10^{-8} M. The concentration of DMSO used in this study (6.4×10^{-8} M, final concentration) did not affect the development of rat embryos, as reported previously by Kitchin and Ebron [7]. Embryos were observed at intervals under a binocular microscope and fixed overnight in 4% paraformaldehyde in 0.1 M phosphate-buffered saline (pH 7.4) at 4°C.

Scanning electron microscopy

Fixed embryos were dehydrated in a graded alcohol series, critical-point dried, mounted on brass stubs with electron-conductive paint (Dotite; Fujikura Kasei, Co., Ltd., Tokyo, Japan), coated with gold in a sputter coater, and observed with a scanning electron microscope.

Light microscopy

Transverse and sagittal 10-μm sections of embryos were prepared by the method of Matsuda [10]. Sections were put on slide glasses, deparaffinized and stained with Mayer's hemalaum. They were enclosed in Entellan (new; E. Merck, AG., Darmstadt, Germany) and examined under a light microscope.

Histochemical procedures

Transverse and sagittal 10-μm sections of embryos were put on slide glasses and deparaffinized. For histochemistry to phalloidin, deparaffinized sections were washed with 20 mM Tris buffer that contained 0.15 M NaCl (pH 7.5), incubated for 30 min at RT with rhodamine-conjugated phalloidin (Wako chemical Ind., Ltd., Osaka, Japan) that had been diluted 1:20 in the buffer. Sections were washed three times with the buffer, enclosed in glycerin jerry (7% gelatin in 50% glycerin containing 0.02% sodium azide) and examined under a fluorescence microscopy (Fluophoto; Nikon, Tokyo, Japan).

RESULTS

Gross and microscopic observations

When rat embryos were cultured for 48 hr in rat serum that contained 2×10^{-8} M cytochalasin D, embryos became C-shaped, with the open part of the C directed ventrally. Their development was almost the same as that of control embryos except in the head region (Table 1). Their cephalic neural plates remained open at the prosencephalon, mesencephalon and rhombencephalon, as shown in Figure 1B. Cephalic neural plates fused in 33-hr-cultured control embryos. However, only elevation and apposition of the neural folds but not fusion were observed in the course of the development of the cytochalasin D-treated embryos (Fig. 2A). The cephalic neural plate was everted in 48-hr-cultured treated embryos (Fig. 2B) and the diencephalon protruded between and over the telencephalic vesicles so that the parts that normally formed the roof of the ventricle were continuous with the skin of the temporal area (Fig. 3A). Transverse sections of the treated embryos showed that the neural plate protruded into the ventricle in the telencephalon (Fig. 3C). A wide space between the neuroepithelium and surrounding mesenchymal cells can be seen in Figure 3C. Anomalies in the neural plate of treated embryos were rather limited in the rhombencephalon (Fig. 3E), as compared with the prosencephalon and the mesencephalon, and part of the rhombencephalon, adjacent to the mesencephalon, showed failure of closure of the neural tube. The rhombencephalic neuroepithelium continued to the neural groove, with both sides closely apposed, in the treated embryos (Fig. 3E) but not in the control embryos (Fig. 3D). The ventricle was more spacious in control embryos than in treated embryos. Trigeminal and facio-acoustic neural crest complexes were observed in the treated embryos as they were in the control embryos (data not shown).

Histochemical observations

In the telencephalic region, neural plates elevated, apposed and everted in cytochalasin D-treated embryos, although control embryos showed fusion of the neural folds and formation of the ventricle. In the 24-hr-cultured control embryos, staining with rhodamine-conjugated phalloidin was observed at the basal region of the lateral margin of the fusing neural folds (Fig. 4A). By contrast, the staining was observed at the surface of the end region of the neural plates

TABLE 1. Effects of cytochalasin D on rat embryos cultured *in vitro* from day 9.5 of gestation for 48 hr

	No. of embryos	No. of embryos with open cephalic neural tube	No. of somites	Crown-rump length (mm)	Head length (mm)
Control	15	0	26.5±1.2	3.52±0.39	1.79±0.17
Cytochalasin D	12	12	25.9±1.2	3.51±0.19	1.62±0.08*

Rat embryos at the head-fold stage were cultured for 48 hr in rat serum with (Cytochalasin D) or without (Control) cytochalasin D (2×10^{-8} M). Mean±S.D. Student's *t*-test was used for statistical analysis. *, Significantly different from the control value ($P<0.01$).

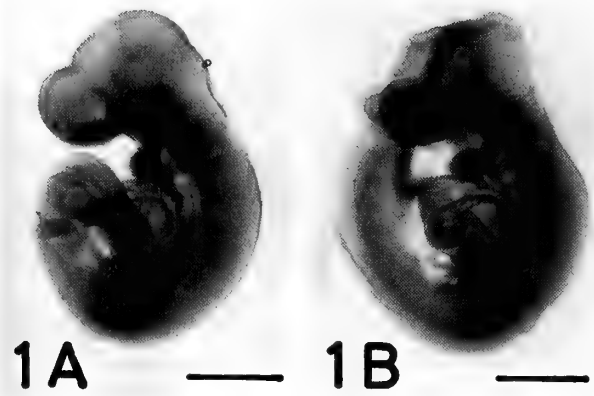

FIG. 1. Gross view of rat embryos at the head-fold stage were cultured in rat serum with (1B) or without (1A) cytochalasin D (2×10^{-8} M) for 48 hr. Fig. 1B shows open an neural tube. Bar, 1 mm.

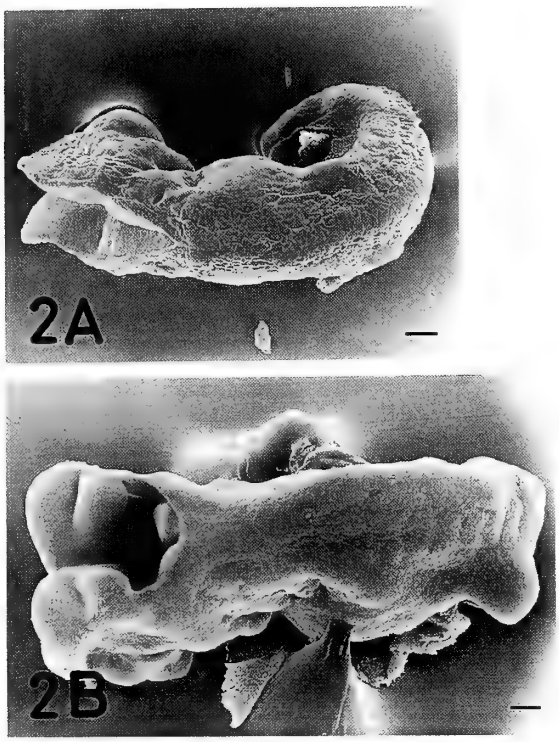

FIG. 2. Scanning electron micrographs of rat embryos. Embryos were cultured for 33 hr (2A) and for 48 hr (2B) in rat serum that contained cytochalasin D (2×10^{-8} M). Fig. 2A shows elevation of the neural folds and Fig. 2B shows eversion of the neural plate. Bar, 100 μm.

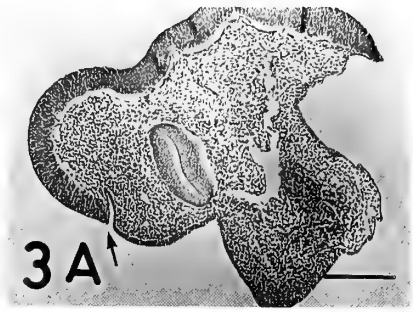

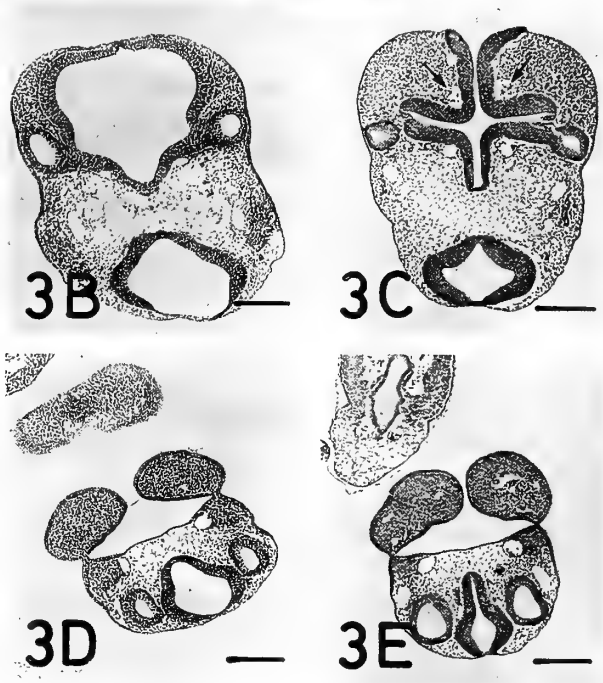

FIG. 3. Anomalies in cytochalasin D-treated rat embryos. Sagittal (3A) and transverse (3B, 3C, 3D and 3E) sections stained with hemalaum. Rat tembryos were cultured in rat serum with (3A, 3C and 3E) or without (3B and 3D) cytochalasin D (2×10^{-8} M) for 48 hr. The diencephalon protrudes between and over the telencephalic vesicles so that parts that normally form the roof of the ventricle are continuous with the skin of the temporal area (3A). An arrow shows the joint that connects the neural plate with the skin. Eversion of diencephalic neuroepithelium is seen in fig. 3C. Arrows indicate the wide space between the neuroepithelium and surrounding mesenchymal cells. The rhombencephalic neuroepithelium continues to the neural groove, the sides of which are closely apposed in the treated embryos (3E). Bars, 250 μm.

in the 24-hr-cultured treated embryos, in which neural plates had opened outwards (Fig. 4B). In 33-hr-cultured control embryos, neural folds fused and the relatively dense staining was observed at the luminal surface of the roof plate. The staining at the luminal surface covered a wide area compared with that at the basal region (Fig. 5A). In contrast, the staining was confined to the edges of the neural folds in the 33-hr-cultured treated embryo (Fig. 5B) in which the neural folds were apposed but not fused. Staining was observed in the roof plate of 36-hr-cultured control embryos (Fig. 6A) but was less in that of 48-hr-cultured control embryos (Fig. 7A) compared with the staining of 36-hr-cultured control embryos. In the treated embryos, neural plates opened outwardly and then everted as time passed. During these processes, staining with rhodamine-conjugated phalloidin was observed at the surface of the neural plates but not at the basal region (Figs. 6B and 7B).

Some parts of the rhombencephalon of the treated

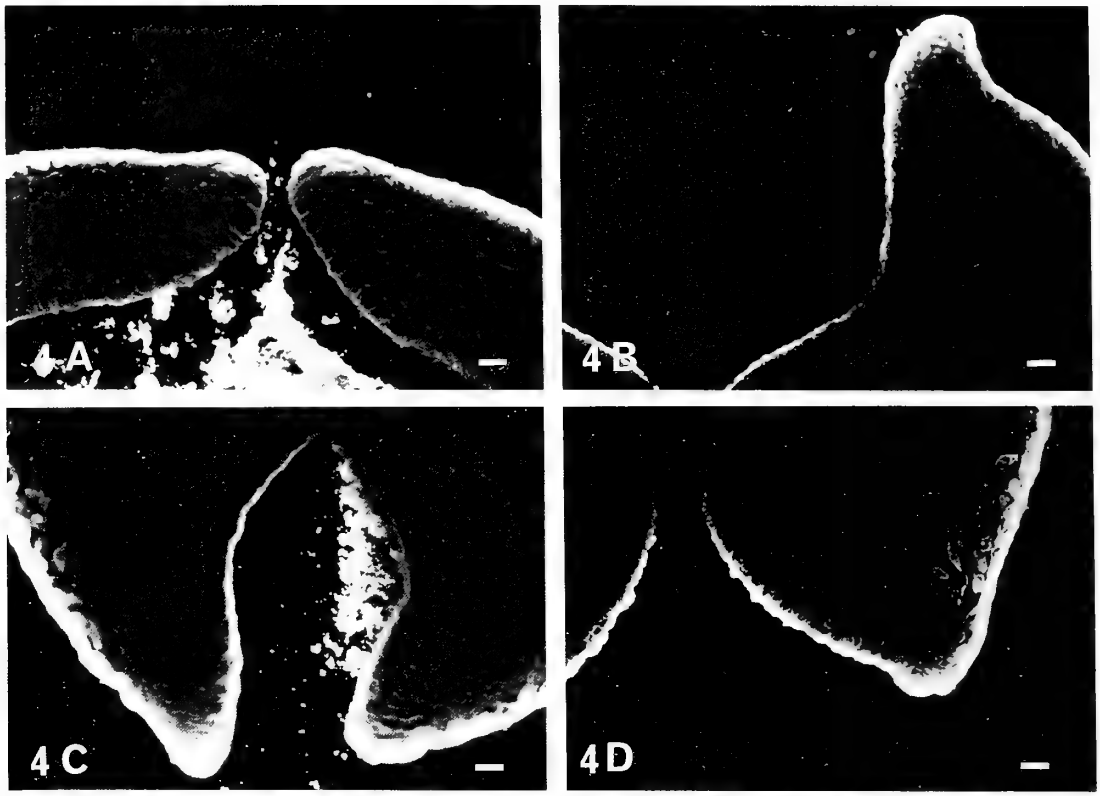

FIG. 4. Distribution of microfilaments in the prosencephalic (4A and 4B) and the rhombencephalic (4C and 4D) neuroepithelium of rat embryos. Transverse sections were stained with rhodamineconjugated phalloidin. Rat embryos at the head-fold stage were cultured for 24 hr in rat serum with (4B and 4D) or without (4A and 4C) cytochalasin D (2×10^{-8} M). Bars, 10 μm.

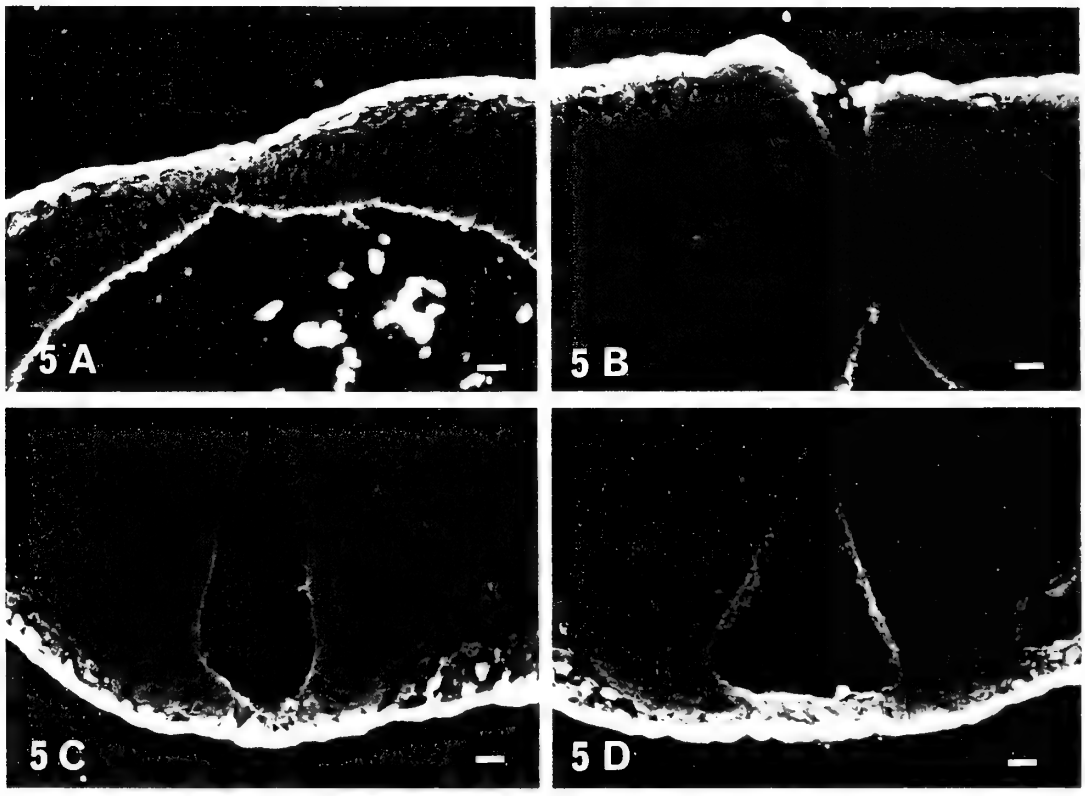

FIG. 5. Distribution of microfilaments in the prosencephalic (5A and 5B) and the rhombencephalic (5C and 5D) neuroepithelium of rat embryos. Transverse sections were stained with rhodamineconjugated phalloidin. Rat embryos as the head-fold stage were cultured for 33 hr in rat serum with (5B and 5D) or without (5A and 5C) cytochalasin D (2×10^{-8} M). Bars, 10 μm.

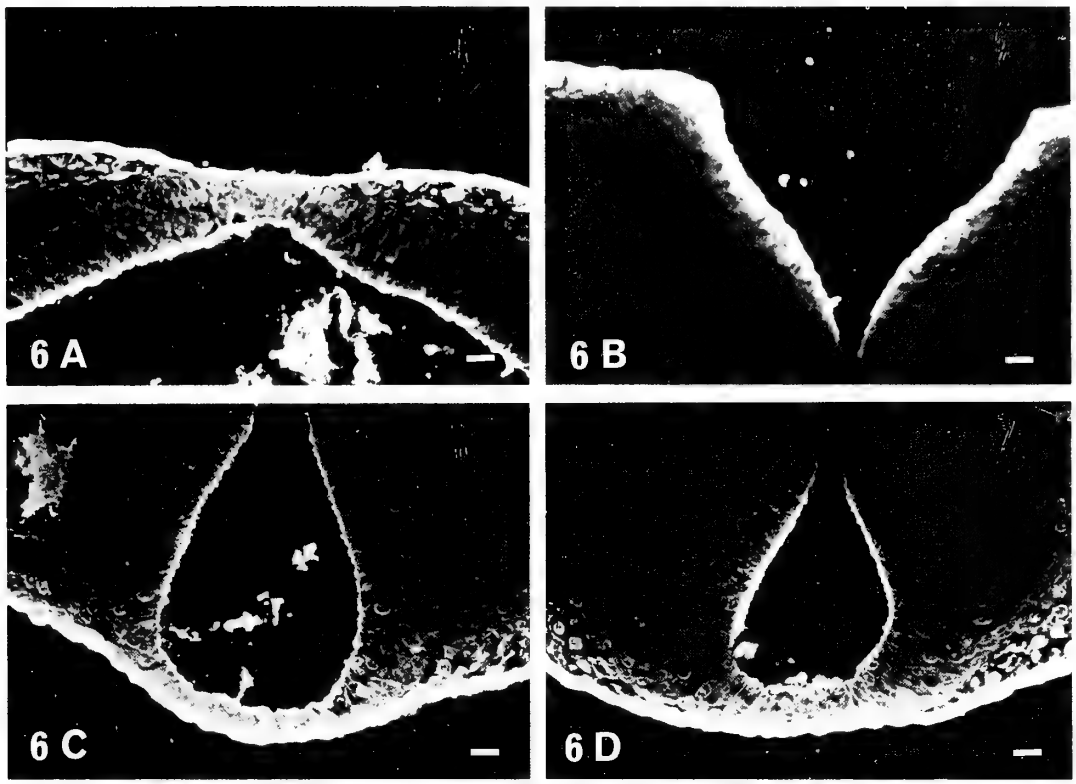

FIG. 6. Distribution of microfilaments in the prosencephalic (6A and 6B) and the rhombencephalic (6C and 6D) neuroepithelium of rat embryos. Transverse sections were stained with rhodamineconjugated phalloidin. Rat embryos at the head-fold stage were cultured for 36 hr in rat serum with (6B and 6D) or without (6A and 6C) cytochalasin D (2×10^{-8} M). Bars, 10 μm.

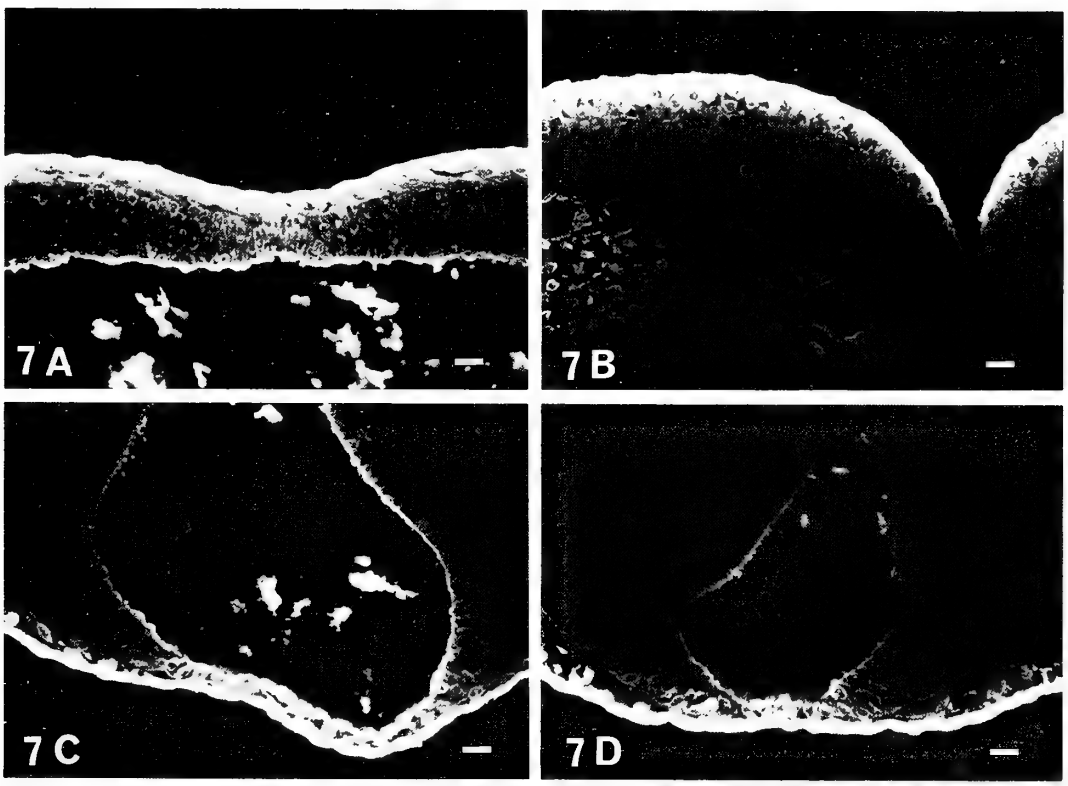

FIG. 7. Distribution of microfilaments in the prosencephalic (7A and 7B) and the rhombencephalic (7C and 7D) neuroepithelium of rat embryos. Transverse sections were stained with rhodamine conjugated phalloidin. Rat embryos at the head-fold stage were cultured for 48 hr in rat serum with (7B and 7D) or without (7A and 7C) cytochalasin D (2×10^{-8} M). Bars, 10 μm.

embryos fused and the staining was detected at the fusing neural folds and in the roof plates as like as control embryos (Figs. 4C, 4D, 5C, 5D, 6C, 6D, 7C and 7D). These figures showed that the area of the staining at the luminal surface of the roof plates spread as the fourth ventricle expanded. As the embryos developed, degree of expansion of the fourth venrticle became different between control and treated embryos and the ventricle was more spacious in the control embryos than in the treated embryos.

DISCUSSION

The results of the present experiments indicate that fusion of the cephalic neural folds in rat embryos can be inhibited by continuous exposure to a relatively low concentration of cytochalasin D (2×10^{-8} M) in vitro. The appearance of the treated embryos resembled to that of the embryos presented by Shepard and Greenaway [22] and by Austin et al. [1] but not those presented by Morriss-Kay and Tuckett [12]. In the investigation of Morriss-Kay and Tuckett [12], collapse of the neural plate to varying extents was apparent in embryos that had been exposed for a short time to a relatively high concentration of cytochalasin D (3×10^{-7} M). This concentration induced death of embryos of C57BL/6 mice within 24 hr although embryos remained alive in 2×10^{-8} M cytochalasin D [17]. It is unclear whether embryos with collapsed neural plates develop exencephaly or not. However, the embryos shown by Shepard and Greenaway [22] and by Austin et al. [1] did develop exencephaly. Therefore, it appears that the embryos obtained in our experimental system should provide a more convenient model for investigations of the mechanism of neurulation.

Neurulation involves formation of the neural plate from the ectoderm, elevation of the neural folds, their apposition and fusion [5, 6, 21]. The results of our experiments indicate that elevation and apposition of the neural folds occur in cytochalasin D-treated embryos but fusion does not. Schoenwolf et al. [20] reported that cytochalasin D did not prevent median furrowing of the neural plate or elevation of the neural folds but did prevent the fusion of neural folds in the chick embryo. Although cytochalasin D produces exencephaly when injected into pregnant mice, the morphological features of such embryos have not been described in detail [1, 22]. It is unclear from the earlier reports whether cytochalasin-induced exencephaly occurs *via* failure of elevation of failure of fusion of the neural folds. However, the fusion process is inhibited both in cadmium-induced exencephaly [28] and in arsenic-induced exencephaly [12]. From these results and the present result, it seems possible that exencephaly occurs as the result of failure of the fusion and not of failure of the elevation or apposition of the neural folds.

Cell shape changes are the basis for morphogenetic movement and the intact microfilaments are required for such changes. The correlation is that in the presence of cytochalasins, microfilaments are disrupted and morphogenesis ceases, and that cytochalasins removal results in microfilament reappearance and resumption of morphogenesis [24]. Cytochalasins reversibly inhibit the growth of microfilaments and degrade preformed microfilaments [2, 24, 29]. Among the cytochalasins, cytochalasin D has a particularly high affinity for contractility-related binding sites but has no effect on hexose transport [3, 11, 26–27]. Thus, the results of our experiments suggest that microfilaments do not play an essential role in the elevation of the neural folds but do play an important role in fusion. Microfilaments are intimately involved in neurulation in amphibian, avian and mammalian embryos [5, 6, 9, 16, 19, 20, 23]. The cited investigations can be divided into three groups in terms of the apparent involvement of microfilaments: microfilaments influenced the elevation of the neural folds [6, 8, 13–14]; they influenced both the elevation and the fusion of the neural folds [9]; and they influenced the fusion of the neural folds [20]. Our study falls into the third group. Although interpretation of the various earlier results is complex, it is possible that a relatively high concentration of cytochalasin D (3×10^{-7} M) affects the elevation and apposition of the neural folds while a relatively low concentration of the drug (2×10^{-8} M) does not affect the elevation but affects the fusion of the neural folds.

The results of the present experiments indicated that when the fusion of the neural plates failed the staining with rhodamine-conjugated phalloidin appeared at the surface of the end region of the neural plates, while the staining was observed at the basal region of the end region of the neural plates in the process of the successful fusion. These results suggest that the state of microfilaments at the end region of the fusing neural plates is intimately related to the fusion. Delicate changes in the distribution of microfilaments may result in changes in cell shape that cause the fusion of the neural plates. The results of our experiments also show that the distribution of microfilaments changed with the moulding of the cephalic neural tube, suggesting that microfilaments play a role not only in fusion but also in the moulding of the cephalic neural tube.

Eversion of the telencephalic neural plates followed failure of fusion of neural folds. Our experimental results revealed that microfilaments at the luminal surface was not observed at the time of apposition in the treated embryos then it appeared with eversion of the neural plates. In the present time, why appearance of microfilaments was not inhibited in the treated embryos is unclear. The various cell types respond with distinctly differing sensitivities to cytochalasins [4] and cells at the luminal surface may be relatively more resistant than the fusing cells, and/or that cytochalasin D may be eliminated from cells at the luminal surface by an active pump, such as the transmembrane pump in tumor cells [18].

REFERENCES

1 Austin WL, Wind M, Brown KS (1982) Differences in the toxicity and teratogenicity of cytochalasins D and E in various mouse strains. Teratology 25: 11–18

2 Bershadsky AD, Vasilieve JM (1988) Cytoskeleton. Plenum Press, New York and London, pp. 13–78

3 Carter SB (1967) Effects of cytochalasins on mammalian cells. Nature 213:261–264

4 Godman GC, Miranda AF (1978) Cellular contractility and the visible effects of cytochalasin. In "Cytochalasins: Biochemical and Cell Biological Aspects" Ed by SW Tanenbaum, Elsevier/North Holland Biomedical Press, Amsterdam, pp 277–429

5 Gordon R (1985) A review of the theories of vertebrate neurulation and their relationship to the mechanics of neural tube birth defects. J Embryol exp Morphol 89: 229–255

6 Karfunkel P (1974) The mechanisms of neural tube formation. Int Rev Cytol 38: 245–271

7 Kitchin KT, Ebron MT (1984) Further development of rodent whole embryo culture: solvent toxicity and water-insoluble compound delivery system. Toxicology 30: 45–57

8 Lee H-Y, Kosciuk MC, Nagele RG, Roisen FJ (1983) Studies on the mechanisms of neurulation in the chick: possible involvement of myosin in elevation of neural folds. J Exp Zool 225: 449–457

9 Lee H-Y, Nagele RG (1985) Studies on the mechanisms of neurulation in the chick: interrelationship of contractile proteins, microfilaments, and the shape of neuroepithelial cells. J Exp Zool 235: 205–215

10 Matsuda M (1990) Fusion of neural folds in the rhombencephalic region of rat embryos. Develop Growth & Differ 32: 383–388

11 Miranda AF, Godman GC, Deitch AD, Tanenbaum SW (1974) Action of cytochalasin D on cells of established lines. I. Early events. J Cell Biol 61: 481–500

12 Morriss-Kay GM, Mottet K (1983) Arsenic-induced exencephaly in the mouse and associated lesions occurring during neurulation. Teratology 28: 399–411

13 Morriss-Kay G, Tuckett F (1985) The role of microfilaments in cranial neurulation in rat embryos: effects of short-term exposure to cytochalasin D. J Embryol exp Morphol 88: 333–348

14 Nagele RG, Lee H-Y (1980) Studies on the mechanism of neurulation in the chick: microfilament-mediated changes in cell shape during uplifting of neural folds. J Exp Zool 213: 391–398

15 New DAT, Coppola PT, Cockroft DL (1976) Comparison of growth *in vitro* and *in vivo* of post-implantation rat embryos. J Embryol exp Morphol 36: 133–144

16 O'Shea KS (1981) The cytoskeleton in neurulation: role of cations. Prog in Anat 1: 35–60

17 Osumi-Yamashita N, Asada S, Eto K (1992) Distibution of F-actin during mouse facial morphogenesis and its perturbation with cytochalasin D using whole embryo culture. J Craniofac Genet Dev Biol 12: 130–140

18 Pearson CK, Cunningham C (1993) Multidrug resistance during cancer chemotherapy-biotechnological solutions to a clinical problem. Tib Tech 11: 511–516

19 Sadler TW, Greenberg DG, Coughlin P, Lessard JL (1982) Actin distribution patterns in the mouse neural tube during neurulation. Science 215: 172–174

20 Schoenwolf GC, Folsom D, Moe A (1988) A reexamination of the role of microfilaments in neurulation in the chick embryo. Anat Rec 20: 87–102

21 Schoenwolf G., Smith JL (1990) Mechanisms of neurulation: traditional viewpoint and recent advances. Development 109: 243–270

22 Shepard TH, Greenaway JC (1977) Teratogenicity of cytochalasin D in the mouse. Teratology 16: 131–136

23 Smedley MJ, Stanisstreet M (1986) Calcium and neurulation in mammalian embryos. II. Effect of cytosleletal inhibitors and calcium antagonists on the neural folds of rat embryos. J Embryol exp Morphol 93: 167–178

24 Spooner BS (1978) Cytochalasins as probes in selected morphogenetic processes. In "Cytochalasins: Biochemical and Cell Biological Aspects" Ed by SW Tanenbaum, Elsevier/North Holland Biomedical Press, Amsterdam, pp 65–89

25 Spooner BS, Wessels NK (1970) Effects of cytochalasin B upon microfilaments involved in morphogenesis of salivary epithelium. Proc Natl Acad Sci USA 66: 360–364

26 Tannenbaum J, Tannenbaum SW, Godman GC (1977) The binding sites of cytochalasin D II. Their relationship to hexose transport and to cytochalasin B. J Cell Physiol 91: 239–248

27 Tannenbaum J (1978) Approaches to the molecular biology of cytochalasin action. In "Cytochalasins: Biochemical and Cell Biological Aspects" Ed by SW Tanenbaum, Elsevier/North Holland Biomedical Press, Amsterdam, pp 547–559

28 Webster WS, Messerle K (1980) Changes in the mouse neuroepithelium associated with cadmium-induced neural tube defects. Teratology 21: 79–88

29 Wessels NK, Spoonner BS, Ash JF, Bradley MO, Ludiena MA, Taylor EL, Wrenn JT, Yamada KM (1971) Microfilaments in cellular and developmental processes. Science 171: 135–143

30 Wiley MJ (1979) The teratogenic effects of cytochalasin D in golden Syrian hamsters. Anat Rec 192:721a

31 Wiley MJ (1980) The effects of cytochalasins on the ultrastructure of neurulating hamster embryos *in vivo*. Teratology 22:59–69

32 Wrenn JT, Wessels NK (1970) Cytochalasin B: effects upon microfilaments involved in morphogenesis of estrogen-induced glands of oviduct. Proc Natl Acad Sci USA 66: 904–908

33 Yamada KM, Spooner BS, Wessels NK (1970) Axon growth: roles of microfilaments and microtubules. Proc Natl Acad Sci USA 66: 1206–1212

ZOOLOGICAL SCIENCE 11: 555–561 (1994)

Effects of Hypophysectomy and Replacement Therapy with Bovine Growth Hormone and Triiodothyronine on the *in Vitro* Uptake of Calcium and Methionine by Scales in the Goldfish, *Carassius auratus*

NORIAKI SHINOBU[1] and YASUO MUGIYA[2]

Department of Biology, Faculty of Fisheries, Hokkaido University, 3-1-1 Minato, Hakodate 041, Japan

ABSTRACT—Using isolated scales, the involvement of bovine growth hormone (bGH) and triiodothyronine (T_3) in scale formation was examined in the hypophysectomized goldfish, *Carassius auratus*. The *in vitro* uptake of calcium and ^{35}S-methionine by scales was used as indices of their calcification and matrix formation, respectively. Hypophysectomy consistently decreased the uptake of these substances with time up to 4 weeks after the operation. The direct addition of bGH or T_3 to the incubation medium had no recovery effect. However, the decreased uptake was restored in the incubation medium with the serum not of hypophysectomized but of sham-operated fish. The acid extract of the hepatopancreas was also effective for stimulating the uptake. The muscle, kidney, and spleen were ineffective for the extract-stimulated uptake. The hepatopancreas-stimulated uptake was also confirmed by the addition of the preincubation media in which the minced hepatopancreas was incubated with various concentrations of bGH or T_3 for 24 hr. These results suggest that bGH and T_3 stimulate scale calcification and matrix formation not via direct but via indirect sequences. A factor(s) secreted from the hepatopancreas in response to bGH and T_3 was considered to exert direct stimulative effects on scale formation.

INTRODUCTION

Teleost scales have been used to determine the age of fish for a long time. They consist of two different layers, the upper osseous layer and the lower fibrillary plate, and grow at their margins by addition of the collagenous osteoid and the subsequent deposition of calcium phosphate on the osteoid. These processes are essentially conducted by scale-forming cells [1] under endocrinological control. Hypophysectomy reduced scale growth in killifish [2, 3] and goldfish [4], and replacement therapy with bovine growth hormone recovered the reduction in killifish [2]. Skeletal tissue formation is also influenced by thyroxin, which is secreted into the blood following the stimulation of thyrotropin from the pituitary. For example, Tanabe [5] reported triiodothyronine-stimulated bone formation and resorption in rainbow trout. Scales were also deteriorated by thyroxine treatment in goldfish [6]. Since these studies were conducted using *in vivo* techniques, the results include direct and indirect effects of the hormones on tissue growth. To our knowledge, the only *in vitro* study in this field was by Takagi *et al.* [7] who examined the effects of temperature, starvation, prolactin, stanniocalcin, and calcitonin on calcium uptake by scales in intact goldfish and reported that only the first treatment reduced the uptake.

In this study, we examined the effect of hypophysectomy and replacement therapy with bovine growth hormone or triiodothyronine on matrix formation and calcification in goldfish scales using an *in vitro* incubation technique. Various tissue extracts were also added to the incubation media to define the direct or indirect effect of the hormones on scale formation.

MATERIALS AND METHODS

Goldfish, *Carassius auratus*, weighing 18–20 g were obtained from a commercial dealer and kept at 23°C under LD 12 : 12 for not less than 2 weeks before use. They were fed fish food pellets *ad libitum* once a day. This experiment was performed from July through November, 1992. The sex of the fish was not considered because their gonads were found to be immature at autopsy.

Hypophysectomy

Hypophysectomy was essentially followed by the method of Yamazaki [8]. Briefly, fish were anesthetized with MS 222 (4–6°C) and fixed sideways. A hole was drilled through the prootic bone between the first and second gill arches and the exposed pituitary was sucked out through a fine pipette. The entire procedure was conducted at 4–5°C to minimize bleeding. Sham-operated fish were subjected to only drilling. They were allowed to recover in 0.25% NaCl tap water.

Blood collection and calcium determination

Blood was collected from the caudal vessels by cutting the tail of the fish and draining it into glass capillaries with or without heparin treatment and then centrifuged to obtain plasma or serum. Plasma calcium concentrations were determined by atomic absorption spectrophotometry. Serum was used for addition to the incubation medium as will be described later.

[1] Present address: Cancer Institute, School of Medicine, Hokkaido University, Kita-ku, Sapporo 060, Japan.
[2] To whom reprint requests should be addressed.

Scale incubation

Hypophysectomized fish were kept in the tap water containing 0.25% NaCl and sacrificed after 1, 2, and 4 weeks. After a quick rinse of the body in 0.1% bleach, scales were removed from the mid dorso-ventral trunk and rinsed three times in cold Ringer solution (NaCl 135, KCl 2.5, $CaCl_2$ 3.2, KH_2PO_4 2.0, $MgSO_4$ 1.0, $NaHCO_3$ 10.0, and Hepes 10.0 mM, pH 7.4) containing streptomycin (100 μg/ml) and penicillin (100 IU/ml). They were individually placed into wells of a tissue culture plate filled with the oxygenated Ringer solution (0.5 ml each) containing the antibiotics, 0.1% glucose, and ^{45}Ca or ^{35}S-methionine (NEN) in a concentration of 7.4 KBq/ml, and incubated at 23°C for 48 hr unless otherwise stated. The incubation medium was changed every 24 hr. These incubation conditions were determined by preliminary experiments. Methionine was chosen as an index of calcifiable matrix formation, because this amino acid occurred only in the Ca^{2+}-binding fraction of the otolith matrix [9]. Special attention was paid not to include regenerating or lateral-line scales.

Radioactive counting

After incubation, scales were rinsed with agitation in distilled water for 24 hr, dried at 85°C for 12 hr, and weighed. In this case, two scales from the same individual were pooled for weighing and radioactive counting. They were placed in counting vials, solubilized in a mixture solution of $HClO_4$ and H_2O_2 (150 μl each) at 80°C for 2 hr, and added to Scintisol EX-H (Wako Pure Chem. Co.) to determine the radioactivity using a liquid scintillation spectrophotometer (Beckman, LS6000 1C).

Hormones and tissue extracts

Bovine growth hormone (bGH, UCB) and triiodothyronine (T_3, Sigma) were dissolved in 0.005 N NaOH (10 μl) and added to the incubation medium to a final concentration of 10, 100, or 1000 ng/ml. Controls received the solvent only. The muscle, kidney, spleen, and hepatopancreas were dissected out from hypophysectomized and sham-operated fish 4 weeks after operation. They were rinsed several times in the Ringer solution, homogenized in 5 M CH_3COOH, and centrifuged at 1500×g and 4°C for 30 min. Supernatants were freeze-dried and stored at −40°C until use. They were dissolved in the Ringer solution at a rate of 250 mg/ml immediately before use and centrifuged at 1500×g and 4°C for 20 min. Supernatants were used as tissue extracts. They were added to the culture medium in a final concentration of 5 mg tissue/ml. Serum obtained from these fish was also added to the incubation medium to a final concentration of 10%.

The hepatopancreas was isolated from hypophysectomized fish 4 weeks after operation, minced in the Ringer solution, and incubated with bGH or T_3 (10, 100, or 1000 μg/ml) for 24 hr. The control incubation only received the solvent (0.005 N NaOH). Supernatants were concentrated to approximately 20 μl and added to the incubation medium in which scales isolated from hypophysectomized fish (hypox scales) were incubated for 48 hr.

RESULTS

Plasma calcium concentrations were approximately 2.7 mM in the sham-operated group. This level decreased to 1.8 mM 1 week after hypophysectomy ($P<0.01$) and remained low throughout an experimental period of 4 weeks (Fig. 1A). This shows that the hypophysectomy was successfully conducted.

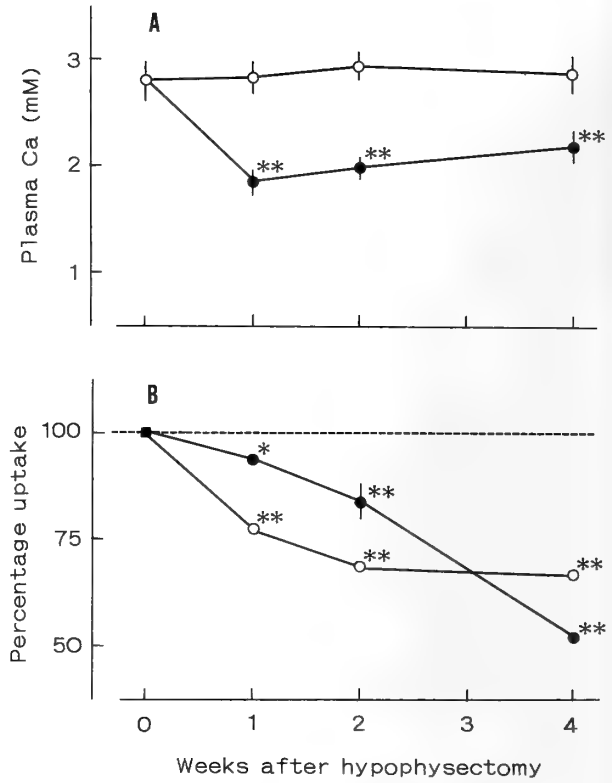

FIG. 1. Time-course related effects of hypophysectomy on plasma calcium concentrations (A, ○: sham-operated; ●: hypophysectomized) and on the *in vitro* uptake of calcium (●) and ^{35}S-methionine (○) by scales (B) in goldfish. Values are means± SE for six fish (A) and for 18 samples (two scales/sample, B) consisting of 36 scales obtained from six individuals. At points where no error bar can be seen, the error lies within the size of the symbol. Horizontal dotted line represents the sham-operated control level (100%). *$P<0.05$ and **$P<0.01$ for each control.

The *in vitro* uptake of calcium and methionine by scales was examined using the same fish. The uptake of these substances showed significant decreases ($P<0.05$ or $P<0.01$) 1 week after hypophysectomy, followed by further decreases to about half of the control level after 4 weeks (Fig. 1B). Time course-related uptake of calcium and methionine by scales was examined 4 weeks after hypophysectomy. The uptake of these substances increased with time up to 72 hr incubation which was the final examination time. However, the rates of uptake were significantly ($P<0.05$) less after 6 hr in the hypophysectomized group versus the sham-operated group, followed by further differences ($P<0.01$) between the two groups (Fig. 2A, B).

Incubation with various concentrations of bGH had no effect on calcium uptake by hypox scales (Fig. 3A). However, methionine uptake was stimulated ($P<0.05$) in a high bGH concentration of 1000 ng/ml (Fig. 3B). Triiodothyronine showed no effects on the uptake of these substances (Fig. 4A, B).

The addition of serum from the sham-operated fish to the incubation medium increased calcium uptake by hypox scales

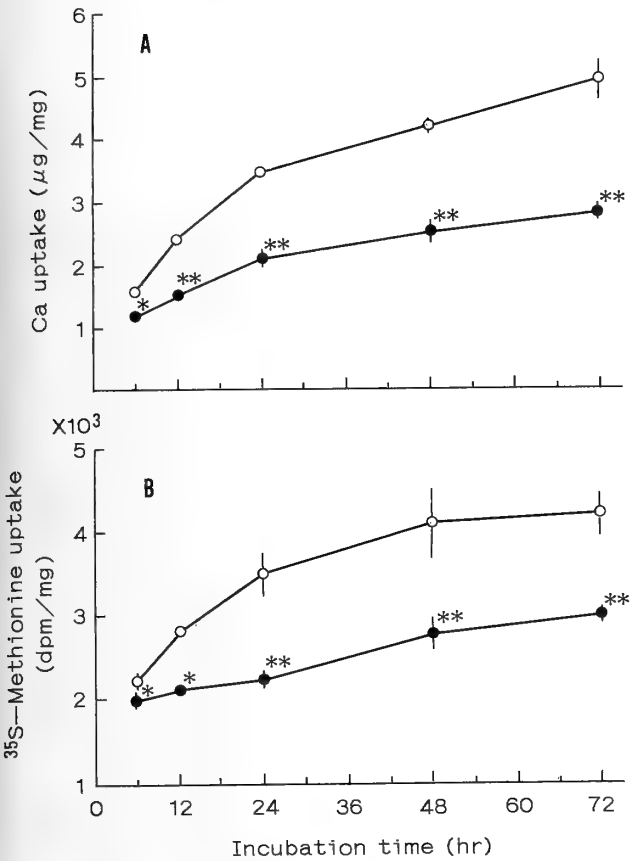

FIG. 2. Time-course related *in vitro* uptake of calcium (A) and ^{35}S-methionine (B) by scales isolated from hypophysectomized goldfish. Open and closed circles represent sham-operated and hypophysectomized fish, respectively. Values are means ± SE for 18 samples (two scales/sample) consisting of 36 scales obtained from six individuals. At points where no error bar can be seen, the error lies within the size of the symbol. $^{*}P<0.05$ and $^{**}P<0.01$ for each control.

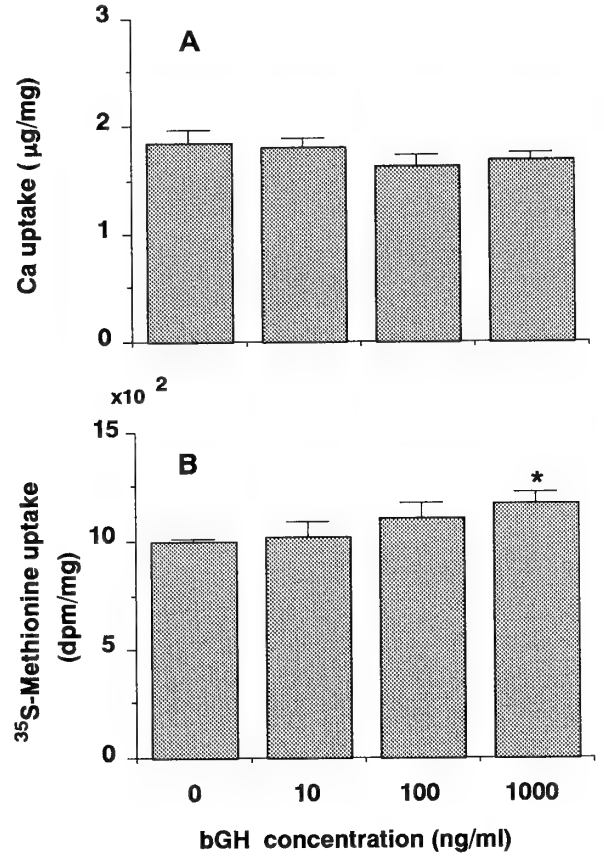

FIG. 3. Effects of various concentrations of bovine growth hormone (bGH) on the *in vitro* uptake of calcium (A) and ^{35}S-methionine (B) by scales isolated from hypophysectomized goldfish. Values are means ± SE for 15 samples (two scales/sample) consisting of 30 scales obtained from five individuals. $^{*}P<0.05$ for the incubation without bGH.

after 24 hr ($P<0.05$) and 48 hr ($P<0.01$) compared with the addition of serum from the hypophysectomized fish (Fig. 5A). Methionine uptake was also stimulated ($P<0.01$) by the addition of the control serum after 48 hr of incubation (Fig. 5B).

Various tissue extracts were added to the incubation media to examine stimulated effects of the extracts on the uptake of calcium and methionine by hypox scales. In this experiment, hypox scales were incubated in the media containing the tissue extracts of either sham-operated (control) or hypophysectomized (experimental) fish. The extracts of the muscle, kidney, and spleen had no effect on calcium uptake by the scales (Fig. 6A). However, the addition of hepatopancreas extract significantly ($P<0.05$) stimulated the uptake. Methionine uptake was not affected by the addition of any extracts between the control and experimental incubations (Fig. 6B). However, the addition of the hepatopancreas extract resulted in the considerably high uptake of methionine in both incubations.

The minced hepatopancreas was preincubated in the media containing various concentrations of bGH for 24 hr and then the media were added to the incubation of hypox scales. Calcium uptake by the scales was stimulated by bGH in a concentration-dependent way up to 1000 ng/ml (Fig. 7A). Methionine uptake also increased in bGH concentrations of 100 and 1000 ng/ml (Fig. 7B).

The preincubation media in which the hepatopancreas was incubated with T_3 in concentrations of 100 and 1000 ng/ml also stimulated calcium uptake by hypox scales (Fig. 8A). However, methionine uptake was stimulated only in a T_3 concentration of 10 ng/ml (Fig. 8B).

DISCUSSION

It is well documented that hypophysectomy reduced ^{45}Ca uptake by scales and their growth in *in vivo* experiments [2, 4, 10]. In the present *in vitro* study, hypox scales showed consistent decreases in the uptake of calcium and methionine with time at least up to 4 weeks after hypophysectomy. The time course-related uptake of these substances was always lower in the hypox scales than the control ones. These facts may indicate that the present incubation technique is

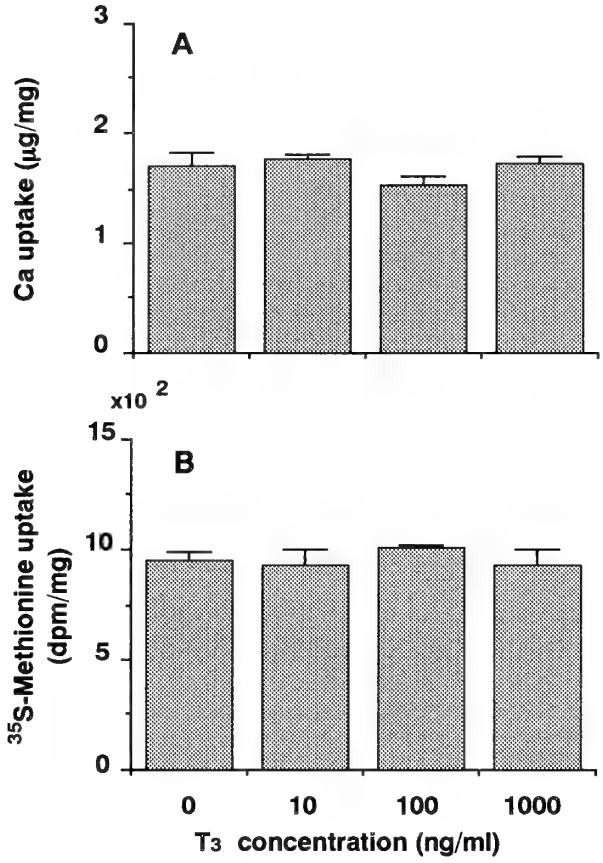

FIG. 4. Effects of various concentrations of triiodothyronine (T_3) on the *in vitro* uptake of calcium (A) and ^{35}S-methionine (B) by scales isolated from hypophysectomized goldfish. Values are means ± SE for 15 samples (two scales/sample) consisting of 30 scales obtained from five individuals.

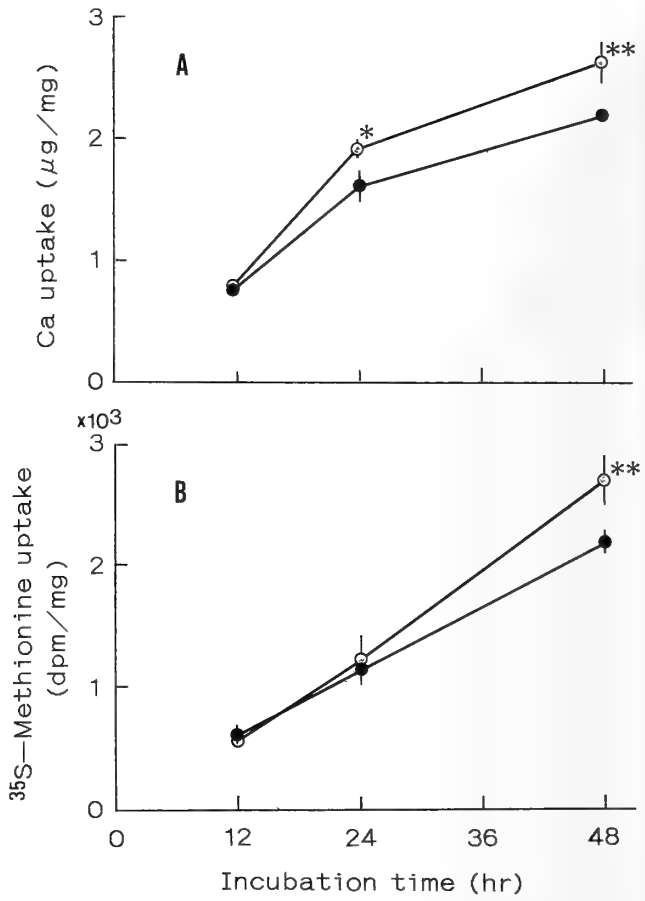

FIG. 5. Effects of serum on the *in vitro* uptake of calcium (A) and ^{35}S-methionine (B) by scales isolated from hypophysectomized goldfish. Sera were obtained from the sham-operated (○) and hypophysectomized (●) fish and added to the incubation media. Values are means ± SE for 15 samples (two scales/sample) consisting of 30 scales obtained from five individuals. At points where no error bar can be seen, the error lies within the size of the symbol. $^*P<0.05$ and $^{**}P<0.01$ for each control.

appropriate enough to evaluate the rates of *in vitro* uptake of calcium and methionine by scales, reflecting the physiological state of the scales. Similarly, Ottaway and Simkiss [11] used the *in vitro* uptake of glycine by scales as an indicator for the instantaneous growth rate of the scales.

Growth hormone is generally accepted to exert a secondary effect of stimulation on bone and cartilage growth via the production of an insulin-like growth factor (IGF) in the liver [12–14]. On the other hand, Isaksson *et al.* [15] and Isgaard *et al.*[16] demonstrated that GH had a direct effect on the growth of these skeletal tissues via the *in situ* production of IGF.

Ash [17] reported that the *in vitro* uptake of ^{35}S-sulfate by the gill cartilage was directly stimulated by GH in rainbow trout. However, Duan and Inui [18] found no such effect of GH on the *in vitro* uptake of ^{35}S-sulfate by the same cartilage in eels. In the present study, the direct addition of GH or T_3 to the incubation media did not show any positive effects on the uptake of calcium and methionine by scales except that a high concentration of GH (1000 ng/ml) stimulated the methionine uptake. Since this concentration greatly exceeds the physiological level, such a positive effect may be attributed to the pharmacological effect of the hormone. Duan and Inui [18] found a time lag between the peak in the plasma level of exogenously administrated GH and the stimulated uptake of sulfate by gill cartilage. Considering these results together, it seems reasonable to conclude that bGH and T_3 have no direct effect on scale formation.

When the serum of sham-operated fish was added to the incubation medium, it effectively stimulated the uptake of both calcium and methionine by hypox scales, while the serum of hypophysectomized fish did not. This suggests that the former serum contains a pituitary-dependent factor which stimulates scale formation. We then identified the tissue responsible for the production of the factor and found that the extract from the hepatopancreas not of hypophysectomized but of sham-operated fish increased calcium uptake by hypox scales. Methionine uptake was stimulated by both extracts. These facts suggest that the hepatopancreas is responsible for the production of the pituitary-dependent factor and that the tissue may include another factor(s) which stimulates methionine uptake by scales, independent of the

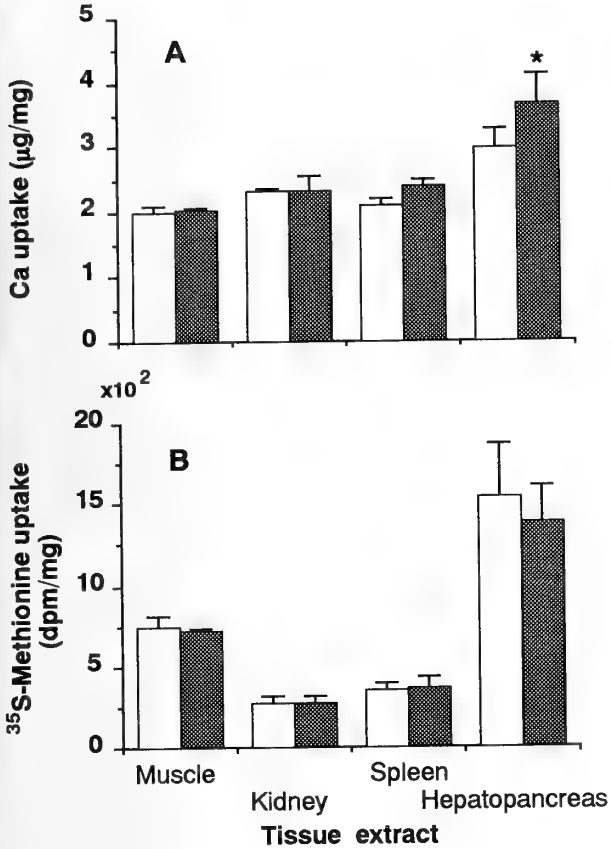

FIG. 6. Effects of various tissue extracts on the *in vitro* uptake of calcium (A) and ^{35}S-methionine (B) by scales isolated from hypophysectomized goldfish. Crude acid extracts were obtained from the four tissues in the hypophysectomized (open column) and sham-operated (shaded column) fish and added to the incubation media. Values are means±SE for 15 samples (two scales/sample) consisting of 30 scales obtained from five individuals. $^*P<0.05$ for the hypophysectomized extract.

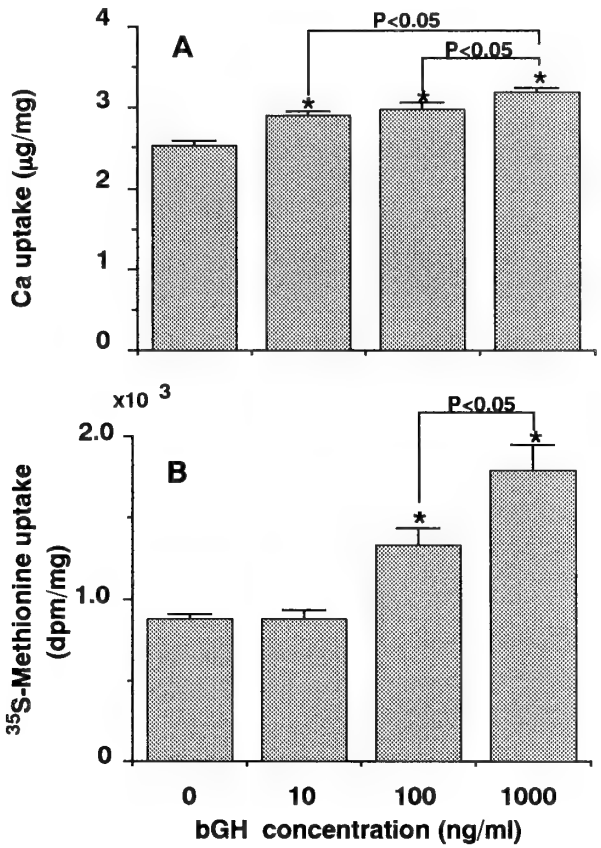

FIG. 7. Effects of the preincubation media on the *in vitro* uptake of calcium (A) and ^{35}S-methionine (B) by scales isolated from hypophysectomized fish. The hepatopancreas was incubated with various concentrations of bovine growth hormone (bGH) and the supernatants were added to the incubation media. Values are means±SE for 15 samples (two scales/sample) consisting of 30 scales obtained from five individulas. $^*P<0.05$ for the incubation without bGH and also between the two groups indicated.

pituitary. Insulin is a candidate for the latter factor because the hepatopancreas extract may inevitably include insulin in goldfish and because insulin stimulates the *in vitro* uptake of ^{35}S-sulfate by the cartilage in eels [19].

We preincubated the minced hepatopancreas of hypophysectomized fish in the presence of bGH or T_3 and then the preincubated media were added to the incubation media in which the uptake of calcium and methionine by hypox scales was examined. The addition of the media induced the stimulated uptake of both substances, showing that in response to the hormones, the hepatopancreas secreted a substance(s) which had stimulative effects on scale growth. Since many studies [19–21] reported that IGF-1, which is synthesized in the liver in response to GH, stimulated ^{35}S-sulfate uptake by the cartilage, we think that the preincubation of the hepatopancreas in the presence of GH produced IGF-1, which might directly stimulate the *in vitro* uptake of calcium and methionine by hypox scales.

Triiodothyronine is known to stimulate the secretion of GH [22, 23] and also to regulate GH receptors in the liver [24]. These facts suggest the necessity of T_3 for GH to produce IGF-1. However, Glasscock *et al.* [25] indicated that T_3 had GH-independent effects on growth stimulation in hypophysectomized rats. In the present study, T_3 stimulated scale formation irrespective of GH effects, suggesting the production of a new factor other than IGF in the T_3-treated hepatopancreas. Further studies are needed to elucidate the sequences of the involvement of T_3 in scale formation.

Bovine growth hormone and T_3 simultaneously stimulated the uptake of calcium and methionine by scales in the present study. Skeletal tissues usually grow by the intimate interaction between inorganic and organic phases. For example, the organic matrix dually functions as a nucleator of crystals and an inhibitor of crystal growth in calcification [26]. Therefore, calcium uptake by scales will be affected by the matrix-related sequences. In the present study, however, effective concentrations of GH and T_3 were different between

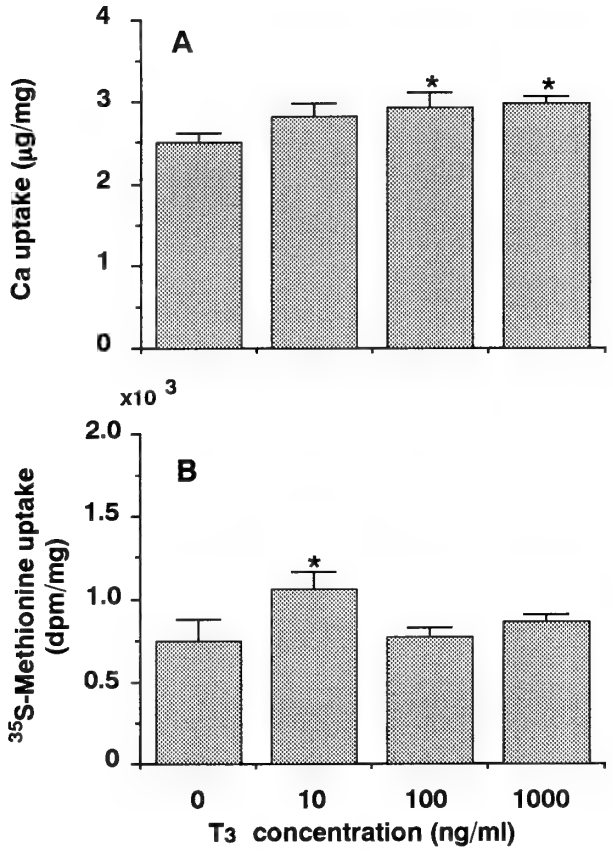

FIG. 8. Effects of the preincubation media on the *in vitro* uptake of calcium (A) and ^{35}S-methionine (B) by scales isolated from hypophysectomized goldfish. The hepatopancreas was incubated with various concentrations of triiodothyronine (T_3) and the supernatants were added to the incubation media. Values are means ± SE for 15 samples (two scales/sample) consisting of 30 scales obtained from five individuals. $^*P<0.05$ for the incubation without T_3.

calcium and methionine uptake. The time-related uptake of these substances was also different between calcium and methionine following hypophysectomy. These results suggest that GH and T_3 did not necessarily exert their stimulative effects on calcium uptake by scales via modification in the matrix formation. Matrix formation and calcification may be, at least in part, under separate control by these hormones.

ACKNOWLEDGMENTS

We are grateful to Mr D. Tahara for his assistance in drawing the figures.

REFERENCES

1 Kobayashi S, Yamada J, Maekawa K, Ouchi K (1972) Calcification and nucleation in fish-scales. Biomineralisation 6: 84–90

2 Pickford GE (1953) A study of the hypophysectomized male killifish, *Fundulus heteroclitus* (Linn.). Bull Bingham Oceanogra Coll 14: 5–41

3 Brehe JE, Fleming WR (1976) Calcium mobilization from acellular bone and effects of hypophysectomy on calcium metabolism in *Fundulus kansae*. J Comp Physiol 110: 159–169

4 Mugiya Y (1990) Long-term effects of hypophysectomy on the growth and calcification of otoliths and scales in the goldfish, *Carassius auratus*. Zool Sci 7: 273–279

5 Tanabe K (1992) Histomorphometric effects of thyroid hormones and thiourea on the pharynx bone in the rainbow trout, *Oncorhynchus mykiss*. Master's dissertation, Faculty of Fisheries, Hokkaido University, Japan

6 Ozaki H, Ikeda Y, Yasuda H (1969) Effects of thyroxine on scale growth in the goldfish (*Carassius auratus* L.). Uloco (2): 22–61 (in Japanese)

7 Takagi Y, Hirano T, Yamada J (1989) *In vitro* measurements of calcium influx into isolated goldfish scales in reference to the effects of putative fish calcemic hormones. Zool Sci 6: 83–89

8 Yamazaki F (1965) Endocrinological studies on the reproduction of the female goldfish, *Carassius auratus* L., with special reference to the function of the pituitary gland. Mem Fac Fish Hokkaido Univ 13: 1–64

9 Asano M, Mugiya Y (1993) Biochemical and calcium-binding properties of water-soluble proteins isolated from otoliths of the tilapia, *Orechromis niloticus*. Comp Biochem Physiol 104B: 201–205

10 Mugiya Y, Odawara F (1988) Effects of hypophysectomy and replacement therapy with ovine prolactin on serum calcium levels, and calcification in otoliths and scales in goldfish. Nippon Suisan Gakkaishi 54: 2079–2083

11 Ottaway EM, Simkiss K (1977) "Instantaneous" growth rates of fish scales and their use in studies of fish populations. J Zool Lond 181: 407–419

12 Daughaday WH, Hall K, Raben MS, Salmon WD, Van den Brande JL, Van Wyk JJ (1972) Somatomedin: proposed designation for sulphation factor. Nature 235: 107

13 Schwander JC, Hauri C, Zapf J, Froesch ER (1983) Synthesis and secretion of insulin-like growth factor and its binding protein by the perfused rat liver: dependence on growth hormone status. Endocrinology 113: 297–305

14 Herington AC, Cornell HJ, Kuffer AD (1983) Recent advances in the biochemistry and physiology of the insulin-like growth factor/somatomedin family. Int J Biochem 15: 1201–1210

15 Isaksson OGP, Jansson JO, Gause IAM (1982) Growth hormone stimulates longitudinal bone growth directly. Science 216: 1237–1239

16 Isgaard J, Nilsson A, Lindahl A, Jansson JO, Isaksson OGP (1986) Effects of local administration of GH and IGF-I on longitudinal bone growth in rats. Am J Physiol 250: E367–E372

17 Ash PJ (1977) Incorporation of [^{35}S] sulphate into mucopolysaccharide by teleost cartilage *in vitro*: the influence of mammalian growth hormone, teleost plasma, and mammalian plasma. Gen Comp Endocrinol 32: 187–194

18 Duan C, Inui Y (1990) Effects of recombinant eel growth hormone on the uptake of [^{35}S] sulfate by ceratobranchial cartilages of the Japanese eel, *Anguilla japonica*. Gen Comp Endocrinol 79: 320–325

19 Duan C, Hirano T (1990) Stimulation of ^{35}S-sulfate uptake by mammalian insulin-like growth factors I and II in cultured cartilages of the Japanese eel, *Anguilla japonica*. J Exp Zool 256: 347–350

20 McCormick SD, Tsai PI, Kelley KM, Nishioka RS, Bern HA (1992) Hormonal control of sulfate uptake by branchial cartilage of coho salmon: role of IGF-I. J Exp Zool 262: 166–171

21 Cao QP, Duguay S, Plisetskaya E, Steiner DF, Chan SJ (1990) Nucleotide sequence and growth hormone-regulated expression of salmon insulin-like growth factor I RNA. Mol Endocrinol 3: 2005–2010

22 DeFesi CR, Fels EC, Surks MI (1984) Triiodothyronine stimulates growth of cultured GC cells by action early in the G1 period. Endocrinology 114: 293–295

23 Casanova J, Copp RP, Janocko L, Samuels HH (1985) 5′-Flanking DNA of the rat growth hormone gene mediates regulated expression by thyroid hormone. J Biol Chem 260: 11744–11748

24 Komourdjian MP, Idler DR (1978) Hepatic mediation of hormonal and nutritional factors influencing the *in vitro* sulfur uptake by rainbow trout bone. Gen Comp Endocrinol 36: 33–39

25 Glasscock GF, Hein AN, Miller JA, Hintz RL, Rosenfeld RG (1992) Effects of continuous infusion of insulin-like growth factor I and II, alone and in combination with thyroxine or growth hormone, on the neonatal hypophysectomized rat. Endocrinology 130: 203–210

26 Crenshaw MA (1982) Mechanisms of normal biological mineralization of calcium carbonates, in "Biological Mineralization and Demineralization" Ed by GH Nancollas, Springer-Verlag, Berlin, pp 243–257

ZOOLOGICAL SCIENCE 11: 563–569 (1994)

Characterization of Androgen Receptors for Testosterone and 5α-Dihydrotestosterone in the Mouse Submandibular Gland

KAZUHIKO SAWADA and TETSUO NOUMURA[1]

Department of Regulation Biology, Faculty of Science, Saitama University, Urawa 338, Japan

ABSTRACT—In the mouse submandibular gland, sex difference becomes evident on day 30, when the granular convoluted tubules (GCT) of the gland rapidly grow in response to drastically increased levels of circulating testosterone and 5α-dihydrotestosterone (DHT) in the male. Testosterone and DHT may act separately on the gland, because the mouse gland can not convert testosterone to DHT. Therefore, we studied properties of the androgen receptor of the mouse submandibular gland using both these circulating androgens as ligands.

Analyses of sucrose density gradient centrifugation and Scatchard plots demonstrated that the mouse submandibular gland contained two types of cytosolic receptors: one is the low-affinity, high-capacity receptor of smaller molecular size at about 3S to be bound with both testosterone and DHT, and the other is the high-affinity, low-capacity DHT specific receptor of larger molecular size at about 8S. The apparent dissociation constant (K_D) of the low-affinity receptor for testosterone and DHT was 0.53–0.62 nM, and that of the high-affinity DHT specific receptor was 0.07–0.11 nM. K_D for each ligand was similar between the sexes and was constant on day 20 through day 90 of age. Maximum bindings of both cytosolic receptors were significantly higher in the male than in the female at 20 and 30 days of age. On the other hand, the cross-competition experiment was allowed to elucidate which androgen was predominant for cytosolic receptors of the mouse gland. When testosterone and DHT were applied at the serum concentrations to the cytosol of the male gland, the cytosolic receptors were bound 28% with testosterone and 72% with DHT on day 20, and they were occupied 60% by testosterone and 40% with DHT on days 30 and 90.

Therefore, these results suggest that the mouse glands may respond to serum DHT to induce cell proliferation of GCT around day 20 and then the gland may respond to both serum testosterone and DHT to induce the early masculine development and maintenance of GCT in fully-stimulated states, and that occurrence of sex difference of the gland may be controlled by androgen binding activities of the receptor around day 20 to 30.

INTRODUCTION

In rodents, the male submandibular gland is larger than the female one and has more complex morphology. The glandular contents of biologically active polypeptides, including nerve growth factor, epidermal growth factor, renin and proteases, are higher in the male than in the female, being responsive to androgens [3, 4, 6, 8, 15, 17, 18, 21, 37]. By histological, ultrastructural and morphometrical studies, both sexes experience a similar morphogenesis of the gland during development, and then the sexual difference arises at 3–4 weeks of age, when the granular convoluted tubules (GCT) grow more rapidly in the male than in the female [12, 14, 20, 28]. In a completely androgen-independent state (neonatal castration and androgen-insensitive Tfm mutation), the gland displays the feminine development [28, 29]. The masculine development of the gland is caused by circulating androgens, testosterone and 5α-dihydrotestosterone (DHT), the latter being more effective [30]. In our CD-1 male mice on day 30 [30], circulating DHT levels are approximately 4-fold over (3.5 ± 0.72 nM), and the serum DHT/testosterone ratio is 2-fold higher (3 : 1 in the ratio) than in male rats at puberty reported [11]. Although both testosterone and DHT are accepted to exert independently their effects as active hormones [31], it is still unknown which molecule is the predominant androgen for the mouse submandibular gland. Therefore, the properties of the androgen receptor of the mouse gland were examined by using both circulating androgens as ligands.

Accepted June 13, 1994
Received April 4, 1994
[1] To whom reprint requests should be addressed.

MATERIALS AND METHODS

Animals

CD-1 mice of both sexes were obtained from Charles River Japan Co. and maintained by randomly mating in our laboratory. The animals were given a commercial diet (CRF-1: Charles River Japan Co.) and tap water *ad libitum* and were kept at 23 ± 1°C under 12 hr artificial illumination (from 8 : 00 to 20 : 00). All animals used in this experiment were castrated 1 week before killing to abolish endogenous androgens.

Preparation of cytosol

Male and female mice were killed on days 20, 30 and 90, and the submandibular glands were quickly removed, stripped free of connective tissues, placed on ice and weighed. All subsequent procedures were performed at 0–4°C. Glands were homogenized in 4–5 volumes of Tris-HCl buffer (10 mM) containing EDTA (1.5 mM), 2-mercaptoethanol (1 mM), and 10% (vol/vol) glycerol (pH 7.4) (TEMG buffer) by a glass-teflon homogenizer. The homogenate was centrifuged at 800 *g* for 15 min. The resulting supernatant was further centrifuged at 100,000 g, and the supernatant obtained was designated as 'cytosol'. The protein concentration of cytosol was determined by BCA protein assay reagent (Pierce Chemical CO.,

Rockford, IL, U.S.A.).

Sucrose gradient centrifugation

Aliquots (200 μl) of cytosol (12.9±1.71 mg protein/ml) were incubated with 1 nM [1,2, 6, 7-^{3}H]testosterone or 1 nM [1, 2, 4, 5, 6, 7-^{3}H]DHT (specific activity, 70 and 103 Ci/mmol, respectively; Amersham) in the presence or absence of a 100-fold molar excess of nonradioactive testosterone or DHT for 3 hr at 0°C. The sample was applied onto a linear 5–20% sucrose density gradient (4 ml) in TEMG buffer prepared by Beckman Density Gradient Former. Centrifugation was performed at 200,000 *g* for 22 hr at 0°C in a Beckman Ultracentrifuge (with a SW55Ti rotor). Fractions of each 4 drops (approximately 200 μl) were collected to a set of test tubes, and the same volume (200 μl) of dextran-coated charcoal suspension (1% activated charcoal and 0.5% dextran T-70 in TEMG buffer, pH 7.2) was added to each tube, and the mixture was incubated for 15 min at 0°C. Then, the bound fractions were separated by centrifugation at 1,500 *g* for 15 min at 0°C. After adding 4 ml scintillation fluid (4 g DPO and 0.2 g POPOP in 1,000 ml toluene containing Triton X-100 (33%, vol/vol)), radioactivity was measured in a Packard Liquid Scintillation Counter (model 3255) with an efficiency of 50% for ^{3}H. Results were expressed as d.p.m. of 400 μl of each bound fraction. Bovine serum albumin (BSA; 4.6S) and human γ-globulin (γ-G; 7S) were used as markers of molecular size.

Assay of cytosolic androgen receptors

Aliquots (100 μl) of cytosol (3.8±0.42 mg protein/ml) were incubated with increasing concentrations (0.025–2 nM) of [^{3}H]testosterone or [^{3}H]DHT in the presence or absence of a 100-fold molar excess of nonradioactive steroids for 3 hr at 4°C. After incubation, the same volume (100 μl) of dextran-coated charcoal suspension was added to each tube, and the mixture was incubated for 15 min at 0°C. Then, the bound fraction were separated by centrifugation at 1,500 *g* for 15 min at 0°C. After adding 4 ml scintillation fluid to 150 μl of bound fraction, radioactivity was measured. Results were expressed as nanomolar or fmol per mg protein of cytosol in 200 μl of the bound fraction.

Cross-competition studies

In the first experiment, aliquots (100 μl) of cytosol from the glands in 90-day-old male and female mice (protein concentration, 7.5±0.84 mg/ml and 4.3±0.12 mg/ml, respectively) were incubated with 1 nM [^{3}H]testosterone or [^{3}H]DHT in the presence of increasing concentrations (1–100 nM) of nonradioactive testosterone or DHT for 3 hr at 4°C. In the second experiment, aliquots (100 μl) of cytosol from the glands of male mice at 20, 30 and 90 days of age (protein concentration, 2.5±0.29 mg/ml, 4.4±0.63 mg/ml and 7.2± 0.71 mg/ml, respectively) were incubated with radioactive testosterone (or DHT) in the presence of nonradioactive DHT (or testosterone) as endogenous competitors at the circulating concentrations for 3 hr at 4°C. Testosterone and DHT, one is radioactive and the other is nonradioactive, were applied at the concentrations of 1.2 nM and 1.5 nM to cytosol from the 20-day-old male gland, and were applied at the concentrations of 10 nM and 3.5 nM to cytosol from the 30- and 90-day-old male glands, respectively. After the incubation, an equal volume (100 μl) of dextran-coated charcoal suspension was added, and the mixture was incubated for 15 min at 4°C. Then, the bound fractions were separated by centrifugation at 1,500 *g* for 15 min at 0°C. After adding 4 ml scintillation fluid to 150 μl of the bound fraction, radioactivity was measured. Results were expressed as percentage of each ligand.

Statistical analysis

Data were statistically analyzed by Mann-Whitney's U-test.

RESULTS

Analysis of cytosolic androgen bindings by sucrose density gradient centrifugation

Sucrose density gradient sedimentation profile of cytosolic androgen receptors from the mouse submandibular gland is shown in Figure 1. On linear 5–20% sucrose gradients, the cytosolic binding for ^{3}H-testosterone was sedimented only a peak at smaller molecular size (about 3S). The ^{3}H-DHT binding in the cytosol was sedimented two peaks at smaller molecular size (about 3S) and larger molecular size (about 8S). These peaks were disappeared by adding each 100-fold molar excess of nonradioactive testosterone or DHT (Fig. 1).

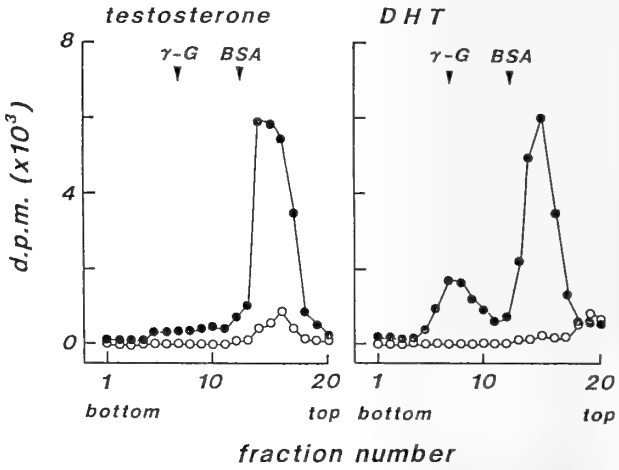

FIG. 1. Sucrose density gradient analysis of cytosolic androgen receptors in the submandibular glands of 90-day-old male mice. Aliquots (200 μl) of cytosol from the submandibular gland were incubated with 1 nM [^{3}H]testosterone or 1 nM [^{3}H]5α-dihydrotestosterone (DHT) in the presence (○) or absence of 100-fold molar excess of nonradioactive androgens (●). Each sample was layered on 5–20% linear sucrose density gradient and centrifuged at 200,000 *g* for 22 hr. Fractions of each four drops were collected. Unbound steroids were removed with dextran-charcoal pellets, and the resultant supernatant (bound fraction) was counted for radioactivity. Data were shown as d.p.m. per fraction. Bovine serum albumin (BSA; 4.6S) and human γ-globulin (γ-G; 7S) were used as markers of molecular size.

Specificity of androgen receptors

To test specificity of cytosolic androgen receptors, aliquots of cytosol from the mouse submandibular gland were incubated with 1 nM [^{3}H]testosterone or 1 nM [^{3}H]DHT in the presence of each 100-fold molar excess of nonradioactive testosterone, DHT, 5α-androstane-3α,17β-diol (3α-diol), 5α-androstane-3β,17β-diol (3β-diol), progesterone, or estradiol-17β (E_2). When ^{3}H-testosterone was used as a ligand, specific binding to cytosolic receptor from the male and female glands was competitively displaced 90% or more by DHT. Similarly, specific binding of ^{3}H-DHT was also dis-

TABLE 1. Specificity of cytosolic androgen receptors from the submandibular glands in male and female mice on day 90

ligands	competitors	% of binding	
		male	female
testosterone	testosterone	0	0
	DHT	8.3±1.69[a]	4.0±3.24
	3α-diol	28.5±7.20	19.8±2.72
	3β-diol	17.0±4.22	16.8±1.14
	progesterone	77.9±11.68	83.1±7.82
	estradiol-17β	35.6±11.07	28.4±2.95
DHT	testosterone	0.4±0.32	7.2±3.30
	DHT	0	0
	3α-diol	31.0±3.80	31.3±7.12
	3β-diol	44.0±8.52	30.9±2.47
	progesterone	72.2±9.91	72.0±7.77
	estradiol-17β	26.7±8.83	30.8±10.21

Aliquots (100 μl) of cytosol of the mouse submandibular glands were incubated with 1 nM [^{3}H] testosterone or 1 nM [^{3}H] 5α-dihydrotestosteroe (DHT) in the presence of 100-fold molar excess of nonradioactive steroids. Data were expressed as percentage of competitors. [a]: mean±S.E.M. (n=3), 3α-diol: 5α-androstane-3α, 17β-diol, 3β-diol: 5α-androstane-3β, 17β-diol.

placed 90% or more by testosterone (Table 1). Specific binding of ^{3}H-testosterone was displaced 71–80% by 3α-diol and 83% by 3β-diol, respectively. 3α- and 3β-Diols competed 69% and 56-70% with the ^{3}H-DHT binding to the receptors, respectively (Table 1). These androgen bindings were also reduced 64–73% by E_2, and progesterone was a poor competitor for the androgen bindings (17–28%) (Table 1).

Scatchard plot analysis

Incubation of the male submandibular gland cytosol with increasing concentrations (0.025–2 nM) of ^{3}H-testosterone or ^{3}H-DHT in the presence or absence of a 100-fold molar excess of nonradioactive ligands revealed the presence of saturable specific binding (Fig. 2). Scatchard plots demonstrated that the cytosol from the 90-day-old male gland contained two binding sites for ^{3}H-DHT: one is high-affinity and low-capacity, and the other is low-affinity and high-capacity. In contrast, ^{3}H-testosterone could bind to only the low-affinity receptor (Fig. 2). Similar data were obtained by the cytosol of the 90-day-old female gland (data not shown). In the glands of 90-day-old males, apparent dissociation constants (K_D) of the high-affinity and the low-affinity receptors for ^{3}H-DHT were 0.08±0.01 nM (n=3) and 0.59±0.05 nM (n=3), respectively. K_D of the low-affinity receptor for ^{3}H-testosterone was 0.59±0.04 nM (n=3) (Table 2). K_D values of the high-affinity receptor for ^{3}H-DHT and of the low-affinity receptors for ^{3}H-testosterone and ^{3}H-DHT were constant through ages examined and showed no sex difference (Table 2).

Maximum binding (Bmax) of the cytosolic receptor was expressed as f mol per mg protein. Through experiments, Bmax of the low-affinity cytosolic receptor was not different between both ligands, but the male Bmax was gradually decreased with age and was rather lower than the female

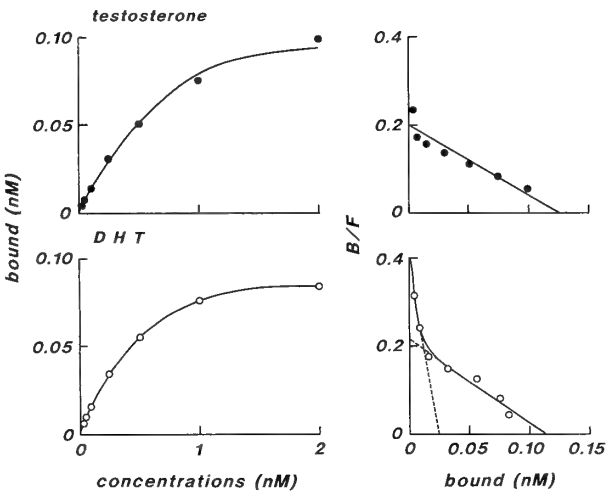

FIG. 2. Saturation and Schatchard plot analyses of [^{3}H]testosterone (●) and [^{3}H]5α-dihydrotestosterone (DHT; ○) binding to cytosol from the submandibular glands of 90-day-old male mice. Aliquots (100 μl) of cytosol from the mouse submandibular gland were incubated with increasing concentrations (0.025–2 nM) of [^{3}H]testosterone or [^{3}H]DHT in the presence or absence of 100-fold molar excess of nonradioactive testosterone or DHT.

Bmax on day 90 (Fig. 3). The male Bmax of the high-affinity cytosolic receptor for ^{3}H-DHT was higher than the female Bmax on days 20 and 30, but also declined with age and became rather lower than the female Bmax on day 90 (Fig. 3).

Cross-competition studies

The cross-competition experiments for the receptor binding were performed in the submandibular glands of 90-day-old male and female mice. When ^{3}H-testosterone was used as ligand, specific binding to the cytosolic receptor showed a decrease in the reverse of increasing concentrations

TABLE 2. Apparent dissociation constant (K_D) of cytosolic androgen receptors from the mouse submandibular glands

sexes	age in days	n	apparent K_D (nM)			
			testostereone		DHT	
			high-affinity	low-affinity	high-affinity	low-affinity
male	20	3	ND	0.58±0.09[a]	0.10±0.01	0.53±0.02
	30	3	ND	0.57±0.01	0.10±0.01	0.55±0.03
	90	3	ND	0.59±0.04	0.08±0.01	0.59±0.05
female	20	3	ND	0.60±0.02	0.10±0.02	0.58±0.09
	30	3	ND	0.57±0.05	0.07±0.02	0.62±0.04
	90	3	ND	0.60±0.06	0.11±0.04	0.60±0.04

Aliquots (100 μl) of cytosol of the mouse submandibular glands were incubated with increasing concentration (0.025–2 nM) of [^{3}H] testosterone or [^{3}H] 5α-dihydrotestosteroe (DHT) in the presence or absence of 100-fold molar excess of nonradioactive testosterone or DHT. Apparent K_D (nM) were analyzed by Scatchard plots. [a]: mean±S.E.M., ND: not detected.

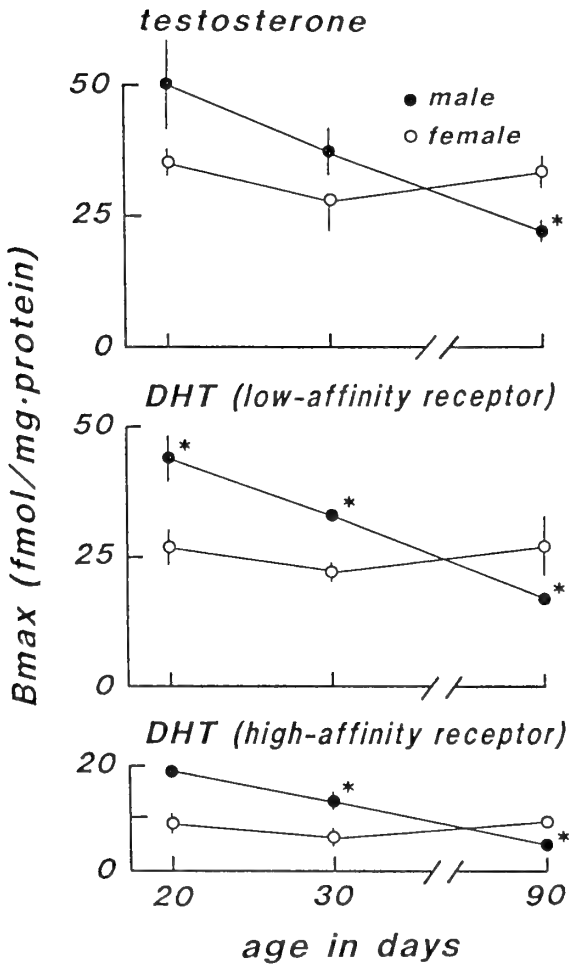

FIG. 3. Maximum binding (Bmax) of [^{3}H]testosterone and [^{3}H] 5α-dihydrotestosterone (DHT) to cytosol from the mouse submandibular gland. Aliquots (100 μl) of cytosol from the mouse submandibular gland were incubated with increasing concentrations (0.025–2 nM) of [^{3}H]testosterone or [^{3}H]DHT in the presence or absence of 100-fold molar excess of nonradioactive testosterone or DHT. Data were analyzed by Scatchard plot, and were expressed as fmol per mg of cytosolic protein. Values are mean±S.E.M., n=3 per group. *:$P<0.05$ vs age matched female (Mann-Whitney's U-test).

of nonradioactive testosterone or DHT. By 100-fold molar excess of the nonradioactive androgens, the ^{3}H-testosterone binding was displaced 90% or more (Fig. 4). When ^{3}H-DHT was used as ligand, nonradioactive DHT competed for the ^{3}H-DHT binding more effectively than nonradioactive testosterone. The displacement of the ^{3}H-DHT binding by 10- and 50-fold molar excess of nonradioactive testosterone was 12–16% lower than those by 10- and 50-fold molar excess of nonradioactive DHT (Fig. 4)

Furthermore, the cross-competition experiment was allowed to elucidate which was a predominant androgen for cytosolic receptors of the mouse submandibular gland when testosterone and DHT were applied at circulating concentrations. In male mice, circulating levels of testosterone and DHT drastically increased between days 20 to 30 (1.2±0.27 nM and 1.5±0.36 nM on day 20 and 10.0±2.05 nM and 3.5±0.72 nM on day 30, respectively) to attain the adult levels [30]. Therefore, testosterone and DHT, one is radioactive and the other is nonradioactive, were applied at the concentrations of 1.2 nM and 1.5 nM to cytosol from the 20-day-old male gland, and were applied at the concentrations of 10 nM and 3.5 nM to cytosol from the 30- and 90-day-old male glands, respectively. In the cytosol from the 20-day-old male gland, the specific binding of ^{3}H-testosterone was displaced 72% by 1.5 nM of nonradioactive DHT (Table 3). The binding of ^{3}H-DHT was displaced only 28% by 1.2 nM of nonradioactive testosterone (Table 3). Therefore, it was presumed that the receptors in the 20-day-old male gland might be bound about 28 parts with testosterone and about 72 parts with DHT. In the cytosol from the glands in 30- and 90-day-old male mice, the binding of ^{3}H-testosterone was displaced 36–41% by 3.5 nM of nonradioactive DHT and the binding of ^{3}H-DHT was displaced 59–61% by 10 nM of nonradioactive testosterone, respectively (Table 3). Therefore, it was presumed that the receptors in the 30- and 90-day-old male glands might be occupied approximately 60 parts by testosterone and 40 parts by DHT.

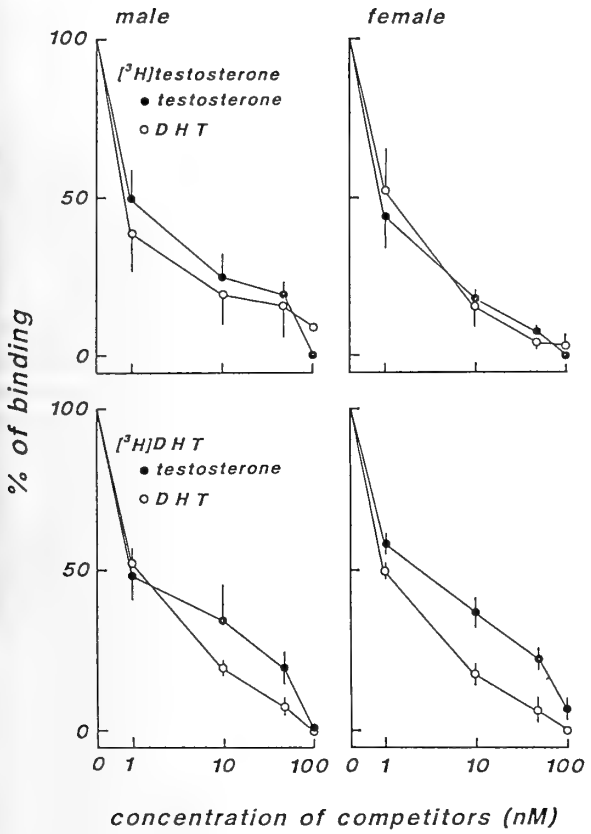

FIG. 4. Cross-competition of [^{3}H]testosterone (upper two panels) and [^{3}H]5α-dihydrotestosterone (DHT; lower two panels) for binding to cytosol from the submandibular glands of 90-day-old male (left two panels) and female (right two panels) mice. Aliquots (100 μl) of cytosol from the mouse submandibular gland were incubated with 1 nM [^{3}H]testosterone or [^{3}H]DHT in the presence or absence of 1, 10, 50 or 100-fold molar excess of nonradioac tive testosterone (●) or DHT (○). Values are mean±S.E.M., n=3 per group.

DISCUSSION

Verhoeven and Wilson have reported that cytosol from the mouse submandibular gland contains two types of DHT binding proteins: one is the high-affinity, low-capacity binding of about 8S size and the other is the low-affinity, high-capacity binding protein of about 3S size [35]. In the present study, the cytosolic binding sites for ^{3}H-DHT in the mouse glands were sedimented in two peaks of about 3S and 8S by a linear 5–20% sucrose density gradient centrifugation (Fig. 1). Scatchard plot analysis also demonstrated that the cytosol from the mouse gland contained two binding sites for ^{3}H-DHT, that is, the high-affinity, low-capacity receptor and the low-affinity, high-capacity receptor (Fig. 2). In contrast, the ^{3}H-testosterone binding site was obtained as only one smaller sedimentation of about 3S by the sucrose gradient centrifugation (Fig. 1), and Scatchard plots showed only the low-affinity receptor to bind with ^{3}H-testosterone (Fig. 2). These results suggest that a larger size of the high-affinity receptor in cytosol from the mouse gland is specific for DHT rather than testosterone. Furthermore, cross-competition showed that ^{3}H-DHT binding was more effectively displaced by nonradioactive DHT than nonradioactive testosterone, when the nonradioactive androgens were applied in 10- and 50-fold molar excess (Fig. 4). This results support the presence of the DHT specific high-affinity receptor in the mouse gland cytosol. On the other hand, both testosterone and DHT could bind to the low-affinity, high-capacity receptor at 3S size in the gland cytosol (Figs. 1 and 2). K_D value of the low-affinity receptor for ^{3}H-testosterone was 0.57–0.60 nM, resembling that of the low-affinity receptor for ^{3}H-DHT (0.53–0.62 nM) (Table 2). Bmax of the low-affinity receptor for ^{3}H-testosterone and ^{3}H-DHT did not differ through 20–90 days of age (Fig. 3), suggesting that the low-affinity receptor of smaller size at 3S in the cytosol could bind both testosterone and DHT.

As described above, cytosol of the mouse gland contained both the high-affinity DHT-specific receptor and the low-affinity androgen receptor. The effect of DHT on growth of the gland is more effective in comparison with that of testosterone [30], suggesting that these DHT effect might be associated with the high-affinity DHT-specific receptor.

Androgen responsiveness of the submandibular glands in young adult mice, containing both the gland weight gain and

TABLE 3. Bindings of ^{3}H-testosterone and ^{3}H-5α-dihydrotestosterone (DHT) to cytosolic receptor from the submandibular glands of male mice, applying nonradioactive testosterone or DHT in the serum concentrations

age in days	n	ligands	competitors	% of binding
20	6	1.2 nM [^{3}H] testosterone	1.5 nM DHT	27.4±7.07[a]
30	5	10 nM [^{3}H] testosterone	3.5 nM DHT	64.0±10.94
90	6	10 nM [^{3}H] testosterone	3.5 nM DHT	59.2±7.97
20	6	1.5 nM [^{3}H] DHT	1.2 nM testosterone	71.1±5.60
30	5	3.5 nM [^{3}H] DHT	10 nM testosterone	38.9±10.35
90	6	3.5 nM [^{3}H] DHT	10 nM testosterone	41.1±9.56

Aliquots (100 μl) of cytosol of the submandibular glands of male mice were incubated with [^{3}H] testosterone or [^{3}H] 5α-dihydrotestosterone (DHT) in the presence or absence of nonradioactive testosterone or DHT in the serum concentrations. Date were expressed as percentage of specific binding to each ligand in the presence of the nonradioactive steroids. [a]: mean±S.E.M.

the mitotic activity of GCT, is significantly higher in the males than in the females [30]. The present study demonstrated that Bmax of both the high- and low-affinity receptors in cytosol were superior in the male gland to those in the female gland on days 20 and 30 (Fig. 3), suggesting that occurrence of sex difference in the gland might be controlled by androgen binding activities of the receptor around these ages. In addition, Bmax of both the high- and low-affinity receptors in cytosol from the male gland gradually declined with age and became lower than those from the female gland by day 90 (Fig. 3). At 90 days of age, androgen-induced DNA synthesis in the male GCT is inferior to that in the female GCT [25], but the female gland is inferior to the male gland morphologically [12, 14, 20, 28] and functionally [3, 4, 6, 8, 15, 17, 18]. The mouse gland contains thyroid hormone receptor [36] as well as androgen receptor, and genetically [38] or drug-induced [10, 15, 16] hypothyroid male mice display a hypofunction of the gland. Thyroid hormones induce a morphological development of GCT [2, 9] and syntheses of biologically active polypeptides [1, 5, 15, 19, 21, 32, 34, 37, 39], independently of androgen action [2, 19, 21, 25, 26, 37, 39]. These results suggest that not only androgens but also thyroid hormones may participate in the maintenance of GCT in the gland of adult mice, morphologically and functionally.

The cytosolic androgen receptors in the male gland increase during postnatal development and attain to adult levels by day 20 [24, 33]. In our male mice, circulating levels of androgens begin to rise on day 20 and drastically increase between days 20 and 30 [30]. On day 20, histological and morphometrical aspects of the mouse gland showed no sex difference, whereas the mitotic activity of GCT in the mouse gland was significantly higher in males than in females [28]. In our male mice, circulating levels of testosterone and DHT were 1.2 ± 0.27 nM and 1.5 ± 0.36 nM, respectively, on day 20 [30]. When 1.2 nM of testosterone and 1.5 nM of DHT were applied to the cytosol from the 20-day-old male glands, about 28% of the cytosolic receptors bound with testosterone and 72% with DHT (Table 3). DHT acts more effectively on the mitotic activity of GCT in the gland than testosterone [30]. Therefore, the mouse gland primarily responds to the serum DHT to induce cell proliferation of GCT. Circulating levels of testosterone and DHT drastically increased between days 20 and 30 (testosterone: 10.0 ± 2.05 nM, DHT: 3.5 ± 0.72 nM) to attain adult levels [30]. When 10 nM of testosterone and 3.5 nM of DHT were applied to the cytosol from the 30- and 90-day-old male glands, the cytosolic receptors were occupied 60% by testosterone and 40% by DHT (Table 3). Testosterone and DHT may act separately on the gland, because the mouse gland can not convert testosterone to DHT [31]. Both androgens cause to increase all the gland weight, the relative occupied area of GCT, the cell height of GCT and the mitotic activity of GCT in the gland, whereas DHT is more effective in comparison with testosterone [30]. In addition, the glandular contents of biologically active polypeptides, including nerve growth factor, epidermal growth factor and renin, begin to increase around 3–4 weeks of age in male mice [8, 12, 13, 18, 23]. These results suggest that the mouse gland responds to both serum testosterone and DHT around days 20 to 30 to induce the early masculine development, morphologically and functionally, and then to maintain GCT in fully-stimulated states until 90 days of age.

The cytosol preparations from the mouse gland used in this experiments were specific for both testosterone and DHT to bind (Table 1). The specific bindings of those preparations to ^{3}H-testosterone and ^{3}H-DHT were reduced 15–44% by applying 100-fold molar excess of nonradioactive 3α- and 3β-diols, showing no difference in the binding competition between 3α- and 3β-diols (Table 1). Some researcher have also reported that 3α-diol does not bind in high-affinity mode to the androgen receptor in various tissues of rats [7, 22, 27]. However, 3α-diol takes effect on growth of the mouse gland and its potency is similar to DHT [31]. The effect of 3α-diol may be attributed to its conversion to active DHT because the gland contains 3α-hydroxysteroid dehydrogenase activity [31], or 3α-diol may specifically bind to its own receptor different from those for testosterone and DHT.

REFERENCES

1 Aloe L, Levi-Montalcini R (1980) Comparative studies on testosterone and L-thyroxine effects on the synthesis of nerve growth factor in mouse submaxillary salivary glands. Exp Cell Res 125: 15–22

2 Aloe L, Levi-Montalcini R (1980) Enhanced differentiation of sexually dimorphic organs in L-thyroxine treated Tfm mice. Cell Tissue Res 205: 19–29

3 Barka T (1980) Biologically active polypeptides in submandibular glands. J Histochem Cytochem. 28: 836–859

4 Byyny RL, Orth DN, Cohen S (1972) Radioimmunoassay of epidermal growth factor. Endocrinology 90: 1261–1266

5 Chao J, Margolius HS (1983) Differential effects of testosterone, thyroxine, and cortisol on rat submandibular gland *versus* renal kallikrein. Endocrinology 113: 2221–2225

6 Clements JA (1989) The glandular kallikrein family of enzymes: tissue-specific expression and hormonal regulation. Endocr Rev 10: 393–419

7 Cunningham GR, Tindall DJ, Means AR (1979) Differences in steroid specificity for rat androgen binding protein and the cytoplasmic receptor. Steroids 33: 261–276

8 Dunn JF, Wilson JD (1975) Developmental study of androgen responsiveness in the submandibular gland of the mouse. Endocrinology 96: 1571–1578

9 Fang J, Yamamoto R, Takatsuka D, Tsuji M, Terada N (1993) Effects of pretreatment with androgen or thyroid hormone on androgen-induced proliferation of granular convoluted tubular cells in mouse submandibular glands. Anat Rec 236: 679–684

10 Fujieda M, Murata Y, Hayashi H, Kambe F, Matsui N, Seo H (1993) Effect of thyroid hormone on epidermal growth factor gene expression in mouse submandibular gland. Endocrinology 132: 121–125

11 George FW, Johnson L, Wilson JD (1989) The effect of a 5α-reductase inhibitor on androgen physiology in the immature male rat. Endocrinology 125: 2434–2438

12 Gresik EW (1980) Postnatal developmental changes in submandibular glands of rats and mice. J Histochem Cytochem 28: 860–870

13 Gresik EW, Barka T (1978) Immunocytochemical localization of epidermal growth factor during the postnatal development of the submandibular gland of the mouse. Am J Anat 151: 1–10

14 Gresik EW, MacRae EK (1975) The postnatal development of the sexually dimorphic duct system and of amylase activity in the submandibular glands of mice. Cell Tissue Res 157: 411–422

15 Gresik EW, Schenkein I, van der Noen H, Barka T (1981) Hormon al regulation of epidermal growth factor and protease in the submandibular gland of the adult mouse. Endocrinology 109: 924–929

16 Gubits RM, Shaw PA, Gresik EW, Onetti-Muda A, Barka T (1986) Epidermal growth factor gene expression is regulated differently in mouse kidney and submandibular gland. Endocrinology 119: 1382–1387

17 Hirata Y, Orth DN (1979) Concentrations of epidermal growth factor, nerve growth factor, and submandibular gland renin in male and female mouse tissue and fluids. Endocrinology 105: 1382–1387

18 Hendry IA (1972) Developmental changes in tissue and plasma concentrations of the biologically active species of nerve growth factor in the mouse, by using a two-site radioimmunoassay. Biochem J 128: 1265–1272

19 Hosoi K, Tanaka I, Ueha T (1981) Induction of epidermal growth factor by tri-iodo-L-thyronine in the submandibular glands of mice with testicular feminization. J Biochem 90: 267–270

20 Jayasinghe NR, Cope GH, Jacob S (1990) Morphometric studies on the development and sexual dimorphism of the submandibular gland of the mouse. J Anat 172: 115–127

21 Kasayama S, Yoshimura M, Oka T (1989) The regulation by thyroid hormones and androgen of epidermal growth factor synthesis in the submandibular gland and its plasma concentrations in mice. J Endocrinol 121: 269–275

22 Krieg M, Horst H-J and Sterba M-L (1975) Binding and metabolism of 5α-androstane-3α,17β-diol and of 5α-androstane-3β, 17β-diol in the prostate, seminal vesicles and plasma of male rats: studies *in vivo* and *in vitro*. J Endocrinol 64: 529–538

23 Kurachi H, Oka T (1986) Regulation of the level of epidermal growth factor by oestrogen in the submandibular gland of female mice. J Endocrinol 109: 221–225

24 Minetti CASA, Valle LBS, Fava-De-Moraes F, Romaldini JH, Oliveira-Filho RM (1986) Ontogenesis of androgen receptors in the mouse submandibular gland: correlation with the developmental profiles of circulating thyroid and testicular hormones. Acta Endocrinol 112: 290–295

25 Oda M, Yamamoto R, Terada N, Nishizawa Y, Takatsuka D, Kitamura Y, Matsumoto K (1992) Maintenance by androgen and thyroid hormone of androgen-induced convoluted tubular cells in mouse submandibular glands. Anat Rec 232: 453–457

26 Okamoto S, Ito M, Kitamura Y, Matsumoto K (1985) Proliferative response of mouse submandibular gland to androgen but not to thyroid hormone. Cell Tissue Kinet 18: 583–588

27 Roselli CE, Horton LE, Resko AJ (1987) Time-course and steroid specificity of aromatase induction in rat hypothalamus-preoptic area. Biol Reprod 37: 628–633

28 Sawada K, Noumura T (1991) Effects of castration and sex steroids on sexually dimorphic development of the mouse submandibular gland. Acta Anat 140: 97–103

29 Sawada K, Noumura T (1992) Sexually dimorphic duct system of the submandibular gland in mouse with testicular feminization mutation (Tfm/Y). Acta Anat 143: 241–245

30 Sawada K, Noumura (1992) Differential effects of testosterone and 5α-dihydrotestosterone on growth in mouse submandibular gland. Zool Sci 9: 803–809

31 Sawada K, Noumura T (1993) Metabolism of androgens by the mouse submandibular gland and effects of their metabolites. Zool Sci 10: 481–488

32 Steidlar, NE, Reade PC (1983) An immunohistochemical and histological study of the influence of the thyroid gland on epidermal growth factor-containing cells in the submandibular salivary glands of mice. J Anat 136: 225–235

33 Takuma T, Nakamura, T, Hosoi K, Kumegawa M (1977) Binding protein for 5α-dihydrotestosterone in mouse submandibular gland. Biochim Biophys Acta 496: 175–181

34 Takuma T, Tanemura T, Hosoda S, Kumegawa M (1978) Effects of thyroxine and 5α-dihydrotestosterone on the activities of various enzymes in the mouse submandibular gland. Biochim Biophys Acta 541: 143–149

35 Verhoeven G, Wilson JD (1976) Cytosol androgen binding in submandibular gland and kidney of the normal mouse and the mouse with testicular feminization. Endocrinology 99: 79–92

36 Walker P. Coulombe P, Dussault JH (1982) Time- and dose-dependent effect of triiodothyronine on submaxillary gland epidermal growth factor concentration in adult female mice. Endocrinology 111: 1133–1139

37 Walker P, Weichsel ME Jr, Hoath SB, Poland RE, Fisher DA (1981) Effect of thyroxine, testosterone, and corticosterone on nerve growth factor (NGF) and epidermal growth factor (EGF) concentrations in adult female mouse submaxillary gland: dissociation of NGF and EGF responses. Endocrinology 109: 582–587

38 Wilson CM, Griffin JE, Reynolds RC, Wilson JD (1985) The interaction of androgen and thyroid hormones in the submandibular gland of the genetically hypothyroid (*hyt*/*hyt*) mouse. Endocrinology 116: 2568–2577

39 Wilson CM, Myhre MJ, Reynolds RC, Wilson JD (1982) Regulation of mouse submaxillary gland renin by thyroxine. Endocrinology 110: 982–989

ZOOLOGICAL SCIENCE 11: 571–576 (1994)

Effects of Sex Steroids on Dopamine Neurons in Cultured Hypothalamus and Preoptic Area Cells Derived from Neonatal Rats

KEIICHI TAKAGI[1] and SEIICHIRO KAWASHIMA

Zoological Institute, Graduate School of Science, University of Tokyo, Bunkyo-ku, Tokyo 113, Japan

ABSTRACT—The effect of sex steroids on the preoptic area and hypothalamic dopamine neurons derived from neonatal rats within 12 hr after birth was studied in primary culture. Testosterone or estradiol-17β was transiently added to the culture medium, and the cellular and medium dopamine contents were measured by an electrochemical detector connected with HPLC. Addition of testosterone (1 nM) for 3 days from day 2 of culture significantly increased cellular dopamine content and greatly increased medium dopamine concentration in the hypothalamic culture at day 14 of culture. Estradiol-17β (1 nM) for 3 days from day 2 of culture also greatly increased medium dopamine concentration at day 14, but it did not alter cellular dopamine content in the hypothalamic culture. Neither testosterone nor estradiol-17β altered the dopamine levels in the culture of the preoptic area cells. These results suggest that the property of cultured hypothalamic dopamine neurons was irreversibly altered by transient treatment with testosterone or estradiol-17β, while that of cultured preoptic dopamine neurons was not affected.

INTRODUCTION

Morphological and functional sex differences are well documented in the central nervous system of mammals [16, 22]. Most of the sex differences in the brain are thought to be developed by steroid hormonal environment during the perinatal critical period in rats and mice, but not by genetic sex [17]. Androgen secreted from the testis during the critical period in male rats induces masculinization of the brain, while the brain without the androgenic influence develops into basic female-type. Exogenously administered testosterone or testosterone propionate during the critical period can shift the female-type brain to the male-type one. On the other hand, castration of male rats on the day of birth effectively generates the female-type brain instead of the male-type. It is considered that androgen not only directly acts on some discrete brain regions, but also manifests their indirect action through neural networks of androgen-sensitive neurons [9, 13]. Therefore, it is difficult by in vivo experiments to clarify whether the sex differences are really generated by direct action of androgens. The cell culture system is one of the effective methods for the study of direct action of androgen.

Dopaminergic systems are deeply concerned with the sexual differentiation of the brain. Perinatal administration of dopamine-related drugs demasculinizes male rats [11, 14]. The preoptic area (POA) and hypothalamus contain four dopamine (DA) neuron groups [4, 12]. Among such dopaminergic groups, the A12 group, also called tuberoinfundibular DA neurons, is located in the periventricular region of the mediobasal hypothalamus including the arcuate nucleus. The neurons of this group extend their axons mainly to the median eminence, and inhibit the release of prolactin from the pituitary. Although no morphological sexual dimorphism has been found in this dopaminergic system, sex difference in the secretion and synthesis of DA has been reported [18]. The A14 group is located in the periventricular region between the POA and anterior hypothalamus. The exact role of the A14 group has not yet been established. DA neurons in this group appear to innervate both the luteinizing hormone-releasing hormone and GABA neurons in the medial POA [10] and the intermediate lobe of the pituitary [7]. Evident sexual dimorphism has been reported in the number and fiber density of DA neurons in the anteroventricular region of the A14 group by Simerly *et al.* [23].

The aim of the present study was to clarify the effects of sex steroids on DA neurons in the periventricular POA (including the A14) and hypothalamus (including the A12) in primary culture. We cultured the cells of each region derived from neonatal rats, and the cultured cells were transiently given testosterone or estradiol-17β during early days of culture. Cellular and medium DA was measured at later days.

MATERIALS AND METHODS

Cell culture

Newborn rats of the Wistar/Tw strain (about 20 pups for one experiment) were used within 12 hr after birth. The sex of animals was disregarded, but the number of male and female rats was about the same. After decapitation, the brain was dissected out and pooled in the ice-cold serum-supplemented medium. The periventricular POA and hypothalamus were separately dissected out as indicated in Figure 1. Since A11 group is more caudally and A13 group is more dorsolaterally located in the hypothalamus, only small population of A11 and A13 DA neurons would be contaminated in

Accepted June 13, 1994
Received April 20, 1994
[1] Present address and correspondence: Department of Physiology, Jichi Medical School, Minamikawachimachi, Tochigi-ken 329-04, Japan.

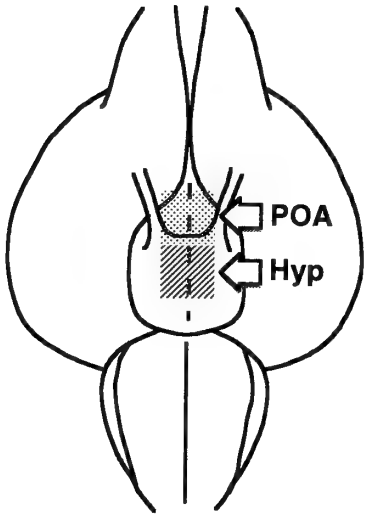

FIG. 1. Schematic diagram of dissected brain areas. Periventricular preoptic area (POA) was dissected out as a tissue clump of about 1 mm width, 1 mm height, and 1 mm depth cube at just rostral to the optic chiasma (hatched square). Periventricular hypothalamus (Hyp) was dissected out as a tissue clump of about 1 mm width, 1 mm height, and 1 mm depth cube at just caudal to the optic chiasma (dashed square).

dissected tissue pieces, if any. Pooled tissues of each brain region were dissociated by the method previously reported [26]. Briefly, the tissue clumps were digested in 1,500 PU/ml dispase (Godosyusei, Tokyo) in the serum-supplemented medium for 15 min at 37°C, followed by gentle pipettings. Enzymatic digestion and mechanical dissociation were repeated several times until most of the tissue clumps were dissociated. The dissociated cell suspension was kept in an ice bath during the dissociation step. After removing debris and remaining tissue masses by passing through a nylon mesh (40 μm in pore size), cell suspension was centrifuged at 1,200 r.p.m. for 5 min. Collected cells were resuspended in a fresh culture medium, and cultivated in each well of 24-well multiwell culture plate (Falcon) at a density of 2.0×10^5 viable cells/well containing 0.4 ml of culture medium. The culture well was kept in an atmosphere of 5% CO_2-95% air at 37°C. Culture medium was replaced at 3-day intervals. To avoid possible effects of steroid hormones in the fetal calf serum (FCS), serum-free medium was routinely used except during the first 2 days of culture. Serum-supplemented medium was DME/F12 without phenol red (Sigma) supplemented with 100 IU/ml penicillin G, 100 μg/ml streptomycin, additional 540 mg/ml glucose, and 15% fetal calf serum (FCS) in the serum-free medium. Serum-free medium was DME/F12 without phenol red supplemented with 100 μM putrescine (Sigma), 30 nM sodium selenite (Sigma), 5 μg/ml insulin (Sigma), 50 μg/ml transferrin (Sigma), 100 IU/ml penicillin G, 100 μg/ml streptomycin, and additional 540 mg/ml glucose. This serum-free medium was able to maintain the POA/hypothalamic neurons for a long period without any steroid hormone, if short preculture period with serum-supplemented medium was placed [25].

Following preculture in a serum-supplemented medium for 2 days, the medium was changed to the serum-free medium with or without steroid hormones. Testosterone (Sigma) or estradiol-17β (Sigma) was dissolved in absolute ethanol, and diluted to 1.0 nM with the serum-free medium. The final concentration of the ethanol was 0.007%. The same percentage of ethanol was added to the control medium. Testosterone at the concentration of 1.0 nM has been reported to facilitate the survival of neurons derived from neonatal rat POA [26]. After 3-day culture in a steroid hormone-containing medium, the medium was replaced to a serum-free medium without steroid hormones, and the cells were continued to be cultured. At day 14 of culture (9 days after the removal of steroids), cellular contents of DA and medium DA concentrations were measured. A few hypothalamic cultures were used for the observation of catecholamine neurons.

Staining of catecholamine neurons

Catecholamine neurons in culture were visualized by glyoxylic acid method [15]. At day 14 of culture, coverslips were briefly rinsed with PBS and immersed into 2% glyoxylic acid in PBS (pH 7.0) containing 20% sucrose for 20 min at 4°C in the dark. Then, the coverslip was dried by hot air for 5 min, and heated at 100°C for 5 min. The coverslip was mounted on a slide glass with liquid paraffin, and cells were observed under a fluorescent microscope. DA and noradrenaline are reported to emit blue fluorescence (emission max.=475 nm) when excited by the light at the wavelength of 415 nm [15].

Measurement of dopamine (DA)

The content of DA was measured by an electrochemical detector connected with a high-performance liquid chromatography (HPLC). Reversed-phase column (TSK ODS-80Ts, Tosoh) was used for the analysis. The mobile phase was composed of 0.15 M NaH_2PO_4, 0.1 mM EDTA, 0.5% sodium octanesulphonic acid, and 5% methanol (pH 3.4). To concentrate and extract DA from the culture medium, method of Porter *et al.* [19] was used with a slight modification. The medium of each group was pooled, acidified with an equal volume of 0.1 M perchloric acid (PCA) −0.4 mM sodium metabisulphate containing internal standard, 3,4-dihydroxybenzylamine (DHBA, Sigma), and stored at −80°C until measurement. After centrifugation at 9,000×g for 10 min and neutralization of supernatant with 1.0 M Tris buffer (pH 8.6), catecholamines were absorbed on activated alumina, back-extracted into 0.3 M PCA −0.4 mM sodium metabisulphate, microfiltered (0.22 μm in pore size), and 50 μl aliquot of the extract was introduced into HPLC. To extract cellular DA content the cells in each well were harvested by a cell-scraper immediately after complete separation of the culture medium, and suspended with 200 μl of 0.1 M PCA and 0.4 mM sodium metabisulphate containing DHBA. The suspended cells were sonicated at 4°C, and stored at −80°C until measurement. After centrifugation at 9,000×g for 10 min, the supernatant was microfiltered, and 50 μl aliquot of this supernatant was directly introduced into HPLC. Recovery of DA (Sigma) in the present procedure was steadily about 85%. To calculate the concentration of DA, the method described by Felice *et al.* [6] was used. DA concentrations and contents were expressed as ng/ml and ng/well (mean±standard error), respectively. Student's t-test was used for analyzing cellular DA contents. For the measurement of DA in the medium, media of each group were all pooled, and therefore, no statistical analysis was applicable.

RESULTS

As we have previously reported [25], the number of neurons in the hypothalamus and POA culture at day 14 of culture was almost stable in the present study. When cultured cells were stained by glyoxylic acid [15] at day 14 of culture, DA neurons were observed as the cells that extended

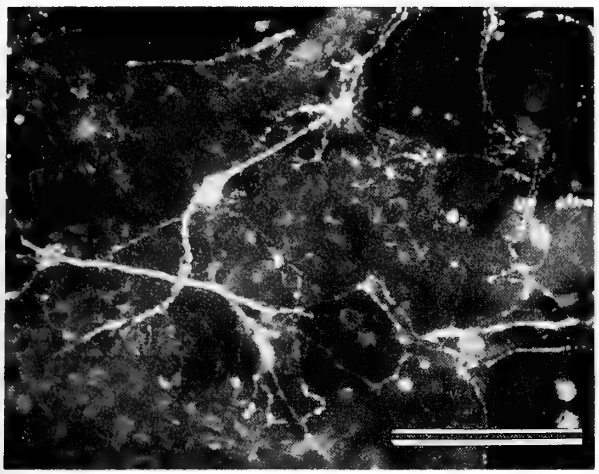

FIG. 2. Fluorescent microphotograph of catecholamine neurons in the hypothalamic cells at day 14 of culture stained by glyoxylic acid method. Catecholamine neurons show very long neurites with numerous branchings and varicosities. Bar=100 μm.

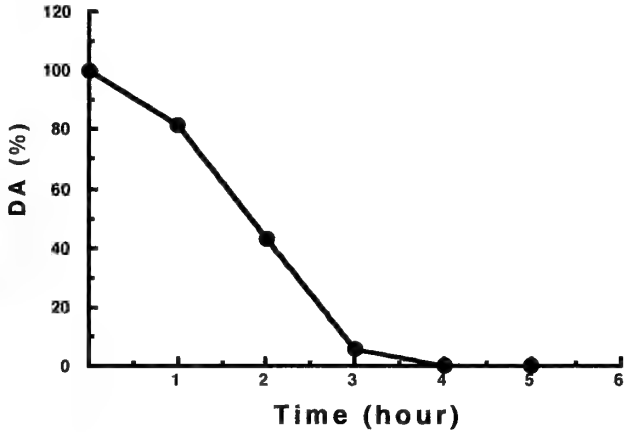

FIG. 4. Decrease of dopamine (DA) in the serum-free culture medium. Dopamine (5 ng/ml) was dissolved in the serum-free medium, and incubated at 37°C in the atmosphere of 5% CO_2-95% air. DA concentration is indicated as percentage of the initial value.

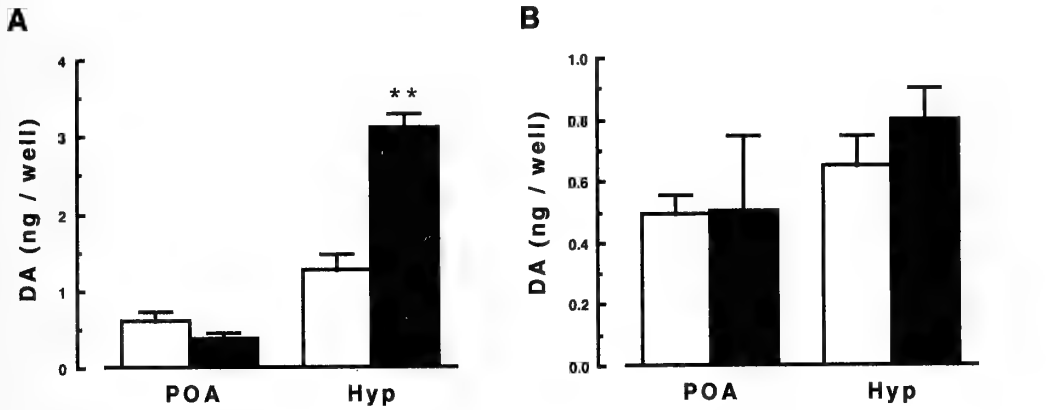

FIG. 3. Cellular dopamine (DA) contents after exposure to 1 nM testosterone (A) or estradiol-17β (B) in cultured preoptic (POA) or hypothalamic (Hyp) cells at day 14 of culture. Each steroid was given for 3 days from day 2 of culture. Open columns indicate control cultures, and solid columns indicate steroid-treated cultures. Each column shows the mean $\pm$ standard error of 3–4 samples. **$P<0.01$ (Student's t-test).

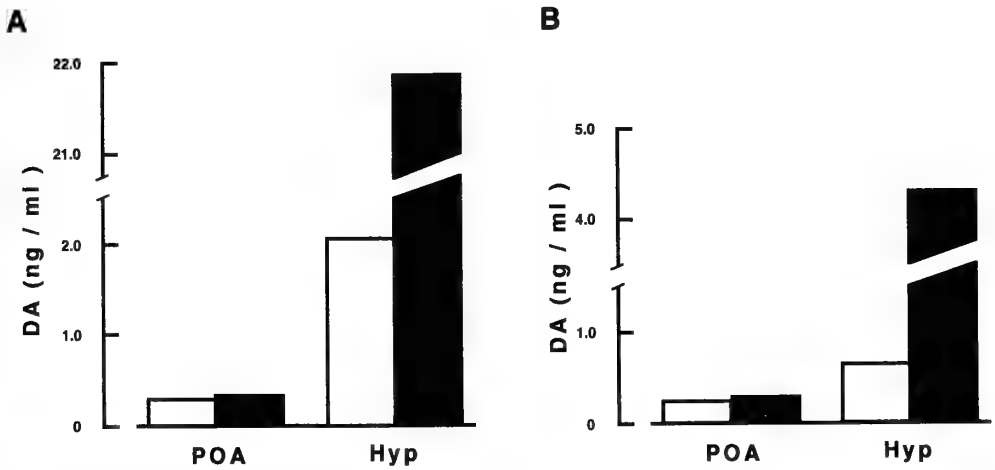

FIG. 5. Medium concentrations of dopamine (DA) after exposure to 1 nM testosterone (A) or estradiol-17β (B) released from the preoptic (POA) or hypothalamic (Hyp) cells at day 14 of culture. Each steroid was given for 3 days from day 2 of culture. Medium was collected from 3–4 wells in each group, and content of DA was measured. Open columns indicate control cultures, and solid columns indicate steroid-treated cultures.

very long neurites with numerous varicosities and branchings (Fig. 2). However, no quantitative morphological comparison was examined in the present study.

As shown in Figures 3A and 5A, exposure to testosterone for 3 days from day 2 of culture increased both cellular contents and medium concentrations of DA in the hypothalamic culture. In the hypothalamic culture, the cellular DA contents were more than 2-fold greater in the cells exposed to testosterone than in the control cells at day 14 of culture (Fig. 3A). DA concentration in the medium was about 10-fold greater in the testosterone-exposed culture than in the control culture (Fig. 5A). Figure 4 shows the time-course decrease of standard DA in the serum-free medium at 37°C without any cell. DA rapidly decreased, and became undetectable after only 4 hrs of incubation. Therefore, measured DA concentrations in the media indicate the released DA during a short period before the termination of culture. Short-term exposure to estradiol-17β tended to increase DA release from the hypothalamic culture, where DA concentration was about 7-fold greater in the medium of estradiol-exposed culture than the control culture(Fig. 5B). However, no significant difference was detected in the cellular DA content between estradiol-exposed and control cultures (Fig. 3B).

Exposure to testosterone failed to alter either cellular content or medium concentration of DA in the POA culture (Figs. 3A and 5A). Cellular DA content in testosterone-exposed POA culture was slightly lower than that in the control culture, but the difference was statistically not significant. The medium DA concentration of testosterone-exposed culture was almost the same as that of the control (Fig. 5A). Exposure to estradiol-17β was not effective in altering cellular or medium DA contents (Figs. 3B and 5B).

DISCUSSION

In the present study, the cultured hypothalamic or POA cells derived from neonatal rats were transiently exposed to 1.0 nM testosterone or estradiol-17β. Both cellular content and medium concentration of DA in the hypothalamic culture were increased after a long time lapse since the exposure to testosterone. Estradiol-17β likewise elevated medium concentration of DA, but was not effective for cellular content. These results indicate that the hypothalamic DA neurons were irreversibly affected by the transient exposure to steroids in primary culture. Because estradiol-17β also effectively elevated the medium DA concentration, conversion of testosterone to estradiol-17β might be playing a role for the effect of testosterone in the alteration of the property of DA neurons. The effect of nonaromatizable androgen, 5α-dihydrotestosterone, should further be tested for convincing this possibility. There are at least three possible explanations on the effect of sex steroids on the cultured hypothalamic DA neurons. The first is the effect on the survival of DA neurons. The second is the effect on the morphology of DA neurons. If axonal branching and/or varicosities of DA neurons are more numerous in the steroid-treated cultures, more DA content in the cells and more release to the medium might occur. However, our preliminary observation (data not shown) by using glyoxylic acid method [15], which fluorochemically stained DA neurons, seemed to point out that the two possibilities were not feasible. The third possibility is the effect on the activity of each DA neuron. If the rate of synthesis and/or release of DA is increased, DA in the cells and culture medium should be increased. In the present study, cellular DA content was more than 2-fold greater in testosterone-treated cultures, while DA concentration in the culture medium was about 10-fold. This result fits well with the third possibility, suggesting that both synthesis and release of DA were increased, where the influence on the release of DA was more marked than on the synthesis.

Although morphological sex difference is absent, the activity of tuberoinfundibular DA neurons shows sexual dimorphism. Demarest *et al.* [5] reported that the concentration of DA in the median eminence was the same in male and female rats, but the basal rates of synthesis and turnover of DA in the median eminence were 2–3 fold greater in the female than in the male. DA content in the portal blood was several times higher in the female rat [3]. Similarly, while there is no sex difference in the number of DA neurons in the tuberoinfundibular system, the amount of tyrosine hydroxylase (TH) mRNA in the ovariectomized female rat was greater than in the male [1, 2]. Demarest *et al.* [5] stated that sex difference in the tuberoinfundibular DA system seems to be determined by the sex steroidal environment during neonatal period as are other sex differences in the brain. Sar [20] reported that considerable percentage of TH-immunopositive neurons in this region incorporated [^{3}H]-estradiol-17β, suggesting that the sex difference in this system was the consequences of the direct effect of sex steroids.

There are several reports on the effect of steroid hormones on the tuberoinfundibular DA neurons. Ovariectomy of female rats decreases the turnover rate of DA in the median eminence, and the administration of estradiol benzoate to the ovariectomized animal recovers the turnover rate [8]. Similarly, administration of estradiol [27] or testosterone [24] increases the turnover rate of DA in the median eminence in castrated male rats. Recently, Yamaguchi *et al.* [28] reported that short-term treatment with estradiol-17β increased spontaneous release of [^{3}H]-DA from cultured tuberoinfundibular cells. In our present experiments, testosterone and estradiol-17β exerted a long-lasting stimulatory effect on the hypothalamic DA neurons. The effect of steroids on the hypothalamic DA neurons in the present study might reflect the sexual differentiation of the tuberoinfundibular DA neurons.

Apparent sexual dimorphism was reported in the number of DA neurons in the POA. The number of DA neurons in the anteroventral periventricular nucleus (AVPvN) is 3–4 fold more in the female rat than in the male [23]. This sexual dimorphism appears to be dependent on the perinatal levels of gonadal steroids, since orchidectomy of newborn males increased and treatment of newborn females

with testosterone decreased the number of TH mRNA-containing cells in the AVPvN [21]. However, there was no significant effect of transient sex steroid exposure in the present study on DA content in the periventricular POA cultures neither in the cells nor in the culture medium. Observation of Sar [20] that there was no coexpression between TH-immunoreactivity and [^{3}H]-estradiol incorporation in the POA suggests the lack of direct response to estrogen in DA neurons in the POA. Gonadal steroid may indirectly influence on the sexual differentiation of DA neurons in the POA.

To conclude, transient exposure either to testosterone or estradiol-17β induced long-lasting effects on the dopaminergic property of cultured hypothalamic cells derived from neonatal rats. Transiently administered testosterone for 3 days from day 2 of culture increased cellular DA content and medium DA concentration at day 14. Transiently administered estradiol-17β also increased medium DA concentration, but cellular content was not affected. These data suggest that transiently administered sex steroids, testosterone or estradiol-17β, irreversibly stimulated the basal level of DA synthesis and release in the hypothalamic culture of neonatal rats. Dopaminergic property of cultured cells derived from the periventricular POA was not affected by the treatments. Alterations of the tuberoinfundibular dopaminergic property by direct effects of sex steroids during critical period seem to be crucial for the determination of sex difference of DA neurons in this area.

ACKNOWLEDGMENTS

This study was supported in part by a Grant-in-Aid for Scientific Research from the Ministry of Education, Science and Culture, Japan and a Research Grant from Zenyaku Kogyo, Ltd. to S. Kawashima.

REFERENCES

1 Arbogast L A, Voogt J L (1990) Sex-related alterations in hypothalamic tyrosine hydroxylase after neonatal monosodium glutamate treatment. Neuroendocrinology 52: 460–467

2 Arbogast L A, Voogt J L (1991) Ontogeny of tyrosine hydroxylase mRNA signal levels in central dopaminergic neurons: development of a gender difference in the arcuate nuclei. Dev Brain Res 63: 151–161

3 Ben-Jonathan N, Oliver C, Weiner H J, Mical R S, Porter J C (1977) Dopamine in hypophysial portal blood of the rat during the estrous cycle and throughout pregnancy. Endocrinology 100: 452–458

4 Dahlström A, Fuxe K (1964) Evidence for the existence of monoamine-containing neurons in the central nervous system. Acta Physiol Scand 62 (Suppl 232): 1–55

5 Demarest K T, Mckay D W, Riegle G D, Moore K E (1981) Sexual differences in tuberoinfundibular dopamine nerve activity induced by neonatal androgen exposure. Neuroendocrinology 32: 108–113

6 Felice L J, Felice J D, Kissinger P T (1978) Determination of catecholamines in rat brain parts by reverse-phase ion-pair liquid chromatography. J Neurochem 31: 1461–1465

7 Goudreau J L, Lindley S E, Lookingland K J, Moore K E (1992) Evidence that hypothalamic periventricular dopamine neurons innervate the intermediate lobe of the rat pituitary. Neuroendocrinology 56: 100–105

8 Gunnet J W, Lookingland K J, Moore K E (1986) Effects of gonadal steroids on tuberoinfundibular and tuberohypophysial dopaminergic neuronal activity in male and female rats. Proc Soc Exp Biol Med 183: 48–53

9 Handa R J, Hines M, Schoonmaker J N, Shryne J E, Gorski R A (1986) Evidence that serotonin is involved in the sexually dimorphic development of the preoptic area in the rat brain. Dev Brain Res 30: 278–282

10 Horvath T L, Naftolin F, Leranth C (1993) Luteinizing hormone-releasing hormone and gamma-aminobutyric acid neurons in the medial preoptic area are synaptic targets of dopamine axons originating in anterior periventricular areas. J Neuroendocrinol 5: 71–79

11 Hull E M, Nishita J K, Bitran D (1984) Perinatal dopamine-related drugs demasculinize rats. Science 224: 1011–1013

12 Hökfelt T, Johansson O, Fuxe K, Goldstein M, Park D (1976) Immunohistochemical studies on the localization and distribution of monoamine neuron systems in the rat brain. 1. Tyrosine hydroxylase in the mes- and diencephalon. Med Biol 54: 427–453

13 Jarzab B, Kaminski M, Gubala E, Achtelik W, Wagiel J, Döhler K D (1990) Postnatal treatment of rats with the β_2-adrenergic agonist salbutamol influences the volume of the sexually dimorphic nucleus in the preoptic area. Brain Res 516: 257–262

14 Kawashima S (1964) Inhibitory action of reserpine on the development of the male pattern of secretion of gonadotropins in the rat. Annot Zool Japon 37: 79–85

15 Lindvall O and Björklund A (1974) The glyoxylic acid fluorescence histochemical method: A detailed account of the methodology for visualization of central catecholamine neurons. Histochemistry 39: 97–127

16 MacLusky N J, Naftolin F (1981) Sexual differentiation of the central nervous system. Science 211: 1294–1303

17 McEwen B S (1981) Neural gonadal steroid actions. Science 211: 1303–1311

18 Moore K E (1987) Interaction between prolactin and dopaminergic neurons. Biol Reprod 36: 47–58

19 Porter J C, Kedzierski W, Aguila-Mansilla N, Jorquera B A (1990) Expression of tyrosine hydroxylase in cultured brain cells: Stimulation with an extractable pituitary cytotropic factor. Endocrinology 126: 2474–2481

20 Sar M (1984) Estradiol is concentrated in tyrosine hydroxylase-containing neurons of the hypothalamus. Science 223: 938–940

21 Simerly R B (1989) Hormonal control of the development and regulation of tyrosine hydroxylase expression within a sexually dimorphic population of dopaminergic cells in the hypothalamus. Mol Brain Res 6: 297–310

22 Simerly R B (1990) Hormonal control of neuropeptide gene expression in sexually dimorphic olfactory pathway. Trends Neurosci 13: 104–110

23 Simerly R B, Swanson L W, Gorski R A (1985) The distribution of monoaminergic cells and fibers in a periventricular preoptic nucleus involved in the control of gonadotropin release: Immunohistochemical evidence for a dopaminergic sexual dimorphism. Brain Res 330: 55–64

24 Simpkins J W, Kalra S P, Kalra P S (1983) Variable effects of testosterone on dopamine activity in several microdissected regions in the preoptic area and medial basal hypothalamus. Endocrinology 112: 665–669

25 Takagi K and Kawashima S (1992) Attempts to improve survival of neurons derived from neonatal rat hypothalamus-

preoptic area in serum-free medium. Zool Sci 9: 293–304

26 Takagi K and Kawashima S (1993) Culture of rat brain preoptic area neurons: Effects of sex steroids. Int J Dev Neurosci 11: 63–70

27 Terry L C, Craig R, Hughes T, Schatzle J, Zorza M, Ortolano G A, Willoughby J O (1985) Hypothalamic monoaminergic activity and pituitary function in male rats with estrogen-induced pituitary hyperplasia. Neuroendocrinology 41: 269–275

28 Yamaguchi M, Koike K, Kadowaki K, Miyake A, Tanizawa O (1991) Short-term treatment with 17β-estradiol enhances spontaneous [^{3}H] dopamine release from cultured rat tuberoinfundibular neurons. J Endocrinol Invest 14: 187–191

ZOOLOGICAL SCIENCE 11: 577–581 (1994)

Identification of Melatonin in Different Organs of the Cricket, *Gryllus bimaculatus*

Masanori T. Itoh[1], Atsuhiko Hattori[2], Yawara Sumi[1] and Takuro Suzuki[2]

[1]*Department of Chemistry,* [2]*Department of Anatomy, St. Marianna University School of Medicine, Sugao, Miyamae-ku, Kawasaki 216, Japan*

ABSTRACT—The possible presence of melatonin (N-acetyl-5-methoxytryptamine) was investigated in different tissues and organs of adult crickets by the use of reversed-phase high-performance liquid chromatography with fluorometric detection and radioimmunoassay. Melatonin was detected in the compound eye, antenna, ovipositor, palp, cercus, leg, wing, brain, ovary, digestive tube and Malpighian tube of the crickets, indicating that melatonin was very widely distributed in the crickets. The results suggest that melatonin in these organs might be involved in the local control of various aspects of rhythmic activity.

INTRODUCTION

Melatonin (N-acetyl-5-methoxytryptamine) was originally found in the vertebrate pineal gland, where its synthesis and secretion exhibit a diurnal rhythm with peak activity at night [1]. It is now widely accepted that the melatonin rhythm of the pineal gland mediates photoperiodic information [18]. Melatonin has also been found in extrapineal organs of vertebrates, such as the retina [9, 19, 24], the Harderian gland [19, 24], the gastrointestinal tract [5] and the brain [13, 17, 20]. However, the function of melatonin in these extrapineal organs remains to be elucidated.

Recently, the presence of melatonin has been demonstrated in some invertebrate species including insects [22]. In insects, melatonin has been identified in the compound eye of the locust [23] and the head of the fruit fly [8]. However, the presence of melatonin in organs other than the compound eye or the head of insects has not yet been reported. The present study investigated the possible presence of melatonin in different tissues and organs of adult crickets, *Gryllus bimaculatus*, using reversed-phase high performance liquid chromatography (RP-HPLC) with fluorometric detection and radioimmunoassay (RIA).

MATERIALS AND METHODS

Animals and preparation of tissues and organs

Adult crickets were maintained under a 12 h light-12 h dark cycle (lights on at 06:00 a.m.) and ambient temperature of 24°C, with food and water *ad libitum* for a minimum of 1 week. The compound eyes, antennae, ovipositors, palpi, cerci, fore-, mid- and hind-legs, wings, brains, ovaries, digestive tubes, Malpighian tubes, and fat bodies were dissected from 20 adult females between 09:00 a.m. and 12:00 noon. The tissues and organs were weighed and homogenized in 2.5 times their volume of ice-cold 0.1 M perchloric acid containing 0.1% ascorbic acid. After centrifugation at 12000 g for 15 min at 4°C, the supernatant was extracted with 4 volumes of chloroform. The chloroform phase was washed twice with 1 ml of distilled water, evaporated and stored at −80°C until RP-HPLC analysis.

RP-HPLC analysis

The tissue or organ extracts were dissolved in 50 μl of 30% methanol in a 50 mM ammonium acetate solution (pH 4.2) for the mobile phase of RP-HPLC. Aliquots of 20 μl of the solution were directly injected into the RP-HPLC system, which was equipped with a Superiox ODS S-5 μm column (4.6×150 mm) (Shiseido Co., Tokyo) and a RF-550 fluorometric detector (Shimadzu Co., Kyoto). The detector was operated at an excitation wavelength of 280 nm and an emission wavelength of 340 nm. The flow rate of the mobile phase was adjusted to 1 ml/min and one-min fractions were collected. All separations were performed isocratically at 24°C. Melatonin and other indole standards were obtained from Sigma Chemical Co. (St. Louis, MO).

RIA of melatonin

Aliquots of RP-HPLC fractions were evaporated and dissolved in 250 μl of 10 mM phosphate buffered saline (pH 7.4) containing 1% bovine serum albumin. The melatonin content of each fraction was determined by RIA [11]. N-[2-aminoethyl-2-^{3}H] melatonin was obtained from Dupont/New England Nuclear (Wilmington, DE). Anti-melatonin serum was provided by Prof. K. Wakabayashi, Gunma University.

RESULTS

Figure 1 shows a typical elution profile of various indole standard solutions; a peak of the melatonin standard appeared at 15.7 min and was clearly separated from those of the other indole compounds examined. Figures 2–7 show elution and RIA profiles obtained from the various organ extracts of the crickets by RP-HPLC and RIA. A peak of melatonin in the elution profiles was tentatively identified by comparison of the retention time with that of the melatonin

Accepted June 16, 1994
Received March 30, 1994

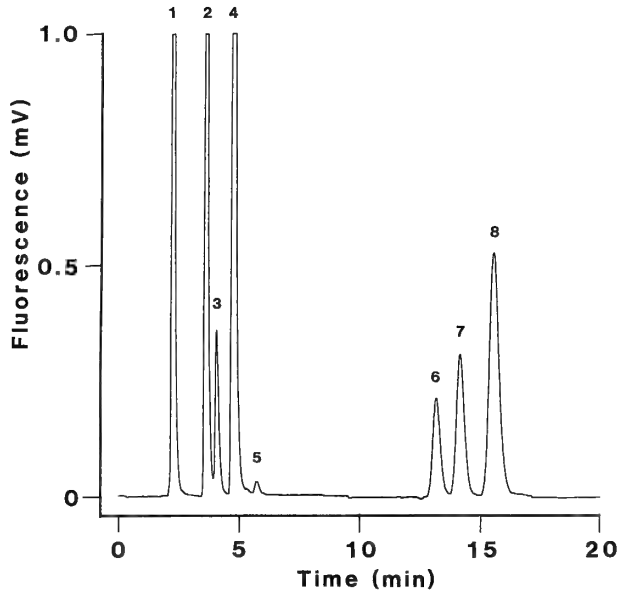

FIG. 1. RP-HPLC elution profile of various indole standards (250 pg). For chromatographic conditions, see text. Peaks: 1) 5-hydroxytryptamine (serotonin); 2) 5-hydroxyindole-3-acetic acid and 5-hydroxytryptophol; 3) N-acetylserotonin; 4) 5-methoxytryptamine; 5) 6-hydroxymelatonin; 6) 5-methoxyindole acetic acid; 7) 5-methoxytryptophol; 8) N-acetyl-5-methoxytryptamine (melatonin).

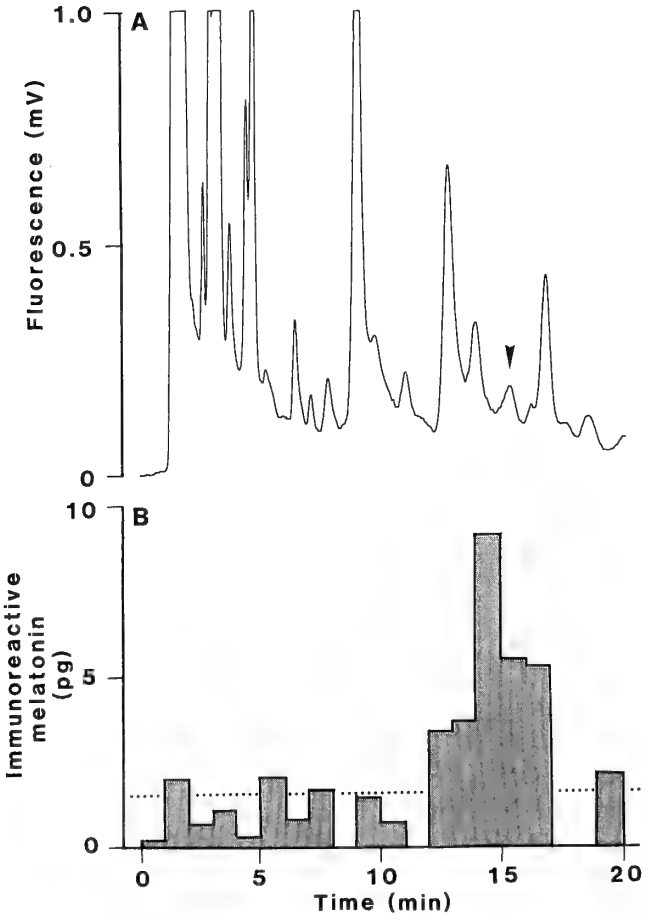

FIG. 2. RP-HPLC elution profile (A) and RIA profile (B) of the compound eye extracts of the crickets. Arrow head in (A) of Figs. 2–7 indicates the elution position corresponding to the melatonin standard. The dotted line in (B) of Figs. 2–7 indicates the detection limit of RIA (1.60 pg/100 μl).

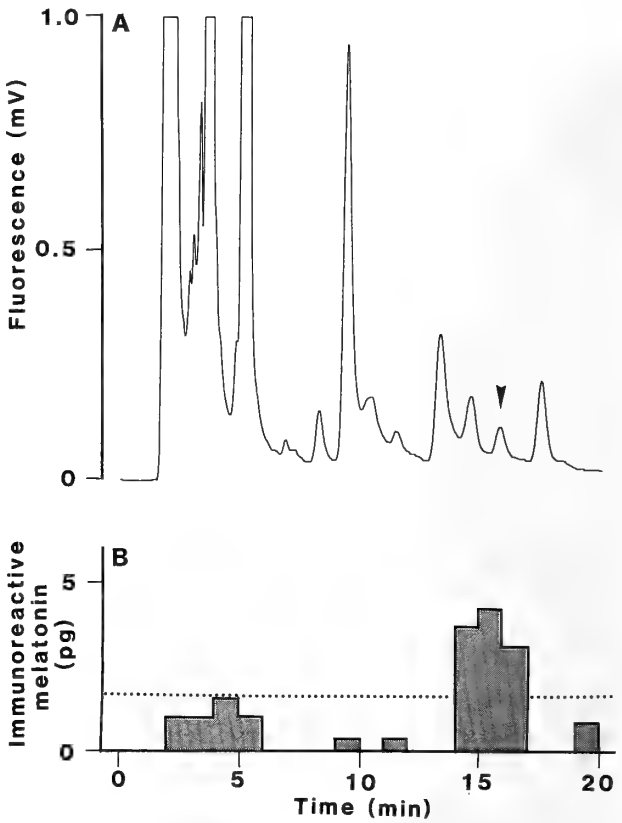

FIG. 3. RP-HPLC elution profile (A) and RIA profile (B) of the antenna extracts of the crickets.

standard as shown in Figure 1. A peak with the identical retention time to that of the melatonin standard was found in extracts of the compound eyes, antennae, ovipositors, brains and ovaries indicated in elution profiles of Figures 2–6. However, no peak with an identical retention time to that of the melatonin standard was detected in the fat body (Fig. 7A). Peaks with identical retention times to those of the other indole standards were also found in the elution profiles obtained from the extracts of these organs.

RIA revealed that the major immunoreactive peak at about 15.7 min corresponded to the endogenous melatonin detected by RP-HPLC, although the peak was broad in some extracts and minor peaks sometimes appeared in the neighborhood of the major peak (Figs. 2–6). The retention time obtained by RP-HPLC and the immunoreactivity detected by RIA confirmed that the peak observed at 15.7 min was due to melatonin. Thus, it was demonstrated that melatonin is present in the compound eye, antenna, ovipositor, brain and ovary as shown in Figures 2–6, and in addition, in the palp, cercus, legs, wing, digestive tube and Malpighian tube, although the elution profiles obtained are not shown. Table 1 shows the melatonin content (pg/cricket) and concentration

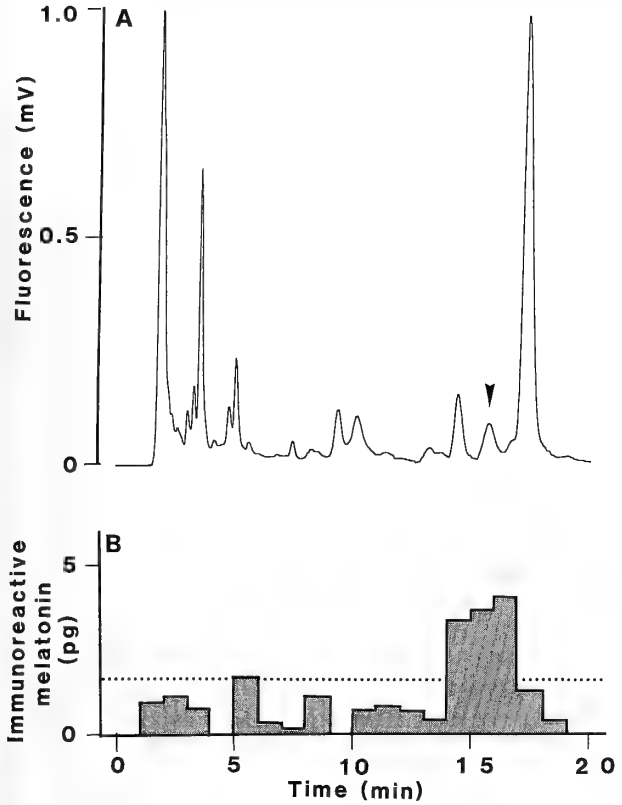

FIG. 4. RP-HPLC elution profile (A) and RIA profile (B) of the ovipositor extracts of the crickets.

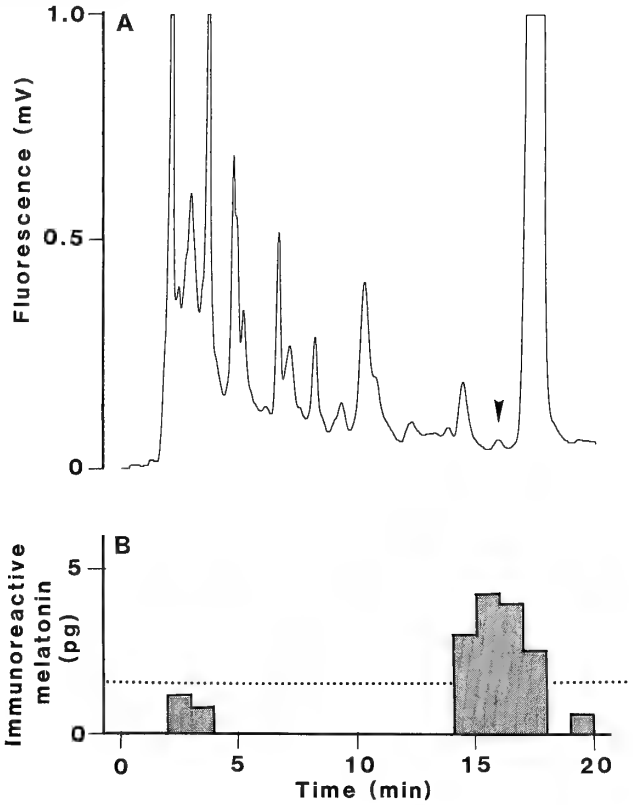

FIG. 6. RP-HPLC elution profile (A) and RIA profile (B) of the ovary extracts of the crickets.

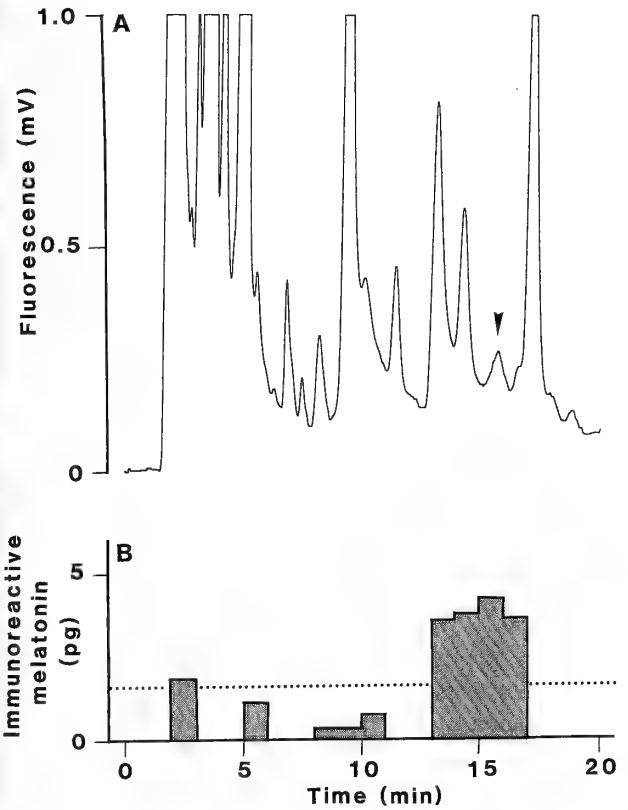

FIG. 5. RP-HPLC elution profile (A) and RIA profile (B) of the brain extracts of the crickets.

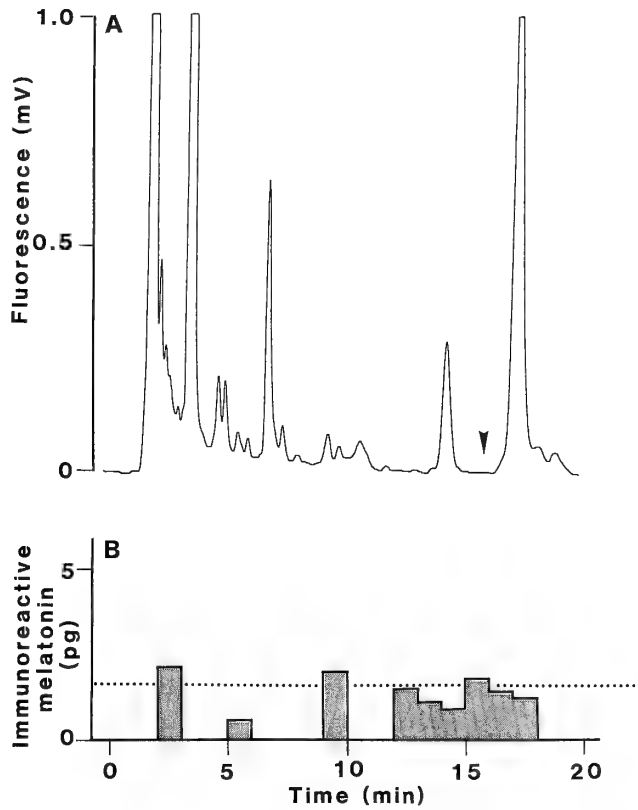

FIG. 7. RP-HPLC elution profile (A) and RIA profile (B) of the fat body extracts of the crickets.

Table 1. Melatonin Content and Concentration in Different Organs of the Adult Cricket

Organ	Content (pg/cricket)	Concentration (pg/g wet tissue)
Compound eye	5.43±1.15	263.48±49.25
Antenna	2.20±0.25	457.50±84.30
Ovipositor	1.91±0.18	240.18±38.81
Palp	2.66±0.50	122.27±16.54
Cercus	2.03±0.32	189.44±27.78
Fore-leg	1.88±0.10	117.32±24.25
Mid-leg	2.15±0.21	104.29± 7.19
Hind-leg	2.51±0.43	37.47±11.42
Wing	1.14±0.19	104.98± 9.78
Brain	1.61±0.10	83.12± 7.97
Ovary	1.91±0.09	30.08± 2.14
Digestive tube	1.70±0.17	20.75± 4.48
Malpighian tube	2.21±0.06	154.68±14.48

Each melatonin content and concentration were calculated by collecting the immunoreactivities of fraction No. 15–17 in the elution profiles obtained. Values are expressed as means and SEM derived from three separate experiments.

(pg/g wet tissue) calculated from the RIA profiles obtained from various organs of the crickets. The concentration in the sense organs, such as compound eye, antenna, ovipositor, palp, cercus, fore- and mid-legs, were usually higher than those of ovary and digestive tube.

Immunoreactive melatonin was unexpectedly detected in the fat body (Fig. 7B), although no peak of melatonin was observed in the elution profile obtained from the fat body (Fig. 7A), and its level was close to the RIA detection limit (1.60 pg/100 μl).

DISCUSSION

The present study gives clear proof of the presence of melatonin in different organs of adult crickets (Figs. 2–6 and Table 1). The proof of the presence of melatonin was obtained by two different methods, RP-HPLC with fluorometric detection and RIA. Since fluorometric detection is quite selective and highly sensitive for indole compounds [14], RP-HPLC with fluorometric detection is well suited to analysis of melatonin or other indole compounds in tissue and organ extracts of insects. However, the major immunoreactive peak at about 15.7 min was broad in some extracts, and weak immunoreactivities were observed at positions which differed from that of the melatonin standard (Figs. 2–6). This indicated that some chemical compounds or indoles other than melatonin in the crickets might interfere with its detection by RIA. Therefore, the melatonin content and concentration in the crickets was determined by collecting only those fractions corresponding to the melatonin peak, excluding all other fractions.

Melatonin in insects has previously been identified in the compound eye of the locust [23] and the head of the fruit fly [8]. The results obtained in the present study were consistent with these previous reports and revealed the presence of melatonin in other organs of the crickets. Melatonin in these organs is considered to be due to endogenous synthesis or uptake from a circulating pool. Activity of N-acetyltransferase, a key enzyme controlling melatonin synthesis in vertebrates, has been found in the brain of the fruit fly [6]. This suggests that melatonin may be synthesized in the brain of crickets. However, N-acetyltransferase activity in organs other than the brain is still unknown in insects. The peaks at about 2.3 and 4.3 min in the elution profile, as shown in Figures 2–7, corresponded to serotonin and N-acetylserotonin, respectively, the precursors of melatonin in vertebrates. This suggests that these precursors are also probably present in the melatonin-containing organs of the cricket and that melatonin may be synthesized in these organs via the same pathway as in vertebrates.

Several reports of the detection of melatonin in different organs of vertebrates have been published, as described in the Introduction. The functions of melatonin in extrapineal organs remain unknown. Several papers suggest that the extrapineal organs of vertebrates also exhibit diurnal rhythms associated with melatonin [17, 21, 25] or N-acetyltransferase activity [3, 4, 9]. Retinal melatonin has been supposed to play a role in circadian regulation of retinal physiology, such as pigment aggregation in the pigment epithelium [16] and shedding of outer segment discs [2]. In addition, gastrointestinal melatonin has been considered to inhibit gastrointestinal motility [10] and sodium absorption in the colon [15]. Based on these studies on vertebrates, we suggest that the melatonin-containing organs of the cricket may rhythmically synthesize melatonin, which may be involved in the local control of various aspects of rhythmic activity. It is also likely that melatonin in these organs is released into the blood and contributes to maintaining the melatonin levels in the systemic circulation, as has been proposed by Huether [12].

Melatonin was detected in various sense organs of the crickets, such as the compound eye, antenna, ovipositor, palp, cercus, fore- and mid-legs (Figs. 2–4 and Table 1) and, moreover, the melatonin concentrations in these sense organs were higher than those in ovary and digestive tube, as shown in Table 1. Sense organs are known to react directly to light, temperature, sound, touch, airmovement, chemical substances, etc. Melatonin inhibits the release of dopamine in rabbit retina [7] and rat hypothalamus [26]. Therefore, melatonin may modulate the activity of sensory cells and the transmission of signals from sensory cells to the central nervous system by influencing the release of neurotransmitters. Melatonin was also detected in the brain of the crickets (Fig. 5). From these facts, we might speculate that melatonin is implicated in the reception, transduction, transmission and integration of environmental information. The significance of the presence of melatonin in different organs should be further investigated.

ACKNOWLEDGMENTS

We thank Prof. K. Wakabayashi, Gunma University for the supply of anti-melatonin serum.

REFERENCES

1 Axelrod J (1974) The pineal gland: a neurochemical transducer. Science 184: 1341–1348

2 Besharse JC, Dunis DA (1983) Methoxyindoles and photoreceptor metabolism: Activation of rod shedding. Science 219: 1341–1343

3 Besharse JC, Iuvone PM (1983) Circadian clock in *Xenopus* eye controlling retinal serotonin N-acetyltransferase. Nature 305: 133–135

4 Binkley S, Hryshchyshyn M, Reilly K (1979) N-acetyltransferase activity responds to environmental lighting in the eye as well as in the pineal gland. Nature 281: 479–481

5 Bubenik GA (1980) Localization of melatonin in the digestive tract of the rat. Effect of maturation, diurnal variation, melatonin treatment and pinealectomy. Horm Res 12: 313–323

6 Dewhurst SA, Croker SG, Ikeda K, McCaman RE (1972) Metabolism of biogenic amines in *Drosophila* nervous tissue. Comp Biochem Physiol 43: 975–981

7 Dubocovich ML (1983) Melatonin is a potent modulator of dopamine release in the retina. Nature 306: 782–784

8 Finocchiaro L, Callebert J, Launay JM, Jallon JM (1988) Melatonin biosynthesis in *Drosophila*: its nature and its effect. J Neurochem 50: 382–387

9 Hamm HE, Meneaker M (1980) Retinal rhythms in chicks: Circadian variation in melatonin and serotonin N-acetyltransferase activity. Proc Natl Acad Sci USA 77: 4998–5002

10 Harlow HJ, Weekly BI (1986) Effect of melatonin on the force of spontaneous contractions of *in vitro* rat small and large intestine. J Pineal Res 3: 277–284

11 Hattori A, Wada M (1985) Diel changes in quail plasma concentration of melatonin under long day, short day and skeleton photoperiods. Proc of 10th Annual Meeting Japan Soc Comp Endocrinol pp 55

12 Huether G (1993) The contribution of extrapineal sites of melatonin synthesis to circulating melatonin levels in higher vertebrates. Experientia 49: 665–670

13 Kopp N, Claustrat B, Tappaz M (1980) Evidence for the presence of melatonin in the human brain. Neurosci Lett 19: 237–242

14 Leechin J (1988) Melatonin and other indoles in the rat pineal. J Chromatogr 428: 206–208

15 Legris GJ, Will PC, Hopfer U (1982) Inhibition of amiloride-sensitive sodium conductance by indoleamines. Proc Natl Acad Sci USA 79: 2046–2050

16 Pang SF, Yew DT (1979) Pigment aggregation by melatonin in the retinal pigment epithelium and choroid of guinea-pigs, *Cavia porcellus*. Experientia 35: 231–233

17 Pang SF, Chow PH, Wong TM, Tso ECF (1983) Diurnal variations of melatonin and N-acetylserotonin in the tissues of quails (*Coturnix* sp.), pigeons (*Columba livia*), and chickens (*Gallus domesticus*). Gen Comp Endocrinol 51: 1–7

18 Reiter RJ (1993) The melatonin rhythm: both a clock and a calendar. Experientia 49: 654–664

19 Reiter RJ, Richardson BA, Hurlbut EC (1981) Pineal, retinal and Harderian gland melatonin in a diurnal species, the Richardson's ground squirrel (*Spermophilus richardsonii*). Neurosci Lett 22: 285–288

20 Sallanon M, Claustrat B, Touret M (1982) Presence of melatonin in various cat brainstem nuclei determined by radioimmunoassay. Acta Endocrinol 101: 161–165

21 Vakkuri O, Rintamaki H, Leppaluoto J (1985) Presence of immunoreactive melatonin in different tissues of the pigeon (*Columba livia*). Gen Comp Endocrinol 58: 69–75

22 Vivien-Roels B, Pevet P (1993) Melatonin: presence and formation in invertebrates. Experientia 49: 642–647

23 Vivien-Roels B, Pevet P, Beck O, Fevre-Montange M (1984) Identification of melatonin in the compound eyes of an insect, the locust (*Locusta migratoria*), by radioimmunoassay and gas chromatography-mass spectrometry. Neurosci Lett 49: 153–157

24 Vivien-Roels B, Pevet P, Dubois MP, Arendt J, Brown GM (1981) Immunohistochemical evidence for the presence of melatonin in the pineal gland, the retina, and the Harderian gland. Cell Tissue Res 217:105–115.

25 Voisin P, Geffard M, Delaage M, Collin JP (1982) An immunological study of melatonin in the pineal organ, retina and plasma of the pigeon. Reprod Nutr Dev 22: 959–971

26 Zisapel N, Laudon M (1982) Dopamine release induced by electrical field stimulation of rat hypothalamus *in vitro*: inhibition by melatonin. Biochem Biophys Res Commun 104: 1610–1616

ZOOLOGICAL SCIENCE 11: 583–588 (1994)

Several Biochemical Alterations from Larval to Adult Types are Independent on Morphological Metamorphosis in a Salamander, *Hynobius retardatus*

Masami Wakahara, Norihisa Miyashita, Akane Sakamoto and Takako Arai

Division of Biological Sciences, Graduate School of Science, Hokkaido University, Sapporo 060, Japan

ABSTRACT—Biochemical transitions from larval to adult types, such as changes in hemoglobin subunits and pattern of excretion of nitrogen wastes, were studied during ontogeny of a salamander, *Hynobius retardatus*, which had been reported to show neotenic reproduction. A transition of hemoglobin subunits in normally metamorphosing and metamorphosed, and T_4-induced precociously metamorphosed *H. retardatus* was analyzed using SDS-PAGE. The transition of hemoglobin subunits from larval to adult types occurred on the same time schedule in both normally metamorphosing and precociously metamorphosed animals. A changeover from ammonotelism to ureotelism was analyzed by determining amounts of ammonia and urea excreted from normal and metamorphosis-arrested animals. A basic changeover from ammonotelism to ureotlism also occurred even in metamorphosis-arrested, aquatic larvae, on the similar time schedule in normally metamorphosing and metamorphosed animals. Because the transition of hemoglobin subunits in the metamorphosis-arrested larvae has been reported to occur on the same time schedule as in the controls, it is concluded that either transitions of hemoglobin subunits from larval to adult or pattern of nitrogen excretion from ammonotelism to ureotelism are independent on the morphological metamorphosis in *H. retardatus*. The substantial separation of biochemical "metamorphosis" from morphological metamorphosis will explain a possible cause of neoteny which has been reported in this species.

INTRODUCTION

Biochemical alterations in metamorphosing amphibian larvae have met with considerable interest as criteria illuminating the evolutionary past of these animnals, or as traits of adaptive significance for the transition from the aquatic to the terrestrial habitat [24]. Among various biochemical alterations, changes in molecular constituents of the body such as blood proteins [6], keratins [18] and hemoglobins subunits [4, 13, 24], and a pattern of nitrogen excretion [6, 17, 24] were extensively studied using many amphibian speceis. For instances, a switch in hemoglobin synthesis is reported to occur at metamorphosis, resulting in the replacement of the larval globin subunits by a set of distinct adult ones [9, 16]. Similarly to the hemoglobin transition, a pattern of nitrogen waste pruducts is known to change during metamorphosis in many species of amphibians which show a shift of habitats from aquatic to terrestrial according to the metamorphosis: excretion of ammonia exceeds that of urea during pre- and prometamorphic stages, whereas the situation is reversed in postmetamorphic and adult stages [24]. The shift from ammonotelism to ureotelism coincides with the metamorphic climax.

Contrary to anurans and ordinary urodelans, something different phenomena are known in neotenic urodelans. Axolotl, a neotenic form of *Ambystoma mexicanum*, has been reported to show the transition of hemoglobins from larval to adult types without any indications of anatomical metamorphosis [5, 13]. Similar has happened in *Hynobius retardatus*, which was reported to show neotenic reproduction in the specific environment of Lake Kuttara, a small volcanous lake not far from Sapporo [19, 20]: the transition of hemoglobin subunits from larval to adult types occurs on the same time schedule in both normally metamorphosing and metamorphosed animals and metamorphosis-arrested larvae [1]. Furthermore, we have recently demonstrated that *H. retardatus* can produce morphologically mature spermatozoa even in larval forms with well developed gills and tail fins when the metamorphosis is arrested by goitrogens [23]. Since *H. retardatus* shows very similar pattern of the transition of hemoglobins to that in the axolotl, and has an ability to undergo neoteny [19, 20], this salamander is expected to have similar biochemical characteristics to the axolotl or other salamanders showing the facultative neoteny. In the present study, a hemoglobin transiton from larval to adult types and a changeover of pattern of the nitrogen excretion from ammonotelism to ureotelism were analyzed using experimentally induced, precociously metamorphosed animals and metamorphsosis-arrested larvae of *H. retardatus*.

Accepted June 17, 1994
Received April 11, 1994

MATERIALS AND METHODS

Animals

Fertilized eggs of *Hynobius retardatus* were collected from several ponds or small streams in the vicinity of Sapporo in the

breeding season. Newly hatched larvae were reared at 10°, either in an aqueous solution of diluted thyroxine (T_4, 6×10^{-8} M) in order to induce a precocious metamorphosis, or in T_4-free solution as controls. Others were reared at a room temperature either in aqueous solution of 0.02% thiourea (TU) plus 0.02% sodium perchlorate (SPC) to arrest the metamorphosis, or goitrogen-free medium as controls. They were fed with live *Tubifex*. After they metamorphosed, they were transferred to a terrarium. Developmental stages were determined according to the normal table for *Hynobius nigrescens* [10].

Identification of hemoglobin subunits

Procedures for preparation of hemolysates from larvae, juveniles and adults were described previously [1]. After the amount of protein was determined using BCA Protein Assay Reagent (Pierce Chem. Co.), the samples were electrophoresed or frozen at −80°C. Samples from very small larvae were combined together because the amount of hemolysate from one larva was too small. Sodium dodecyl sulfate-polyacrylamide gel electrophoresis (SDS-PAGE) was performed according to Laemmli [11], using 15% separating gels [1]. All electrophoresed gels were stained with Coomassie Brilliant Blue.

Determination of amount of ammonia and urea

Each experimental larva or juvenile was placed in a Petri dish or grass beaker with a cover of proper size filled with 20 ml of 20 mM phosphate buffer (pH 6.8) for 24 hr. After removing unnecesary solids from the solution including excretion of laevae or juveniles with a centrifugation (3000 g, 7 min), a part of the samples was directly used for determination of amounts of ammonia as well as urea. The amount of ammonia was determined by means of phenol-chloramine T-spectrophotometry [8]. The amount of urea was determined according to the procedure by Archibald [2]. Three to 6 larvae or juveniles were used for one determination.

RESULTS

Larval development under various rearing conditions

Fig. 1 shows time courses of development in *H. retardatus* which were reared at 10°C, either in T_4 or T_4-free media. At 10°C which was employed to retard the metamorphosis in controls in order to make conspicuous the effects of T_4, the progress in larval development and metamorphosis was relatively slow. Almost all control larvae developed to stage 63, fully grown larval stage just before metamorphosis [10], 100–110 days after hatching [1]. Contrary to this, the larvae treated with T_4 developed much faster: they reached stage 63 approximately 50 days after hatching.

A wide variation in the progress in larval development and metamorphosis was observed at 10°C: some controls could complete metamorphosis by 180 days, but others could not complete even after 250 days of hatching (cf. [1]). At the end of this experiment (250 days after hatching), the average developmental stage of controls was stage 67.3, almost completion of morphological metamorphosis. The animals which were reared in T_4 completed metamorphosis approximately by 130 days after hatching. This indicated convincingly that exogeneously applied T_4 accelerated the metamorphosis in experimental groups for 60–90 days.

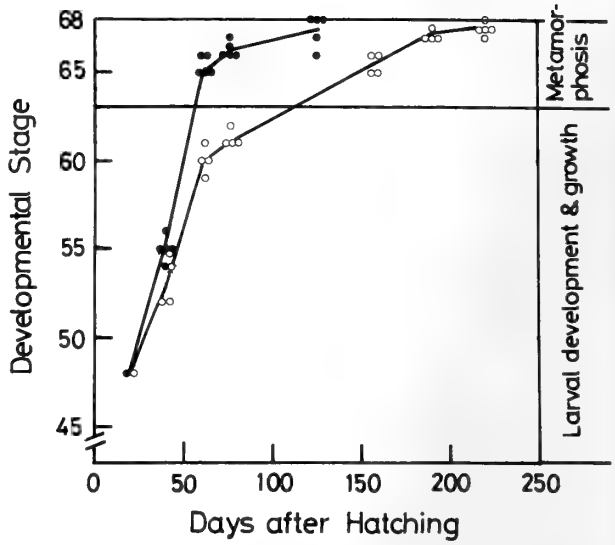

FIG. 1. Progress in larval developmental stages in *Hynobius retardatus*. Larvae just after hatching were reared in thyroxine (T_4) (closed circles) or T_4-free (open circles) media at 10°C. The larval developmental stages were determined according to Iwasawa and Yamashita [10]. The larvae treated with T_4 reach stage 63, fully grown larval stage just before metamorphosis, approximately by 50 days after hatching, whereas almost all controls develop to stage 63 after 100–110 days of hatching. The animals treated with T_4 complete metamorphosis by 130 days after hatching, whereas almost all controls metamorphose 220 days after hatching.

When the larvae were reared in an aqueous solution of thiouea (TU) and sodium perchlorate (SPC) at a room temperature, morphological metamorphosis was basically blocked at stage 64–65. Although all controls metamorphosed by 70 days after hatching, proceeding of the metamorphosis in the goitrogen-treated larvae was extremely retarded or basically arrested (see Fig. 5 of [1]). No larvae treated with goitrogens completed morphological metamorphosis within this experiment (250 days after hatching). All larvae reared in goitrogens had external gills and well developed tail fins which were characteristic to aquatic forms, and appeared to adapt to the water habitat (Fig. 2).

Hemoglobin transition

Fig. 3 shows electrophoretic profiles of hemoglobin subunits from normally metamorphosing and metamorphosed animals reared at 22°C and 10°C. Typical larval globins were separated into 2 bands (L1 and L2) on SDS-PAGE. Approximate molecular weights of them were 13700 and 15000. Adult hemoglobins were shown to be composed of 3 fractions (A1 to A3) whose molecular weights were estimated as 14000, 15000 and 15500, respectively. Adult type subunits were already detected in the larvae of 35 days after hatching at 22°C (Panel A, lane a, arrowheads). Similarly to this, adult type subunits were observed in the larvae of 126 days after hatching at 10°C. Inversely, the larval type bands were getting faint (Panel B, lane a, arrowhead). In the larvae of 189 days (when the average developmental stage

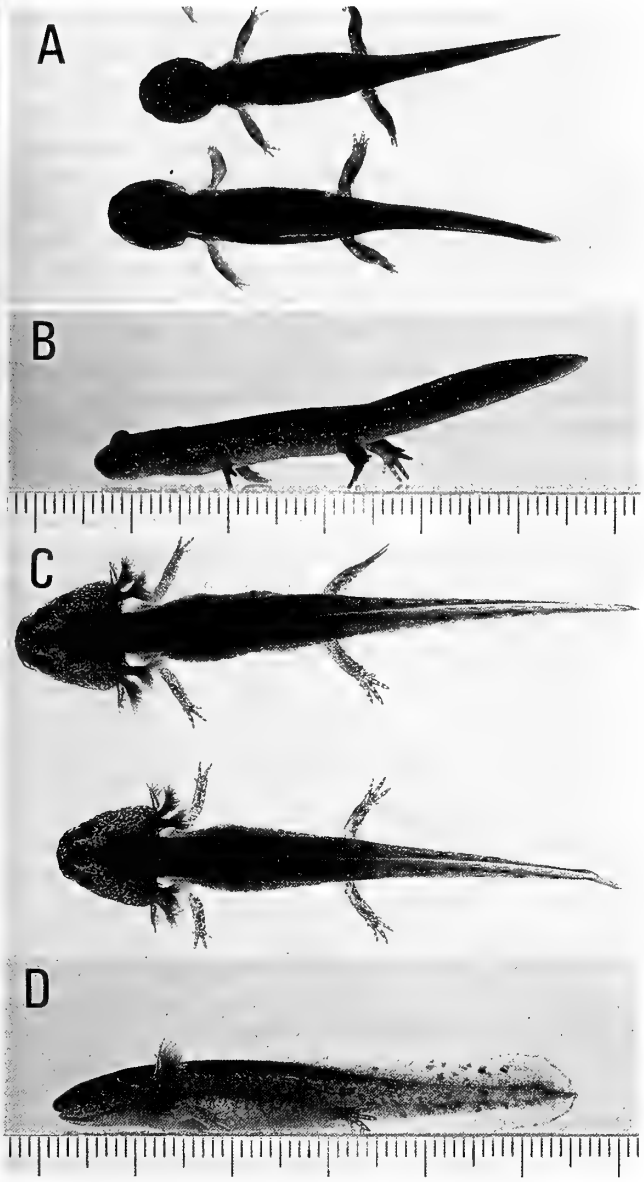

FIG. 2. External morphology of metamorphosed *Hynobius retardatus* and metamorphosis-arrested larvae. Larvae just after hatching were reared in an aqueous solution of thiourea plus sodium perchlorate or in the goitrogen-free (control) media at room temperature. Dorsal (A) and lateral (B) views of metamorphosed controls on 68 days after hatching. Dorsal (C) and lateral (D) views of metamorphosis-arrested larvae of the same age as the metamorphosed controls. All controls complete metamorphosis 70 days after hatching and shift to terrestrial habitats. Metamorphosis-arrested larvae have well developed external gills and tail fins, and fully adapt to the aquatic habitat.

was stage 66.5), the larval bands could not be detected on SDS-PAGE (Panel B, lane c). This indicates that the transition of hemoglobins from larval to adult types finishes before the completion of morphological metamorphosis in the larvae reared at 10°C.

Fig. 4 shows electrophoretic profiles of hemolysates from T_4-treated and T4-free animals reared at 10°C. Adult bands did not detected on 40 days after hatching (lanes a, b, c), but

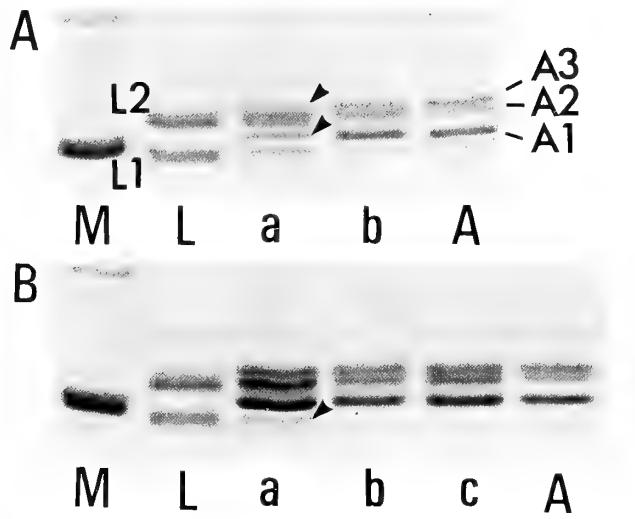

FIG. 3. Typical electrophoregrams of hemoglobins in *Hynobius retardatus*. Time courses in the transition of hemoglobins from larval to adults types at 22°C (A) and 10°C (B) were analyzed on SDS-PAGE. Panel A, lane M, molecular marker (top, 20K, bottom, 14K); L, hemolysate from typical larvae (3 days after hatching); a, 35 days after hatching; b, 68 days after hatching; A, hemolysate from typical adult. Larval hemoglobins are separated into 2 bands (L1 and L2). Adult globins are separated into 3 bands, A1 to A3. Adult type subunits are clearly seen in 35 days larvae (lane a, arrowheads). Panel B, lane M, molecular marker; L, typical larvae; a, 126 days after hatching; b, 159 days after hatching; c, 189 days after hatching; A, typical adult. Larval type subunits are getting faint in 126 days (lane a, arrowhead) and disappeared in 189 days larvae (lane c).

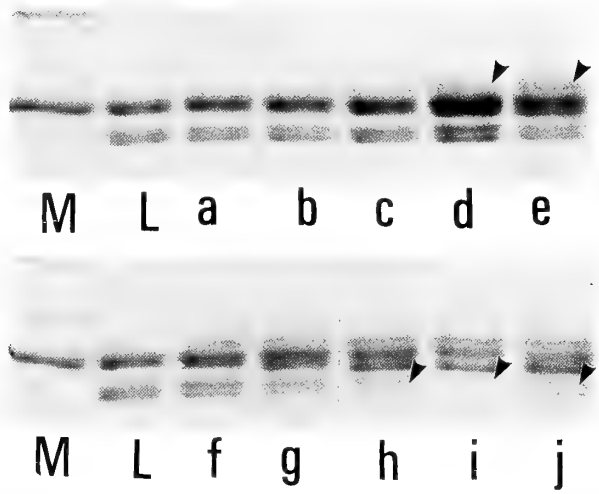

FIG. 4. Electrophoretic profiles on SDS-PAGE showing the transition of hemoglobins from larval to adult types. Hemolysates were prepared from precociously metamorphosed (T_4-treated) and control (T_4-free) animals at 10°C. Lane M, molecular marker (top, 20 K, bottom, 14 K); lane L, typical larval hemolysate; lanes a and b, control, 40 days; lane c, T_4-treated, 40 days; lane d, control, 68 days; lane e, T_4-treated, 68 days; lane f, control, 78 days; lane g, T_4-treated, 78 days; lane h, control, 157 days; lanes i and j, T_4-treated, 157 days. Adult type subunits appear on 68 days after hatching in both T_4-treated, and T_4-free animals (arrowheads on lanes d and e). Larval type subunits in the controls are getting faint on the same time cources as in the precociously metamorphosed animals (arrowheads on lanes h, i and j).

faintly appeared on 63 days after hatching in both T_4-treated, precociously metamorphosing animals (lane e) and T_4-free, normal control (lane d). Similarly to these, disappearance of larval bands in precociously metamorphosed animals began on the same time schedule as in the controls (lanes h, i, j; 157 days after hatching).

Pattern of nitrogen excretion

Amount of nitrogen (N) out of ammonia and urea excreted from larvae and juveniles during the ontogeny in normal controls and in the metamorphsosis-arrested larvae was determined at the level of μg N/body wight (g)/day. Fig. 5 shows combined data from three different experiments demonstrating changeover from ammonotelism to ureotelism during the ontogeny and in the metamorphosis-arrestesd larvae of *H. retardatus*. Each point on the graph indicates an average of 3 to 6 determinations using individual larvae or juveniles, respectively. Although considerable variations were found in each experiment, it was clear a major nitrogen

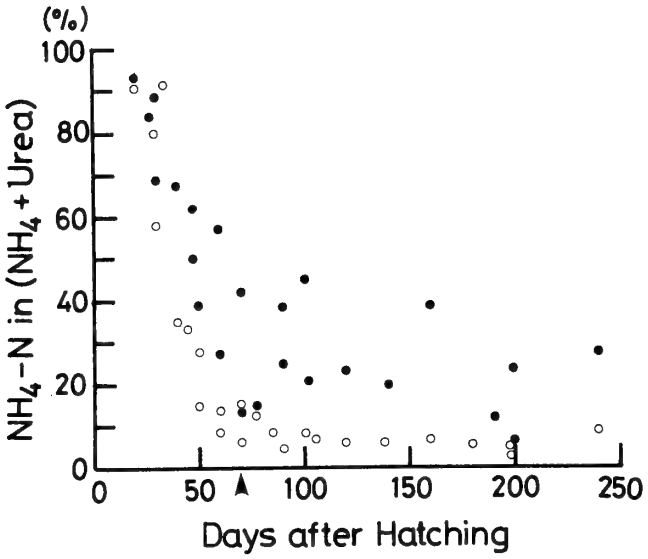

FIG. 5. Changes in the pattern of nitrogen excretion from ammonotelism to ureotelism in *Hynobius retardatus*. Amounts of ammonia and urea excreted from individual animals were measured respectively, and ratio of ammonia-nitrogen (NH_4-N) to total-(NH_4+urea)-N was calculated. An arrowhead on abscissa indicates the completion of metamorphosis in controls. In the controls (open circles), approximately 90% of the (NH_4+urea)-N is ammonia before and during early metamorphosis. After the metamorphosis, the ratio of ammonia-N to the (NH_4+urea)-N is maintained at 5–10% (in average, 7.0±3.3%) level. In the metamorphosis-arrested larvae (closed circles), approximately 80–90% of the (NH_4+urea)-N is ammonia during the early larval stages, similarly to the controls. After the controls completed metamorphosis, the ratio of ammonia-N in the metamorphosis-arrested larvae gradually decreases to the level of 10–40% (in average, 25.0±12.0%). Level of the ratio of ammonia-N to the (NH_4+urea)-N in controls after the metamorphosis is significantly lower than in the metamorphosis-arrested larvae ($p<0.01$ in Student's t test). These are combined data from three different experiments. Each point indicates an average of 3 to 6 determinations using individual larvae or juveniles, respectively.

waste was ammonia in larval stages both in control and metamorphosis-arrested groups. In the controls (Fig. 5, open circles), approximately 90% of nitrogenous wastes (nitrogens of ammonia plus urea) was ammonia before metamorphosis and during early metamorphosis. During metamorphosis, however, the ratio of ammonia-N drastically decreased and then maitained at a 5–10% level after the metamorphosis. In metamorphosis-arrested larvae (Fig. 5, closed circles), the pattern of nitrogen excretion was basically same as in the controls during early development: approximately 80–90% of nitrogenous wastes was ammonia. After the controls completed metamorphosis, the major nitrogen waste products gradually change from ammonia to urea in the metamorphosis-arrested larvae, even though they showed typical larval forms morphologically (Fig. 2). Timing of the increase in urea excretion (conversely the decrease in ammonia excretion) in the metamorphosis-arrested larvae was a little later than that in the controls. Furthermore, the level of ammonia excreted from the controls after metamorphosis (in average, 7.0±3.3% of total nitrogen) was significantly lower than that of the metamorphosis-arrested larvae (25.0±12.0%).

DISCUSSION

Transition of hemoglobin subunits

Although the beginning and completion of the metamorphosis are accelerated in T_4-treated animals for 50–90 days compared with the normal controls reared at 10°C, the transition of the hemoglobin subunits from larval to adult types occurs on the same time schedule in both control and experimental groups. This suggests convincingly that though exogeneously applied thyroid hormone induces precocious metamorphosis at the morphological level, it does not induce biochemical precocious "metamorphosis". This result supports furthermore our previous results, which demonstrated the hemoglobin transition occurred even in metamorphosis-arrested larvae on the same time schedule as in the controls [1], and is consistent with the observations showing the transition was completely independent on the morphological metamorphosis in axolotl [5, 13].

Because hemoglobins from metamorphosing larvae of *H. retardatus* were separated into 8 different polypeptides on the two-dimentional electrophoresis [1], the globin subunits are considered to be encoded by 8 different genes, 4 larval and 4 adult genes whose expressions are developmentally regulated. In many anurans, it is reported that the larval hemoglobin subunits stop being produced after a thyroid hormone treatment due to the down-regulation of the corresponding genes, whereas the genes coding the adult hemoglobin subunits are up-regulated [25]. Contrary to these, an earlier observation demonstrated that the hemoglobin transition in *Xenopus laevis* was determined more by chronological age, or size, or some other independent factors, rather than the hormonal control by thyroid hormones [14]. The present results which have shown an independence of the

transition of hemoglobin subunits on exogeneously applied T_4 are consistent with the latter: the hemoglobin transiton in *H. retardatus* is possibly determined by chronological age.

Pattern of nitrogen excretion

The conversion of the pattern of nitrogen excretion has been thought to be controlled internally by the effects of thyroid hormones [24] and/or externally by environmental conditions where the animals are placed [3, 12, 15]. Since the transition occurred during the climax of metamorphosis in normal controls (Fig. 5), it is assumed that increasing concentrations of the circulating thyroid hormones play some roles on this transition in *H. retardatus* as well. This explanation is consistent with the fact that the level of the urea excretion was relatively lower in the metamorphosis-arrested larvae than in the controls, probably due to a shortage of thyroid hormones in the former.

Because the goitrogens used in this experiment are considered to suppress substantially the thyroid activity [23], concentrations of the circulating thyroid hormones in the metamorphosis-arrested laevae was expected to be very low so that the morphological metamorphosis was basically arrested [1, 23]. In spite of the fact, a substantial transition from ammonotelism to ureotelism occurred in the metamorphosis-arrested larvae, though the timing of the transition was a little later than the conspicuous transition in the controls (Fig. 5). Because it has been reported that a major nitrogen excretion in the axolotl is urea [21], it seems possible that the metamrophosis-arrested larvae in *H. retardatus* excrete nitorogenous wastes as urea, even though they adapted to the aquatic habitat. A possible explanation for this is as follows: the substantial transition from ammonotelism to ureotelism in the metamorphosis-arrested larvae is regulated by thyroid hormones of very low concentrations which are insufficient to induce morphological metamorphosis. This will explain a retardation of the transition, and an insufficient transition in the metamorphosis-arrested larvae compared with the controls (Fig. 5).

The detoxication of ammonia constitutes an important biochemical adaptation to the restriction of water supply in amphibians which shift from aquatic to terrestrial habitats [3]. Thus, *Xenopus laevis*, which lives in aquatic forms even after metamorphosis, excretes major nitrogen waste products as ammonia [17, 24]. Furthermore, changes in the pattern of nitrogen excretion from ammonotelism to ureotelism have been reported after adult *Xenopus* has been exposed to restricting water supply [3], or high osmolarity [15]. From this point of view, aquatic larvae of *H. retardatus* which have been treated with the goitrogens and axolotl need not to change the pattern of nitrogen excretion from ammonotelism to ureotelism, because they are surrounded by a lot of water and fully adapted to an aquatic habitat. The fact that the ratio of ammonia-nitrogen excreted from metamorphosis-arrested larvae (10–40%, in average $25.0\pm2.0\%$) was considerably higher than that from controls (5–10%, in average $7.0\pm3.3\%$) will answer to this: although a substantial transiton is expected to be induced by thyroid hormones of very low concentrations, an aquatic environment resulting from the incompletion of the metamorphosis affects on the mechanism of nitrogen excretion, probably on the activity of enzymes of the ornithine cycle in liver [12]. Thus, the alteration of nitrogen excretion in *H. retardatus* will be regulated by a combination of hormonal controls and environmental conditions. Since it was difficult to treat separately hormonal (internal) and environmental (external) conditions, degrees of their involvement in the transiton of nitrogen excretion were not examined in this study. Determinations of the concentrations of circulating thyroid hormones are necessary to elucidate these, and now in progress.

Heterochrony in phenotypic expression

Although the transition of hemoglobin subunits from larval to adult types occurs on the same time schedule in both normally metamorphosing and metamorphosis-arrested animals [1], the transition of nitrogen excretion from ammonotelism to ureotelism in the metamorphosis-arrested larvae occurs a little later than in the controls. Furthermore, it has been reported that the gonadal development is much earlier than the somatic development in metamorphosis-arrested *Hynobius* [23]. These chronological differences in phenotypic expression or development imply possible differences in the sensitivity to thyroid hormones among various tissues. Since axolotls are reported to be able to produce thyroid hormones at a very low level, and accomplish a number of cryptic metamorphic processes [22], different tissues or cells will behave differently in response to the thyroid hormones. Thus, it is possible that the morphological or anatomical metamorphosis such as disappearance of external gills and tail fins is accelerated by relatively high concentrations of circulating thyroid hormones, but that the biochemical "metamorphosis" such as the transition of nitrogen excretion is regulated by very low concentrations of thyroid hormones and/or in part by environmental conditions. The transition of hemoglobin subunits and the developement of germ cells will be regulated by some other factors, rather than the hormonal control by thyroxine. These heterochronic phenotypic expressions or development will be fundamental causes of the reported neoteny in this species [7].

REFERENCES

1 Arai T, Wakahara M (1993) Hemoglobin transition from larval to adult types in normally metamorphosing, metamorphosed and metamorphosis-arrested *Hynobius retardatus*. Zool Sci 10: 637–644

2 Archibald RM (1945) Colorimetric determination of urea. J Biol Chem 157: 507–518

3 Balinski JB (1961) Adaptation of nitrogen metabolism to hyperosmotic environment in Amphibia. J Exp Zool 215: 335–350

4 Cardellini P, Sala M (1979) Metamorphic variations in the hemoglobins of *Bombina variegata* (L.). Comp Biochem Physiol 64B: 113–116

5 Ducibella T (1974) The occurrence of biochemical metamorphic events without anatomical metamorphosis in the axolotl. Devel Biol 38: 175–186

6 Frieden E (1961) Biochemical adaptation and anuran metamorphosis. Am Zool 1: 115–149

7 Gould SJ (1977) "Ontogeny and Phylogeny". Harvard University Press, Cambridge

8 Grismer MR (1937) Colorimetric determination of ammonia. Bull Soc Chim Biol 19: 1000–1006

9 Hosbach HA, Widmer HJ, Andreas A-C, Weber R (1982) Expression and organization of the globin genes in *Xenopus laevis*. In "Embryonic Development, Part A: Genetic Aspects". Ed by MM Burger, Weber R, Alan R Liss, New York, pp 115–125

10 Iwasawa H, Yamashita K (1991) Normal stages of development of a hynobiid salamander, *Hynobius nigrescens* Stejneger. Jpn J Herpetol 14: 39–62 (in Japanese with English Abstract)

11 Laemmli UK (1970) Cleavage of structural proteins during the assembly of the head of bacteriophage T4. Nature 227: 680–685

12 Lee AR, Silove M, Katz U, Balinski JB (1982) Urea cycle enzymes and glutamate dehydrogenase in *Xenopus laevis* and *Bufo viridis* adapted to high salinity. J Exp Zool 221: 169–172

13 MacLean N, Jurd RD (1972) The control of haemoglobin synthesis. Biol Rev 47:393–437.

14 MacLean N, Turner S (1976) Adult hemoglobin in developmentally retarded tadpoles of *Xenopus laevis*. J Embryol Exp Morph 35:261–266

15 McBean RL, Goldstein L (1970) Accelerated synthesis of urea in *Xenopus* during osmotic stress. Am J Physiol 219: 1124–1130

16 Moss B, Ingram VM (1968) Hemoglobin synthesis during amphibian metamorphosis II. Synthesis of adult hemoglobin following thyroxine administration. J Mol Biol 32: 481–504

17 Munro AF (1953) The ammonia and urea excretion of different species of Amphibia during their development and metamorphosis. Biochem J 54: 29–36

18 Nishikawa A, S-Nishikawa K, Miller L (1992) Spatial, temporal, and hormonal regulation of epidermal keratin expression during development of the frog, *Xenopus laevis*. Devel Biol 151: 145–153

19 Sasaki M (1924) On a Japanese salamander, in Lake Kuttarush, which propagates like the axolotl. J Coll Agr Hokkaido Imp Univ 15: 1–36

20 Sasaki M, Nakamura, H (1937) Relation of endocrine system to neoteny and skin pigmentation in a salamander, *Hynobius lichenatus* Boulenger. Annot Zool Japon 16: 81–97

21 Schultheiss H (1977) The hormonal regulation of urea excretion in the Mexican axolotl (*Ambystoma mexicanum* Cope). Gen Comp Endocrinol 31: 45–52

22 Tompkins R (1978) Genetic control of axolotl metamorphosis. Am Zool 18: 313–319

23 Wakahara M (1994) Spermatogenesis is extraordinarily accelerated in metamorphosis-arrested larvae of a salamander, *Hynobius retardatus*. Experientia 50: 94–98.

24 Weber R (1967) Biochemistry of amphibian metamorphosis. in "The Biochemistry of Animal Development, vol 2". Ed by R Weber Academic Press, New York, pp 227–310

25 Widmer BA, Andreas AC, Niessing J, Hosbach HA, Weber R (1981) Comparative analysis of cloned larval and adult globin cDNA sequences of *Xenopus laevis*. Devel Biol 88:325–332

ZOOLOGICAL SCIENCE 11: 589–595 (1994)

Colony Formation via Sexual and Asexual Reproduction in *Salmacina dysteri* (Huxley) (Polychaeta, Serpulidae)

EIJIROH NISHI[1] and MORITAKA NISHIHIRA[2]

[1]*Amakusa Marine Biological Laboratory, Kyushu University, Amakusa, Kumamoto 863-25 and* [2]*Biological Institute, Faculty of Science, Tohoku University, Aoba-ku, Sendai 980, Japan*

ABSTRACT—Reproduction and colony formation in the tubicolous serpulid polychaete *Salmacina dysteri* (Huxley) were investigated on the Okinawan coral reef. Numerous individuals of this species aggregate and construct an arborescent pseudo-colony which is formed by physiologically unconnected individuals. This species reproduces both sexually and asexually. The proportion of the two modes of reproduction varied according to the position of individuals in the colony. Growing tips of colony branches included more asexually reproducing worms, while basal or central parts of a colony contained more sexually mature ones. The predominant mode of reproduction in a colony changed with colony size. In colonies with < about 500 worms, asexual reproduction was more frequent than sexual reproduction, but in colonies with >2,000 worms, sexual reproduction predominated.

INTRODUCTION

Annelids show various modes of reproduction, such as sexual and asexual reproduction, dioecism and hermaphroditism, brooding and broadcast spawning, viviparity, external and internal fertilization, *etc.* [18]. Among the polychaetes, asexual reproduction is least mode of reproduction. Detailed reproductive processes have been reported in many polychaete families, and the colonial status was achieved through asexual budding in cirratulids [7], spionids [21], sabellids and serpulids [8]. Asexual cloning is seen in *Dodecaceria concharum* and *D. fewkesi* [1, 7], and *D. fewkesi* builds separate male and female colonies through asexual reproduction [1]. Gibson [7] noted that, the colonies of all asexually reproducing species of *Dodecaceria* can theoretically be produced from a single ovum. The relationship between asexual cloning and colony forming process has not been previously studied in polychaetous annelids.

Individuals of *Salmacina dysteri* form calcareous, arborescent aggregations, which lack physiological connections between individual worms [6, 15]. We use the term "pseudo-colony" for such an aggregation according to Knight-Jones & Moyse [10]. *Salmacina dysteri* can perform various reproductive modes; worms may be male, female, or hermaphroditic, and reproduce asexually budding [14, 15]. The interaction among these modes has not been known up to now in pseudo-colonial polychaetes, though interaction of sexual and asexual reproduction has been detected in eucolonial organisms, which have physiological connections, especially in relation to the age or size of the colony [2, 11].

In the present study, we analyze the interaction of sexual and asexual reproduction according to size or age of the pseudo-colony of *S. dysteri*.

Accepted July 4, 1994
Received July 26, 1993

SAMPLING SITES AND MATERIALS

Field studies were conducted on Sesoko Island (26° 38'N, 127° 52'E), Okinawa, South-western Japan (Fig. 1). Two study sites were selected; 1) a mass of a concrete block artificial reef set off Sesoko Island, and 2) the vertical wall of the pier in Hamasaki Port. The former was at a depth of about 10 m, the latter 2 m to 4 m. The

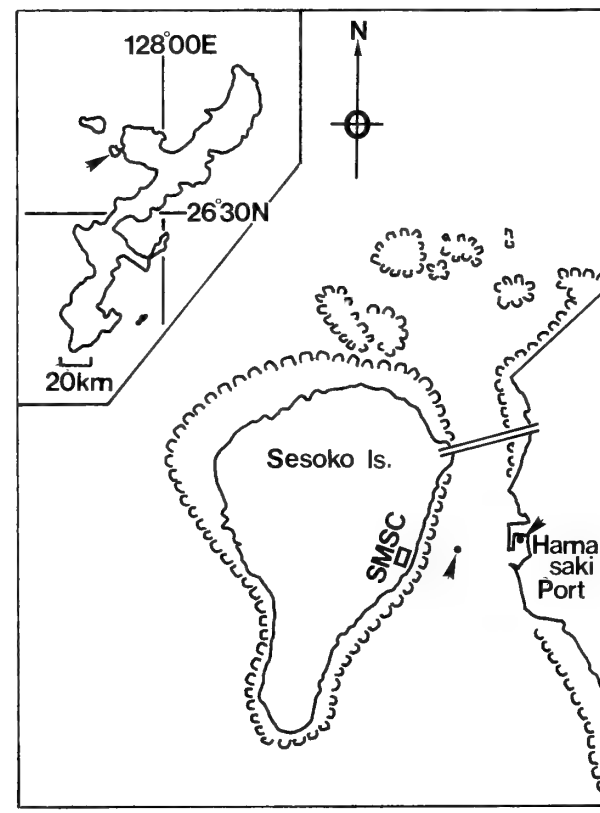

FIG. 1. Map of the study area. Arrow in the inserted map shows Sesoko Island, two dots pointed with arrows show the sampling points. SMSC, Sesoko Marine Science Center.

bottoms of both sites were covered by sand or mud substrata. The sea water temperature of these sites ranged from 18 to 32°C during the year [12]. The pseudo-colonies of *Salmacina dysteri* were found attaching to hard substrata such as dead coral skeletons, concrete blocks, bivalve shells, etc. at a depth of 5 m to 10 m.

Pseudo-colonies of *S. dysteri* were arborescent, and looked like a dead eu-colony of a finely branching coral *Seriatopora histrix* (Fig. 2; similar shaped pseudo-colonies were found at the port of Iwaya, Awajishima, Central Japan [22]). Pseudo-colonies 5 to 10 cm in diameter (which include 500 to 2000 worms per colony) were common. The size of a mature individual is 2 to 3 mm in length including a branchial crown, and 0.2 mm in width. The branchial crown consists of 4 pairs of white filaments, an operculum is absent [9]. The thorax and abdomen are red, each having 6–7 and 8–25 segments respectively.

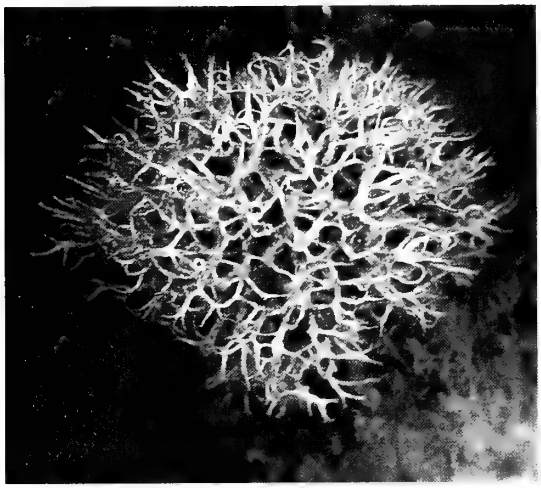

FIG. 2. Arborescent colony of *Salmacina dysteri*, about 20 cm in diameter.

METHODS

Identification of species

Salmacina dysteri and sympatric related species can only be separated based on their collar setal morphology or teeth distributional pattern [13]. Scanning electron microscopy (SEM) was used for the identification of *S. dysteri*. For SEM, worms were fixed in 2.5% glutaraldehyde buffered in seawater, rinsed, dehydrated, dried with a critical-point dryer using liquid CO_2, and coated with gold-palladium. Usually, 5 to 20 worms were selected at random from a pseudo-colony, then viewed with the SEM and checked for their collar setal morphology.

Inter-colonial variation of the proportion of juveniles

The number of juveniles with a small body was recorded separately from the number of adults. Pseudo-colonies were collected between April and June 1989. Juveniles were separated by their body size into two categories. Juveniles which were sexually produced had 3 pairs of branchial filaments and a thin semi-transparent tube [16]. Their thoracic and abdominal segments were short and had fewer segments (3–8) than adults (10–25). By contrast, juveniles which had originated from buds by asexual reproduction had 8 branchial filaments [13] and wide abdominal segments which were comparable to those of adults. These asexually produced juveniles had 4–5 thoracic and 7–10 abdominal segments. After 1 month following settlement of larvae or 2 weeks from the release of a bud from the stock, these juveniles could not be identified from each other or from adult worms.

Inter- and intra-colonial variation of reproductive modes

In order to know the inter- and intra-pseudo-colonial variations of reproductive modes, the numbers of sexually mature and asexually reproducing worms were recorded for some pseudo-colonies. Materials were collected between April and June 1989 to minimize seasonal effects. Individuals in the male phase have white segments, whereas those in the female phase have brown ovoid eggs in the coelom or the tube. Asexually reproducing worms have a bud in various developmental stages in their abdomen. If the worm with adult size and morphology lacked a bud on its abdomen or eggs and embryos in the abdomen or tube, it was treated as an immature worm or juvenile. In this paper, sexually mature worms represent, male, female, and hermaphroditic worms. Asexually reproducing female or male worms rarely appeared (unpublished data). However, the samples analyzed in this study did not contain a worm reproducing sexually and asexually simultaneously.

Experimental halving of pseudo-colony

To study the effect of pseudo-colony size on the reproductive mode, six pseudo-colonies with various sizes (ranging from 8–11 cm, averaging 9 cm in diameter) were selected, and about half of each colony was sampled to check the proportion of reproductive worms. The remaining half (about 4 cm in diameter) was left as it was on the substrate. Six weeks later, these latter halves were collected to check the proportion of reproductive worms. This field experiment was conducted between July and August, 1989. About 50–80% of worms (100 to 200 worms) in each pseudo-colony were examined under an dissecting microscope. The worms were collected from all positions of a colony to minimize intra-pseudo-colonial variation of reproductive modes.

Effect of pseudo-colony age on reproductive modes

In order to know the effect of age on reproductive modes, the relationship between progressed time (month) from initial observation and reproductive ability was tentatively calculated from field experiments conducted between April 1989 and July 1990. Seventeen small pseudo-colonies about 3 to 5 cm in diameter (with an estimated age 2 to 5 months from settlement) were selected, then only a part of a branch (10 to 50 worms) was collected and checked for reproductive ability. All the colonies remained in the field. After some (1 to 6) months, 2, 3 or 4 colonies were re-collected and checked for their reproductive activity. This

experiment was initiated in spring or summer months. When we check their reproductive ability, because intracolonial variation of reproductive modes may appear [14], worms were collected from various positions (peripheral, middle and central positions) within a pseudo-colony.

Induction of asexual budding in solitarily reared worms

A total of 70 sexually mature worms with calcareous tubes were reared solitarily for 1 month in glass dishes (8 cm in diameter, 10 ml in capacity) in a natural light regime. The water temperature was 22–28°C. Diatoms were added as food each week. Ten fragmented branches (containing 10 to 30 worms) with calcareous tubes were taken from a central part of a large colony about 10 cm in diameter. They were then also reared in separate dish after identifying sex of each worm if possible.

Aggregation during larval settlement

In order to know whether larvae aggregate during the settlement event, trochophore larvae at the 3 setiger stage were gathered from 5 pseudo-colonies by breaking the tubes of brooding females, and released in 4 sets of petri-dishes (9 cm in diameter, 120 ml in capacity). After 1 week, almost all of the larvae had settled, gregariously or solitarily. If tubes of settled worms touched other tubes, it was categorized as aggregation.

RESULTS

Intra-colonial variation of two reproductive modes

Within a single pseudo-colony, particularly larger ones, peripheral parts had a higher proportion of asexually reproducing worms than basal and lower middle parts (Benferroni's t-test, $P<0.05$, Fig. 3). The proportion of sexually mature worms was higher in the basal and lower middle parts (Benferroni's t-test, $P<0.05$). Between the lower and upper middle parts, the difference in the proportions of sexually mature and asexually reproducing worms were not significant (Benferroni's t-test, $P>0.05$).

Inter-colonial variation of the proportion of juveniles

It was possible to discriminate between juveniles produced sexually and asexually. In a single pseudo-colony, there were both juveniles produced by sexual and asexual reproduction in various proportions (Fig. 4). The proportion of sexually produced juveniles was higher in larger colonies than in smaller ones. The positive correlation between the proportion of sexually produced juveniles and colony size was significant ($r=0.678$, $P<0.01$).

Inter-colonial variation of two reproductive modes

The pseudo-colonies of *S.dysteri* consisted of many worms in various stages of their life cycles. Newly formed smaller pseudo-colonies (<200 worms) usually contained mostly sexually immature and asexually reproducing worms, but larger ones (>2000 worms) contained abundant hermaphroditic worms (Fig. 5). The proportion of hermaphroditic worms seems to be correlated with pseudo-colony size (in terms of total number of worms) ($r=0.802$, $P<0.01$). However, the correlation between the number of males and pseudo-colony size was not significant ($r=0.385$, $P>0.05$). The proportion of asexually reproducing worms

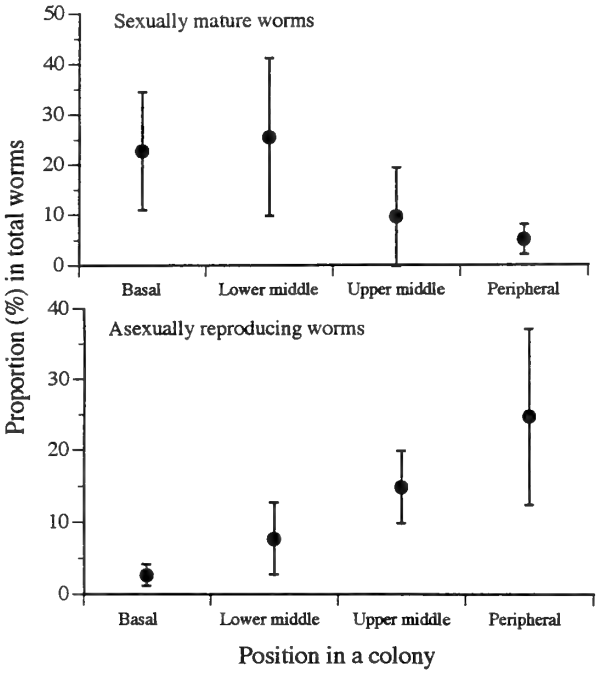

FIG. 3. Proportion of sexually mature and asexually reproducing worms in different parts of 3 colonies of *Salmacina dysteri*. Three colonies were examined between April and June (colonies 5, 8, and 10 cm in diameter), 1989. Ten to 20 worms were examined from 4 parts of each colony, vertical line shows the S.D.

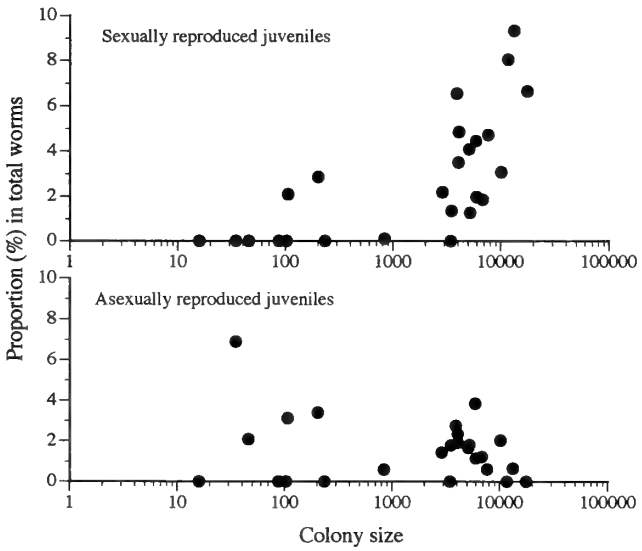

FIG. 4. Relationship between colony size (in terms of number of worms) and proportions of sexually (top graph) and asexually (lower graph) reproduced juveniles in *Salmacina dysteri*.

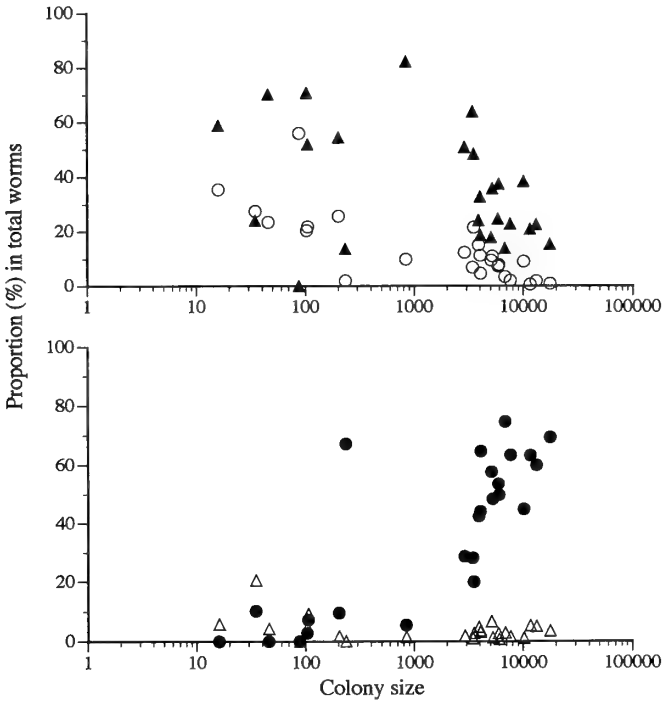

FIG. 5. Relationship between colony size (in terms of the number of worms) and abundance of reproducing worms which have a normal adult shape (with 8 branchial filaments and >10 abdominal segments) in *Salmacina dysteri*. All colonies were collected between April and June, 1989. Whole worms were examined except for the largest 5 colonies where only 60 to 70% were checked. ○, asexually reproducing worms (upper graph); ▲, immature worms (upper graph); △, males (lower graph); ●, hermaphroditic worms (lower graph).

was negatively correlated with the size of the pseudo-colony ($r=-0.759$, $P<0.01$).

Relationship between estimated pseudo-colony age and reproductive modes

The relationship between pseudo-colony age (expressed by month from initial observation) and the proportion of the mode of reproduction is depicted in Fig. 6. A pseudo-colony survived a maximum of 6 months from the initiation of observation. The growth rate of the pseudo-colony was roughly estimated. The growth of the pseudo-colony was about 1–2 cm in diameter per month.

Since the growth of pseudo-colonies was not studied from the initiation of the pseudo-colony formation (i.e., settlement of larvae), the age of pseudo-colonies was estimated from the preliminary growth experiment (unpublished data); the age of pseudo-colonies with a diameter of 1–2 cm (2 to10 worms in a pseudo-colony) seemed to be 1 month from the settlement, that with 3 cm in diameter (about 20 to 30 worms) 2 months, and that with a 4 cm diameter (about 40 to 60 worms) 3 months. The pseudo-colonies with an estimated age of about 3 to 5 months (1 to 3 months in Fig. 6) contained few sexually reproduced worms, but contained many asexually reproducing worms (20–30% of the total number). In pseudo-colonies more than 6 months (4 to 6

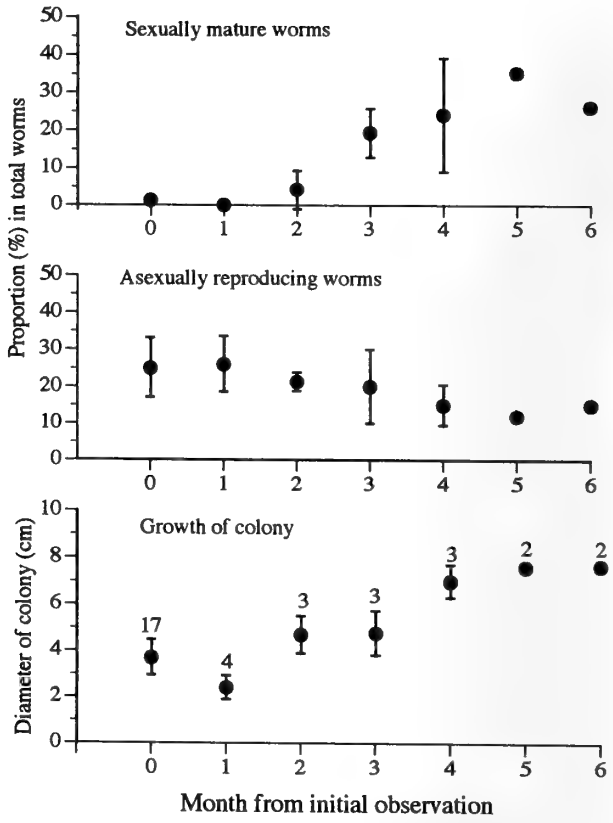

FIG. 6. Relationship between months from initial observation and proportion of sexually (male plus hermaphroditic worms) (upper graph) and asexually (middle graph) reproducing worms in *Salmacina dysteri*. Observations were conducted between April, 1989 and July, 1990, and initiated from small size, 3 to 5 cm in diameter (estimated age of which being 2 to 5 months after the settlement). After some months, worms representing about 20 to 50% of the total worms in a collected colony were examined. Worms were collected from basal, middle, and peripheral parts of the colony to mitigate intra-colonial reproductive variation. The number on the bar in the lower graph shows the number of colonies analyzed. Lower graph; change in colony size (mean±S.D) during observation.

months in Fig. 6), both sexually mature and asexually reproducing worms were found, but the former were more abundant than the latter. The proportion of sexually mature worms (male and hermaphroditic worms) increased with time from initial observation ($r=0.757$, $P<0.01$). The proportion of asexually reproducing worms showed an negative correlation with time from initial observation ($r=-0.589$, $P<0.01$).

Experimental halving of pseudo-colony size

The broken pseudo-colonies still showed a significant sexual reproductive capability 2 weeks after the artifical break, but within 1 to 2 months, they increased the proportion of asexual reproduction to a degree comparable to that of pseudo-colonies of the same size class (Table 1). The decrease in the proportion of sexually mature worms appeared in all pseudo-colonies examined. On the contrary, an increase in proportion of asexually mature worms was detected

TABLE 1. Sexually mature and asexually reproducing worms before and after the experimental halving in 6 pseudo-colonies of *Salmacin adysteri*

Colony	Diameter (cm) of colony	Proportion (%) of sexually mature worms		Proportion (%) of asexually reproducing worms	
		before	after	before	after
1	12	65	37	28	61
2	11	64	47	24	42
3	10.5	24	18	15	34
4	9	54	10.5	22	24
5	8.5	30	21	20	18
6	7.5	17	8	18	21
Average		42.3	23.5	21.2	33.3
S.D.		21.2	15.4	4.6	6.6

TABLE 2. Settlement of 3-setigerous larvae of *Salmacina dysteri* in a petri-dish, known number of larvae were released and settlers were counted after 1 week

Replicates	No. of larvae		Number of aggregations	No. of worms in an aggergation		No. (%) of worms solitarily settled
	released	settled		mean ± S.D.	range	
1	50	45	7	3.6±1.59	2–6	21(46.6)
2	50	42	5	4.8±2.40	2–8	18(42.8)
3	40	25	3	5.3±2.86	2–9	9(36.0)
4	90	71	8	5.3±3.56	2–11	29(40.8)

in all colonies examined except for one pseudo-colony. The average changes were not significant in both sexually mature and asexually reproducing worms (Benferroni's *t*-test, $P > 0.05$).

Induction of asexual budding in solitarily reared worms

In the laboratory culture of solitary worms, sexually mature worms were observed to absorb gonads and produce buds within 2 to 3 weeks after the start of the culture (25 among 70 worms). In the culture of fragmented branches, almost all the males and hermaphroditic worms ceased sexual reproduction and started to produce buds for asexual reproduction after 3 to 4 weeks from the start of the laboratory culture, or produced large amounts of calcareous tubes after the experimental fragmentation.

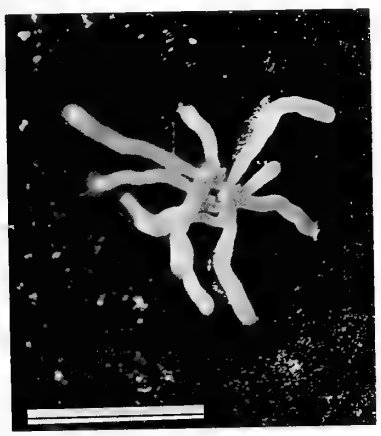

FIG. 7. An aggregation of 11 sexually reproduced juveniles of *Salmacina dysteri* in a petri-dish. Scale bar represents 1 cm.

Aggregation during larval settlement

The larvae settled solitarily or in aggregation with a varying number of individuals (Fig. 9 & Table 2). The difference between numbers of settled worms solitarily and those in aggregation was not significant (Chi-square and *G*-test, $P > 0.05$). Aggregations were formed mostly on the vertical wall of a petri-dish. Only 5 aggregations were formed on the bottom.

DISCUSSION

Intra-colonial variation of the two reproductive modes

The proportion of the two reproductive modes varied according to the positions in the colony (Fig. 3). A lower proportion of sexually mature worms was found in the tips of growing branches in *S. dysteri*. It may be explained in terms of 1) allocation of colony resources to growth rather than gamete production, as in numerous eu-colonial organisms [4, 5, 17, 19], or 2) individual age. The peripherally positioned worms in a pseudo-colony seem to be younger than the centrally positioned ones because asexually produced buds extend their tubes in an outer direction over the stock worm.

In the aggregating polychaete *Pygospio elegans*, as food availability decreased according to their density-increment, sexual reproduction was induced [20, 21]. Similarly, food availability may regulate the commencement of sexual and asexual reproduction in *S. dysteri*. The position of worms in

a colony seems to affect the availability of suspended food: centrally located worms receive less food, while peripheral worms receive an adequate food supply. This may result in more sexual reproductive ability in central colony positions than peripheral ones. Subsequently, larger pseudo-colonies seem to contain a higher proportion of worms located centrally (below 2 cm from the edge of a pseudo-colony) than smaller pseudo-colonies.

Inter-colonial variation of reproductive modes

Generally, the proportion of sexually mature worms increased with the pseudo-colony size in *S. dysteri*, but, in a rare case, a small pseudo-colony showed a high proportion of sexual reproduction (Fig. 5). The small pseudo-colony seems to have been freshly damaged, so the highest ability of sexual reproduction might have been retained. This possibility could be tested by breaking of large pseudo-colonies. The broken pseudo-colonies still showed a significant sexual reproductive capability 2 weeks after the artifical break, but within 1 to 2 months, they increased the proportion of asexual reproduction to a degree comparable to that of pseudo-colonies of the same size class (see the result of experimental halving and Table 1).

The age of a pseudo-colony may be a factor affecting the reproductive mode (see Figs. 5 and 6). However, we concluded that the size of a colony is the most important factor affecting the reproductive mode, based on the result of experimental halving, induction of asexual reproduction in solitarily reared worms, and inter-colonial variation of reproductive modes (Fig. 5).

Factors leading to pseudo-colony formation in Salmacina dysteri

Bosence [3] and ten Hove [8] discussed the ecology of serpulid polychaetes and listed various factors which cause their aggregation. These factors are, physical environmental factors, larval aggregation, brooding, asexual budding, response to light in the larval stage, larval retention, limited substrate availability, biotic factors such as space competition or predation, and possibly high primary productivity. In *S. dysteri*, some of these factors might also be working in the pseudo-colony construction process. We could not test the effect of environmental factors on the pseudo-colony formation. However, the following factors seem important in pseudo-colony formation; brooding, retention of larvae near the parent pseudo-colony, settlement of larvae on conspecific pseudo-colonies, and budding. Larger colonies seem to have the capacity to produce and retain more larvae in their near vicinity (Fig. 4), and thus can grow more rapidly than smaller colonies. Aggregation during larval settlement did not always occur (Table 2). However, it will contribute pseudo-colony formation if partially.

ACKNOWLEDGMENTS

We are grateful to Dr. T. Kikuchi, and Dr. T. Yamasu, for providing facilities and suggestions during this work. We also thank Mr. S. Nakamura, for his help in collecting worm colonies, Dr. Harry A. ten Hove and Dr. J. H. Bailey-Brock for critical reading of our manuscript and anonymous reviewers for their comments and advice. This work was partly supported by the Grant in Aid for Scientific Research on Priority Area (#204) 'Dispersal Mechanisms', and Priority Area (#319), Project "Symbiotic Biosphere: An Ecological Complexity Promoting the Coexisting of Many Species" from the Ministry of Education, Science and Culture, Japan.

REFERENCES

1 Berkeley E, Berkeley C (1954) Notes on the life history of the polychaete *Dodecaceria fewkesi* (nom. n.). J Fish Res Bd Canada 11: 326–334

2 Boardman RS, Cheetham AH, Oliver, Jr WA (1973) Introducing coloniality. In "Animal colonies" Ed by Boardman RS, Cheetham AH, Oliver, Jr WA, Stroudsburg, PA Dowden, Hutchinson & Ross, pp v-ix

3 Bosence DWJ (1979) The factors leading to aggregation and reef formation in *Serpula vermicularis* L. In "Biology and systematics of colonial organisms" Ed by Larwood G, Rosen BR, Academic Press, London, New York and San Francisco pp 299–318

4 Brazeau DA, Lasker HR (1990) Sexual reproduction and external brooding by the Caribbean gorgonian *Briareum asbestinum*. Mar Biol 104: 465–474

5 Connell JH (1973) Population ecology of reef-building corals. In "Biology and ecology of coral reefs, Vol 2, Ed by Jones OA, Endean R, Academic Press, New York, pp 205–246

6 Faulkner GH (1930) The anatomy and the histology of bud formation in the serpulid *Filograna implexa* together with some cytological observations on the nuclei of the neoblasts. J Linn Soc London 37: 109–189

7 Gibson PH (1977) Reproduction in the cirratulid polychaetes *Dodecaceria concharum* and *D. pulchra*. J Zool London 182: 89–102

8 ten Hove HA (1979) Different causes of mass occurrence in serpulids. In "Biology and systematics of colonial organisms" Ed by Larwood G, Rosen BR, Academic Press, London, New York and San Francisco, pp 281–298

9 Huxley TH (1855) On hermaphrodite and fissiparous species of tubicolar annelid *Protula dysteri*. Edinb Phil J New Ser 1: 113–129

10 Knight-Jones EW, Moyse J (1961) Intraspecific competition in sedentary marine animals. Symp Soc Exp Biol 15: 72–95

11 Larwood G, Rosen BR (1979) The biology and systematics of colonial organisms. Academic Press, New York and London, 589 pp

12 Nakamura S (1984) Record of air temperature, surface water temperature and chlorinity at Sesoko in 1983. Galaxea 3: 105

13 Nishi E (1993) Notes on reproductive biology of some serpulid polychaetes at Sesoko Island, Okinawa, with brief accounts of setal morphology of three species of *Salmacina* and *Filograna implexa*. Mar Foul 10: 11–16

14 Nishi E, Nishihira M (1992) Colony formation via sexual and asexual reproduction in the serpulid *Salmacina dysteri* (Annelida, Polychaeta). Zool Sci 9: 1293 (abstract)

15 Nishi E, Nishihira M (1993) Hermaphroditisms, brooding, and gamete production in the serpulid *Salmacina dysteri* (Polychaeta, Sedentaria). Publ Amakusa Marine Biol Lab 12: 1–11.

16 Nishi E, Yamasu T (1992) Brooding and development of a serpulid tube worm *Salmacina dysteri* (Huxley) (Annelida, Polychaeta). Bull Coll Sci, Univ Ryukyus 54: 107–121

17 Rinkevich B, Loya Y (1979) The reproduction of the Red Sea

coral *Stylophora pistillata*. II. Synchronization in breeding and seasonality of planula shedding. Mar Ecol Prog Ser 1: 146–152

18 Schroeder PC, Hermans CO (1975) Annelida: Polychaeta. In "Reproduction in marine invertebrates Vol 3" Ed by Giese AC & Pearse JS, Academic Press, New York & London, pp 1–213

19 Wallace CC (1985) Reproduction, recruitment and fragmentation in nine sympatric species of the coral genus *Acropora*. Mar Ecol Prog Ser 88: 217–233

20 Wilson Jr WH (1983) The role of density dependence in a marine infaunal community. Ecology 64: 295–306

21 Wilson Jr WH (1985) Food limitation of asexual reproduction in a spionid polychaete. Int J Invertebrate Repr Dev 8: 61–65

22 Yamanishi R. (1978) Occurrence of *Salmacina dysteri* at Iwaya, Awajishima. Nature study 24:9–11 (in Japanese)

ZOOLOGICAL SCIENCE 11: 597–604 (1994)

Molecular Phylogenetic Status of the Iriomote Cat *Felis iriomotensis*, Inferred from Mitochondrial DNA Sequence Analysis

RYUICHI MASUDA[1,2,5], MICHIHIRO C. YOSHIDA[1,2], FUMIHARU SHINYASHIKI[3] and GEN BANDO[4]

[1]*Chromosome Research Unit, Faculty of Science,* [2]*Division of Biological Science, Graduate School of Environmental Earth Science, Hokkaido University, Sapporo 060,* [3]*Okinawa International University, Okinawa 901-22, and* [4]*Asahiyama Zoo, Asahikawa 078, Japan*

ABSTRACT—To investigate the molecular phylogenetic status of the Iriomote cat *Felis iriomotensis*, partial sequences of the mitochondrial 12S rRNA gene (373 bases) and the cytochrome b gene (402 bases) were determined by using the polymerase chain reaction-product direct sequencing technique and then compared with those of seven other feline species. Six Iriomote cats examined in this study showed no intraspecific variation for both genes. The sequence comparisons and the molecular phylogenetic trees indicated that the Iriomote cat is very closely related to the leopard cat *Felis bengalensis*, which is a widespread species throughout southern and eastern Asia, and that it is reasonable for these two felines to be classified to the same genus. Based on sequence data, the Iriomote cat was estimated to have diverged from the leopard cat arround or less than 0.2 million years ago, and this concurs with the previously reported geological isolation date of the Ryukyu Arc from the Chinese continent. Our results suggest that the geographic barrier has led the fixation of some unique morphological characters into the Iriomote cat population while both the Iriomote cat and the leopard cat still retain very close genetic characters.

INTRODUCTION

The Iriomote cat was discovered in 1965 on Iriomote Island which is located about 200 km east of Taiwan, and Imaizumi [12] examined the morphological characters and classified this feline as a new genus and a new species *Mayailurus iriomotensis*. Since the discovery, some versions of the Felidae classification based on the morphological characters and distribution have been presented as reviewed by Nowak [25]. Although each version recognized the Iriomote cat as a distinct species, the genus nomenclature differed as shown in Table 4. Wurster-Hill *et al.* [36] reported that the G-banding karyotype of the Iriomote cat (2 n =38) was indistinguishable from that of the leopard cat. However, no other analysis on the phylogeny of the Iriomote cat has been reported so far.

On the other hand, the Iriomote cat is one of the most endangered species in Japan. Izawa *et al.* [14, 15] reported that the population of the Iriomote cat was estimated to be about 100 individuals. For the purpose of conservation and management, it is important and also very urgent to clarify the taxonomic position and the genetic characters of this feline.

A molecular genetic approach provides reliable information on the phylogenetic relationships between species. Especially, since the mitochondrial DNA (mtDNA) evolves more rapidly than the nuclear DNA [3], mtDNA sequence analysis is a useful way to study the evolution of closely related species including carnivores [17, 23, 30, 32].

In this study, partial sequences of the mitochondrial 12S rRNA gene and the cytochrome b gene of the Iriomote cat were determined and then compared with those of several other feline species. Based on sequence comparisons, we investigated the phylogenetic status of the Iriomote cat and presented the genetic evidence that this feline is very closely related to the leopard cat, which is a widespread species throughout southern and eastern Asia.

MATERIALS AND METHODS

Sample sources and DNA extraction

Tissues specimens were obtained from six Iriomote cats and seven other feline species as described in Table 1. Five Iriomote cats were killed by traffic or other accidents on Iriomote Island [16, 27]. One individual died at the Okinawa Children Land Zoo. Since the family Viverridae and the Hyenidae were reported to be closer to the Felidae than other carnivores [31], the suricate (SSU1) from the Viverridae was used as an outgroup species (Table 1). Species names were according to the nomenclature of Nowak [25]. DNAs were extracted from the frozen muscle, kidney, liver, heparinized whole blood or cultured skin fibroblasts, according to the phenol/proteinase K/sodium dodecyl sulfate (SDS) method of Sambrook *et al.* [28] with some modifications [23].

PCR amplification for single-stranded DNAs

The mitochondrial 12S rRNA and cytochrome b gene regions were PCR-amplified using the procedure of Kocher *et al.* [20] with a slight modification [23]. Primers for the 12S rRNA gene [17], L1091 (5'-AAACTGGGATTAGATACCCCACTAT-3') and H1478 (5'-GAGGGTGACGGGCGGTGTGT-3') were designed by referring to the published sequences of Kocher *et al.* [20]. Referring to the

Accepted June 24, 1994
Received March 4, 1994
[5] To whom correspondence should be addressed.

TABLE 1. The Iriomote cats and other feline species examined in this study

Species	Common name	Code	Source; Collecting locality if known
Felis iriomotensis	Iriomote cat	FIR	5 individuals (FIR1, 2, 3, 4, 5) stocked at Univ. of Ryukyus; obtained from Iriomote Island, Okinawa
			1 individual (FIR6) kept at Okinawa Children Land Zoo; captured on Iriomote Island
Felis bengalensis	Leopard cat	FBE	2 individuals (FBE1, 2) from Okinawa Children Land Zoo; originated from Thailand (FBE1)
Felis lynx	Lynx	FLY	2 individuals (FLY1, 2) from Asahiyama Zoo, Asahikawa; originated from Siberia
Felis catus	Domestic cat	FCA	2 individuals (FCA1, 2) obtained in Sapporo
Felis pardalis	Ocelot	FPA	1 individual (FPA1) from Asahiyama Zoo
Panthera pardus	Leopard	PPA	2 individuals, PPA1 (studbook no. 173) and PPA2 (studbook no. 161) from Asahiyama Zoo; originated from Siberia
Panthera uncia	Snow leopard	PUN	2 individuals, PUN1 (studbook no. Sapporo 9) and PUN2 (studbook no. Nagoya 4) from Asahiyama Zoo
Panthera tigris	Tiger	PTI	1 individual (PTI1) from Ueno Zoological Gardens; originated from Sumatra
Suricata suricatta	Suricate	SSU	1 individual (SSU1) from Kobe Oji Zoo

report of Irwin *et al.* [13], primers for the cytochrome b gene were designed as L14724 (5′-GATATGAAAAACCATCGTTG-3′) and H15149 (5′-CTCAGAATGATATTTGTCCTCA-3′) [23]. Primer names identify the light (L) or heavy (H) strand and the 3′ end-position of the primer in the human mtDNA sequence [1]. These oligonucleotides were synthesized on an Applied Biosystems 391 DNA synthesizer.

Symmetric PCR was performed with a GeneAmp PCR reagent kit (Perkin-Elmer/Cetus) according to the manufacturer's instruction. In brief, 50 μl of mixture contained 10 mM Tris (pH 8.3), 50 mM KCl, 1.5 mM $MgCl_2$, 0.001% (w/v) gelatin, each NTP at 200 μM, 1.25 U of *Taq* DNA polymerase, each primer at 250 nM, and 100 ng of the extracted DNA or 1–5 μl of the simply purified DNA as a template. Each cycle consisted of denaturing at 94°C for 1 min, annealing at 50–60°C for 0.5–1 min, and extension at 72°C for 1 min. After 30–35 cycles, the extension reaction was completed by incubation at 72°C for 10 min.

Asymmetric PCR was done to amplify single-stranded DNAs according to the method of Gyllensten and Erlich [9]. The procedures were basically the same as symmetric PCR, except for use of a 1:100 (2.5 nM:250 nM) ratio of the two primers and 1 μl of the symmetric PCR product in 100 μl of the mixture.

Direct sequencing of PCR-amplified single-stranded DNAs

The asymmetric PCR product was concentrated using a Centricon-30 microconcentrator (Amicon), and 7 μl was sequenced with 10 ng of primer for the L or H strand, [^{32}P] dCTP (Amersham), and T7 DNA polymerase (United States Biochemical), according to the dideoxynucleotide chain reaction method [29]. The internal primer for the 12S rRNA sequencing was designed as 5′-GGTTTGCTGAAGATGGCGGTATATAG-3′ (the heavy strand) [17]. For the cytochrome b sequencing, the internal primers were synthesized as 5′-GACACAACAACCGCCTTCTC-3′ (the light strand) and its complement 5′-GAGAAGGCGGTTGTTGTGTC-3′ (the heavy strand). Reaction products were electrophoresed on 6% polyacrylamide gels containing 7 M urea. Gels were dried and exposed to Fuji RX X-ray films for 1–5 days.

Sequence analysis

Sequence alignment and construction of phylogenetic tree by the neighbor-joining method [26] were performed using the Clustal V computer software [11]. Numbers of nucleotide substitutions per site were estimated for multiple substitutions using Kimura's two-parameter method [18]. The bootstrap method [7] was used in the Clustal V to assess the degree of support for internal branches of the phylogenetic tree.

RESULTS

The 12S rRNA sequence of the Iriomote cat

Using the PCR product-direct sequencing technique, partial sequences (373 bases) of the mitochondrial 12S rRNA genes were determined in the Iriomote cat and seven other feline species (Fig. 1). Sequence differences and numbers of transitions/transversions obtained from all pairwise comparisons were shown in Table 2.

The six Iriomote cats (FIR1-6) showed the same sequence (Fig. 1). One (FBE1) of the two leopard cats shared the identical sequence with the Iriomote cats. Between FIR1-6/FBE1 and the other leopard cat (FBE2), there was only one transitional difference (C→T) at the nucleotide position (nt) 301 and the sequence difference was 0.3% (1/373 bases). Higher sequence differences (2.4–4.6%, 9–17/373 bases) were observed between the Iriomote cat and the other feline species (Table 2). For examination of the degree of multiple substitutions, the transversional difference per site was plotted against the transitional difference per site (Fig. 3).

The cytochrome b sequence of the Iriomote cat

Partial sequences (402 bases) of the mitochondrial cytochrome b genes were determined in the Iriomote cats and other feline species. Although the PCR amplification was completed on two specimens (PPA1 and PPA2) of the leopards, the sequencing ladders on the X-ray film were unreadable due to a mixture of more than two kinds of molecule populations, suggesting the heteroplasmy of

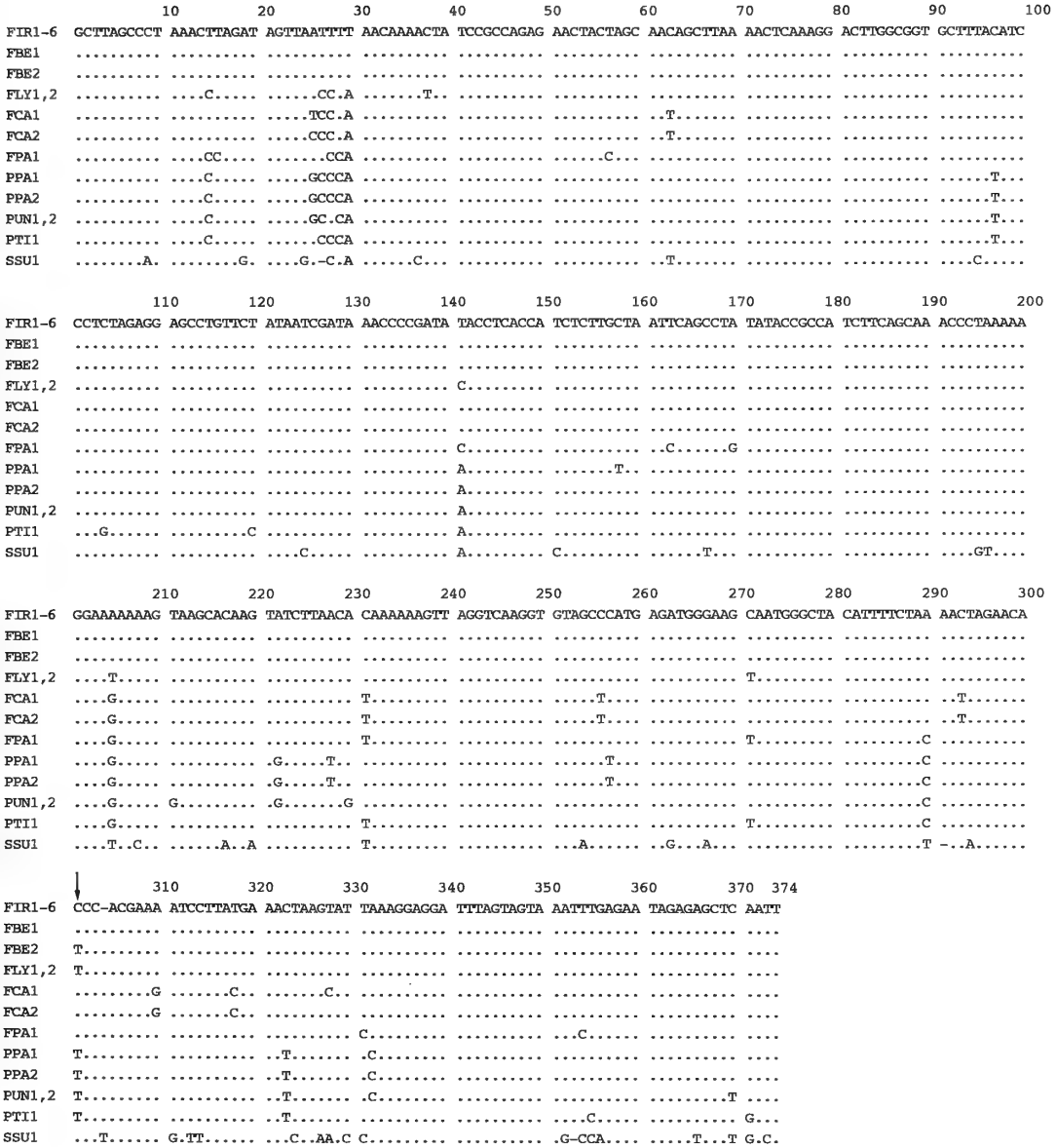

FIG. 1. Alignment of the 12S rRNA sequences from the Iriomote cat and other feline species. Species codes refer to those in Table 1. Dots indicate identities with nucleotides in the Iriomote cat seuqence (FIR1–6). Dashes denote gaps. The sequence of the Iriomote cat was identical with that of one leopard cat (FBE1). An arrow shows the substitution site, nt 301, between FIR1–6/FBE1 and another leopard cat (FBE2).

mtDNA sequences or the existence of mtDNA-like sequence(s) in the nuclear genome (data not shown). The cytochrome b region of FPA1 could not be amplified probably due to the mismatch of primer sequences, while the 12S rRNA region could be amplified from the same DNA sample.

No intraspecific variation was observed among the six Iriomote cats (FIR1–6) (Fig. 2). Two leopard cats (FBE1 and FBE2) shared identical sequences (Fig. 2). The sequence difference between the Iriomote cat and the leopard cat was 0.5% (2/402 bases) (Table 3). The two substitutions were transitional; G→A (FIR-FBE) at nt 108 and A→G at nt 354 (Fig. 2). Each substitution was synonymous and occurred at the third position in codon; one codon (CTG or CTA) including nt 108 encoded the proline and the other (ATA or ATG) including nt 354 encoded the methionine. Between the Iriomote cat and the other feline species excluding the leopard cat, the sequence differences were 10.4–13.2% (42–53/402 bases) (Table 3). The relationships between the transversional difference per site and the transitional difference per site were shown in Figure 3.

Phylogenetic trees

Phylogenetic trees of the 12S rRNA and the cytochrome b sequences were constructed using the neighbor-joining method, based on the numbers of nucleotide substitutions per site which were estimated by Kimura's two-parameter

TABLE 2. Percentage differences (above diagonal) and numbers of transitions/transversions (below diagonal) for mitochondrial 12S rRNA sequences (373 bases)

Code	FIR1-6*	FBE1	FBE2	FLY1,2*	FCA1	FCA2	FPA1	PPA1	PPA2	PUN1,2*	PTI1	SSU1**
FIR1-6*	—	0	0.3	2.4	3.2	3.0	4.0	4.6	4.3	4.3	4.6	10.8
FBE1	0/0	—	0.3	2.4	3.2	3.0	4.0	4.6	4.3	4.3	4.6	10.8
FBE2	1/0	1/0	—	2.1	3.5	3.2	4.3	4.3	4.0	4.0	4.3	11.1
FLY1,2*	7/2	7/2	6/2	—	3.8	3.5	3.5	3.8	3.5	4.0	3.2	11.1
FCA1	10/2	10/2	11/2	12/2	—	0.5	5.1	5.4	5.1	5.6	5.1	11.1
FCA2	9/2	9/2	10/2	11/2	2/0	—	4.8	5.1	4.8	5.4	4.8	11.1
FPA1	13/2	13/2	14/2	11/2	17/2	16/2	—	5.1	4.8	5.4	4.0	11.4
PPA1	12/5	12/5	11/5	9/5	15/5	14/5	16/3	—	0.3	1.9	3.2	13.0
PPA2	11/5	11/5	10/5	8/5	14/5	13/5	15/3	1/0	—	1.6	3.0	12.7
PUN1,2*	11/5	11/5	10/5	10/5	16/5	15/5	17/3	5/2	4/2	—	3.5	12.7
PTI1	13/4	13/4	12/4	8/4	15/4	14/4	13/2	9/3	8/3	10/3	—	11.4
SSU1**	27/13	27/13	28/13	30/11	28/13	28/13	31/11	36/12	35/12	35/12	31/11	—

* Six individuals of the Iriomote cat (FIR1-6), two of the lynx (FLY1 and FLY2), and two of the snow leopard (PUN1 and PUN2) showed no intraspecific sequence variation in each species.
** For comparison of SSU1 and feline species, three sites of gaps were eliminated.

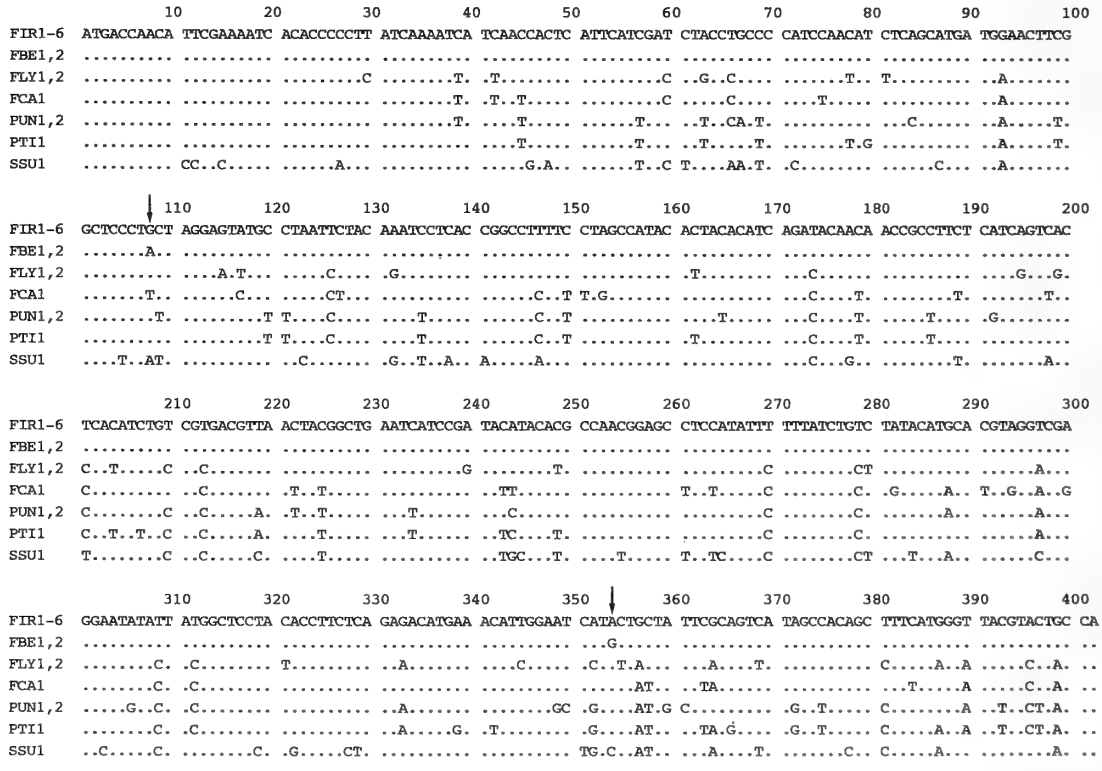

FIG. 2. Alignment of the cytochrome b sequences from the Iriomote cat and other feline species. Species codes refer to those in Table 1. Dots indicate identities with nucleotides in the Iriomote cat sequences (FIR1–6). Arrows show two substitution sites, nt 108 and nt 354, between the Iriomote cats (FIR1–6) and the leopard cats (FBE1 and FBE2).

method (Fig. 4). The Iriomote cats (FIR1–6) and the leopard cats (FBE1, 2) were clustered with 95% (the 12S rRNA tree) and 100% (the cytochrome b tree) bootstrap values. The species of the genus *Panthera* were clearly separated from the other felines with 76% (the 12S rRNA tree) and 100% (the cytochrome b tree) bootstrap values. Since the suricate (SSU1), which is included in the family Viverridae, was most distantly separated from the other species, SSU1 was used as an outgroup to set a root of the tree.

TABLE 3. Percentage differences (above diagonal) and numbers of transitions/transversions (below diagonal) for mitochondrial cytochrome b sequences (402 bases) of the Iriomote cat and other feline species

Code	FIR1–6*	FBE1,2*	FLY1,2*	FCA1	PUN1,2*	PTI1	SSU1
FIR1–6*	—	0.5	10.4	11.2	13.2	12.9	15.7
FBE1,2*	2/0	—	11.0	11.4	13.7	13.4	15.4
FLY1,2*	37/5	39/5	—	11.9	13.7	11.4	16.9
FCA1	39/6	40/6	45/3	—	12.2	12.4	16.9
PUN1,2*	46/7	48/7	49/6	44/5	—	6.7	18.2
PTI1	45/7	47/7	40/6	45/5	25/2	—	17.7
SSU1	46/17	45/17	46/22	45/23	49/24	47/24	—

* Six individuals of the Iriomote cat (FIR1–6), two of the leopard cat (FBE1 and FBE2), two of the lynx (FLY1 and FLY2), and two of the snow leopard (PUN1 and PUN2) showed no intraspecific sequence variation in each species.

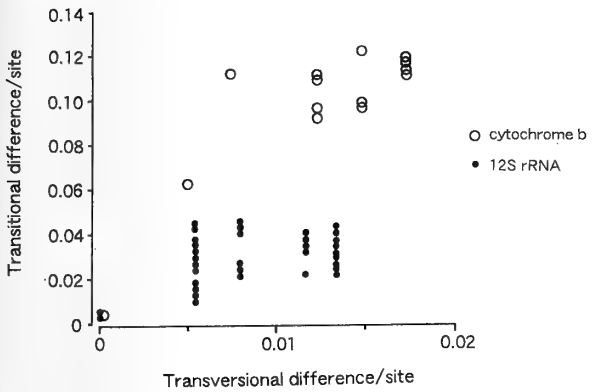

FIG. 3. The transversional difference per site was plotted against the transitional difference per site in pairwise comparisons at the 12S rRNA gene (closed circles) and the cytochrome b gene (open circles). The comparison with the suricate as an outgroup was not included.

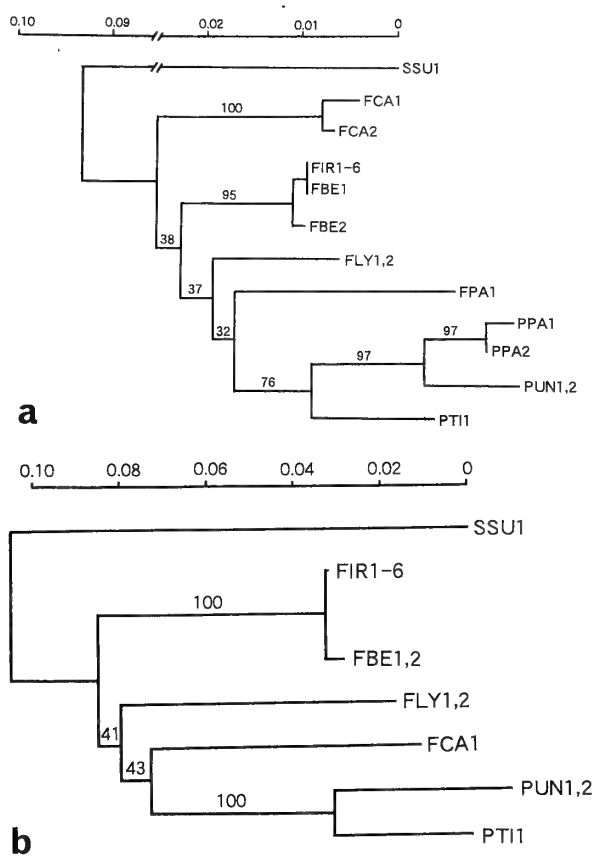

FIG. 4. Phylogenetic trees of the 12S rRNA (a) and the cytochrome b (b) sequences constructed by the neighbor-joining method. The numbers of nucleotide substitutions per site, indicated by the scale, were estimated using Kimura's two parameter method [18]. Bootstrap values above branches were derived from 500 replications.

DISCUSSION

MtDNA phylogeny of the feline species

From sequence comparisons, it was clarified that the saturation due to the multiple substitutions at the same site is being approached for transitions in the feline 12S rRNA gene (Fig. 3), similar to the previous reports of other animals [2, 4, 30]. In the cytochrome b gene, the multiple substitutions seem to have reached the saturation (Fig. 3). This result is in agreement with the previous observation [30] that the cytochrome b gene evolves faster than does the 12S rRNA gene in mammals.

Despite of the substitution rate difference between the two genes, the Iriomote cat (FIR1–6) and the leopard cat (FBE1, 2) were clustered and separated from the other feline species with high bootstrap values in both the 12S rRNA tree and the cytochrome b tree: 95% in the 12S rRNA tree and 100% in the cytochrome b tree (Fig. 4). This indicates that the Iriomote cat is closely related to the leopard cat with a high confidence. The *Panthera* species were clustered with high bootstrap values: 76% in the 12S rRNA tree and 100% in the cytochrome b tree (Fig. 4). Our results of the phylogenetic status of the *Panthera* species support the previous reports by the microcomplement fixation method [5] and the shorter sequences of the 12S rRNA gene [17]. The difference in topology between the 12S rRNA tree and the cytochrome b tree (Fig. 4) seems to reflect the substitution rate difference between the two genes and the absence of the ocelot (FPA) and the leopard (PPA) in the cytochrome b tree. Since the suricate (SSU1) from the family Viverridae was most distantly separated from the species of the family Felidae, this species was used to set a root of the tree.

MtDNA sequence similarity between the Iriomote cat and the leopard cat

The difference of the cytochrome b sequences was 0.5% (2/402 bases) between the Iriomote cat (FIR1–6) and the leopard cat (FBE1, 2) (Table 3, Fig. 2). The 12S rRNA sequences of six Iriomote cats (FIR1–6) were identical to that of one leopard cat (FBE1) and different by 0.3% (1/373 bases) from that of the other leopard cat (FBE2) (Table 2,

Fig. 1). The close relationship between the Iriomote cat and the leopard cat supports the previous report of Wurster-Hill *et al.* [36], in that the karyotypes of both felines were indistinguishable. However, it must be noticed that the karyological identity is not always in agreement with the molecular similarity. Wurster-Hill and Centerwall [35] reported that the species of the genus *Panthera* have identical karyotypes. By contrast with their karyological data, our molecular results indicated that the 12S rRNA sequence difference (1.6–3.5%, 6–13/373 bases) among the *Panthera* species is not always very low, as compared with the sequence difference among the other feline species (Table 2).

Between the two leopards (PPA1, 2) and between the two domestic cats (FCA1, 2), the intraspecific differences for the 12S rRNA sequences were 0.3% and 0.5%, respectively (Table 2). The sequence difference (0–0.3%) between the Iriomote cat (FIR1–6) and the leopard cat (FBE1, 2) is comparable to these intraspecific variations. Therefore, it is not reasonable for the two felines to be classified to distinct genera.

The leopard cat is widespread in Asia and has the geographic variation of the morphological characters [21]. Glass and Todd [8] reported on the presence or absence of the second premolar (P2) as a quasi-continuous variation in various leopard cat populations, while Imaizumi [12] described that the P2 is absent in the Iriomote cat. Moreover, Glass and Todd [8] considered that the Iriomote cat's key characters reported by Imaizumi [12] are polymorphic in the leopard cat, and suggested that the fixation of the P2 absence in the Iriomote cat population may show a result of the genetic drift in an island population [8]. Wozencraft [34] assigned the Iriomote cat to the synonym of the leopard cat based on the morphological characters (Table 4). Our results together with the previous taxonomic reports [8, 34] suggest that the geographic isolation has led the fixation of some unique morphological characters in the Iriomote cat population while both this feline and the leopard cat still retain very close genetic characters. Since the leopard cat is distributed in many islands of Asia, it is quite necessary to examine the genetic and morphological variations in each island population, and to compare them with the characters of the Iriomote cat population.

Divergence time of the Iriomote cat

In order to clarify the evolutionary origin of the Iriomote cat, it is important to estimate the divergence time of this feline from the leopard cat, which is a widespread species in Asia. Wayne *et al.* [33] estimated divergence time of various carnivore species based on the microcomplement fixation method. Their data showed that the divergence time between the domestic cat and the tiger is about 4.5 million years (Myr) ago. In our results, the sequence difference between the domestic cat (FCA1) and the tiger (PTI1) was 12.4% for the cytochrome b gene (Table 3). Based on these values, the substitution rate of the cytochrome b gene was calculated to be 1.38%/Myr. Between the Iriomote cat (FIR1–6) and the leopard cat (FBE1, 2), the sequence difference was 0.5% for the cytochrome b gene (Table 3). Using the calculated substitution rate and the sequence difference, the divergence time of the Iriomote cat and the leopard cat was estimated to be 0.18 Myr ago. On the other hand, since the cytochrome b gene was reported to diverge at a rate of at least 2.5%/Myr in mammals [13, 24], the Iriomote cat was estimated to have diverged from the leopard cat less than 0.20 Myr ago. Thus, the two divergence times estimated in different ways were in good agreement with each other.

Kimura *et al.* [19] with the geological data reported that the land bridge connecting the Ryukyu Arc and the Chinese continent existed intermittently from 0.24 to 0.02 Myr ago and that the land bridge subsided about 0.02 Myr ago. Our estimated divergence time of both felines is in agreement with the geological isolation date of the Ryukyu Arc. In fact, the leopard cats live in Taiwan, which is located about 200 km west of Iriomote Island [21]. It is still interesting that the Iriomote cat is distributed only on Iriomote Island among many islands of the Ryukyus. After isolation from the Chinese continent, the Ryukyu Islands may have undergone geological and environmental changes, and the ancestors of

TABLE 4. Nomenclatures of the Iriomote cat and the leopard cat, cited from previously proposed classifications

	Researcher (year)					
	Imaizumi (1967)	Ewer (1973)	Hemmer (1978)	Leyhausen (1979)	Nowak (1991)	Wozencraft (1993)
Iriomote cat						
Genus	*Mayailurus*	*Mayailurus*	*Prionailurus*	*Prionailurus*	*Felis*	Synonym of
Subgenus	—	—	*Mayailurus*	—	*Mayailurus*	the leopard cat
Species	*iriomotensis*	*iriomotensis*	*iriomotensis*	*iriomotensis*	*iriomotensis*	
Leopard cat						
Genus		*Prionailurus*	*Prionailurus*	*Prionailurus*	*Felis*	*Prionailurus*
Subgenus		—	*Prionailurus*	—	*Prionailurus*	—
Species		*bengalensis*	*bengalensis*	*bengalensis*	*bengalensis*	*bengalensis*
Reference	[12]	[6]	[10]	[22]	[25]	[34]

the Iriomote cats may have been able to survive only on Iriomote Island. Further paleontological studies will elucidate their past distribution on the islands.

Controversy on nomenclatures in the Felidae classification

The Iriomote cat was reported to have primitive morphological characters and was named *Mayailurus iriomotensis* as a new genus and a new species [12]. The genus name of the Iriomote cat was, however, different among several versions of the Felidae classifications presented so far. In Table 4, the nomenclatures of the Iriomte cat and the leopard cat were extracted from the previous classifications. Our results based on mtDNA sequence analysis support the classifications in that the Iriomote cat is included in the same genus as the leopard cat. As shown in Table 4, Hemmer [10], Leyhausen [22], and Nowak [25] all classified the two felines to one genus, but there is some disagreement between their classifications on the other feline species, especially the *Panthera* species. Hemmer [10] assigned the snow leopard to *Uncia uncia*, while the leopard and the tiger were named *Panthera pardus* and *P. tigris*, respectively. In Leyhausen's classification [22], the snow leopard was assigned to *Uncia uncia*, while the leopard was *Panthera pardus* and the tiger was *Neofelis tigris*. Thus, Hemmer [10] and Leyhausen [22] divided these three big felines into two or three genera. By contrast, Nowak [25] included all of these big felines in one genus *Panthera*. In our results, the *Panthera* species, which have identical karyotypes [35], were clustered with a high confidence (Fig. 4). Considering the classification throughout the feline species, therefore, Nowak's classification [25] was adopted in this report, although he classified the Iriomote cat and the leopard cat into the different subgenera, *Mayailurus* and *Prionailurus*, respectively.

This is the first report on the molecular phylogeny of the Iriomote cat, inferred from mtDNA sequences. The phylogenetic understanding is the basis and the first step to know the genetic diversity of the Iriomote cat population for the purpose of conservation and management.

SEQUENCE AVAILABILITY

The nucleotide sequence data reported in this paper will appear in the GSDB, DDBJ, EMBL, and NCBI nucleotide sequence databases with the following accession numbers: for the 12S rRNA sequences, D28888 (FIR), D28889 (FBE1), D28890 (FBE2), D28891 (FLY), D28892 (FCA1), D28893 (FCA2), D28894 (FPA), D28895 (PPA1), D28896 (PPA2), D28897 (PUN), D28898 (PTI), D28899 (SSU): for the cytochrome b sequences, D28900 (FIR), D28901 (FBE), D28902 (FLY), D28903 (FCA), D28904 (PUN), D28905 (PTI), D28906 (SSU).

ACKNOWLEDGMENTS

We thank Dr. M. Izawa, Department of Biology, University of the Ryukyus, for supplying specimens and invaluable advice of the Iriomote cat. We are grateful to R. Kuwae and T. Kinjo, Okinawa Children Land Zoo, and K. Murata, Kobe Oji Zoo, for contribution of specimens. We are also indebted to Dr. M. Yoneda, Japan Wildlife Research Center, for valuable advice and Dr. M. Kimura, University of the Ryukyus, for geological suggestion. All specimens of the Iriomote cats were examined under the permission of the Envionmental Agency and the Agency for Cultural Affairs of Japan. This work was supported in part by a research grant from the Sumitomo Foundation.

REFERENCES

1 Anderson S, Bankier AT, Barrell BG, De Bruijn MHL, Coulson AR, Drouin J, Eperon IC, Nierlich DP, Roe BA, Sanger F, Schreier PH, Smith AJH, Staden R, Young IG (1981) Sequence and organization of the human mitochondrial genome. Nature 290: 457–465

2 Brown GG, Simpson MV (1982) Novel features of animal mtDNA evolution as shown by sequences of two rat cytochrome oxidase subunit II genes. Proc Natl Acad Sci USA 79: 3246–3250

3 Brown WM, George MJr, Wilson AC (1979) Rapid evolution of animal mitochondrial DNA. Proc Natl Acad Sci USA 76: 1967–1971

4 Brown WM, Prager EM, Wang A, Wilson AC (1982) Mitochondrial DNA sequences of primates: Tempo and mode of evolution. J Mol Evol 18: 225–239

5 Collier GE, O'Brien SJ (1985) A molecular phylogeny of the Felidae: Immunological distance. Evolution 39: 473–487

6 Ewer RF (1973) The Carnivores. Cornell Univ Press, New York

7 Felsenstein J (1985) Confidence limits on phylogenies: An approach using the bootstrap. Evolution 39: 783–791

8 Glass GE, Todd NB (1977) Quasi-continuous variation of the second upper premolar in *Felis bengalensis* Kerr, 1792 and its significance for some fossil lynxes. Z Saugetierk 43: 62–64

9 Gyllensten UB, Erlich HA (1988) Generation of single-stranded DNA by the polymerase chain reaction and its application to direct sequencing of the HLA-DQA locus. Proc Natl Acad Sci USA 85: 7652–7656

10 Hemmer H (1978) The evolutionary systematics of living Felidae: Present status and current problems. Carnivore 1: 71–79

11 Higgins DG, Bleasby AJ, Fuchs R (1992) Clustal V: Improved software for multiple sequence alignment. Comput Appl Biosci 8: 189–191

12 Imaizumi Y (1967) A new genus and species of cat from Iriomote, Ryukyu Islands. J Mamm Soc Japan 3: 75–108

13 Irwin DM, Kocher TD, Wilson AC (1991) Evolution of the cytochrome *b* gene of mammals. J Mol Evol 32: 128–144

14 Izawa M, Doi T (1991) Status of conservation and management of two species of Felidae in Japan. Honyurui Kagaku [Mammalian Science] 31: 15–22 (in Japanese with English abstract)

15 Izawa M, Doi T, Ono Y (1991) Ecological study on the two species of Felidae in Japan. In "Wildlife Conservation" Ed by N Maruyama, B Bobek, Y Ono, W Regelin, L Bartos, PR Ratcliffe, Sankyo, pp 141–143

16 Izawa M, Sakaguchi N, Okamura M, Yasuda N, Akuzawa M, Mochizuki M (1993) Records of deaths of Iriomote cat, *Felis iriomotensis* II. Island Studies in Okinawa 11: 107–112 (in Japanese with English abstract)

17 Janczewski DN, Yuhki N, Gilbert DA, Jefferson GT, O'Brien SJ (1992) Molecular phylogenetic inference from saber-toothed cat fossils of Rancho La Brea. Proc Natl Acad Sci USA 89: 9769–9773

18 Kimura M (1980) A simple method for estimating evolutionary rate of base substitutions through comparative studies of nucleotide sequences. J Mol Evol 16: 111–120

19 Kimura M, Matsumoto T, Nakamura T, Otsuka H, Nishida S, Aoki M, Ono T, Danno K (1992) Diving survey of the Kerama Saddle in the eastern margin of the Okinawa Trough: Probable sunken land-bridge during the last glacial age. Proc JAMSTEC Symp Deep Sea Res: 107–133 (in Japanese with English abstract)

20 Kocher TD, Thomas WK, Meyer A, Edwards SV, Pääbo S, Villablanca FX, Wilson AC (1989) Dynamics of mitochondrial DNA evolution in animals: Amplification and sequencing with conserved primers. Proc Natl Acad Sci USA 86: 6196–6200

21 Lekagul B, McNeely JA (1988) Mammals of Thailand. Saha Karn Bhaet, Bangkok

22 Leyhausen P (1979) Cat behavior. Garland STPM Press, New York

23 Mausda R, Yoshida MC (1994) Nucleotide sequence variation of cytochrome b genes in three species of weasels, *Mustela itatsi*, *Mustela sibirica*, and *Mustela nivalis*, detected by improved PCR product-direct sequencing technique. J Mamm Soc Japan 19: 33–43

24 Meyer A, Kocher TD, Basasibwaki P, Wilson AC (1990) Monophyletic origin of Lake Victoria cichlid fishes suggested by mitochondrial DNA sequences. Nature 347: 550–553

25 Nowak RM (1991) Walker's Mammals of the World. 5th ed, Johns Hopkins Univ Press, Baltimore

26 Saitou N, Nei M (1987) The neighbor-joining method: A new method for reconstructing phylogenetic trees. Mol Biol Evol 4: 406–425

27 Sakaguchi N, Izawa M (1992) Records of deaths of Iriomote cat, *Felis iriomotensis*. Island Studies in Okinawa 10: 25–35 (in Japanese with English abstract)

28 Sambrook J, Fritsch EF, Maniatis T (1989) Molecular Cloning: A Laboratory Manual. 2nd ed, Cold Spring Harbor Laboratory, New York

29 Sanger F, Nicklen S, Coulson AR (1977) DNA sequencing with chain-terminating inhibitors. Proc Natl Acad Sci USA 74: 5463–5467

30 Thomas RH, Schaffner W, Wilson AC, Pääbo S (1989) DNA phylogeny of the extinct marsupial wolf. Nature 340: 465–467

31 Wayne RK, Benveniste RE, Janczewski DN, O'Brien SJ (1989) Molecular and biochemical evolution of the Carnivora. In "Carnivore Behavior, Ecology, and Evolution" Ed by JL Gittleman, Cornell Univ Press, New York, pp 465–494

32 Wayne RK, Jenks SM (1991) Mitochondrial DNA analysis implying extensive hybridization of the endangered red wolf *Canis rufus*. Nature 351: 565–568

33 Wayne RK, Van Valkenburgh B, O'Brien SJ (1991) Molecular distance and divergence time in canivores and primates. Mol Biol Evol 8: 297–319

34 Wozencraft WC (1993) Order Carnivora. In "Mammal Species of the World: A Taxonomic and Geographic Reference, 2nd ed" Ed by DE Wilson and DM Reeder, Smithsonian Institution Press, Washington, pp 279–348.

35 Wurster-Hill DH, Centerwall WR (1982) The interrelationships of chromosome banding patterns in canids, mustelids, hyena, and felids. Cytogenet Cell Genet 34: 178–192

36 Wurster-Hill DH, Doi T, Izawa M, Ono Y (1987) Banded chromosome study of the Iriomote cat. J Hered 78: 105–107

ZOOLOGICAL SCIENCE 11: 605–612 (1994)

A Molecular Phylogeny of the Family Mustelidae (Mammalia, Carnivora), Based on Comparison of Mitochondrial Cytochrome b Nucleotide Sequences

RYUICHI MASUDA* and MICHIHIRO C. YOSHIDA

Chromosome Research Unit, Faculty of Science, and Division of Biological Science, Graduate School of Environmental Earth Science, Hokkaido University, Sapporo 060, Japan

ABSTRACT—To study the phylogenetic relationships between the species of the family Mustelidae, by using the improved polymerase chain reaction-product direct sequencing technique, nucleotide sequences (375 bases) of the mitochondrial cytochrome b gene were determined on ten species from five genera of the Mustelidae and three species of other carnivore families, all of which are distributed in or around Japan. The molecular phylogenetic tree indicated a clear separation of five genera: *Mustela* and *Martes* from the subfamily Mustelinae, *Lutra* and *Enhydra* from the subfamily Lutrinae, and *Meles* from the subfamily Melinae. This clustering agreed with the previously reported morphological and karyological taxonomy. Furthermore, the relationships between the intrageneric species were discussed in more detail. This is the first report on the molecular phylogeny throughout the Japanese species of the Mustelidae, inferred from the mitochondrial DNA sequences.

INTRODUCTION

The family Mustelidae, which includes 64 species, has been most diversified in the order Carnivora which consists of more than 230 species [10]. The distribution of the mustelid species is widespread on a global scale. However, detailed relationships between the species in this family have not been fully examined.

In Japan, ten species of the Mustelidae are known: *Mustela itatsi* Temminck, 1844; *Mustela sibirica* Pallas, 1773; *Mustela nivalis* Linnaeus, 1766; *Mustela erminea* Linnaeus, 1758; *Mustela vison* Schreber, 1777; *Martes melampus* (Wagner, 1840); *Martes zibellina* (Linnaeus, 1758); *Meles meles* (Linnaeus, 1758); *Lutra lutra* (Linnaeus, 1758); *Enhydra lutris* (Linnaeus, 1758). At present, the latter two aquatic species have become endangered in Japan. *Mustela sibirica*, which is native on Tsushima Islands, and *Mustela vison* were introduced to Japan from Korea and North America, respectively. Obara [32] suggested that *Mustela erminea* is an ancestral type with karyological characters similar to *Mustela itatsi, Mustela nivalis*, and *Martes melampus*. *Meles meles* was karyologically separated from the other species of the Mustelidae [32]. However, the phylogenetic relationships throughout Japanese mustelid species have yet to be resolved.

A molecular genetic approach provides important information on the relationships between closely related species. Since the mitochondrial DNA (mtDNA) evolves more rapidly than the nuclear DNA [8], the mtDNA analysis is a useful method for the phylogenetic study [5, 7, 16]. Recently, the advent of polymerase chain reaction (PCR) led the advance in nucleotide sequence analysis from small amounts of DNA [29, 30, 33, 34]. Moreover, the PCR technology also developed the mtDNA analysis for the evolutionary study of many animal species including carnivores [23, 25, 39, 40, 42]. Previously, we reported the improved PCR product-direct sequencing technique and characterization of nucleotide sequence variations of the mitochondrial cytochrome b genes on three weasel species: *M. itatsi, M. sibirica*, and *M. nivalis* [27]. In that report, we showed that the analysis of this gene is useful for examination of the genetic difference between closely related species.

In this study, we determined partial nucleotide sequences of the cytochrome b genes for ten species of the Mustelidae and other carnivores using the improved PCR product-direct sequencing technique. Based on sequence comparison, we presented the molecular phylogeny of intra- and intergeneric species in the Mustelidae and discussed the relationships between them, as compared with the previously reported karyological and morphological data.

MATERIALS AND METHODS

Animals and DNA extraction

Animals examined in this study were listed in Table 1. Muscle tissues were dissected from each animal and frozen at −80°C or preserved in 70% ethanol. Total DNAs were extracted according to the phenol/proteinase K/sodium dodecyl sulfate (SDS) method of Sambrook *et al.* [36] with simplified modifications [27]. In brief, a small piece (about 2×2×2 mm) of tissue was excised with a scalpel and washed several times with 1 ml of STE buffer (0.1 M NaCl/10 mM Tris/1 mM EDTA). Using a small glass homogenizer, the tissue was homogenized with 500 μl of STE buffer containing a final concentration of 0.5% SDS and 5 μg/ml of proteinase K. After incubation at 37°C overnight, the homogenate was extracted twice

Accepted June 27, 1994
Received Jan 31, 1994
* To whom correspondence should be addressed.

TABLE 1. Species of the family Mustelidae and other carnivore families analyzed in this study

Species	Code	Common name	No. examined	Source (Collecting locality if known)
Family Mustelidae				
Mustela itatsi	MIT	Japanese weasel	2*	Rishiri Town Museum and Shiretoko Museum (Rishiri Island and Abashiri-gun, Hokkaido; ref. [26]**)
Mustela sibirica	MSI	Siberian weasel	2*	Kitakyushu Museum of Natural History (Onga-gun, Fukuoka Pref.; ref. [26]**)
Mustela erminea	MER	Stoat or ermine	1	Shiretoko Museum (Shari-cho, Hokkaido)
Mustela nivalis	MNI1	Least weasel	1	Iwate Prefectural Museum (Kunohe-gun, Iwate Pref.)
Mustela nivalis	MNI2	Least weasel	1	Shiretoko Museum (Shari-gun, Hokkaido; ref. [26]**)
Mustela vison	MVI	American mink	2*	Shiretoko Museum (Shari-gun, Hokkaido)
Martes melampus	MME	Japanese marten	1	Iwate Prefectural Museum (Morioka-shi, Iwate Pref.)
Martes zibellina	MZI	Sable	2*	Shiretoko Museum (Shari-cho and Kiyosato-cho, Hokkaido)
Meles meles	MEL	Japanese badger	1	(Ohno-gun, Gifu Pref.)
Lutra lutra	LLU	River otter	2*	Kobe Oji Zoo (originated from Russia)
Enhydra lutris	ELU	Sea otter	1	Suma Aqualife Park (originated from North Pacific)
Family Ursidae				
Selenarctos thibetanus	STH	Asiatic black bear	1	(Ohno-gun, Gifu Pref.)
Family Otariidae				
Zalophus californianus	ZCA	California sea lion	1	Kobe Oji Zoo (originated from North America)
Family Phocidae				
Phoca vitulina	PVI	Harbor seal	—	ref. [4]***

* Two individuals showed no intraspecific sequence variation.
** The cytochrome b sequences were cited from our previous paper [27].
*** The cytochrome b sequence was cited from the previously published paper of Arnason and Johnsson [4].

with an equal volume of phenol/chloroform (1:1) and once with chloroform/isoamyl alcohol (24:1). All procedures were done in 1.5 ml microcentrifuge tubes. STE buffer extracted by the same procedure was used as a negative control in the following PCR amplification.

Symmetric and asymmetric PCR amplification

Partial regions of the mitochondrial cytochrome b genes were PCR-amplified using the method of Kocher *et al.* [25] with some modifications [27]. Referring to the published information of Irwin *et al.* [23], primer sequences were designed as L14724 (5′-GATATG-AAAAACCATCGTTG-3′) and H15149 (5′-CTCAGAATGATA-TTTGTCCTCA-3′) by the consensus between the mtDNA sequences of the human [2], the bovine [3], and the mouse [6]. Primer names identify the light (L) or heavy (H) strand and the 3' end-position of the primer in the human mtDNA sequence [2]. Primers were synthesized on an Applied Biosystems 391 DNA synthesizer.

Symmetric PCR was done for the amplification of double-stranded DNAs with a GeneAmp PCR reagent kit (Perkin-Elmer/Cetus) according to the manufacturer's instruction. A total volume of 50 μl of the reaction mixture included 10 mM Tris (pH 8.3), 50 mM KCl, 1.5 mM $MgCl_2$, 0.001% (w/v) gelatin, each dNTP at 200 μM, 1.25 U of *Taq* DNA polymerase, each primer at 250 nM, and 1–5 μl of the extracted DNA solution as a template. Each cycle was programed by denaturing at 94°C for 1 min, annealing at 50°C for 1 min, and extension at 72°C for 1 min. After 35 cycles, the extension reaction was completed by incubation at 72°C for 10 min.

Asymmetric PCR was performed to generate single-stranded DNAs according to the method of Gyllensten and Erlich [14]. The PCR procedure was basically the same as symmetric PCR, except for 30 cycles of reaction, a 1:100 (2.5 nM:250 nM) ratio of two primers, and 1 μl of the symmetric PCR product as a DNA template in 100 μl of the reaction mixture.

Direct sequencing of PCR products and sequence analysis

Single-stranded DNAs produced by asymmetric PCR were concentrated using a Centricon-30 microconcentrator (Amicon), and 7 μl of the concentrated DNA was sequenced with 10 ng of the PCR primer for the L or H strand, [^{32}P] dCTP (Amersham), and T7 DNA polymerase (United States Biochemical), according to the dideoxynucleotide chain reaction method [37]. Reaction products were electrophoresed on 6% polyacrylamide gels containing 7 M urea. Gels were dried and exposed to Fuji RX X-ray films for 1–5 days.

Sequence analysis and phylogenetic tree construction by the neighbor-joining method [35] were performed with the Clustal V computer software [18]. Numbers of nucleotide substitutions per site were estimated for multiple substitutions using Kimura's two-parameter method [24]. Bootstrap methods [13] were used in the Clustal V to assess the degree of support for internal branches of the tree. Cytochrome b sequences of MIT (Accession No. D26130), MSI (Accession No. D26132), and MNI2 (Accession No. D26133) were cited from our previous report [27]. PVI sequence was obtained from the published paper of Arnason and Johnsson [4].

RESULTS

From a small piece of each animal tissue, total DNAs were extracted with the simplified method, and the partial

(a)

```
          10         20         30         40         50         60         70         80
MIT   ATGACCAACA TTCGCAAAAC CCACCCACTA ACCAAAATCA TCAACAACTC ATTCATTGAC TTACCCGCCC CATCAAACAT
MSI   .......... .......... .......T.. .......... .......... ....G..... C.T..... ..........
MER   .......... ....T..... T......T.. .......... .......... ...T..C... C.C.....T. ..........
MNI1  .......... ....T..... T........G .......... .......... .......... C.C.....T. ..........
MNI2  .......... ....T..... T........G .......... .......... .......... C.C.....T. ..........
MVI   .......... ....T..... .......T.. ........T. .......... .........T C....T..T. ..........
MME   .......... ....T..... T......... G.T....... .......T.. ......C... .....T..T. ..........
MZI   .......... ....T..... T......... G......... .......T.. ......C... .....T..T. ..........
MEL   .......... ....T...T. G......... .........C .......T.. ...T...... C.......A. ....C..T..
LLU   .......... .......... T......T.. G......... .......... GC....C..T C.......G. ....G..T..
ELU   .......... ....T..G.. ...T..C... .....G.... .......... ......C... C.......A. ..........
PVI   .......... .C..A..... ...T...... .TA.....T. .......... ......C... C.....A.A. .......T..
ZCA   .......... ....A...GT A..T.....G G.......T. ......GT.. .C.T..C... C.G...A.A. ....T.....
STH   .......... .CT.A..... ...T...T.. G......... .T........ .C.......T C.C..A..A. .......T..

          90         100        110        120        130        140        150        160
MIT   TTCAGCGTGA TGAAACTTCG GCTCCCTTCT CGGAATCTGC CTAATTATTC AGATTCTTAC AGGTTTATTT TTAGCTATAC
MSI   C.....A... .......... .......... .......... .......... .......... .......... .....C....
MER   C.....A... .......... .......C.. .......... .....C.... .......... .......... .....C..G.
MNI1  C.....A... .......... .T.....C.. .......... ..T....... .......... .......... .....C..G.
MNI2  C.....A... .......... .......... .......... ..T....... .......... .......... .....C..G.
MVI   C.....A... .......... .G.....A.. .......... ......C... .A........ ...C.....C .....C....
MME   ...C..A... .......... .......C.. T......... .....CC.A. .......... .......... C....C....
MZI   ...C..A... .....T.... .......C.. T........T ..G..CC.A. .......... .......... C....C....
MEL   C.....A... ........T. .A.....C.. T......... .....CC.A. .A..C..... .........C C....C....
LLU   ......A... .....T..T. .A.....A.. A....CT... T....CC... .......... .......... .....C....
ELU   C.....A... .......... .A.....A.. ......T... T....CC... .......... .......... ..........
PVI   C..G..A... ........T. .A..T..... .......... .....CC.G. ....CT.A.. ...C.....C C....C....
ZCA   C.....A... ........T. .A.....C.. ..C.GCA... T..GCCT.A. .A..C..A.. ...CC.T..C C.........
STH   C.....A... ........T. .A........ ....G.A... ...G..C.A. .......A.. ...CC..... C....C....

          170        180        190        200        210        220        230        240
MIT   ACTATACATC GGACACAGCC ACAGCCTTTT CATCAGTCAC CCATATCTGT CGAGACGTCA ACTATGGCTG AATCATCCGA
MSI   .......... A......... .......... .......... ......T... .......... .......... ..........
MER   .T..C..... A......... ........C. .......... ...C.....C .......... ....C..... ..........
MNI1  .......... A..T...... .......... .......... ...C...... .......... ....C..... ...T......
MNI2  .......... A..T...... .......... .......... ...C...... .......... ....C..... ...T......
MVI   ....C..... A........T .......... .......... T.....T..C ........T. .T.....T.. ......T...
MME   ....C..... A......... ........C. .......... ...C..T..C .......... ....C..A.. ...T......
MZI   ....C..... A......... ........C. ....G..... ...C..T..C .......... ....C..... G..T..T...
MEL   .T..C...C. A.....CA.T ..C.....C. .......T.. A..C...... ........T. .......... ......T...
LLU   ....C..... A......A.. ........C. ........G. A..C.....C .......... ....C..... G..T......
ELU   .T........ A......A.. ........C. ........G. .........C .......... ....C..... ...T.....G
PVI   ....C..C.. A......A.. ........C. .......A.. ...C.....C ........A. ....C..... .........T
ZCA   .......C.. A.....CA.. .......... .......... ...C..T..C .......... ....C..... ..........
STH   .......... A...G..A.T .......... ....G...G. ...C..T..C .........C .T..C..A.. ...T......

          250        260        270        280        290        300        310        320
MIT   TATATACATG CAAACGGAGC CTCCATATTC TTTATCTGCC TGTTCCTACA CGTAGGGCGA GGCTTATATT ACGGATCCTA
MSI   ..C.....C. .......... T......... ..C....... .......... .......... ..T....... .......T..
MER   ..C.....C. .......... T......... ..C....... .A........ ......A... .......... ....T..T..
MNI1  ..C....... .......... T.....G... .....T.... .A........ ......A... .......... .T..T..T..
MNI2  ..C....... .......... T......... .....T.... .A........ ......A... .......... .T..T..T..
MVI   ........C. ....T..... T......... ...G.T...T .......... T.....A... .......... .T.....T..
MME   ..C....... .C.....G.. T......... ..C....... .......G.. ...C..A..G ...C....C. .T.....T..
MZI   .......... .C.....G.. T......... ..C....... .......G.. ...C..A..G ..T.....C. .T.....T..
MEL   .....G..C. .T..T..... .......... .......... .A...T.... T.....A... ...C...... ..........
LLU   ..C.....C. .......... .......... ..C....... .......... T.....A..C ...C.G..C. .......T..
ELU   ..C....... .......... A......... .....T.... .A........ T.....A... ..A.....C. .T.....T..
PVI   ...C.T..C. ....T..... T........T ..C....... .A.A.A.G.. T.....A... ..AC.G.... ....C.....
ZCA   ..C..G..C. ....T..... .......... .......... .C.A.A.G.. ......A... ..AC.G..C. ..........
STH   .......... .......... ......G... ..C....... .A...A.... ......A..G .....G.... .T..C..T..
```

```
                330        340        350        360        370   375
MIT   TATATTCACC GAAACATGAA ACATCGGCAT TATCTTATTA TTCGCAGTCA TAGCA
MSI   .......... .......... .......... .........G .......... .....
MER   .......C.. .......... ....T..... .......... .......... .....
MNI1  .......T.. .......... .......... .......... .......... .....
MNI2  .......T.. .......... .......... .......... .......... .....
MVI   ......TC.T .......... .T..T..T.. C......C.. ...A....A. .....
MME   .....A.C.. ........G. ....T..... C...C..... ........T. .....
MZI   .....A.C.. ........G. ....T..T.. C...C..... .......... .....
MEL   .......C.T .......... .T.....T.. C.....G... ...A....A. .....
LLU   .......C.T .......... ...CT..T.. ...TC..C.. ......AC.. .....
ELU   C.....TT.. .......... ....T..T.. .G.....C.. ...A....T. .....
PVI   C.C......A ..G....... .......... ....C.C... ...A.C.... ....T
ZCA   ..C.C.A..A .......... ....T..... C...C.CC.. ..TA..A... ....T
STH   CC..C..T.A .......... .T..T...TA CG..C.CC.. ..TA....T. ....C
```

(b)

```
                10         20         30         40         50         60         70         80
MIT   MTNIRKTHPL TKIINNSFID LPAPSNISAW WNFGSLLGIC LIIQILTGLF LAMHYTSDTA TAFSSVTHIC RDVNYGWIIR
MSI   .......... ........V. .......... .......... .......... .......... .......... ..........
MER   .......... .......... .......... .......... .......... .......... .......... ..........
MNI1  .......... .......... .......... .......... .......... .......... .......... ..........
MNI2  .......... .......... .......... .......... .......... .......... .......... ..........
MVI   .......... .......... .......... .......... ..L....... .......... .......... ..........
MME   .......... A......... .......... .......... ..L....... .......... .......... ..........
MZI   .......... A......... .......... .......... ..L....... .......... .......... ..........
MEL   ......S... ...L...... .......... .......... ..L....... ......P..T .......... ..........
LLU   .......... A......L.. .......... ........T. ..L....... .........T ......A... ..........
ELU   .......... .......... .......... .......... ..L....... .........T ......A... ..........
PVI   .......... M......... ..T....... .......... ..L....... .........T .......... ..........
ZCA   ......V... A....S.L.. ..T....... .......AA. .AL....... .........T .......... ..........
STH   ....W..... A......L.. .......... ........V. .VL....... ........AT ......A... ...H......

                90         100        110        120   125
MIT   YMHANGASMF FICLFLHVGR GLYYGSYMFT ETWNIGIILL FAVMA
MSI   .......... .......... .......... .......... .....
MER   .......... .......... .........P .......... .....
MNI1  .......... .......... .........S .......... .....
MNI2  .......... .......... .........S .......... .....
MVI   .......... .V........ .........P .......... .T...
MME   .......... .......... ........YP .......... .....
MZI   .......... .......... ........YP .......... .....
MEL   .......... .......... .........P .......... .T...
LLU   .......... .......... .........P ....T..... ..T..
ELU   .......... .......... .........S .......V.. .T...
PVI   .L........ ....YM.... .......T.. .......... .T...
ZCA   .......... ....YM.... .......TL. .......... .TI..
STH   .......... .....M.... .......LLS ......YV.. .T...
```

FIG. 1. Cytochrome b sequences in species of the family Mustelidae. a: nucleotide sequences (375 bases) obtained by the PCR product-direct sequencing technique. b: amino acid sequences (125 amino acids) deduced from nucleotide sequences (a). Characters are nucleotide or amino acid codes recommended by IUPAC-IUB. Dots denote identity with nucleotides or amino acids of MIT.

region of the mitochondrial cytochrome b gene was successfully amplified by symmetric and asymmetric PCRs. Using the direct sequencing technique of single-stranded DNAs, nucleotide sequences (375 bases) were determined without any gap or insertion in all species (Fig. 1a).

Two individuals from each of the five mustelid species (*Mustela itatsi, M. sibirica, M. vison, Martes zibellina*, and *Lutra lutra*) showed no intraspecific sequence variation, indicating the possible close relationships between the two individuals: samples of *M. itatsi, M. sibirica*, and *M. vison* were originated from the introduced small populations, and two specimens of *M. zibellina* were collected from the close localities in Hokkaido, and two individuals of *L. lutra* were brought from Russia and kept in the zoo (Table 1). *Mustela*

TABLE 2. Percentage differences (above diagonal) and numbers of transitions/transversions (below diagonal) for cytochrome b nucleotide sequences (375 bases) of the Mustelidae and other carnivore species

Code	MIT	MSI	MER	MNI1	MNI2	MVI	MME	MZI	MEL	LLU	ELU	PVI	ZCA	STH
MIT	—	4.3	8.3	7.5	6.7	12.3	12.3	13.1	14.7	14.4	11.7	17.1	20.0	18.7
MSI	15/1	—	6.4	7.2	6.4	11.2	12.3	13.1	15.7	13.9	12.3	16.8	20.0	17.9
MER	28/3	22/2	—	5.3	5.1	11.7	9.3	10.7	13.3	11.5	10.4	15.5	18.9	17.9
MNI1	24/4	24/3	19/1	—	0.8	12.5	11.5	12.5	15.7	14.9	10.7	18.1	20.5	17.1
MNI2	21/4	21/3	18/1	3/0	—	12.3	11.2	12.3	15.7	14.7	10.4	17.6	20.5	17.1
MVI	41/5	36/6	38/6	40/7	39/7	—	14.7	14.9	13.1	15.7	13.1	18.9	21.3	17.6
MME	38/8	37/9	26/9	33/10	32/10	46/9	—	3.5	16.3	13.3	13.9	18.4	20.0	18.1
MZI	42/7	41/8	32/8	38/9	37/9	48/8	12/1	—	16.8	13.6	14.9	19.7	21.6	19.5
MEL	41/14	44/15	35/15	43/16	43/16	38/11	47/14	50/13	—	16.5	16.5	16.3	18.4	21.1
LLU	46/8	43/9	34/9	46/10	45/10	54/5	38/12	40/11	50/12	—	12.8	18.7	19.2	18.4
ELU	36/8	37/9	30/9	30/10	29/10	44/5	40/12	45/11	48/14	42/6	—	17.3	19.5	17.1
PVI	43/21	41/22	36/22	45/23	43/23	49/22	44/25	50/24	34/27	47/23	44/21	—	15.7	18.7
ZCA	54/21	53/22	47/24	52/25	52/25	58/22	50/25	57/24	48/21	49/23	52/21	43/16	—	18.4
STH	50/20	48/19	50/17	46/18	46/18	47/19	48/20	52/21	55/24	49/20	44/20	51/19	50/19	—

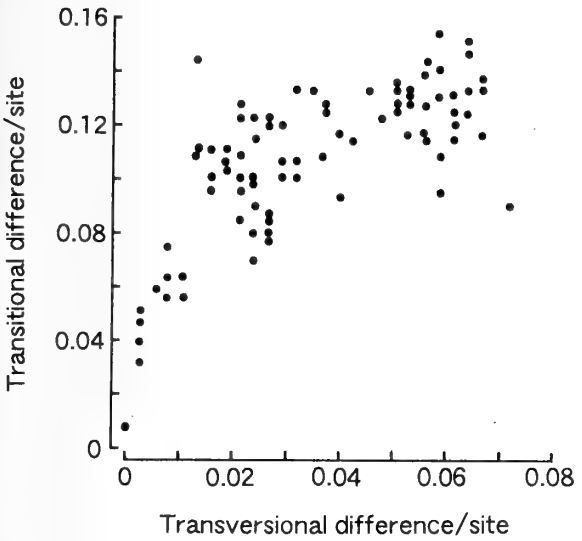

FIG. 2. The transitional difference per site was plotted against the transversional difference per site in pairwise comparisons of cytochrome b nucleotide sequences.

nivalis from Iwate Prefecture (MNI1) showed 0.8% (3/375 bases) sequence difference from that from Hokkaido (MNI2) (Tables 1 and 2). From each of the other five mustelid species, one sample was examined (Table 1). Percentage sequence differences and numbers of transitions/transversions obtained from all pairwise comparisons were shown in Table 2.

In Figure 2, the transitional difference per site was plotted against the transversional difference per site. These differences were positively related among the mustelid species and the high transition bias was observed (Fig. 2).

Among the mustelid species, percentage differences were between 4.3 and 16.8% (3–63/375 bases) (Table 2). Outgroup species including *Phoca vitulina* (PVI), *Zalophus californianus* (ZCA), and *Selenarctos thibetanus* (STH) showed 15.5–21.6% (58–81/375 bases) sequence differences from the mustelid species (Table 2).

Among the *Mustela* species except for *M. vison* (MVI), sequence differences were between 4.3 and 8.3% (3–31/375

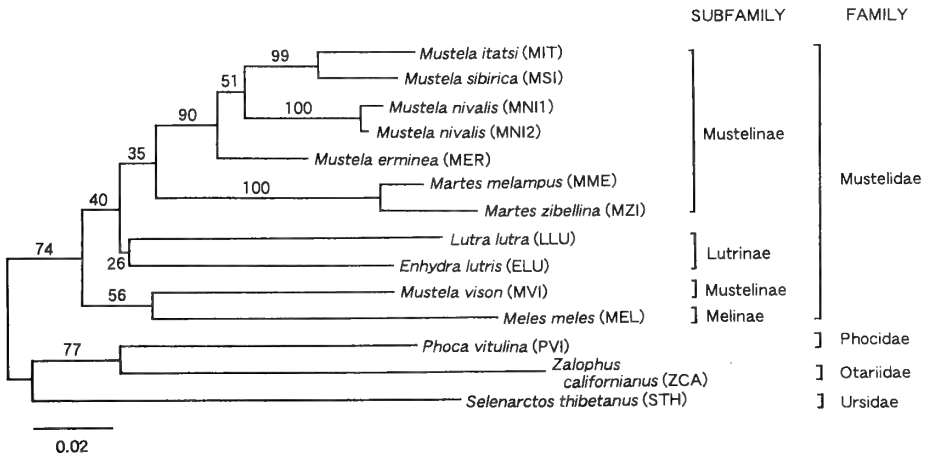

FIG. 3. Phylogenetic tree of cytochrome b nucleotide sequences constructed by the neighbor-joining method and Kimura's two-parameter method. The scale bar indicates an evolutionary distance of 0.02 substitution per site. Numbers above branches are bootstrap probability values based on 500 replications.

bases) (Table 2). MVI showed higher differences (11.2–12.5%, 42–47/375 bases) from the other *Mustela* species. Two species of the genus *Martes, M. melampus* (MME) and *M. zibellina* (MZI), showed 3.5% (13/375 bases) difference between them. These two *Martes* species differed by 9.3–14.9% (35–56/375 bases) of sequences from the *Mustela* species. *Meles meles* (MEL), *Lutra lutra* (LLU), and *Enhydra lutris* (ELU) showed relatively higher differences (10.4–16.8%, 39–63/375 bases) from those of the *Mustela* and *Martes* species (Table 2). Amino acid sequences deduced from nucleotide sequences were shown in Figure 1b.

The phylogenetic tree of cytochrome b nucleotide sequences was constructed using the neighbor-joining method, based on the matrix of the numbers of nucleotide substitutions per site expected by Kimura's two-parameter method (Fig. 3). The species of the genus *Mustela* in the subfamily Mustelinae, except for MVI, were separated from the other mustelid species with 90% bootstrap value. Two species of the genus *Martes*, MME and MZI, were clustered with 100% bootstrap value. MVI was distantly related to the cluster of the subfamily Mustelinae. LLU and ELU from the subfamily Lutrinae were grouped into the same lineage, although the bootstrap value was low (26%). MEL, the subfamily Melinae, was positioned distantly from the other mustelid species. Among outgroup species, ZCA was closer to PVI than STH.

DISCUSSION

In this study, we examined the molecular phylogenetic relationships between the species of the family Mustelidae which are distributed in or around Japan. Using the DNA extraction and the PCR product-direct sequencing techniques improved by us, the cytochrome b nucleotide sequences (375 bases) were successfully determined (Fig. 1a). The amino acid sequences (Fig. 1b) deduced from the nucleotide sequences indicated that synonymous mutations were more numerous than nonsynonymous ones. This pattern of nucleotide substitution is similar to that reported in previous works [7, 9, 17, 28, 38]. The high transition bias was observed, and the transitional difference was positively related to the transversional one among the mustelid species (Fig. 2). Our findings agree with the previous reports and reflect the initial high transition bias of mtDNA, which gradually decreases over time as transversions are accumulated [7, 9, 11, 17, 19]. Since the high transition bias was found among the intrafamilial species which showed relatively higher sequence homology, Kimura's two-parameter method [24] was used for estimating numbers of nucleotide substitutions per site in the phylogenetic tree construction.

The molecular phylogenetic tree of the cytochrome b nucleotide sequences (Fig. 3) revealed that the species of the Mustelidae were divided into three major clusters: the first which includes four species (MIT, MSI, MNI, and MER) of the genus *Mustela*, the second which includes two species (MME and MZI) of the genus *Martes*, and the third which includes LLU and ELU. MEL and MVI were distantly related to the other mustelid species. The results suggest a monophyletic grouping of each genus, except for MVI in the *Mustela*. According to the Carnivora classifications by Ewer [12] and Wozencraft [44], the family Mustelidae was divided into at least four subfamilies: Mustelinae, Lutrinae, Melinae, and Mephitinae. The classification of subfamilies was shown on the phylogenetic tree in Figure 3. Our results support the classification of subfamilies, except for the position of MVI (Fig. 3).

In the previous study [27], we reported a clear distinction of the cytochrome b sequences between *M. itatsi* (MIT) and *M. sibirica* (MSI). The present study throughout the Japanese mustelid species indicated that MIT and MSI, though genetically distinct, were clustered and separated from the other *Mustela* species with the high bootstrap value (99%) (Fig. 3). By contrast, Wozencraft [45] proposed that MIT is a synonym of MSI, based on the morphological similarity. Ewer [12] and Nowak [31] classified the Japanese weasel as MSI, but they did not recognize MIT in the classification of the *Mustela* species. On the one hand, Imaizumi [22] classified MIT and MSI as two subspecies of *M. sibirica, M. s. itatsi* and *M. s. coreana*, respectively, based on the difference of a ratio of the tail length to the head and body lengths (the T-HB ratio): about 0.4 in *M. s. itasti* and greater than 0.5 in *M. s. coreana*. In the previous study [27], using the T-HB ratio we unambiguously identified MIT (0.39–0.41 of five specimens) and MSI (0.53–0.56 of two specimens). Between specimens identified as MIT and MSI, sequence difference was 4.3% [27]. Although this value is somewhat smaller than those among the *Mustela* species revealed in the present study (5.1–8.3% excluding MVI, Table 2), its magnitude apparently exceeds the intraspecific level. The intraspecific differences of the cytochrome b sequences were 0.8% in MIT [27] and 0.8% in *M. nivalis* (Table 2). In addition, Wayne and Jenks [41] reported the intraspecific differences of the canine cytochrome b sequences: 0.3–1.3% in the coyote *Canis latrans* and 0.3–0.5% in the gray wolf *C. lupus*. Therefore, we concluded that it is reasonable for MIT and MSI to be classified as distinct species.

Two specimens of *M. nivalis* collected from Iwate Prefecture (MNI1) and Hokkaido (MNI2) showed 0.8% (3/375 bases) nucleotide difference (Table 2), all of which were synonymous (Fig. 1b). Obara [32] reported the karyotype differences between M. nivalis from Aomori Prefecture (2n=38) and that from Hokkaido (2n=42), and he proposed that these two animals are distinct species, *M. namiyei* and *M. nivalis nivalis*, respectively. *M. nivalis* from the Eurasian Continent, which has the karyotype (2n=42) [26] similar to the Hokkaido type, was proposed as an ancestral type of *M. nivalis* occurring in Japan [32]. Although, in this study, a karyotype could not be analyzed on MNI1 and MNI2, their collecting localities (Iwate, close to Aomori, and Hokkaido, respectively) suggest that MNI1 and MNI2 may have different karyotypes as shown by Obara's data [32]. However, the sequence difference (0.8%) between MNI1 and MNI2 was much smaller than the interspecific difference within the

genus *Mustela* (Table 2), indicating that they are not distinct species. Since the two MNI types are karyologically different and geographically isolated, it seems to be reasonable that they are classified as subspecies. Further studies on more specimens from Honshu and Hokkaido are, however, still necessary to conclude whether the two types are subspecies or distinct species.

It is interesting that *M. vison* (MVI) was outside of the monophyletic grouping of the genus *Mustela* in the phylogenetic tree (Fig. 3). Holmes [20], by a cladistic analysis, divided the genus *Mustela* into four monophyletic groups: the first which consisted of only MVI, the second which included *M. sibirica* and other species, the third which included *M. nivalis, M. erminea,* and other species, and the last which consisted of different species from our study. Our results support Holmes' classification of the genus *Mustela* and the position of MVI.

Two species of the genus *Martes, M. melampus* (MME) and *M. zibellina* (MZI), were grouped with 100% bootstrap value and they were closer to the genus *Mustela* (Fig. 3), supporting the morphological classification in that both the *Martes* and the *Mustela* are classified into the subfamily Mustelinae [12, 44]. The cytochrome b sequence difference between MME and MZI was 3.5% (13/375 bases) (Table 2), all of which were synonymous mutations (Fig. 1b). Previous morphological reports indicate that MME and MZI may be conspecific [1, 15]. In fact, the sequence difference (3.5%) between MME and MZI is smaller than the interspecific differences (4.3–8.3%) within the genus *Mustela* including MIT, MSI, MER, and MNI (Table 2), but it is larger than the intraspecific differences such as: 0.8% for MNI (Table 2), 0.8% for MIT [27], 0.3–0.5% for *C. lupus* [42]. As compared with these sequence differences, it is reasonable for MME and MZI to be classified as distinct species.

Lutra lutra (LLU) was grouped with *Enhydra lutris* (ELU) (Fig. 3). This concurs with morphological classifications of Ewer [12] and Wozencraft [44] that these two aquatic species were classified into the subsfamily Lutrinae.

Meles meles (MEL) was distantly related to the other mustelid species (Fig. 3), in agreement with the karyological taxonomy by Obara [32]. Morphologically, MEL was classified into the subfamily Melinae by Ewer [12] and Wozencraft [44]. Hosoda *et al.* [21] reported the phylogenetic relationship among carnivore species including MIT, MNI, MME, and MEL, based on the restriction fragment length polymorphisms of the nuclear ribosomal DNA. Our finding basically agree with the result of Hosoda *et al.* [21] on the four species.

Among outgroup species, *Zalophus californianus* (ZCA) was closer to *Phoca vitulina* (PVI) than *Selenarctos thibetanus* (STH), supporting the previous findings from the DNA hybridization analysis of Wayne *et al.* [41]. Our results also agree mostly with the karyological phylogeny on these species reported by Wurster and Benirschke [46] and Wozencraft [43].

This is the first report on the molecular phylogeny throughout the Japanese species of the family Mustelidae, inferred from the mtDNA sequences. The relationships between the intergeneric species and between the intrageneric species were examined in detail, based on the cytochrome b sequence comparison. As a whole, the molecular phylogenetic tree was in agreement with the previously reported karyological and morphological taxonomy.

SEQUENCE AVAILABILITY

The nucleotide sequence data reported in this paper will appear in the GSDB, DDBJ, EMBL, and NCBI nucleotide sequence data bases with the following accession numbers; D26515 for MER; D26516 for MNI1; D26517 for MVI; D26518 for MME; D26519 for MZI; D26520 for MEL; D26521 for LLU; D26522 for ELU; D26523 for STH; D26524 for ZCA.

ACKNOWLEDGMENTS

We thank Dr. M. Baba of Kitakyushu Museum of Natural History, S. Dakemoto, Y. Masuda of Shiretoko Museum, K. Murata of Kobe Oji Zoo, M. Sato of Rishiri Town Museum, F. Sekiyama of Iwate Prefectural Museum for supplying specimens. We are also grateful to Dr. N. Saitou of the National Institute of Genetics for helpful advice on computer software.

REFERENCES

1 Anderson E (1970) Quaternary evolution of the genus *Martes* (Carnivora, Mustelidae). Acta Zool Fennica 130: 1–132

2 Anderson S, Bankier AT, Barrell BG, De Bruijn MHL, Coulson AR, Drouin J, Eperon IC, Nierlich DP, Roe BA, Sanger F, Schreier PH, Smith AJH, Staden R, Young IG (1981) Sequence and organization of the human mitochondrial genome. Nature 290: 457–465

3 Anderson S, De Bruijn MHL, Coulson AR, Eperon IC, Sanger F, Young IG (1982) Complete sequence of bovine mitochondrial DNA: Conserved features of the mammalian mitochondrial genome. J Mol Biol 156: 683–717

4 Arnason U, Johnsson E (1992) The complete mitochondrial DNA sequence of the harbor seal, *Phoca vitulina*. J Mol Evol 34: 493–505

5 Avice JC (1991) Ten unorthodox perspectives on evolution prompted by comparative population genetic findings on mitochondrial DNA. Annu Rev Genet 25: 45–69

6 Bibb MJ, Van Etten RA, Wright CT, Walberg MW, Clayton DA (1981) Sequence and gene organization of mouse mitochondrial DNA. Cell 26: 167–180

7 Brown WM (1985) The mitochondrial genome of animals. In "Molecular Evolutionary Genetics" Ed by RJ MacIntyre, Plenum Press, New York, pp 95–130

8 Brown WM, George MJr, Wilson AC (1979) Rapid evolution of animal mitochondrial DNA. Proc Natl Acad Sci USA 76: 1967–1971

9 Brown WM, Prager EM, Wang A, Wilson AC (1982) Mitochondrial DNA sequences of primates: Tempo and mode of evolution. J Mol Evol 18: 225–239

10 Corbet GB, Hill JE (1991) A World List of Mammalian Species. 3rd ed, Oxford Univ Press, Oxford

11 DeSalle R, Freedman T, Pragner EM, Wilson AC (1987) Tempo and mode of sequence evolution in mitochondrial DNA of Hawaiian *Drosophila*. J Mol Evol 26: 157–164

12 Ewer RF (1973) The Carnivores. Cornell Univ Press, New

York

13 Felsenstein J (1985) Confidence limits on phylogenies: An approach using the bootstrap. Evolution 39: 783–791

14 Gyllensten UB, Erlich HA (1988) Generation of single-stranded DNA by the polymerase chain reaction and its application to direct sequencing of the HLA-DQA locus. Proc Natl Acad Sci USA 85: 7652–7656

15 Hagmeier EM (1961) Variation and relationships in North American marten. Canadian Field-Naturalist 75: 122–138

16 Harrison RG (1989) Animal mitochondrial DNA as a genetic marker in population and evolutionary biology. Trends Ecol Evol 4: 6–11

17 Hedges SB, Bezy RL, Maxson LR (1991) Phylogenetic relationships and biogeography of xantusiid lizards, inferred from mitochondrial DNA sequences. Mol Biol Evol 8: 767–780

18 Higgins DG, Bleasby AJ, Fuchs R (1992) Clustal V: Improved software for multiple sequence alignment. Comput Appl Biosci 8: 189–191

19 Hixon JE, Brown WM (1986) A comparison of the small ribosomal RNA genes from the mitochondrial DNA of the great apes and humans: Sequence divergence, structure, evolution, and phylogenetic implications. Mol Biol Evol 3: 1–18

20 Holmes T (1985) A phylogeny of the Mustelinae (abstract). Am Soc Mammal, 65th Annu Meeting Abstr p 60

21 Hosoda T, Suzuki H, Yamada T, Tsuchiya K (1993) Restriction site polymorphism in the ribosomal DNA of eight species of Canidae and Mustelidae. Cytologia 58: 223–230

22 Imaizumi Y (1960) Coloured Illustrations of the Mammals of Japan. Hoikusha, Osaka (in Japanese)

23 Irwin DM, Kocher TD, Wilson AC (1991) Evolution of the cytochrome *b* gene of mammals. J Mol Evol 32: 128–144

24 Kimura M (1980) A simple method for estimating evolutionary rate of base substitutions through comparative studies of nucleotide sequences. J Mol Evol 16: 111–120

25 Kocher TD, Thomas WK, Meyer A, Edwards SV, Pääbo S, Villablanca FX, Wilson AC (1989) Dynamics of mitochondrial DNA evolution in animals: Amplification and sequencing with conserved primers. Proc Natl Acad Sci USA 86: 6196–6200

26 Mandahl N, Fredga K (1980) A comparative chromosome study by means of G-, C-, and NOR-bandings of the weasel, the pygmy weasel and stoat (*Mustela*, Carnivora, Mammalia). Hereditas 93: 75–83

27 Masuda R, Yoshida MC (1994) Nucleotide sequence variation of cytochrome b genes in three species of weasels, *Mustela itatsi*, *Mustela sibirica*, and *Mustela nivalis*, detected by improved PCR product-direct sequencing technique. J Mamm Soc Japan 19: 33–43

28 Meyer A, Wilson AC (1990) Origin of tetrapods inferred from their mitochondrial DNA affiliation to lungfish. J Mol Evol 31: 359–364

29 Mullis K, Faloona F, Scharf S, Saiki R, Horn G, Erlich H (1986) Specific enzymatic amplification of DNA in vitro: The polymerase chain reaction. Cold Spring Harbor Symp Quant Biol 51: 263–273

30 Mullis KB, Faloona FA (1987) Specific synthesis of DNA *in vitro* via a polymerase-catalyzed chain reaction. Methods Enzymol 155: 335–350

31 Nowak RM (1991) Walker's Mammals of the World, 5th. Johns Hopkins Univ Press, Baltimore

32 Obara Y (1991) Karyosystematics of the mustelid carnivores of Japan. Honyurui Kagaku [Mammalian Science] 30: 197–220 (in Japanese with English abstract)

33 Saiki RK, Scharf S, Faloona F, Mullis KB, Horn GT, Erlich HA, Arnheim N (1985) Enzymatic amplification of β-globin genomic sequences and restriction site analysis for diagnosis of sickel cell anemia. Science 230: 1350–1354

34 Saiki RK, Gelfand DH, Stoffel S, Scharf SJ, Higuchi R, Horn GT, Mullis KB, Erlich HA (1988) Primer-directed enzymatic amplification of DNA with a thermostable DNA polymerase. Science 239: 487–491

35 Saitou N, Nei M (1987) The neighbor-joining method: A new method for reconstructing phylogenetic trees. Mol Biol Evol 4: 406–425

36 Sambrook J, Fritsch EF, Maniatis T (1989) Molecular Cloning: A Laboratory Manual. 2nd ed, Cold Spring Harbor Laboratory, New York

37 Sanger F, Nicklen S, Coulson AR (1977) DNA sequencing with chain-terminating inhibitors. Proc Natl Acad Sci USA 74: 5463–5467

38 Smith MF, Patton JL (1991) Variation in mitochondrial cytochrome *b* sequence in natural populations of South American akodontine rodents (Muridae: Sigmodontinae). Mol Biol Evol 8: 85–103

39 Thomas RH, Schaffner W, Wilson AC, Pääbo S (1989) DNA phylogeny of the extinct marsupial wolf. Nature 340: 465–467

40 Thomas WK, Pääbo S, Villablanca FX, Wilson AC (1990) Spatial and temporal continuity of kangaroo rat populations shown by sequencing mitochondrial DNA from museum specimens. J Mol Evol 31: 101–112

41 Wayne RK, Benveniste RE, Janczewski DN, O'Brien SJ (1989) Molecular and biochemical evolution of the Carnivora. In "Carnivore Behavior, Ecology, and Evolution" Ed by JL Gittleman, Cornell Univ Press, New York, pp 465–494

42 Wayne RK, Jenks SM (1991) Mitochondrial DNA analysis implying extensive hybridization of the endangered red wolf *Canis rufus*. Nature 351: 565–568

43 Wozencraft WC (1989) The phylogeny of the recent Carnivora. In "Carnivore Behavior, Ecology, and Evolution" Ed by JL Gittleman, Cornell Univ Press, New York, pp 495–535

44 Wozencraft WC (1989) Classification of the recent Carnivora. In "Carnivore Behavior, Ecology, and Evolution" Ed by JL Gittleman, Cornell Univ Press, New York, pp 569–593

45 Wozencraft WC (1993) Order Carnivora. In "Mammal Species of the World: A Taxonomic and Geographic Reference, 2nd ed" Ed by DE Wilson and DM Reeder, Smithsonian Inst Press, Washington, pp 279–348

46 Wurster DH, Benirschke K (1968) Comparative cytogenetic studies in the Order Carnivora. Chromosoma 24: 336–382

ZOOLOGICAL SCIENCE 11: 613–623 (1994)

Phylogeny of Cerataphidini Aphids Revealed by Their Symbiotic Microorganisms and Basic Structure of Their Galls: Implications for Host-Symbiont Coevolution and Evolution of Sterile Soldier Castes

TAKEMA FUKATSU[1], SHIGEYUKI AOKI[2], UTAKO KUROSU[3] and HAJIME ISHIKAWA[1]

[1]*Zoological Institute, Faculty of Science, University of Tokyo, Hongo, Bunkyo-ku, Tokyo 113,* [2]*Laboratory of Biology, College of General Education, Rissho University, Magechi 1700, Kumagaya, Saitama 360-01, and* [3]*Laboratory of Entomology, Tokyo University of Agriculture, Sakuragaoka, Setagaya-ku, Tokyo 156, Japan*

ABSTRACT—We collected more than 40 species of aphids of Cerataphidini and related groups, which cover all the Cerataphidini genera ever described, and examined their symbiotic system histochemically. The Cerataphidini aphids were divided into two groups in terms of their symbiotic system; species with prokaryotic intracellular symbionts in mycetocytes which are typical of Aphididae species in general, and those with yeast-like extracellular symbionts in the hemocoel and fat body which are quite exceptional in Aphididae. The species with yeast-like symbionts, 12 out of 39 species examined, were further divided into three groups in terms of morphology of their symbionts. This division based on the symbionts coincided well with the division of genera based on morphology of the insects, with the only exception of "*Cerataphis*" *bambusifoliae*. We postulate that harboring the yeast-like symbiont is an apomorphic state, and evolved only once in Cerataphidini. It is also pointed out that the galls of Cerataphidini aphids fall into two types, single-cavity galls and multiple-cavity galls, based on the basic plan and structure. The multiple-cavity gall was considered to be apomorphic and of a single origin in Cerataphidini. Thus, the tribe Cerataphidini is constituted by two major monophyletic groups, one characterized by yeast-like symbionts and the other by multiple-cavity galls. A phylogenetic hypothesis on the evolutionary history of Cerataphidini is proposed. Also we discuss a possible origin and function of the yeast-like symbiont, taxonomic treatment of problematic taxa in Cerataphidini, and the effects of acquisition of novel symbionts on the evolution of host aphids.

INTRODUCTION

So far, some 4000 species of aphids (Homoptera, Aphididae) have been described. Almost all of them harbor microbial intracellular symbionts in the cytoplasm of mycetocytes, huge cells in the abdomen specialized for this purpose [11]. Judging from their ultrastructure and sensitivity to antibiotics, the symbionts are evidently of prokaryotic nature [22, 25]. Since they are passed from one to the next generation of the host insects by ovarial transmission and have no free-living state [11, 25], they can be regarded as a maternally inherited genetic element like mitochondria. The symbionts are not propagated when taken out of the host cells [23, 34]. The aphids show retarded growth and become sterile when deprived of their symbionts [27, 43]. It has been demonstrated that the symbionts serve as an important component in the pathway of amino acid metabolism [13, 24]. Thus, the aphids and their intracellular symbionts are intimately mutualistic with each other. Morphological, histological, biochemical and molecular biological lines of evidence have consistently suggested that the intracellular symbionts of various aphids are of a single origin; they have been derived from a bacterial species that was acquired by the common ancestor of the present aphids [11, 19, 37, 38, 40]. Molecular phylogenetic analyses revealed that the symbionts constitute a monophyletic group, *Buchnera*, a genus closely related to *Escherichia coli* [41].

Although the prokaryotic intracellular symbionts are highly conserved amongst Aphididae, several aphids have been reported to have a different symbiotic system. Four *Cerataphis* species [*C. fransseni* (= *variabilis*), *C. lataniae, C. freycinetiae* and *C. orchidearum*], *Glyphinaphis bambusae* and *Hamiltonaphis styraci* have been shown to contain neither mycetocytes nor intracellular symbionts but harbor yeast-like eukaryotic extracellular symbionts in the hemocoel and fat body [9, 10, 17, 30]. All these exceptional aphids belong to the tribe Cerataphidini, which prompted us to investigate this group extensively.

In the present study, we examine the symbiotic system of Cerataphidini aphids, and demonstrate that they are divided into two groups; species with intracellular symbionts and those with yeast-like ones. Based on the symbiont types and basic structure of the galls, which are shown to be stable characters in aphids in general but polymorphic in Cerataphidini, we analyze phylogenetic relationships in this group.

Accepted July 11, 1994
Received May 16, 1994

BACKGROUND ON CERATAPHIDINI

Systematics of Cerataphidini

The tribe Cerataphidini is a relatively small aphid group which embraces more than 60 species chiefly found in tropical/subtropical areas of southeastern Asia [14, 20]. Figure 1 is a proposed phylogeny for subfamilies of Aphididae based on morphological characters [21]. The family Aphididae is composed of many subfamilies, one of which is Hormaphidinae. This subfamily is divided into three tribes, one of which is Cerataphidini. So far, ten genera have been placed under the tribe Cerataphidini, although there are some problems in the taxonomic treatment as will be mentioned later.

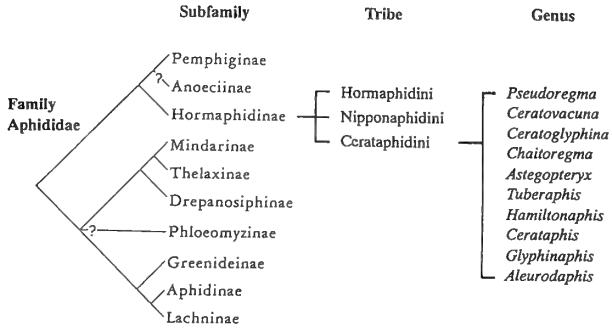

FIG. 1. Phylogeny of Aphididae and position of Cerataphidini.

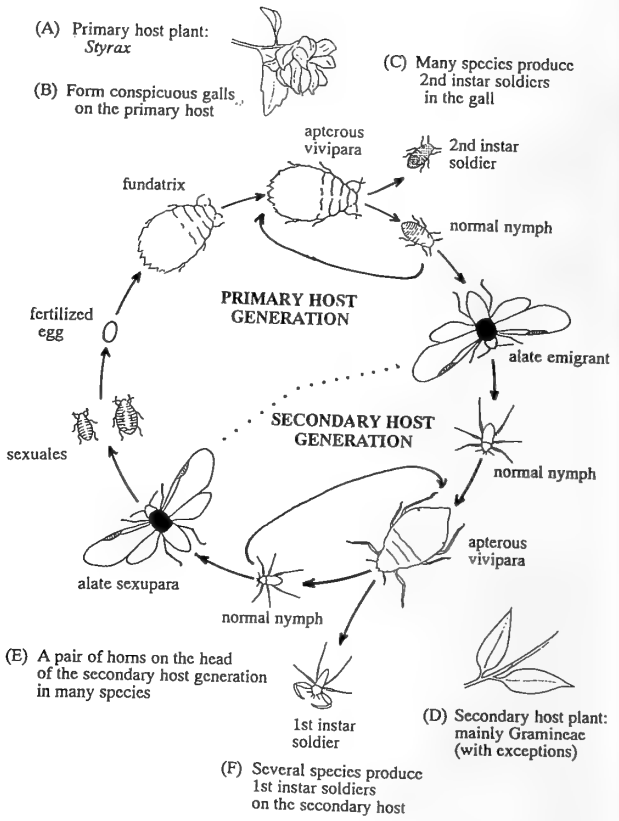

FIG. 2. Life cycle of Cerataphidini aphids. (A)-(F) indicate important characteristics of Cerataphidini.

Life cycle of Cerataphidini

Species of the tribe Cerataphidini mainly have host-alternating life cycles. The primary hosts are trees of the single genus *Styrax* (Fig. 2A) on which they induce galls of various shapes (Fig. 2B). All the species whose gall-generations have been examined produce 2nd instar soldiers (Fig. 2C). They are associated with various plants as the secondary hosts, but in many cases Gramineae (bamboos and grasses) (Fig. 2D). The secondary host generation, with a pair of horns on the head in general, is quite different in morphology from the conspecific primary host generation (Fig. 2E). Several species produce 1st instar soldiers on the secondary host (Fig. 2F). This is a life cycle typical of Cerataphidini. However, for most of the species, the entire life cycle is still unknown. Many can persist on the secondary host for years without sex. Some (*e.g. Hamiltonaphis styraci*) have a monoecious life cycle with sex on the primary host.

Production of soldiers in Cerataphidini

In eusocial aphids, including Cerataphidini, two types of nymphs are produced, normal nymphs (reproductives-to-be) and soldiers. The soldiers have the following characteristics: 1) They attack predatory intruders, often in a self-sacrificing manner. 2) They are 1st or 2nd instar nymphs and do not molt further, so that they do not reproduce. 3) They morphologically differ from the conspecific normal nymphs of the same instar [1].

Table 1 shows the characteristics of two types of soldiers of Cerataphidini. On the primary host plant, they produce 2nd instar soldiers, which are characterized by sclerotized exoskeleton, in the gall. The soldiers attack intruders by stinging with the stylets, and clean their gall by pushing off honeydew globules and shed skins. On the other hand, all species of *Pseudoregma* and some species of *Ceratovacuna* produce 1st instar soldiers on the secondary host. They are armed with a pair of sharp horns on the head and powerful forelegs. When encountering with a predator, they clutch it by the forelegs and pierce its body with the horns.

MATERIALS AND METHODS

Insect materials

Thirty-nine species of Cerataphidini aphids were collected from Japan, Taiwan, Java, Sumatra and Malaysia (Table 2). For the outgroup of Cerataphidini, two Hormaphidini and two Nipponaphidini species were also collected. The collected insects were immediately fixed and preserved in alcoholic formalin (ethanol : formalin : acetic acid = 16 : 6 : 1).

Histochemical procedures

The fixed insects were decapitated in 70% ethanol, dehydrated and cleared through ethanol-xylene series, and embedded in Para-

TABLE 1. Differences between two types of Cerataphidini soldiers

	Primary-host soldiers	Secondary-host soldiers
Instar	2nd	1st
Host plant on which soldiers are produced	*Styrax*	Gramineae and Zingiberaceae
Colony in which soldiers are produced	In gall	Exposed
Morphology	Without horns on frons; forelegs not always thickened.	With sharp horns on frons; forelegs always thickened.
Attacking behavior	Stinging a predator with stylets	Piercing a predator with horns
Do soldiers also work?	Yes	No
Soldier-producing genera	More than 7 genera:[a] *Pseudoregma, Ceratovacuna, Ceratoglyphina, Astegopteryx, Tuberaphis, Hamiltonaphis* and *Cerataphis*	Only 2 genera: *Pseudoregma* and *Ceratovacuna*

[a] "*Astegopteryx*" *vandermeermohri* also produces 2nd instar soldiers (Kurosu and Aoki, unpublished data).

TABLE 2. Cerataphidini aphids examined in this study

Genus	Species	Locality	Host
(CERATAPHIDINI)			
Pseudoregma	*alexanderi*	T	Sc
	koshunensis	J, T	Sc
	bambucicola	J	Sc
	panicola	J	Sc
	nicolaiae	M	Sc
	sundanica	M, S, V	Sc
	pendleburyi	S	Sc
Ceratovacuna	*lanigera*	T, S	Sc
	japonica	J	Sc
	nekoashi	J	Pr
	longifila	T	Sc
	keduensis	M	Sc
Ceratoglyphina	*styracicola*[a]	T	Pr, Sc
	bambusae	M	Sc
Chaitoregma	*tattakana*	T	Sc
Astegopteryx	*bambucifoliae*	J, T	Sc
	formosana	T	Sc
	muiri	M	Sc
	bambusae	M	Sc
	malaccensis	S	Sc
	rappardi	M	Sc
	roepkei	S	Pr
	pandani	V	Sc
"*Astegopteryx*"[b]	*vandermeermohri*	S	Pr
Tuberaphis	*coreana*	J	Sc
	taiwana	T	Pr
	loranthi	S	Sc
	takenouchii	T	Sc
	leeuweni[c]	S	Pr
	sumatrana[d]	S	Pr
Hamiltonaphis	*styraci*	J	Pr
Cerataphis	*fransseni*	J, T, M	Pr, Sc
	lataniae	M	Sc
	freycinetiae	M	Sc
	pothophila	M	Sc
	bambusifoliae	T	Sc
Glyphinaphis	*bambusae*	T	Sc
Aleurodaphis	*blumeae*	J	Sc
	sp.[e]	J	Sc
(HORMAPHIDINI)			
Hormaphis	*betulae*	J	Pr
Hamamelistes	*miyabei*	J	Pr
(NIPPONAPHIDINI)			
Nipponaphis	*distyliicola*	J	Pr
Neothoracaphis	*yanonis*	J	Pr

In the column of "Locality", J, collected in Japan; M, in Malaysia; S, in Sumatra; T, in Taiwan; V, in Java. In the column of "Host", Pr, collected from the primary host plant; Sc, from the secondary host plant.

[a] The Taiwanese population has been referred to as *Ceratoglyphina bambusae* before. However, since it is distinct from the nominate Javanese population, we use the name *C. styracicola* in this paper. [b] This species was originally described as a member of *Astegopteryx* but clearly does not belong to it. A new genus should be made to accept the species. [c),d)] Both were described as members of *Astegopteryx*, but no doubt belong to the genus *Tuberaphis* (Aoki *et al.*, unpublished data). [e] Described in Moritsu [39].

plast plus (Monoject). Tissue sections of 3–5 μm thick were prepared on a rotary microtome and mounted on gelatin-coated microscope slides.

The tissue sections were immunohistochemically stained with anti-symbionin antiserum [18] by which prokaryotic intracellular symbionts were specifically stained in deep brown. They were also subjected to periodic acid-Schiff (PAS) staining to visualize yeast-like extracellular symbionts selectively in deep red or purple. The stained tissue sections were observed under a Normarski differential interference microscope.

RESULTS AND DISCUSSION

I. *Histochemical examination of symbiotic microorganisms of various Cerataphidini aphids*

Among 39 Cerataphidini species we examined histochemically, all species of *Pseudoregma, Ceratovacuna, Ceratoglyphina, Chaitoregma, Astegopteryx* and *Aleurodaphis*, and *Cerataphis bambusifoliae* and "*Astegopteryx*" *vandermeermohri* harbored typical intracellular symbionts as in usual aphids. On the other hand, all species of *Tuberaphis*, all but one species of *Cerataphis, Hamiltonaphis styraci* and *Glyphinaphis bambusae* possessed PAS-positive budding particles in the hemocoel and fat body. The particles were apparently yeast-like extracellular symbionts. There were no species that had both the intracellular symbionts and yeast-like extracellular ones.

The species with yeast-like symbionts were divided into three groups in terms of morphology of their symbionts. The symbionts of *Hamiltonaphis* and *Cerataphis* were slender in shape (Fig. 3A) while those of *Tuberaphis* were roundish (Fig. 3B). Distinct from either type, the symbionts of *Glyphinaphis* were larger in size and of rather irregular shape with multiple budding sites (Fig. 3C).

These results are summarized in Table 3 with information on host plants, gall type, and soldiers.

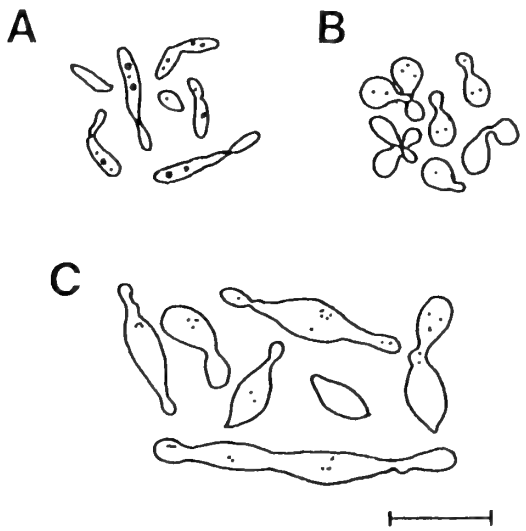

Fig. 3. Three types of yeast-like symbionts found in Cerataphidini. A, slender type (*Hamiltonaphis styraci*); B, roundish type (*Tuberaphis sumatrana*); C, large irregular type (*Glyphinaphis bambusae*). Bar represents 20 μm.

II. *Occurrence of yeast-like extracellular symbionts in Cerataphidini: congruence with present classification*

This study revealed that there are a number of Cerataphidini species with yeast-like extracellular symbionts in place of prokaryotic intracellular symbionts which are typical of Aphididae in general. Yeast-like symbionts were found in all examined species of *Tuberaphis, Hamiltonaphis styraci* and *Glyphinaphis bambusae* (the sole members of the respective monotypic genera), and all examined species of *Cerataphis* but *C. bambusifoliae*. No species of the other genera had yeast-like symbionts. In addition, the shape of yeast-like symbionts varied between, not within, genera. Thus, occurrence of yeast-like symbionts accorded well with the generic classification of the tribe Cerataphidini, which has been mainly based upon morphological characters of the secondary host generation. The only problematic species is *Cerataphis bambusifoliae*. Treatment of this species (referred to as "*Cerataphis*" *bambusifoliae* in the following sections) will be discussed in section VII.

III. *Monophyly of the Cerataphidini species with yeast-like symbionts*

Almost all aphid species (but some Cerataphidini species) harbor prokaryotic microorganisms in the cytoplasm of specialized cells, mycetocytes, in the abdomen [11, 19]. The intracellular symbionts (so-called primary symbionts) of various aphids hold a number of characters in common irrespective of the phylogenetic or taxonomic positions of their hosts. The mycetocytes that house them are large, round and uninucleated, and located between the gut and ovarioles forming cell-aggregates called mycetomes [11]. The symbionts are globular with a diameter of 3–5 μm and gram-negative with a thin rudimentary cell wall [19, 24]. They also represent peculiar characters at the molecular level that are not found among related free-living bacteria [19]. Thus, it has been thought that the intracellular symbiosis of aphids is of a single origin. This idea is also supported by recent molecular phylogenetic analyses. Based on 16S rRNA sequences, it was found that the symbionts of various aphids constitute a monophyletic group in bacteria, and the genus *Buchnera* was erected to accept them [41]. The molecular phylogeny of the symbionts showed good congruence with the phylogeny of their host aphids based on morphological characters [40]. These studies consistently suggest that the intracellular symbionts have been derived from a prokaryote that was acquired by the common ancestor of the present Aphididae species. The establishment of the symbiotic association was estimated to be as old as 160–280 million years ago by 16S rRNA molecular clock calibrated by fossil records of aphids [38].

Therefore, the common ancestor of Cerataphidini must have harbored prokaryotic intracellular symbionts, plesiomorphy of the symbiotic system. In fact, its sister groups, Hormaphidini and Nipponaphidini, possess intracellular symbionts (see Table 3). The finding of a number of Cerataphidini aphids possessing yeast-like extracellular symbionts, apomorphy of the symbiotic system, suggests that prokaryotic intracellular symbionts were replaced by extracellular yeast symbionts in the course of evolution of Cerataphidini. It is quite likely that the replacement occurred only once because such replacement is supposedly rare in aphids, found only in Cerataphidini. Thus, evidence from the symbiont type corroborates the hypothesis that the species with yeast-like symbionts constitute a monophyletic group in Cerataphidini.

TABLE 3. Symbiont type, gall type, host plants, and occurrence of soldiers of the Cerataphidini aphids examined

Genus[a]	Species[b]	Symbiont[c]	Gall[d]	Primary Host	Secondary Host	2nd instar Soldier	1st instar Soldier
(CERATAPHIDINI)							
Pseudoregma	*alexanderi*	intracellular	—	—	Gramineae	—	present
	koshunensis	intracellular	multiple	*Styrax*	Gramineae	present	present
	bambucicola	intracellular	multiple	*Styrax*	Gramineae	present	present
	panicola	intracellular	—	—	Gramineae	—	present
	nicolaiae	intracellular	—	—	Zingiberaceae	—	present?
	sundanica	intracellular	—	—	Zingiberaceae	—	present
	pendleburyi	intracellular	—	—	Gramineae	—	present
Ceratovacuna	*lanigera*	intracellular	—	—	Gramineae	—	absent
	japonica	intracellular	multiple	*Styrax*	Gramineae	present	present
	nekoashi	intracellular	multiple	*Styrax*	Gramineae	present	absent
	longifila	intracellular	—	—	Gramineae	—	present
	keduensis	intracellular	—	—	Gramineae	—	absent
Ceratoglyphina	*styracicola*	intracellular	multiple	*Styrax*	Gramineae	present	absent
	bambusae	intracellular	—	—	Gramineae	—	absent
Chaitoregma	*tattakana*	intracellular	—	—	Gramineae	—	absent
Astegopteryx	*bambucifoliae*	intracellular	multiple	*Styrax*	Gramineae	present	absent
	formosana	intracellular	—	—	Gramineae	—	absent
	muiri	intracellular	—	—	Zingiberaceae	—	absent
	bambusae	intracellular	—	—	Gramineae	—	absent
	malaccensis	intracellular	—	—	Gramineae	—	absent
	rappardi	intracellular	—	—	Palmae	—	absent
	roepkei	intracellular	multiple	*Styrax*	****	present	****
	pandani	intracellular	—	—	Pandanaceae	—	absent
"*Astegopteryx*"	*vandermeermohri*	intracellular	single	*Styrax*	—	present	—
Tuberaphis	*coreana*	roundish yeast	—	—	Loranthaceae	—	absent
	taiwana	roundish yeast	single	*Styrax*	—	present	—
	loranthi	roundish yeast	—	—	Loranthaceae	—	absent
	takenouchii	roundish yeast	single	*Styrax*	Loranthaceae	present	absent
	leeuweni	roundish yeast	single	*Styrax*	****	present	****
	sumatrana	roundish yeast	single	*Styrax*	—	present	—
Hamiltonaphis	*styraci*	slender yeast	single	*Styrax*	****	present	****
Cerataphis	*fransseni*	slender yeast	single	*Styrax*	Palmae	present	absent
	lataniae	slender yeast	—	—	Palmae	—	absent
	freycinetiae	slender yeast	—	—	Pandanaceae	—	absent
	pothophila	slender yeast	—	—	Araceae	—	absent
	orchidearum[e]	slender yeast	—	—	Orchidaceae	—	absent
	bambusifoliae	intracellular	—	—	Gramineae	—	absent
Glyphinaphis	*bambusae*	large yeast	—	—	Gramineae	—	absent
Aleurodaphis	*blumeae*	intracellular	—	—	Compositae	—	absent
	sp.	intracellular	—	—	Balsamina-ceae	—	absent
(HORMAPHIDINI)							
Hormaphis	*betulae*	intracellular	single	*Hamamelis*	Betulaceae	absent	absent
Hamamelistes	*miyabei*	intracellular	single	*Hamamelis*	—	absent	—
(NIPPONAPHIDINI)							
Nipponaphis	*distyliicola*	intracellular	single	*Distylium*	Fagaceae	absent	absent
Neothoracaphis	*yanonis*	intracellular	single	*Distylium*	Fagaceae	absent	absent

"—", information not available; "****", without the secondary host generation because of monoecy on the primary host. [a] Genera with yeast symbionts are underlined; [b] Species with yeast symbionts are underlined; [c] Yeast symbionts are underlined; [d] Multiple, multiple-cavity gall; single, single-cavity gall. The former galls are underlined;[e] This species was not examined in this study, but its symbiont was described by Buchner [10].

Further phylogenetic inferences can be drawn from the morphology of yeast-like symbionts. The three symbiont types (Fig. 3) are sufficiently distinct from one another and invariable within the morphologically well-defined genera *Cerataphis, Glyphinaphis* and *Tuberaphis*, suggesting that the symbiont types reflect phylogenetically related aphid groups.

IV. *Monophyly of the Cerataphidini species forming multiple-cavity galls*

In addition to the symbiont type, it has been revealed that the basic plan and structure of galls is a key character to reconstruct the phylogenetic relationship in Cerataphidini (Kurosu and Aoki, unpublished data).

All the Cerataphidini aphids whose primary host generations have been described form galls on *Styrax* trees (see Fig. 2). Although their galls show conspicuous diversity in shape [12], they fall into two categories, single-cavity type and multiple-cavity type, based on the basic structure and the mode of gall formation. *Cerataphis* [44], *Hamiltonaphis* [3] and *Tuberaphis* [6, 7] species, and "*Astegopteryx*" *vandermeermohri* [12; Kurosu and Aoki, in preparation] form galls of the former type, while *Pseudoregma* [4, 5], *Ceratovacuna* ([31]; Kurosu and Aoki, unpublished data), *Ceratoglyphina* [8, 32] and *Astegopteryx* [33] species form galls of the latter type (see Table 3). Single-cavity galls have a single cell which contains the fundatrix and its offspring. This is a simple and the commonest type of aphid galls, and is found among various aphid groups including Hormaphidini and Nipponaphidini [20], the sister groups of Cerataphidini. In contrast, multiple-cavity galls have a number of subgalls each having a cavity, and are found only in Cerataphidini. The formation process and structure of galls of this type (see [31]) are so unique and complex that the multiple-cavity gall is no doubt apomorphic, and probably evolved only once in Cerataphidini. Thus, argumentation on the gall type supports the hypothesis that the species forming multiple-cavity galls constitutes a monophyletic group in Cerataphidini.

Chaitoregma tattakana, the sole member of the monotypic genus, though its gall has yet been unknown, probably belongs to this group because it well resembles *Pseudoregma* and *Ceratovacuna*, members of the group, in morphology.

V. *Phylogeny and evolution of Cerataphidini*

Figure 4 is a phylogenetic tree of Cerataphidini aphids based on the consideration above. Beside each taxon, the character states of its symbiont and gall are indicated. Important evolutionary events are estimated and also indicated on the tree. The tribe Cerataphidini is composed of two major monophyletic groups; one, characterized by yeast-like extracellular symbionts, contains *Hamiltonaphis, Cerataphis, Glyphinaphis* and *Tuberaphis* species, and the other, characterized by multiple-cavity galls, embraces *Pseudoregma, Ceratovacuna, Astegopteryx, Chaitoregma* and *Ceratoglyphina*. "*Astegopteryx*" *vandermeermohri* has neither of the apomorphic characters; it harbors normal intracellular symbionts and forms a single-cavity gall. Therefore, this species by itself constitutes a third group.

Phylogenetic positions of the remaining problematic taxa, "*Cerataphis*" *bambusifoliae* and *Aleurodaphis*, will be discussed in section VII.

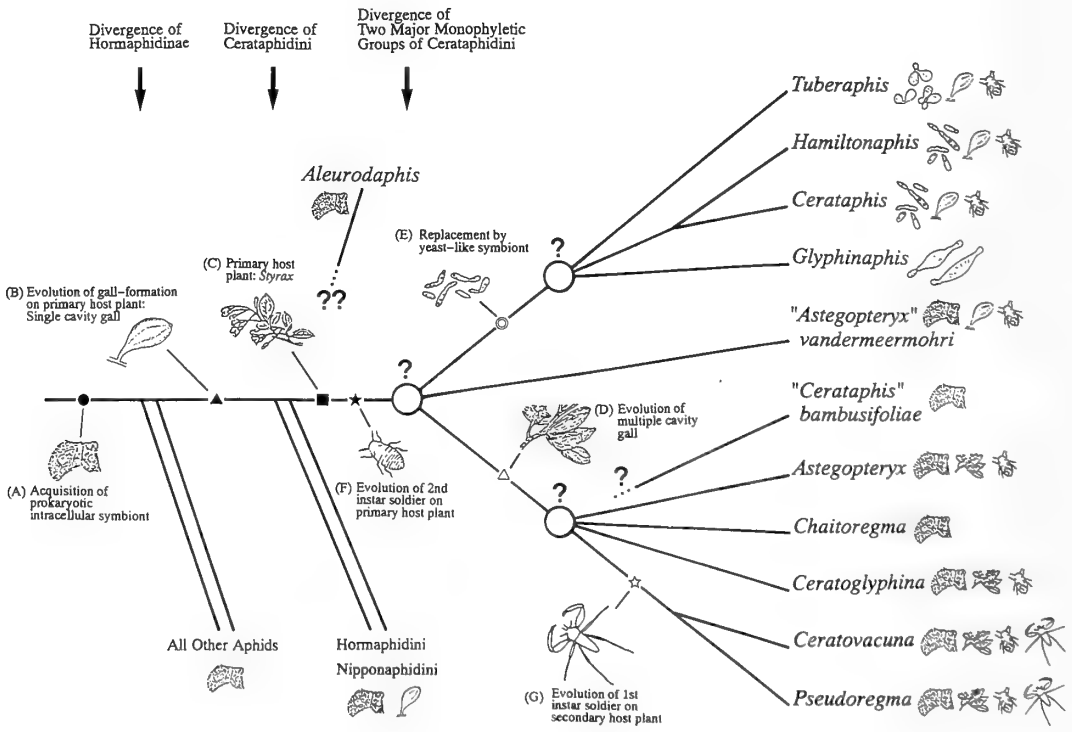

FIG. 4. Phylogenetic relationship among Cerataphidini aphids based on the types of symbionts and the basic structure of galls.

Let us follow the evolutionary course of Cerataphidini on the phylogeny we proposed. In the common ancestor of the family Aphididae, the root of the tree, a prokaryotic intracellular symbiont was acquired (Fig. 4A). Then the subfamily Hormaphidinae branched from the other aphids. In the common ancestor of Hormaphidinae, the ability to form galls on the primary host plant might have evolved (Fig. 4B). The Hormaphidinae ancestor then diverged into three tribes, Hormaphidini, Nipponaphidini and Cerataphidini. The common ancestor of Cerataphidini acquired the primary host *Styrax* on which it formed a single-cavity gall (Fig. 4C). Then the Cerataphidini diverged into two major lines, the multiple-cavity gall group and the yeast-like symbiont group. In the common ancestor of the former group, the ability to form a multiple-cavity gall evolved (Fig. 4D). In the common ancestor of the latter group, a yeast-like microbe replaced the original intracellular symbiont (Fig. 4E). The latter group further diverged into three subgroups which harbor slender, roundish, and large yeast symbionts, respectively.

VI. *Evolution of two types of sterile soldier castes in Cerataphidini*

In aphids, it has been demonstrated that eusociality has evolved at least four times; once in *Colophina* (Pemphiginae, Eriosomatini), once in *Pemphigus* (Pemphiginae, Pemphigini) and twice in Cerataphidini (Hormaphidinae) [1, 28]. Among all eusocial insects ever known, the tribe Cerataphidini is particularly interesting in that it produces two distinct types of sterile soldier castes in different stages of the life cycle (Fig. 2 and Table 1). Because of fundamental differences in instar, morphology, stages in the life cycle at which they are produced, and attacking behavior between them, it was strongly suggested that the two types of soldiers evolved independently. Considering the fact that 2nd instar soldiers are found ubiquitously whereas 1st instar soldiers are restricted to two genera in Cerataphidini, it was pointed out that the former is of more ancient origin than the latter [2].

Now we can reconstruct the evolution of the two types of soldiers in Cerataphidini in relation to the phylogeny. Beside each taxon of the phylogenetic tree, occurrence of the soldiers is indicated (Fig. 4). The 2nd instar soldiers are found from a number of genera covering the two major monophyletic groups and "*Astegopteryx*" *vandermeermohri*. Thus, it is concluded that the 2nd instar soldier evolved in the common ancestor of the present Cerataphidini aphids (Fig. 4F). In contrast, the 1st instar soldier occurs only in *Pseudoregma* and *Ceratovacuna*. This suggests that it evolved after the two major monophyletic groups had diverged, likely in the common ancestor of the two genera (Fig. 4G).

It should be noted, however, that the evolutionary course of 1st instar soldiers in Cerataphidini may be more complicated. All species of *Pseudoregma* produce 1st instar soldiers while about a half of *Ceratovacuna* species do so. Thus, a single acquisition of 1st instar soldiers as shown in Figure 4 is, though quite likely, a minimal estimate.

VII. *Treatment of problematic taxa, "Astegopteryx" vandermeermohri, "Cerataphis" bambusifoliae, and Aleurodaphis*

"*Astegopteryx*" *vandermeermohri* is a phylogenetically interesting species because it keeps both symbiont type and gall type plesiomorphic. This suggests that "*A.*" *vandermeermohri* diverged from other lines at an early stage of Cerataphidini evolution when neither yeast-like symbiont nor multiple-cavity gall had evolved (Fig. 4). Although it has been placed under the genus *Astegopteryx* tentatively, it is evident that a new genus should be erected to accept this species.

"*Cerataphis*" *bambusifoliae* is the most problematic species in Cerataphidini. *Cerataphis* species have the following characters in common; the apterous adult has a pair of frontal horns, the head and the three thoracic segments completely fused, the first seven abdominal segments completely fused, and well-developed marginal wax plates [42]. Indeed, the apterous adult of "*C.*" *bambusifoliae*, having these characters, resembles those of other *Cerataphis* species very much (Fig. 5), although it differs from the latter in that the tips of the horns are rounded and that its secondary host plants are bamboos. Based solely on morphology, one could not help placing "*C.*" *bambusifoliae* under the genus *Cerataphis* as some taxonomists did [35, 45]. However, we found that it does not harbor yeast-like symbionts but intracellular symbionts, indicating that it belongs to a clade distinct from that with yeast-like symbionts. This finding suggests that "*C.*" *bambusifoliae* would be placed in a new genus, although further supporting evidence is needed to make final conclusion. If so, its remarkable morphological resemblance to *Cerataphis* is due to parallelism or remaining plesiomorphic characters. Since its gall is still unknown, it is uncertain whether "*C.*" *bambusifoliae* belongs to the monophyletic group forming multiple-cavity galls (Fig. 4).

It has been unclear whether the genus *Aleurodaphis* really belongs to Cerataphidini. Cerataphidini aphids have the following characteristics in common: 1) They form galls on the primary host *Styrax*. 2) They produce 2nd instar soldiers on the primary host. 3) Their secondary hosts are monocots, most of which are Gramineae (with several exceptions). 4) They have sharp horns on the head (with several exceptions). All these characters are lacking or unknown in *Aleurodaphis*. Aoki and Usuba [7] suggested that "*Astegopteryx*" *takenouchii* is the primary host generation of an *Aleurodaphis* species based on the morphology of its nymphs. However, recent discovery of its secondary host generation (Kurosu *et al.*, unpublished data) and the examination of its symbionts in this study demonstrated that it belongs to *Tuberaphis*. It is still uncertain whether *Aleurodaphis* is a member of Cerataphidini (Fig. 4). However, recent molecular phylogenetic studies suggest that this genus should be placed outside the tribe Cerataphidini (Fukatsu and Ishikawa, unpublished data).

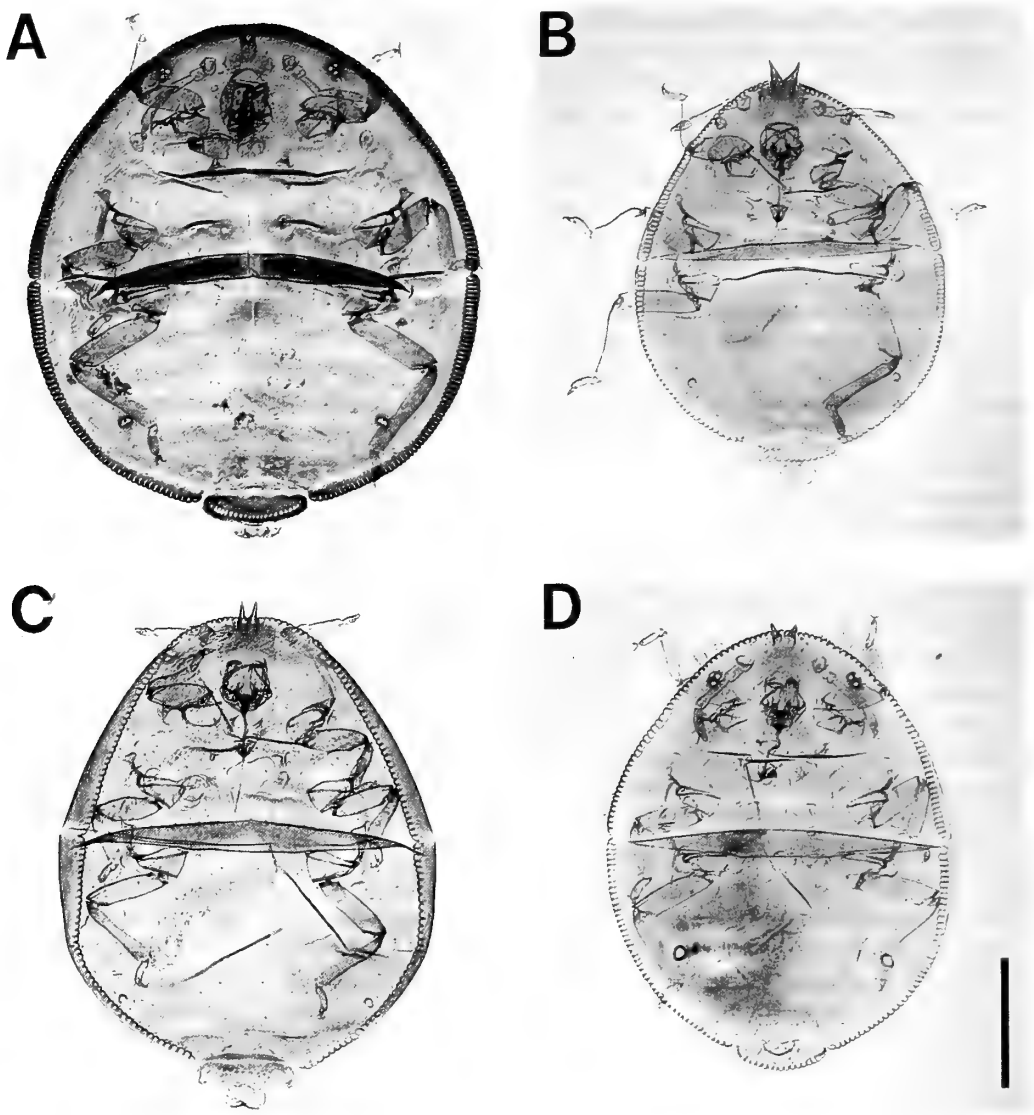

FIG. 5. Apterous adults (secondary host generation) of *Cerataphis* species and "*Cerataphis*" *bambusifoliae*. A, "*C.*" *bambusifoliae*; B, *C. fransseni*; C, *C. freycinetiae*; D, *C. pothophila*. Bar represents 0.4 mm.

VIII. *On the origin of yeast-like symbionts*

It became clear that a kind of yeast-like organisms displaced the original intracellular symbiont in a lineage of Cerataphidini. Observation of the ultrastructure showed that it is no doubt a fungus [17]. Then, what kind of fungus was it? How did it infect the insect and displace the original symbiont? Why is there no species with both yeast and bacterial symbionts now? Although there is little evidence to answer these questions, it may be useful to speculate possible scenarios and to develop hypotheses.

The extracellular symbionts of Cerataphidini look like budding yeasts. However, it is difficult to specify fungi related to them because budding unicellular fungi are known from various groups of Eumycetes [36]. One way to investigate this is to determine the sequences of 18S rRNA of the yeast-like symbionts to construct molecular phylogeny among fungi.

One possible explanation for the origin of the yeast-like symbiont is that it was derived from a parasitic or pathogenic fungus. It is conceivable that in an ancestral Cerataphidini species a parasitic fungus lost its harmful effects on the host and became a symbiont, just as has been proposed as a plausible scenario of the origin of endosymbiotic associations in general [15, 29, 37].

Interestingly, Kolb [30] reported casual occurrence of a parasitic fungus in *Pseudoregma panicola*. In the specimens of this species from Java, she found yeast-like microbes in addition to the typical intracellular symbionts. They were localized in the hemolymph and fat body, but not in embryos. The extra yeasts were probably not symbiotic but parasitic since they were found from only a part of the individuals she examined. In fact, we failed to discover such yeasts although we examined many specimens of *P. panicola* collected in Japan. Such a parasitic fungus might have been the

original form of the yeast symbionts found among present Cerataphidini aphids.

In spite of our extensive studies on the symbiotic system of Cerataphidini, there was no species that harbored both the intracellular and extracellular symbionts. This suggests that the newcomer yeasts sooner or later displaced the original intracellular symbionts. It seems that there are several possible factors that facilitated the symbiont replacement. A candidate is the difference in transmission efficiency between the symbionts. The symbionts of aphids are passed from one to the next generation by ovarial transmission in which embryos at a very early stage are infected by the symbionts of a small number. The symbionts have to infect a restricted part, follicle peg, which transiently appears at the posterior pole of early embryos [11]. Therefore, if the yeast symbionts are more efficient in the transmission than the intracellular ones, the former will replace the latter as the host's generations go on. Since this process is of exponential nature, the replacement might have completed within a small number of generations. The hypothetical difference in efficiency is, though circumstantial, supported by the following anatomical observations: since intracellular symbionts are confined in the cytoplasm of mycetocytes, they have to go out of the cell into the hemocoel to infect embryos. In contrast, yeast symbionts are always located in the hemocoel, and thus more accessible to the embryos. Even if there is no difference in the mean efficiency, random drift may result in fixation of either type. The other candidates are direct interactions between the two types of symbionts. The two symbionts may compete for resources and energy in the same host insect. If one can utilize them better, it will overwhelm and expel the other. Usually microorganisms produce antibiotic substances. Actually, it has been suggested that symbiotic yeasts of planthoppers, *Laodelphax striatellus* and *Nilaparuata lugens*, produce antibiotics that prevent pathogens from infecting their hosts [16]. Likewise, the yeast symbionts might have chemically expelled the intracellular ones.

Yeast-like endosymbionts are also known from various homopterans and other groups of insects [11]. The relationship of Cerataphidini symbionts to them is an interesting problem which should be pursued by molecular phylogenetic approaches.

IX. *On the function of yeast-like symbionts*

At present, there is no direct information on the function of the yeast-like symbionts of Cerataphidini aphids. However, it should be noted that all the Aphididae species ever examined harbor symbiotic microorganisms without exception; most of them have intracellular prokaryotes and only some Cerataphidini species extracellular yeasts. When the intracellular symbionts are destroyed, the host aphids show retarded growth and become sterile [27, 43]. It has been demonstrated that the intracellular symbionts work as an important component in the pathway of amino acid metabolism [13, 24]. These facts indicate that symbiotic microorganisms are essential for aphids in general. In some Cerataphidini aphids, since they are free from the intracellular symbionts, it is quite likely that extracellular yeasts are also essential for their host aphid by making, for example, nutritional contributions to the host. To prove this, however, physiological studies on the yeast-like symbionts and their hosts will be necessary.

X. *Effects of acquisition of novel symbionts on the evolution of host aphids: neutral or advantageous?*

Almost all Cerataphidini species belong to either of the two major monophyletic groups, one of which has been subjected to the symbiont replacement while the other has not (Fig. 4). Because the two groups are derived from a common ancestor, comparison between them may provide a clue to estimate the effects of acquisition of a novel symbiotic system on the evolution of host aphids. In other words, the former group provides an experimental data set (species subjected to the symbiont replacement) whereas the latter provides a control data set (species not subjected to it) under the common phylogenetic constraints. When various characters were compared between the two groups, however, there were found little essential differences. They possess common morphological characters to such an extent that they are reasonably included in the same tribe Cerataphidini. Their life cycles are not out of the framework shown in Figure 2. Only 16 of more than 60 Cerataphidini species have yeast-like symbionts, suggesting that the lineage that acquired yeast-like symbionts has experienced no frequent speciation. In short, it is likely that the yeast-like symbiont simply displaced the original intracellular symbiont without drastic effects on the evolution of host aphids.

Also, there are abundant examples corroborating frequent occurrences of neutral invasion of microbes in aphids. Buchner [11] reported that roughly half of the aphids he examined possessed another intracellular prokaryotes (secondary symbionts) in addition to the universal primary symbionts. They have apparently been acquired many times in various lineages independently [19]. Monosymbiotic and disymbiotic species are frequently found together in a single clade, without any remarkable phenotypic differences. For example, in the monophyletic group of Cerataphidini forming multiple-cavity galls (see Fig. 4), several species of *Ceratoglyphina, Pseudoregma* and *Ceratovacuna* were disymbiotic while the others were monosymbiotic (unpublished data). These facts suggest that the secondary symbionts have no essential roles for the hosts but are rather neutral companions.

Almost all homopteran insects, including Aphididae, harbor one or several species of endosymbiotic microorganisms [11]. It is believed that they have established a special niche, feeding only on nutritionally-unbalanced plant sap all through their life, with the help of the symbionts. In fact, many homopterans have been shown to be absolutely dependent on their symbionts [13, 26]. These facts suggest that the endosymbiosis has been derived from the common ances-

tor of the present Homoptera. On the other hand, it is frequently observed that different endosymbiont florae are found even in a single homopteran lineage [11]. Thus, it is no doubt that in many lineages foreign microbes have repeatedly invaded the established symbiotic associations, coexisting or replacing the original endosymbionts [19, 37]. Moran and Baumann [37] suggested that such replacement events could be governed by host adaptations favoring one or the other microbial type and/or by evolution of the microbes themselves. We agree with them, but emphasize that many of the invasion and replacement events may be neutral rather than advantageous to the hosts, and that the neutrality should be responsible for a large part of the conspicuous diversity of endosymbiotic systems of Homoptera we can observe now.

ACKNOWLEDGMENTS

We thank Dr T. Yahara for reading through the manuscript critically and Mr D.L. Stern for a part of samples of Cerataphidini aphids. This research was supported by Grants-in-Aid to H. I. for General (No. 01440004) and Developmental (No. 01840028) Research and for Scientific Research on Priority Areas, "Symbiotic Biosphere: Ecological Interaction Network Promoting the Coexistence of Many Species" (No. 03269102) from the Ministry of Education, Science and Culture of Japan. This research was also supported by a grant from Kirin Brewery Co., Ltd. T.F. is supported by a JSPS (Japan Society for the Promotion of Science) Predoctoral Fellowship for Japanese Junior Scientists with Research Grant 3191.

REFERENCES

1 Aoki S (1987) Evolution of sterile soldiers in aphids. In "Animal Societies: Theories and Facts" Ed by Y Ito, JL Brown, J Kikkawa, Japan Sci. Soc. Press, Tokyo, pp 53–65

2 Aoki S, Kurosu U (1989) Two kinds of soldiers in the tribe Cerataphidini (Homoptera: Aphidoidea). J Aphidol 3: (Proceedings of Fourth National Symposium on Aphidology, Shimla-1988) 1–7

3 Aoki S, Kurosu U (1990) Biennial galls of the aphid *Astegopteryx styraci* on a temperate deciduous tree, *Styrax obassia*. Acta Phytopathol Ent Hungarica 25: 57–65

4 Aoki S, Kurosu U (1991) Host alternation of the aphid *Pseudoregma koshunensis* (Homoptera) in Taiwan. New Entomol 40: 31–33

5 Aoki S, Kurosu U (1992) Gall generations of the soldier-producing aphid *Pseudoregma bambucicola* (Homoptera). Jpn J Ent 60: 359–368

6 Aoki S, Kurosu U (1993) The gall, soldiers and taxonomic position of the aphid *Tuberaphis taiwana* (Homoptera). Jpn J Ent 61: 361–369

7 Aoki S, Usuba S (1989) Rediscovery of "*Astegopteryx*" *takenouchii* (Homoptera, Aphidoidea), with notes on its soldiers and hornless exules. Jpn J Ent 57: 497–503

8 Aoki S, Yamane S, Kiuchi M (1977) On the biters of *Astegopteryx styracicola* (Homoptera, Aphidoidea). Kontyu, Tokyo 45: 563–570

9 Aoki S, Kurosu U, Fukatsu T (1993) *Hamiltonaphis*, a new genus of the aphid tribe Cerataphidini (Homoptera). Jpn J Ent 61: 64–66

10 Buchner P (1958) Eine neue Form der Endosymbiose bei Aphiden. Zool. Anz. 160: 222–230

11 Buchner P (1965) Endosymbiosis of Animals with Plant Microorganisms. Interscience, New York

12 Docters van Leeuwen-Reijnvaan J, Docters van Leeuwen WM (1926) Zoocecidia of the Netherlands East Indies. Drukkerij de Unie, Batavia

13 Douglas AE (1989) Mycetocyte symbiosis in insects. Biol Rev 64: 409–434

14 Eastop VF (1977) Worldwide importance of aphids as virus vectors. In "Aphids as Virus Vectors" Ed by KF Harris, K Maramorosch, Academic Press, New York, pp 3–62

15 Ewald PW (1987) Transmission modes and evolution of the parasitism-mutualism continuum. Ann New York Acad Sci 503: 295–306

16 Fredenhagen A, Kenny P, Kita H, Komura H, Naya Y, Nakanishi K, Nishiyama K, Sugiura M, Tamura S (1986) Role of intracellular symbiotes in planthoppers. In "IUPAC Proceedings, Pesticide Sciences and Biotechnology" Ed by R Greenhalgh, TR Roberts, Blackwell, Oxford, pp 181–188

17 Fukatsu T, Ishikawa H (1992) A novel eukaryotic extracellular symbiont in an aphid, *Astegopteryx styraci* (Homoptera, Aphididae, Hormaphidinae). J Insect Physiol 38: 765–773

18 Fukatsu T, Ishikawa H (1992) Synthesis and localization of symbionin, an aphid endosymbiont protein. Insect Biochem Molec Biol 22: 167–174

19 Fukatsu T, Ishikawa H (1993) Occurrence of chaperonin 60 and chaperonin 10 in primary and secondary bacterial symbionts of aphids: Implications for the evolution of an endosymbiotic system in aphids. J Mol Evol 36: 568–577

20 Ghosh AK (1985) Hormaphidinae: distribution, phylogeny and systematics. In "Evolution and Biosystematics of Aphids" Polska Akademia Nauk, pp 303–336

21 Heie OE (1980) The Aphidoidea (Hemiptera) of Fennoscandia and Denmark. I. General part. The families Mindaridae, Hormaphididae, Thelaxidae, Anoeciidae, and Pemphigidae. Fauna Ent Scand 8: 1–236

22 Hinde R (1971) The fine structure of the mycetome symbiotes of the aphids *Brevicoryne brassicae, Myzus persicae*, and *Macrosiphum rosae*. J Insect Physiol 17: 2035–2050

23 Hinde R (1971) Maintenance of aphid cells and the intracellular symbiotes of aphids *in vitro*. J Invertebr Pathol 17: 333–338

24 Houk EJ (1987) Symbionts. In "Aphids, their Biology, Natural Enemies and Control 2A" Ed by AK Minks, P Harrewijn, Elsevier, Amsterdam, pp 123–129

25 Houk EJ, Griffiths GW (1980) Intracellular symbiotes of Homoptera. Ann Rev Ent 25: 161–187

26 Ishikawa H (1989) Biochemical and molecular aspects of endosymbiosis in insects. Int Rev Cytol 116: 1–45

27 Ishikawa H, Yamaji M (1985) Symbionin, an aphid endosymbiont-specific protein I. Production of insects deficient in symbiont. Insect Biochem 15: 155–163

28 Ito Y (1989) The evolutionary biology of sterile soldiers in aphids. Trends Ecol Evol 4: 69–73

29 Jeon KW (1987) Change of cellular "pathogens" into required cell components. Ann New York Acad Sci 503: 359–371

30 Kolb G (1963) Die Endosymbiose der Thelaxiden unter besonderer Berueeksichtigung der Hormaphidinen und ihrer Embryonalentwicklung. Z Morphol Oekol Tiere 53: 185–241

31 Kurosu U, Aoki S (1990) Formation of a "cat's-paw" gall by the aphid *Ceratovacuna nekoashi* (Homoptera). Jpn J Ent 58: 155–166

32 Kurosu U, Aoki S (1991) Incipient galls of the soldier-producing aphid *Ceratoglyphina bambusae* (Homoptera). Jpn J Ent 59: 663–669

33 Kurosu U, Aoki S (1991) The gall formation, defenders and

life cycle of the subtropical aphid *Astegopteryx bambucifoliae* (Homoptera). Jpn J Ent 59: 375–388

34 Lanham UN (1968) The Blochmann bodies: hereditary intracellular symbionts of insects. Biol Rev 43: 269–286

35 Liao HT (1976) Bamboo aphids of Taiwan. Q J Taiwan Mus 29: 499–586

36 Lodder J (1970) The Yeasts, A Taxonomic Study, 2nd ed, North-Holland Pub. Co., Amsterdam-London.

37 Moran N, Baumann P (1994) Phylogenetics of cytoplasmically inherited microorganisms of arthropods. Trends Ecol Evol 9: 15–20

38 Moran NA, Munson MA, Baumann P, Ishikawa H (1993) A molecular clock in endosymbiotic bacteria is calibrated using the insect hosts. Proc R Soc Lond B 253: 167–171

39 Moritsu M (1983) Aphids of Japan in Colors. Zenkoku-Noson-Kyoiku-Kyokai, Tokyo. (In Japanese.)

40 Munson MA, Baumann P, Clark MA, Baumann L, Moran NA, Voegtlin DJ, Campbell BC (1991) Evidence for the establishment of aphid-eubacterium endosymbiosis in an ancestor of four aphid families. J Bacteriol 173: 6321–6324

41 Munson MA, Baumann P, Kinsey MG (1991) *Buchnera* gen. nov. and *Buchnera aphidicola* sp. nov., a taxon consisting of the mycetocyte-associated, primary endosymbionts of aphids. Int J Syst Bacteriol 41: 566–568

42 Noordam D (1991) Hormaphidinae from Java (Homoptera, Aphididae). Zool Verh Leiden 270: 1–525

43 Ohtaka C, Ishikawa H (1991) Effects of heat treatment on the symbiotic system of an aphid mycetocyte. Symbiosis 11: 19–30

44 Stern DL, Aoki S, Kurosu U. (1994) The life cycle and natural history of the tropical aphid *Cerataphis fransseni* (Homoptera, Hormaphididae), with reference to the evolution of host alteration. J Natural History in press

45 Takahashi R (1925) Aphididae of Formosa, part 4. Dept Agr Gov Res Inst Formosa Rept 16: 1–65

ZOOLOGICAL SCIENCE 11: 625–627 (1994)

[RAPID COMMUNICATION]

Different Gene Expression of Mouse Transforming Growth Factor α between Pregnant Mammary Glands and Mammary Tumors in C3H/He Mice

Toshio Harigaya[1], Satoshi Tsunoda[2], Masako Mizuno[2], and Hiroshi Nagasawa[2]

[1]*Laboratory of Functional Anatomy and* [2]*Experimental Animal Research Laboratory, Faculty of Agriculture, Meiji University, Tama-ku, Kawasaki-shi, Kanagawa 214, Japan*

ABSTRACT—Mouse transforming growth factor alpha (TGFα) gene expression was determined by reverse transcriptase-polymerase chain reaction (RT-PCR) method in pregnant mammary glands and mammary tumors in C3H/He mice. Both normal pregnant and tumorous mammary tissues expressed mRNA for mouse TGFα. When primers from rat TGFα cDNA sequence as well as those in the previous report [12] were used, the PCR amplified products were the same sizes in both normal pregnant mammary gland and tumor. However, there were obviously different PCR products between pregnant mammary gland and tumor in case of using primers according to the mouse TGFα cDNA sequence. In tumors, various sizes of PCR products were detected in addition of a predicted size. This is unlikely the experimental artifact, but the polymorphic TGFα gene expression is induced in mammary tumors.

INTRODUCTION

Transforming growth factor alpha (TGFα), which is a 50 amino acid polypeptide, was originally isolated from the conditioned medium of a murine sarcoma virus transformed cell line. TGFα shares approximately 30% homology with epidermal growth factor (EGF) and acts through binding with EGF receptors [5, 13]. Human tumors and tumor cell lines often express TGFα [7, 11] and TGFα expression has also been identified in normal cells, including human keratinocytes [4] and human and rodent mammary epithelial cells [15]. Furthermore, direct evidence has been provided for an autocrine role of TGFα in normal mammary gland cells [2]. Matsui *et al.* [9] and Halter *et al.* [6] reported the morphological abnormalities of mammary glands associated with the expression (production) of human transforming growth factor α (hTGFα) in (C57BL×DBA) hybrid transgenic mice bearing hTGFα cDNA under the control of the mouse mammary tumor virus (MMTV) enhancer/promoter. Enhanced mammary tumorigenesis associated with an elevation of mammary DNA synthesizing enzyme activity was also reported in MMTV/hTGFα transgenic female mice [10]. These reports suggest that this growth factor has functional roles in normal mammary gland and involves in mammary tumorigenesis. Snedeker *et al.* [12] have identified TGFα and EGF in the mouse mammary glands at different development stages: TGFα like EGF was localized to the proliferated epithelial cell layers of the terminal end-buds.

We are investigating the endocrine participation in the effect of TGFα on normal and neoplastic mammary development. In this study, we found the different gene expression of mouse TGFα between pregnant mammary glands and mammary tumors.

MATERIALS AND METHODS

Animals

C3H/He strain mice maintained by the brother x sister mating in this laboratory were used. Females were mated with males at 2 months of age and the day of the presence of vaginal plug was designated as day 1 of pregnancy. Three mice were killed by decapitation under the light ether anesthesia at 9:00–10:00 hr on 18–19 days of pregnancy. The remaining animals were retired after the 3rd lactation and were checked for palpable mammary tumors once a week. Three mice carrying mammary tumors were killed at 20 to 25 months of age when the tumor sizes reached approximately 1 cm in a diameter. At autopsy, the unilateral third thoracic mammary gland or the portion of mammary tumors was immediately removed and stored at −70°C until use for the extraction of RNA.

RNA isolation and the detection of TGFα mRNA

Total RNA was isolated from 100 mg of frozen mammary tissue by the acid guanidinium thiocyanate-phenol-chloroform extraction method [3]. TGFα mRNA expressed in the mammary gland was determined by reverse transcriptase-polymerase chain reaction (RT-PCR) method. The RT-PCR was performed with cloned moloney murine leukemia virus (MMLV) reverse transcriptase and Taq DNA polymerase (Perkin Elmer Cetus, Norwalk, CT, USA) according to the procedure of supplier's recommendation. The cDNA obtained

Accepted June 27, 1994
Received May 9, 1994

by a reverse transcriptase reaction was provided for PCR and amplified for 40 cycles (1 cycle=94°C-1 min, 55°C-2 min, 72°C-2 min) in a program temperature control system (Astec, Fukuoka, Japan). Two sets of primers for TGFα were used for PCR. In the first experiment, we tried to detect mRNA for mouse TGFα according to the method of Snedeker *et al.* [12] using the same primers both sense and antisense strands derived from the rat TGFα sequences [8] corresponded at amino acids −32 to −26 (5′-GGACAGCTCGCT-CTGCTAGCG-3′) for a sense strand and at 103 to 97 (5′-CTTCTC-GTGTCTGCAGACGAG-3′) for an antisense strand, respectively (Fig. 1). In the second experiment, the primers were corresponded to the mouse TGFα precursor sequence [14]. The sense strand was as same region as that from rat sequence that was 100% match for mouse TGFα sequence. The antisense strand was at nucleotides 158–141 (5′-AGTGGATCAGCACACAGGT-3′). The predicted sizes of amplified products of TGFα are 408 bp with first primers and 349 bp with second primers, respectively (Fig. 1). β-Actin primers according to the mouse sequence [1], amino acids 35–41 (5′-GTGG-GCCGCTCTAGGCACCA-3′) and 116–108 (5′-CGGTTGGCCT-TAGGGTTCAGGGGGG-3′) were used for RT-PCR control reaction.

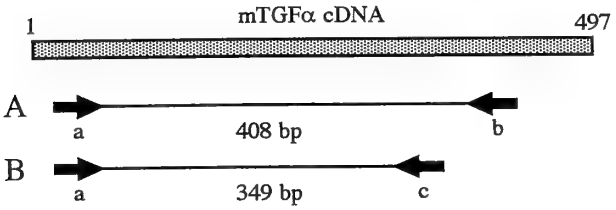

FIG. 1. Expected amplified cDNA regions by PCR. Arrow heads with a, b and c mean sense and antisense primer regions and directions used in this study. PCR product of 408 bp with a and b primers from rat sequence (A), and 349 bp with a and c primers from mouse sequence (B). Primer a region is same in both rat and mouse TGFα cDNAs.

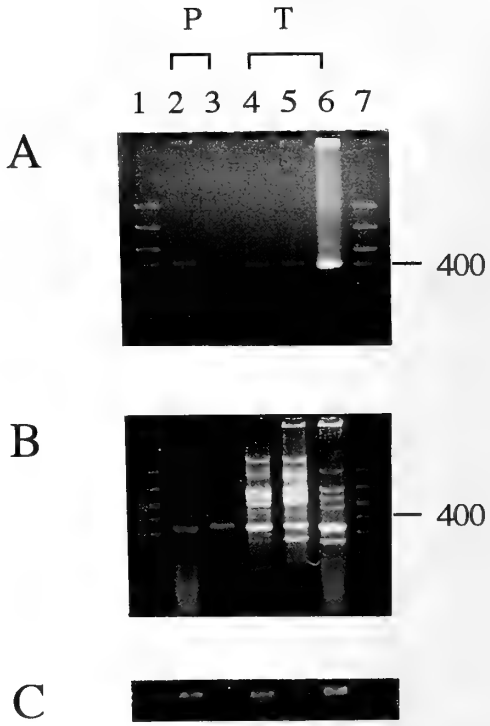

FIG. 2. RT-PCR products with different primers. A and B indicate the results using primers set A and set B depicted in Fig. 1, respectively. Each sample from pregnant mammary glands (P) in lane 2 and 3 and tumors (T) in lane 4, 5 and 6 are shown. Lane 1 and 7 indicate molecular weight markers. Molecular weight size of 400 bp is indicated on the right side of A and B. C indicates the control RT-PCR products (245 bp) in all samples obtained with β-actin primers.

RESULTS AND DISCUSSION

In the first experiment, RT-PCR products of TGFα were detected in two of three samples of normal pregnant mammary glands and in all three samples of mammary tumors. The amplified cDNAs were the same single bands of predicted size of 408 bp in all samples detected (Fig. 2A). In one sample of pregnant mammary glands, no amplified product of TGFα was observed, though the PCR product of β-actin was amplified. Next, we tried to change an antisense primer to the sequence corresponded to the mouse TGFα precursor sequence [14], because the former antisense primer from rat sequence found to be formed dimers and not completely identical to mouse TGFα sequence. In the second experiment, a single band of PCR products was detected in two of three samples of pregnant mammary glands as well as that of the first experiment (Fig. 2B). However, multiple sizes of amplified products were detected in all samples of mammary tumors. When PCR conditions were more stringent (annealing temperature=60–65°C), the same results were obtained (data not shown). The PCR products using β-actin primers were detected in all samples determined (Fig. 2C).

In this study, it is suggested that a single class of TGFα gene is expressed in the pregnant mammary gland of C3H/He mice. This result supports the report of Snedeker *et al.* [12] that TGFα gene expression was induced in proliferating mammary tissues. The same size of PCR product was also detected in the mammary tumor using primers derived from rat TGFα cDNA sequence. Using primers from mouse TGFα cDNA sequence, a single size of PCR product was detected again in pregnant mammary glands. However, in mammary tumors, multiple gene expressions of TGFα were observed using primers from the mouse sequence. This is not due to the experimental artifact because there was only a single band in the normal pregnant mammary gland using the same PCR condition. When the annealing temperature was increased to 65°C, the same result was obtained. It is also unlikely that these primers were annealed to the cDNAs for other growth factors, like EGF, because no sequence was found by a homology search in DNA sequence database. It is probably that multiple copy gene of mouse TGFα and/or alternative splicing induces several sizes of mRNA which could not be detected by rat primers because of a little difference of nucleotide sequence. The expression pattern seems to be depend on animals since the sizes and densities of

some PCR products were not identical among tumor samples determined. It might be caused in the different developmental stage of each tumor under different transcriptional control or splicing. In a normal physiological condition, only a normal way of splicing from a single transcript is occurred.

In tumorigenesis, several transcripts from multiple copy gene can be involved by its expression with some transcription factor(s) that is inhibited in a normal physiological state. However, it is not known whether mammary tumor is induced by polymorphic TGFα proteins as the result of the multiple gene expressions. Another possibility that other unknown TGFα like mRNAs which have the same sequence as mouse primer are expressed in tumors will be still remained. In the present experiment, at least, the obvious difference of characteristic between normal and neoplastic mammary glands is demonstrated in mRNA expressions determined by PCR with homologous TGFα primers, and it will be useful for determination of neoplastic characteristics in mouse mammary glands.

ACKNOWLEDGMENTS

Authors thank Human Genome Center, Institute of Medical Science, The University of Tokyo to use FASTA program for a DNA sequence homology search. This work was supported in part by a Grant in Aid from the Ministry of Education, Science and Culture, Japan, and a Grant for Special Project from Institute of Science and Technology, Meiji University.

REFERENCES

1 Alonso S, Minty A, Bourlet Y, Buckingham M (1986) J Mol Evol 23: 11–22

2 Bates S E, Valverius E M, Ennis B W, Bronzert D A, Sheridan J P, Stampfer M R, Mendelsohn J, Lippman M E, Dickson R B (1990) Endocrinology 126: 596–607

3 Chomczynski P, Sacchi N (1987) Anal Biochemistry 162: 156–159

4 Coffey R J, Derynck R, Wilcox J N, Bringman T S, Goustin A S, Moses H L, Pittelkow M R (1987) Nature 328: 817–820

5 Derynck R (1988) Transforming growth factor α. Cell 54: 593–595

6 Halter S A, Dempsey P, Matsui Y, Stokes M K, Deal R G, Hogan B L M, Coffey R J (1992) Amer J Pathol 140: 1131–1146

7 Hawburger A W, Pinnarmanei G (1993) Proc Soc Exp Biol Med 202: 64–68

8 Lee D C, Rose T M, Webb N R, Todaro G J (1985) Nature 313: 489–491

9 Matsui Y, Halter S A, Holt J T, Hogan B L M, Coffey R J (1990) Cell 61: 1147–1155

10 Mizuno M, Sakamoto S, Harigaya T, Mori T, Nagasawa H (1994) In Vivo: in press

11 Mydro J H, Michaeli J, Cordo C C, Goldenberg A S, Heston W D W, Fair W R (1989) Cancer Res 49: 3407–3411

12 Snedeker S M, Brown C F, DiAugustine R P (1991) Proc Natl Acad Sci USA 88: 276–280

13 Todaro G J, Fryling C, DeLarco J E (1980) Proc Natl Acad Sci USA 77: 5258–5262

14 Vaughan T J, Pascall J C, Brown K D (1992) Biochim Biophys Acta 1132: 322–324

15 Zajchowski D, Band V, Pauzine N, Tager A, Stampfer M, Sarger R (1988) Cancer Res 48: 7041–7047

ERRATA

1) In Vol. 11, No. 1, p 133
   dtudying→studying
   characteristics→characteristic
   In general→In general
   Lowe→Lord
   resorces→resources
   lief-history→life-history
   Amont→Among

2) In Vol. 11, No. 1, p 134
   sized→sizes

3) In Vol. 11, No. 1, p 135, Table 4
   0.19→1.19

4) In Vol. 11, No. 1, p 135
   results→result

5) In Vol. 11, No. 1, p 136
   sized→sizes
   Although→Although
   (plastic asymptonic, growth)
   →(plastic asymptonic growth)
   differenc→difference
   urichin→urchin
   jawa→jaws
   Bioology→Biology
   rtythrogramma→*erythrogramma*

6) In Vol. 11, No. 1, p 137
   Bio Essays→BioEssays

Development
Growth & Differentiation

Published Bimonthly by the Japanese Society of Developmental Biologists
Distributed by Business Center for Academic Societies Japan, Academic Press, Inc.

Development, Growth and Differentiation (ISSN 0012–1592) is published bimonthly by The Japanese Society of Developmental Biologists. Annual subscription for Vol. 35 1993 U. S. $ 191,00, U. S. and Canada; U. S. $ 211,00, all other countries except Japan. All prices include postage, handling and air speed delivery except Japan. Second class postage paid at Jamaica, N.Y. 11431, U. S. A.

Outside Japan: Send subscription orders and notices of change of address to Academic Press, Inc., Journal Subscription Fulfillment Department, 6277, Sea Harbor Drive, Orlando, FL 32887–4900, U. S. A. Send notices of change of address at least 6–8 weeks in advance. Please include both old and new addresses. U. S. A. POSTMASTER: Send changes of address to *Development, Growth and Differentiation,* Academic Press. Inc., Journal Subscription Fulfillment Department, 6277, Sea Harbor Drive, Orlando, FL 32887–4900, U. S. A.

In Japan: Send nonmember subscription orders and notices of change of address to Business Center for Academic Societies Japan, 16–9, Honkomagome 5-chome, Bunkyo-ku, Tokyo 113, Japan. Send inquiries about membership to Business Center for Academic Societies Japan, 16–9, Honkomagome 5-chome, Bunkyo-ku, Tokyo 113, Japan.

Air freight and mailing in the U. S. A. by Publications Expediting, Inc., 200 Meacham Avenue, Elmont, NY 11003, U. S. A.

POWERFUL PARTNERS FOR LONG-TERM PATCH CLAMPING

The MHW-3 water hydraulic micromanipulator features a refined slide mechanism and a 5:1 hydro/mechanical ratio to keep drift to an absolute minimum — just 1/17.5th of earlier, oil-based hydraulic units. Consequently, patch recording is accurate and reliable over extended periods. The MHW-3 has a full, pipette movement range of 2mm in ultra-fine 0.2μm graduations to allow fine remote control movement in all three axes, thereby providing exceptionally precise specimen pinpointing.

The MHW-30 features a movement range of 10mm, minimum graduations down to 1μm, and a 1:1 hydraulic system.

Three-Dimensional Water Hydraulic Micromanipulators

with coarse and fine manipulation

MHW-3 and MHW-30

For further information and maintenance service:

NARISHIGE JAPAN

NARISHIGE SCIENTIFIC INSTRUMENT LAB.

9-28, Kasuya 4-chome, Setagaya-ku, Tokyo 157, Japan
Phone: (INT-L) 81-3-3308-8233 Fax: (INT-L) 81-3-3308-2005 Telex: NARISHIGE J27781

U.S. NARISHIGE INTERNATIONAL INC.
404 Glen Cove Avenue, Sea Cliff, New York 11579, U.S.A.
Telephone: +1 (516) 759-6167 Telefax: +1 (516) 759-6138

NARISHIGE INTERNATIONAL LTD.
Unit 7, Willow Business Park, Willow Way, London SE26 4QP, UK
Telephone: +44 (0) 81-699-9696 Telefax: +44 (0) 81-291-9678

ZOOLOGICAL SCIENCE

VOLUME 11 NUMBER 4 AUGUST 1994

CONTENTS

INDEXED IN:
Current Contents/LS and AB & ES,
Science Citation Index,
ISI Online Database,
CABS Database, INFOBIB

Issued on August 15
Front cover designed by Saori Yasutomi
Printed by Daigaku Letterpress Co., Ltd.,
Hiroshima, Japan

ISSN 0289-0003

An International Journal

ZOOLOGICAL SCIENCE

Vol. 11 No.5

October 1994

PHYSIOLOGY
CELL and MOLECULAR BIOLOGY
GENETICS
IMMUNOLOGY
BIOCHEMISTRY
DEVELOPMENTAL BIOLOGY
REPRODUCTIVE BIOLOGY
ENDOCRINOLOGY
BEHAVIOR BIOLOGY
ENVIRONMENTAL BIOLOGY and ECOLOGY
SYSTEMATICS and TAXONOMY

published by Zoological Society of Japan
distributed by Business Center for Academic Societies Japan
VSP, Zeist, The Netherlands

ZOOLOGICAL SCIENCE

The Official Journal of the Zoological Society of Japan

The Zoological Society of Japan:
Toshin-building, Hongo 2–27–2, Bunkyo-ku,
Tokyo 113, Japan. Phone 03-3814–5461
Fax 03-3814-5352

ZOOLOGICAL SCIENCE is devoted to publication of original articles, reviews and rapid communications in the broad field of Zoology. The journal was founded in 1984 as a result of unification of Zoological Magazine (1888–1983) and Annotationes Zoologicae Japonenses (1897–1983), the former official journals of the Zoological Soceity of Japan. An annual volume consists of six regular numbers and one supplement (abstracts of papers presented at the annual meeting of the Zoological Society of Japan) of more than 850 pages. The regular numbers appear bimonthly.

MANUSCRIPTS OFFERED FOR CONSIDERATION AND CORRESPONDENCE CONCERNING EDITORIAL MATTERS should be sent to:

Dr. Tsuneo Yamaguchi, Editor-in-Chief, Zoological Science, Department of Biology, Faculty of Science, Okayama University, Okayama 700, Japan, in accordance with the instructions to authors which appear in the first issue of each volume. Copies of instructions to authors will be sent upon request.

SUBSCRIPTIONS. ZOOLOGICAL SCIENCE is distributed free of charge to the members, both domestic and foreign, of the Zoological Society of Japan.To non-member subscribers within Japan, it is distributed by Business Center for Academic Societies Japan, 5–16–9 Honkomagome, Bunkyo-ku, Tokyo 113. Subscriptions outside Japan should be ordered from the sole agent, VSP, Godfried van Seystlaan 47, 3703 BR Zeist (postal address: P. O. Box 346, 3700 AH Zeist), The Netherlands. Subscription rates will be provided on request to these agents. New subscriptions and renewals begin with the first issue of the current volume.

[Publication of Zoological Science has been supported in part by a Grant-in-Aid for Publication of Scientific Research Results from the Ministry of Education, Science and Culture, Japan.]

ZOOLOGICAL SCIENCE 11: 631–632 (1994)

OBITUARY

Juro Ishida (1908–1994)

In deep sorrow, we have to announce that Dr. Juro Ishida, Professor Emeritus of the University of Tokyo, passed away at the age of 86 on July 22, 1994. He had suffered from a thrombosis in the brain for the last several years and had hardly been able to carry out his duties as chief director of the Ito Foundation for the Advancement of Fish Biology, which was the last sign of his devotion to science. We deeply regret the loss of our teacher and of this very influential zoologist, developmental physiologist and biochemist. Juro Ishida was born in 1908 in Gohtsu-city in Shimane Prefecture. After graduation from Matsue Higher School, he entered the Imperial University of Tokyo (now the University of Tokyo), majoring in zoology. He then went on to the graduate school of that university and studied experimental zoology under the guidance of Professors Naohide Yatsu and Tokusuke Goda.

While in the graduate course, he became a researcher in the Mitsui Institute of Marine Biology near Shimoda, Shizuoka Prefecture, where he was actively engaged in studying digestive proteases in some marine vertebrates and invertebrates. Soon afterward, this line of study led him to his monumental discovery of a hatching protease in sea urchin embryos in 1936. This was the first documentation of the hatching enzyme in echinoderms. Afterward he moved from the Mitsui Institute to the Division of Fisheries, Department of Agriculture and Forestry, the Karafuto Agency, and lived in Karafuto (now Sakhalin in Russia) for one and a half years. Then in 1938 he resumed his graduate studies at the Imperial University of Tokyo. He continued research work in basic biology again under the guidance of Professor Tokusuke Goda, who was developing physiological chemistry in the field of zoology in Japan. During the period of his graduate studies, Ishida devoted himself to the study on proteolytic phenomena in animal tissues, for example, proteolytic activity in mammalian liquor folliculi in relation to its ovulatory activity and regulation of the autolytic activity of some tissues.

In 1942, he became a lecturer at the Biological Institute, Faculty of Science, Nagoya Imperial University (now Nagoya University). One and a half years later, he was appointed Associate Professor in the Institute. There he started his research work succeeding in 1944 in the first identification and physiological analysis of the hatching enzyme of the teleost (medaka), *Oryzias latipes*. He obtained the degree of Dr. Sc. in 1945. He also made further studies on the sea urchin hatching enzyme that he had discovered previously. During his time in Nagoya, his interest seemed to be concentrated on hatching phenomena, and later on the fertilization of sea urchins, a research carried out in cooperation with Dr. Eizo Nakano, his first student at Nagoya. Besides his own experimental investigation of hatching, Ishida dug out the historical fact that the first experimental study on enzymatic hatching in animals was done in 1910 by a Japanese investigator, Ikumo Moriwaki. He introduced Moriwaki's work to Japanese zoologists in 1944. Moreover, in 1948 he published two excellent books on the hatching enzyme and animal hatching. They were the first comprehensive monographs on animal hatching published anywhere in the world.

In 1950, Ishida moved to the Zoological Institute, Faculty of Science, the University of Tokyo as an Associate Professor. After 1951, he was joined gradually by students who were not only interested in Ishida's research project but who were also attracted to his unauthoritarian and affable personality. When Ishida was building his research group at the University of Tokyo, the remarkable progress in biological sciences after the World War II was just bursting and a flood of information on research in biochemistry and physiology done during and after the war mostly in the U.S.A. was surging into Japan to fill the wartime blank. With intensive interest in extensive fields of biochemistry and developmental biology, Ishida energetically introduced the newest information and trends in these scientific fields to his students and to all other zoologists and students of biology in Japan. Thus, we are greatly indebted to Ishida for accumulation and increase in our knowledge of trends in biochemistry and developmental physiology after the World War II. The so-called "Ishida School" comprised more than 25 his students. Many of them, though active and diligent, were unique and tough in their character and not so docile. Ishida, however, treated his students generously and impartially to help them mature responsibly at their own will and pace. This style of guidance has brought it about that among his former students there are experts in fields ranging from social biology to molecular biology, as well as in biochemistry and developmental physiology.

In 1956, he moved to the Biological Institute, College of General Education of the University of Tokyo at Komaba as Professor, while maintaining his laboratory at the Zoological Institute and setting up a new laboratory at Komaba. The subjects of research for his students were various depending on the interest of his students as well as his own: those related to the hatching enzyme, fertilization, metabolism of spermatozoa, metabolic changes during embryonic development, metabolism of endocrine organs, mitochondrial activity, muscle proteins and muscular contraction, and digestive enzymes. More than one hundred papers dealing with the above mentioned subjects were published from his laboratory over about 10 years. Being deeply impressed by the publication list of Ishida's laboratory, Professor John Runnstrom, the leader of the Swedish school in the field of developmental physiology at that time, highly praised Ishida for his interest, insight and activity in so a great variety of fields of physiological chemistry when he introduced Ishida at a meeting of the Royal Academy of Sciences of Sweden. The research projects born in his laboratory have been extended and developed markedly by his former students and their students. During the latter half of his time at Komaba, he actively committed himself to the establishment of a new Laboratory of Cooperative Biology in a new Department of Pure and Applied Sciences of the Komaba College. This new laboratory aimed at educating a new type of biologist well-grounded in physical and chemical science. He considered Dr. Norbert Wiener to be an example of such a scientist. This laboratory is well known to be adhering to Ishida's goals even now, nearly 30 years after its establishment.

In 1965, he moved back again to the Zoological Institute and headed his new laboratory of Developmental Physiology until 1968 when he retired from the University of Tokyo. After retirement, he continued for 5 years to teach biology as a Professor in the Department of Biology, Faculty of Science and Engineering, Saitama University, and for more 5 years in the Department of Biology, Faculty of Science, Toho University. At Saitama University, he successfully undertook painstaking administrative work as Dean of the Faculty and Acting President of the University, during a period when all Japanese universities, including Saitama University, encountered difficult problems, because of the students' movement. At Toho University, he enjoyed talking about biology to his young students, even while he was still quite busy in administration as a councillor and a member of the board of trustees.

Ishida belonged to many academic societies such as the Zoological Society of Japan, the Japanese Society of Developmental Biologists, the Japan Society for Cellular Chemistry (now the Japan Society for Cell Biology), the Japanese Biochemical Society, and the International Society of Developmental Biology. He made a great contribution to these societies by serving as secretary, councillor, or member of the advisory board. Even after his death, his influence will continue to stimulate progress in physiological chemistry and developmental physiology in Japan. Dr. Ishida is survived by his beloved wife, Michiyo, five children and twelve grandchildren.

SHIGETOSHI TAGUCHI[1], TOHRU NAKAZAWA[2] KATSUTOSHI ISHIHARA[3] and KENJIRO YAMAGAMI[4]

[1] Takada-cho, Kohoku-ku, Yokohama
[2] Department of Biology, Faculty of Science, Toho University
[3] Department of Regulation Biology, Faculty of Science, Saitama University, and
[4] Life Science Institute, Sophia University

ZOOLOGICAL SCIENCE 11: 633–645 (1994)

REVIEW

The Genetic Analysis of Neuropeptide Signaling Systems

MARTHA A. O'BRIEN and PAUL H. TAGHERT

Department of Anatomy and Neurobiology, Box 8108, Washington University School of Medicine, 660 South Euclid Avenue, Saint Louis, MO 63110, USA

INTRODUCTION

One of the important achievements of neuroscience in the last decade is the recognition that neurons release and respond to a very large number of signaling molecules. Many of these regulatory molecules are neuropeptides. They play both general and specific roles in the neural control of physiology, behavior and development. Neuropeptides are typically small molecules that are made as part of larger precursor forms; many different neuropeptides are often derived from the same precursor [101]. Such biologically active peptides are released along with classical transmitters and individual neurons are known to express and to release, in coordinate fashion, the products of several neuropeptide genes.

These features of co-synthesis and co-release of several neuropeptides suggest that they may have shared functions. Physiology and pharmacology have already revealed much about the functions of individual neuropeptides. However, we remain ignorant about the functions of the majority of neuropeptides, and are almost completely ignorant about the physiological processes that are controlled by sets of co-synthesized peptides. This feature presents an especially difficult problem for functional analysis because the biologically active agents may be working individually or in concert. Traditional analyses of neuropeptide functions are pharmacological and are often frustrated by the lack of specific antagonists by which to interrupt peptide action. Surgical experiments may remove the source of peptide secreting neurons, but such experiments must be controlled for variables unrelated to peptide action. In this regard, genetics can be extremely useful because it addresses questions regarding the function of molecules *in vivo* and should prove a useful complement to other forms of experimental analysis for the study of neuropeptide systems.

The significance of a genetic analysis stems from many features. First it is performed *in vivo*, and hence does not rely on choice of assay, nor does it preclude the analysis of multiple target sites. Second, it may address gene function in its entirety and so may consider the coordinate roles of distinct neuropeptides that are co-synthesized and released. Third, it provides the means to study animals that are chronically deficient in neuropeptide signaling, and so, can test the consequences of the disruption of such regulatory pathways. Finally, available methods permit the re-introduction of gene sequences (by germ line transformation) so as to test and extend hypotheses derived from observations of mutant phenotypes. Our intention in this review is to consider the prospects for a genetic analysis of neuropeptide signaling in simple systems, especially in the fruit fly, *Drosophila* and in the nematode, *C. elegans*. We principally focus on one gene, that encoding several FMRFamide-related neuropeptides, as a basis by which to evaluate the prospects for the approach. We survey the recent progress in the characterization and genetic analysis of other neuropeptide genes in systems amenable to genetics. Finally, we consider 'model system' studies of molecules that perform related functions within the broad category of neuropeptide signaling, and we discuss novel techniques by which genes encoding such molecules may be identified and targeted for genetic analysis.

Received August 29, 1994

INVERTEBRATE *FMRFamide* GENES

FMRFamide-related peptides have been isolated from species as diverse as coelenterates and mammals. The authentic tetrapeptide, Phe-Met-Arg-Phe-amide, has been found in mollusks and annelids; most other examples are extended at the amino-terminus. In invertebrates, genes encoding FMRFamide-like peptides have been cloned in the mollusks, *Aplysia* [88, 105], *Helix* [56], and *Lymnaea* [54, 86], in the nematode, *Caenorhabditis* [84], and the fruit fly, *Drosophila* [63, 94, 95, 103]. Sequence homologies indicate they are ancestrally related to the vertebrate opioid and corticotrophin releasing factor neuropeptide genes [105]. Pharmacological studies have shown that FMRFamide and related peptides in invertebrates have diverse physiological effects: they are cardioactive [51, 75, 79] and increase neurally-induced tension in skeletal muscles (e.g., [16]). In the central nervous system, FMRFamide-related peptides alter specific motor patterns and affect behavioral states. In mollusks, FMRFamide decreases or abolishes patterned motorneuron activity involved in feeding [55, 59].

The analysis of genes encoding FMRFamide

neuropeptides in animals as different as snails, worms and insects provides an opportunity to define the differences in gene structure and expression that have evolved over considerable evolutionary time. It has been argued that such evolutionary comparisons provide a basis with which to identify functionally important regions of a gene (e.g., [4, 43]). Among these diverse species, the *FMRFamide* gene appears to have retained several salient features, but also displays a remarkable amount of species-specific gene structure.

At least two genes encode FMRFamide-related neuropeptides in *Drosophila*. *Drosophila FMRFamide* generates several extended FMRFamide sequences [12, 95]. The existence of a second gene (called *dromyosuppressin-dms*) has been inferred from peptide sequence analysis [66]. As described in a later section, *dms* is likely to encode an extended FLRFamide. The *Drosophila FMRFamide* gene has a simple structure: a single intron separates a short 5' untranslated leader from the exon encoding a single prohormone precursor [12, 95]. The entire transcription unit in flies comprises only ~6 kb and transcription appears limited to the production of a single RNA. In the nematode, *C. elegans*, Li and colleagues have defined a single copy gene (called *flp-1*) that is split into 6 exons and that encodes a small precursor from which several N-terminally extended FMRFamide-like peptides are produced [84, 92]. In the snail, *Lymnaea*, the *FMRFamide* gene spans more than 20 kb and is composed of several exons that are differentially spliced to produce alternative RNAs. In a striking finding, Burke and colleagues found that the FMRFamide RNAs in the snail alternatively produce two different polyproteins: these prohormones produce short and long forms of FMRFamide-related peptides, respectively [11, 87]. Short forms (also referred to generically as "tetrapeptides") include authentic FMRFamide and FLRFamides. Long forms (also referred to generically as "heptapeptides") include peptides 6–10 amino acids long and represent N-terminally extended forms of the FMRFamide peptide family (e.g. GDPFLRFamides, [11, 87], also see [13]). In Figure 1, we schematize the organization of these diverse *FMRFamide* genes in various species to highlight what we emphasize as differences.

The contribution of RNA splicing to the generation of FMRFamide neuropeptide diversity varies greatly according to the animal examined. As mentioned earlier, the *Drosophila* gene does not appear to be spliced into alternative RNAs. The nematode *flp-1* gene displays some alternative splicing to generate either of two precursors that differ by the presence of one additional FMRFamide-like peptide [84]. RNA splicing appears most important in the case of the molluscan FMRFamide systems: the short versus long peptide precursor phenotype of *Lymnaea* is solely determined by this mechanism.

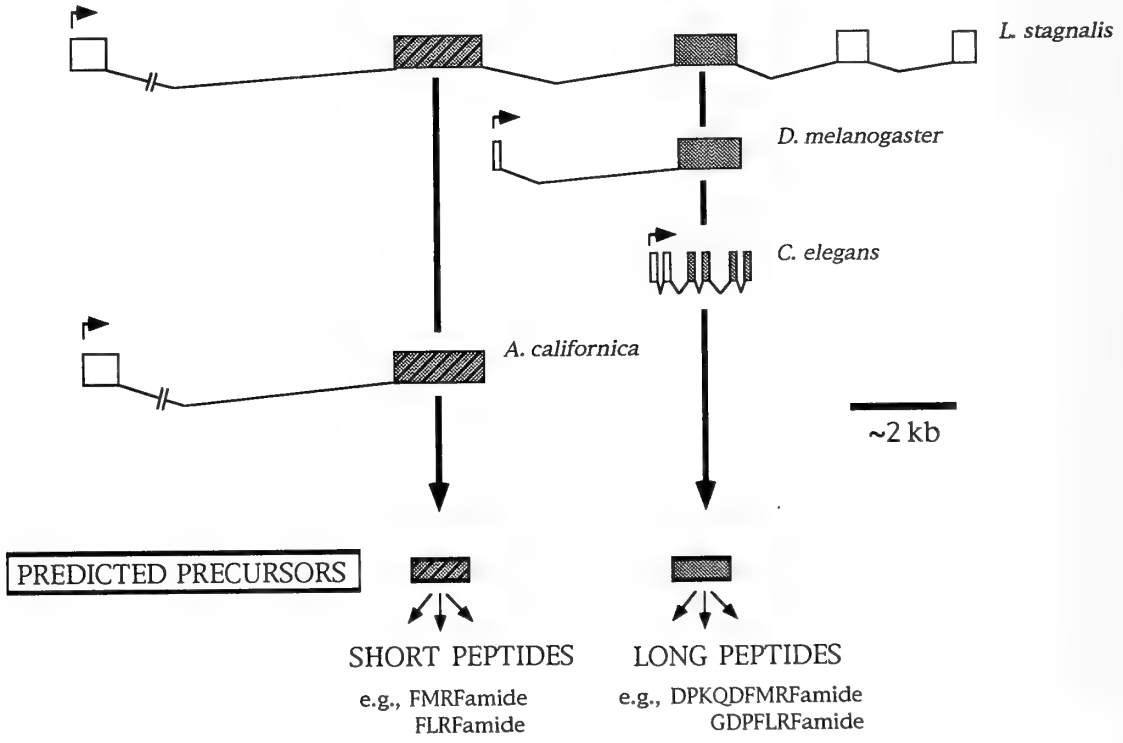

FIG. 1. Schematic organization of several genes that encode FMRFamide-related neuropeptides. Boxes indicate the position and number of exons; thin lines that connect the boxes represent intronic sequences. The sizes are only approximate representations. The small arrows at the front of genes indicate the positions of transcription start sites. In the case of *Aplysia*, the number of exons and the position of the start site are inferred (see [105]). The marking within certain exons indicates the positions of sequences that encode pro-FMRFamide precursors: the cross-hatched stippling represents exons that encode "short peptide" precursors; the stippling without cross-hatching represents exons that encode "long peptide" precursors.

The *Drosophila* and *C. elegans* FMRFamide precursors appear similar to the long (heptapeptide) precursor of the snail according to several criteria (Fig. 2). First, the length of the encoded peptides are similar and all are extended in the N-terminal direction. Secondly, the peptides are arranged similarly within the precursor, such that most are separated from each other by only a single basic residue. This residue is likely to be the site of endoproteolytic cleavage, an event which liberates the individual peptides from the precursor. In contrast, the *Lymnaea* tetrapeptide (short) precursor retains a characteristic acidic spacer region of 6 to 8 amino acids between the repeated FMRFamide coding units. In addition, the coding units themselves are most often flanked by dibasic residues. This is similar to the arrangement of the *Aplysia FMRFamide* gene which encodes multiple copies of the tetrapeptide with acidic spacer regions between each copy. Interestingly, the long (heptapeptide) forms of FMRFamide-related peptides have not been detected in *Aplysia*; whether the exon that encodes the long forms is absent in that animal (see Fig. 1) or whether this reflects a post-transcriptional change has not been defined. In the case of the snails, the fly and the worm, experiments suggest that the *FMRFamide* genes here defined are each present in single copy. It appears unlikely therefore, that flies and

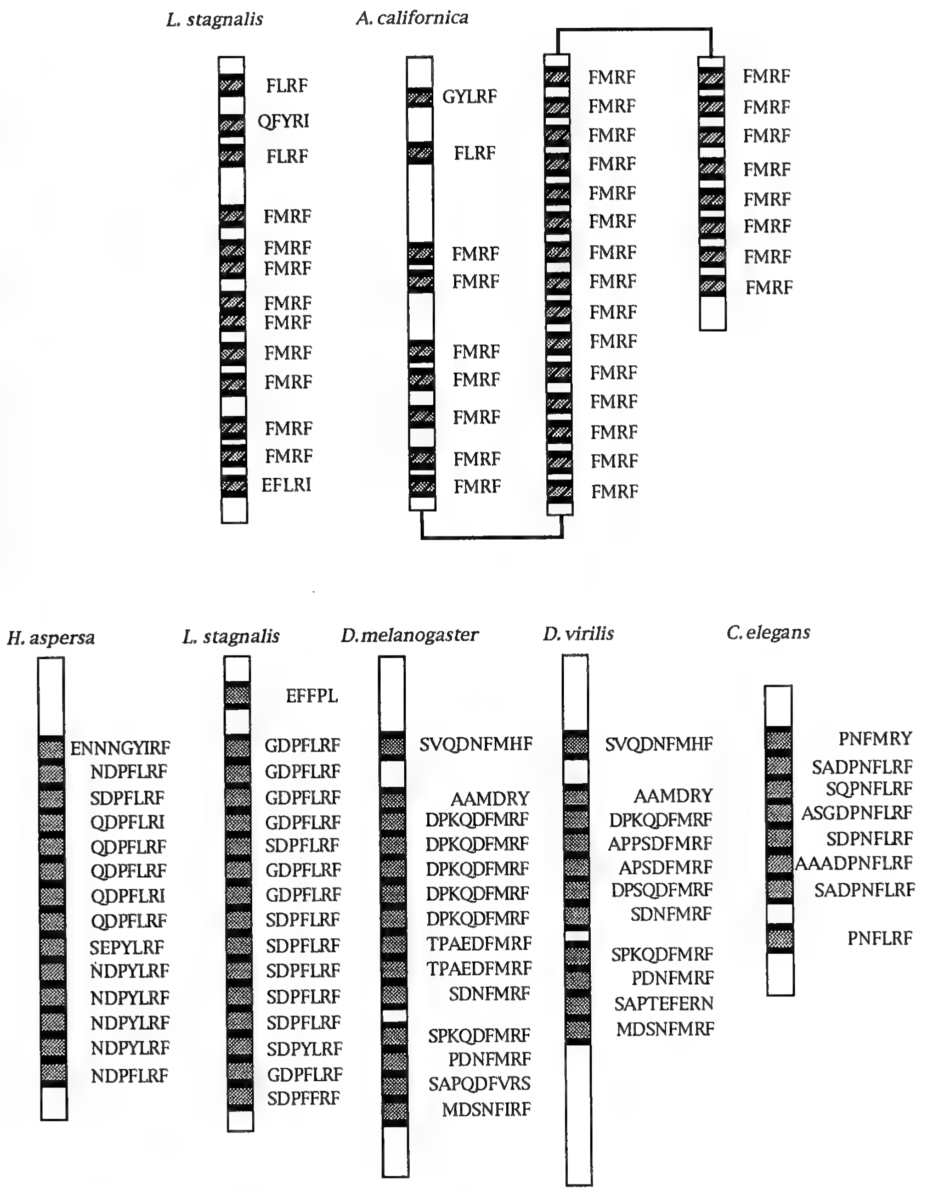

FIG. 2. Schematic representation of several precursors encoding FMRFamide-related neuropeptides. The top half of the figure illustrates the short (tetrapeptide) precursors from *Lymnaea* and *Aplysia*. The lower half illustrates the long (heptapeptides, etc.) precursors from two molluscan species, two fly species, and from the nematode. The size of the precursors are only approximate representations. The short FMRFamide peptides are denoted with cross-hatched stipples, the long FMRFamide peptides with stipples only. Basic cleavage sites are shown with black bars; amidation sites are present following each peptide (not shown). Note that the short peptides are typically separated from each other by spacer regions and the long peptides are not.

worms contain other, as yet uncharacterized, genes that are more related to the snail *FMRFamide*. Rather, this appears to be a case wherein the difference in the biology of the animals have promoted and/or permitted a divergence of *FMRFamide* gene structure.

TRANSCRIPTIONAL REGULATION OF THE *FMRFamide* GENE

The FMRFamide neuropeptide phenotype is associated with a stereotyped though heterogeneous group of neurons. This association appears to be stable over considerable evolutionary time: in flies, the pattern of neurons is highly reproducible between species separated by an estimated 60 Myr [103]. The same observation was made for distinct nematode species [93]. This strong linkage of neuropeptide phenotype with neuronal cell type suggests that the functions of the transmitters are intimately tied to the functions of particular neurons and to the synaptic circuits in which those neurons participate. We do not known whether these FMRFamide-expressing neurons participate in a common functional circuit, or whether they subserve independent roles in the animal. Nevertheless, our understanding of the rules that produce precise patterns of neuropeptide gene expression throughout development could contribute directly to the elucidation of neuropeptide function. The establishment of these individual neuronal properties requires the restriction of gene expression to specific neurons and it exemplifies a fundamental problem in developmental neurobiology. The *Drosophila FMRFamide* neuropeptide gene is a useful model with which to address this issue because its expression is restricted to a small group of neurons in the central nervous system (CNS) that is stereotyped such that individual neurons can be followed throughout development.

In vivo analyses of promoters for several neuronal genes have begun to define the mechanisms underlying such phenotypic complexity. Highly restricted patterns of reporter gene expression have been seen using regulatory fragments of neural-specific genes. For example, Young, *et al.* [110] reported that *oxytocin* gene expression was closely mimicked in mice bearing a 5.2 kb DNA fragment from the *oxytocin/vasopressin* locus. The organization of regulatory elements that underlie more widespread patterns of gene expression have also been described. Deletion analysis of the *Drosophila choline acetyltransferase* promoter revealed the presence of multiple regulatory elements, whose removal led to the absence of reporter gene expression in subsets of the normal pattern [49]. For the *Dopa decarboxylase* gene of *Drosphila*, deletion and mutation analyses have suggested that its expression by any single cell type depends on cell type-specific enhancer elements and a common, tissue-specific regulatory element that is required for expression by all *Ddc* neurons [10, 36, 43]. Similarly, in the *fushi tarazu*, *even-skipped*, and *sevenless* genes of *Drosophila*, numerous *cis*-regulatory elements act in concert to produce complex patterns of expression [35, 24, 5, 6].

In the CNS of the *Drosophila* larva, the FMRFamide pattern consists of ~50 neurons that are distributed throughout the brain and ventral nerve cord [97]. Following metamorphosis, there is an increase in the number of neurons expressing the gene to a total of ~120 [70, 97]. Based on position and axonal projections, there neurons represent ~15 discrete cell types including large neuroendocrine cells and interneurons in the ventral ganglion, central brain and sensory neuropils. Recent studies using reporter gene expression and germ line transformation methods [96], (M. Roberts, S. Renn and P. Taghert, unpublished) have generated evidence for three principal conclusions regarding the regulation of the *FMRFamide* gene. First, that an 8 kb fragment containing upstream and intragenic regions of the *FMRFamide* gene contains sufficient regulatory information to direct the appropriate pattern of transcription (and therefore peptide expression) to the normal complement of ~15 neuronal cell types. Second, that separate regions of this fragment are required for expression by different neuronal cell types. Third, that neuropeptide gene expression in individual cell types, the OL visual system neurons and the Tv neuroendocrine neurons, is produced by small, non-overlapping DNA regions that display the properties of cell type-specific enhancers. This information is schematized in Figure 3.

The first conclusion stems from studying the activity of an 8 kb fragment of the *FMRFamide* gene. This activity is sufficient to direct *lacZ* expression *in vivo* with a pattern and intensity that is nearly indistinguishable from that of the endogenous gene. This correspondence suggested that the pattern and level of *FMRFamide* gene expression is largely determined by transcriptional control mechanisms. Furthermore, the loss of β-gal immunoreactivity from specific cell types following transformation with the deletion constructs suggested that control regions within the *FMRFamide* promoter are distributed throughout the 8 kb of flanking and intragenic sequences (Fig. 3). The distributed organization of required elements is consistent with previous studies of tissue-specific gene expression, which have suggested that transcription is regulated by multiple modular enhancers [104, 23, 27, 25, 35, 21]. Similar to many of these studies, the *FMRFamide* gene contains a broadly distributed set of regulatory regions that appear to control different subsets of the cellular pattern. One of these regions, from −476 to −162, can act as a cell type-specific enhancer for a single neuronal type, the OL2 group [96]. Thus, within a large regulatory domain that controls gene expression by many neuronal cell types, this small region is sufficient for expression by a single cell type.

More recent studies have indicated the presence of a second cell type-specific promoter. An adjacent region of the promoter (from −922 to −476 bp) can direct reporter gene expression to a different set of FMRFamide neurons, the neuroendocrine Tv cells (M. Roberts, S. Renn, and P. Taghert, unpublished). These data suggest that certain regulatory elements of the *FMRFamide* gene are autonomous

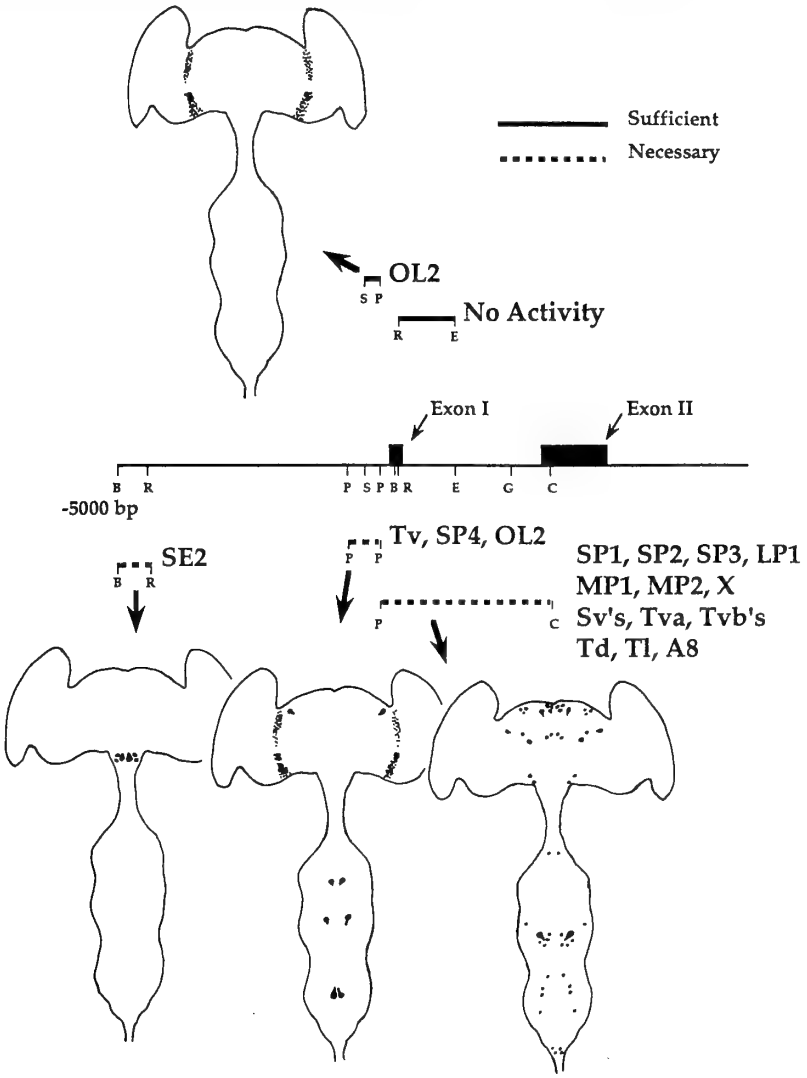

FIG. 3. A schematic that illustrates the positions of DNA regions within the *FMRFamide* promoter that control cell type-specific *lacZ* gene expression. The *FMRFamide* gene is diagrammed in the center of the figure with the two exons indicated as black boxes. Restrictions abbreviations include: B (*Bam*HI), R (*Eco*RI), P (*Pst*I), S (*Sal*I), E (*Spe*I) G(*Bgl*II), C (*Cla*I). Below the gene, the dotted lines and corresponding drawings summarize results of deletion analysis. These regions are necessary for *lacZ* expression in the indicated neurons. Above the gene, the results of the enhancer constructs are summarized. The 300 bp fragment lying 162 bp 5' to exon I is sufficient to direct expression of the reporter gene by a heterologous promoter in the OL2 neurons. The names of neuronal cell types that express the *FMRFamide* gene are presented as abbreviations (e.g, SE2, OL2, etc.); see ref. [96] for a more complete description. Reprinted with permission of Cell Press.

enhancers, capable of directing expression to individual cell types. Accordingly, not all of the diverse neurons that share this specific neuropeptide phenotype share a common transcriptional control. Instead, the parallel regulation of these distinct enhancers in different cell types results in the full pattern of *FMRFamide* expression. Some of the elements appear specific for particular cell types, while others appear to contribute to many cell types in coordinate fashion. In addition, ectopic reporter gene expression, both within the CNS and in other tissues [96], (M. Roberts, S. Renn, and P. Taghert, unpublished) indicates the presence of negative transcriptional elements as well. This model shares may features with ones that describe the activation of the pair-rule genes *hairy* and *eve* in individual stripes across the *Drosophila* blastoderm [28, 40, 74]. Certain individual stripes of gene expression are controlled by discrete enhancer regions; other stripes are coordinately controlled by a common regulatory domain.

Aspects of this model have many important implications for the regulation of *FMRFamide* gene expression. For example, the use of independent enhancers could provide a very high degree of flexibility in the evolutionary modification of gene expression, at the level of single cell types. A possible example of such evolutionary modification is illustrated by two neurons called Tv and Tva. Although these two cells share a common cell body position, axonal target,

and neuroendocrine function, different regions of the *FMRFamide* promoter are required for their respective expression (Fig. 3). Furthermore, both the Tv and Tva cells are present and morphologically differentiated in larval stages (D. Zitnan and P. Taghert, unpublished), but only the Tv neurons have detectable levels of *FMRFamide* expression at this time. In contrast, both the Tv and Tva neurons in *D. virilis* are FMRFamide-immunoreactive in larval stages [103]. This subtle difference between closely related species may result from the modified use of independent, cell type-specific enhancers. Further analysis of the regulatory domains and their molecular controls should contribute to our understanding of neurotransmitter phenotypes in the brain. As outlined below, related questions of interest include those of comparative regulation: How similar are the regulatory domains for different neuropeptide genes? When coordinately expressed in the same neuronal cell type, are they independently or jointly regulated? The precision of studies of identifiable neurons of simple systems, when combined with the power of genetic transformation techniques, makes it now possible to address such fundamental questions directly.

GENETIC ANALYSIS OF NEUROPEPTIDE FUNCTIONS

As described earlier, neuropeptide systems are not easily dissected because they display complex patterns of cellular expression and because they employ several strategies to generate diversity of peptide sequences. For this reason, genetics could be useful to analyze neuropeptide systems at many levels. There are thirteen copies of structurally-related neuropeptides on the *Drosophila* proFMRFamide precursor. Many of the individual peptides are indeed processed from the precursor, as determined by purification from tissue homogenates [63, 66]. This arrangement of multiple, biologically active molecules is reminiscent of numerous neuropeptide precursor structures. The proenkephalin and prothyrotropin-releasing hormone precursors of mammals, for example, each contain multiple copies of their respective biologically active peptide sequences [26, 50].

A genetic analysis will allow us to ask fundamental questions about the role(s) of a complex neuropeptide precursor *in vivo*. First, does the gene serve an essential function? By studying animals that are chronically deficient in the production of these molecules, we hope to learn if the survival of the animal depends on their function, or whether other neuropeptides share overlapping functions. Also, to what extent do the different co-synthesized neuropeptides act coordinately? Does the inclusion of many related neuropeptides on one precursor indicate functional amplification, or redundancy? Further, does the gene play a similar role in all the neurons in which it is expressed, or is it contributing to the execution of diverse neural activities? By manipulating gene structure in a mutant background, it should be possible to assess the importance of the sequence, copy number and arrangement of specific neuropeptides on a complex precursor molecule.

While very little information is available concerning the roles of insect FMRFamide peptides, some possible functions have been suggested by direct pharmacological analysis. In *Drosophila*, several of the neuropeptides encoded by the proFMRFamide precursor modulate neurally-evoked tension in larval somatic muscle (R. Hewes and P. Taghert, unpublished). In locusts, FMRFamide and related peptides have similar effects on skeletal muscle contractions in the leg [19]. In the blowfly, *Calliphora*, some but not all endogenous FMRFamide-like neuropeptides induce fluid secretion from isolated salivary glands [18]. Whether these diverse *in vitro* tissue reponses correspond to actual physiological events *in vivo* awaits genetic confirmation.

Genetic studies of *Drosophila FMRFamide* have begun to define its chromosomal locus (Fig. 4). The gene is present in single copy and is located at position 46C of the 2nd chromosome [94]. No mutant stocks were available, so deficiency stocks were first generated which have relatively large deletions in the surrounding region. These served to define the locus and to provide a starting point for mutagenesis experiments. Ultimately, these deficiency stocks helped to define a 50-60 kb region surrounding the *FMRFamide* gene and they were used to identify lethal mutations residing within this interval [71]. Because so little is known about the functions of *Drosophila FMRFamide*, we could not accurately predict the severity or quality of phenotypes from a hypomorphic or null allele. We mutagenized flies with ethyl methane sulfonate which generally produces point mutations. Screening for the most severe phenotype (lethality) was the first step and resulted in the identification of three genes within the 50–60 kb surrounding region which give a lethal phenotype when mutated (Fig. 4). These three genes with lethal mutant phenotypes appear to be neighbors of *FMRFamide*, but not *FMRFamide* itself. These results raised the possibility that the *FMRFamide* gene may not be an essential gene; they also point out two principal limitations to the identification of neuropeptide gene mutations.

The first limitation involves the probability of mutating a complex neuropeptide gene to a null phenotype by chemical mutagenesis. Such genes encode polyprotein precursors that, by their design, incorporate redundant sequence elements (e.g., Fig. 2). This design feature reduces the chances that a single base pair alteration will necessarily affect the basic functioning of the entire protein. This feature may also operate in wild type populations to lessen the consequences of spontaneous mutations due to environmental mutagens. The second complication involves the likelihood that a profound phenotype will result from a *bona fide* mutation in a neuropeptide gene. While the logic of neuropeptide signaling is yet to be defined, it almost certainly includes highly redundant signals that may be cosynthesized and/or derived from distinct precursors. This functional redundancy reduces the chances that the absence of any given group of neuropeptides will generate a distinctive phenotype.

Given these limitations, it is useful to consider alterna-

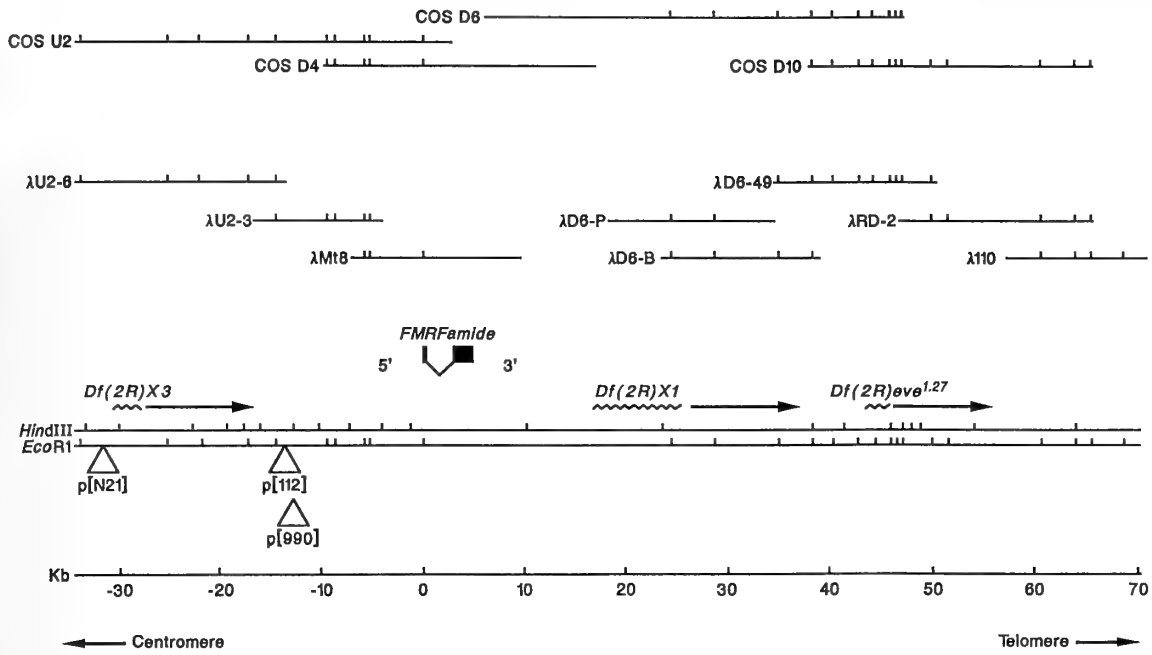

FIG. 4. Genomic map of the 46C region surrounding the *FMRFamide gene*. Cosmid (Cos) clones and lambda (λ) phage clones are shown above the schematized *FMRFamide* gene. *Hind* III and *Eco*RI restriction maps are illustrated below the schematized gene. Deficiency endpoints are denoted by a wavy line and the direction of the deletion from the endpoint is noted by an arrow. P element insertions are illustrated with a triangle and the insertion designation. (See ref. [71]). Reprinted with permission of the Genetics Society of America.

tive methods to analyze neuropeptide systems genetically. In this regard, transposable elements offer useful complimentary approaches to initiate novel genetic analyses. Insertional mutagenesis is useful because it can be employed as a molecular screen and therefore is not dependent on the ability to predict a phenotype. For example, with respect to the *Drosophila FMRFamide* gene, a "local hop" strategy of mobilizing P elements [107] was used to identify a stock bearing an insertion ~15 kb upstream of the gene [71]. This insertion disrupts a neighboring gene and hence is not useful by itself to define FMRFamide functions. Nevertheless, such proximity encourages the hope that reiterations of the experiment will produce the more specific insertional event desired. A similarly-conceived screen in *C. elegans* has resulted in the identification of a stock bearing a transposable element (Tc1) inserted within the *flp-1* promoter (C. Li, per. communication). Excision of this insert should permit a detailed examination in the near future of worms that are deficient in the production of FMRFamide neuropeptides. The utility of transposable elements for the analysis of neuropeptide systems is also evident in the use of enhancer trap screens, as we discuss in a later section.

OTHER NEUROPEPTIDE SYSTEMS IN *DROSOPHILA*

We have outlined studies of the *FMRFamide* gene in model systems as a means of introducing outstanding questions relating to neuropeptide structure, expression and functions. Molecular genetic studies have also been initiated for several other *Dorosophila* neuropeptide genes, including those encoding the drosulfakinins [65], the eclosion hormone [39], and the adipokinetic hormone [90]. Their chromosomal positions are 81F, 90B, and 64AB, respectively. A gene encoding dromyosuppressin, an extended FLRFamide-related neuropeptide, has also been inferred [66], and is discussed due to its potential relationship to the *FMRFamide* gene. Genetic analyses in all these cases are in their initial stages; however, the available molecular information provides the basis for addressing questions about function and regulation of expression. Notably, this section does not review several pertinent studies of neuropeptides in *Drosophila* for which the genes have not yet been cloned. We refer the reader to a recent review by Nässel [64] for a discussion of this substantial body of information.

I. Drosulfakinin

Questions regarding function and regulation are especially pertinent for neuropeptides derived from conserved evolutionary families. Among neuropeptide systems being investigated in *Drosophila*, in addition to FMRFamide, drosulfakinin, is also a member of an -RFamide family with apparent homologues in both vertebrates and invertebrates. The *drosulfakinin* (*dsk*) gene [65] was cloned using oligonucleotide probes based on the conserved amino acid sequences of the vertebrate gastrin and cholecystokinin (CCK) peptides, as well as another insect neuropeptide, leucosulakinin, from the cockroach [60, 61]. Two of three encoded peptides in the pro-dsk precursor are *Drosophila* homologues of the gastrin and CCK family of vertebrate peptides, while

the third is novel [65]. Two features suggest that insect dsk and vertebrate gastrin/CCK systems may display conservation of functions and/or receptor structure. First, the closest homology resides in the C-terminal pentapeptide and there is a tyrosine just N-terminal to the pentapeptide. The C-terminal pentapeptide and the sulfated tyrosine are thought to be necessary for activity of the gastrin/CCK peptides [62]. Secondly, in vertebrates, gastrin and CCK are gastrointestinal-brain peptides with implicated functions in digestion, feeding behavior and satiety [100]. A dsk peptide also has been localized in the brain [106] and gut [67]. A genetic analysis will be essential for determining if the expression of the dsk peptides reflects a conserved function in digestion and feeding behavior.

II. Dromyosuppressin

Dromyosuppressin (dms) was purified from *Drosophila* extracts with an anti-RFamide antibody [66]. Its sequence (TDVDHVFLRFamide) was not among those deduced from the *FMRFamide* or *dsk* genes; this indicated a separate genomic locus. The dms peptide shares sequence homology with leucomyosuppressin from the cockroach [37], and neomyosuppressin from the flesh fly [22], peptides that both have myoinhibitory effects. A specific antibody against the TDVDHV portion of the peptide was generated and used to demonstrate that this peptide is expressed in the CNS and in the gut [57]. The degree to which the *dms* and *FMRFamide* genes are evolutionarily related will be an important issue to resolve. Dms does not co-localize with the dsk peptides [106]; the possibility of co-localization with the peptides encoded by *FMRFamide* has not yet been addressed. Co-localization of distinct RFamide-neuropeptides would support a hypothesis that these genes may have retained similar promoter/regulatory regions. Equally important are the functional consequences derived from the relationship between *FMRFamide* and *dms*. A genetic analysis of these two genes in flies will be important for determining the degree to which their functions are unique and non-overlapping.

III. Eclosion hormone

Eclosion hormone (EH) is a neuropeptide that triggers ecdysis behaviors in insects [109]. The *EH* gene in *Drosophila* was cloned by homology using sequences from the tobacco hornworm, *Manduca sexta* [39]. In both species, the precursor is remarkably simple: a signal sequence is followed by a single, conserved 62 amino acid peptide (there is a possible additional 9 amino acid cleavage product in *Drosophila* [38, 39]). The *EH* gene has an extremely discrete expression pattern in both *Manduca* and *Drosophila*; transcripts are found in only two pair of neurons in the brain of *Manduca* [38] and in one pair in *Drosophila* [39]. In *Manduca*, the EH cell axons exit the proctodeal (hindgut) nerve along which there are neurohaemal release sites. However, it has also been established that these neurons release EH directly within the CNS from their axonal processes. The role of EH in triggering ecdysis behaviors is primarily accomplished *via* this direct access to the CNS [34]. While much useful information concerning EH action has accumulated from classic pharmacological and physiological experiments, the genetic analysis of EH could address more directly its long term roles in neuromodulation (e.g., in releasing stage-specific behaviors). Also, the full scope of its actions at non-neuronal sites could be defined; several non-neuronal target tissues for the neuropeptide have already been identified [34, 77, 99]. Likewise, a molecular genetic analysis of *EH* could address the basis for its highly restricted spatial expression and its potential regulation by genes involved in generating circadian outputs [83]. Existing deficiency stocks for the *EH* chromosomal locus, and a well-defined function *in vivo* provide a substantial basis for initiating these genetic studies.

IV. Adipokinetic hormone

The *adipokinetic hormone* (*AKH*) gene encodes a neuropeptide involved in lipid mobilization during flight in insects [102]. The gene was cloned in *Drosophila* based on the known peptide sequence of *Drosophila* AKH [89, 90]. In the grasshopper and locust, there are two closely-related forms of AKH (called I and II). They are the products of different genes, although the genes display some similarities [68, 69]. AKH I and II are co-localized and co-released, but they are not synthesized in equivalent amounts and the ratios of the two forms change during development. The precise regulation of the AKH I and II peptide stoichiometry throughout development is maintained *via* several mechanisms [72].

First, dimerization of the two precursors contributes to the stoichiometry of the processed peptides. AKH I and II are synthesized as precursors including a signal peptide, the AKH peptide, and a carboxy-terminal peptide or AKH precursor related peptide (APRP) of unknown function [32]. The precursors dimerize both as homodimers and heterodimers before the processing cleavage steps, thus producing AKH I, AKH II, and three dimeric APRPs [31, 32, 98]. Secondly, there are additional transcriptional and translational mechanisms to regulate the stoichiometry [20]. Finally, there is an increase in the number of AKH expressing cells during development, which increases the overall levels [48]. Interestingly, these co-localized and co-expressed genes have quite different 5' flanking regions, suggesting they have evolved different regulatory mechanisms [69]. Despite a considerable understanding of the mechanisms underlying this precise stoichiometry of the AKHs and APRPs, the utility of this complex peptidergic system is not well defined. The *in vivo* functions of AKH II and the APRPs are not known; it is hypothesized that AKH II has a larval function and that the APRPs may be involved in other metabolic processes related to flight [72]. In *Drosophila*, there appears to be a single *AKH* gene [90]. A comparison of its promoter region with that of the grasshopper AKH I and II promoter regions could provide insight into the evolution of distinct regulatory regions of highly related genes. The AKH-

APRP arrangement within the precursor is preserved in *Drosophila* although the APRP peptide sequence is not well-conserved. A genetic dissection of the *Drosophila adipokinetic hormone* gene would help to evaluate the physiological significance of their co-synthesis.

NEUROPEPTIDE GENES IN OTHER INSECTS

The study of neuropeptides at the biochemical, physiological, and developmental level has an extensive history in insects [47, 108]. More recently these studies have taken a molecular approach, thus offering the prospect of a genetic analysis of several additional neuropeptide systems. Two neuropeptide genes, recently cloned in other insects, are important in the neuroendocrine pathways controlling molting and metamorphosis, and may have homologues in *Drosophila*. These are the *prothoracicotropic hormone* (*PTTH*) gene, cloned from the silkmoth [1, 45] and the *allatostatin* (*AST*) gene, cloned from the cockroach [17]. PTTH, initiates the molting process by stimulating synthesis of ecdysone (the molting hormone) by the prothoracic glands. AST inhibits juvenile hormone synthesis by the corpora allata. Antibodies that display specificity to these two important developmental neurohormones both cross-react in *Drosophila* [111]. Furthermore, CNS extracts from *Drosophila* stimulate ecdysone production by the ring gland. This suggests an endogenous PTTH-like activity [33, 73]. The degree to which the neuroendocrine circuits regulating molting and metamorphosis are conserved between lepidopterans and dipterans has not been resolved (see [78]). A molecular genetic approach to this system should be very informative. Two additional neuropeptide genes cloned in other insects are considered in detail here because they illustrate two prominent features of neuropeptide systems that have not been presented in our previous examples: 1) peptides co-synthesized on the same precursor serving distinct temporal functions and 2) neuropeptide genes comprising a multi-gene family.

The *diapause hormone* (*DH*) neuropeptide gene, recently cloned in *B. mori*, [46, 85] and *H. zea* [15] provides a striking example of distinct functions for peptides encoded on the same precursor. Sequence analysis of the deduced DH precursor revealed that a distinct bioactive neuropeptide, the pheromone biosynthesis activating neuropeptide (PBAN), was co-synthesized. Although PBAN and DH are structurally related (they share a pentapeptide C-terminus), at least some of their functions appear to be distinct at different developmental stages. Diapause hormone induces diapause in the embryo in *Bombyx* while PBAN stimulates pheromone biosynthesis in the adult; thus peptides derived from a common precursor may have very distinct times at which they function [85]. Whether these are the exclusive functions of these peptides, or whether they have additional overlapping functions is not known. Such questions await answers in a genetically tractable system, like *Drosophila*, wherein the composition of a neuropeptide precursor may be manipulated and then returned to the animal for evaluation *in vivo*. While the biological functions of putative DH and PBAN homologues in *Drosophila* have not been described, this issue of functional complexity applies to any of several neuropeptide precursors that generate diverse final products.

The neuropeptide genes currently being investigated in *Drosophila* display much variation in precursor complexity, and in the degree to which the peptides they encode have retained sequence conservation through evolution. It is notable however, that they are similar in that each represents a single copy within the haploid genome. For comparative purposes, it is worth mentioning that in other insects and in other animals, neuropeptide genes are often members of large gene families (e.g., [91]). Bombyxin, an insulin-related neurohormone from the silkmoth, *Bombyx mori*, provides an extreme example of a neuropeptide multigene family. Purification of the neurohomone revealed that there were several isoforms of the protein; it is now known that this heterogeneity is due in large part to genetic diversity [41]. There are numerous bombyxin genes (>20), at least four of which were found clustered in the genome [44]. These genes are categorized into four families [41, 42]; genes are paired such that distinct members of two related families are adjacent and in the opposite orientation [44]. This arrangement could facilitate coordinated expression of related gene families. It is hypothesized that different pairs of bombyxin genes are expressed at different stages of development. A neuropeptide multi-gene family has not been identified in flies, but a molecular genetic analysis of such a gene family could help us to understand its functional significance and its regulatory interactions.

RECEPTORS AND PROCESSING ENZYMES

The enzymes responsible for processing of neuropeptide precursors and the receptors with which neuropeptides interact are important control points in the functional circuits underlying neuropeptide signaling. Their involvement would also be better defined by a molecular genetic analysis. Because genes of both types of molecules have been cloned in *Drosophila*, we include a brief summary of that information here.

Two genes related to the mammalian *furin* processing enzyme genes have been cloned (D*fur1* and D*fur2*; [30, 80, 81]. The furin protein is related to the yeast protein which is a serine endoprotease, with specificity for paired basic amino acid residues. There are four transcripts of the D*fur1* gene generated by alternative splicing [82]. *In situ* hybridization to two of these transcripts indicated that they have non-overlapping expression patterns in the embryo, suggesting different physiological roles [82]. With multiple proprotein processing enzyme genes and multiple transcripts from these genes, there may be a high degree of specificity in processing of *Drosophila* proproteins, and neuropeptide precursors, in particular. An *in vivo* mutational analysis of this rapidly expanding family of peptide processing genes will be an

important step in sorting out this specificity.

The identification of diverse neuropeptide receptors is beginning to match the diversity of neuropeptides themselves in vertebrates. This field is ripe for investigation in an organism that readily allows for genetic manipulation. To date, three identified neuropeptide receptors have been cloned in *Drosophila*, two different tachykinin receptors [52, 58] and a neuropeptide Y receptor [53]. These three receptors are developmentally regulated with peaks of expression in late embryogenesis. The spatial and temporal regulation of neuropeptide receptors clearly may have functional consequences for neuropeptide action; this is another reason why *in vivo* studies of all components of neuropeptide systems are essential for a comprehensive understanding of the function of this diverse class of signaling molecules.

ENHANCER DETECTOR LINES REVEAL DISCRETE NEUROENDOCRINE NEURON EXPRESSION PATTERNS

An alternative approach to a genetic screen for genes involved in neuropeptide signaling is a molecular screen. The advantage of a molecular screen is that it does not require consideration of potential mutant phenotype. For example, P element enhancer detector lines in *Drosophila* can be screened for expression patterns that include identified peptidergic neurons. In these lines, a β-galactosidase gene construct inserts into the fly genome. The reporter gene is constructed to require enhancer activity for robust expression; in principle, that activity derives from single neighboring genes of the host [2, 3, 29]. The significance of this method derives not only from the ease with which novel genes may be cloned, but also from the provision of direct means by which they may be subsequently mutated. The P element insertion can be mobilized and imprecise, mutating excisions can be detected (e.g., [7, 71]).

In insects, a certain class of peptidergic cells are often distinguished by their size, their axonal projections, and the large amount of secretory neuropeptides that they synthesize and store [64]. We utilized these anatomical features to screen several hundred nervous systems from developing adult *Drosophila* in which a GAL4-containing P element [9] had been mobilized. From this small-scale screen, we found several interesting patterns that are dominated by the inclusion of previously identified neuroendocrine neurons (P. Taghert, A. Schaefer, and M. O'Brien, unpublished). It should be emphasized that in most cases, the pattern of expression is not exclusive to these neurons, or even to the nervous system. The search image that we employed simply required a high level of expression and some exclusivity to certain identifiable, peptidergic neurons.

In Figure 5 is shown examples of two patterns - a general and a specific. The first is numbered P9 and it displays a pattern of gene expression in one to two hundred neurons scattered throughout the CNS. These include several identified peptidergic neurons as indicated by (i) co-expression of peptide immunoreactivities: for FMRFamide [103], allatostatin [111], or proctolin (P. Taghert, unpublished); or as indicated by (ii) axonal projections that, by terminating is neurohaemal sites, indicate a neuroendocrine, peptidergic function [64, 97]. We hypothesize that the indicated gene product may be a protein that is widely expressed by cells that secrete large amounts of peptides. There are several identified peptidergic neurons that do not express this reporter

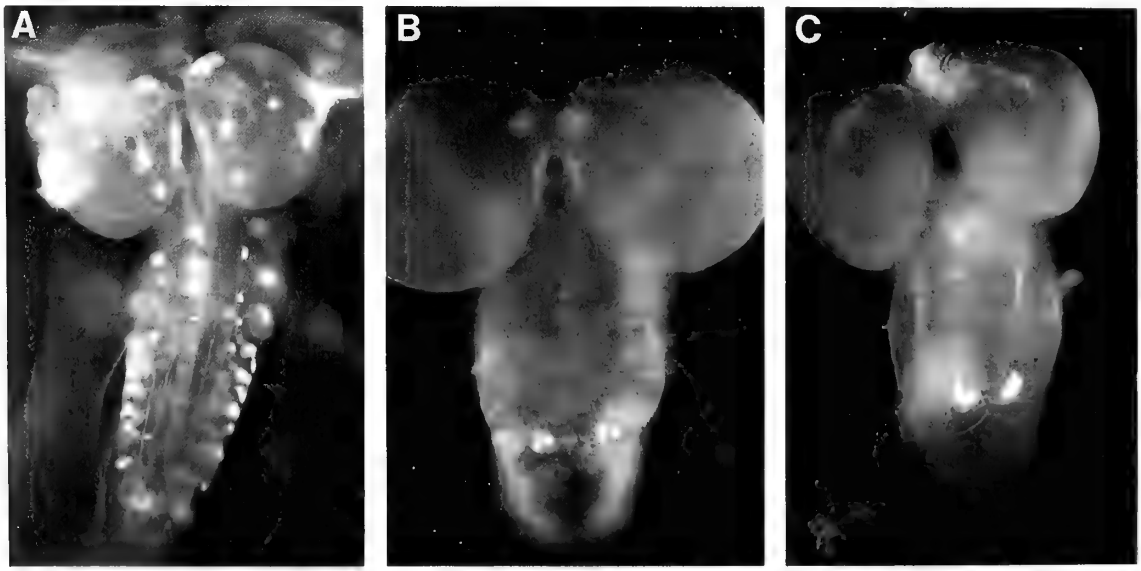

FIG. 5. Enhancer trap expression of beta-galactosidase in two lines of *Drosophila*. (A) The P[9] line is expressed in >100 neurons of the larval CNS; many are identifiable by their axonal projections and/or by their peptide immunoreactivities as peptidergic neurons. (B) The P[3] line expressed beta-galactosidase at low levels in many cells of the abdominal neuromeres of the CNS and at high levels by 14 large identifiable neuroendocrine neurons. Six of these neurons are also specifically labeled by antibodies to the molluscan neuropeptide myomodulin, as shown in (C). All examples shown are 3rd instar larval CNSs that were stained with anti-β-gal antibodies (A and B) or anti-myomodulin antibodies (C); primary antibodies were visualized by subsequent application of a fluorescent secondary antibody.

gene. Therefore, if the P9 gene serves a general secretory function, it may not be unique in its capacity.

The more specific pattern, numbered P3, displays very weak expression in widespread regions of the CNS and very strong expression in fourteen specific neurons; twelve of these are identified peptidergic neurons. In addition, there is peripheral expression in four peritracheal cells [29] per segment. An antiserum to the molluscan neuropeptide myomodulin [14] specifically labels twenty neurons in the *Drosophila* CNS, and these include six of the fourteen P3-positive neurons; this same antibody also labels two of the four P3-positive peritacheal cells per segment (M. O'Brien and P. Taghert, unpublished). In all, there is a remarkable coincidence to the spatial patterning of P3 and molluscan myomodulin-immunoreactivity. These limited observations indicate that there is a large amount of useful information to be acquired from the further examination and manipulation of enhancer detector lines.

CONCLUSIONS

In this review, we have summarized the strengths and weaknesses of analyzing neuropeptide signaling systems with genetic techniques (see also [76]). In all, we believe that the advantages far outweight the difficulties of initiating such studies. Beyond describing their sequences and their spatial patterns of expression, there are several fundamental properties of neuropeptides that remain to be defined. These include: the precise roles that such molecules play *in vivo*; the degree to which these physiological and bahavioral roles are effected by groups of neuropeptides acting in concert; whether precise neuropeptide expression (i.e., a close association with specific synaptic circuits) is a critical feature of their functioning (see [8] for a recent discussion of this point); the degree to which other molecules involved in signaling (e.g., biosynthetic enzymes, neuropeptide receptors) are points of regulation for proper signaling processes. The ability to manipulate transmitter gene expression *in vivo* will be the principal means of defining these properties and thus evaluating the contributions of neuropeptide signaling systems. Among the model systems that are amenable to genetics, there exists a wealth of interesting physiology, development, and behavior for which diverse neuropeptide systems have been indicated to play major regulatory roles. With the advent of molecular genetic techniques with which to manipulate neuropeptide signaling systems *in vivo*, we can look forward to substantial progress in further elucidating chemical signaling within the nervous system.

ACKNOWLEDGMENTS

We thank Chris Li, Randall Hewes, Susan Renn, Marie Roberts and Anneliese Schaefer for permission to cite unpublished results. We thank Klaude Weiss for the anti-myomodulin antiserum. We are grateful to Rod Murphey, David Shepard and Kim Kaiser for their permission and assistance in screening GAL4 insertion lines. Unpublished work from our laboratory was supported by grants from the National Institutes of Health and the National Science Foundation.

REFERENCES

1 Adachi-Yamada T, Iwami M, Kataoka H, Suzuki A, Ishizaki H (1994) Eur J of Biochem 220: 633–643
2 Bellen HJ, O'Kane C, Wilson C, Grossniklaus U, Pearson RK, Gehring WJ (1989) Genes & Dev 3: 1288–1300
3 Bier E, Vaessin H, Sheperd S, Lee K, McCall K, Barbel S, Akerman L, Caretto R, Uemura T, Grell E, Jan LY, Jan YN (1989) Genes & Dev 3: 1273–1287
4 Blackman RK, Meselson M (1986) J Mol Biol 188: 499–515
5 Botwell DDL, Kimmel BE, Simon MA, Rubin GM (1989) Proc Nat Acad Sci USA 86: 6245–6249
6 Botwell DDL, Lila T, Michael WM, Hackett D, Rubin GM (1991) Proc Nat Acad Sci USA 88: 6853–6857
7 Bourgouin C, Lundgren SE, Thomas JB (1992) Neuron 9: 549–561
8 Bowers CW (1994) Trends in Neurosci 17: 315–320
9 Brand AH, Perrimon N (1993) Development 118: 401–415
10 Bray SJ, Johnson WA, Hirsh J, Heberlein U, Tjian R (1988) EMBO J 7: 177–188
11 Bright K, Kellett E, Saunders SE, Brierly M, Burke J, Benjamin PR (1993) J Neurosci 13: 2719–2729
12 Chin A, Reynolds E, Scheller RH (1990) DNA and Cell Biology 9: 263–271
13 Cottrell GA, Price DA, Doble KE, Hettle S, Sommerville J, MacDonald M (1992) Biol Bull 183: 113–122
14 Cropper EC, Tenenbaum R, Kolks MAG, Kupferman I, Weiss KR (1987) Proc Nat Acad Sci USA 84: 5483–5486
15 Davis MT, Vakharia VN, Henry J, Kempe TG, Raina AK (1992) Proc Natl Acad Sci USA 89: 142–146
16 Doble KE, Greenberg JJ (1982) Neuropeptides 2: 157–167
17 Donly BC, Ding Q, Tobe SS, Bendena WG (1993) Proc Natl Acad Sci USA 90: 8807–8811
18 Duve H, Johnson AH, Sewell JC, Scott AG, Orchard I, Rehfield JF, Thorpe A (1992) Proc Natl Acad Sci USA 89: 2326–2330
19 Evans PD, Myers CM (1986) J Exp Biol 126: 403–422
20 Fischer-Lougheed J, O'Shea M, Cornish I, Losberger C, Roulet E, Schulz-Aellen M-F (1993) J Exp Biol 177: 223–241
21 Fisher JA, Maniatis T (1983) Cell 53: 451–461
22 Fónagy A, Schoofs L, Proost P, Vandamme J, Bueds H, Deloof A (1992) Comp Biochem Physiol 102C: 239–245
23 Garabedian MJ, Sheperd BM, Wesink PC (1986) Cell 53: 451–461
24 Goto T, Macdonald P, Maniatis T (1989) Cell 57: 413–422
25 Grosfeld F, Assendelft GB, Greaves DR, Kollias G (1987) Cell 51: 975–985
26 Gubler U, Seeburg P, Hoffman BJ, Gage LP, Udenfriend S (1982) Nature (Lond) 295: 206–208
27 Hammer RE, Krumlauf R, Camper SA, Brinster RL, Tilghman SM (1987) Science (Wash) 235: 53–58
28 Harding K, Hoey T, Warrior R, Levine M (1989) EMBO J 8: 1205–1212
29 Hartenstein V, Jan YN (1992) Roux's Arch Dev Biol 201: 194–220
30 Hayflick JS, Wolfgang WJ, Forte MA, Thomas G (1992) J Neurosci 12: 705–717
31 Hekimi S, Burkhart W, Moyer M, Fowler E, O'Shea M (1989) Neuron 2: 1363–1368
32 Hekimi S, Fischer-Lougheed J, O'Shea M (1991) J Neurosci

11: 3246–3256
33 Henrich VC, Pak MD, Gilbert LI (1987) J Comp Physiol (B) 157: 543–549
34 Hewes RS, Truman JW (1991) J Comp Physiol (A) 168: 697–707
35 Hiromi Y, Gehring WJ (1987) Cell 50: 963–974
36 Hirsh J (1989) Dev Genetics 10: 232–238
37 Holman GM, Cook BJ, Nachman RJ (1986) Comp Biochem Physiol 85C: 329–333
38 Horodyski FM, Riddiford LM, Truman JW (1989) Proc Natl Acad Sci USA 86: 8123–8127
39 Horodyski FM, Ewer J, Riddiford LM, Truman JW (1993) Eur J Biochem 215: 221–228
40 Howard KR, Struhl G (1990) Development 110: 1223–1231
41 Ishizaki H, Suzuki A. (1992) In "The Peptidergic Neuron Vol 92" Ed by J Joose, RM Buijis, FJH Tilders, Prog in Brain Res, Elsevier Press, Amsterdam, pp 1–14
42 Iwami M, Adachi T, Kondo H, Kawakami A, Suzuki Y, Nagasawa H, Suzuki A, Ishizaki H (1990) Insect Biochem 20: 295–303
43 Johnson WA, McCormick CA, Bray SJ, Hirsh J (1989) Genes & Dev 3: 676–686
44 Kawakami A, Iwami M, Nagasawa H, Suzuki A, Ishizaki H (1989) Proc Natl Acad Sci USA 86: 6843–6847
45 Kawakami A, Kataoka H, Oka T, Mizoguchi, A, Kimura-Kawakami M, Adachi T, Iwami M, Nagasawa H, Suzuki A, Ishizaki H (1990) Science (Wash) 247: 1333–1335
46 Kawano T, Kataoka H, Nagasawa H, Isogai A, Suzuki A (1992) Biochem and Biophys Res Comm 189: 221–226
47 Kelly TJ, Masler EP, Menn JJ (1994) In "Insect Neuropeptides: current status and avenues for pest control Vol 551" Ed by PA Hedin, JJ Menn, RM Hollingsworth Natural and Engineered Pest Management Agents, Washington D.C., ACS Symposium Series, pp 292–319
48 Kirschenbaum SR, O'Shea M (1993) Development 118: 1181–1190
49 Kitamoto T, Ikeda K, Salvaterra PM (1992) J Neurosci 12: 1628–1639
50 Lechan RM, Wu P, Jackson IM, Wolf H, Cooperman S, Mandel G (1986) Science (Wash) 231: 159–161
51 Li C, Calabrese RL (1987) J Neurosci 7: 595–603
52 Li XJ, Wolfgang W, Wu YN, North RA, Forte M (1991) EMBO J 10: 3221–3229
53 Li X-J, Wu Y-N, North RA, Forte M (1992) J Biol Chem 267: 9–12
54 Linacre A, Kellett E, Saunders S, Bright K, Benjamin PR, Burke JF (1990) J Neurosci 10: 412–419
55 Lloyd PE, Frankfurt M, Stevens P, Kupfermann I, Weiss KR (1987) J Neurosci 7: 1123–1132
56 Lutz EM, Macdonald M, Hettle S, Price DA, Cottrell GA, Sommerville J (1992) Mol Cell Neurosci 3: 373–382
57 McCormick J, Nichols R (1993) J Comp Neurol 338: 278–288
58 Monnier D, Colas J-F, Rosay P, Hen R, Borrelli E, Maroteaux L (1992) J Biol Chem 267: 1298–1302
59 Murphy AD, Lukowiak K, Stell WK (1985) Proc Natl Acad Sci USA 82: 7140–7144
60 Nachman RJ, Holman GM, Haddon WF, Ling N (1986) Science (Wash) 234: 71–73
61 Nachman RJ, Holman GM, Haddon WF (1988) Peptides 9: 137–143
62 Nachman RJ, Holman GM, Haddon WF, Hayes TK (1989) Peptide Res 2: 171–177
63 Nambu JR, Murphy-Erdosh C, Andrews PC, Feistner GJ, Scheller RH (1988) Neuron 1: 55–61
64 Nässel DR, Bayraktaroglu E, Dirckson H (1994) Zool Sci 11: 15–31
65 Nichols R, Schneuwly SA, Dixon JE (1988) J Biol Chem 263: 12167–12170
66 Nichols R (1992) J Mol Neurosci 3: 213–218
67 Nichols R (1992) Mol Cell Neurosci 3: 342–347
68 Noyes BE, Schaffer MH (1990) J Biol Chem 265: 483–489
69 Noyes BE, Schaffer MH (1993) DNA and Cell Biol 12: 509–516
70 O'Brien MA, Schneider LE, Taghert PH (1991) J Comp Neurol 304: 623–638
71 O'Brien MA, Roberts MS, Taghert PH (1994) Genetics 137: 121–137
72 O'Shea M, Rayne RC (1992) Experientia 48: 430–438
73 Pak JW, Chung KW, Lee CC, Kim K, Namkoong Y, Koolman J (1992) J Insect Physiol 38: 167–176
74 Pankratz MJ, Seifert E, Gerwin N, Billi B, Nauber U, Jackle H (1990) Cell 61: 309–317
75 Price DA, Greenberg MJ (1977) Prep Biochem 7: 261–281
76 Restifo LL, White K (1990) Adv Insect Physiol 22: 115–219
77 Reynolds SE (1977) J Exp Biol 70: 27–37
78 Riddiford LM (1993) In "The Development of *Drosophila melanogaster* Vol II" Ed by CM Bate, A Martinez-Arias, Cold Spring Harbor: Cold Spring Harbor Press, pp 899–939
79 Robb S, Packman LC, Evans PD (1989) Biochem Biophys Res Comm 2: 850–856
80 Roebroek AJM, Pauli IG, Zhang Y, Van de Ven WJM (1991) FEBS Letters 289: 133–137
81 Roebroek AJM, Creemers JWM, Pauli IGL, Boaert, T, Van de Ven WJM (1992) J Biol Chem 267: 17208–17215
82 Roebroek AJM, Creemers JWM, Pauli IGL, Bogaert T, Van de Ven WJM (1993) EMBO J 12: 1853–1870
83 Rosbash M, Hall JC (1989) Neuron 3: 387–398
84 Rosoff ML, Burglin TR, Li C (1992) J Neurosci 12: 2359–2361
85 Sato Y, Oguchi M, Menjo N, Imai K, Saito H, Iketa M, Isobe M, Yamashita O (1993) Proc Natl Acad Sci USA 90: 3251–3255
86 Saunders SE, Bright K, Kellet E, Benjamin PR, Burke JF (1991) J Neurosci 11: 740–744
87 Saunders SE, Kellet E, Bright K, Benjamin PR, Burke JF (1992) J Neurosci 12: 1033–1039
88 Schaefer M, Picciotto MR, Kreiner T, Kaldany R-R, Taussig R, Scheller RH (1985) Cell 41: 457–467
89 Schaffer MH, Noyes BE, Slaughter CA, Thorne GC, Gaskell SJ (1990) Biochem J 269: 315–320
90 Schaffer MH, Noyes BE (1992) Soc Neurosci Abs 18: 466, 11
91 Scheller RH, Jackson JF, McAllister LB, Schwartz JH, Kandel ER, Axel R (1982) Cell 28: 707–719
92 Schinkmann K, Li C (1992) J Comp Neurol 316: 251–260
93 Schinkmann K, Li C (1994) Mol Brain Res 24: 238–246
94 Schneider LE, Taghert PH (1988) Proc Natl Acad Sci USA 85: 1993–1997
95 Schneider LE, Taghert PH (1990) J Biol Chem 265: 6890–6895
96 Schneider LE, Roberts MS, Taghert PH (1993) Neuron 10: 279–291
97 Schneider LE, Sun ET, Garland DJ, Taghert PH (1993) J Comp Neurol 337: 446–460
98 Schulz-Aellen MF, Roulet E, Fischer-Lougheed J, O'Shea M (1989) Neuron 2: 1369–1373
99 Schwartz LM, Truman JW (1982) Science (Wash) 215: 1420–1421
100 Sodersten P, Forsberg G, Bednar I, Linden A, Qureshi GA

(1992) In "The Peptidergic Neuron Vol 92" Ed by J Joosse, RM Buijs, FHJ Tilders, Prog. in Brain Res, Elsevier, Amsterdam, pp 335–344

101 Sossin WS, Fisher JM, Scheller RH (1989) Neuron 2: 1407–1417

102 Stone JV, Mordue W, Batley KE, Morris HR (1976) Nature (Lond) 263: 207–211

103 Taghert PH, Schneider LE (1990) J Neurosci 10: 1929–1942

104 Tamura T, Kunert C, Postlethwait J (1985) Proc Nat Acad Sci USA 82: 7000–7004

105 Taussig R, Scheller RH (1986) DNA 5: 453–461

106 Tibbetts MF, Nichols R (1993) Neuropeptides 24: 321–325

107 Tower JG, Karpen H, Craig N, Spradling AC (1993) Genetics 133: 347–359

108 Truman JW, Taghert PH (1983) In "Brain Peptides" Ed by D Kreiger, M Brownstein, J Martin, John Wiley & Sons, pp 165–181

109 Truman JW (1992) In "The Peptidergic neuron Vol 92" Ed by J Joosse, RM Buijs, FJH Tilders, Prog in Brain Res, Elsevier, Amsterdam, pp 361–374

110 Young WSI, Reynolds K, Shepard EA, Gainer H, Castel M (1990) J Neuroendo 2: 917–925

111 Zitnan D, Sehnal F, Bryant P (1993) Dev Biol 156: 117–135

ZOOLOGICAL SCIENCE 11: 647–662 (1994)

REVIEW

Cell Signaling Mechanisms for Sperm Motility

MASAAKI MORISAWA

Misaki Marine Biological Station, School of Science, University of Tokyo, Misaki, Miura, Kanagawa 238-02, Japan

INTRODUCTION

Signal transduction mechanisms have been shown by many studies to regulate a number of cell functions in animals and plants. Binding of ligands to receptors and opening or closing of ion channels are the main triggers of these mechanisms.

Spermatozoa have long received attention due to their vigorous motility. There is too much evidence that the basic mechanochemical mechanism of flagellar motility is ATP-induced sliding of microtubules, the energy for sliding being due to ATPase activity associated with the dynein arms on the outer doublet microtubule [53]. Recent studies on sperm motility have been focused on the cell signaling mechanism for initiation of motility: completely immotile, such as teleost sperm and low motility sperm, such as mammalian sperm in the male reproductive organ, start to become motile on spawning and ejaculation. Activation of sperm motility as well as their respiration and attraction to eggs, which occurs after the initiation of motility and in response to substances released from the egg, are attractive subjects for analysis of the mechanisms underlying cell signaling. This article reviews results obtained mainly in the author and his collaborates (Chapter II and III) and other laboratories (Chapter IV) on possible regulatory mechanisms of sperm motility with two different types of trigger, changes in the external ionic or osmotic environment and ligand-receptor binding.

II INITIATION OF SPERM MOTILITY BY SIGNALS FROM THE ENVIRONMENT

Many physical and chemical factors, such as mechanical dilution, change in the environmental O_2-CO_2 tension, pH and heavy metal concentrations, have been suggested to initiate sperm motility (for review, see ref. [104]). However, Morisawa and Suzuki actually first demonstrated that external signals initiate motility of sperm of teleost fishes [107]. Their finding opened the way to analyze and clarify cell signaling systems related to motility of sperm cells.

Received September 19, 1994

A Domain controlling flagellar motility located in the basal region of the sperm flagellum of salmonid fishes

Spermatozoa of salmonid fishes such as rainbow trout and chum salmon are completely quiescent when the semen is diluted in the medium containing millimolar concentrations of K^+, but show motility when the semen is suspended in K^+-free medium [107, 110]. The seminal plasma of salmonid fishes contains a high concentration of K^+ and the spawning ground, fresh water of rivers has a low K^+ content [104]. Thus the experimental condition of low K^+ concentration is similar to that in natural conditions on spawning; release from the suppression of K^+ on spawning in freshwater causes the initiation of sperm motility. The effects of Na^+ and K^+ on sperm motility have also been investigated in amphidromous salmonidform species, the ayu, *Plecoglossus altivelis* [185].

Reduction of the K^+ concentration surrounding sperm on spawning in freshwater, that is, the first event triggering the initiation of sperm motility, may cause the efflux of K^+ through the K^+ channel, since blockers of the K^+ channel such as tetraethylammonium, Ba^{2+} and triphenil tin, suppress K^+ efflux and sperm motility [170, 171]. Hyperpolarization of the plasma membrane induced by K^+ efflux occurs during motility initiation of trout sperm in K^+-free medium [15, 52, 169]. A blocker of the Ca^{2+} channel, verapamil, also inhibits trout sperm motility [41, 170]. The K^+-dependent immotility of sperm can be reversed by the addition of Ca^{2+} [9, 170], implicating the occurrence of Ca^{2+} influx through the Ca^{2+} channel for initiation of motility. Okuno and Morisawa [134] showed that a low concentration of Ca^{2+} of less than $10^{-8.5}$ M is necessary for reactivation of demembranated trout sperm and that 10^{-8} M Ca^{2+} is inhibitory. Furthermore, when the cAMP concentration in the reactivating solution was changed, the concentration of Ca^{2+} for conversion of demenbranated sperm from the motile to the immotile state was not altered, suggesting that the Ca^{2+}-dependent regulating system of flagellar movement is independent of a cAMP-induced initiation mechanism. Boitano and Omoto [16] recently found that the addition of other divalent cations besides Ca^{2+} can activate trout sperm motility in the presence of K^+, suggesting that the effect of Ca^{2+} is not specific. They measured the ability of these divalent cations to hyperpolarize the membrane potential and proposed that membrane hyperpolarization rather than Ca^{2+}

influx is the trigger for the initiation of sperm motility. Short term intrusion of Ca^{2+} has not been detected [170], but, measurements of the fluorescence intensity of Quin-2, Fura-2 or Fluo-3 with a fluorescence spectrometer [16, 171] or by microfluorometry using a highly sensitive video camera [171] suggest the occurrence of increase in intracellular Ca^{2+} concentration on initiation of sperm motility. Possibly membrane hyperpolarization induces increase in intracellular Ca^{2+} from intracellular storage site [16] and the environment of sperm cells, resulting in initiation of sperm motility (Fig. 7) as well as in induction of other systems related to sperm motility.

Demembranated spermatozoa require cAMP for initiation of axonemal movement [108]. Cyclic AMP synthesized by adenylyl cyclase [114], which is known to be activated by increased intracellular Ca^{2+} in mammalian spermatozoa [69], induces activation of cAMP-dependent protein kinase (A-kinase) in the initiation of trout sperm motility [115]. The kinase phosphorylates and activates tyrosine kinase, since phosphorylation of Motility Initiating Phospho-Protein (MIPP) [77], with a molecular weight of 15,000 [112], occurs at tyrosine residue (Fig. 7). Several results suggest the activation of tyrosine kinase by activated A-kinase [63, 115].

MIPP was extracted from the semen of rainbow trout and the testis of chum salmon, and was isolated by affinity chromatographies [63 ,77]. The liver of chum salmon does not contain any phosphoprotein that corresponds to MIPP. Inhibitor of protein kinase, H-9 and a random copolymer of glutamate and tyrosine [63], and tyrosine-specific protein kinase, genistein [77], inhibit phosphorylation of the protein. During the purification procedure, MIPP migrates together with a 38 kDa phosphoprotein and a 45 kDa phosphoprotein, which may be the phosphorylating enzyme of MIPP (Fig. 1). Recent studies by western blotting showed that the 38 kDa and 45 kDa proteins are derived from the 72 kDa phosphoprotein, which may be the enzyme phosphorylating MIPP, e.g., tyrosine kinase (unpublished data).

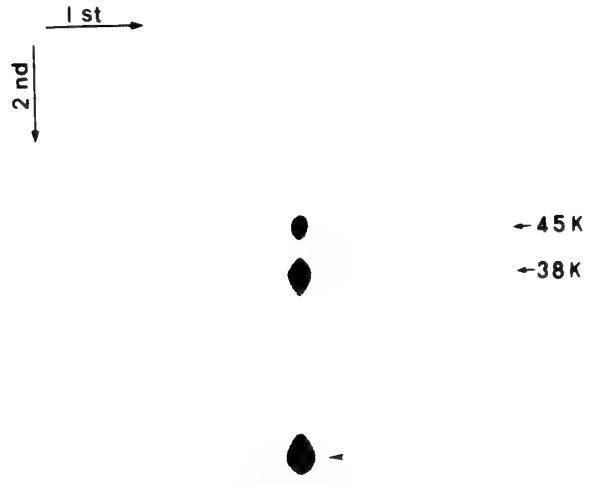

FIG. 1. Evidence for a phosphoprotein complex. The MIPP-complex which includes a 15 kDa motility initiating phosphoprotein (MIPP) and its phosphorylating activity i.e. tyrosine kinase, was purified from salmon sperm flagella using Blue Sepharose CL-613. The fraction from Sepharose was phosphorylated with radioactive ATP, and subjected to non-denaturing electrophoretic fractionation on 5% polyacrylamide gel. The first-dimensional gel was soaked in the sample buffer for SDS-polyacrylamide gel electrophoresis. Then electrophoresis in the second dimension was carried out in 12.5% gel. The autoradiogram is shown. The position of MIPP is indicated by an arrowhead. From Jin *et al.* [77].

Of 64 clones that were positive for a protein complex containing MIPP by ELISA, 11 clones were positive by western blotting assay [78] and three monoclonal antibodies, FMI7, FMI17 and FMI27, inhibited both the initiation of axonemal movement of the demembranated sperm and phosphorylation of MIPP (Fig. 2). Immunofluorescence staining of the demembranated sperm with the three monoclonal antibodies showed that the antigens were located in the basal region of the sperm flagellum (Fig. 3). An iontophoretic technique showed that when Ca^{2+} and cAMP were applied along the flagellar of intact and demembranated sperm, respectively, initiation of flagellar motility occurred when the second messengers were attached to the basal region of the flagellum (Okuno, Morisawa; unpublished data). Our studies by immunohistochemistry and iontophoresis strongly suggest that the cell signaling systems that are involved in the control of flagellar movement are located in the basal region of the flugellum in salmonid fishes (Fig. 7).

B Osmotic shrinkage or swelling of sperm mediating motility controlling systems in freshwater and marine teleosts and amphibians

Spermatozoa of marine teleosts, such as the puffer fish and flounder, and freshwater cyprinid teleosts, such as the carp, goldfish [107, 109, 127], zebrafish [167] and pejerrey [157], and of amphibians, such as toads, frogs [74] and newt [60] are quiescent in solutions with or without electrolytes when the osmolality is isotonic with that of the seminal plasma (almost 300 mOsm kg^{-1}), but become motile when the semen is diluted with a hypotonic solution for freshwater teleosts and amphibians and with a hypertonic solution for marine teleosts. Osmolality also has the same effect on the motility of lamprey sperm [83]. The osmolality-dependent initiation of sperm motility also mimics that in the environment on spawning of these animals in natural conditions.

Conversion of motility to immotility and vice versa, of sperm in freshwater cyprinid teleosts and marine teleosts occurs on changing the external osmolality [167]. As shown in Figure 4A, increase and decrease in osmolality of the environment caused reversible initiation and termination of sperm motility in a marine teleost, the puffer fish. Conversely, decrease and increase in osmolality caused reversible initiation and termination of sperm motility in the freshwater teleost, the zebrafish. Similar changes were observed in sperm of an amphibian, *Xenopus* (Inoda, Morisawa; unpublished data). These results suggest that osmolality reversibly regulates sperm motility. Furthermore, motility of demembranated sperm of freshwater and marine teleosts can be

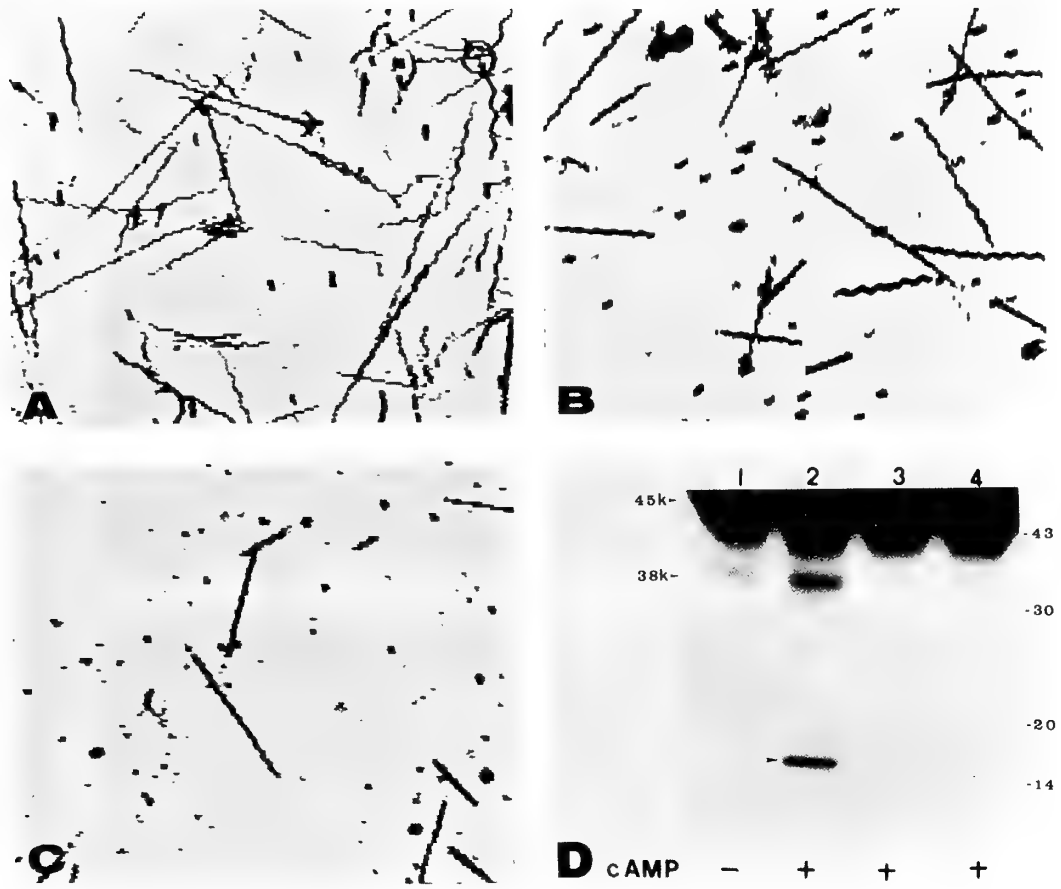

FIG. 2. Inhibition of trout flagallar motility and phosphorylation of the MIPP-complex by monoclonal antibodies to the MIPP-complex. Demembranated spermatozoa of rainbow trout obtained by Triton X-100 extraction were treated with normal mouse serum (A), monoclonal antibody from clone 2E11.2.2 (B) and monoclonal antibody from clone 2E7.1.1 (C), and their motility in reactivating solution containing cAMP and ATP was photographed. The image of tracks of heads which are driven by axonemal movement were observed as lines under a microscope. Motility of sperm in A, B, and C is 70%, 29% and 12%, respectively. For (D), the MIPP-complex partially purified from chum salmon sperm was preincubated with monoclonal antibodies and the cAMP-dependent phosphorylation was monitored by conventional procedures. Lane 1, negative control without cAMP; lane 2, positive control with cAMP; lane 3, after preincubation with clone 2E7.1.1; lane 4, after preincubation with clone 2E11.2.2. No phosphorylation of 15kDa MIPP(arrowhead) or 38 kDa protein was detected in lane 3 and 4. From Jin *et al.* [78]

manipulated repetitively by changing the environmental ion concentration (Fig. 4B). The demembranated sperm of both a marine teleost, the puffer fish and a freshwater teleost, the zebrafish, are immotile in reactivating solution containing 150 mM K^+, which may be equivalent to their intracellular K^+ concentration. Increase and decrease, and decrease and increase in the K^+ concentration of the reactivating solution caused initiation and termination of the motility of demembranated sperm of the puffer fish and zebrafish, respectively. Measurement of the intracellular K^+ concentration $[K^+]_i$ of sperm of a marine teleost, the puffer fish, by the null point analysis with a K^+/H^+ ionophore, nigericine [6], showed that $[K^+]_i$ increased during the initiation of sperm motility at hypertonic osmolality. These findings suggest that increase in osmolality around sperm causes increase in $[K^+]_i$ which affects the flagellar axoneme, resulting in initiation of flagellar motility. In hypertonic solution, puffer fish spermatozoa appear shrunken under a microscope. Moreover, the volume of the sperm pellet is less in hypertonic solution than that in isotonic solution, suggesting that increase in $[K^+]_i$ is due to decrease in cell volume by extrusion of water in hypertonic conditions. In the freshwater teleost, the carp, the cell volume increases in hypertonic conditions [109] and $[K^+]_i$ may possibly decrease.

The change of external osmolality is obviously harmful to cell structures and functions. In general, hypo- or hyperosmolality causes disruption of cells by their swelling or shrinkage. The volume of swollen or shrinken blood cells and bacteria is readjusted by cell signaling systems [57]; decrease in the cell volume in thymic lymphocytes after swelling is accomplished by loss of KCl and water from the cells by Ca^{2+}-activation of ion channels. In sperm of marine invertebrates, however, swelling of the head is observed immediately after immersion in hypotonic seawater and then structures are completely destroyed. Diluted Ringer solution causes spiralling of mammalian sperm tails and loss of

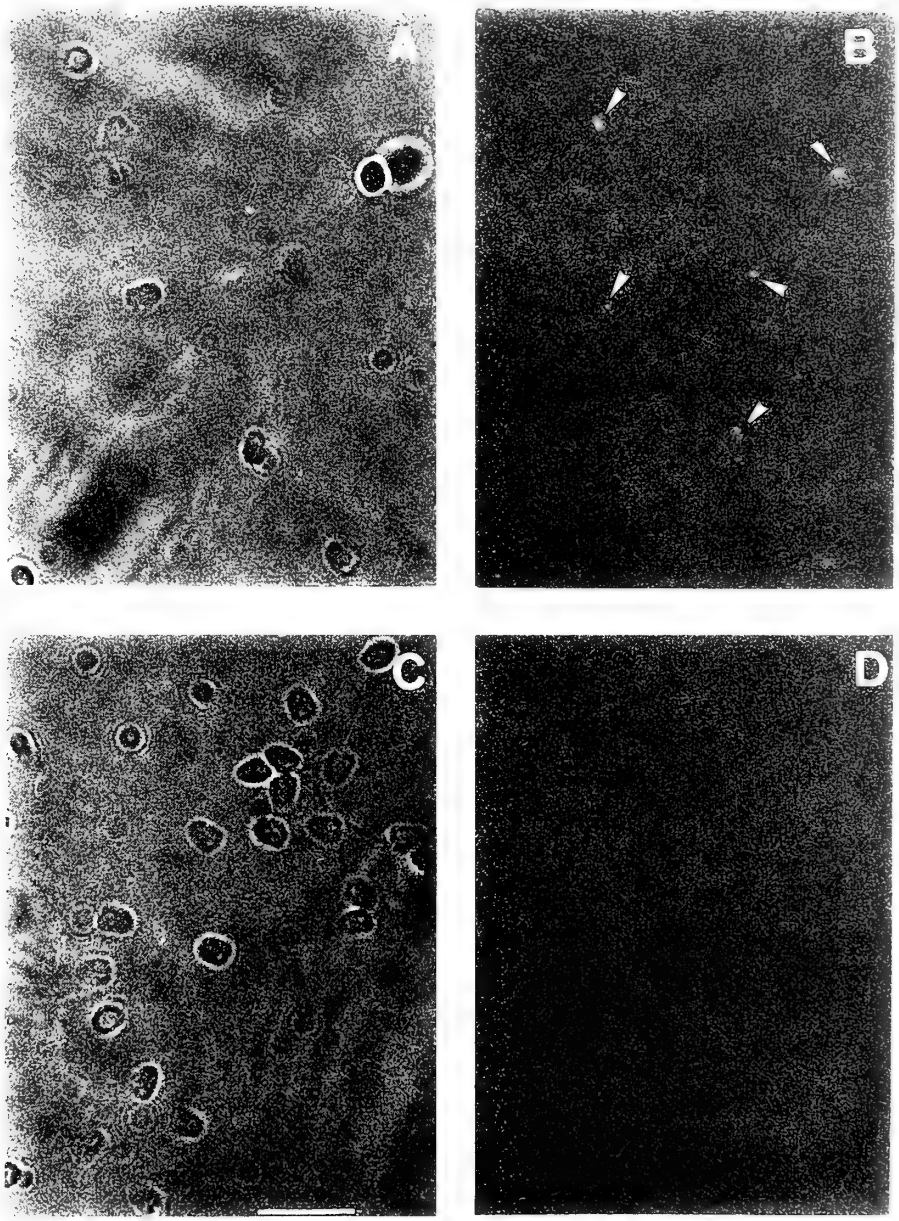

FIG. 3. Evidence for the presence of the MIPP-complex in the basal region of the flagellum. Rainbow trout spermatozoa were attached to the surface of a glass slide and then permeabilized with 0.05% Tween 20. Samples were treated with monoclonal antibody FM17 (A, B) or control mouse gammma globulin (C, D). FITC-labeled horse anti-mouse IgG was used as the secondary antibody. A, C; phase-contrast images. B, D; fluorescence images of the same fields as A, B, respectively. The bar represents 10 μm. FITC fluorescence is detected in the basal region of flagella(white arrowhead) in B. From Jin *et al.* [78].

motility [46, 47]. Swollen or shrunken sperm heads and fragments of tails of sperm of amphibians and marine teleosts were observed in hypo- or hyper-tonic solutions, respectively. Nevertheless, change in external osmolality acts as a trigger for cell signaling systems in sperm. At spawning, mature males and females of fishes come close to each other and release sperm and eggs simultaneously [155]. The duration of sperm motility of teleosts is generally short [107]. Thus, during the short period of approach of sperm to eggs, shrinkage or swelling of sperm cells by change of the environmental osmolality occurs and concomitantly increase or decrease in $[K^+]_i$ occurs (Table 2). The drastic changes of homeostasis in sperm cells may change the mechanochemical properties of the motile apparatus of the flagellum axoneme, resulting in initiation of sperm motility in freshwater and marine teleosts and amphibians.

It is still unknown how increase or decrease in $[K^+]_i$ induces the cascade of events for initiation of sperm motility in freshwater cyprinid and marine teleosts and amphibians, but possible contributions of Ca^{2+} and intracellular pH, $[pH]_i$ have been proposed in marine teleosts [127]. In the two species of puffer fish, *Takifugu niphobles* and *T. pardalis*, a chelating agent, EGTA, had no influence on the osmolality-dependent initiation of sperm motility, suggesting that ex-

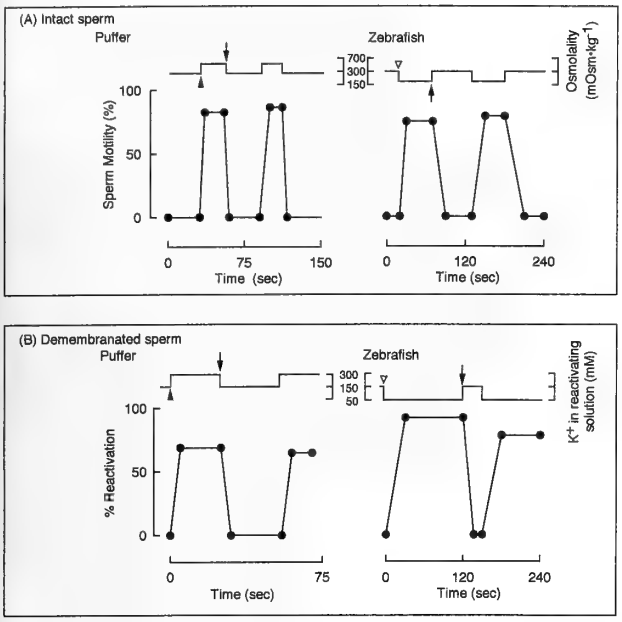

FIG. 4. Repetitive induction of motility in intact and demembranated spermatozoa of a freshwater cyprinid and marine teleost. (A) Spermatozoa of the puffer fish and zebrafish diluted with isotonic 150 mM NaCl solution (300 $mOsmKg^{-1}$) were completely immotile. But when 5 M NaCl was added to puffer fish sperm to increase osmolality (700 $mOsmKg^{-1}$, arrowhead) or Hepes buffer was added to zebrafish sperm to decrease the osmolality (150 $mOsmKg^{-1}$, white arrowhead), the spermatozoa became fully motile. The motility was lost on return of the spermatozoa to solution of isotonic osmolality (arrows). (B) Demembranated sperm of the puffer fish and zebrafish suspended in reactivating solution containing 150 mM K^+ which is equivalent to the $[K^+]_i$ showed no axonemal movement. Upon transfer of the immotile sperm to reactivating solution containing 300 mM high K^+ (puffer fish, arrowhead) or 50 mM low K^+ (zebrafish, white arrowhead), the sperm axoneme became motile. In both case, motility stopped on return to 150 mM K^+ (arrows). Note that the initiation and termination of activity of both intact and demembranated sperm was reversible on changing the external osmolality and K^+ concentration of the reactivating solution. From Takai and Morisawa (original figure).

tracellular Ca^{2+} has no effect on motility initiation. Increase in intracellular Ca^{2+}, $[Ca^{2+}]_i$, on initiation of sperm motility in hypertonic solution was detected by measuring the fluorescence of Quin-2 loaded in sperm as the Quin-2/AM form. The increase occurred in the absence of external Ca^{2+}. In isotonic solution spermatozoa were immotile, however, when Ca^{2+} was introduced into the sperm by treatment with Ca^{2+} ionophore, motility was initiated. Further studies on the role of Ca^{2+} in osmolality-dependent motility initiation are necessary.

Decrease in $[pH]_i$ on initiation of trout sperm motility was reported, but artificial decrease of $[pH]_i$ did not activate motility, suggesting that $[pH]_i$ is independent of motility initiation in salmonid sperm [15, 52, 113]. The possible role of $[pH]_i$ in the initiation of sperm motility was suggested in marine teleosts. Motility of spermatozoa of the flounder, *Kareius bicoloratus*, and the puffer fish, *T. niphobles*, was initiated at isotonic osmolality when $[pH]_i$ was increased by NH_4Cl or $(NH_4)_2SO_4$ [127]. Furthermore, increase and decrease of the pH of reactivating solution caused the initiation and termination of motility in demembranated sperm (data not shown), suggesting that $[pH]_i$ is another factor regulating the intracellular signaling system for the initiation of sperm motility. However, it is still unknown, whether activation of the Na^+/H^+ exchange mechanism by osmotic effects on the plasma membrane of teleost sperm occurs as reported in blood cells [57]. In addition, controversial results of increase or no increase of $[pH]_i$ on osmolality-induced initiation of motility have been obtained using different pH-sensitive fluorescent dyes [127, 167].

III SPERM ACTIVATION AND CHEMOTAXIS INDUCED BY SIGNALS FROM THE EGG

After initiation of sperm motility by the signals of change in the ionic or osmotic environment, the motility is sometimes increased in response to secretions released from the eggs or the female reproductive organs. Sperm chemotaxis toward eggs occurs under the influence of a chemo-attractant released from the egg to complete fertilization. In some cases, such as in the herring and *Ciona*, these secretions may act not only to increase motility and chemotaxis, but also to trigger initiation of motility if this is not initiated by change of the environment upon release from the genital pore.

A Sperm motility initiating and activating peptides in fishes

Teleost spermatozoa have certain advantages for use in studies on sperm-egg interaction at fertilization. They lack an acrosome, and so signal transduction mechanisms in sperm activation and initiation of motility do not overlap acrosome-related events. Sperm activation and chemotaxis occur near the egg micropyle, which is a hole perforated the chorion at the animal pole of the egg through which the sperm move toward the egg, and the plasma membranes of the sperm and egg fuse directly with each other at fertilization.

The motility of spermatozoa of three species of Japanese bitterlings is initiated in fresh water and then the spermatozoa move by rotating toward the micropyle where they accumulate and then disperse. The sperm accumulating substance that is present and diffuses out near the micropyle is a dialyzable substance of low molecular weight that is resistant to heat and alcohol, but destroyed by trypsin treatment [162–165]. A jelly-like flask covering the animal pole of the lamprey egg attracts and aggregates spermatozoa [151]. The spermatozoa move quickly and aggregate in egg water, suggesting that the sperm attracting and aggregating substance is released from the egg, although no studies on its chemical nature and distribution have been reported.

Spermatozoa of the herring, *Clupea palasii*, that are immotile or only slightly motile in diluted seawater or in isotonic solution, start to move actively when they come in contact or nearly in contact with the egg surface [192, 197] or near the egg surface [116]. A few spermatozoa swim active-

ly at the vegetal hemisphere and in regions far from the eggs [116, 192]. The factor for activation of sperm requires Ca^{2+} and is supposed to be a protein [193]. As shown in Figure 5, herring spermatozoa are completely immotile in a solution isotonic to the seminal plasma, but about 20% of the sperm start swimming at a speed of about 170 μm/sec in hypertonic 60–70% seawater. The number of motile sperm and their speed of swimming (about 200 μm/sec) increase when egg seawater is added, suggesting that a sperm activating substance is released from the eggs [116]. This substance was purified from egg water by gel filtration and isoelectric focusing. In this way five different herring sperm-activating peptides (HSAPs) were obtained with isoelectric points of 4.8, 4.9, 5.0, 5.1 and 5.4. The molecular weight of the major peptide (pI=5.1) was found to be 8.1 kDa by mass spectrometry [128].

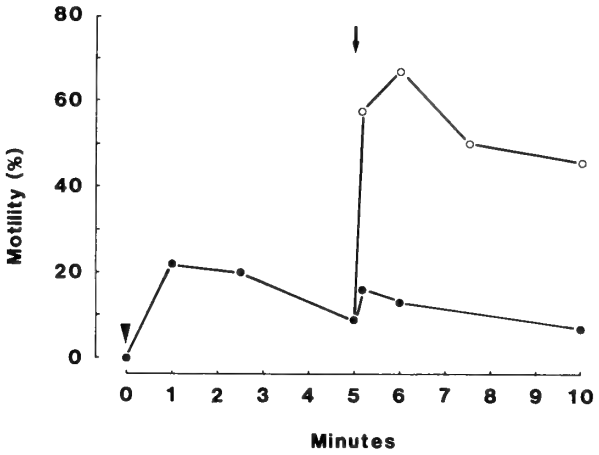

FIG. 5. Initiation and activation of motility of herring sperm. Herring eggs were incubated in seawater for 1 hr at 4°C. The supernatant named egg water, was obtained by low speed centrifugation. Semen was diluted with 80% seawater (arrowhead) and sperm motility was monitored (●). Then egg water (○) or 80% seawater (●) was added (arrow), and monitoring of motility was continued. Motility was initiated in about 20% of the spermatozoa on exposure to seawater. Motility was initiated in almost all spermatozoa by exposure to egg factor. From Morisawa *et al.* [116]

Detailed observations on sperm behavior around the micropyle area of a herring egg were reported by Yanagimachi *et al.* A preparation of spermatozoa in which less than 0.1% were moving in diluted 50% seawater began to move actively as they came in contact with the micropyle area. In this experiment, one egg was placed in 10–12 ml of Ringer solution [197], which may cause the dispersion and dilution of HSAPs released from the egg in the large volume of Ringer solution, and so sperm activation around the egg may not have been detected. In the author's experiment, washing of 70 herring eggs with 6 ml of isotonic 300 mM NaCl solution resulted in depletion of HSAPs activity of the eggs (unpublished data).

The radially arranged grooves located around the egg micropyle of the freshwater cyprinid fish Rosy-barb, *Barbus conchonius*, are reported to guide spermatozoa into the micropyle [1]. The micropyle area of the herring egg chorion possesses a factor which enhances sperm motility and attracts or guides spermatozoa into the micropyle [197]. The activity of the factor is lost on treatment with trypsin or acidic sea water. Pillai *et al.* [139] purified the factor, sperm motility initiating factor (SMIF) from an acid seawater extract of herring eggs and identified it as a glycoprotein with molecular weight of 105 kDa. HSAPs and SMIF may function during approach of herring sperm to the egg at fertilization. After partial initiation of motility by increase in the osmolality around the spawned sperm, HSAPs released from eggs cause further motility initiation and activation of immotile sperm, resulting in fully motile spermatozoa. When the activated sperm come in contact with the micropyle area, SMIF further activates sperm motility and guides sperm into the micropyle (Table 2) to complete the fusion of the plasma membrane of gametes.

B Sperm activation and chemotaxis in hydrozoans and ascidians

The first observation of sperm chemotaxis in animals was that of sperm accumulation near the germinal vesicle of the egg in the hydromedusa, *Spirocodon saltatrix* [42]. Evidence for sperm chemotaxis was accumulated in the Hydroids, *Campanularia, Tubularia, Gonotyrea* and *Clava etc.*, in hydromedusa (for review, see ref. [99]). In siphonophores [23] as well as in a leptomedusae [95], spermatozoa are attracted or agglutinated at a point on the egg surface that is the site of emission of the polar bodies. The diameter of circular trajectories of sperm, progressively decreases near the cupule, the site of sperm attraction and entrance in siphonophores or the tip of pipette containing cupule extract.

Ciona sperm exhibit both typical activation of motility and chemotaxis under the influence of eggs [93, 97]. Our recent studies on the both events in the ascidians *Ciona intestinalis* and *C. savignyi* showed that a sperm-activating and -attracting factor (SAAF) is released from the egg itself (Fig. 6) rather than the follicle cells [93], and that the sperm-activating and -attracting activities of the egg disappear at the time of completion of fertilization [198].

There are conflicting reports with regard to the site of sperm entrance into the egg in ascidians. In *Styela*, the spermatozoon enters near the vegetal pole of the egg [34]; in *Phallucia*, the spermatozoon enters near the animal pole and then is carried to the vegetal pole area by ooplasmic segregation [154]; *Molugla* sperm bind at any site on the egg surface and then are carried to the vegetal pole area [149]. In *Ciona*, spermatozoa are attracted to the vegetal pole of a naked egg suggesting that the attractant is released from the vegetal pole (Fig. 6, see ref. [198]). The sperm-activating and -attracting substance is a dialyzable, heat-stable, probably nonproteinacious small molecule and controls both activation and attraction by different mechanisms [198]).

The second messengers, cAMP and Ca^{2+} have received

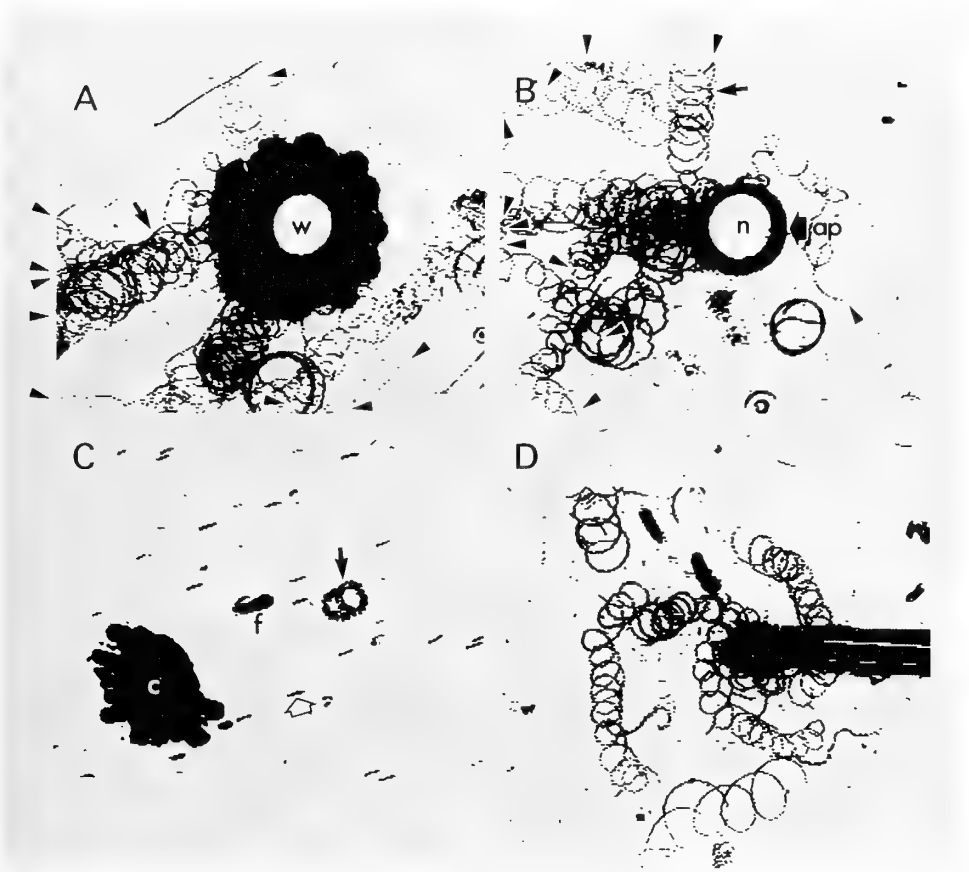

FIG. 6. Sperm activation and attraction activities of *Ciona* eggs and purified sperm-activating and -attracting factor (SAAF). A, B and C: A follicle cell (f), chorion (c), and naked egg (n) were separated from a whole egg (w) and placed in sperm suspension. (A) Sperm are seen around the whole egg. (B) Sperm are seen on the left side of the naked egg. Polar bodies (ap) appeared on the right portion (arrow) suggesting that sperm were attracted toward the vegetal pole of the egg. (C) Sperm are seen to be immotile around the follicle cell and chorion. D: The tip of a capillary containing SAAF inserted into a sperm suspension. The sperm were attracted toward the SAAF moving with circular trajectories. Sperm trajectries are shown as continuous circular lines. Black spots indicate the heads of immotile sperm. Arrowheads show the beginning points of sperm trajectories. From Yoshida *et al.* [198, 199].

considerable attention as regulators of activation and attraction of *Ciona* sperm. The Ca^{2+}-chelator EGTA suppresses sperm motility of *Ciona* and addition of Ca^{2+} results in activation of motility, suggesting the participation of Ca^{2+} in sperm activation [111]. Furthermore, a recent study by Yoshida *et al.* [199] showed that flunarizine, a T-type (transient type) Ca^{2+}-channel selective antagonist, inhibits activation of *Ciona* sperm by SAAF, and that sperm activation does not occur and cAMP is not synthesized in Ca^{2+}-free seawater. The level of cAMP increase concomitantly with the activation of sperm motility in the presence of Ca^{2+}. Thus it is thought that SAAF causes Ca^{2+} influx through T-type Ca^{2+}-channels and synthesis of intracellular cAMP. The cAMP induces motility of the axoneme, the motile apparatus in the flagellum, resulting in activation of *Ciona* spermatozoa (Fig. 7). Activation of axonemal movement by cAMP is known to occur in parallel with cAMP-dependent phosphorylation of proteins including dynein heavy-chain components [19, 135]. Therefore, one pathway regulating sperm motility in *Ciona* occurs along the whole length of the sperm flagellum except for limited portion, although another pathway such as that known in salmonid fishes (Fig. 7) is still possible.

The chemotactic behavior of siphonophore sperm cannot be observed in Ca^{2+}-free seawater and the wave form of sperm flagella is symmetrical in Ca^{2+}-free or low-Ca^{2+} seawater in the presence of sperm attractant or the calcium ionophore A23187 [39]. The wave form becomes asymmetrical when the Ca^{2+} concentration is increased [38], suggesting that the chemoattractant from the cupule might modulate flagellar asymmetry and generate the chemotactic response (Table 2). The requirement of Ca^{2+} for sperm chemotaxis toward the egg was also observed in an ascidian [93]. SAAF, the sperm-attracting and -activating factor of *Ciona*, also requires Ca^{2+} for the modulation of chemotactic behavior of the sperm as well as for induction of activation. However, cAMP, an intracellular factor for activation of *Ciona* sperm, is independent of sperm chemotaxis, because increase in cAMP by treatment of sperm with teophilline, a phosphodiesterase inhibitor did not induce chemotaxis [199]. Chemotaxis of *Ciona* sperm does not occur in Ca^{2+}-free seawater in the presence of SAAF, but spermatozoa are attracted toward the tip of a capillary containing SAAF by

TABLE 1. Properties of sperm chemoattractants in marine invertebrates

	MW range (kDa)	Heat Stability	Protease Sensitivity	Species-specificity	Ref.
Hydrozoans					
Anthomedusae	5–14	+	?	+	92, 96
(Sessile)	<1	+	+	−	92, 96
Limunomedusae	>5	+	?	+	92, 96
Leptomedusae	<1	+	?	+	92, 97
Siphonophore	20–25	+	+	+	23, 40
Coral	<0.5	(lipid like substance)		+	32, 33
Mollusca					
Chiton	?	?	?	−	94
Echinoderms					
sea urchin	1–2	+	+	+	160, 187
starfish	10–12	+	+	+, −	140
brittle star	?	?	?	+	98
sea cucumber	?	?	?	−, +	98
Chordata					
Ciona	<12–14	+	−	−	99, 199

progressive decrease in the diameter of the sperm track with proximity to the attractant source (Fig. 6). Generally, symmetry of the flagellar wave form generates a linear sperm trajectory, whereas flagellar asymmetry generates narrow and circular trajectories. A high Ca^{2+} concentration causes asymmetrical waves in demembranated sea urchin spermatozoa [18, 22]. From the data on Ca^{2+} control of flagellar asymmetry in siphonophore sperm chemotaxis, Cosson *et al.* [37] proposed the following hypothetical model for the generation of chemotaxis: "When spermatozoa swim close to a gradient of attractant, binding of a few attractant molecules to the sperm cells induces a transient calcium influx which, in turn, increases flagellar asymmetry and narrows the sperm trajectory". In *Ciona*, the motility of intact sperm is suppressed by Ca^{2+} channel antagonists in the presence of SAAF. Thus Ca^{2+} influx through Ca^{2+} channels by the action of SAAF may increase the asymmetrical beating of the axoneme resulting in the induction of chemotactic behavior of spermatozoa (Fig. 7).

In animals, the chemical nature of sperm attractant is considered to be a peptide or protein with a molecular weight varying from 1 to 2 kDa [158] in the sea urchin to 20–25 kDa in siphonophores [40]. Sperm chemotaxis is highly species-specific, whereas the sperm chemoattractants from three *Tubularia*, coral and chiton have no species specificity. In *Ciona intestinalis* and *C. savignyi*, the egg of each species can activate and attract the sperm of both species, suggesting no species specificities in SAAF of *Ciona* (Table 1). SAAF is a dialyzable, small molecular weight compound of less than 12–14 kDa that is heat-stable and resistant to proteases such as trypsin, thermolysin, and pronase E, suggesting that it may not be a protein. Recently, coral sperm chemoattractant was also proposed to be a low molecular weight nonproteinacious substance [32, 33]. During purification of SAAF by column chromatographies, the sperm-activating and -attracting activities are always co-eluted (unpublished data). Furthermore, spermatozoa exhibit "turn", which is an index of chemotactic behavior of sperm, near the purified SAAF. Thus it seems that one kind of molecule (SAAF) mediates two different pathways: Ca^{2+}- and cAMP-dependent sperm activation, and sperm attraction which is regulated by Ca^{2+} alone.

IV INITIATION AND ACTIVATION OF SPERM MOTILITY AND SPERM CHEMOTAXIS IN OTHER ANIMALS

A Sea urchins and other invertebrates

In sea urchin, alkalization of the inside of sperm cells by efflux of CO_2, a volatile inhibitor of sperm motility [79] at spawning and efflux of H^+ by Na^+/H^+ antiport [125] induce activation of dynein ATPase, resulting in the initiation of sperm motility [26]. Concomitantly with energy consumption after the initiation of sperm motility, ATP is supplied through the phosphorylcreatine shuttle [178] to confer the sperm with full motility (Fig. 7). Increase of $[pH]_i$ by a factor released from egg jelly also induces activation of respiration and motility of sea urchin sperm.

The first evidence for sperm activation in invertebrates was the observation of increase in sperm motility of the annelid *Nereis* and the sea urchin, *Arbacia* in egg seawater containing secretions of eggs [86], but demonstration of a sperm activating substance in egg jelly was established by the studies of Ohtake [129, 130]. Sperm activating peptides with a sequence of 10 amino acids were purified from the egg jelly of the sea urchin, *Hemicentrotus pulcherrimus* [159] and *Strongylocentrotus purpuratus* [51, 58] and named as speract. Numerous peptides such as resact in Arbacia punctulata [160] and mosact in *Clypeaster japonicus* [161] *etc.* were subsequently purified, and their amino acid sequences were deter-

mined. They are given a systematic nomenclature based on the taxonomic order of the species by Suzuki [158]; SAP-I in the order Echinoida; SAP-II in the order Arbacioida; SAP-III in the order Clypeasteroida, and SAP-IV in the Diadematoida.

Extensive studies on signal transduction occurring in activation and sperm chemotaxis in sea urchin sperm have been conducted by Garbers and his colleagues (Fig. 7). Receptors for speract and resact which are located in the plasma membrane of sperm were identified and characterized as acidic glycoproteins with molecular weights of 77 kDa and 160 kDa, respectively [11, 43, 44, 152]. A 160 kDa protein from *A. punctulata* was identified as guanylyl cyclase [152]. Guanylyl cyclase is considered to be associated with the receptor of speract [152, 177] since a large amount of the enzyme is present in *S. purpuratus* testis [177] and is activated by speract [14]. Guanylyl cyclase itself is the receptor for atrial natriaretic peptide (ANP) [168] which has the physiological effects of causing natriuresis, diuresis, *etc.* The receptors of both ANP and resact are proteins penetrating the plasma membrane. The amino acid sequences of the receptors for resact and ANP have similarity in their intracellular portions, but little in their extracellular portions [25]. The fact that the receptors of sperm activating peptides act as receptors for ANP in mammalian tissue, indicates that similar cell signaling mechanisms have different physiological functions in different tissues or organs throughout the animal kingdom.

Upon exposure to speract or resact, guanylyl cyclase in sperm is stimulated and the cGMP level increases [12, 50, 142]. Guanylyl cyclase is predominantly in a high molecular weight and phosphorylated active form, and is converted to a low molecular weight, dephosphorylated form with low activity on exposure to speract and resact [13, 143, 188]. The peptides also induce phosphorylation of membrane proteins in the presence of GTP [14]. From these findings, it is possible that binding of the peptides to the receptor which is located close to guanylyl cyclase causes elevation of cGMP level, resulting in phosphorylation of proteins. The guanylyl cyclase becomes a dephosphorylated inactive form.

Speract and monesine, an ionophore capable of causing Na^+/H^+ exchange, induce both Na^+/H^+ exchange and activation of spermatozoa [59, 144]. The activation of the Na^+/H^+ exchange by speract occurs through hyperpolarization of the plasma membrane caused by K^+ efflux [85]. It is also suggested that Ca^{2+} influx occurs through activation of Na^+/H^+ exchange by speract [150]. Recently, Cook and Babcock proposed that cGMP activates a K^+ channel with the resulting cascade of hyperpolarization of the plasma membrane, activation of Na^+/H^+ exchange and increase in $[pH]_i$. The alkalization causes activation of adenylyl cyclase and elevation of cAMP which induces Ca^{2+} influx through activation of the Ca^{2+}-channel [35, 36]. Ca^{2+} and phosphorylation of protein cause downstream events for initiation and activation of sperm motility (Fig. 7). Recently, receptors for sperm activating peptides were also identified in Japanese sea urchins, *Hemicentrotus pulcherrimus, Clipeaster japonicus, etc.* [61, 200] and the roles of membrane hyperpolarization, Ca^{2+} and $[pH]_i$ in sperm functions [62, 66] were investigated in the species.

Ca^{2+} requirement for sperm chemotaxis in hydrozoans and ascidians has been discussed in Chapter III B. Activity as a chemoattractant has been reported only for resact among the egg peptides of sea urchins [187]. Speract has no chemotactic activity. Extracellular Ca^{2+} is required for this activity. In the case of resact-induced chemotaxis, the track diameter of sperm trajectories increases and the sperm swim in straighter trajectories, somewhat different from the sperm chemotaxis reported in siphonophores [39] and *Ciona* [198]. In addition to functioning in sperm activation and chemotaxis, speract can potentiate the effect of a high molecular weight acrosome reaction inducing substance from egg jelly through increase in the cAMP level [191]. Both paths of cell signaling mechanism, i.e. cGMP-dependent protein phosphorylation and increase in $[pH]_i$ and $[Ca^{2+}]_i$ finally cause activation of sperm, such as increase in respiration and motility, chemotaxis and induction of the acrosome reaction (Fig. 7).

Cyclic AMP-dependent phosphorylation plays a key role in the activation of sperm motility in the sea urchin [20, 76] and starfish [76]. According to Ishiguro *et al.*, a fraction obtained from a Triton X-100 extract of sea urchin or starfish sperm, contains cAMP-dependent protein kinase and a protein factor associated with the enzyme. The phosphorylated form of the protein factor is a prerequisite for reactivation of demembranated sperm, suggesting the requirement of phosphoprotein for the initiation and activation of sperm motility [76]. Gibbons and Gibbons [54] reported that addition of cAMP has no effect on motility of the demembranated sperm. Cyclic AMP sometimes does not affect demembranated sperm prepared by Triton X-100 treatment from very fresh sea urchin spermatozoa. However, preincubation of sperm at room temperature made them susceptible to cAMP-dependent reactivation, indicating that dephosphorylation occurs during demembranation of sperm, which leads to their quiescence [76]. Phosphorylation of proteins by the cAMP system may have an important role in regulation of axonemal movement in echinoderms.

An extensive cascade system for the sperm functions was demonstrated in silkworm, *Bonbyx mori* by Osanai and his colleagues (Table 2). During the process from formation of spermatozoa to fertilization; (a) spermatogenesis in the testis, (b) transfer of two types of spermatozoa, apyrene and eupyrene spermatozoa, to the vesicula seminalis and their storage in it, (c) ejaculation from male glands into the busa copulatrix of a female to form the spermatophore, (d) disappearance of apyrene spermatozoa, and completion of fertilization, "initiatorine" a specific endopeptidase acts as the trigger for sperm maturation and initiation of arginine degradation cascade for an energy-yielding [136]. Apyrene spermatozoa require the initiatorine and a cyclic nucleotide, cAMP or cGMP for activation of flagellar movement [137],

suggesting that second messenger-dependent cell signaling mechanisms and enhancement of energy metabolism have key role for the regulation of sperm function in insect.

B Mammals and chickens

Control of the motility of mammalian spermatozoa occurs at two critical stages. One is at ejaculation; when motility is initiated for the first time in the life span of the sperm. The other control occurs when the sperm reach the upper portion of the female reproductive tract; where sperm motility is stimulated, or "hyperactivated", and sperm become sensitized to stimuli for inducing the acrosome reaction through the process of capacitation which enables them to penetrate the zona pellucida surrounding the egg.

In marine invertebrates such as the sea urchin, and in teleosts, such as the trout, puffer fish, and zebrafish, spermatozoa are completely quiescent in undiluted semen. However, the degree of motility of mammalian sperm in undiluted semen varies with the species. Samples from the distal part of the cauda epididymis contain many motile sperm [123] in the rabbit (25%), bull (35%) and especially man (60%). Sperm with low motility have also been found in this region [123] in the rat (2%), mouse (1%) and hamster (1%). It is uncertain whether the observed motility represents the true *in situ* motility within the epididymis. Motility is initiated in a considerable proportion of the spermatozoa on mixing with the seminal plasma flushed from the accessory glands and ejaculated into the female reproductive tract.

Nevo [124] showed that CO_2 completely inhibited the motility of bull sperm, suggesting that an anaerobic CO_2-rich condition in the male reproductive tract suppresses sperm motility before ejaculation (Table 2). Cascieri *et al.* [24] found that bull sperm are already partially motile before dilution and suggested that reduction of mechanical restraint through dilution is a factor for initiation of sperm motility. Storey [156] reported that some motile sperm can be obtained from the epididymis of the rabbit, and suggested that initiation of sperm motility at ejaculation is caused by both release from physical restraint and access to oxygen. The motility of rat sperm is suppressed by the restraint of a mucin-like glycoprotein, named immobilin present in epididymal fluid, and release from the restraint at ejaculation is proposed to be a factor for motility initiation [183]. Glycerylphosphocholine [181], carnitine [65], and a proteinaceous factor [182] have also been proposed as factors for restrain of rat sperm.

Stimulatory effects of Ca^{2+} (e.g. [120]) and effect of cyclic nucleotides (e.g. [75, 101, 122, 153, 186]) on the motility of many mammalian spermatozoa have been reported. The cyclic AMP level is low in immotile sperm but rapidly increases on initiation of motility. Furthermore, demembranated mammalian sperm show initiation of motility in the presence of cAMP in reactivating solution [75, 87, 101, 190]. There may be several pathways and following system for induction of sperm motility is possible. The epididymal fluid contains phosphodiesterase and a little Ca^{2+}, thus spermatozoa are immotile or slightly motile in the epididymis where they have a low intracellular cAMP content and low external Ca^{2+} level. In some mammalian species whose seminal plasma has a high Ca^{2+} content [123, 173], spermatozoa become motile on supplementation of Ca^{2+} from the seminal plasma at ejaculation, which causes rapid cAMP synthesis to induce motility.

A stimulatory effect of sodium bicarbonate on porcine spermatozoa in the seminal plasma has also been noted. A low molecular weight sperm motility activating factor, which increases cAMP by activation of adenylyl cyclase, was found in the porcine seminal plasma [131] and was identified as $NaHCO_3$ by Okamura *et al.* [132]. $NaHCO_3$ activates adenylyl cyclase, motility, and respiration in the sperm of many mammalian species such as porcine, bovine, rat, mouse, dog and human sperm [132, 153]. Anion channel blockers enhance the accumulation of endogeneous HCO_3^-, and sperm are activated by inhibition of the efflux of HCO_3^- derived from CO_2, suggesting that intracellular HCO_3^- stimulates adenylyl cyclase [166]. The roles of proteases in the regulation of sperm motility have been studied extensively by Gagnon [49], and Inaba and his colleagues recently focused attention on the relation of proteasomes to sperm motility [70–73]. A trypsin-like proteinase which binds to the plasma membrane of epididymal sperm and inhibits adenylyl cyclase, and a proteinase inhibitor in the seminal plasma were recently reported by Okamura *et al.* [133]. They proposed cascade system for initiation of mammalian sperm motility: namely, suppression of proteinase activity by the seminal proteinase inhibitor at ejaculation causes activation of HCO_3^--stimulated adenylyl cyclase, resulting in the rapid synthesis of cAMP, a second messenger that proceeds the further cascade mechanism of sperm motility initiation (Fig. 7). Bovine sperm, in contrast, contain a trypsin-like protease that activates adenylyl cyclase [80].

Changes in external ionic conditions such as in Ca^{2+} and HCO_3^- level and subsequent elevation of the cAMP level appears to be a major signal pathway in the triggering system for initiation of motility in mammalian sperm (see above) as well as other species such as teleosts, tunicates and sea urchins (see Chapter II and Chapter III A). Increase in $[pH]_i$ is also a factor regulating mammalian sperm motility [7, 8]. A type II regulatory subunit of cAMP-dependent protein kinase (RII) [126], with a molecular weight of 55–56 kDa [17], is the target of phosphorylation mediated by cAMP. The 56 kDa phosphoprotein, i.e. RII in mammalian sperm, was named axokinin [174]. Calmodulin, on the other hand, is known to be a mediator of signal transduction in calcium-regulated flagellar motility through protein phosphatase activity [173]. The facts that the sperm RII related to the calmodulin-dependent protein phosphatase is present in mammalian sperm [175], and that RII and the protein phosphatase are associated with dynein ATPase activity [172], suggest that both cAMP-dependent phosphorylation and Ca^{2+}-calmodulin-dependent dephosphorylation pathways regulate the ATP-induced sliding of the microtubule and control the process of initiation of mammalian sperm motility (Fig.

TABLE 2. Factors for regulation of sperm motility in animals

Specie	Motility	External signal	Membrane response	Internal factor	Ref.
Siphonophore	chemotaxis	peptide	Ca^{2+} channel	Ca^{2+}	39
Horseshoe crab	initiation & activation	peptide Zn removal			27–29, 31, 180
Silkworm	activation	endopeptidase		energy yielding, cAMP, cGMP	136, 137
Sea urchins*	initiation activation chemotaxis	CO_2, Zn addition speract etc resact	Na^+/H^+ exchange ANP-receptor hyperpolarization	pH cGMP, cAMP Ca^{2+}	30, 79 45 45
Starfish	initiation chemotaxis	Zn removal peptide			102 140
Ciona*	initiation activation chemotaxis	SAAF SAAF SAAF	Ca^{2+}-channel Ca^{2+}-channel Ca^{2+}-channel	Ca^{2+}, cAMP Ca^{2+}, cAMP Ca^{2+}	111 198, 199 198, 199
Herring	initiation & activation chemotaxis	osmolality, HSAPs HSAPs SMIF SMIF			116, 128, 139 139
Salmonids*	initiation	K^+	hyperpolarization	Ca^{2+}, cAMP	78, 104, 107
FW teleosts SW teleosts Amphibians	initiation initiation initiation	osmolality osmolality osmolality	cell swelling cell shrinkage	K^+ decrease K^+ increase	107, 167 107, 127, 167 60, 74
Chicken	initiation	temperature	temperature pass Ca^{2+} influx	temp effect phosphoprotein	2–5
Mammals*	initiation hyperactivation chemotaxis	HCO^-_3, Ca^{2+}, CO_2 peptide	protease activity	Ca^{2+}, cAMP, pH Ca^{2+}, cAMP, pH	36, 131–133, 172, 189, 194 141, 201

* see detail; Fig. 7

7).

Hyperactivated motility of spermatozoa (hyperactivation) in mammals is a distinct, vigorous motility [194, 195] exhibiting high amplitude, crawling, serpentine, whiplash and frenzied or contorted flagellar movements, and is considered to play a significant role in fertilization. There are many reports on hyperactivated patterns of sperm flagella and their roles in fertilization, and there is some evidence for the contribution of a cell signaling system to the induction of hyperactivation (Table 2). Cyclic AMP synthesis in hamster sperm is enhanced when the sperm are incubated in a medium causing hyperactivation [121, 189]. The demembranated sperm exhibit hyperactivated motility in the presence of cAMP [101]. Ca^{2+} is related to the phenomenon [88, 138]. Probably calcium influx and a Ca^{2+}-calmodulin system are involved in hyperactivation of mammalian sperm [189, 196], but these possibilities have not yet been demonstrated conclusively.

N-Formylmethionyl peptides, which are chemoattractants for neutrophils and macrophages have a chemotactic effect on human spermatozoa [55]. Recent studies showed that human spermatozoa accumulate in follicular fluid *in vitro* [141] and that atrial natriaretic peptide, a known activator of particulate guanylyl cyclase, induces activation and attraction of spermatozoa [201].

Chicken sperm are unique in showing a response to temperature [2]. They are immotile at a body temperature of 40–41°C, but become motile on decrease in temperature to 30–35°C. The motility of demembranated chiken sperm also exhibit the same response to change of temperature, i.e. immotile and motile at a high and low temperature, respectively, suggesting that temperature change directly affects the flagellar motile apparatus, the axoneme to regulate sperm motility. Decrease in the intracellular Ca^{2+} level at 40°C immobilizes sperm and the subsequent addition of Ca^{2+} at 40°C causes initiation of sperm motility [176]. However, such effects of Ca^{2+} are not observed with demembranated sperm [3], suggesting that Ca^{2+} may not have a direct effect on the axoneme but that its effect is mediated by soluble substances that are removed in the demembranation procedure. Cyclic AMP also does not affect the motility of demembranated sperm [2], but a recent study suggested that cAMP-independent phosphorylation of a 43 kDa protein is necessary for induction of motility of chiken sperm at low temperature [4]. These results suggest that temperature controls the motility by at least two pathways: by a direct action on the motile apparatus, the axoneme, and by an indirect action through the change in $[Ca^{2+}]_i$ and the protein phosphorylation process (Table 2). The contribution of type 1 protein phosphatase to the initiation of chicken sperm motility was recently demonstrated [5].

C Roles of zinc in regulation of sperm motility

Zinc apparently contributes to the activation of respiration and motility in marine invertebrates such as the sea urchin, starfish and horseshoe crab and in mammals (Table 2). The motility of sea urchin sperm is not increased by addition of zinc or copper but is reduced by metal-chelating agents such as EDTA and amino acids [146]. Clapper *et al.* [30] reported that metal chelators and SH reagents cause removal of zinc from sperm, a delay in motility initiation, and a decrease of $[pH]_i$. Zinc is absorbed and the motility and

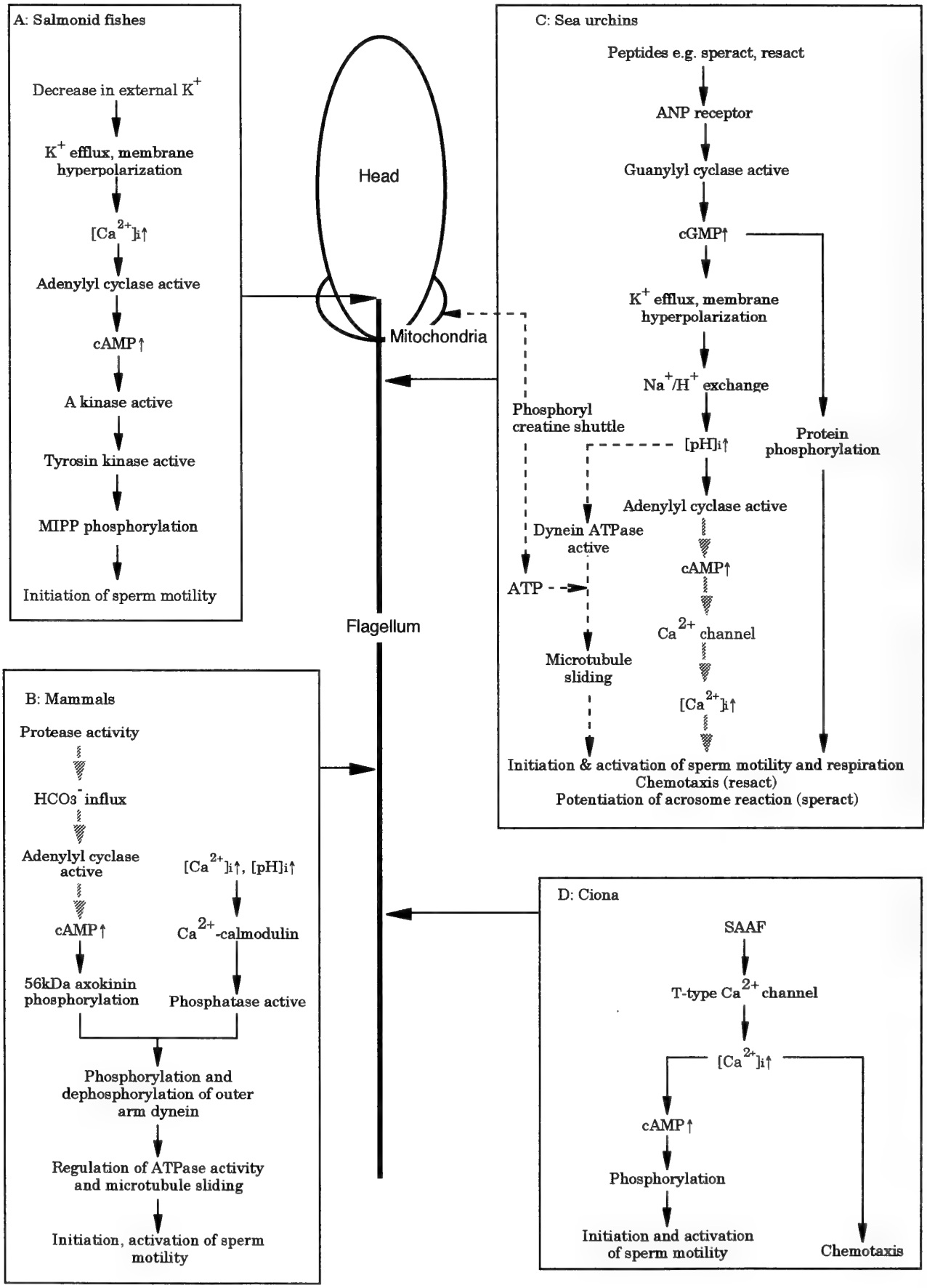
A: Salmonid fishes
Decrease in external K+
K+ efflux, membrane hyperpolarization
[Ca2+]i↑
Adenylyl cyclase active
cAMP↑
A kinase active
Tyrosin kinase active
MIPP phosphorylation
Initiation of sperm motility
Head
Mitochondria
Flagellum
C: Sea urchins
Peptides e.g. speract, resact
ANP receptor
Guanylyl cyclase active
cGMP↑
K+ efflux, membrane hyperpolarization
Na+/H+ exchange
[pH]i↑
Phosphoryl creatine shuttle
Protein phosphorylation
Adenylyl cyclase active
Dynein ATPase active
cAMP↑
ATP
Ca2+ channel
Microtubule sliding
[Ca2+]i↑
Initiation & activation of sperm motility and respiration
Chemotaxis (resact)
Potentiation of acrosome reaction (speract)
B: Mammals
Protease activity
HCO3- influx
Adenylyl cyclase active
[Ca2+]i↑, [pH]i↑
cAMP↑
Ca2+-calmodulin
56kDa axokinin phosphorylation
Phosphatase active
Phosphorylation and dephosphorylation of outer arm dynein
Regulation of ATPase activity and microtubule sliding
Initiation, activation of sperm motility
D: Ciona
SAAF
T-type Ca2+ channel
[Ca2+]i↑
cAMP↑
Phosphorylation
Initiation and activation of sperm motility
Chemotaxis

$[pH]_i$ recover on subsequent addition of zinc, suggesting that the increase of $[pH]_i$ resulting from exposure of sperm to zinc in sea water, is a possible cause of initiation of motility of sea urchin sperm. In contrast, the respiration and motility of starfish sperm are increased by chelators which reduced the level of zinc [102, 184]. Starfish spermatozoa initially contain zinc, but release it into the surrounding seawater, upon dilution and motility activation [100], suggesting that this release of zinc causes initiation of sperm motility. The concentrations of heavy metals in sea urchin sperm have been measured [105] and the effect of zinc on microtubule proteins [106], for example conformational changes of flagellar protein [103] and tubulin assembly [67], and sheet polymer formation [81, 84] have been studied.

In the horseshoe crab, *Limulus polyphemus*, spermatozoa are immotile upon dilution in seawater and become motile on release of a peptide from the eggs [27, 29]. Mobilization of intracellular Ca^{2+} and an increase in the cAMP level have been correlated with initiation of motility by a crude egg extract of the horseshoe crab as well as the starfish [180]. Trace metals and divalent cations are also involved in the regulating sperm motility of the horseshoe crab [28, 31]. Zinc is absorbed by the sperm from the surrounding medium and inhibits their motility, whereas removal of zinc from the sperm by treatment with a chelating agent causes initiation of sperm motility [31].

There are several reports that the semen or spermatozoa of mammals such as dogs, humans and rats, contain a high concentration of zinc (see [89, 148]). Zinc is closely associated with sulfhydryl groups and disulfide linkages and is concentrated in the sperm tail [64]. Sperm contain heavy metals [48, 90, 148], and their removal from the sperm with a chelating agent [148] enhances or inhibits sperm motility [82, 91, 145, 147] as well as in marine invertebrates (see above). Thus zinc may be necessary for regulation of sperm motility in various phyla, from invertebrates to vertebrates.

V CONCLUSIONS

Drastic change in the motility state occurs in the life history of spermatozoa. During transit of sperm from the testis to the epididymis or vas deferens, spermatozoa generally acquire the potential for motility [117, 179], although there are some exceptions [10], and cAMP, Ca^{2+} and pH are known to be important regulators of the process [68, 118, 119]. The subject of "acquisition of sperm motility" was not included in this review.

Even though spermatozoa have capacity to move, their motility is more or less suppressed in the epididymis or vas deferens by factors present in the fluid part of the semen. Assuming that the motility observed in the undiluted sperm samples represents that within a male reproductive organ, such as the epididymis or sperm duct, spermatozoa are completely quiescent in sea urchins [56] and teleosts [107], whereas the spermatozoa in some species, especially some mammals, are motile to a certain degree [123]. On spawning into an aquatic environment in species with external fertilization or at ejaculation into the female reproductive tract after mixing with the seminal plasma in species with internal fertilization, sperm change from an immotile or slightly motile state to a fully motile state, named "initiation of sperm motility". Then their motility is activated, "activation of sperm motility", and they are attracted toward eggs, "sperm chemotaxis".

The cell signaling systems underlying these changes in motility are various. However, the external signals for initiation of sperm motility on spawning and ejaculation are basically changes in the environment of inorganic components such as CO_2, ions including Ca^{2+} and zinc or in non-chemical stimuli, such as osmolality and temperature. Activation and chemotaxis, in contrast, are caused by exposure to organic compounds, mainly peptides or proteins released from the female. The spermatozoa of *Ciona* and the herring, remain quiescent or only slight motile for a while after spawning. In such cases, initiation and activation of sperm motility may be induced simultaneously on stimulation by an organic substance from the female. In both species as well as in *Arbacia punctulata*, one substance, such as SAAF, HSAPs or resact may have the ability to induce plural phenomena. For instance, SAAF from *Ciona* eggs causes initiation, activation, and chemotaxis of sperm spawned in seawater.

Internal cascade systems for sperm motility are triggered by several factors, mainly second messengers, such as cyclic nucleotides and Ca^{2+}, and seem to converge upon the phosphorylation and dephosphorylation of proteins through several kinds of protein kinases and phosphatases which would be related to axonemal movement. The phosphorylation of protein for initiation of motility was found to occur at two different sites. Cyclic AMP-dependent phosphorylation of motility initiating phosphoprotein (MIPP) in salmonid fishes is suggested to occur in the basal portion of the flagellum, possibly the centriolar region, whereas both cAMP-dependent phosphorylation of axokinin and calmodulin-dependent dephosphorylation of dynein ATPase appear to occur all along the whole length of the axoneme and to modulate sliding of microtubules in mammalian spermatozoa (Fig. 7). The molecular mechanism indispensable for the control of flagellar motility has generally been thought to be distributed along the axoneme. In a recent review, however Brokaw discusses the special function of the basal end of the flagellum [21]. In initiation of chicken sperm motility, the

FIG. 7. Proposed cell signaling mechanisms underlying the initiation and activation of sperm motility, and chemotaxis in the sea urchin, *Ciona*, salmonid fishes and mammals. A: from Morisawa M. (this review). B: from Okamura *et al.*(shaded line, [133]); Tash JS (black line, [172]). C: from Domino SE and Garbers DL(black line, [45]); Cook SP and Babcock DF (shaded line, [36]); Tombes RM and Shapiro BM (dotted line, [178]). D: From Yoshida *et al.* [199]

external temperature directly affects the axoneme and Ca^{2+} controlling the functions of other systems in soluble components, suggesting the presence of two systems for motility initiation in different portions of the sperm cell.

The facts that chemoattractants have been shown to modify the flagellar asymmetry in a Ca^{2+}-dependent manner in siphonophores [39] and in *Ciona* [199], suggest a role of the attractants in regulation of $[Ca^{2+}]_i$. However, the target of Ca^{2+} has not been identified. For initiation and activation of sperm motility, the main cell signaling pathway is cyclic nucleotide-dependent, whereas the chemotactic behavior of sperm may be modulated by Ca^{2+} rather than cAMP.

Efforts to identify the molecular mechanisms of cell signaling for the regulation of sperm motility should contribute to our understanding of general mechanisms of cell signaling in cells.

ACKNOWLEDGMENTS

I thank my colleagues Drs. Hiroshi Hayashi, Sachiko Morisawa, Makoto Okuno, Katsumi Ishida, Hideki Ohtake, Ken-ichi Manaka, Satomi Tanimoto and Zong Xuan Jin, and the graduate students of Misaki Marine Biological Station, Syoji Oda, Hiroyuki Takai and Manabu Yoshida whose findings have been discussed in this review. I am also indebted to Dr. Hideo Mohri, Professor Emeritus of the University of Tokyo for his encouragement. This work was supported by Grants-in-Aid from the Ministry of Education, Science and Culture of Japan.

REFERENCES

1 Amanze D, Iyengar A (1990) Development 109: 495–500
2 Ashizawa K, Suzuki Y, Okauchi K (1989) J Reprod Fert 86: 263–270
3 Ashizawa K, Maeda S, Okauchi K (1989) J Reprod Fert 86: 271–276
4 Ashizawa K, Katayama S, Tsuzuki Y (1992) Biochem Biophys Res Commun 185: 740–745
5 Ashizawa K, Wishart GJ, Tomonaga H, Nishinakama K, Tsuzuki Y (1994) FEBS Letters 350: 130–134
6 Babcock DF (1983) J Biol Chem 258: 6380–6389
7 Babcock DF, Rufo GA, Lardy HA (1983) Proc Natl Acad Sci USA 80: 1327–1331
8 Babcock DF, Pfeiffer DR (1987) J Biol Chem 262: 15041–15047
9 Baynes SM, Scott AP, Damson AP (1981) J Fish Biol 19: 259–267
10 Bedford JM (1979) In "The Spermatozoon" Ed by DW, Fawcett, JM Bedford Urban and Schwarzenberg, Baltmore-Munich, pp 7–21
11 Bentley JK, Shimomura H, Garbers DL (1986) Cell 45: 281–288
12 Bentley JK, Tubb DJ, Garbers DL (1986) J Biol Chem 261: 14859–14862
13 Bentley JK, Garbers DL (1986) Biol Reprod 35: 1249–1259
14 Bentley JK, Khatra AS, Garbers DL (1987) J Biol Chem 262:15708–15713
15 Boitano S, Omoto CK (1991) J Cell Sci 98: 343–349
16 Boitano S, Omoto CK (1992) Cell Motil Cytoskelt 21: 74–82
17 Brandt H, Hoskins DD (1980) J Biol Chem 255: 982–987
18 Brokaw CJ (1979) J Cell Biol 82: 401–411
19 Brokaw CJ (1982) Cell Motil 1: 185–189
20 Brokaw CJ (1984) Ann NY Acad Sci 438: 132–141
21 Brokaw CJ (1994) Cell Motil Cytoskelt 28: 199–204
22 Brokaw CJ, Josslin R, Bobrow L (1974) Biochem Biophys Res Commun 58: 795–800
23 Carré D, Sardet C (1981) Biol Cell 40: 119–128
24 Cascieri M, Amann RP, Hammerstedt RH (1976) J Biol Chem 251: 787–793
25 Chinkers M, Garbers DL, Chang MS, Lowe DG, Chin H, Goeddel DV, Schulz S (1989) Nature 338: 78–83
26 Christen R, Schackmann RW, Dahlquist FW, Shapiro BM (1983) Exp Cell Res 149: 289–294
27 Clapper DL, Brown GG (1980) Dev Biol 76: 341–349
28 Clapper DL, Brown GG (1980) Dev Biol 76: 350–357
29 Clapper DL, Epel D (1982) Gamete Res 6: 315–326
30 Clapper DL, Davis JA, Lamothe PJ, Patten C, Epel D (1985) J Cell Biol 100: 1817–1824
31 Clapper DL, Lamothe PJ, Davis JA, Epel D (1985) J Exp Zool 236: 83–91
32 Coll JC, Bowden BF, Clayton MN (1990) Chemistry in Britain August: 761–763
33 Coll JC, Miller RL (1991) In "Comparative Spermatology 20 Years After" Ed by B Baccetti, Ravan Press, New York, pp 129–134
34 Conklin EG (1905) J Acad Natl Sci Philadelphia 13: 1–126
35 Cook SP, Babcock DF (1993) J Biol Chem 268: 22402–22407
36 Cook SP, Babcock DF (1993) J Biol Chem 268: 22408–22413
37 Cosson MP (1990) In "Controls of Sperm Motility: Biological and Clinical Aspects" Ed by C Gagnon, CRC press, Boca Raton, pp 103–135
38 Cosson MP, Carré D, Cosson J, Sardet C (1983) J Submicrosc Cytol 15: 89–93
39 Cosson MP, Carré D, Cosson J (1984) J Cell Sci 68: 163–181
40 Cosson J, Carré D, Cosson MP (1986) Cell Motil Cytoskelt 6: 225–228
41 Cosson MP, Billard R, Lelellier L (1989) Cell Motil Cytoskelt 14: 424–434
42 Dan JC (1950) Biol Bull 99: 412–415
43 Dangott LJ, Garbers DL (1987) Ann NY Acad Sci 513: 274–285
44 Dangott LJ, Jordan JF, Bellet RA, Garbers DL (1989) Proc Natl Acad Sci USA 86: 2128–2132
45 Domino SE, Garbers DL (1990) In "Controls of Sperm Motility: Biological and Clinical Aspects" Ed by C Gagnon, CRC Press Boca Raton, pp 91–101
46 Drevius LO (1963) Nature 197: 1123–1124
47 Drevius LO, Erickson H (1966) Exp Cell Res 42: 136–156
48 Foresta C, DeCarlo E, Zorzi M, Rossato M, Finelli L (1990) Acta Eur Fertil 21: 305–308
49 Gagnon C, Lamirande ED (1987) In "New Horizons in Sperm Cell Research" Ed by H Morri Japan Sci. Soc. Press, Tokyo, Gordon and Breach Sci. publ., New York, pp 205–214
50 Garbers DL (1992) Cell 71: 1–4
51 Garbers DL, Watkins HD, Hansbrough JR, Smith A, Misono KS (1982) J Biol Chem 257: 2734–2737
52 Gatti J-L, Billard R, Christen R (1990) J Cell Physiol 143: 546–554
53 Gibbons IR (1981) J Cell Biol 91: 107s–124s
54 Gibbons BH, Gibbons IR (1972) J Cell Biol 54: 75–97
55 Gnessi L, Ruff MR, Fraioli F, Pert, CB (1985) Exp Cell Res 161: 219–230
56 Gray J. (1928) Br J Exp Biol 5: 337–344
57 Grinstein S, Rothstein A, Cohen S (1985) J Gen Physiol 85:

765–787
58 Hansbrough JR, Garbers DL (1981) J Biol Chem 256: 1447–1452
59 Hansbrough JR, Garbers DL (1981) J Biol Chem 256: 2235–2241
60 Hardy MP, Dent JN (1986) J Exp Zool 240: 385–396
61 Harumi T, Yamaguchi M, Suzuki N (1991) Dev Growth Differ 33: 67–73
62 Harumi T, Hoshino K, Suzuki N (1992) Dev Growth Differ 34: 163–172
63 Hayashi H, Yamamoto K, Yonekawa H, Morisawa M (1987) J Biol Chem 262: 16692–16698
64 Hidiroglou M, Knipfel JE (1984) J Dairy Sci 67: 1147–1156
65 Hinton BT, Brooks DE, Dott HM, Setchell BP (1981) J Reprod Fert 61: 59–64
66 Hoshino K, Shimizu T, Sendai Y, Harumi T, Suzuki N (1992) Dev Growth Differ 34: 403–411
67 Haskins KM, Zanbola RR, Boling JM, Lee YC, Himes RH (1980) Biochem Biophys Res Commun 95: 1703–1709
68 Hoskins DD, Vijayaraghavan S (1990) In "Control of Sperm Motility: Biological and Clinical Aspects" Ed by C Gagnon, CRC Press, Boca Raton, Boston pp 53–62
69 Hyne RV, Garbers DL (1979) Biol Reprod 21: 1135–1142
70 Inaba K, Morisawa M (1991) Biomed Res 12: 435–437
71 Inaba K, Akazome Y, Morisawa M (1992) Biochem Biophys Res Commun 182: 667–674
72 Inaba K, Morisawa M (1992) Biol Cell 76: 329–333
73 Inaba K, Akazome Y, Morisawa M (1993) J Cell Sci 104: 907–915
74 Inoda T, Morisawa M (1987) Comp Biochem Physiol 88A: 539–542
75 Ishida K, Okuno M, Morisawa S, Mohri T, Mohri H, Waku M, Morisawa M (1987) Dev Growth Differ 29: 47–56
76 Ishiguro K, Murofushi H, Sakai H (1982) J Cell Biol 92: 777–782
77 Jin ZX, Nakajima T, Morisawa M, Hayashi H (1994) J Biochem 115: 552–556
78 Jin ZX, Inaba K, Manaka K, Morisawa M, Hayashi H (1994) J Biochem 115: 885–890
79 Johnson CH, Clapper DL, Winkler MM, Lee HC, Epel D (1983) Dev Biol 98: 493–501
80 Johnson RA, Jakobs KH, Schultz G (1985) J Biol Chem 260: 111–121
81 Kamimura S, Mandelkow E (1992) J Cell Biol 118: 865–875
82 Keller DW, Polakoski KL (1975) Biol Reprod 13: 154–157
83 Kobayashi W (1993) Zool Sci 10: 281–285
84 Larsson H, Wallin M, Edström A (1976) Exp Cell Res 100: 104–110
85 Lee HC, Garbers DL (1986) J Biol Chem 261: 16026–16032
86 Lillie FR (1913) J Exp Zool 14: 515–574
87 Lindemann CB (1978) Cell 13: 9–18
88 Lindemann CB,Goltz JS, Kanous KS, Gardner TK, Olds-Clarke P (1990) Mol Reprod Dev 26: 69–77
89 Lindholmer CH, Eliasson R (1972) Int J Fertil 17: 153–160
90 Lindholmer CH (1973) Fert Steril 24: 521–526
91 Magnus O, Brekkel L, Abholm T, Puvis K (1990) Arch Androl 24: 159–166
92 Miller RL (1974) Amer Zool 14: 467–486
93 Miller RL (1975) Nature 254: 244–245
94 Miller RL (1977) J Exp Zool 200: 203–212
95 Miller RL (1978) J Exp Zool 205: 385–402
96 Miller RL (1979) Mar Biol Berlin 53: 115–124
97 Miller RL (1982) Amer Zool 22: 827–840
98 Miller RL (1985) J Exp Zool 234: 383–414
99 Miller RL (1985) In "Biology of Fertilization Vol 2" Ed by CB Metz, A Monroy Academic Press, New York pp 275–337
100 Mizuno T (1956) J Fac Sci Univ Tokyo Sect. IV 7: 478–487
101 Mohri H, Yanagimachi R (1980) Exp Cell Res 127: 191–196
102 Mohri H, Fujiwara A, Daumae M, Yasumasu I (1990) Dev Growth Differ 32: 375–381
103 Morisawa M (1976) J Mechanochem Cell Motil 3: 239–245
104 Morisawa M (1985) Zool Sci 2: 605–615
105 Morisawa M, Mohri H (1972) Exp Cell Res 70: 311–316
106 Morisawa M, Mohri H (1974) Exp Cell Res 83: 87–94
107 Morisawa M, Suzuki K (1980) Science 210: 1145–1147
108 Morisawa M, Okuno M (1982) Nature 295: 703–704
109 Morisawa M, Suzuki K, Shimizu H, Morisawa S, Yasuda K (1983) J Exp Biol 107: 95–103
110 Morisawa M, Suzuki K, Morisawa S (1983) J Exp Biol 107: 105–113
111 Morisawa M, Morisawa S, DeSantis R (1984) Zool Sci 1: 237–244
112 Morisawa M, Hayashi H (1985) Biomed Res 6: 181–184
113 Morisawa M, Morisawa S (1986) Zool Sci 3: 979 (abstract)
114 Morisawa M, Ishida K. (1987) J Exp Zool 242: 199–204
115 Morisawa M, Morisawa S (1990) In "Control of Sperm Motility: Biological and Clinical Aspects" Ed by C Gagnon CRC Press, Boca Raton, pp 137–151
116 Morisawa M, Tanimoto S, Ohtake H (1992) J Exp Zool 264: 225–230
117 Morisawa S, Morisawa M (1986) J Exp Biol 126: 89–96
118 Morisawa S, Morisawa M (1988) J Exp Biol 136: 13–22
119 Morisawa S, Ishida K, Okuno M, Morisawa M (1990) Mol Reprod Dev 34: 420–426
120 Morita Z, Chang MC (1970) Biol Reprod 3: 169–179
121 Morton B, Albagli L (1973) Biochem. Biophys Res Commun 50: 697–702
122 Morton B, Harrigan-Lum J, Albagli L, Joose T (1974) Biochem Biophys Res Commun 56: 372–379
123 Morton B, Sagadraca R, Fraser C (1978) Fertil Steril 29: 695–698
124 Nevo AC (1965) J Reprod Fert 9: 103–107
125 Nishioka D, Cross N (1978) In "Cell Reproduction" Ed by ER, Dirksen, DM Prescott, DF Fox, Academic Press, New York, pp 403–413
126 Noland TD, Abumrad NA, Beth AH, Garbers DL (1987) Biol. Reprod. 37: 171–180
127 Oda S, Morisawa M (1993) Cell Motil Cytoskelt 25: 171–178
128 Oda S, Igarashi Y, Ohtake H, Sakai K, Shimizu N, Morisawa M (1994) Dev Growth Differ (in press)
129 Ohtake H (1976) J Exp Zool 198: 303–312
130 Ohtake H (1976) J Exp Zool 198: 313–322
131 Okamura N, Sugita Y (1983) J Biol Chem 258: 13056–13062
132 Okamura N, Tajima Y, Soejima A, Masuda H, Sugita Y (1985) J Biol Chem 260: 9699–9705.
133 Okamura N, Onoe S, Kawamura K, Tajima Y, Sugita Y (1990) Biochem Biophys Acta 1035: 83–89
134 Okuno M, Morisawa M (1989) Cell Motil Cytoskelt 14: 194–200
135 Opresko LK, Brokaw CJ (1983) Gamete Res 8: 201–218
136 Osanai M, Aigaki T, Kasuga H (1987) In "New Horizons in Sperm Cell Research" Ed by H Mohri, Japan Sci. Soc. Press Tokyo/Gordon and Breach Sci. Publ. New York, pp 185–195
137 Osanai M, Kasuga H, Aigaki T (1989) J Insect Physiol 35: 401–408
138 Pilikian S, Adeleine P, Czyba JC, Ecochard R, Guerin JF,

Mimouni P (1991) Int J Androl 14: 167–173
139 Pillai MC, Shields TS, Yanagimachi R, Cherr GN (1993) J Exp Zool 265: 336–342
140 Punnett T, Miller RL, Yo B-H (1992) J Exp Zool 262: 87–96
141 Ralt D, Goldenberg M, Fetterolf P, Thompson D, Dor J, Mashiach S, Garbers DL, Eisenbach M (1991) Proc Natl Acad Sci USA 88: 2840–2844
142 Ramarao CS, Garbers DL (1985) J Biol Chem 260: 8390–8396
143 Ramarao CS, Garbers DL (1988) J Biol Chem 263: 1524–1529
144 Repaske DR, Garbers DL (1983) J Biol Chem 258: 6025–6029
145 Riffo M, Leiva S, Astudillo J (1992) Int J Androl 15: 229–237
146 Rothschild R, Tuft RH (1950) J Exp Biol 27: 59–72
147 Saito S, Bush IM, Mackengie AR, Whitemore Jr WF (1967) Invest Urol 4: 546–555
148 Saito S, Zeitz L, Bush IM, Lee R, Whitemore Jr WF (1969) Am J Physiol. 213: 749–752
149 Sawada T, Schatten G (1989) Dev Biol 132: 331–342
150 Schackmann RW, Chock PB (1986) J Biol Chem 261: 8719–8728
151 Schartan O, Montalenti G. (1942) Biol Zentralbl 61: 473
152 Shimomura H, Dangott LJ, Garbers DL (1986) J Biol Chem 261: 15778–15782
153 Si Y, Okuno M (1993) Mol. Reprod Dev 36: 89–96
154 Speksnijder JF, Jaffe LF, Sardet C (1989) Dev Biol 133: 180–184
155 Stacy N E, Liley N R (1974) Nature 247: 71–72
156 Storey BT (1975) Biol Reprod 13: 1–9
157 Strüssmann CA, Renard P, Ling H, Takashima F (1994) Fish Sci 60: 9–13
158 Suzuki N (1989) In "Bioorganic Marine Chemistry Vol. 3" Ed by PJ Scheuer: Springer-Verlag, Berlin pp 47–70
159 Suzuki N, Nomura K, Ohtake H, Isaka S (1981) Biochem Biophys Res Commun 99: 1238–1244
160 Suzuki N, Shimomura H, Radany EW, Ramarao CS, Ward GE, Bentley JK, Garbers DL (1984) J Biol Chem 259: 14874–14879
161 Suzuki N, Kurita M, Yoshino K, Kajiura H, Nomura K, Yamaguchi M, (1987) Zool Sci 4: 649–656
162 Suzuki R (1958) Embryologia 4: 93–102
163 Suzuki R (1959) Embryologia 4: 359–367
164 Suzuki R (1959) Annot Zool Jpn 32: 105–111
165 Suzuki R (1961) Annot Zool Jpn 34: 24–39
166 Tajima Y, Okamura N (1990) Biochem Biophys Acta 1034: 326–332
167 Takai H, Morisawa M (1994) J Cell Sci (submitted)
168 Takayanagi R, Inagami T, Snajdar RM, Inada T, Tamura M, Misono KS (1987) J Biol Chem 262: 12104–12113
169 Tanimoto S, Imae Y, Morisawa M (1988) Zool Sci 5: 1281(abstract)
170 Tanimoto S, Morisawa M (1988) Dev Growth Differ 30: 117–124
171 Tanimoto S, Kudo Y, Nakazawa T, Morisawa M (1994) Mol Reprod Dev (in press)
172 Tash JS (1990) In "Controls of Sperm Motility:Biological and Clinical Aspects" Ed by C Gagnon, CRC Press, Boca Raton, pp 229–240
173 Tash JS, Means AK (1982) Biol Reprod 28: 75–104
174 Tash JS, Hidaka H, Means AR (1986) J Cell Biol 103: 649–655
175 Tash JS, Krinks M, Patel J, Means RL, Klee CB, Means AR (1988) J Cell Biol 106: 1625–1633
176 Thomson MF, Wishart GJ (1991) J Reprod Fert 93: 385–391
177 Thorpe DS, Garbers DL (1989) J Biol Chem 264: 6545–6549
178 Tombes RM, Shapiro BM (1985) Cell 41: 325–334
179 Tournade A (1913) C R Soc Biol 74: 738–744
180 Tubb DJ, Kopf GS, Garbers DL (1979) J Reprod Fert 56: 539–542
181 Turner TT, D'addario D, Howard SS (1978) Biol Reprod 19: 1095–1101
182 Turner TT, Giles RD (1982) Am J Physiol 242: R199-R203
183 Usselman MC, Cone RA (1983) Biol Reprod 29: 1241–1253
184 Utida S, Nanao S (1956) J Fac Sci Univ Tokyo Sect IV 7: 505–514
185 Utugi K (1993) Jpn. J Ichthyol 40: 273–278
186 VandeVoort CA, Tollner TL, Overstreet JW (1994) Mol Reprod Dev 37: 299–304
187 Ward GE, Brokaw CJ, Garbers DL, Vacquier VD (1985) J Cell Biol 101: 2324–2329
188 Ward GE, Moy GW, Vacquier VD (1986) In "Molecular and Cellular Bioloby of Fertilization" Ed by J Hedrick, Plenum Press, New York
189 White DR, Aitken RJ (1989) Gamete Res 22: 163–177
190 White IG, Voglmayr JK (1986) Biol Reprod 34: 183–193
191 Yamaguchi M, Niwa T, Kurita M, Suzuki N (1987) Dev Growth Differ 30: 159–167
192 Yanagimachi R (1957) Annot Zool Japon 30: 114–119
193 Yanagimachi R, Kanoh Y (1961) J Fac Sci Hokkaido Univ Ser 6 11: 487–494
194 Yanagimachi R (1969) J Reprod Fert 18: 275–286
195 Yanagimachi R (1970) J Reprod Fert 23: 193–196
196 Yanagimachi R (1988) In "Physiology of Reproduction" Ed by E Knobil *et al*. Raven Press, New York
197 Yanagimachi R, Cherr GN, Pillai MC, Boldwin JD (1992) Dev Growth Differ 34: 447–461
198 Yoshida M, Inaba K, Morisawa M. (1993) Dev Biol 157: 497–506
199 Yoshida M, Inaba K, Ishida K, Morisawa M (1994) Dev Growth Differ (in press)
200 Yoshino K, Suzuki N (1992) Eur J Biochem 206: 887–893
201 Zamir N, Riven-Kreitman R, Manor M, Makler A, Blumberg S, Ralt D, Eisenbach M (1993) Biochem Biophys Res Commun 197: 116–122

ZOOLOGICAL SCIENCE 11: 663-666 (1994)

Relationships between the Slope of the Oxygen Equilibrium Curve and the Cooperativity of Hemoglobin as Analyzed Using a Normalized Oxygen Pressure Scale

MICHIYORI KOBAYASHI*, KAZUKO KITAYAMA, GAKU SATOH, KEN-ICHI ISHIGAKI[1] and KIYOHIRO IMAI[2]

Department of Biology, Faculty of Science, [1]Information Processing Center, Niigata University, Niigata 950-21 and [2]Department of Physiology, Medical School, Osaka University, Suita, Osaka 565, Japan

ABSTRACT—The oxygen equilibrium curve (OEC) for hemoglobin, which is usually expressed as a S *vs.* P plot, was expressed by normalizing P by P_{dmax}, where S is oxygen saturation, P is partial pressure of oxygen, and P_{dmax} is P at which the slope of the usual OEC is maximized. The maximal slope of normalized OEC gives $P_{dmax} \cdot S'_{max}$, where S'_{max} is the maximal slope of the usual OEC, a measure for the oxygen transport efficiency of hemoglobin. Here, the term "efficiency" is used in the sense that the oxygen release from hemoglobin becomes more sensitive to oxygen pressure changes as S'_{max} becomes larger. An analysis using 38 sets of published oxygen equilibrium data for human adult hemoglobin under various experimental conditions showed that (a) expressing OEC by means of S *vs.* P/P_{dmax} or S *vs.* log P is advantageous for analyzing the slope of OEC compared to usual S *vs.* P plot and (b) while the OEC differs depending on experimental conditions, S'_{max} varies in close linear correlation to n_{max} (the maximal slope of the Hill plot which measures oxygen binding cooperativity), and $P_{dmax} \cdot S'_{max}$ is almost equal to $n_{max}/4$. Thus, the parameter expressing oxygen transport efficiency is closely related to the parameter expressing oxygen binding cooperativity.

INTRODUCTION

The sigmoid shape of the oxygen equilibrium curve (OEC) of hemoglobin (Hb) is physiological significant since the oxygen release from hemoglobin is sensitively regulated in response to the oxygen demands of tissue. The sigmoid character of OEC is ascribed to cooperative oxygen binding arising from heme-heme interactions. Cooperativity has been conventionally measured by the Hill coefficient, n_{max}, which is defined as the maximal slope of the Hill plot, i.e., log [S/(1-S)] *vs.* log P plot, where S and P are the oxygen saturation of hemoglobin and partial pressure of oxygen, respectively [2, 9]. The entire OEC is well described by the Adair equation [1] as follows:

$$S = \frac{(K_1P + 3K_1K_2P^2 + 3K_1K_2K_3P^3 + K_1K_2K_3K_4P^4)}{(1 + 4K_1P + 6K_1K_2P^2 + 4K_1K_2K_3P^3 + K_1K_2K_3K_4P^4)} \quad (1)$$

Here, K_i (i=1 to 4) is the intrinsic equilibrium constant for the ith oxygen binding step (stepwise Adair constant).

The efficiency of oxygen transport by hemoglobin is assessed by the first derivative of S, (S'(=dS/dP)), with respect to P. Plotting S' against P yields a bell-shaped curve. The ordinate and abscissa readings at the top of the curve give the maximal oxygen transport efficiency, S'_{max}, and the partial oxygen pressure at that point, P_{dmax}, respectively. Our recent analysis [6] using 38 sets of published accurate oxygen equilibrium data including Adair constant values showed that S_{nmax} (S at which n_{max} occurs) does not agree with S_{dmax} (S at $P=P_{dmax}$), the latter mostly being 0.38 irrespective of the experimental conditions. This indicates that the point on the OEC at which cooperativity is maximized is not necessarily the same as the point at which the oxygen transport efficiency is maximized. In the previous analysis, P_{dmax} varied widely depending on the overall oxygen affinity, usually measured by P_{50} (oxygen pressure at half oxygen saturation).

In the present paper, we describe a specific way of drawing the OEC in which the abscissa is normalized by P_{dmax}. By using this normalization, the maximal slope of OEC as a measure of oxygen transport efficiency is found to be closely related to oxygen binding cooperativity.

METHODS

The experimental data used for the present analysis were taken from 38 sets of published oxygen equilibrium data for human adult hemoglobin (Hb A) [3, 4, 5, 8] obtained at 25°C under a variety of solutions conditions such as pH (6.5, 7.4 and 9.1), Cl^- concentration (2.6 mM, 7 mM and 100 mM), 2,3-diphosphoglycerate concentration (0 and 2 mM), inositol hexaphosphate concentration (0 and 2 mM) and CO_2 pressure (0 and 40 mmHg). These data included Adair constant values obtained by a nonlinear least-squares curve-fitting method. These Adair constant values were used for calculating various parameters and the construction of curves that appear in the present study.

All computations were carried out on a personal computer model PC-9821 Ap2 using MS-FORTRAN (Nippon Electric Co.,

Accepted August 17, 1994
Received June 9, 1994
* To whom all correspondence should be addressed.

Tokyo).

RESULTS AND DISCUSSION

Normalization of the OEC abscissa

It was shown in our previous analysis [6] that the S' value strongly depends on the position of the OEC along the abscissa: S'_{max} was inversely related to the parameters expressing the position of OEC, such as P_{dmax} or P_{50} (P at S = 0.5). It is therefore expected that the dependence of S'_{max} on the position of the OEC becomes less distinct if P is made dimensionless by normalizing it with some parameter representing the position of OEC along the abscissa. We used P_{dmax} as this parameter. Figure 1 shows three examples of normalized OEC determined in different solutions. The parameter values for three OECs are listed in Table 1.

TABLE 1. Parameter values for three examples of OEC

	Solution conditions	P_{50} (mmHg)	P_{dmax} (mmHg)	S'_{max} (mmHg^{-1})	n_{max}
OEC A	pH 9.1, 2.6 mM Cl^-	1.04	0.75	0.67	2.35
OEC B	pH 9.1, 0.1 M Cl^-	2.13	1.68	0.36	2.73
OEC C	pH 7.4, 0.1 M Cl^- 5% CO_2	7.84	6.65	0.11	3.15

These normalized OECs are located at roughly similar positions, taking into account that the P_{dmax} value for the 38 OECs varied from 0.75 to 15.48 mmHg. If other OECs are plotted together, they would be close to curve C. This normalization allows us to analyze the shape of OEC in a more direct way.

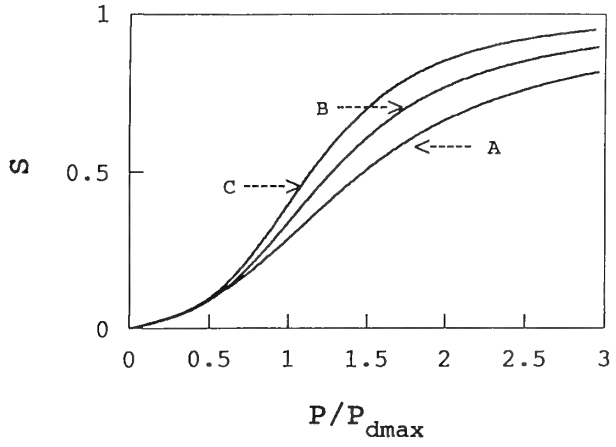

FIG. 1. Oxygen equilibrium curves (OEC) of human Hb A normalized by P_{dmax}. OEC data taken from Imai [3]. S, fractional oxygen saturation; P, partial pressure of oxygen; P_{dmax}, P at which S'(=dS/dP) is maximized. Solution are given in Table 1.

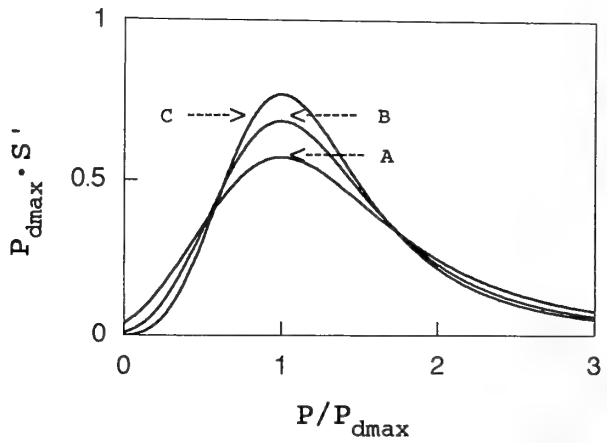

FIG. 2. P_{dmax}·S' *vs.* P/P_{dmax} plots for human Hb A. S' is the first derivative of S with respect to P. The OEC data sets are the same as those in Fig. 1.

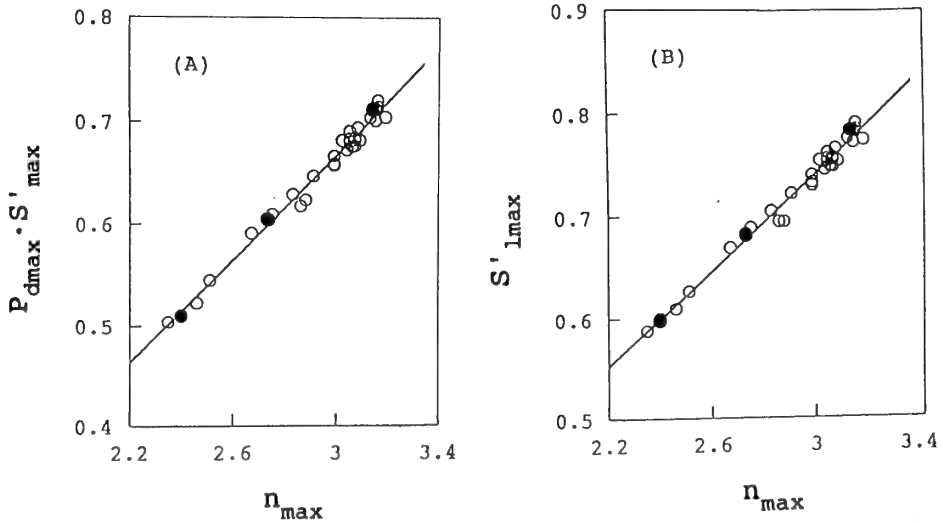

FIG. 3. Correlation between P_{dmax}·S'_{max} and n_{max} (A) and between S'_{lmax} and n_{max} (B) for human Hb A. The P_{dmax}·S'_{max} values were calculated from the slope of normalized OECs at $P/P_{dmax}=1$ for the 38 OEC data sets [3–5, 8]. S'_{lmax} is the maximal slope of the S *vs.* log P plot (see Fig. 4). The OEC data sets are the same as in Fig. 3 A. Closed circles are the data sets shown in Fig. 1.

Relation between the maximal slope of normalized OEC and n_{max}

The slope of normalized OEC gives the P_{dmax}·S' value. In Figure 2, the same sets of data as in Figure 1 are plotted by means of P_{dmax}·S' *vs.* P/P_{dmax}, yielding bell-shaped curves. As opposed to the previous S' *vs.* P plot [6], the tops of the bell-shaped curves in Figure 2 are located at the same position along the normalized abscissa. At the top where $P/P_{dmax}=1$, the P_{dmax}·S' value is maximized. The higher the top (or the larger the P_{dmax}·S'_{max} value), the larger the n_{max} value.

Figure 3 (A) shows the correlation's between P_{dmax} ·S'_{max} and n_{max} for the 38 sets of OEC data. These two parameters are closely correlated, showing a linear regression:

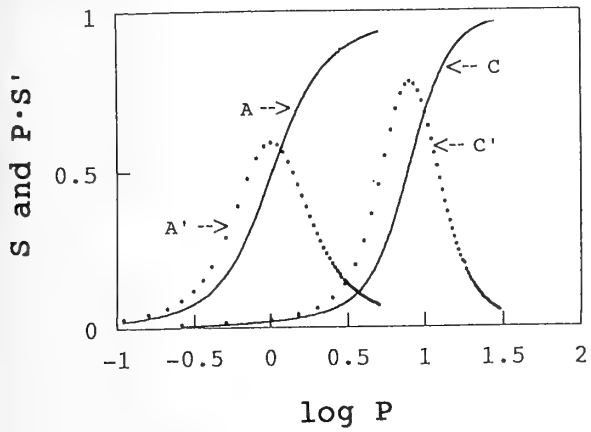

FIG. 4. S *vs.* log P plots (solid lines) and S'·P *vs.* log P plots (dotted lines) of human Hb A. Two of the three OEC data sets in Fig. 1 were used. P·S' was calculated from the slope of the S vs. log P plot (Eq. (3)).

$$P_{dmax}\cdot S'_{max} = 0.25\cdot n_{max} - 0.09 \ (r=0.98). \qquad (2)$$

The coefficient values indicate that P_{dmax}·S'_{max} is roughly equal to 1/4 of n_{max} and the maximal slope of the normalized OEC is closely related to oxygen binding cooperativity.

Relation between the maximal slope of the S vs. log P plot and n_{max}

Expressions of OEC by means of a S *vs.* log P plot are advantageous in the sense that changes in overall oxygen affinity are converted to parallel displacement of OEC along the abscissa and comparison of the shape is easy.

Figure 4 shows two sets of OEC data chosen from the three sets in Figure 1 as expressed by S *vs.* log P and their slope as a function of log P. Since

$$dS/d\log P = P\cdot dS/dP = P\cdot S', \qquad (3)$$

P_{dmax}·S'_{max} can be calculated from the slope of the S *vs.* log P plot at $P=P_{dmax}$, yielding the same linear regression as Eq. (2). The maximal slope (S'_{lmax}) of the S *vs.* log P plot also yielded a similar linear regression:

$$S'_{lmax} = 0.23\cdot n_{max} + 0.04 \ (r=0.98) \qquad (4)$$

(see Fig. 3(B)). Interestingly, the maximal slope occurred in the narrow range of S: S=0.49 to 0.54. or at S=0.52± 0.01SD for all 38 data sets.

Eqs. (2) and (4) indicate that P_{dmax}·S'_{max} is related to S'_{lmax}. In fact, these two quantities showed a very close correlation:

$$P_{dmax}\cdot S'_{max} = 1.08\cdot S'_{lmax} - 0.133 \ (r=0.999). \qquad (5)$$

Since P_{dmax}·S'_{max} varied from 0.5 to 0.7 while S'_{lmax} varied from 0.6 to 0.8 depending on the solutions, the latter can be a rough approximation for the former. Thus, the maximal slope of the S *vs.* log P plot gives basically the same information as that of the S *vs.* P/P_{dmax} plot. The constant term of the right-hand side of Eq. (5) originates from the constant terms in Eqs. (2) and (4). There is no theoretical necessity for these 3 terms to be zero since these 3 equations are empirical.

Basis for the relation between P_{dmax}·S'_{max} and n_{max} and its significance

It holds that

$$n = d\log [S/(1-S)]/d\log P$$
$$= [(1/(S(1-S))]\cdot dS/d\log P \qquad (6)$$

where n is the slope of the Hill plot at a given P value [8]. From Eqs. (3) and (6) it follows that

$$P\cdot S' = S(1-S)\cdot n. \qquad (7)$$

At $P=P_{dmax}$, the S values for the 38 OEC data sets are approximately equal to 0.38 [4] and n is somewhat smaller than n_{max}. Thus, $P_{dmax}\cdot S'_{max}\simeq 0.24\cdot n_{max}\simeq n_{max}/4$. As described above, S'_{lmax} is roughly equal to P_{dmax}·S'_{max}, and the former occurs around S=0.5. Furthermore, n at S=0.5 is only insignificantly smaller than n_{max}. Therefore, $P_{dmax}\cdot S'_{max}\simeq 0.5(1-0.5)\cdot n_{max}=n_{max}/4$. These approximations would be more concise if the OEC expressed by S *vs.* log P was more symmetric and thereby the values of P_{dmax}, P_{50} and P_{nmax} (at which n_{max} occurs) were closer to each other.

The present analysis has shown that (a) the expression of OEC by means of S *vs.* P/P_{dmax} or S *vs.* log P is advantageous for analyzing the slope of OEC compared to a conventional S *vs.* P plot and (b) S'_{max} is closely related to n_{max}, while P_{dmax}·S'_{max} is approximately equal to $n_{max}/4$. Thus, the parameter expressing oxygen transport efficiency is closely related to the parameter expressing oxygen binding cooperativity. However, it should be stressed here that the values of P or S at which oxygen transport is maximized do not necessarily agree with those at which cooperativity is maximized [6].

We also analyzed the same OEC data as used in the present study using the two-state allosteric model of Monod *et al.* [7] instead of the Adair scheme, and obtained essentially the same results. The present method of analysis has the

advantage that P_{dmax} can easily be evaluated from the inflection point of the usual OEC (S *vs.* P) and thus allowing the easy construction of the normalized OEC (S *vs.* P/P_{dmax}).

ACKNOWLEDGMENTS

We thank Dr. Hideki Akiyama, Niigata University for helpful comments. This study was supported in part by grants from Ajinomoto Co., Tokyo to Imai K.

REFERENCES

1 Adair GS (1925) The hemoglobin system, VI. The oxygen dissociation curve of hemoglobin. J Biol Chem 63: 529–545

2 Hill AV (1910) The possible effects of the aggregation of the molecule of haemoglobin on its dissociation curves. J Physiol (London) 40: 4–7

3 Imai K (1982) Allosteric effects in haemoglobin. Cambridge University Press, London, New York, pp 107–203

4 Imai K, Yonetani T (1975) pH dependence of the Adair constants of human hemoglobin. Non-uniform contribution of successive oxygen binding to the alkaline Bohr effect. J Biol Chem 250: 2227–2231

5 Imaizumi K, Imai K, Tyuma I (1982) Linkage between carbon dioxide binding and four-step oxygen binding to hemoglobin. J Mol Biol 159: 703–719

6 Kobayashi M, Ishigaki K, Kobayashi M, Imai K (1994) Shape of the haemoglobin-oxygen equilibrium curve and its oxygen transport efficiency. Respir Physiol 95: 321–326

7 Monod J, Wyman J, Changgeux J-P (1965) On the nature of allosteric transitions: A possible model. J Mol Biol 12:88–118

8 Tyuma I, Imai K, Shimizu K (1973) Analysis of oxygen equilibrium of hemoglobin and control mechanism of organic phosphates. Biochemistry 12: 1491–1498

9 Wyman J (1964) Linked functions and reciprocal effects in hemoglobin: a second look. Adv Protein Chem 19: 228–286

ZOOLOGICAL SCIENCE 11: 667–674 (1994)

Identification of Putative Photoreceptor Cells in the Siphon of a Clam, *Ruditapes philippinarum*

HIDEYUKI KARAKISAWA[1], SATOSHI TAMOTSU[2], AKIHISA TERAKITA[3] and KOHZOH OHTSU[1]

[1]*Ushimado Marine Laboratory, Faculty of Science, Okayama University, Ushimado, Oku, Okayama 701-43,* [2]*First Department of Physiology, Hamamatsu University School of Medicine, Hamamatsu 431-31 and* [3]*Institute of Biology, Faculty of Education, Oita University, Oita 870-11, Japan*

ABSTRACT—A clam, *Ruditapes philippinarum* responds to light by siphonal retraction and valve adduction. Sensitivity to light was seen widely diffused on the siphon, so attempts to identify possible photoreceptor cells were made in the distal portion of the siphon which is most sensitive. Histological investigations by light- and electron-microscopy revealed microvilli arising from the epithelial cells of the outer and inner surfaces of the siphon. Immunohistochemical experiments using anti-squid-rhodopsin serum in conjunction with FITC or streptavidin-biotin revealed specific binding of the anti-serum to the microvillar layer of the outer and inner epithelial cells. It is therefore suggested that the epithelial cells may contain a visual pigment in the microvilli and so function as a primitive photoreceptor.

INTRODUCTION

The phylum Mollusca includes a wide variety of forms, which have evolved a correspondingly diverse range of visual organs, from 'simple' eyes comprising relatively few cells to sophisticated organs with a lens, pupil and a complex retina [14]. The cephalopods (octopuses and squids), for examples catch mobile prey and, relying heavily on vision, have developed eyes comparable to those of vertebrates. Many gastropods, which generally move about slowly on the sea bed have a relatively simple 'eye spot' [6–8]. The bivalves are filter feeders, which are usually attached to the substrate and except for Pectinidae [1] and Cardiidae [2, 22] generally lack sophisticated photoreceptive organs. Instead, they have a primitive photoreceptive system consisting of scattered photoreceptor cells which have been demonstrated indirectly by recording light-activated impulses from the pallial nerves in *Spisula, Mya* and *Venus* ([10], for review see [24]).

It is clear from preliminary behavioral observations that many bivalves of the family Veneridae respond to light but the organs of photoreception have yet to be identified. *Ruditapes phillipinarum*, a common venerid in Japan, shows siphonal retraction and valve adduction in response to either an increase or decrease in background light. Preliminary investigations on *Ruditapes*, with a small light spot of about 1 mm in diameter, indicated that photosensitivity was widely distributed over the siphon, suggesting that photoreceptor cells are scattered throughout the regions. The aim of the present investigations was to identify the photoreceptor cells in the most sensitive region: the distal portion of the siphon.

[3] Present Address: Department of Biophysics, Faculty of Science, Kyoto University, Kyoto 606-1, Japan.

Accepted August 30, 1994
Received May 30, 1994

MATERIALS AND METHODS

Small specimens of *Ruditapes philippinarum* (Adam & Reeve, 1850), were collected near the Ushimado Marine Laboratory or purchased from fish shops. Prior to the experiments, the clams were dark-adapted or kept under dim red light for more than 4 hr. The tip of the siphon was then removed from the animals and used for the experiments described below.

Microscopy

For light-microscopical observations, isolated siphons were fixed in Bouin's fluid for a day, dehydrated through a graded series of ethanols and embedded in paraffin wax. Sections of 4 μm thick were stained with hematoxylin-eosin.

For electron-microscopical observations, isolated siphons were fixed with 1% glutaraldehyde in 0.1 M sodium-cacodylate buffer (pH 7.4) and 0.4 M sucrose for about 4 hr at room temperature. The material was post-fixed with 1% osmium tetroxide and 1% potassium ferrocyanide in 0.1 M sodium cacodylate (pH 7.4) and 0.4 M NaCl. The samples were dehydrated through a graded series of ethanols and embedded in epoxy-resin (TAAB Laboratories). Ultrathin sections were stained with 1% alcoholic uranyl acetate and then 0.1% lead citrate and examined with a Hitachi H-500H electron microscope.

Immunohistochemistry

To investigate whether or not the siphons of *Ruditapes* contain a visual pigment (rhodopsin), an anti-rhodopsin serum was prepared. A procedure to purify a *Ruditapes* rhodopsin has not yet been estabilished. Instead, a squid (*Todarodes pacificus*) rhodopsin was used for immunization.

The anti-squid rhodopsin serum was prepared as follows. The *Todarodes* rhodopsin was extracted and purified according to the procedure reported by Nashima *et al* [16]. Rhodopsin obtained was further purified with sodium dodecyl sulfate-polyacrylamide gel electrophoresis (SDS-PAGE). A rhodopsin band was collected and dissolved in phosphate-buffered saline. Immunization was carried out by injecting the dissolved sample containing rhodopsin (about 50

μg protein) into a mouse 3 times, every 3 weeks. Prepared mouse anti-squid rhodopsin serum recognized the rhodopsin bands in western blot analysis of *Todarodes* retina and immunohistochemically outer segments of photoreceptor cells of *Todarodes* retina.

Isolated siphons were fixed with 4% paraformaldehyde in 0.1 M phosphate buffer (pH 7.4) containing 0.4 M sucrose under dim red light for more than 8 hr at 4°C. The siphons were cryoprotected by soaking in the same buffer solution containing 30% sucrose for 2 hr and then embedded in OCT compound (Miles Scientific, No. 4583) for freezing in liquid nitrogen. The frozen samples were sectioned at 5 μm or 15 μm with a cryotome (Bright, Model OTF) at −20°C.

Thicker sections of 15 μm were first treated with 0.1% Triton X-100 for 15 min and then with 0.02% glycine for 2 hr to block non-specific autofluorescence. The sections were primarily reacted with the anti-rhodopsin serum, diluted 200 times, for 2 hr at room temperature and secondarily with fluorescein isothiocyanate(FITC)-conjugated goat anti-mouse IgG for 3 hr at room temperature. For the control, the anti-rhodopsin serum was absorbed with purified *Todarodes* rhodopsin. Phosphate buffer (0.1M) was used in a series of experiments. Stained sections were observed by epifluorescence.

To avoid autofluorescence involved in the immunofluorescence technique, localization of rhodopsin was also investigated by using a modified avidin-biotin complex (ABC) immunohistochemical technique, i.e., Streptavidin-Biotin (SAB) method (Nichirei, Histofine, SAB-PO(M) kit). Thinner sections of 5 μm and the same anti-rhodopsin serum as that described above (but diluted 500 times with buffer) were used. A series of reactions were performed according to the kit protocol. Sections were counterstained with hematoxylin.

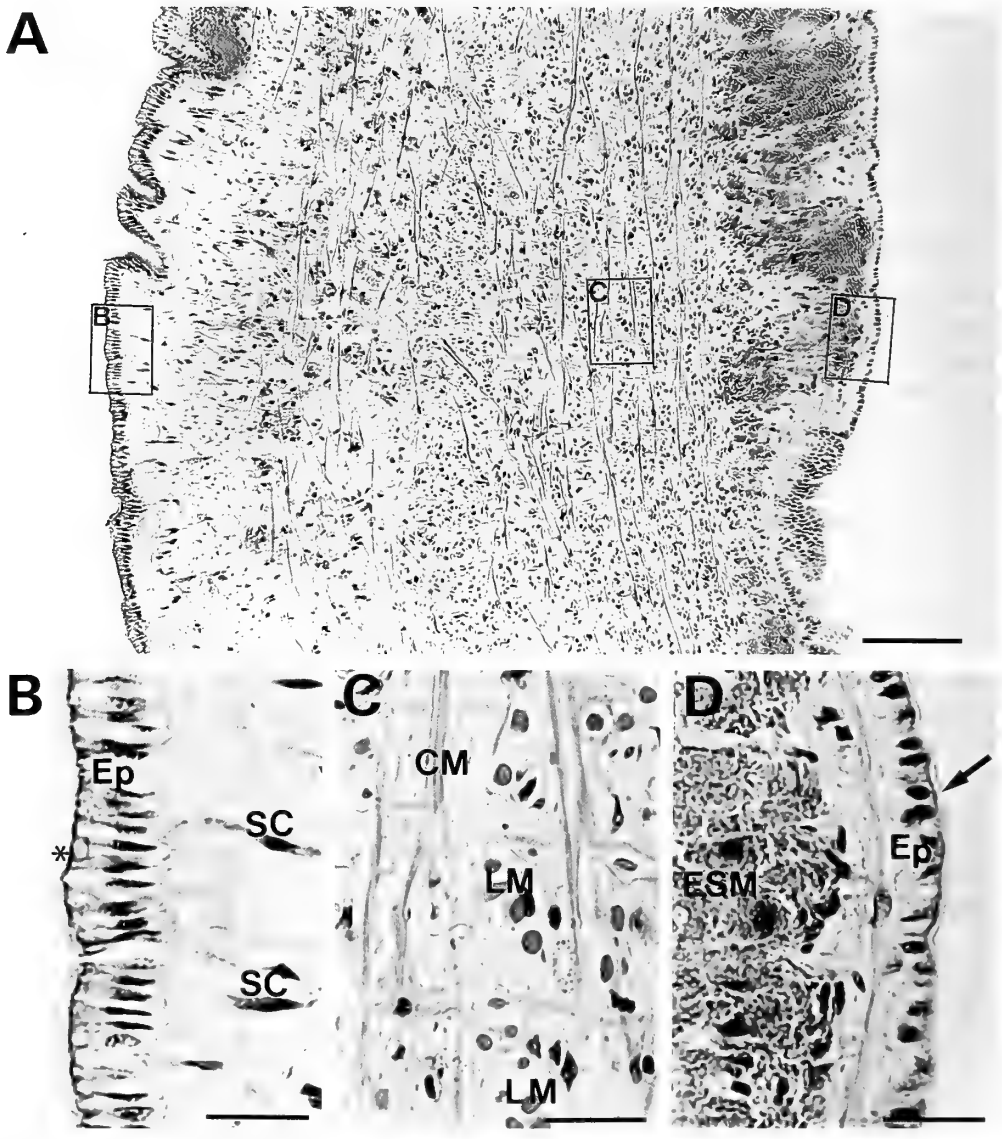

FIG. 1. Light micrographs of a transverse section through the siphonal wall. (A) Low power view. The left and right boundaries correspond to the outer and inner walls of the siphon, respectively. (B)-(D) Insets shown in (A) at higher magnification. (B) Outer epithelium. Note the translucent layer (asterisk) overlying the epithelium (Ep). Cells presumed to be sensory cells (SC) extend fine processes distally and proximally. (C) Muscle tissue of siphon, consisting of circular (CM) and longitudinal (LM) muscles. (D) Inner epithelium. Arrow indicates the outermost translucent layer, similar to that in B. Below the inner epithelium are aggregations of eosin sensitive matter (ESM). Scale bars 100 μm in A, 20 μm in B-D.

RESULTS

Light microscopical observations

The siphon of *Ruditapes* consists of inhalent and exhalent tubes fused with each other on one side, having a figure-8-like form in cross-section. Figure 1A shows a cross-sectional view through the siphonal wall. As magnified in Figure 1B, the extreme outer surface of the siphon is covered with a translucent layer (asterisk in B), which is stained with neither hematoxylin nor eosin, under which columnar cells with elliptical nuclei proximally are present. Cells presumed to be sensory cells lie below an outer epithelial layer (outer EPL) and extend fine processes distally towards the outer surface and proximally towards the central region of the siphonal wall. The central region is occupied with circular and longitudinal muscles which intermingle with each other (Fig. 1C). The inner wall of the siphon is also covered with a layer of cells somewhat thinner than that of the outer ones (Fig. 1D). The translucent layer is also seen along the surface of an inner epithelial layer (inner EPL). Additionally, there are large aggregations of material staining with eosin throughout the region below the inner EPL (Fig. 1A, D). It is emphasized that no structures (such as eye cup, reflecting tapetum and lens) featuring differentiated photoreceptor organs were observed. There were, at least light-microscopically, no apparent differences between the inhalent and exhalent siphons.

Immunohistochemical observations

To investigate the location of photoreceptive pigment, rhodopsin, the siphon was searched by using an anti-serum against squid rhodopsin. Greenish specific fluorescence due to conjugated FITC was observed as a layer along the free surface of the outer EPL (Fig. 2A). This fluorescence was not seen when anti-rhodopsin serum was absorbed by purified squid rhodopsin: only dim yellow autofluorescence remained along the line of cell bodies in the outer EPL (Fig. 2B).

The inner EPL also fluoresced on their free surface, although somewhat weaker than the outer EPL (Fig. 2C). In addition, intense fluorescence was detected throughout the region below the inner EPL (Fig. 2C). Fluorescence in both areas disappeared in the control and dim yellow autofluorescence remained along the line of cell bodies in the inner EPL (Fig. 2D).

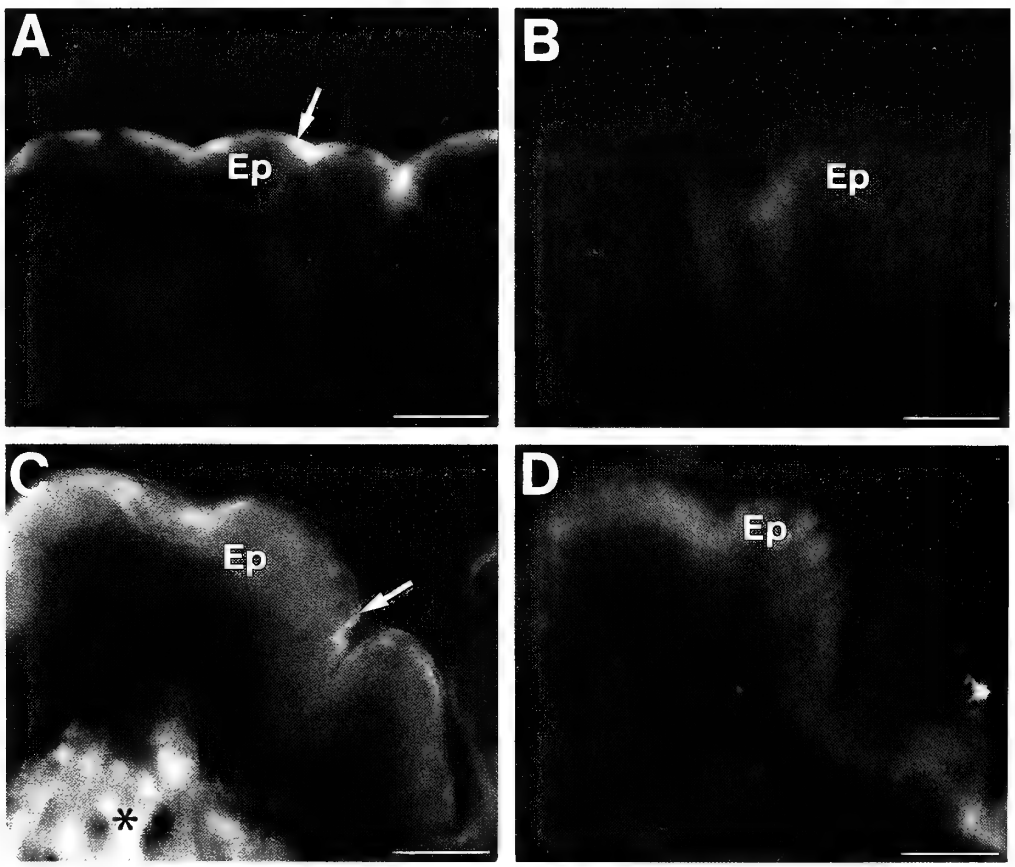

FIG. 2. Fluorescence micrographs of the epithelia of the siphon immunostained with anti-rhodopsin serum using the FITC method. (A) A fluorescing layer (arrow) along the free surface of the outer epithelium (Ep). (B) Control. Anti-rhodopsin serum was blocked by purified rhodopsin. Little fluorescence appears. (C) A fluorescing layer (arrow) along the free surface of the inner epithelium (Ep). Intense fluorescence (asterisk) was found throughout the region below the inner epithelium (cf. ESM in Fig. 1D), (D) Control of C, using anti-rhodopsin serum blocked by purified rhodopsin. Most fluorescence (cf. that indicated by the arrow and asterisk in C) disappeared leaving auto-fluorescence from the cell bodies of the inner epithelium. Scale bars, 20 μm.

To avoid the auto-fluorescence seen when using FITC, the anti-rhodopsin serum was also used in conjunction with the Streptavidin-Biotin (SAB) method. As was the case for FITC, binding of the antiserum was restricted to the extreme surface of the outer EPL (Fig. 3A) and lost in the control with the antiserum which was absorbed by purified squid rhodopsin (Fig. 3B). The inner EPL gave similar results (Fig. 3C, D). However, weaker specific binding than that of the inner EPL was found throughout the region just below the inner EPL (Fig. 3C), corresponding to the strong specific fluorescence observed with FITC (Fig. 2C).

Identification of immunoreactive cells

To identify the cells positive to anti-rhodopsin serum, the ultrastructure of the siphon was investigated (Fig. 4). As shown in the light-microscopical observations, the electron-microscopic observations reveal that the outer surface of the siphon is covered with epithelial cells (outer EPCs)(10–20 μm in length, 4–7 μm in width) which are anchored by connective tissue through a basement membrane (Fig. 4A). A nucleus occupies the base of each cell and a number of vesicles and mitochondria are present distally. Some cells have tightly packed electron-dense melanin-like granules. Numerous microvilli (3–5 μm in length, 50–100 nm in diameter) arise from the free surface of the outer EPCs, forming a layer which coincides in position with the translucent layer observed in the light microscope (Fig. 1).

The inner epithelial cells (inner EPCs) (3–10 μm in length, 4–7 μm in width) have less vesicles than the outer EPCs, but otherwise basically resemble the outer EPCs (Fig. 4B). The microvilli (0.5–3 μm in length, 50–100 nm in diameter) are also observed on the free surface of the inner EPCs. Beneath the layer of the connective tissue underlying the inner EPCs, cells with tightly packed granules (0.3–0.4 μm in diameter) are seen in groups (Fig. 4B). They correspond in position to the eosin-sensitive matters (ESM) in Figure 1D and will hereafter be referred to as 'granular cells'.

Although much less frequently, two other types of cell, are found among the outer and inner EPCs. One type has many 'cilia' on the free surface, and the other has shorter

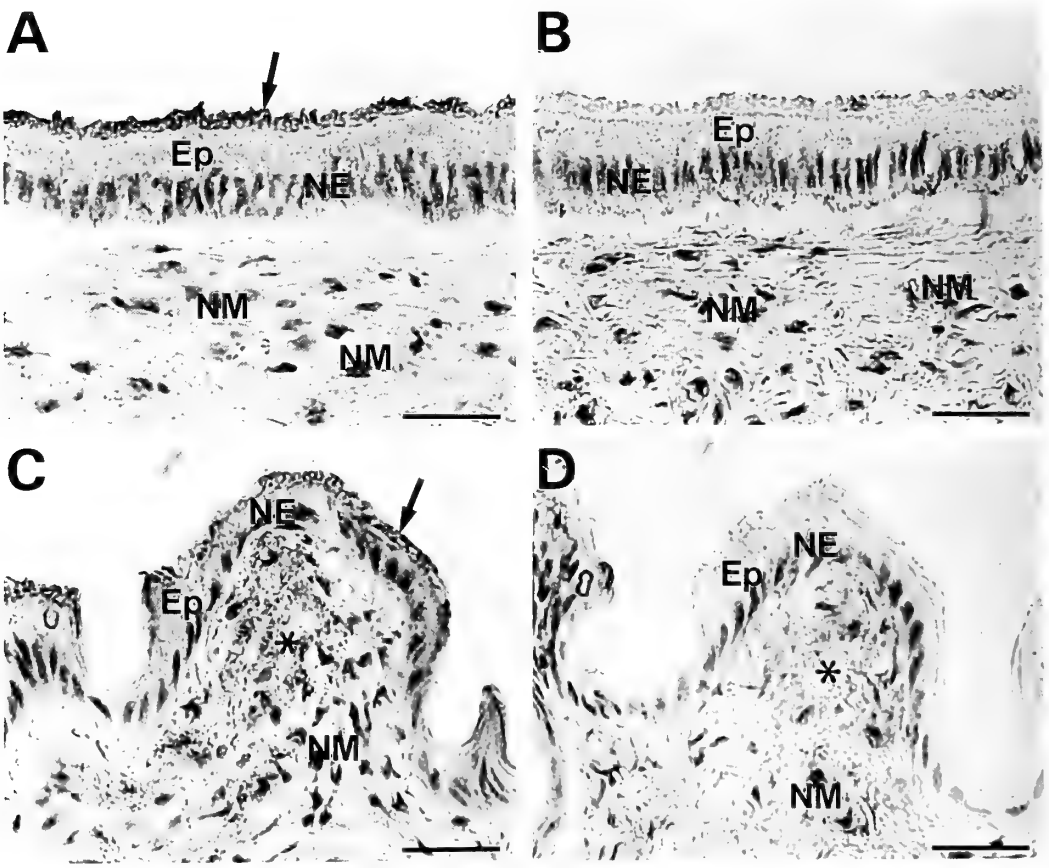

FIG. 3. Light micrographs of the outer (A, B) and inner (C, D) surfaces of the siphon immunostained with anti-rhodopsin serum using the SAB method, counterstained with hematoxylin. (A) A dark layer of positive staining (arrow) appears along the free surface of the outer epithelium (Ep). (B) Control. Anti-rhodopsin serum blocked by purified rhodopsin does not stain the free surface of the outer epithelium. The hematoxylin-stained nuclei of the outer epithelium (NE) and muscles (NM) remain unchanged between A and B. (C) The free surface of inner epithelium (Ep) stained with the anti-serum (arrow). Weaker binding (asterisk) appears throughout the region below the inner epithelium. (D) Control of C, using rhodopsin-blocked anti-serum. The nuclei (NE, NM) counter-stained with hematoxylin remain unchanged but the staining seen in C does not appear. Scale bars, 20 μm.

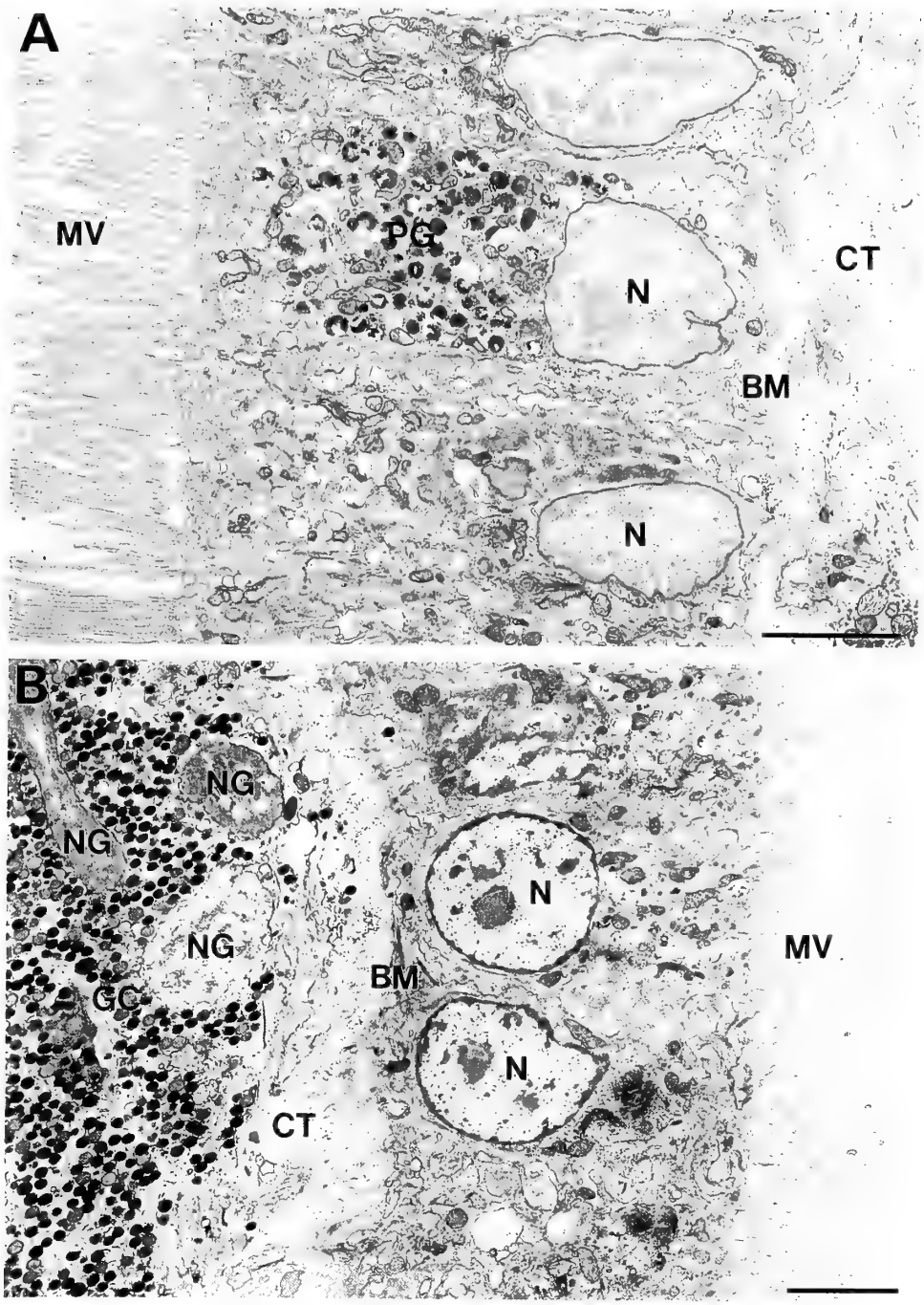

FIG. 4. Electron micrographs of the outer (A) and inner (B) walls of the siphon. Note the characteristic microvilli arising from the outer and inner EPCs, and the granular cells (GC) with numerous compacted granules. (Abbreviations) BM, basement membrane; CT, connective tissue; MV, microvilli; N, nuclei of epithelial cells; NG, nuclei of granular cells; PG, pigment granules. For explanations, see text. Scale bars, 3 μm.

microvilli, forming a concaved 'pit'-like structure distally (Fig. 5A). Cilia could not be found in the latter even in a series of continuous sections. Both 'ciliary' and 'pit' cells extend microtuble-containing fine processes distally between the outer and inner EPCs (Fig. 5B, C) and have nuclei proximally (not shown in Fig. 5). It is clear from their appearance and position that they correspond to the sensory cells in Figure 1B. The central region of the siphonal wall is mostly occupied by the circular and longitudinal muscles, with scattered nerve bundles and fine nerve processes (Fig. 5D). However, differentiated photoreceptor cells comparable to those in eyes were never found in the siphon of *Ruditapes*.

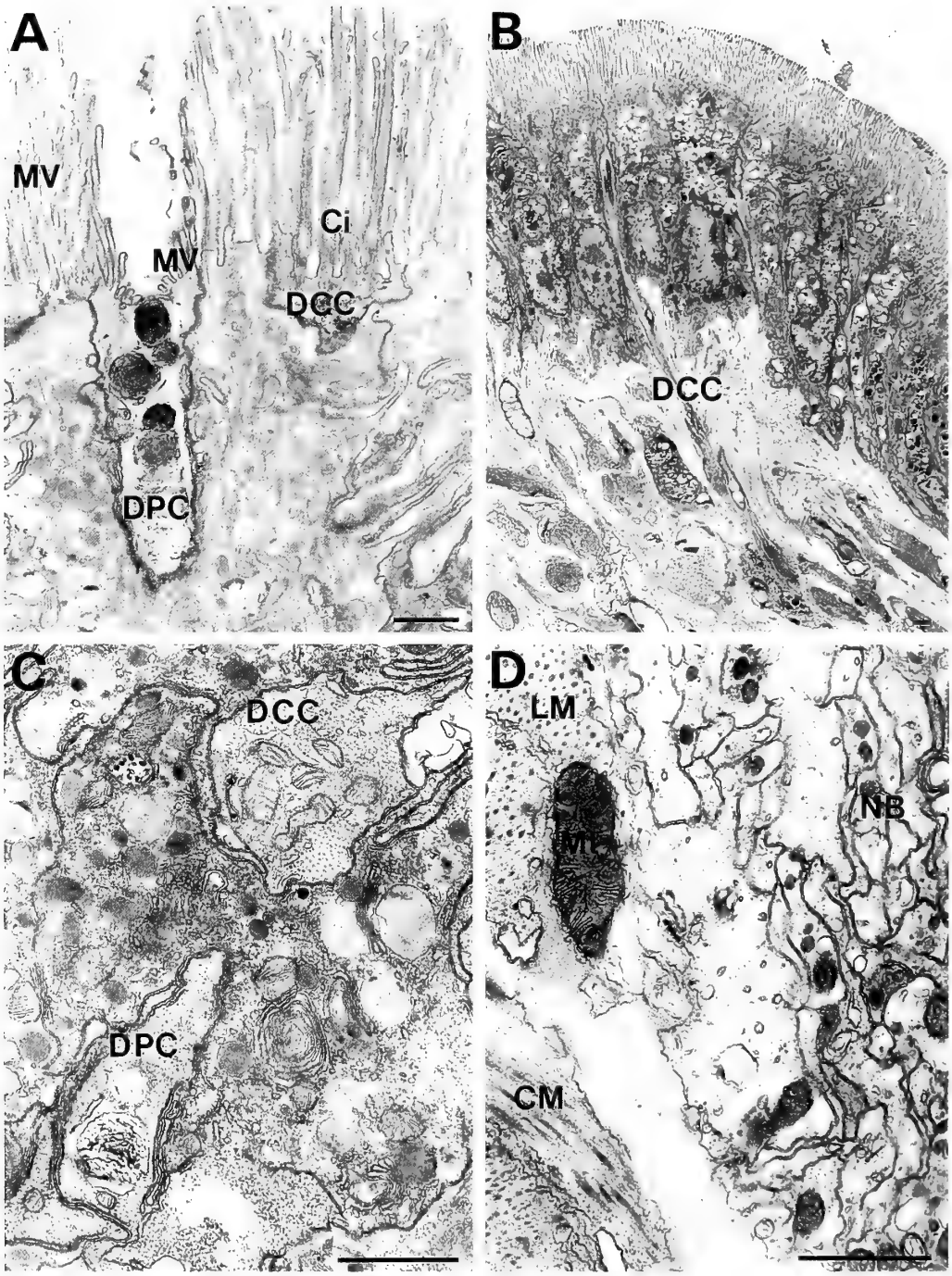

FIG. 5. Electron micrographs showing the distal processes of the ciliary cells (DCC) and pit cells (DPC), and nervous tissue. (A) Higher magnification showing cilia (Ci) of the ciliary cells, and a pit cell with its short microvilli (MV) in the outer epithelium of the siphon. (B) Lower magnification showing a fine distal process projecting from a ciliary cell. (C) A cross section of the distal processes of the ciliary and pit cells, showing many microtubules. (D) A cross section of the nerve bundle (NB) in the central region of the siphonal wall. CM, circular muscle; LM, longitudinal muscle. Scale bars, 1 μm.

DISCUSSION

It is unknown whether or not the mouse anti-squid rhodopsin serum used here cross-react with the *Ruditapes* rhodopsin, because a procedure to purify the *Ruditapes* rhodopsin has not yet been established. *Todarodes* and *Ruditapes*, however, belong to the same phylum, it is conceivable that their visual pigments will have sufficient homology for the anti-squid rhodopsin serum to cross-react with the *Ruditapes* rhodopsin.

The electron-microscopical observations revealed characteristic microvilli on the free surfaces of the outer and inner

EPCs (Fig. 4). It is suggested from the position of the microvilli (Figs. 2–4) and the appearance of the binding site of the anti-rhodopsin serum that the microvilli of the outer and inner EPCs contain rhodopsin-like immunoreactivity. The fact that the specific binding occurs in the overall surfaces of the outer and inner epithelia supports the idea above, because cells other than the EPCs, such as the ciliary and pit cells, are distributed only sparsely on both epithelia.

Intense fluorescence due to conjugated FITC was seen throughout the region beneath the inner epithelium (Fig. 2C). It is clear from electron-microscopical observations of the identical region (Fig. 4) that the fluorescence originates from groups of the granular cells. They can be seen scattered in the inner wall of the siphon with a low power dissecting microscope but their function remains to be investigated. In the SAB method, on the other and, the granular cells stained somewhat weakly with the serum (Fig. 3C, D). This inconsistency seems partly to be attributed to thickness of sections (15 μm in FITC, 5 μm in SAB). However, we should be cautious to decide whether or not the fluorescence of the granular cells is specific.

Although no differentiated photoreceptor cells were found in the siphon, *Ruditapes* clearly responds to illumination or shading of the siphon. The most probable candidate photoreceptor cells are the outer and inner EPCs which are provided with microvilli which show rhodopsin-like immunoreactivity. However, as has been known so far, photoreceptor cells which are able to transmit light information to secondary neurons and so on, and to induce effector responses are always nervous origin cells. Non-nervous cells such as epithelial cells have no axons and usually generate neither slow graded potentials nor action potentials. However, it has been reported in many hydroids (Cnidaria) that the epithelial cells generate electrically conductive action potentials which are able to excite nerves through electrical contact [13, 17]. Additionally, it has been reported in echinoids [21] and vertebrates [15] that pigment cells of non-nervous origin are directly photoresponsive. It may not therefore be unlikely that the outer and inner EPCs of *Ruditapes* siphon are photosensitive and pass light information to effector muscles through neihbouring nerves such as the ciliary and pit cells. Microvilli like those of the outer and inner EPCs are common in many molluscan epithelial cells (4, 11, 19, 20, 23) and their vertically projected appearance from the epithelial surface is reminiscent of those of primitive photoreceptor cells of some molluscs [3, 8, 9].

Crisp [5] has reported 2 types of sensory cells presumed to be mechanoreceptors cells (type I) and photoreceptor cells (type II) in the epithelium of a marine gastropod, *Nassarius*. The type I cells with cilia resemble the ciliary cells in *Ruditapes*. Type II cells with regressed cilia resemble the pit cells in *Ruditapes* except that the latter has no cilia. Based on morphology alone, the ciliary cells might be mechanoreceptive. The pit cells have short microvilli and a concaved distal portion, which rather suggest a chemoreceptive function. This does not necessarily mean that the ciliary and pit cells are not photosensitive, because directly photosensitive nerves are widely known in extraocular photoreceptive systems [18, 24].

Light [12] suggested from the light-microscopical observations of the siphon of *Mya*, that the pear-shaped cells may be photoreceptor cells. In *Ruditapes*, however, cells comparable to those of *Mya* could not be found, although there is presently no sufficient information on the ultrastructure of the pear-shaped cells.

ACKNOWLEDGMENTS

We thank Dr. Y. Kito, Osaka University, for his kind gift of purified squid rhodopsin and also Dr. I. G. Gleadall, Ohu University, for his useful comments and correcting the manuscript.

REFERENCES

1 Barber VC, Evans EM, Land MF (1967) The fine structure of the eye of the mollusc *Pecten maximus*. Z Zellforsch 76: 295–312

2 Barber VC, Land MF (1967) Eye of the cockle, *Cardium edule*: anatomical and physiological investigations. Experientia 23: 677–678

3 Brandenburger JL, Eakin RM (1970) Pathway of incorporation of vitamine A $^3H_2$ into photoreceptors of a snail, *Helix aspersa*. Vision Res., 10: 639–653.

4 Chia Fu-S, Koss R (1982) Fine structure of the larval rhinophores of the nudibranch, *Rostanga pulchra*, with emphasis on the sensory receptor cells. Cell Tiss Res 225:235–248

5 Crisp M (1971) Structure and abundance of receptors of the unspecialized external epitherium of *Nassarius reticulatus* (Gastropoda, Prosobranchia). J Mar Biol Ass U K 51: 865–890

6 Gillary HL, Gillary EW (1979) Ultrastructual features of the retina and optic nerve of *Strombus luhuanus*, a marine gastropod. J Morphol 159: 89–116

7 Jacklet JW (1969) Electrophysiological organization of the eye of *Aplysia*. J Gen Physiol 53: 21–42

8 Katagiri Y, Katagiri N, Fujimoto K (1985) Morphological and electrophysiological studies of a multiple photoreceptive system in a marine gastropod, *Onchidium*. Neurosci Res (Suppl 2): 1–15

9 Kataoka S, Yamamoto T-Y (1981) Diurnal changes in the fine structure of photoreceptors in an abalone, *Nordotis discus*. Cell Tissue Res 218: 181–189.

10 Kennedy D (1960) Neural photoreception in a lamellibranch mollusc. J. Gen. Physiol., 44: 277–299.

11 Lane N J (1963) Microvilli on the external surfaces of gastropod tentacles and body-walls. Quart J Micr Sci 104: 495–504

12 Light VE (1930) Photoreceptors in *Mya arenaria*, with special reference to their distribution, structure, and function. J Morphol Physiol 49: 1–43

13 Mackie GO, Passano LM (1968) Epithelial conduction in Hydromedusae. J Gen Physiol 52: 600–621

14 Messenger JB (1981) Comparative physiology of vision in molluscs. In "Handbook of Sensory Physiology Vol VII/6C" Ed by H Autrum, Springer-Verlag, Berlin, Heidelberg, New York, pp 93–200

15 Naora H, Takabatake I, Iga T (1988) Spectral sensitivity of melanophores of a freshwater teleost, *Zacco temmincki*. Comp Biochem Physiol 90A: 147–149

16 Nashima K, Mitsudo M, Kito Y (1979) Molecular weight and

structural studies on cephalopod rhodopsin. Biochim Biophys Acta 579:155–168

17 Ohtsu K (1980) Electrical activities in the subtentacular region of the anthomedusan *Spirocodon saltatrix* (Tilesius). Biol Bull 159: 376–393

18 Ohtsu K (1983) UV-visible antagonism in extraocular photosensitive neurons of the anthomedusa, *Spirocodon saltatrix* (Tilesius) J Neurobiol 14:145–155

19 Osborne N N, Cottrell G A (1971) Distribution of biogenic amines in the slug, *Limax maximus*. Z Zellforsch 112: 15–30

20 Paillard C, Le Pennec M (1993) Ultrastructural studies of the mantle and the periostracal lamina in the manila clam, *Ruditapes philippinarum*. Tissue Cell 25:183–194

21 Weber W, Danbach M (1974) Light-sensitivity of isolated pigment cells of the sea urchin *Centrostephanus longispinus*. Cell Tiss Res 148: 437–440

22 Wilkens LA (1984) Ultraviolet sensitivity in hyperpolarizing photoreceptors of the giant clam *Tridacna*. Nature 309: 446–448

23 Wright B R (1974) Sensory structure of the tentacles of the slug, *Arion ater* (Pulmonata, Mollusca) 1. Ultrastructure of the distal epithelium, receptor cells and tentacular ganglion. Cell Tiss Res 151:229–244

24 Yoshida M (1979) Extraocular photoreception. In "Handbook of Sensory Physiology Vol VII/6A" Ed by H Autrum, Springer-Verlag, Berlin, Heidelberg, New York, pp 581–640

ZOOLOGICAL SCIENCE 11: 675–680 (1994)

Immunoreactivities to Rhodopsin and Rod/Cone Transducin Antisera in the Retina, Pineal Complex and Deep Brain of the Bullfrog, *Rana catesbeiana*

Tomoko Yoshikawa[1], Yumi Yashiro[1], Tadashi Oishi[1]*, Koichi Kokame[2] and Yoshitaka Fukada[2]

[1]*Department of Biology, Faculty of Science, Nara Women's University, Nara 630 and* [2]*Department of Pure and Applied Sciences, College of Arts and Sciences, University of Tokyo, Tokyo 153, Japan*

ABSTRACT—Birds and lower vertebrates are known to have extra-retinal photoreceptors in the pineal complex and deep brain. Although the photoreceptive function of the pineal complex has been investigated well, the exact location and nature of the deep brain photoreceptors are not known. In this study we tried to localize visual pigments and signal transduction proteins immunohistochemically in the brain of bullfrogs (*Rana catesbeiana*). The retina, and the brain with the pineal and the frontal organ were fixed with Zamboni's fixative and/or Bouin's solution. Immunoreactivities to three antisera against bovine rhodopsin (Rh-As), α-subunits of bovine rod (anti-pTrα) and cone transducin (anti-pTcα) were shown in the retina, pineal, frontal organ and hypothalamus. The retina and pineal were immunopositive to both Rh-As and anti-pTrα, whereas the frontal organ was immunopositive to only Rh-As and the hypothalamus was immunopositive to all three antisera. The cells which were immunoreactive to Rh-As, anti-pTrα and anti-pTcα were observed in the preoptic nucleus and suprachiasmatic nucleus in the hypothalamus. The shape of these immunoreactive cells in the hypothalamus was round or spindle-like with one or two immunoreactive nerve processes most of which were perpendicular to the ventricular surface. Western blot analysis of the hypothalamus, pineal and frontal organ demonstrated immunoreactive bands molecular weight of which corresponded to those of the retina (34 kDa, 38 kDa and 41 kDa). Thus, visual pigments and transducin-like proteins seem to exist in the hypothalamus as well as the pineal complex of frogs.

INTRODUCTION

Birds and lower vertebrates are known to have extra-retinal photoreceptors, such as the pineal complex including the frontal organ in frogs and the parietal eye in lizards and deep brain photoreceptors. In the quail pineal, at least two types of photoreceptor cells are known [8, 14], and in the pineal and frontal organs of frogs, there are at least three types of photoreceptor cells [14, 20].

Since Benoit's pioneer works [1], many studies on the deep brain photoreceptors have been done in avian species. The photoreceptors which mediate photoperiodism may well lie in the medio-basal hypothalamus [10, 18] according to a local illumination experiment established by Oishi and Kato [15]. Action spectra for the photoperiodic responses suggested the involvement of rhodopsin-like photopigment in the hypothalamus in intact quail [5, 6] and in blinded and pinealectomized quail [16]. In immunohistochemical studies, Silver *et al.* [19] reported that there were cells labeled with an opsin antibody in two distinct regions, the lateral septum and the infundibular region of the hypothalamus. But they failed to detect opsin in immunoblot analysis. Although Oishi, Yoshikawa and Yashiro (unpublished data) also showed positive results, Foster *et al.* [7] could not detect any immunopositive cells to opsin antibodies in the quail hypothalamus.

The cells at the ventricular border of septum in lizards were labeled with opsin antibodies, and opsins and retinals were detected in the anterior brain by immunoblot analysis and high performance liquid chromatography analysis, respectively [9].

In frogs, responses to white light stimulation can be recorded electrophysiologically from diencephalon and mesencephalon [2, 3]. Chromophores of rhodopsin, 11-cis and all-trans retinal, were also detected in the ventral part of brain including the hypothalamus [14].

Since antibodies against α-subunits of bovine rod and cone transducins (Trα and Tcα, respectively) have been developed and shown to react to rod and cone outer segments, respectively, in bovine [13] and chicken retinas [12], these antisera can classify the rod type and cone type photoreceptors and signal transductions. In this study, we tried to reveal the existence and localization of rhodopsin and transducins in the retina, pineal comlex and deep brain in the bullfrog by means of immunohistochemistry and immunoblot analysis.

MATERIALS AND METHODS

Experimental animals

Adult bullfrogs (*Rana catesbeiana*) were obtained from a local breeder.

Accepted September 12, 1994
Received May 23, 1994
* To whom correspondence should be addressed

Immunohistochemistry

The eyes and brains with the pineal and frontal organ were dissected (N=13). The tissues were fixed with Zamboni's fixative and/or Bouin's solution. After the tissues were dehydrated through graded alcohols, they were embedded in paraffin and sectioned at 4～6 μm. Deparaffinized sections were washed in PBS and immersed in 0.3% H_2O_2 in methanol to remove endogenous peroxidase.

As described previously [17], sections thus prepared were treated with ABC (abidin-biotin peroxidase complex) method. Briefly, after PBS wash, the sections were incubated with diluted normal serum (30 min), with primary antisera (over night at 4°C) , with biotinylated antibody solution (60 min), and with Vectastain ABC reagent (Vector, Burlingame) (30 min). Then peroxidase activities were demonstrated by diaminobenzidine (DAB; Nacalai Tesque, Kyoto) solution. The sections were washed in PBS for 30 min between each incubation. Normal serum, primary antisera, biotinylated antibody and ABC reagent were diluted with 0.3% triton X-100 in PBS. All processes except the incubation with primary antisera described above were done at room temperature. Anti-bovine rhodopsin antiserum (Rh-As, dilution: ×1000 or ×500 as described by Kawata *et al.* [11]), and antisera against synthetic oligopeptides [13] specific to α-subunits of bovine rod and cone transducins (anti-pTrα and anti-pTcα, respectively, dilution: ×500 as described by Kokame *et al.* [12]) were used as the primary antisera.

The preparations were observed with a Nomarski differential interference microscope.

Western blotting

The retina, hypothalamus, pineal, frontal organ, hypophysis and cerebrum were dissected out from six frogs and frozen in dry-ice alcohol and kept in a deep freezer (−85°C) until use. Each tissue except the retina was homogenized in 1% digitonin in PBS, and the retina was homogenized in saline. The homogenates were centrifuged (15000 rpm for 20 min), and each pellet was homogenized in 1% digitonin in PBS and centrifuged again. The supernatant was used for western blotting. Protein extracts were applied to 12% polyacrylamide gel and electrophoretically separated. Proteins in the gel were transferred to a Poly Screen sheet (Du Pont, Boston), and then, treated with the ABC method. Following processes, except the incubation with primary antisera were done at room temperature. The sheet of Poly Screen was incubated with 1% skim milk in PBS for 1 hour to block non-specific reaction, and then primary antiserum (over night at 4°C) and biotinylated secondary antibody (1 hour) diluted with 1% skim milk in PBS. Poly Screen sheet was washed with 1% skim milk in PBS between these incubations. Then the sheet was washed with 0.05% Triton X-100 in PBS to remove skim milk, and incubated with Vectastain ABC reagent. DAB solution or western blot chemiluminescence reagent (Du Pont, Boston) was used to visualize immunoreactive bands.

RESULTS

Immunohistochemistry

The outer segments and some parts of inner segments of rods in the retina were immunopositive to Rh-As (Table 1)

TABLE 1. Results of immunohistochemistry in the retinal and extra-retinal photoreceptors of bullfrogs

		Retina	Pineal	Frontal organ	Hypothalamus
Rh-As	B	++	++	++	++
	Z	++	++		−
	Z+B	++	++		+
anti-pTrα	B	−	−	−	++
	Z	++	−		−
	Z+B	++	+	−	+
anti-pTcα	B	−	−	−	++
	Z	−	−		−
	Z+B	−	−	−	+

Tissues were fixed with Bouin's solution (B), Zamboni's fixative (Z) or a combination of Zamboni's fixative and Bouin's solution (Z+B).
+: immunopopsitive, −: immunonegative

FIG. 1. Immunohistochemistry of the photoreceptor cells in the retina fixed with Zamboni's fixative. Anti-pTrα labeled rod outer (►) and inner segment (►) (A), but did not label cone cells (→). There were no immunoreactive cells to anti-pTcα (B). Scale bar=20 μm.

FIG. 2. Immunohistochemistry of the pineal fixed with Zamboni's fixative and Bouin's solution. The outer segments of the pinealocytes were stained with anti-pTrα (►) (A). There were no immunoreactivities to anti-pTcα (B). Scale bar=40 μm.

FIG. 3. Immunohistochemistry of the frontal organ fixed by Zamboni's fixative and Bouin's solution. There were no immunoreactivities to anti-pTcα. Scale bar=100 μm.

FIG. 4. Immunohistochemistry in the hypothalamus fixed with Bouin's solution. Three antisera were used ; Rh-As (A), anti-pTrα (B) and pTcα (C). Stained cells were located near the third ventricle (V). There were no differences in the extent of immunoreactivity and distribution of immunoreactive cells among each antiserum. The immunoreactive cells distributed in the suprachiasmatic nucleus (C1) and preoptic nucleus (A1, B1). The cells showed round or spindle-like shape and had immunoreactive nerve processes (►), most of which were perpendicular to the ventricular surface in cross sections. These cells have immunopositive cytoplasm (→) and immunonegative nucleus (→) (A2, B2 and C2). The diameter of these cells was 9.7～21.5 μm, and the average was 15.0 μm. A1, B1, C1 : Scale bar=100 μm. A2, B2, C2 : Scale bar=20 μm.

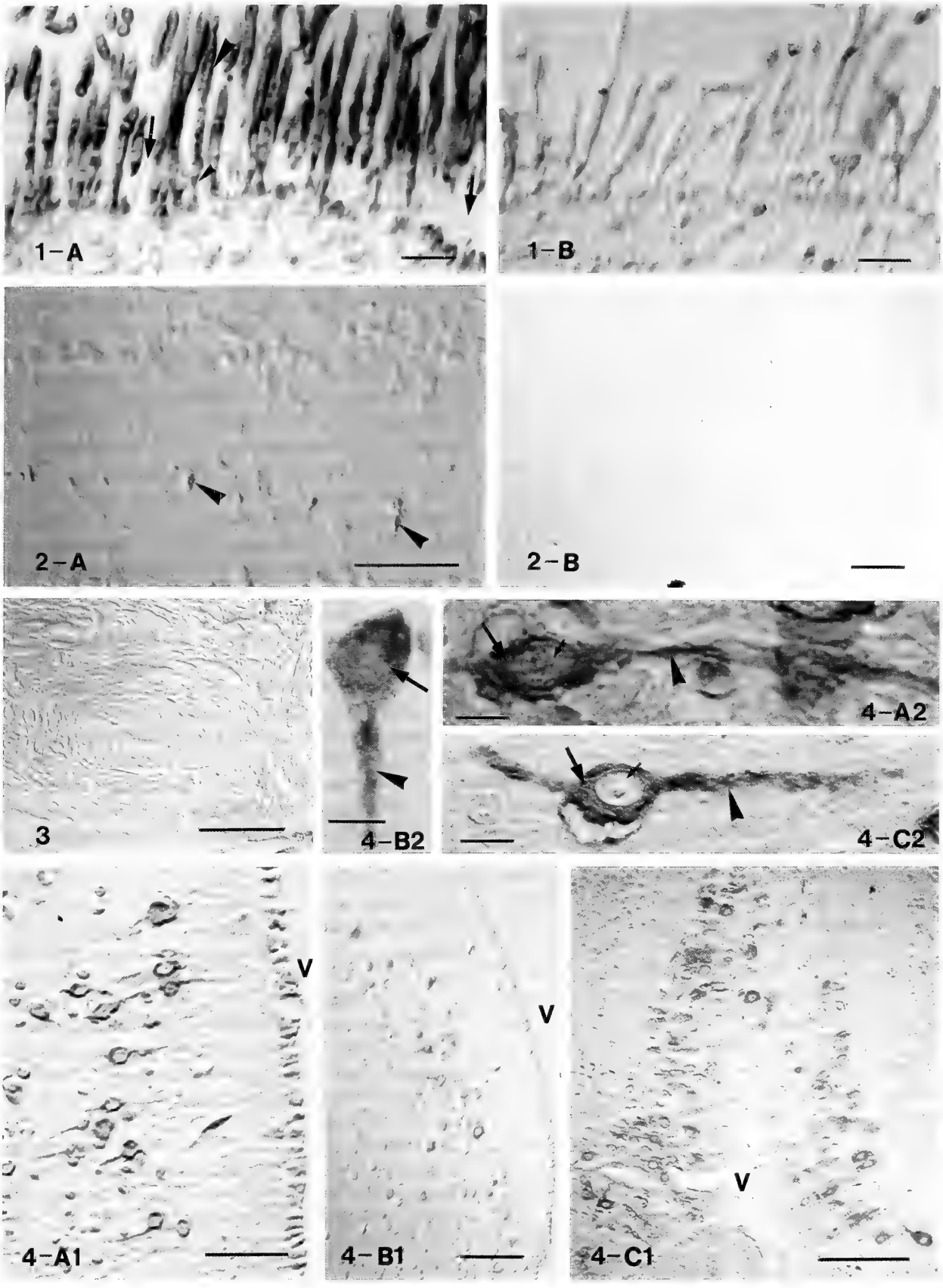
1-A
1-B
2-A
2-B
3
4-B2
4-A2
4-C2
V
4-A1
V
4-B1
V
4-C1

and anti-pTrα (Fig. 1-A), while there were no immunoreactivity to anti-pTcα (Fig. 1-B). But there were some differences in the immunoreactivities to anti-pTrα depending on the fixative used (Table 1), i.e., the result was negative when Bouin's solution was used. Cone cells were immunonegative to all three antisera.

The outer segments and cell bodies of many pinealocytes were immunopositive to Rh-As (Table 1). The outer segments of some pinealocytes were immunopositive to anti-pTrα (Fig. 2-A), while the other cells were immunonegative to the antiserum. But the positive immunoreactivities to anti-pTrα were obtained only in the pineal fixed with a combination of Zamboni's fixative and Bouin's solution, showing difference depending on the fixative used (Table 1). There were no cells immunopositive to anti-pTcα (Fig. 2-B).

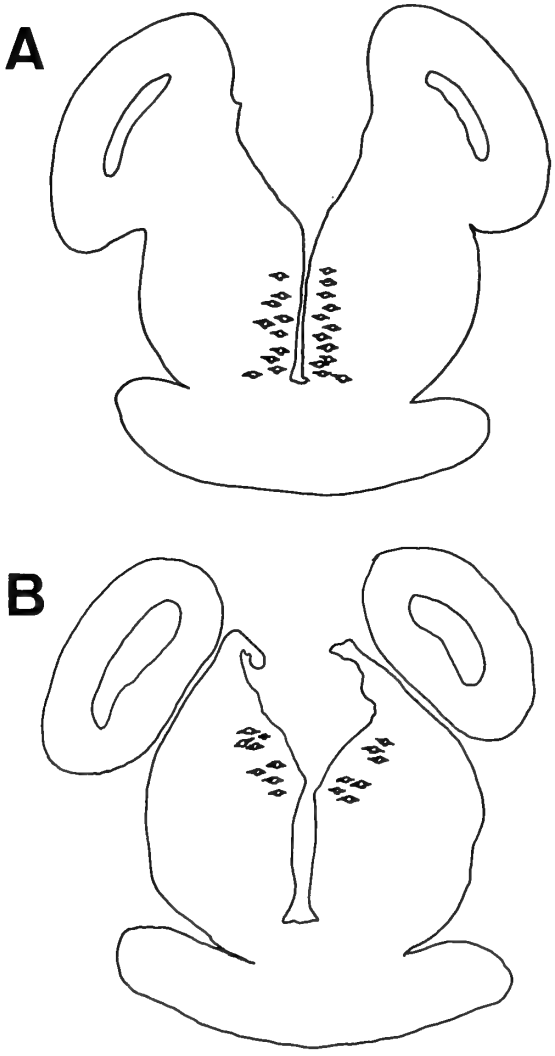

FIG. 5. Schematic drawing of cross sections of the brain. The areas where immunoreactive cells located were shown (A, B). These areas corresponded to the suprachiasmatic nucleus (A) and preoptic nucleus (B) in the hypothalamus. The immunoreactive cells in the suprachiasmatic nucleus were located in front of the preoptic nucleus. Population density of these cells was higher in the suprachiasmatic nucleus than in the preoptic nucleus.

The frontal organ was immunopositive to Rh-As but immunonegative to both anti-pTrα and anti-pTcα (Fig. 3, Table 1).

The cells in the hypothalamus near the third ventricle were immunopositive to all three antisera (Rh-As, anti-pTrα and anti-pTcα) (Fig. 4-A, B, C). The area where the immunopositive cells were observed was divided into two parts (Fig. 5), and these areas corresponded to the suprachiasmatic nucleus and preoptic nucleus. There were the pineal and choroid plexus in the upper part of third ventricle of the area. The immunoreactive cells in the suprachiasmatic nucleus were located in front of the preoptic nucleus. Population density of immunopositive cells was higher in the suprachiasmatic nucleus (Fig. 4-C1) than in the preoptic nucleus (Fig. 4-A1, B1). The results obtained from serial sections suggest that all three immunoreactive substances were localized in one and the same cells. The shape of immunoreactive cells was round or spindle-like with one or two immunoreactive nerve processes, most of which were perpendicular to the ventricular surface in cross sections (Fig. 4-A1, C1). In sagittal sections, immunoreactive nerve processes were not observed, indicating that the direction of nerve processes is perpendicular to the sagittal axis. There were no differences in the extent of immunoreactivity among each antiserum. No particular structures except the nucleus were observed in the immunoreactive cells (Fig. 4-A2, B2, C2). All these cells had immunopositive cytoplasm and immunonegative nucleus. The diameter of these cells ranged from 9.7 μm to 21.5 μm, and the average was 15.0 μm. In the hypothalamus, there were some differences in immunoreactivities among the fixatives used (Table 1), i.e., the immunoreactivities to all three antisera became unclear when Zamboni's fixative was used.

Positive immunoreactivities to Rh-As and anti-pTrα were observed in the retina, pineal and hypothalamus, but the immunoreactivity to anti-pTcα was positive only in the hypothalamus (Table 1).

Western blot analysis

Immunoblot analysis of retinal extracts with Rh-As demonstrated two bands, molecular weights of which were 34 kDa and 36 kDa, and the analysis with anti-pTrα and anti-pTcα demonstrated a band of 41 kDa and 38 kDa, respectively (Fig. 6). In the extracts of the hypothalamus, pineal and frontal organs, 34 kDa band was demonstrated with Rh-As (Fig. 6). There were immunoreactive bands to anti-pTcα in the extracts of the hypothalamus and cerebrum, molecular weights of which were 38 kDa and 120~130 kDa (Fig. 6). Some bands except those described above were also demonstrated by immunoblot analysis, but they were non-specific bands to the antisera, because those bands were demonstrated without the primary antisera.

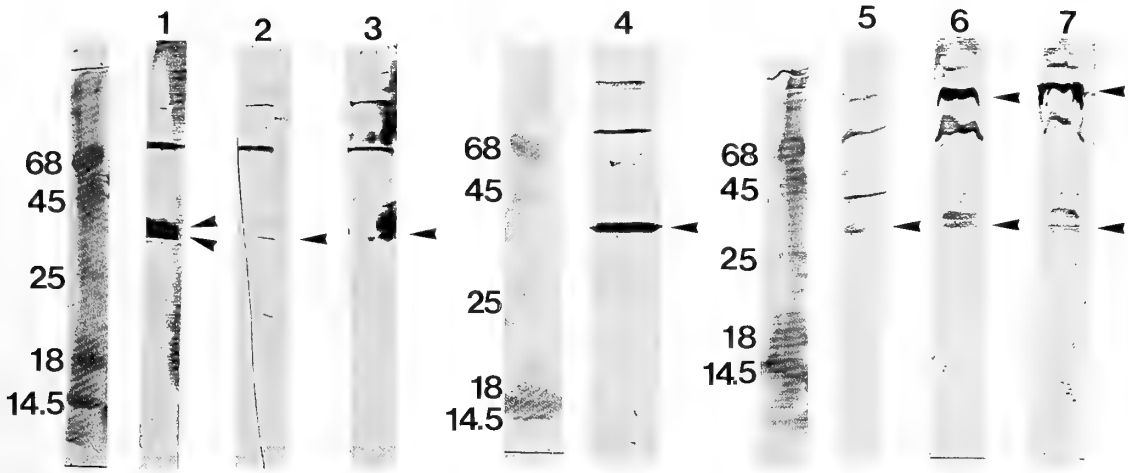

FIG. 6. Immunoblot analysis of protein extracts from tissues. Immunoreactive bands were indicated by arrow heads (►). Immunoreactive bands to Rh-As were detected in the extracts of retina (lane 1) (34 kDa, 36 kDa), pineal (lane 2) and hypothalamus (lane 3) (34 kDa). An immunopositive band to anti-pTrα was detected in the retinal extract (lane 4) (41 kDa), and those to anti-pTcα were detected in the extracts of retina (lane 5) (38 kDa), hypothalamus (lane 6) and cerebrum (lane 7) (38 kDa, 120~130 kDa).

DISCUSSION

The present study using Rh-As in the retina and pineal complex confirmed our previous results [11, 14]. Since the pineal was immunopositive to antibodies against Rh and pTrα (Fig. 2), the pineal might also have rod-like photoreceptors and a signal transduction system. Since the frontal organ was immunoreactive to Rh-As but not to anti-pTrα and -pTcα (Fig. 3), the signal transduction system in the frontal organ might be different from the retina or transducin molecules might have sequences different from bovine transducins, and can not be identified by the antibodies used. There were some immunoreactive cells to the antisera against photoreceptor proteins (rhodopsin and transducins) in the suprachiasmatic nucleus and preoptic nucleus of the hypothalamus (Fig. 4). Immunoblot analysis of the hypothalamus with Rh-As demonstrated an immunoreactive band and the molecular weight corresponded to 34 kDa band of the retina (Fig. 6). Masuda *et al.* [14] detected 11-cis and all-trans retinal in the ventral part of the frog diencephalon including the hypothalamus. These results indicate that visual pigments, chromophores and proteins involved in the signal transduction of light exist in the hypothalamus of frogs. The mesencephalic and diencephalic unit of the blinded and pinealectomized frogs showed electrophysiological responses to light [2, 3]. These responses might be induced by photoreception through rhodopsin system. From the immunohistochemical results of serial sections, we suppose these immunoreactive substances to the three antisera are localized together in the same cells in the hypothalamus.

When the retinas were fixed with Bouin's solution, the outer segments of photoreceptor cells were immunopositive to Rh-As and immunonegative to anti-pTrα. However, they were immunopositive to both Rh-As and anti-pTrα when Zamboni's fixative or a combination of Zamboni's fixative and Bouin's solution was used. The same results were obtained from the retina of Japanese quail (*Coturnix coturnix japonica,* unpublished data). Since rhodopsin is bound to disk membranes and transducins are peripheral proteins, differences in the immunoreactivity depending on the fixatives and tissues might be due to differences in characters of proteins. When the hypothalamus was fixed with Bouin's solution, there was an intense immunoreactivity to all these antisera (Fig. 4), while there were no immunoreactivities when it was fixed with Zamboni's fixative. When fixed with Zamboni's fixative and then Bouin's solution, there was a weak immunoreactivity (Table 1). Thus, the immunoreactivity of the hypothalamus to the antisera was different from the retina depending on each fixative used. Since we do not know how photoreceptor proteins are localized in the cells of the hypothalamus, immunohistochemistry using an electron microscope is now in progress in our laboratory.

Immunoblot analysis with Rh-As and anti-pTrα in retinal extracts clearly demonstrated immunoreactive bands. The result with Rh-As corresponded to those reported by Fong *et al.* [4]. Other bands showed very weak immunoreactivities, though they were specific to each antiserum.

Locomotor activity of blinded frogs (*Xenopus*) can be entrained to light-dark cycles (Fujisawa, Harada, Kegasawa and Oishi, in preparation). Since the pineal of *Xenopus* is not developed well, the results indicate that the deep brain photoreceptor (probably hypothalamus) is involved in the entrainment of circadian rhythms as the extra-retinal and extra-pineal photoreceptor. Our results suggest that the visual pigments involved in these phenomena are rhodopsin-like substances and that the signal transduction is mediated by transducin-like substances.

Foster *et al.* [9] reported opsin localization and existence of retinoids in the brain of lizards. There were immunopositive cells to a monoclonal antibody against opsin in the brain of ring doves [19]. These results in addition to our present results indicate that rhodopsin-like photopigments involved

in the brain photoreceptor prevail among birds and lower vertebrates.

REFERENCES

1 Benoit J (1935) Stimulation par la lumière artificielle du développement testiculaire chez des canards aveuglés par énucléation des globes oculaires. Comp Rend Soc Biol 120: 136–139

2 Cadusseau J, Galand G (1980) Electrophysiological evidence for white light sensitivity of the encephalon in eyeless and pinealectomized frogs. Exp Brain Res 40: 339–341

3 Cadusseau J, Galand G (1981) Electrophysiological recordings of an extraocular and extrapineal photoreception in the frog encephalon. Brain Res 219: 439–444

4 Fong SL, Landers RA, Bridges CDB (1985) Varieties of rhodopsin in frog rod outer segment membranes: analysis by isoelectric focusing. Vision Res 25: 1387–1397

5 Foster RG, Follett BK (1985) The involvement of a rhodopsin-like photopigment in the photoperiodic response of the Japanese quail. J Comp Physiol A 157: 519–528

6 Foster RG, Follett BK, Lythgoe JN (1985) Rhodopsin-like sensitivity of extra-retinal photoreceptors mediating the photoperiodic response in quail. Nature 313: 50–52

7 Foster RG, Korf HW, Schalken JJ (1987) Immunochemical markers revealing retinal and pineal but not hypothalamic photoreceptor systems in the Japanese quail. Cell Tissue Res 248: 161–167

8 Foster RG, Schalken JJ, Timmers AM, De Grip WJ (1989) A comparison of some photoreceptor characteristics in the pineal and retina. 1. The Japanese quail (*Coturnix coturnix*). J Comp Physiol A 165: 553–563

9 Foster RG, Garcia-Fernandez JM, Provencio I, De Grip WJ (1993) Opsin localization and chromophore retinoids identified within the basal brain of the lizard *Anolis carolinensis*. J Comp Physiol A 172: 33–45

10 Homma K, Sakakibara Y (1971) Encephalic photoreceptors and their significance in photoperiodic control of sexual activity in Japanese quail. In "Biochronometry" Ed by Menaker M, Natl. Acad. Sci., Washington DC, pp 333–341

11 Kawata A, Oishi T, Fukada Y, Shichida Y, Yoshizawa T (1992) Photoreceptor cell types in the retina of various vertebrate species: immunocytochemistry with antibodies against rhodopsin and iodopsin. Photochem Photobiol 56: 1157–1166

12 Kokame K, Fukada Y, Shichida Y, Okada M, Honda Y, Yoshizawa T (1993) Identification of the α-subunits of rod and cone transducin in chicken photoreceptor cells. Exp Eye Res 57: 135–140

13 Lerea CL, Somers DE, Hurley JB, Klock IB, Bunt-Milam AH (1986) Identification of specific transducin α subunits in retinal rod and cone photoreceptors. Science 234: 77–80

14 Masuda H, Oishi T, Ohtani M, Michinomae M, Fukada Y, Shichida Y, Yoshizawa T (1994) Visual pigments in the pineal complex of the Japanese quail, Japanese grass lizard and bullfrog: immunocytochemistry and HPLC analysis. Tissue Cell 26: 101–113

15 Oishi T, Kato M (1968) Pineal organ as a possible photoreceptor in photoperiodic testicular response in Japanese quail. Mem Fac Sci Kyoto Univ Ser Biol 2: 12–18

16 Oishi T, Ohashi K (1993) Effects of wavelengths of light on the photoperiodic gonadal response of blinded-pinealectomized Japanese quail. Zool Sci 10: 757–762

17 Oishi T, Kawata A, Hayashi T, Fukada Y, Shichida Y, Yoshizawa T (1990) Immunohistochemical localization of iodopsin in the retina of chicken and Japanese quail. Cell Tissue Res 216: 397–401

18 Oliver J , Jallageas M, Baylé JD (1979) Plasma testosterone and LH levels in male quail bearing hypothalamic lesions or radioluminous implants. Neuroendocrinology 28: 114–122

19 Silver R, Witkovsky P, Horvath P, Alones V, Barnstable CJ, Lehman MN (1988) Coexpression of opsin-and VIP-like-immunoreactivity in CSF-contacting neurons of the avian brain. Cell Tissue Res 253: 189–198

20 Vigh B, Vigh-Teichmann I (1986) Three types of photoreceptors in the pineal and frontal organs of frogs: ultrastructure and opsin immunoreactivity. Arch Histol Jap 49: 495–518

ZOOLOGICAL SCIENCE 11: 681–691 (1994)

The Phagocytes in Hemolymph of *Halocynthia roretzi* and Their Phagocytic Activity

SHIN-ICHI OHTAKE, TAKEYUKI ABE, FUMIO SHISHIKURA, and KUNIO TANAKA

Department of Biology, Nihon University School of Medicine, Oyaguchi Itabashi, Tokyo 173, Japan

ABSTRACT—The phagocytes in hemolymph of *Halocynthia roretzi* and their phagocytic activity *in vitro* were studied by electron microscopy. Hemocytes were ultrastructurally classified as follows: Large granular amebocytes (LGs), small granular amebocytes (SGs), eight types of vacuolated or vesicular cells, dense granular cells and lymphoid cells. The vacuolated or vesicular cells, V1-V8, were distinguished from each other by the size of vacuole and the nature of inclusions. The identification of phagocytic cells and possible targets were examined *in vitro*. Freshly collected hemolymph was incubated with latex beads (LB) of 1, 5, 26 μm in diameter, SRBC, *Escherichia coli* or small pieces of tunic. Small granular amebocytes actively ingested all the particles except the 26 μm-LB. They surrounded the tunic pieces and the 26 μm-LB. LGs ingested only 1 μm-LB. Their activity was, however, weaker than that of SGs. We could not find any phagocytosed particles in other hemocytes during a 30 min incubation. Furthermore, the plasma factor(s) that activated the phagocytosis to SRBC, did not influence that to the LB.

INTRODUCTION

The basic strategies of self defense mechanism of higher vertebrates are the innate immunity including phagocytosis or encapsulation and the acquired immunity. Immunological specificity and acquired memory are essential features of vertebrate immunological competence [19]. Tunicates and vertebrates are thought to have derived from the same ancestor. However, evidence concerning immunological responses on tunicates is limited. As in vertebrates, the recognition and reaction system of foreignness is a function of the hemocytes and hemolymph plasma in ascidians. Humoral defense factors reported on ascidian hemolymph are natural aggulutinins [3, 12, 32, 34, 36] and antimicrobial factors [2, 20]. Immunoglobulins and complement cascade have, however, not yet been determined in the plasma of these animals. Immunological specificity and memory are yet to be clearly demonstrated in ascidians.

The innate cellular defense mechanisms such as phagocytosis to foreign materials may be important in these animals. Many authors observed phagocytosis or encapsulation when foreign bodies were introduced into the tunic, or the vascular system. For example, carbon particles which were injected into the tunic of the body wall of *Halocynthia aurantium* were phagocytosed by hyaline amebocytes [30], glass fragments which were inserted into the branchial sac of *Molgula manhattensis* were encapsulated by vanadocytes [1] and parasitic copepods in some ascidians were encapsulated by host cells [6, 23]. Recently, electron microscopic observations of hemocytes of ascidians have accumulated, although the knowledge of functional characterization of the cellular reaction to defense mechanism is still limited [4, 7, 15, 22, 24, 32, 37]. We therefore wanted to define the phagocytic cell of *H. roretzi*. This ascidia can be purchased from cultivators and kept in a laboratory aquarium, and the responses of its hemocytes toward foreign materials are easily observable *in vitro*.

In this paper, the classification of hemocytes, the identification of phagocytic cells in *Halocynthia roretzi* and their possible targets were studied *in vitro* by electron microscopy. The twofold aim of the present paper is to clarify the influence of plasma factors, pH and Ca^{2+}, Mg^{2+} ions in phagocytic activity for different targets.

Accepted July 13, 1994
Received May 6, 1994

MATERIALS AND METHODS

Animals and hemocytes

Cultured solitary ascidians, *Halocynthia roretzi*, purchased from fisheries at Mutsu Bay, Asamushi, Aomori prefecture were used. The animals were maintained in laboratory aquaria containing natural sea water at 7–10°C without feeding and used for experiments within three weeks. Their morphological features did not change during that period. The hemolymph was collected into sterilized ice-cold tubes by cutting the tunic at the bottom of the body or from the space just beneath the tunic papilla at the upper part of the animal with a sterilized plastic syringe.

Preparations for electron microscopy

The hemocytes were suspended into 0.1% glutaraldehyde in 1.5% NaCl solution buffered with 0.2 M sodium cacodylate at pH 7.4. They were packed into a pellet by centrifugation (225×*g*, 5 min) 2 hr after fixation. The pellet was continuously fixed in the same fixative for 22 hr at room temperature and post-fixed in 1% osmium tetroxide in the same buffer for 2 hr on ice. Epoxy resin sections stained with uranyl acetate and lead citrate were observed with a JEM 100T electron microscope (Japan Electron Optics, Tokyo). The count of cell numbers with electron microscopy was performed on the sections

cut out from the different blocks taken from one fixed specimen.

Phagocytosis and encapsulation

The inorganic and organic targets used for phagocytosis or encapsulation were: Latex beads (LB) of 1.03 μm (small LB), 4.62 μm (middle LB) and 25.7 μm (large LB) in diameter as inorganic targets; fresh red blood cells of sheep (SRBC) (Nippon Bio-Test Inc.), SRBC fixed for 24 hr in 1% glutaraldehyde (gSRBC), *Escherichia coli* W3630 (a gift from Professor Masaya Kawakami, Kitasato University School of Medicine) and tunic pieces cut into 2 mm cubes (TP) as organic targets. The organic targets, except for the TPs, were washed three times in phosphate-buffered saline (PBS) and suspended in Pantin's artificial sea water (NaCl 23.51 g, $MgCl_2 \cdot 6H_2O$ 10.685 g, KCl 0.725 g, $CaCl_2$ 1.119 g, Na_2SO_4 3.937 g/l) [25] buffered with 20 mM HEPES (*N*-2-hydroxyethyl-piperazine-*N'*-2-ethanesulfonic acid) at pH 7.2 (ASW). The freshly collected hemolymph and the washed hemocytes after being suspended in various media were incubated with these targets at 23 ± 1°C with agitation every minute. The hemocytes were fixed at 5, 10, 20 and 30 min of the incubation time for electron and light microscopic observations. The final concentrations of targets in incubation media were: LB, 0.05 w/v%; SRBC, 2.5×10^7 cells/ml; gSRBC, 2.9×10^7 cells/ ml; *E. coli*, $1.3–1.6 \times 10^8$ cells/ml and TP, 5 pieces in 3 ml.

Effects of Ca^{2+}, Mg^{2+} and pH on phagocytosis of washed hemocytes

The pH of the hemolymph collected was immediately adjusted to 5.6 with one tenth volume of Ca^{2+}- and Mg^{2+}- free ASW containing 50 mM MES ([N-morpholino]ethanesulfonic acid) and 0.1 M EDTA for the prevention of hemocytes aggregation. Hemocytes were washed three times in Ca^{2+}- and Mg^{2+}- free acid ASW and resuspended in the following incubation media: ASW, Ca^{2+}- and Mg^{2+}-free neutral ASW containing 0.54 mM EDTA ($Ca^{2+} \cdot Mg^{2+}$ free ASW), ASW buffered with 20 mM MES at pH 5.6 (acid ASW) and Ca^{2+}- and Mg^{2+}- free acid ASW containing 0.54 mM EDTA ($Ca^{2+} \cdot Mg^{2+}$ free acid ASW). These media were used after sterilization by an autoclave. Each hemocyte suspension was incubated with small LB at 23 ± 1°C with agitation every minute. The final concentration of hemocytes and small LB were 2×10^7 cells/ml and 1×10^8 particles/ml, respectively. After dilution with ASW at 5, 10 and 20 min of the incubation, an aliquot of the mixture was poured on a slide glass and settled for 5 min in order for the hemocytes to adhere onto the glass surface and extend their pseudopodia. Specimens were poured off ASW, dried in air and stained with May-Grünward Giemsa solution. The phagocytic activity was shown as the ratio of the number of SG ingesting small LB to that of total SG counted under a light microscope.

The effect of hemolymph plasma on the phagocytic activity

After washing three times with $Ca^{2+} \cdot Mg^{2+}$ free acid ASW, the hemocytes (3×10^7 cells/ml) were incubated with SRBC or middle LB in their own plasma, plasma diluted with ASW or ASW. The concentration of the target particles was adjusted to the same as of the hemocytes. The phagocytic activities of SG in each medium for 20 min at 23 ± 1°C was measured with a light microscope in the same way as in the previous experiment.

RESULTS

Types and distribution of hemocytes

The mean density of cells in hemolymph from 5 animals was $2–3 \times 10^7$ cells per milliliter and did not markedly change during the 30 days' cultivation at 7–10°C in our aquaria. The twelve types of hemocytes, which were distinguished under an electron microscopic observation, were as follows: Small granular amebocytes (SGs), large granular amebocytes(LGs), dense granular cells, lymphoid cells and eight types of vacuolated or vesicular cells, V1-V8, which were classified by the size of the vacuole and the nature of inclusions (Fig. 1 and 2). Some intermediate and immature cells were occasionally observed besides the typical types.

Table 1 shows the composition of hemocytes which were measured in five animals from different batches reared in aquaria for 1–17 days. The percentages of SG, LG and V2 were not significantly different among the animals, that of other vacuolated cells, however, differed for each animal.

Small granular amebocyte (SG) (Fig. 1A) The nucleus of SG was irregular in shape and was usually in the center of the cell. Smooth tubulo-vesicular components of various sizes, some of which included electron dense material, and small granules about 0.2–0.4 μm in diameter were observed in the cytoplasm. The granules consisted of homogeneous and electron dense material, which was always more electron dense than LG, and some granules showed elongated shapes. The Golgi apparatus was at the peripheral region of the nucleus. The SG was obviously phagocytes, because several phagosomes, which varied in size and content, were scattered in the cytoplasm. Occasionally, the SG engulfed and degraded a hemocyte. These cells extended the pseudopodia in every direction and possessed high mobility on a slide glass. The SG was the only phagocytic hemocyte identified with a light microscope. The phagocytic processes of SRBC and middle LB by these cells were easily observed *in vitro*.

Large granular amebocyte (LG) (Fig. 1B) These cells were another type of granular amebocytes and their density was the second in line. The shape of the LG fixed immediately after collection was round but it changed to a rod shape about 8–13 μm in length with an irregular shaped nucleus *in vitro*. The Golgi apparatus and the rough endoplasmic reticulum were observed near the nucleus. Most of the cytoplasm was filled with spherical granules about 0.4–0.6 μm in diameter, larger than that of the SG and contained finely granular and homogeneous contents limited by a membrane. The LG elongated and extended its pseudopodia and some granules swelled *in vitro*. Bundles (50–125 nm in diameter) of short filaments (10–20 nm in diameter) appeared just beneath the cell surface when these cells were fixed by Karnovsky's fixative. They interlaced and were parallel to the membrane surface of both LG and SG.

Lymphoid cell (Fig. 1C) The lymphoid cells were about 3–5 μm in diameter and their cytoplasm had features similar to the lymphocytes of vertebrates.

Dense granular cell (Fig. 1D) The cells have a round shape about 4–5 μm in diameter. Extended types like SG and LG were not observed. The granules in the cytoplasm had a oval shape (about 0.4×0.6 μm) like the granules of the LG, and had almost the same electron density as the granules of

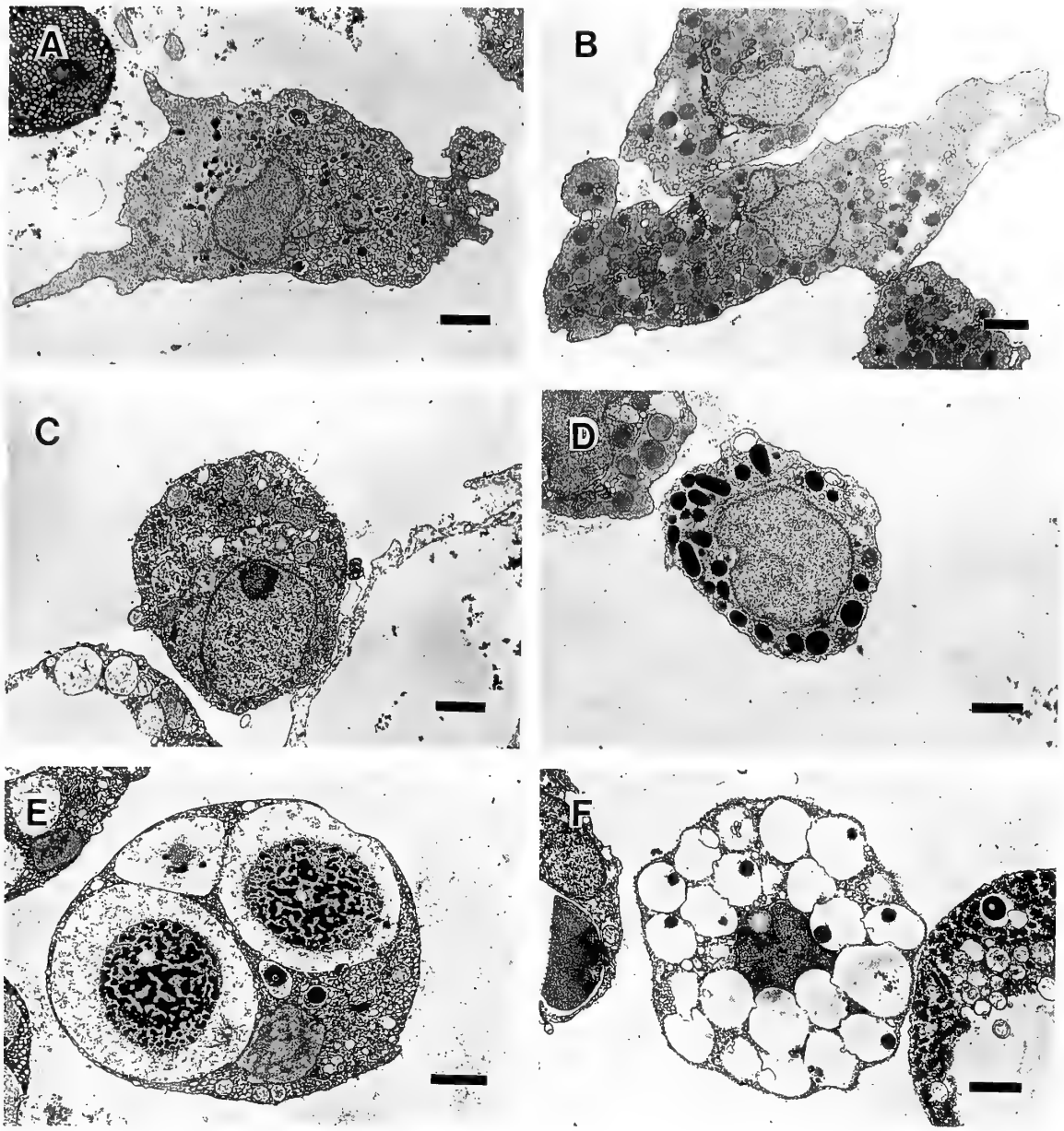

FIG. 1. The hemocyte types of *H. roretzi*. A: small granular amebocyte (SG), B: large granular amebocyte (LG), C: lymphoid cell (LY), D: dense granular cell (DG), E: V1, F: V2. Scale bars=1 μm.

the SG and were always more dense than the granules of LG.

Vacuolated or vesiculated cells The rest of the hemocytes were vacuolated or vesiculated cells. We distinguished eight types.

V1 (Fig. 1E) These cells were the most abundant cells in the hemolymph. They had a few large vacuoles, many small vesicles and a few small oval mitochondria in the cytoplasm, and an irregular shaped nucleus located at a peripheral side of the cytoplasm. It appeared that the vesicles fused each other to increase their sizes and their contents. They could finally become large vacuoles.

V2 (Fig. 1F) Many spherical vacuoles about 1–1.8 μm in size filled the cytoplasm with a nucleus at the central part of the cells. This type probably corresponds to a globular cell. Fine and dense granules were observed in the vacuoles.

V3 (Fig. 2A) Cells of this type had about ten vacuoles on one side of the cytoplasm in each section. Each vacuole contained electron dense and crescent-shape material.

V4 (Fig. 2B) These cells had many vacuoles and some of them contained fine granules or debris-like substance.

V5 (Fig. 2C) These cells were about 10–13 μm in diameter. The most characteristic feature of these cells was the existence of numerous vesicles about 0.2–0.6 μm in diameter and the well developed Golgi apparatus. The vesicles included very fine granules and the larger ones contain fibrous material. Their cytoplasm was stained basophilic by Wright or May-Grünward Giemsa stain.

V6 (Fig. 2D) Vacuoles with a homogeneous fine granular

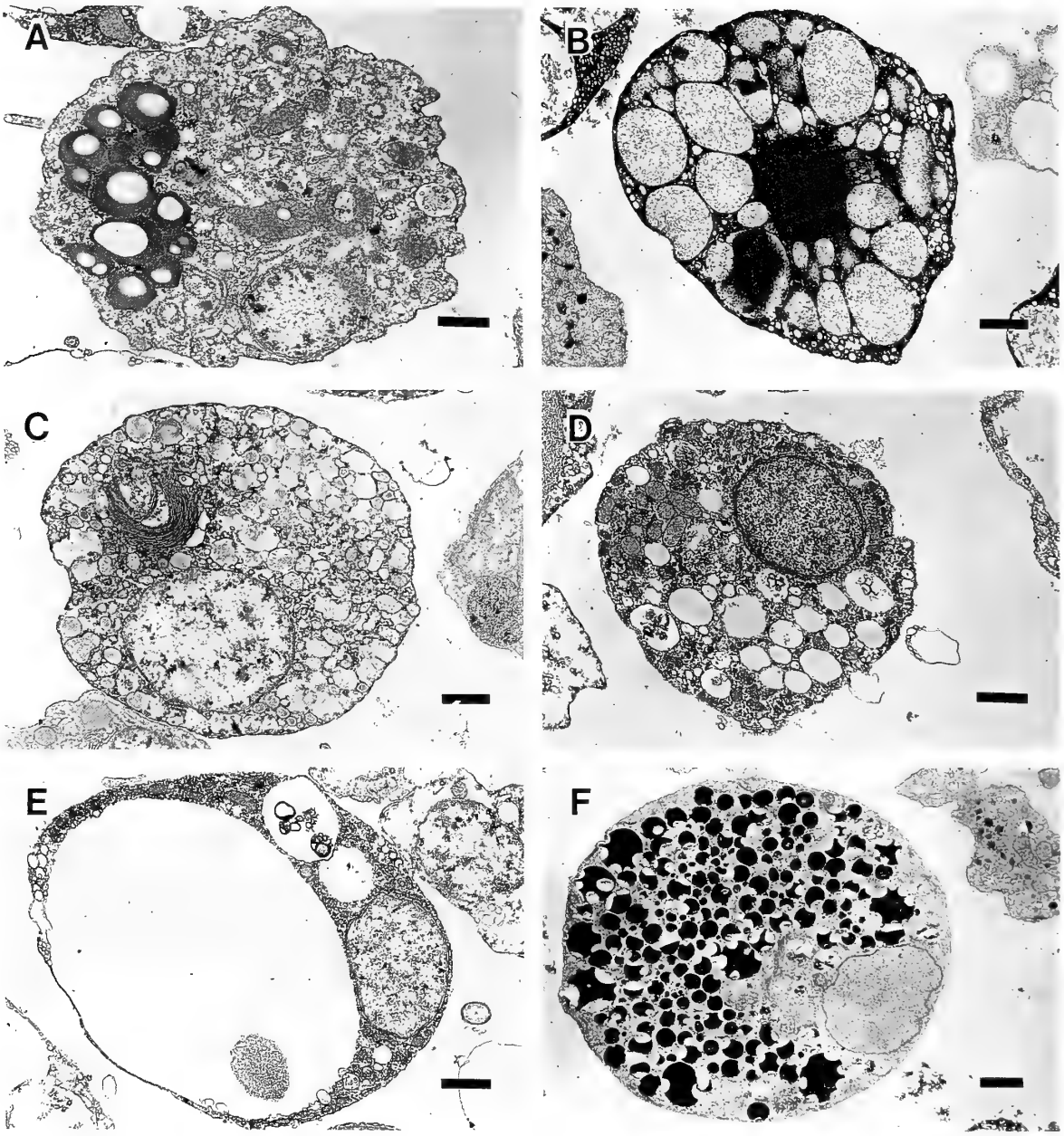

FIG. 2. The hemocyte types of *H. roretzi* (continued). A-F: V3-V8. Scale bars=1 μm.

content and vesicles in various sizes filled the cytoplasm. The nucleus was located peripherally in the cytoplasm.

V7 (Fig. 2E) This is a signet ring cell, very rare in the hemolymph of *H. roretzi*. These cells are about 6–12 μm in diameter and they have a single large vacuole occasionally containing granular material. The nucleus and their cytoplasm were located in the periphery of the cell.

V8 (Fig. 2F) Cells of this type were filled with a lot of very electron dense vacuoles and had an eccentric and crescent shape which could be an artificial result from the fixative used. The nucleus of these cells was located at a peripheral side of the cytoplasm.

Electron and light microscopic observations on phagocytosis and encapsulation to some inorganic and organic targets

When the hemolymph was mixed with small LB *in vitro*, many SGs were actively phagocytosed (Fig. 3). But only a part of the LGs could ingest a few small LBs (Fig. 4). It was observed in a sample taken one minute after mixing that a SG was extending its pseudopods to encircle a particle and had already ingested particles in the phagocytic vacuoles in its cytoplasm. In Fig. 3 eleven particles can be seen in the cytoplasm of one SG fixed 10 min after the onset of incubation.

The phagocytic activity to small LB by LG was less than that by the SG. Though many particles were observed among LGs in an aggregate induced in the hemolymph after

TABLE 1. The hemocyte composition in the hemolymph of *H. roretzi*

Cell types	Composition (%)
Small granular amebocyte	29.8±1.6
Large granular amebocyte	10.7±4.8
Dense granular cell	0.4±0.2
Lymphoid cell	0.4±0.1
Vacuolated or vesicular cell	
V1	42.2±6.0
V2	5.4±2.6
V3	3.1±0.8
V4	3.0±1.4
V5	2.4±0.9
V6	2.1±0.9
V7	0.4±0.1
V8	0.2±0.1

Percentage values represent the mean±SD of five animals from different batches kept in an aquarium for 1–17 days.

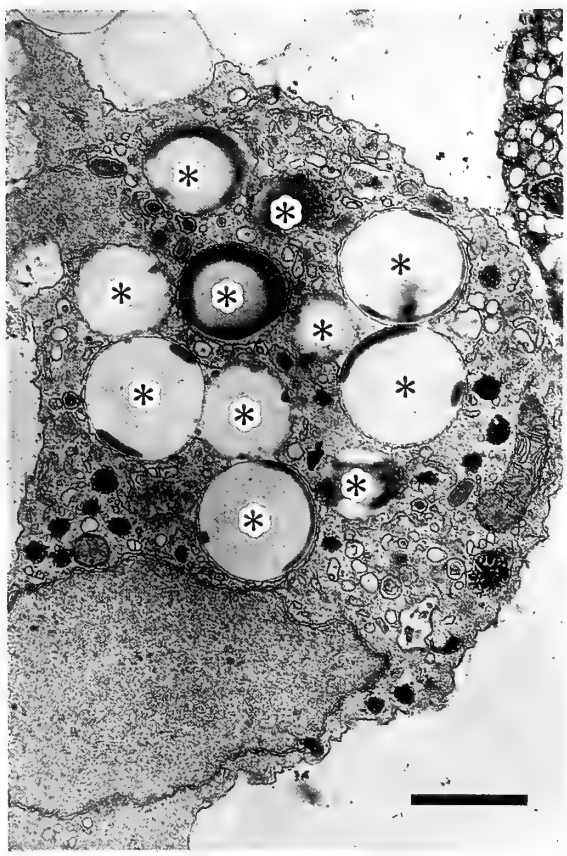

FIG. 3. A SG ingesting small LB (*). Eleven LBs are seen in the cytoplasm of a SG 10 min after the incubation. Scale bar=1 μm.

the addition of small LBs (Fig. 4). The numbers of SGs and LGs, which phagocytosed small LBs in the hemolymph *in vitro*, increased with the progress in the incubation time (Table 2). Twenty percent of SGs have already ingested the

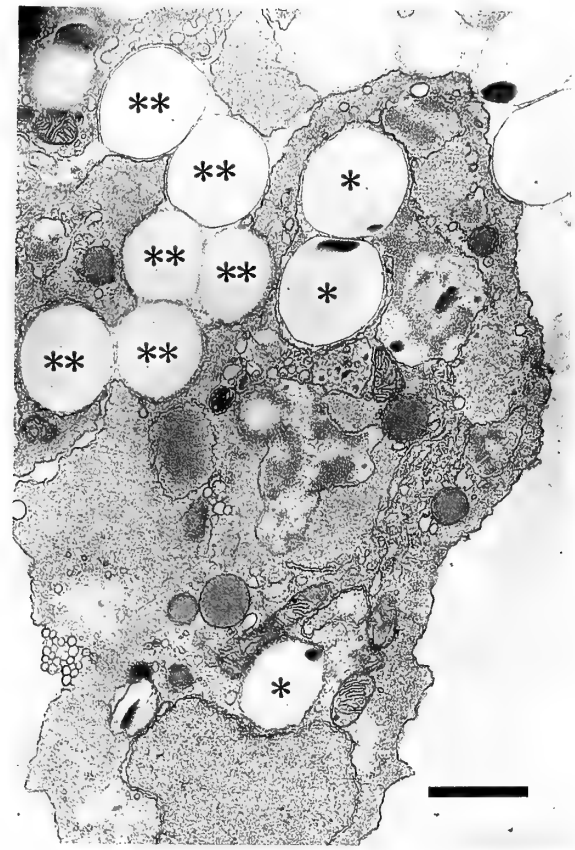

FIG. 4. A LG ingesting 3 small LBs 10 min after the mixing. *: Small LB in the cytoplasm. **: Small LB outside of cells. Scale bar=1 μm.

TABLE 2. The time-dependent increase of the numbers of SG and LG phagocytosing small LB

Hemocytes	Number of cells ingesting small LB			
	1 min	5 min	10 min	30 min
SG	254/1283 (19.8%)	711/1433 (49.6%)	990/1346 (73.6%)	1153/1293 (89.2%)
LG	0/411 (0%)	16/350 (5.0%)	23/413 (5.6%)	27/290 (9.3%)
Others*	0	0	0	0

Values express the number of phagocytosing SGs (LGs)/total SGs (LGs) in the sum of results obtained from three different animals. Parcentages are shown in parenthesis. *: Hemocytes more than 3000 were counted in every observations.

particles within one minute of the incubation and 89% of SGs ingested the particles for 30 min. Only 9.3% of LGs phagocytosed the particles even 30 min after the onset of incubation, and the number of LBs ingested in the cells was less than that of SGs. We could not find any phagocytosed particle in the cytoplasm of other hemocyte types though we counted more than 3000 cells under electron microscopic observations.

When middle LBs were applied to the hemolymph as targets almost the same size as SGs, only the SGs were able to

FIG. 5. A SG ingesting 3 middle LBs (*) in the cytoplasm after the 30 min incubation. Scale bar=1 μm.

FIG. 7. A SG ingesting glutaraldehyde fixed SRBC (*) 5 min after mixing. gSRBCs which were caught by pseudopodia (upper), already ingested in the cytoplasm (middle) and just included (lower) are shown. Scale bar=1 μm.

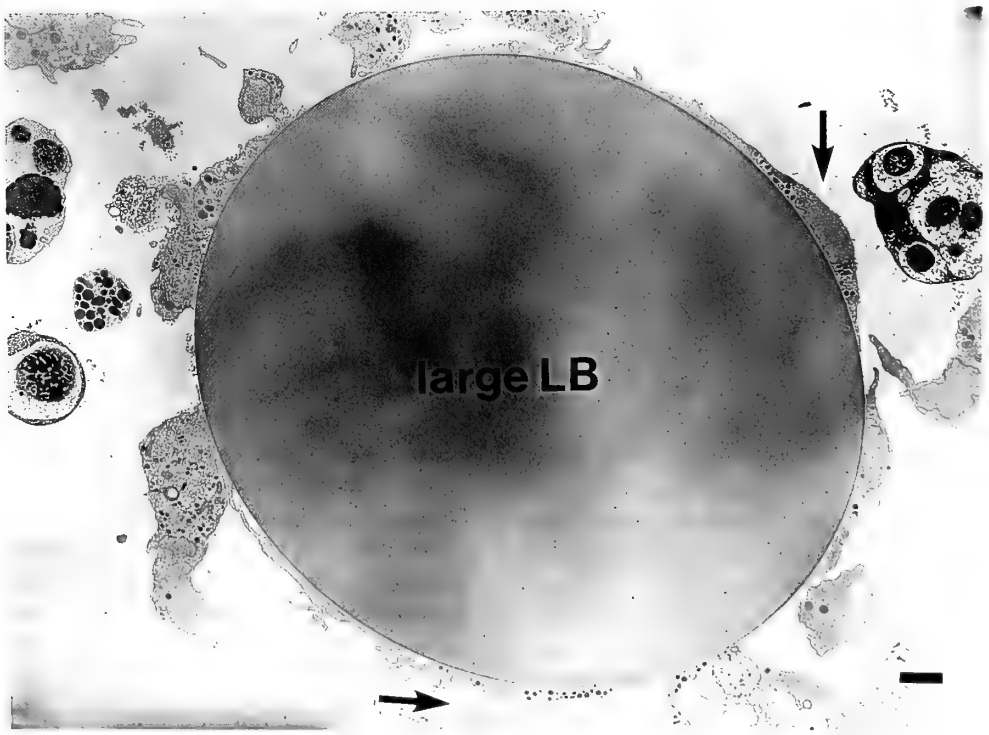

FIG. 6. SGs adhering to the surface of a large LB after the 30 min incubation. Arrows indicate SGs. Scale bar=2 μm.

ingest particles within the 30 min incubation (Fig. 5). No middle LB was observed in hemocytes of other types even 30 min after the onset of incubation.

When large LBs were added into the hemolymph, SGs adhered on the surface of large LBs to encapsulate them by elongation and the spreading of their pseudopodia (Fig. 6).

The organic particles, SRBC, gSRBC or *E. coli*, were also phagocytosed only by SGs in the hemolymph. Figure 7 shows gSRBCs which have been ingested in a SG, just included and caught by pseudopodia in a sample fixed five min after mixing. In this sample, the surface of the pseudopodia does not always make contact with the surface of the targets. *E. coli* was also well ingested by SGs but not by LGs although some of the LGs were able to phagocytose small LBs which have almost the same size as *E. coli* (about 1 μm in diameter) (Fig. 8).

When the hemolymph was incubated with pieces of the tunic dissected from the same animals, SGs tightly spread over a tunic piece and became a single layer surrounding it 30 min later (Fig. 9).

The comparison of phagocytic activity of hemocytes toward different targets

The phagocytic ability of SG and LG in the hemolymph *in vitro* toward different foreign particles was compared in 30 minute-incubation of hemolymph using small, middle and large LB as inorganic targets and SRBC, gSRBC and *E. coli* as organic targets (Table 3). The phagocytic reaction of the SGs to the inorganic targets was more intense than to the

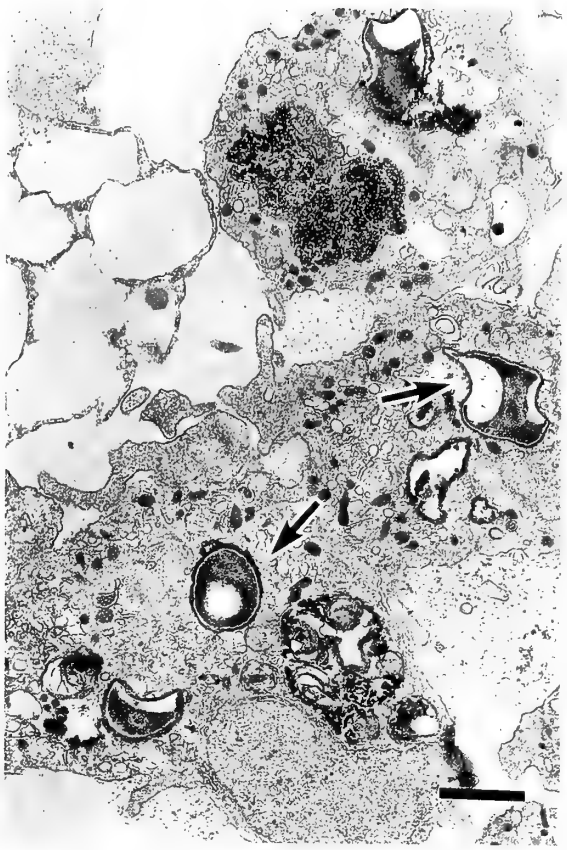

FIG. 8. A SG ingesting *E. coli* (arrows) 10 min after mixing. Scale bar=1 μm.

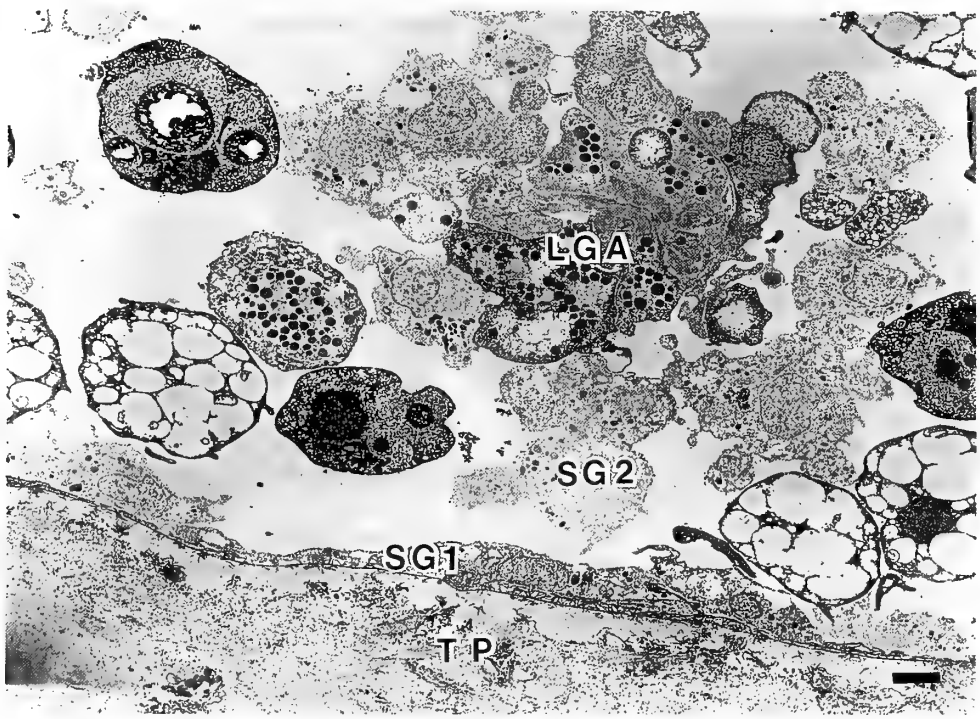

FIG. 9. SGs spreading over the surface of a tunic piece and surrounding an aggregate of LGs 30 min after incubation. SG1: The SG covering the surface of a tunic piece, SG2: The SG surrounding an aggregate of LGs, LGA: An aggregate of LG, TP: A tunic piece incubated with the hemolymph. Scale bar=2 μm.

TABLE 3. The phagocytic activity of hemocytes toward different targets

Targets	% of cell ingesting targets		
	SG	LG*	Others**
Latex beads (ϕ 1.03 μm)	89.3±0.3	10.1±1.47	0
(ϕ 4.62 μm)	83.2±2.54	0	0
SRBC	74.8±2.32	0	0
gSRBC	78.2±5.0	0	0
E. coli	79.9±3.25	0	0

Values represent the mean±SD of experiments from three animals as percentages of cells ingesting the particle of the total number of each cell type. Hemocytes were incubated with particles for 30 min. *: LGs more than 300 were counted in every experiment. **: Hemocytes more than 3000 were counted in every experiment.

organic ones and that to small LB was the highest. The reaction to the gSRBC was stronger than to the SRBC and almost the same as that to *E. coli*. On the other hand, the LGs showed low phagocytic activity only toward small LB.

The effect of Ca^{2+} and Mg^{2+} ions, and low pH on the phagocytic activity of SG

The effect of Ca^{2+} and Mg^{2+}, and pH on the phagocytic activity of SG to small LB was tested using washed hemocytes. The phagocytic activity was measured under light microscopy after a May-Grünward Giemsa stain. The results are summarized in Table 4. SG was easily identified by the following characteristics in the light microscopic preparates: Adhering to a slide glass with elongated pseudopodia and containing acidophilic fine granules in the cytoplasm. In the hemolymph, 53% of SGs phagocytosed the particles for five min and 77% for 20 min of the incubation time. When the hemocytes were washed and resuspended in ASW, the phagocytic activity of the SG became stronger than in the hemolymph. Further, when the washed hemocytes were suspended in acid ASW and/or Ca^{2+}·Mg^{2+} free ASW, more than 80% of SGs have phagocytosed the small LB within five min and 94% of the cells within 20 min of incubation. The phagocytic activity in these media was significantly higher than in the hemolymph.

TABLE 4. The effect of the incubation media on the phagocytic activity of SGs against small LB

Incubation media	% of SG ingesting small LB		
	Incubation time		
	5 min	10 min	20 min
Normal hemolymph	52.9±6.39	61.2±4.41	77.0±3.73
ASW	73.6±6.68*	82.2±5.41*	86.6±4.72*
Ca^{2+}·Mg^{2+} free ASW	84.1±3.16**	92.9±3.36**	93.9±3.42**
Acid ASW	83.9±3.84**	91.8±3.97**	93.7±2.51**
Ca^{2+}·Mg^{2+} free acid ASW	88.3±4.12**	90.6±4.07**	93.8±2.27**

Values represent the mean±SD of experiments from five animals as percentage of SGs ingesting small LB of a total SGs. *: The values of ASW were significantly higher than those of normal hemolymph ($P<0.01$). **: The values of Ca^{2+}·Mg^{2+} free ASW, Acid ASW and Ca^{2+}·Mg^{2+} free acid ASW were higher than those of normal hemolymph and normal ASW ($P<0.01$).

The effect of hemolymph plasma on phagocytosis of SGs

Hemocytes and hemolymph plasma were obtained from the same animal. The washed hemocytes were resuspended in the hemolymph plasma, the diluted plasma or ASW and incubated with SRBC or middle LB for 20 min. The concentration of target particles was adjusted so it was the same as the hemocyte concentration in each experiment (3×10^7 cells/ml). The results are shown in Table 5. SGs actively phagocytosed the middle LB without any significant difference between those in ASW and those in plasma. On the other hand, the phagocytic activity of SG to SRBC was significantly influenced by the concentration of plasma in the incubation mixture. Within 20 min after the start of incubation 71% of SGs phagocytosed the SRBC in the hemolymph, but only 39% of SGs phagocytosed the SRBC in ASW. The higher the plasma concentration was in the incubation medium, the more the active SGs increased.

TABLE 5. The effect of plasma on the phagocytic activity of SGs

Media	% of SG ingesting targets	
	SRBC	middle LB
ASW	39.1±1.86[a]	69.2±3.08[f]
ASW : Plasma=9 : 1	41.6±4.93[b]	—
ASW : Plasma=1 : 1	56.5±5.24[c]	—
Plasma	67.0±1.97[d]	—
Hemolymph	71.0±4.55[e]	69.9±2.99[g]

Values represent the mean±SD of experiments from five animals. The plasma used was obtained from the same individual as for the cell sourse. Hemocytes were incubated with particles for 20 min. Significant differences are recognized between a and c; b and c; and c and d ($P<0.01$) but not between a and b; d and e; and f and g.

LG aggregation induced by the addition of foreign particle and TP

The addition of foreign particles into the hemolymph induced the aggregation of LGs, even if they were TPs from the same animal. The granules of LGs in the center of the aggregate swelled and fused each other (Fig. 4, 9). It was also observed that SGs were surrounding the aggregate of LGs (Fig. 9) in the same manner as with large LB and TP.

DISCUSSION

There are many reports which propose and demonstrate the relationship of the structure of ascidian hemocytes to various functions such as nutrition [11], tunic formation [9,

10], heavy metal accumulation [9, 21], germ cell formation [11] and immune responses [1, 19, 34]. A wide variety of cell types found among different species and their various functions are well known. Overton [24], using *Perophora viridis*, has reported with a special reference to the fine structure of vanadocyte. Milanesi and Burighel [22] and Burighel *et al.* [7] distinguished six cell types based on the fine structure in *Botryllus schlosseri*. It is generally believed that six to nine cell types of hemocytes are found in the hemolymph of ascidians [35], however, the relationship between the physiological roles and morphological characters is not clear.

Recently, Sawada *et al.* [28] classified ten groups of living hemocytes of *H. roretzi* (two types of phagocytes, three types of granular cells, four types of vacuolated cells and lymphoid cells) according to vital staining, autonomous fluorescence and the effect of NH_4 ions in the presence of EGTA at pH 6.0, where hemocytes were adhering or spreading on glass. Zhang *et al.* [37] identified nine types of hemocytes in *H. roretzi* according to their ultrastructural characteristics. Fuke and Fukumoto [15] classified hemocytes of *H. roretzi* into nine types by electron microscopy with reference to their appearance by light microscopy (vacuolated cells, hyaline amoebocytes, small amoebocytes, granular amoebocytes, macrogranular cells, globular cells, lymphocyte-like cells, large basophilic cells, and large granular cells).

Referring to the above results, we classified hemocytes of *H. roretzi* into twelve types on ultrastructural findings as follows: SG, LG, lymphoid cells, dense granular cells and eight types of vacuolated or vesicular cells, V1-V8, which were distinguished by the size of vacuoles and the nature of the inclusion. Table 6 shows our classification as we believe it corresponds to Sawada *et al.* [28] and Fuke and Fukumoto [15]. The dense granular cells, V3, V4, V6 and V7 that we observed are not described by them.

Ascidians have got two defense mechanisms against foreign materials (bacteria, certain species of copepoda, non-self tissues). The first, known as humoral responses, involves natural agglutinins [3, 12, 32, 34, 36] and bactericidines [2, 20]. We also found in the hemolymph plasma of *H. roretzi*, the existence of protease and its inhibitor, which are activated by contact with the tunic *in vitro* (Unpublished data). The second is cellular responses that include inflammatory-like reactions, phagocytosis, encapsulation and histocompatibility [1, 26, 31, 35].

Phagocytic activities of several ascidians' hemocytes were reported under experimental conditions. Small particulate foreign bodies were introduced into the tunic or vascular system, and were phagocytosed by hyaline and granular leucocytes [35]. Carmine particles were phagocytosed readily in the cytoplasm of amebocytes and trypan blue could be identified in cytoplasm of amebocytes and vacuoles of signet ring cells after intracardial injections into *Molgula manhattensis* [1]. Fuke [13] reported phagocytic activity in *H. roretzi* of the following cells: Vesicular cells, fine granular ameboid cells, minute granular cell, small vacuolated cells and large basophilic cells. On the other hand Sawada *et al.* [28] confirmed phagocytic activity toward SRBC in three groups of hemocytes of *H. roretzi*. But they supposed that the pahgocytes of this species consist of two types of amebocyte (p-1, p-2). Although many types of the hemocytes showed certain signs of endocytosis under electron microscopic studies in other ascidians, only one type of cells is called the phagocyte or the macrophage because these cells frequently contain one or more cells in their cytoplasm [22, 24]. In our present electron and light microscopic observations, however, only SGs showed active pahgocytic activity toward not only inorganic targets like LB but organic targets

TABLE 6. The names and symbols provided by us for each cell type and the corresponding names by Sawada *et al.* and by Fuke & Fukumoto

Cell types	Corresponding names	
	Sawada *et al.** LM	Fuke & Fukumoto** TEM
Small granular amebocyte	p1 and p2	Hyaline amoebocyte and Small amoebocyte
Large granular amebocyte	g1	Granular amoebocyte
Dense granular cell		
Lymphoid cell	Lymphoid cell	Lymphocyte-like cell
Vacuolated or vesicular cell		
V1	v3	Vacuolated cell T2
V2		Globular cell
V3		
V4		
V5	g2	Large basophilic cell
V6		
V7		
V8	g3	Large granular cell

*: According to Sawada *et al.* [28]. **: According to Fuke & Fukumoto [15].

like SRBC as well. We suppose that the clearing and elimination of foreign substances, such as bacteria, are mainly performed by the phagocytosis of SGs. The meaning of the phagocytosis carried out by a small number of LGs toward small LB only is not clear. LGs may have pahgocytic subpopulation(s) or they may exert their phagocytic activity in free cell conditions but lose it after their aggregation. The aggregation of LGs *in vitro* was induced within five min by the addition of small pieces of tunic or other foreign materials used in this experiment and the adhesion of SGs around LG-aggregate was also observed (details of the aggregate formation are not shown).

The encapsulation responding toward copepods have been naturally observed in the outer wall of the peribranchial cavity or within the gill cavity. The parasites were surrounded by a thin membrane of host tissue [6, 23]. The process of encapsulation has been studied in *M. manhattensis* in which hemocytes responsible for encapsulation reactions are vanadocytes and signet ring cells. These cells coat the glass fragment inserted in the branchial tissue [1]. In general, hemocytes responsible for the encapsulation reactions belong to those of the vacuolated category, predominantly the morula cell [35]. In the present observations, however, SG was the only responsible hemocyte for the encapsulation reaction of this species. It is not clear whether the differences of cell types responding for encapsulation reflected the differences of species, of cell appearance or of unique experimental conditions.

SGs readily ingested LBs in every condition of experimental media. As LBs used in this experiment protrude $-COOH^-$ group on their surface, they may easily have contact with the plasma membrane of SGs. In mammalian macrophages, anionic molecules are better inducers of phagocytosis than either neutral or cationic species [8]. The phagocytic activity of SGs toward gSRBC was higher than that of non-treated SRBC (Table 3). Usually, the outer surface of protein molecules exposes hydrophilic molecules. After denaturation, like in a treatment with glutaraldehyde, the hydrophobic groups are exposed to aqueous solvent. The increase in surface hydrophobicity could act as a marker, which would allow non specific recognition of macrophage [27, 33].

The highest phagocytic activity of SGs toward small LB was observed in Ca^{2+}·Mg^{2+} free acid ASW (Table 4). Because the aggregation of LGs and the adhesion of SGs to LG-aggregates were depressed in these condition, the chance of SGs striking their targets may have been increased.

Immunoglobulins are not known in the hemolymph plasma in ascidians. However, it has been suggested that ascidians have lectins that act as opsonin for foreign materials [3, 32]. The present experiment clearly demonstrates that humoral factor(s) in the hemolymph plasma play a significant role in the phagocytosis of SGs toward SRBC, but not toward middle LB.

Our results suggest that SGs play a part in the clearing and elimination of foreign materials together with a certain plasma factor and SGs and LGs play important roles in hemostasis and wound healing in *H. roretzi*.

ACKNOWLEDGMENTS

The author wishes to thank Dr. T. Numakunai and the staff of Asamushi Marine Biological station of Tohoku University for their kind support in supplying the animals. We also thank Prof. R. M. Gerling, Nihon University School of Medicine, for reading the manuscript.

REFERENCES

1 Anderson, RS (1971) Cellular responses to foreign bodies in the tunicate *Molgula manhattensis* (DeKay). Biol Bull, 141: 91–98

2 Azumi K, Yokosawa H, Ishii S (1990) Halocyamines: Novel antimicrobial tetrapeptide-like substances isolated from the hemocytes of the solitary ascidian *Halocynthia roretzi*. Biochemistry 29: 159–165

3 Azumi K, Ozeki S, Yokosawa H, Ishii S (1991). A novel lipopolysaccharide-binding hemagglutinin isolated from hemocytes of the solitary ascidian, *Halocynthia roretzi*: It can agglutinate bacteria. Dev Comp Immunol 15: 9–16

4 Azumi K, Satoh N, Yokosawa H (1993) Functional and structural characterization of hemocytes of the solitary ascidian, *Halocynthia roretzi*. J Exp Zool 265: 309–316

5 Botte L, Scippa S (1977) Ultrastructural study of vanadocytes in *Ascidia malaca*. Experientia 33: 80–81

6 Bresciani J, Lützen J (1960) *Gonophysema gullmarensis* (Copepoda parasitica). An anatomical and biological study of an endoparasite living in the ascidian *Ascidiella aspersa*. I. Anatomy. Cha Biol mar 1: 157–184

7 Burighel P, Milanesi C, Sabbadin A (1983) Blood cell ultrastructure of the ascidian *Botryllus schlosseri* L. II. Pigment cells. Acta Zool (Stockh.) 64: 15–23

8 Cohn ZA, Parks E (1967) The regulation of pinocytosis in mouse macrophages. II. Factors inducing vesicle formation. J Exp Med 125: 213–230

9 Endean R (1955a) Studies of the blood and tests of some Australian ascidians. I. The blood of *Pyura stolonifera* (Heller). Aust J mar Freshwat Res 6: 35–59

10 Endean R (1955b) Studies of the blood and tests of some Australian ascidians. III. The formation of the test of *Pyura stolonifera* (Heller). Aust J mar Freshwat Res 6: 157–164

11 Fujimoto H, Watanabe H (1976) The characterization of granular amoebocytes and their possible roles in the asexual reproduction of the polystyelid ascidian, *Polyzoa vesiculiphora*. J Morph 150: 623–638

12 Fuke TM, Sugai T (1972) Studies on the naturally occurring hemagglutinin in the coelomic fluid of an ascidian. Biol Bull 143: 140–149

13 Fuke TM (1979) Studies on the coelomic cells of some Japanese ascidians. Bull Mar Biol St Asamshi, Tohoku Univ 16: 143–159

14 Fuke M (1990) Self and nonself recognition in the solitary ascidian, *Halocynthia roretzi*. In "Defense Molecules" Ed by JJ Marchalonis, CL Reinisch, Alan R.Liss, New York, pp 107–117

15 Fuke M, Fukumoto M (1993) Correlative fine structural, behavioral, and histochemical analysis of ascidian blood cells. Acta Zool (Stockh.) 74: 61–71

16 Gansler H, Pfleger K, Seifen E,Bielig H-J (1963) Submikroskopische Struktur von Vanadocyten. Ein Beitrag zur Vanadin-

Anhäufung bei Tunicaten. Experientia 19: 232–234

17 George, WC (1939) A comparative study of the blood of the tunicates. Quart J Micros Sci 81: 391–428

18 Hildemann WH, Reddy AL (1973) Phylogeny of immune responsiveness: marine invertebrates. Fed Proc 32: 2188–2194

19 Hildemann WH (1974) Phylogeny of immune responsiveness in invertebrates. Life Sci 14: 605–614

20 Johnson PT, Chapman FA (1970) Comparative studies on the *in vitro* response of bacteria to invertebrate body fluids. II. *Aplysia californica* (sea hare) and *Ciona intestinalis* (tunicate). J Invert Pathol 16: 259–267

21 Michibata H, Hirata J, Uesaka M, Numakunai T, Sakurai H (1987) Separation of vanadocytes: Determination and characterization of vanadium ion in the separated blood cells of the ascidian, *Ascidia ahodori*. J Exp Zool 244: 33–38

22 Milanesi C, Burighel P (1978) Blood cell ultrastructure of the Ascidian *Botryllus schlosseri*. I. Hemoblast, granulocytes, macrophage, morula cell and nephrocyte. Acta zool (Stockh.) 59: 135–147

23 Monniot C (1963) *Kystodelphys drachi* n. g. n. sp., copépode enkysté dans une branchie d'Ascidie. Vie Milieu 14: 263–273

24 Overton J (1966) The fine structure of blood cells in the ascidian *Perophora viridis*. J Morph 119: 305–326

25 Pantin CFA (1948) Notes on Microscopical Technique for Zoologists. Cambridge Univ. Press, London, pp 63–68

26 Parrinello N, Patricolo E, Canicatti C (1984) Inflammatory-like reaction in the tunic of *Ciona intestinalis* (tunicata). I. Encapsulation and tissue injury. Biol Bull 167: 229–237

27 Rabinovitch M (1969) Phagocytosis of modified erythrocytes by macrophages and L2 cells. Exptl Cell Res 56: 326–332

28 Sawada T, Fujikura Y, Tomonaga S, Fukumoto T (1991) Classification and characterization of ten hemocytes types in the tunicate *Halocynthia roretzi*. Zool Sci 8: 939–950

29 Schlumpberger JM, Weissman IL, Scofield VL (1984) Separation and labeling of specific subpopulations of *Botryllus* blood cells. J Exp Zool 229: 401–411

30 Smith MJ (1970) The blood cells and tunic of the ascidian *Halocynthia aurantium* (Pallas). II. Histochemistry of the blood cells and tunic. Biol Bull 138: 379–388

31 Tanaka K (1973) Allogeneic inhibition in a compound ascidian, *Botryllus primigenus* Oka. II. Cellular and humoral responses in "nonfusion"reaction. Cell Immunol 7: 427–443

32 Warr GW, Decker JM, Mandel TE, DeLuca D, Hudson R, Marchalonis JJ (1977) Lymphocyte-like cells of the tunicate, *Pyura stolonifera*: Binding of lectins, morphological and functional studies. AJEBAK 55: 151–164

33 Wilkinson PC (1976) Recognition and response in mononuclear and granular phagocytes. Clin exp Immunol 25: 355–366

34 Wright RK, Cooper EL (1975) Immunological maturation in the tunicate *Ciona intestinalis*. Amer Zool 15: 21–27

35 Wright RK (1981) Urochordates. In "Invertebrate Blood Cells Vol 2" Ed by NA Ratcliffe and AF Rowley, Academic Press, London, pp 565–626

36 Yokosawa H, Sawada H, Abe Y, Numakunai T, Ishii S (1982) Galactose-specific lectin in the hemolymph of solitary ascidian, *Halocynthia roretzi*: Isolation and characterization. Biochem Biophys Res Commun 107: 451–457

37 Zhang H, Sawada T, Cooper EL,Tomonaga S (1992) Electron microscopic analysis of Tunicate (*Halocynthia roretzi*) hemocytes. Zool Sci 9: 551–562

ZOOLOGICAL SCIENCE 11: 693–700 (1994)

Changes at the Egg Surface during the First Maturation Division in the Spider *Achaearanea japonica* (Bös. *et* Str.)

HIROHUMI SUZUKI* and AKIO KONDO

Department of Biology, Faculty of Science, Toho University, 2-1, Miyama 2 chome, Funabashi-shi, Chiba 274, Japan

ABSTRACT—Changes at the egg surface during the first maturation division were examined in the spider *Achaearanea japonica* under the light and electron microscope. Newly laid eggs had already accepted a sperm nucleus. The nuclear division of the primary oocyte had occurred parallel to the egg surface and then the meiotic spindle developed perpendicular to the egg surface to complete the division. The cell membrane began to invaginate from the egg surface immediately after oviposition. Then the lumen of the invagination became wider and the large yolk granules became organized into an outer columnar layer and an inner spherical mass. The outer layer of the "vitelline membrane" appeared to be formed by the contents of periplasmic granules, which were newly detected in the present study. These granules discharged their contents by exocytosis. The formation of the outer layer after entrance of the sperm nucleus suggests that the "vitelline membrane" of the spider egg is equivalent to a fertilization membrane and is not a true vitelline membrane.

INTRODUCTION

The eggs of spiders are generally considered to be surrounded by two egg membranes: an outer membrane, the chorion; and an inner membrane, the so-called "vitelline membrane". According to Kondo [5], in lycosid spiders, a single membrane corresponding to the outer layer of the "vitelline membrane" is located between the chorion and the cell membrane 30 min after oviposition. The "vitelline membrane" then becomes distinguishable under the light microscope after formation of the main layer has started. Kondo suggested that the "vitelline membrane" bore some resemblance to the fertilization membrane. Suzuki and Kondo [13] described how, in the theridiid spider *Achaearanea japonica*, the main layer was formed under the outer layer by the matrix of vesicles that had been discharged by exocytosis. In the present study, we examined the changes that occur at the egg surface in newly laid eggs during the first maturation division in *A. japonica*. We discuss the possibility that the "vitelline membrane" could be referred to as the fertilization membrane and we identify the origin of the outer layer of the fertilization membrane.

MATERIALS AND METHODS

Mature female specimens of *Achaearanea japonica* (Bös. *et* Str.) lay eggs in middle and late summer, and about 100 eggs are released at each oviposition. The eggs are spherical and 0.5 mm in diameter. Eggs laid naturally on the campus of Toho University were used for the present study.

The eggs were covered with oviposition fluid immediately after oviposition. Before this fluid hardened, the eggs were ellipsoidal. It was difficult to isolate each egg without injury. Fixation of an entire mass was more effective at the earlier stages and, therefore, the eggs were immersed in fixative at the site of their collection.

Each egg mass was harvested 10 min after oviposition and was carried to the laboratory. The oviposition fluid usually took at least 20 min to dry up and then the eggs ceased to stick together. The physical properties of the egg membrane, such as its elasticity and permeability to fixatives, changed during the evaporation of the oviposition fluid. For example, an egg covered with the fluid was elastic and fragile while a dry egg was less elastic and firm. In the latter case, fixation after puncturing of the egg with a tungsten needle in the fixative was more effective than fixation without puncturing.

For light microscopy, eggs were fixed in a mixture of 2.5% glutaraldehyde and 2% paraformaldehyde in 0.1 M phosphate buffer (pH 7.4) that contained 0.2 M sucrose. Samples dehydrated in a graded alcohol series were embedded in methacrylate resin (Technovit 7100; Kulzer, Wehrheim, Germany). The resin-embedded specimens were sectioned at 1–5 μm with a glass knife on an ultramicrotome (type 4800; LKB-Produkter, Stockholm, Sweden). The sections were stained with Mayer's acid-haemalum and eosin.

For fine-structural observations, the eggs were prefixed at room temperature for 3 hr in a mixture of 2% paraformaldehyde and 2.5% glutaraldehyde in 0.1 M phosphate buffer (pH 7.4) that contained 0.2 M sucrose. During fixation, the eggs were cut in half with a tungsten needle. After rinsing for more than one hour with the same buffer plus 0.2 M sucrose, the samples were postfixed at room temperature for one hour in 2% osmic acid in 0.1 M phosphate buffer (pH 7.4) without sucrose. After rinsing with the same buffer without sucrose, the samples were dehydrated in a graded alcohol series, transferred to propylene oxide and embedded in epoxy resin (Quetol 812; Nisshin EM, Tokyo). Ultrathin sections were cut with a diamond knife on the ultramicrotome, stained with uranyl acetate and lead citrate and examined under an electron microscope (JEM-1210; JEOL, Tokyo). Thick sections were prepared simultaneously and these sections were stained with toluidine blue for light microscopy.

Accepted August 24, 1994
Received June 3, 1994
* To whom correspondence should be addressed.

RESULTS

Light microscopy

By the time oviposition occurred, the egg had already accepted a sperm nucleus which was visible at a depth of about 50 μm from the egg surface (Fig. 1). The cytoplasm was distributed at the surface of each egg as a layer of periplasm of 10–20 μm in thickness (Fig. 1). The egg contained many large yolk granules of 10–40 μm in diameter and these granules were deeply stained by eosin and by toluidine blue.

Evidence for the first maturation division of the oocyte, which was in the telophase, was visible in the periplasm (Fig. 2). The meiotic spindle was oriented parallel to the egg surface. The spindle curved toward the center of the egg in its equatorial region, resembling a cup in terms of shape.

The egg membrane appeared to consist only of a chorion with a rough external surface and a smooth internal surface (see Fig. 5).

Ten minutes after oviposition, the meiotic spindle of the first maturation division was oriented obliquely with respect to the surface in some eggs (Fig. 3), while in other eggs two sets of daughter chromosomes were oriented perpendicularly to the surface of the egg (Fig. 4a, b). In the latter case, the meiotic spindle was not clearly discernible and a deeply located set of chromosomes was visible about 40 μm from the surface of the egg.

Twenty minutes after oviposition, the large yolk granules consisted of two layers: an outer layer of radial columns and an inner layer that was a spherical mass (Fig. 5). Two chromosome plates were observed, situated close to each other (Fig. 5). One of them, located at the surface of the spherical mass of the large yolk granules, was that of the secondary oocyte and the other, located in the periplasm or in the cytoplasm accompanied by radial columns of large yolk granules, was that of the first polar body. Protrusion of the cytoplasm of the first polar body from the periplasm was not observed. The yolk mass resembled an aggregation of irregular polygons in live eggs at this stage (Fig. 6).

Electron microscopy

At the time oviposition occurred, many microvilli were observed on the surface of the egg (Fig. 7). The main components of the cytoplasm were fatty granules and vesicles. The fatty granules, 1–2.5 μm in diameter, had a moderately electron-dense matrix and their limiting membranes were often obscure. Vesicles were 1–6 μm in diameter and contained a slightly electron-opaque matrix. Some small yolk granules of less than 5 μm in diameter were observed. Both large and small yolk granules had smooth surfaces and their limiting membranes were not visible for the most part. The yolk granules were very electron-dense. Mitochondria were either oval or rod-shaped and had a very electron-dense matrix. Granules that could be divided into the following two types were detected for the first time in the present study and they were designated "periplasmic granules". Periplasmic granules of the first type were ellipsoidal with a long axis of 0.3–0.5 μm, and each contained membrane-like material (Fig. 8). Periplasmic granules of the second type were spherical, 0.2–0.4 μm in diameter, and contained a very electron-dense matrix (Fig. 8). Periplasmic granules that appeared to be intermediate between the two types were also observed (Fig. 9). The glycogen granules were very electron-dense and clusters of glycogen granules were observed near the large yolk granules.

Electron micrographs of maturation divisions were unavailable because of our failure to stain the thick, epoxy resin-embedded sections.

A structure corresponding to the "vitelline membrane", which was usually found at later stages of development, was not observed at the surface of the egg. The chorion was composed of a weakly electron-dense basal layer of 0.25 μm in thickness and electron-dense spherules of 0.5–0.8 μm in diameter (Fig. 7). The spherules were attached to the outer surface of the basal layer.

Within two minutes after oviposition, microvilli became less prominent and the periplasmic granules migrated to the outermost region of the periplasm (Fig. 10).

Three minutes after oviposition, the microvilli had disappeared entirely. The membrane-like material and the very electron-dense matrix of periplasmic granules were discharged at the egg surface by exocytosis, and the egg surface was enveloped discontinuously by a thin membrane or mucous material (Figs. 11 and 12). The cell membrane had invaginated sporadically at intervals of 25–50 μm toward the center of the egg (Fig. 13), and the tips of invaginations extended to a depth of about 25 μm from the egg's surface. Vesicles were often arranged in sequence beyond the tips of invaginations (Fig. 14).

Fifteen minutes after oviposition, the surface of the egg was completely enveloped by a thin membrane and an underlying layer of mucous material (Fig. 15). The chorion was not in contact with this newly formed envelope. Exocytosis of periplasmic granules was still observed at this time.

Twenty minutes after oviposition, the cell membrane had invaginated to a distance of 25–30 μm from the surface of the egg. The lumen of each invagination became wider from a depth of about 5 μm to the tip, and large yolk granules were arranged into an outer layer of radial columns and an inner spherical mass (Fig. 16). At this time, a membrane of about 30 nm in thickness was located between the chorion and the cell membrane (Fig. 17). The discontinuity of the membrane with the chorion and the cell membrane indicated that it was the outer layer of a fertilization membrane. Microvilli were again observed but the number of periplasmic granules had decreased markedly.

DISCUSSION

The chorion

The egg membranes of spiders are considered to consist of a chorion and a "vitelline membrane". The chorion of

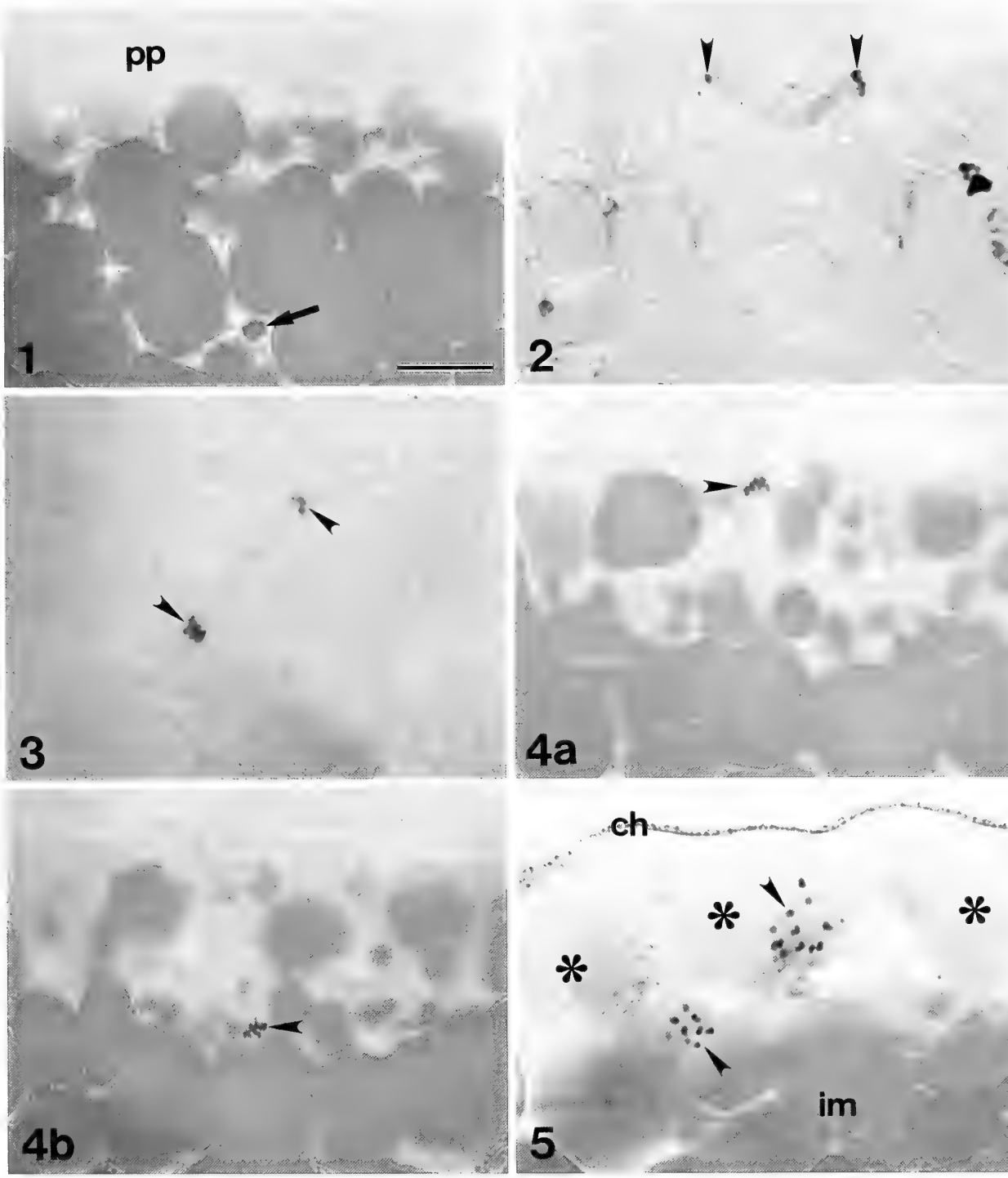

FIGS. 1–5. Surfaces of newly laid eggs during the first maturation division (Technovit-embedded sections). Scale bar=20 μm. arrowheads, chromosomes. Fig. 1. Just at the time of oviposition. The egg includes many large yolk granules and has accepted a sperm nucleus (arrow). The cytoplasm is distributed at the egg surface as periplasm (pp). Fig. 2. Just at the time of oviposition. The nuclear division of the primary oocyte at telophase is visible in the periplasm. The division occurs parallel to the egg surface. The spindle becomes cup-shaped. Fig. 3. Ten minutes after oviposition. The meiotic spindle lies obliquely with respect to the egg surface. Figs. 4a and 4b. Ten minutes after oviposition. Two sections from a serially sectioned egg. Two sets of daughter chromosomes are located perpendicular to the egg surface. The chromosomes in Fig. 4a will be those of the first polar body, and those in Fig. 4b will be those of the secondary oocyte. Fig. 5. Twenty minutes after oviposition. The large yolk granules are arranged as an outer layer of radial columns (asterisks) and an inner spherical mass (im). Two chromosome plates are visible. One of them, located at the surface of the spherical mass of the large yolk granules, is that of the secondary oocyte and the other, located in the periplasm and in the cytoplasm accompanied by a radial column of the large yolk granules, is that of the first polar body. ch, chorion.

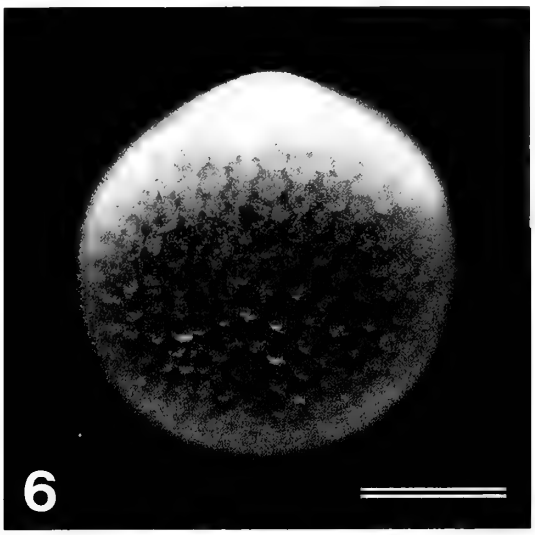

FIG. 6. A live egg in liquid paraffin, twenty minutes after oviposition. The yolk mass appears to be divided into irregular polygons. Scale bar=0.2 mm.

Achaearanea japonica consists of a basal layer and spherules. The fine structure of the chorion is similar to that of eggs of lycosid spiders [5]. No such spherules have been described in the ovarian eggs of *Heptathela kimurai* [10], *Plexippus paykulli* [11] and *Cupiennius salei* [12]. Kondo and Chaki [6] reported mature eggs that were enclosed by spherules in the ovarian cavity of *Nephila clavata*. In spiders, the spherules should attach to the basal layer of the chorion when eggs are released into the ovarian cavity.

Lambert [7] reported that, in *Epeira cinerea*, the spherules floated away freely when living eggs were immersed in alcohol and he concluded that they were not structurally a part of the chorion. This phenomenon was not observed in *A. japonica*. When live eggs of *A. japonica* were shaken in a solution of sodium hypochlorite, the spherules easily became detached from the basal layer and each egg membrane became transparent. Moreover, many craters were visible on the surface of the basal layer under the scanning electron microscope (Suzuki and Kondo, unpublished data). Each crater probably corresponded to a site at which a spherule had been attached, and attached spherules would make the egg appear opaque. Since the egg membrane of *Heptathela kimurai* is transparent [14], it would be of interest to determine whether spherules are present in the chorion of this primitive spider.

The outer layer of the fertilization membrane

It has been generally accepted that the "vitelline mem-

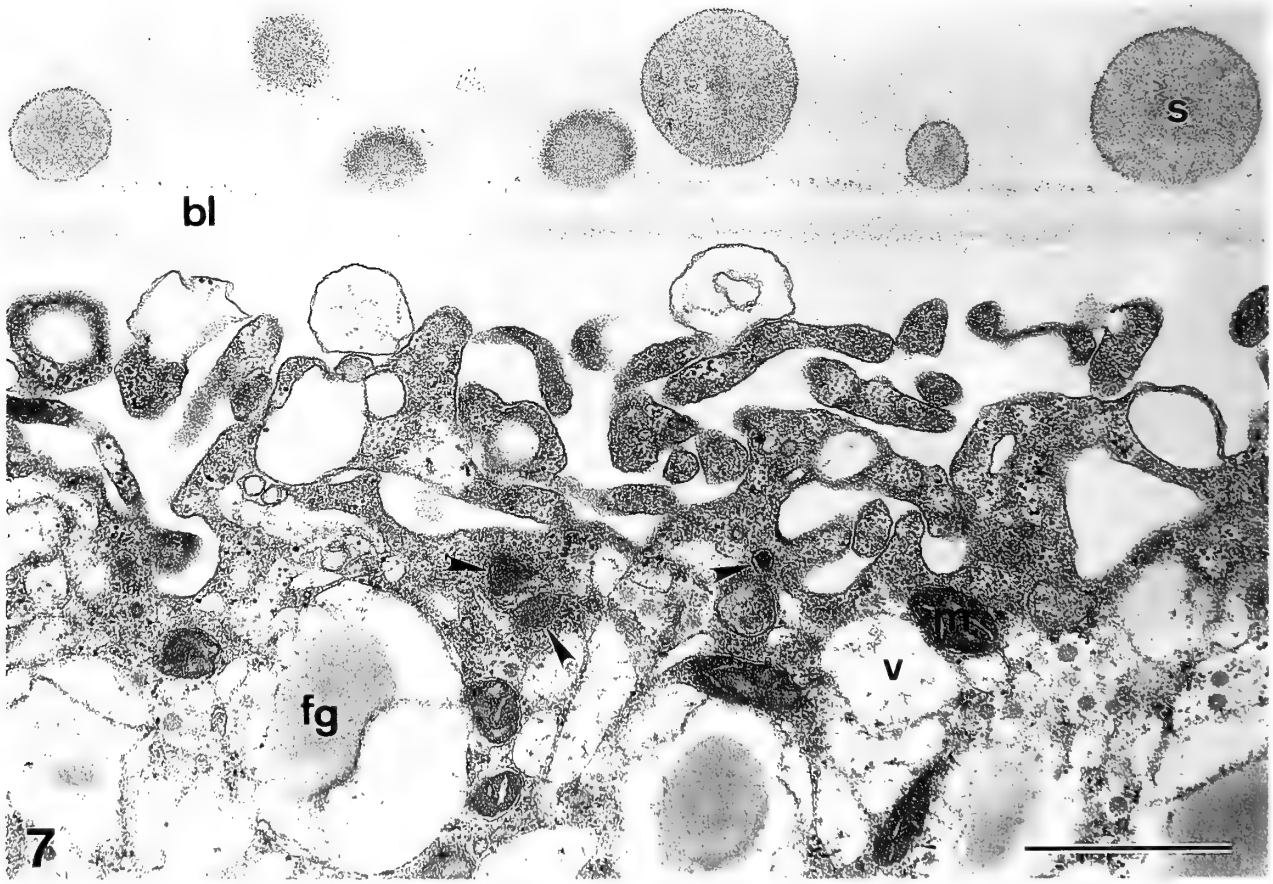

FIG. 7. The egg surface just at the time of oviposition. The chorion is composed of a basal layer (bl) and spherules (s). The cell membrane extrudes many microvilli. No "vitelline membrane" is visible under the chorion. Scale bar=1 μm. arrowheads, periplasmic granules; fg, fatty granule; m, mitochondrion; v, vesicle.

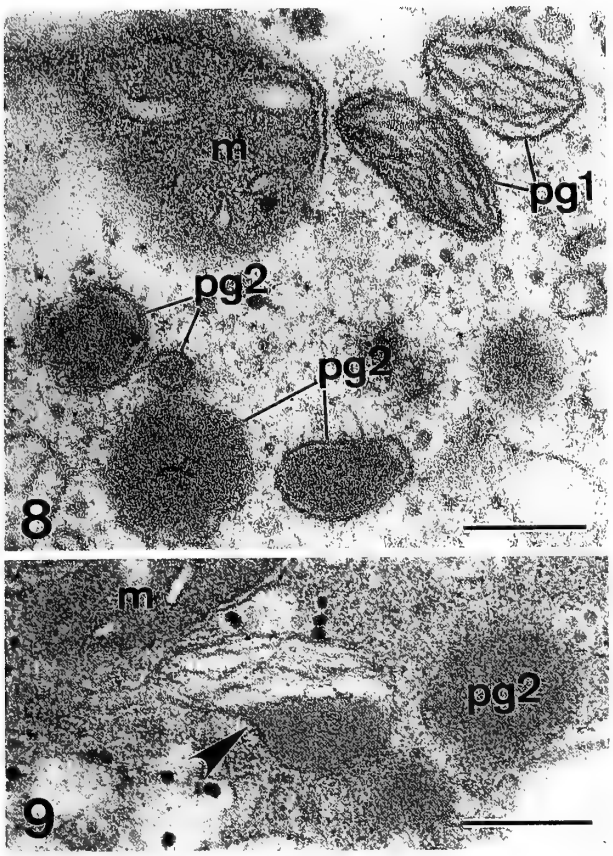

FIG. 8. Electron micrograph showing periplasmic granules. Periplasmic granules of the first type (pg1; see text) are ellipsoidal and contain membrane-like material. Granules of the second type (pg2; see text) are spherical and contain a very electron-dense matrix. Scale bar=0.2 μm. m, mitochondrion.

FIG. 9. Periplasmic granule of the transitional type (arrowhead; see text), which is intermediate between granule of the first type and that of the second type. Scale bar=0.2 μm. m, mitochondrion; pg2, periplasmic granule of the second type.

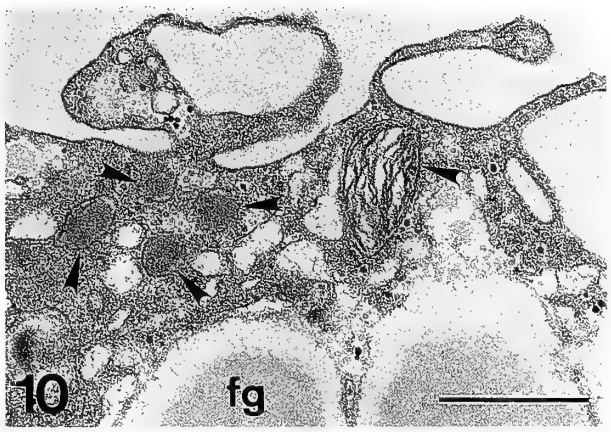

FIG. 10. The surface of the egg, two minutes after oviposition. Microvilli are faintly visible (compare with Fig. 7). Periplasmic granules (arrowheads) are found at the outermost region of the periplasm. Scale bar=0.5 μm. fg, fatty granule.

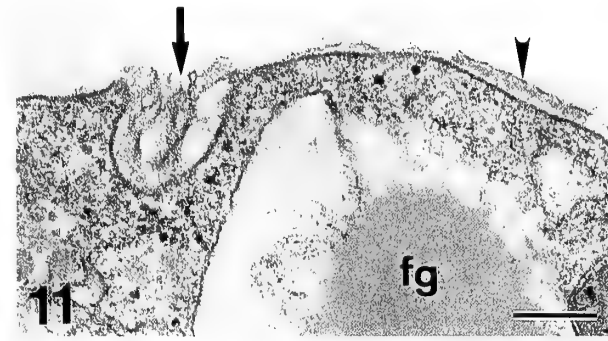

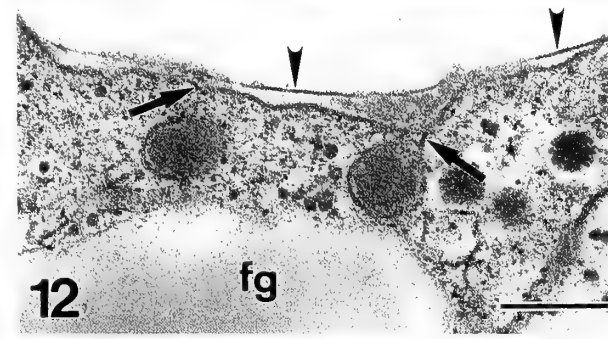

FIG. 11. The surface of the egg, three minutes after oviposition. A periplasmic granule is discharging its membrane-like contents (arrow). Discontinuous regions of mucous material are visible on the surface of the egg (arrowhead). Scale bar=0.2 μm. fg, fatty granule.

FIG. 12. The surface of the egg, three minutes after oviposition. Two periplasmic granules are discharging their very electron-dense matrix (arrows). Discontinuous thin membranes can be seen on the surface of the egg (arrowheads). Scale bar=0.2 μm. fg, fatty granule.

brane" is located within the chorion in spider eggs. According to Kondo [5], in lycosid spiders, only a thin outer layer of the "vitelline membrane", which cannot be recognized by light microscopy, is present 30 min after oviposition. The "vitelline membrane" is nearly complete at the 16-nucleus stage after formation of the main layer has started. Kondo suggested that the "vitelline membrane" bears some resemblance to the fertilization membrane in terms of its formation.

The origin of the outer layer of the fertilization membrane was clarified in the present investigation. In *A. japonica*, just at the time of oviposition, when the egg had already accepted the sperm nucleus, no structure corresponding to an outer layer was visible. Such a structure appeared for the first time as a discontinuous thin membrane or a discontinuous layer of mucous material on the surface of the egg. Fifteen minutes after oviposition, the surface of the egg was enveloped completely by a thin membrane and an underlying layer of mucous material. The contents discharged on the egg surface from the periplasmic granules appeared to form the outer layer of the fertilization membrane.

From the existence of an intermediate type of granule, we can conclude that the contents of the two types of periplasmic granule may have the same components. Both the membrane-like material and the very electron-dense

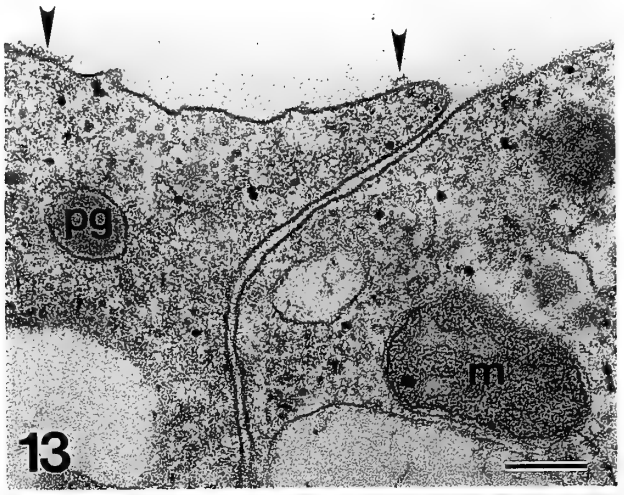

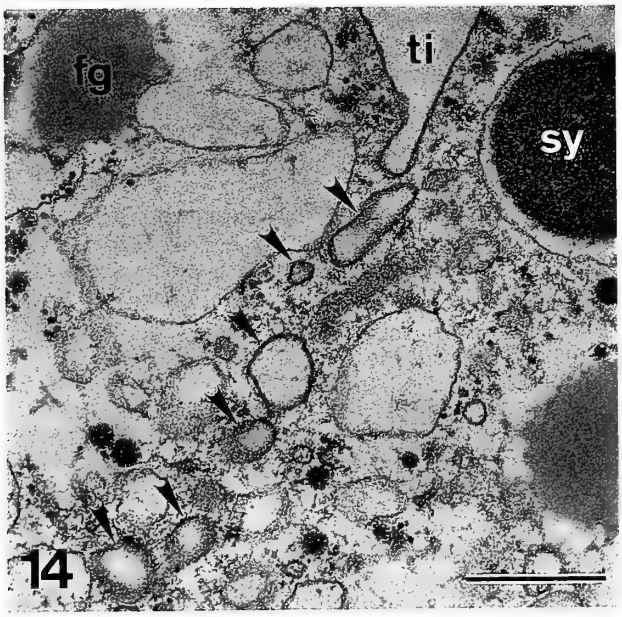

FIG. 13. Invagination of the cell membrane, three minutes after oviposition. Mucous material is visible on the surface of the egg (arrowheads). Scale bar=0.2 μm. m, mitochondrion; pg, periplasmic granule.

FIG. 14. Vesicles (arrowheads) arrayed at the tip of an invagination (ti), three minutes after oviposition. The elongation of the invagination of the cell membrane may be the result of the fusion of these vesicles. Scale bar=0.5 μm. fg, fatty granule; sy, small yolk granule.

matrix may, therefore, be able to form the mucous material. This mucous material may gradually harden from the outer side to form the outer layer of the fertilization membrane. The outer layer was observed as a membrane of 30 nm in thickness 20 min after oviposition. According to Suzuki and Kondo [13], the main layer of the "vitelline membrane" is formed by the matrix of vesicles that is discharged by exocytosis 30 min after oviposition. The formation of the outer layer and that of the main layer may be successive processes that require different materials.

In many animals other than spiders, the vitelline membrane is already complete by the time oviposition occurs.

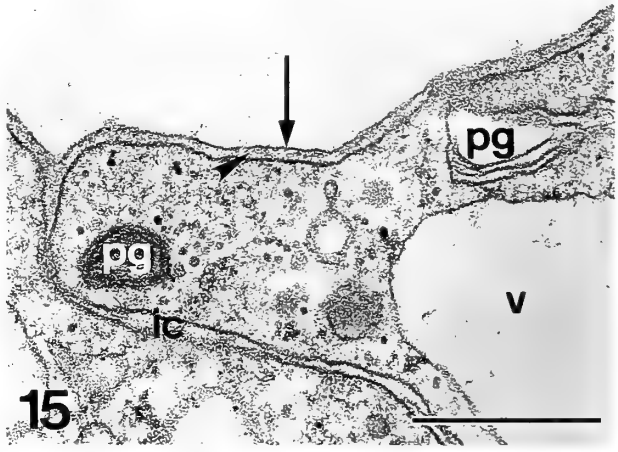

FIG. 15. The surface of the egg, fifteen minutes after oviposition. The surface is completely enveloped by a thin membrane (arrow) and an underlying layer of mucous material (arrowhead). The periplasmic granule (pg) on the right is discharging its contents. Scale bar=0.5 μm. ic, invaginating cell membrane; v, vesicle.

The formation of the outer layer after oviposition or after the entrance of the sperm nucleus suggests that the "vitelline membrane" of the spider egg is equivalent to the fertilization membrane and is not a true vitelline membrane. Suzuki and Kondo [13] postulated the incorporation of sperm into spider eggs in the ovarian cavity.

Invagination of the cell membrane and the arrangement of large yolk granules

The many microvilli found on the egg surface just at the time of oviposition may have participated in uptake of yolk materials during oogenesis. It has been reported in other spiders that the microvilli are formed at the vitellogenic stage [10–12]. In *A. japonica*, the microvilli disappeared prior to the exocytosis of periplasmic granules that resulted in formation of the outer layer of the fertilization membrane and then they appeared again prior to the formation of the main layer of the fertilization membrane.

In *A. japonica*, the cell membrane began to invaginate between 2 and 3 min after oviposition. The cell membrane that was extruded as microvilli might be utilized initially for the formation of invaginations. By contrast, the elongation of the invaginations of the cell membrane may be the result of the fusion of small vesicles, which were seen to be arrayed beyond the tip of each invagination. Some authors have reported polygonal mesh-work structures that corresponded in size to the underlying yolk masses in the periplasm in eggs of other spiders [2–4, 7, 8]. The edges of such polygons should correspond to the regions of invaginations of the cell membrane. Locy [8] and Kautzsch [3] reported that the polygons were smaller in one hemisphere than in the other in two species of *Agelena*. In *Achaearanea japonica*, no remarkable differences in the sizes of polygons were observed.

The lumen of each invagination of the cell membrane became wider and the large yolk granules were organized into

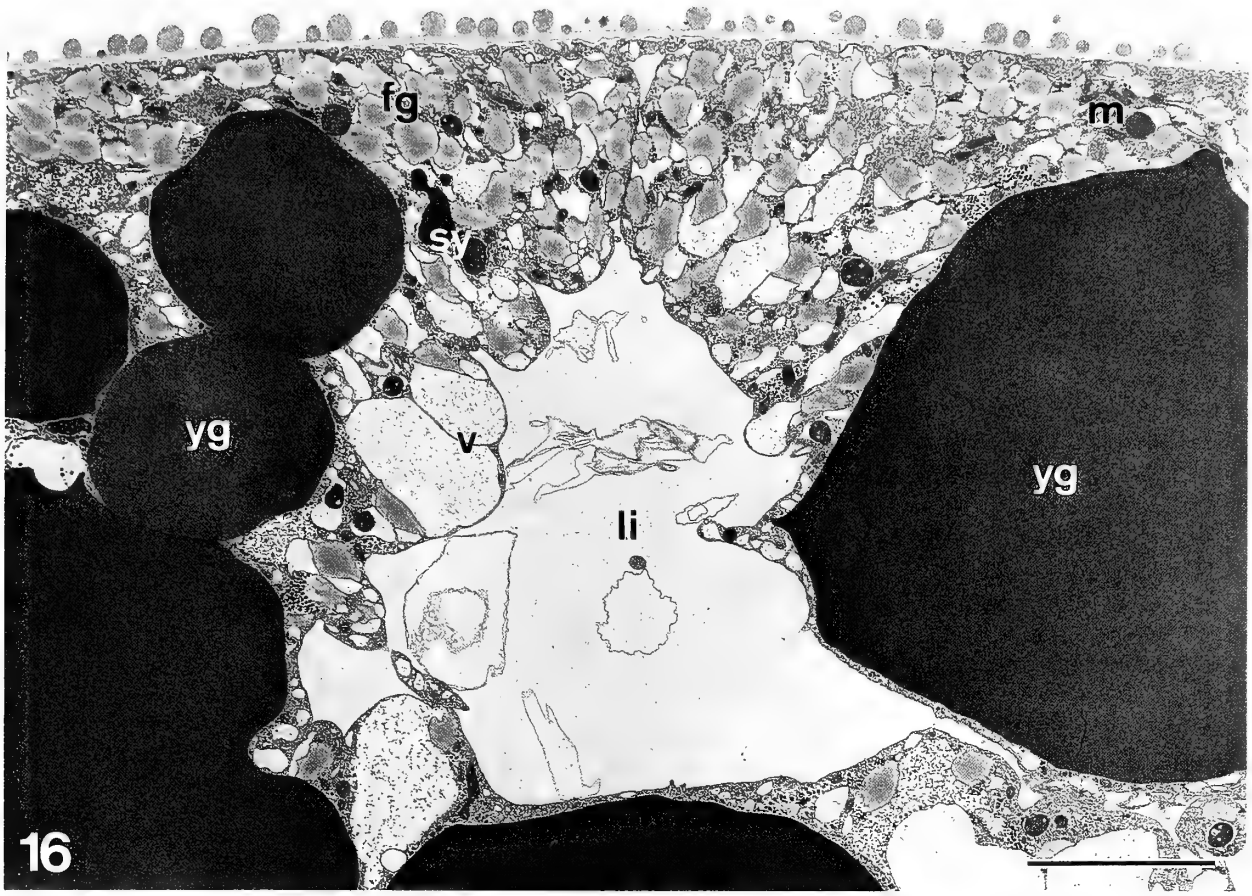

FIG. 16. Low-magnification view of the surface of an egg, twenty minutes after oviposition. The lumen of an invagination of the cell membrane (li) becomes wider and the large yolk granules (yg) become organized into radial columns in the outer region of the yolk mass (compare with Fig. 5). Scale bar=5 μm. fg, fatty granules; sy, small yolk granules; m, mitochondria; v, vesicles.

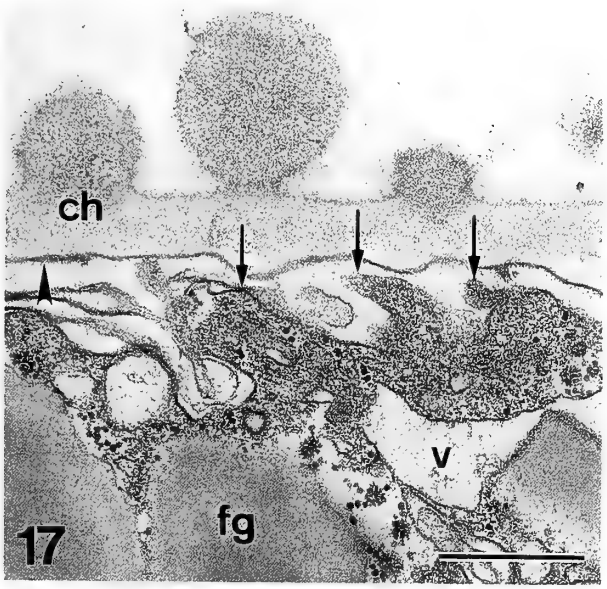

FIG. 17. High-magnification view of a portion of Figure 16. Arrowhead indicates the outer layer of the fertilization membrane. The cell membrane extrudes microvilli (arrows). Scale bar=0.5 μm. ch, chorion; fg, fatty granule; v, vesicle.

outer radial columns and an inner spherical mass. Montgomery [9] described this double structure of large yolk granules in *A. tepidariorum*. However, he failed to observe the invagination of cell membranes.

The first maturation division

Few investigations of egg maturation in spiders have been reported. Montgomery [9] described the first meiotic spindle in *A. tepidariorum*, which is oriented perpendicularly to the egg surface at the time that oviposition occurs. In *A. japonica*, the first meiotic spindle was oriented parallel to the egg surface at oviposition, and then the spindle was oriented perpendicularly to the egg surface for completion of nuclear division. This process may be explained in terms of the rotation of the meiotic spindle. The rotation may terminate prior to oviposition in *A. tepidariorum*. Fernández *et al.* [1] suggested the active participation of microtubules in the rotation of the first meiotic spindle in the leech *Theromyzon rude*.

It is unclear from the present study whether or not the first polar body is eliminated from the egg via the fusion of invaginating cell membranes. Reliable staining to the thick sections is required for further observations at the fine-

structural level.

REFERENCES

1 Fernández J, Olea N, Téllez V, Matte C (1990) Structure and development of the egg of the glossiphoniid leech *Theromyzon rude*: reorganization of the fertilized egg during completion of the first meiotic division. Dev Biol 137: 142–154

2 Holm Å (1954) Notes on the development of an orthognath spider, *Ischnothele karschi* Bös. & Lenz. Zool Bidr Uppsala 30: 109–221

3 Kautzsch G (1909) Über die Entwicklung von *Agelena labyrinthica* Clerck. Zool Jb Anat 28: 477–538

4 Kishinouye K (1891) On the development of Araneina. J Coll Sci Imp Univ Tokyo 4: 55–88

5 Kondo A (1969) The fine structures of the early spider embryo. Sci Rep Tokyo Kyoiku Daigaku Sec B 14: 47–67

6 Kondo A, Chaki E (1991) Histological studies on the ovaries of the golden silk spider, *Nephila clavata* L. Koch, before and after oviposition. Proc Arthropod Embryo Soc Jpn 26: 9–10

7 Lambert AE (1909) History of the procephalic lobes of *Epeira cinerea*. A study in arachnid embryology. J Morphol 20: 413–459

8 Locy WA (1886) Observations on the development of *Agelena nævia*. Bull Mus Com Zool 12: 63–103

9 Montgomery TH (1908) On the maturation mitoses and fertilization of the egg of *Theridium*. Zool Jb Anat 25: 237–250

10 Ōsaki H (1971) Electron microscope studies on the oocyte differentiation and vitellogenesis in the liphistiid spider, *Heptathela kimurai*. Annot Zool Japon 44: 185–209

11 Ōsaki H (1972) Electron microscope studies on developing oocytes of the spider, *Plexippus paykulli*. Annot Zool Japon 45: 187–200

12 Seitz KA (1971) Licht-und elektronenmikroskopische Untersuchungen zur Ovarentwicklung und Oogenese bei *Cupiennius salei* Keys. (Araneae, Ctenidae). Z Morph Tiere 69: 283–317

13 Suzuki H, Kondo A (1994) The second maturation division and fertilization in the spider *Achaearanea japonica* (Bös. *et* Str.). Zool Sci 11: 433–439

14 Yoshikura M (1955) Embryological studies on the liphistiid spider, *Heptathela kimurai*. Part 2. Kumamoto J Sci Ser B 2: 1–86

ZOOLOGICAL SCIENCE 11: 701–705 (1994)

Ultrastructural Study of Endogenous Energy Substrates in Spermatozoa of the Sea Urchins *Arbacia lixula* and *Paracentrotus lividus*

Masatoshi Mita[1], Atsuko Oguchi[2], Sakaé Kikuyama[2], Rosaria De Santis[3] and Masaru Nakamura[4]

[1]*Teikyo Junior College, Shibuya-ku, Tokyo 151,* [2]*Department of Biology, School of Education, Waseda University, Shinjuku-ku, Tokyo 169-50,* [3]*Department of Cell Biology, Stazione Zoologica 'Anton Dohrn', Villa Comunale, Napoli 80121, Italy, and* [4]*Department of Biology, Faculty of Medicine, Teikyo University, Hachioji, Tokyo 192-03, Japan*

ABSTRACT—Spermatozoa of the sea urchins, *Arbacia lixula* and *Paracentrotus lividus*, use endogenous triglyceride (TG) and phosphatidylcholine (PC), respectively, to produce energy for swimming. The present study examined ultrastructurally the location of TG and PC available for utilization in energy metabolism in spermatozoa of these species. The *A. lixula* spermatozoon contained several lipid globules in the midpiece proximally from the head. After incubation with seawater, TG levels decreased and morphological changes in the lipid globules were observed. Some lipid globules lost their smooth spherical shape, and their surface became irregular and uneven. Vacuoles of various sizes and forms also appeared near the lipid globules. In contrast, *P. lividus* spermatozoa possessed lipid bodies, instead of lipid globules, in the space between the mitochondrial outer and inner membranes. After incubation with seawater, the lipid bodies became small and finally disappeared, coincident with a decrease in the level of PC. These results strongly suggest that TG and PC, as endogenous substrates providing energy for motility, are stored in the lipid globules of *A. lixula* spermatozoa and the lipid bodies of *P. lividus* spermatozoa, respectively.

INTRODUCTION

Sea urchin spermatozoa obtain energy for flagellar movement from oxidation of an endogenous substrate [14–16]. In our recent study, following incubation in seawater, a decrease in the level of endogenous triglyceride (TG) was observed in the spermatozoa of the sea urchin *Arbacia lixula*, which belongs to the order Arbacioida, whereas in spermatozoa of *Paracentrotus lividus*, of the order Echinoida, the content of phospholipids, particularly phosphatidylcholine (PC), decreased [10]. Whereas the spermatozoa of *P. lividus* are generally composed of various phospholipids and cholesterol, *A. lixula* spermatozoa additionally contain TG [10]. The preferential hydrolysis of TG and PC is related to the properties of lipase and phospholipase A_2, respectively [10]. Glycogen and glucose are present in trace amounts in both species [10]. These findings suggest that *A. lixula* spermatozoa obtain energy for swimming through oxidation of endogenous TG, whereas *P. lividus* spermatozoa use mainly PC as a source for energy metabolism. Similar findings have been obtained for spermatozoa of other species of sea urchins belonging to the orders Arbacioida [6] and Echinoida [9, 11, 12]. The energy-metabolic system in sea urchin spermatozoa appears to differ between the Arbacioida and Echinoida.

It has been demonstrated that the sperm midpiece of *Glyptocidaris crenularis* (Arbacioida) contains a single mitochondrion and lipid globules [8]. The lipid globule is spherical and located in the posterior region between the basis of the mitochondrion and the plasma membrane. Similar lipid globules have been observed in spermatozoa of *Arbacia punctulata* [2, 4] and *Brissopsis lyrifera* [1]. Since there is a concomitant decrease in the level of intracellular TG in *G. crenularis* spermatozoa [8], it is assumed that the lipid globules contain TG, which is available for utilization in energy metabolism.

In contrast, it has been shown that the sperm midpiece of *Hemicentrotus pulcherrimus* (Echinoida) contains several lipid bodies within the mitochondrion [7]. This lipid body differs from the lipid globules, because the former is located inside the mitochondrion and it is relatively small in comparison with lipid globules. Following the initiation of swimming, the lipid bodies in *H. pulcherrimus* spermatozoa become small, coincident with a decrease in the level of PC [7]. Presumably, the lipid bodies within the mitochondria of spermatozoa are reservoirs of endogenous PC substrate. To obtain additional information on the energy metabolism of spermatozoa of the sea urchins *A. lixula* and *P. lividus*, the present study was undertaken to determine whether the sperm midpiece in both species contains lipid bodies or lipid globules. Furthermore, the relationship between these lipid inclusions and energy metabolism was examined.

MATERIALS AND METHODS

Materials

Spawning of stored spermatozoa of the sea urchins *A. lixula* and *P. lividus* was induced by injecting 0.5 M KCl into the coelomic

Accepted August 24, 1994
Received May 16, 1994

cavity. Semen was always collected freshly as 'dry sperm' and kept undiluted on ice. The number of spermatozoa was calculated on the basis of protein concentration, which was determined using a Micro BCA protein assay kit (Pierce, IL). The protein content per 10^9 spermatozoa was 0.5 ± 0.1 mg in both species.

Incubation of spermatozoa

Dry sperm were diluted 100-fold in artificial seawater (ASW) consisting of 458 mM NaCl, 9.6 mM KCl, 10 mM $CaCl_2$, 49 mM $MgSO_4$, and 10 mM Tris-HCl at pH 8.2. After dilution and incubation at 20°C, the sperm suspension was centrifuged at $3,000 \times g$ for 5 min at 0°C.

Determination of PC and TG concentrations

Total lipids were extracted from spermatozoa using the method of Bligh and Dyer (1959). PC and TG levels were determined by high-performance thin-layer chromatography (HPTLC), as described previously [5, 11, 12].

Preparation for electron microscopy

Dry sperm were diluted 100-fold in ASW and incubated at 20°C. At appropriate intervals, the spermatozoa were prefixed in 2.5% glutaraldehyde ASW solution for 40–60 min; a volume of sperm suspension was mixed with the same volume of 5% glutaraldehyde in 80% ASW. The prefixed spermatozoa were rinsed with ASW and post-fixed with 1% OsO_4 for 2 hr. After dehydration in a graded series of ethanol solutions, the specimens were embedded in epoxy resin, and ultrathin sections were cut on a Reichert Ultracut ultramicrotome. After staining the specimens with lead citrate, they were observed using a Hitachi 7000 electron microscope.

Reagents

The TG and PC standards were purchased from Sigma Chemical Co. (St. Louis, MO). All reagents and solvents were of analytical grade. HPTLC plates (silica gel 60) were obtained from E. Merck (Darmstadt, Germany).

RESULTS

It has been demonstrated that the level of TG in *A. lixula* and of PC in *P. lividus* spermatozoa decreases, respectively, after 1 hr of incubation in seawater [10]. Confirming this, the PC level decreased gradually when dry sperm of *P. lividus* had been diluted and incubated for 15, 30, 45, and 60 min in ASW (Fig. 1a). About 23 μg PC was contained in 10^9 spermatozoa. During incubation for 1 hr, about 5 μg PC was consumed by the spermatozoa. Although *A. lixula* spermatozoa contained PC (about 22 $\mu g/10^9$ sperm), the PC content did not change significantly during incubation (Fig. 1a). In contrast, the level of TG in *A. lixula* spermatozoa decreased following incubation in ASW (Fig. 1b). About 3 μg of TG was consumed in 10^9 spermatozoa during incubation for 1 hr. TG was present in a trace amount (<1 $\mu g/10^9$ sperm) in *P. lividus* spermatozoa [10].

The sea urchin spermatozoon consists of a head, a midpiece and a tail. In longitudinal sections through spermatozoa of *A. lixula*, the midpiece was observed to consist of a single mitochondrion and several lipid globules (Fig. 2a). All spermatozoa contained these lipid globules, which were mostly spherical and homogeneously dense in appearence, and located distally in the sperm midpiece (Fig. 3a), distributed in a band nearest the flagellum (Fig. 3b).

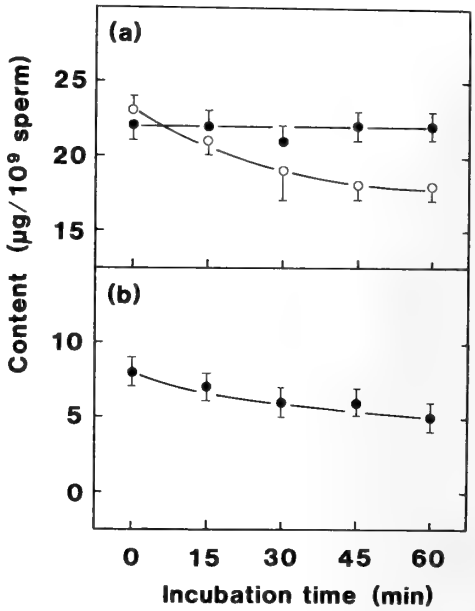

FIG. 1. Changes in levels of phosphatidylcholine (a) and triglyceride (b) in *A. lixula* (●) and *P. lividus* (○) spermatozoa following incubation in seawater. Dry sperm were diluted 100-fold and incubated in seawater at 20°C. Each value is the mean of four separate experiments. Vertical bars show S.E.M.

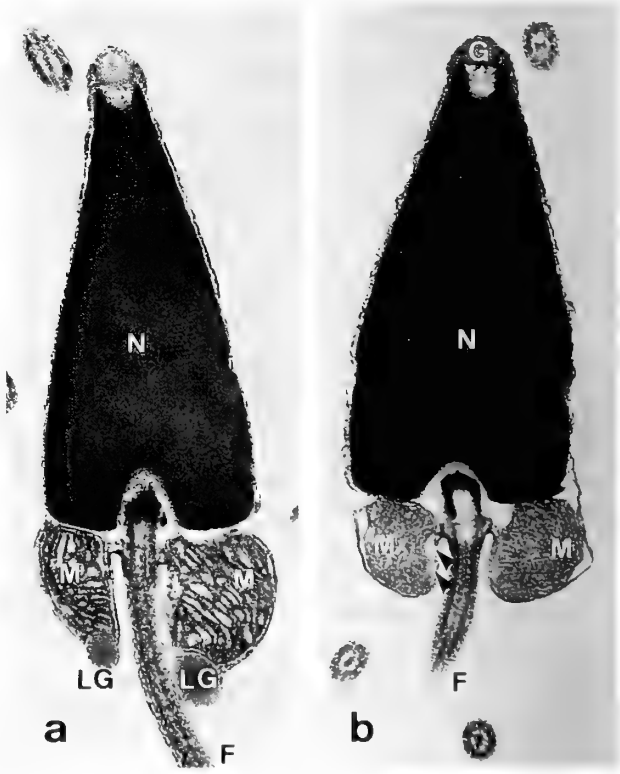

FIG. 2. Longitudinal section through a spermatozoon of *A. lixula* (a) and *P. lividus* (b). Arrow heads show lipid bodies. F: flagellum, G: acrosomal granule, LG: lipid globule, M: mitochondrion, N: nucleus. ×25,000.

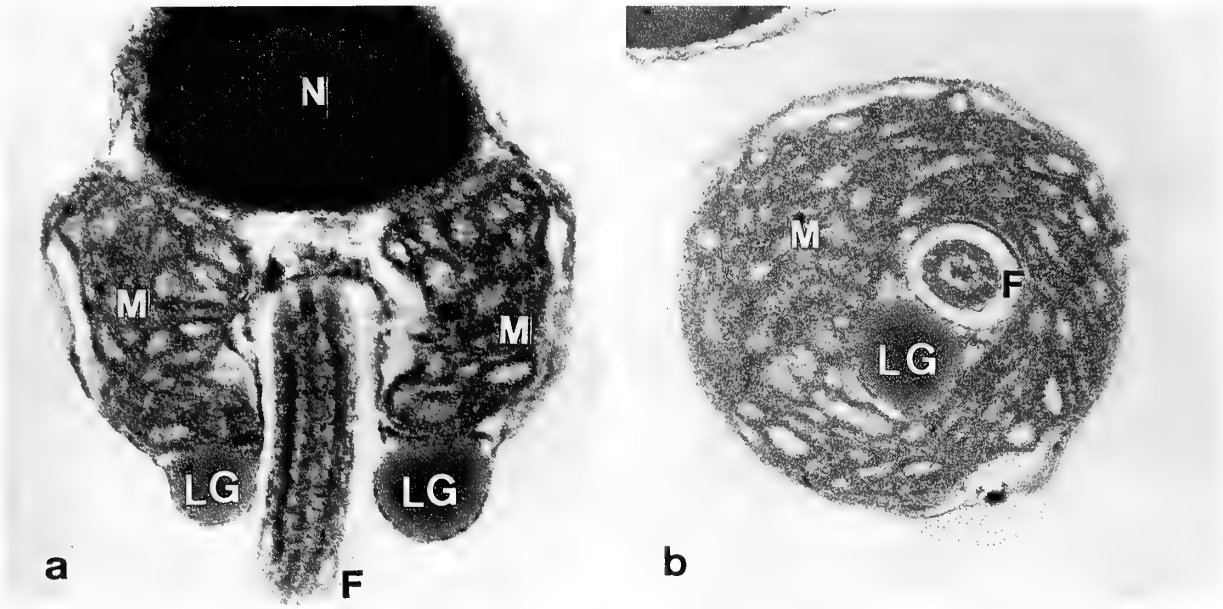

FIG. 3. Longitudinal (a) and transverse (b) sections through the mitochondrial region of *A. lixula* spermatozoa before incubation in seawater. F: flagellum, LG: lipid globule, M: mitochondrion, N: nucleus. ×55,000.

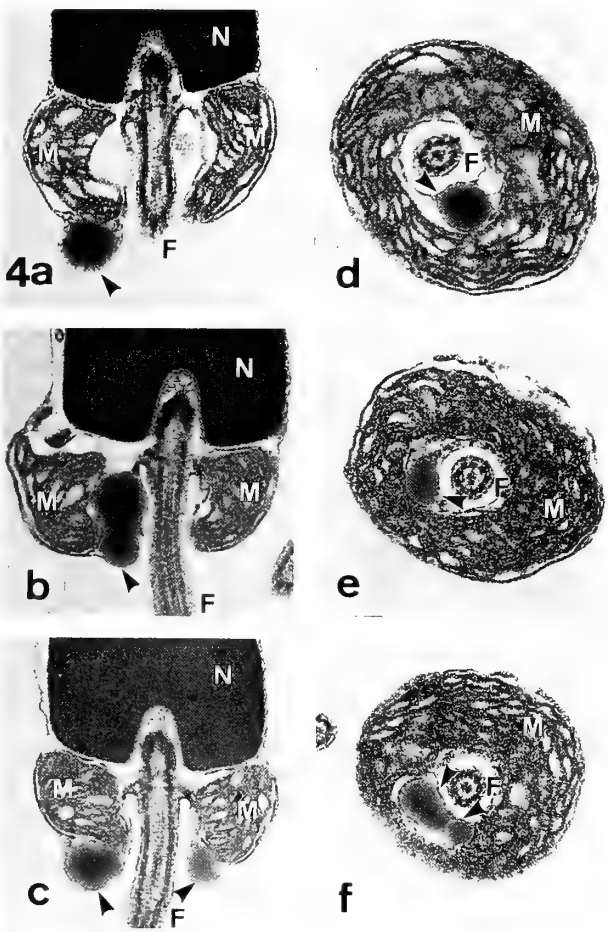

FIG. 4. Longitudinal (a-c) and transverse (d-f) sections through the mitochondrial region of *A. lixula* spermatozoa after incubation in seawater for 10 min (a, d), 30 min (b, e) and 60 min (c, f). Arrow heads show lipid globules. F: flagellum, M: mitochondrion, N: nucleus. ×27,000.

Longitudinal and transverse sections of the midpieces of *A. lixula* spermatozoa were examined after incubation in ASW. After incubation for 10 min, there was little evident change in the lipid globules (Figs. 4a and d). After 30 min of incubation, some lipid globules had lost their smooth spherical shape, and their surface had become irregular and uneven (Figs. 4b and e). After 60 min of incubation, irregular and uneven globules appeared frequently (Figs. 4c and f).

In contrast to *A. lixula*, the midpiece of the *P. lividus* spermatozoon did not contain lipid globules (Fig. 2b). A region between the mitochondrial outer and inner membranes was dilated in a band nearest the flagellum and contained low-electron-density lipid bodies (Fig. 5), similar to those observed in the spermatozoa of *H. pulcherrimus* [7]. These lipid bodies were irregular in profile and smaller than lipid globules. After 10 min of incubation in ASW, lipid bodies were still present (Figs. 6a and d), and a gap was also observed to have opened between the plasma membrane and the mitochondrial outer membrane. At 30 min after incubation, the lipid bodies had become small (Figs. 6b and e) and by 60 min, the lipid bodies and inner ring of the mitochondrion had finally disappeared (Figs. 6c and f). However, various structural features of the mitochondrion, such as the number of cristae and the thickness of the membranes, did not change during incubation in ASW.

DISCUSSION

This study showed that lipid globules were present in spermatozoa of *A. lixula* of the order Arbacioida (Fig. 2a) and that lipid bodies were present in those of *P. lividus* of the order Echinoida (Fig. 2b). The lipid globules were located distant from the mitochondrion, in the midpiece proximally from the head (Fig. 3), whereas the lipid bodies were distri-

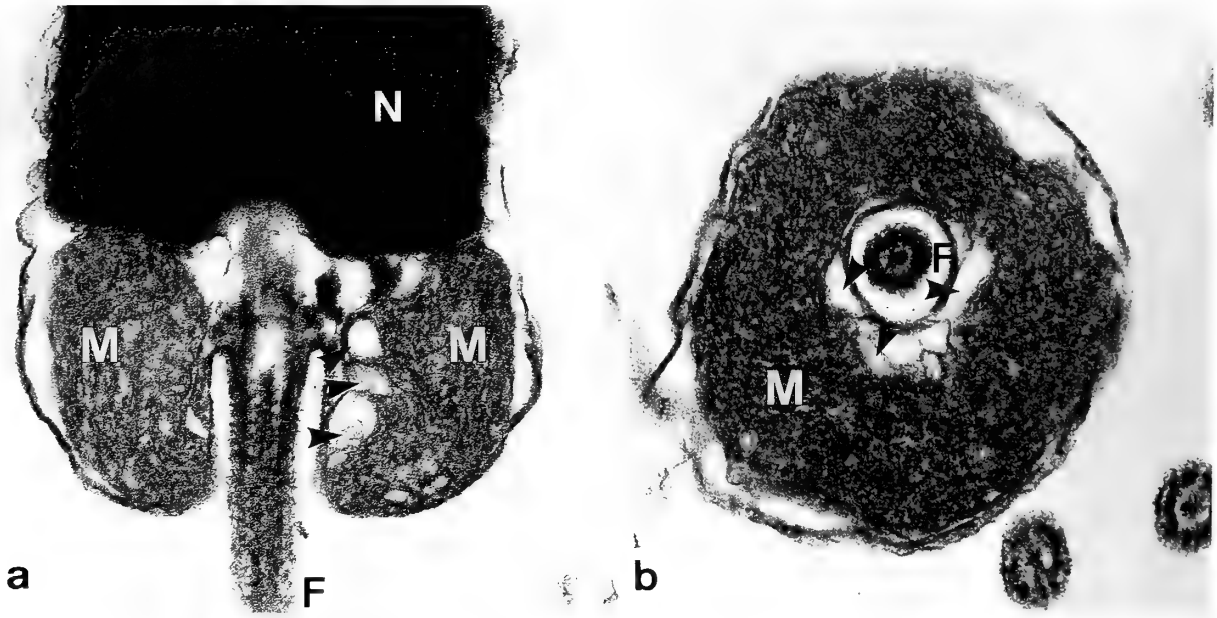

FIG. 5. Longitudinal (a) and transverse (b) sections through the mitochondrial region of *P. lividus* spermatozoa before incubation in seawater. Arrow heads show lipid bodies. F: flagellum, M: mitochondrion, N: nucleus. ×55,000.

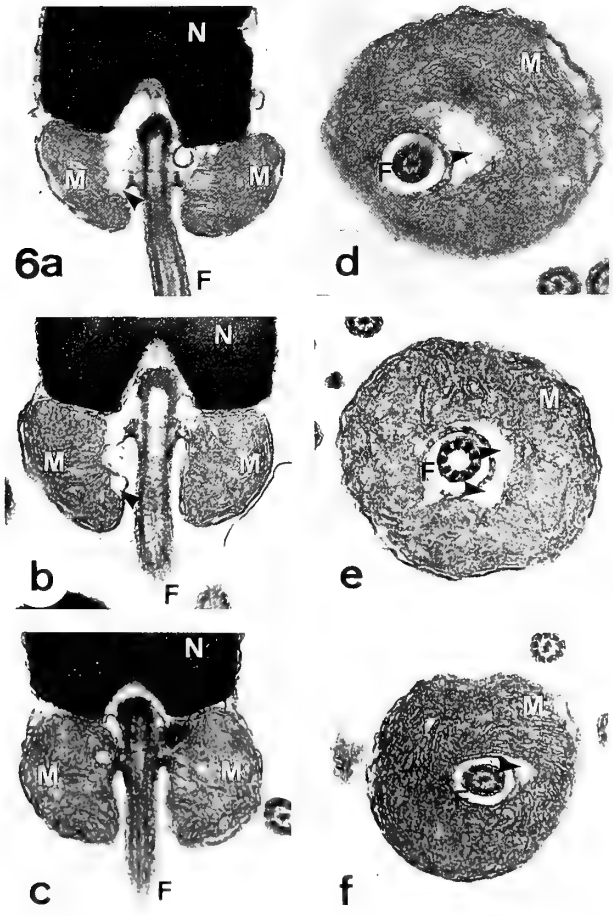

FIG. 6. Longitudinal (a-c) and transverse (d-f) sections through the mitochondrial region of *P. lividus* spermatozoa after incubation in seawater for 10 min (a, d), 30 min (b, e) and 60 min (c, f). Arrow heads show lipid bodies. F: flagellum, M: mitochondrion, N: nucleus. ×27,000.

buted within the mitochondrion (Fig. 5). Morphological changes in both the lipid globules (Fig. 4) and lipid bodies (Fig. 6) were observed after incubation, suggesting that digestion of these inclusions occurs simultaneously with activation of energy metabolism.

The several lipid globules were found to be mostly spherical in the midpieces of *A. lixula* spermatozoa before incubation (Figs. 3 and 4), but they became irregular and uneven after incubation. Previous studies have shown that the total volume of lipid globules in spermatozoa of *G. crenularis* is reduced during incubation, concomitantly with a decrease in the level of TG [8]. The present study also revealed a decrease of TG levels in spermatozoa of *A. lixula* after incubation (Fig. 1b), as described previously [10]. Therefore it is possible that TG available for utilization in energy metabolism is contained in the lipid globules of *A. lixula* spermatozoa.

In contrast, PC is the substrate used for energy metabolism in *P. lividus* spermatozoa [10]. This study also showed that the lipid bodies shrank and disappeared (Fig. 6) in parallel with changes in the level of PC (Fig. 1a). These observations suggest that PC available for use in energy metabolism is related to the appearance of lipid bodies. Similar findings have been obtained in spermatozoa of other sea urchins of the order Echinoida [7, 9]. Thus possibly, the lipid bodies within mitochondria are reservoirs of PC as an endogenous substrate.

With regard to the substrate used for energy metabolism in sea urchin spermatozoa, it is interesting that TG and PC are stored in lipid globules and lipid bodies, respectively. Neither TG nor lipid globules are present in spermatozoa of Echinoida sea urchins, such as *P. lividus* (Figs. 1 and 2) and *H. pulcherrimus* [7]. Therefore it is assumed that the Echi-

noida spermatozoa, which have lost their lipid globules, are provided with a system for metabolism of phospholipids, particularly PC, in lipid bodies within mitochondria.

ACKNOWLEDGMENTS

This work was supported by the Japanese Society for Promotion of Science (JSPS) and the Italian National Research Council (CNR).

REFERENCES

1 Afzelius BA, Mohri H (1966) Mitochondria respiring without exogenous substrate. A study of aged sea urchin spermatozoa. Exp Cell Res 42: 10–17

2 Bernstein MH (1962) Normal and reactive morphology of sea urchin spermatozoa. Exp Cell Res 27: 197–209

3 Bligh EG, Dyer WJ (1959) A rapid method of total lipid extracion and purification. Can J Biochem 37: 911–917

4 Longo FJ, Anderson E (1969) Sperm differentiation in the sea urchins *Arbacia punctulata* and *Strongylocentrotus purpuratus*. J Ultrastruct Res 27: 486–509

5 Macala LJ, Yu RK, Ando S (1983) Analysis of brain lipids by high performance thin-layer chromatography and densitometry. J Lipid Res 24: 1243–1250

6 Mita M (1991) Energy metabolism of spermatozoa of the sea urchin *Glyptocidaris crenularis*. Mol Reprod Dev 28: 280–285

7 Mita M, Nakamura M (1992) Ultrastructural study of an endogenous energy substrate in spermatozoa of the sea urchin *Hemicentrotus pulcherrimus*. Biol Bull 182: 298–304

8 Mita M, Nakamura M (1993) Lipid globules at the midpieces of *Glyptocidaris crenularis* spermatozoa and their relation to energy metabolism. Mol Reprod Dev 34: 158–163

9 Mita M, Nakamura M (1993) Phosphatidylcholine is an endogenous substrate for energy metabolism in spermatozoa of sea urchins of the order Echinoidea. Zool Sci 10: 73–83

10 Mita M, Oguchi A, Kikuyama S, Yasumasu I, De Santis R, Nakamura, M (1994) Endogenous substrates for energy metabolism in spermatozoa of the sea urchins *Arbacia lixula* and *Paracentrotus lividus*. Biol Bull 186: 285–290

11 Mita M, Ueta N (1988) Energy metabolism of sea urchin spermatozoa, with phosphatidylcholine as the preferred substrate. Biochim Biophys Acta 959: 361–369

12 Mita M, Ueta N (1989) Fatty chain composition of phospholipids in sea urchin spermatozoa. Comp Biochem Physiol 92B: 319–322

13 Mita M, Ueta N (1990) Phosphatidylcholine metabolism for energy production in sea urchin spermatozoa. Biochim Biophys Acta 1047: 175–179.

14 Mita M, Yasumasu I (1983) Metabolism of lipid and carbohydrate in sea urchin spermatozoa. Gamete Res 7: 133–144

15 Mohri H (1957) Endogenous substrates of respiration in sea-urchin spermatozoa. J Fac Sci Univ Tokyo Sec IV 8: 51–63

16 Rothschild Lord, Cleland KW (1952) The physiology of sea-urchin spermatozoa. The nature and location of the endogenous substrate. J Exp Biol 41: 66–71

ZOOLOGICAL SCIENCE 11: 707–711 (1994)

The Effect of Glucocorticoids on the Activity of Monoamine Oxidase and Superoxide Dismutase in the Rat Interscapular Brown Adipose Tissue

GORDANA CVIJIĆ, RATKO RADOJIČIĆ, ŽANA MATIJAŠEVIĆ and VUKOSAVA DAVIDOVIĆ[1]

Institute of Physiology and Biochemistry, Faculty of Biology, University of Belgrade, Akademski Trg 16, 11000 Belgrade, Yugoslavia

ABSTRACT—The effect of dexamethasone (DEX) and corticosterone (COR) on the activity of monoamine oxidase (MAO), copper-zinc superoxide dismutase (CuZn SOD) and manganese superoxide dismutase (Mn SOD) in the rat interscapular brown adipose tissue (IBAT) were studied. DEX (1 mg/kg, i.p. for two days) significantly increased MAO activity in the IBAT as compared to the corresponding controls. On the contrary, COR, in the corresponding dose (5 mg/kg), did not affect MAO activity in the IBAT. DEX also markedly enhanced the activity of both SODs in the tissue studied, while COR was ineffective. The results suggest that there exist the differences in the effect between the synthetic glucocorticoid, such as DEX, and COR, which is a natural glucocorticoid in the rat, on the activity of IBAT enzymes studied.

INTRODUCTION

The major role of brown adipose tissue (BAT) is heat production. This specialized tissue is considered to be an effector of non-shivering [10], and diet induced thermogenesis [21]. Heat production within the BAT results from the oxidation of fatty acids in mitochondria [3] without the involvement of ATP synthesis. The main regulator of the BAT activity is noradrenaline [12], which is released from the sympathetic nerve terminals, present within the tissue. The BAT metabolic activity can be modified by a number of hormones. For example, COR reduces this activity [11] whereas adrenalectomy causes its increase [14]. On the other hand, it is known that the increased oxygen consumption in the BAT may induce the generation of oxygen free radicals in mitochondria [1]. These free radicals are very toxic and hence aerobic organisms possess anti-oxidant enzymes which maintain their intracellular concentration at a low level preventing the membrane destruction. The main enzyme, which dismutates superoxide anion radicals (O_2^-) into H_2O_2 plus O_2^- is superoxide dismutase (SOD). The rat IBAT contains a relatively high content of the two main forms of SOD: CuZn SOD and Mn SOD residing in the cytosol and in the matrix of mitochondria respectively [20]. Besides, in the processes of catecholamine deamination with MAO, H_2O_2 is produced [4, 24]. Thus, the changes in the activity of some enzymes of the anti-oxidant system (SODs), along with the changes in the activity of MAO, an enzyme involved in the metabolism of noradrenaline, which is the main regulator of BAT activity, could be relevant indicators of metabolic alterations in the BAT under the hormonal influence. In order to elucidate this possibility we have studied the effect of dexamethasone and corticosterone on the activities of MAO and on two antioxidant enzymes of the superoxide dismutase family, the CuZn SOD and Mn SOD, in IBAT.

MATERIALS AND METHODS

Experiments were carried out on male rats of the Wistar strain, weighing 193–227 g at the beginning of the experiment. The animals were previously acclimated to 21±1°C, maintained under intermittent 12 hr periods of light and dark and given food and water *ad lib*. The rats were divided into 4 groups. The first group consisted of animals treated with dexamethasone (ICN, Galenika) dissolved in saline, in dose of 1 mg/kg body weight *i.p.* for 2 days. The second group of rats (control) was treated in the same way but with the saline only. The rats of the third group received corticosterone (Sigma, Chemical Co., St Louis, MO, USA) in dose of 5 mg/kg body weight, *i.p.* for 2 days. Before the injection, corticosterone was dissolved in a small amount of ethanol and diluted with saline. Parallelly, the fourth group of rats was treated with vehicle (ethanol-saline) only. On day 3 of the experiment all the animals were decapitated and their IBAT removed, placed in the appropriate medium, weighed and prepared for the measurement of the enzyme activities. Namely IBAT from each rat was minced and divided into two portions. One portion was then homogenized in cold 0.9% KCl, and used for determination of MAO activity with ^{14}C-triptamine bisuccinate as a substrate by the method of Wurtman and Axelrod [25]. The results obtained are expressed as pmol/mg of proteins/min of incubation. Total protein content was measured by the method of Lowry [18].

Another IBAT portion was homogenized at 0–4°C using 0.25 M sucrose, 0.05 M Tris and 0.1 nM EDTA adjusted to pH 7.4, with HCl. The homogenates were sonicated (at 50 W for 30 s in a Bronson model B-12 sonicator) to release the Mn SOD. The

Accepted August 1, 1994
Received April 18, 1994
[1] To whom requests of reprints should be addressed.

homogenates were then centrifuged at 6,000×g for 15 min. The supernatant was centrifuged at 85,000×g for 90 min and used for the determination of CuZn SOD and Mn SOD activities. SOD activity in the cytosol (CuZn SOD) and mitochondria (Mn SOD) was determined by the epinephrine method of Misra and Fridovich [19] and expressed as units of SOD/mg of proteins. One unit of SOD was defined as the amount of protein inhibiting the oxidation of epinephrine by 50% under the appropriate reaction conditions. Blood glucose concentration was measured with a glucose analyser (Exactech) using Dextrostix reagent strips.

IBAT mitochondria were prepared by the method of Slinde *et al.* [23] and mitochondrial protein content was estimated [18]. All results have been presented as means±SEM. Statistical significance of differences between groups was evaluated by Student's t-test.

RESULTS

Effect of dexamethasone and corticosterone on the body weight, blood glucose, total protein and mitochondrial protein content

Dexamethasone significantly lowered body weight ($P<0.005$), whereas corticosterone produced a marked body weight gain ($P<0.005$) in relation to the corresponding controls (Table. 1). At the same time, dexamethasone

TABLE 1. Effects of dexamethasone and corticosterone on body weight, IBAT weight, blood glucose, total protein and mitochondrial protein content

Treatment	Saline (Control)	Dexamethasone	Saline + Alcohol	Corticosterone
Initial body weight (g)	193.00±1.70*	221.00±3.80	227.00±3.00	224.00±5.30
Final body weight (% of initial values)	107.77	92.76	104.85	114.73
Blood glucose (nmol/l)	6.60±0.31*	6.90±1.60	6.74±2.20	7.01±1.80
IBAT weight per body weight (mg/g)	0.91	1.22	1.03	0.95
IBAT total protein content (mg/ml homog.)	5.06±0.22*	4.83±0.33	4.91±0.28	4.40±0.13
Mitochondrial protein content (mg/ml homog.)	0.30±0.02	0.26±0.03	0.29±0.01	0.17±0.01

* Mean±S.E.M. (n=6)

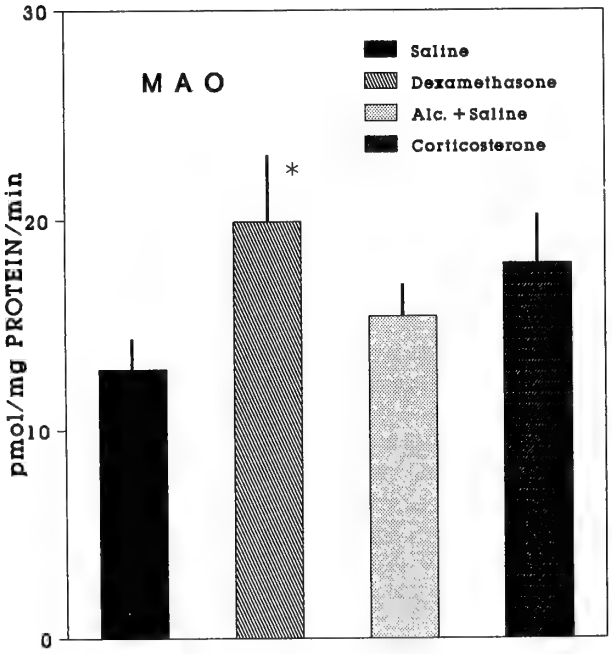

FIG. 1. The effect of dexamethasone (1 mg/kg b.w. *i.p.* for two days) or corticosterone (5 mg/kg b.w. *i.p.* for two days) on the MAO activity in the rat IBAT. Values (pmol of indol acetic acid formed per mg of protein per min of incubation) are given as means±SEM of six animals. Difference from the saline control: $*P<0.05$.

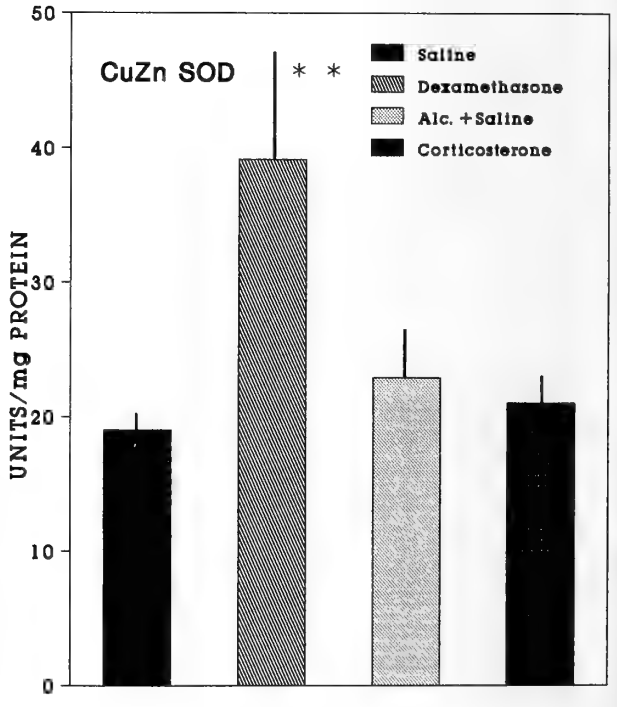

FIG. 2. The effect of dexamethasone (1 mg/kg b.m. *i.p.* for two days) or corticosterone (5 mg/kg b.m. *i.p.* for two days) on the CuZn SOD activity in the rat IBAT. Values (units per mg of protein) are given as means±SEM of six animals. Difference from the saline control: $**P<0.025$.

caused a significant increase in the IBAT weight (34%, $P<0.005$), whereas corticosterone had no effect on the weight of this tissue. Both glucocorticoids showed any significant effect neither on the blood glucose level nor on the total IBAT protein content. In contrast to dexamethasone, which exerted no effect on the mitochondrial protein content, corticosterone significantly reduced it ($P<0.005$).

Effects of dexamethasone and corticosterone on the MAO activity in the rat IBAT

Dexamethasone significantly increased MAO activity in the IBAT ($P<0.05$) as compared to the saline treated controls (Fig. 1). The values for control and dexamethasone-treated animals were 14.22 ± 1.43 and 19.91 ± 3.13 pmol/mg protein/min, respectively. However, corticosterone did not markedly change the activity of this catecholamine degrading enzyme in the tissue. The respective values for control and corticosterone-treated rats were 15.42 ± 1.53 and 17.91 ± 2.30 pmol/mg protein/min.

Effects of dexamethasone and corticosterone on the CuZn SOD and Mn SOD activities in the rat IBAT

It is evident from Figure 2 that dexamethasone significantly increased CuZn SOD activity in the IBAT ($P<0.025$). The values for control and dexamethasone-treated rats were 18.98 ± 1.27 and 39.14 ± 8.40 U/mg protein respectively. Similarly, a marked enhance in Mn SOD activity in the IBAT of rats was obtained by dexamethasone treatment (Fig. 3). The respective values for the control and dexamethasone treated animals were 2.02 ± 0.30 and 4.30 ± 0.82 U/mg protein ($P<0.025$). On the other hand, corticosterone did not influence the activity of either of the SOD forms in the IBAT (Figs. 2 and 3) in respect to corresponding controls (control 22.90 ± 3.87; corticosterone-treated 21.03 ± 2.08 U/mg protein, for CuZn SOD and control 3.43 ± 0.85; corticosterone treated 4.43 ± 0.18 U/mg protein, for Mn SOD).

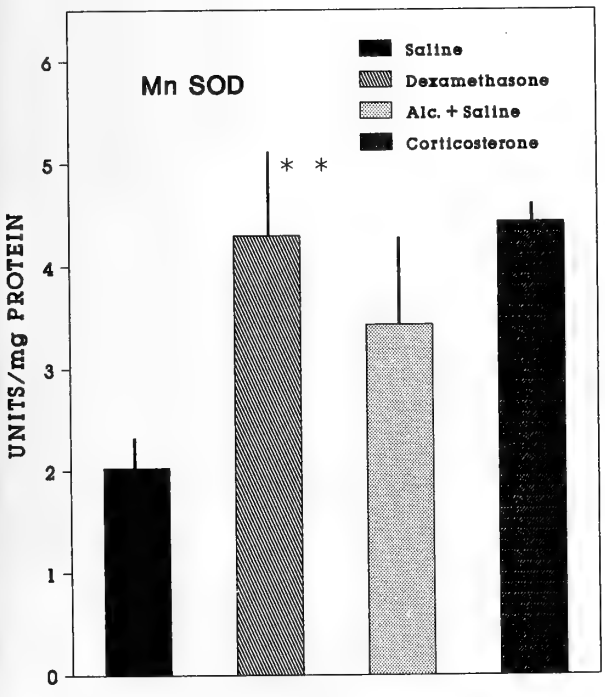

FIG. 3. The effect of dexamethasone (1 mg/kg b.m. *i.p.* for two days) or corticosterone (5 mg b.m. *i.p.* for two days) on the Mn SOD activity in the rat IBAT. Values (units per mg of protein) are given as means ± SEM of six animals. Differences from the saline control: $^{**}P<0.025$.

DISCUSSION

In the present study we observed that dexamethasone significantly lowered body weight, which is in accordance with the results of Fleck *et al.* [9]. This is probably the consequence of the stimulating effect of this hormone on the IBAT metabolic activity which leads to the increased energy expenditure [16]. However, corticosterone produced the significant body weight gain, which probably resulted from its inhibitory action on the secretion of corticotrophin releasing hormone (CRH). Namely, it is known that CRH enhances the sympathetic activity in the IBAT and increases energy expenditure [2, 7]. Therefore, it is possible to suppose that exogenously applied corticosterone inhibits CRH secretion and consequently, the sympathetic nervous system activity in the IBAT as well as the energy expenditure, which results in the body weight gain. We have also shown that dexamethasone markedly increased the IBAT weight while corticosterone had no significant effect. This increase in the IBAT weight, which is not accompanied by the change in the IBAT total protein content, may result from the possible intense lipogenesis, induced by insulin, the release of which is stimulated by dexamethasone [13].

Our results also clearly indicate the different actions of two glucocorticoids, dexamethasone and corticosterone, on the activity of catecholamine degrading enzyme MAO and the main enzymes for antioxidant defence, CuZn SOD and Mn SOD, in the IBAT of rats. Namely, dexamethasone, a highly potent synthetic glucocorticoid, the half life of which in the circulation is markedly longer than that of corticosterone, increased the activity of all IBAT enzymes studied. At the same time, short-term treatment of rats with corticosterone, which is a natural glucocorticoid in the rats, did not change markedly either the activity of catecholamine degrading enzyme MAO or the activity of any of the two SOD forms. However, the mechanism of action by which glucocorticoids alter MAO and SODs activities, *in vivo*, is still unknown. It is not known whether dexamethasone and corticosterone exert the direct effect on the activity of all enzymes studied, or their influence is mediated by changes in the CRH production and consequently in the activity of IBAT innervating sympathetic nerves. In fact our results concerning the stimulating effect of dexamethasone on the activity of the main enzymes for antioxidant defence and on catecholamine degrading enzyme MAO in the IBAT are apparently not in agreement with general idea that corticoids have a depressing effect on IBAT activity and thermogenin content in rodents

[15, 22]. However, having in mind the observations that the prolonged dexamethasone treatment can increase thermogenin content and thermogenin mRNA expression [16], it is possible to suppose that this glucocorticoid, acting directly on the IBAT, increases both metabolic and MAO activities. Therefore, under the present experimental conditions the production of free radicals might be enhanced and consequently the induction of enzymes for antioxidant defence.

Unlike dexamethasone, corticosterone did not change significantly either the activity of MAO or that of either of the two SOD forms. The failure of corticosterone to affect these activities might have been predicted if we bear in mind the following evidence: first, corticosterone is one "antibrown fat" hormone [11, 15] which inhibits the metabolic activity of BAT [26]; second, corticosterone reduces in rats both the integrated sympathetic nervous system activity and direct sympathetic activity within the IBAT, as judged by the decreased urinary noradrenaline excretion and noradrenaline turnover rate in the IBAT [5], and finally, it is well known that changes in the circulating corticosterone level induce reciprocal effects in hypothalmic CRH production [26]. Namely, York [26] showed that CRH, given centrally, increases the firing rate of sympathetic innervation of IBAT in both, lean and obese rats. Le Feuvre *et al.* [17] also observed that central administration of CRH produces an activation of the brown adipose tissue thermogenesis in the rats. Since CRH enhances sympathetic activity, it is possible to suppose that exogenously applied corticosterone inhibits the production of CRH, by a negative feed-back mechanism, decreasing in this way both the sympathetic nervous system activity and noradrenaline turnover in the IBAT [5]. Therefore, under these experimental conditions, the production of free radicals and consequently the increase in the activity of SODs were not possible. Bearing in mind the data mentioned above, it may be concluded that the differences in the effect between dexamethasone and corticosterone on the activity of IBAT enzymes studied result from the different pathways of their action. It seems that dexamethasone acts directly on the IBAT through glucocorticoid (GR) receptors, the existence of which was proved by Feldman [8]. These receptors have a few times higher affinity for dexamethasone than for corticosterone [6]. However, corticosterone probably acts indirectly through the changes in the activity of efferent sympathetic nerves, which innervate this specialized tissue.

ACKNOWLEDGMENTS

This research was supported by the Ministry of Science and Technology of Serbia (Contract No. 0319).

REFERENCES

1 Barja de Quiroga G, Lopez-Torres M, Perez-Campo R, Abelenda M, Paz Nava M, Puerta L (1991) Effect of cold acclimation on GSH, antioxidant enzymes and lipid peroxidation in brown adipose tissue. Biochem J 277: 289–292

2 Brown UR, Fisher LA, Spiess J, Rivier J, Rivier C, Vale W (1982) Corticotropin releasing factor: action on the sympathetic nervous system and metabolism. Endocrinology 111: 928–931

3 Bukowiecki IJ, Follea N, Lupien J, Paradis A (1981) Metabolic relationships between lipolysis and respiration in rat brown adipocytes. J Biol Chem 256: 12840–12848

4 Cohen G (1985) Oxidative stress in the nervous system. In "Oxidative Stress" Ed by H Sies, Academic Press, New York, pp 383–401

5 Davidović V, Vasilev I, Stojanović-Šušulić V (1992) Dependence of the sympatho-adrenal activity on the nutritional status in corticosterone treated rats. Comp Biochem Physiol 101A: 309–312

6 De Kloet ER (1991) In "Brain Corticosteroid Receptor Balance and Homeostatic Control vol. 12", Frontiers in Neuroendocrinology, Ed by F Ganong and L Martini, Raven Press, New York, pp 95–164

7 Egawa M, Yoshimatsu H, Bray GA (1990) Effect of corticotropin releasing hormone and neuropeptide Y on electrophysiological activity of sympathetic nerves to interscapular brown adpose tissue. Neuroscience 34: 771–775

8 Feldman D (1978) Evidence that brown adipose tissue is a glucocorticoid target organ. Endocrinology 103: 2091–2097

9 Fleck C, Thong TN, Braunlich H (1988) Relation between renal and hepatic excretion of drugs: IX: Acceleration of phenol red-excretion via kidney and liver in rats of different ages by dexamethasone treatment. Exp Pathol 34: 161–169

10 Foster DO, Frydman ML (1978) Nonshivering thermogenesis in the rat. II Measurements of blood flow with microspheres point to brown adipose tissue as the dominant site of the calorigenesis induced by noradrenaline. Can J Physiol Pharmacol 56: 110–122

11 Galpin KS, Henderson RG, James WPT, Trayhurn P (1983) GDP binding to brown adipose tissue mitochondria of mice treated chronically with corticosterone. Biochem J 214: 265–268

12 Girardier L, Seydoux J (1986) Neural control of brown adipose tissue. In "Brown Adipose Tissue" Ed by P Trayhurn, DG Nicholls, Edward Arnold, London, pp 122–151

13 Granneman JG, Campbell RG (1984) Effects of sucrose feeding and denervation on lipogenesis in brown adpose tissue. Metabolism 33: 257–268

14 Himms-Hagen J (1985) Brown adipose tissue metabolism and thermogenesis. Ann Rew Nutr 5: 69–94

15 Holt S, York DA (1982) The effect of adrenalectomy on GDP binding to brown adipose tissue mitochondria on obese rats. Biochem J 20: 819–822

16 Jacobsson A, Nedergaard J, Cannon B (1986) α- and β-adrenergic control of thermogenin mRNA expression in brown adipose tissue. Bioscience Reports 6: 621–631

17 Le Feuvre RA, Rothwell NJ, Stock MJ (1987) Activation of brown fat thermogenesis in response to central injection of corticotropin releasing hormone in the rat. Neuropharmacolo gy 26: 1217–1221

18 Lowry OH, Rosebrough NJ, Faar AL, Randall RJ (1951) Protein measurement with the folin phenol reagent. J Biol Chem 193: 265–275

19 Misra HP, Fridovich I (1972) The role of superoxide anion in the autooxidation of epinephrine and a simple assay for super oxide dismutase. J Biol Chem 247: 3170–3175

20 Petrović VM, Spasić M, Saičić ZS, Milić B, Radojičić R (1987) Superoxide dismutase activity in the cytosol of brown adipose tissue and liver during an acute and chronic exposure of rats to cold. Bull Acad Serbe Sci 27: 99–108

21 Rothwell NJ, Stock MJ (1979) A role for brown adipose tissue in diet-induced thermogenesis. Nature 281: 31–35

22 Rothwell NJ, Stock MJ, York DA (1984) Effects of adrenalectomy on energy balance, diet-induced thermogenesis and brown adipose tissue in adult cafeteria-fed rats. Comp Bochem Physiol 78A: 565–569

23 Slinde G, Pederson JI, Flatmark T (1975) Sedimentaton coefficient and buoyant density of brown adpose tissue mitochondria from guinea-pigs. Anal Biochem 65: 581–588

24 Spina MB, Cohen G (1989) Dopamine turnover and glutathione oxidation: implications for Parkinsons disease. Proc Natl Acad Sci USA 86: 1389–1400

25 Wurtman RJ, Axelrod J (1963) A sensitive and specific assay for the estimation of monoamine oxidase. Biochem Pharmacol 12: 1439–1440

26 York DA (1989) Cortcosteroid inhibiton of thermogenesis in obese animals. Proc Nutr Soc 48: 231–235

ZOOLOGICAL SCIENCE 11: 713–716 (1994)

Amino Acid Sequence of Sardine Calcitonin and Its Hypocalcemic Activity in Rats

NOBUO SUZUKI[1], YASUHIRO NOSÉ[1], YOICHI KASÉ[1], YUICHI SASAYAMA[1], YOSHIO TAKEI[2], HIROMICHI NAGASAWA[2], TAKUSHI X. WATANABE[3], KIICHIRO NAKAJIMA[3] and SHUMPEI SAKAKIBARA[3]

[1]*Department of Biology, Faculty of Science, Toyama University, Gofuku 3190, Toyama 930,* [2]*Ocean Research Institute, Tokyo University, Minamidai 1-15-1, Nakano, Tokyo 164, and* [3]*Peptide Institute Incorporated, Protein Research Foundation, Ina 4-1-2, Minoh, Osaka 562, Japan*

ABSTRACT—A novel calcitonin (CT) was isolated from the spotlined sardine, *Sardinops melanostictus*. The primary structure of sardine CT was determined as follows: H-Cys-Ser-Asn-Leu-Ser-Thr-Cys-Ala-Leu-Gly-Lys-Leu-Ser-Gln-Glu-Leu-His-Lys-Leu-Gln-Ser-Tyr-Pro-Arg-Thr-Asn-Val-Gly-Ala-Gly-Thr-Pro-NH_2. This amino acid sequence was different from that of salmon CT in 4 amino acid residues at positions 8th, 21th, 27th and 29th. As judged by the international method of CT bioassay, hypocalcemic activity of sardine CT was calculated as 4156 IU/mg. When compared for durability of CTs, it was found that sardine CT was significantly more potent than that of salmon CT. This is the first report of CT from a marine species of teleost.

INTRODUCTION

Calcitonin (CT) is a hormone, composed of 32 amino acid residues [9]. The primary structures of CTs from 3 species of teleosts (salmon [4], eel [5] and goldfish [6]), have been sequenced to date. However, CT from teleost which inhabits the sea throughout its life, has not yet been isolated. Marine teleosts are always exposed to high ambient Ca in which its level is 2–3 times higher than serum Ca levels. On the other hand, it is known that in mammals, bile is an important pathway for Ca excretion [12], and that CT stimulates excretion of Ca into the bile [11]. It is reported that also in marine teleosts, bile Ca concentrations are 3–7 times higher than serum Ca levels, which are higher than those of fresh water fish [2, 7]. Therefore, if teleosts CTs play a similar role in Ca regulation of bile as in mammals, CT might be more important in marine teleosts. In fact, it is reported that administration of salmon CT to a marine teleost (kelp bass) produced significant hypocalcemia, although there are many conflicting results regarding the effect of CT when it was administered to fresh water fishes [1]. In the present study, the primary structure of sardine CT was studied as one of the representatives of CTs from marine teleosts. Hypocalcemic activity of sardine CT was also examined by the rat bioassay.

MATERIALS AND METHODS

Purification of sardine CT

Three hundred twenty individuals of spotlined sardine (*Sardinops melanostictus*) were provided by fishermen in May 1993 in Toyama Bay. Pharyngeal tissue including UBG was dissected out, and immediately frozen until use. Sardine CT was purified according to the method reported for ray CT [8].

The crude extract of sardine UBG was subjected to reverse-phase high performance liquid chromatography (RP-HPLC) on an ODS-120T column (4.6×250 mm, Tosoh) with a linear gradient elution from 20 to 80% CH_3CN in 0.1% trifluoroacetic acid (TFA) for 60 min. In each fraction eluted, the presence of CT-specific immunoactivity was examined using Western blotting method with salmon CT polyclonal antiserum. The immunopositive fraction was further purified on the same column with a linear gradient from 40 to 80% CH_3OH in 0.1% TFA for 50 min.

The purified sardine CT was subjected to a protein sequencer (Model 473A, Applied Biosystems). After determining the primary structure, sardine CT was synthesized with a peptide synthesizer (Model 430A, Applied Biosystems). Furthermore, retention time of the synthetic sardine CT in RP-HPLC was compared with that of natural sardine CT.

Rat bioassay

Hypocalcemic activity of synthetic sardine CT was examined using synthetic one and compared with that of synthetic salmon CT by using rat bioassay according to Uchiyama *et al.* [10]. Each rat received 1 pM of sardine CT or 1 pM of salmon CT, contained in 400 μl of vehicle solution (0.9% saline solution containing 0.1% bovine serum albumin, pH 4.6). The same volume of vehicle solution was also administered to rat as a control. Blood was sampled before (zero hr) and at 0.5, 1, 2 and 3 hr after administration of CT or vehicle.

Serum Ca and Na concentrations were determined with atomic absorption spectrophotometer (180–70 type, Hitachi-Zeeman). Furthermore, the area between the serum Ca curve and the initial (zero) level was taken as a measure of the hormone response or control during the 3 hr period after administration, as reported previously [6]. In this warp, the duration of the hypocalcemic potency of the hormone could be expressed quantitatively. Data were analyzed by Student's *t*-test.

Accepted August 24, 1994
Received April 7, 1994

RESULTS

Purification and amino acid sequence of sardine CT

At first, an aliquot of 1/10 volume of crude extraction was subjected to RP-HPLC (Fig. 1). Location of the peak of sardine CT was sought on the result of Western blotting (shown by the arrow in Fig. 1). The consequence obtained in the second subjecting with a different solvent system of RP-HPLC are also exhibited in Figure 2. Then, the purification of sardine CT is judged from the single peak obtained. A half amount of eventual sample was subjected to a peptide sequencer to determine the amino acid sequence of sardine CT which is as follows: H-Cys-Ser-Asn-Leu-Ser-Thr-Cys-Ala-Leu-Gly-Lys-Leu-Ser-Gln-Glu-Leu-His-Lys-Leu-Gln-Ser-Tyr-Pro-Arg-Thr-Asn-Val-Gly-Ala-Gly-Thr-Pro-NH_2

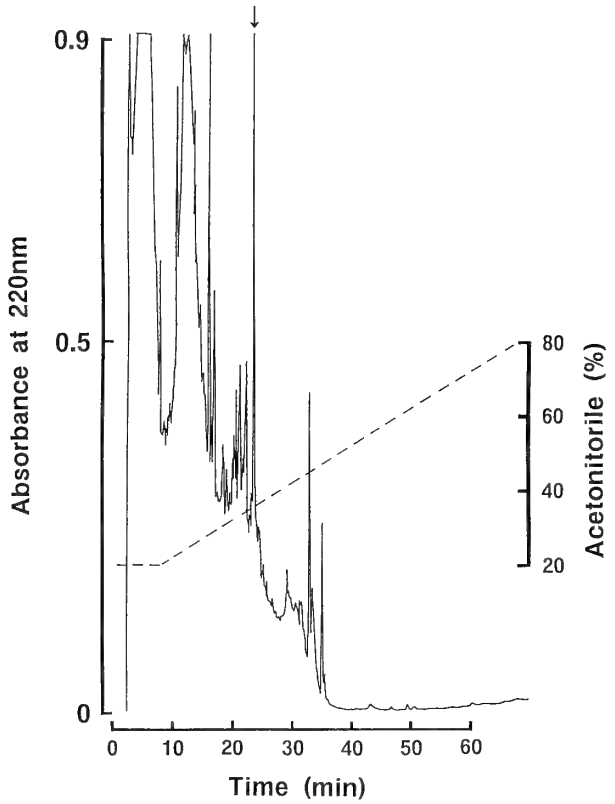

FIG. 1. Reverse phase HPLC on an ODS-120T column. Sample: crude extract of ultimobranchial glands of sardine; flow rate: 1 ml/min; Solvent system: linear gradient elution from 20 to 80% CH_3CN in 0.1% trifluoroacetic acid for 60 min. Arrow indicates the peak containing sardine calcitonin.

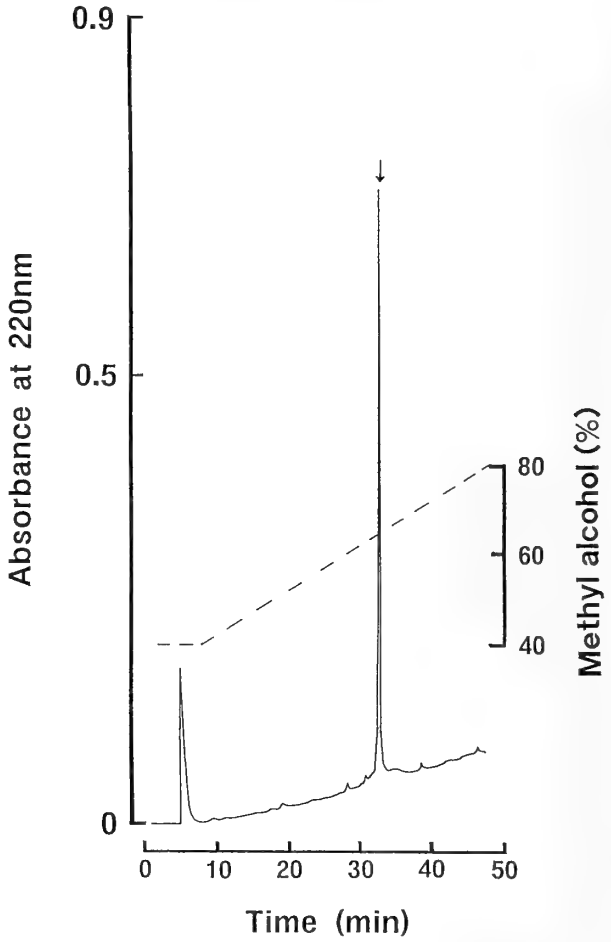

FIG. 2. Reverse phase HPLC on an ODS-120T column. Sample: the peak containing sardine calcitonin; flow rate: 1 ml/min; Solvent system: linear gradient elution from 40 to 80% CH_3OH in 0.1% trifluoroacetic acid for 50 min. Arrow indicates the peak of purified sardine calcitonin.

(Fig. 3). Furthermore, it was known that retention time of the synthesized CT in RP-HPLC was coincident with that of natural sardine CT.

Hypocalcemic potency of sardine CT by rat bioassay

Administration of 1 pM of sardine CT evoked significant hypocalcemia at 0.5 hr ($P<0.001$), 1 hr ($P<0.001$) and 2 hr after ($P<0.05$). (Fig. 4). On the other hand, administration of salmon CT produced smaller declines in serum Ca levels than these obtained for sardine CT (Fig. 4). Hypocalcemic

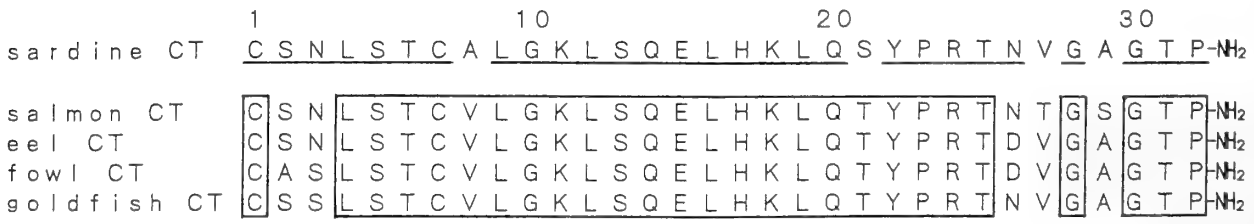

FIG. 3. Amino acid sequences of sardine calcitonin and other calcitonins. The identical amino acid residues in salmom lineage are boxed. Amino acid residues of sardine CT, which are identical to salmon calcitonin are underlined.

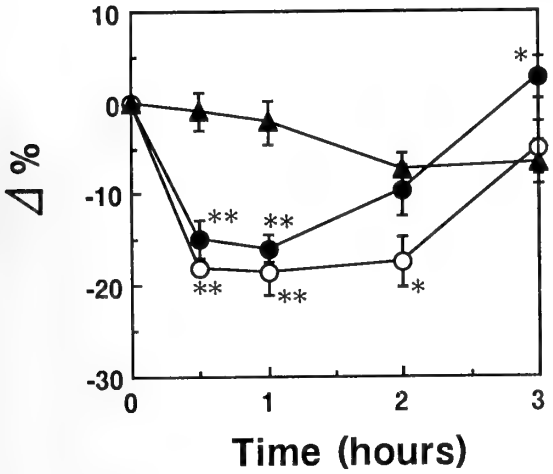

FIG. 4. Changes in serum Ca levels after administrations of either 1 pmol of sardine calcitonin (○), 1 pmol of salmon calcitonin (●) or vehicle (▲). Vertical bars indicate ± SE. The number of rats used were 10 individuals for sardine CT, 10 individuals for salmon CT and 6 individuals for vehicle. * and ** indicate significant differences from vehicle-$P<0.05$ and $P<0.001$, respectively.

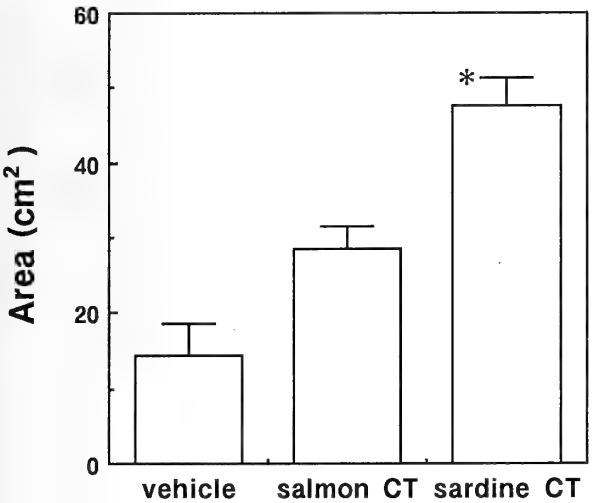

FIG. 5. Total areas below the initial level of serum Ca after administrations of either 1 pmol of sardine calcitonin or salmon calcitonin during 3 hour. Vertical bars indicate ± SE. * indicates significant difference from salmon CT-$P<0.001$

activity evoked after administration of salmon CT was recovered by 2 hr. The areas below the initial levels are shown in Figure 5. The area of the nonspecific declines caused by the vehicle solution was 14.4 ± 4.1 cm^2. The respective values of sardine CT and salmon CT were 47.7 ± 3.8 cm^2 and 28.4 ± 3.0 cm^2. The area of the former was significantly larger than that of the latter ($P<0.001$).

Serum Na levels did not change during 3 hr after administration, and remained at about 330 mg/100 ml (data not shown).

DISCUSSION

Eleven kinds of CTs have been sequenced to date. These are classified into 3 lineages: human lineage (human, rat and rabbit), porcine lineage (porcine, cattle, sheep and dog) and salmon lineage (salmon, eel, fowl and goldfish) [6]. Recently, we purified stingray CT from a cartilaginous fish [8], which appears to belong to another lineage. The primary structure of sardine CT sequenced in the present study demonstrates that it should be placed with the salmon lineage. In composition of amino acids, the sardine CT differs from eel CT (at positions 8th, 21th and 26th; homology 91%), from goldfish CT (at positions 3th, 8th and 21th; homology 91%), from salmon CT (at positions 8th, 21th, 27th and 29th; homology 88%), and from fowl CT (at positions 2th, 3th, 8th, 21th and 26th positions; homology 84%). Thus, it seems that among the salmon lineage, the sardine CT is more similar to eel and goldfish CTs in term of amino acid compositions. These results also imply that there is no distinction in amino acid components of CTs between fresh water teleosts and marine teleosts. The primary structure of CT appears to be well conserved among teleosts. Homology between sardine CT and mammalian CTs is low, 47–50% in human lineage and 38–47% in porcine lineage. However, similarity of sardine CT to ray CT is relatively high (69%).

As judged from declines in serum Ca levels of rat at 1 hr after administration, the activity of sardine CT was calculated as 4,156 IU/mg, as against a value of salmon CT which is reported as 3,500 IU/mg [3]. Furthermore, the present study demonstrates that sardine CT is more effective than salmon CT as its effect is of larger potency and long lasting.

ACKNOWLEDGMENTS

We are grateful to Messrs. H. Uragami, K. Nunome, H. Nunome, M. Hata, F. Matsusita, A. Yatsuhashi and K. Ikeda for their kind assistance at sampling of sardines.

REFERENCES

1 Glowacki J, O'sullivan J, Miller M, Wilkie DW, Deftos LJ (1985) Calcitonin produces hypocalcemia in leopard sharks. Endocrinology 116: 827–829

2 Hickman C, Trump BE (1969) In "Fish physiology Vol 1" Ed by WS Hoar and DJ Randall, Academic Press, New York and London, pp 91–239

3 Homma T, Watanabe M, Hirose S, Kanai A, Kangawa K, Matsuo H (1980) Isolation and determination of the amino acid sequence of chicken calcitonin I from chicken ultimobranchial glands. J Biochem 100: 459–467

4 Niall HD, Keutmann HT, Copp DH, Potts JT Jr (1969) Amino acid sequence of salmon ultimobranchial calcitonin. Proc Natl Acad Sci USA 64: 771–778

5 Otani M, Yamaguchi H, Megro T, Kitazawa S, Watanabe S, Orimo H (1976) Isolation and characterization of calcitonin from pericardium and esophagus of eel. J Biochem 79: 345–352

6 Sasayama Y, Ukawa K, Kai-ya H, Oguro C, Takei Y, Watanabe TX, Nakajima K, Sakakibara S (1993) Goldfish calcitonin:

purification, characterization and hypocalcemic potency. Gen Comp Endocrinol 89: 189–194

7 Suzuki N, Sasayama Y (1992) Changes of mineral concentrations of body fluids in some seawater fishes transferred to diluted seawater. Proc Jap Soc Comp Endocrinol **1992**: 41

8 Takei Y, Takahashi A, Watanabe TX, Nakajima K, Sakakibara S, Sasayama Y, Suzuki N, Oguro C (1991) New calcitonin isolated from the ray, *Dasyatis akajei*. Biol Bull 180: 485–488

9 Reginster JY (1993) Calcitonin for prevention and treatment of osteoporosis. Am J Med 95 (Suppl 5A): 44–47

10 Uchiyama M, Yoshihara M, Murakami T, Oguro C (1978) Presence of a hypocalcemic factor in the ultimobranchial gland of snake. Gen Comp Endcrinol 36: 59–62

11 Yamaguchi M, Yamamoto T (1979) Effects of various calcitonins on calcium concentrations in the bile and serum of thyroparathyroidectomized rats. Chem Pharm Bull 27: 1671–1674

12 Yamaguchi M, Yamamoto T, Hasegawa A (1979) Physiological significance of calcium excretion into the bile of rats. Chem Pharm Bull 27: 3137–3139

ZOOLOGICAL SCIENCE 11: 717–724 (1994)

Evidence for Non-steroidal Gonadal Regulator(s) of Gonadotropin Release in the Goldfish, *Carassius auratus*

WEI GE and RICHARD E. PETER

Department of Zoology, University of Alberta, Edmonton, Alberta, Canada T6G 2E9

ABSTRACT—In mammals, it is well documented that in addition to steroidal hormones, gonads also produce a variety of non-steroidal proteins and peptides that can feed back to regulate pituitary gonadotropin secretion. The best studied among these non-steroidal substances are inhibin and activin. The present study demonstrates that in sharp contrast to mammalian gonadal extracts which usually have inhibitory effects on mammalian gonadotropin secretion due to inhibin, the aqueous goldfish gonadal extracts stimulate pituitary gonadotropin-II (GTH-II) release in goldfish. Interestingly, the actions of the goldfish gonadal extracts are similar to our previously reported effects of porcine follicular fluid on goldfish GTH-II release. The stimulatory activities of goldfish ovarian extracts and the pituitary resopnsiveness to this stimulation fluctuate dramatically with the ovarian development. The results presented in this paper support our previous findings that porcine inhibin and activin stimulate goldfish gonadotropin release and the immunoreactive inhibin and activin subunits are present in the goldfish gonads.

INTRODUCTION

McCullagh first described 60 years ago that animal gonads produced non-steroidal substances that influenced gonadotropin (GTH) secretion. The term "inhibin" was proposed to designate a putative factor in the aqueous extracts of bull testes that could prevent the appearance of castration cells in the anterior pituitary gland [20]. The putative gonadal "inhibin" was later demonstrated to be a selective non-steroidal inhibitor of follicle-stimulating hormone (FSH) secretion. During the past decades, inhibin activity of suppressing basal FSH release has been demonstrated in various gonadal preparations such as follicular fluids [5–7, 13, 17, 21, 35, 40], ovarian extracts [2, 3, 36], testicular extracts [12, 23, 33, 36], rete testis fluids [1] and seminal plasma [4, 32] from a variety of mammalian species including pigs, cows, sheep, rodents, horses and humans.

With the development of a specific biossay to monitor the purification process for inhibin, four laboratories simultaneously purified inhibin molecules from porcine [15, 22, 28] and bovine follicular fluid [29] in 1985. During the separation of inhibin from porcine follicular fluid, another novel protein was isolated that stimulated FSH release from cultured rat pituitary cells and was named FSH releasing protein (FRP) [38] or activin [16]. Biochemical characterization revealed that activin is structurally related to inhibin [16, 38]. The stimulatory actions of activin in the gonadal preparations are believed to be overridden and masked by the potent inhibitory actions of inhibin on FSH release, which results in an overall inhibitory effect of the aqueous extracts from gonads. In addition to inhibin and activin, a variety of other protein or peptide factors of gonadal origin which had either stimulatory or inhibitory effects on pituitary GTH release have been identified in mammals [14, 18, 27, 31, 32, 34, 42]; however, studies on these factors are fragmentary compared to those on inhibin and activin.

The purpose of this study was to provide preliminary evidence for the presence of non-steroidal substances in the goldfish gonads that may regulate pituitary GTH secretion. The present work serves as an initial point for future studies on the identities of such molecules. A protocol similar to that used in mammals was adopted in the present work; however, a pituitary fragment perifusion system was used as the bioassay instead of static culture of pituitary cells. In common carp, a closely related species to goldfish, two chemically distinct GTHs have been identified and designated GTH-I and GTH-II; however unlike mammalian FSH and luteinizing hormone (LH), which have distinct biological functions, carp GTH-I and GTH-II possess the same biological activites in goldfish, in terms of stimulation of gonadal steroidogenesis and induction of oocyte final maturation [39]. Since the radioimmunoassay for GTH-I was not available, the present study was based on the measurement of GTH-II using carp GTH-II as the standard in the assay.

MATERIALS AND METHODS

Experimental animals

Common or comet variety goldfish (*Carassius auratus*) of mixed sex (approximately 25 g) were purchased from Grassyfork Fisheries Co., Martinsville, IN, USA or Ozark Fisheries, Stoutland, MO, USA. Fish were acclimated to 17±1°C and a simulated natural photoperiod of Edmonton, and fed a commercial trout food, for at least one week before use. Animals were anaesthetized with 0.05% tricaine methanesulphonate before handling.

Tissue extracts

Mature goldfish ovaries were homogenized with a Polytron homogenizer and extracted in phosphate-buffered saline (PBS, 50 mM+0.8% NaCl, pH 7.4) (1 : 1.5, weight:volume) containing 0.01 M

Accepted September 8, 1994
Received July 13, 1994

phenylmethylsulfanyl fluoride (PMSF, a proteinase inhibitor) for 3 hr at 4°C. The homogenates were centrifuged for 1 hour at 20,000×g. The supernatants were treated with Dextran-coated charcoal (30 mg/ml charcoal, 3 mg/ml Dextran) for 30 min to remove endogenous steroids. After centrifugation, the supernatants were dialysed (with 12 kD cut-off) against double distilled water for 24 hr, lyophilized, and stored at −20°C for subsequent use. Testosterone and estradiol levels in the crude goldfish ovarian extract (CGOE) were 0.12±0.05 and 0.20±0.11 ng/10 mg CGOE, respectively.

Extracts from the ovaries of sexually regressed and recrudescing fish, testes and muscles were prepared following the same procedures described above. The ovarian fluid was collected by centrifuging the ovulated eggs. CGOEs prepared from regressed, recrudescing and mature ovaries are designated CGOE-reg, CGOE-rec and CGOE-mat, respectively. The ovary was judged at dissection as regressed if no vitellogenic oocytes were visually evident, as recrudescing if vitellogenic oocytes could be seen, and as mature (=prespawning) if the ovary appeared full of large yolky oocytes.

Perifusion of pituitary fragments

For bioassay, an *in vitro* pituitary perifusion system was used as described by Marchant *et al.* [19]. Briefly, the whole pituitaries were collected from goldfish of mixed sexes and cut into small fragments (<0.05 mm^3) with a McIlwain tissue chopper (Mickle Laboratory Engineering Co. Ltd., Guildford, Surrey, England). The fragments were then washed three times with medium M199 and loaded between two layers of Cytodex beads (Pharmacia, Uppsala, Sweden) in mini-columns (3 pituitaries/column). The fragments were perifused with medium M199 with Hank's salts, 0.35 g/litre $NaHCO_3$, 25 mM Hepes, antibiotics and 0.1% BSA (M199-H-BSA, pH 7.2) at 17°C. The effects of long-term and short-term exposure to CGOE of the perifused pituitary fragments on GTH-II secretion were examined. For the long-term approach, the pituitary fragments were exposed to CGOE-mat-containing medium (1 mg/ml) for 24 hr at the perifusion rate of 5 ml/hr. The perifusion rate was increased to 15 ml/hr 2 hr before collecting the media in fractions, and the treatment with CGOE continued. After the fraction collection started, a series of 2 min 20 nM salmon gonadotropin-releasing hormone (sGnRH) pulses were applied at 60 min intervals. The treatment with CGOE-mat was terminated after the second pulse of sGnRH and the medium was changed to normal M199-H-BSA. In short-term tests, the fragments were perifused with medium M199-H-BSA for at least 15 hr at the flow rate of 5 ml/hr before any treatments were given (preincubation) to stabilize the basal release of GTH-II and the flow rate was changed to 15 ml/hr 2 hr before collecting the media in fractions. CGOEs and other tissue extracts were applied for short periods of time (2 or 20 min) as specified in each experiment. In both long-term and short-term tests, the same amounts of BSA were used as control. The perifusion media were collected at 5 min intervals unless otherwise specified and the GTH-II concentrations in the fractions measured with a heterologous carp GTH-II radioimmunoassay as described by Peter *et al.* [25] and Van der Kraak *et al.* [39]

Data analysis

In long-term experiments, the hormone levels in the twelve fractions with the lowest values from each column were averaged and defined as the "basal" level. The hormone levels in all fractions from the same column were expressed as a percentage of this average (% basal) in order to demonstrate any long-term trends in GTH-II secretion, as well as to allow the data from different columns and different experiments to be pooled. In short-term experiments, the data were expressed as either % basal or as a percentage of average levels in the three fractions before each individual treatment was applied (% prepulse). For calculating the hormone responses, the areas under the response peaks were determined. Briefly, the average hormone concentration in the three fractions immediately before each treatment pulse (prepulse, P) was determined. Any value higher than P plus one SEM was considered to be a part of the response peak. P was subtracted from each value in the peak and the differences summed and expressed as a percentage of the basal level of the column, which was defined as the hormone response (GTH-II response).

Statistical analysis was performed by using Student's t-test or one way ANOVA followed by Fisher's least significance difference (LSD) comparison.

RESULTS

Long-term effects of CGOE-mat on GTH-II release

The pituitary fragments in the perifusion column were perifused with CGOE-mat (1 mg/ml) for 24 hr before the perifusates were collected in fractions (pretreatment) and the treatment continued for 2 hr after the collection started (concurrent treatment) (Fig. 1). A series of sGnRH pulses (20 nM, 2 minutes) was applied at 60 min intervals after 24 hr pretreatment with CGOE-mat. CGOE-mat treatment was terminated after the second sGnRH pulse. Pretreatment of goldfish pituitary fragments with CGOE-mat caused an increase in GTH-II release ranging from about 130% to 230% basal. The same amount of BSA in the control columns did not affect the basal levels of GTH-II release. Notably, after terminating perifusion with CGOE-mat and switching to normal medium M199-H-BSA, the basal GTH-II secretion rapidly decreased to the levels (107±26% basal before the third sGnRH pulse) comparable to those in the control columns (110±15% basal before the third sGnRH pulse). In addition to the stimulatory effects on basal GTH-II secretion, continuous perifusion with CGOE-mat also potentiated sGnRH-stimulated GTH-II release; the GTH-II response to the first two sGnRH pulses in the presence of CGOE-mat was significantly greater than in the control columns. The GTH-II response to sGnRH decreased and became comparable to that in the control columns after the switch to normal medium M199-H-BSA.

Short-term effects of CGOE-mat on GTH-II release

To demonstrate whether CGOE has any acute effects on pituitary GTH-II release, CGOE-mat of different doses was applied to goldfish pituitary fragments in perifusion in a pulse of 20 min (Fig. 2). CGOE-mat caused an apparent dose-dependent and rapid release of GTH-II. BSA had no effects on the release of GTH-II from the pituitary fragments.

Effects of other tissue extracts on GTH-II release

Similar to the ovarian preparation, the testicular extract also had strong stimulatory actions on GTH-II release while the ovarian fluid induced a relatively smaller stimulatory

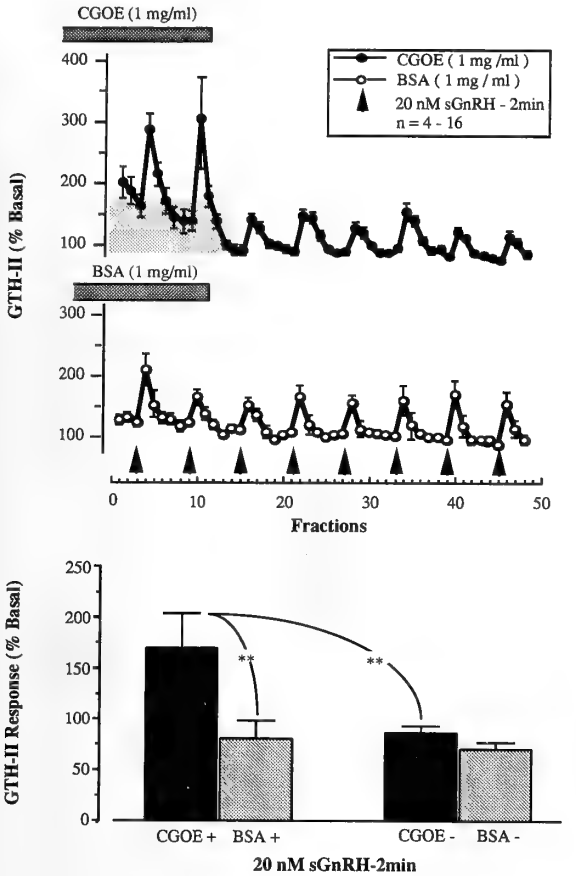

FIG. 1. Long-term effects of CGOE-mat on basal and sGnRH-stimulated goldfish GTH-II release by perifused pituitary fragments from sexually regressed fish. The fragments were perifused with either 1 mg/ml BSA (control) or 1 mg/ml CGOE-mat for 24 hr before collecting the media. A series of 2 min pulses of 20 nM sGnRH was given at 60 min intervals after the fraction collection started. After the second pulse of sGnRH, perifusion with CGOE-mat and BSA was discontinued, and the media changed to normal medium M 199-H-BSA. The perifusate was collected at 10 min intervals. Values are the average of 4–16 columns of separate experiments. The horizontal bars represent concurrent treatments with CGOE-mat and BSA, and the shaded area highlights the elevated basal level of GTH-II. *Lower panel*: GTH-II responses (mean ± SEM, n = 12–56) to sGnRH quantified as described in the Materials and Methods. +, in the presence of CGOE-mat or BSA; −, in the absence of CGOE-mat or BSA. **Significant difference ($p < 0.001$, Student's t-test).

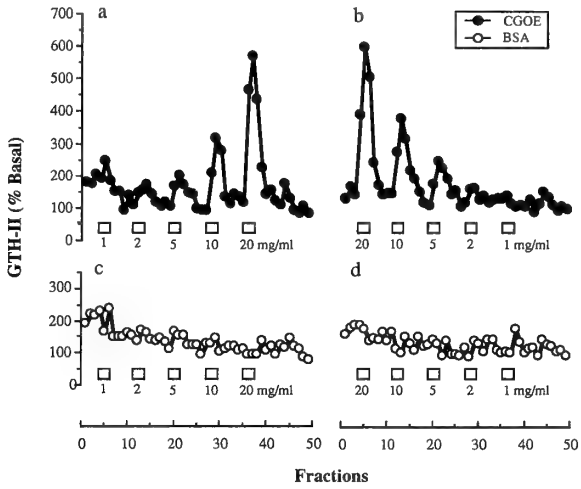

FIG. 2. Short-term effects of CGOE-mat on goldfish. CGOE-mat (a and b) and BSA (control, c and d) were applied for 20 minutes from low dose to high dose (a and c) and from high dose to low dose (b and d) in separate columns, respectively. The perifusate was collected at 10 min intervals. The square symbols represent 20 minute exposure to CGOE-mat or BSA.

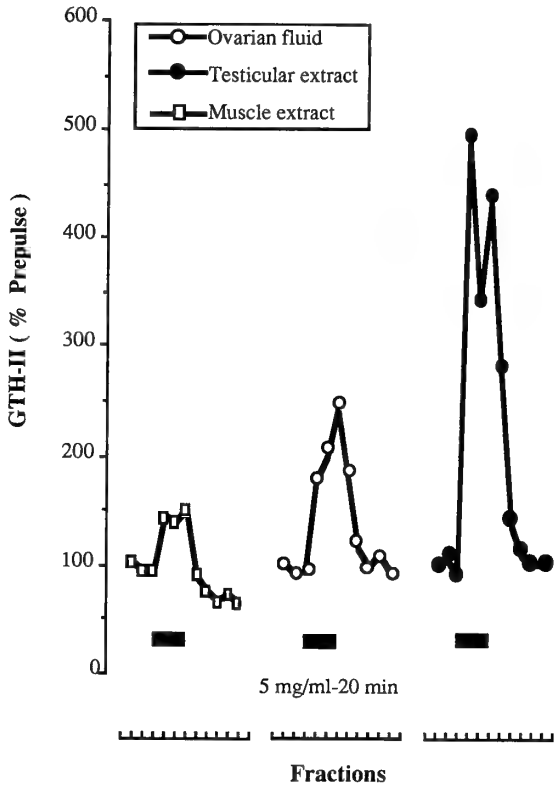

FIG. 3. Effects of extracts from different tissues on goldfish gonadotropin secretion from perifused pituitary fragments. The pituitaries were collected from sexually regressed goldfish. Extracts were applied for 20 minutes at a dosage of 5 mg/ml. The perifusate was collected at 10 min intervals. The values are the average of two columns.

effect. The muscle extract caused only minor increase in GTH-II release (Fig. 3).

Seasonal changes in the effectiveness of the ovarian extracts in stimulating GTH-II release

During the reproductive cycle, the goldfish ovary undergoes major morphological and physiological changes. CGOE from different stages of ovarian development was prepared and tested in the goldfish pituitary fragment perifusion to determine if the *in vitro* stimulatory effects on GTH-II release change with the reproductive cycle. The stimulatory effects of CGOE (5 mg/ml, 2 min) on GTH-II release showed evident seasonality (Fig. 4). Among the three preparations, CGOE-rec was the most effective in stimulating

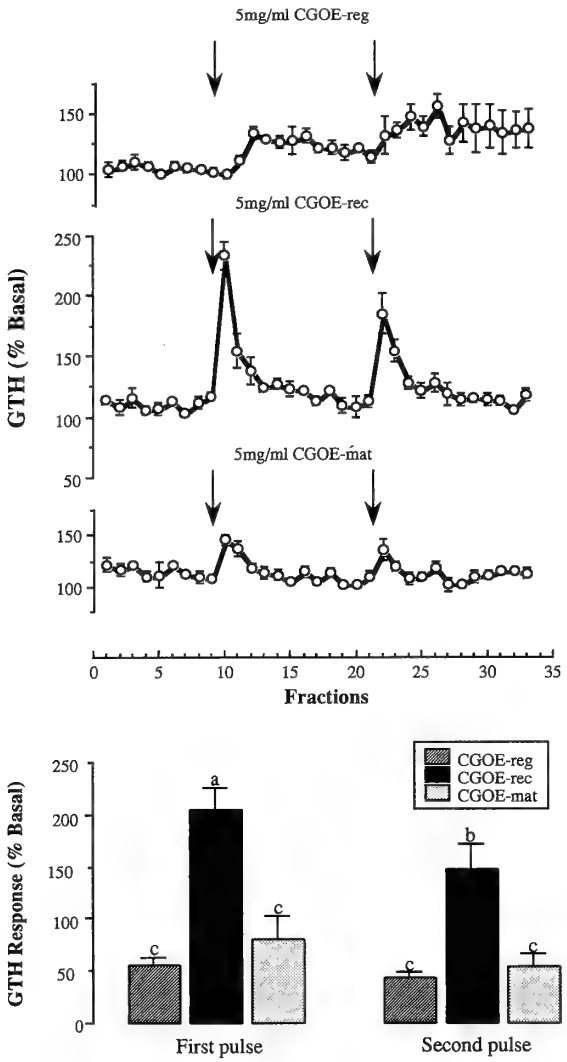

FIG. 4. Effects of CGOE from different stages of ovarian development on goldfish gonadotropin release. The pituitaries were collected from early recrudescing goldfish. The values are the average of four columns. *Lower panel*: GTH-II responses (mean±SEM, n=4) to CGOEs (5 mg/ml, 2 min) from different ovarian stages quantified as described in the Materials and Methods. Different letters above each column indicate significant difference ($p<0.05$, ANOVA followed by LSD comparison).

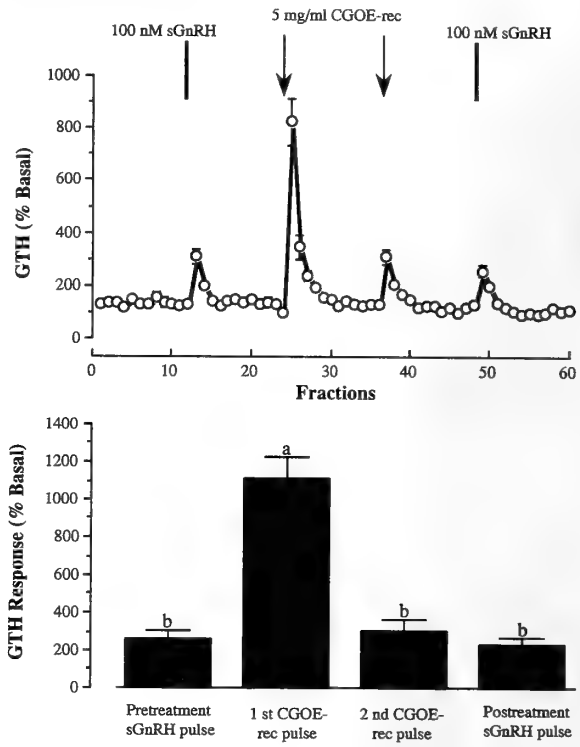

FIG. 5. Effects of CGOE-rec on goldfish GTH-II release by perifused pituitary fragments from recrudescing fish. After overnight preincubation, two 2 min pulses of CGOE-rec were applied to the pituitary fragments at a 60 min interval. sGnRH (2 min pulse) was used as pre- and post-treatment control. Values are the average of five columns. *Lower panel*: GTH-II responses (mean±SEM, n=5) quantified as described in the Materials and Methods. Different letters above each column indicate significant difference ($p<0.05$, ANOVA followed by LSD comparison).

GTH-II release compared to CGOE-reg and CGOE-mat. Interestingly, the pituitary fragments appeared to become refractory to the treatment with CGOE-rec, as the GTH-II response to the second pulse of CGOE-rec significantly decreased compared to that to the first pulse.

The desensitizing effect of CGOE-rec on GTH-II response

The desensitizing effect of CGOE-rec on GTH-II response observed in the above experiment was further confirmed in a separate experiment in which the GTH-II response to CGOE-rec reached a much higher level (Fig. 5). Two sGnRH pulses at the maximal dose (100 nM, 2 min) were given as pre- and post-treatment control. The GTH-II response to the first pulse of CGOE-rec was significantly higher than that to the maximal dose of sGnRH; however, the GTH-II response to the second pulse of CGOE-rec was reduced in magnitude to a level similar to the response to sGnRH. Interestingly, the GTH-II response to the post-treatment sGnRH pulse was not affected by the action of CGOE-rec. The desensitization of the GTH-II response to CGOE-rec was then examined with intervals of 30, 60 and 120 min between the two CGOE-rec pulses (Fig. 6). The desensitizing effect of CGOE-rec continued to occur with a pulse interval of 120 min. The GTH-II responses to the post-treatment sGnRH pulse remained unchanged.

Seasonality of GTH-II responsiveness to CGOE-rec

Two separate experiments were performed using the pituitaries from sexually regressed (gonad weight/total body weight X 100%, gonadosomatic index, GSI=0.90±0.93%; mean±SD) and recrudescing (GSI=3.73±3.59%) goldfish to determine if the seasonal gonadal cycle influences the pituitary GTH-II responsiveness to CGOE-rec (Fig. 7). The GTH-II responses to both sGnRH and CGOE-rec by pituitary fragments from sexually regressed goldfish were

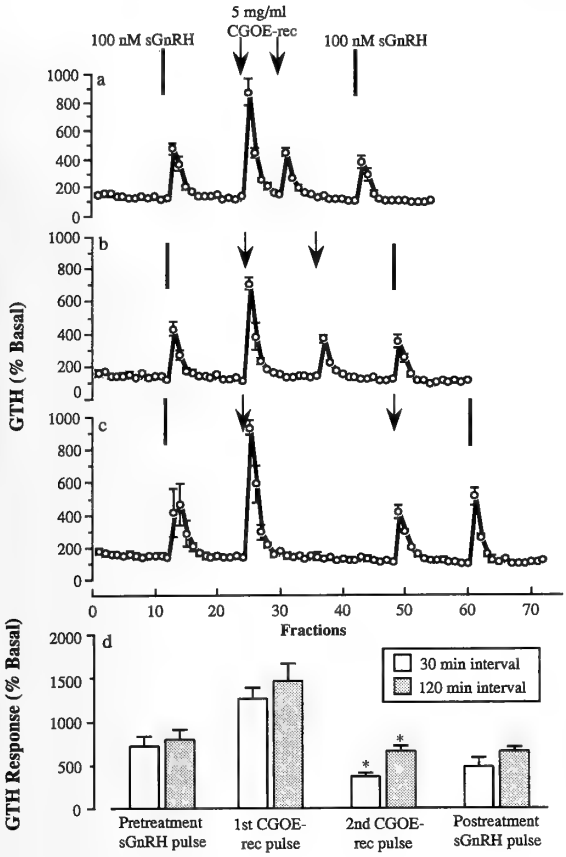

FIG. 6. Effects of CGOE-rec on goldfish GTH-II release by perifused pituitary fragments from recrudescing fish. Two 2 min pulses of CGOE-rec were applied to the pituitary fragments at 30 (a), 60 (b) and 120 (c) min intervals, respectively. sGnRH (2 min pulse) was used as internal pre- and post-treatment control. Values are the average of two (60 min interval) or three columns. *Panel d*: GTH-II responses (mean±SEM, n=3) to sGnRH and CGOE-rec quantified as described in the Materials and Methods. * Significantly different from the corresponding response to the first CGOE-rec pulse ($p<0.05$, Student's t-test). The quantification for the 60 min interval was not shown because only two columns were included in this experiment.

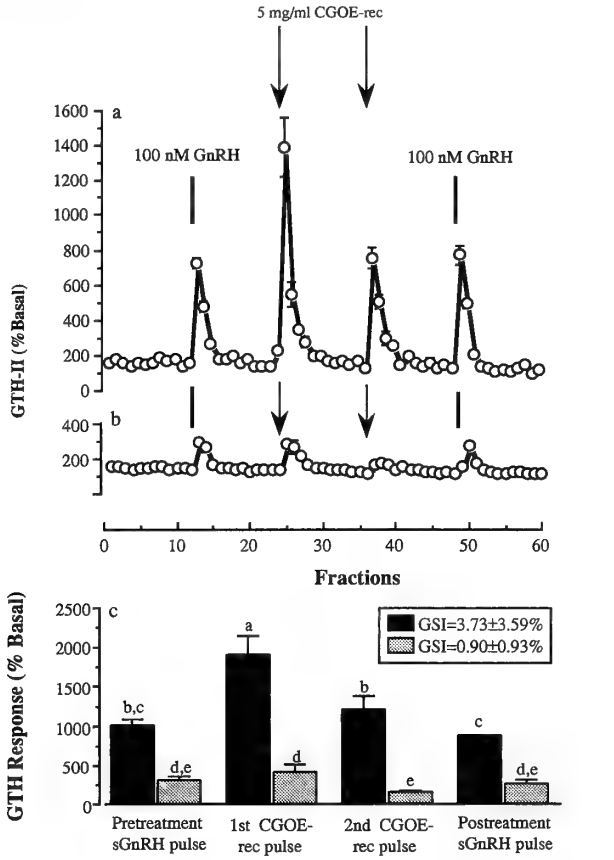

FIG. 7. Effects of gonad developmental stage on the pituitary GTH-II responsiveness to CGOE-rec. Two separate experiments were performed using goldfish at sexually recrudescing (a) and regressed (b) stages. Values are the average of three (a) or four (b) columns. *Panel c*: GTH-II responses (mean±SEM, n=3–4) to sGnRH and CGOE-rec quantified as described in the Materials and Methods. Different letters above each column indicate significant difference ($p<0.05$, ANOVA followed by LSD comparison).

low, and the GTH-II release stimulated by CGOE-rec was similar to that induced by sGnRH. With the pituitaries from sexually recrudescing goldfish, both sGnRH and CGOE-rec caused larger GTH-II responses compared to the pituitaries from regressed fish, with the magnitude of CGOE-rec-induced GTH-II release becoming significantly higher than that of sGnRH-stimulated GTH-II response.

Interaction between dopamine and CGOE-rec on GTH-II release

Dopamine (DA) is a potent hypothalamic inhibitor of basal and sGnRH-stimulated GTH-II release in goldfish [26]. To show whether DA affects CGOE-rec action, the perifused pituitary fragments were exposed to continuous treatment with 1 μM DA during which the first pulse of CGOE-rec was applied (Fig. 8). Treatment with DA caused a slight decrease in basal GTH-II release; however, the GTH-II re-

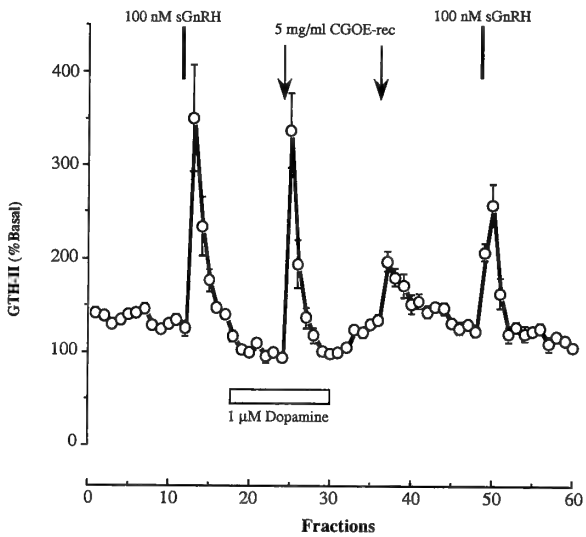

FIG. 8. Effects of dopamine on CGOE-rec-stimulated goldfish GTH-II release. The pituitaries were collected from fully regressed goldfish as those used in Figure 7b. Values are the average of four columns.

sponse stimulated by CGOE-rec was not reduced compared to that in the absence of DA (the GTH-II release by the pituitary fragments from the regressed goldfish in Fig. 7b).

DISCUSSION

Crude aqueous extracts from goldfish ovaries exhibit stimulatory effects on both basal as well as sGnRH-stimulated GTH-II release after long term treatment. Furthermore, the extracts from both goldfish ovaries and testes have acute stimulatory actions on pituitary GTH-II release in perifusion, with pulsatile treatment for as short as 2 minutes eliciting a rapid response of GTH-II release. This is in contrast to mammalian studies on gonadal fluids and extracts that generally have inhibitory effects on pituitary GTH, expecially FSH, release, attributed to the actions of inhibin [41]. Another feature of the present results that is distinct from those in mammalian species is the acute response to CGOE and testicular extract. Although the acute effects of CGOE appear to be similar to that induced by GnRH, some evidence indicates that the novel stimulatory factor(s) in CGOE are different from GnRH. First, the extracts had been subjected to dialysis with 12 kD cut-off point to remove small molecules including small peptides; therefore, the putative stimulatory factors in the foldfish gonadal extracts are likely to have molecular weight of more than 12 kD. Second, even though CGOE-rec exhibits a strong desensitizing effect on the GTH-II response to the subsequent treatment, the desensitization of the response to CGOE-rec does not reduce the GTH-II response to sGnRH stimulation, suggesting that the desensitization is specifically related to the actions of CGOE-rec and is independent of sGnRH.

One interesting aspect of the GTH-II-releasing activity of goldfish ovarian extracts is that the stimulatory actions change significantly with the developmental stages of the ovary, with CGOE-rec being the most effective compared to CGOE-reg and CGOE-mat. Furthermore, the pituitary responsiveness to CGOE-rec also varies significantly with the development of gonads. The GTH-II responsiveness to CGOE-rec increases significantly when the fish enter sexual recrudescence and maturation, similar to the seasonal variations in responsiveness to GnRH in goldfish (C.K. Murthy and R.E. Peter, unpublished results); however, the increase in the GTH-II response induced by CGOE-rec is even higher. The increase in the action of CGOE-rec compared to CGOE-reg and CGOE-mat, and the significantly higher GTH-II responsiveness to CGOE-rec by the pituitaries from sexually recrudescing fish correlate well with the onset of ovarian recrudescence and the associated increase in plasma GTH-II levels [11, 24, 37], implying that the stimulatory factor(s) in CGOE-rec might be involved in initiating these changes.

Interestingly, although DA is potent in suppressing basal and GnRH-induced GTH-II secretion in goldfish [26], DA does not affect CGOE-rec-stimulated GTH-II release. This suggests that there may be a stimulatory pathway for GTH-II in goldfish that is independent of the tonic inhibition by the hypothalamic DA.

In mammals, a variety of factors have been identified in gonadal preparations that can either stimulate or inhibit pituitary GTH release [14, 18, 27, 31, 32, 34, 41, 42]. Therefore, any observed actions of a crude preparation only reflect a net effect depending on the relative amounts, potencies and the complex interactions of all active substances present in the mixture. This also applies to the goldfish gonadal extracts used in the present study. With overwhelming evidence in mind for the inhibitory effects of mammalian gonadal preparations on pituitary GTH secretion, the stimulatory actions of the goldfish gonadal extracts on pituitary GTH-II release described above are unexpected, although it has been reported that *Tilapia* seminal plasma and testicular extract are also stimulatory to GTH release from the pituitary fragments in perifusion [30]. The nature of the putative stimulatory factors in goldfish gonads remains unknown and additional studies are needed to identify these factors and characterize their biochemical and biological properties.

Our previous studies showed that inhibin and activin-containing porcine follicular fluid (pFF), purified porcine inhibin A and activin A have stimulatory actions on goldfish GTH-II release [8]. The stimulatory effects of porcine inhibin on goldfish GTH-II release is in sharp contrast to its well-documented inhibitory actions in mammalian species. Furthemore, both porcine inhibin and activin have acute effects on goldfish GTH-II release in pituitary fragment perifusion, and their actions are not suppressed by DA. Interestingly, inhibin and activin-containing pFF is surprisingly similar to CGOE in terms of long-term and short-term effects on GTH-II release in goldfish, and both pFF and CGOE-rec have strong desensitizing effects on GTH-II response [8]. Using domain-specific antibodies, the immunoreactive inhibin and activin subunits have been demonstrated in the goldfish gonads [9]. We have recently cloned and sequenced goldfish activin βA and βB subunits, and demonstrated that inhibin and activin β subunits are highly conserved throughout vertebrates [10]. Toghther with the results presented in the present paper, these previous results suggest that inhibin and activin-like molecules in the goldfish gonads may, at least partially, contribute to the unique stimulatory actions of goldfish gonadal extracts.

ACKNOWLEDGMENTS

We thank the International Development Reserch Centre of Canada for Scholarship and the Alberta Heritage Foundation for Medical Research for Studentship support of W. G. Research was supported by grant A6371 from the Natural Sciences and Engineering Research Council of Canada to R.E.P

REFERENCES

1 Bardin CW, Morris PL, Chen CL, Shaha C, Voglmayr J, Rivier J, Spiess J, Vale W (1987) Testicular inhibin: structure and

regulation by FSH, androgens and EGF. In "Inhibin-Non-steroidal Regulation of Follicle Stimulating Hormone Secretion" Ed by HG Burger, DM de Kretser, JK Findlay, M Igarashi, Raven Press, New York, pp 179–190

2 Channing CP, Gordon WL, Liu WK, Ward DN (1985) Physiology and biochemistry of ovarian inhibin. Proc Soc Exp Biol Med 178: 339–361

3 Chappel SC (1979) Cyclic fluctuations in ovarian FSH-inhibiting material in golden hamster. Biol Reprod 21: 447–453

4 Chari S, Duraiswami S, Franchimont P (1978) Isolation and characterization of inhibin from bull seminal plasma. Acta Endocrinol 87: 434–448

5 Chari S, Hopkinson CRN, Daume E, Sturnz G (1979) Purification of inhibin from human ovarian follicular fluid. Acta Endocinol 90: 157–166

6 de Jong FH, Sharpe RM (1976) Evidence for inhibin-like activity in bovine follicular fluid. Nature 263: 71–72

7 Fujii T, Hoover DJ, Channing CP (1983) Changes in inhibin activity, and progesterone, oestrogen and androstenedione concentrations, in rat follicular fluid throughout the oestrous cycle. J Reprod Fertil 69: 307–314

8 Ge W, Chang JP, Peter RE, Vaughan J, Rivier J, Vale,W (1992) Effects of porcine follicular fluid, inhibin-A, and activin-A on goldfish gonadotropin release *in vitro*. Endocrinology 131: 1922–1929

9 Ge W, Cook H, Peter RE, Vaughan J, Vale W (1993a) Immunocytochemical evidence for the presence of inhibin and activin-like proteins and their localization in goldfish gonads. Gen Comp Endocrinol 89: 333–340

10 Ge W, Gallin WJ, Strobeck C, Peter RE (1993b) Cloning and sequencing of goldfish activin subunit genes: strong structural conservation during vertebrate evolution. Biochem Biophys Res Commun 193: 711–717

11 Kobayashi M, Aida K, Hanyu I (1988) Hormone changes during the ovulatory cycle in goldfish. Gen Comp Endocrinol 69: 301–307

12 Koegh EJ, Lee VWK, Rennie GC, Burger HG, Hudson B, de Kretser DM (1976) Selective suppression of FSH by testicular extracts. Endocrinology 98: 997–1004

13 Koiter TR, Schaaf-Verdonk GCJ, Kuiper H, Pols-Valkhof N, Schunling GA (1983) Control of follicle-stimulating hormone secretion by steroid-free bovine follicular fluid in the ovariectomized rat. J Endocrinol 99: 1–8

14 Li CH, Ramasharma K, Yamashiro D, Chung D (1987) Gonadotropin-releasing peptide from human follicle fluid: isolation, characterization, and chemical synthesis. Proc Natl Acad Sci USA 84: 959–962

15 Ling N, Ying S-Y, Ueno N, Esch F, Denoroy L, Guillemin R (1985) Isolation and partial characterization of a Mr 32,000 protein with inhibin activity from porcine follicular fluid. Proc Natl Acad Sci USA 82: 7217–7221

16 Ling N, Ying S-Y, Ueno N, Shimasaki S, Esch F, Hotta M, Guillemin R (1986) Pituitary FSH is released by a heterodimer of the β subunits of the two forms of inhibin. Nature 321: 779–782

17 Lumpkin MD, DePaolo LV, de Negro-Vilar A (1984) Pulsatile release of follicle-stimulating hormone in ovariectomized rats is inhibited by porcine follicular fluid (inhibin). Endocrinology 114: 201–206

18 Manjunath, R. (1984) Gonadotropin release stimulatory and inhibitory proteins in bull seminal plasma. In "Gonadal Proteins and Peptides and their Biological Significance" Ed by MR Sairam, LE Atkinson, World Scientific, Singapore, pp 49–61

19 Marchant TA, Fraser RA, Andrews PC, Peter RE (1987) The influence of mammalian and teleost somatostatins on the secretion of growth hormone from goldfish (*Carassius auratus* L) pituitary fragments *in vitro*. Regul Peptides 17: 41–52

20 McCullagh DR (1932) Dual endocrine activity of the testes. Science 76: 19–20

21 Miller KF, Wesson JA, Ginther OJ (1979) Changes in concentrations of circulating gonadotropins following administration of equine follicular fluid to ovariectomized mares. Biol Reprod 21: 867–872

22 Miyamoto K, Hasegawa Y, Fukuda M, Iganashi M, Kangaw V, Matsuo H (1985) Isolation of porcine follicular fluid inhibin of 32 kDa. Biochem Biophys Res Commun 129: 396–403

23 Murthy S, Ramasharma HMK, Moudgal NR (1979) Studies on purification of sheep testicular inhibin. J Reprod Fertil (Suppl) 26: 61–70

24 Peter RE (1981) Gonadotropin secretion during reproductive cycles in teleosts: influences of environmental factors. Gen Comp Endocrinol 45: 294–305

25 Peter RE, Nahorniak CS, Chang JP, Crim LW (1984) Gonadotropin release from the pars distalis of goldfish, *Carassius auratus*, transplanted beside the brain or into the brain ventricles: additional evidence for gonadotropin-release-inhibitory factor. Gen Comp Endocrinol 55: 337–346

26 Peter RE, Chang JP, Nahorniak CS, Omeljaniuk RJ, Sokolowska M, Shih SH, Billard R (1986) Interactions of catecholamines and GnRH in regulation of gonadotropin secretion in teleost fish. Recent Prog Horm Res 42: 513–548

27 Ramasharma K, Sairam MR, Seidah NG, Chretien M, Manjunath P, Schiller PW, Yamashiro D, Li CH (1984) Isolation, structure, and synthesis of a human seminal plasma peptide with inhibin-like activity. Science 223: 1199–1202

28 Rivier J, Spiess J, McClintock R, Vaughan J, Vale W (1985) Purification and partial characterization of inhibin from porcine follicular fluid. Biochem Biophys Res Commun 133: 120–127

29 Robertson DM, Foulds LM, Leversha L, Morgan FJ, Hearn MTW, Burger HG, Wettenhall REH, de Kretser DM (1985) Isolation of inhibin from bovine follicular fluid. Biochem Biophys Res Commun 126: 220–226

30 Rubin-Kedem H, Levavi-Zermonsky B, Yaron Z (1989) Factors in tilapia testes affecting gonadotropin secretion from perifused pituitary gland: a preliminary study. Gen Comp Endocrinol 74: 316–317

31 Schenken RS, Hodgen GD (1986) Follicle-stimulating hormone blocks estrogen-positive feedback during the early follicular phase in monkeys. Fertil Steril 45: 556–560

32 Sheth AR, Arabatti N, Carlquist M, Jornvall H (1984) Characterization of a polypeptide from human seminal plasma with inhibin (inhibition of FSH secretion) like activity. FEBS Lett 165: 11–15

33 Sheth AR, Joshi LR, Moodbidri SB, Rao SS (1979) Characterization of a gonadal factor involved in the control of FSH secretion. J Reprod Fertil (Suppl) 26: 71–85

34 Sopelak VM, Hodgen GD (1984) Blockade of the estrogen-induced luteinizing hormone surge in monkeys: a nonsteroidal, antigenic factor in porcine follicular fluid. Fertil Steril 41: 108–113

35 Summerville JW, Schwartz NB (1981) Suppression of serum gonadotropin levels by testosterone and porcine follicular fluid in castrate male rats. Endocrinology 109: 1442–1447

36 Torney AH, Robertson DM, de Kretser DM (1991) Characterization of inhibin and related proteins in bovine fetal testicular and ovarian extract: evidence for the presence of inhibin subunit products and FSH-suppressing protein. J Endocrinol 133: 111–120

37 Trudeau VL, Peter RE, Sloley BD (1991) Testosterone and

estradiol potentiate the serum gonadotropin response to gonadotropin-releasing hormone in goldfish. Biol Reprod 44: 951–960

38 Vale W, Rivier J, Vaughan J, McClintock R, Corrigan A, Woo W, Karr D (1986) Purification and characterization of an FSH releasing protein from porcine ovarian follicular fluid. Nature 321: 776–779

39 Van der Kraak G, Suzuki K, Peter RE, Itoh H, Kawauchi H (1992) Properties of common carp gonadotropin I and gonadotropin II. Gen Comp Endocrinol 85: 217–229

40 Williams AT, Lipner H (1981) Negative feedback control of gonadotropin secretion by chronically administered estradiol and porcine follicular fluid (gonadostatin) in ovariectomized rats. Endocrinology 109: 1496–1501

41 Ying S-Y (1988) Inhibins, activins, and follistatins: gonadal proteins modulating the secretion of follicle-stimulating hormone. Endocr Rev 9: 267–293

42 Ying S-Y, Ling N, Bohlen P, Guillemin R (1981) Gonadocrinins: peptides in ovarian follicular fluid stimulating the secretion of pituitary gonadotropins. Endocrinology 108: 1206–1215

ZOOLOGICAL SCIENCE 11: 725–730 (1994)

Age-dependent Changes Related to Reproductive Development in the Odor Preference of Blowflies, *Phormia regina*, and Fleshflies, *Boettehersica peregrina*

AZUSA NAKAGAWA[1], AKIFUMI IWAMA and ATSUO MIZUKAMI

Tsukuba Research Center SANYO Electric Co., Ltd., Tsukuba, Ibaraki 305 Japan

ABSTRACT—We investigated the preference for the odor of decaying meat in a T-maze using female and male blowflies, *Phormia regina*, with one of two nutritional histories (protein-containing or protein-free diet), and compared them with fleshflies, *Boettehersica peregrina*. The preference showed age-dependent changes, which differed according to sex and nutritional history. Females in both nutrition groups showed a high preference for the odor. The preference of protein-fed females showed cyclic variations corresponding to the ovarian cycle, while the protein-deficient group, which never oviposited having immature eggs, did not exhibit cyclic changes and their preference remained high. These results suggest that the preference for the odor may be associated with the ovarian cycle. In males, both nutrition groups showed significant changes with age. The preference of protein-deficient males changed similarly to that of females, whereas protein-fed males were not attracted by the odor. This also suggests that the preference for the odor may be related to reproductive development. With *B. peregrina*, which has different reproductive natures from *P. regina*, the age-dependent changes in the preference did not differ so markedly with sex and nutritional history as with *P. regina*.

INTRODUCTION

The blowfly, *Phormia regina* (Meigen), needs decaying meat as an essential protein source for the development of eggs and reproductive glands in the early days of adulthood, and as an adequate substrate for subsequent oviposition. It can survive on carbohydrates and water only, and completes its normal life span [18]. However, without dietary protein, its eggs and accessory reproductive glands stop developing at three days after eclosion [15, 21], and juvenile hormones [24] or ecdysteroids [23] are not produced. Mated females lay their eggs on decaying meat, whereas they seldom lay on fresh meat. The protein consumption of female blowflies is known to reach a peak during egg development and after oviposition [4]. In males, a moderate amount of protein is consumed during the first day or two after eclosion [4]. Protein uptake is likely to be closely connected to the reproductive development or cycle in both female and male blowflies.

The mechanism of carbohydrate intake has been well studied from both behavioral and physiological aspects [12]. With protein uptake, however, much less is known about what sensory inputs are necessary and what mechanisms regulate it [4, 16, 17]. Olfaction is likely to play an important role in insect behaviors such as feeding and mating. Blowflies of the genus *Calliphora* have been shown to have carrion receptors which specifically respond to the odor of decaying meat [6, 14]. It is supposed that the ability to detect the odor of decaying meat is indispensable to blowflies' lives. Thus, the response to the odor of decaying meat may change during the course of protein feeding and with the reproductive cycle.

Various studies have indicated that chemosensory functions of insects interact with the neuro-hormonal changes associated with the reproductive cycles [5]. For example, in blowflies, the sensitivity of the taste labellar chemosensilla varies depending on the ovarian cycle or related factors [1, 2, 19, 20]. In olfaction, the antennal receptors of mosquitoes have been shown to be associated with the reproductive cycle [9~11]. However, in blowflies, though age-dependent change in olfactory sensitivity has been observed [7, 8], the interaction with the reproductive cycle is not clear.

P. regina is a convenient species to use in studies of the putative factors influencing chemosensory functions, since it is easy to produce two different reproductive states in flies with the same sex, by feeding them protein-containing or protein-free diet. In this study, we investigated the preference for the odor of decaying meat using female and male blowflies, *Phormia regina*, of different ages, with one of two nutritional histories (protein-containing or protein-free diet). In addition, we compared the preference of *P. regina* with that of fleshflies, *Boettehersica peregrina*, the reproductive nature of which differs from that of *P. regina*. We found that the preference for the odor changed with age and depended on sex and nutrition, suggesting that it may be related to the reproductive functions in both females and males.

MATERIALS AND METHODS

Animals

Blowflies (*Phormia regina*, Meigen) and fleshflies (*Boettehersica*

Accepted July 23, 1994
Received April 18, 1994
[1] To whom correspondence should be addressed.

peregrina) were reared in this laboratory. Larvae of *P. regina* were raised on artificial medium (5 g of casein, 5 g of dry yeast, 0.1～0.2 g of agar powder and one drop of lanolin in 36 ml of a solution, one liter of which contained 0.45 g of NaCl, 0.01 g of KCl, 0.013 g of $CaCl_2 \cdot 2H_2O$, 0.01 g of $NaHCO_3$, 0.382 g of $NaH_2PO_4 \cdot 2H_2O$ and 0.3875 g of K_2HPO_4). Larvae of B. peregrina were given pork liver. Larvae and pupae were kept in the dark. Adult flies, separated according to sex within 24 hr after eclosion, were kept in a light:dark cycle of L12:D12. The temperature was maintained at 23±1°C. Adults were raised on 2 kinds of diet. The protein-fed group of *P. regina* was raised on a diet of water, brown sugar and pork liver. That of *B. peregrina* was given minced pork meat instead of pork liver. The protein-free groups of both species were fed on water and 0.1 M sucrose solution. The age of flies is designated as day 0, 1, 2, etc, day 0 being the day of eclosion. The protein-fed group of female *P. regina* was divided further into two groups, mated and unmated. To obtain mated flies, the same number of females and males were put into a cage on day 4 and reared together thereafter. *B. peregrina* females were used without mating.

Determining odor preference in a T-maze

Preferences for the odor were tested in a T-maze, which consisted of a central chamber (40×40×35 mm) and two choice tubes (33×400 mm) (Fig. 1). The apparatus was made of transparent acrylic plates and tubes. One of the choice tubes was attached to the odor source and the other was left open. The right/left orientation of odor and control was randomized for each test. As the odor source, we used about 30 g of decaying meat (minced beef stored at 23°C for 1 week).

Flies were starved by giving only water for 24 hr before testing. Twenty to 40 flies for one trial were shaken into the central chamber, which was shut off from the choice tubes by thin plates. A vacuum hose was attached to the central chamber and air was drawn through by a small pump (6 liters/min). Then, the plates were slid up and the odor of decaying meat or fresh air was allowed to flow through the choice tubes. After 2 min, the plates were slid down and the flies which had moved into the choice tubes or remained in the central chamber were counted. Each fly was used once only. The ages of the flies used were 1 to 12 days for *P. regina* and 1 to 9 days for *B. peregrina*. The numbers of female and male blowflies with one of two nutritional histories were 72 to 328 and tests were done four to ten times for each age. For fleshflies, 43 to 267 were used at two to eight tests. Each series of experiments for each group was done at random. Tests were performed at the same time of the day (10:00 a.m. to 3:00 p.m.) from May to October. Ambient temperatures were 24±2°C and relative humidities were >70%.

Acetic acid or alcohol are attractants for flies at lower concentrations but deterrents at higher concentrations [12]. When we used a high concentration of acetic acid as the odor source (100 μl of 10 M solution on 5×5 cm filter paper), flies moved into the choice tube opposite to the odor source. At low concentration (10^{-2} M), flies tended to go to the odor source. Thus, the preference for the odor was indicated by the number of flies moving into the choice tube on the odor side.

When we used decaying meat as the odor source, 20% to 50% of the flies remained in the central chamber. In 2 min experiments, once flies had gone into one of the choice tubes, they were seldom observed to return to the central chamber or to go into the other choice tube. We estimated the preference for the odor by the ratio of the total numbers of flies moving into the odoriferous tube in all trials to the sum of those in both choice tubes, excluding the flies remaining in the central chamber. These ratios were calculated for each age, sex and nutrition group.

RESULTS

We investigated the preferences for the odor of decaying meat in female and male blowflies, *Phormia regina*, with one of two nutritional histories at each day after eclosion. The preference in each group of flies changed in an age-dependent manner, which also depended on nutritional history (protein-containing or protein-free diet) and sex. We give below full details of the age-dependent changes of *P. regina* and a comparison with those of fleshflies, *Boettehersica peregrina*.

Odor preferences of blowflies

Females:

On the day after eclosion (day 1), females were not attracted to the odor of decaying meat, but subsequently their preference increased (Fig. 2A). The age-dependent change in preference in the protein-fed group showed cyclic variations between 60 and 90% (Fig. 2A). The changes in preference with age were significant between days 1 and 2, days 3 and 4 ($P<0.01$: Chi-squared test), days 4 and 5, and days 9 and 10 ($P<0.05$). In these experiments, the protein-fed flies were mated on day 4 and were observed to oviposit mainly on days 5～6, 8 and 10. A few eggs were also laid on day 11. The cycle of change in the preference corresponded to the ovarian cycle. The preference reached a peak before the first oviposition. During the ovipositions, the preference

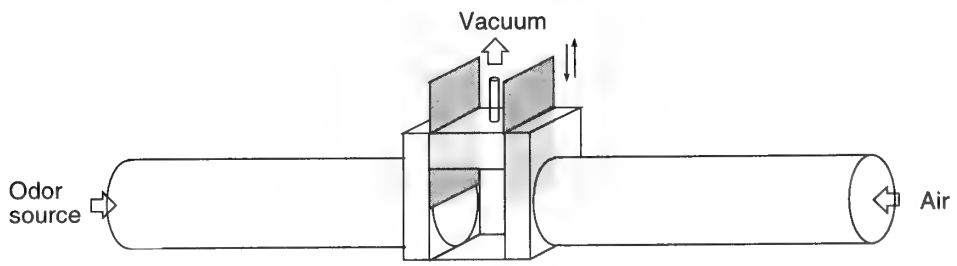

FIG. 1. T-maze. The maze consists of the central chamber and two choice tubes. The central chamber is shut off from the choice tubes by thin plates. One of the choice tubes is attached to the odor source. Suction applied at the central chamber draws air through both choice tubes.

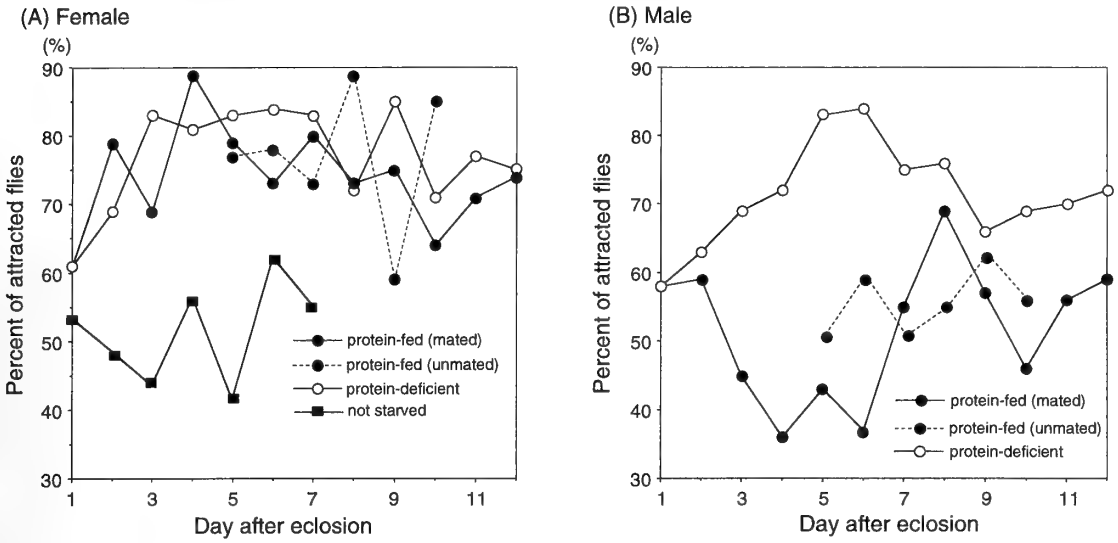

FIG. 2. The preference for the odor of decaying meat of female (A) and male (B) blowflies, *P. regina*. The odor preference of female and male blowflies is shown for each day and each nutrition group (protein-fed and protein-deficient). Results are expressed as the ratio of flies moving into the odoriferous tube to the sum of those in both choice tubes, excluding flies remaining in the central chamber.

decreased and subsequently increased. When flies were not mated, we also observed oviposition on days 6~7, 9 and 12, but the ovarian cycle was one day later than that of the mated flies. In unmated females, the age-dependent change in preference also showed cyclic variations (Fig. 2A). However, significant differences were found between mated and unmated females at days 8, 9 ($P<0.05$) and 10 ($P<0.01$). The cyclic variations of unmated females were one day later than those of mated flies, as was the ovarian cycle. In addition, the range of variation was larger than that of the mated females ($P<0.05$ between days 7 and 8, and $P<0.01$ between days 8 and 9 and days 9 and 10).

In the protein-deficient females, the preference increased with age and reached a peak on day 3; it then remained high but showed a slight tendency to decrease (Fig. 2A). As a whole, the preference of protein-deficient females was a little stronger than that of protein-fed flies (Fig. 2A), showing significant differences at days 3, 6 and 9 ($P<0.05$). Protein-deficient blowflies were never observed to mate or, of course, to oviposit. In contrast with the age-dependent change in protein-fed females which showed cyclic variations corresponding to the ovarian cycle, the preference in the protein-deficient group remained high from day 3 to day 7 and then showed similar cyclic variations between days 8 and 12 ($P<0.05$ between days 2 and 3 and days 7 and 8). There was no correlation between the changes of preference with age of both nutrition groups (the Pearson correlation coefficient was 0.55).

In the above experiments, the flies had been starved for 24 hr before testing. We also measured the preference for the odor daily using the same group of females without prior starvation. Their preference was about 50% and lower than that of the starved flies ($P<0.01$ on days 2~5 and 7) (Fig. 2A). However, their preference increased to 60% during oviposition ($P<0.01$ bewteen days 5 and 6), while the preference of starved flies decreased during oviposition and subsequently increased.

With protein-fed females, the activity in a T-maze (the proportion of flies moving into both choice tubes to all flies used) was 50% at the time of eclosion and increased to about 80%, then decreased thereafter to about 60%. Protein-deficient females tended to show slightly higher activity than the protein-fed flies, but the difference was significant only on day 8 ($P<0.05$).

Males:

With male blowflies, the age-dependent change in the odor preference showed a significant difference between the 2 nutrition groups (on days 3~6, $P<0.01$ and on day 7, $P<0.05$) (Fig. 2B). On day 1, males were not attracted to the odor as much as females. Thereafter, the preference of protein-deficient males increased gradually and reached a peak on day 6 followed by a slow decrease (Fig. 2B). These changes in preference with age were not significant throughout the tested period ($P>0.05$).

On the other hand, the preference of protein-fed males decreased from day 2 ($P<0.05$ between days 2 and 3) (Fig. 2B). Protein-fed males were not greatly attracted to the odor of decaying meat, except on days 2 and 8. They were even repelled by the odor on days 4 and 6. When flies were not mated, the preference was stronger than that of mated males, but there was no significant difference between mated and unmated males except at day 6 ($P<0.05$) (Fig. 2B).

The degree of activity was similar in both nutrition groups, increasing to about 70% gradually from day 0 (43%) and decreasing later to about 50%.

We then compared the preferences of the two sexes with the same nutritional history. Protein-fed females and males

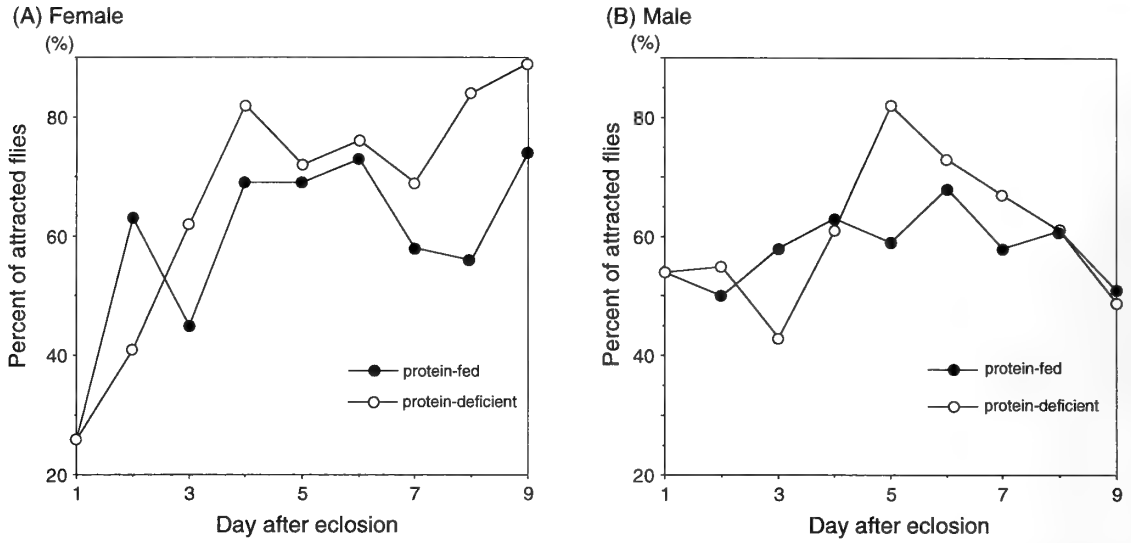

FIG. 3. The preference for the odor of the decaying meat of female (A) and male (B) fleshflies, *B. peregrina*. The preferences are shown for days 1 to 9 in each nutrition group. Results are expressed as described in Fig. 2.

differed significantly. The preference of females was much stronger than that of males (on days 2~7, $P<0.01$; on days 9 ~12, $P<0.05$) (Fig. 2). On the other hand, protein-deficient flies showed a difference between the sexes only on day 3 ($P<0.05$) and day 9 ($P<0.01$), though the change in females was more rapid and their preference remained high longer (Fig. 2). Correlation was found between the changes of preference with age of female and male protein-deficient flies (the Pearson correlation coefficient was 0.64). Females were slightly more active than males and, the difference became greater with time.

Odor preference of fleshflies

We made the same tests using fleshflies, *B. peregrina*. In this species, the preferences of each group also showed age-dependent changes (Fig. 3).

Females:

Both nutrition groups of female fleshflies showed similar age-dependent changes in their preference (Fig. 3A). The preferences increased with age and tended to remain high during the period we examined. There was no significant difference between both nutrition groups except on day 4 ($P<0.05$) and day 8 ($P<0.01$), though the preference in the protein-deficient group was a little greater than that of the protein-fed flies. The age-dependent changes in female fleshflies were similar to those in blowfly females, but fleshflies did not show such clear cyclic variations as the blowflies did.

Males:

The age-dependent change in protein-fed male fleshflies was not striking (Fig. 3B). Their preference remained low, but they were not repelled by the odor, in contrast to the equivalent group of *P. regina*. In addition, no significant difference was found between the nutrition groups of *B. peregrina* males, except on day 5 ($P<0.01$) (Fig. 3B). Nutrition had little effect on the age-dependent change of preference of males as well as of females. With the same nutritional history, the difference between the sexes was small (Fig. 3). In the protein-deficient group, the differences were found on days 4, 8 and 9 ($P<0.01$) (Fig. 3). No difference was observed between males and females in the protein-fed group, except on day 1 ($P<0.05$), in marked contrast to *P. regina*. The degree of activity of all 4 groups of fleshflies was similar to that of each other and to that of the equivalent group of blowflies.

DISCUSSION

Our results showed that the odor preference of *P. regina* exhibited age-dependent change influenced by sex and nutrition.

Both nutrition groups of females showed a strong preference. The reason that females are attracted by the odor of decaying meat is thought to be for feeding and oviposition. Two reasons are likely to induce blowflies to feed: First, they must ingest protein as adults to develop their eggs and accessory reproductive glands completely [15, 21], and they need decaying meat as protein food sources. Next, they search for decaying meat in order to satisfy their hunger because they have been starved for 24 hr before the experiments.

Belzer indicated that the peaks of female protein consumption corresponded to the ovarian cycles [4]. Thus, it is reasonable that the preference for the odor, which is probably closely connected to protein feeding, should change with the ovarian cycle. We found that the preference of protein-fed females did indeed show cyclic variations corresponding to the ovarian cycle. In addition, unmated protein-fed females showed cyclic variations one day later than those of the mated flies, while their ovarian cycles also occurred one day later

than those of mated individuals. These facts suggest that the preference for the odor may reflect the need for protein feeding corresponding to the ovarian cycle. This is also supported by the fact that the age-dependent change of protein-deficient females, which never oviposit, did not show correlation with that of protein-fed flies. Furthermore, the fact that the preference of the protein-deficient females reached its peak on day 3 and remained high thereafter suggests that they seek for a protein source in order to complete the maturation of their eggs. This is also suggested by the fact that the preference of protein-deficient females was somewhat stronger than that of the protein-fed flies. In addition, we observed that protein-fed flies began to mate on day 4, whereas protein-deficient flies were never observed to mate. The maturation of eggs or glands is likely to influence the mating behavior as well as the odor preference of the flies.

Blowflies are also thought to be attracted by the odor of decaying meat as a means of satisfying their hunger, regardless of the ovarian cycle. The period of starvation before testing is likely to have increased their preference for the odor, since the preference of unstarved females was weaker than that of starved females.

Moreover, blowflies must search for appropriate oviposition sites. Olfaction has been shown to be very important in the oviposition behavior of blowflies [3]. Our previous experiments showed that flies were able to choose the oviposition site by detecting the odor of decaying meat (paper in preparation). Blowflies are thought to recognize the odor of decaying meat as indicating a suitable oviposition site. We observed that the preference reached a peak after oviposition and decreased during oviposition. It is likely that the preference for the odor primarily reflects the need for protein corresponding to the ovarian cycle, not site-seeking for oviposition. However, in unstarved females, the preference increased during oviposition, supporting the association with site-seeking for oviposition. Stoffolano et al. suggested that during the first ovarian cycle females obtained protein for oögenesis from another source than the oviposition substrate [22]. Thus it is possible that the protein feeding associated with the ovarian cycle and that relating to site-seeking for oviposition may be manifested differently in the odor preference detected in a T-maze.

On the other hand, the preferences were strong in both nutrition groups and the age-dependent change observed with protein-deficient females was identical to that of protein-fed flies after day 7. Therefore, the odor preference may also correlate with some age-related factors, which are probably independent of the ovarian cycle. Previous studies have demonstrated that olfactory sensitivity in female blowflies increases as the females age, regardless of their feeding history [7, 8]. This age-dependent increase is likely to correlate with other features of maturation in the early days after eclosion, such as development of the flight muscles [8]. In addition, the age-related decrease in sensitivity was suggested to be due to an increasing number of inoperative sensilla [19, 20]. It is not clear whether the odor preference in females is related to these phenomena.

In males, the age-dependent change in preference differed significantly depending on nutrition. Protein-deficient males showed increasing preference with age, as did the females, whereas, interestingly, protein-fed males were not attracted by the odor but rather repelled by it. Males also need dietary protein in adulthood for the development of their reproductive glands [21]. In addition, males were shown to consume a moderate amount of protein during the first day or two after eclosion but little or none thereafter [4]. The preferences of both nutrition groups on days 1 and 2 are considered to correspond to protein consumption in the early period. The preference of protein-deficient males, which subsequently increases, might result from the flies searching for protein food sources to develop their glands. Thus, the odor preference of males is probably related to their reproductive development. However, we do not fully understand why protein-fed males were not attracted by the odor and even repelled by it, although they had been starved before the experiments. As a rule, among calliphorids, males do not appear to frequent carrion or live animals to the same extent as females [22]. In protein-fed males with completely developed reproductive glands, some other behavior such as mating is likely to override the need to search for food. If the odor of conspecific females is used as the stimulus, the odor preferences of two nutrition groups of males may be reversed. Stoffolano indicated that sex influenced the sensitivity change in sugar receptors of blowflies but not in that of the salt cells [20], probably because of the metabolic difference related to reproductive functions. The difference in the effects of nutritional history on the preference of both sexes may also be influenced by the metabolic difference by sex.

In fleshflies, *B. peregrina*, the age-dependent changes in odor preference were not so strongly different between the sexes and nutrition groups. *B. peregrina* is ovoviviparous, unlike *P. regina*. Mating was observed to begin on day 2 or 3 after eclosion even with protein-deficient fleshflies, as well as with protein-fed flies, whereas protein-deficient *P. regina* was never observed to mate. Oviposition was not observed until day 10. The fleshflies *Sarcophaga bullata*, which are ovoviviparous like *B. peregrina*, are considered to be incipient autogenous and protein-free diet leads to egg maturation though not completely [15]. A protein-free diet may not have such a critical influence on oögenesis of *B. peregrina* as it does with *P. regina*. Therefore, the effect of nutrition may only slightly influence the odor preference of both groups of *B. peregrina* females. However, we observed a slightly stronger preference in the protein-deficient group than in the protein-fed flies, and an increase in the preference on day 9 (the day before oviposition), also suggesting the influence of the ovarian cycle. With males, a protein-rich diet did not cause them to be repelled by the odor and, similarly, protein deficiency had only a small effect in increasing the preference for the odor. The reproductive nature of *B. peregrina* differs from that of *P. regina*; therefore, the

influence of a protein diet may have a smaller differential effect on the age-dependent changes in each group of *B. peregrina* than it does with *P. regina*.

Thus, it is likely that factors related to the ovarian cycle in females and to the development of reproductive glands in males influence the olfactory sensitivity of the flies. Flies may take advantage of these variations associated with their reproductive functions to seek dietary protein, adapting themselves to achieve adequate behavior at that time. We do not fully understand the mechanism regulating olfactory behavior; there may be a central mechanism involving endocrine and neural systems which regulates the olfactory sensitivity. Juvenile hormone, which plays an important role in controlling oögenesis in many insects [13], has been suggested to increase the sensitivity of labellar salt cells in blowflies [1]. A humoral mechanism related to the reproductive cycle is likely to affect the sensitivity of olfactory receptor. Further physiological investigations are necessary to clarify the regulatory mechanisms.

ACKNOWLEDGMENTS

We wish to thank Dr. A. Shiraishi, Kyushu University, for kindly providing flies from his culture. This study was supported in part by grants from Commercial Equipment Systems Of SANYO Electric Co., Ltd.

REFERENCES

1 Angioy AM, Liscia A, Crnjar R, Pietra P (1983) An endocrine control mechanism for chemosensillar activity in the blowfly. Experientia 39: 545–546

2 Angioy AM, Liscia A, Pietra P (1983) Cyclic sensitivity variations in the labellar chemosensilla of *Calliphora*. Experientia 39: 546–547

3 Barton Browne L (1960) The role of olfaction in stimulation of oviposition in the blowfly, *Phormia regina*. J Insect Physiol 5: 16–22

4 Belzer WR (1978) Patterns of selective protein ingestion by the blowfly *Phormia regina*. Physiol Entomol 3: 169–175

5 Blaney WM, Schoonhoven LM, Simmonds MSJ (1986) Sensitivity variations in insect chemoreceptors; a review. Experientia 42: 13–19

6 Boeckh J, Kaissling KE, Schneider D (1965) Insect olfactory receptors. Cold Spring Harbor Symp Quant Biol 30: 263–280

7 Bowdan E (1982) Effect of age and nutrition on the responses of female blowflies (*Phormia regina*) to the odor from a proteinaceous source. Ent exp & appl 32: 1–6

8 Crnjar R, Yin CM, Stoffolano JGJr, Tomassini Barbarossa I, Liscia A, Angioy AM (1990) Influence of age on the electroantennogram response of the female blowfly (*Phormia regina*) (Diptera: Calliphoridae). J Insect Physiol 36: 917–921

9 Davis EE, Takahashi FT (1980) Humoral alteration of chemoreceptor sensitivity in the mosquito. Olfaction and Taste 7: 139–142

10 Davis EE (1984) Development of lactic acid-receptor sensitivity and host-seeking behavior in newly emerged female *Aedes aegypti* mosquitoes. J Insect Physiol 30: 211–215

11 Davis EE, Haggart DA, Bowen MF (1987) Receptors mediating host-seeking behavior in mosquitoes and their regulation by endogenous hormones. Insect Sci Applic 8: 637–641

12 Dethier VG (1976) The Hungry Fly. Harvard University Press, Cambridge, Mass.

13 Englemann F (1970) The Physiology of Insect Reproduction. Pergamon Press, New York

14 Kaib M (1974) Die Fleisch-und-Blumenduftrezeptoren auf der Antenne der Schmeissfliege *Calliphora vicina*. J Comp Physiol 95: 105–121

15 Pappas C, Fraenkel G (1977) Nutritional aspects of oogenesis in the flies *Phormia regina* and Sarcophaga bullata. Physiol Zool 50: 237–246

16 Rachman NJ (1980) Physiology of feeding preference patterns of female black blowflies (*Phormia regina* Meigen) I. The role of carbohydrate reserves. J Comp Physiol 139: 59–66

17 Rachman NJ (1982) Physiology of feeding-preference patterns of female black blowflies (*Phormia regina* Meigen): alterations in responsiveness to salts. J Insect Physiol 28: 625–630

18 Rasso SC, Fraenkel G (1954) The food requirements of the adult female blowfly, *Phormia regina* (Meig.) in relation to ovarian development. Ann Entomol Soc Amer 47: 638–645

19 Rees CJC (1970) Age dependency of response in an insect chemoreceptor sensillum. Nature 227: 740–742

20 Stoffolano JGJr (1973) Effect of age and diapause on the mean impulse frequency and failure to generate impulses in labellar chemoreceptor sensilla of *Phormia regina*. J Gerontol 28: 35–39

21 Stoffolano JGJr (1974) Influence of diapause and diet on the development of the gonads and accessory reproductive glands of the black blowfly, *Phormia regina* (Meigen). Can J Zool 52: 981–988

22 Stoffolano JGJr, Bartley MM, Yin CM (1990) Male and female *Phormia regina* (Diptera: Calliphoridae) trapped at different baits in the field. Ann Entomol Soc Am 83: 603–606

23 Yin CM, Zou BX, Stoffolano JGJr (1990) Ecdysteroid activity during oogenesis in the black blowfly, *Phormia regina* (Meigen). J Insect Physiol 36: 375–382

24 Zou BX, Yin CM, Stoffolano JGJr, Tobe SS (1989) Juvenile hormone biosynthesis and release during oocyte development in *Phormia regina* Meigen. Physiol Ent 14: 233–239

ZOOLOGICAL SCIENCE 11: 731–735 (1994)

Changes of Mycetocyte Symbiosis in Response to Flying Behavior of Alatiform Aphid (*Acyrthosiphon pisum*)

YUICHI HONGOH and HAJIME ISHIKAWA*

Zoological Institute, Faculty of Science, University of Tokyo, Hongo, Bunkyo-ku, Tokyo 113, Japan

ABSTRACT—Prior to migratory flight of alatiform aphids, their total volume of mycetocyte was greatly reduced. Since in this period they ingest little food, it is likely that they develop the flight muscles at the cost of their mycetocytes. In this period, not only the size and number of the mycetocyte but also the density of endosymbionts in the cell decreased. Starving aphids resulted in a sharp decrease in the total volume of mycetocyte, which was reversed by refeeding, suggesting that aphids consume their mycetocytes harboring endosymbionts as a nutrient source on their physiological demands.

INTRODUCTION

Most groups of the family Aphidoidea harbor prokaryotic endosymbionts within specialized cells, mycetocytes, in the haemoceal [2, 5]. The symbiosis between aphid and its symbiont has so highly evolved that one can no longer do without the other. Aposymbiotic aphids produced by treating with antibiotics exhibit severe defects such as retarded growth and low fecundity, while the symbionts isolated from aphids cannot multiply themselves [6]. Although some indirect evidence suggests that the symbionts synthesize and supply vitamins, amino acids, and sterols to the host [2, 4, 5, 10, 11, 12], there still remain many questions unanswered about the relationship between aphid and its symbiont.

In order to further clarify this symbiotic interaction, it will be essential to know how the physiological conditions of aphid affect the mycetocyte in which the symbionts are housed. Douglas and Dixon reported variations in number and size of mycetocytes of *Megoura viciae and Acyrthosiphon pisum* with age and morph in detail [3]. They revealed that the number of mycetocytes decreases consistently after birth, and that the reported rate of decline is higher in alatae than in apterae. They also reported that the mycetocyte size increases over larval stages and soon after the final ecdysis the median size shows a declining curve in both apterae and alatae are due to the difference in growth rate, or number of embryos which vertically receive symbionts.

Unlike apterae, alatae are driven to flight a few days after the final ecdysis to settle on new host plants and start larviposition [8]. During this period alatae undergo morphological and physiological changes such as hardening of the wing and cuticle, and degeneration of the flight muscles.

We studied the changes of mycetocytes in the two morphs of *A. pisum* after the final ecdysis. The data showed that the marked changes in number, size, and color of mycetocytes take place over the first several days. It was also revealed that in the same period the density of endosymbionts in the mycetocyte changes considerably. We also studied the effect of starvation on the condition of the mycetocyte of the two morphs. The present results will lend a clue to look into how the host controls the symbionts in response to its own physiological conditions.

MATERIALS AND METHODS

Insect materials

A long established parthenogenetic clone of pea aphids, *Acyrthosiphon pisum* (Harris) was maintained on young broad bean plants, *Vicia faba* (L.) at 20°C with photoperiod of 16 hr. Uniform nutritional conditions were retained in the following procedures. Adult apterae were placed on seedlings of the two-leaf stage to obtain nymphs with the average density of 10 per seedling. To obtain alatae, parental apterae were kept in a relatively high density.

Under these conditions used, the 4th stage spanned from day 5 to 7 of birth, the final ecdysis occurred on day 7 or 8, and the larviposition started on day 9 or 10 (apterae) and day 11–13 (alatae).

Starvation of insects

Starvation of insects was conducted on 1–2 days after the final ecdysis, when their cuticle had not completely hardened yet, indicating that the insects were before flight.

The aphids to be starved were transferred to petri dishes with moist filter papers to prevent desiccation, and returned to fresh host plants 3 days later.

Measurement of number and size of mycetocytes

The mycetocytes were isolated by dissecting insects submerged in buffer (35 mM Tris-HCl, pH 7.6 containing 10 mM $MgCl_2$, 25 mM KCl and 250 mM sucrose) on petri dish covered with agars, and the number and diameter of mycetocytes were determined under a stereoscopic microscope (15×6.3). In this method, mycetocytes, unless very small in size, were easily discriminated from other fat body cells and embryos. The number of mycetocytes was expressed as mean±SD. The volume of mycetocytes was calculated from the diameter measured with a micrometer and expressed as mean±SD of median values of about 30 round-shaped cells per individual. The total volume of mycetocytes was calculated based on the number and

Accepted September 8, 1994
Received March 29, 1994
* To whom all correspondence should be addressed.

mean diameter for each individual and expressed as mean ± SD.

Relative growth rates of the aphids and their mycetocytes were calculated from the fresh body weight and volume, respectively [1].

The statistic analysis was conducted on Welch's method.

Density of endosymbionts

The density of endosymbionts in the mycetocyte was estimated measuring the number of symbiont in 0.5 μm-thick sections of mycetocytes under a light microscope. The isolated mycetocytes were fixed in the phosphate-buffered (pH 7.6) 1.5% formaldehyde −1.5% glutaraldehyde fixative, then dehydrated, cleared, and embedded in resin (Technovit 7100, Kulzer). The sections were stained with Toluidine blue or hematoxylin-eosin.

RESULTS

Number and size of mycetocyte

The changes in number and size of the mycetocytes with age and morph are shown in Fig. 1.

Most alatae used in this study exhibited the flight behavior on day 2–4 of final ecdysis. They were usually found walking on the wall of the experimental cage, and returned to the host plants within a day. For convenience's sake, only the insects before flight were referred to day 1, those showing the flight behavior were referred to day 3, and those settling on host plants after flight were referred to day 4.

After the final ecdysis, the mean number of mycetocytes per aphid decreased slowly in apterae (−15%, $P<0.01$, between day 0 and day 3) and rapidly in alatae (32%, $P<0.01$, between day 0 and day 3) (Fig. 1). In alatae, the decrease in number stopped on the re-settling on the host plant on day 4, and the number of mycetocytes somewhat increased thereafter ($P<0.05$, between day 3 and day 9) (Fig. 1), though no dividing mycetocyte was detected throughout this period under a microscope.

The median size of mycetocyte was changed with age, also in a different manner between in apterae and in alatae (Fig. 2). In apterae, the size increased regularly over 4th instar stage to the beginning of larviposition ($P<0.01$, between day 0 and day 3). The relative growth rates (r.g.r) from day −1 to 2 were 0.29 $mm^3\ mm^{-3}day^{-1}$ and 0.30 $mgmg^{-1}day^{-1}$ for mycetocyte and insect, respectively. Afterward, the size of mycetocyte was kept unchanged or slightly decreased (Fig. 2). By contrast, in alatae, the size of mycetocyte decreased steeply between day 0 and day 3 ($P<0.01$), r.g.r. being −0.57 $mm^3mm^{-3}day^{-1}$ and −0.18 $mgmg^{-1}day^{-1}$ for mycetocyte and insect, respectively. Then the size turned to a sharp increase to restore that on day 0 ($P<0.01$, between day 3 and day 4; $P<0.01$, r.g.r.: 0.28 $mm^3mm^{-3}day^{-1}$, 0.15 $mgmg^{-1}day^{-1}$, between day 3 and day 9,) (Fig. 2).

Figure 3 shows the change in total volume of mycetocytes per aphid. In apterae, the total volume increased until the onset of larviposition ($P<0.01$, r.g.r.: 0.21 $mm^3mm^{-3}day^{-1}$, 0.30 $mgmg^{-1}day^{-1}$), and gradually decreased thereafter. Unlike in apterae, in alatae the total volume decreased rapidly between day 0 and day 3 ($P<0.01$,

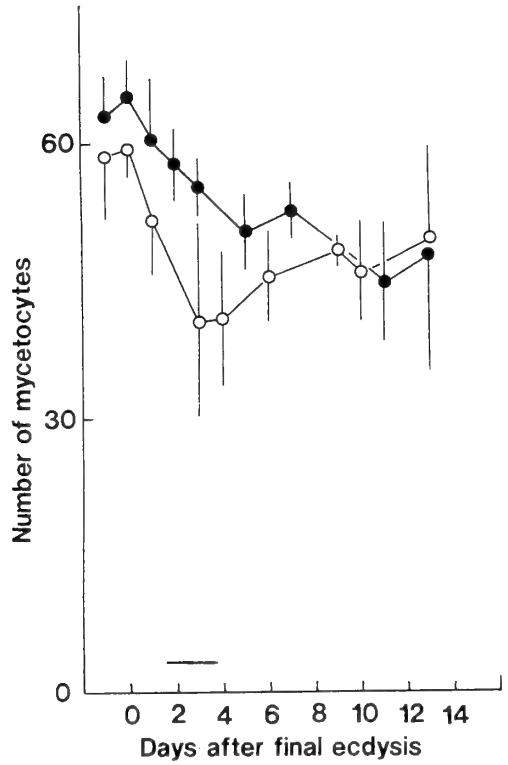

FIG. 1. Changes in number of mycetocyte per insect individual. Each value was expressed as mean ± SD. Closed symbols, apterae, n=10 to 25; open symbols, alatae, n=10 to 56. Horizontal bar designates the flying period.

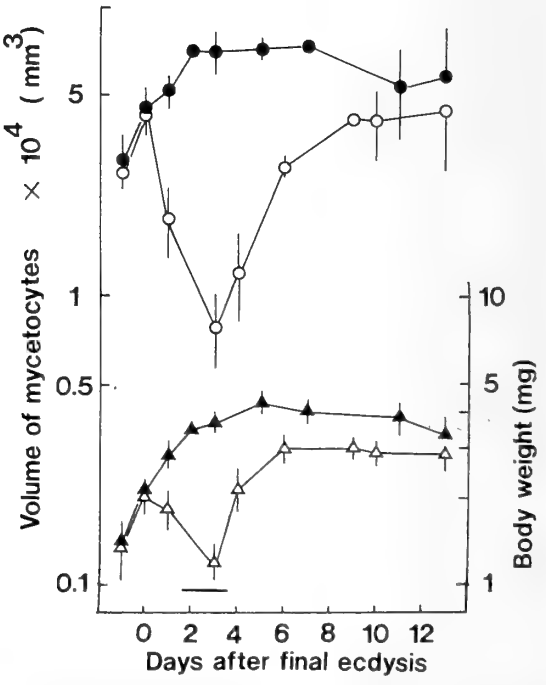

FIG. 2. Changes in median volume of mycetocytes (circles) and fresh body weight (triangles). Each value was expressed as mean ± SD. Closed symbols, apterae, n=10 to 25; open symbols, alatae, n=10 to 56. Horizontal bar designates the flying period.

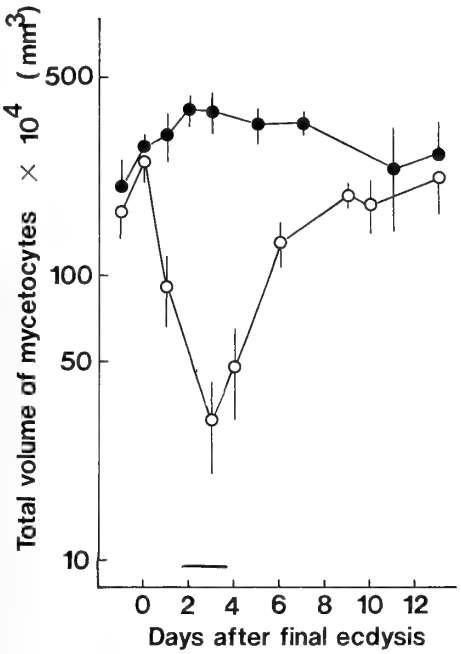

FIG. 3. Changes in total mycetocyte volume per insect individual. Total mycetocyte volume was calculated based on the number and mean diameter of mycetocytes for each individual. Each value was expressed as mean±SD. Closed symbols, apterae; open symbols, alatae.

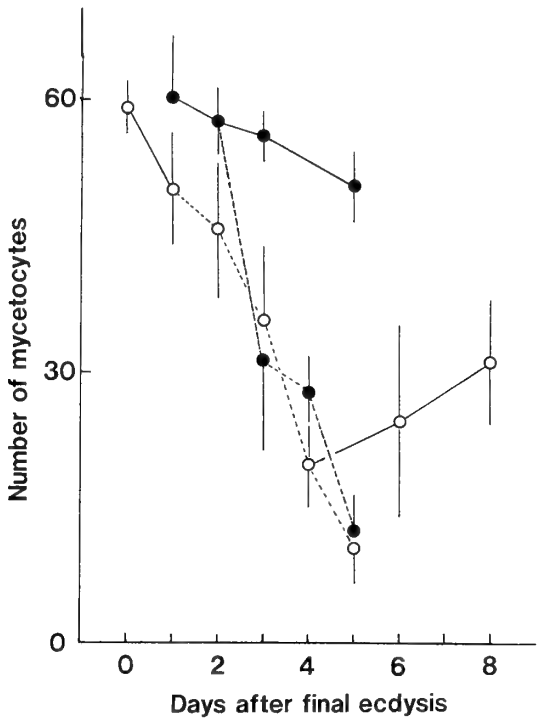

FIG. 4. Effects of starvation on number of mycetocyte per insect individual. Solid and dotted lines represent changes in fed and starved aphids, respectively. Each value was expressed as mean±SD. Closed symbols, apterae, n=5 to 12; open symbols, alatae, n=5 to 10.

r.g.r.: $-0.70\,mm^3mm^3day^{-1}$, $-0.18\,mgmg^{-1}day^{-1}$), then increased between day 3 and day 9 ($P<0.01$, r.g.r.: $0.30\,mm^3mm^{-3}day^{-1}$, $0.16\,mgmg^{-1}day^{-1}$).

Density of endosymbiont

In the flying stage of alatae, when the size of mycetocytes marked the lowest value, the density of endosymbionts was also lowered. On re-settling, the density recovered 78% of the value on day 0 (Table 1).

TABLE 1. Variation in symbiont density with behavior in alatae

day (age)	behavior	n	density ($*10^5/mm^2$)
0 (4th instar)	settling	3	2.7±0.2
3 (adult)	flying	8	1.5±0.1
6 (adult)	settling	4	2.1±0.1

Density was calculated by counting the total symbionts within several squares (15×15 μm) on a 0.5 μm seciton around a median line of mycetocyte, and expressed as mean±SD. 'n' Represents cell number surveyed. The values obtained were significantly ($P<0.05$) different from one another.

Interestingly, the color of mycetocytes also changed at the flying stage in alatae. In apterae and larval stage of alatae, mycetocytes were usually colorless and transparent. As the mycetocytes in alatae became smaller in number and size after the final ecdysis, the cells took on the condensed green. On settling of the insect, the condensed green re-

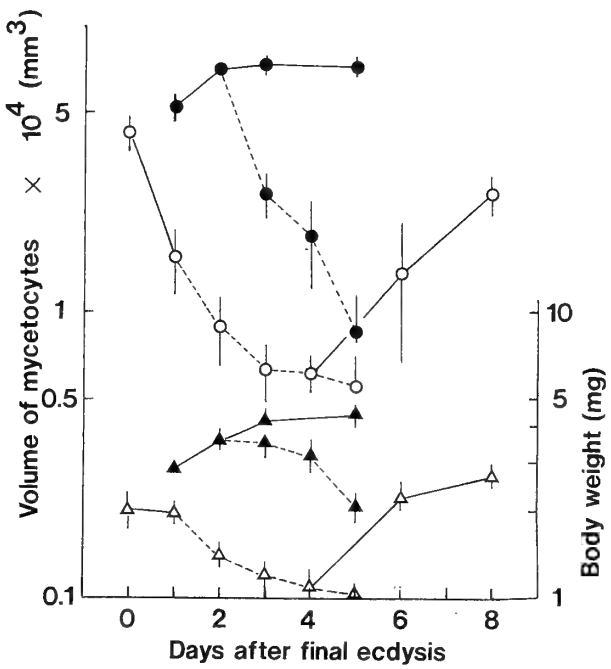

FIG. 5. Effects of starvation on volume of mycetocyte (circles), and fresh body weight (triangles). Solid and dotted lines represent changes in fed and starved aphids, respectively. Each value was expressed as mean±SD. Closed symbols, apterae; open symbols, alatae.

mained only partially on mycetocytes, then faded away after all.

Effects of starvation on total volume of mycetocyte

Apterae starved for 2 days did not much reduce their body weight (−12%), but the number and size of their mycetocytes declined by 45% and 75%, respectively (Figs. 4 and 5), and the total mycetocyte volume per aphid decreased rapidly down to 12% of the mean value on day 2 ($P<0.01$, r.g.r.: $-1.2\,mm^3mm^{-3}day^{-1}$, $0.18\,mgmg^{-1}day^{-1}$, for 3 days' starvation) (Fig. 6).

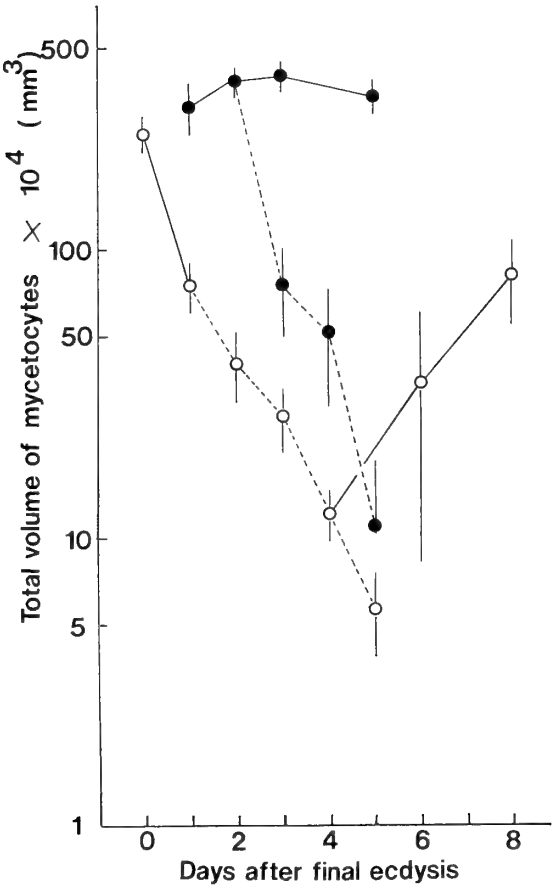

FIG. 6. Effects of starvation on total mycetocyte volume per insect individual. Solid and dotted lines represent changes in fed and starved aphids, respectively. Closed symbols, apterae; open symbols, alatae.

Unlike apterae, alatae decreased the number, volume and total volume of their mycetocyte spontaneously for the first one day after the final ecdysis even without starvation, and the starvation did not much reinforce the relative declining rate of the volume. In alatae, the decrease in the total mycetocyte volume was more gentle than in apterae ($P<0.01$, r.g.r: $-0.60\,mm^3mm^{-3}day^{-1}$, $0.20\,mgmg^{-1}day^{-1}$, for 3 days' starvation). When the starved alatae were transferred back to host plants, the total volume of mycetocytes and the aphid body weight began to increase rapidly, and 2 to 3 days later they started larviposition. The increase in number of mycetocytes after refeeding was also significant ($P<0.01$, between day 4 and day 7) (Fig. 4).

DISCUSSION

The present result on the changes in number and size of the mycetocyte in apetrae with age largely confirmed the results of the previous study [3]. In addition, our results on alatae provided several new findings with respect to the change of mycetocyte in response to their flight and feeding behavior.

Changes in number and size of the mycetocyte after the final ecdysis were quite different due to morph (Figs. 1 and 2). As a result, the change in the total volume of the mycetocyte was also remarkably different between the two morphs (Fig. 3). The most marked difference was represented by a steep decrease in size of the mycetocyte in alatae over 3 days after the final ecdysis (Fig. 2). This period exactly coincides with the period in which alatiform aphids develop their flight muscles to take off for migratory flight. Our previous study revealed that over the first two days after the final ecdysis alatae decrease their body weight, and the protein content of their indirect flight muscle increases in inverse proportion to their body weight [7].

In this period, alatae of *A. pisum*, like those of *Tuberolachnus salignus*, are not likely to ingest appreciable amount of food [7, 9], which suggests that their flight muscle goes on developing without supply of nutrients by feeding. And the fact that the sharp decrease of total mycetocyte volume had started when the whole body weight was not much reduced imply that this change is controlled selectively. In this context, the present results suggested that the putative source of nutrients for the developing muscle is the mycetocyte containing endosymbionts, since in alatae the rise and fall of the total volume of mycetocytes for the first several days after the final ecdysis was in exact inverse relation to that of the protein content of indirect flight muscle [7]. The result that not only the total volume of mycetocytes but also the density of endosymbionts in the mycetocyte decreased in this period (Table 1) may indicate that the endosymbionts rather than the mycetocyte itself serve as major nutrient sources.

The possibility that the mycetocyte harboring endosymbionts serve as a nutrient source to the host was also sustained by the experiments in which aphids were kept starved (Fig. 6). As far as aphids were kept starved, their total mycetocyte volume was consistently decreased at a much higher rate than that of the decline of their body weight, suggesting that under the nutritionally adverse conditions aphids will reduce their endosymbiotic system unfalteringly in order to preserve their own life at the cost of the endosymbionts. This situation has been most typically demonstrated with alatae at the teneral period. Starving them, on one hand, induced a sharp decline of their total mycetocyte volume (Fig. 6), and, on the other hand, prevented their indirect flight muscle from breaking down [7]. When the nutritional conditions were improved by refeeding, their total mycetocyte volume im-

mediately restored the original value, suggesting that the change is reversible in nature.

It had been rather unexpected that upon settling and refeeding of alatae their mycetocyte were tuned to increase in not only total volume (Fig. 3) but also cell number (Fig. 1). Refeeding after the starvation also resulted in increase in number of mycetocytes (Fig. 4). It is likely that under the nutritionally adverse conditions part of mycetocytes are decreased in size to the extent in which they are hardly distinguishable from fat body cells surrounding them, and that they restore the original size on refeeding. In any case, our conclusion that aphids survive the nutritionally adverse conditions at the cost of their endosymbionts will not be hurt. It is interesting to know what mechanisms make it feasible for the cells to change their size so extremely, and yet, reversibly.

Finally, it should be described that the present results concern only the maternal symbiosis. For the present, it is just a matter of conjecture whether or not under the adverse conditions aphids reduce the total symbiosis including that of their embryos. It would be very interesting to know under which circumstances, if at all, aphid embryos cooperate with their mother by reducing their own symbiosis.

ACKNOWLEDGMENTS

This research was supported by Grants-in-Aid for General Research (No. 03454020) and for Scientific Priority Areas, "Symbiotic Biosphere: Ecological Interaction Network promoting the Coexistence of Many Species" (No. 04264103) from the Ministry of Education, Science and Culture of Japan.

REFERENCES

1 Adams JB, von Emden HF (1972) The biological properties of aphids and their host plant relationships. In "Aphid Technology" Ed by von Emden HF, Academic Press, London, pp. 48–104

2 Bühner P (1965) "Endosymbiosis of Animals with Plant Microorganisms", Interscience, New York.

3 Douglas AE, Dixon AFG (1987) The mycetocyte symbiosis of aphids: variation with age and morph in virginoparae of *Megoura viciae* and *Acyrthosiphon pisum*. J Insect Physiol 33: 109–113

4 Ehrhardt P (1968) Einfluss von Ernahrungsfaktoren auf die Entwicklung von Safte saugenden Insekten unter besonderer Berucksichtigung von Symbionten. Z Parasitkde 31: 38–66

5 Houk EJ, Griffiths GW (1980) Intracellular symbiotes of the Homoptera. A Rev Ent 25: 161–187

6 Ishikawa H (1989) Biochemical and Molecular Aspects of Endosymbiosis in Insects. Int Rev Cytol 116: 1–45

7 Kobayashi M, Ishikawa H (1993) Breakdown of indirect flight muscles of alatae aphids (*Acyrthosiphon pisum*) in relation to their flight, feeding and reproductive behavior. J Insect Physiol 39: 549–554

8 Kring JB (1972) Flight behavior of aphids. A Rev Ent 17: 461–492

9 Mittler TE (1958) Studies on the feeding and nutrition of *Tuberolachnus salignus* (Gmelin) 3. The nitrogen economy. J Exp Biol 35: 626–638

10 Mittler TE (1971) Dietary amino acid requirements of the aphid *Myzus persicae* affected by antibiotic uptake. J nutr 101: 1023–1028

11 Sasaki T, Ishikawa H (1991) Growth and reproduction of the symbiotic and aposymbiotic pea aphids, *Acyrthosiphon pisum* maintained on artificial diets. J Insect Physiol 37: 749–756

12 Srivastava PN, Auclair JL, and Srivastava U (1983) Effect of nonessential amino acids on phagostimulation and maintainance of the pea aphid, *Acyrthosiphon pisum*. Can J Zool 61: 2224–2229

ZOOLOGICAL SCIENCE 11: 737–743 (1994)

Seven Types of Tunic Cells in the Colonial Ascidian *Aplidium yamazii* (Polyclinidae, Aplousobranchia): Morphology, Classification, and Possible Functions

EUICHI HIROSE*[1], TERUHISA ISHII[2], YASUNORI SAITO[2] and YASUHO TANEDA[3]

[1]*Biological Laboratory, College of Agriculture and Veterinary Medicine, Nihon University, Fujisawa, Kanagawa 252,* [2]*Shimoda Marine Research Center, University of Tsukuba, Shimoda, Shizuoka 415, and* [3]*Department of Biology, Faculty of Education, Yokohama National University, Yokohama, Kanagawa 240, Japan*

ABSTRACT—Seven types of tunic cells and multicellular vesicles are described in the tunic of the polyclinid ascidian *Aplidium yamazii*: spherical tunic cells (t. c.), phagocytic t. c., elongated t. c., filopodial t. c., micro-granular t. c., morula-like t. c., and macro-granular t. c. The spherical tunic cells are characterized by their spherical cell bodies filled with round granules. Some of these cells are located on the outside of the tunic, and they are probably released from the tunic. The phagocytic tunic cells are irregularly shaped and are motile. They contain phagosomes and vesicles laden with round granules, which are probably derived from the contents of the phagosomes. It is thought that the phagocytic tunic cells filled with the granules become the spherical tunic cells that are released from the tunic. The elongated tunic cells have thin cell bodies with long cellular processes extending from them. These processes appear to connect with each other and possibly form a contractile network in the tunic. The tunic vesicle is a hollow multicellular vesicle composed of thin flattened cells and cuboidal granular cells. The cuboidal cells of the tunic vesicle often contain a large amount of rough endoplasmic reticulum, indicating a high level of protein synthesis, and they may secrete some components of the tunic. The functions of the other tunic cells, i.e., filopodial tunic cell, micro-granular tunic cell, morula-like tunic cell, and macro-granular tunic cell, are not clear.

INTRODUCTION

Ascidian bodies are completely covered with the tunic, which is a leathery or gelatinous matrix containing cellulosic fibrils [1, 20]. There are several different kinds of tunic cells distributed within the tunic. In this sense, the ascidian tunic is not merely a covering, but is a living tissue performing some biological functions. In colonial species, the tunic is also a shared tissue among the clonal individuals and possibly involves some events that are characteristic of colonial organisms (e.g., budding of zooids [14, 15], coordination of zooids [10], allorecognition between colonies [18], *etc.*).

Tunic cell morphology and classification have been described for a few groups of colonial ascidians. In botryllid ascidians, which have an interzooidal (common) vascular system, there are only two or three types of tunic cells [8, 9, 22], and hemocytes infiltrating from the vascular system are involved in some events occurring in the tunic, such as the allogeneic rejection reaction between colonies [7, 19]. On the other hand, aplousobranchian species, lacking an interzooidal vascular system, usually possess various types of tunic cells. For instance, six types of tunic cells are recognized in the aplousobranchian didemnid *Leptoclinides echinatus* [5]. In the species without tunic vessels, it is difficult for the hemocytes to respond quickly to the events occurring in the tunic, because they have to migrate for a long distance. These aplousobranchian species are, therefore, likely to have more types of tunic cells for dealing with these events than do the species with an interzooidal vascular system, such as botryllids.

Recently, we reported that a particular type of tunic cell shows phagocytic activity in the aplousobranchian polyclinid *Aplidium yamazii* [6]. Another type of tunic cell probably has another function in the tunic. In order to understand the various biological events in the tunic, it is necessary to describe and classify the tunic cells in this species. The present study deals with the classification of the tunic cells of *A. yamazii* based on light and electron microscopical observations. We also discuss the possible functions of some of these tunic cells.

MATERIALS AND METHODS

Animals

The colonies of *Aplidium yamazii* were collected in Nabeta Bay, Shimoda (Shizuoka Pref., Japan). They were attached to glass slides with cotton thread and were reared in culture boxes immersed in Nabeta Bay. The colonies grew and spread on the glass slides.

Light and electron microscopy

A living colony was sliced transversely as thin as possible (about

Accepted July 13,1994
Received April 14, 1994
* To whom all correspondence should be addressed.

0.5 mm or less) with a razor blade and mounted with seawater. The live specimens were observed under a light microscope equipped with Nomarski differential interference contrast (DIC) optics.

A colony was cut into pieces and fixed in 2.5% glutaraldehyde-0.1 M sodium cacodylate-0.45 M sucrose (pH 7.4) for 2 hr on ice. These colony pieces were then washed in 0.1 M sodium cacodylate-0.45 M sucrose (pH 7.4), and postfixed in 1% osmium tetroxide-0.1 M sodium cacodylate (pH 7.4) for 1 to 1.5 hr on ice. The specimens were dehydrated through an ethanol series, cleared with *n*-butyl glycidyl ether, and embedded in low viscosity epoxy resins. Thick sections were stained with toluidine blue for light microscopy (LM). For transmission electron microscopy (TEM), thin sections were stained with uranyl acetate and lead citrate, and they were examined in a Hitachi HS-9 transmission electron microscope at 75 kV.

Recording of cell motility

The motility of tunic cells was recorded using a time-lapse videocassette recorder AG-6010 (National, Japan). A colony was sliced with a razor blade, mounted with seawater, and observed by a microscope equipped with Nomarski DIC optics and a video camera WV-1800 (National, Japan). The recording was performed about 1/60 of the actual speed.

Staining of microfilaments with phalloidin-fluorescein isothiocyanate (FITC)

Microfilaments were visualized in colony slices by labeling with phalloidin-FITC. A colony was cut into slices with a razor blade. The slices of the colony were fixed with 3.5% formaldehyde in Ca^{2+}-free artificial seawater (CFSW; Jamarine Lab., Japan) for 10 min, permeabilized with 0.1% Triton X-100 in CFSW for 5 min, and washed with phosphate buffered saline (PBS). They were incubated with 1 μg/ml phalloidin-FITC (Sigma) in PBS for 30 min and then were rinsed extensively with PBS. The specimens were observed under a microscope equipped with epifluorescence and Nomarski DIC optics.

RESULTS

Morphology and classification of tunic cells

We identified seven types of tunic cells based on their morphology: spherical tunic cells (t. c.), phagocytic t. c., elongated t. c., filopodial t. c., micro-granular t. c., morula-like t. c., and macro-granular t. c. The micro-granular and macro-granular t. c. are fewer in number than the other types. There are also hollow multicellular vesicles, called tunic vesicles, in the tunic.

Spherical t. c. (Fig. 1): These are one of the prominent tunic cell types. They are characterized by a spherical cell shape and round granules (about 1 to 1.5 μm in diameter) that occupy the bulk of the cells (Fig. 1, A and B). The granules show a variety of electron densities, and each of them is contained in a vesicle. The tunic cuticle often surrounds the cells distributed near the cuticle (Fig. 1A). This indicates that these cells are present outside the tunic. Some of the spherical t. c. appear to be released from tunic surface (Fig. 1, C and D).

Phagocytic t. c. (Fig. 2): This is the most prominent type of tunic cell, being distributed throughout the tunic. These cells are characterized by phagocytic activity, as described previously [6]. The phagocytic tunic cells often have phagosomes containing disorganized structures, and some of them also engulf other tunic cells. They also contain round granules, 1.5 μm or less in diameter. The granules of 1 to 1.5 μm in diameter are similar in morphology to those of the spherical t. c. described above. The cells containing no or few granules have an irregularly shaped cell body with numerous filopodia, whereas the cells containing many granules have a relatively thicker cell body with fewer filopodia. Some of the phagocytic tunic cells filled with granules are similar in morphology to the spherical t. c. (Fig. 2C).

Elongated t. c. (Fig. 3): These cells are flat and extend cellular processes that are often 70 μm or greater in length. They often have vacuoles, but no prominent granule in the cytoplasm. The cellular processes appear to contact those of neighboring elongated t. c. and probably form a network of these cells.

Filopodial t. c. (Fig. 4): These cells are usually distributed near the tunic cuticle. Under Nomarski DIC optics, the cells have a stellate shape and radiate filopodia (Fig. 4A). They often have vacuoles, but no prominent granules. Because of the limited information from thin sections, it is difficult to define the filopodial tunic cells in TEM. There are nongranular amoeboid tunic cells near the tunic cuticle, and they are the most probable candidates for the filopodial t. c. (Fig. 4B).

Micro-granular t. c. (Fig. 5): These cells are characterized by electron-dense granules of about 0.2 μm in diameter. They are irregularly shaped and protrude pseudopodia. It is impracticable to discriminate between this type of cell and the phagocytic t. c. in LM.

Morula-like t. c. (Fig. 6): These cells closely resemble morula cells, which are a kind of hemocyte that has been described in many other ascidians [21]. The greater part of these cells is occupied by several vacuoles filled with electron-dense materials (Fig. 6A). The cells that are distributed close to the epidermis of zooids are often elliptically shaped, whereas the others are round.

Fig. 1. Spherical tunic cells. Arrowheads indicate the tunic cuticle. A) The cell surrounded by the tunic cuticle. B) The cells in a live specimen under Nomarski DIC. C) The cell, half-released from the tunic, in the thick sections stained with toluidine blue. D) A part of the cell projecting out from the tunic (arrow). Scale bars=5 μm (A, C and D) and 50 μm (B).

Fig. 2. Phagocytic tunic cells. Arrowheads indicate phagosomes containing disorganized structures. Scale bars=5 μm.

Fig. 3. Elongated tunic cells (arrows) in a live specimen (Nomarski DIC, A) and in thin section (TEM, B). Scale bars=50 μm (A) and 5 μm (B).

Fig. 4. A filopodial tunic cell in a live specimen (Nomarski DIC, A) and a possible candidate in thin section (TEM, B). Scale bars=10 μm (A) and 5 μm (B).

Fig. 5. A micro-granular tunic cell. Scale bar=2 μm.

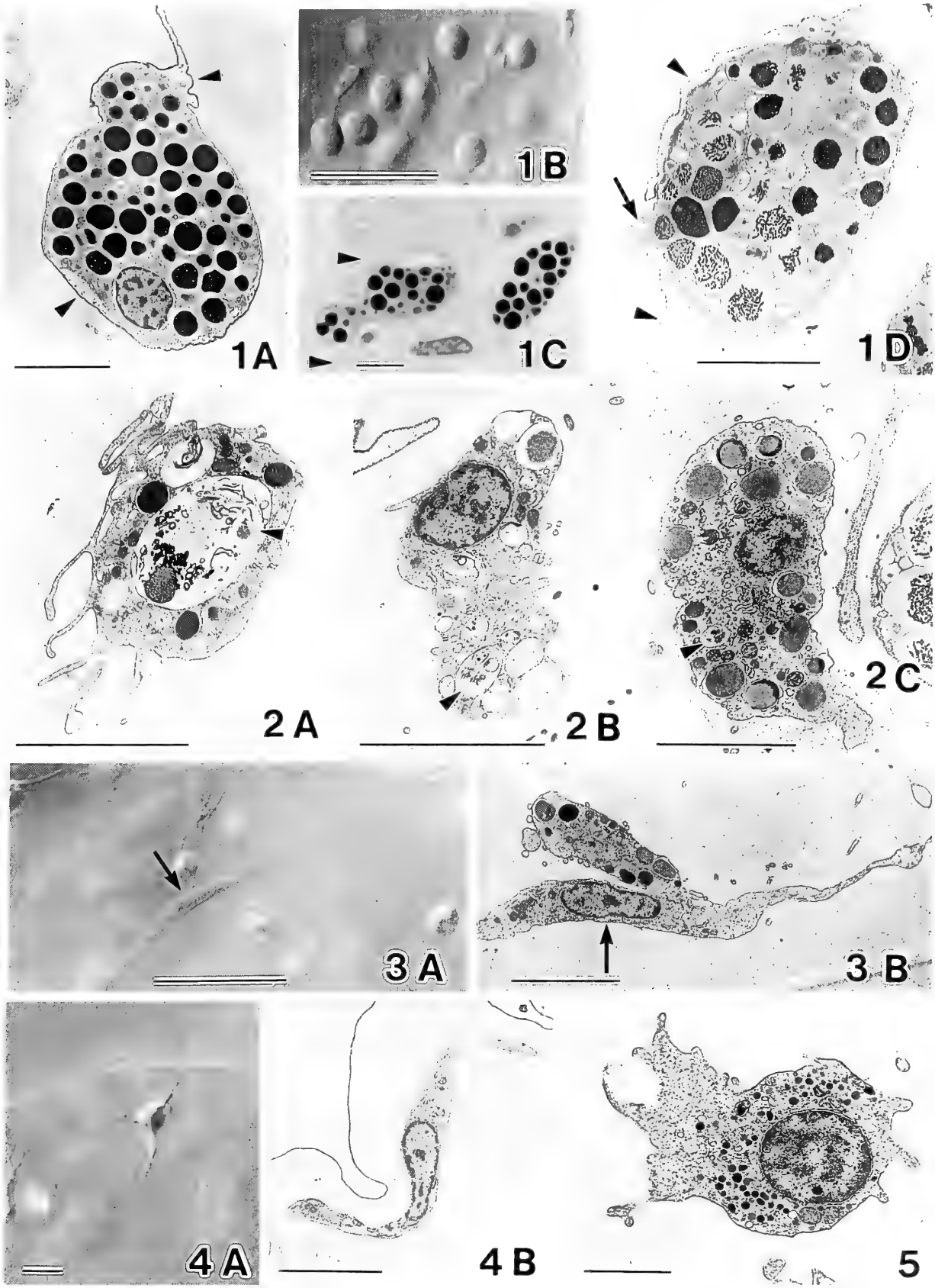
1A
1B
1C
1D
2A
2B
2C
3A
3B
4A
4B
5

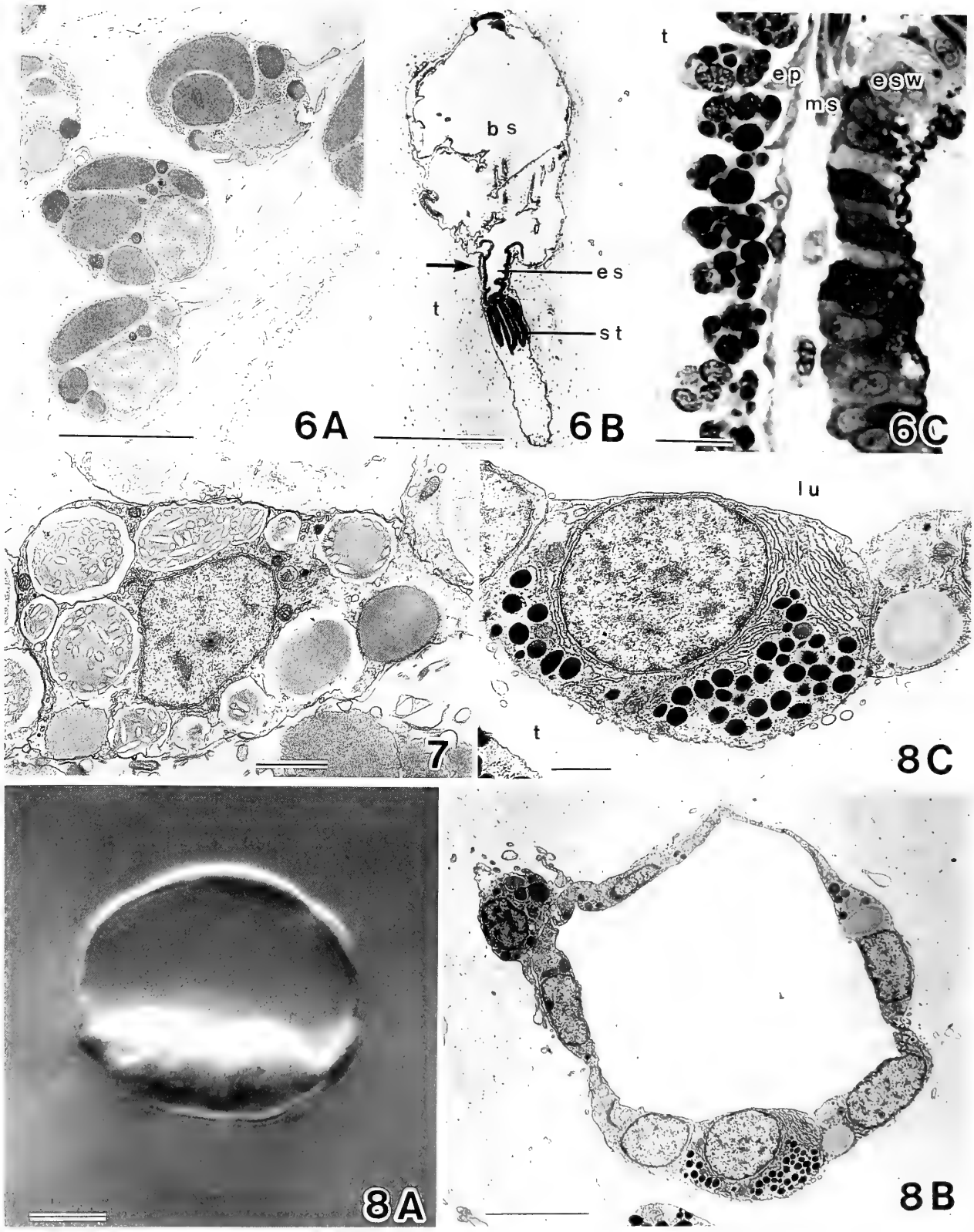

Fig. 6. A) Morula-like tunic cells. B) A transverse section of a zooid. Arrow indicates the cells arranged in a row adjacent to the epidermis. C) Enlargement of the area indicated by arrow in B. B and C are thick sections stained with toluidine blue. bs, branchial basket; ep, epidermis; es, esophagus; esw, esophageal wall; ms, mesenchymal space; st, stomach=t, tunic. Scale bars=5 μm (A), 50 μm (B), and 10 μm (C).

Fig. 7. A macro-granular tunic cell. Scale bar=2 μm.

Fig. 8. Tunic vesicles. A) Nomarski DIC in a live specimen. B) TEM. C) Cuboidal cells of tunic vesicles (enlargement of B). lu, lumen of tunic vesicles; t, tunic. Scale bars=10 μm (A), 5 μm (B),, and 2 μm (C).

Many morula-like t. c. surround the anterior-most abdominal epidermis that covers the esophagus (Fig. 6, B and C). These cells are arranged in a row adjacent to the epidermis. The area of this aggregative cell distribution is limited, and the cells do not encircle this area like a collar.

Macro-granular t. c. (Fig. 7); These are distributed close to the epidermis of the zooid and usually form a cell mass. They are characterized by round vacuoles each of which contains a large granule approximately 2 μm in diameter. The granule is not homogeneous, and there are many electron-lucent areas lined with electron-dense substances in each granule.

Tunic vesicle (Fig. 8): There are hollow multicellular vesicles in the tunic. Simple epithelial cells form the wall of the vesicle, and they consist of at least two cell types: thin flattened cells and cuboidal granular cells. The flattened cells contain some mitochondria and occasionally a few moderately dense granules (about 1 μm in diameter). The cuboidal granular cells are characterized by electron-dense granules of 0.3 to 0.4 μm in diameter and a large amount of rough endoplasmic reticulum (RER) (Fig. 8C). In both cell types, we did not find a prominent basal lamina on either the tunic side or the inner side.

Distribution and composition of tunic cells

Tunic cells of each type are not distributed homogeneously in the tunic. Preliminary analysis of the distribution and composition of each cell type was carried out in the thick sections stained with toluidine blue (Table 1). The seven types of tunic cells described here were grouped into three types, because some cell types were not classified perfectly in the thick sections. Namely, "amoeboid type" includes phagocytic, filopodial, micro-granular, and elongated t. c., and "morula-like type" includes morula-like and macro-granular t. c. The numbers of each cell type were determined in three different areas of the tunic: beneath the tunic cuticle; around the zooid (abdomen), including the area where morula-like t. c. are aggregatively distributed; and the peripheral part of the colony. The spherical t. c. was relatively abundant in the subcuticular area and rare around the zooid. In contrast, many of the morula-like t. c. were found around the zooids. The epidermal vesicles were often distributed around the colony periphery.

TABLE 1. Differential cell counts of tunic cells in three different tunic area

Cell type[2]	Number (%) of cells in[1]: Subcuticle	Abdomen	Periphery
Spherical	37 (14)	3 (1)	5 (7)
Amoeboid	217 (83)	190 (72)	62 (86)
Morula-like	9 (3)	70 (27)	1 (1)
Epidermal vesicle[3]	0 (0)	1 (<1)	4 (6)
Total	263	264	72

[1] Subcuticle=subcuticular area (within 50 μm below tunic cuticle) around branchial siphon; Abdomen=around the abdomen of zooids (within 50 μm along abdominal epidermis); Periphery=peripheral parts of the colony, excluding subcuticular area.

[2] The three cell types listed here represent all seven types described in the text because of the difficulty of classification in thick sections (see text).

[3] Each epidermal vesicle is counted as a single cell, although it is a multicellular structure.

Cell motility and cellular microfilaments

Many of phagocytic t. c. migrate actively in the tunic, and some others that extend filopodia radially do not migrate. Filopodial t. c. that are distributed near the cuticle usually repeatedly contract and expand, but do not change position in the tunic, whereas elongated t. c. rarely contract. Spherical t. c. and morula-like t. c. are not motile. The tunic vesicles do not migrate in the tunic, and each of them repeatedly contracts and expands. Under a light microscope, it is very difficult to distinguish the micro-granular t. c. and the macro-granular t. c. from some of the phagocytic t. c. and the morula-like t. c., respectively, and thus, the cell motility of these two cell types is uncertain in this study. The speed of cell migration could not be measured because of three-dimensional migration of the tunic cells in the tunic slices.

Phalloidin-FITC stains the cellular microfilaments (espe-

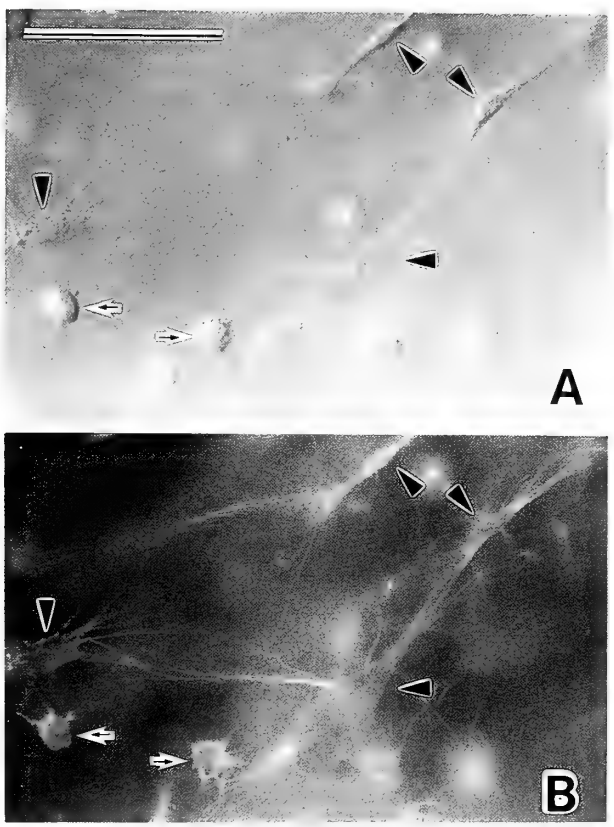

FIG. 9. Paired images of tunic slices stained with phalloidin-FITC (Nomarski DIC for A, fluorescent microscopy for B). Arrow, phagocytic tunic cell; arrowhead, elongated tunic cell. Scale bar=50 μm.

cially the filopodia) of the phagocytic t. c., filopodial t. c. and elongated t. c. (Fig. 9). The filopodia of the elongated t. c. appear to connect with one another, thereby possibly forming a cellular network in the tunic. The other tunic cells show only weak fluorescence at their cell periphery.

DISCUSSION

The present study describes seven types of tunic cells and a type of multicellular vesicle in the colonial ascidian *Aplidium yamazii*. The possible functions of some of the tunic cells are discussed, based on morphological findings.

Spherical t. c. are characterized by their spherical cell shape and are filled with round granules. Many spherical t. c. are distributed in the subcuticular area of the tunic, and some of them are released from the tunic. It is not known how they move to the outside of the tunic, since the time-lapse video recording shows their immotility. Release of tunic cells has been reported in a solitary ascidian, *Ciona intestinalis*: the large granule cell in the adult tunic [2] and the large single vacuole cell and the type B cell in the metamorphosing embryo [11, 12]. According to these reports, these tunic cells are presumed to migrate from the mesenchymal space between the epidermis and the peribranchial epithelium, cross the epidermis, and finally reach the outside of the tunic cuticle. These excreted cells in *C. intestinalis* have a large vesicle containing electron-dense materials, and they differ in structure from the spherical t. c. that are multigranular. It is possible that the excreted cells of *C. intestinalis* and *A. yamazii* originate from different tissues, respectively.

Phagocytic t. c. are characterized by phagocytic activity and have phagosomes and round granules. Peroxidase activity was demonstrated exclusively within the vesicles laden with granules, and this suggests that the granules may be derived from the contents of the phagosomes [6]. The structures of the round granules are similar to those of spherical t. c., and phagocytic t. c. filled with granules appears to be intermediate in form between phagocytic t. c. and spherical t. c. Based on these observations, we suppose that the course of differentiation to become phagocytic/spherical t. c. is as follows: 1) The young phagocytic tunic cell has a thin cell body and numerous protruding filopodia. 2) The round granules are produced from the contents of phagolysosomes. 3) In accordance with the increase of granules, the cell body becomes thicker and roundish. 4) The cells that are full of granules differentiate into spherical t. c. and then are excreted from the tunic as waste.

The long cellular processes of elongated t. c. appear to connect with each other to form a cellular network in the tunic. Mackie and Singla [10] reported a network of cells in the tunic of two colonial species, *Diplosoma listerianum* and *D. macdonaldi*. The cells forming the network are called myocytes; they stain with NBD-phallacidin and show contractility. The myocytes are usually multipolar with long cellular processes, and the net of myocytes itself is supposed to conduct impulses that trigger its contraction, according to electrophysiological studies [10]. In the tunic of the *Diplosoma*, Mackie and Singla [10] also described filopodial cells that are restricted to the surface layer of the tunic. The filopodial cell in the *Diplosoma* probably corresponds to the filopodial t. c. in *A. yamazii*. In *Diplosoma*, the filopodial cells and the myocytes are distributed separately in the tunic. According to Mackie and Singla [10], "filopodial cells are restricted to the surface layer of the tunic, while the myocyte lie deeper." This is probably true for filopodial t. c. and elongated t. c. in *A. yamazii*. In *Leptoclinides echinatus*, six types of tunic cells are described by means of LM for paraffin sections and by scanning electron microscopy [5], and the "elongated tunic cell" in this species is similar in cell shape to the elongated t. c. in *A. yamazii*.

Tunic vesicles (or epidermal vesicles) have been reported in two colonial ascidians: *Aplidium* (=*Amaroucium*) *constellatum* [3, 4] and *Polycitor proliferus* [16, 17]. These studies reported that tunic vesicles are the result of evagination from the epidermis of zooids during the late embryonic stage. Oka and Usui [17] assumed, on the basis of their histological examinations, that the tunic vesicles are constantly formed, even in adult colonies. They also supposed that the tunic vesicles in *P. proliferus* secrete some adhesive substance to fix the colony to the substratum. In *A. yamazii*, the cells of tunic vesicles contain a large amount of RER and many granules, suggesting synthetic and secretory activity.

In general, tunic cells are thought to originate from hemocytes that pass through the epidermis. In *Aplidium* (= *Amaroucium*) *yamazii*, Nakauchi [13] has reported that "many tunic cells surrounding the neck of the abdomen become free from the zooid, and they migrate into the tunic" during the last stage of budding. In the present study, we have also found that many morula-like t. c. aggregate in the tunic around the epidermis covering the esophagus (neck of abdomen). This possibly indicates that morula-like t. c. originate from morula cells of hemocytes that have passed through the epidermis at this area. Since morula-like t. c. are, however, a kind of differentiated cell, they will not differentiate into other types of tunic cells, such as phagocytic t. c. or elongated t. c. This observation, therefore, cannot support the idea that these cell aggregation is a source of all types of tunic cells in *A. yamazii*. The origin of each type of tunic cell still remains unresolved.

ACKNOWLEDGMENTS

The present study is the contribution no. 573 from Shimoda Marine Research Center. We wish to thank the staff members of Shimoda Marine Research Center for their assistance and hospitality.

REFERENCES

1 De Leo G, Patricolo E, D'Ancona Lunetta G (1977) Studies on the fibrous components of the test of *Ciona intestinalis* Linaeus. I. Cellulose-like polysaccharide. Acta Zool (Stockh.) 58: 135–141

2 De Leo G, Patricolo E , Frittita G (1981) Fine structure of the

tunic of *Ciona intestinalis* L. II. Tunic morphology, cell distribution and their functional importance. Acta Zool 62: 259–271

3 Grave C (1920) The origin, function and fate of the test-vesicles of *Amaroucium constellatum*. Anat Rec 17: 350

4 Grave C (1921) *Amaroucium constellatum* (Verrill). II. The structures and organization of the tadpole. J Morphol 36: 71–101

5 Hirose E (1992) Tunic cells in *Leptoclinides echinatus* (Didemnidae, Ascidiacea): An application of scanning electron microscopy for paraffin embedding specimens. Hiyoshi Rev Natur Sci Keio Univ 11: 5–8

6 Hirose E, Ishii T, Saito Y, Taneda Y (1994) Phagocytic activity of tunic cells in the colonial ascidian *Aplidium yamazii* (Polyclinidae, Aplousobranchia). Zool Sci 11: 203–208

7 Hirose E, Saito Y, Watanabe H (1990) Allogeneic rejection induced by cut surface contact in the compound ascidian, *Botrylloides simodensis*. Invert Reprod Dev 17: 159–164

8 Hirose E, Saito Y, Watanabe H (1991) Tunic cell morphology and classification in botryllid ascidians. Zool Sci 8: 951–958

9 Izzard CS (1974) Contractile filopodia and in vivo cell movement in the tunic of the ascidian, *Botryllus schlosseri*. J Cell Sci 15: 513–535

10 Mackie GO, Singla CL (1987) Impulse propagation and contraction in the tunic of a compound ascidian. Biol Bull 173: 188–204

11 Mancuso V (1983) Cell types in the tunic of the metamorphosing *Ciona* embryo: Large single vacuole cells. Acta Embryol Morphol Exper 4: 119–126

12 Mancuso V (1986) Type B cells in the metamorphosing *Ciona intestinalis* embryos. Acta Embryol Morphol Exper 7: 27–33

13 Nakauchi M (1970) Asexual reproduction in *Amaroucium yamazii* (a colonial ascidian). Publ Seto Mar Biol Lab 17: 309–328

14 Nakauchi M, Kawamura K (1974) Experimental analysis of the behavior of buds in the ascidian, *Aplidium multiplicatum*. I. Rep Usa Mar Biol Stn21: 29–38

15 Nakauchi M, Kawamura K (1978) Additional experiments on the behavior of buds in the ascidian, *Aplidium multiplicatum*. Biol Bull 154: 453–462

16 Oka H (1943) Metamorphosis of *Polycitor mutabilis* (ascidiae compositae). Annot Zool Jpn 22: 54–58

17 Oka H, Usui M (1944) On the growth and propagation of the colonies in *Polycitor mutabilis* (ascidiae compositae). Sci Rep Tokyo Bunrika Daigaku, Sec B, 103: 25–53

18 Taneda Y, Saito Y, Watanabe H (1985) Self or non-self discrimination in ascidians. Zool Sci 2: 433–442

19 Taneda Y, Watanabe H (1982) Studies on colony specificity in the compound ascidian, *Botryllus primigenus* Oka. I. Initiation of "nonfusion" reaction with special reference to blood cell infiltration. Dev Comp Immunol 6: 43–52

20 Van Daele Y, Revol J-F, Gaill F, Goffinet G (1992) Characterization and supramolecular architecture of the cellulose-protein fibrils in the tunic of the sea peach (*Halocynthia papillosa*, Ascidiacea, Urochordata). Biol Cell 76: 87–96

21 Wright RK (1981) Urochordate. In "Invertebrate Blood Cells Vol 2" Ed by NA Ratcliffe, AF Rowley, Academic Press, London, pp 565–626

22 Zaniolo G (1981) Histology of the ascidian *Botryllus schlosseri* tunic: In particular, the test cells. Boll Zool 48: 169–178

ZOOLOGICAL SCIENCE 11: 745–752 (1994)

Aminergic and Acetylcholinesterase-positive Innervation in the Cerebral Arterial System and Choroid Plexus of the Newt *Triturus pyrrhogaster*, with Special Reference to the Plexus Innervation

Kōichi Andō[1] and Nobuhiko Ōkura[2]

[1]*Biological Laboratory, Department of Regional Culture, Faculty of International Studies of Culture, Kyushu Sangyo University, Matsukadai, Higashi-ku, Fukuoka 813, and* [2]*Zoological Laboratory, Faculty of Agriculture, Kyushu University, Fukuoka 812, Japan*

ABSTRACT—The pattern of cerebrovascular noradrenergic or adrenergic (NA) and acetylcholinesterase-positive (AChE) innervation in the newt was investigated. The cerebral arterial tree of this urodelan species was dually innervated by both NA and AChE nerves, with a lesser density of the latter type. NA nerves innervating the major cerebral arteries sometimes originated from NA-containing nerve cells intrinsic to these vessel walls. Another finding worthy of attention was that a large number of NA and AChE nerves were concentrated in the microvascular-epithelial regions of the choroid plexuses, especially the venule loop in the most outer part of the lateral and third plexuses, despite a poor supply of these two nerve types along the entire length of the cerebral arterial tree. This and other findings suggest that NA and cholinergic mechanisms are responsible for the microcirculation and transport action within the choroid plexus in the nutrition of the newt brain via the cerebrospinal fluid. In addition, basophil leucocytes emitted a brilliant greenish yellow fluorescence after formaldehyde gas-treatment. From the combination of the standard excitation and emission spectra and the shifting pattern of these two spectra after HCl vapor treatment, it is expected that specific granules of the newt basophil leucocytes contain not only serotonin and/or catecholamines, but also a substantial amount of fluorescent components other than these biogenic amines and histamine.

INTRODUCTION

It is well established that the major cerebral arteries in mammals are richly innervated by sympathetic noradrenergic and parasympathetic acetylcholinesterase-positive (AChE) nerves with approximately the same density [37]. Dual innervation by these two populations of nerves has also been demonstrated in the choroid plexus, the special vascular-epithelial structure for the secretion of the cerebrospinal fluid (CSF) in the brain ventricles [6, 8, 9, 20, 21].

In urodelan amphibians, Tsuneki and Ouji [34] and Tsuneki et al. [35] demonstrated the absence of blood vessels in the bulk of the brain parenchyma in the Japanese salamanders belonging to the family Hynobiidae. They also pointed out the dense aggregation of brain neuronal perikarya in the periventricular region facing the CSF, the periventricular gray matter, in a variety of urodeles. The urodelan choroid plexus is known to be well vascularized and large relative to the whole brain [13, 17]. Furthermore, a large volume of blood in the brain of this amphibian group has been reported to flow toward the choroid plexus [12]. For these reasons, it has been suggested that the choroid plexus in urodelan amphibians may act as a major site for the supply of nutrients and oxygen to the brain, and for the exit of brain metabolic substances such as carbon dioxide. Thus, it is a matter of interest to explore the neurogenic mechanisms by which the urodelan choroid plexus, as well as their cerebral arterial system, is regulated.

Our previous studies showed a unique pattern of noradrenergic or adrenergic (NA) innervation, and AChE innervation in both the cerebral arterial tree and choroid plexus of some anuran amphibians [2, 31, 32]. The major cerebral arteries of the Japanese toad, the leopard frog, and the bullfrog receive a relatively rich supply of NA nerves , with a poor supply (the former two species) and lack (the latter one) of AChE nerves, while those of the clawed toad have only a few or no aminergic and AChE nerves. Within the choroid plexuses of the Japanese toad, bullfrog, and leopard frog, NA nerves are densely distributed along the arteri al system, but were very poor in the plexus proper consisting of the venule, capillary net and epithelium. In contrast, extremely rich NA innervation has been found in close association with the microvascular-epithelial regions of the choroid plexus in the clawed toad. There are no AChE nerves in the choroid plexuses of these four anuran amphibians, except for a few fibers with very weak enzyme activity in the clawed toad. The present formaldehyde histofluorescence and AChE staining studies on an urodelan species, the newt, are directed

Accepted July 14, 1994
Received April 27, 1994

ACA anterior cerebral artery, AR anterior ramus, BA basilar artery, CCA cerebral carotid artery, FSA first spinal artery, H hypophysis, MCA middle cerebral artery, OC optic chiasma, PCA posterior cerebral artery, PCMT posterior communicating artery, PR posterior cerebral artery, P-L lateral choroid plexus, P-III third choroid plexus, P-IV fourth choroid plexus, TB terminal branch

toward more precise understanding of aminergic and AChE neuronal influence on the choroid plexus as well as the cerebral arterial tree of amphibians.

MATERIALS AND METHODS

Thirty five adult Japanese newts, *Triturus pyrrhogaster*, were used. To clarify the vascular supply of the brain and choroid plexus, five newts were infused through the heart with India ink containing 10% gelatin and placed in ice-cold water. The brain was rapidly removed from the skull and fixed with 10% formalin. Choroid plexuses were then harvested from the lateral, third and fourth ventricles.

Formaldehyde fluorescence and AChE histochemistry

The animals were perfused through the heart with cold Ringer's solution under ethyl ether anesthesia. The brain was removed either immediately, or after perfusion with 4% buffered formaldehyde. The cerebral arterial tree and the choroid plexus were then carefully dissected out from the unfixed or fixed brains. For demonstration of aminergic neurons, the materials obtained from unfixed brains were stretched over nonfluorescent glass slides and transferred to a desiccator to be dried in vacuo over P_2O_5 for 1 h. Air-dried materials were treated with formaldehyde vapor obtained from paraformaldehyde (relative humidity=47%) for 1 h at 80°C [10]. To detect AChE-positive neurons, the arteries and choroid plexuses fixed in formaldehyde for 1 h at 4°C were maintained in Karnovsky's medium without acetylcholine iodide for 30 min at 4°C and then incubated in complete medium containing 2×10^{-4} M tetraisopropyl pyrophosphoramide as an inhibitor of nonspecific cholinesterase activity for 1–5 h at 20°C [18]. The detailed procedures of formaldehyde histofluorescence and AChE staining have been described elsewhere [1].

Microspectrofluorimetry

Microspectrofluorimetric identification of the fluorescent materials induced by formaldehyde gas was carried out using a Nikon SPM-RFL system in accordance with the method of Kojima et al. [19] To differentiate between noradrenaline or adrenaline and two other biogenic amines, dopamine and serotonin, slides were subjected to HCl vapor treatment [3]; the whole-mount preparations on quartz slides were exposed to the vapor of a fresh sample of concentrated HCl solution at room temperature for 1 to 10 min in a closed Petri dish, and then mounted in glycerol under quartz coverslips. All spectra were corrected and expressed as relative quanta versus wavelength.

RESULTS

Angioarchitecture of the cerebral arterial system and choroid plexus

The posterior cerebral artery (PCA) arose from the anterior ramus (AR) to form the anterior circulation of the cerebral arterial tree, together with the middle and anterior cerebral arteries (Fig. 1). On the other hand, the posterior ramus (PR) joined the terminal branches (TB) of the basilar artery (BA) at the midline of the upper part of the medulla oblongata, and formed the posterior circulation. At the level where the right and left PR ran caudally along the

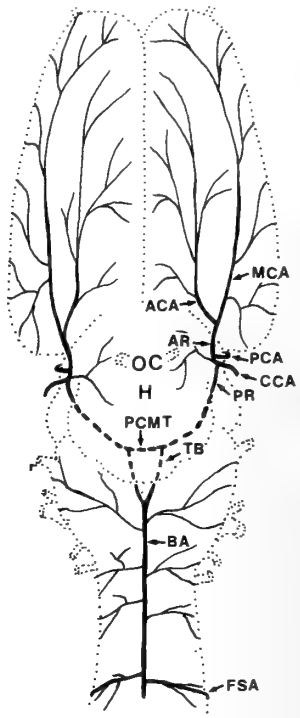

FIG. 1. Diagram of arterial supply to the brain of the newt (ventral view).

caudal portion of the hypophysis, they communicated through the posterior communicating trunk (PCMT). No anterior communicating artery was found between the right and left anterior circulations, so that the circle of Willis was not complete.

The choroid plexuses from the lateral and third ventricles (P-L, P-III) were large in proportion to the brain size, and appeared with a butterfly wing-like profile (Fig. 2). The lateral and third choroidal arteries arising from the PCA ramified over the plexus proper, so that they made up a fine and well-developed capillary network between the ependymal (epithelial) cell layer and stroma. The outermost part of the P-L and P-III were fringed with the venule lining. The choroid plexus from the fourth ventricle (P-IV) was triangular in shape, and was supplied by branches from both the PR and the BA.

Formaldehyde fluorescence

Aminergic innervation

A few thick fluorescent fiber bundles, which entered the cranial cavity along the internal carotid artery (ICA) via the carotid canal, ran longitudinally along the AR or PR toward the anterior or posterior circulations (Fig. 3AB). Such fluorescent fiber bundles were also seen to ascend along the wall of the caudal part of the BA via the first spinal artery (FSA) which corresponds to the vertebral artery in mammals, and to meet with the descending fiber bundles via the ICA around the TA (Fig. 3CD). A small number of thin fibers emanated from fluorescent fiber bundles and were distributed spirally or circularly along the major cerebral arteries of the

FIG. 2. Photomicrograph of the lateral (L) and third (III) choroid plexuses. C: Capillary net. Arrows indicate the venule lining running along the plexus outer margin. ×18.

anterior and posterior circulations with approximately equal density (Table 1). Interestingly, a few nerve cells emitting a strong greenish yellow-fluorescence, which showed a simple multipolar or pseudomultipolar profile, were situated singularly on the walls of the cerebral carotid artery (CCA), the intracranial part of the ICA, and the AR in some individuals (Figs. 3B). Their axons ran parallel to, or spirally toward the major arteries of the anterior circulation. Some of these also descended towards the posterior circulation, and could be followed up to the rostral part of the BA.

The innervation density of aminergic nerves in the choroid plexuses from all the ventricles was significantly higher compared to that observed in the major cerebral arteries (Fig. 4A, Table 1). A few fluorescent fiber bundles on the lateral and third choroidal arteries, which branched out from thick fiber bundles on the PCA via the CCA, spread radially when they entered the corresponding choroid plexuses, and built up a well-defined and dense network of thin varicose fibers over the whole of the microvascular-epithelial region. The nerve supply was much more prominent along the venule loop in the outermost part, in comparison to the capillary net (Fig. 4B). The density of aminergic nerves in the P-IV was approximately the same as that observed in the P-L and P-III. There were no fluorescent nerve cells in any choroid plexuses examined.

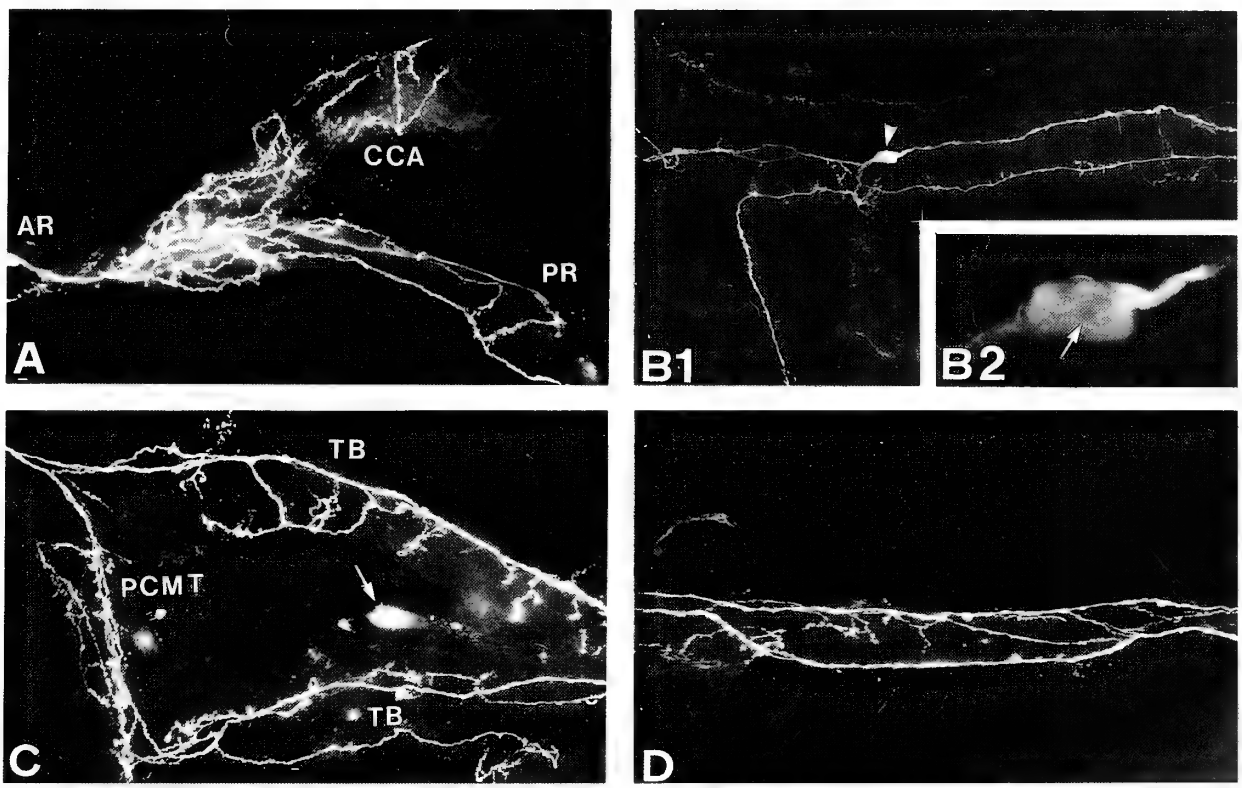

FIG. 3. Fluorescence photomicrographs of whole-mounts showing (nor) adrenergic innervation in the major cerebral arteries. A: Cerebral carotid artery (CCA), and anterior and posterior rami (AR, PR). B: Anterior ramus. Arrowhead indicates single aminergic nerve cell located at the wall of the AR, and arrow indicates its nucleus. C: Posterior communicating trunk (PCMT) and terminal branch (TB). Arrow indicates basophil leucocyte. D: Basilar artery. A, C, D ×165; B1 ×100; B2 ×500.

TABLE 1. Density of NA and AChE nerves in the major cerebral arteries and choroid plexuses of the newt

	Arteries								Choroid plexuses		
	ACA	MCA	PCA	AR	CCA	PR	TB	BA	P-L	P-III	P-IV
NA	+	+	+	+	+	+	+	+	++	++	++
AChE	+	+	+	+	+	+	+−	+−	++	++	+

The relative number of nerve fibers was graded arbitrarily. − absent; + a few fibers; ++ dense fibers.

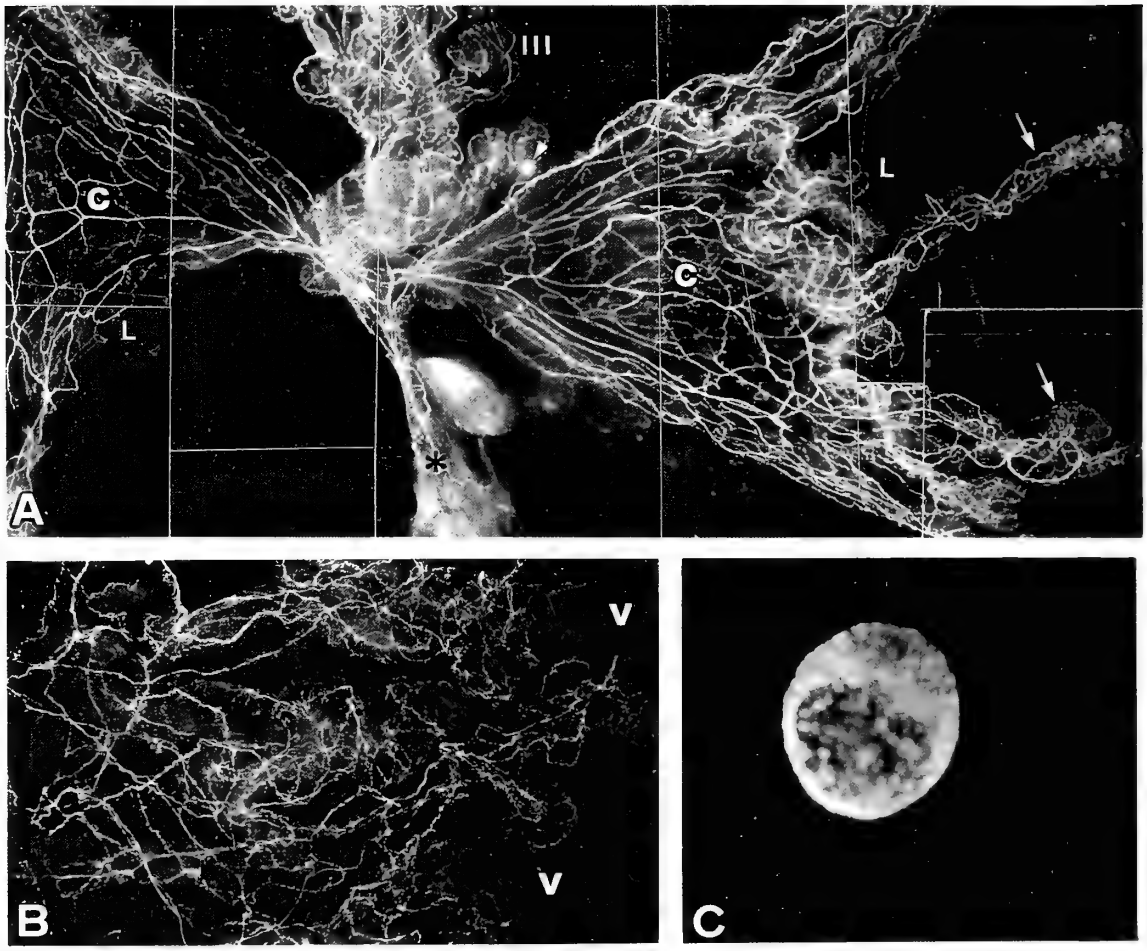

FIG. 4. Fluorescence photomicrographs of whole-mounts showing (nor)adrenergic innervation in the choroid plexuses (A, B), and of a blood smear showing fluorescent basophil leucocytes (C). A: Lateral (L) and third (III) choroid plexuses, capillary net (C). Arrows indicate venule lining, and arrowhead indicates basophil leucocyte. Asterisk indicates choroidal artery arising from the posterior cerebral artery. B: Venule lining of the third choroid plexus and ventricle (v). C: Basophil leucocyte. A ×66; B ×132; C ×500.

Basophil leucocyte

Specific granules filling the cytoplasm of the basophil leucocytes emitted a brilliant greenish yellow-fluorescence after treatment with formaldehyde gas for 1 h (Fig. 4C), but did not show such fluorescence without formaldehyde treatment. A longer irradiation with ultraviolet light, as was also the case with water treatment, resulted in a striking extinction of fluorescence.

Microspectrofluorimetric analysis

The excitation and emission spectra of the greenish-yellow fluorescent ganglion cells and nerves showed large peaks at about 410 and 480 nm, respectively, with a small peak in the excitation spectrum at 330 nm (Fig. 5A). After exposure to HCl vapor for 5 min or more, the maximum peak of the excitation spectrum shifted to 330–340 nm, concomitant with a striking lowering of the peak at 410 nm, while the emission maximum was remained unchanged. During the course of HCl treatment, the fluorescence faded very rapidly. This is a typical pattern characteristic of adrenaline or noradrenaline [3].

The standard excitation spectrum of fluorescent basophil leucocytes showed a large peak at about 415 nm and a small peak at about 330 nm, and the emission spectrum had a broad

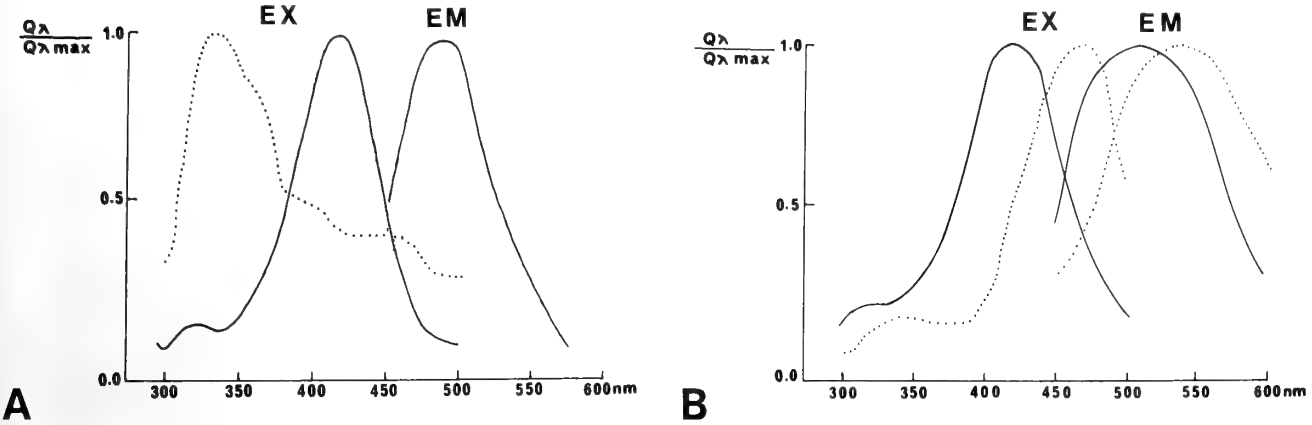

FIG. 5. Excitation (EX) and emission (EM) spectra of fluorescent nerve cells in the walls of the anterior ramus (A) and of fluorescent basophil leucocytes (B). —: after formaldehyde gas treatment only; ---: after formaldehyde gas treatment followed by treatment with HCl vapor for 5 min or more. All spectra were corrected and expressed as relative quanta.

peak ranging from 495 to 515 nm (Fig. 5B). After HCl vapor treatment, the greenish-yellow fluorescence changed into a yellowish color with no detectable level of fading. Both the large and small peaks on the excitation spectrum shifted to about 480 and 350 nm, respectively, and the maximum emission peak also shifted to around 520–540 nm.

AChE staining

A few thick fiber bundles that were stained intensely for AChE reaction were consistently present on the CCA (Fig. 6A), but none were found in the walls of the FSA to BA. AChE fiber bundles on the CCA ran rostrally and caudally towards the anterior and posterior circulations. The density of AChE nerves in the major cerebral arteries appeared to be lower, particularly along the BA, than that of NA nerves (Fig. 6, Table 1), although it was difficult to follow the precise distribution pattern owing to the high level of non-nervous AChE-activity in the vessel walls themselves except for the wall of the CCA.

AChE-positive nerves supplying the P-L and P-III also showed high-level activity of this enzyme, and were apparently rich compared to those supplying the P-IV and the major cerebral arteries. These positive nerves were distributed in a manner similar to NA nerves (Fig. 6D, Table 1): the axons from AChE fiber bundles on the choroidal stem arteries formed a well-developed meshwork of thin fibers over the microvascular-epithelial regions, with a preference for the venule lining in the outermost part, rather than for the capillary-epithelial complex. There were no ganglionic structures positive for AChE in the choroid plexuses from all the ventricles, as well as in the walls of the major cerebral arteries in all parts of the brain.

DISCUSSION

Species differences

The present study documented for the first time the innervation pattern of NA and AChE nerves in the cerebral arterial tree and choroid plexus of the newt. The supply of these two types of cerebral perivascular nerves to the major cerebral arteries of this urodele, which is characterized by a lesser density of AChE nerves, is less rich than those of the Japanese toad and leopard frog [31, 32], but is not as poor as that of the clawed toad [2]. In contrast, the innervation of choroid plexus by NA nerves in the newt is distinctly denser than that observed in the Japanese toad, bullfrog, and leopard frog [31, 32], although it is not as prominent as that of the clawed toad [2]. The P-L and P-III of this urodelan species also have a richer AChE innervation comparable in density to the NA innervation, receiving the most abundant supply of AChE nerves of the various amphibian choroid plexuses investigated to date. The distribution of NA and AChE nerves projecting to the newt choroid plexus, unlike the NA innervation in the Japanese toad and bullfrog, but like that in the clawed toad [2], is predominant in both the microvascular system and epithelium, particularly along the venule loop in the P-L and P-III. Thus, each of the amphibian species investigated has its own characteristic pattern of plexus innervation by NA and AChE nerves that is quite different from the innervation pattern seen in the major cerebral arteries.

Source and pathway of aminergic and AChE innervation

It is well known that sympathetic ganglia typical of higher vertebrates are not present in the cyclostomes, the most primitive vertebrate, but many aminergic (serotonin-containing) nerve cells are scattered over, or clustered along the cardiovascular system [27]. Indeed, the major cerebral arteries of the lamprey, a member Cyclostome species, are innervated by serotonergic nerve cells intrinsic to these vessel walls [15]. In most cases in newts, NA nerves innervating the major cerebral arteries are all of extracranial origin (presumably from cervical sympathetic chain ganglia) as reported in anuran amphibians [2, 31, 32], and pass through the ICA and FSA to reach the cranial cavity. However, we have demonstrated that a few NA nerve cells occur on the

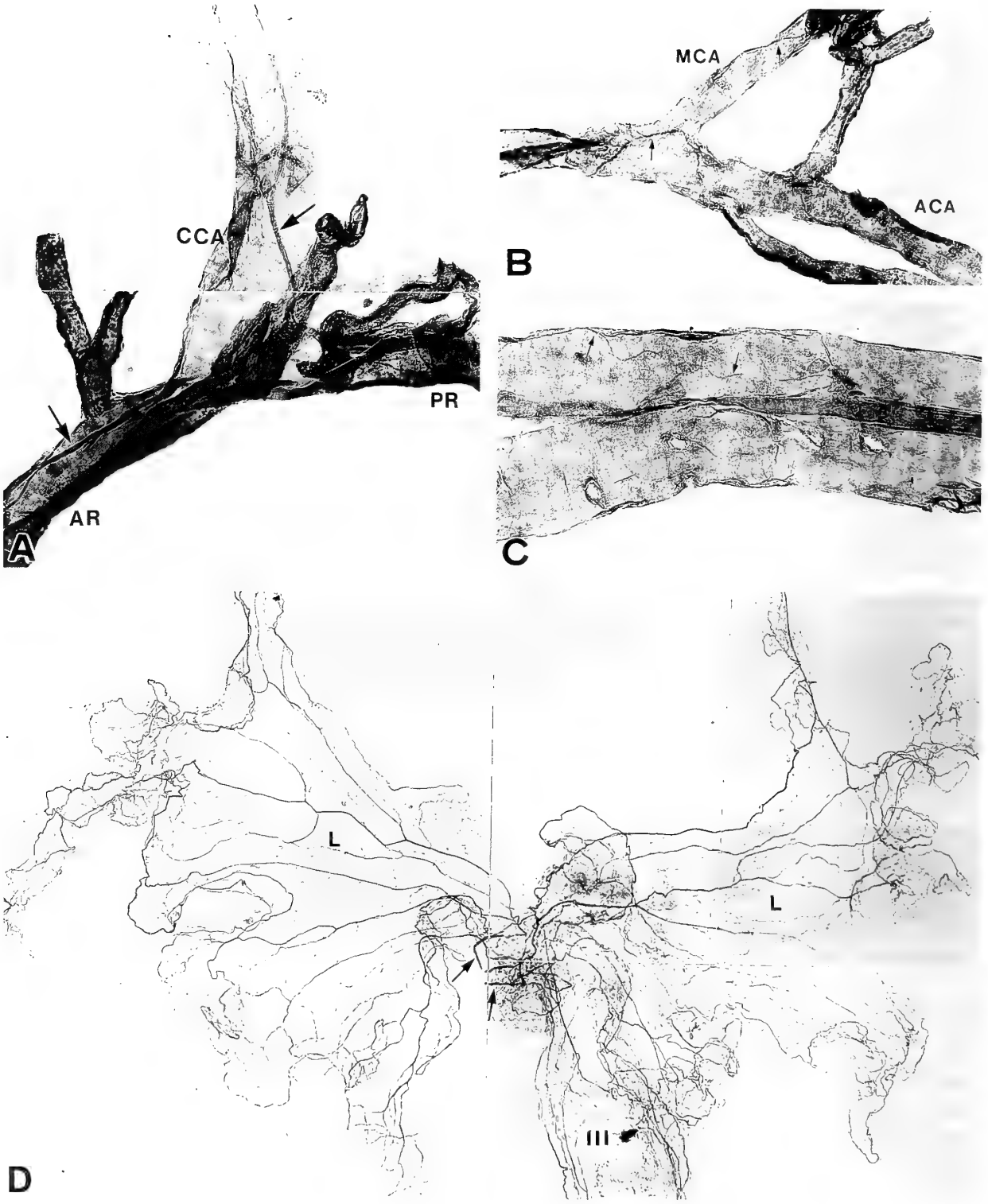

FIG. 6. AChE staining in whole-mounts of the major cerebral arteries (A, B and C) and choroid plexuses (D). A: Cerebral carotid artery (CCA) and anterior and posterior rami (AR, PR). B: Middle and anterior cerebral arteries (MCA, ACA). C: Terminal branch of the basilar artery. Large arrows indicate thick fiber bundles positive for AChE. Small arrows indicate AChE nerve fibers. Note a high non-nervous AChE activity in the walls of the major cerebral arteries. D: Lateral (L) and third (III) choroid plexuses. Arrows indicate AChE fiber bundles on the choroidal stem arteries that extend over the plexus proper. A, B, C ×125; D ×50.

walls of the major cerebral arteries in some individuals, and some of the fluorescent nerves in fact originate there. Such a primitive profile of aminergic innervation that is maintained even now by the newt cerebral circulation emphasizes further the concept of amphibian phylogeny that urodelan amphibians are much more primitive than anurans.

The present study has clearly shown the wide spread of NA axons within fluorescent fiber bundles which run along the choroidal stem arteries via the ICA or FSA over the choroid plexus in the newt. Similar sources and vascular pathways of extracranial NA nerves for plexus innervation have also been noticed in the Japanese toad and bullfrog [2]. However, this pattern cannot be regarded as a common feature of the plexus NA innervation in amphibian, since our previous study revealed that NA nerves within the choroid plexuses of the clawed toad originate in the axons from NA ganglion cells located at the plexus stroma [2]. Furthermore, the possibility that the axons from NA nerve cells intrinsic to the major cerebral arteries may contribute, to some extent, to the plexus innervation cannot be excluded in some newts.

In the newt, AChE fiber bundles, unlike the results of formaldehyde histofluorescence, were found only along the ICA. This finding, in addition to the lack of nerve cells positive for AChE throughout the pial vasculature and choroid plexus, seem to indicate that AChE nerves supplying the cerebral arterial tree of this urodelan species come from the ICA alone, and then extend to the choroid plexus via the corresponding choroidal arteries in a manner preferential for the P-L and P-III. Although it is difficult to make an exact identification between parasympathetic cholinergic neurons and sympathetic or sensory neurons soley by AChE staining, it is generally accepted that high concentrations of AChE are located in parasympathetic cholinergic neurons, and low levels of the enzyme activity are associated with sympathetic or sensory neurons [29]. AChE nerves contributing to the rich innervation of the newt choroid plexus, as well as the fiber bundles present on the ICA, were stained strongly with this enzyme reaction, and thus are probably parasympathetic in nature.

Functional implications

No neurogenic influence on choroid plexus function has been reported for amphibian. However, the two major effects of NA nerves on plexus vascular-epithelial function, inhibition of CSF production by the epithelial cells, and manipulation of active transport between the CSF compartment and blood, have been shown in mammals [5, 7, 11, 22–26]. In addition, AChE nerves have been suggested to exert vasodilatory effects in the cerebral circulation [4]. Therefore, the rich innervation of NA and AChE nerves focused on the microvascular system and epithelium within the choroid plexus in the newt, despite a less rich supply of the two nerve types along its cerebral arterial tree, must be considered in relation to the secretomotor and transport actions essential for the functioning of these plexus elements. Since the critical role of the choroid plexus for the brain nutrition and metabolism via the CSF has been proposed on the basis of the brain structures characteristic of urodelan amphibians including the newt [28, 34, 35], it might deeply participate in the regulation of such plexus functions. In this regard, distinct species differences in the innervation density and regional distribution of NA and AChE nerves in amphibian choroid plexuses may involve species-specific NA and cholinergic mechanisms responsible for CSF production from epithelial cells, and the exchange of oxygen, nutrients and metabolic products between this special vascular-epithelial structure and brain parenchyma.

Basophil leucocytes

The specific granules of basophil leucocytes of the newt, which comprise about 48% of total leucocytes [16] and contain only a trace amount of histamine [33], emitted brilliant greenish-yellow fluorescence after exposure to formaldehyde gas. The standard excitation (EX) and emission (EM) spectra of these fluorescent granules were different from those of the formaldehyde gas-induced fluorescence in the turtle basophil leucocytes (EX/EM max: 470/495 nm) [14] and in the histamine (EX/EM max: 380/450 nm) [36]. The findings presented here suggests that the specific granules in the newt basophil leucocytes mainly consist of serotonin and/or catecholamines (dopamine, noradrenaline, adrenaline), considering the remarkably high fading rate of fluorescence after water treatment and irradiation with ultraviolet light. However, the shifting pattern of EX and EM spectra after HCl vapor treatment, which did not coincide with those of serotonin (EX/EM max: 390/530 nm), dopamine (EX/EM max: 320 and 365/490 nm), or (nor) adrenaline (EX/EM max: 320/490) [3, 30], leads to the speculation that the newt basophil leucocytes also contain substantial amounts of fluorescent components other than these biogenic amines. Further biochemical research must be carried out before any firm conclusion can be made on this matter.

ACKNOWLEDGMENTS

This work was supported by a grant from Kyushu Sangyo University in Japan. We are grateful to Prof. T. Shiraishi, Zoological Laboratory, Faculty of Agriculture, Kyushu University, Dr. H. Hayashi, University of Occupational and Environmental Health, and Dr. H. Hasegawa, School of Medicine, University of the Ryukyu, for their encouragement and advice.

REFERENCES

1 Andō K (1981) A histochemical study on the innervation of the cerebral blood vessels in bats. Cell Tissue Res 217: 55–64

2 Andō K, Tagawa T, Ishikawa A, Takamura H, Yasuzumi, F (1986) A comparative study of the innervation of the choroid plexus in amphibia. Experientia 42: 394–398

3 Björklund A, Ehinger B, Falck B (1968) A method for differentiating dopamine from noradrenaline in tissue sections by microspectrofluorometry. J Histochem Cytochem 16: 263–270

4 Duckles SP (1986) Cholinergic innervation of cerebral arteries.

In "Neural regulation of brain circulation" Ed by C Owman and J E Hardebo, Elsevier, Amsterdam, pp 235–243

5 Edvinsson L, Håkanson R, Lindvall M, Owman C, Svensson K-G (1975) Ultrastructural and biochemical evidence for a sympathetic neural influence on the choroid plexus. Exp Neuro 48: 241–251

6 Edvinsson L, Nielsen K, Owman C (1973) Cholinergic innervation choroid plexus in rabbits and cats. Brain Res 63: 500–503

7 Edvinsson L, Nielsen K, Owman C (1973) Sympathetic nervous influence on the blood circulation and carbonic anhydrase activity in the choroid plexus. Stroke 4: 368

8 Edvinnson L, Nielsen KC, Owman C, West KA (1974) Adrenergic innervation of the mammalian choroid plexus. Am J Anat 139: 299–308

9 Edvinsson L, Owman C, Rosengren E, West KA (1972) Concentration of noradrenaline in pial vessels, choroid plexus, and iris during two weeks after sympathetic ganglionectomy or decentralization. Acta physiol Scand 85: 201–206

10 Falck B (1962) Observation on the possibility of the cellular localization of monoamines by a fluorescence method. Acta Physiol Scand 56 (Suppl): 1–25

11 Haywood JR, Vogh BP (1979) Some measurements of autonomic nervous system influence on production of cerebrospinal fluid in the cat. J Pharmacol Exp Ther 208: 341–346

12 Heisey SR (1968) Brain and choroid plexus blood volumes in vertebrates. Comp Biochem Physiol 26: 486–498

13 Hinton WA (1953) The choroid plexus of the lateral and third ventricles of tailed amphibia. J Comp Neurol 99: 545–559

14 Iijima T (1977) A histochemical study of the innervation of cerebral blood vessels in the turtle. J Comp Neurol 176: 307–314

15 Iijima T, Wasano T (1980) A histochemical and ultrastrucural study of serotonin-containing nerves in cerebral blood vessels of the lamprey. Anat Rec 198: 671–680

16 Ishizuka H, Inokawa J, Taguchi T, Igarashi, H (1975) Granulopoiesis in the newt. J Med Soc Toho Japan 22: 65–77

17 Isomura H (1959) Studies on the angioarchitecture of the brain in the urodela. Fukuoka Acta Medica 50: 3185–3200

18 Karnovsky MJ, Roots L (1964) A direct coloring thiocholine method for cholinesterase. J Histochem Cytochem 12: 219–221

19 Kojima H, Kuwahara M, Anraku S, Onogi K, Ito R (1978) Fluorescence histochemical and chemical analyses of catecholamines in bullfrog adrenals. Acta Histochem Cytochem 10: 350–357

20 Lindvall M (1979) Fluorescence histochemical study on regional differences in the sympathetic nerve supply of the choroid plexus from various laboratory animals. Cell Tissue Res 198: 261–267

21 Lindvall M, Edvinsson L, Owman C (1977) Histochemical study on regional differences in the cholinergic nerve supply of the choroid plexus from various laboratory animals. Exp Neurol 55: 152–159

22 Lindvall M, Edvinsson L, Owman C (1978) Sympathetic nervous control of cerebrospinal fluid production from the choroid plexus. Science 201: 176–178

23 Lindvall M, Edvinsson L, Owman C (1979) Effect of sympathomimetic drugs and corresponding receptor antagonists on the rate of cerebrospinal fluid production. Exp Neurol 64: 132–145

24 Lindvall M, Owman C (1981) Autonomic nerves in the mammalian choroid plexus and their influence on the formation of cerebrospinal fluid. J Cereb Blood flow Metab 1: 245–266

25 Lindvall M, Owman C, Winbladh B (1981) Sympathetic influence on transport function in the choroid plexus of rabbit and rat. Brain Res 223: 160–164

26 Lindvall M, Owman C, Winbladh B (1982) Sympathetic influence on sodium-potassium activated adenosine triphosphatase activity of rabbit and rat choroid plexus. Brain Res Bull 9: 761–763

27 Nilsson S (1983) Autonomic nerve function in the vertebrates. Springer-Verlag, New York

28 Nilsson C, Lindvall-Axelsson M, Owman C (1992) Neuroendocrine regulatory mechanisms in the choroid plexus-cerebrospinal fluid system. Brain Research Reviews 17: 109–138

29 Owman C, Edvinsson L, Nielsen KC (1974). Autonomic neuoreceptor mechanisms in brain vessels. Blood Vessels 11: 2–31.

30 Prasada Rao PD, Hartwig HG (1974) Monoaminergic tracts of the diencephalon and innervation of the pars intermedia in *Rana temporaria*. A fluorescence and microspectrofluorimetric study. Cell Tissue Res 151: 1–26

31 Tagawa T, Andō K, Wasano T, Iijima T (1979) A histochemical study on the innervation of cerebral blood vessels in the bullfrog. J Comp Neurol 183: 25–32

32 Tagawa T, Ishikawa A, Su WC, Okamoto K (1989) Autonomic innervation of intra- and extra-cranial arteries in the Am phibia. Zool Sci 6: 233–239

33 Takaya K (1969) The relationship between mast cells and histamine in phylogeny with special reference to reptiles and birds. Arch histol Jap 30: 401–402

34 Tsuneki K, Ouji M (1988) Absence of vessels in the brain of six species of primitive salamanders. Zool Sci 5: 847–853

35 Tsuneki K, Ouji M, Akiyoshi H, Ichikawa, K (1986) Absence of blood vessels in the brain parenchyma of hynobiid salamanders. Experientia 41: 1400–1402

36 Van Orden III, L S (1970) Quantitative histochemistry of biogenic amines. A simple microspectrofluorometer. Biochem Pharmacol., 19: 1105–1117

37 Wasano T (1979) Innervation of the cerebral blood vessels of vertebrates. Acta Anat Nippon 54: 65–84

ZOOLOGICAL SCIENCE 11: 753–757 (1994)

Estimation of Phylogenetic Relationships among Japanese Brown Frogs from Mitochondrial Cytochrome b Gene (Amphibia: Anura)

TOMOKO TANAKA[1], MASAFUMI MATSUI[1] and OSAMU TAKENAKA[2]

[1]*Graduate School of Human and Environmental Studies, Kyoto University, Kyoto 606-01 and* [2]*Primate Research Institute, Kyoto University, Inuyama, Aichi 484, Japan*

ABSTRACT—We investigated phylogenetic relationships among five species of Japanese brown frogs by the analysis of nucleotide sequences in the cytochrome b gene of mitochondrial DNA (mtDNA). The sequence of the 251-base pairs, which cover approximately 22% of the cytochrome b gene, was determined by PCR-Direct sequencing method. Phylogenetic relationships were analyzed by UPGMA, neighbor-joining, maximum-likelihood, and maximum parsimony analyses. The sequences only slightly varied within one population of *Rana japonica*. Intraspecific variation in sequences varied among species, and *R. tagoi* showed more pronounced variation than did *R. ornativentris*. *Rana japonica* and *R. tagoi* share 2n=26 chromosomes with each other, but the former was closer to *R. pirica* and *R. ornativentris*, both with 2n=24, than to the latter. Phylogenetic relationships estimated from the nucleotide sequence of the cytochrome b gene generally conformed to the idea hitherto proposed chiefly on the bases of morphological and ecological evidences.

INTRODUCTION

Recently, DNA sequences have often been used to infer phylogenetic relationships among various animal groups [11]. Moreover, PCR (Polymerase Chain Reaction: [19]) enables us easily to obtain many DNA fragments for determination of the nucleotide sequences.

In evolutionary studies, mitochondrial DNA (mtDNA) is more often used than nucleic DNA. This is because mutation occurs at much higher rates in mtDNA than in nucleic DNA. Such a rapid rate of change in mtDNA is effective in investigating evolutionary relationships among population of a species and/or among closely related species [4, 13]. In addition, mtDNA is simple, because of its maternal inheritance [25], and is suitably used as a molecular clock by which we can determine the time elapsed since each divergence point in the phylogenetic tree [25]. Nucleotide sequences in cytochrome b gene of mtDNA have recently been successfully employed to estimate phylogenetic relationships of various animals representing a wide range of divergence time [2, 3, 8, 12].

The genus *Rana* contains approximately 300 species [7], and 19 species of this genus occur in Japan. Among them, brown frogs of the *Rana temporaria* group, consist a rather large group, including eight species: *R. japonica, R. tsushimensis, R. okinavana, R. tagoi, R. sakuraii, R. pirica, R. ornativentris*, and *R. dybowskii* [16]. Although these frogs can be grouped into two types by the number of diploid chromosomes (2n=24 or 26), they all are quite similar in morphology, and it is hard to infer their phylogenetic relationships [17].

Accepted May 31, 1994
Received September 12, 1994

We investigated a phylogenetic relationship of Japanese brown frogs from nucleotide sequences in the cytochrome b gene in mtDNA by the following approaches: 1) Analysis of polymorphism within one population of *R. japonica*; 2) Analysis of the geographic distribution of polymorphisms in *R. tagoi* and *R. ornativentris*; 3) Estimation of phylogenetic relationships among five species of brown frogs using several methods that have different assumptions.

MATERIALS AND METHODS

DNA sources

We examined a total of 36 frogs as shown in Appendix. *R. tagoi* from Kyoto contains two sympatric populations that differ in the body size (Large type and Small type: [26]). *Rana catesbeiana* was used as an outgroup taxon from morphological studies made by Dubois [5].

Liver, muscle, heart and egg were immediately removed from sacrificed individuals under deep anesthesia with acetone chloroform and stored at −80°C. Frozen tissue samples (10 mg-100 mg) were homogenized at 4°C using a homogenizer in 1.5 ml of a solution containing 0.25 M sucrose, 0.01 M Tris-HCl , and 1 mM EDTA, pH 7.4–7.6. The homogenate was centrifuged at 600×g for 2 min at 4°C. The aqueous phase was transferred to a new tube and centrifuged at 5500×g for 20 min at 4°C. The pellet was suspended in STE (10 mM Tris/Cl pH 8.0, 100 mM NaCl, 1 mM EDTA pH 8.0). Mitochondrial fraction was lysed by the addition of 1% sodium dodecyl sulfate. Proteins were digested with proteinase K (0.1 mg/ml) for 3 hr at 52°C. The solution was treated with phenol and chloroform/isoamyl alcohol and DNA was precipitated with ethanol. DNA precipitates were dried and dissolved in 1ml of TE (10 mM Tris/HCl, 1mM EDTA, pH 8.0) and 50 μl was subjected to PCR amplification.

Amplification and sequencing of mitochondrial cytochrome b gene

Mitochondrial sequences containing cytochrome b gene were

amplified by PCR. Primers for amplification and sequencing were designed according to the method of Kocher et al. [15] on the basis of conserved areas of nucleotide sequences of humans [1] and *Xenopus laevis* [21]. Primers were synthesized using a ABI/381A DNA synthesizer. Sequences of primers were L14850 (5′-TCTCCGCATGATGAAACTTCGGCTC-3′) and H15168 (5′-AAGTTTGTAATTACTGTGGCCCCTC-3′). The numbering system followed that of the human sequence [1]. DNA segment was purified by TaKaRa/EASYTRAP™ Ver.2 Kit after electrophoresis in a 4% NuSieve GTG (FMC BioProducts) agarose gel. Sanger dideoxy reaction [23] was carried out using Pharmacia/Cycle Sequencing Kit and two primers, L14850 and H15150 (5′-TCAGAATGATATTTGGCCTC-3), respectively.

Data Analysis

Genetic relationships among taxa were estimated based on the pairwise matrix of distance calculated by Kimura's 2-parameter model [14]. When a taxon included several haplotypes, we considered the one which appeared most frequently as a representative haplotype for the taxon. UPGMA algorithm [24] and a neighbor-joining method [22], using the program included with PHYLIP [6], were applied to the data set. In the latter analysis, we located a root at the midpoint of the longest path. Using the branch-and bound algorithm in version 3.5C of PHYLIP [6], we bootstrapped the data set 1,000 times to obtain a consensus tree.

In addition to above phenetic analyses, a continuous maximum-likelihood (CONTML) analysis was made using the program included with version 3.5C of PHYLIP [6].

The sequence data were also subjected to a cladistic parsimony analysis using version 3.0 of PAUP [28], and the branch-and-bound algorithm to find the shortest trees. We again bootstrapped the data set 1,000 times, using the branch-and-bound algorithm, to obtain approximate confidence on the tree.

In the analyses of neighbor-joining, maximum-likelihood, and maximum parsimony, a transition-to-transversion ratio was assumed to be 2.0.

RESULTS

Intraspecific differences

We could determine the nucleotide sequence of 251 bp in the Japanese brown frogs' cytochrome b gene. The nucleotide sequence within one population of *R. japonica* from Tateyama, Chiba showed three different haplotypes (type 1–3). The type 1, 2, and 3 appeared in seven (58.3%), three (25%), and two samples (16.7%), respectively. These three types differed from each other by 2 bp, and therefore, similarities between them were invariably 99.2%.

The nucleotide sequences of two samples from a Large type population of *R. tagoi* from Kyoto showed a difference in 2 bp. The similarity between them was 99.2%, which value was identical to those obtained among different haplotypes within one population of *R. japonica*. Differences in nucleotide sequences among six populations of *R. tagoi* collected from five different localities of Tohoku to Kyusyu were 8–17 bp. Similarities among these populations ranged from 93.2–96.8%, which were smaller than the similarity found within a population. The pattern of variation among populations was very complex, and a simple geographic cline was not observed. For instance, the sample of the Large type population from Kyoto was quite dissimilar in the sequence to that of the sympatric Small type population. On the other hand, this Small type was similar in sequences to specimens from Aomori or Kochi, both are fairly remote from Kyoto geographically.

The two samples of *R. ornativentris* from Toyama differed in 2 bp, with the similarity value of 99.2%, which was equal again to the similarity found within a population of *R. japonica* or *R. tagoi*. Differences in nucleotide sequences among five populations of *R. ornativentris* from Tohoku to Kyusyu regions were 2–10 bp, and similarities ranged from 99.2 to 96.0%. These values were larger than those found among populations of *R. tagoi*. The five populations could be roughly divided into northeastern (Aomori and Toyama) and southwestern (Hyogo, Kochi and Oita) groups by the degree of similarities in sequences.

Interspecific differences

Within the five brown frogs' cytochrome b sequences,

FIG. 1. Aligned sequences of a 251-bp segment of the cytochrome b gene from five brown frogs and *R. catesbeiana* as an outgroup. Dots indicate identity to the sequence of *R. japonica*.

TABLE 1. Pairwise comparisons of cytochrome b sequences among five Japanese brown frog species and one outgroup taxon *Rana catesbeiana*. The percentage sequence differences are shown in the above diagonal, and the distance obtained by Kimura's 2-parameter model [14] are shown below.

	1	2	3	4	5	6
1. *R japonica*	—	88.8	86.9	88.0	86.9	83.7
2. *R. ornativentris*	0.1158	—	88.4	88.0	85.3	83.7
3. *R. pirica*	0.1397	0.1149	—	86.5	85.3	83.3
4. *R. t. tagoi*	0.1303	0.1247	0.1440	—	97.2	85.3
5. *R. sakuraii*	0.1444	0.1573	0.1583	0.0283	—	85.3
6. *R. catesbeiana*	0.1851	0.1796	0.1857	0.1640	0.1640	—

251 bp, (Table 1), all of 57 substitutions occurred at first and third positions of codons. On the other hand, there were no replacements at second positions. The number of nucleotide substitution at first and third position of codons were 2, 55, respectively. Both of them at first position of codon were transitions (i. e. the interchange of pyrimidines, C⇔T ,or purines, A⇔G). Transition occurred approximately five times as frequently as transversion (i. e. a change from a purine to a pyrimidine or vice versa) at third position of codon. Although most of nucleotide replacement were silent mutations, amino acid replacement occurred only in the sequence of *R. japonica*. The amino acid residue changed from phenylalanin to Leucine.

Figure 2A shows the tree obtained from the pairwise matrix of genetic distance (Table 1) with UPGMA method.

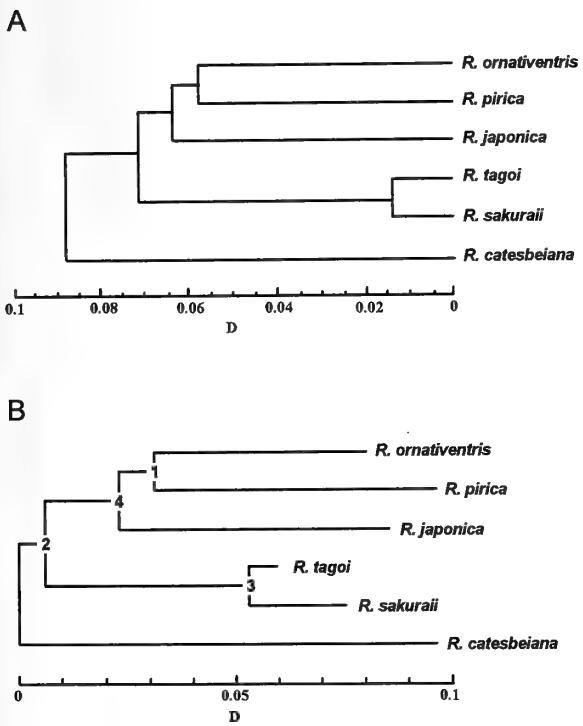

FIG. 2. A UPGMA phenogram (A) and a neighbor-joining tree (B) constructed from a distance matrix obtained from nucleotide sequences by the Kimura "2-parameter" model. The latter tree was rooted at the midpoint of the longest path. Numbers on the nodes in B correspond to those shown in Table 2.

In this tree, the outgroup species, *R. catesbeiana*, is clearly separated from the ingroup five species of brown frogs. In the ingroup, *R. tagoi* and *R. sakuraii* constitute a cluster and split from another cluster of all the remaining species. In the latter cluster, *R. pirica* and *R. ornativentris* formed a subcluster, and split from another subcluster of *R. japonica*. The tree constructed by the neighbor-joining method (Fig. 2B) showed a topology identical to the UPGMA tree. The ingroup relationships of brown frogs were supported in 805/1,000 bootstrap iterations. Within the ingroup, the sister relationship of *R. tagoi* and *R. sakuraii* was nearly completely supported (998/1,000 bootstrap iterations), while the sister relationship of *R. ornativentris* and *R. pirica* was supported in only 512/1,000 iterations. The relation of the latter two species with *R. japonica* was more strongly supported (770/1,000 iterations).

The maximum-likelihood analysis, using *R. catesbeiana* as an outgroup, produced a result identical to that obtained by the two analyses discribed above, although the tree contained a collapsing branch in which the 95% confidence interval includes zero (Table 2).

In the parsimony analysis, only one shortest tree, with a minimum of 94 steps and a consistency index of 0.707 (excluding uninformative characters) was produced. The topology of this tree slightly differed from that found in the above analyses. The sister relationship of *R. pirica* and *R.*

TABLE 2. Branch lengths and their approximate confidence intervals obtained in the maximum likelihood analysis for Japanese brown frogs, with an outgroup taxon *R. catesbeiana*. Nodes are those shown in Fig. 2B

Branch between nodes		Branch length	Approximate confidence interval
R. catesbeiana	2	0.11775	0.07052, 0.16629
2	3	0.04541	0.01373, 0.07739
3	*R. tagoi*	0.00398	0.00000, 0.01354
3	*R. sakuraii*	0.02441	0.00428, 0.04553
2	4	0.02908	0.00123, 0.05717
4	*R. japonica*	0.06004	0.02492, 0.09540
4	1	0.02592	0.00210, 0.04993
1	*R ornativentris*	0.04886	0.01681, 0.08121
1	*R. pirica*	0.06706	0.03043, 0.10369

ornativentris was less strongly supported (338/1,000 bootstrap iterations) than that of *R. japonica* and *R. ornativentris* (569/1,000 iterations).

DISCUSSION

The four nucleotide replacements found in a population of *R. japonica* from Tateyama, Chiba were transitions, all of which being silent substitutions in the third position of codons. It is well-known that transitions occur more frequently than transversions. The variation in sequences within a population of *R. japonica* from Tateyama, Chiba, was very low, and suggested that only a few samples may represent features of the sequence specific to a population or a taxon. This assumption was supported by low haplotype variations within population exhibited by *R. tagoi* from Kyoto (a population of the large type) and *R. ornativentris* from Oyama, Toyama.

There were great differences in nucleotide sequences between the large and the small type of *R. tagoi* from Kyoto, and the degree of difference (similarity=94.6%) roughly equaled to those found among populations that are geographically remote (e. g., 94.4% between populations from Aomori and Miyazaki). This genetic divergence was concordant with differentiations found in morphology and ecology of the two types [26, 27]. Previous studies on isozymes and blood proteins in several populations of *R. tagoi* from west Japan suggested that genetic differentiation has proceeded well within this species [20]. Differentiation of nucleotide sequences also seemed to have progressed well in this species. In order to clarify further genetic differentiation in this species, we must investigate larger number of populations in detail. On the other hand, differences in nucleotide sequences among populations of *R. ornativentris* were lower than in *R. tagoi*. This may indicate that the genetic divergence occurred more recently in this species than in *R. tagoi*.

Like most other ranid frogs, *R. tagoi, R. sakuraii*, and *R. japonica*, have diploid chromosomes of 2n=26 [9]. However, in none of the trees constructed by varying methods, *R. japonica* constituted a cluster with the remaining two species. Instead, *R. japonica* was clustered with the subcluster of *R. pirica* and *R. ornativentris* both with 2n=24 chromosomes. Green and Borkin [10] reported similarly remote phylogenetic relationships of *R. tagoi* and *R. japonica* through the analysis of isozymes. These results suggest an early divergence of *R. tagoi*, and probably of *R. sakuraii*, from the other brown frogs, and this is in agreement with a high degree of specialization of these two species in reproductive strategies, i. e., breeding in underground, small streams (*R. tagoi*) or under the stones of montane streams (*R. sakuraii*) unlike others that breed in open, still water [18].

Unlike the above three species, *R. pirica* and *R. ornativentris* have 2n=24 chromosomes, and have been regarded as closely related with each other from isozyme, acoustic, and morphological evidences [17]. These two species formed a group in UPGMA, neighbor-joining, and maximum-likelihood trees, but their sister relationship was not always strongly supported as shown by a low value of bootstrap iterations (512/1,000) in the consensus tree obtained by the neighbor-joining method. Further, in the parsimony analysis, *R. ornativentris* formed a group not with *R. pirica*, but with *R. japonica*, although the topology of the tree was not strongly supported (569/1,000 bootstrap iterations). This finding suggests equally remote relationships of *R. pirica* and *R. japonica* to *R. ornativentris*, that have never been pointed out before. Further studies of these species from various approaches will reveal the validity of the present findings.

This study suggested that differences in nucleotide sequences would increase in the order of within a population, among populations, and among species. Generally, nucleotide sequences of cytochrome b gene are regarded as good indicators for evaluating intraspecific and/or interspecific variation of brown frogs. Determinations and comparisons of nucleotide sequences of longer areas would clarify divergence times in Japanese brown frogs, in addition to intraspecific and/or interspecific phylogenies.

ACKNOWLEDGMENTS

We received help in the acquisition of tissue samples from T. Tanabe, Y. Misawa, T. Sugahara and K. Kasugai. T. Hikida helped in the statistic analyses. Part of the study was supported by the National Geographic Society (No. 4505–91) to M. Matsui.

REFERENCES

1 Anderson S, Bankier AT, Barrell BG, de Bruijin MHL, Coulson AR, Drouin J, Eperon IC, Nierlich DP, Roe BA, Sanger F, Schreier PH, Smith AJH, Staden R, Young IG (1981) Sequence and organization of the human mitochondrial genome. Nature 290: 457–465

2 Arnason U, Gullberg A (1994) Relationship of baleen whales established by cytochrome b gene sequence comparison. Nature 367: 726–728

3 Bowen BW, Nelson WS, Avise JC (1993) A molecular phylogeny for marine turtles: Trait mapping, rate assessment, and conservation relevance. Proc Natl Acad Sci USA 90: 5574–5577

4 Brown WM, George MJ, Wilson AC (1979) Rapid evolution of animal mitochondrial DNA. Proc Natl Acad Sci USA 76: 1967–1971

5 Dubois A (1992) Notes sur la classification des Ranidae (Amphibians Anoures). Bull Mens Soc Linn Lyon 61: 350–352

6 Felsenstein J (1993) PHYLIP (phylogeny inference package) Version 3.5c. Distributed by the author. Dept Genet Univ Washington, Seattle.

7 Frost DR (1985) Amphibian Species of the World: A Taxonomic and Geographical Reference. Allen Press, Lawrence, Kansas, i. v. pp, 732

8 Graybeal A (1993) The phylogenetic utility of cytochrome b: Lessons from bufonid frogs. Mol Phylogenet Evol 2:256–269

9 Green DM (1983) Evidence for chromosome number reduction and chromosomal homosequenciality in the 24chromosome Korean frog *Rana dybowskii* and related species. Chromosoma 88: 222–226

10 Green DM, Borkin LJ (1993) Evolutionary relationships of eastern Palearctic brown frogs, genus *Rana*: Paraphyly of the

24-chromosome species group and the significance of chromosome number change. Zool J Linn Soc 109: 1–25

11 Hillis DM, Moritz C (1990) Molecular Systematics. Sinauer Associates, Inc., Sunderland, Massachusetts.

12 Irwin DM, Kocher TD, Wilson AC (1991) Evolution of the cytochrome b gene of mammals. J Mol Evol 32: 128–144

13 Kessler LG, Avise JC (1984) Systematic relationships among waterfowl (Anatidae) inferred from restriction endonuclease analysis of mitochondrial DNA. Syst Zool 33: 370–380

14 Kimura M (1980) A simple method for estimating evolutionary rates of base substitutions through comparative studies of nucleotide sequences. J Mol Evol 16: 111–120

15 Kocher TD, Thomas WK, Meyer A, Edwards SV, Pääbo S, Villablanca FX, Wilson AC (1989) Dynamics of mitochondrial DNA evolution in animals: Amplification and sequencing with conserved primer. Proc Natl Acad Sci USA 86: 6196–6200

16 Maeda N, Matsui M (1993) Frogs and Toads of Japan, 3rd edition. Bun-ichi Sogo Shuppan, pp 207

17 Matsui M (1991) Original description of the brown frog from Hokkaido, Japan (Genus *Rana*). Jpn J Herpetol 14: 63–78

18 Matsui T, Matsui M (1990) A new brown frog (genus *Rana*) from Honshu, Japan. Herpetologica 46: 78–85

19 Mullis KB, Faloona FA (1987) Specific synthesis of DNA in vitro via a polymerase catalyzed chain reaction. Methods Enzymol 155:335–350

20 Nishioka M, Ohta S, Sumida M (1987) Intraspecific differentiation of *Rana tagoi* elucidated by electrophoretic analyses of enzymes and blood proteins. Sci Rep Lab Amphibian Biol Hiroshima Univ 9: 97–133

21 Roe BA, Ma D, Wilson RK, Wong JF-H (1985) The complete nucleotide sequence of the *Xenopus laevis* mitochondrial genome. J Biol Chem 260: 9759–9774

22 Saitou N, Nei M (1987) The neighbor-joining method: A new method for reconstructing phylogenetic trees. Mol Biol Evol 4: 406–425

23 Sanger F, Nicklen S, Coulson AR (1977) DNA sequencing with chain-terminating inhibitors. Proc Natl Acad Sci USA 74: 5463–5467

24 Sneath PHA, Sokal RR (1973) Numerical Taxonomy. W H Freemen, San Francisco

25 Stringer CB (1990) The Emergence of Modern Humans. Scientific American 263: 68–74

26 Sugahara T (1990) Reproductive ecology of *Rana tagoi tagoi* at Kitayama in Kyoto. Jpn J Herpetol 13: 145

27 Sugahara T, Matsui M (1993) Morphometric comparisons in two types of *Rana tagoi tagoi* from Kumogahata, Kyoto. Jpn J Herpetol 15: 83

28 Swofford DL (1990) Users Manual for PAUP Version 3.0: Phylogenetic analysis using parsimony. Illinois Natural History Survey, Champaign, Illinois.

APPENDIX
SPECIMENS EXAMINED

A total of 36 frogs are stored at the Graduate School of Human and Environmental Studies, Kyoto University and in T. Sugahara private collection.

Rana japonica (n=12): Tateyama-shi, Chiba (n=12).
Rana tagoi (n=7): Towadako-machi, Aomori (n=1); Hayakawa-cho, Yamanashi (n=1); Kyoto-shi, Kyoto (Kyoto-L=Large type of Sugahara [26]) (n=2); Kyoto-shi, Kyoto (Kyoto-S=Small type of Sugahara [26]) (n=1); Tosayama-mura, Kochi (n=1); Gokase-cho, Miyazaki (n=1).
Rana sakuraii (n=4): Okutama-machi, Tokyo (n=2); Kiyokawa-mura, Kanagawa (n=1); Miyama-cho, Kyoto (n=1).
Rana pirica (n=3): Obihiro-shi, Hokkaido (n=1); Sapporo-shi, Hokkaido (n=2).
Rana ornativentris (n=6): Towadako-machi, Aomori (n=1); Oyama-machi, Toyama (n=2); Sasayama-cho, Hyogo (n=1); Tosayama-mura, Kochi (n=1); Bungotakada-shi, Oita (n=1).
Rana catesbeiana (n=4): Inuyama-shi, Aichi (n=2); Bungotakada-shi, Oita (n=2).

ZOOLOGICAL SCIENCE 11: 759–762 (1994)

[RAPID COMMUNICATION]

Differences in Flicker Fusion Frequencies of the Five Spectral Photoreceptor Types in the Swallowtail Butterfly's Compound Eye

TAKANAO NAKAGAWA and EISUKE EGUCHI[1]

Department of Biology, Yokohama City University, 22-2 Seto, Kanazawa-ku, Yokohama 236, Japan

ABSTRACT—Intracellular recordings were used to measure flicker fusion frequencies (FFF's) as a function of light intensity (I) in the five types of spectral receptors (UV, violet, blue, green and red) in the compound eye of the butterfly, *Papilio xuthus*. FFF's in all receptor types increase with light intensities when stimulus I's are less than I_{50} (the I that generates 50% of the maximum response amplitude, Vmax, in the V-log I curve). FFF's in all receptor types are maximum at I's between approximately $I_{50}+0.5$ and $I_{50}+1$ log unit. At stronger I's FFF's of blue and green receptors decrease gradually but remain above 80% of the maximum FFF's. But UV, violet and red receptors maintain nearly maximal FFF's at I's above I_{50}. Maximum FFF's of green (107 Hz) and the blue (103 Hz) receptors are significantly higher than those of UV (90 Hz) and violet (82 Hz) receptors.

INTRODUCTION

Flicker fusion frequency (FFF) is a common measure of temporal resolution in vision. It marks the critical frequency at which discrete individual responses to or perception of a flickering light just become fused into a continuous response or perception.

Interspecific differences in temporal resolution of photoreceptors have been reported in Hymenopteran insects [8] and in Dipteran insects [6]. Do photoreceptors of different spectral sensitivities in a single retina have different temporal resolutions? In *Drosophila*, FFF's of peripheral retinula cells (R1-6) are about three times higher than those of central retinula cells (R7, 8). In these experiments, the eyes were selectively adapted with monochromatic light, and the responses were recorded by ERG method which are partially integrated retinal responses [4]. Yet the details of how primary visual processes determine different FFF's in the various types of spectral receptor cells are not known. The butterfly is an insect with compound eyes which cover an unusual wide spectral range [1] and therefore this insect is particularly suitable to investigate this problem. Here we report the first case about comparison of the temporal resolution of the different spectral classes of photoreceptor cells using definitive intracellular techniques.

In the compound eye of the swallowtail butterfly, *Papilio xuthus*, five spectral types of photoreceptors were identified by intracellular recordings. They have respective peak sensitivities around 360 nm (UV), 400 nm (violet), 460 nm (blue), 520 nm (green) and 600 nm (red) [1]. In the present study, electrical responses to flickering light were measured by intracellular recordings from the five photoreceptor types. The FFF's of each type were determined as a function of I.

MATERIALS AND METHODS

Animals, eye preparation, light stimuli and intracellular recording methods were the same as those used previously [2]. Since temperature can affect FFF [4], all experiments were carried out at a controlled room temperature between 22 and 24°C. The insects were dark adapted for 30 min previous to the experiments.

Flicker at various frequencies was produced by rotating a disc with an open sector allowing the beam to pass through. The waveform of each resulting light flash was an asymmetrical trapezoid with no background light. The light and dark periods were equal and fixed. The frequency and phase of the flashes were recorded with a photo-diode connected to the oscilloscope.

We used glass microelectrodes filled with 3M KCl. Since electrode resistance affects the recording condition, noise level, we measured with electrodes which had resistance of 70–80 MΩ. We rejected electrodes which had resistance of lower than 70 MΩ or higher than 80 MΩ for measurements.

When a photoreceptor cell was successfully impaled, its spectral type was determined with isoquantal flashes of monochromatic light of 22 interference filters each with a half band-width of 10 nm and a peak transmission ranging from 290 to 700 nm. The quantum flux of these monochromatic flashes at the corneal surface was adjusted with the optical wedge to 3×10^{10} photons/cm^2.s as measured with a radiometer (Model-470D, Sanso).

Then the V-log I curve for that cell was determined with monochromatic light flashes at each receptor's peak wavelength (λ_{max}). In these experiments I_{50} was defined as the stimulus light intensity evoking a response amplitude 50% of the maximum (V_{max}). This provided a physiological reference point for each cell studied. Stimulus durations for the V-log I measurements were 30 msec.

Then responses to flickering light were measured. Response

[1] To whom correspondence should be addressed.

Accepted September 16, 1994
Received June 24, 1994

amplitudes, peak to peak, were averaged. And a response amplitude of 0.5 mV, just strong enough to be discriminated from the background noise, was taken as the threshold for FFF. Flickering light intensity was increased stepwise from weak light intensity, and FFF was determined for each intensity. By these considerations the experimental artifacts can be minimized, and therefore the results obtained here are supposed to reflect almost the actual FFF's.

In the present experiments, responses to light flicker were measured only from photoreceptors which showed resting membrane potentials over 50 mV and a V_{max} response greater than 40 mV to a single flash stimulus. Therefore, our threshold criterion of 0.5 mV for FFF corresponds roughly to 1% of the maximal flash response. Each series of measurements took about 30 min. The reference intensity of each monochromatic light (Log=0) at the corneal surface corresponded to 1×10^{13} photons/cm^2.s.

RESULTS AND DISCUSSION

The data recorded here are based overall on intracellular recordings from 10 UV, 8 violet, 4 blue, 13 green, and 4 red photoreceptor cells. All responded to brief test stimuli of $I_{test}=I_{50}+2$ log units with at least 40 mV depolarization and were active long enough to make three or more series of flicker measurements at different stimulus intensities.

Our preliminary experiments indicated that the logarithm of the flicker response amplitudes (V) declined linearly with flicker frequencies (F) as expressed mathematically as follows:

$$V = a^{-bF}$$

where a and b are constants. The experiments also revealed

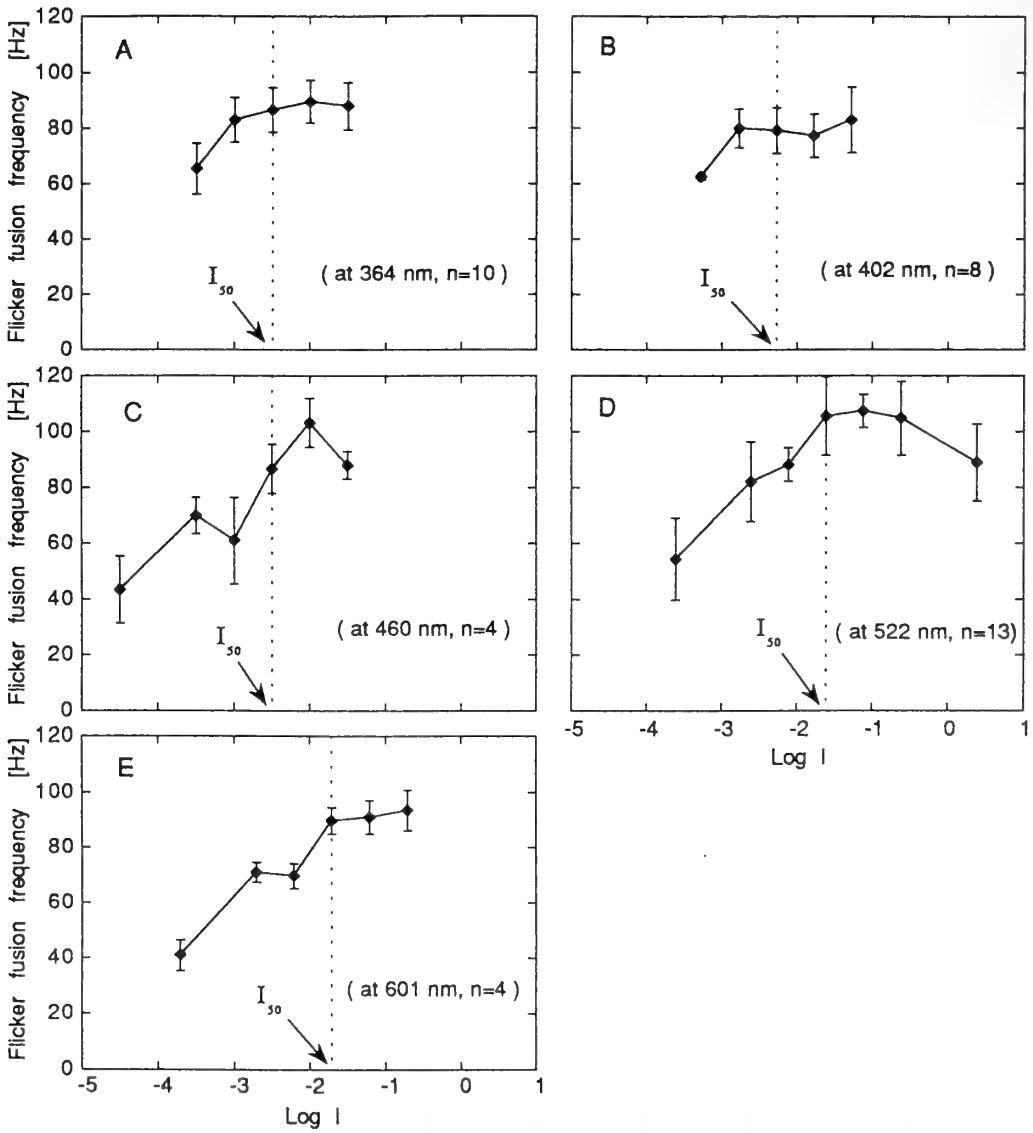

FIG. 1 A-E. FFF as a function of log I for the five types of spectral receptors: UV (**A**), violet (**B**), blue (**C**), green (**D**), and red (**E**). Intracellular recordings were made by 3M KCl-filled glass microelectrodes with resistances of 70–80 MΩ. Resting potentials were −50 to −70 mV. Bars indicate standard deviations. Wavelength of light stimulus is indicated in the parenthesis. Dotted vertical lines indicate I_{50} for each spectral receptors. I_{50} (UV)$=3.23\times10^{10}$ photons/cm^2/s. I_{50} (violet)$=5.31\times10^{10}$ photons/cm^2/s. I_{50} (blue)$=3.18\times10^{10}$ photons/cm^2.s. I_{50} (green)$=2.45\times10^{11}$ photons/cm^2/s. I_{50} (red)$=1.96\times10^{11}$ photons/cm^2.s.

that all five types of spectral receptor cells had almost the same gradients (b in the equation) in the linear relation between F and logarithm of V (Data not shown).

In green receptor (Fig. 1D), FFF's increased with stimulus intensities from 55 Hz at the light intensity of $I_{50}-2$ (log unit) to 105 Hz at I_{50}, then the FFF's stayed nearly constant between 104 and 107 Hz with intensities from I_{50} to $I_{50}+1$. At $I_{50}+2$ which produced nearly saturated responses to flash light stimulus, the FFF finally decreased to 90 Hz. The UV and blue receptors (Fig. 1A, C) followed nearly the same curve as the green receptor. The violet receptor (Fig. 1B), however, did not decrease its FFF's at strong light intensities (I_{50} to $I_{50}+1$), but yielded nearly constant FFF's between 79–83 Hz. In contrast, the FFF's for the red receptor (Fig. 1E) kept on increasing at all light intensities tested up to $I_{50}+1$.

Comparison shows that the green receptor has an FFF_{max} at 107 Hz with an intensity of $I_{50}+0.5$, next the blue receptor at 103 Hz with $I_{50}+0.5$, the red receptor at 95 Hz (or more) with $I_{50}+1$, the UV receptor at 90 Hz with $I_{50}+0.5$. The violet receptor had the lowest FFF at 82 Hz with $I_{50}+1$. A statistical analysis using a student's *t*-test among the highest FFF's, shows that there are significant differences between green-UV, green-violet, blue-UV and blue-violet receptors. The actual highest FFF's of violet and red receptors may be a little higher than those described above, because both receptors still showed increases in FFF's even at the highest intensities so far examined (Fig. 1). The FFF's of violet and red receptors were not recorded at strong light intensities above $I_{50}+2$ in the present experiments because their physiological condition usually deteriorated rather rapidly during intracellular recordings.

The present experiments demonstrate that there are significant differences in FFF_{max} for the five spectral types of *Papilio* photoreceptors previously reported [1]. The green and blue receptors have significantly higher FFF_{max}'s (107, 103 Hz) than do the UV(90 Hz) and violet receptors (83 Hz) (Fig. 2). If the green and blue receptors of *Papilio* are critical for scanning details of objects such as the green foliage of trees and other plants against the sky, their high FFF_{max}'s would likely increase temporal acuity for perceiving this visual pattern, particularly when flying. If so, the lower temporal acuities of the butterfly's UV and violet receptors may function in other ways to be determined. Presumably the UV receptor aids in discriminating UV light reflection of certain flowers [3] and may be, as it is in honeybees, important for discrimination of polarized light from the blue sky [9].

There are several methods to evaluate photoreceptor's temporal resolution. Those are FFF, frequency-response functions by using sinusoidally modulated stimulus, and impulse responses by using very brief flash stimulus. The reason of our choice of flicker fusion method was facility to compare quantitatively temporal resolution in wider stimulus intensity range and to find optimal stimulus intensity of maximal temporal resolution. And limitation of our experimental apparatus was also the reason of measurement by flicker fusion method. Flicker fusion method should be used with care about some aspects, because FFF may differ depending on recording condition, signal to noise ratio. We took care in following aspects to reduce errors of FFF caused by experimental condition, 1) the electrode resistances were kept in 70–80 MΩ, 2) experimental temperature was controlled in 22–24°C, 3) we only measured from photoreceptors which showed the maximal response amplitude of over 40 mV to single flash stimulus, 4) in 1950's and 60's, FFF's were measured by ERG and decided by researcher's own eyes, but in present study 0.5 mV of threshold amplitude was used for definition of FFF, and this definition of FFF by criteria threshold amplitude was used in both intracellular recordings [7] and ERG recordings [5].

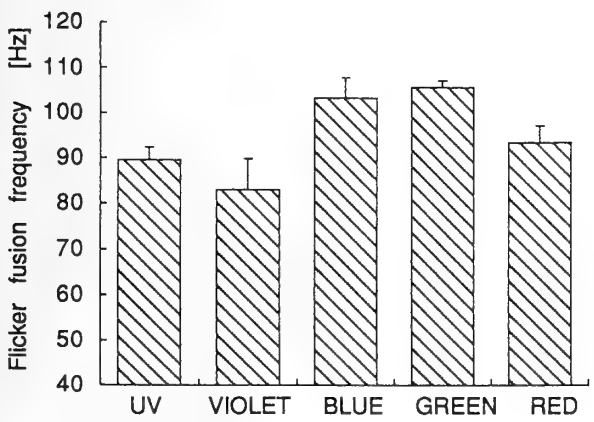

FIG. 2. Comparison of FFF_{max} for 10 UV, 8 violet, 4 blue, 13 green and 4 red receptors. The FFF_{max}'s of green and blue receptors taken together are significantly higher than those of UV and violet receptors with a probability of less than 0.05 that this difference would occur by chance (Student's *t*-test). *Bars* indicate standard errors of the means.

ACKNOWLEDGMENTS

We are very grateful to to Dr.Talbot H Waterman (Yale University) for his critical reading of the manuscript and to Dr. Simon B Laughlin (Cambridge University) for his helpful comments on the manuscript. This work was supported by Grants-in-Aid to E. Eguchi from the Ministry of Education, Science, and Culture of Japan.

REFERENCES

1 Arikawa K, Inokuma K, Eguchi E (1987) Naturwissenschaften 74: 297–298

2 Bandai K, Arikawa K, Eguchi E (1992) J Comp Physiol A 171: 289–297

3 Barth FG (1985) In "Insects and flowers" Princeton Univ Press, Princeton, New Jersey, pp 116–122

4 Cosens D, Spatz HC (1978) J Insect Physiol 24: 587–593

5 Green DG, Siegel IM (1975) Science 188: 1120–1122

6 Laughlin SB, Weckström M (1993) J Comp Physiol A 172: 593–609

7 Nowak LM, Green DG (1983) Vision Res 23: 845–849

8 Souza JM de, Ventura DF (1989) J Comp Physiol A 165: 237–245
9 Wehner R, Rossel S (1985) In "Experimental behavioral ecology and sociobiology" Ed by B Hölldobler, M Lindauer, Fischer, Stuttgart New York, pp 11–53

ZOOLOGICAL SCIENCE 11: 763–766 (1994)

[RAPID COMMUNICATION]

Identification of Protein C in Sera of the Frogs, *Rana nigromaculata* and *Rana brevipoda*

MASAHISA NAKAMURA[1], MASAYUKI SUMIDA, TOMOYO YAMANOBE[2] and MIDORI NISHIOKA

Laboratory for Amphibian Biology, Faculty of Science, Hiroshima University, 1-3-1 Kagamiyama, Higashi-Hiroshima, Hiroshima 724, and [2]Central Laboratory of Analytical Biochemistry, School of Medicine, Teikyo University, 2-11-1 Kaga, Itabashi-ku, Tokyo 173, Japan

ABSTRACT—When sera from the frogs, *Rana* (*R.*) *nigromaculata* and *Rana* (*R.*) *brevipoda*, were run on starch-gel electrophoresis (SGE), several bands were seen in an electrophoretic pattern of proteins. This pattern on SGE appeared the same at stages XIV, XV and XXI, and in the adult frog, *R. niguromaculata*. However, the pattern at stage X was different. A protein, designated "protein C", did not appear clearly at this stage, but afterwards. This protein was the second richest among serum proteins of mature frogs. Protein C (Mr=180 kD, when estimated by SDS-PAGE) was obtained after SGE and then subjected to an NH_2-terminal sequence analysis. Sequences of protein C from *R. nigromaculata* and *R. brevipoda* were NH_2-TDPMYVIFIPQTLXE for the first 15 amino acids and NH_2-TDPHYVIFKG for the first 10 amino acids, respectively. Homology search of GenBank sequences indicated no significant similarity with any known proteins. The results suggest that protein C is a new protein, and that it may play an important role(s) in the serum after stage X in these species.

INTRODUCTION

In order to understand the process of inheritance of a number of characters in amphibians, it is necessary to determine a locus of each gene in the chromosomes. Only a few studies of amphibians have focused on this topic so far [4–6]. This is probably due to difficulties in matching characters with the chromosomes carrying genes. However, by comparison of an electrophoretic pattern of proteins with constitution of bivalent chromosomes in oocytes of female backcrosses among Japanese pond frogs, it is possible to determine which chromosome is carrying a gene for each protein. Nishioka *et al.* [5, 6] determined the loci of five albino genes and 23 genes controlling 3 blood proteins and 13 enzymes on the chromosomes of mature offspring produced from female hybrids between *R. nigromaculata* and *R. brevipoda*, and male parents. They also showed that the gene of one of three blood proteins, designated "protein C", is located on chromosome No. 9. When proteins in sera from two species, *R. nigromaculata* and *R. brevipoda*, were run on starch gel-electrophoresis (SGE) and stained with amido black, several distinct bands were seen. The richest protein was albumin [5], but other proteins including protein C have not been identified yet. To clarify the relationship between a gene and a character, identification of protein C is essential. This study was undertaken to determine developmental change of protein C in the serum and to identify this protein in the frogs, *R. nigromaculata* and *R. brevipoda*.

MATERIALS AND METHODS

Experimental animals

Mature male frogs, *R. nigromaculata* and *R. brevipoda* collected in the Hiroshima district and the Okayama district, respectively, and female hybrids between these two species were used. For electrophoretic analysis of serum proteins, only offsprings from a pair of *R. niguromaculata* were used. The ovulation of a mature female was induced by bull frog pituitaries. Fertilization was then carried out artificially. Tadpoles in metamorphic stages and mature frogs were fed on boiled spinach or two-spotted crickets [7]. The developmental stage of tadpoles was determined according to Taylor and Kollros [8].

Starch-gel electrophoresis (SGE)

SGE was carried out as previously described [5]. In order to obtain blood samples, 0.1 ml of Ringer's solution containing 200 units of heparin was injected into frog's body cavities. After anesthetization with ether for mature frogs, or with MS-222 [0.01% (w/v); Sankyo] in H_2O for tadpoles, laparotomy was conducted. Blood was taken from the heart with a syringe and subjected to centrifugation at 600×g for 3 min at room temperature to remove blood cells. Sera thus obtained were stored at −20°C until use. For SGE each serum was absorbed in a small piece of filter paper (Whatman, No. 3; 3×7 mm) and placed into a well in a 12% starch-gel (16×18 cm, 6 mm thick) produced in a buffer (A) containing 20 mM boric acid, 0.68 mM EDTA and 21 mM Tris-HCl (pH 8.0). Proteins were run

Accepted July 23, 1994
Received January 12, 1994
[1] To whom correspondence should be addressed.

on SGE at 18.8 V/cm for 4 hr at 2°C in the 10× A (pH 8.0). After electrophoresis, each gel was cut into two slices. One slice was stained with amido black 10B [1% (w/v), Sigma] to identify the spot to which protein C migrated. The other was left unstained to extract protein C. Spots retaining protein C were cut off and boiled for 5 min in 1 ml of a 2% SDS sample buffer [2]. Boiled samples were centrifuged at 5000×g for 10 min at room temperature (Kubota 1900). The resultant supernatant was used to determine the heterogeneity of proteins on SDS-PAGE using a 12% polyacrylamide gel and an NH_2-terminal sequence analysis.

SDS-PAGE

Proteins were heat-denatured in SDS sample buffer and electrophoresed on a discontinuous 12% acrylamide gel [2].

NH_2-terminal sequence analysis

Protein C extracted from starch gels with a 2% SDS sample buffer [2] was prepared for NH_2-terminal sequence analysis using a sample preparation cartridge (ProSpin™; Applied Biosystems) by a protocol made by Applied Biosystems. An automated protein sequence analysis was carried out on an Applied Biosystems Model 470A gas-liquid phase protein sequencer connected on-line to an Applied Biosystems Model 120A HPLC [1, 3].

RESULTS AND DISCUSSION

The electrophoretic pattern of serum proteins from *R. nigromaculata* and *R. brevipoda* revealed four distinct bands, as shown in Figure. 1. These four bands were previously designated A, B, C and D on the basis of their mobility on SGE [5]. The biggest band A is albumin [5]. There were two bands at the position of A or C in the electrophoretic pattern of serum proteins from a hybrid between these two species (Fig. 1; lane 2). However, only one band of A or C appeared in the serum of *R. nigromaculata* and *R. brevipoda* (Fig. 1; lanes 1 and 3). Therefore, two proteins corresponding to the band A or C must be a product from a codominant allele on the respective chromosome.

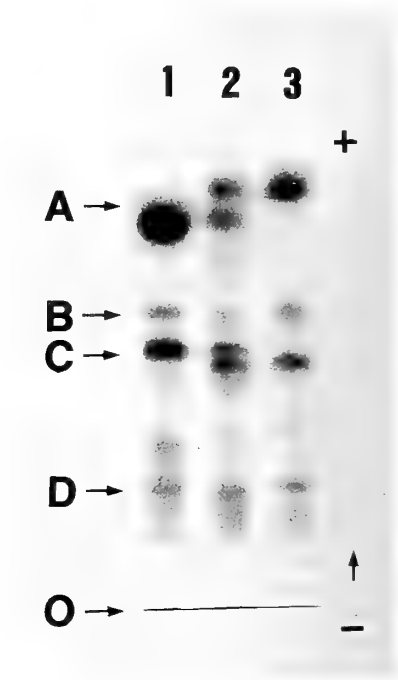

FIG. 1. Electrophoretic pattern of serum proteins of mature frogs on SGE. Proteins in the serum of two species of mature Japanese pond frogs were electrophoresed on a 12% starch-gel and stained with amido black as described in MATERIALS AND METHODS. Letters on the left side of the panel indicate protein A (A), protein B (B), protein C (C), protein D (D) and the original position before SGE (O), respectively. Proteins were mobilized from a cathode (−) to an anode (+) as indicated by an arrow. Lane 1, a male *R. brevipoda*; lane 2, a female hybrid between two species and lane 3, a male *R. nigromaculata*.

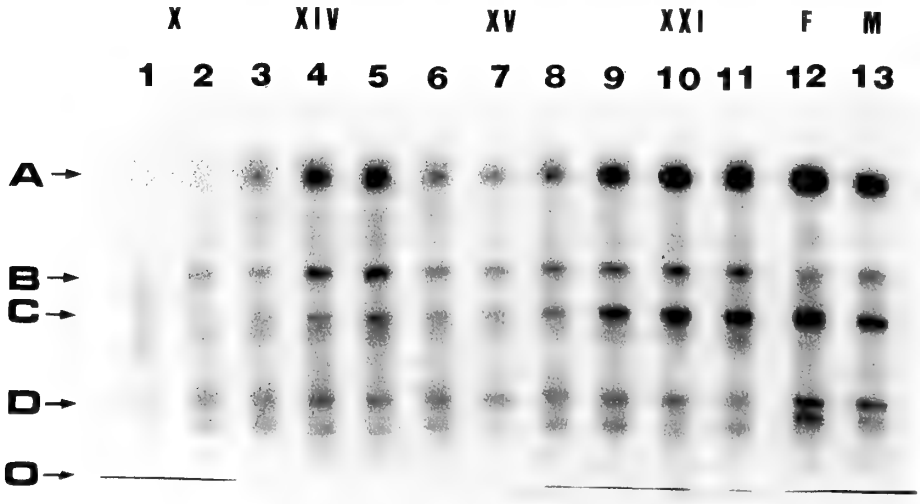

FIG. 2. Developmental pattern of serum proteins of *R. nigromaculata* on SGE. Proteins in the serum from various stages of *R. nigromaculata* were electrophoresed and stained with amido black. See the legend to Figure 1 for details. Letters at the top designate developmental stages. Lanes 1–2, stage X (X); lanes 3–5, stage XIV (XIV); lanes 6–8, stage XV (XV); lanes 9–11, stage XXI (XXI); lane 12, a mature female (F), and lane 13, a mature male (M).

Next, the developmental pattern of serum proteins of *R. nigromaculata* was determined. Five bands were observed at all the stages examined except for stage X (Fig. 2), while four bands were observed in Fig. 2. The appearance of 4 or 5 bands in the electrophoretic pattern probably depends on whether band D is a singlet or doublet (see Figs. 1 and 2). Nishioka *et al.* [5, 6] also found that the appearance of a 5 band pattern, the 5th band having the slowest mobility, depended on the particular blood sample. Hence, the amount of protein in this 5th band probably varies from individual to individual. Protein C did not appear clearly at stage X, while band B did (Fig. 2). Band A (albumin) was also very faint at this stage. Furthermore, protein C was not the second richest protein in the serum of *R. niguromaculata* before stage XIV, but at stage XXI. The pattern at stage XXI was the same as that in the adult (Fig. 2).

The developmental change in body weights of *R. nigromaculata* was depicted in Figure 3. The body weight of this species rapidly increases after stage X and declines beyond stage XIX. The appearance of protein C and albumin in the serum is probably associated with rapid growth in tadpoles of *R. nigromaculata*.

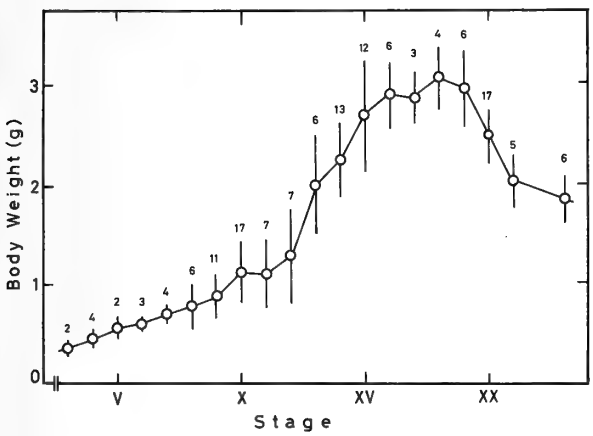

FIG. 3. Developmental change in body weights of *R. nigromaculata*. Body weights of tadpoles of *R. nigromaculata* during early development were determined. Bars indicate the mean ± SD. Values on the top of bars represent the number of animals used.

When protein C from the serum of *R. brevipoda* was run on SGE, extracted with the SDS sample buffer and then run on SDS-PAGE, only one band with Mr = 180 kD was observed (Fig. 4; lane b). The Mr of protein C from *R. nigromaculata* was also 180 kD when estimated on SDS-PAGE (data not shown). The abundance of this protein appeared second among serum proteins of mature frogs (Fig. 4; lane a), which was compatible with the result obtained from SGE (see Fig. 1). The most abundant protein with Mr = 74 kD seemed to be albumin, because it immunoreacted with sheep antisera raised against *Xenopus laevis* albumin on an immunoblot analysis (data not shown).

To identify protein C, the NH_2-terminal amino acid sequence was determined. As shown in Fig. 5, the sequence

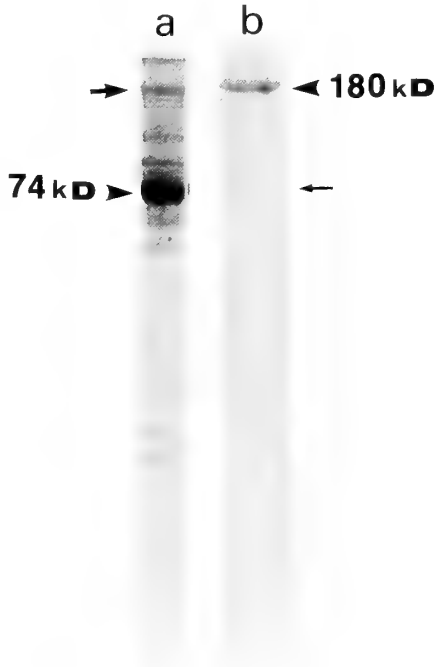

FIG. 4. Profile of proteins on SDS-PAGE. Crude serum (a) and protein C (b) of *R. brevipoda* obtained after SGE were then run on SDS-PAGE and stained with Coomassie brilliant blue R (Sigma) [2]. A large arrow indicates protein C in the crude serum. The richest protein with Mr = 74 kD is likely to be albumin (see Results). A small arrow indicates a position of albumin that migrates on SDS-PAGE. Thirty and three μg of proteins were loaded for lanes a and b, respectively.

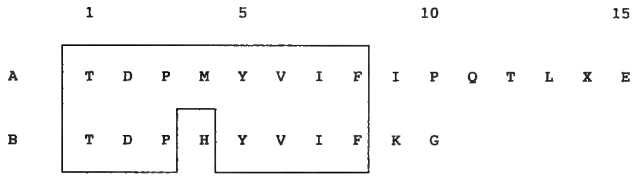

FIG. 5. The NH_2-terminal amino acid sequence of protein C in sera of two species, *R. nigromaculata* (A) and *R. brevipoda* (B). The homologous area is blocked.

of the first 15 amino acids of protein C from *R. nigromaculata* and the first 10 amino acids from *R. brevipoda* revealed that they were not identical, but probably in the same family. The heterogeneity of amino acid compositions between two proteins could be one reason why they showed different mobility on SGE (see Fig. 1), as they have the same Mr of 180 kD. Comparison of these sequences with the existing protein data base held by GenBank showed no significant identity with any previously described protein. Possible reasons for this include; (1) the molecular size of protein C is fairly large, (2) efforts to determine the amino acid sequence of such proteins deduced from their cDNAs have been made mainly in studies of animals other than amphibians, and (3) there should naturally be a substantial difference in amino acid composition of proteins from frogs and other animals. Taking all these possible factors into consideration, it is

conceivable that no significant homology of protein C to others could be observed, even when the field was narrowed to serum proteins.

It is of great interest to note that protein C appears in the serum of the frog, *R. nigromaculata* when body weight increases rapidly. Protein C must have an imporant function(s) in the serum of this species, but there is no evidence for this at the present time. To allow understanding of its molecular structure and physiological role(s), the nucleotide sequence of its cDNA should be determined right away.

ACKNOWLEDGMENTS

We would like to thank to Dr. D.R. Schöenberg, Uniformed Services University of the Health Science, for the generous gift of sheep antisera against *Xenopus laevis* serum albumin. Partial support for this work was provided by Grant-in-Aid to MN (No. 06640867) from the Ministry of Education, Science and Culture of Japan.

REFERENCES

1 Kennedy TE, Gawinowicz MA, Barzilai A, Kandel ER, Sweatt JD (1988) Proc Natl Acad Sci USA 85: 7008–7012

2 Laemmli UK (1970) Nature 227: 680–685

3 Nakamura M, Moriya M, Baba T, Michikawa Y, Yamanobe T, Arai K, Okinaga S, Kobayashi T (1993) Exp Cell Res 205: 101–110

4 Nishioka M, Ohtani H (1986) Sci Rep Lab Amphibian Biol Hiroshima Univ 8: 1–27

5 Nishioka M, Ohtani H, Sumida M (1980) Sci Rep Lab Amphibian Biol Hiroshima Univ 4: 127–184

6 Nishioka M, Ohtani H, Sumida M (1987) Sci Rep Lab Amphibian Biol Hiroshima Univ 9: 1–52

7 Nishioka M, Matsuura M (1977) Sci Rep Lab Amphibian Biol Hiroshima Univ 2: 165–185

8 Taylor AC, Kollros JJ (1946) Anat Rec 94: 7–24

Development
Growth & Differentiation

Published Bimonthly by the Japanese Society of Developmental Biologists
Distributed by Business Center for Academic Societies Japan, Academic Press, Inc.

Development, Growth and Differentiation (ISSN 0012–1592) is published bimonthly by The Japanese Society of Developmental Biologists. Annual subscription for Vol. 35 1993 U. S. $ 191,00, U. S. and Canada; U. S. $ 211,00, all other countries except Japan. All prices include postage, handling and air speed delivery except Japan. Second class postage paid at Jamaica, N.Y. 11431, U. S. A.

Outside Japan: Send subscription orders and notices of change of address to Academic Press, Inc., Journal Subscription Fulfillment Department, 6277, Sea Harbor Drive, Orlando, FL 32887–4900, U. S. A. Send notices of change of address at least 6–8 weeks in advance. Please include both old and new addresses. U. S. A. POSTMASTER: Send changes of address to *Development, Growth and Differentiation,* Academic Press. Inc., Journal Subscription Fulfillment Department, 6277, Sea Harbor Drive, Orlando, FL 32887–4900, U. S. A.

In Japan: Send nonmember subscription orders and notices of change of address to Business Center for Academic Societies Japan, 16–9, Honkomagome 5-chome, Bunkyo-ku, Tokyo 113, Japan. Send inquiries about membership to Business Center for Academic Societies Japan, 16–9, Honkomagome 5-chome, Bunkyo-ku, Tokyo 113, Japan.

Air freight and mailing in the U. S. A. by Publications Expediting, Inc., 200 Meacham Avenue, Elmont, NY 11003, U. S. A.

POWERFUL PARTNERS FOR LONG-TERM PATCH CLAMPING

The MHW-3 water hydraulic micromanipulator features a refined slide mechanism and a 5:1 hydro/mechanical ratio to keep drift to an absolute minimum — just 1/17.5th of earlier, oil-based hydraulic units. Consequently, patch recording is accurate and reliable over extended periods. The MHW-3 has a full, pipette movement range of 2mm in ultra-fine 0.2μm graduations to allow fine remote control movement in all three axes, thereby providing exceptionally precise specimen pinpointing.

The MHW-30 features a movement range of 10mm, minimum graduations down to 1μm, and a 1:1 hydraulic system.

Three-Dimensional Water Hydraulic Micromanipulators

with coarse and fine manipulation

MHW-3 and MHW-30

For further information and maintenance service:

NARISHIGE JAPAN

NARISHIGE SCIENTIFIC INSTRUMENT LAB.
9-28, Kasuya 4-chome, Setagaya-ku, Tokyo 157, Japan
Phone: (INT-L) 81-3-3308-8233 Fax: (INT-L) 81-3-3308-2005 Telex: NARISHIGE J27781

U.S. NARISHIGE INTERNATIONAL INC.
404 Glen Cove Avenue, Sea Cliff, New York 11579, U.S.A.
Telephone: +1 (516) 759-6167 Telefax: +1 (516) 759-6138

NARISHIGE INTERNATIONAL LTD.
Unit 7, Willow Business Park, Willow Way, London SE26 4QP, UK
Telephone: +44 (0) 81-699-9696 Telefax: +44 (0) 81-291-9678

ZOOLOGICAL SCIENCE

VOLUME 11 NUMBER 5 OCTOBER 1994

CONTENTS

INDEXED IN:
Current Contents/LS and AB & ES,
Science Citation Index,
ISI Online Database,
CABS Database, INFOBIB

Issued on October 15
Front cover designed by Saori Yasutomi
Printed by Daigaku Letterpress Co., Ltd., Hiroshima, Japan

ISSN 0289-0003

An International Journal

ZOOLOGICAL SCIENCE

Vol. 11 No.6

December 1994

PHYSIOLOGY
CELL and MOLECULAR BIOLOGY
GENETICS
IMMUNOLOGY
BIOCHEMISTRY
DEVELOPMENTAL BIOLOGY
REPRODUCTIVE BIOLOGY
ENDOCRINOLOGY
BEHAVIOR BIOLOGY
ENVIRONMENTAL BIOLOGY and ECOLOGY
SYSTEMATICS and TAXONOMY

published by Zoological Society of Japan
distributed by Business Center for Academic Societies Japan
VSP, Zeist, The Netherlands

ZOOLOGICAL SCIENCE

The Official Journal of the Zoological Society of Japan

The Zoological Society of Japan:
Toshin-building, Hongo 2–27–2, Bunkyo-ku,
Tokyo 113, Japan. Phone 03-3814–5461
Fax 03-3814-5352

ZOOLOGICAL SCIENCE is devoted to publication of original articles, reviews and rapid communications in the broad field of Zoology. The journal was founded in 1984 as a result of unification of Zoological Magazine (1888–1983) and Annotationes Zoologicae Japonenses (1897–1983), the former official journals of the Zoological Soceity of Japan. An annual volume consists of six regular numbers and one supplement (abstracts of papers presented at the annual meeting of the Zoological Society of Japan) of more than 850 pages. The regular numbers appear bimonthly.

MANUSCRIPTS OFFERED FOR CONSIDERATION AND CORRESPONDENCE CONCERNING EDITORIAL MATTERS should be sent to:

Dr. Tsuneo Yamaguchi, Editor-in-Chief, Zoological Science, Department of Biology, Faculty of Science, Okayama University, Okayama 700, Japan, in accordance with the instructions to authors which appear in the first issue of each volume. Copies of instructions to authors will be sent upon request.

SUBSCRIPTIONS. ZOOLOGICAL SCIENCE is distributed free of charge to the members, both domestic and foreign, of the Zoological Society of Japan.To non-member subscribers within Japan, it is distributed by Business Center for Academic Societies Japan, 5–16–9 Honkomagome, Bunkyo-ku, Tokyo 113. Subscriptions outside Japan should be ordered from the sole agent, VSP, Godfried van Seystlaan 47, 3703 BR Zeist (postal address: P. O. Box 346, 3700 AH Zeist), The Netherlands. Subscription rates will be provided on request to these agents. New subscriptions and renewals begin with the first issue of the current volume.

[Publication of Zoological Science has been supported in part by a Grant-in-Aid for Publication of Scientific Research Results from the Ministry of Education, Science and Culture, Japan.]

ZOOLOGICAL SCIENCE 11: 767–780 (1994)

REVIEW

Comparison of Gustatory Transduction Mechanisms in Vertebrate Taste Cells

TOSHIHIDE SATO, TAKENORI MIYAMOTO and YUKIO OKADA

Department of Physiology, Nagasaki University School of Dentistry, Sakamoto, Nagasaki 852, Japan

INTRODUCTION

Animals in various classes of vertebrates live in different environments, such as the water, the underground, the surface of lands or the sky, and eat different types of foods. Therefore, it is supposed that various vertebrates have different sensitivities to a variety of chemicals.

Investigations of gustatory transduction mechanisms in taste cells have been carried out with varying vertebrate species, such as catfish, frog, mudpuppy, salamander, mouse, rat, gerbil and hamster. Comparison of gustatory research data obtained in different species of vertebrates must be done carefully because their living environments and food customs differ from each other. When an interpretation of the experimental data obtained from the taste nerve in some animal is given on the basis of taste cell functions, the taste cell data from the same or similar species should be used. Some confusion may happen when the properties of gustatory neural responses in one species are explained by the properties of the taste cell responses in a quite different species. Some researchers confuse an understanding of gustatory nerve and cell data because of citing unadequate references.

In this review we attempted to compare gustatory transduction mechanisms obtained in various mammalian taste cells (rat, mouse, hamster) and amphibian taste cells (frog, salamander, mudpuppy), which were mostly studied with microelectrode techniques and patch electrode techniques. Although there are many review articles which mentioned gustatory transduction mechanisms [9, 30, 41, 43–45, 47, 84], few have carefully compared those in different vertebrates [9, 45].

GUSTATORY TRANSDUCTION IN FROG TASTE CELLS

1. *Characteristics of taste cell responses*

Several species of frogs and toads have been used for investigation of taste mechanisms. Figure 1 illustrates receptor potentials in frog taste cells induced taste stimuli [92]. Figure 2 shows relationships between stimulus concentration

Received October 26, 1994

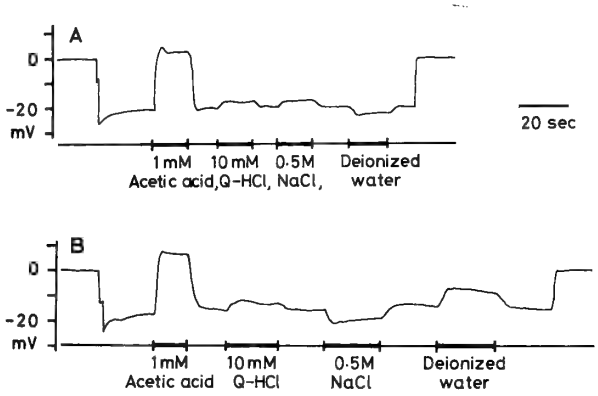

FIG. 1. Intracellular receptor potentials of a frog taste cell in response to acetic acid, quinine-HCl (Q-HCl), NaCl and deionized water. Record A is from a taste cell of the apical region and record B from a taste cell of the proximal region of the tongue. The vertical deflection at the left shows a penetration of taste cell and that at the right a withdrawal of the cell. From [92].

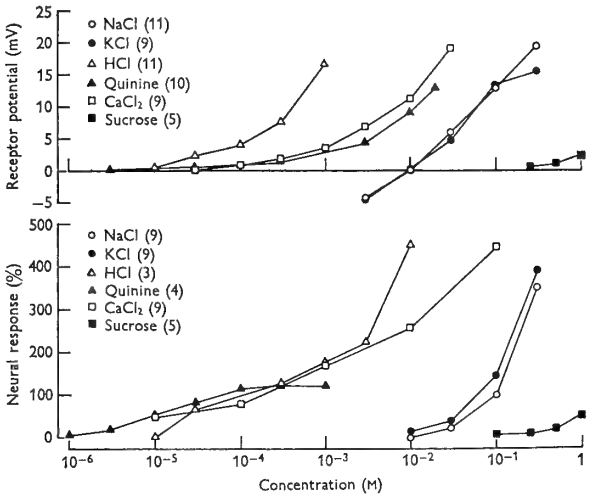

FIG. 2. Relationships between taste stimulus concentration and response magnitude, obtained from the frog taste cell (upper graph) and from the frog glossopharyngeal nerve (lower graph). Stimuli were indicated by different symbols. Each point represents the mean value of the maximum magnitude of receptor potentials and gustatory neural responses obtained from several experiments, the number of which is indicated by a numeral inside a parenthesis after each stimulus. In all the experiments taste receptors were preadapted to 0.01 M-NaCl before each stimulation. From [4].

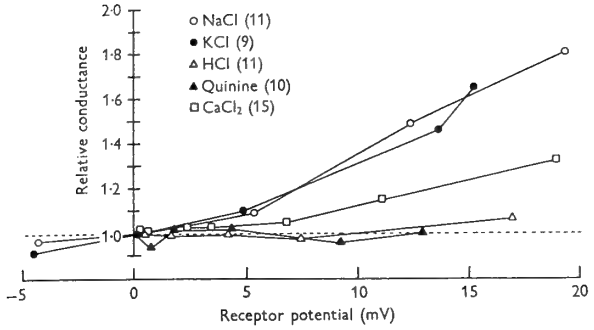

FIG. 3. Relationships between the receptor potential amplitude and the relative conductance magnitude in frog taste cells. The latter represents the ratio of the electrotonic potential magnitudes between rested and stimulated state. Numeral inside the parenthesis is number of taste cells sampled. From [4].

and response magnitude in gustatory cells (upper) and in gustatory nerves (lower) [4]. Salt, bitter and acid stimuli elicit large responses in both gustatory cells and nerves, but sweet stimuli elicit small responses. Intracellular receptor potentials in response to four basic taste stimuli and water stimulus are depolarizing or hyperpolarizing. However, depolarizations are dominant for salt, acid and bitter stimuli. Depolarization in response to water is found in the taste cells in the proximal region of the tongue [92] (Fig. 1). Conductance change during generation of receptor potentials is shown in Figure 3 [4]. Conductance is increased for salt, acid and sucrose but reduced slightly for quinine-HCl (Q-HCl) [4, 53, 69, 87, 97]. The conductance change during water stimulation shows two types [72]: reduction or increment depending on cell types. Frog taste cells can produce spike potentials in response to electrical stimulation [5, 54, 56].

Frog and toad taste organs on the dorsal surface of the tongue are located on the top of the fungiform papillae. Each fungiform has a large disc-shaped structure of 100–300 μm in diameter which is termed the taste disc rather than the taste bud. There are several types of taste disc cells. Classification and nomenclature of the disc cells are controversial [31, 36, 80, 116]. Usually two types of taste cells are distinguished depending on their structure. All the taste cells are innervated by the glossopharyngeal nerves. There are gap junctions between supporting cell and taste cell and between taste cells in the taste disc [86].

In frog taste cell membrane, voltage-gated ion channels (several types of K^+ channels, Na^+ channel, Ca^{2+} channel) and ligand-gated ion channels (Na^+ channel, K^+ channel, non-selective cation channel, Cl^- channel) are found. However, their physiological functions in gustatory transductions are unclear and under investigation [5–8, 25–27, 54–58, 60, 75].

Recently, most studies on gustatory transduction mechanisms in frog taste cells are carried out in our laboratory with microelectrode and patch pipette techniques. Therefore, studies on anuran amphibians are focused on our experimental data.

2. Salt taste

The taste cell membrane can be divided into the apical receptive membrane exposed to the oral cavity and the basolateral membrane. The former is usually bathed in the superficial fluid (SF) and the latter in the interstitial fluid (ISF). The amplitudes of the receptor potentials in frog taste cells induced by salt stimuli are greatly decreased when interstitial Na^+ and Ca^{2+} are replaced with choline$^+$, tetramethylammonium$^+$, tetraethylammonium$^+$ [55, 59, 87, 90, 93]. Addition of 5 mM Co^{2+} and 3 μM tetrodotoxin (TTX) to ISF does not affect the receptor potentials. This indicates that TTX-insensitive cation channels in the basolateral membrane play an important role in generation of the receptor potentials [55].

After the normal ionic composition of SF and ISF of the frog tongue is changed with low-concentration Na^+ saline, the relationships between membrane potentials and receptor potentials in a frog taste cell evoked by various concentrations of NaCl and various types of salts can be analyzed to examine the permeability of the taste-receptive membrane to cations and anions (Fig. 4). In this situation, the mean reversal potentials for depolarizing potentials of a taste cell in response to 0.05, 0.2, and 0.5 M NaCl are -40.0, 6.4, and 28.8 mV, respectively [59]. When adding an anion channel blocker, SITS (4-acetamide-4′-isothiocyanostilbene-2,2′-disulfonic acid), to a NaCl stimulus, the reversal potential for receptor potential with NaCl plus SITS becomes about twice larger than that with NaCl alone [59]. This result indicates that Na^+ and Cl^- of the NaCl stimulus permeate the apical receptive membrane. Previously Akaike and Sato [3] suggested that cation and anion of salt stimuli directly permeate the receptive membrane in frog taste cells.

Reversal potentials for 0.2 M NaCl, LiCl, KCl, and NaSCN in frog taste cells are 6.4, 25.4, −1.0, and −7.8 mV, respectively, indicating that permeability of the apical taste receptive membrane to cations of the Cl- salts is of the order of $Li^+ > Na^+ > K^+$ and that the permeability to anions of the Na^+ salts is $SCN^- > Cl^-$ [59]. These results indicate that

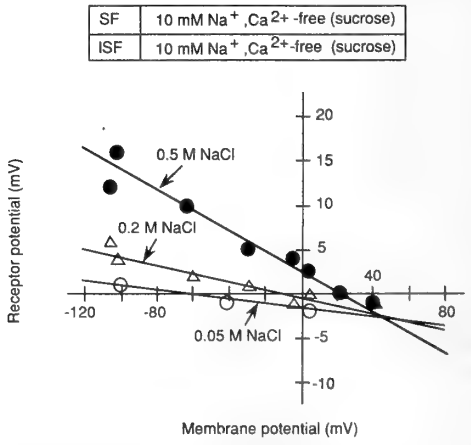

FIG. 4. Relationship between membrane potentials and receptor potentials induced by NaCl stimuli in a frog taste cell. Superficial fluid (SF) and interstitial fluid (ISF) used are shown above the graph. From [59].

the NaCl stimulus-induced receptor potential in a frog taste cell results from an inflow of Na^+ and Cl^- across cation and anion channels on the taste-receptive membrane, as well as an inflow of interstitial Na^+ across cation channels on the basolateral membrane. Salt-induced receptor currents in frog taste cells are recorded with single microelectrode or patch pipette voltage clamping method [58, 73]. Recently, Miyamoto *et al.* found salt stimulus-gated K^+ channels in the frog receptive membrane which show a high permeability to Na^+ [57, 58, 60]. Fig. 5 illustrates a tentative diagram of NaCl signal transduction in a frog taste cell [55, 59, 60].

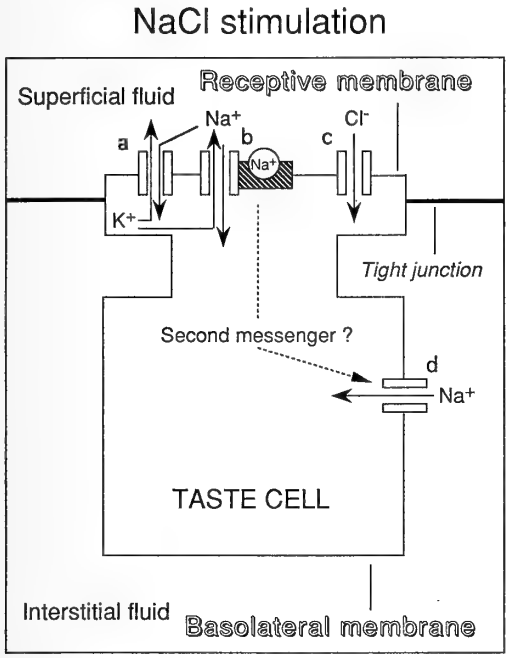

FIG. 5. Schematic drawing of transduction of a NaCl stimulus into receptor potential in a frog taste cell. a, cation channel; b, K^+ channel; c, anion channel; d, cation channel. Voltage-dependent channels, such as Na^+-, K^+- and Ca^{2+}-channels, which are related to generation of spike potentials of the taste cell are removed in this and other figures.

Patch pipette studies with excised patch membranes indicate that there are K^+ channels, nonselective cation channels, and Cl^- channels of various conductances in the apical receptive membrane of frog taste cells [25–27]. However, contribution of these channels to salt signal transduction has not yet been clarified.

Amiloride-blockable Na^+ channels exist in the frog taste cell membrane [8, 55, 66]. Miyamoto *et al.* with *in situ* taste cells could not find a change in NaCl-induced receptor potential following 50 min adaptation of the receptive membrane to 0.1 mM amiloride [55]. Therefore, it is likely that amiloride-blockable Na^+ channels may exist in the basolateral membrane of frog taste cells. The Na^+ channels do not contribute directly to salt signal transduction in frog taste cells.

3. Sour taste

The removal of Na^+, Ca^{2+}, and Cl^- from the normal ISF does not affect the receptor potential in a frog taste cell induced by acid stimuli such as acetic acid and HCl [53]. Interstitial 100 mM K^+ saline also does not affect the acid response [53]. The receptor potential is reduced greatly when Ca^{2+} is removed from the superficial normal saline, but is increased when the Ca^{2+} concentration is elevated [53, 95] (Fig. 6). Similar responses are seen in the frog gustatory nerve [67]. The removal of superficial Cl^- does not affect the receptor potential. The receptor potential elicited by an acid stimulus under superficial Ca^{2+}-free saline is partly caused by Na^+ [53]. Li^+, K^+, NH_4^+, or choline$^+$ substitutes for Na^+ in producing the receptor potential. The receptor potential is unaffected by superficial TTX, but is blocked by superficial Ca^{2+} antagonists such as Co^{2+} and Cd^{2+}. Sr^{2+} and Ba^{2+} substitute for Ca^{2+} in generating the receptor potential [53]. The receptor potentials observed under various concentrations of superficial Ca^{2+} becomes smaller when Na^+ is present in the SF, indicating a competition between Ca^{2+} and Na^+ passing through a Ca^{2+}-permeable conductance in the apical receptive membrane [53].

These findings indicate that a large portion of the recep-

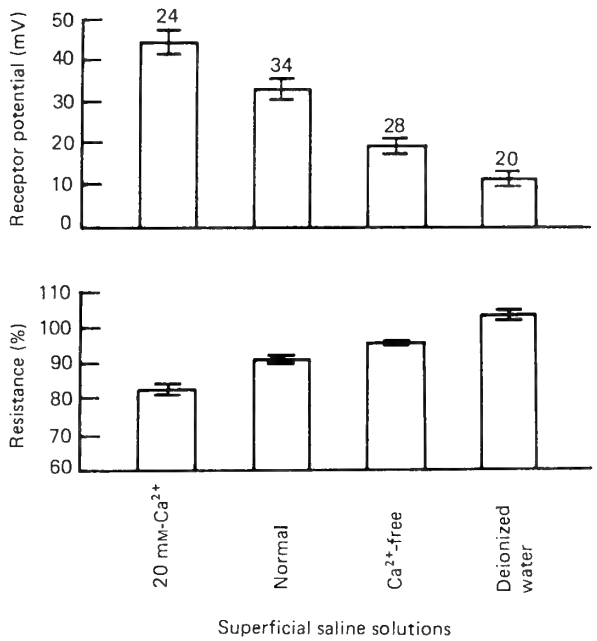

FIG. 6. Relation between the amplitude of receptor potentials and the amplitude of input resistance induced by 1 mM-HCl in frog taste cell. The tongue surface is adapted to 20 mM-Ca^{2+}, normal, Ca^{2+}-free saline solutions and deionized water. The resistance is expressed as a percentage of the control in the unstimulated state. The absolute value of the input resistance in the unstimulated state is 62 ± 6 MΩ with 20 mM-Ca^{2+} saline, 54 ± 5 MΩ with normal (1.8 mM-Ca^{2+}) saline, 53 ± 7 MΩ with Ca^{2+}-free saline and 64 ± 7 MΩ with deionized water. No significant differences are found in any pairs of these figures. From [53].

tor potential induced by acid stimuli is concerned with proton-gated Ca^{2+} channels on the taste-receptive membrane [53]. Both divalent (Ca^{2+}, Sr^{2+}) and monovalent (Na^+, Li^+, K^+, NH_4^+, choline$^+$) cations can pass through the Ca^{2+} channel. Even after the tongue surface is adapted to pure water, the amplitude of acid-induced response in a taste cell remains as large as 35% of the control (Fig. 6). After 0.1 mM DCCD (N,N'-dicyclohexylcarbodiimide), a proton pump inhibitor, is added to SF, the acid response is greatly suppressed, indicating a contribution of proton transporter on the receptive membrane to the acid-induced receptor potential [74].

The receptor current from a dissociated frog whole taste cell can be recorded with a patch pipette filled with 100 mM CsCl. Application of 0.1 mM acetic acid stimulus containing 80 mM $BaCl_2$ to the cell initiates an inward current of about −50 pA at the holding potential of −40 mV [75]. After the taste-receptive membrane alone is damaged, the receptor current induced by acetic acid stimulus containing the $BaCl_2$ greatly decreases, indicating that the inward receptor current is induced by Ba^{2+} passing across proton-gated Ca^{2+} channels on the apical receptive membrane. Cation permeability of the proton-gated Ca^{2+} channel is: $P_{Ca}:P_{Ba}:P_{Sr}:P_{Na}:P_{Cs}$ $=1.87:1.17:0.73:0.99:1.00$ [75]. Therefore, this channel should be called rather a proton-gated nonselective cation channel than the proton-gated Ca^{2+} channel.

It is concluded that most of the acid-induced response in a frog taste cell is generated by a current carried through the proton-gated cation channel of the apical receptive membrane, and that the remaining portion of the acid response is generated by current carried through a DCCD-sensitive proton transporter of the receptive membrane [53, 74] (Fig. 7).

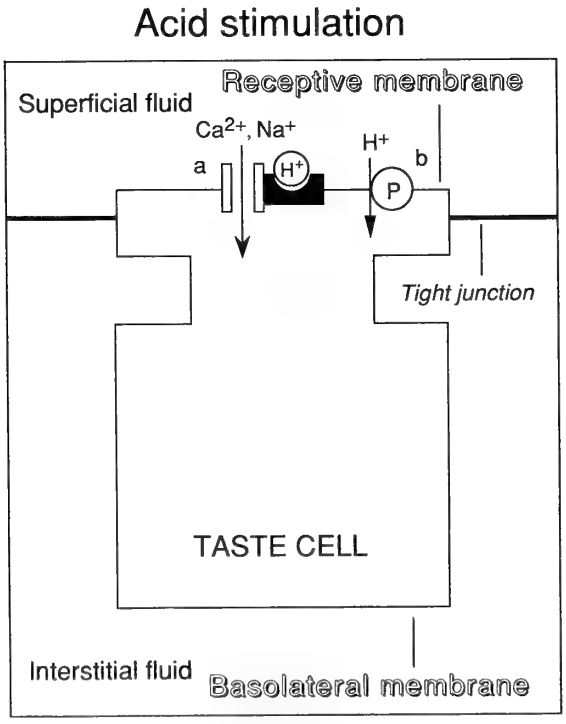

FIG. 7. Schematic drawing of transduction of an acid stimulus into receptor potential in a frog taste cell. a, proton-gated nonselective cation channel; b, H^+-transporter.

4. Bitter taste

The ionic mechanism of the receptor potential in a frog taste cell elicited by quinine-HCl (Q-HCl) has been studied. The frog taste cells whose receptive membranes are adapted to normal saline and deionized water generate depolarizing receptor potentials at Q-HCl concentrations higher than 2 and 0.01 mM, respectively [69]. The input resistance of the taste cell during Q-HCl stimulation increases slightly [4, 69, 97]. The receptor potential does not change even when the membrane potential level is greatly changed. The magnitude of the receptor potential is increased by reducing the concentration of superficial Cl^- on the taste-receptive membrane (Fig. 8), but is independent of the concentration of superficial Na^+ [69, 97].

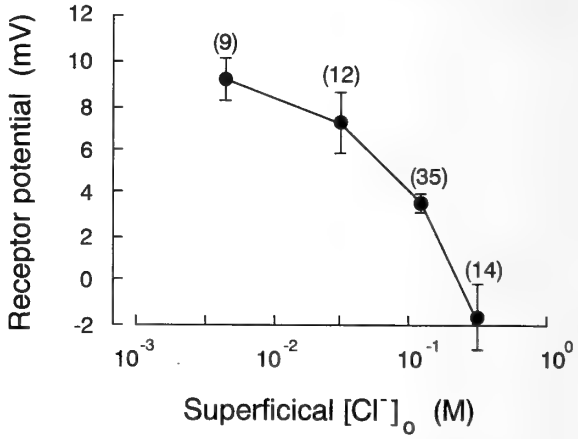

FIG. 8. Relationship between concentration of superficial Cl^- and amplitude of Q-HCl-induced responses in frog taste cells. Numerals in parentheses are numbers of taste cells sampled. From [69].

Injection of Cl^- into a frog taste cell greatly increases the receptor potential [69]. The magnitude of the receptor potential is greatly decreased by removing interstitial Na^+ or Cl^-, or both, surrounding the basolateral membrane of the taste cell. Furosemide (1 mM) added to the ISF decreases the receptor potential to 15%, while interstitial ouabain (0.1 mM) and superficial SITS (0.1 mM) do not influence it [69, 97]. From these results, we can conclude [69, 94, 96, 98]: (1) an electroneural Na^+/Cl^- cotransport occurs through the basolateral membrane of a frog taste cell in the resting state, so that Cl^- accumulates inside the cell. (2) Q-HCl stimulation induces the active secretion of Cl^- across the taste receptive membrane, resulting in a depolarizing receptor potential (Fig. 9).

5. Sweet taste

The frog taste cell generates a depolarizing receptor potential accompanying a remarkable reduction of input

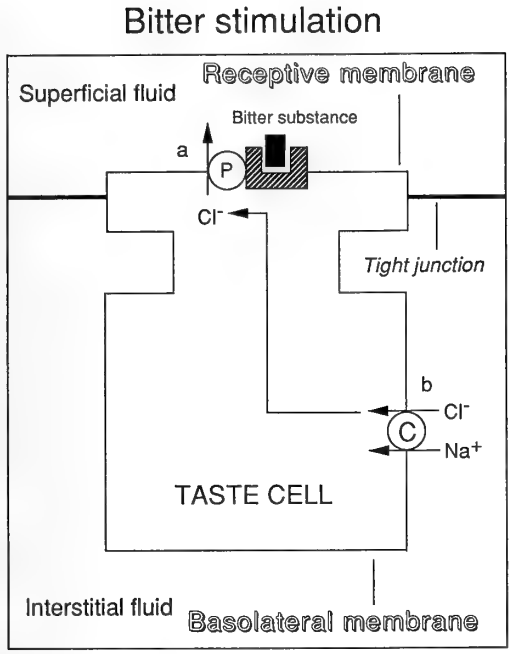

FIG. 9. Schematic drawing of transduction of a bitter stimulus into receptor potential in a frog taste cell. a, Cl^- pump; b, electroneutral Na^+/Cl^- cotransporter.

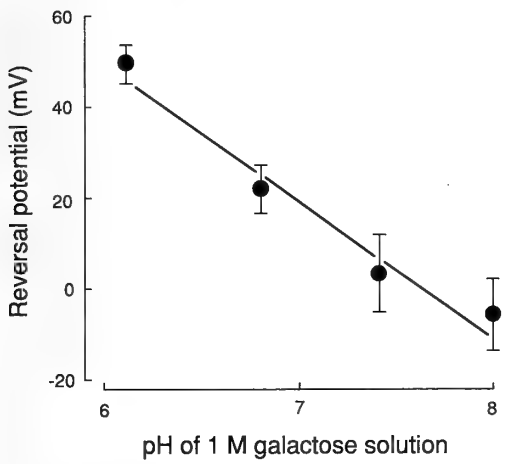

FIG. 10. Relationship between pH of 1 M galactose and reversal potential for receptor potentials in frog taste cells. Points are means from three or four taste cells; bars are SE. From [71].

resistance in response to stimulation with galactose and sucrose [71]. The magnitude of the receptor potential in response to a galactose solution increases linearly with decreasing pH in the pH range 6–8, but remains constant above pH 8 [71]. The reversal potential is increased by only 29 mV by a 10-fold increase in the H^+ concentration of the stimulus, suggesting that there are pH-dependent and pH-independent components in the mechanism generating the receptor potential [71] (Fig. 10). Superficially added blockers of anion channels (0.1 mM SITS) have no effect on the receptor potential. Na^+-free, Ca^{2+}-free, and K^+-free ISF do not affect the receptor potential, but the elimination of Cl^- from the ISF largely abolishes it [71]. Interstitial 0.1 mM DCCD completely inhibits the receptor potential, and interstitial 0.1 mM N-ethylmaleimide decreases the potential to 40% of the control value [71]. Lowering the pH of ISF from 7.2 to 6.3 greatly decreases the receptor potential. It is concluded that part of the receptor potential in frog taste cells induced by sugar stimuli may be produced by an inflow of H^+ through the taste-receptive membrane [71] (Fig. 11). The intracellular pH of the taste cell may be regulated by a Cl^--dependent H^+ pump in the basolateral membrane [71].

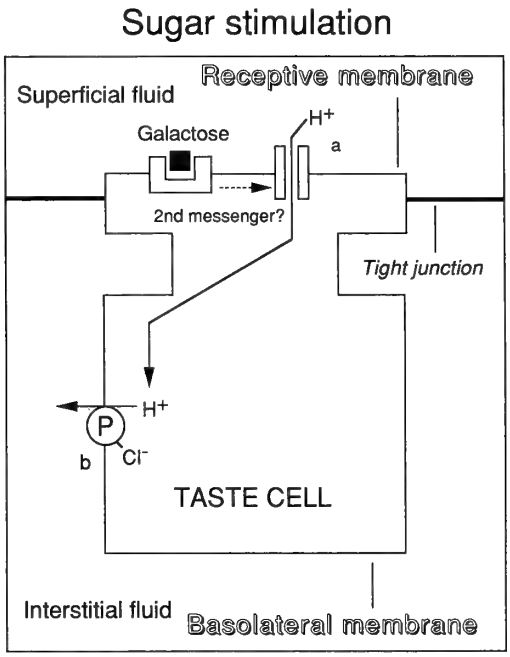

FIG. 11. Schematic drawing of transduction of a sugar stimulus into receptor potential in a frog taste cell. a, H^+ channel; b, Cl^--dependent H^+ pump.

6. *Water taste*

The frog taste cell located in the proximal portion of the tongue generates a depolarizing receptor potential that averages 10 mV in response to stimulation with deionized water [72]. Water-sensitive taste cells are classified into two types: Cl^--dependent and Cl^--independent. In Cl^--dependent cells whose input resistance is decreased or unchanged by deionized water, the magnitude of the water-induced depolarization decreases with an increase in concentration of superficial Cl^- in contact with the receptive membrane and with addition of blockers of anion channels (0.1 mM SITS and 0.1 mM DIDS) to deionized water [72]. The reversal potential for the depolarization in this type shifts according to the concentration of superficial Cl^- [72]. These properties of the responses are consistent with those of the glossopharyngeal nerve, which innervates the taste disc. In Cl^--independent cells whose input resistance is increased by deionized water, the reversal potential is approximately equal to the equilibrium potential for K^+ at the basolateral membrane [72]. The water-induced response of the glossopha-

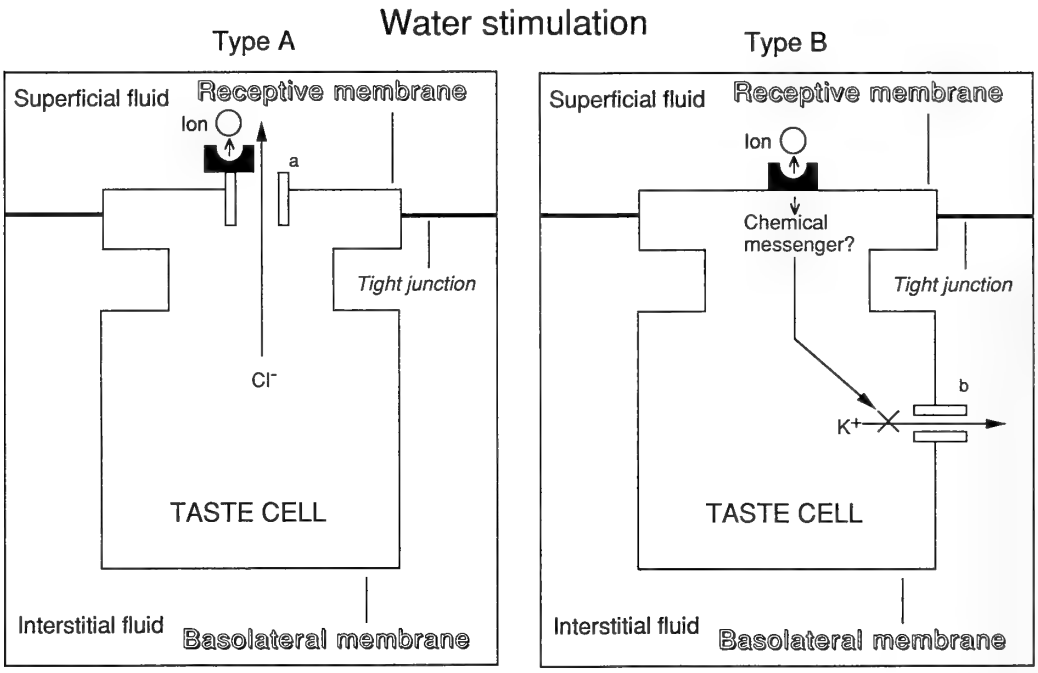

FIG. 12. Schematic drawing of transduction of a water stimulus into receptor potential in frog taste cells. The type A is Cl^--dependent, water-sensitive taste cell, and the type B is Cl^--independent, water-sensitive taste cell. a, Cl^- channel; b, K^+ channel. X means block of channel.

ryngeal nerve is decreased to about 60% of the control value by addition of interstitial 2 mM Ba^{2+}. K^+ channels of approximately 40 pS are found in the frog taste cell membrane [6, 26, 27]. The activities of these channels are blocked by cAMP in the presence of ATP and cAMP-dependent protein kinase [6, 27]. The frog taste cells *in situ* depolarized by intracellular injection of cAMP and cGMP have been found [68]. Probably, the K^+ channels are related to a depolarization of Cl^--independent, water-sensitive frog taste cells, which is accompanied with increase of the membrane resistance. It is concluded that the water-induced receptor potential is produced by Cl^- secretion through the taste-receptive membrane in about 70% of Cl^--dependent, water-sensitive frog taste cells (type A in Fig. 12), while it is generated by an inhibition of the resting K^+ conductance of the basolateral membrane in the remaining 30% of Cl^--independent, water sensitive taste cells [72] (the type B in Fig. 12).

GUSTATORY TRANSDUCTION IN TAILED AMPHIBIAN TASTE CELLS

1. *Cellular organization of taste buds*

In tailed amphibians, taste buds are found over the whole dorsal surface of the tongue [16]. The glossopharyngeal nerve innervates the taste buds. Taste buds contain three types of cells: dark, light and basal cells [82]. The basal cells can be further divided into two types: undifferentiated stem cell and Merkel-like cell [19]. The dark and light cells have an elongated, bipolar structure and are regarded as taste receptor cells which extend apical processes to the taste pore.

2. *Types of ionic channels in taste cells*

Taste cells of the mudpuppy, *Necturus*, are electrically excitable and generate action potential in response to taste stimuli [38, 81]. Some basal cells also possess the action potential [13]. Using the patch-clamp technique, it has been confirmed that taste cells in tailed amphibians possess a variety of voltage-dependent currents, such as a TTX-sensitive Na^+ current, a L-type Ca^{2+} current and several K^+ currents [39, 51, 106]. The role of the action potential is unclear. The action potential may be necessary to activate the Ca^{2+} current underlying a neurotransmitter release. The microelectrode study in mudpuppy taste cells [48] identified a Ca^{2+}-dependent chloride conductance which might terminate the depolarizing responses elicited by taste stimuli [108]. Electrical coupling has been observed between a group of taste cells in mudpuppy taste buds [117]. It is thought that such groups may form an organization unit within taste buds. The taste cell-basal cell synapse also has been identified in a lingual slice preparation [22].

3. *Salty taste*

In whole-cell recordings from taste cells in the tiger salamander, *Ambystoma*, it has been shown that Na^+ influx through amiloride-sensitive Na^+ channels mediates transduction of Na^+ salts into receptor potentials [107] (Fig. 13). Amiloride reduces a sustained Na^+ current in isolated salamander taste cells (Fig. 14) and inhibits a NaCl-induced neural response in the animals, suggesting that these channels are located in the apical receptive membrane. The drug, however, does not block the neural response elicited by NaCl in the mudpuppy [50]. Alternatively, an apically-located K^+ channels mediate transduction of K^+ salts in the mud-

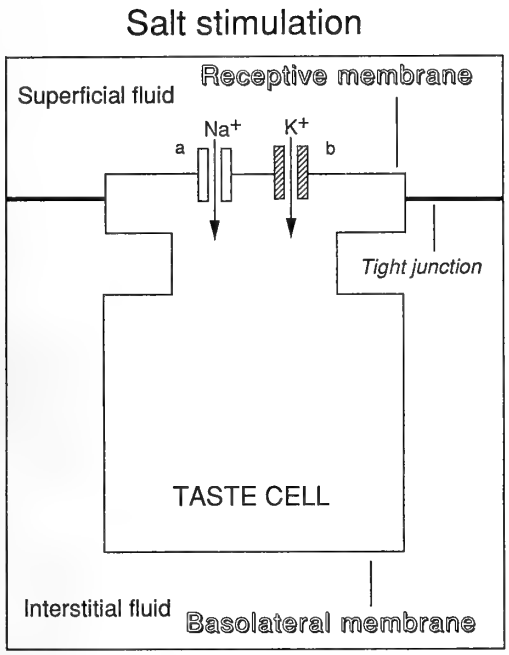

FIG. 13. In tiger salamander, Na^+ ions directly pass through apical amiloride-sensitive Na^+ channels (a). Alternatively, in mudpuppy, K^+ ions also directly pass through apical TEA-sensitive K^+ channels (b).

puppy taste cells [40, 42]. It is likely that K^+ flux through the channel can depolarize taste cells. The dominant sensitivity of K^+ salts in the mudpuppy has already been reported with the microelectrode technique [115].

4. Bitter and sour tastes

In the mudpuppy, block of the apically-located K^+ channels may mediate the transduction of several taste stimuli, including sour, bitter and $CaCl_2$ stimuli (Fig. 15). Patch-clamp and microelectrode studies have shown that these stimuli all reduce the voltage-dependent K^+ current in the mudpuppy taste cells [12, 39, 40]. Since the voltage-dependent K^+ current is restricted to the apical membrane of the taste cells [83], the K^+ channels are directly exposed to taste stimuli. Recent investigation with single channel recording also has indicated that the channels are all blocked by citric acid and quinine applied to outer surface of the channels [17] (Fig. 16). Since these channels exhibit a significant open probability at rest, block of the channels can produce depolarization in taste cells. Similar results have been obtained in the tiger salamander taste cells [107]. The taste cells in the animals, however, generate the inward current accompanied by conductance increase in response to sour stimuli. The blocking mechanism may result in a lack of discrimination among those taste stimuli [14], although single unit analysis of the glossopharyngeal nerve response has suggested the discrimination between the sour and bitter tastes in the mudpuppy [85]. The cross-adaptation analysis of the glossopharyngeal nerve between taste stimuli and K^+ channel blockers still has not been made.

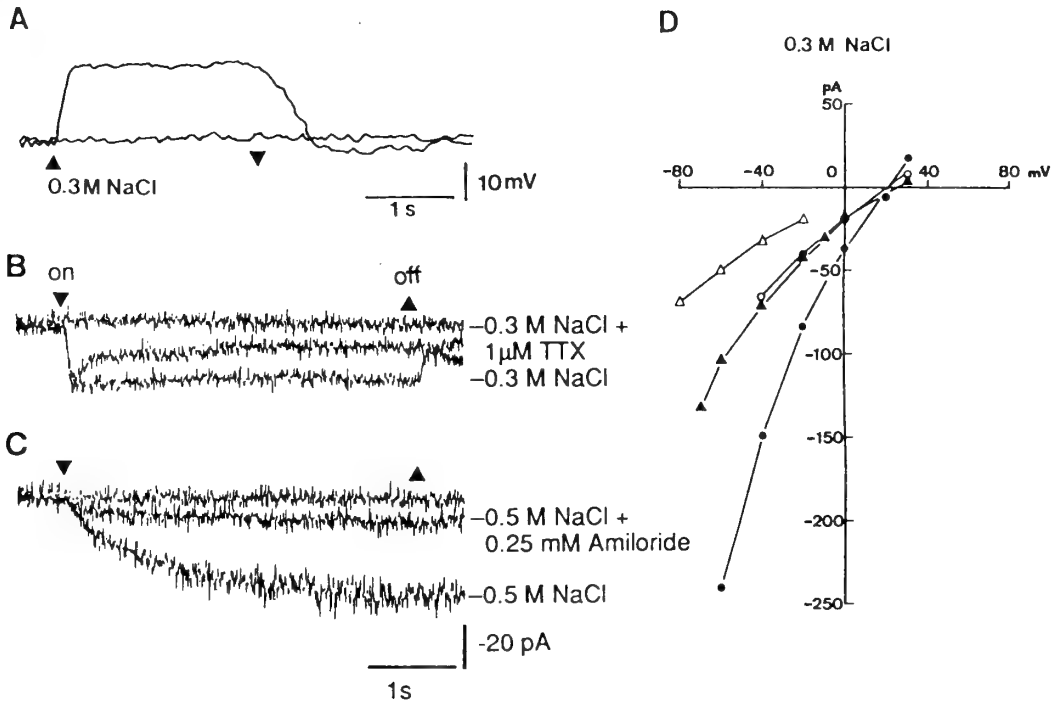

FIG. 14. NaCl-induced taste cell responses in tiger salamander. Application of 0.3 M NaCl induces a depolarization in a current-clamped taste cell (A). 0.3 M NaCl induces a sustained inward current in a voltage-clamped taste cell. The inward currents are partially blocked by TTX (B) and amiloride (C). Effect of holding potential on 0.3 M NaCl-induced inward currents in four taste cells (D). The data are obtained by the whole cell recordings from isolated taste cells. From [107].

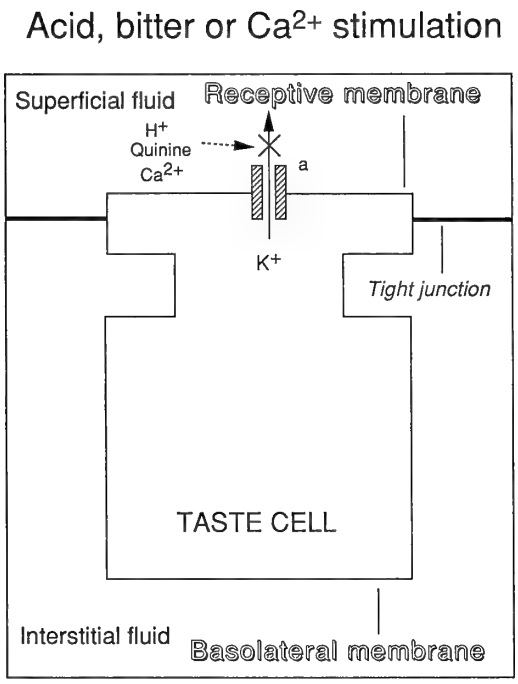

FIG. 15. Schematic drawing of mechanism of transduction of acid, bitter and $CaCl_2$ stimuli into receptor potentials in tailed amphibian taste cells. In tailed amphibians, acids, quinine and Ca^{2+} depolarize taste cells by direct block of apical K^+ channels (a). This diagram comes from [12, 39, 107].

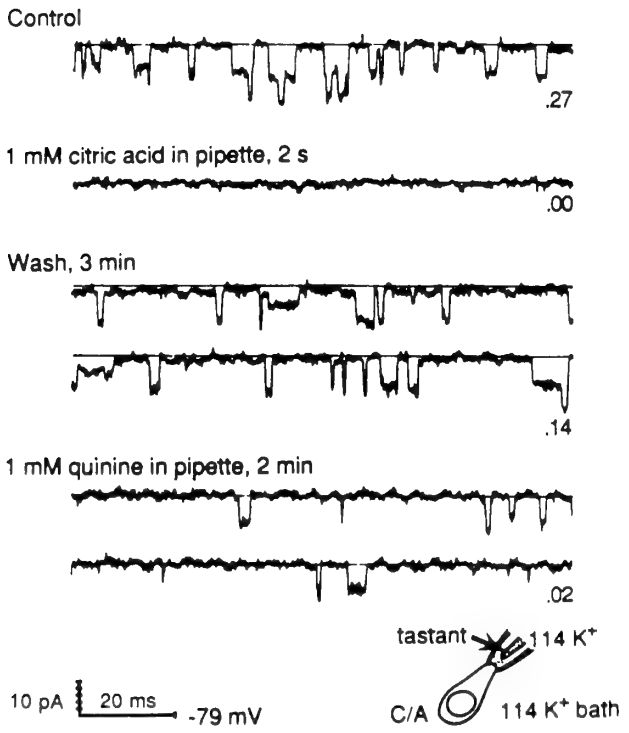

FIG. 16. Effect of citric acid and quinine, applied via pipette perfusion, on apical K^+ channels in a cell-attached patch of a mudpuppy taste cell. Citric acid and quinine block the channels directly. The recording pipette is put on the apical membrane and stimuli are also applied via the pipette perfusion (diagram at the bottom). From [17].

GUSTATORY TRANSDUCTION IN MAMMALIAN TASTE CELLS

1. *General properties of gustatory responses*

The taste cells are tightly packed in the taste bud. Taste buds in the tongue exist in three types of lingual papillae: fungiform, foliate and vallate. The fungiform papillae are located on the anterior two thirds of the tongue surface and are innervated by the chorda tympani nerve, which has higher sensitivity to salty and sweet tastes. The foliate and vallate papillae are located on the posterior and lateral surfaces of the tongue, respectively and are innervated by the glossopharyngeal nerve, showing higher sensitivity to sour and bitter tastes [79] (Fig. 17).

Ultrastructural observation indicates that four types of taste bud cells, dark (type I), light (type II), intermediate (type III) and basal cells, exist in a taste bud. It is believed that only type III cells which have synaptic contact with the gustatory nerve are gustatory cells, and basal cells situating at the bottom of taste bud are a stem cell of taste cells. Usually, type I, II and III cells excepting basal cells cannot be distinguished from one another by light microscopic figures. In electrophysiological studies with intracellular microelectrodes, taste bud cells are clarified into taste cells and non-taste cells by responsivity to taste stimuli [78]. Taste

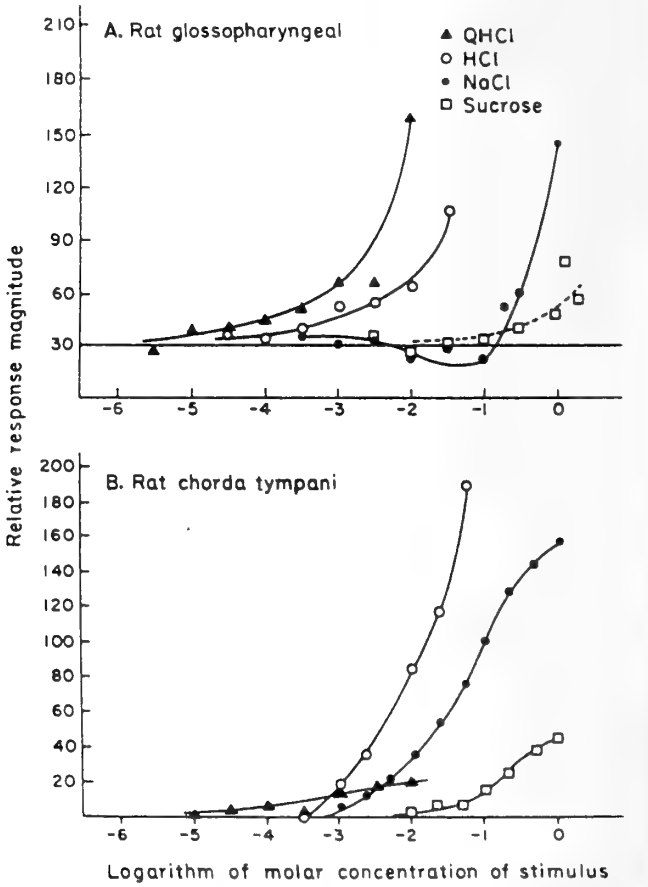

FIG. 17. Comparison of relative response magnitudes for rat glossopharyngeal and chorda tympani nerves. The responses in the two nerves are equated at 1 M NaCl. From [79].

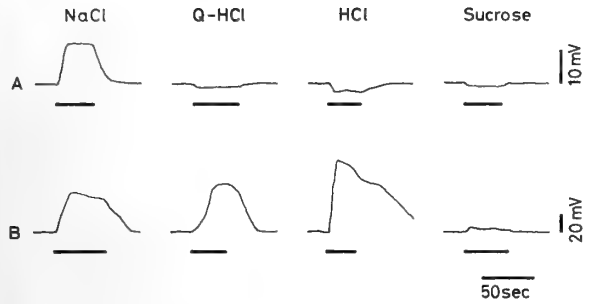

FIG. 18. Intracellularly recorded receptor potentials of rat taste cells in response to four basic taste stimuli. Taste stimuli: 0.5 M NaCl, 0.02 M Q-HCl, 0.01 M HCl, and 0.5 M sucrose. Horizontal bars under the records show the duration of stimulus application. The records A and B are obtained from two taste cells adapted to water. From [91].

cell responses consist of a depolarization, a hyperpolarization and an intermediate response [89, 91, 110, 112] (Fig. 18).

The resting potential and the input resistance of taste cells obtained by an intracellular recording method are −30 to −50 mV and 10 to 300 MΩ, respectively when the cells in rat and hamster are adapted to water [88]. The mean resting potential becomes small when adapted to saline solutions [89]. The whole-cell clamp experiments show that isolated rat taste cells have a zero-current potential of −50 to −70 mV, an input resistance of 1–3 GΩ and a membrane capacitance of 3–5 pF [11]. During gustatory stimulation with basic substances changes in input resistance of rat taste cells are shown in Table 1. The input resistance increases for all stimuli excepting salt stimuli [89, 94].

TABLE 1. Change in input resistance of rat taste cells at the peaks of receptor potentials elicited by four basic taste stimuli

Taste stimuli	Resistance (%)*	Receptor potential (mV)†	No. of cells
0.5 M NaCl	62±4	25±2	44
0.1 M $CaCl_2$	73±8	24±5	11
0.02 M Q-HCl	178±16	9±2	42
0.01 M HCl	148±8	11±2	34
0.5 M sucrose	138±12	3.4±2.5	26

* The values (mean±SE) are expressed as percent of control input resistance under 41.4 mM NaCl.
† The values are mean±SE under 41.4 mM NaCl adaptaion. From [89].

Spontaneous and tastant-induced firings of action potentials in mammalian taste cells are observed with the patch clamp method [11], but are not with the intracellular recording method [77, 88, 89, 94, 109, 110]. This discrepancy may be partially derived from inactivation of voltage-dependent channels by a damage-induced depolarization by a microelectrode [11]. The role of the action potentials is unclear, but these may be necessary for initiating a transmitter release under a low density of Ca^{2+} channels in mammalian taste cells [11]. At least five kinds of voltage-dependent ionic channels: TTX-sensitive Na^+ channel, transient K^+ channel, outwardly-rectifying K^+ channel, L- and T-type Ca^{2+} channels, and a ligand-dependent channel, amiloride-sensitive Na^+ channel are involved in the rat taste cell membrane [2, 11, 29, 102]. 4-aminopyridine-sensitive, tetraethylammonium-sensitive and cyclic-nucleotide-blockable channels are included in a group of K^+ channels [2, 11, 102].

2. Salty taste

Microelectrode studies suggest that depolarizations in response to salt stimuli are concerned with activation of cation channels accompanied with a decrease of membrane resistance [77, 89, 109]. Schiffman *et al.* [99] first suggested that the amiloride-sensitive Na^+ channels contribute to salty taste transduction in humans. This hypothesis has been supported by many neurophysiological experiments. Amiloride greatly suppresses the chorda tympani nerve responses to NaCl and LiCl, but does not the response to KCl [15, 20, 32, 65]. Recently, localization of amiloride-sensitive Na^+ channel at the apical membrane of taste cells is clarified by noninvasively recording action potentials and currents from a fungiform papilla [10, 28]. Therefore, it is primarily accepted that salt taste transduction occurs through amiloride-sensitive Na^+ channels in mammalian taste cells of the fungiform papillae (Fig. 19). Amiloride-sensitive Na^+ current is confirmed in isolated taste cells of hamster with whole-cell recording (Fig. 20) [29].

Since amiloride can not suppress the whole salt response, the residual salt response is possibly mediated by different

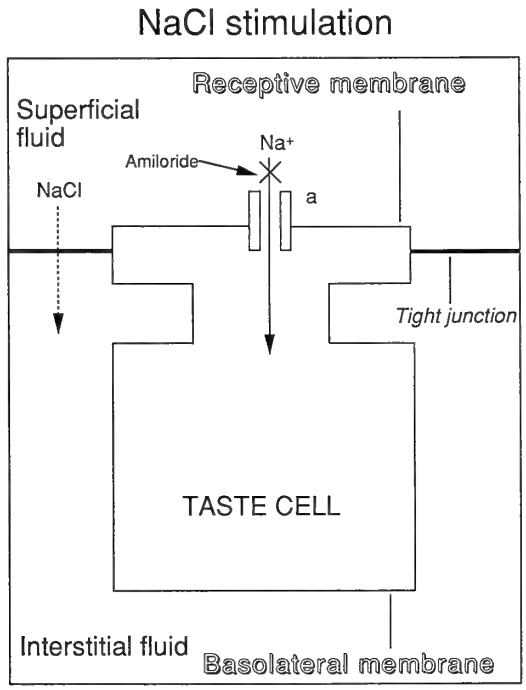

FIG. 19. Schematic drawing of salt signal transduction in mammalian taste cells. Na^+ directly passes through an amiloride-sensitive Na^+ channel (a). Both Na^+ and Cl^- are considered to pass through tight junction from mucosal side to serosal side, resulting in a transepithelial potential change (dotted arrow). From [118].

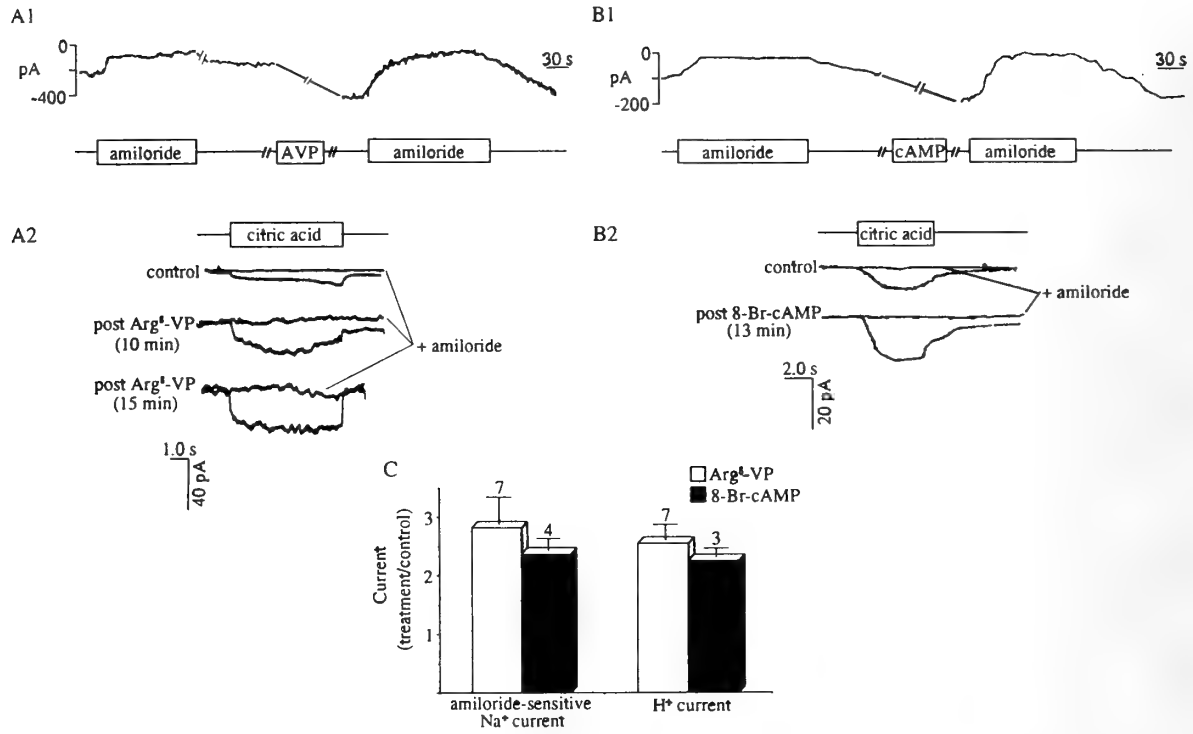

FIG. 20. Suppressive effect of amiloride on response of taste cells isolated from hamster fungiform papillae to citric acid and its enhancement by arginine-vasopressin (Arg^8-VP) and cAMP. Currents blocked by 30 μM amiloride (I_{Na}) are enhanced after treatment with Arg8-VP (AVP) (10 mU/ml for 15 min) (A1) or 0.25 mM 8-bromo-cAMP (cAMP or 8-Br-cAMP) (B1). Current responses to citric acid stimulation ($I_H{}^+$) are also enhanced following treatment with Arg^8-VP (A2) or 0.25 mM 8-Br-cAMP (B2). (C) Mean enhancement of I_{Na} and $I_H{}^+$ by Arg^8-VP and 8-Br-cAMP. From [29].

mechanisms. Amiloride sensitivity of several Na^+ salts is dependent on the size of the anions [23]. However, several anion channel blockers do not affect the salt responses of the chorda tympani nerve [21]. Therefore, Ye *et al.* [118] have proposed a hypothesis that field potentials generated by anion permeability through the pericellular pathway in the taste bud influence salt signal transduction (Fig. 19).

Amiloride-sensitivity of salt responses in the rat chorda tympani changes during development or after Na^+-deprivation [34]. Currents through amiloride-sensitive Na^+ channels in isolated hamster taste cells are enhanced by arginine-vasopressin and cAMP (Fig. 19) [29]. Similar plasticity of NaCl response is known in frog gustatory system [70]. These results suggest a great plasticity in density of amiloride-sensitive Na^+ channels in mammalian taste cells as in other Na^+-absorbing epithelia [114].

The glossopharyngeal nerve in mammals shows a low sensitivity to salts, and the salt response in glossopharyngeal nerve is never affected by amiloride [24]. This indicates that no amiloride-sensitive Na^+ channels are expressed in the taste cells of foliate and circumvallate papillae. The transduction of salt stimuli other than Na^+ salts has not been examined well so far with exception of suppression of KCl response by 4-AP, a potassium channel blocker, in rat chorda tympani nerve [37]. However, other potassium channel blockers such as tetraethylammonium, $BaCl_2$ and quinidine do not reduce KCl response. The suppression of KCl response by 4-AP is 40%. Thus, the mechanism mediating the residual response may be attributed to adsorption of cations and surface potential change on the taste cell membrane after 4-AP suppression [63, 64].

3. *Sour Taste*

For the transduction mechanism of sour taste, no conclusive model has been proposed. It is postulated that in hamster taste cells H^+ included in acid stimuli passes through amiloride-sensitive Na^+ channels, resulting in a depolarization of taste cells [28, 29] (Fig. 19). This hypothesis is consistent with the previous observation in rats [77]. However, amiloride blocks the response to both NaCl and HCl in hamster [33], but does not in monkey [32] and human [99]. Amiloride blocks HCl response in only sodium-selective nerve fiber carrying primarily the information for salty taste in hamster [33] and in rat [65]. Other pathways underlying the transduction mechanism for sour taste stimuli should be pursued in future even if amiloride-sensitive Na^+ channel pathway may play some role in sour taste transduction in mammals.

The decrease of membrane conductance during acid stimuli in rat taste cells has been observed with the intracellular recording method [89]. This might happen if the high density of K^+ channels is localized at the apical membrane [17, 27]. In addition, it should be noted that proton induces an increase of anionic conductance in lingual epithelia, result-

ing in a permeation of small cations in the paracellular pathway [100].

4. Bitter taste

Receptors coupled to G-protein and second messengers are believed to mediate gustatory responses to some bitter substances. Akabas *et al.* [1] have shown that a bitter substance, denatonium, increases an intracellular Ca^{2+} level in some taste cells of the circumvallate papillae in rat. The increased Ca^{2+} is suggested to be released from intracellular Ca^{2+} stores. Biochemical and histochemical studies have shown that IP_3 receptors are present on the endoplasmic reticulum in the apical membrane region of taste cells [35]. Other bitter substances, such as sucrose octaacetate and strychnine, also increase an IP_3 level in mouse taste cells [101]. These data suggest that a bitter substance activates G-protein coupled phospholipase C after binding to the receptor, causing an IP_3 production and a subsequent release of Ca^{2+} from intracellular stores. The released Ca^{2+} may trigger a transmitter release regardless of a depolarization of taste cell membrane (Fig. 21).

Another bitter substance quinine produces a depolarization accompanied by a decrease of the membrane conductance in rat taste cells [77, 89]. Quinine does not induce a Ca^{2+}-release from intracellular stores in taste cells of rat circumvallate papillae [35]. In mouse taste cells, denatonium strongly depresses voltage-dependent outward K^+ currents [102], whereas in rat taste cells denatonium, strychnine and 4-AP do not inhibit voltage-dependent K^+ currents [2]. In guinea-pig taste cells, denatonium does not induce any increase of intracellular Ca^{2+} level [76]. These findings indicate that there may be a species-specific variety in the transduction mechanisms of bitter taste stimuli.

Recently a taste-specific G-protein, gustducin is found, which leads to the activation of phosphodiesterase and in turn decreases the intracellular cAMP concentration [49]. Gustducin is believed to be a possible candidate for the mediator of bitter taste transduction. Amphiphilic substances including bitter and non-sugar sweeteners directly activate G-proteins reconstituted into phospholipid vesicles [62]. Multiple transduction pathways probably exist in bitter transduction mechanisms.

5. Sweet taste

Sweet transduction is related to receptor-mediated mechanisms. Two different models have been proposed to explain the transduction of sweet taste stimuli into a depolarization in taste cells. In the first model [103, 111], binding of sweet molecules to receptor followed by activation of G-

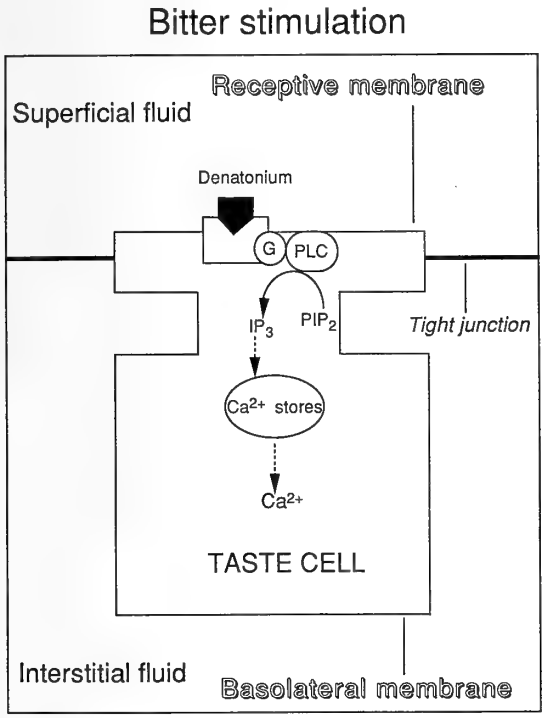

FIG. 21. Schematic drawing of bitter signal transduction in a mammalian taste cell. Bitter substance is thought to have a specific binding site. The formation of bitter substance-receptor molecule complex stimulates IP_3 production via G-protein-coupled PI-turnover. IP_3 induces Ca^{2+}- release from internal Ca^{2+}-stores, and the released Ca^{2+} directly triggers transmitter release without the membrane depolarization. G: G-protein, PLC: Phospholipase C, PIP_2: Inositol 4,5-biphosphate, IP_3: inositol 1,4,5-triphosphate. The data come from [1, 35, 101].

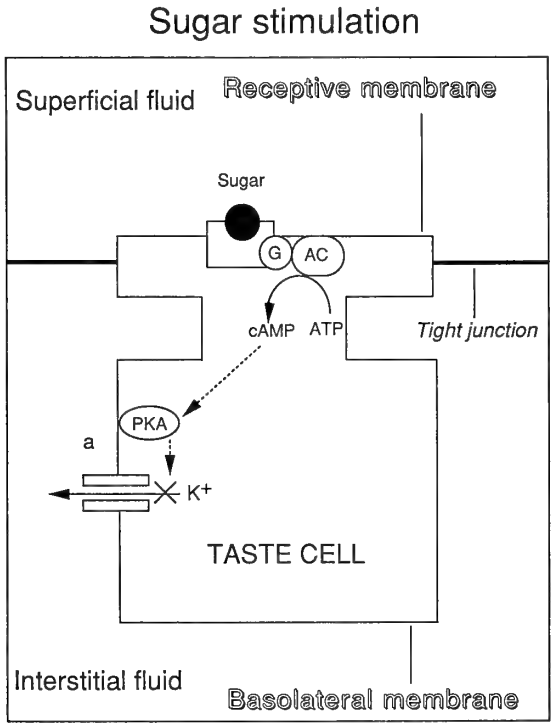

FIG. 22. Schematic drawing of sweet signal transduction in a mammalian taste cell. The binding of sugar to the specific receptor molecule stimulates G-protein-coupled cAMP-production sequence, resulting in activation of a cAMP-dependent protein kinase (PKA). The block (X) of K^+ channels (a) by phosphorylation via PKA induces a depolarization. G: G-protein, AC: Adenylate cyclase, PKA: cAMP-dependent protein kinase. The data come from [103, 111].

protein mediates activation of adenylate cyclase and production of cAMP. cAMP blocks a resting K^+ conductance by activation of protein kinase A, resulting in a depolarization in taste cells (Fig. 22). The second model [52] is that binding of sweet stimuli to receptors opens an amiloride-sensitive cation conductance, leading to a depolarization.

Sucrose induces a decrease or no change of the membrane conductance during depolarizing response in rat [89] and mouse taste cells [110]. Tonosaki and Funakoshi [111] observed a taste cell depolarization in response to an injection of cAMP or cGMP which is accompanied by a decrease of the membrane conductance. Biochemical studies show that sucrose causes a concentration-dependent rise in adenylate cyclase activity in the taste buds of rat [103], pig [61] and cattle [61]. The activation of adenylate cyclase by sucrose stimulation requires the presence of GTP [103] and is blocked by a specific sweet taste inhibitor [104]. Cummings *et al.* (1993) reported that nearly every taste bud responsive to sweeteners also responds to cyclic-nucleotides [18]. These results support the first model. However, biochemical studies indicate that saccharin does not stimulate adenylate cyclase activity in contrast to sucrose [61, 104]. Therefore, it is possible that natural and artificial sweeteners mediate differential transduction mechanisms [62].

Ozeki [77] indicates that sucrose induces an increase of ionic permeability in the rat taste cell membrane because of increase in the membrane conductance. It has been shown that sweeteners induce a short circuit current across the lingual epithelium and amiloride inhibits the chorda tympani response to sweeteners [52]. These results support the second model. The same mechanism is insisted in human sweet taste [99]. In contrast, there are many negative reports in which amiloride or cations in the mucosal solution never affect the responses to sweeteners in mouse [112], hamster [11, 33] or monkey [32]. Amiloride-insensitive conductance located at the basolateral membrane of taste cell may be activated by sugar stimuli.

Recently investigation using northern blot analysis and *in situ* hybridization demonstrates that amiloride-sensitive Na^+ channels are expressed in not only gustatory but also non-gustatory tissue of the lingeal epithelial layer [46]. This means that a large amount of Na^+ is transported from mucosal solution to interstitial fluid through amiloride-sensitive Na^+ channels in taste and non-taste cells when a high concentration of Na^+ is exposed to mucosal side. Tastant is known to induce a secretion of saliva containing more than 10 times the basal concentration of Na^+ [46], and consequently amiloride-sensitive Na^+ channels can modulate the responses to all tastants including sweeteners.

Recently another sweet taste transduction pathway has been proposed with gerbil taste cells [113]. It has been suggested that some sweet amino acids increase intracellular IP_3, and release Ca^{2+} from the internal store, and the released Ca^{2+} may directly release a transmitter substance from taste cells.

ACKNOWLEDGMENTS

This work was supported in part by Grants-in Aid for Special Project Research, Co-operative Research, Developmental Scientific Research and Scientific Research from the Ministry of Education, Science and Culture of Japan, and by Grant-in-Aid from the Human Frontier Science Program Organization.

REFERENCES

1 Akabas M H, Dodd J, Al-Awqati Q (1988) Science 242:1047–1050
2 Akabas M, Dodd J, Al-Awqati Q (1990) J Membr Biol 114:71–78
3 Akaike N, Sato M (1976) Comp Biochem Physiol 55A: 383–391
4 Akaike N, Noma A, Sato M (1976) J Physiol 254: 87–107
5 Avenet P, Lindemann B (1987) J. Membr Biol 97: 223–240
6 Avenet P, Hoffman F, Lindemann B (1988) Nature 331: 351–354
7 Avenet P, Hoffman F, Lindemann B (1988) Comp Biochem Physiol 90A: 681–685
8 Avenet P, Lindemann B (1988) J Membr Biol 105: 245–255
9 Avenet P, Lindemann B (1989) Membr Biol 112: 1–8
10 Avenet P, Lindemann B (1991) J Membr Biol 124:33–41
11 Béhé P, DeSimone J A, Avenet P, Lindemann B (1990) J Gen Physiol 96: 1061–1084
12 Bigiani A R, Roper S D (1991) Science 252: 126–128
13 Bigiani A R, Roper S D (1993) J Gen Physiol 102: 143–170
14 Bowerman A G, Kinnamon S C (1994) Chem Senses 19: 303–315
15 Brand J G, Teeter J H, Silver W L (1985) Brain Res 334: 207–214
16 Cummings T A, Delay R J, Roper S D (1987) J Comp Neurol 261: 604–615
17 Cummings T A, Kinnamon S C (1992) J Gen Physiol 99: 591–613
18 Cummings T A, Powell J, Kinnamon S C (1993) J Neurophysiol 70: 2326–2336
19 Delay R J, Taylor R, Roper S D (1993) J Comp Neurol 335: 606–613
20 DeSimone J A, Heck G L, Mierson S, DeSimone S K (1984) J Gen Physiol 83: 633–656
21 Elliott J E, Simon S A (1990) Brain Res 535: 9–17
22 Ewald D A, Roper S D (1992) J Neurophysiol 67: 1316–1324
23 Formaker B K, Hill D L (1988) An analysis of residual NaCl taste response after amiloride. Am J Physiol 255: R1002–R1007
24 Formaker B K, Hill D L (1991) Physiol Behav 50: 765–769
25 Fujiyama R, Miyamoto T, Sato T (1993) NeuroReport 5: 11–13
26 Fujiyama R, Miyamoto T, Sato T (1994) In "Olfaction and Taste XI" Ed by K Kurihara, N Suzuki, H Ogawa, Springer-Verlag, Tokyo, p 109
27 Fujiyama R, Miyamoto T, Sato T (1995) Pflügers Arch: in press
28 Gilbertson T A, Avenet P, Kinnamon S C, Roper S D (1992) J Gen Physiol 100: 803–824
29 Gilbertson T A, Roper S D, Kinnamon S C (1993) Neuron 10: 931–942
30 Gilbertson T A (1993) Current Opinion Neurobiol 3: 532–539
31 Graziadei P P C, DeHan R S (1971) Acta Anat 80: 563–603
32 Hellekant G, DuBois G E, Roberts T W, Wel H van der (1988)

Chem Senses 13: 89–93
33 Hettinger T P, Frank M E (1990) Brain Res 513: 24–34
34 Hill D L, Mistretta C M (1990) Trends Neurosci 13: 188–195
35 Hwang P M, Verma A, Bert D S, Snyder S H (1990) Proc Natl Acad Sci USA 87: 7395–7399
36 Jaeger C B, Hillman (1976) In "Frog Neurobiology" Ed by R Linas, W Precht, Springer-Verlag, Berlin, pp. 588–606
37 Kim M, Mistretta C M (1993) Brain Res 612: 96–103
38 Kinnamon S C, Roper S D (1987) J Physiol 383: 601–614
39 Kinnamon S C, Roper S D (1988) J Gen Physiol 91: 351–371
40 Kinnamon S C, Roper S D (1988) Chem Senses 13: 115–121
41 Kinnamon S C (1988) Trends Neurosci 11: 491–496
42 Kinnamon S C, Dionne V E, Beam K G (1988) Proc Natl Acad Sci USA 85: 7023–7027
43 Kinnamon S C, Getchell T. (1991) In "Smell and Taste in Health and Disease" Ed by T V Getchell, R L Doty, L M Bartoshuk, J B Snow Jr, Raven Press, New York, pp 145–172
44 Kinnamon S C, Cummings T A (1992) Annu Rev Physiol 54: 715–731
45 Kurihara K (1990) Jpn J Physiol 40: 305–324
46 Li X-J, Blackshaw S, Snyder S H (1994) Proc Natl Acad Sci USA 91: 1814–1818
47 Margolskee R F (1993) BioEssays 15: 645–650
48 McBride D W Jr, Roper S D (1991) J Membr Biol 124: 85–93
49 McLaughlin S K, McKinnon P J, Margolskee R F (1992) Nature 357: 563–569
50 McPheeters M, Roper S D (1985) Chem Senses 10: 341–352
51 McPheeters M, Barber A J, Kinnamon S C, Kinnamon J C (1994) J Comp Neurol 346: 601–612
52 Mierson S, DeSimone S K, Heck G L, DeSimone J A (1988) J Gen Physiol 92: 87–111
53 Miyamoto T, Okada Y, Sato T (1988) J Physiol 405: 699–711
54 Miyamoto T, Okada Y, Sato T (1988) Brain Res 449: 369–372
55 Miyamoto T, Okada Y, Sato T (1989) Comp Biochem Physiol 94A: 591–595
56 Miyamoto T, Okada Y, Sato T (1991) Zool Sci 8: 835–845
57 Miyamoto T, Okada Y, Sato, T, Yamada Y, Brand J G, Teeter J H (1992) Chem Senses 17: 112
58 Miyamoto T, Okada Y, Fujiyama R, Sato T (1992) Jpn J Physiol 42 (Suppl): S204
59 Miyamoto T, Okada Y, Sato T (1993) Comp Biochem Physiol 106A: 489–493
60 Miyamoto T, Fujiyama R., Okada Y, Sato T (1994) In "Olfaction and Taste IX" Ed by K Kurihara, N Suzuki, H Ogawa, Springer-Verlag, Tokyo , p 108
61 Naim M, Ronen T, Striem B J, Levinson M, Zehavi U (1991) Comp Biochem Physiol 100B: 455–458
62 Naim M, Seifert R, Nürnberg B, Grünbaum L, Schulz G (1994) Biochem J 297: 451–454
63 Nakamura M, Kurihara K (1990) Brain Res 524: 42–48
64 Nakamura M, Kurihara K (1991) Comp Biochem Physiol 100A: 661–665
65 Ninomiya Y, Funakoshi M (1988) Brain Res 451: 319–325
66 Okada Y, Miyamoto T, Sato T (1986) Jpn J Physiol 36: 139–150
67 Okada Y, Miyamoto T, Sato T (1987) Comp Biochem Physiol 88A: 487–490
68 Okada Y, Miyamoto T, Sato T (1987) Biochim Biophys Acta 904: 187–190
69 Okada Y, Miyamoto T, Sato T (1988) Brain Res 450: 295–302
70 Okada Y, Miyamoto T, Sato T (1991) Comp Biochem Physiol 100A: 693–696
71 Okada Y, Miyamoto T, Sato T (1992) J Exp Biol 162: 23–36
72 Okada Y, Miyamoto T, Sato T (1993) J Exp Biol 174: 1–17
73 Okada Y, Miyamoto T, Sato T (1993) Comp Biochem Physiol 106A: 37–41
74 Okada Y, Miyamoto T, Sato T (1993) Comp Biochem Physiol 105A: 725–728
75 Okada Y, Miyamoto T, Sato T (1994) J Exp Biol 187: 19–32
76 Orola C N, Yamashita T, Harada N, Amano H, Ohtani M, Kumazawa T (1992) Acta Otolaryngol 112: 120–127
77 Ozeki M (1971) J Gen Physiol 58: 688–699
78 Ozeki M, Sato M (1972) Comp Biochem Physiol 41A: 391–407
79 Pfaffmann C, Fisher G L, Frank M K (1967) In "Olfaction and Taste II" Ed by T Hayashi, Pergamon Press, Oxford, pp 361–381
80 Richter H -P, Avenet P, Mestres P, Lindemann B (1988) Cell Tissue Res 254: 83–96
81 Roper S D (1983) Science 220: 1311–1312
82 Roper S D (1989) Annu Rev Neurosci 12: 329–353
83 Roper S D, McBride D W Jr (1989) J Membr Biol 109: 29–39
84 Roper S D (1992) J Neurosci 12: 1127–1134
85 Samanen D W, Bernard R A (1981) J Comp Physiol A 143: 151–158
86 Sata O, Okada Y, Miyamoto T, Sato T (1992) Comp Biochem Physiol 103A: 99–103
87 Sato T, Beidler L M (1978) J Gen Physiol 66: 735–763
88 Sato T (1980) Prog Neurobiol 14: 25–67
89 Sato T, Beidler L M (1982) Comp Biochem Physiol 73A: 1–10
90 Sato T, Sugimoto K, Okada Y (1982) Jpn J Physiol 32: 459–462
91 Sato T, Beidler L M (1983) Comp Biochem Physiol 75A: 131–137
92 Sato T, Ohkusa M, Okada Y, Sasaki M (1983) Comp Biochem Physiol 76A: 233–239
93 Sato T, Sugimoto K, Okada Y, Miyamoto T (1984) Jpn J Physiol 34: 973–983
94 Sato T (1986) Prog Sensory Physiol 6: 1–37
95 Sato T, Okada Y, Miyamoto T (1987) Ann N Y Acad Sci 510: 23–26
96 Sato T, Okada Y, Miyamoto T (1989) In "Chemical Senses Vol. 1, Receptor Events and Transduction in Taste and Olfaction" Ed by J G Brand, J H Teeter, R H Cagan, M R Kare, Marcel Dekker, New York, pp 115–136
97 Sato T, Okada Y, Miyamoto T (1994) Physiol Behav 56: in press
98 Sato T, Okada Y, Miyamoto T (1994) In "Olfaction and Taste XI" Ed by K Kurihara, N Suzuki, H Ogawa, Springer-Verlag, Tokyo, pp 96–99
99 Schiffman S S, Lockhead E, Maes F W (1983) Proc Natl Acad Sci USA 80: 6130–6140
100 Simon S A, Garvin J L (1985) Am J Physiol 249:C398–C408
101 Spielman A I, Huque T, Whitney G, Brand J G (1992) In "Sensory Transduction" Ed by D P Corey, S D Roper, Rockefeller University Press, New York, pp 307–324
102 Spielman A I, Mody I, Brand J G, Whitney G, MacDonald J F, Salter M W (1989) Brain Res 503:326–329
103 Striem B J, Pace U, Zehavi U, Naim M, Lancet D (1989) Biochem J 260:121–126
104 Striem B J, Yamamoto T, Naim M, Lancet D, Jakinovich W Jr, Zehavi U (1990) Chem Senses 15: 529–536
105 Striem B J, Naim M, Lindemann B (1991) Cell Physiol Biochem 1:46–54
106 Sugimoto K, Teeter J H (1990) J Gen Physiol 96: 809–834
107 Sugimoto K, Teeter J H (1991) Chem Senses 16: 109–122

108 Taylor R, Roper SD (1994) J Neurophysiol 72: 475–478
109 Tonosaki K, Funakoshi M (1984) Comp Biochem Physiol 78A:651–656
110 Tonosaki K, Funakoshi M (1984) Chem Senses 9:381–387
111 Tonosaki K, Funakoshi M (1988) Nature 331:354–356
112 Tonosaki K, Funakoshi M (1989) Comp Biochem Physiol 92A:181–183
113 Uchida Y, Miyamoto T, Sato T (1994) Chem Senses 19: in press
114 Van Driessche W, Zeiske W (1985) Physiol Rev 65:833–903
115 West C H K, Bernard R A (1978) J Gen Physiol 72: 305–326
116 Witt M (1993) Cell Tissue Res 272: 59–70
117 Yang J, Roper S D (1987) J Neurosci 7: 3561–3565
118 Ye Q, Heck G L, DeSimone J A (1993) J Neurophysiol 70:167–178

ZOOLOGICAL SCIENCE 11: 781–795 (1994)

REVIEW

Regeneration and Pattern Formation in Planarians: Cells, Molecules and Genes

JAUME BAGUÑÀ, EMILI SALÓ, RAFAEL ROMERO, JORDI GARCIA-FERNÀNDEZ, DAVID BUENO, ANNA MA MUÑOZ-MARMOL, JOSE RAMON BAYASCAS-RAMIREZ AND ANDREU CASALI

Departament de Genètica, Facultat de Biologia, Universitat de Barcelona, Diagonal 645, 08071 Barcelona, Spain

ABSTRACT—The process of regeneration in freshwater planarians (Platyhelminthes; Turbellaria; Tricladida) is reviewed. Long-standing questions such as time and role of wound healing, the origin of blastema cells and the time and mode of determination of lost structures have come to be solved in recent years due to the use of old and new cell labelling and transplantation methods. In most turbellarian species wound healing occurs in less than 1 hour. Sound evidence has been produced to support the origin of blastema cells from undifferentiated stem-cells or neoblasts, and determination of lost structures takes place during the first two days of regeneration following a disto-proximal sequence. These results suggest that epithelial-mesenchymal interactions, brought up by wound healing, may be instrumental, through cell-cell interactions or activating transient morphogenetic gradients, in setting the early pattern of lost structures upon the equivalent blastema and postblastema cells. We are fully ignorant, however, on the molecular nature of substances playing such roles as well as on how positional information along the antero-posterior and dorso-ventral axes is set and maintained in the intact organism and reset again and transmitted to blastema cells in regenerating organisms.

Molecular biology and recombinant DNA techniques brought into the field of planarian regeneration in the last 10 years have opened new research perspectives but produced limited results. As expected, signals, receptors and transducing molecules which activate cell proliferation and differentiation in planarians were found to be not different to those known to operate in other activated systems. Instead, monoclonal antibodies (mAbs) against positional specific antigens have recently been obtained and found to be very sensitive to changes in positional values during regeneration. Homeobox containing genes, namely those belonging to the HOM/Hox Antennapedia class have been detected and sequenced in different species. Whether or not they are clustered in the genome, how are they expressed along the antero-posterior body axis in both intact and regenerating organisms, and how are they linked to the positional markers detected by mAbs are key questions to answer and a matter of intense research. Finally, the recent finding of active transposable elements in some species of planarians opens the way to obtain transformed neoblasts and, ultimately, transgenic planarians. When available, this would represent an extremely useful tool to study cell lineage, as well as to test the function of cloned genes and to induce loss and gain of function mutations. Based on these results and perspectives, a new research agenda is suggested.

GENERAL MORPHOLOGICAL AND FUNCTIONAL BACKGROUND

Because of their high regenerative power, planarians have been one of the favorite organisms for studying the cellular and molecular mechanisms leading to pattern restoration. With the exception of hydras, it is difficult to think of any other organisms which are able to regenerate a new individual from a tiny fragment (down to 1/300th according to Morgan [67] or approximately to 1×10^4 cells according to Montgomery and Coward [64]) of their bodies. This has generated a continuous, though a bit rambling, interest to study the cellular and molecular basis of such process in planarians. However, despite almost a century of intensive studies and the existence of a vast literature on the subject, several problems remain still unsolved and no general model has been produced and accepted.

Among planarians, freshwater triclads (phylum Platyhelminthes, class Turbellaria, order Seriata, suborder Tricladida) are the best known animals due to their easy culture and handling under laboratory conditions. They have been and still are, the most widely used turbellarian in experimental research of regeneration (see [6, 9, 12, 36] for general references). Freshwater planarians are characterized by being triploblastic, acoelomates, unsegmented organisms and by the lack of circulatory, respiratory and skeletal structures. They belong to the first group of organisms with defined bilateral symmetry, antero-posterior polarity and centralized (brain ganglia) nervous system with longitudinal nerve cords and sense organs. The digestive system consists of a pharynx and a blind, three-branched and diverticulated gut lacking an anus. A solid mass of tissue, the parenchyma,

Received November 7, 1994

fills the space between the cellular monostratified ciliated epidermis and the gut, and surrounds the internal organs. The parenchyma consists of several non-proliferating differentiated cell types and a particular class of undifferentiated, mitotic, multipotential stem cells, usually called neoblasts [4, 7, 27]. In cellular terms, planarians can be considered to be made of two main compartments: 1) a proliferative compartment formed by a single, morphologically identifiable, population of multipotent stem-cells or neoblasts (approx. 20–30% of the total number of cells) which give rise, by differentiation, to all differentiated functional cell types, while maintaining its own population by cell proliferation [3, 51, 52] and 2) a functional compartment, made by 12–15 non-proliferating differentiated cell types (approx. 75–80% of total cells) that are continuously replaced during the life-time of the individual. The stem-cell nature of neoblasts have been demonstrated by light and electron microscopy studies of differentiation in several cell types of freshwater triclads (epidermal cells: [27, 41, 100]; rhabdite cells [40, 55]; muscle cells [41, 69, 97]; nerve cells [96]; gastrodermal cells [42]; germ cells[35]) as well as in some species of different orders of Turbellaria and Cestoda using thymidine labelling [24, 25, 80, 108].

Besides their ample power of regeneration, freshwater planarians are also known for their ability to grow and to shrink in volume and length continuously, depending on body size, temperature, and food availability. Quantitative cellular studies of both processes have shown that they depend on the daily balance between cells born by cell proliferation and cells lost by cell lysis and death [5, 85, 86]. When temperature and food are kept at the optimum (which varies for different species) planarian remains in steady-state since a balance holds between the number of cells (neoblasts) produced by proliferation and the number of cells lost from the functional compartment [85]. Several lines of evidence (see below) indicate that the neoblasts of the intact organism, which mainly function as the stem cells for daily cell renewal [4], are similar (actually identical) to the undifferentiated cells of the regenerative blastema, the latter arising directly from the former [91, 93].

REGENERATION: A BRIEF OUTLINE

When a planarian is cut, the epithelium around the wound rapidly closes up (due to the contraction of the underlying circular and longitudinal muscles) and a thin film of epidermal cells from the stretched old epidermis covers it. Below the wound epithelium (which does not proliferate), groups of undifferentiated cells aggregate to form a few layers of cells. These cells increase in number by the basal addition of new undifferentiated cells formed by cell division in the underlying parenchyma. At one day of regeneration, this accumulation of undifferentiated cells is externally visible due to its unpigmented character, and is called the regenerative blastema. In subsequent days, the blastema grows exponentially due to a combination of cell migration and cell proliferation [91, 93]. Several studies have shown that despite growing in size and cell number, blastema cells do not divide [70, 91]. From this, it has been suggested that blastema grows by the continuous entrance at its base of undifferentiated cells, produced by cell division in the old stump (postblastema). Using chromosomal ploidy, and fluorescent markers [93] it has been shown that cells forming the blastema are of local origin; that is, cells originally placed farther than 500 μm from the wound boundary are barely detected in 3- and 5-days old blastemata. After 4–6 days of regeneration, new structures are differentiated within the blastema and postblastema areas following a disto-proximal sequence. The lost structural pattern is thus restored and normal body proportions are finally attained after 3–4 weeks of regeneration.

REGENERATION: THE UNSOLVED QUESTIONS

Although some of the unsolved problems of planarian regeneration have been reviewed recently [6, 9, 36], we would like to consider some of the hottest points of uncertainty, new results bearing on them, and new research strategies addressed to answer them. Standing among them, we will discuss the time and role of wound healing, the origin of blastema cells, the spatial and temporal sequences of pattern determination, and the molecules and genes presumably involved in positional signaling and pattern formation.

Wound healing

Although some literature exists on the timing of wound healing in planarians, no agreement has been reached on the precise time when healing is complete and (if any) on its functional role. Although both questions would appear to be trivial, it seem not to be so if we consider the possible roles of epithelial-mesenchymal interactions in early pattern formation and whether or not an asymmetrical covering by the wound epithelium [18] plays any role in establishing the antero-posterior polarity of the regenerant.

Estimates of the timing of wound healing in freshwater triclads range from 10–15 min [18] or 30–45 min [90], to several hours and even days (see [82, 103] for references). In the microturbellarian *Microstomum lineare* (order Macrostomida) a thin wound epidermis with widely spaced cilia and microvilli covers the whole wound area one hour after cutting [78]. Using light microscopy and scanning electron microscopy (Fig. 1), we have shown in the triclads *Dugesia(G)tigrina*, *Dugesia(G)polychroa* and *Dugesia(D)gonocephala* that healing is complete within 30 min after cutting [6, 90]. This supports the earlier values reported by Chandebois [18]. In our view, longer healing times in most of reports were due to unproper fixation methods that burst the delicate film of wound epithelium giving the false impression of non healed wounds.

As the wound epithelium no longer adheres to the basement membrane of the stump epidermis but lies over parenchymal tissues, the stage is set for epithelial-mesenchymal interactions to occur. These interactions may

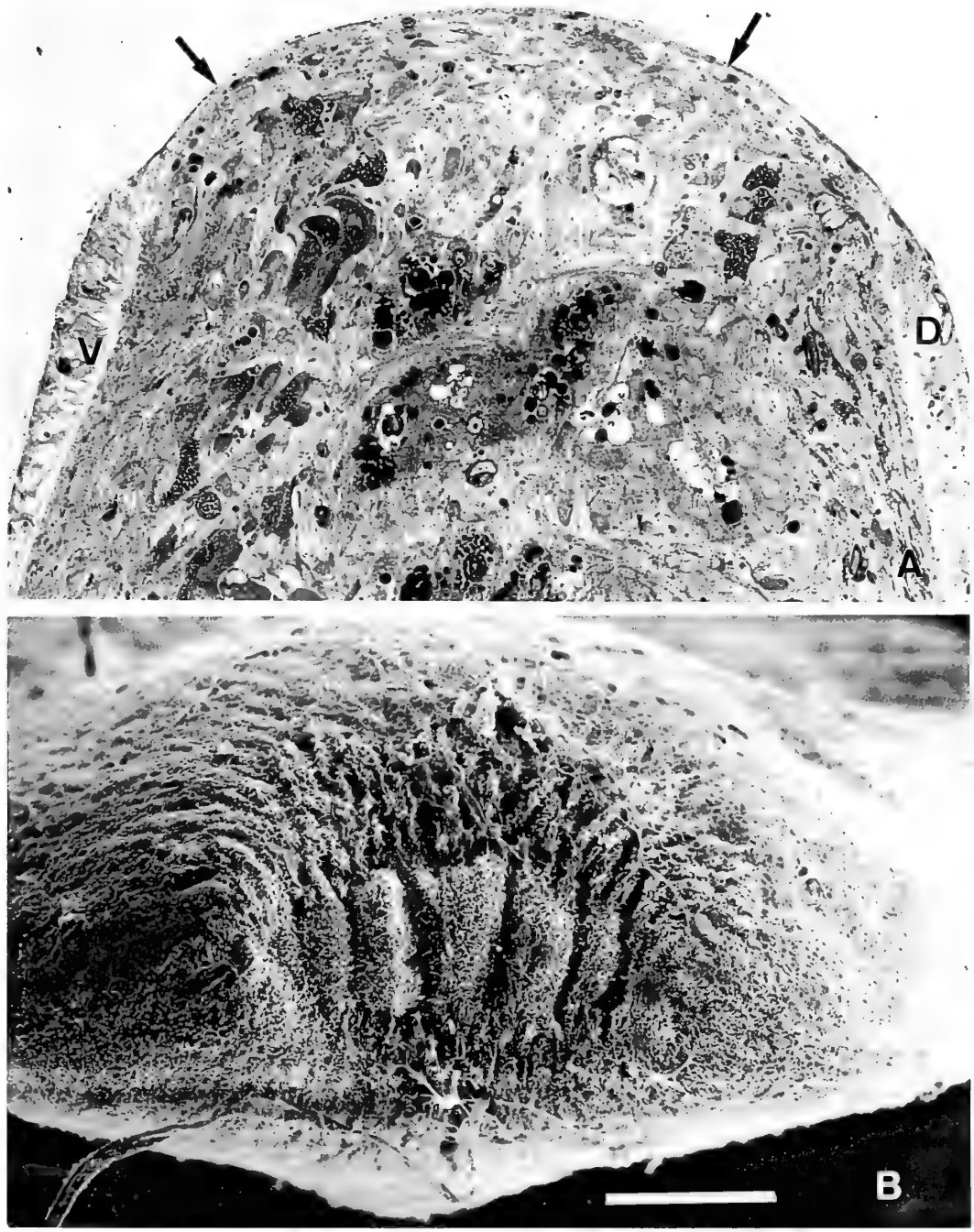

FIG. 1. A. Light micrograph of a tail fragment of *Dugesia(S)polychroa* one hour after cutting. Sagittal section. Arrows point to the very thin stretched wound epithelium. D: dorsal epithelium; V: ventral epithelium. ×1000. B. Scanning electron micrograph (SEM) of the wound area of *Dugesia(D)gonocephala* one hour after cutting. Frontal view. The wound is already covered by a ciliated epithelium. Bar, 100 μm. Dorsal is to the top, ventral to the bottom.

play a dual role. First, as it has been shown in different developmental and regenerating systems [19, 88], the epithelium induces the expression of several homeobox-containing genes in mesodermal cells. These genes seem important to maintain cell proliferation and to set early pattern formation. In turn, the mesoderm seems to be crucial to maintain the integrity of the epithelium. Second, as first suggested by Chandebois [18] in regenerating planarians, an asymmetrical covering of the stump by the wound epithelium (dorsal epithelium covering it in anterior regeneration, ventral in posterior regeneration) would suggest a key role for such tissue in maintaining the antero-posterior polarity and in setting early pattern formation. This model assumes extreme antero-posterior positional values for dorsal and ventral epidermis respectively.

The role of epithelial-mesenchymal interactions in re-

generating planarians has so far not been substantiated. The use of potential inhibitors of such interactions (e.g. cytochalasin B, Concanavalin A) and the induction of supernumerary structures by barrier insertions gave no clear answers (Ribas and Baguñà, unpublished data). Moreover, no candidate molecule and/or gene have so far been spotted. At present, a sound approach to find them would be to screen cDNA planarian libraries with degenerate oligonucleotides to the conserved regions of the msh-homeobox containing genes, present from hydras to vertebrates (Saló *et al.*, work in progress). Another set of interesting genes to search would be the planarian homologues of genes such as *hedgehog* of *Drosophila* and *Sonic hedgehog* of Vertebrates that belong to the Transforming Growth Factor Beta (TGF-β) superfamily, as well as members of the Fibroblast Growth Factor (FGF) family. Products of these genes have been shown to play key roles in establishing the antero-posterior polarity in the development of *Drosophila* imaginal discs and in limb bud formation in Vertebrates [45, 48] through epithelial-mesenchymal interactions.

Evidence for asymmetrical covering is pervasive [18] but only indirect, and new approaches (e.g. regenerating chimaeric double-dorsal and double-ventral organisms [6]) have not been attempted. To validate Chandebois' proposal of asymmetrical covering, differential labelling of dorsal and ventral epidermis is needed. From a collection of monoclonal antibodies (mAbs) obtained against antigens of the intact planarian *Dugesia(G)tigrina*, several epithelium-specific mAbs were obtained. Among them, EPI-1 stains specifically the dorsal epithelium, and EPI-2 the ventral one (Bueno, Baguñà and Romero, unpublished data) though their expression during wound healing has not been studied. Mechanical influences of wound healing on pattern formation processes should not be overlooked. Mead [61, 62] has shown that short antero-posterior fragments made by two transverse cuts across the body were more likely to regenerate abnormally (e.g. two heads, abnormal heads) when the interval between the two cuts was 5 or 12 min than when it was 1.5 min. These results indicate that events occurring shortly after a cut is made significantly affect structure patterning and proportioning of the regenerate. As muscle contraction plays a major role in bringing the two epithelia together, it would be interesting to study how the three-dimensional pattern of muscle layers in the head and tail regions, may affect differentially the pattern of wound closure. This is being studied by double-staining of muscle cells with phalloidin-rhodamine and the muscle-specific monoclonal antibody TMUS-13 (Romero, Cebrià and Baguñà, unpublished data).

The origin of blastema cells

In most regenerating systems, blastema cells arise by dedifferentiation of functional cells. In planarians, it has been a matter of debate whether dedifferentiated cells or a population of undifferentiated cells, the neoblasts, are the main source of blastema cells. In the last fifty years, this issue has been polarized into what is called the "neoblasts versus dedifferentiation" controversy, between the so-called "neoblast theory" and the "dedifferentiation theory" (see [4, 101] for a statement on the controversy, and [6, 9, 36] for general reviews). Although in the the last decade several evidence was obtained for each theory (see [37] for the dedifferentiation theory, and [7] for the neoblast theory), the issue is still unresolved. Meanwhile, careful electron microscopy studied have failed to provide evidence for dedifferentiation, but have strongly supported the differentiation of several differentiated cell types from neoblasts. A definite proof of the exclusive (or even a main) role of neoblasts awaits a differential and permanent marking of neoblasts and differentiated cells and tracing the lineage of these cells (see below) in both intact and regenerating organisms.

As a way to obtain such markers, several attempts for raising monoclonal antibodies specific to neoblasts have been undertaken. So far, all of them proved unsuccesful [87, 99]. A more fruitful and simpler approach may be to purify neoblasts from a specific donor strain, to stain them either with the lipophilic dyes DiI and DiO or with the nuclear stains DAPI or Hoetsch 33243, and to introduce such cells into irradiated organisms of a host strain following the method described in Baguñà *et al.* [7]. At different periods after injection, the number and types of labelled cells, clonally derived from each injected donor neoblast, could be monitored and its potentialities assessed. Conversely, purified differentiated cells from donor strains may also be stained with such dyes and their capacity to dedifferentiate, both in intact and regenerating organisms, may be determined following identical procedures. Suspensions of neoblasts and differentiated cells are easily stained with DiI and DAPI. Injected neoblasts proliferate into hosts tissues, form clones of different sizes, and several labelled differentiated cell types appear at the edges of the clone (Cebrià, Romero and Baguñà, unpublished observations). When DiI-labelled differentiated cells were injected, no cells were seen to dedifferentiate and the cells fade away in 15–20 days due to the normal cell turnover. In agreement with the "neoblast theory", these results support a main role of neoblasts both in the daily cell turnover and as a source of blastema cells during regeneration.

Pattern formation during regeneration or when, where and how are antero-posterior structures determined

By pattern formation during regeneration we mean the spatio-temporal laying down of the lost structures, and the cellular, molecular and genetic mechanisms involved in it. The main points of debate are when and where groups of cells which are to become particular regions, organs or tissues of the regenerant are determined, whether this process occurs sequentially or simultaneously along the body axes and, in the former case, whether it does in a proximo-distal or disto-proximal direction.. Moreover, which genes control it is the ultimate, and main, unsolved question. Despite decades of intense research, pattern formation in planarians is very

poorly understood. Some models have been proposed and some molecules invoked (see [12, 63, 110, 111] for general references). However, twenty five years after being proposed, none of the models have been substantiated and none of the postulated molecules have ever been isolated.

Determination of missing anterior structures in caudal regenerants was studied [90] using transplantation methods previously used in hydra to estimate determination of head structures [58]. Two set of experiments were carried out. First, heads were grafted at different positions along the antero-posterior body axis of an anteriorly cut organism to estimate when the grafted head no longer inhibits the regeneration of a new head (time of head determination) or a new pharynx (time of pharynx determination) in the host (Fig. 2). Second, blastemata at different stages of regeneration were grafted to regenerating host organisms to estimate its ability to inhibit the regeneration of a new head in the host (Fig. 3). This inhibitory capacity would indicate when the grafted blastema is determined to be a head. The first set of experiments showed that head determination in anteriorly regenerating organisms is a very early event (3–12 hr at 24°C, 6–24 hr at 17°C) whereas determination of the pharynx occurs slightly later (12–36 hr), both happening within a narrow strip of tissue (0–500 μm) below the wound when the blastema has not been formed or is barely visible [90]. The second set of experiments showed that the inhibitory capacity of blastemal structures increases steadily (20 to 32 hr old blastemas), long before overt differentiation starts (3–4 days). As regards the spatial laying down of new structures, it is important to point out that head ganglia appear within the blastema itself or at the junction between blastema and postblastema, whereas other structures such as the pharynx are entirely patterned within the old stump (postblastema) area. These results suggested a mixed morphallactic-epimorphic model of pattern formation in planarians with an early morphallactic phase in which pattern is set in a disto-proximal sequence within a narrow strip of tissue below the wound to be amplified later on by epimorphosis [91]. As regards particular mechanisms to set the pattern, either cell-cell interactions driven by early epithelial-mesenchymal interactions during wound healing, or transient gradients of morphogenetic substances set by an still undisclosed mechanism, could be envisaged though no data has so far been obtained to support any of them.

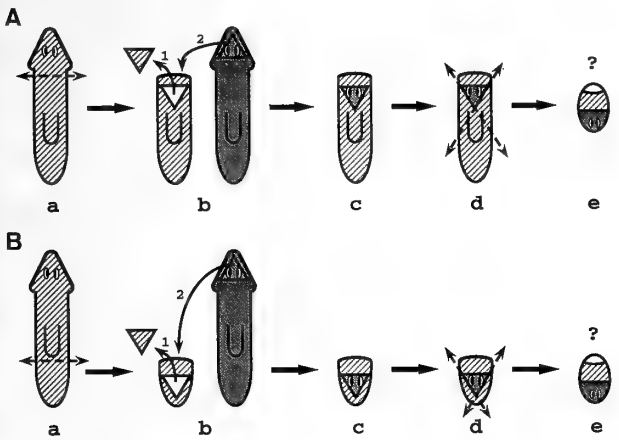

FIG. 2. Grafting method used to estimate the period when the head is determined in postcephalic (A) and postpharyngeal (B) regenerating fragments of *Dugesia(G)tigrina* (slightly modified from Saló [90]). Host organisms (hatched) are cut (a) at postcephalic and postpharyngeal levels. A triangular prepharyngeal or caudal piece is cut from the host and discarded (1). In its place, a cephalic piece from the donor (stippled) is grafted (2) in inverted polarity (b,c). The grafted head is trimmed (d) and the appearance of the eye spots in the anterior blastema (unfilled) indicates if the head has been determined. Time of head determination in the host could be estimated making grafts at different times after cutting the host. When grafts are made soon after cutting the grafted head inhibits the formation of a new head by the host. The time (in hours) when grafted heads no longer inhibits the formation of a new head in the host is taken as the time of head determination.

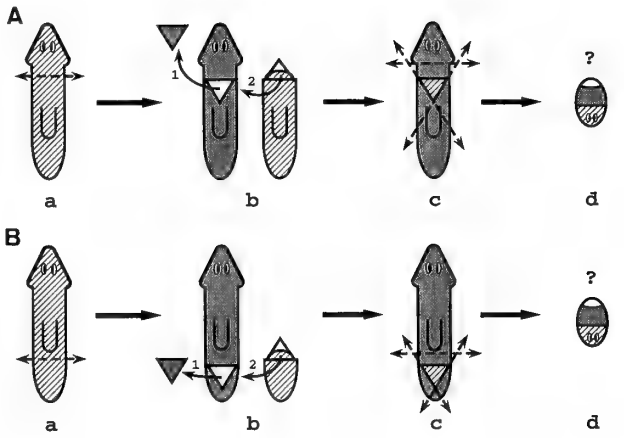

FIG. 3. Grafting method used to estimate when head blastemas acquire the capacity to inhibit formation of a new head. Steps and symbols as in Figure 2, the only difference being that a blastema instead of a full head is grafted into the host (b2).

The differentiation of new structures and the emergence of the new pattern

Since freshwater planarians do not incorporate tritiated thymidine into their cells, differentiation of new structures in regenerating organisms has been mainly studied by electron microscopy. Epidermal cells [40], gastrodermal cells [42], muscle cells [41, 70, 97] and nerve cells [96] have been particularly well studied. In most cases, blastemal neoblasts have been shown to be the source of these cells, though claims for dedifferentiation have also been reported [50, 104]. The canonnical time-course of differentiation starts between 2 and 4 days with the regeneration of the epidermis from migrating parenchymal rhabdite-cells, that come from undifferentiated neoblasts. These cells cross the basal membrane and squeezes among the stretched old epidermal cells [40, 43]. Newly differentiating muscle cells, showing small nascent myofibril bundles in the cytoplasm close to the nuclear envelope or rough endoplasmic reticulum, are discernible in the third day at the periphery of the blastema, beneath the basal lamina. Later on (4–6 days), these newly

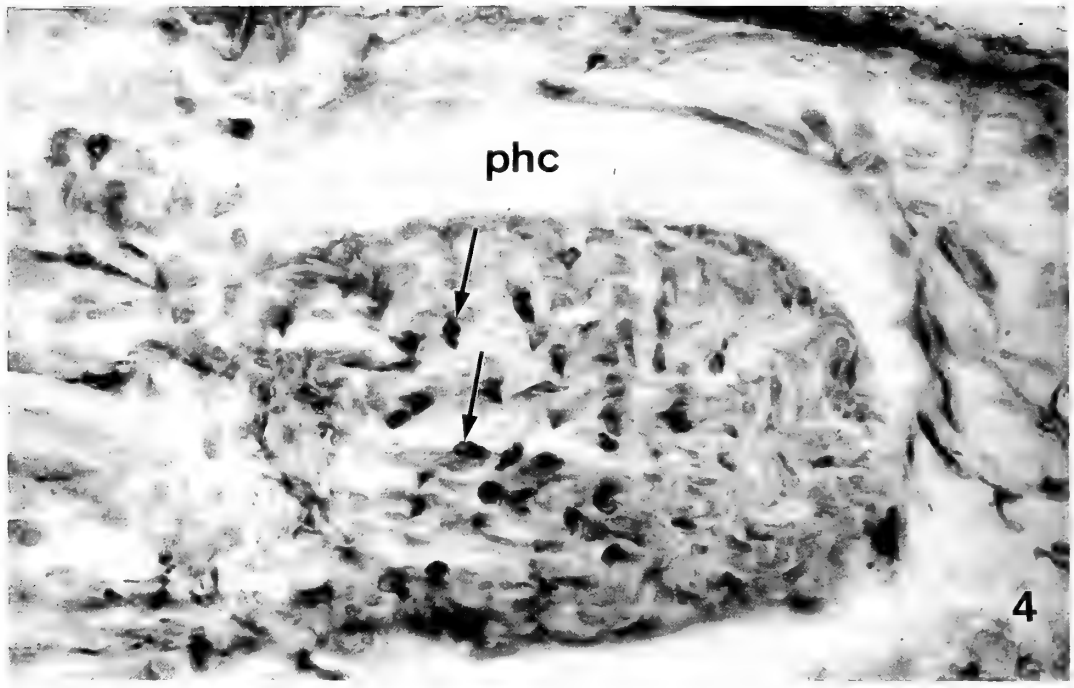

FIG. 4. Pharynx of a 4-day regenerant of *Dugesia(G)tigrina* stained with the muscle specific monoclonal antibody TMUS-13. Immunopositive cells (arrows) are myoblasts at the early stages of differentiation into mature muscle cells. ×400. Sagittal section. The anterior (cephalic) part is to the left, and the dorsal side to the top. phc: pharynx cavity.

developing muscle cells extend cellular projections towards the basal lamina, enlarge the contractile apparatus and establish myoneural connections. At 6 days fully formed muscle cells are observed [41, 70, 97]. A similar chain of events has been described for nerve cells differentiating from neoblasts [96].

Regeneration of the pharynx has been also a source of relevant information. The pharynx appears from a group of undifferentiated cells clustering far from the wound. From this cluster, a slit forms separating the new epithelium of the pharynx from that of the pharynx cavity. Although the precise mechanism by which the pharynx grows is still uncertain (see [2] for a particular mechanism), muscle cells precursors have been detected by the monoclonal antibody TMUS-13 [13] (Fig. 4) and by phalloidin fluorescein staining as early as three days of regeneration. These cells are alike to neoblasts. Later, these cells elongate, and the pattern of longitudinal, circular and radial fibers unfolds from an early anarchic stage to the precise array seen in later stages (Cebrià Romero and Baguñà, unpublished results).

As regards cell differentiation, regeneration in microturbellarian species have been particularly informative. These groups do incorporate both tritiated thymidine and bromodeoxyuridine. Studies using both nucleotides have been carried out in asexually reproducing and in regenerating *Microstomum lineare* (order Macrostomida) and *Stenostomum leucops* (order Catenulata) by Palmberg [79]. Recently cut worms were incubated for 1 hr in tritiated thymidine and examined at 1, 6, 12 and 25 hr of regeneration. As soon as 1 hr after cutting an abundance of labelled cells were found behind the pharynx in the mesenchyme and gastrodermis. Some of them were clearly migrating cells. Ultrastructural studies show them to be undifferentiasted cells alike to neoblasts. Some specific ultrastructural features suggested the presence of two different, intermingling populations of stem cells: the parenchymal neoblasts and the gastrodermal neoblasts. Six hours after decapitation, a group of labelled cells were found at the wound border but also in the central parts of organ primordia. These organs (brain, ciliated pits, and pharynx) consist of aggregations of labelled neoblasts. The differentiation always begins at the core of the aggregate, and new cells are recruited peripherally by further cell migration and proliferation. Several flame cells of the protonephridia were also labelled at that time. Between 12 and 25 hr, the new epidermis is formed by labelled new epidermal cells intermixed with the unlabelled old epidermal cells. Labelling was also very conspicuous in the new subepidermal cell layers. It should be pointed out, however, that some nerve cells and muscle cells within the new organs were not labelled and, conversely, that some labelled neoblasts did not differentiate. The existence of both labelled differentiated cells and labelled but still mitotic cells 2 days after thymidine incorporation indicates that neoblasts consist of heterogeneous class of cells, some differentiating very early and others having several rounds of proliferation before differentiation. Further evidence for the existence of different subpopulations of neoblasts was that 2 day-regenerating heads had a substantial number of unlabelled cells, either neoblasts and differentiated cells (e.g. flame cells, nerve cells and muscle cells). As first pointed out by Saló and Baguñà

[91] in freshwater triclads, this suggests the existence of a population of slowly cycling neoblasts which spend most of their cycle time in G_2. Moreover, the differentiation of neoblasts into unlabelled flame cells at 6 hr may indicate that G_2 neoblasts, as well as those in G_1, can differentiate very rapidly into any cell type.

Although impressive these data appear to be for planarian standards, it is still an unsolved problem how the stem cells are determined to stand in G_2 or triggered to proliferate and differentiate. In the last years, several growth factors, neuropeptides and metabolites have been shown to have clear or circumstancial effects on neoblast proliferation (see [9], for a review of the most recent literature). However, neither a clear cell proliferation test has been devised nor any of these presumptive factors has been shown to act directly on neoblast proliferation. On the other hand, how the time-course of neoblast proliferation and differentiation is integrated within pattern formation mechanisms is even less understood. To tackle these problems the new tools from molecular biology and molecular genetics appear to be the clue.

THE MOLECULAR APPROACH TO REGENERATION IN PLANARIANS

A considerable attention has been given recently to signals, membrane receptors and transducing molecules which activates cell proliferation and differentiation in planarians. The main results found are in no way different to those obtained for other activated systems. The neurotransmitters, serotonin, noradrenaline and dopamine [59], neuropeptides and growth factors such as substance P, substance K, Hydra Head Activator, Epidermal Growth Factor (EGF) and Fibroblast Growth Factor (FGF) [8, 9], and simple molecules such as cyclic AMP, calcium ions, putrescine, spermidine and spermine [59, 94], have been found to activate at low concentrations the rate of regeneration and the mitotic rate in regenerating organisms and, in some cases, in cultured planarian cells. Nothing is known on membrane receptors in planarians with the exception of an src-related cytoplasmic tyrosine kinase, recently reported by Burgaya *et al.* [15], whose expression does not change during regeneration. Indirect evidence for different kinds of membrane receptors come from the activation of protein kinase A (PKA) and protein kinase C (PKC) mediated by adenylate cyclase and cAMP and by diacylglycerol, respectively [66]. In addition, phorbol esters (e.g. 12-O-tetradecanoylphorbol-13-acetate, TPA), can substitute for diacylglycerol and activated PKC inducing a high rate of proliferation and the induction of transplantable tumours in treated planarians [39]. Finally, preliminary data on the presence of a Ras protein in a Platyhelminth (the cestode *Diphyllobothrium dendriticum*) has been recently reported [46].

Variation in the levels of some of these substances, and the effects of some of their antagonists, have been monitored and linked to DNA, RNA and protein synthesis as well as to protein phosphorylation, cell proliferation and differentiation and even to pattern formation (see [8, 65] for detailed references). As expected, the results show that the mechanisms by which cells are activated to proliferate and differentiate in planarian regeneration are, in many respects, similar to those of other cellular systems (for comprehensive reviews see [17, 81]).

Are molecular changes seen after cutting the result of differential activation of otherwise silent genes or do they result from the enhanced and/or decreased activities of genes and gene products already active in the intact organism? In other words, do organisms such as planarians, with continuous cell turnover, need to activate specific genes to regenerate? Two sets of previous data strongly support a main role for quantitative over qualitative variation. The first set involves published data [29, 53, 54] on the effects of RNA and protein synthesis inhibitors on regeneration and can be summarized as follows: 1) actinomycin D (act D) applied to hatched or very young regenerating planarians inhibited the increase in RNA synthesis seen after cutting, gave a normal, though smaller, blastema, but did not impair pattern formation and cell differentiation; 2) protein synthesis, monitored by ^{3}H-leucine incorporation was not affected by act D; 3) cycloheximide inhibited protein synthesis as well as regeneration; 4) the capacity to regenerate in the presence of act D decreased during growth being lost in the adult; and 5) the lost capacity in adults could be restored after repeated (at least two) cuttings separated at 3–10 days intervals [112]. Altogether, these results clearly suggest the existence of a stable population of messenger RNA involved probably in functions such as proliferation, cell movement, and cell differentiation which are going on continuously in the intact organism, and are only enhanced after cutting. The second set of data comes from regeneration of X-ray irradiated planarians. After a dose of 8000 rads, cell division stops, the number of neoblasts decreases exponentially to become zero at two weeks after irradiation [90], and the organism dies at four-six weeks post-irradiation. When cut within the first 2 days after irradiation, planarians form a small (down to 15–20% of normal size) and transient blastema that, before disintegration, differentiates all the missing structures albeit on a smaller scale. This capacity decreases as long as the interval between irradiation and cutting increase, being lost at 3 days after irradiation. Again, this suggests that the cellular and molecular machinery in intact adult planarians is in an activated state and that regeneration could be a mere quantitative enhancement of this state.

A further proof for quantitative variation stems from the patterns of protein synthesis and protein content during cephalic regeneration in the planarian *Dugesia(G)tigrina* detected by high resolution two-dimensional electrophoresis (2D-PAGE) [20, 21]. Fluorographic 2D-PAGE patterns indicate that less than 5% of protein synthesized show significant changes during regeneration, these being mainly quantitative. The pattern of protein changes suggest two main phases of coordinate expression of sets of genes: an early one, linked to the cellular, biochemical and physiologi-

cal reaction to amputation and to early body repatterning (0–2 days), and a late one linked to organogenesis and cell differentiation processes (3–7 days). Hence, cephalic regeneration in planarians is carried out through quantitative changes in a small number of proteins, and most quantitative changes concentrate at early and late stages of regeneration. In addition, post-translational modifications seem important to explain variations in content in a fair number of proteins. Altogether, the effects of RNA and protein inhibitors, data from X-ray irradiation and data from 2D-PAGE patterns point to a major role for quantitative changes over qualitative (all or none) variation.

We should bear in mind, however, that 2D-PAGE, though highly sensitive for separating polypeptides, only resolves less than 10% of protein synthesized [57, 74]. Besides, the proteins detected belong to those synthesized at relatively high rates, and certainly would not give information on the proteins synthesized in low amounts to which most regulatory proteins belong. Hence, to know whether or not qualitative variations actually exist, more sophisticated analytical techniques such as very high-resolution 2D-PAGE (including powerful computer software data analysis), differential screening of cDNA libraries, and, most notably, finding and studying the changes in expression of individual genes known to play major roles in other developmental systems, are clearly needed.

THE DAWN OF MOLECULAR GENETIC ANALYSIS TO REGENERATION: NEW TOOLS FOR OLD THEMES

To establish how the lost pattern is first reset and how new structures and organs appear during regeneration, molecular markers of the early stages of pattern formation and cell differentiation are clearly needed. This would allow visualisation of the pattern before morphogenesis and overt differentiation takes place, as well as to detect the appearance of new primordia in itegrated structures (e.g. new ganglia along the longitudinal nerve cord and new gut diverticula).

Which is the soundest approach to detect such markers and the genes that code them involved in pattern formation during regeneration? In the last decade several attempts have been undertaken. Two-dimensional electrophoresis (2D-PAGE) of different regions along the a-p axis has spotted specific regional markers: one for the head region, some for the pharynx, a single one for the caudal area and several for the central areas of the body [20]. Regrettably, none of these potential markers have been further studied. Differential screening of cDNA libraries between different stages of regeneration or between different body regions in planarians have not been attempted. Given the paucity of results in other regenerating systems (e.g. Hydra [56], Amphibians [105],...), and the fact that most genes detected with this technique belonged to highly transcribed or to house-keeping class genes, it is questionable that such approach may give interesting results in planarians in which most genes seem to be on. A better approach would be to use the Polymerase Chain Reaction (PCR) technique to amplify those messages specifically enhanced in the blastema and postblastema areas at the early or late stages of regeneration. To our knowledge this approach has not been tried so far in planarians.

Monoclonal antibodies

A powerful approach to detect markers of early territorial determination makes use of monoclonal antibodies (mAbs). Two collections of mAbs against antigens of the freshwater triclads *Dugesia(G)tigrina* and *Phagocatta vivida*, showing cell type and regional specificites have been obtained [87, 99]. These collections have two main applications. First, cell type specific mAbs (e.g. against nerve cells, muscle cells, epithelial cells and so on) could be used to monitor when and where specific cell types first appear during the regeneration of specific organs and tissues. Two specific mAbs to the epithelia of the pharynx and the pharynx cavity (TCAV-1 and TCAV-2), a mAb against muscle cells (TMUS-13), and one against cianophylic secretory cells of the pharynx (TF-9.1) have been used to monitor when the primordia of the pharynx cavity and the pharynx itself first appears and unfolds during regeneration [14]. On the other hand, a collection of mAbs that stain all muscle cells (TMUS-13) or specific subsets (e. g. longitudinal (TMUS-46.2), circular or dorso-ventral muscles) are at present being used to monitor how the new pattern of muscles appear within the blastema and, most importantly, how the new and the old pattern interconnect (Cebrià Bueno, Baguñà and Romero, unpublished observations).

The second and main application of mAbs is as markers of specific areas or regions along the antero-posterior (a/p) and dorso-ventral (d/v) axes. This allows to study the temporal and spatial appearance of these structures during regeneration. This approach has been used succesfully in several systems, among them in regenerating hydra [44]. Information on the specific order of appearance of such structures will be instrumental to pick up the best model of pattern formation in planarians among those suggested in the past. Of the mAbs obtained in the planarian *Dugesia(G)tigrina* two are particularly relevant. One mAb, the TCEN-49, detects an antigen, TCEN-49Ag, that stains all cells from the central area of the body with the exception of epithelial cells. Anterior (head) cells and posterior (tail) cells are not stained (Fig. 5). As these cells are not related by lineage but by position, TCEN-49 may confer positional identity to the central body area. The other mAb, TNEX-59, has a complementary labelling as it stains the nuclei of all cells in the cephalic and caudal regions with a decreasing disto-proximal gradient in intensity (Fig. 6). Again, cells within these regions are not related by lineage; so, TNEX-59 may confer positional identity to both head and tail areas. Interestingly, all epithelial cells are highly and uniformly stained by TNEX-59.

Changes in TCEN-49 expression have been monitored during both anterior and posterior regeneration [13]. When

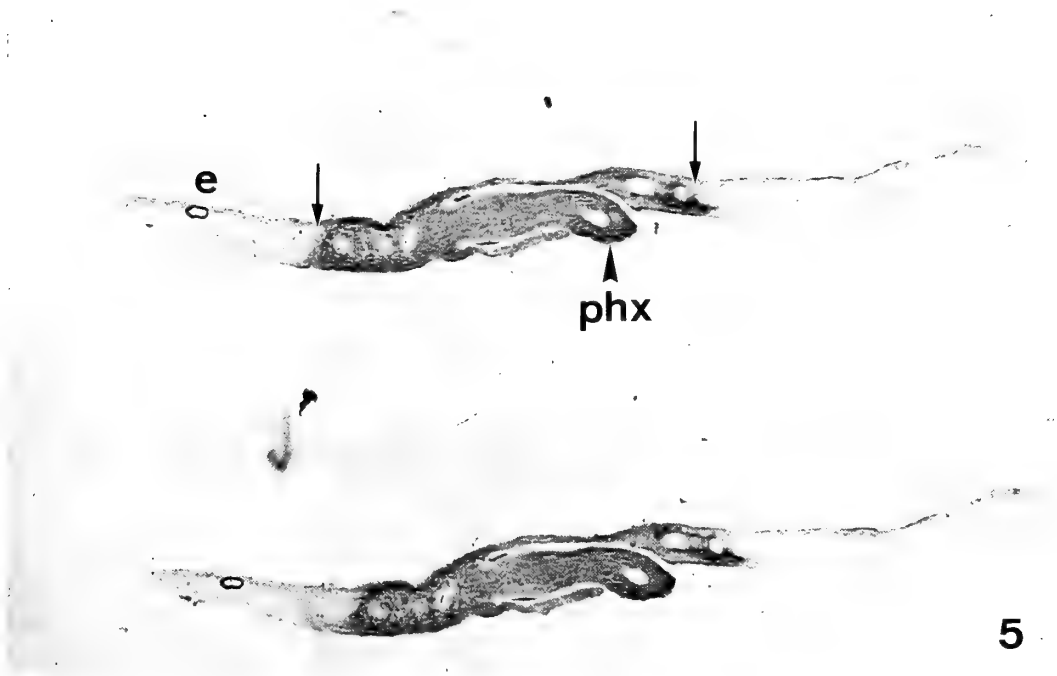

FIG. 5. Consecutive paraffin sections of *Dugesia(G)tigrina* immunostained with the monoclonal antibody TCEN-49. Sagittal sections, ABC method. The anterior part is to the left and the dorsal side to the top. Arrows indicate the anterior and posterior boundaries of the TCEN-49 positive central body area. e: eye spot; phx: pharynx. ×50.

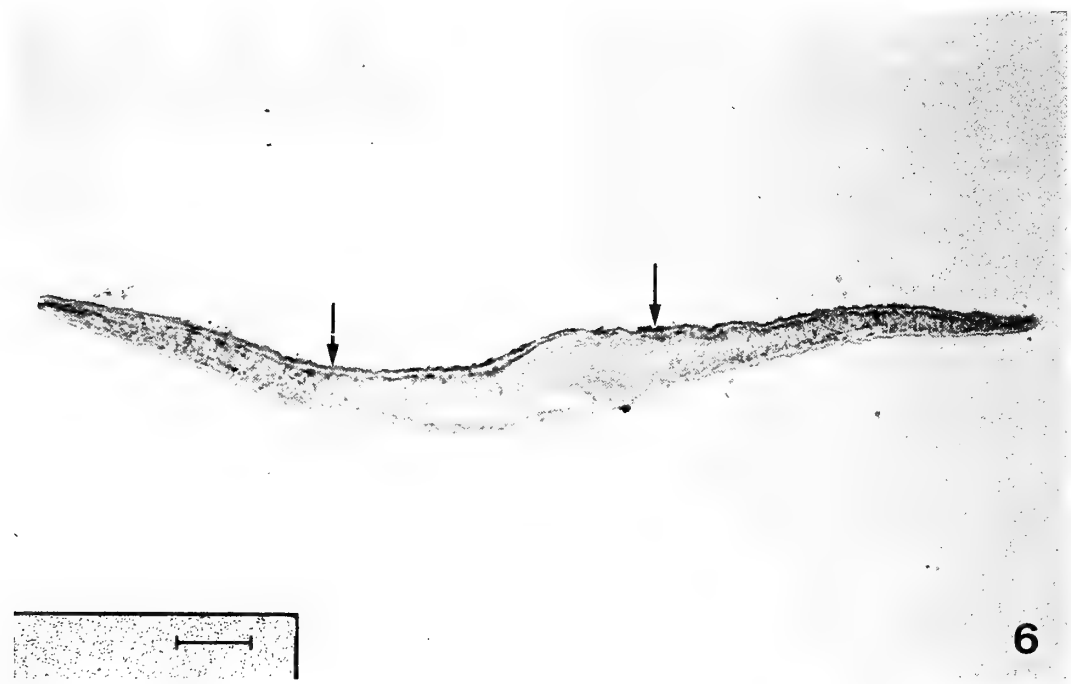

FIG. 6. *Dugesia(G)tigrina* immunostained with the monoclonal antibody TNEX-59. Sagittal section, ABC method. Nuclei of terminal regions (head and tail) are stained forming a decreasing concentration gradient. Central body regions are negative. The anterior part to the left and the dorsal side to the top. Arrows indicate the approximate boundaries between negative and positive TNEX-59 areas. Bar: 300 μm. ×50.

the cut bisects the area of expression, the staining recedes very quickly in the most distal area of both anterior and posterior regenerants. At 2 days no TCEN-49 positive cells are seen within the newly formed blastema. Later on, new boundaries are progressively established within the stump region. When the cut is made far from the boundaries of TCEN-49 positive area (e.g. a tail fragment regenerating a new head and the central area), a few small round TCEN-49

positive cells appear at 1 day of regeneration just at the boundary where the new pharynx will form. The number of positive cells increases at 2–3 days, a new anterior boundary is established and, later on, new cells are recruited in a disto-proximal sequence. These results indicate that expression of TCEN-49 is very sensitive to changes in positional values thought to occur close to the wound area during the early stages of regeneration. Whatever the mechanism that turns on or off its expression during regeneration, TCEN-49 seems a very valuable marker to monitor the early determination of central body areas. Since the mAb TNEX-59 seems to be specific for terminal areas (either head or tail) double staining with TNEX-59 and TCEN-49 of regenerating tails or heads will help to describe in molecular terms how the new pattern unfolds and to pick up the pattern formation model that best fits the data (Bueno, Romero and Baguñà, work in progress).

Homeobox-containing genes

Re-setting and re-specifying the pattern along the antero-posterior (a/p) body axis is the main event in any regenerating system. In the early embryonic development of all the organisms studied so far this role is fulfilled by a specific class of homeobox containing genes, the so-called *Antennapedia*-class (for reviews see [34, 47, 49, 60]). Homeobox containing genes code for transcription factors involved in the control of pattern formation and cell determination and differentiation. Its main feature is a 180 bp DNA sequence, the homeobox, that codifies for 60 residues, the homeodomain, with a specific motif the helix-turn-helix that binds DNA. The homeobox has been shown to be highly conserved from sponges to mammals which promptly suggested a key role in the development of most organisms.

The number of homeobox containing genes is over 500 (see [26] for a thorough recent compilation). Those involved with the antero-posterior axis specification (the *Antennapedia* class), are clustered in the genome (HOM/Hox clusters, or Hox for short), and are expressed along the a/p axis in a conserved order that is colinear with their positions in the genome. Hox genes are ubiquitously distributed from Cnidarians [98] to Vertebrates [60] and their remarkable similarity in genome organization and function have been taken to represent apomorphic features defining the whole animal kingdom [102]. Its main function is to give positional identity within homogeneous field of cells and transform them into a series of unique pattern elements along the a/p body axis. It is therefore to be expected that these genes play a similar role during regeneration; that is, to transform the homogeneous blastema and postblastema fields into discrete lost pattern elements.

To search for these genes in planarians, several laboratories performed direct screening of planarian cDNA or genomic libraries with heterologous probes from *Drosophila* and other organisms. No Hox genes were found. This apparent failure was later found to be due to the strong bias in planarians, as in other lower metazoans, toward using codons with an adenine or thymine in the third position. To circumvent this problem, two basic approaches were tried: 1) screening of cDNA libraries with degenerated oligonucleotides corresponding to the most conserved amino acid sequence from the helix-3 of the homeodomain [16]; and 2) PCR amplification of genomic DNA or cDNA using two sets of degenerated oligonucleotides corresponding to helices 1 and 3 of the homeodomain.

The first approach yielded the first two homeobox-containing genes in Platyhelminthes, Dth-1 and Dth-2 [31]. They belong to the NK family and have tissue-specific expression. *In situ* hybridization shows Dth-1 in cells of the gastrodermis and in a few scattered cells surrounding it that may correspond to neoblasts differentiating into gut cells [32]. Dth-2 is expressed in the peripheral parenchyma, with a higher expression in dorsal and lateral regions than in ventral regions. During regeneration, the expression of both genes is not enhanced at early stages, though a slight increase, probably linked to gut differentiation, is seen at later stages for Dth-1. Screening of cDNA and genomic libraries of *Dugesia(G)tigrina* using PCR and degenerated oligonucleotides has yielded, so far, 13 homeobox containing genes that belong to the paired-like (1), paired (1), POU (3) and, most importantly, to the *Antennapedia* family (8) (Table 1). Similar studies in other species of free-living and parasitic Platyhelminthes have detected homeobox genes belonging to the *Antennapedia*, NK, *paired, engrailed* and POU families [10, 73, 77, 107].

Homeobox containing genes of the POU family have been described from *Caenorhabditis elegans* to mammals (see [89] for review). They code for a protein with two highly conserved domains: the POU-specific domain and the POU homeodomain. Based on homologies of both domains, POU genes have been grouped into 5 subclasses (POU-I to POU-V). They are mainly expressed in the central nervous system. Sequence comparison showed that *Dugesia(G)tigrina* POU-box genes DtPOU-1 and DtPOU-2 belong to the subclass POU-III and DtPOU-3 belongs to the subclass POU-IV. DtPOU-1 is identical over the entire POU-domain to the DjPOU-1 from *Dugesia(D)japonica* reported by Orii *et al.* [76]. In planarians, POU-box genes are weakly expressed. Northern blots of DtPOU-1 and 2 were negative (Miralles and Saló, unpublished data) whereas a faint single band appeared for DjPOU-1 in Northern blots of *Dugesia(D)japonica* [76]. A quantitative study of DjPOU-1 expression using reverse transcription and PCR (RT-PCR) showed higher expression in head regions as compared to central and tail regions and puzzling changes in expression during regeneration [76]. *In situ* hybridizations have given, so far, no results. Western blots using polyclonal antibodies raised against a fussion protein labels a 57 KDa protein of the expected size. Preliminary immunocytochemical studies using monoclonal antibodies show a specific staining in the nuclei of brain nerve cells surrounding the neuropil of *Dugesia(G)tigrina* (Casali, Romero and Saló, unpublished data).

PCR of cDNA and genomic DNA using homeobox

TABLE 1. Number of different genes from each homeobox class (with the exception of the HOM/Hox class) in the freshwater planarian *Dugesia(G)tigrina*

Class	prd-like	prd	NK	POU III	POU IV
Number identified	1, Dtprd1	1, Dtpax-6	2, Dth-1, Dth-2	2, DtPOU-1 DtPOU-2	1, DtPOU-3
Approach	PCR of genomic DNA and total cDNA	PCR of genomic DNA	cDNA screening with degenerate oligonucleotides	PCR of genomic DNA and cDNA screening with degenerate oligonucleotides	PCR of genomic DNA
Primers	Helix 1, 3	Prd domain	Helix 3	Helix A Helix 3	Helix A Helix 3
Type and number of clones isolated	6 cDNA 1 genomic		12 cDNA 7 genomic	1 cDNA 2 genomic (DtPOU-1)	4 genomic
Similarity	*unc-4* *Ceh-10* *Smox-3*	*Aniridia* *Small eye* *ey*	*NK-2* *TTF-1* *Nkx-2* *Eghbx-3*	*DjPOU-1* *Cf1a*	*Unc-86*
Function	?	Determination of eye?	Gut and subepidermal cell determination and or differentiation	Nerve cell expression?	?

The number and type of independent clones isolated, similarity to known homeobox genes and presumed function are indicated. Sequences used for comparison were from the EMBL and SwissProt databases. Nomenclature, abbreviations and a brief description of the homeobox genes referred to can be found in the recent compilation of Duboule [26]. For further details, see text.

TABLE 2. Number of different genes from the HOM/Hox class in the freshwater planarian *Dugesia(G)tigrina*

HOM/Hox Class	lab/Hox1	pb/Hox2	Dfd/Hox4	Scr/Hox5	Antp, Ubx, AbdA/Hox 6/8	AbdB/Hox9/10
Number identified	1, DtoxA	1, DtoxB	1, DtoxE	1, DtoxC	2, DtoxF, DtoxD	1, DtoxH
PCR approach	blastema cDNA	genomic DNA and total cDNA	genomic DNA and blastema cDNA	blastema cDNA	genomic DNA and cDNA from intact and regenerating libraries	blastema cDNA
Primers	Helix 1, 3	Helix 1, 3	Helix 1, 3	Helix 1, 3	Helix 1, 3	Helix 1, 3
Type and number of clones isolated			7 cDNA clones	5 cDNA clones	3 cDNA and 7 genomic clones	4 genomic clones
Similarity	*lab/Hox1;* *PwoxA;* *PwoxB;* *EtoxA;* *Fhhbx1.*	*pb/hox2*	*Dfd/Hox4* *Smox1* *EtoxB* *Fhhbx2*	*Scr/Hox5*	*Antp/Hox6* *PwoxC* *PwoxD* *EtoxC* *Dthox1=DtoxF*	*AbdB/Hox9* *PwoxE*

The number and type of independent clones isolated, similarity to known HOM/Hox genes and presumed function are indicated. Sequences used for comparison were from the EMBL and SwissProt databases. Nomenclature, abbreviations and a brief description of the homeobox genes referred to can be found in the recent compilation of Duboule [26]. For further details, see text.

primers of the *paired* family have detected two genes: Dtpax-6 which belongs to the subclass Pax-6 of the paired family (Callaerts, Saló and Gehring, unpublished data), and Dtprd1 belonging to the close paired-like family (Muñoz-Marmol and Saló, unpublished data). The subclass Pax-6 includes the gene *eyeless* of *Drosophila* and the genes *small eye* and *aniridia* of mouse and man respectively. Loss of function of these genes causes severe anomalies in the eyes. In addi-

tion, Pax-6 genes have been found to be expressed in the eyes of several animal groups [83]. It is therefore highly probable that eyes of planarians express Dtprd2. If this is so, this would be an unvaluable genetic marker to monitor eye determination during regeneration. As regards Dtprd1 expression, Northern blots and RNase protection assays were negative though quantitative PCR of anterior and posterior body regions of intact organisms and during regeneration showed a faint constant expression. Western blots using polyclonal antibodies raised against a Dtprd1 fussion protein label a 32 KDa protein of the expected size. Preliminary immunocytochemical studies show expression of Dtprd1 in clusters of still unidentified cells in the peripheral ventral parenchyma (Muñoz-Marmol and Saló, unpublished observations).

Seven Hox Antp-like homeobox genes (PWoxA to PWoxH) have been reported by PCR of genomic DNA in the freshwater planarian *Phagocata woodworthii* [10]. The reactions gave bands of 146 bp that were purified, cloned and sequenced. Comparison to a list of over 350 homeodomain sequences indicated that PWoxA and B were both closely related to labial from *Drosophila* and to Hox1 from the mouse, PWoxC and D belonged to the Antp/Ubx/abd-A class from *Drosophila*, PWoxE could be placed within the Abd-B class whereas PWox F and G were likely duplications within the lineage leading to *Phagocata* and could represent either the anterior (lab, pb) or the medial (Dfd/Scr or Antp/Ubx/abd-A) groups. Using a similar approach, eight Hox genes (DtHoxA to DtoxH) that belong to the Antp class have been obtained from the freshwater triclad *Dugesia(G)tigrina* (Saló *et al.*, unpublished data). Genomic or cDNA clones of some of these PCR amplified fragments bearing the whole homeobox and flanking regions (368 to 687 bp) were isolated from *Dugesia(G)tigrina* libraries and sequenced. With the exception of DtHoxG, they were assigned to the cannonical orthologous groups from *Drosophila* and the mouse and compared to other Hox genes from Platyhelminthes (Table 2). Further characterization and sequencing of these genes and studies of their expression patterns in intact and regenerating organisms using whole mount *in situ* hybridization are underway.

Flatworms are generally considered to be the modern representatives of the earliest bilateral organism (reviewed in [106, 109]). Molecular phylogenies based on 18S rDNA sequences strongly supports this suggestion [1, 84]. The Hox genes found in *Dugesia(G)tigrina* bear an almost one to one correspondence to the main classes described in *Drosophila*. As Hox genes appear clustered in the genome and expressed in order along the a/p axis in all organisms studied so far, it is highly probable that a similar structural and functional organization do exist in planarians. To check it two different approaches are presently being tried: first, chromosome walking in the genomic library; second, Southern blots of large fragments of genomic DNA isolated by pulse field electrophoresis (Saló *et al.*, unpublished data).

The almost endless capacities of adult planarians to grow, shrink and regenerate suggest that pattern formation mechanisms must be always on. If, as expected, planarian Hox genes are clustered and expressed in order along the a/p axis, this pattern must be evident in the adult intact organism and should be somehow turned on again during regeneration. Probes from some of the Hox genes of *Dugesia(G)tigrina* are presently being tested using *in situ* hybridization on whole mounts or on sagittal paraffin sections from intact and regenerating individuals. According to the patterns found in the embryonic development of *Drosophila* and some vertebrates [60] and in regenerating hydras [98], two different patterns in the intact organism could be anticipated; either a nested expression of several Hox genes that would determine in a combinatorial way different regions along the body or a region-specific expression that may determine such regions in a one to one basis (for a more detailed explanation see [95]). As regards regeneration, three are the main issues to be asked. First, are Hox genes activated following a disto-proximal or a proximo-distal sequence? Second, who activates and how is set up the same Hox gene expression pattern? Finally, how Hox genes specify the different regions; in other words, do we have any hints on down-stream genes regulated by the Hox genes in planarians? While *in situ* hybridization will provide soon clear answers to the first question, only potential candidate molecules could be called for to answer the second. Prominent among them are members of the Transforming Growth Factor Beta (TGF-β) family such as activin and *decapentaplegic* (dpp), members of the segment-polarity genes of *Drosophila* like as *wingless* (wg) and *hedgehog* (hh) as well as the Fibroblast Growth Factor (FGF) family, shown in different systems (Amphibians [38], *Drosophila* [11, 22], chick [28, 71]) to play a key role coordinating growth and patterning. In the chick limb, it has been proposed that signals from the ZPA (Zone of Polarizing Activity) such as retinoic acid (RA) and the product of the gene *Sonic hedgehog* (Shh), acting in conjunction with the FGF4 from the Apical Ectodermal Ridge (AER) activates Hox expression and other downstream genes involved in mesoderm respecification [72]. In planarians it is sound to suggest that some undisclosed product (s) induced by epithelial-mesenchymal interactions activates the expression of Hox genes within the blastema and postblastema which, in turn, would activate specific downstream genes to generate the specific lost structures. In this context, the products detected by the mAbs TCEN-49 and TNEX-59 may belong to such downstream genes. Using these mAbs and probes from the Hox genes, the classical transplantation experiments performed in the last 100 years can be performed again and reinterpreted in molecular terms.

IS REGENERATION IN PLANARIANS STILL WORTH TO BE STUDIED OR SHALL WE FOLLOW MORGAN'S FOOTSTEPS?

Near the turn of this century, T.H. Morgan made both theoretical and experimental contributions to the problem of

how polarity is maintained along the antero-posterior body axis during regeneration in planarians and other organisms. Morgan proposed a model whereby polarity was due to a "gradation of materials" along the body axis [68]. In this model head and tail "stuffs" were distributed asymmetrically throughout the worm. Although this hypothesis formally explained most results and represented the first suggestion of a morphogenetic gradient accounting for a developmental process, it is well know that he felt that "he will never understand the phenomena of development and regeneration" and, wisely, turn to study the problem of inheritance. In general terms we are no better than Morgan at his time. The main problem remains the same as 100 years ago: how is a set of complex regions made from a few thousand homogeneous blastema cells covered by a thin ectodermal sheet? Thus, shall we stick with planarians or shall we follow Morgan's footsteps and turn to the mouse, the zebrafish or to the stars of the field *Drosophila* and *C. elegans*?

A trivial argument to stick to planarians is their unparalleled power to regenerate. However, when the non amenability of planarians, and turbellarians as a whole, to classical genetic analysis is considered, this advantage turns into nothing. However, two recent developments have dramatically changed this gloomy situation. First, the availability of molecular markers and genes, namely regional-specific mAbs and the Hox genes, involved in pattern formation is leading for the first time to examine the molecular basis of regeneration and to redescribe in molecular terms the classical experiments of induction of extra regions in normal or inverted polarity (see [12] for a review). Second, the finding that a subpopulation of neoblasts is totipotent and can be used to transform planaria provides a potentially powerful tool for studying planarian regeneration [7]. So, one may envision making use of clonally expanded neoblasts to create clonally derived planaria [9]. If these planaria are derived from neoblasts containing random integrations of a reporter gene, it should be possible to screen for worms exhibiting interesting patterns of reporter gene expression. This type of screening is referred to as an enhancer trap screen [75]. Ultimately, these screenings should make possible the identification of genes expressed in a region-specific manner in regenerating tissues, thereby providing insight into the mechanisms that determine neoblast fate during regeneration.

THE ULTIMATE TOOL: TRANSGENIC PLANARIA

The two steps necessary for developing transgenic planaria are to introduce exogenous DNA into neoblasts and to establish conditions allowing stable integration of this DNA into the neoblast genome. Different techniques and parameters of introduction of DNA into neoblasts are presently under study (Newman, García-Fernàndez, Saló and Baguñà, work in progress). However, it is the recent finding in the planarian *Dugesia(G)tigrina* of several DNA sequences similar to the transposable *mariner* element of *Drosophila* [33] that may provide an excellent method to integrate exogenous DNA in planaria. There are ~7000 copies of this element in the *D. tigrina* genome and these elements seem to code for an active transposase ([30] and García-Fernàndez *et al.* (submitted for publication)). The fact that none of these elements are detected in the genome of several species of turbellarians, among them species close to *Dugesia(G)tigrina* such as *Dugesia(S)mediterranea, Dugesia(S)polychroa* and *Dugesia(D)gonocephala*, provide a straightforward way of testing planarian *mariner-1* as a general integrative vector. Briefly, a general vector including a non-autonomous *mariner-1* element, a selectable marker gene (e.g. the neomycin phosphotransferase gene under control of a planarian active promoter), and a reporter gene coding for reporter proteins such as beta-galactosidase (β-gal) or the jellyfish Green Fluorescent Protein can be constructed. By electroporating *D. mediterranea* neoblasts with this plasmid it should be possible to select for cells resistant to neomycin (neo^R) which will also express the reporter gene product. After clonal expansion, these transformed neoblasts can be introduced to neoblast-depleted *D. mediterranea* and transgenic planarian obtained.

The methods outlined above could also be extended to introduce planarian genes such as HOM/Hox, NKs, prd,...under the control of inducible (e.g. heat shock) promoters to activate their expression in regions where they are not normally expressed and monitor the molecular and morphological changes induced. This would be equivalent to gain of function mutations and may give insights into gene function and gene or gene product interactions in planarians. Conversely, methods to inactivate the normal function of a gene could be also devised, this being equivalent to loss of function mutations. When these methods are developed, a potentially powerful tool for understanding many aspects of planarian biology will be available. At present, this knowledge is out of our reach due to the lack of classical genetic analysis in planarians (for a recent discussion see Baguñà *et al.* [6, 9])

A NEW RESEARCH AGENDA

The upshot of this new work is that a specific research agenda can be formulated. The main questions to be addressed can be summarized as follows:

1) Which is the best available method to obtain long-lasting labelled neoblasts: by introduction of reporter genes via *mariner*-derived vectors or through virus-derived vectors? Can these transformed cells be the key to show the totipotent nature of some neoblasts and the cell lineage of blastema cells or would the transient expression of some molecular markers (DAPI, DiI, CellTracker) be enough?

2) What is the role of the wound epithelium and the underlying parenchyma cells in setting the antero-posterior polarity of the regenerating organisms? Do epithelial-mesenchymal interactions turn on the homologous genes of the TGF-β and FGF families within the blastema? Are there any other growth factors involved? Which is the role, if any, of msh-homeobox containing genes?

3) Are HOM/Hox genes clustered in the planarian genome? Which is the pattern of expression of the HOM/Hox genes in the intact organism: is it nested or region-specific? Are HOM/Hox genes activated via growth factors induced during wound healing? Are the homologues of *Drosophila* head-specific genes such as *orthodenticle* (otd) and *empty spiracles* (ems) and of tail (caudal) specific genes such as *even-skipped* (eve) present in planarians? If so, are they activated during regeneration?

4) Are region-specific antigens detected by the monoclonal antibodies TCEN-49 and TNEX-59 down-stream genes controlled by the HOM/Hox genes?

5) Can *mariner*-derived vectors be instrumental to obtain transgenic planarians? Can these vectors mediate transformation in all turbellarian orders? If so, would they be the key to obtain transgenic organisms from those orders with cannonical spiral development such as Polycladida, Acoela and Catenulida?

The answer to even some of these questions will constitute the best argument to stick to planarians and to consider Morgan's forsake a wise idea whose time has passed.

ACKNOWLEDGMENTS

The authors wish to thank to all people which in the past 15 years have contributed to any of the results mentioned in this review. Carme Auladell, Maria Ribas, Joan Collet, Ferran Burgaya, Joaquim Prats, Marta Riutort, Salvador Carranza, Montserrat Corominas, Agustí Miralles, Marc Pellicer, Eduard Batlle, Marc Aureli Soriano and Lluís Espinosa are particularly acknowledged. We would also thank Francesc Cebrià for sharing unpublished results. The senior authors (JB, ES and RR) wish to thank the help and advise along these years of Drs K. Agata (Himeji Institute of Technology, Japan), R. Ehrlich (Universidad de Montevideo, Uruguay), W. Gehring (Biozentrum, Basel, Switzerland), V. Gremigni (Università di Pisa, Italia), T.S. Okada (Okazaki National Research Institutes, Japan), H. Orii (Himeji Institute of Technology, Japan), M. Reuter (Abo Akademi, Abo, Finland), R. Rieger (Universitat Innsbruck, Austria), and R. Steele (University of California, Irvine, USA). The financial support in the last 10 years of the Dirección General de Investigación Científica y Técnica (Ministerio de Educación y Ciencia, Spain) and the Comissió Interdepartamental de Recerca i Innovación Tecnològica (Generalitat de Catalunya) is warmly acknowledged.

REFERENCES

1 Adoutte A and Phillipe H (1993) In "Comparative Molecular Neurobiology" Ed by Y Pichon, Birhauser Verlag, Basel, pp 1–34
2 Asai E (1991) Zool Sci 8: 775–784
3 Baguñà J (1976) J Exp Zool 195: 53–64
4 Baguñà J (1981) Nature 290: 14–15
5 Baguñà J and Romero R (1981) Hydrobiologia 84: 181–194
6 Baguñà J, Saló E, Collet J, Auladell MC, Ribas M (1988) Fortschr Zool 36: 65–78
7 Baguñà J, Saló E, Auladell MC (1989) Development 107: 77–86
8 Baguñà J, Saló E and Romero R (1989) Int J Dev Biol 33: 261–266
9 Baguñà J, Romero R, Saló E, Collet J, Auladell MC, Ribas M, Riutort M, García-Fernàndez J, Burgaya F, Bueno D (1990) In "Experimental Embryology in Aquatic Plants and Animals" Ed by HJ Marthy, Plenum Press, New York, pp 129–162
10 Bartels JL, Murtha MT, Ruddle FH (1993) Mol Phylogenetics Evol 2: 143–151
11 Basler K and Struhl G (1994) Nature 368: 208–214
12 Bronsted HV (1969) Planarian Regeneration. Pergamon Press, Oxford, pp 1–270
13 Bueno D, Espinosa Ll, Soriano MA, Batlle E, Baguñà J, Romero R (1994) Hydrobiologia (in press)
14 Bueno D, Batlle E, Soriano MA, Espinosa Ll, Baguñà J, Romero R (1994) Hydrobiologia (in press)
15 Burgaya F, García-Fernandez J, Riutort M, Baguñà J, Saló E (1994) Oncogene 9: 1267–1272
16 Burglin TR, Finney M, Coulson A, Ruvkun G (1989) Nature 341: 239–243
17 Cantley LC, Auger KR, Carpenter C, Duckworth B, Graziani A, Kapeller R, Soltoff S (1991) Cell 64: 281–302
18 Chandebois R (1980) Devel Growth Differ 22: 693–704
19 Coelho CND, Upholt WB, Kosher RA (1993) Development 156: 303–306
20 Collet J (1990) Ph D Thesis, University of Barcelona, pp 1–247
21 Collet J and Baguñà J (1993) Electrophoresis 14: 1054–1059
22 Couso JP, Bishop SA, Martínez-Arias A (1994) Development 120: 621–636
23 Dorey AE (1965) Quart J micr Sci 106: 142–172
24 Drobysheva IM (1986) Hydrobiologia 132: 189–193
25 Drobysheva IM (1988) Fortschr Zool 36: 97–101
26 Duboule D (1994) Guidebook to the Homeobox Genes. Oxford Univ. Press, Oxford pp 1–284
27 Ehlers U (1992) Microfauna Marina 7: 311–321
28 Fallon JF, Lopez A, Ros MA, Savage MP, Olwin BB (1994) Science 263: 104–107
29 Gabriel A and Le Moigne A (1971) Z Zellforsch 115: 426–441
30 García-Fernàndez J (1992) Ph D Thesis, University of Barcelona, pp 1–221
31 García-Fernàndez J, Baguñà J, Saló E (1991) Proc Natl Acad Sci USA 88: 7338–7342
32 García-Fernàndez J, Baguñà J, Saló E (1993) Development 118: 241–253
33 García-Fernàndez J, Marfany G, Baguñà J, Saló E (1993) Nature 364: 109–110
34 Gehring W (1987) Science 236: 1245–1252
35 Gremigni V (1974) Boll Zool 41: 359–377
36 Gremigni V (1988) Zool Sci 5: 1153–1163
37 Gremigni V and Miceli C (1980) Wilhelm Roux's Arch Dev Biol 188: 107–113
38 Gurdon JB, Harger P, Mitchell A, Lemaire P (1994) Nature 371: 487–492
39 Hall F, Morita M, Best JB (1986) J Exp Zool 240: 211–227
40 Hori I (1978) J Electron Microsc 27: 89–102
41 Hori I (1983) Cell Differ 12: 155–163
42 Hori I (1985) J Submicrosc Cytol 17: 569–581
43 Hori I (1991) Hydrobiologia 227: 19–24
44 Javois LC (1990) J Exp Zool 254: 155–164
45 Johnson RL, Riddle RD, Tabin CJ (1994) Curr Opin Genet Dev 4: 535–542
46 Karlsted KA, Wikgren BJ, Paatero GI (1990) Acta Academiae Aboensis 50: 59–66
47 Kenyon C (1994) Cell 78: 175–180
48 Kingsley DM (1994) Genes Dev 8: 133–146

49 Krumlauf R (1994) Cell 78: 191–201
50 Kudoh M, Teshima H, Teshirogi W (1991) Hydrobiologia 227: 47–56
51 Lange CS (1968) Int J Radiat Biol 13: 511–530
52 Lange CS (1985) In "Stem Cells" Ed by CS Potten, Churchill Livingstone, Edinburgh, pp 29–66
53 Le Moigne A and Gabriel A (1971) Z Zellforsch 115: 442–460
54 Le Moigne A and Gabriel A (1973) C R Acad Sc Paris 276: 1741–1743
55 Lentz TL (1967) J Ultrastruct Res 17: 114–126
56 Lesh-Laurie GE, Brooks DC, Hood RL (1986) Dev Growth Differ 28: 53–56
57 Lovell-Badge RH, Evans MJ, Bellairs R (1985) J Embryol Exp Morph 85: 65–80
58 MacWilliams HK (1983) Dev Biol 96: 217–238
59 Martelly I and Franquinet R (1984) Trends Biochem Sci 8: 468–471
60 McGinnis W and Krumlauf R (1992) Cell 68: 283–302
61 Mead RW (1991) Hydrobiologia 227: 25–30
62 Mead RW (1991) J Exp Zool 259: 69–77
63 Meinhardt H (1993) Dev Biol 157: 321–333
64 Montgomery JR and Coward SJ (1974) Trans Am Microsc Soc 93: 386–391
65 Moraczewsky J, Martelly I, Franquinet R (1986) Hydrobiologia 132: 223–227
66 Moraczewski J, Martelly I, Franquinet R, Castagna M (1987) Comp Biochem Physiol 87B: 703–707
67 Morgan TH (1898) Arch Entwicklungsmech 7: 364–397
68 Morgan TH (1905) J Exp Zool 2: 495–506
69 Morita M and Best JB (1984) J Exp Zool 229: 413–424
70 Morita M and Best JB (1984) J Exp Zool 229: 425–436
71 Niswander L, Tickle C, Vogel A, Booth I, Martin GR (1993) Cell 75: 579–587
72 Niswander L, Jeffrey S, Martin GR, Tickle C (1994) Nature 371: 609–612
73 Oliver G, Vispo M, Mailhos A, Martínez C, Sosa-Pineda B, Fielitz W, Ehrlich R (1992) Gene 121: 337–342
74 O'Farrell PH (1975) J Biol Chem 250: 4007–4021
75 O'Kane CJ and Gehring WJ (1987) Proc Natl Acad Sci USA 84: 9123–9127
76 Orii H, Agata K, Watanabe K (1993) Biochem Biophys Res Commun 192: 1395–1402
77 Orii H, Miyamoto T, Agata K, Watanabe K (1994) Hydrobiologia (in press)
78 Palmberg I (1986) Hydrobiologia 132: 181–188
79 Palmberg I (1990) Protoplasma 158: 109–120
80 Palmberg I and Reuter M (1983) Int J Invertebr Reprod 6: 197–206
81 Panayotou G and Waterfield MD (1993) BioEssays 15: 171–177
82 Pedersen KJ (1976) Wilhelm Roux's Arch Dev Biol 179: 251–273
83 Quiring R, Walldorf U, Kloter U, Gehring W (1994) Science 265: 785–789
84 Riutort M, Field KG, Turbeville JM, Raff RA, Baguñà J (1992) Can J Zool 70: 1425–1439
85 Romero R (1987) Ph D Thesis, University of Barcelona, pp 1–282
86 Romero R and Baguñà J (1988) Fortschr Zool 36: 283–289
87 Romero R, Fibla J, Bueno D, Sumoy L, Soriano MA, Baguñà J (1991) Hydrobiologia 227: 73–79
88 Ros MA, Lyons G, Kosher RA, Upholt WB, Coelho CND, Fallon JF (1993) Development 116: 811–818
89 Ruvkun G and Finney M (1991) Cell 64: 475–478
90 Saló E (1984) Ph D Thesis, University of Barcelona, pp 1–312
91 Saló E and Baguñà J (1984) J Embryol Exp Morphol 83: 63–80
92 Saló E and Baguñà J (1986) J Exp Zool 237: 129–135
93 Saló E and Baguñà J (1989a) Development 107: 69–76
94 Saló E and Baguñà J (1989b) J Exp Zool 250: 150–161
95 Saló E, Muñorz-Marmol A, Bayascas-Ramírez JR, García-Fernàndez J, Miralles A, Casali A, Corominas M, Baguñà J (1994) Hydrobiologia (in press)
96 Sauzin MJ (1967) Bull Soc Zool France 92: 313–318
97 Sauzin MJ (1967) Bull Soc Zool France 92: 613–616
98 Shenk MA, Bode H, Steele RE (1993) Development 117: 657–667
99 Shirakawa T, Sakurai A, Inoue T, Sasaki K, Nishimura Y, Ishida S, Teshirogi W (1991) Hydrobiologia 227: 81–91
100 Skaer RJ (1965) J Embryol Exp Morphol 13: 129–139
101 Slack JMW (1980) Nature, Lond 288: 760
102 Slack JMW, Holland PWH, Graham CF (1993) Nature 361: 490–492
103 Spiegelman M and Dudley PL (1973) J Morphol 139: 155–184
104 Teshirogi W (1986) Hydrobiologia 132: 207–216
105 Tsonis PA, Mescher AL, Del Rio-Tsonis K (1992) Biochem J 281: 665–668
106 Valentine JW (1989) Proc Natl Acad Sci USA 86: 2272–2275
107 Webster PJ, Mansour TE (1992) Mech Dev 38: 25–32
108 Wikgren BJP, Gustafsson MKS and Knuts GM (1971) Z Parasitenk 36: 131–139
109 Willmer P (1990) Invertebrate Relationships. Cambridge Univ. Press, Cambridge
110 Wolff E (1962) In "Regeneration" Ed by D Rudnick, The Ronald Press, New York, pp 53–84
111 Young DA (1983) Differentiaton 25: 1–4
112 Ziller C (1973) C R Acad Sc Paris 277: 1365–1368

ZOOLOGICAL SCIENCE 11: 797–806 (1994)

Sex Chromosome Differentiation in the Japanese Brown Frog, *Rana japonica* I. Sex-related Heteromorphism of the Distribution Pattern of Constitutive Heterochromatin in Chromosome No. 4 of the Wakuya Population

IKUO MIURA

Laboratory for Amphibian Biology, Faculty of Science, Hiroshima University, Higashihiroshima 724, Japan

ABSTRACT—To clarify the sex-related differences of chromosomes in the Japanese brown frog, *Rana japonica*, its chromosomes were analyzed by C- and late replication banding techniques. This species was characterized by ♂XY/♀XX sex chromosomes. There were three types (A, O and B) of chromosome No. 4 with respect to C-banding pattern. The type A had a C-band at the basal portion of the long arm, the type O had no such band, and the type B had double bands at the corresponding region. Almost all (97.6%) of the females examined showed the AA type and 2.4% the AO type, while 85.7% of the males examined showed the AO type, 10.7% the AA type, 1.2% the OO type and 2.4% the AB type. Histological examination of the testes of these AA, OO and AB males and the sex ratio of their offspring with AA females revealed that the OO and AB males were genetic XY males, while the AA males were composed of spontaneously sex-reversed XX females and genetic XY males. These results suggest that the genetic XY males of AA and the presumably genetic XX female of AO were produced by a recombination between the C-band in chromosome No. 4 and the site of a male-determining gene on the same chromosome. The OO male was probably produced from a mating of an XY male of AO with an XX female of AO.

INTRODUCTION

Sex chromosomes in amphibians vary widely among species [16, 18, 19] and populations [3, 7, 12, 20] with respect to a degree of differentiation. This feature presumably reflects the primitive differentiation of the sex chromosomes in amphibian species. Accordingly, cytogenetic and genetic examination of the amphibian sex chromosomes is important in comprehending why and how the chromosomes including sex determining genes have differentiated into the so-called distinguishable sex chromosomes by changing their external appearance.

The Japanese brown frog, *Rana japonica*, is widely distributed in Honshu except for Aomori Prefecture, Shikoku and Kyushu. Its sex-determining mechanism has been well examined by breeding experiments and sex-reversal [6, 10, 11]. However, sex chromosomes of this species have not been identified by conventional staining [8, 9, 13, 21, 22] and banding methods [4]. In recent years, C- and replication banding techniques have been used in amphibian species to demonstrate minor innerstructural changes taking place in the Y or W chromosome, which is apparently identical with the X or Z chromosome [2, 15, 17]. Thus, the present study attempts to clarify the sex-related differences of chromosomes in *Rana japonica* using these banding techniques.

MATERIALS AND METHODS

Animals

Specimens of *Rana japonica* Günther used in this study were collected from the paddyfields in Wakuya-machi, Toda-gun, Miyagi Prefecture situated in the northeastern area of Honshu, Japan.

Accepted October 17, 1994
Received April 27, 1994

Chromosome preparation and banding techniques

Mitotic metaphases were obtained by the *in vitro* blood cell culture [12]. A frog was first anesthetized with ether. After incision of the skin (about 1.5 cm in length) at the rear of the tympanum, the branchial vein and/or the muscular-cutaneus vein was cut with iridectomy scissors and watchmaker's forceps, and the blood was collected with a glass pipette containing 0.01～0.02 ml of heparin solution (10 mg/ml RPMI1640). The injury to the skin was healed without any proper treatment. 0.1～0.2 ml of blood was cultured in 2 ml of medium composed of 60% RPMI1640, 20% calf serum, 20% redistilled deionized water and 3% phytohemagglutinin (M) with penicillin and streptomysin at final concentrations of 100 Iu/ml and 100 μg/ml, respectively, at 25°C for 3–5 days. After the hypotonic treatment with 0.075M KCl solution, the cells were fixed in Carnoy's fluid (acetic acid : methanol = 1 : 3). Chromosome spreads were then prepared using the conventional air-drying method.

C-banding was performed according to the method of Sumner [23] with slight modifications. Chromosome preparations aged one day were treated with 0.2 N HCl for 40 min, and they were incubated in 5% $Ba(OH)_2$ solution at 35°C.

Late replication bands were produced mainly by the method of Takayama *et al.* [24]. The period of G_2 phase in the lymphocyte cell-cycle of this species was estimated at 2 hours (data not shown). Therefore, in order to visualize the chromosomal regions replicated during about four hours in late S phase, after 3–5 days of growth of non-synchronized peripheral lymphocytes *in vitro*, 5-bromodeoxyuridine was added to the cultures 6 h before the cell harvest (final concentration 10^{-4} M). Colchicine was added 4 h before the harvest to make the final concentration 10 μg/ml. The BrdU-chromosome preparations were kept for 1–2 days at room temperature, and then stained with 3% Giemsa solution diluted in 2% 4Na-EDTA aqueous solution for 3–5 minutes at 40°C.

Cross experiments and histological preparation

Cross experiments were performed in February. Ovulation was accelerated by injecting suspension of bullfrog pituitaries into the abdominal cavity. For histological observation, gonads fixed in Navashin's fluid were sectioned (10–12 μm in thickness) and stained with Delafield's haematoxylin and eosin.

RESULTS

Mitotic chromosomes

a. Conventional Giemsa staining

Rana japonica collected from Wakuya had, without exception, 26 chromosomes in diploid, comprising five large and eight small chromosome pairs, and chromosome No. 10 had the large, remarkable secondary constriction at the middle portion of the long arm, as reported previously in this species [8, 9, 13, 21, 22]. One homologue of chromosome pair 4 was slightly shorter than the other in the males, while in the females each was similar in size (Fig. 1).

b. C-banding

Chromosomes of this species were characterized by dark and well defined C-bands at the basal portions of both arms (Fig. 2). Each of the five large pairs could be identified by the length, shape and C-banding pattern (Fig. 3). Nos. 1, 2, 4 and 5 were metacentric, and No. 3 was submetacentric. Because No. 1 was largest and No. 5 was smallest, they were discernible from three other chromosome pairs. Though it was similar in size and shape to No. 5, the following type O of No. 4 was clearly distinguished from No. 5 by the unique

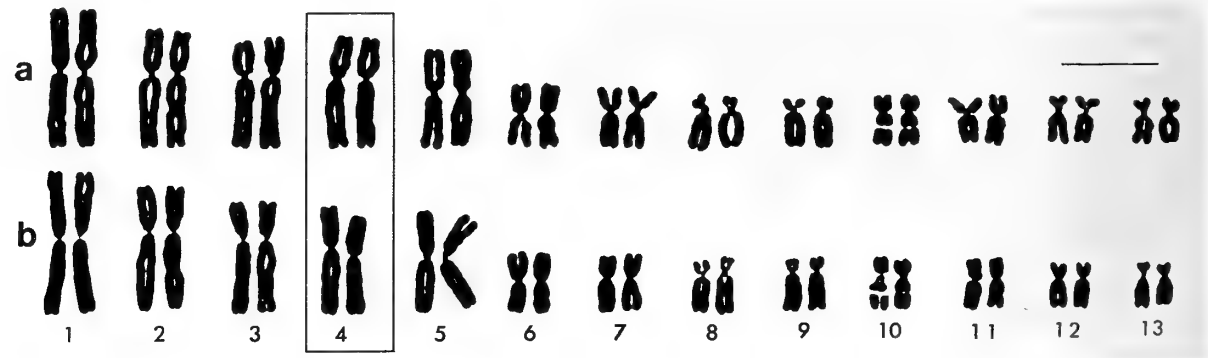

FIG. 1. The karyotypes of *Rana japonica* from the Wakuya population by conventional Giemsa staining: (a) female and (b) male. No. 4 chromosomes are boxed. Bar, 10 μm.

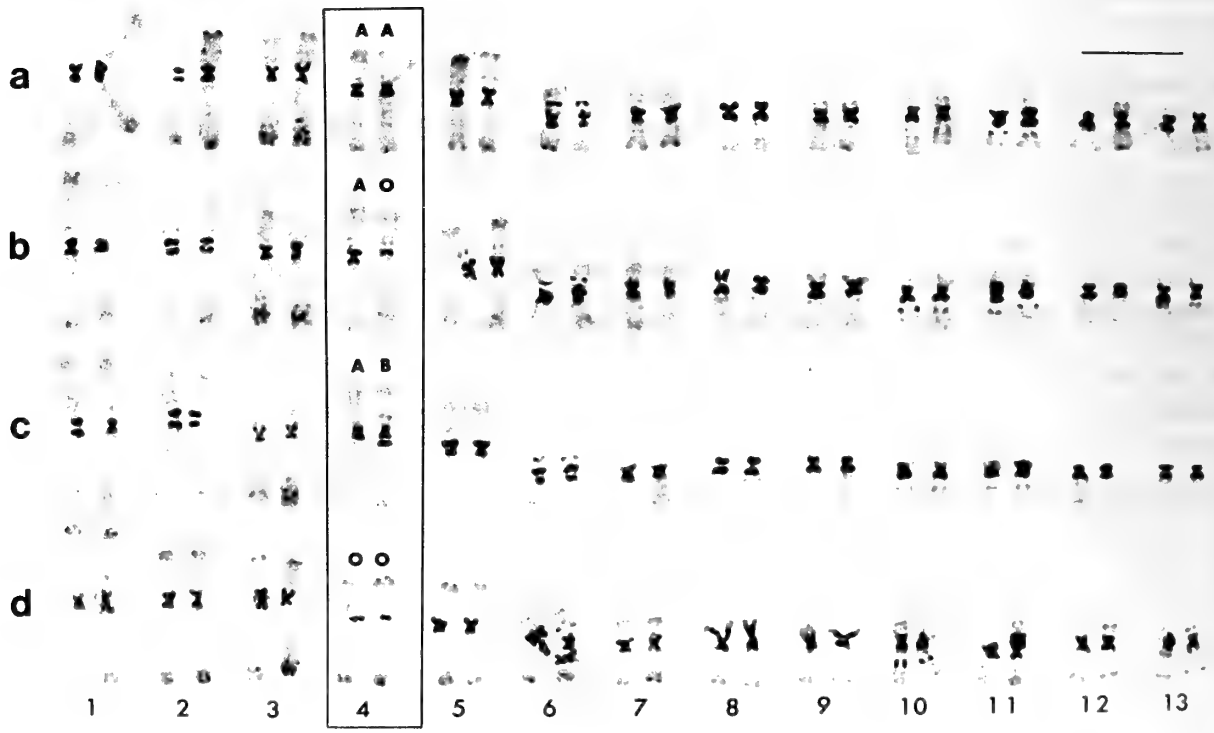

FIG. 2. C-banded karyotypes of *Rana japonica* from the Wakuya population: (a) female of AA type (AA1), (b) male of AO type (AO1), (c) male of AB type (AB1) and (d) male of OO type (OO1). No. 4 chromosomes are boxed. Bar, 10 μm.

C-banding pattern (Figs. 2 and 3). No. 3 was easily identified by its shape and three subterminal weak bands of the long arm, which were pointed out by arrowheads in Fig. 3. Nos. 2 and 4 were similar in shape, although No. 2 was somewhat larger than No. 4. Moreover, No. 2 had three weak C-bands: two sequential bands in the intermediate region of the short arm, and one interstitial band of the long arm. These two bands of the short arm were often observed, while one of the long arm only rarely. In contrast, No. 4 had four weak bands: one subterminal and one proximal bands of the short arm and two interstitial bands of the long arm. Bands of the short arm were frequent, while those of the long arm rare. Therefore, Nos. 2 and 4 could be distinguished from each other by these four frequently observable weak bands of the short arms, as pointed out by arrowheads in Fig. 3. In addition, these two chromosomes could also be distinguished on the basis of dark and well defined pericentromeric bands. For No. 2, two pericentromeric bands on short and long arms got separated from each other, whereas for No. 4 they often appeared joined together due to their close location (Figs. 2–4).

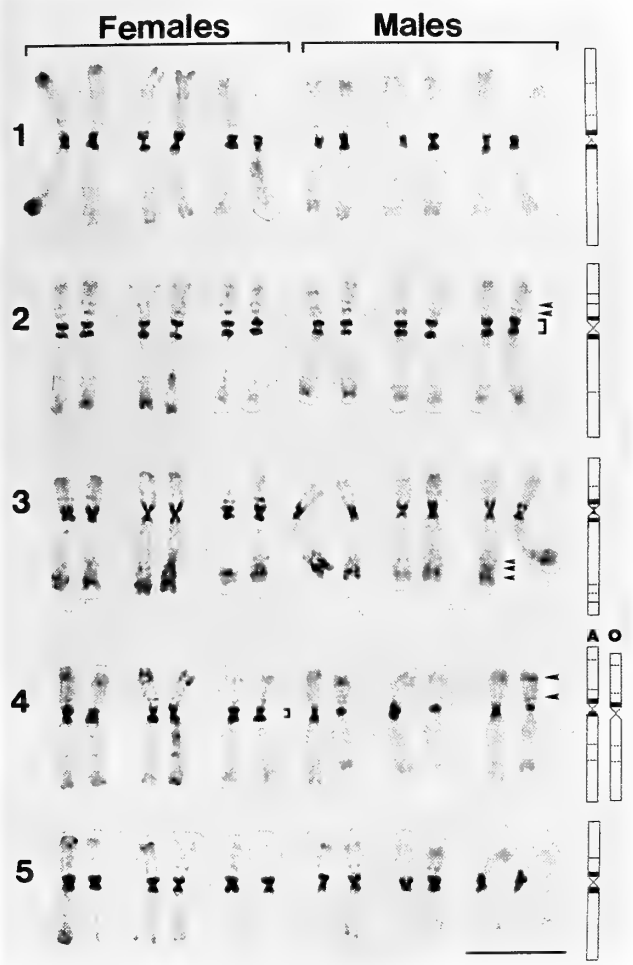

FIG. 3. Partial C-banded karyotypes of three females and three males. Chromosomes 1~5 are presented. Chromosome number is indicated on the left side. Idiogram showing C-banding patterns of chromosomes 1~5 is arranged on the right side. The arrowheads point to C-bands that characterize chromosomes 2, 3 and 4. Distance between the two pericentromeric bands on chromosomes 2 and 4 is shown by a short vertical bar. Bar, 10 μm.

When C-banded karyotypes of 125 specimens were examined, No. 4 chromosome was divided into three types (A, O and B) with respect to C-banding pattern (Fig. 2). Type A chromosome had a band at the basal portion of the long arm like other chromosomes, type O had no such band, and type B had double bands at the corresponding region. Type O chromosome was slightly shorter than type A at a ratio of 0.931 ± 0.011 (standard error), calculated from 30 metaphases of 11 males. And, type B was slightly longer than type A at a ratio of 1.099 ± 0.021, calculated from eight metaphases of two males. As shown in Table 1, of the 41 females examined, 40 were homomorphic (AA), and the remaining one was heteromorphic (AO). In contrast, of the 84 males examined, 72 were heteromorphic (AO), nine, homomorphic (AA), one, homomorphic (OO), and two, heteromorphic (AB). These observations show that the C-band located at the basal portion of the long arm of chromosome No. 4 is sex-linked. There were no definite banding differences between the A chromosomes of AA females and AA males, and also between the AO chromosomes of the AO males and AO female (Fig. 4). The C-bands in other chromosomes showed no such sex-related heteromorphism.

c. Late replication banding

The 140–141 late replicated bands were identified in the haploid chromosome set (Fig. 5). These bands showed characteristic pattern of each chromosome, making exact identification of all the chromosomes possible (Fig. 6). For chromosome No. 4, seven bands were equally confirmed in the short arms of the type A and O chromosomes, while nine and eight bands were visualized in the long arms of the type A and type O chromosomes, respectively (Fig. 7). The first band from the basal region of the long arm of the type A chromosome, which corresponded to the C-band at the basal portion of the long arm, was not detected in the type O

TABLE 1. Number of mitotic metaphases used for chromosome analyses and the banding pattern of chromosome No. 4 in the Wakuya population of *Rana japonica*

Sex	No. of analyzed frogs	No. of mitotic metaphases observed (photographed)			C-band type of chromosome No. 4
		Giemsa staining	C-banding	LR-banding	
Female	40	14 (14)	643 (165)	116 (116)	AA
	1	—	11 (11)	—	AO
Total	41	14 (14)	654 (176)	116 (116)	
Male	9	—	160 (46)	2 (2)	AA
	72	17 (17)	1352 (167)	29 (29)	AO
	2	—	40 (18)	—	AB
	1	—	20 (10)	—	OO
Total	84	17 (17)	1572 (241)	31 (31)	

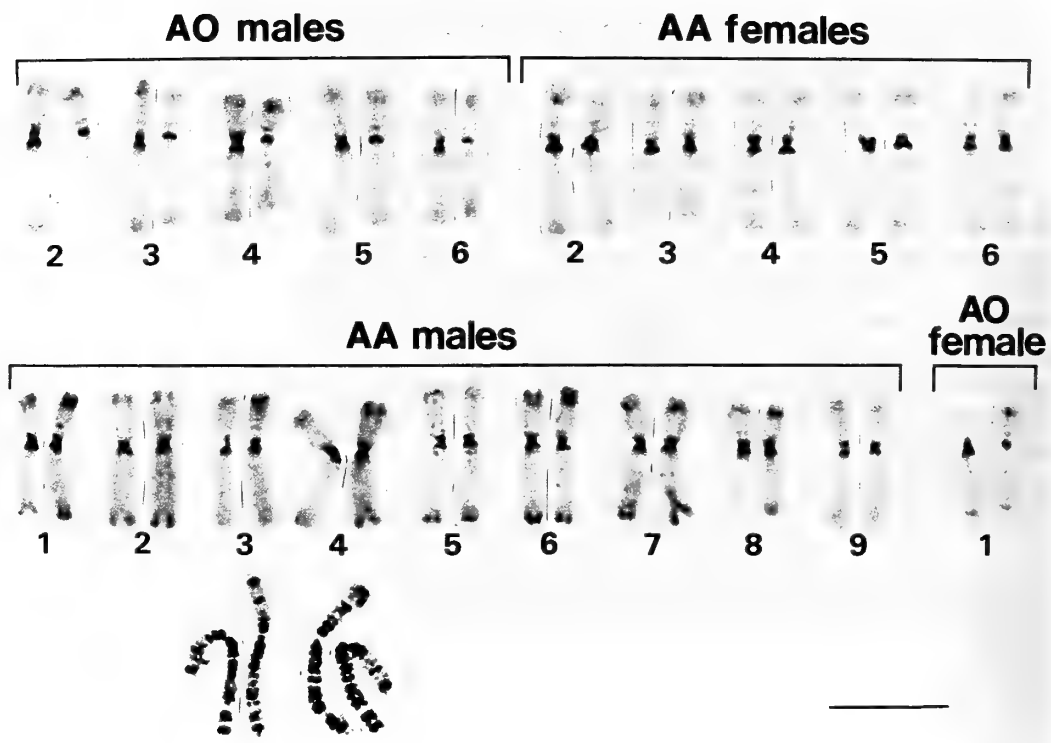

FIG. 4. C-banding patterns of the No. 4 chromosomes from five AO males (AO2~6), five AA females (AA2~6), nine AA males (AA1~9) and one AO female (AO1). Individual numbers are shown under the C-banded chromosome pairs. Late replication banding patterns of the No. 4 chromosomes from AA3 and AA4 males are shown under their C-banded chromosome pairs. Bar, 10 μm.

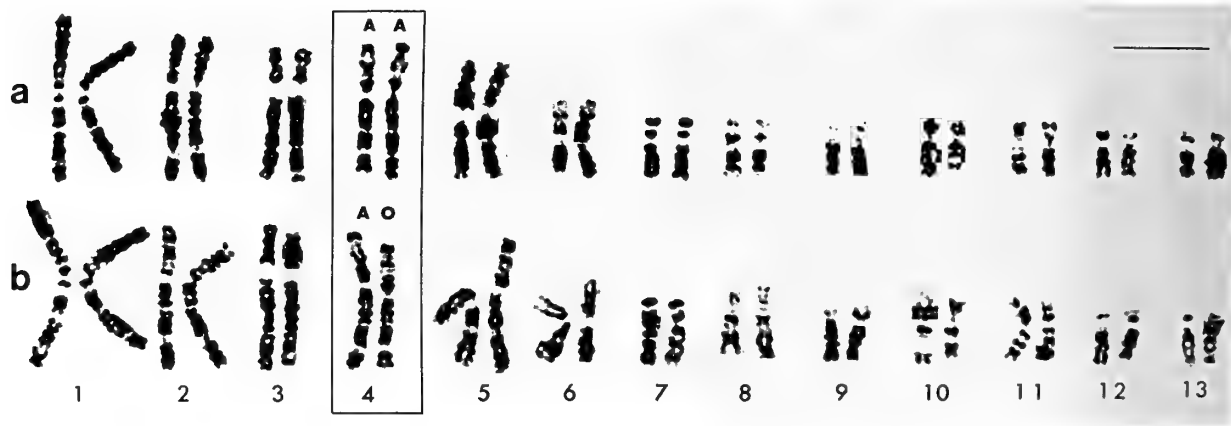

FIG. 5. Late replication banded karyotypes of *Rana japonica* from the Wakuya population: (a) female of AA type (AA1) and (b) male of AO type (AO15). No. 4 chromosomes are boxed. Bar, 10 μm.

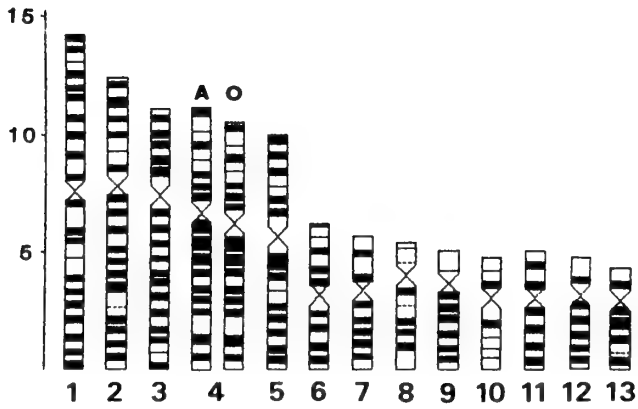

chromosome. The patterns of the remaining bands of the type A chromosome were identical with those of the type O chromosome. Between the two A chromosomes of the AA males, there were no differences of banding patterns (Fig. 4). In the remaining chromosomes there were no differences in the banding patterns between females and males.

FIG. 6. Idiogram showing late replication banding pattern of haploid chromosome set in *Rana japonica*. Scale on the left side shows relative chromosome length.

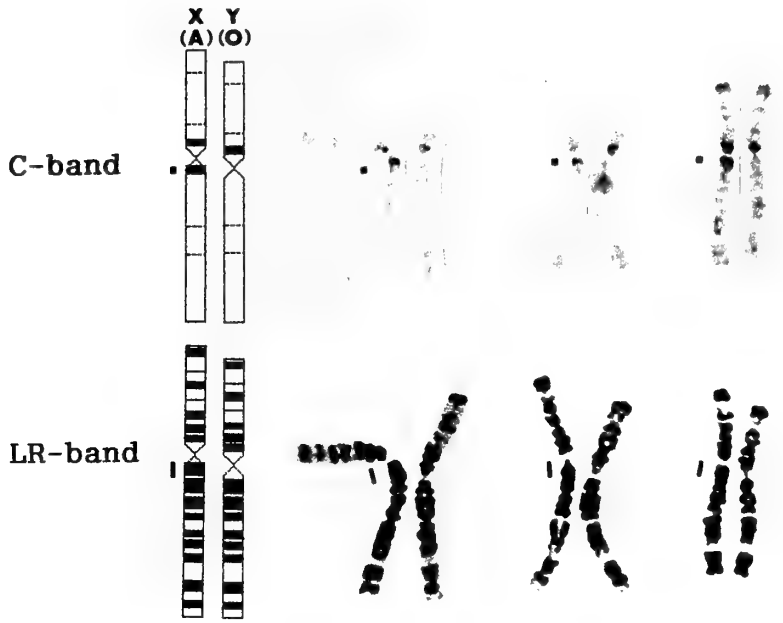

FIG. 7. Selected No. 4 chromosomes in a male of AO type (AO15) after C-banding and LR-banding. C-banding was performed after destaining of the LR-banded chromosome preparation. Almost all regions along the A and O chromosomes are homologous except the basal portions of the long arms, which are indicated by dots or bars.

Meiotic chromosomes

The pairing of the chromosomes at first meiotic metaphase was examined in the AO males. Identification of chromosome pair No. 4 was difficult, even in the C-banded metaphases, owing to the considerable spiraling and condensation of each bivalent (Fig. 8). Therefore, the number of large rod-shaped bivalents included in a complement was counted. The results are shown in Table 2. The number of complements containing one large rod-shaped bivalent varied considerably between males examined (17.9~66.7%). Consequently, during meioses of the AO males of *R. japonica*, it seems that each homologue of chromosome pair 4 does not always pair in an end to end fashion, thus differing from the sex-bivalents of mammals and also those of other frogs having highly evolved sex chromosomes.

Examination of the genetic sex of AA, AB and OO males

By C-banding analyses of the mitotic chromosomes, a

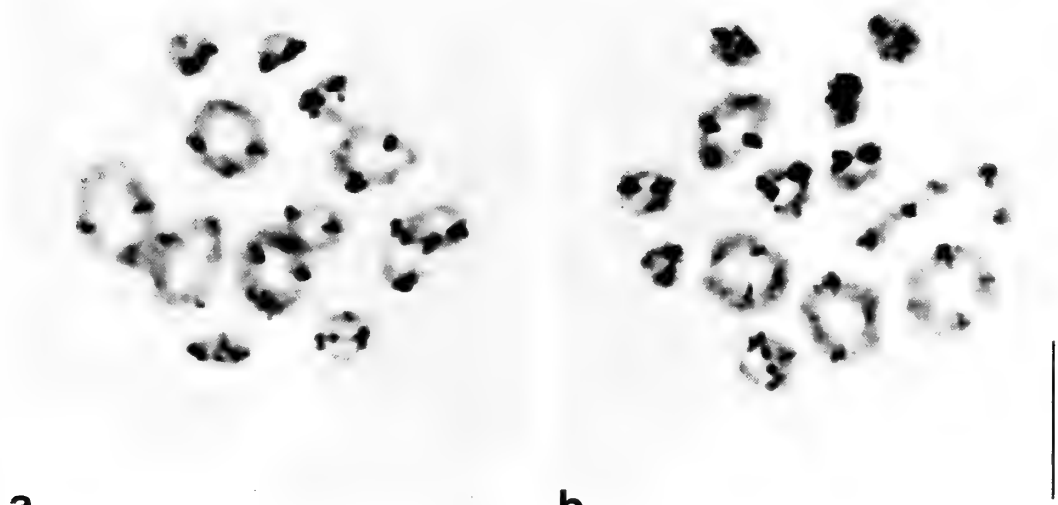

FIG. 8. First meiotic metaphase plates of the AO male (AO5) after C-banding. (a) This complement consists of five large and eight small ring-shaped bivalents. (b) Four large and eight small ring-shaped bivalents and one large rod-shaped bivalent. Bar, 10 μm.

TABLE 2. Pairing of the chromosomes at first meiotic metaphases of ten AO males

Individual No.	No.of meioses	No. of meiotic complements containing 0–5 large rod-shaped bivalents						No. of meioses including univalents
		0	1	2	3	4	5	
AO5	207	**167**	37 (17.9%)	0	0	0	0	3
AO6	209	**152**	53 (25.4%)	3	0	0	0	1
AO7	212	**132**	71 (33.5%)	8	0	0	0	1
AO8	210	7	**140** (66.7%)	47	11	0	0	5
AO9	214	22	**116** (54.2%)	64	7	0	0	5
AO10	210	12	**113** (53.8%)	67	13	0	0	5
AO11	210	85	**106** (50.5%)	16	2	0	0	1
AO12	200	4	**89** (44.5%)	85	17	2	0	3
AO13	218	1	56 (25.7%)	**146**	10	0	0	5
AO14	210	5	89 (42.4%)	**92**	22	2	0	0
Total	2100	587	870 (41.4%)	528	82	4	0	29

small number of males of AA, AB and OO and a female of AO that do not fit the ♂AO/♀AA system were found. Two cases can be supposed for the explanation of this fact. One is due to sex-reversal and the other to a recombination between a C-band at the basal portion of the long arm of chromosome No. 4 and a site of a male-determining gene located on the same chromosome. If sex-reversal could occur, AA males should be sex-reversed females and an AO female a sex-reversed male. And, an OO would be a genetic YY male produced from mating of a genetic XY male of AO with a sex-reversed XY male of AO. If this is true, some structural abnormality characteristic of transforming gonads might be observed in their testes. Therefore, the histological structure of testes was carefully examined.

a. Structure of testis

All the AA, AB and OO males examined had typical testes with normal structure except the two AA males (AA1, AA7), each of which had an auxocyte within the seminiferous tubule (Fig. 9a). Thus, these two males (AA1, AA7) seem to be spontaneously sex-reversed females.

In order to confirm the genetic sex of the AA males (AA1~5), the AB male (AB1) and the OO male (OO1), they were crossed with AA females, and the sex-ratio of the offspring was examined. Although the AO female laid a number of eggs, they did not begin to cleave at all. Therefore, the sex-ratio of the offspring between the AO female and an AO male could not be examined.

b. Sex of the offspring

Four AO males were mated with six AA females as controls, and five AA males, one OO and one AB males were mated with the six AA females. The percentage of normally cleaved eggs was low (21.0~35.2%) in the matings of the

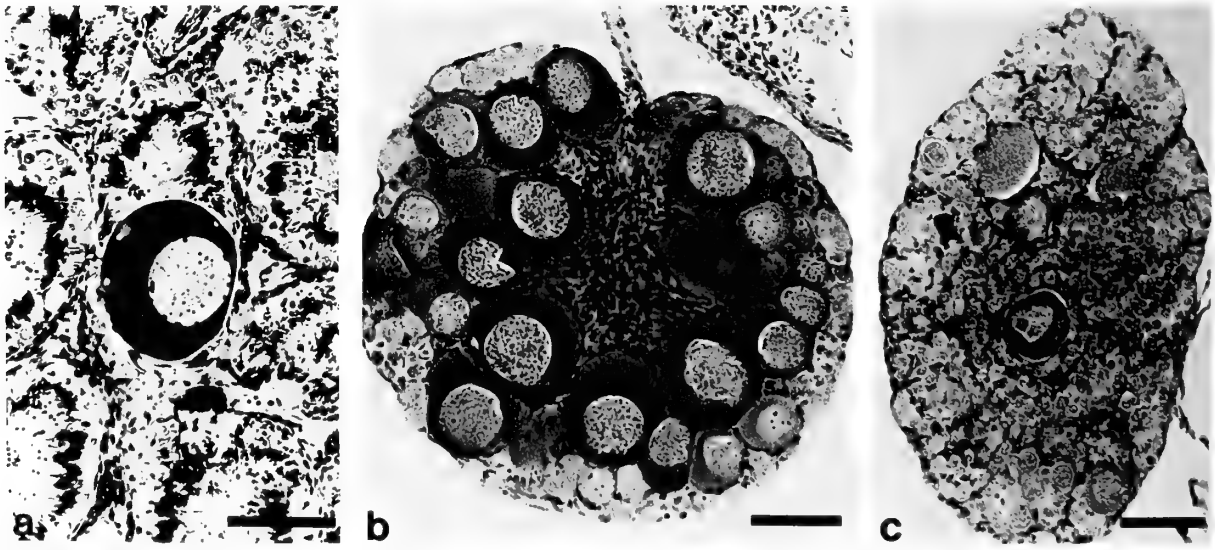

FIG. 9. Cross sections of gonads in an adult male (a) and 1~1.5-month-old frogs after metamorphosis (b and c). (a) Testis of AA7 male with a growing auxocype in the seminiferous tubule. (b) Gonad of a hermaphrodite, transforming from ovary into testis. (c) Gonad of a hermaphrodite having small groups of oocytes in testis. Bars, 100 μm.

AA2, AA5 and AB1 males, while high (72.8~99.6%) in other matings (data not shown). The sex of young frogs within 1.5 months after metamorphosis and adults of six months or one year old obtained from these matings was examined.

The results are shown in Table 3. In control matings, out of a total of 1061 frogs, 526 were females and 535 (50.4%) were males. The sex-ratio was just 1:1 (Table 3). 13 young frogs were hermaphrodites, the gonads of which were testes as a whole, where nearly all the gonia were surrounded with rete cells and there were no ovarian cavities, although there were small groups of oocytes (Fig. 9c).

In experimental matings using the AA males, two types of sex ratio were found. The offspring of the AA2 and AA4 males were females and males at a ratio of about 1:1, which is one type. Nine hermaphrodites at young frog stage were similar to those in the controls, having testes with some oocytes. On the other hand, almost all of the offspring from the AA1, 3 and 5 males were females, which is the other type. Twenty-one hermaphrodites at the young frog stage contained 15 hermaphrodites that had testes with some oocytes similar in histological structure to those of the controls, and six that had gonads at the beginning of sex-reversal, where a multiplication of rete cells was found in the medullary parts of the gonads and in the cortical parts there were abundant oogonia and young oocytes (Fig. 9b). Sex-ratio of offspring from the AB male and the OO male was about 1:1 (Table 3).

These sex-ratios reveal that the three AA males (AA1, 3 and 5) are spontaneously sex-reversed XX females, while the two AA males (AA2 and 4) as well as the AB and OO males are genetic XY males (Table 4).

Inheritance of the C-band in chromosome No. 4

Segregation of the three kinds of C-bands (O, A and B) in chromosome No. 4 was examined in the offspring from the above matings (Table 5). In the control matings of the AO males with the AA females, all the females examined showed the AA type and all the males examined the AO type. In the experimental mating of the AB male with the AA female, all of the females showed the AA type and all of the males the AB type. From these results, the O chromosome of the AO males and the B chromosome of the AB male could be considered Y chromosomes and inheritable to the next generation. In the experimental matings of the AA males with the AA females, all the frogs examined were of the AA type. Likewise, in the experimental mating of the OO male with the AA female, all the frogs examined were of the AO type. These results show that no addition or deletion of the C-band at the basal portion of the long arm of chromosome No. 4 occurred in the course of gametogenesis, or during the development and growth of these males.

TABLE 3. Sex of offspring in the matings of five AA, one AB and one OO males with AA females

Series	Parents		No. of metamorphosed frogs (%)	1~1.5-month-old frogs whose sex was examined					Six months- or one-year old frogs examined			Sex of all frogs examined		
	Female	Male		Total	♀	♂	⚥E	⚥C	Total	♀	♂	Total	♀	♂ (%)
Cont.	AA1	AO1	189	117	52	65			48	29	19	165	81	84 (50.9)
	AA2	AO2	196 (87.9)	114	56	57		1	48	24	24	162	80	82 (50.6)
	AA3	AO3	207 (87.0)	111	48	61		2	73	37	36	184	85	99 (53.8)
	AA4	AO3	195 (91.1)	181	87	87		7				181	87	94 (51.9)
	AA5	AO4	190 (79.2)	111	52	56		3	67	44	23	178	96	82 (46.1)
	AA6	AO4	206 (90.4)	191	97	94						191	97	94 (49.2)
	Total		994 (87.0)	825	392	420		13	236	134	102	1061	526	535 (50.4)
Exp.	AA1	AA1	153	81	60	5	4	12	55	42	13	136	102	**34 (25.0)**
	AA2	AA2	90 (21.5)	47	25	22			43	15	28	90	40	50 (55.6)
	AA2	AA3	194 (59.1)	99	93	1	2	3	68	55	13	167	148	**19 (11.4)**
	AA3	AA4	211 (69.9)	104	62	41		1	80	36	44	184	98	86 (46.7)
	AA4	AA4	196 (85.2)	192	89	95		8				192	89	103 (53.6)
	AA5	AA5	126 (32.1)	61	61	0			55	55	0	116	116	**0 (0.0)**
	AA6	AA5	106 (31.8)	99	99	0						99	99	**0 (0.0)**
	3 males (AA1, 3 and 5)			340	313	6	6	15	178	152	26	518	465	53 (10.2)
	2 males (AA2 and 4)			343	176	158		9	123	51	72	466	227	239 (51.3)
	AA2	AB1	90 (15.6)	52	29	23			35	17	18	87	46	41 (47.1)
	AA5	OO1	300 (82.9)	197	99	96		2	73	34	39	270	133	137 (50.7)
	AA6	OO1	210 (87.1)	184	103	81						184	103	81 (44.0)
	Total		510 (84.6)	381	202	177		2	73	34	39	454	236	218 (48.0)

⚥E, hermaphrodite whose gonad was at the beginning of sex-reversal from ovary into testis
⚥C, hermaphrodite whose gonad was testis as a whole with some oocytes

TABLE 4. Testes and the male offspring of nine AA males, two AB males and one OO male of *Rana japonica* collected from the Wakuya population

Individual No.	Growing auxocytes	Male offspring (%)	Presumed sex chromosome constitution
AA1	+	25.0	XX
AA2	−	55.6	XY
AA3	−	11.4	XX
AA4	−	50.3	XY
AA5	−	0.0	XX
AA6	−	NE	?
AA7	+	NE	XX
AA8	−	NE	?
AA9	−	NE	?
AB1	−	47.1	XY
AB2	NE	NE	?
OO1	−	48.0	XY

NE, not examined
+, detected −, not detected

TABLE 5. Segregation of C-bands on chromosome No. 4 in the offspring from matings of AO, AA, AB and OO males with AA females

Series	Parents		Sex	No. of analyzed frogs	C-band type of chromosome No. 4		
	Female	Male			AA	AO	AB
Cont.	AA2	AO2	Female	14	14	0	0
			Male	14	0	14	0
	AA5	AO4	Female	10	10	0	0
			Male	12	0	12	0
	Total		Female	24	24	0	0
			Male	26	0	26	0
Exp.	AA1	AA1	Female	1	1	0	0
			Male	2	2	0	0
	AA2	AA2	Female	1	1	0	0
			Male	1	1	0	0
	AA2	AA3	Female	2	2	0	0
			Male	1	1	0	0
	AA3	AA4	Female	1	1	0	0
			Male	2	2	0	0
	Total		Female	5	5	0	0
			Male	6	6	0	0
	AA2	AB1	Female	17	17	0	0
			Male	18	0	0	18
	AA5	OO1	Female	3	0	3	0
			Male	2	0	2	0

DISCUSSION

Male heterogamety in the sex-determining mechanism of Rana japonica

Moriwaki [10] obtained 16 parthenogenetic diploids (seven males and nine females) of *Rana japonica* by cold treatment of unfertilized eggs after pricking them with a glass needle. When one of these males was mated with a normal female caught in the field, the progeny were all females [11]. Kawamura and Yokota [6] performed sex-reversal of genetic females of *R. japonica* into phenotypic males by an injection of testosterone propionate at the tadpole stage. All the injected larvae became mature males. When 12 of these males were mated with normal females, the progeny from four of these males were females and males with the ratio 1:1, while almost all of the progeny from the remaining eight males were females. These two experiments clearly show that the males which produced only female progeny in the matings with normal females are sex-reversed XX females, and consequently, in *R. japonica* the male is the heterogametic sex (♂XY/♀XX system). The present C-banding analysis of the chromosomes with the Wakuya population of *R. japonica* has demonstrated that chromosome pair 4 was heteromorphic (AO) in the males and homomorphic (AA) in the females for a C-band at the basal portion of the long arm. When the AO males were mated with AA females, all the male offspring were of the AO type and all the female offspring were of the AA type. Thus, it is clear that the C-band located at the basal portion of the long arm of chromosome No. 4 is sex-linked, and chromosome No. 4 is a sex chromosome itself.

Lower amount of constitutive heterochromatin on the Y chromosome than on the X chromosome

In general, much more constitutive heterochromatin has been accumulated in the Y or W chromosomes than in the X or Z chromosomes of mammals, birds and some lower vertebrates. In contrast, the amounts of constitutive heterochromatin distributed in the Y chromosomes (O) were less than in the X chromosomes (A) in *Rana japonica*. This is one of the unique features for the sex chromosomes of *R. japonica* elucidated in this study. Sex chromosomes similar to those of *R. japonica* have so far been found in the marsupial frog, *Gastrotheca walkeri* [18]. The C-banded karyotype exhibits a large amount of constitutive heterochromatin in the pericentromeric region of each of the chromosomes including X, while the Y chromosome contains an extremely low amount of constitutive heterochromatin at the centromeric region. Such Y chromosomes have been reported also in Japanese Gold fish and Chinese Funa [14] and the Asian black turtle, *Siebenrockiella crassicollis* [1]. In *Rana japonica*, amplification of the heterochromatin occurred in the pericentromeric regions of all the chromosomes, but only the basal portion of the long arm of the Y chromosome escaped from the occurrence possibly by the sex-specific innerstructural change, which may be one of the initial steps

on the differentiation of the Y chromosomes.

Various morphs of the X and Y chromosomes within a species

The other unique feature for the sex chromosomes of *R. japonica* confirmed in this study is the presence of the AA, OO and AB males and the AO female within the ♂AO/♀AA system. Four of the nine AA males were found to be spontaneously sex-reversed females, because almost all of the progeny from these three males when mated with the AA females were females, and one AA male included a growing auxocyte within the seminiferous tubule of the testis (Table 4). Other two AA males were found to be genetic XY males, because the progeny of these two males when mated with the AA females were females and males in the ratio 1 : 1. The OO male was also found to be a genetic XY male, not a YY male, judging by the 1 : 1 sex ratio of the progeny. This OO male may have been produced from a mating of an AO male of XY with an AO female of XX in the field. The AO female may not be a sex-reversed XY male, but an XX genetic female, because sex-reversal of genetic XY male into phenotypic female is firmly resisted in *Rana* species [5]. The heteromorphic AB male was also found to be a genetic XY male on the basis of the sex ratio of 1 : 1 in the progeny, and the B chromosome was found to be a Y chromosome from chromosome analysis of the progeny, where all males were of the AB type and all females were of the AA type.

Thus, in the Wakuya population two morphs (A and O) of the X chromosomes and three morphs (O, A and B) of the Y chromosomes coexist. The south American frog, *Gastrotheca psuestes*, is characterized by ♂XY/♀XX sex chromosome system, and it was shown that in 11 males the XY chromosomes are still homomorphic, but in 15 males the Y chromosome displays a prominent telomeric C-band in the long arm, which is absent in the X [19]. The North American salamander, *Aneides ferreus*, is characterized by ♀ZW/♂ZZ sex chromosomes in the Vancouver island populations, while in the northern California populations all males are homomorphic (telocentrics/telocentrics), and the females are either homomorphic (T/T) or heteromorphic (T/metacentrics) [7, 20]. In the two species referred to above, the frequency of specimens with the morph of the Y or W chromosome which is identical to the X or Z in appearance is relatively high, 42.3% in *Gastrotheca pseustes* and 26.9% in *Aneides ferreus*. By contrast, for *Rana japonica* the genetic XY males of AA rarely occurred at the frequency of 2.4% (2/84)~6.0% (5/84); if the uncertain three AA males are all sex-reversed XX females, the number of the genetic XY males of AA would be two in total, and if those are all genetic XY males, it would be five. Furthermore, a genetic XX female of AO occurred at the similar frequency of 2.4% (1/41). Thus, it is reasonable to infer that in *R. japonica* the XY males of the AA type and the XX female of the AO type were produced through a recombination between the site of a C-band at the basal portion of the long arm of chromosome No. 4 and the site of a male-determining gene on the same chromosome during male meiosis. Since the late replication banding patterns in the euchromatic regions of the A and O chromosomes were almost identical with each other and both AO and autosomal bivalents of the ring-like appearance were formed in male meiosis, the A and O chromosomes may be genetically homologous, and crossing over should occur at the euchromatic regions of XY (AO) as often as autosomes.

Consequently, chromosome No. 4 of *R. japonica* is a sex chromosome without doubt. However, sex-linkage of the C-band on chromosome No. 4 is incomplete. Therefore, the heteromorphic situation of the sex chromosomes will possibly not be held in this population, if the number of recombinants and sex-reversed females increases in future generations. Such unstable heteromorphism of the sex chromosomes may reflect the primitive state of sex chromosome differentiation.

Iizuka [4] has performed C- and Ag-banding analyses on the chromosomes of *R. japonica* with the Hitachi-ota population from Ibaraki Prefecture, but failed to identify the sex chromosomes. Therefore, in order to know whether such a peculiar differentiation of the sex chromosomes is a restricted system only to the Wakuya population under present study, or whether other different types of sex chromosome exist in this species, it is necessary to do an extensive chromosomal analysis of various geographic populations.

ACKNOWLEDGMENTS

I wish to express my sincere thanks to M. Nishioka of Hiroshima University for her constant guidance in the course of this work. I am also deeply indebted to K. Saitoh of Aomori University for his valuable advice. I wish to thank Setsuko Saitoh for her help in collecting specimens used in this study.

REFERENCES

1 Carr JL, Bickham JW (1981) Sex chromosomes of the Asian black pond turtle, *Siebenrockiella crassicollis* (Testudines: Emydidae). Cytogenet Cell Genet 31: 178–183

2 Green DM (1988) Heteromorphic sex chromosomes in the rare and primitive frog *Leiopelma hamiltoni* from New Zealand. J Heredity 79 (3): 165–169

3 Green DM (1988) Cytogenetics of the endemic New Zealand frog, *Leiopelma hochstetteri*: Extraordinary supernumerary chromosome variation and a unique sex-chromosome system. Chromosoma 97: 55–77

4 Iizuka K (1989) Constitutive heterochromatin and nucleolus organizer regions in Japanese brown frogs, *Rana japonica* and *Rana ornativentris*. Jpn J Herpetol 13(1): 15–20

5 Kawamura T, Nishioka M (1977) Aspects of the reproductive biology of Japanese anurans. In "Reproductive Biology of Amphibians" Ed by DH Taylor, SI Guttman, Plenum Publishing Corporation, New York, London pp103–139.

6 Kawamura T, Yokota R (1959) The offspring of sex-reversed females of *Rana japonica* Guenther. J Sci Hiroshima Univ Ser B Div 1 18: 31–38

7 Kezer J, Sessions SK (1979) Chromosome variation in the plethodontid salamander, *Aneides ferreus*. Chromosoma 71: 65–80

8 Kobayashi M (1962) Studies on reproductive isolation mechanisms in brown frogs II. Hybrid sterility. J Sci Hiroshima Univ Ser B Div 1 20: 157–179

9 Kuramoto M, Furuya E, Takegami M, Yano K (1974) Karyotypes of several species of frogs from Japan and Taiwan. Bull Fukuoka Univ Educ PtIII 23: 67–78

10 Moriwaki T (1957) Studies on matured parthenogenetic frogs I. The development and the reproductive ability. J Sci Hiroshima Univ Ser B Div 1 17: 13–32

11 Moriwaki T (1959) Studies on matured parthenogenetic frogs II. The offspring of a male parthenogenetic frog. J Sci Hiroshima Univ Ser B Div 1 18: 45–50

12 Nishioka M, Miura I, Saitoh K (1993) Sex chromosomes of *Rana rugosa* with special reference to local differences in sex-determining mechanism. Sci Rep Lab Amphibian Biol Hiroshima Univ 12: 55–81

13 Nishioka M, Okumoto H, Ueda H, Ryuzaki M (1987) Karyotypes of brown frogs distributed in Japan, Korea, Europe and North America. Sci Rep Lab Amphibian Biol Hiroshima Univ 9: 165–212

14 Ojima Y, Ueda T, Narikawa T (1979) A cytogenetic assessment on the origin of the gold-fish. Proc Japan Acad 55(B): 58–63

15 Schempp W, Schmid M (1981) Chromosome banding in Amphibia VI. BrdU-replication patterns in Anura and demonstration of XX/XY sex chromosomes in *Rana esculenta*. Chromosoma 83: 697–710

16 Schmid M, Haaf T, Geile B, Sims S (1983) Chromosome banding in Amphibia VIII. An unusual XY/XX-sex chromosome system in *Gastrotheca riobambae* (Anura, Hylidae). Chromosoma 88: 69–82

17 Schmid M, Olert J, Klett C (1979) Chromosome banding in Amphibia III. Sex chromosomes in *Triturus*. Chromosoma 71: 29–55

18 Schmid M, Steinlein C, Feichtinger W, de Almeida CG, Duellman WE (1988) Chromosome banding in Amphibia XIII. Sex chromosomes, heterochromatin and meiosis in marsupial frogs (Anura, Hylidae). Chromosoma 97: 33–42

19 Schmid M, Steinlein C, Friedl R, de Almeida CG, Haaf T, Hillis DM, Duellman WE (1990) Chromosome banding in Amphibia. XV. Two types of Y chromosomes and heterochromatin hypervariability in *Gastrotheca pseustes* (Anura, Hylidae). Chromosoma 99: 413–423

20 Sessions SK, Kezer J (1987) Cytogenetic evolution in the plethodontid salamander genus *Aneides*. Chromosoma 95: 17–30

21 Seto T (1965) Cytogenetic studies in lower vertebrates, II Karyological studies of several species of frogs (Ranidae). Cytologia 30: 437–446

22 Sumida M (1981) Studies on the Ichinoseki population of *Rana japonica*. Sci Rep Lab Amphibian Biol Hiroshima Univ 5: 1–46

23 Sumner AT (1972) A simple technique for demonstrating centromeric heterochromatin. Exp Cell Res 75: 304–306

24 Takayama S, Taniguchi T, Iwashita Y (1981) Application of the 4Na-EDTA Giemsa staining method for analysis of DNA replication pattern. CIS 31: 36–38

ZOOLOGICAL SCIENCE 11: 807–815 (1994)

Sex Chromosome Differentiation in the Japanese Brown Frog, *Rana japonica* II. Sex-linkage Analyses of the Nucleolar Organizer Regions in Chromosomes No. 4 of the Hiroshima and Saeki Populations

IKUO MIURA

Laboratory for Amphibian Biology, Faculty of Science, Hiroshima University, Higashihiroshima 724, Japan

ABSTRACT—The Wakuya population of the Japanese brown frog, *Rana japonica*, from Miyagi Prefecture (northeast of Honshu, Japan) is characterized by ♂XY/♀XX sex chromosomes. The sex chromosomes are the fourth largest (No. 4) in the complement; the Y chromosome is distinguished from the X and autosomes by its C- and late replication banding patterns. In the present study, somatic chromosomes of this species were examined with two populations from Hiroshima and Saeki of Hiroshima Prefecture (southwest of Honshu) by C-, late replication and Ag-banding techniques, with special attention to chromosome No. 4. However, sex-related differences in shape and banding pattern were not found in any chromosomes, inclusive of No. 4. Since nucleolar organizer regions (NORs) were present in chromosome pair 4 in one of the two populations, linkage of the NOR in chromosome No. 4 to the sex was examined in the backcrossed offspring between these two populations. As a result, the NOR in chromosome No. 4 was not linked to the sex. Therefore, a male determining gene may not be on chromosome No. 4 in these two populations of Hiroshima Prefecture.

INTRODUCTION

Previous cytogenetic and genetic studies demonstrated that the Japanese brown frog, *Rana japonica*, from the Wakuya population is characterized by a ♂XY/♀XX sex chromosome system [10]. The sex chromosomes are the fourth largest chromosomes in the complement. The males are of the AO type and the females of the AA type for the C-band located at the basal portion of the long arm. Cross experiments revealed that sex-linkage of the C-band was persisted to the next generation.

Rana japonica is widely distributed in Japan, and comprises genetically differentiated populations. For example, the karyotypes of the Hiroshima (southwestern Honshu) and Ichinoseki (northeastern Honshu) populations are slightly different from each other, and there exists a reproductive isolation of incomplete male hybrid sterility between them [19]. Thus, it is expected that in the Hiroshima population, the sex chromosomes have accomplished differentiation in a manner different from those of the Wakuya population.

In the present study, chromosome analyses using C- and late replication banding techniques were performed in *Rana japonica* from the two populations, Hiroshima in a plain and Saeki in a mountanious region, of Hiroshima Prefecture. However, the diploid chromosomes showed no sex-related heteromorphism in their banding patterns.

Furthermore, the position of nucleolar organizer region (NOR) in the chromosomes of these two populations was examined by Ag-staining. In the Hiroshima population, the NORs were present in only chromosome pair 10 like other *Rana* species [16], whereas in the Saeki population they were demonstrated in chromosome pairs 4 and 10. A NOR is associated with a sex chromosome in four anuran species [1, 5, 14, 17]. Then, in order to elucidate if chromosomes No.4 in these two populations of Hiroshima Prefecture are sex-related like those in the Wakuya population, backcrossed progeny were produced between the Hiroshima and Saeki populations, and the relationship between the NORs in No.4 chromosomes and the sex was examined.

Accepted July 29, 1994
Received April 27, 1994

MATERIALS AND METHODS

Specimens were collected in Hiroshima City, and Saeki-cho, Saeki-gun, Hiroshima Prefecture. The numbers of frogs and mitotic metaphases analyzed by the conventional Giemsa staining and various banding techniques are shown in Table 1.

Mitotic metaphase cells were obtained by the blood cell culture as described earlier [10]. Chromosome slides were prepared by the conventional air-drying method. C- and late replication bandings were performed as described earlier [10]. Ag-staining for the demonstration of NORs was done according to '1-step method' of Howell and Black [6].

Cross experiments were performed from February to March. Ovulation was accelerated by injection of the suspension of bullfrog pituitaries into the abdominal cavity.

RESULTS

Chromosome analyses

a. Conventional Giemsa staining

The diploid complement of 26 chromosomes, consisting of five large and eight small chromosome pairs was confirmed in both sexes of these populations (Fig. 1). In the Hiroshima population, a large secondary constriction was observed

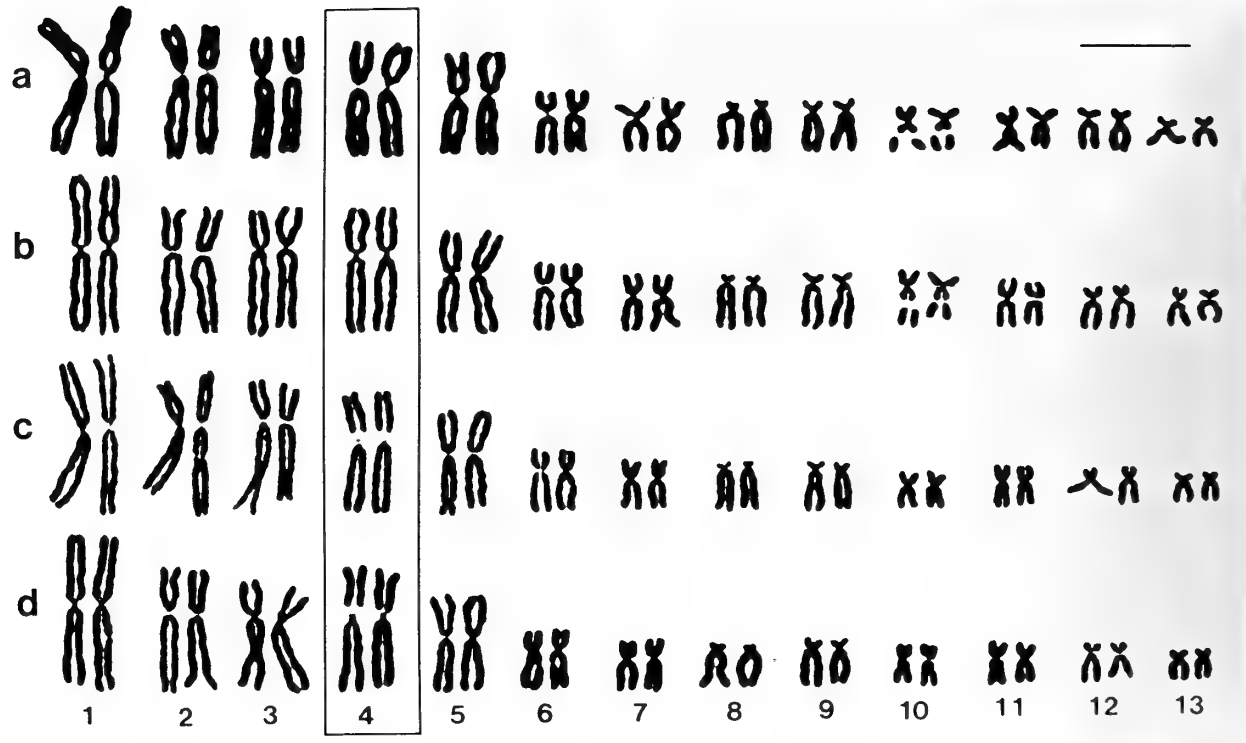

FIG. 1. Karyotypes of *Rana japonica* from the Hiroshima (a, female; b, male) and Saeki (c, female; d, male) populations by the conventional Giemsa staining. No. 4 chromosomes are boxed. Bar, 10 μm.

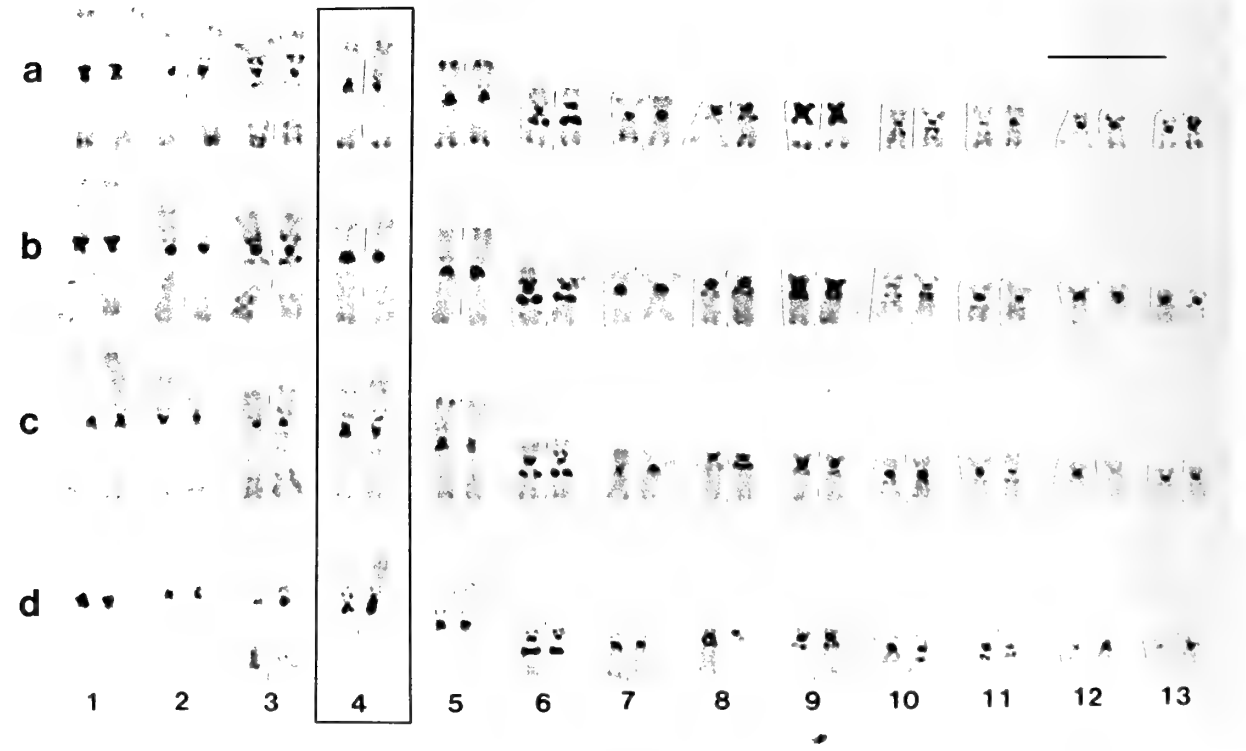

FIG. 2. C-banded karyotypes of *Rana japonica* from the Hiroshima (a, female; b, male) and Saeki (c, female; d, male) populations. No. 4 chromosomes are boxed. Bar, 10 μm.

in the middle portion of the long arm of chromosome No. 10, whereas in the Saeki population such secondary constriction was observed in the basal portion of the short arm of chromosome No. 4 and sometimes in chromosome No. 10. No heteromorphic sex chromosomes were distinguished in either population.

b. C-banding and late replication banding (LR banding)

Constitutive heterochromatin was distributed mainly in the centromeric region of each chromosome (Fig. 2). The amounts were very low compared to those in the Wakuya population [10]. None of the chromosomes, inclusive of No. 4, showed any sex-related heteromorphism of C-banding patterns in either population.

The late replication banding patterns of mitotic chromosomes were analyzed with two males from the Hiroshima population and eight frogs (♀4, ♂4) from the Saeki population. A total of 131 late replication bands in the haploid set was identified (Fig. 3). No heteromorphism in the LR banding patterns was found in either sex of the Saeki population. These two populations of Hiroshima Prefecture and the Wakuya population showed similar LR-band patterns, with the exception of those bands corresponding to the C-bands (Fig. 4).

c. Ag-staining

Since marked secondary constrictions were observed, as described above, in the conventionally Giemsa-stained chromosomes, their presence and location were examined again by Ag-staining for the demonstration of NORs (Table 1; Fig. 5). The location and number of NORs on chromosomes of one complement showed no cell to cell variation within a specimen. In the Hiroshima population, the NOR was restricted to the middle portion of the long arm of chromosome No. 10. In the Saeki population, the NOR was identified in the basal portion of the short arm of chromosome No. 4, in addition to that in No. 10 (Fig. 5). Although the NORs in chromosome pair 4 of the Saeki population were invariably observed in both homologues of all the females and males examined (4^+4^+), they were not always present in chromosome No.10: in the two females, they were detected in both homologues (10^+10^+), but in the five females, the NOR was detected only in one homologue (10^+10^-). The remaining 13 females and two males had no NOR in any regions of chromosome No. 10 (10^-10^-).

Analysis of linkage between the NOR in chromosome No. 4 and the sex

Analyses of chromosomes in the Hiroshima and Saeki populations by various banding techniques failed to detect any sex-related heteromorphism. However, the similarities in the late replication banding patterns in chromosomes No. 4 of the two populations of Hiroshima Prefecture and the Wakuya population suggest that the No. 4 chromosomes in these populations are homologous in structure (Fig. 4). Therefore, it is speculated that chromosomes No. 4 in these two populations of Hiroshima Prefecture are sex chromosomes but not differentiated morphologically. So, the NOR located in chromosome No. 4 of the Saeki population was utilized as a marker for the analysis of linkage with the sex. Males heteromorphic for the NOR in chromosome No. 4 (4^+4^-) were produced by crossing females (4^+4^+) of the Saeki population with males (4^-4^-) of the Hiroshima population and *vice versa*, then they were backcrossed to the females (4^+4^+) of the Saeki population. The linkage of the NOR in chromosome pair 4 with the sex was examined in the backcrossed offspring.

a. Sex ratios of the hybrids and backcrossed hybrids

Almost all of the hybrids between genetically differenti-

FIG. 3. Late replication banded karyotypes of *Rana japonica* from the Hiroshima (a, male) and Saeki (b, female; c, male) populations. No. 4 chromosomes are boxed. Bar, 10 μm.

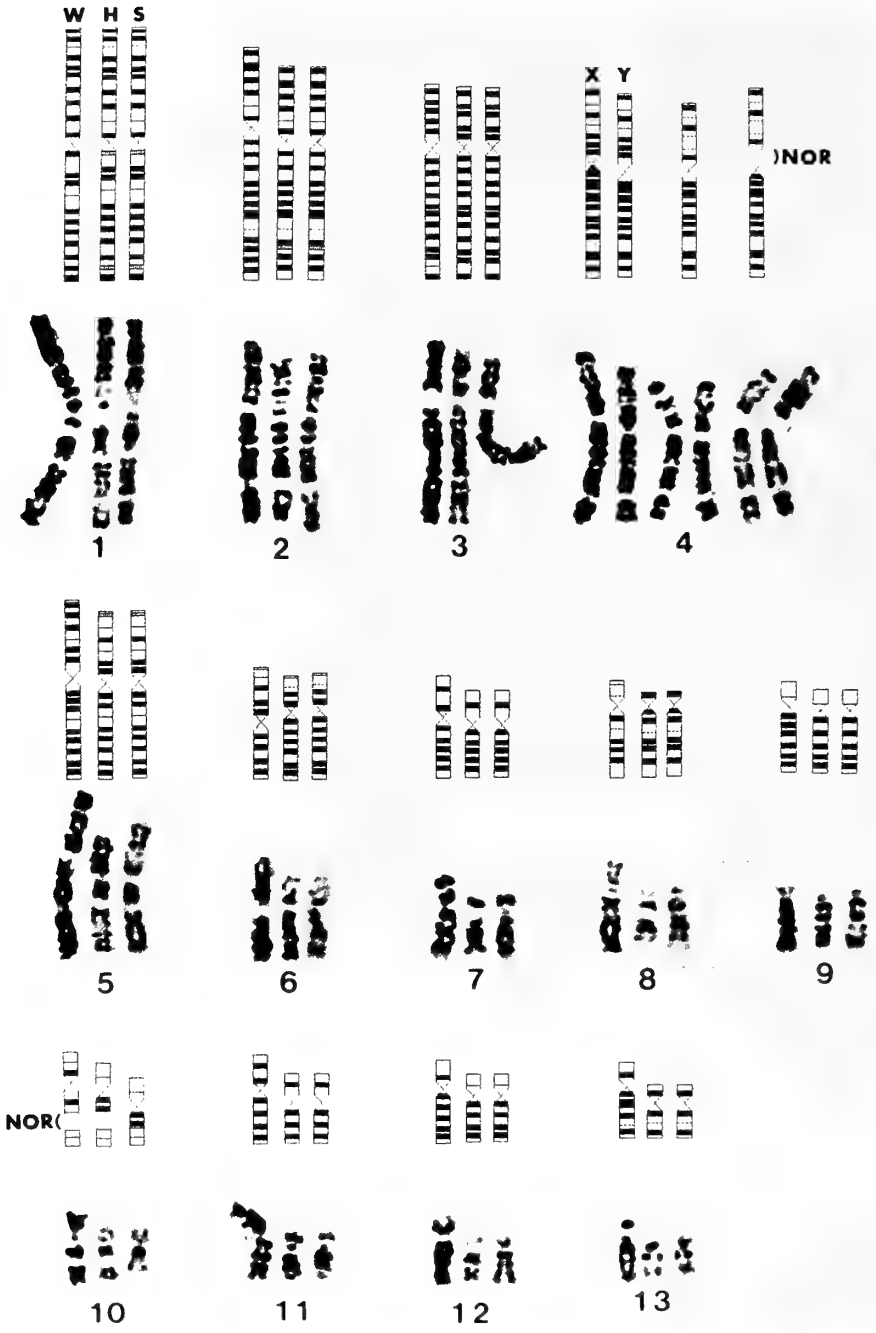

FIG. 4. Comparison of the late replication banding patterns in the chromosomes of males from the Wakuya (W), Hiroshima (H) and Saeki populations (S). The haploid chromosome sets of the three populations are arranged except chromosome pair 4, of which both homologues are presented. Almost all of the banding patterns in the 13 chromosome pairs are homologous between these populations except for the bands corresponding to C-bands.

ated populations of *Rana japonica* are known to become males by sex-reversal [19]. Thus, it is necessary to check the sex ratio of hybrids and backcrossed offspring between the Hiroshima and Saeki populations. The frogs from the Hiroshima population are symbolized here for description as H and those from the Saeki population as S, respectively.

The sex of hybrids and control frogs was examined within six months after metamorphosis (Table 2). The sex ratios of control offspring and experimental offspring were approximately 1:1, except in the matings using the S2 and S3 females. The S2 female produced an approximately equal number of females and males in the control mating, while in the experimental mating with the H2 male, the number of male offspring was a little higher than those of female offspring (71.0%). The S3 females produced a slight majority of male offspring in both the control (63.6%) and experimental (63.9%) matings.

The sex of the offspring of the hybrid males (SH and HS) backcrossed to the S females was examined within a month after metamorphosis (Table 3). The sex-ratios of the

TABLE 1. Number of frogs and mitotic metaphases analyzed by the conventional staining and various banding techniques

Population	Sex	No. of frogs	No. of mitotic figures analyzed				NORs	
			G	C	LR	Ag	No. 4	No. 10
Hiroshima	Female	1	2	6	—	—		
		4	—	—	—	40	4^-4^-	10^+10^+
	Male	3	10	14	13	—		
		4	—	—	—	40	4^-4^-	10^+10^+
	Total	12	12	20	13	80		
Saeki	Female	7	16	13	42	—		
		13	—	—	—	106	4^+4^+	10^-10^-
		5	—	—	—	26	4^+4^+	10^+10^-
		2	—	—	—	13	4^+4^+	10^+10^+
	Male	9	36	29	42	—		
		2	—	—	—	20	4^+4^+	10^-10^-
	Total	38	52	42	84	165		

G, Conventional Giemsa staining C, C-banding
LR, Late replication banding Ag, Ag-staining
$^+$ and $^-$ in the right superscript indicate the presence and absence of a NOR, respectively, in one homologue

offspring from the SH male hybrids were about 1 : 1 in all the series. In contrast, those offspring from the HS male hybrids were about 1 : 1 in four of the six matings, whereas in the remaining two matings of the HS4 and HS6 male hybrids, the number of males was a little higher than that of females. The slight majority of males observed in these hybrids and backcrossed offspring suggests that there is a slight incompatibility of interaction of the Hiroshima nuclear genome to the Saeki cytoplasm.

Inheritance of the NOR in chromosome No. 4

The phenotypes of NORs in chromosomes No. 4 were examined with the offspring of hybrid males (4^+4^-, 4^-4^+) between the two populations, Hiroshima and Saeki, backcrossed with females (4^+4^+) of the Saeki population. If the NOR in chromosome pair 4 was linked to the sex, then the backcrossed offspring from the SH hybrid males (4^+4^-) should be heteromorphic (4^+4^-) for the NOR in males and homomorphic (4^+4^+) in females, whereas those from the HS hybrid males (4^+4^+) should be homomorphic (4^+4^+) in males and heteromorphic (4^+4^-) in females. The sex and phenotypes of the NORs in backcrossed offspring were examined within a month after metamorphosis (Table 4). In all the matings using the SH and HS male hybrids, the frequency of each NOR type (4^+4^+ or 4^+4^-) in chromosome No. 4 did not show any significant differences between the female and male offspring. Similar results were obtained regarding the phenotypes of NORs in chromosome pair 10. These results reveal that the NOR in chromosome No. 4, as well as that in No. 10, is not linked to the sex.

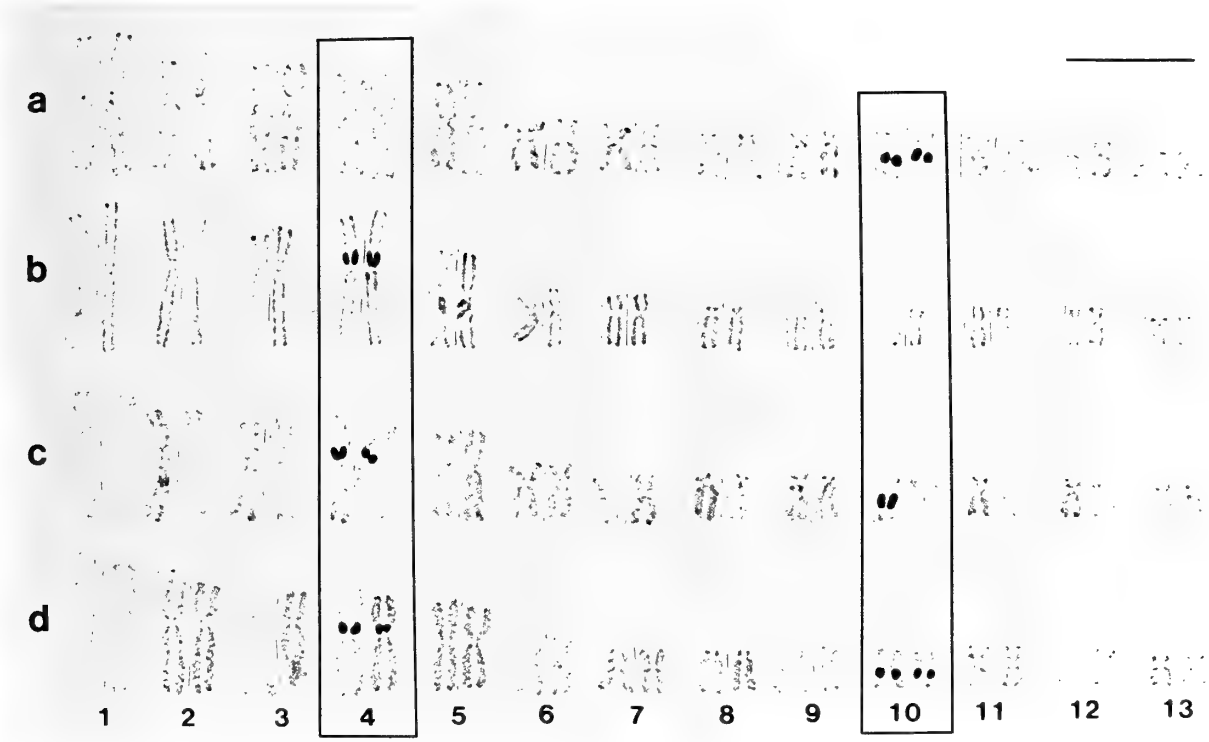

FIG. 5. Karyotypes of *Rana japonica* from the Hiroshima and Saeki populations by Ag-staining: (a) female of the Hiroshima population with NORs in both homologues of chromosome pair 10, (b) female of the Saeki population with NORs in both homologues of chromosome pair 4, (c) female of the Saeki population with NORs in both homologues of chromosome pair 4 and one of pair 10 and (d) female of the Saeki population with NORs in both homologues of chromosome pairs 4 and 10. Nos. 4 and 10 chromosomes are boxed. Bar, 10 μm.

TABLE 2. Sex of hybrids between the Hiroshima and Saeki populations

Series		Parents Female	Parents Male	No. of eggs	No. of metamorphosed frogs (%)	No. of No. of frogs whose sex was examined Total	♀	♂ (%)
Cont.	Hiroshima (H)	H1	H1	47	35 (74.5)	17	9	8 (47.1)
		H2	H2	75	18 (24.0)	6	3	3 (50.0)
		H3	H3	105	87 (82.9)	54	23	31 (57.4)
		H3	H4	116	87 (75.0)	42	17	25 (59.5)
		Total		343	227 (66.2)	119	52	67 (56.3)
	Saeki (S)	S1	S1	123	25 (20.3)	14	7	7 (50.0)
		S2	S1	121	84 (69.4)	82	38	44 (53.7)
		S3	S2	45	33 (73.3)	33	12	21 (63.6)
		S4	S2	209	31 (14.8)	9	7	2 (22.2)
		Total		498	173 (34.7)	138	64	74 (53.6)
Exp.	H×S	H1	S1	116	86 (74.1)	67	33	34 (50.7)
		H2	S1	117	98 (83.8)	94	45	49 (52.1)
		H3	S2	178	93 (52.2)	66	30	36 (54.5)
		Total		411	277 (67.4)	227	108	119 (52.4)
	S×H	S1	H1	171	36 (21.1)	12	7	5 (41.7)
		S2	H2	105	78 (74.3)	69	20	49 (71.0)
		S2	H3	103	71 (68.9)	64	30	34 (53.1)
		S3	H4	138	93 (67.4)	83	30	53 (63.9)
		S4	H4	234	37 (15.8)	23	15	8 (34.8)
		S5	H5	250	125 (50.0)	98	50	48 (49.0)
		Total		1001	440 (44.0)	349	152	197 (56.4)

TABLE 3. Sex of the backcrossed offspring

Series	Parents Female	Parents Male	No. of eggs	No. of metamorphosed frogs (%)	No. of frogs whose sex was examined Total	♀	♂ (%)
S×SH	Sw1	SH1	60	29 (48.3)	16	6	10 (62.5)
	Sw2	SH1	413	99 (24.0)	94	39	55 (58.5)
	Sw3	SH1	413	60 (14.5)	55	29	26 (47.3)
	Sw4	SH1	266	238 (89.5)	135	69	66 (48.9)
	Sw4	SH2	251	129 (51.4)	91	50	41 (45.1)
	Total		1403	555 (39.6)	391	193	198 (50.6)
S×HS	Sw1	HS1	209	157 (75.1)	113	52	61 (54.0)
	Sw1	HS2	222	194 (87.4)	142	76	66 (46.5)
	Sw2	HS3	211	98 (46.4)	77	40	37 (48.1)
	Sw5	HS4	168	95 (56.5)	82	28	54 (65.9)
	Sw5	HS5	278	214 (77.0)	104	62	42 (40.4)
	Sc6	HS6	548	98 (17.9)	72	23	49 (68.1)
	Total		1636	1856 (52.3)	590	281	309 (52.4)

w, field-caught
c, control series

TABLE 4. Phenotypes of the NORs in chromosomes Nos. 4 and 10 of the backcrossed offspring

Parents			Backcrossed offspring									
Female	Male	Sex	No. of frogs	NOR of No. 4		χ^2	P (%)	NOR of No. 10			χ^2	P (%)
				4^+4^+	4^+4^-			10^+10^+	10^+10^-	10^-10^-		
Sw1	SH1	Female	2	1	1			1	1	0		
(++, ++)	(+−, −+)	Male	0	0	0			0	0	0		
Sw2	SH1	Female	2	2	0			0	2	0		
(++, −−)	(+−, −+)	Male	3	1	2	2.22	13.6	0	2	1	0.83	36.1
Sw3	SH1	Female	11	7	4			2	5	4		
(++, +−)	(+−, −+)	Male	17	9	8	0.31	57.6	7	8	2	2.99	22.4
Sw4	SH1	Female	6	2	4			3	3	0		
(++, ++)	(+−, −+)	Male	18	13	5	2.90	8.8	8	10	0	0.06	81.3
Sw4	SH2	Female	9	6	3			9	0	0		
(++, ++)	(+−, −+)	Male	12	7	5	0.15	69.7	9	3	0	2.63	10.5
Total		Female	30	18	12							
		Male	50	30	20	0.00	100.0					
		Total	80	48	32							
Sw1	HS1	Female	7	4	3			3	4	0		
(++, ++)	(−+, +−)	Male	15	4	11	1.92	16.6	4	11	0	0.58	44.8
Sw1	HS2	Female	7	4	3			3	4	0		
(++, ++)	(−+, +−)	Male	13	10	3	0.85	35.7	8	5	0	0.64	42.3
Sw2	HS3	Female	6	4	2			0	4	2		
(++, −−)	(−+, +−)	Male	8	8	0	3.11	7.8	0	3	5	1.17	28.0
Sw5	HS4	Female	7	2	5			0	4	3		
(++, −−)	(−+, +−)	Male	35	17	18 (2)	0.94	33.2	0	22 (1)	13 (1)	0.08	77.6
Sw5	HS5	Female	9	5	4			0	5	4		
(++, −−)	(−+, +−)	Male	4	2	2	0.03	85.3	0	3	1	0.44	50.6
Sc6	HS6	Female	6	2	4			0	5	1		
(++, −−)	(−+, +−)	Male	10	7	3	2.05	15.2	0	6	4	0.95	33.0
Total		Female	42	21	21							
		Male	85	48	37 (2)	0.47	49.1					
		Total	127	69	58 (2)							

Values in parentheses show the number of triploids
The NOR phenotypes in chromosome Nos. 4 and 10 of the parents are indicated by + and − in parentheses: The first two symbols is the phenotype of No. 4 and the second one is that of No. 10

DISCUSSION

Interpopulation variation in the sex chromosome differentiation

Chromosome analyses using C-banding demonstrated that in *Rana japonica* from the Wakuya population in the northeastern area of Honshu, constitutive heterochromatin are characteristically distributed in the basal portions of both arms of each chromosome, and further chromosome pair 4 shows the heteromorphic pattern (AO) in males and homomorphic (AA) in females for the C-band located in the basal portion of the long arm. Thus, in this population, chromosome pair 4 is considered sex chromosomes of the ♂XY/♀XX system [10].

On the contrary, the present study showed that the heteromorphic XY sex chromosomes were not distinguished in the C-banded karyotypes of the Hiroshima and Saeki populations. Moreover, no sex-related heteromorphism of banding patterns could be detected by late replication banding analysis in the chromosomes of Saeki population. The nucleolar organizer regions (NORs), which can be visualized by Ag-staining [4] in mitotic metaphase chromosomes, are localized in the middle portions of the long arms of chromosomes No. 10 in many of *Rana* species [9, 16], inclusive of *R. japonica* from the Hitachi-ota [7] and the Hiroshima studied here. In the Saeki population, however, site of NOR was found in the basal portion of the short arm of chromosome No. 4, with or without that in chromosome No. 10. When sex chromosomes are associated with NORs, the NOR in the Y chromosome, or the W chromosome, is degenerated in some anuran species such as the marsupial frog, *Gastrotheca riobambae* [17], the American tree frog, *Hyla femoralis* [1]

and the Japanese bell-ring frog, *Buergelia buergeli* [14], while it is active in other species such as *Leiopelma hamiltoni* from New Zealand [5]. In *Rana japonica* from Saeki population, the NORs were present in both homologues of chromosome pair 4 without showing any sex-specific heteromorphism in the females and males.

The position of NOR found in the short arm of chromosome No. 4 of Saeki population is very close to the site of the sex-specific C-band found in the basal portion of the long arm of the Wakuya population. Therefore, if a male determining gene is still in chromosome No. 4 in the Hiroshima and Saeki populations, the NOR in chromosome No. 4 should be linked to the sex in the backcrossed progeny between the two populations. The NORs in chromosomes No. 4 of these populations are applicable to the linkage analysis with a sex because of the following facts. First, the location and number of NORs on chromosomes of one complement showed no cell to cell variation within a specimen. Second, each of the NOR phenotypes of the hybrids and backcrossed offspring was segregated at a ratio expected from the phenotypes of their parents, showing that the activity of the NORs in chromosome pair 4 is not affected by the number of the NORs in chromosome No. 10 of the same complement. The results of examination showed that the NOR in chromosome No. 4 was not linked to the sex. Thus, a male determining gene may not be on chromosome No. 4 in both Hiroshima and Saeki populations. However, no chromosomal mutations at a late replication band level, such as inversion or reciprocal translocation including chromosome No. 4, could be detected in these two populations of Hiroshima Prefecture.

A comparable case is the North American salamander *Aneides ferreus* [8, 18]. In *ferreus* I group, chromosome 13 is variable in shape and not related to the sex. On the other hand, No.13 in *ferreus* II group is related to sex and this group is characterized by the ♀ZW/♂ZZ sex chromosomes. A possible explanation of this case is, as in the case of *R. japonica*, that a dominant female determining gene is not on chromosome No.13 in the *ferreus* I group.

Instability of the location of a male determining gene in anuran species

The heteromorphic XY sex chromosomes are characteristic of the European water frog *Rana esculenta*, as proved by the replication banding method [15]. The karyotype of this species is very similar to those of the Japanese pond frogs, *Rana brevipoda* and *R. nigromaculata*, and its XY sex chromosomes correspond to chromosome pair 3 of the two Japanese pond frog species, the arm ratio of which is the lowest among the five large chromosome pairs [12]. In *Rana brevipoda* from Maibara, Japan, its sex-linked enzyme locus is ME-B (malic enzyme), which is located also in chromosome No. 3, while in the same species from Konko and *R. nigromaculata*, MPI (mannose phosphate isomerase) and SORDH (sorbitol dehydrogenase) are sex-linked and located in chromosome No. 4 [11, 13]. In addition, various enzyme loci that are linked to the sex have been known in American frogs, *Rana pipiens* complex [20], *R. catesbeiana* [2], and *R. clamitans* [3]. These facts indicate that a dominant male determining gene in anurans is unstable in its location within a species or between closely related species.

Such instability of the chromosomal location of a male determining gene observed in *R. japonica* in the present study and some frog species may cause the scarcity of amphibian species with highly evolved sex chromosomes. In the next step of research, it is important to examine whether a male determining gene in the frog species is movable or whether there are multiple genes functioning as a dominant male determining factor.

ACKNOWLEDGMENTS

I wish to express my sincere thanks to Professor Midori Nishioka of Hiroshima University for her constant guidance in the course of this work. I am deeply indebted to Professor Kazuo Saitoh of Aomori University for his valuable advice on this work.

REFERENCES

1 Anderson K (1991) Chromosome evolution in Holarctic *Hyla* treefrogs. In "Amphibian Cytogenetics and Evolution" Ed by DM Green, SK Sessions, Academic Press, San Diego, pp 299–331

2 Elinson RP (1981) Genetic analysis of developmental arrest in an amphibian hybrid (*Rana catesbeiana*, *Rana clamitans*). Devel Biol 81: 167–176

3 Elinson RP (1983) Inheritance and expression of a sex-linked enzyme in the frog, *Rana clamitans*. Biochem Genet 21(5/6): 435–442

4 Goodpasture C, Bloom SE (1975) Visualization of nucleolar organizer regions in mammalian chromosomes using silver staining. Chromosoma 53: 37–50

5 Green DM (1988) Heteromorphic sex chromosomes in the rare and primitive frog *Leiopelma hamiltoni* from New Zealand. J Hered 79(3): 165–169

6 Howell WM, Black DA (1980) Controlled silver-staining of nucleolus organizer regions with a protective colloidal developer: a 1-step method. Experientia 36: 1014–1015

7 Iizuka K (1989) Constitutive heterochromatin and nucleolus organizer regions in Japanese brown frogs, *Rana japonica* and *Rana ornativentris*. Jpn J Herpetol 13(1): 15–20

8 Kezer J, Sessions SK (1979) Chromosome variation in the plethodontid salamander, *Aneides ferreus*. Chromosoma 71: 65–80

9 King M (1990) Amphibia. In "Animal Cytogenetics Vol 4/2" Ed by B John, C Gwent, Gebrüder Borntraeger, Berlin·Stuttgart

10 Miura I (1994) Sex chromosome differentiation in the Japanese brown frog, *Rana japonica* I. Sex-related heteromorphism of the distribution pattern of constitutive heterochromatin in chromosome No. 4 of the Wakuya population. Zool Sci 11 (6): 797–806

11 Nishioka M, Ohtani H, Sumida, M (1987) Chromosomes and the sites of five albino gene loci in the *Rana nigromaculata* group. Sci Rep Lab Amphibian Biol Hiroshima Univ 9: 1–52

12 Nishioka M, Okumoto H, Ryuzaki M (1987) A comparative study on the karyotypes of pond frogs distributed in Japan, Korea, Europe and North America. Sci Rep Lab Amphibian

Biol Hiroshima Univ 9: 135–163

13 Nishioka M, Sumida M (1989) The position of sex-determining gene in different populations of *Rana nigromaculata* and *Rana brevipoda*. Zool Sci 6(6): 1110

14 Ohta S (1986) Sex determining mechanism in *Buergeria buergeri* (Schlegel) I. Heterozygosity of chromosome pair No. 7 in the female. Sci Rep Lab Amphibian Biol Hiroshima Univ 8: 29–43

15 Schempp W, Schmid M (1981) Chromosome banding in Amphibia VI. BrdU-replication patterns in Anura and demonstration of XX/XY sex chromosomes in *Rana esculenta*. Chromosoma 83: 697–710

16 Schmid M (1978) Chromosome banding in Amphibia II. Constitutive heterochromatin and nucleolus organizer regions in Ranidae, Microhylidae and Rhacophoridae. Chromosoma 68: 131–148

17 Schmid M, Haaf T, Geile B, Sims S (1983) Chromosome banding in Amphibia VIII. An unusual XY/XX-sex chromosome system in *Gastrotheca riobambae* (Anura, Hylidae). Chromosoma 88: 69–82

18 Sessions SK, Kezer J (1987) Cytogenetic evolution in the plethodontid salamander genus *Aneides*. Chromosoma 95: 17–30

19 Sumida M (1981) Studies on the Ichinoseki population of *Rana japonica*. Sci Rep Lab Amphibian Biol Hiroshima Univ 5: 1–46

20 Wright DA, Richards CM, Frost JS, Camozzi AM, Kunz BJ (1983) Genetic mapping in amphibians. Isozymes: Current topics Biol Med Res 10: 287–311

ZOOLOGICAL SCIENCE 11: 817–820 (1994)

Mixed-Incubation of Allogeneic Hemocytes in Tunicate *Halocynthia roretzi*

TOMOO SAWADA[1] and SHIN-ICHI OHTAKE[2]

[1]*Department of Anatomy, Yamaguchi University School of Medicine, Ube, Yamaguchi 755, and* [2]*Department of Biology, Nihon University School of Medicine, Oyaguchi, Itabashi, Tokyo 173, Japan*

ABSTRACT—We developed a new convenient method to examine self-nonself compatibility of tunicate, *Halocynthia roretzi,* by reactions in a mixture of hemocytes. Tunicate hemolymph samples of 100 μl each, harvested from two individuals and containing approximately 10^6 cells, were mixed and incubated for 12–20 hr at 15–23°C. This incubation of hemocyte-mixture resulted in two definite types of phenomena: i.e., presence and absence of alloreactivity which was represented by intensive discharge of hemocyte contents and amorphous precipitation of hemocyte clusters with brown pigmentation. Such alloreactivity exsisted in most nonself combinations, while the incubation of hemocytes from single tunicate (autologous control) did not exhibit any of them. Autologous controls and certain several nonself combinations showed a simple accumulation of hemocytes, as forming buttons at the center of U-bottomed culture wells. Consequently, those nonself combinations were judged as non-reactive or compatible. Autologous controls and the non-reactive nonself combinations formed large spherical aggregates which did not adhere to the culture wells and were evidently different from the amorphous clusters found in alloreactive hemocyte mixtures. Furthermore, we confirmed the consistency between the alloreactivity measured by mixed-hemocyte-incubation (MHI-assay) and that measured by contact reaction. The procedure for MHI-assay in U-bottomed culture plate was simple, and compatibility could be judged without microscopic observation. Thus, MHI-assay will be an effective method to test self-nonself compatibility of numerous number of combinations using a large number of tunicates, that will be required in studying genetic background of tunicate allogeneic recognition.

INTRODUCTION

Allogeneic reactions of tunicate hemocytes are well-known and very important, which has been concerned in the argument of phylogenic development of allogeneic recognition in immune systems [1]. Because tunicate is one of the most primitive animals of phylum Chordata, allogeneic recognition of them has been studied in relation to vertebrate allo-recognizing system [17]. Early studies of tunicate allogeneic recognition were performed using colonial tunicates mainly on the allogeneic discrimination at colony-fusion [6, 14]. Contact reaction between allogeneic hemocytes was reported as one of allogeneic responses in several solitary tunicates hemocytes [2]. Recently, allograft rejection [8, 10], a proliferative response by a hemocyte subpopulation following allogeneic stimuli [9] and cytotoxic activity against allogeneic hemocytes [5] were demonstrated also in solitary tunicates.

The genetic control of allogeneic compatibility has been studied both in solitary [2, 3, 8] and in colonial species [11, 12, 15], but cellular mechanisms of allogeneic recognition require more intensive studies. To proceed experimental studies on tunicate allogeneic responses, more convenient and quick method has been required to clarify the compatibility of all combinations among tunicates used in experiments. Therefore, we accomplished a convenient incubation of mixtures of nonself hemocytes in solitary tunicates, and examined the consistency between the compatibility in mixed-incubation and that measured by contact reaction.

Accepted November 14, 1994
Received August 8, 1994

MATERIALS AND METHODS

Hemocytes

Tunicates, *Halocynthia roretzi*, were collected at Mutsu-bay in northeastern Japan. Hemocytes were harvested as the hemolymph using 1 ml plastic syringes from the space beneath epithelium at tunic papilla (without any anti-coagulant).

Mixed-hemocyte-incubation assay (MHI-assay)

Hemolymph from two different tunicates (100 μl for each which contained approximately 10^6 cells) was mixed and incubated in 96-well culture plate for 12–20 hr at 15–23°C. As controls, hemolymph was mixed with autologous hemolymph (100 μl to 100 μl) and was incubated at the same condition. Both flat-bottomed and U-bottomed 96-well plates were used. Flat-bottomed well plates were used for microscopic observation, at first. Then, we preferred U-bottomed 96-well plates for more convenient assay to check button-formation, in which the result was demostrated more clearly.

Contact reaction

The contact reaction between hemocytes of two different (allogeneic) tunicates was observed according to Fuke [2]: hemolymph was diluted five times with sea water and mixed with 5× diluted hemolymph from another tunicate. A mixture of hemolymph was mounted on a glass slide, and hemocyte behavior was observed continuously for 60–90 min. Alloreactivity was judged by the occurrence of cell-to-cell adhesion which led to explosive devacuolation or degranulation on both cells. Usually such devacuolation and degranulation left a numerous amount of debris of hemocytes with brown prigmentation.

Microscopic observation in sections

The hemocyte-mixture after incubation was fixed with 0.1% glutaraldehyde in 1.5% NaCl solution buffered with 0.2 M sodium cacodylate (pH. 7.4) for 24 h at room temparature, and then post-fixed in 1% osmium tetroxide in the same buffer of ice cold for 2 hr. Hemocytes were embedded in Epok 812 (Oken Co. Tokyo), and thick sections (1 μm) were stained with toluidine blue.

RESULTS

Mixed-hemocyte-incubation of nonself combinations

In most nonself combinations, the mixture of hemolymph (nonself hemocyte-mixture) started to become brown within 30 min. But, incubation of hemolymph from a single tunicate (autologous controls) did not result in any pigmentation at least 12–20 hr. There were several certain combinations between nonself tunicates whose hemocyte-mixture did not show the pigmentation.

Within 12–20 hr, hemocytes of autologous control setteled on the bottom to make thick hemocyte layer. Large and spherical aggregates of hemocytes were formed in such layer. Those aggregates were observed as transparent spheres or as dark spheres embedded in accumulated hemocytes (Fig. 1-a). Similar aggregates were also formed in the nonself combinations whose hemocyte-mixture did not become pigmented. These spherical aggregates did not adhere to culture wells. On the other hand, hemocyte-mixture in most of nonself combinations formed a numerous number of amorphous aggregates with brown pigmentation and adhering to the bottom (Fig. 1-b).

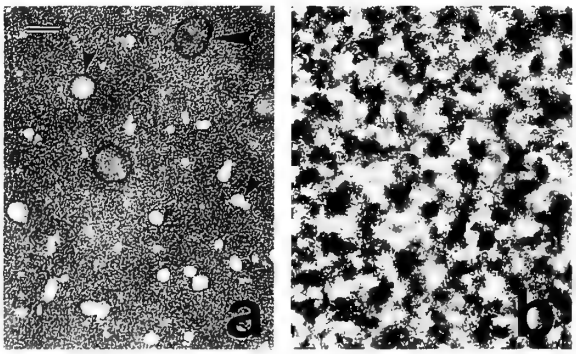

FIG. 1. Hemocytes in MHI-assay (flat-bottom wells) after 12 hr incubation. a: Hemocytes incubated in autologous control. Spherical aggregates were formed, and appeared as dark (large arrow head) or clear (small arrow heads) spheres which were embedded in homogeneous back-ground by accumulated hemocytes. b: Hemocytes incubated in nonself reactive combination. All hemocytes clamped to form amorphous clusters. Bar=200 μm.

We used the precipitation of amorphous aggregates and the brown pigmentation as a marker of alloreactivity in the following studies. Table 1 shows the presence or absence of the alloreactivity as described above, among eight tunicates No. 1–8 using flat-bottomed wells. As shown in Table. 1,

TABLE 1. Alloreactivity among tunicate No. 1–8, in mixed hemocyte incubation

	No. 1	No. 2	No. 3	No. 4	No. 5	No. 6	No. 7	No. 8
No. 1	$-^{(c)}$	+	+	$-^{**}$	+	+	±	+
No. 2	+	$-^{(c)}$	+	+	+	+	+	+
No. 3	+	+	$-^{(c)}$	+	+	+	+	+
No. 4	$-^{**}$	+	+	$-^{(c)}$	+	+	+	$-^{**}$
No. 5	+	+	+	+	$-^{(c)}$	+	+	+
No. 6	+	+	+	+	+	$-^{(c)}$	+	+
No. 7	+	+	+	±	+	+	$-^{(c)}$	+
No. 8	+	+	+	$-^{**}$	+	+	+	$-^{(c)}$

Hemolymph was mixed with nonself hemolymph (100 μl+ 100 μl). In autologous controls (c), hemolymph was added to autologous hemolymph. Presence and absence of alloreactivity are indicated by + and − respectively. Intermediate cases are indicated by ±. Non-reactive nonself combinations in contact reaction are indicated by asterisks (**). Two of nonself combinations (No. 1 *vs.* No. 4 , and No. 4 *vs.* No. 8) did not exhibit alloreactivity, despite the presence of alloreactivity between No. 1 and No. 8.

No. 4 was not reactive to both of No. 1 and No. 8, while No. 1 was alloreactive against No. 8. We obtained a few intermediate results on flat-bottomed wells, 2 out of 56 wells of nonself combinations. In the intermediate cases, brown pigmentation and amorphous hemocyte aggregates appeared with also a few spherical and transparent aggregates similar to those of autologous controls.

When MHI-assay was accomplished in a U-bottomed 96-well plate, hemocytes of non-reactive mixtures (auto-

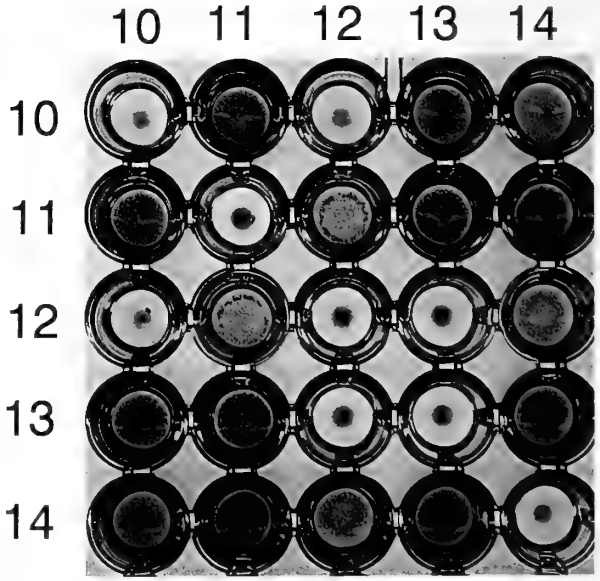

FIG. 2. Hemocyte in MHI-assay (in U-bottomed wells) after 18 hr incubation. Allogeneic reactivity among 5 tunicates (No. 10–14) examined. Hemocytes in autologous controls and two of nonself combinations (10 *vs.* 12, and 12 *vs.* 13) accumulated into the center of the wells to form white buttons (non-reactive). On the other hand, hemocytes in most nonself combinations spread on the bottom surface as brown precipitation.

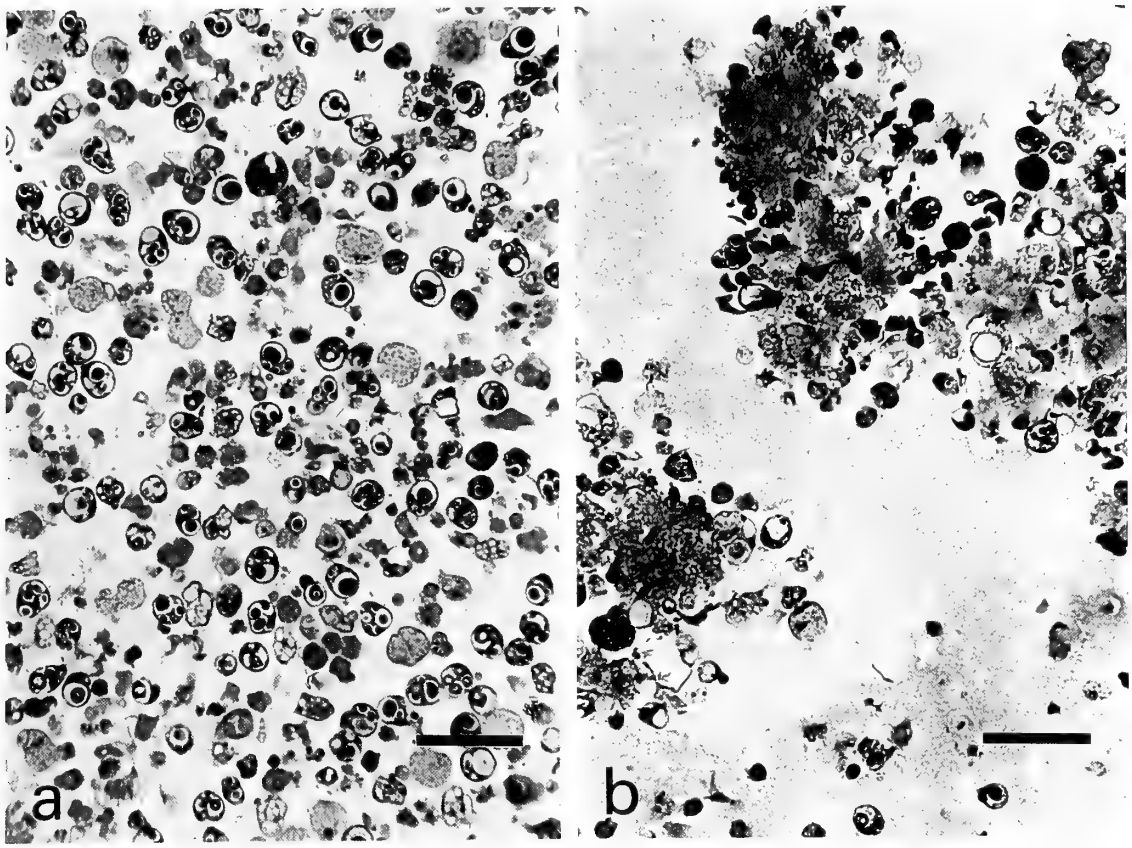

FIG. 3. Thick section of the hemocyte mixture. a: In hemocyte-mixture of non-reactive nonself combination, the hemocytes did not aggregate even after incubation for 18 hr. b: In alloreactive combination, hemocytes formed amorphous aggregates involving multiple hemocyte types and material discharged from granulated and vacuolated cells surrounded the aggregates. Bar=50 μm.

logous controls and non-reactive nonself hemocyte-mixtures) accumulated at the center of the bottom and formed white buttons in culture wells. Hemocytes of reactive nonself-mixtures (most of nonself combinations) formed brown precipitation adhering and spreading on the whole area of the bottom (Fig. 2). No intermediate cases regarding white-button formation appeared in MHI-assay using U-bottomed plates, while certain variety existed in degrees of the brown pigmentation.

Contact reaction

For all the combinations examined by MHI-assay, alloreactivity in contact reaction was examined. Contact reaction occured in all the combinations reactive in MHI-assay and in the combinations exhibiting an intermediate result in flat-bottomed culture wells (Table 1). On the other hand, contact reaction was negative not only in autologous controls but also in all the non-reactive nonself combinations (Table 1). The alloreactivity tested in U-bottomed culture wells was also consistent with that examined by contact reaction.

Observation in sections

In thick sections of the precipitated amorphous clusters in alloreactive hemocyte-mixtures, almost all types of hemocytes were involved in aggregation. Discharged material from hemocytes was observed surrounding those aggregates (Fig. 3-a). Autologous controls did not include the aggregates of multiple cell types (Fig. 3-b).

DISCUSSION

Alloreactivity in tunicates

The previous studies on the various allogeneic reactivities of tunicates have suggested certain differences in alloreactivity patterns between tunicates and mammalian T-lymphocyte system [3, 4, 13, 16, 17]. In tunicates, any pairs sharing at least one allele of histocompatibility-gene seemed to be compatible, suggesting a system to recognize the absence of self-markers. Contact reaction was reported as occuring in this manner [2, 3], and the alloreactivity as measured by MHI-assay here also exhibited such typical pattern similar to the previous reports. Each tunicate of a non-reactive pair has a different alloreactive repertoire. In addition, the alloreactivity as measured by MHI-assay and by contact reaction was consistent with each other.

Although cellular mechamism and responsible cells for the alloreactivity have not been defined yet, MHI-assay and contact reaction seemed to be somehow related to cytotoxicity, by numerous cell death and discharge of cytoplasmic

contents. Cytotoxic activity of hemocytes was proved against allogeneic [5] as well as xenogeneic cells [7] also in other solitary tunicates, whereas our preliminary date in *Styela clava*, *Halocynthia hispida*, and *Chelysoma siboja* showed no definite reactivity in MHI-assay. Thus, MHI-assay seems to be applicable only to *Halocynthia roretzi*, so far. However, Akita *et al.* (personal communication) detected phenoloxidase-activity in the supernatant of mixed-hemocyte-incubation of alloreactive combinations. Despite that we did not examine such enzymic activity, it seems possible that more delicate research to detect such enzymic activity may demonstrate the presence of alloreactivity in mixed-hemocyte-incubation using other tunicate species.

MHI-assay as to examine alloreactivity of tuicates

We demonstrated for the first time that tunicate alloreactivity is evidently exhibited in mixed-incubation of nonself hemocytes. Although we obtained a few unclear results in MHI-assay using flat-bottomed wells, an improvement to use U-bottomed wells could eliminate such unclear cases. This MHI-assay using U-bottomed wells is simple and does not require microscopic examination to judge the results. It would allow us to check easily a large number of nonself combinations at once without killing or injuring tunicates. Therefore, investigators will be able to use the same crews of tunicates for further experiments after alloreactivity was mesured. Thus, MHI-assay is quite effective to check alloreactivity (compatibility) in tunicates, at least in *Halocynthia roretzi*. Especially the MHI-assay seems to be effective in the study of genetic background of tuicate allogeneic recognition.

ACKNOWLEDGMENTS

We thank the staff of Asamushi Marine Biological Station of Tohoku University for their support in supplying tunicates.

REFERENCES

1 Cooper EL, Rinkevich B, Uhlenbruck G, Valembois P (1992) Invertebrate immunity: another viewpoint. Scand J Immunol 35: 247–266

2 Fuke MT (1980) "Contact reaction" between xenogeneic or allogeneic coelomic cells of solitary ascidians. Biol Bull 158: 304–315

3 Fuke MT, Nakamura I (1985) Pattern of cellular alloreactivity of solitary ascidian, *Halocynthia roretzi*, in relation of genetic control. Biol Bull 169: 631–637

4 Fuke M (1990) Self and nonself recognition in the solitary ascidian, *Halocynthia roretzi*. In "Defense Molecules" Ed by JJ Marchalonis and CL Reinisch, UCLA Symposium on Molecular and Cellular Biology New Series Vol. 121, Wiley-Liss, New York, pp 107–117

5 Kelly KL, Cooper EL, Reftos DA (1992) *In vitro* allogeneic cytotoxicity in the solitary urochordates. J Exp Zool 262: 202–208

6 Oka H, Watanabe H (1960) Problems of colony specificity in compound ascidians. Bull Mar Biol Stn Asamushi 10: 153–155

7 Parrinello N, Arizza V, Cammarata M, Parrinello DM (1992) Cytotoxic activity of *Ciona intestinalis* (Tunicate) hemocytes: Properties of the in vitro reaction against erythrocyte targets. Dev Comp Immunol 17: 19–27

8 Raftos DA, Briscoe DA (1990) Genetic basis of allograft rejection in *Styela plicata*. J Heredity 81: 96–100

9 Raftos DA, Cooper EL (1991) Proliferation of lymphocyte-like cells from the solitary tunicate, *Styela clava*, in response to allogeneic stumuli. J Exp 260: 391–400

10 Raftos DA, Tait NN, Briscoe DA (1987) Allograft rejection and alloimmune memory in the solitary urochordate, *Styela plicata*. Dev Comp Immunol 11: 343–351

11 Rinkevich B, Shapira M, Weissman IL, Saito Y (1992) Allogeneic responses between three remote populations of the cosmopolitan ascidian *Batrullus schlosseri*. Zool Sci 9: 989–994

12 Rinkevich B, Weissman IL (1992) Incidents of rejection and indifference in Fu/HC incompatible protochordate colonies. J Exp Zool 263: 105–111

13 Smith LC, Davidson EH (1992) The echinoid immune system and the phylogenetic occurence of immune mechanisms in deuterostomes. Immunol Today 13: 356–361

14 Tanaka, K (1973) Allogeneic inhibiton in a compound ascidian, *Botryllus primigenus* Oka. II. Cellular and humoral responses in "nonfusion" reaction. Cell. Immunol. 7: 427–443

15 Taneda Y, Saito Y, Watanabe H (1985) Self or nonself discrimination in ascidians. Zool Sci 2: 433–442

16 Watanabe H, Taneda Y (1982) Self or non-self recognition in compound ascidians. Amer Zool 22: 775–782

17 Weissman IL, Saito Y, Rinkevich B (1990) Allorecognition histocompatibility in a protochordate species: is the relationship to MHC semantic or structural? Immun Rev 113: 227–241

ZOOLOGICAL SCIENCE 11: 821–824 (1994)

Localization of Connectin-like Proteins in the Giant Sarcomeres of Barnacle Muscle

SAORI MAKI, SUMIKO KIMURA, and KOSCAK MARUYAMA

Department of Biology, Faculty of Science, Chiba University, Chiba 263, Japan

ABSTRACT—In the giant sarcomeres of barnacle adductor muscle (sarcomere length at rest, ~10 μm), there were ~5000 kDa connectin-like protein and 1200 kDa projectin that reacted with monoclonal antibodies to vertebrate skeletal muscle connectin, SM1 and 3B9, respectively. Immunofluorescence microscopy showed that the ~5000 kDa protein linked the myosin filament to the Z line and extensible upon stretch and projectin was localized on the myosin filament. On removal of myosin and actin, both proteins moved to the side of the Z line. These behaviors were the same as those of the giant sarcomeres of crayfish claw muscle, suggesting that projectin is bound to the ~5000 kDa protein.

INTRODUCTION

Connectin is the largest protein (~3000 kDa) in vertebrate striated muscle. It links the myosin filament to the Z line as a spring (for reviews, see [8, 12]).

In invertebrate muscle there is a biodiversity in the connectin family proteins. Twitchin (753 kDa) in *C. elegans* bodywall muscle [1, 2] and projectin (1200 kDa) in arthropod striated muscle [3, 7, 10, 11] are well characterized. In addition, ~3000 kDa proteins are present in annelid bodywall muscle [5], crayfish claw muscle [7] and some insect muscle [3]. In the regular sizes of sarcomeres of crayfish and insect striated muscles, projectin connects the Z line to the myosin filament [7, 10]. On the contrary, in the giant sarcomeres of crayfish claw muscle, 3000 kDa connectin-like protein links the Z line and the myosin filament, whereas projectin is bound onto the myosin filament [7].

The present work demonstrates that ~5000 kDa connectin-like protein links the Z line and the myosin filament in the giant sarcomeres of barnacle adductor muscle and projectin is mainly localized in the A band.

MATERIALS AND METHODS

Materials

Barnacle, *Tetraclita squamosa japonica*, was collected at the Kominato Marine Biological Laboratory, Chiba University, and reared for a week in our laboratory. There are several kinds of muscles in barnacle: striated muscle (ventral squtal depressor, lateral squtal depressor and adductor) and smooth muscle (targal depressor) as shown in Figure 1 [9]. The giant sarcomere, 10 μm at rest, is present in adductor muscle and mainly used for the present study. The sarcomere lengths of other striated muscles at rest were approximately 4.6 μm (ventral squtal depressor) and 6.7 μm (lateral squtal depressor), respectively.

SDS gel electrophoresis

Each muscle was homogenized in 3 volumes of an SDS solution (10% SDS, 40 mM dithiothreitol, 10 mM EDTA, and 0.1 M Tris-HCl buffer, pH 8.0), boiled for 3 min and clarified at 15,000×*g* for 20 min. Laemmli's 2–8% polyacrylamide gels were used for electrophoresis [6].

Accepted October 17, 1994
Received September 5, 1994

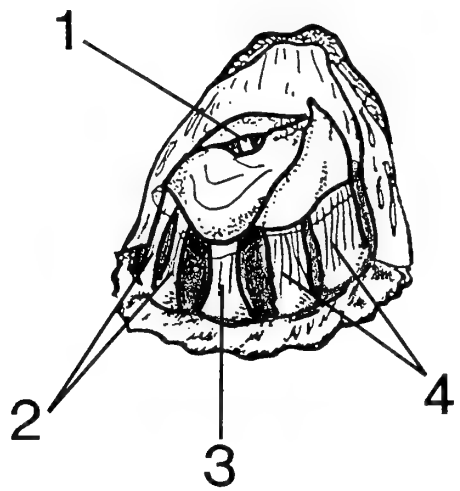

FIG. 1. Barnacle muscle. Modified from Matsuno and Hirota [9]. 1, adductor; 2, ventral squtal depressor; 3, lateral squtal depressor; 4, targal depressor.

Immunoblots

Monoclonal antibodies to chicken breast muscle connectin, SM1 [4] and 3B9 [4] and polyclonal antibodies to crayfish claw muscle [3] were used. The electrophoresed gel bands were electrophoretically transferred to a nitrocellulose sheet and treated with the antibodies described above. Bound antibodies were detected after the treatment with horseradish peroxidase-conjugated anti-rabbit IgG (Bio-Rad) or anti-mouse IgG (DAKOPATTS, Copenhagen).

Immunofluorescence microscopy

Freshly skinned fibers of barnacle adductor muscle were fixed at a given sarcomere length in the relaxing solution (3 mM ATP, 2.5 mM $MgCl_2$, 10 mM EGTA, 100 mM KCl, 10 mM phosphate buffer, pH 7.5 and 0.5% Triton X-100) containing 3.5% formaldehyde. The fixed muscle fibers were gently homogenized in the relaxing solution and blocked for 30 min with the relaxing solution containing

1% bovine serum albumin. The sample on a slide glass was treated with the antibodies for 90 min followed by the treatment with FITC-labelled anti-rabbit IgG or anti-mouse IgG (Cappel, West Chester, PA.). A Leitz Ortholax-2 fluorescence microscope was used for observation.

RESULTS

Connectin- and Projectin-like Proteins of Barnacle Adductor Muscle

Figure 2b shows SDS gel electrophoresis pattern of barnacle adductor muscle. There was a very high molecular weight protein the mobility of which was significantly slower than 3000 kDa rabbit skeletal muscle α-connectin (Fig. 2a). The molecular mass of the former protein was certainly larger than 3000 kDa. There is no method to estimate the molecular mass of the barnacle protein and, therefore, it is tentatively assumed to be ~5000 kDa. In addition, there were several bands corresponding to crayfish projectin (1200 kDa).

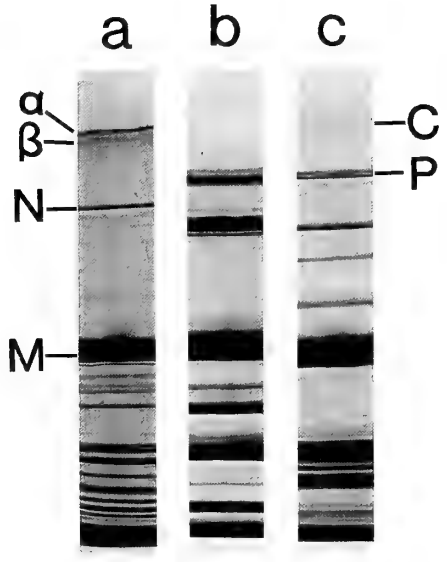

Fig. 2. SDS gel electrophoresis pattern of barnacle adductor muscle. a, rabbit skeletal muscle; b, barnacle adductor muscle; c, crayfish closer muscle. α, β, α-and β-connectin; N, nebulin; M, myosin heavy chain; C, connectin like protein; P, projectin.

Immunoblots revealed that SM1, monoclonal antibody to chicken breast muscle α-connectin, reacted with barnacle ~5000 kDa protein (Fig. 3b). 3B9, monoclonal antibody to chicken breast muscle β-connectin reacted with several bands including projectin (Fig. 3c). Anti-crayfish claw muscle projectin antibodies reacted with barnacle projectin-like protein (Fig. 3d). A faint band above projectin also reacted with the antiserum (Fig. 3d).

Immunofluorescence Localization of Barnacle Connectin and Projectin

The immunofluorescence microscopy using SM1 revealed that the epitopes to SM1 were localized in the I band near the Z line at a sarcomere length of 12.9 μm (Fig. 4a). When the sarcomere length was increased to 19.2 μm by stretch, a weak but significant band appeared in the I band in addition to the strongly fluorescent band near the Z line (Fig. 4b). This observation suggested that the ~5000 kDa protein was extensible upon stretch.

Fig. 3. Immunoblots of barnacle adductor muscle. a, Amido Black stain; b, treated with SM1; c, treated with 3B9; d, treated with antiserum to crayfish claw muscle projectin.

On the other hand, 3B9 stained the whole A band and the fluorescent band did not change when muscle was stretched from a sarcomere length of 14.6 μm to 17.5 μm (Fig. 4c, d). The antiserum to crayfish projectin also stained the A band of barnacle adductor muscle. It was likely that projectin was localized on the A band. Since the width of the fluorescence band was slightly larger than that of the A band, it is likely that projectin somewhat extruded from the edge of the A band (Fig. 4c, d).

When barnacle adductor myofibrils were extracted with 0.6 M KCl to remove myosin, the density of the A band decreased (Fig. 5b, e). The fluorescence due to SM1 binding remained in the I band near the Z line (Fig. 5b). On the other hand, fluorescence due to 3B9 binding disappeared in the middle of the A band and remained at the A-I junction region (Fig. 5e). This must have been due to the removal of myosin at the center of the A band, and it seems that some projectin was dissolved away together with myosin.

When the myofibrils were treated with 0.6 M KI to remove both myosin and actin, only the Z lines remained (Fig. 5c, f). The SM1 fluorescence and also the 3B9 fluorescence were recognized near the Z lines (Fig. 5c, f). It is to be noted that the Z line itself was not fluorescent (Fig. 5f). Thus it appears that the ~5000 kDa protein together with projectin retracted toward the Z line, when myosin was completely solubilized away.

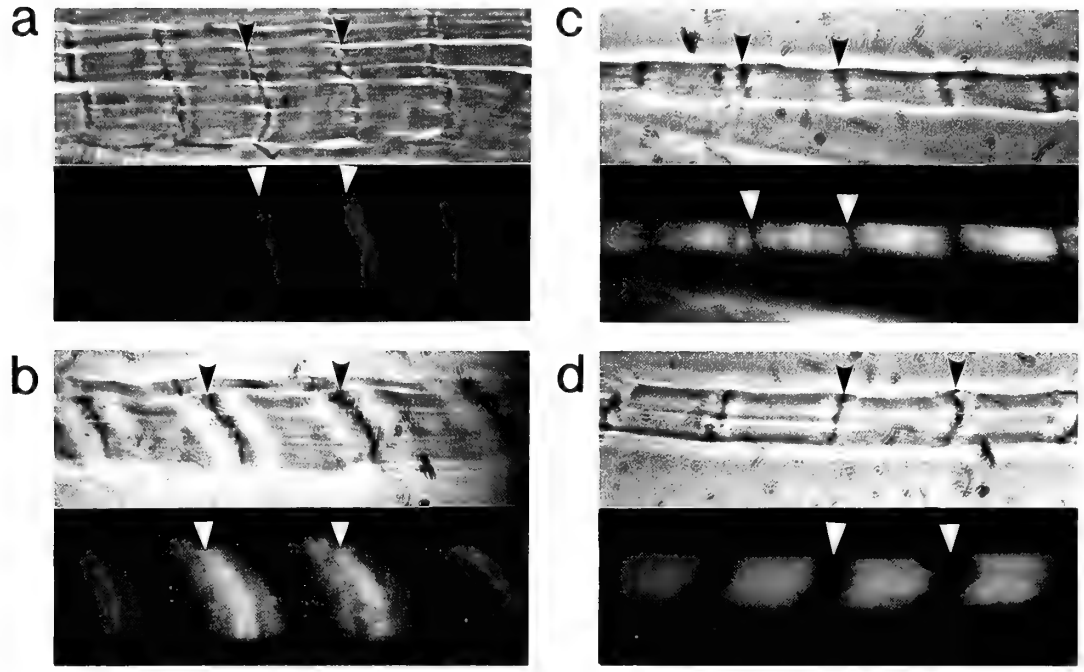

FIG. 4. Immunofluorescence of barnacle adductor muscle. a, treated with SM1, sarcomere length, 12.9 μm. b, *ibid.*, 19.2 μm. c, treated with 3B9, 14.6 μm. d, *ibid.*, 17.5 μm. Upper, phase contrast image; lower, fluorescence image. Arrowhead indicates Z line. Bar, 20 μm.

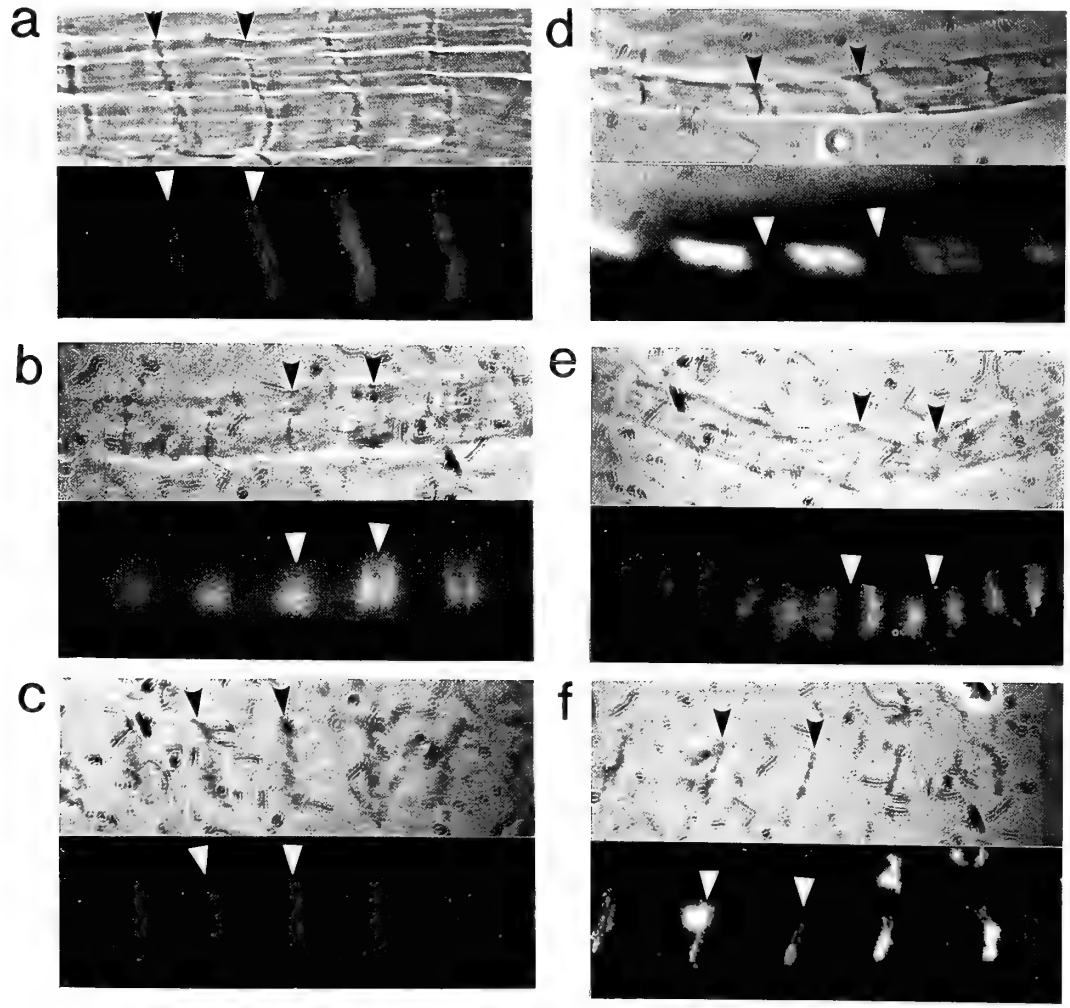

FIG. 5. Immunofluorescence of myosin-dissolved barnacle muscle. a, d, control; b, e, treated with 0.6 M KCl; c, f, treated with 0.6 M KI. a, b, c, treated with SM1; d, e, f, treated with 3B9. Arrowhead indicates Z line. Bar, 20μm.

DISCUSSION

In invertebrate muscle a variety of elastic filamentous proteins are known: 753 kDa twitchin (*C. elegans* bodywall muscle) [1, 2] and 1200 kDa projectin (arthropod striated muscle) [3, 7, 10, 11] and ~3000 kDa connectin-like proteins [3, 5, 7]. Monoclonal antibodies to vertebrate skeletal muscle connectin, 3B9 and SM1 crossreact with projectin [3, 7] and connectin-like protein [5, 7], respectively. In the present study, 3B9 reacted with 1200 kDa projectin-like protein and SM1 reacted with ~5000 kDa connectin-like protein of barnacle adductor muscle. Although isolation of each protein was not done, it was likely that these two kinds of proteins were filamentous proteins (cf. ref. [7]).

It is to be mentioned that the barnacle ~5000 kDa protein is even larger than the 4000 kDa protein of polychaete bodywall muscle [5]. It is of interest to note that the barnacle adductor ~5000 kDa protein is the largest in size among connectin family proteins. The mobilities of barnacle striated muscle connectin-like proteins were in the following: ventral squtal depressor (similar to rabbit skeletal muscle α-connectin)>lateral squtal depressor (similar to 4000 kDa polychaete bodywall muscle protein [5]>adductor ~5000 kDa.

Barnacle projectin was shown to be localized on the myosin filament using 3B9. The same immunofluorescence pattern was observed when antiserum to crayfish projectin was used instead of 3B9. This localization of projectin was similar to that in the giant sarcomeres of crayfish claw muscle (closer) [7]. However, it appears that barnacle projectin somewhat extruded from the edge of the myosin filament (Fig. 4c, d). When myosin was completely solubilized by 0.6 M KI, projectin retracted to the side of the Z line together with the ~5000 kDa protein. Thus it seems that projectin bound to the ~5000 kDa protein. These relationships between projectin and the connectin-like protein were the same as crayfish claw muscle projectin [7].

Immunofluorescence microscopy showed that connectin-like protein was localized in the I band and extensible upon stretch (Fig. 4a, b). It is very likely that it linked the myosin filament to the Z line, since it moved toward the Z line, when myosin was completely solubilized (cf. [7]).

Thus the elastic structure of barnacle giant sarcomere is very similar to that of giant sarcomeres of crayfish claw muscle [7]. A scheme of the elastic filaments of barnacle adductor muscle is depicted in Figure 6.

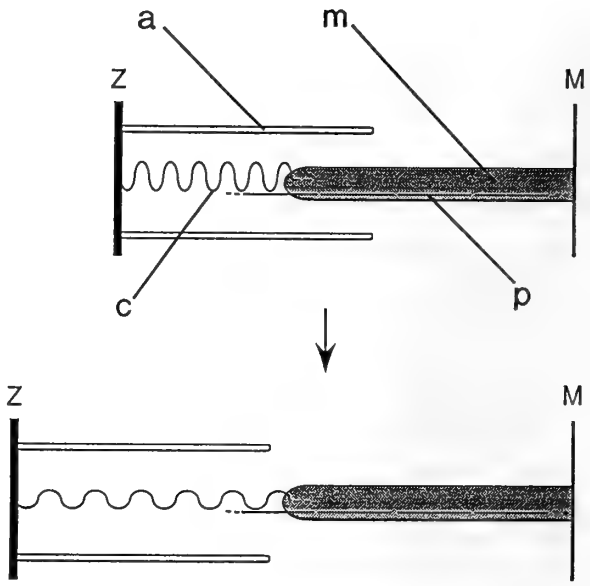

Fig. 6. A scheme of the elastic filaments in barnacle adductor sarcomere. Z, Z line; M, M line; a, actin filament; m, myosin filament; c, connectin; p, projectin.

REFERENCES

1 Benian GM, Kiff JE, Neckelmann N, Moerman DG, Waterston RH(1989) Sequence of an unusually large protein implicated in regulation of myosin activity in *C. elegans*. Nature 342: 45–501

2 Benian GM, Lhernault SW, Morris ME (1993) Additional sequence complexity in the muscle gene, unc-22, and its encoded protein, twitchin, of *caenorhabditis elegans*. Genetics 134: 1097–1104

3 Hu DH, Matsuno A, Terakado K, Matsuura T, Kimura S, Maruyama K (1990) Projectin is an invertebrate connectin (titin): Isolation from crayfish claw muscle and localization in crayfish claw muscle and insect flight muscle. J Muscle Res Cell Motil 11: 497–511

4 Itoh Y, Suzuki T, Kimura S, Ohashi K, Higuchi H, Sawada H, Shimizu T, Shibata M, Maruyama K (1988) Extensible and less-extensible domains of connectin filaments in stretched vertebrate skeletal muscle sarcomeres as detected by immunofluorescence and immunoelectron microscopy using monoclonal antibodies. J Biochem 104: 504–508

5 Kawamura Y, Suzuki J, Kimura S, Maruyama K (1994) Characterization of connectin-like proteins of obliquely striated muscle of a polychaete (annelida). J Muscle Res Cell Motil in press

6 Laemmli UK (1970) Cleavage of structural proteins during the assembly of the head of bacteriophage T4. Nature 227: 680–685

7 Manabe T, Kawamura Y, Higuchi H, Kimura S, Maruyama K (1993) Connectin, giant elastic protein, in giant sarcomeres of crayfish claw muscle. J Muscle Res Cell Motil 14: 654–665

8 Maruyama K (1994) Connectin, an elastic protein of striated muscle. Biophy Chem 50: 73–85

9 Matsuno A, Hirota S (1989) Ultrastructural investigations on themuscular systems in the barnacle, *Tetraclita squamosa japonica*. Tissue and Cell 21: 863–874

10 Nave R, Weber K (1990) A myofibrillar protein of insect muscle related to vertebrate titin connects Z-band and A-band:purification and molecular characterization of invertebrate mini-titin. J Cell Sci 95: 535–544

11 Saide JD (1981) Identification of a connecting filament protein in insect fibrillar flight muscle. J Mol Biol 153: 661–679

12 Trinick J (1991) Elastic filaments and giant proteins in muscle. Curr Cell Biol 3: 112–119

ZOOLOGICAL SCIENCE 11: 825–839 (1994)

Stages of Normal Development in the Medaka *Oryzias latipes*

TAKASHI IWAMATSU

Department of Biology, Aichi University of Education, Kariya 448, Japan

ABSTRACT—Unfertilized eggs of *Oryzias latipes* were artificially inseminated and incubated at 26±1°C. Careful observation of the process of embryonic development by light microscopy allowed division of the process into 39 stages based on diagnostic features of the developing embryos. The principal diagnostic features are the number and size of blastomeres, form of blastoderm, extent of epiboly, development of the central nervous system, number and form of somites, optic and otic development, development of the notocord, heart development, blood circulation, the size and movement of the body, development of the tail, membranous fin development, and development of such viscera as the liver, gallbladder, gut tube, spleen and swim (air) bladder. After hatching, development of the larvae (fry) and young can be divided into five stages based on such diagnostic features as fins, scales and the secondary sexual characteristics.

INTRODUCTION

The genus *Oryzias* (the medaka), which inhabits fresh and brackish waters from India throughout South-east Asia across Wallace's line to Timor, Sulawesi, Luzon, and Japan, is unique among common laboratory teleosts. The natural breeding season of *Oryzias latipes* extends from mid-April to late September in Japan. Oocyte maturation occurs at night [8, 10], and ovulation at dawn [2, 12]. Under regular daily photoperiod with more than 13 hours of artificial lighting [32], ovulation occurs about one hour before the onset of the light period, and oviposition occurs for one hour before and after the onset of the light period throughout the year. Recently, it has been shown that oocytes can be induced to mature and to ovulate *in vitro* without any exogenous hormone if they are removed from the ovary less than 12 hour before the onset of the light period and incubated in culture medium [12]. The eggs develop to the hatching stage within 10 days at 26°C. Embryonic development in *O. javanicus* [15] and *O. latipes* follows the typical teleostean pattern; therefore, these transparent eggs are excellent and very convenient materials for investigating fish embryogenesis.

The normal developmental process of *O. latipes* has been reported in Japanese by several investigators [4, 6, 11, 21, 22, 23, 24] and in English by Kirchen and West [22] and Yamamoto [30]. In these reports, the descriptions of stage 1 to stage 27 are in good agreement. However, except for our reports [6, 11] the descriptions of later stages (St. 28 to St. 33–36) of development are rough, sketchy and not based on detailed observations of the development of tissues and organs. Last year, the present author presented in Japanese more detaied descriptions of the developmental process of *O. latipes* in "The Biology of the Medaka" [13]. The definitions of the developmental stages of *O. latipes* provide a foundation for studying the embryology of this fish. The purpose of the present report is to present the information in English and includes some additional observations on the develomental course in reference to the data of the early investigators.

Accepted October 17, 1994
Received August 2, 1994

MATERIALS AND METHODS

Mature *Oryzias latipes* were purchased from a local fish farm (Yamato-koriyama, Nara-Prefecture) and kept in freshwater in glass aquaria (35×30×60 cm) under artificial reproductive conditions (10 hr dark, 14 hr light; 26–28°C). A measured amount of a powdered diet was supplied at least 6 times daily. The *Oryzias* spawn eggs every day about 9:00 (the onset of light). Ovaries with ovulated eggs in the ovarian lumen were routinely removed into saline [10] by laparotomizing females after pithing their brains. Unfertilized eggs were released from the ovarian lumen by tearing the ovarian sac. Long attaching filaments on each egg were carefully grasped with watchmaker forceps and cut off with the blunt tip of a glass bar while the egg was pulled away. Eggs were then transferred to a small petri dish containing saline and artificially inseminated by immersing them in a fresh sperm suspension in saline. The sperm suspension was prepared by squeezing sperm out of the testes of mature males.

Fertilized eggs were incubated in a stender dish (water depth 40 mm) first for two days in diluted (50%) sterile saline (26±0.5°C) containing methylene blue (2 ppm), and then in diluted saline without methylene blue. Eggs were observed using a special glass slide with a chamber (ca. 1 mm high) so constructed that the cover slip exerted a slight pressure on the chorion of the fertilized egg. By pushing the cover slip in various directions an egg could be rotated and the embryo could be held in any orientation. Each egg was used only once for observations. In some cases, it was necessary to dechorionate fertilized eggs by a convenient method [14] to allow observation of certain features.

OBSERVATIONAL RESULTS AND DESCRIPTIONS

Stage 0 ***Unfertilized eggs*****:**

The mature unfertilized egg is an oblate spheroid measuring average 1,245.9±3.9 μm (n=122) in horizontal diameter and a little less (average 1,169.9±4.0 μm, n=122) in vertical diameter. The egg proper is closely surrounded by a thick egg envelope, the chorion. The perivitelline space between the chorion and the vitellus is very difficult to

recognize using a light microscope. The micropyle located in the chorion at the animal pole is a small trumpet- or funnel-like structure. A number of short villi (non-attaching filaments; average 200.3±4.7/egg, n=38) are distributed over the whole surface of the chorion. At spawning, eggs are held together in clumps by a tuft of long attaching filaments (average 29.6±1.3/egg, n=38) on the chorion surface in the vegetal pole area of each egg [13].

A large, transparent yolk sphere is located in the center of each unfertilized egg. The cortical alveoli (vesicles, ca. 0.4–45 μm in diameter) and oil droplets are embedded at random in the cortical cytoplasm. The cortical alveoli contain a transparent colloidal material and usually one or sometimes a few spherical bodies [16]. The size of the oil droplets usually varies according to differences in the temperature during and after oocyte maturation, in the time after ovulation and among the individual females.

Stage 1 (3 min) ***Activated egg stage*:**

When an egg is stimulated by a spermatozoon arriving at the vitelline surface through the micropyle, a transient wave of increase in cytoplasmic free calcium starts at the point of sperm attachment [5, 33]. The cortical alveoli in the vicinity of the micropyle also begin to break down (exocytosis of alveolar contents) about 9 sec after sperm attachment [17]. The wave of exocytosis begins to propagate over the whole egg surface and ends at the vegetal pole 154 sec after its beginning. As a result of the exocytosis of cortical alveoli into the narrow space between the chorion and the vitellus, the chorion thins and hardens [25] as it separates from the vitellus to form a wide perivitelline space. Swollen spherical bodies secreted from the cortical alveoli are faintly visible in the perivitelline space. A transient "contractile wave" of cortical cytoplasmic layer follows the wave of exocytosis [9, 15]. Due to the oscillatory contractions following this distinct contractile wave, the cortical cytoplasm progressively accumulates toward the animal pole to form a thick cytoplasmic layer [1, 26]. At 7–8 minutes after sperm entry, the second polar body is extruded onto the surface of the cytoplasm at the center of the area where the germinal vesicle broke down during oocyte maturation.

Stage 2 ***Blastodisc stage*:**

The male and the female pronuclei migrate toward and associate with each other at the center of the thick cytoplasmic disc at the animal pole. Chromosomes then appear and divide into two groups at the poles of the spindle marking the end of this stage.

a (30 min). Oscillatory contractions cause the peripheral cortical cytoplasm to migrate toward the animal pole where it forms a convex, lens-shaped blastodisc. Meanwhile, oil droplets migrate toward the vegetal pole and begin coalescing.

b (60 min). The layer of cortical cytoplasm covering the yolk sphere is very thin except where it forms the cap-shaped blastodisc. By the end of this stage, most of the oil droplets from the animal hemisphere have already migrated to the vegetal hemisphere. Two dimple-like pits on the blastodisc serve as markers to locate the future blastomeres.

Stage 3 (1 hr 5 min) ***2 cell stage*:**

The first cleavage plane is at a right angle to the axis between the second polar body (meiotic spindle) and the micropyle in 60–79% of eggs. The two blastomeres are highly rounded just after cleavage, but are comparatively flat just before the second cleavage.

Stag 4 (1 hr 45 min) ***4 cell stage*:**

The second cleavage furrow develops on the two blastomeres at a right angle to the first cleavage plane. It deepens until each blastomere is divided into 2 of the same size. The oil droplets are larger but fewer and gather toward the vegetal pole

Stage 5 (2 hrs 20 min) ***8 cell stage*:**

The third cleavage plane is parallel to the first and divides the 4 blastomeres into 8 blastomeres. The blastoderm has bilaterally symmetrical rows of blastomeres and elongates along the axis of the second cleavage plane.

Stage 6 (2 hrs 55 min) ***16 cell stage*:**

The fourth cleavage plane, which is parallel to the second, divides the 2 rows of 4 blastomeres into 4 rows of 4 blastomeres.

Stage 7 (3 hrs 30 min) ***32 cell stage*:**

The fifth cleavag plane divides the marginal 12 lastomeres meridionally into 24, and the central 4 blastomeres horizontally into 8 thereby forming 2 layers, an outer and an inner layer, in the central region. The number of marginal cells is 14. The number of marginal cells is 14. These observatios agree with those of Matui [24], Gamo and Terajima [4] and Iwamatsu [11] but differ from the earlier reports of Kamito [21, cf. 30] in which cleavage was reported to continue to occur meridionally at least through the 32 cell stage.

Stage 8 (4 hrs 5 min) ***Early morula stage*:**

The planes of the sixth and later cleavages are difficult to precisely trace. The blastomeres (64–128) have different cleavage planes depending on their positions within the dome-shaped blastoderm and are arranged in 3 layers. The peripheral blastomeres (21–24) are flattened in shape. The cells (30–35 μm in diameter) are arranged in 3–4 layers but are still easily dissociated from each other [31].

Stage 9 (5 hrs 15 min) ***Late morula stage*:**

The blastodermal cells (256–512 blastomeres) are smaller than those of the previous stage and the number of marginal cells (30–40) has increased. The blastodermal cells (central region, 25–35 μm in diameter) now form 4–5 layers.

Stage 10 (6 hrs 30 min) ***Early blastula stage*:**

The blastoderm (about 1,000 cells) is still high (thick) as in the late morula stage, although its inner cells (20–30 μm in diameter) are smaller. According to Kageyama [19], the 11th cleavage still takes place synchronously. Nuclei from the marginal cells (40, cf. [19]) migrate out of the cells and are distributed in a few rows in the periblast (cortical syncytial layer).

Stage 11 (8 hrs 15 min) ***Late blastula stage*:**

Projection of the underside of the blastoderm (central cells, about 20 μm in diameter) into the yolk sphere is observed. In this stage, some blastomeres begin to cleave asynchronously and to migrate [20]. Several (5–6) rows of periblast nuclei are visible around the blastoderm.

Stage 12 (10 hrs 20 min) ***Pre-early gastrula stage*:**

The blastoderm has flattened down onto the yolk sphere so that its outer surface follows the curvature of the yolk sphere. The cell layers are slightly thicker on one side. The diameter of the cells in the central region of the blastoderm remains about 20 μm.

Stage 13 (13 hrs) ***Early gastrula stage*:**

The blastoderm begins to expand (epiboly, about 1/4 of the yolk sphere) over the surface of the yolk sphere, and the presumptive region of the embryonic shield arises as a thickened margin (dorsal lip) of the blastoderm. It is difficult to recognize the boundaries of the flattened marginal cells. The diameter of the cells in the central region of the blastoderm is 15–20 μm.

Stage 14 (15 hrs) ***Pre-mid gastrula stage*:**

Epiboly progressively advances and the blastoderm covers about 1/3 of the yolk sphere. The germ ring is well-defined, and the embryonic shield increases in size. Weak, rhythmically undulating movements [3, 29] begin to occur on the blastoderm but not on the uncovered yolk sphere.

Stage 15 (17 hrs 30 min) ***Mid gastrula stage*:**

A streak is visible in the midline of the embryonic shield projecting into the germ ring area. The blastoderm covers about 1/2 of the yolk sphere. The nuclei of the marginal periblast are barely visible on the yolk sphere.

Stage 16 (21 hrs) ***Late gastrula stage*:**

The blastoderm covers 3/4 of the yolk sphere, and the embryonic shield (body) becomes more clearly visible as a narrow streak. The enveloping layer expands uniformly over the yolk sphere until this stage [18].

Stage 17 (1 day 1 hr) ***Early neurula stage*** **(Head formation):**

The yolk sphere is nearly covered by the thin blastoderm leaving a small area around the vegetal pole (yolk plug) exposed. The head (rudimentary brain) is recognized anteriorly in the distinct embryonic body. A beak-like mass of cells is seen in front of the head. A few small vacuoles (Kupffer's vesicles) appear at the underside of the caudal (posterior) end of the body, which is in contact with a small blastopore.

Stage 18 (1 day 2 hrs) ***Late neurula stage*** **(Optic bud formation):**

The brain and nerve cord in the arrow-shaped embryonic body develop as a solid rod of cells. A solid optic bud (rudimentary eye vesicle) appears on each side of the cephalic end. The beak-like cell mass is still visible. The Kupffer's vesicles enlarge somewhat. A small part of the yolk sphere still forms a blastopore at the vegetal pole.

Stage 19 (1 day 3 hrs 30 min) ***2 somite stage*:**

A groove appears in the dorsum of each optic lobe. At the end of this stage (3 somites), two slight knobs are recognized behind the optic vesicles. The blastopore is completely closed. The expansion of the enveloping layer is accomplished without an accompanying increase in the number of constituent cells [18].

Stage 20 (1 day 7 hrs 30 min) ***4 somite stage*:**

A paired placode of otic (auditory) vesicles appears at the posterior region of the head. Depressions begin to form at the dorsal surface of the eye vesicles. Three parts of the brain (the fore-, the mid- and the hind-brain) are discernible.

Stage 21 (1 day 10 hrs) ***6 somite stage*** **(Brain and otic vesicle formation):**

The optic vesicles differentiate to form the optic cups and the lenses begin to form. The small otic vesicles appear, but they lack otolith. The three regions of the brain are well-defined, and the *neural fold (neurocoele)* is seen as a median line along the body. The flat body cavity is recognized on the surface of the yolk sphere bilateral to the mid-brain and hind-brain.

Stage 22 (1 day 14 hrs) ***9 somite stage*** **(Appearance of heart anlage):**

The tubular heart (heart anlage) appears underneath the head from the posterior end of the mid-brain to the anterior end of the hind-brain. The anlage of the hatching enzyme gland (cell mass) appears at the centroventral side of the hind-brain [28]. The body cavity extends further toward the posterior end of the eye vesicles. Melanophores appear on the yolk sphere. Incomplete lenses are present in the eyes, and the vesicular otocyst is defined.

Stage 23 (1 day 17 hrs) ***12 somite stage*** **(Formation of tubular heart):**

The anterior portion of the straight-tubed heart reaches beneath the posterior end of the eye vesicle. A pair of semi-circular Cuvierian ducts (blood vessels) and the vitello-caudal vein begin to form on the yolk sphere. Kupffer's vesicles shrink. The neurocoele is formed in the fore-, mid-

and hind-brains. The spherical optic lenses are completed. A blood island becomes pronounced in the ventral region between the 6th and 11th somites. The anterior (the 3rd-5th) somites assume a slightly dog-legged shape. The oil droplets have coalesced into a single large drop.

Stage 24 (1 day 20 hrs) ***16 somite stage*** **(Start of heart beating):**

The anterior portion of the heart, which exhibits a slow (about 33–64/min) pulsation, extends up to the anterior end of the forebrain. Cuvierian ducts and the vitello-caudal vein are still incomplete. Kupffer's vesicles have almost disappeared. Otoliths are not yet present in the otic vesicles. The embryonic body encircles nearly 1/2 of the yolk sphere. The gut (digestive) tube is observed ventral to the dogleg-shaped somites.

Stage 25 (2 days 2 hrs) ***18–19 somite stage*** **(Onset of blood circulation):**

When blood circulation begins, the spherical blood cells are first pushed out of the blood island (7th-15th somites) toward the vitello-caudal vein (Fig. 1). The blood is pumped (70–80 heartbeats/min) from the heart out into the anterior cardinal vein and the dorsal aorta roots. The dorsal aorta branching off the perceptible bulbus arteriosus is paired anteriorly with continuations extending to the head as the internal carotid arteries. The carotid artery splits to form the optic plexus, which connects with the left and right ducts of Cuvier. The left and right dorsal aorta roots run caudally until they join to form the dorsal aorta. The dorsal aorta is unpaired through the trunk region and continues into the tail as the vitello-caudal artery (Fig. 1). A countercurrent of the blood stream from the heart into the aorta is still observed.

Otoliths appear as two conglomerates of small granules lying against the inner surface of each well-expanded otocyst. The embryonic body encircles nearly 7/12 of the yolk sphere. The dogleg-shaped somites form a herringbone pattern between the 3rd and 10th somites. Kupffer's vesicles have disappeared completely. The bulge of the liver anlage appears at the 1st-3rd somites just posterior to the future position of the left pectoral fin in the 19 somite stage.

Stage 26 (2 days 6 hrs) ***22 somite stage*** **(Development of guanophores and vacuolization of the notochord):**

Blood containing globular blood cells is pumped out beyond the anterior region of the hind-brain. The caudal vein is observed is the region from the 1st to the 14th somites. The tip of the tail is completely free of the yolk sphere. The anlage of the liver, which first appeared at the 19 somite stage, is not yet well-developed. Red-brown colored guanophores, which first appeared at the ventral side of the mid-brain in the 20 somite embryo, are more clearly seen. Vacuolization of the notochord starts at its anterior region. Differentiating choroidea of the eyes begin to darken due to melanization.

Stage 27 (2 days 10 hrs) ***24 somite stage*** **(Appearance of pectoral fin bud):**

The tip of the tail where the notochord attaches is pointed. The embryonic body with the tail free from the yolk sphere encircles 5/8 of the yolk sphere. The rudiments of the pectoral fins protrude from the body trunk behind the base of the Cuvierian ducts. The eminences of liver rudiment are clearly seen on the left side beneath the 1st-3rd somites, and the gut tube can be seen beneath the 1st-13th somites curving to the left-ventral in the region between the 1st and 3rd somites. The arterial end of the heart has shifted to the right. The tail is free of the yolk sphere, and its vein is observed from the 10th to the 16th somites.

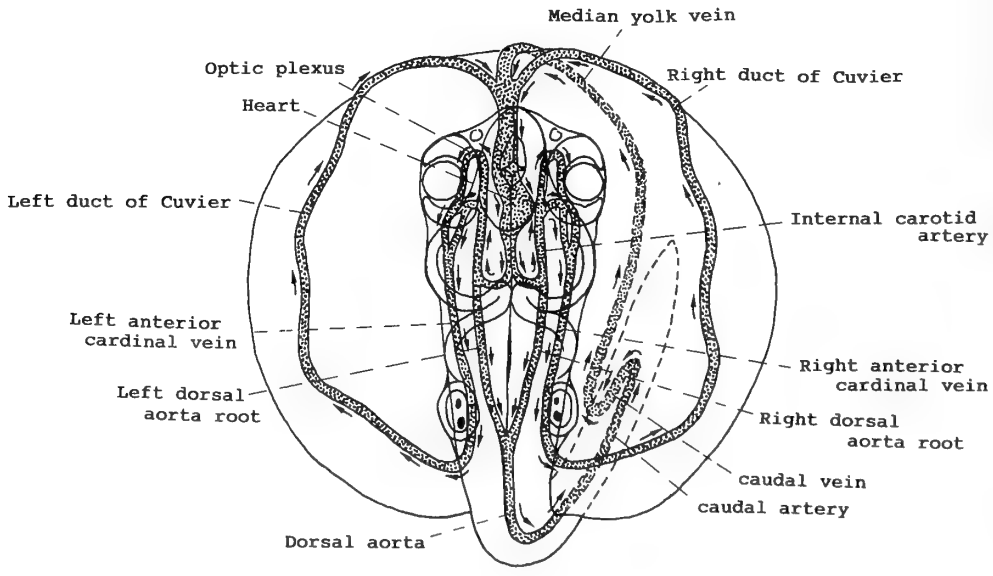

FIG. 1. Embryonic circulatory system at the early stage of blood circulation in the medaka, *Oryzias latipes*.

Stage 28 (2 days 16 hrs) ***30 somite stage*** **(Onset of retinal pigmentation):**

The embryonic body with a caudal vein between the 10th and 22th somites encircles about 2/3 of the yolk sphere. Pigmentation advances around the retina, and several melanophores occupy the dorsal wall of the viscera beneath the 1st to the 5th somites. The bulge of the liver becomes definitive in the left side of the 3rd to 4th somites. The anlage of the pancreas appears as a ventral eminence on the right side beneath and slightly anterior to the 3rd somite. Three sinuous portions of the vitelline veins consisting of the left and right ducts of Cuvier and 4 sinuous portions of the vitello-caudal vein meander on the yolk sphere. The blood cells (8.7 μm in diameter) flatten slightly. The posterior of the two otoliths in each otocyst is slightly larger than the anterior.

Stage 29 (3 days 2 hrs) ***34 somite stage*** **(Internal ear formation):**

The embryonic body encircles about 3/4 of the yolk sphere. The anlage of the pineal gland is recognized as a disc-shaped, round structure at the dorsal surface of the 3rd ventricle. In the heart, the sinus venosus, atrium, ventricle and bulbus arteriosus are differentiated. There is a large, transparent membranous protrusion inside the outer wall and another inside the inner wall of the otic vesicle (internal ear formation). In the region posterior to the eye (where gills will form), a group of large hatching enzyme cells has differentiated from endodermal cells [7, 28]. A ventral eminence is prominent behind the otic vesicles, and another eminence (the presumptive swim bladder) is discernible at the ventral side of the 3rd somite. The pectoral fin is apparent, and membranous fins are also seen in the tail, which has 19 somites beyond the gut tube. Guanophores begin to disperse on the dorsal surface of the body trunk. The anterior tip of the notochord is located where the branches of the dorsal aorta join.

Stage 30 (3 days 10 hrs) ***35 somite stage*** **(Blood vessel development):**

The embryonic body covers nearly 5/6 of the yolk sphere. Branches of arteries supplying blood to the anterior musculature in the body trunk, the gills and the brain are observed. The hepatic vein of the liver drains into the left duct of Cuvier. Two transparent and membranous protrusions (will become semicircular canals) are seen inside the outer wall of each otocyst.

Stage 31 (3 days 23 hrs) ***Gill blood vessel formation stage*****:**

Large cells of the hatching enzyme gland migrate up to the region under the central part of the eye, which now has a cornea. Blood circulation is seen in the gill arches. Pigmentation of the melanophores in the choroidea proceeds as a dark network in the eye. The pronephric kidney appears as a bright structure adjacnet to the 1st somite. The transparent, colorless gallbladder first appears at the posterior region of the liver. Four transparent, membranous protrusions (the structures of the internal ear) are recognized in the otic vesicles. The anterior region of the oral cavity is formed. The tail has 21 somites and a membranous fin which is wider on the ventral side.

Stage 32 (4 days 5 hrs) ***Somite completion stage*** **(Formation of pronephros and air bladder):**

The swim (air) bladder is recognized as a transparent vacuolar body beneath the 3rd somite, and the distinct kidneys (pronephroi) lie in contact with the bilateral sides of the notochord in the 1st somite. In the otic vesicles, a tubular (semicircular canals) membranous labyrinth can be seen. In the posterior end of the tail, the somites are indistinct. The number of whole somites counted is 30. Two hours later, the blood stream is twisted in the posterior end on the tail.

Stage 33 (4 days 10 hrs) ***Stage at which notochord vacuolization is completed*****:**

The tail tip has not yet reached within interocular distance of the eye. Because the eyeball (choroidea) is very dark, the lenses can be seen only with strong transillumination. The notochord is completely vacuolized to the end of the tail. The pineal gland is distinct at the dorsal surface of the vascularized forebrain. The tips of the membranous margins of the pectoral fins reach the 4th somite.

Stage 34 (5 days 1 hr) ***Pectoral fin blood circulation stage*****:**

The tip of the caudal fin has several melanophores and reaches the eye. Blood circulation is apparent in the pectoral fins, which frequently move (flutter). The choroidea of the eye becomes so black that it is almost impervious to light.

Stage 35 (5 days 12 hrs) ***Stage at which visceral blood vessels form*****:**

The tip of the caudal fin reaches beyond the posterior border of the eye. Guanophores are distributed from the head to the vicinity of the tail tip. Blood circulates through the internal tissues of the head and the viscera to Cuvier's ducts. The tubular structure of the spinal cord is revealed. The opening of the oral cavity to the mouth and the presence of several pit organs on the frontal bone can be recognized.

Stage 36 (6 days) ***Heart development stage*****:**

The tip of the tail reaches the otic vesicle. Guanophores and melanophores are distributed on the dorsal wall (peritoneum) of the peritoneal cavity beneath the 1st to the 4th somites. The extent of flexion of the atrio-ventricular region of the heart increases so that in a lateral view, the atrium and the ventricle lie adjacent to each other.

Stage 37 (7 days) ***Pericardial cavity formation stage*****:**

The tip of the tail lies just past the otic vesicle (total length ca. 3.1 mm). The pharyngeal teeth are visible in the posterior region of the gills between the otic vesicles. The

pericardial cavity (cardiac sac) surrounding the heart is easily observed. The slowly moving gut tube has a narrow lumen.

Stage 38 (8 days) ***Spleen development stage*** **(Differentiation of caudal fin begins):**

The tip of the tail extends beyond the otic vesicle (total length ca. 3.6 mm), and the rudiments of the caudal fin rays can be seen within the round membranous fin. The spleen is recognized as a small reddish globule dorsal to the gut tube beneath the left region of the 3rd-4th somites. The gut tube curves to the left between the 1st and the 4th somites, appearing to detour around the swim bladder (3rd-4th somites). A large well-developed gallbladder can be identified by its yellow or yellowish green tint. Both eyes move actively at the same time accompanying movement of the mouth and the pectoral fins.

Stage 39 (9 days) ***Hatching stage*****:**

The tip of the tail extends to the base of the pectoral fin or to the posterior region of the swim bladder (total length 3.8 ~4.2 mm). After hatching, the internal wall of the swim bladder expands remarkably.

Cells of hatching gland have already disappeared. The embryos dissolve the inner layers of the chorion [27], tear the single outer layer by moving the body and escape from the chorion tail-first.

Stage 40 ***1st fry stage*****:**

This period extends from hatching until fin rays appear in the caudal and pectoral fins (total length, ~about 4.5 mm).

Stage 41 ***2nd fry stage*****:**

This period begins after the appearance of jointed rays in the pectoral fins and continues until fin rays appear in the dorsal and anal fins (total length, ~about 5.5 mm).

Stage 42 ***3rd fry stage*****:**

This stage follows the appearance of ventral fin rays and scales in addition and extends to the formation of the jointed fin rays in the dorsal and anal fins (total length, ~about 7 mm).

Stage 43 ***1st young fish stage*****:**

This is the period before the secondary sexual characteristics are manifested (total length, ~about 22 mm).

Stage 44 ***2nd young fish stage*****:**

At this stage the mature fish ejaculate sperm and spawn eggs (total length, about 23 mm~).

REFERENCES

1 Abraham VC, Gupta S, Fluck RA (1993) Ooplasmic segregation in the medaka (*Oryzias latipes*) egg. Biol Bull 184: 115–124.

2 Egami N (1954) Effect of artificial photoperiodicity on time of oviposition in the fish, *Oryzias latipes*. Annot Zool Japon 27: 57–62.

3 Fluck RA, Jaffe LF (1988) Electrical currents associated with rhythmic contractions of the blastoderm of the medaka, *Oryzias latipes*. Comp Biochem Physiol 89A: 603–613.

4 Gamo H, Terajima I (1963) The normal stage of embryonic development of the medaka, *Oryzias latipes*. Jap J Ichthyol 10: 31–38. (in Japanese with English summary)

5 Gilkey JC, Jaffe LF, Ridgway EB, Reynolds GT (1978) A free calcium wave traverses the activating egg of the medaka, *Oryzias latipes*. J Cell Biol 76: 448–466.

6 Hiraki M, Iwamatsu T (1979) Histological observations on developmental process of the medaka egg. Bull Aichi Univ Educ 28 (Nat Sci): 73–78. (in Japanese)

7 Ishida J (1944) Hatching enzyme in the fresh-water fish, *Oryzias latipes*. Annot Zool Japon 22: 137–154.

8 Iwamatsu T (1965) On fertilizability of pre-ovulation eggs in the medaka, *Oryzias latipes*. Embryologia 8: 327–336.

9 Iwamatsu T (1973) On the mechanism of ooplasmic segregation upon fertilization in *Oryzias latipes*. Jap J Ichthyol 20: 73–78.

10 Iwamatsu T (1974) Studies on oocyte maturation of the medaka, *Oryzias latipes*. II. Effects of several steroids and calcium ions and the role of follicle cells on *in vitro* maturation. Annot Zool Japon 47: 30–42.

11 Iwamatsu T (1976) The medaka as a biological material. III. Observations of developmental process. Bull Aichi Univ Educ 25 (Nat Sci): 67–89. (in Japanese)

12 Iwamatsu T (1978) Studies on oocyte maturation of the medaka, *Oryzias latipes*. VI. Relationship between the circadian cycle of oocyte maturation and activity of the pituitary gland. J Exp Zool 206: 355–363.

13 Iwamatsu T (1993) The biology of the medaka. pp 324, Scientist Co, Tokyo. (in Japanese)

14 Iwamatsu T, Fluck RA, Mori T (1993) Mechanical dechorionation of fertilized eggs for experimental embryology in the medaka. Zool Sci 10: 945–951.

15 Iwamatsu T, Hirata K (1984) Normal course of development of the Java medaka, *Oryzias javanicus*. Bull Aichi Univ Educ 33 (Nat. Sci): 87–109.

16 Iwamatsu T, Ohta T (1976) Breakdown of the cortical alveoli of medaka eggs at the time of fertilization, with paticular reference to the possible role of spherical bodies in the alveoli. Wilhelm Roux's Arch 180: 297–309.

17 Iwamatsu T, Onitake K, Yoshimoto Y, Hiramoto Y (1991) Time sequence of early events in fertilization in the medaka egg. Develop Growth & Differ 33: 479–490.

18 Kageyama T (1980) Cellular basis of epiboly of the enveloping layer in the embryo of medaka, *Oryzias latipes*. I Cell architecture revealed by silver staining method. Develop Growth & Differ 22: 659–668.

19 Kageyama T (1987) Mitotic behavior and pseudopodial activity of cells in the embryo of *Oryzias latipes* during blastula and gastrula stages. J Exp Zool 244: 243–252.

20 Kageyama T (1988) How do the waves of nuclear divisions occur in the yolk syncytial layer of medaka embryos. Stud Hun Nat, No 22, 103–117. (in Japanese)

21 Kamito A (1928) Early development of the Japanese killifish (*Oryzias latipes*), with notes on its habits. Jour Coll Agr Univ Tokyo 10: 21–38.

22 Kirchen RV, West ER (1976) The Japanese medaka: Its care and development. pp 36, Carolina Biological Supply Co, Burlington, North Carolina.

23 Kubo I (1935) Spawning behavior and early development in *Oryzias latipes*. Yoshoku-kaishi 5: 1–9. (in Japanese)

24 Matui K (1949) Illustration of the normal course of development in the fish, *Oryzias latipes*. Jap J Exp Morph 5: 33–42. (in Japanese)

25 Ohtsuka E (1960) On the hardening of the chorion of the fish egg after fertilization. III. Mechanism of chorion hardening in *Oryzias latipes*. Biol Bull 118: 120–128.

26 Sakai TY (1964) Studies on the ooplasmic segregation in the egg of the fish, *Oryzias latipes*. Embryologia 8: 129–134.

27 Yamagami (1981) Mechanisms of hatching in fish: Secretion of hatching enzyme and enzymatic choriolysis. Amer Zool 21: 459–471.

28 Yamamoto M (1963) Electron microscopy of fish development. I. Fine structure of the hatching glands of embryos of the teleost, *Oryzias latipes*. J Fac Sci Tokyo Univ IV, 10: 115–121.

29 Yamamoto T (1931) Studies on the rhythmical movements of the early embryos of *Oryzias latipes*. II. Relation between temperature and the frequency of the rhythmical contractions. J Fac Sci Tokyo Univ IV, 2: 153–162.

30 Yamamoto T (1975) Stages in the development. In "Medaka (Killifish): Biology and Strains" (Yamamoto T ed), pp 59–72. Keigaku Publ Co, Tokyo.

31 Yokoya S (1966) Cell dissociation and reaggregation in early stage embryo of the teleost, *Oryzias latipes*. Sci Rep Tohoku Univ 32: 229–236.

32 Yoshioka H (1963) On the effects of environmental factors upon the reproduction of fishes. 2. Effects of short and long day-lengths on *Oryzias latipes* during spawning season. Bull Fac Fish Hokkaido Univ 14: 137–151.

33 Yoshimoto Y, Iwamatsu T, Hiramoto Y (1986) The wave pattern of free calcium release upon fertilizationin medaka and sand dollar eggs. Develop Growth & Differ 28: 583–596.

ABBREVIATION

ab: swim (air) bladder
af: anal fin
ag: artery globe
an: anus
at: attaching filament
bc: body cavity
bd: blastodisc
bi: blood island
bl: beak-like mass of cells
bm: blastomere
br: branchiostegal ray
bv: blood vessel
ca: cortical alveolus
cd: Cuvierian duct
cf: caudal fin
ch: chorion
cn: cornea
cv: caudal vein
da: dorsal aorta
df: dorsal fin
dl: dorsal lip of blastopore
ea: otic (ear) vesicle
em: embryonic body
ev: otic (ear) vesicle rudiment
ey: optic (eye) vesicle
fb: forebrain
fr: fin ray
g: gill
gb: gallbladder
gp: guanophore
gt: gut tube
h: heart rudiment
ha: atrium of heart
hb: hind-brain
hg: hatching gland cell
hv: ventricle of heart
kv: Kupffer's vesicle
l: lens
lj: lower jaw
lv: liver
mb: mid-brain
mc: marginal cell
mf: membranous fin
ml: membrane labyrinth
mp: micropyle
mv: median yolk vein
n: naris
no: notochord
od: oil droplet
o: operculum
op: olfactory pit
ot: otolith
pa: protoplasmic accumulation
pb: protobrain
pf: pectoral fin
pi: pineal gland
pn: nucleus of periblast
pr: pronephros
ps: perivitelline space
s: scale
sc: spinal cord
sm: somite
sp: spleen
uj: upper jaw
uo: urinogenital orifice
v: non-attaching filament
vf: ventral fin
vl: vein of liver
y: yolk sphere

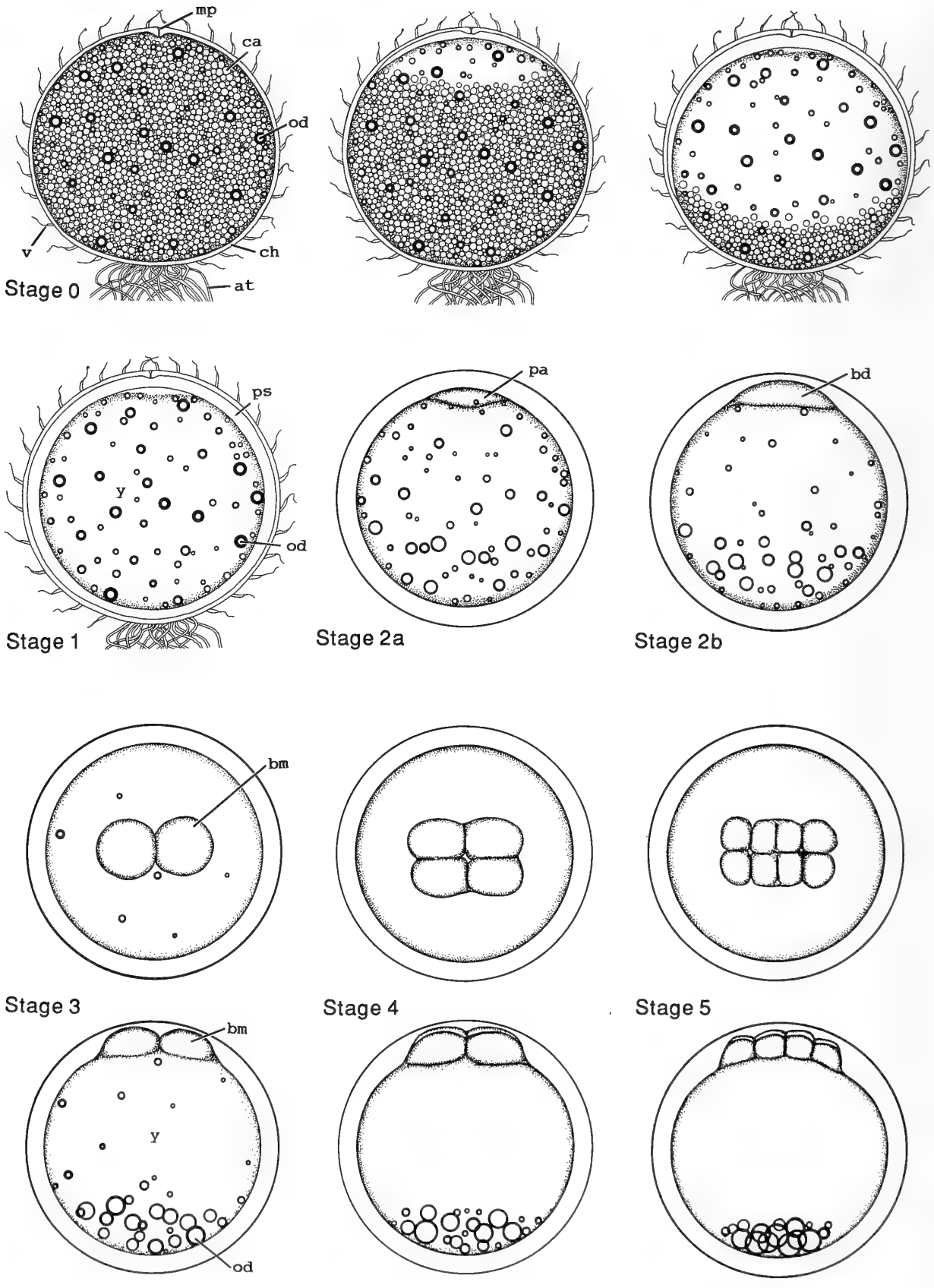
mp
ca
od
v
ch
at
Stage 0
ps
y
od
Stage 1
pa
Stage 2a
bd
Stage 2b
bm
Stage 3
Stage 4
Stage 5
bm
y
od

Plate 1

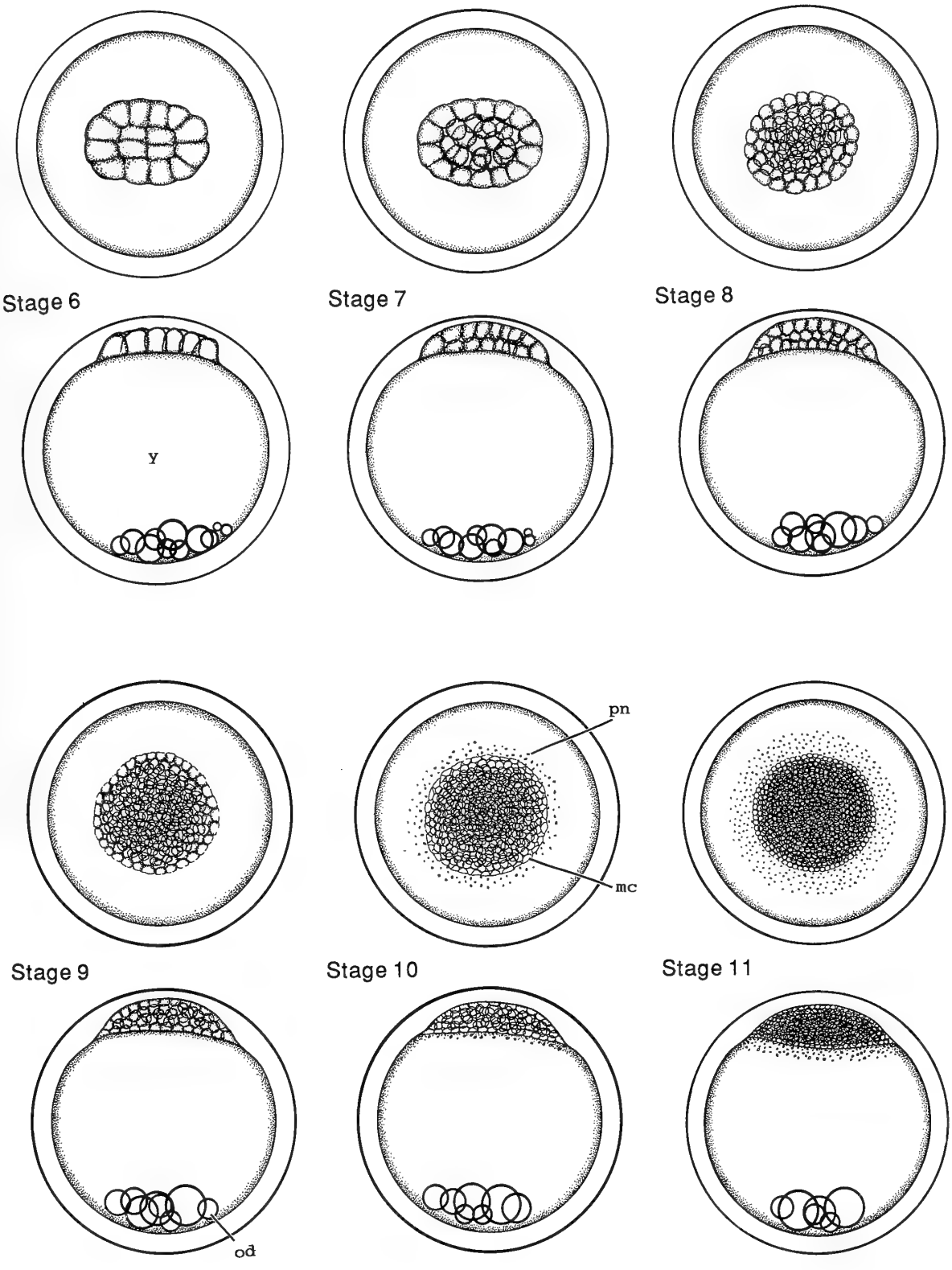

Plate 2

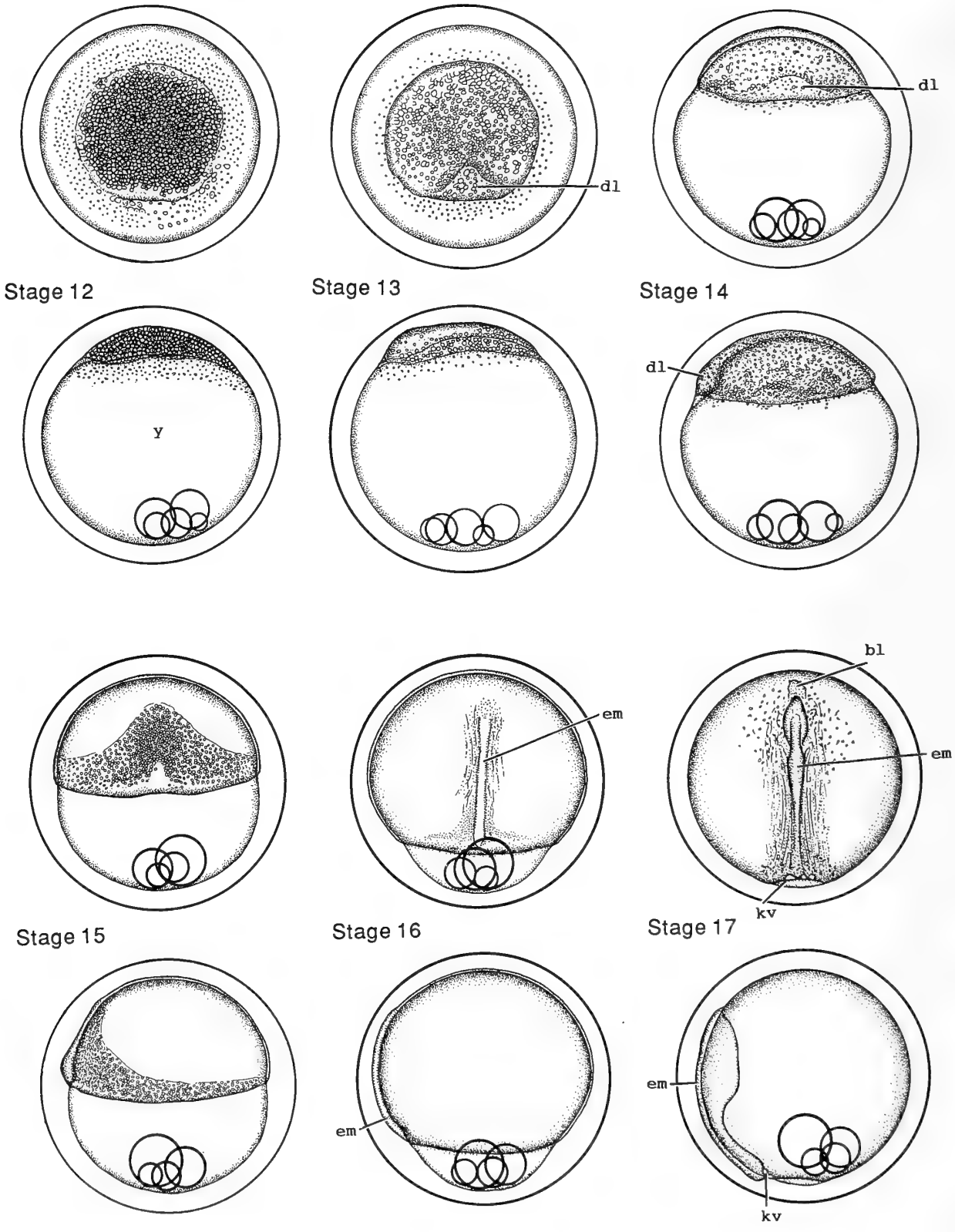
dl
dl
Stage 12
Stage 13
Stage 14
y
dl
em
em
bl
em
kv
Stage 15
Stage 16
Stage 17
em
em
kv

Plate 3

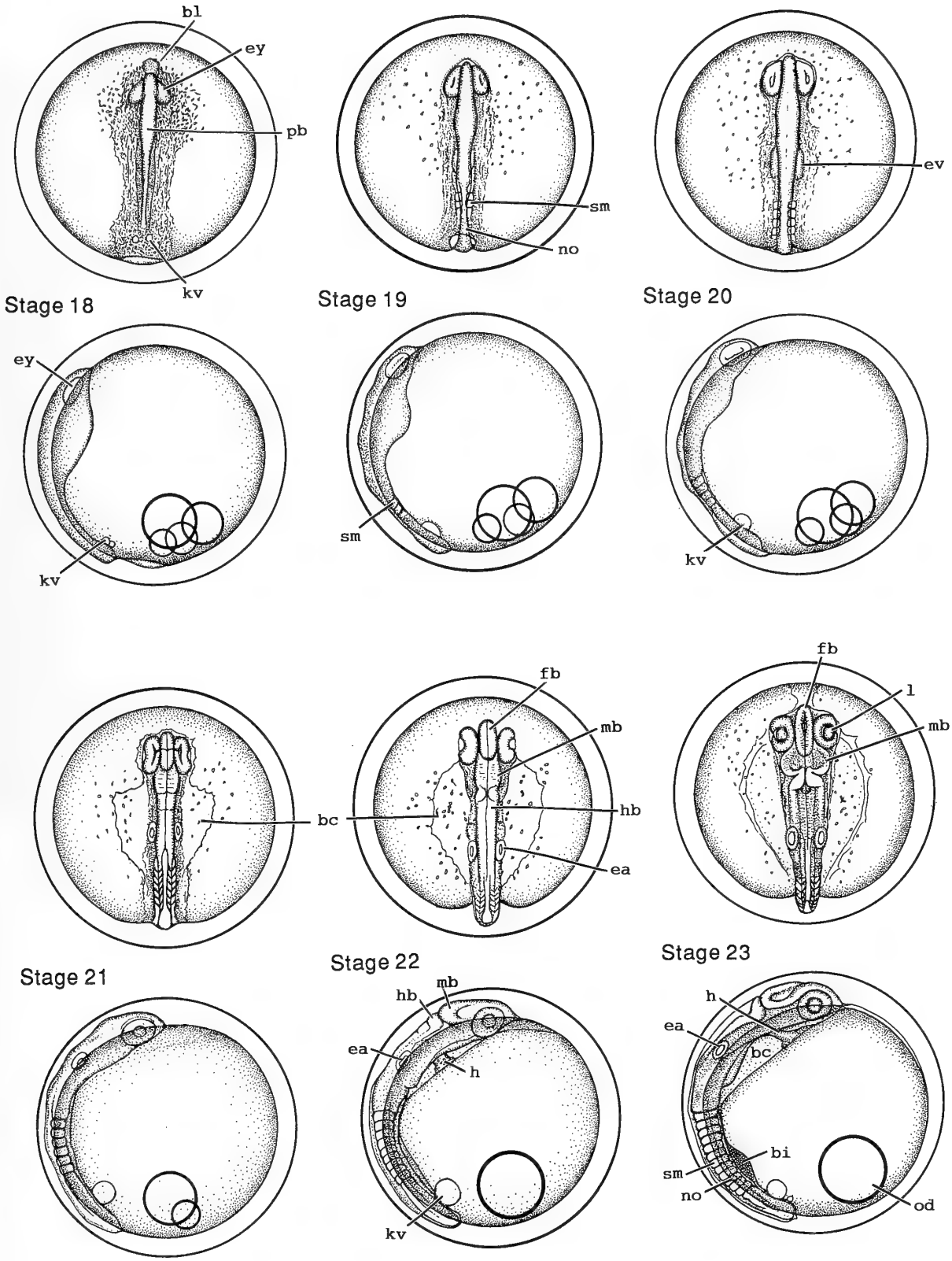
bl
ey
pb
kv
Stage 18
sm
no
Stage 19
ev
Stage 20
ey
kv
sm
kv
fb
mb
bc
hb
ea
Stage 21
Stage 22
fb
l
mb
Stage 23
mb
hb
ea
h
kv
h
ea
bc
bi
sm
no
od

Plate 4

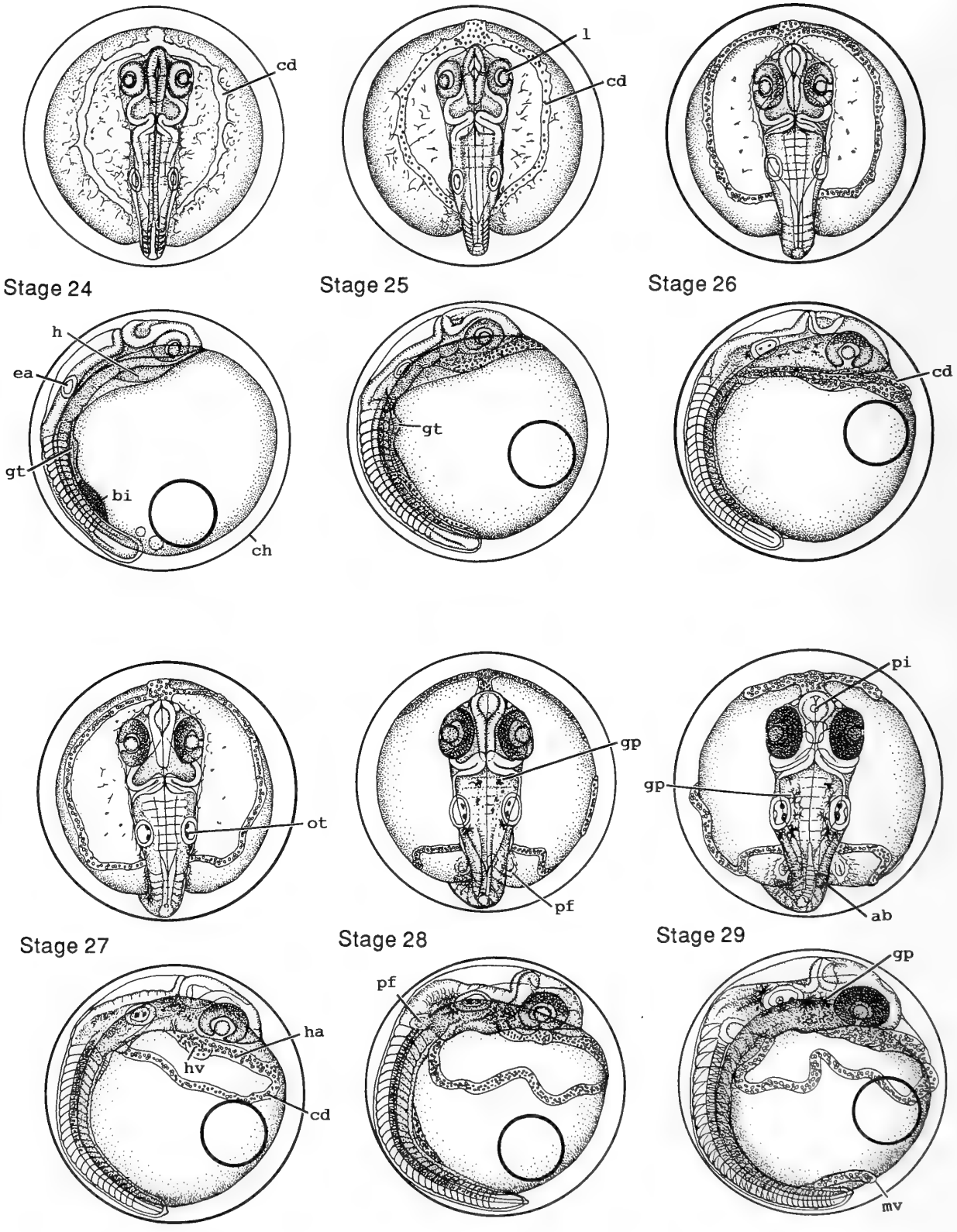
cd
l
cd
Stage 24
Stage 25
Stage 26
h
ea
gt
bi
ch
gt
cd
ot
gp
pf
pi
gp
ab
Stage 27
Stage 28
Stage 29
ha
hv
cd
pf
gp
mv

Plate 5

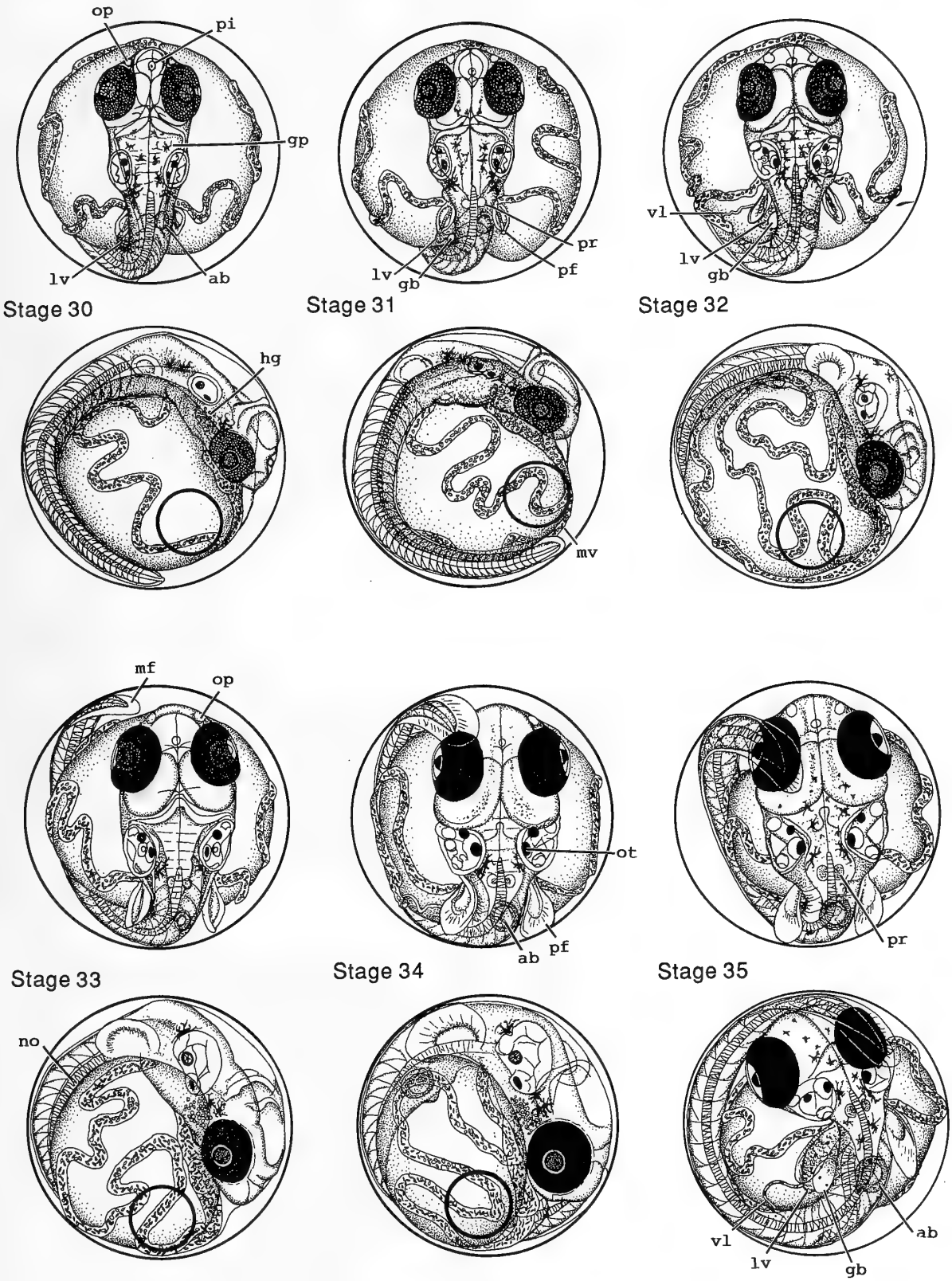
op
pi
gp
lv
ab
Stage 30
lv
gb
pr
pf
Stage 31
vl
lv
gb
Stage 32
hg
mv
mf
op
Stage 33
ot
ab
pf
Stage 34
pr
Stage 35
no
vl
lv
gb
ab

Plate 6

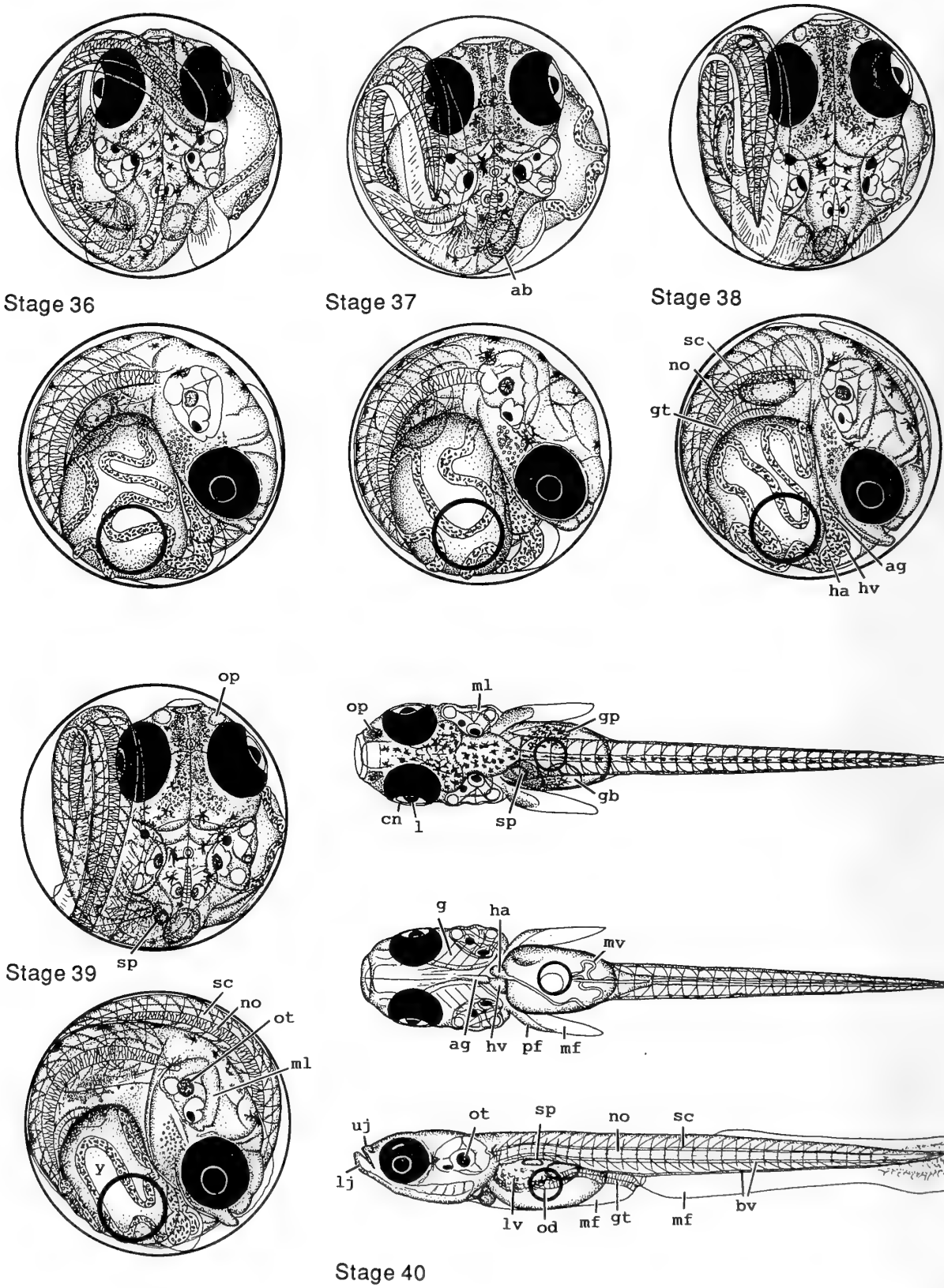
ab
Stage 36
Stage 37
Stage 38
sc
no
gt
ag
ha
hv
op
sp
Stage 39
op
ml
gp
gb
cn
l
sp
g
ha
mv
ag
hv
pf
mf
sc
no
ot
ml
y
uj
ot
sp
no
sc
lj
lv
od
mf
gt
mf
bv
Stage 40

Plate 7

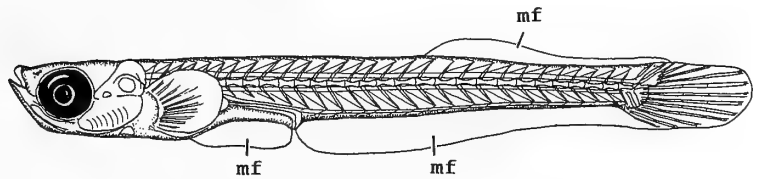

Stage 40

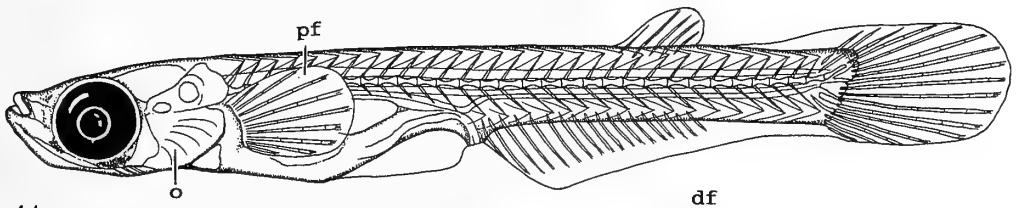

Stage 41

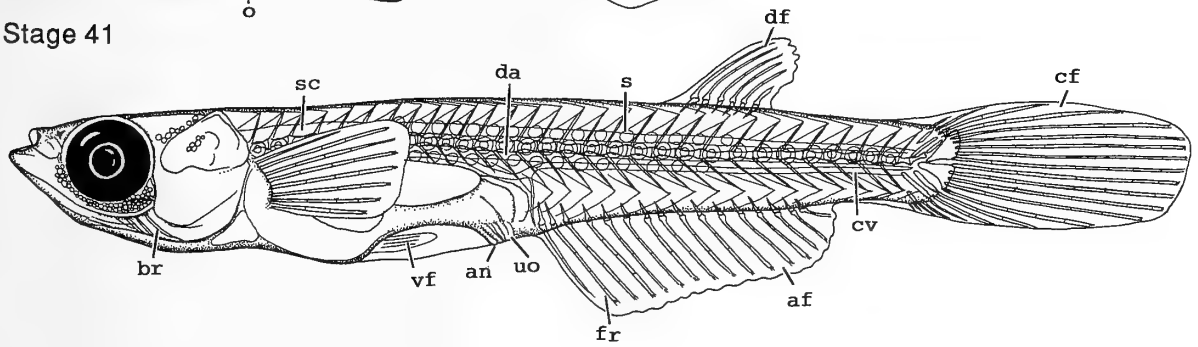

Stage 42

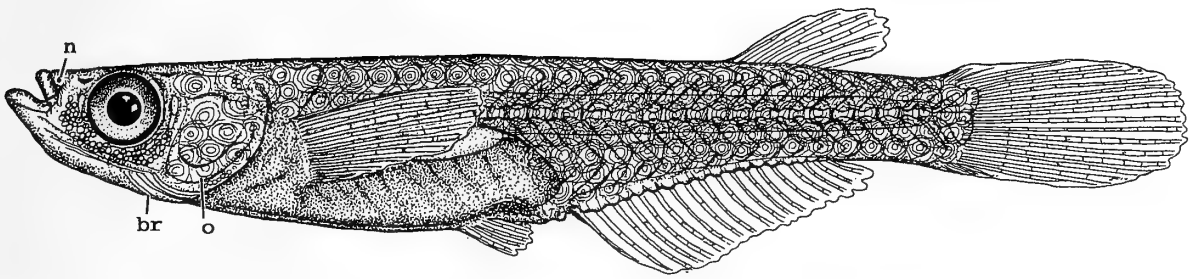

Stage 43

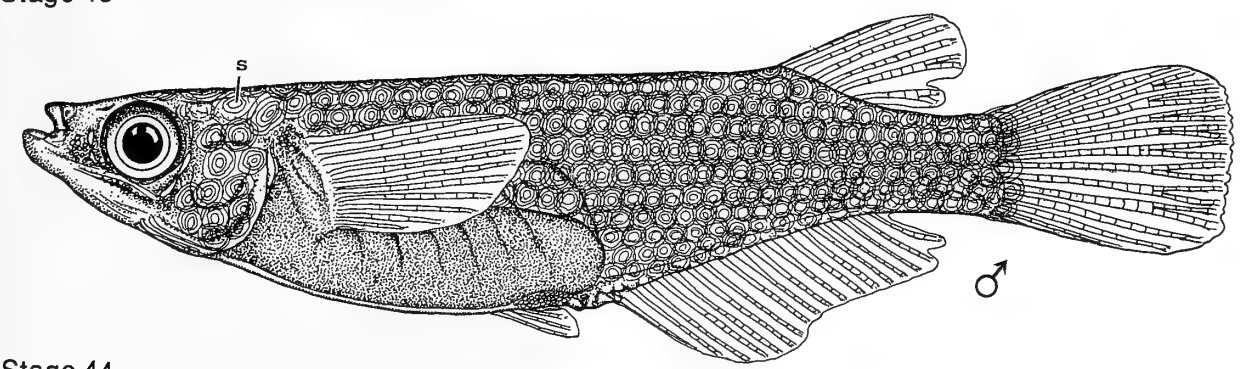

Stage 44

Plate 8

ZOOLOGICAL SCIENCE 11: 841–846 (1994)

Mouse TGFα Gene Expression in Normal and Neoplastic Mammary Glands and Uteri of Four Strains of Mice with Different Potentials for Mammary Gland Growth and Uterine Adenomyosis

Toshio Harigaya[1)], Satoshi Tsunoda[2)], Hidenori Yokoyama[2)], Kazutoshi Yamamoto[3)] and Hiroshi Nagasawa[2)]

[1)]*Laboratory of Functional Anatomy and* [2)]*Experimental Animal Research Laboratory, Meiji University, 1-1-1 Higashimita, Tama-ku, Kawasaki-shi, Kanagawa 214, and* [3)]*Department of Biology, School of Education, Waseda University, Shinjuku-ku, Tokyo 169-50, Japan*

ABSTRACT—The expression of TGFα mRNA and the protein localization in the mammary glands were determined by RT-PCR and immunohistochemical staining methods, respectively, in four strains of mice (SHN, SLN, GR/A and C3H/He), which had different potentials for normal and neoplastic mammary gland growth and uterine adenomyosis. TGFα gene expression was detected in some virgin and pregnant mammary glands of 4 strains and in all lactating glands of SHN, GR/A and C3H/He mice, but not in SLN. The results of immunohistochemical staining of pregnant and lactating mammary glands corresponded well with those of RT-PCR in all strains except SLN. These suggest that there is a strain-related difference in the pattern of TGFα gene expression during the reproductive states. Meanwhile, little difference was observed among strains in TGFα gene expression after retirement; in retired mammary glands, some samples expressed TGFα mRNA and all samples were stained positively in 4 strains. All samples of mammary tumors showed both TGFα mRNA expression and immunohistochemically positive staining. Neither RT-PCR nor immunohistochemical staining showed positive results in uterus in all strains except one sample in GR/A. All findings in this study indicate that TGFα expression itself is not always directly related to the potentials for normal and neoplastic mammary gland growth and uterine adenomyosis in mice. In all strains, several different sizes of PCR products were observed besides the predicted size of product in mammary tumors and lactating and/or retired mammary glands. These suggest that mammary glands may possess sooner or later neoplastic characteristics that include an over expression of TGFα during and after reproductive states.

INTRODUCTION

Four strains of mice (SHN/Mei, SLN/Mei, GR/AMei and C3H/HeMei) maintained in this laboratory have different potentials for mammary gland growth and uterine adenomyosis. In virgins, normal mammary gland growth is marked in order of SHN, GR/A, C3H/He and SLN [23] and the onset of precancerous mammary hyperplastic alveolar nodules (HAN) is earlier in SHN and GR/A than in C3H/He and SLN [20]. The mammary tumor potential in virgins is the highest and the lowest in SHN and C3H/He, respectively and intermediate in GR/A and SLN [21]. In SHN, virgins have the similar mammary tumor potential to breeders [19], but not in the other three strains, whose mammary tumor incidence are higher in breeders than in virgins (Nagasawa, unpublished). Furthermore, GR/A strain has an additional characteristic of the development of pregnancy-dependent mammary tumor (PDMT), which appears at the middle of pregnancy, reaches the maximal size at the end of pregnancy, then regresses and disappears soon after parturition regardless of lactation [1, 15]. In these four strains, almost all mice with mammary tumors also develop uterine adenomyosis, a benign pathological disorder of endometrial tissues, glands and stroma, which invade with the myometrium [14]. The degree of progression of the lesion is higher in SHN and SLN than in GR/A and C3H/He [21].

TGFα is a 50-amino acid mitogenic polypeptide. Expression of TGFα has been identified in human tumors and tumor cell lines [6, 10, 16] and in normal cells including human keratinocytes [5] and human and rodent mammary glands [12, 32], suggesting that TGFα has functional roles in both normal and neoplastic mammary gland growths. TGFα has also been found to express in uterus [7, 27]. These studies tempted us to examine the mouse TGFα gene expression in normal and neoplastic mammary glands and uteri of the four strains of mice. This paper deals with this problem.

MATERIALS AND METHODS

Animals

Three females of each strain were used as virgins at 2 months of age. Some others were mated with littermate males at 2 to 3 months of age and the day when vaginal plug was found was designated as day 1 of pregnancy. Pregnant mice were divided into 3 groups; Group I was killed on day 18 or 19 of pregnancy. Group II was allowed to deliver and killed on day 12 of lactation. Group III was retired after the 2nd or the 3rd lactation, checked for palpable mammary tumors every 7 days and killed in 1–2 weeks after the first

Accepted October 3, 1994
Received July 25, 1994

tumor appearance. All mice were killed by decapitation under the light ether anesthesia and blood was collected from the trunk.

In pregnant and lactating animals, a portion of the unilateral inguinal glands was fixed in Bouin's solution and used for immunohistochemical staining of mouse TGFα protein. The remaining mammary tissues were divided into two parts; one was stored at −70°C and another in acetone for determination of TGFα mRNA and nucleic acid contents, respectively. In virgins and the retired animals, the unilateral third thoracic gland was prepared for the wholemount evaluation. A portion of the inguinal glands was fixed in Bouin's solution for immunohistochemical staining of mouse TGFα protein. The remaining tissues were stored at −70°C for determination of TGFα mRNA. Furthermore, in GR/A mice, the PDMT was surgically removed on day 18 or 19 of the 2nd pregnancy, and used for RT-PCR and immunohistochemical staining.

All mice were maintained in aluminum cages (18×35×15 cm) with wood shavings individually (pregnant or lactating mice) or 4 to 5 each (virgins and retired mice) in an animal room that was air-conditioned (20–22°C and 50–70% relative humidity), artificially illuminated (14 hr of light from 5:00 am to 7:00 pm) and ventilated 16 times/hour. They were provided with a commercial diet (Lab MR Breeder; Nihon Nosan Kogyo KK, Yokohama, Japan) and water *ad libitum*.

Mammary nucleic acid contents

Mammary tissue in acetone was further defatted and dried with hot alcohol-ether and dry matter was weighed. Nucleic acids were extracted with trichloroacetic acid by the method of Schneider [28]. DNA and RNA contents were determined by the diphenylamine [3] and the orcinol [13] reactions, respectively, and expressed with mg/100 mg dry fat-free tissue (DFFT).

Normal and preneoplastic mammary gland growth

The wholemount preparations were examined under 10-fold magnification. The degree of end-bud formation was rated from 1 to 7 in increments of 1 according to the previous report [26]. The area surrounding the tops of ducts was measured by the computerized digitizer (PIAS; Model LA-525, Tokyo, Japan) and used as the index of duct growth. The number and the area of preneoplastic mammary hyperplastic alveolar nodules (HAN) were also counted.

Serum prolactin level

Blood was collected from the trunk, left at room temperature for 8 hr, kept in the refrigerator overnight, and centrifuged at 1000×g for 20 min at 4°C. Serum was stored at −20°C until the radioimmunoassay was performed. Serum level of prolactin was determined by homologous radioimmunoassay according to the previous method [31].

RNA isolation and detection of mouse TGFα mRNA

Total RNA was isolated from 100 mg of frozen mammary tissue by the acid guanidium-phenol-chloroform method [4]. TGFα mRNA expressed in the mammary gland was determined by reverse transcriptase-polymerase chain reaction (RT-PCR) method with cloned moloney murine leukemia virus (MMLV) reverse transcriptase and Taq DNA polymerase (Perkin Elmer Cetus, Norwalk, CT, USA) according to the procedure of supplier's recommendation. The PCR was performed for 40 cycles (1 cycle=94°C for 1 min, 65°C for 2 min and 72°C for 2 min) in a program temperature control system (Astec, Fukuoka, Japan). The sense and antisense primers according to the mouse TGFα cDNA sequence [30] were used for PCR as described previously [8].

β-Actin primers according to the mouse sequence [2] were used for RT-PCR control reaction as reported previously [8].

Immunohistochemical staining

Inguinal mammary glands, mammary tumors and uterus were fixed in Bouin's solution, embedded in paraffin and sectioned at 6 μm. Immunohistochemical staining of TGFα was performed by streptavidin-biotin (SAB) technique using Histofine SAB-PO(R) Kit (Nichirei, Tokyo, Japan) as described previously [9]. Rabbit anti-rat TGFα serum (Peninsula Lab, Taylorway, Ca, USA) was used as primary antiserum (1:1000 dilution). The sample was judged as positive staining when at least one stained cell in the tissue was observed immunohistochemically in three slide glasses on which several sections of each tissue sample were mounted.

RESULTS

Growth and function of the mammary gland and the serum level of prolactin (Tables 1 and 2)

TABLE 1. General features of virginal and retired mammary glands in each strain (MEAN±SEM)

	No of mice	Age (days)	Body weight (g)	Mammary gland		HAN			Mammary tumor		Serum prolactin level (ng/ml)
				Rating	Area (mm^2)	Number (/mouse)	Area (mm^2)		Onset age (day)	Growth rate (%/week)	
Virgin											
SHN	3	61	24.0±0.9	2.0±0	230±9						188±7
SLN	3	63	24.0±0.8	1.0±0*	227±20						129±11
GR/A	3	62	17.8±0.7*	1.3±0.2	142±12*						180[2]
C3H/He	3	65	23.4±0.6	1.7±0.2	226±32						159±10
Retired											
SHN	5	290±28	34.0±1.0	2.8±0.2	329±16	30.0±6.0	1.2±0.1	(150)[1]	280±2	83±18	92±9
SLN	3	326±61	35.5±1.8	2.8±0.3	225±21*	6.5±2.1*	1.3±0.2	(20)[1]	307±62	60±13	104±16
GR/A	4	352±31	28.3±1.4*	3.1±0.4	280±22*	13.8±2.5*	1.3±0.1	(55)[1]	330±33	36±6	124±8
C3H/He	8	564±70	43.8±2.4*	2.5±0.4	249±29*	25.6±2.7	2.8±0.7*	(205)[1]	490±71*	50±6	100±16

[1]: Number of HAN measured
[2]: Mean of two samples
*: Significantly different from SHN at $P<0.05$

TABLE 2. General features of pregnant and lactating mammary glands in each strain (MEAN±SEM)

	No of mice	Age (days)	Body weight (g)	Litter size	Pup's growth rate on day 12 (%/day 1)	Rearing rate on day 12 (%)	Mammary gland			Serum prolactin level (ng/ml)
							DNA (mg/100 mg DFFT[1])	RNA (mg/100 mg DFFT)	RNA/DNA	
Pregnant										
SHN	3	135±14	43.8±2.4				4.09±0.53	3.95±0.73	0.97±0.15	109±9
SLN	3	88±4	36.6±1.3				4.56±0.74	5.95±1.03	1.31±0.36	349±84
GR/A	3	97±6	36.9±1.2				5.10±0.54	3.83±0.22	0.75±0.04	142[2]
C3H/He	3	121±1	42.5±1.6				4.52±0.59	6.27±2.36	1.39±0.55	85±5
Lactating										
SHN	3	160±3	35.9±0.9	7.0±1.0	360±72	100	1.49±0.23	12.00±1.27	8.09±1.20	225±11
SLN	3	160±8	37.1±1.0	8.7±1.3	260±54	100	1.99±0.24	12.39±2.40	6.24±0.85	165±21
GR/A	3	154±12	28.7±0.3*	8.7±0.7	199±20*	100	2.48[2]	8.75[2]	3.54[2]	366±93
C3H/He	3	144±93	39.2±2.4	6.0±0.6	440±6	94±6	1.75±0.12	9.42±3.47	5.40±2.21	206±94

[1]: Dry fat-free tissue
[2]: Mean of two samples
*: Significantly different from SHN at $P<0.05$

In body weight in virgin, lactating and retired groups and pup's growth rate on day 12 of lactation, GR/A was apparently smaller than the other 3 strains, among which little difference was observed. There was little difference among strains in body weight at the end of pregnancy. Nucleic acid contents in mammary glands, which indicate the mammary activities, differed little among strains except RNA/DNA ratio in lactation, which was smaller in GR/A.

Rating and area of mammary glands of virgins in SLN and GR/A, respectively, were lower than those of SHN. Mammary areas of retired SLN, GR/A and C3H/He mice were smaller than that of SHN. Number of HAN per mouse was lower in SLN and GR/A than in SHN and C3H/He, and the area of HAN was the highest in C3H/He. While C3H/He developed mammary tumors later than did the other strains, no apparent difference was seen among strains in the growth of tumors.

There is no significant difference in serum prolactin level among strains compared to SHN at any stage examined.

mRNA expression and immunohistochemical staining of TGFα (Table 3 and Fig. 1)

In virgin or pregnant animals, 1 out of 3 samples from virgin SHN and pregnant SLN and 2 out of 3 samples from other strains expressed mRNA for TGFα. Immunohistochemically, 3 or 2 out of 3 samples from each strain, showed the positive staining of TGFα.

In lactating animals, all samples expressed mRNA and

TABLE 3. Frequency of TGFα gene expression in mammary glands and uteri of each strain

		SHN		SLN		GR/A		C3H/He	
		PCR	IH[1]	PCR	IH	PCR	IH	PCR	IH
Mammary gland	Virgin	1/3[2]	3/3	2/3	2/3	2/3	3/3	2/3	3/3
	Pregnant	2/3	2/3	1/3	3/3	2/3	2/3	2/3	2/3
	Lactating	3/3 (3/3)[3]	3/3	0/3	3/3	3/3	3/3	3/3 (2/3)	3/3
	Retired	1/5 (1/1)	5/5	1/3 (1/1)	3/3	1/4 (1/1)	4/4	1/7 (1/1)	7/7
Tumor	Retired	5/5 (4/5)	5/5	3/3 (1/3)	3/3	4/4	4/4	7/7 (6/7)	7/7
PDMT[4]	Pregnant					3/4			
Uterus	Retired	0/3	0/3	0/3	0/3	0/3	1/3	0/3	0/3

[1]: Immunohistochemical staining
[2]: Positive samples/all samples
[3]: Samples detected different sizes of PCR products/positive samples
[4]: Pregnancy dependent mammary tumor

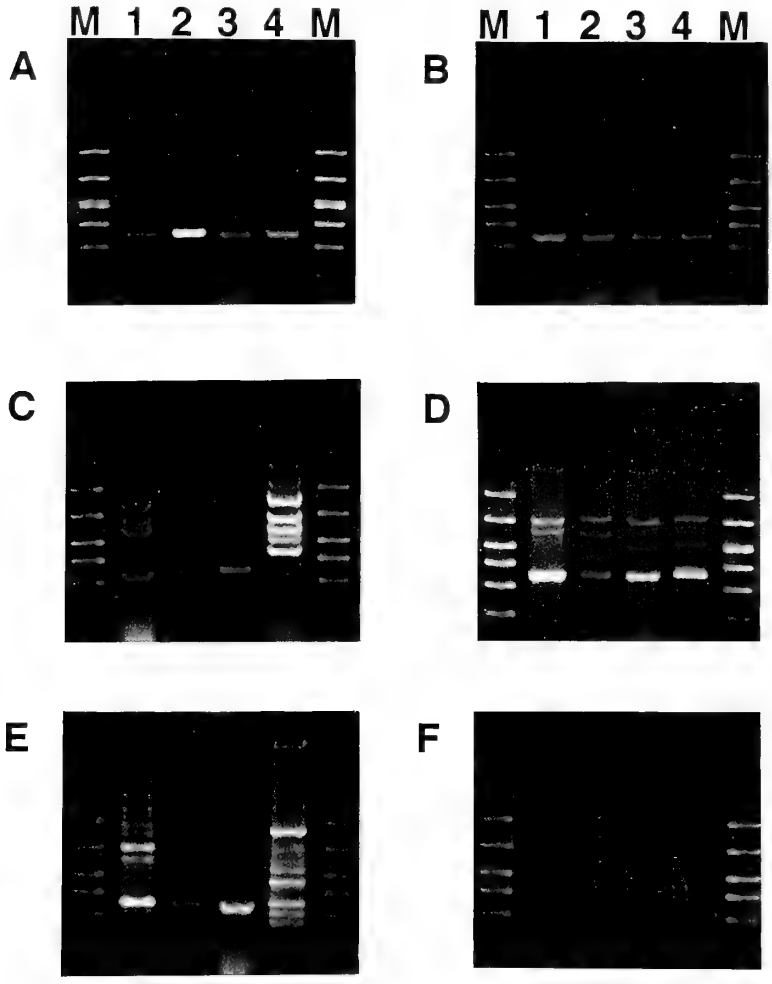

FIG. 1. Agarose gel electrophoresis of RT-PCR products in four strains of mice. Lane 1, 2, 3 and 4 indicate the representative results in SHN, SLN, GR/A and C3H/He, respectively. Lane M indicates molecular size marker of DNA. Panel A, B, C, and D indicate the results from virgin, pregnant, lactating and retired mammary glands, respectively. E and F indicate the results from mammary tumor and uterus, respectively.

showed positive staining in four strains, except for mRNA in SLN, in which no sample was positively detected. Furthermore, various sizes of PCR products [8] were detected in 3 and 2 out of 3 samples in SHN and C3H/He strains, respectively (Fig. 1).

In retired animals, only 1 out of 3 to 7 samples of normal glands from four strains expressed mRNA, all of which showed various sizes of PCR products. On the other hand, all samples examined showed positive staining immunohistochemically in any strain. In these glands, positive cells were always stained in stroma cells, but not in alveolar epithelial cells (Fig. 2).

In mammary tumors, all samples of four strains examined expressed mRNA and were stained positively. Eighty percent (4/5), 33.3%(1/3), 0% (0/4) and 85.7% (6/7) showed obviously several PCR products including predicted size in SHN, SLN, GR/A and C3H/He, respectively. TGFα gene expression was also observed in 3 of 4 samples of the PDMT in GR/A mice. However, the size of PCR product was only a single band of 349 bp (Fig. 1).

In uteri, none of samples from four strains expressed TGFα mRNA or protein, except 1 sample of GR/A, which showed the positive staining of TGFα immunohistochemically.

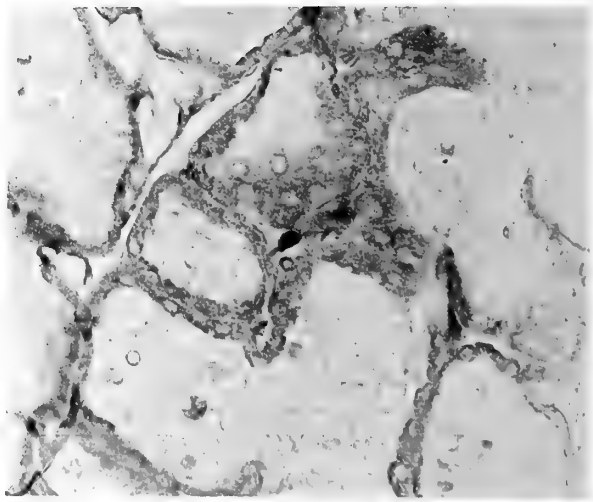

FIG. 2. Immunohistochemical localization of TGFα in the lactating mammary gland. $\times$350

DISCUSSION

All observations in this study on the mammary gland growth and function of four strains are generally in good accord with those reported previously [17, 18, 20–25].

These indicate that mammary gland characteristics change little for generations in these highly inbred strains.

In pregnant mammary glands of SHN, GR/A and C3H/He, 2 out of 3 samples showed both mRNA expression and localization of TGFα. On the other hand, in SLN, only 1 out of 3 samples expressed mRNA, whereas all 3 samples stained positively. It is also the case in lactating glands. Both mRNA and protein detection of TGFα were observed in all samples examined in the former 3 strains. In SLN, however, all samples were stained only immunohistochemically, but none reacted by RT-PCR. These results suggest that there were some differences between SLN and the other three strains in the time, the period and/or the significance of TGFα function on mammary glands during pregnancy and lactation, although no difference was observed among strains in the resultant mammary gland features.

In retired mammary glands of 4 strains, all samples showed positive staining immunohistochemically and some also expressed TGFα mRNA, indicating little strain related difference in the pattern of mammary gland TGFα expression in retired glands. All mammary tumor samples examined from 4 strains showed positive expression and staining of TGFα in the retired animals. These may reflect the continued growth of tumors in all strains with no marked difference as observed in this study. It is noteworthy that the pattern of TGFα expression of tumor cells is like to that of the lactating cells. This would support the continued proliferation of mammary cells even during lactation in high mammary tumor strains of mice (Nagasawa, unpublished).

No TGFα gene expression in uteri of old mice of four strains, most of which had adenomyosis, is in good accord with the results obtained in young CD-1 mice [27]. However, in that study, estrogen enhanced the TGFα expression. Therefore, some hormone treatment accelerating adenomyosis would modify TGFα expression in these old mice. In any case, all findings in this study indicate that TGFα expression itself is not always directly related to the potentials for normal and neoplastic mammary gland growth and uterine adenomyosis in mice.

The expression of TGFα mRNA in lactating mammary glands in SHN, GR/A and C3H/He strains observed in this study is not agreeable with the results reported by Snedeker et al. [29]. TGFα expression in their study was observed in mammary glands during virginal and pregnant stages, but not in lactation in BALB/c and CD-1 mice. Meanwhile, TGFα mRNA was detected in the lactating mammary glands of rats [11]. These reports suggest the possibility of the species- and/or strain-related difference in mammary TGFα gene expression during the reproductive states, which was hypothesized by Snedeker et al. [29].

Not only PCR products of normal predicted size, but also the products with various sizes found in mammary tumors [8] were observed in the lactating glands of SHN and C3H/He and normal and neoplastic mammary glands of retired animals of all strains except GR/A. In GR/A strain, TGFα gene expression was detected, but only the single band was observed in all neoplastic glands of retired and the PDMT of pregnant animals. Although it is unknown the meaning of the various sizes of PCR products [8], these would suggest that mammary glands possess sooner or later neoplastic characteristics during or after the reproductive states, while it does not always correlate with mammary tumorigenic potentials.

ACKNOWLEDGMENTS

This work was supported in part by the Grant-in-Aid from the Ministry of Education, Science and Culture, Japan, and a Grant for Special Project from Institute of Science and Technology, Meiji University.

REFERENCES

1 Aidells BD, Daniel CW (1976) Hormone-dependent mammary tumors in strain GR/A mice. III. Effectiveness of supplementary hormone treatments in inducing tumorous phase growth. J Natl Cancer Inst 57: 527–537

2 Alonso S, Minty A, Bourlet Y, Buckingham M (1986) Comparison of three actin-coding sequences in the mouse; Evolutionary relationships between the actin genes of warm-blooded vertebrates. J Mol Evol 23: 11–22

3 Burton K (1956) A study of the conditions and mechanism of the diphenylamine reaction for the colorimetric estimation of deoxyribonucleic acid. Biochem J 62: 315–325

4 Chomczynski P, Sacchi N (1987) Single-step method of RNA isolation by acid guanidium thiocyanate-phenol-chloroform extraction. Anal Biochem 162: 156–159

5 Coffey RJ, Derynck R, Wilcox JN, Bringman TS, Goustin AS, Moses HL, Pittelkow MR (1987) Production and auto-induction of transforming growth factor-α in human keratinocytes. Nature (London) 328: 817–820

6 Derynck R, Goeddel DV, Ullrich A, Guttermam JU, Williams RD, Bringman TS, Berger WH (1987) Synthesis of messenger RNAs for transforming growth factor α and β and the epidermal growth factor receptor by human tumors. Cancer Res 47: 707–712

7 Han VKM, Hunter III ES, Prati RM, Zendegui JG, Lee DC (1987) Expression of rat transforming growth factor alpha mRNA during development occurs predominantly in the maternal decidua. Mol Cell Biol 7: 2335

8 Harigaya T, Tsunoda S, Mizuno M, Nagasawa H (1994) Different gene expression of mouse transforming growth factor α between pregnant mammary glands and mammary tumors in C3H/He mice. Zool Sci 11: 625–627

9 Harigaya T, Yokoyama H, Tsunoda S, Nagasawa H (1994) Immunohistochemical localization of transforming growth factor α in mouse mammary glands and mammary tumors. Acta Histochem Cytochem 27: 279–282

10 Hawburger AW, Pinnarmanei G (1993) Interferon-induced enhancement of transforming growth factor-α expression in a human breast cancer cell lines. Proc Soc Exp Biol Med 202: 64–68

11 Liscia DS, Merlo G, Ciardiello F, Kim N, Smith GH, Callahan R, Salomon DS (1990) Transforming growth factor-α messenger RNA localization in the developing adult rat and human mammary gland by in situ hybridization. Dev Biol 140: 123–131

12 Liu SC, Sanfilipo B, Pewoteau I, Derynick R, Salamon DS, Kidwall WR (1987) Expression of transforming growth factor α

(TGFα) in differentiated rat mammary tumors; Estrogen induction of TGFα production. Mol Endocrinol 1: 683–692

13 Medjbaum W (1939) Uber die Bestimmung Kleiner Pentosemengen, Insbesondere in Derivaten der Adenylsaure. Z Physiol Chem 258: 117–120

14 Mori T, Nagasawa H (1989) Multiple endocrine syndrome in SHN mice: Mammary tumors and uterine adenomyosis. In Progressive Stages of Neoplastic Growth Vol 5, Ed by HE Kaiser, Kluwer Acad Publ, Dordreckt, pp 121–130

15 Mühlbock O (1965) Note on a new inbred mouse-strain GR/A. Eur J Cancer 1: 123–124

16 Mydlo JH, Micaeli J, Cordo CC, Goldenbreg AS, Heston WDW, Fair WR (1989) Expression of transforming growth factor α and epidermal growth factor receptor RNA in neoplastic and non-neoplastic human kidney tissue. Cancer Res 49: 3407–3411

17 Nagasawa H, Amano K, Araki M (1992) Relationship between pup growth, mother weight, food or water intake in four strains of mice. In Vivo 6: 69–72

18 Nagasawa H, Forukosi K (1985) Effects of concurrent pregnancy and lactation on reproduction in four strains of mice. Lab Anim Sci 35: 142–145

19 Nagasawa H, Furuichi R, Sakamoto S, Yamamoto K. (1993) The similar mammary tumor potentials in virgins and breeders of SHN mice. Exp Anim 42: 631–634

20 Nagasawa H, Konishi R (1987) Precancerous mammary hyperplastic alveolar nodules in four strains of virgin mice with different mammary tumor potentials: influence of chronic caffeine ingestion. Eur J Cancer Clin Oncol 23: 1019–1023

21 Nagasawa H, Konishi R, Naito T, Ohmiya S, Mori T (1987) Relationship between mammary tumorigenesis and uterine adenomyosis in four strains of mice. In Vivo 1: 237–240

22 Nagasawa H, Koshimizu U (1989) Difference in reproductivity and offspring growth between litter numbers in four strains of mice. Lab Anim (UK) 23: 357–360

23 Nagasawa H, Naito T, Namiki H (1987) Mammary gland growth and serum levels of prolactin and growth hormone in four strains of male mice comparison with females. Life Sic 40: 1473–1478

24 Nagasawa H, Naito T, Mori T (1988) Difference in response to mammotropic hormones of mammary growth and uterine adenomyosis among four strains of mice. In Vivo 2: 171–176

25 Nagasawa H, Yamasaki H, Namiki H (1987) Effects of 2-(hydroxyphenyl) indole on mammary gland growth and uterine adenomyosis in four strains of mice. In Vivo 1: 141–146

26 Nagasawa H, Yanai R, Nakajima Y, Namiki H, Kikuyama S, Shiota K (1980) Inhibitory effects of potassium thiocyanate on normal and neoplastic mammary development in female mice. Eur J Cancer 16: 473–480

27 Nelson GK, Takahashi T, Lee DC, Luetteke NC, Bossert NL, Ross K, Eitzman BE, McLachlan JA (1992) Transforming growth factor-α is a potential mediator of estrogen action in the mouse uterus. Endocrinology 131: 1657–1664

28 Schneider WC (1945) Phosphorus compounds in animal tissue. J Biol Chem 161: 293–303

29 Snedeker SM, Brown CF, DiAugustine RP (1991) Expression and functional properties of transforming growth factor-α and epidermal growth factor during mouse mammary gland ductal morphogenesis. Proc Natl Acad Sci USA 88: 276–280

30 Vaughan TJ, Pascall JC, Brown KD (1992) Nucleotide sequence and tissue distribution of mouse transforming growth factor-α. Biochim Biophys Acta 1132: 322–324

31 Yamamoto K, Kikuyama S (1982) Radioimmunoassay of prolactin in plasma of bullfrog and tadpoles. Endocrinol Jap 29: 159–167

32 Zajichowski D, Band V, Pauzine N, Tager A, Stampfer M, Sarger R (1988) Expression of growth factors and oncogenes in normal and tumor-derived human mammary epithelial cells. Cancer Res 48: 7041–7047

ZOOLOGICAL SCIENCE 11: 847–853 (1994)

Androgen-induced Differentiation of the Fibrocartilage of Os Penis Cultured *in vitro*

RYUTARO MURAKAMI*, KAZUSHIGE MIYAKE and IKUO YAMAOKA

Department of Biology, Faculty of Science, Yamaguchi University, Yamaguchi 753, Japan

ABSTRACT—Primordia of the fibrocartilage of os penis of the rat were cultured in vitro in the presence of testosterone, and the effects of testosterone on the expression of type I collagen, type II collagen, vimentin, the activity of alkaline phosphatase (ALP), and Alcian blue-stainable extracellular matrix (ECM) were examined histochemically. Explants cultured in the presence of testosterone formed fibrocartilage while control explants cultured without testosterone formed fibroblastic tissue. Type II collagen, ALP, and Alcian blue stainable ECM were detected only in the explants that had been cultured with testosterone. Calcification of the fibrocartilage was observed in explants that had been cultured for 21 days. By contrast, levels of type I collagen and vimentin increased in explants cultured with or without testosterone. These results demonstrate that testosterone induces terminal differentiation of the fibrocartilage while some histological markers of fibrocartilage can be expressed in the absence of testosterone.

INTRODUCTION

The penis of rodents includes a skeletal structure that is called os penis (baculum). In the rat, os penis is composed of a proximal and a distal segment. The proximal segment of os penis is a Haversian bone with hyaline growth cartilage at its proximal end. The distal segment of os penis is fibrocartilage that gradually becomes ossified after puberty [1–7]. While normal female rats do not have skeletal tissues in the clitoris, bones and cartilages homologous to the os penis can be induced in the clitoris by neonatal treatment with androgen [8–10]. Fetal genital tubercles, in which primordia of the os penis are recognizable in both sexes, can form os penis when transplanted beneath the renal capsule of adult male rats or castrated males that have been treated with androgens [11]. In a previous study, we showed that genital tubercles cultured in vitro can form skeletal elements in the presence of androgens [12]. In addition, the cells of the primordia of os penis acquire androgen-binding capacity during the fetal period [13]. These results indicate that the development of os penis depends on androgens, and that the primordia of os penis are direct targets of androgens. Since the cells that form the skeletal tissues of os penis have distinct cytological characteristics, os penis provides a useful system for studies of cell differentiation caused by androgens. Among the skeletal elements of os penis, the fibrocartilage of the distal segment is a relatively large and non-complex tissue that is composed of chondrocytes and extracellular matrix (ECM). In previous studies, we demonstrated that the ECM of the fibrocartilage of the distal segment contains type I and type II collagens as major components [14], and that the chondrocytes of the fibrocartilage also express strong alkaline phosphatase (ALP) activity, which has been shown to appear in other calcifying tissues, prior to the calcification that occurs after puberty [10]. We also found that the cytoplasm of the chondrocytes is rich in intermediate filaments that react with vimentin-specific antibodies (unpublished data). These histological characteristics provide good markers of the phenotypic differentiation of this fibrocartilage. In order to analyze the role of androgens in the differentiation of the fibrocartilage, primodia of the fibrocartilage were cultured in vitro in the presence and in the absence of testosterone, and the phenotypic expression of various markers was examined.

Accepted November 14, 1994
Received August 1, 1994

MATERIALS AND METHODS

Culture in vitro of the primordium of the distal segment of os penis

Rats of the Wistar Imamichi strain (Imamichi Institute for Animal Reproduction, Oomiya, Japan) were used. The animals were mated during the night and copulation was confirmed the next morning by the presence of spermatozoa in the vaginal smear. The conceptus was designated as being 0.5 days old at noon of this day. Pregnant rats were killed by cervical dislocation and genital tubercles were excised from male and female fetuses. At this stage, a primordium of the distal segment of os penis can be recognized as a mass of mesenchymal cells under a dissection microscope. The genital tubercles were treated with 1 mM EDTA in Tyrode's solution for 15 minutes, and the primordium of the distal segment was isolated with microscissors. The primordia were cultured in vitro essentially as described in a previous report [12]. The isolated explants were laid on a Millipore filter (pore size, 1.2 μm), placed on a stainless-steel grid in a glass dish, and cultured in DMEM supplemented with 20% fetal bovine serum (FBS), 0.2 mM ascorbic acid phosphate, 20 mM β-glycerophosphate, and 10 ng/ml testosterone. In control experiments, no testosterone was added to the medium or cyproterone acetate, an anti-androgen [15], was added at 1 ng/ml to the culture medium to avoid any possible effects of androgens that might be present in FBS. Serum-free medium (ASF301; Ajinomoto, Tokyo, Japan) was also used to avoid potential androgenic effects of the serum. The explants were cultured at 37°C for 7, 10, 12, 14, or 21 days. The culture medium was replaced every three days. The cultured explants were fixed with 95% ethanol for one hour at 4°C, embedded in paraffin (m.p. 46–48°C), sectioned at 4–6 μm and

processed for immunofluorescence or enzyme histochemistry. Some sections were stained with Alcian blue-hematoxylin-eosin for detection of the Alcian blue-stainable ECM that is characteristic of cartilage. To examine calcification of the fibrocartilage, some sections were stained with alizarin red S. Some samples were processed for transmission electron microscopy (TEM) for an examination of calcification.

Immunohistochemical staining specific for type I and type II collagens and vimentin

The paraffin sections were deparaffinized with xylene, rehydrated through a graded ethanol series, washed with PBS and then with water. In order to remove glycosaminoglycans, which might inhibit the binding of antibodies to extracellular collagen fibers, sections were treated with a 0.5% solution of testicular hyaluronidase (Type IS, Sigma, St Louis, MO) in 0.2 M acetate buffer (pH 4.8) for 40 minutes at 37°C. After washing with PBS, adjacent serial sections were incubated either in rabbit antiserum against calf type I collagen (Advance, Tokyo, Japan; diluted 1:40) in PBS, or in rabbit antiserum against calf type II collagen (Advance; diluted 1:150) for one hour at 37°C, then they were washed with PBS and incubated with FITC-conjugated goat antibodies against rabbit IgG (Miles Laboratories, Naperville, IL; diluted 1:64) for one hour at 37°C. Sections were examined with an epifluorescence microscope. For vimentin-specific immunofluorescence, rehydrated sections were incubated in goat antiserun against human vimentin (Sigma; diluted 1:20) for one hour at 37°C, washed in PBS and incubated in FITC-conjugated rabbit antibodies against goat IgG (Sigma; diluted 1:64) for one hour at 37°C.

Histochemical detection of alkaline phosphatase (ALP) activity

The cultured explants were fixed, embedded, sectioned, and deparaffinized as described above. Rehydrated sections were stained for ALP activity by the azo dye method. Naphtol AS-BI phosphate in 0.1 M Tris buffer (pH 9.0) was used as a substrate and Fast red violet L.B. salt was used as the coupling agent. The reaction was allowed to proceed at 37°C for ten minutes.

RESULTS

The numbers of explants examined after each culture period are summarized in Table 1. Since the development of explants taken from male and female fetuses was identical, the following descriptions do not include the sex of the fetuses from which genital tubercles had been removed.

TABLE 1. Number of explants examined after each period in culture

Medium	Culture period (days)				
	0[1]	7	10	14	21
(+Testosterone)					
DMEM		8	9	27	6
ASF		1	1	4	2
	9				
(Control)					
DMEM		6	6	16	4
DMEM+CA[2]		3			2
ASF		2	1	9	2

1. 20.5-day-old fetuses
2. Cyproterone acetate

Development of fibrocartilage in explants during culture in vitro with testosterone

The primordium of the distal segment of os penis was recognized as a mesenchymal condensation in the genital tubercle of the fetus on day 20.5 of gestation (Fig. 1). At this stage, the cells appeared undifferentiated, with scant extracellular matrix (ECM) around them (Fig. 2). Cells in explants that had been cultured for 7 days with testosterone were larger, and fibrous ECM became apparent (Fig. 3). By day 10, the ECM had increased in volume, and differentiated chondrocytes were visible that were associated with ECM that was stained by Alcian blue (Fig. 4). By day 14, a large number of the cells in the explants had differentiated into mature chondrocytes with a hypertrophic appearance, and the ECM around the chondrocytes was heavily stained with Alcian blue (Fig. 5). In controls cultured without testosterone (DMEM+FBS, DMEM+FBS+cyproterone acetate, or ASF), the cells became enlarged and fibrous ECM also increased in volume during culture. However, the explants remained much smaller than those cultured with testosterone. Cells in the control explants did not differentiate into chondrocytes even after 2 or 3 weeks in culture but formed fibroblastic tissue (Fig. 6). Explants cultured with cyproterone acetate also formed fibroblastic tissue, but explants were very small after 2 weeks of culture. The time courses of development of the explants were consistent among explants after each respective period in culture, and details are summarized in Table 2.

TABLE 2. Developmental events in explants

Developmental events	Culture period (days)				
	0[1]	7	10	14	21
Fibrous ECM					
+Testosterone	+	+	++	++	++
Control	+	+	+	+	+
Alician blue-stainable ECM					
+Testosterone	−	−	+	++	++
Control	−	−	−	−	−
Chondrocytes					
+Testosterone	−	−	+	++	++
Control	−	−	−	−	−

1. 20.5-day-old fetuses

Expression of type I and type II collagens in explants cultured with testosterone

In the primordium of the distal segment of os penis after 20.5 days of gestation, the fine fibrous extracellular matrix was weakly immunostained with antiserum specific for type I collagen (Fig. 7). Type II collagen was not detected at this stage. After 7 days in culture, the fibrous extracellular matrix of the explants was strongly positive for type I collagen

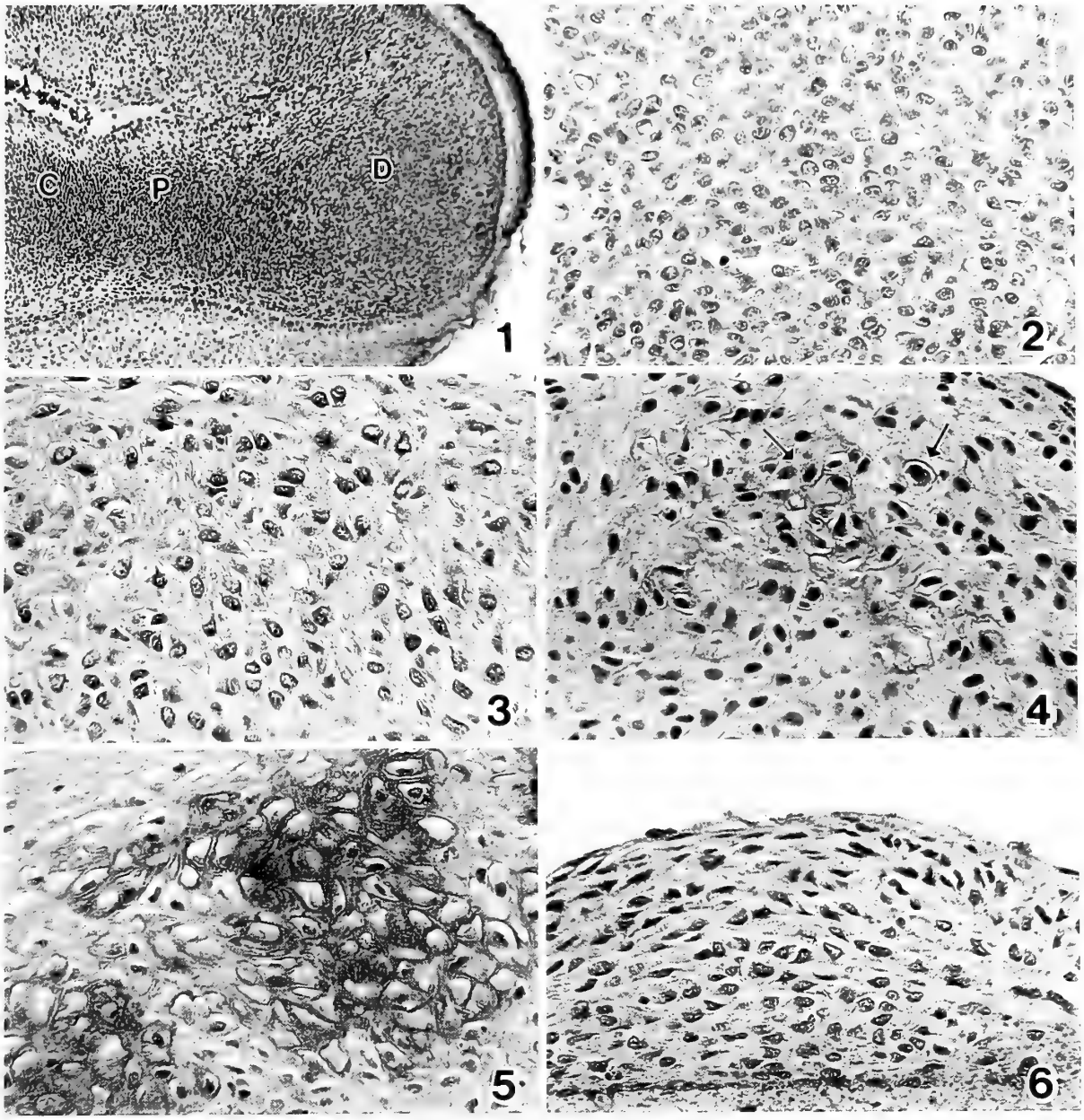

FIG. 1–6. Development of fibrocartilage in explants. Histological sections were stained with Alcian blue-hematoxylin-eosin.

FIG. 1. Longitudinal section of the male genital tubercle of a 20.5-day-old fetus. Primordia of the corpus cavernosum penis (C), proximal segment of os penis (P), and distal segment of os penis are recognizable. 130×.

FIG. 2. Section of the primordium of the fibrocartilage of a 20.5-day-old fetus. Cells are undifferentiated at this stage. 500×.

FIG. 3. Section of an explant after 7 days in culture with testosterone. Cells are large and fibrous ECM is visible. 500×.

FIG. 4. Section of an explant after 10 days in culture with testosterone. Chondrocytes are recognizable (arrows). The ECM around chondrocytes can be stained with Alcian blue. 500×.

FIG. 5. Section of an explant after 14 days in culture with testosterone. A large number of the cells are now mature chondrocytes with a hypertrophic appearance. The ECM around chondrocytes is heavily stained with Alcian blue. 500×.

FIG. 6. Section of a control explant after 14 days in culture. Cells have formed fibroblastic tissue with fibrous ECM. The explant was much smaller than explants that had been similarly cultured with testosterone. 500×.

(Fig. 8). Type II collagen was not detected. On day 10, type I collagen was detected in the ECM throughout the explant, but the fluorescence was diffuse, especially in the inner region of the explant (Fig. 9a). At this stage, chondrocytes appeared in the explants, and type II collagen was detected for the first time in the ECM around clusters of chondrocytes (Fig. 9b). On day 14, a large fraction of the cells in the explants was found to have differentiated into

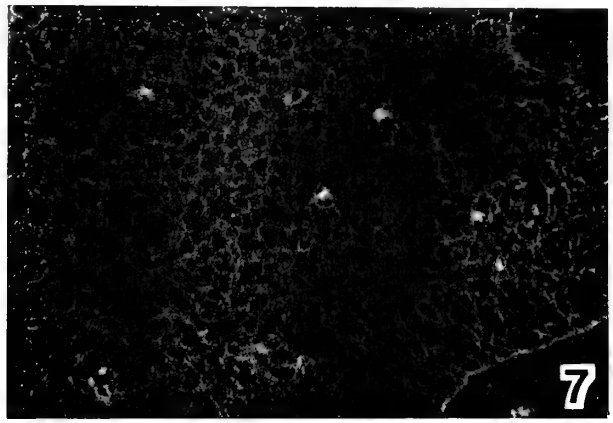

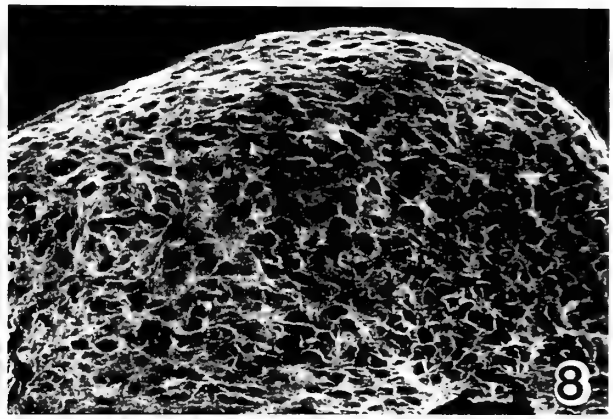

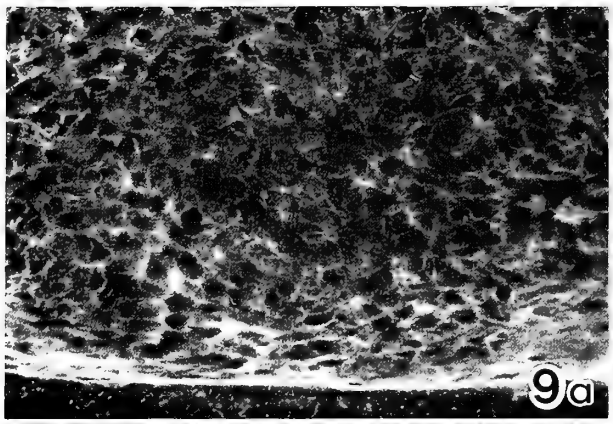

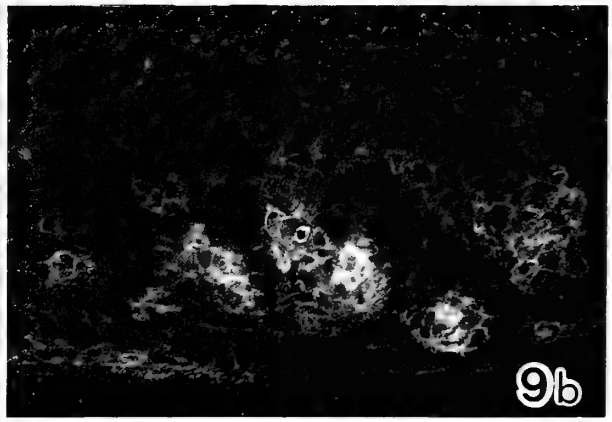

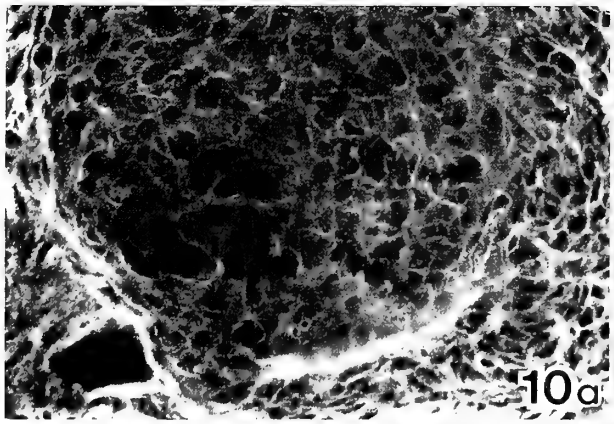

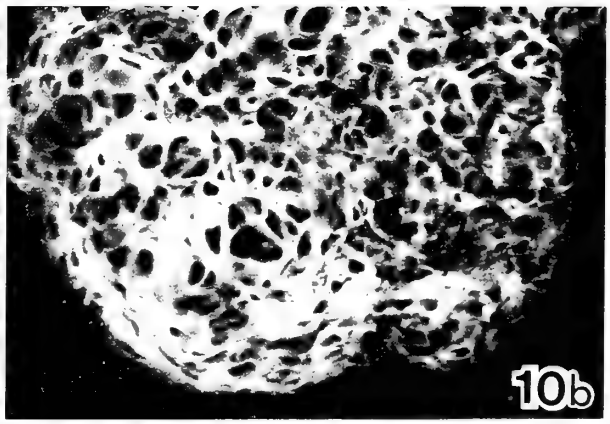

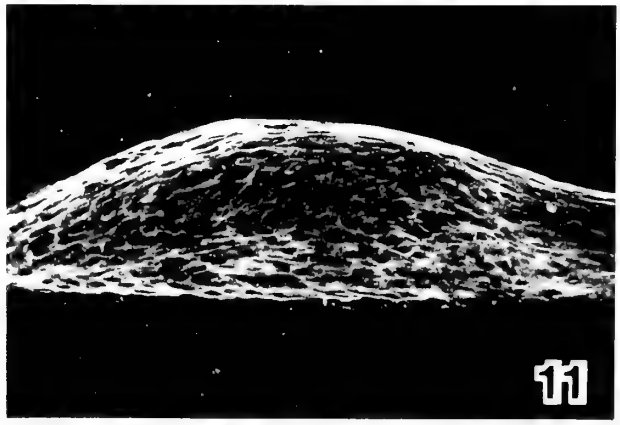

FIG. 7–11. Immunofluorescent staining for type I and type II collagens in explants. 250×.

FIG. 7. Immunofluorescence specific for type I collagen in the primordium of the fibrocartilage from a 20.5-day-old fetus. The fine fibrous ECM is weakly positive. 250×.

FIG. 8. Immunofluorescence specific for type I collagen in an explant after 7 days in culture with testosterone. Fibrous ECM is strongly

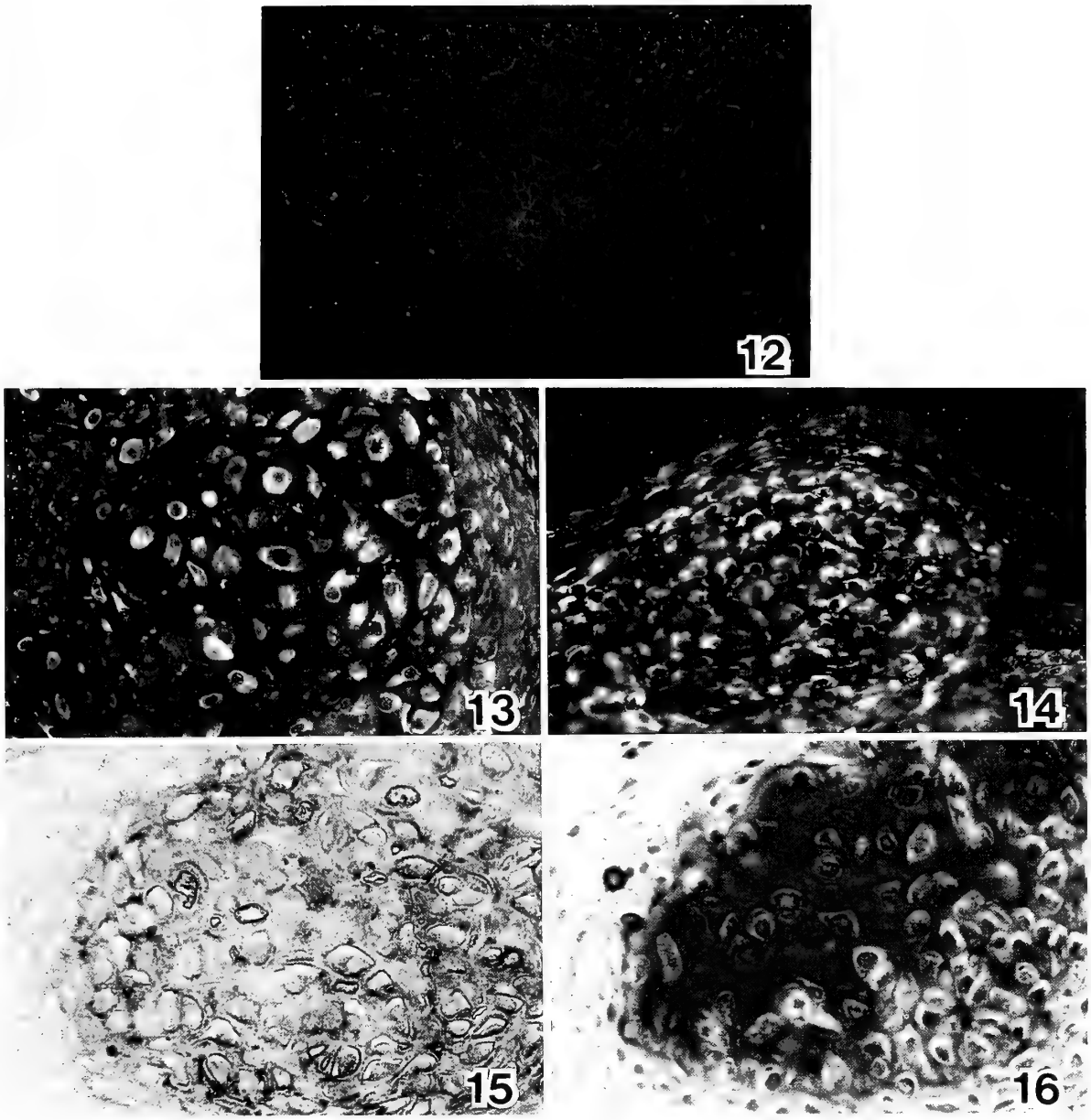

FIG. 12. Immunofluorescence specific for vimentin in the primordium of the fibrocartilage in a 20.5-day-old fetus. The cytoplasm of the cells is weakly immunopositive. 250×.

FIG. 13. Immunofluorescence specific for vimentin in an explant after 14 days in culture with testosterone. The cytoplasm of chondrocytes is strongly positive. 250×.

FIG. 14. Immunofluorescence specific for vimentin in a control explant after 14 days in culture. The cytoplasm of cells is strongly positive. 250×.

FIG. 15. Histochemical detection of ALP activity in an explant after 21 days in culture with testosterone. Chondrocytes are positive for ALP. 250×.

FIG. 16. Staining with alizarin red S for detection of calcification in a section adjacent to that in Fig. 15. The fibrocartilage is heavily calcified. 250×.

---

positive. 250×.

FIG. 9a. Immunofluorescence specific for type I collagen in an explant after 10 days in culture with testosterone. Fluorescence from the inner region of the explant is diffuse. 250×.

FIG. 9b. Immunofluorescence specific for type II collagen in a section adjacent to that in Fig. 9a. Small clusters of chondrocytes are positive for immunostaining. 250×.

FIG. 10a. Immunofluorescence specific for type I collagen in an explant after 14 days in culture with testosterone. Immunoreactivity in the inner region of the explant, in which a mass of fibrocartilage has formed, is weaker than in the outer region. 250×.

FIG. 10b. Immunofluorescence specific for type II collagen in a section adjacent to that in Fig. 10a. The ECM of the fibrocartilage is strongly immunostained. 250×.

FIG. 11. Immunofluorescence specific for type I collagen in a control explant after 14 days in culture. The fibrous ECM is strongly positive. 250×.

chondrocytes. The ECM of the explants was positive for type I collagen. However, the immunoreactivity in the inner region of the explants, where most of the cells had become mature chondrocytes with a hypertrophic appearance, was weaker than had been previously observed (Fig. 10a). Staining for type II collagen was intense in the ECM around the mature chondrocytes (Fig. 10b). In the controls that had been cultured without testosterone, fibrous materials in the ECM of the explants were heavily stained for type I collagen after 7 days of culture (Fig. 11), while type II collagen was not detected at any stage. The expression of type I collagen was also detected in explants that had been cultured in serum-free medium (ASF301) or in medium that contained cyproterone acetate.

These results were consistent among explants after each respective period in culture, and details are summarized in Table 3.

Expression of vimentin in explants

Cells in the primordium of the distal segment of a fetus after 20.5 days of gestation were weakly stained with vimentin-specific antibodies (Fig. 12). On day 14 of culture, all the cells in explants cutured with or without testosterone were heavily stained for vimentin (Figs. 13 and 14, Table 3).

ALP activity and calcification

ALP activity first became detectable after 10 days in culture in clusters of chondrocytes in the explants that had been cultured with testosterone. On days 14 and 21, strong ALP activity was detected in the fibrocartilage (Fig. 15). Calcification of the fibrocartilage was observed after 3 weeks in culture (Fig. 16). In controls, neither ALP activity nor calcification was detected (Table 3).

TABLE 3. Immunohistochemical and histochemical detection of features of differentiation of the fibrocartilage

Feature	Culture period (days)				
	0[1]	7	10	14	21
Type I collagen					
+testosterone	+ (2)	++ (4)	++ (4)	++ (8)	++ (2)
control	+ (2)	++ (4)	++ (2)	++ (6)	++ (1)
Type II collagen					
+testosterone	− (2)	− (4)	+ (4)	++ (8)	++ (2)
control	− (2)	− (4)	− (2)	− (6)	− (1)
Vimentin					
+testosterone	+ (2)			++ (4)	
control	+ (2)			++ (3)	
ALP					
+testosterone		− (1)	+ (2)	++ (2)	++ (2)
control				− (2)	− (1)
Calcification					
+testosterone		− (3)	− (5)	− (7)[2]	+ (4)
control		− (2)	− (2)	− (4)	− (3)

( ): Numbers of explants examined
1. 20.5-day-old fetuses
2. Small electron-dense particles were observed

DISCUSSION

Sexual dimorphism in mammalian external genitalia is determined, for the most part, by the hormonal secretions of the testis: androgens induce the development of the male phenotype, and the absence of gonads results in the female phenotype [16]. Mesenchymal cells have been shown to be essential for the development of sexual dimorphism in accessory sex organs, and they have been shown to be primary targets of androgens in developing prostatic glands [17, 18], mammary glands [19], the prepuce, and the penis [13]. However, responses of the mesenchymal cells to androgens and subsequent processes of cell differentiation have not previously been investigated in detail because most of the mesenchymal cells do not have distinctive histological characteristics that can be used as markers of cell differentiation. The stimulatory effects of androgens on the proliferation of cells in epiphyseal cartilage have been reported [20], but effects on undifferentiated precursor cells of cartilage have not been studied. Os penis of the rat provides a useful system with which cellular responses to androgens can easily be investigated because it has distinct histological and cytological markers and its development has been characterized in detail [10–14]. In the present study, it was found that explants of the primordium of the distal segment of os penis, when cultured in vitro, formed fully mature fibrocartilage in the presence of testosterone. Calcification of the fibrocartilage was also observed. Results obtained in the present study clearly demonstrate the essential role of the androgen in the differentiation of the fibrocartilage in the penis. The explants expressed histological markers characteristic of the fibrocartilage of os penis, namely, type I and type II collagens, Alcian blue-stainable ECM, vimentin, and ALP. Control explants cultured without testosterone formed fibroblastic tissue with fibrous ECM that contained type I collagen, and the cells in the control explants expressed vimentin, even though the latter explants were smaller than those cultured with testosterone. No type II collagen or ALP activity was detected in controls. These results demonstrate that the expression of type I collagen and vimentin does not depend on testosterone, while the expression of type II collagen, Alcian blue-stainable ECM, and ALP depends on exposure to testosterone (Table 4). Since the reactivity specific for type I collagen became weaker in the regions in which mature chondrocytes appeared, it is possible that the synthesis of type I collagen is suppressed in mature chondrocytes.

TABLE 4. Dependence on testosterone of the development of various features of the differentiation of the fibrocartilage

Feature	+Testosterone	Control
Type I collagen	+	+
Type II collagen	+	−
Vimentin	+	+
ALP	+	−
Calcification	+	−

In our experiments, the responses to testosterone differed among the various markers, suggesting that the effect of testosterone is a qualitative one, namely, the induction of the terminal differentiation of the fibrocartilage, rather than a general anabolic effect. The cytological markers analyzed here all represent the end products of the translation of genes. Hence, the results obtained do not necessarily reflect the direct activation of specific genes by testosterone. If we are to clarify the molecular actions of testosterone that lead to the differentiation of the fibrocartilage of os penis, it is important that we determine whether testosterone (or its metabolite, dihydrotestosterone) directly activates transcription of the genes for type II collagen and ALP. The system for culture in vitro of the fibrocartilage of os penis described herein should be useful for studies of the differentiation of cells that is caused by androgens.

REFERENCES

1 Beresford WA, Burkart S (1977) The penile bone and anterior process of the rat in scanning electron microscopy. J Anat 124: 589–597

2 Beresford WA, Clayton SP (1977) Intracerebral transplantation of the genital tubercle in the rat: the fate of the penile bone and cartilages. J Anat 123: 297–311

3 Yoshida H, Kadota, A, Fukunishi, R (1980) Effects of testosterone propionate on neonatal and prepubertal development of os penis in male rats. Exp Anim 29: 39–43

4 Vilmann H (1982) Os penis of the rat. III. Formation and growth of the bone. Acta Morphol Neerl-Scand 20: 309–318

5 Rasmussen KK, Vilmann H, Juhl M (1986) Os penis of the rat. V. The distal cartilage process. Acta Anat 125: 208–212

6 Yamamoto M (1987) Histology of the os penis of rat. I. Light microscopic structure of the distal segment and possible origin of its osteocytes. Teikyo Med J 10: 303–313

7 Williams-Ashman, HG (1990) Epigmatic features of penile development and functions. Perspectives Biol Med 33: 335–374

8 Glucksmann A, Cherry CP (1972) The hormonal induction of an os clitoridis in the neonatal and adult rat. J Anat 112: 223–231

9 Yoshida H, Huggins CB (1980) Induction of ossification in the clitoris of neonatal female rats by administration of androgens. Endocrinology 106: 1956–1959

10 Murakami R, Mizuno T (1984) Histogenesis of the os penis and os clitoridis in rats. Dev Growth Differ 26:419–426

11 Murakami R (1986) Development of the os penis in genital tubercles cultured beneath the renal capsule of adult rats. J Anat 149:11–20

12 Murakami R, Mizuno T (1984) Culture organotypique du tubercule génital de foetus de Rat: induction de l'os pénien par testostérone. C R Soc Biol 178: 576–579

13 Murakami R (1987) Autoradiographic studies of the localisation of androgen-binding cells in the genital tubercles of fetal rats. J Anat 151: 209–219

14 Murakami R (1987) Immunohistochemical and immunoblot analyses of collagens in the developing fibrocartilage in the glans penis of the rat. Acta Morphol Neerl-Scand 25: 279–282

15 Neumann F, Elger W, Kramer M (1966) Development of vagina in male rats by inhibiting androgen receptors with an anti-androgen during the critical phase of organogenesis. Endocrinology 78: 628–632

16 Jost A (1965) Gonadal hormones in the sex differentiation of the mammalian fetus. In "Organogenesis" Ed by RL De Haan and H Ursprung, Holt, Reinehart & Winston, New York, pp 611–628

17 Lasnitzki I, Mizuno T (1980) Prostatic induction: interaction of epithelium and mesenchyme from normal wild-type mice and androgen-insensitive mice with testicular feminization. J Endocrinol 85: 423–428

18 Takeda H, Mizuno T, Lasnitzki I (1985) Autoradiographic studies of androgen-binding sites in the rat urogenital sinus and postnatal prostate. J Endocrinol 104: 87–92

19 Kratochwil K, Schwarz P (1976) Tissue interaction in androgen response of embryonic mammary rudiment of mouse: identification of target tissue for testosterone. Proc Natl Acad Sci USA 73: 4041–4044

20 Sömjen D, Mor Z, Kaye AM (1994) Age dependence and modulation by gonadectomy of the sex-specific response of rat diaphyseal bone to gonadal steroids. Endocrinology 134: 809–814

ZOOLOGICAL SCIENCE 11: 855–857 (1994)

Adult Diapause Induced by the Loss of Water Surface in the Water Strider, *Aquarius paludum* (Fabricius)

TETSUO HARADA*

Department of Biology, Faculty of Science, Osaka City University, Osaka 558, Japan

ABSTRACT—Adults of *Aquarius paludum* collected in autumn were reared on a water surface or, alternatively, on a wet-paper surface under 10L-14D at 20±2°C. After the photoperiod was changed to 15.5L-8.5D terminating reproductive diapause, the percent of individuals adopting diapause posture decreased from more than 50% to 20% on the water surface, while more than 50% of the individuals on the wet paper continued to show diapause posture for 35 days. Moreover the adults placed on the wet paper surface were less fecund than those on the water surface.

INTRODUCTION

Water striders of the genera *Aquarius, Limnoporus*, and *Gerris* are predatory bugs living on the surface of the bodies of fresh water [18]. In general, they survive winter as adults at overwintering sites on land, appear and reproduce on the water surface in spring and summer [18]. Loss of water surface by desiccation in spring and summer means loss of habitat for water striders and that situation seems to make them choose for flying to other water surfaces or for entering diapause behaviorally and reproductively at the site without water surface until water returns. Wilcox and Maier [20] reported that adults of a water strider, *Aquarius remigis* estivated facultatively with diapause posture during summer in damp area underneath stream bed-rocks when a pool in a small stream became dry. Estivation is common among insects and can be induced by relatively predictable factors of environment, such as photoperiod and temperature, or by unpredictable factors, such as wet or dry condition [1, 2, 13, 19]. Wilcox and Maier [20] showed the evidence for behavioral association with a damp-microhabitat, but not for specific cues that instigated the striders' diapause behavior in *Aquarius remigis*. In the case of water striders, the loss of water surface may be an important cue to induce estivation including diapause behavior and reproductive diapause. However, this point has not been studied so far.

Overwintered (long-winged) adults of *Aquarius paludum* kept under outdoor conditions laid eggs shortly after they were moved from fallen leaves to the water surface at the beginning of March, although the transfer to water surfaces was earlier than in nature [8]. This earlier reproduction suggests that the water surface is a cue that induces the maturation of the reproductive system. Conversely, the lack of water surface in reproductive season might be a causal factor of reproductive suppression or diapause.

Accepted October 17, 1994
Received August 2, 1994

* Present address: Biological Laboratory, Faculty of Education, Kochi University, Kochi 780, Japan

The present work aims at examining the effects of loss of water surface on diapause posture by adults and reproduction.

MATERIALS AND METHODS

Fifth instar nymphs destined to overwinter as adults were collected from a pond in Sakurai (34°31'N, 135°22'E), Nara Prefecture, Japan in the middle of October, 1992, and allowed to complete development under outdoor conditions. Males and females with the same wing form were paired just after emergence and held in individual plastic pots. Adults grown under short-days enter diapause, and the diapause is kept under short-days and terminated by long-days [7, 10]. Pairs were kept on water under a short-day (10L-14D) at 20±2°C for 20 days to remain diapause.

After that, some of them were moved onto wet paper. The rest was maintained on the water surface. Five days later, the photoperiod was changed to 15.5L-8.5D terminating reproductive diapause. Adults were checked every 1–2 days at 13:00 to see if they had adopted a diapause-posture (positioning of all six legs along the body to resemble a stick). In this study, the preoviposition period, which was defined as the days after the change to the long-day, and the number of eggs were examined evey 1–2 days.

The plastick pots, 14 cm in diameter and 5 cm in depth, were used for the rearing of adults and filled with water to a depth of 5–10 mm or with wet-paper on the bottom, and each pot was provided with a wooden stick, about 1 cm in diameter and 12 cm long, for oviposition or resting site. Water striders could walk on the wet paper and the stick was kept wet. Therefore the main difference between the two conditions was that in mechanical stimulus on the tarsa of the legs. The water and wet paper were exchanged every day and the striders were fed on flies *Fannia canicularis* L. every day at the rate of one per one pair.

RESULTS AND DISCUSSION

On the water surface, females began to lay eggs at 14–16 days after the change to the long-day photoperiod (Table 1). On the other hand, some of the females on the wet paper began to lay eggs as much as 10 days later, though the rest began to do so at the same time as those on the water surface. The number of eggs per female on the wet paper was similar

TABLE 1. Influence of shortage of water surface on the oviposition process

Preoviposition period (days)*	On wet paper	On water surface
	19.6±8.1 (7)	15.7±1.9 (6)
Number of eggs**		
0–5 days	29.3±14.7 (7)	40.0±13.0 (6)
5–10	48.6±26.9 (7)	52.0±22.2 (6)
10–15	36.3±21.8 (7)#	79.2±30.2 (6)
15–20	31.4±17.9 (7)#	55.2±18.2 (5)
20–25	23.0±22.8 (7)#	91.6±15.5 (5)
25–30	6.0±4.7 (4)#	67.8±23.5 (5)
Total fecundity***	180.4±105.8 (5)#	398.4±80.4 (5)

Values are mean±S.D. (n).
* Days after the change to the long-day photoperiod.
** Number every 5th day after the onset of oviposition.
*** Total number of eggs for 30 days after the onset of oviposition.
# $P<0.05$ on Mann-Whitney U-statistics for differences between the two conditions.

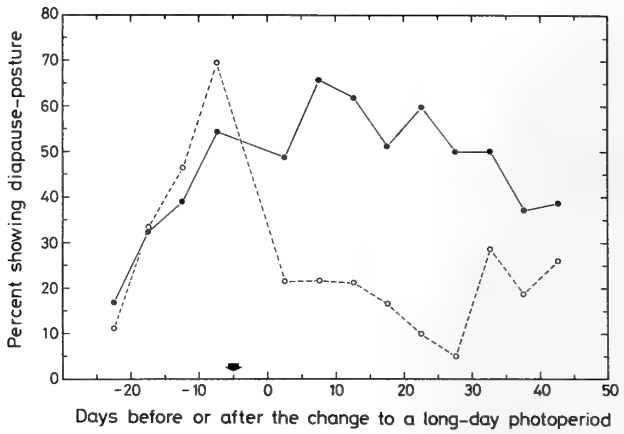

FIG. 1. Effect of a shortage of water surface on diapause-posture under 15.5L-8.5D at 20±2°C. Symbols are based on data obtained for 5 days. Open and solid circles are for the adults maintained on the water surface and wet paper, respectively. The day when adults were transferred onto the wet paper is shown with an arrow. n=28–96 for each 5 days in the wet-paper-group; n=16–72 in the water-surface-group.

to that on the water surface over the first 10 reproductive days (Table 1). After that, females on the water surface continued to lay 50–95 eggs per female and per 5 days over days 10–52 after which time they died (Table 1). However, on the wet paper, the number of eggs decreased (Table 1) and four of seven females finally stopped laying eggs 20–30 days after the onset of oviposition. The four females had no or only a few matured oocytes in their ovaries at the time they died, while the females on water surface had matured ones more than 20. In addition to seven females in Table 1, two females survived for 23 or 33 days after the change to the long-day without laying eggs and died on the wet paper.

Under the short-day photoperiod, the percent adopting diapause posture increased up to more than 50% on both the water surface and the wet paper (Fig. 1). On the water surface, the high number of individuals showing diapause posture decreased to 20% after the change to the long-day photoperiod. On the wet paper, however, diapause posture was mostly maintained for 35 days. The number was significantly higher on the wet paper than on the water surface through the 35th day after the change to the long-day photoperiod (χ^2-test: $P<0.05$). The number of females adopting diapause behavior was similar to that of males in both groups throughout the entire rearing period.

The loss of water surface induces the prolonged preoviposition period by some females and makes the adults take a diapause posture even under the photoperiod terminating adult diapause. These results suggest that the unpredictable loss of water surface is a factor delaying the termination of winter-diapause in spring. Moreover the dramatical decrease in fecundity and the following reproductive diapause which are caused by water loss imply the adopting of summer diapause in the case of dessication during reproductive season.

Polymorphism for dispersal ability or tendency is wide spread among insect species [3, 4, 11, 12]. Some studies on Gerridae and Gryllidae show that the proportion of winged adults, flight propensity or performance, development and maintainance of flight muscle, allocation of energy to triglycerides (flight fuel), ovarian development, and fecundity are genetically correlated and this series of correlatd traits can be called the migratory syndrome [5, 6, 14, 15, 16, 17]. *Aquarius remigis* of which the estivating adults were observed [20] show these traits with low dispersal tendency [6]. *A. paludum* also show relatively higher extent of wing reduction than other Japanese *Aquarius* and *Gerris* species excluding *G. amembo* [9, 10]. Therefore, when water in habitats goes dry, the adopting of diapause, which can be induced by the loss of water surface in *A. paludum*, is proposed to be also another negatively correlated trait for dispersal tendency.

ACKNOWLEDGMENTS

I would like to thank Professor Dr. John R. Spence, Department of Biological Sciences, University of Alberta, for invaluable and critical comments on this study.

REFERENCES

1 Beck SD (1980) Insect Photoperiodism. Academic Press, New York, 2nd ed, 387 pp.
2 Danks HV (1987) Insect Dormancy: an Ecological Perspective. Biological Survey of Canada, Ottawa, 439 pp.
3 Davis MA (1980) Variation in flight duration among individual *Tetraopes* beetles: implications for studies of insect flight. J Insect Physiol 26: 403–406
4 Davis MA (1980) The flight duration and migratory ecology of the red milkweed beetle (*Tetraopes tetraophthalmus*). Ecology 65: 230–234
5 Fairbairn DJ (1994) Wing dimorphism and the migratory syndrome: correlated traits for dispersal tendency in wing dimorphic

insects. In "Proceedings of Memorial and International Symposium on Dispersal Polymorphism of Insects" Ed by F Nakasuji, K Fujisaki, Okayama Univ., Okayama, pp 143–152

6 Fairbairn DJ, Desranleau L (1987) Flight threshold, wing muscle histolysis, and alary polymorphism: correlated traits for dispersal tendency in the Gerridae. Ecol Entomol 12: 13–24

7 Harada T (1991) Effects of photoperiod and temperature on phototaxis in a water strider, *Gerris paludum insularis* (Motschulsky). J Insect Physiol 37: 27–34

8 Harada T (1993) Reproduction by overwintering adults of water strider, *Aquarius paludum* (Fabricius). Zool Sci 10: 313–319

9 Harada T, Taneda K (1989) Seasonal changes in alary dimorphism of a water strider, *Gerris paludum insularis* (Motschulsky). J Insect Physiol 35: 919–924

10 Harada T, Numata H (1993) Two critical day lengths for the determination of wing forms and the induction of adult diapause in the water strider, *Aquarius paludum*. Naturwissenschaften 80: 430–432

11 Harrison RG (1980) Dispersal polymorphisms in insects. Ann Rev Ecol Syst 11: 95–118

12 Johnson CG (1969) Migration and Dispersal of Insect by Flight, Methuen, London, 763 pp

13 Masaki S (1980) Summer diapause. Ann Rev Entomol 25: 1–25

14 Palmer JO (1985) Migration: Mechanisms and Adaptive Significance. Contributions to Marine Science, 27 (Supplement): 663–673

15 Roff DA (1990) Antagonistic pleiotropy and the evolution of wing dimorphism in the sand cricket, *Gryllus firmus*. Heredity 65: 169–177

16 Roff DA (1994) Evidence that the magnitude of the trade-off in a dichotomous trait is frequency-dependent. Evolution 48: (in press)

17 Roff DA, Fairbairn DJ (1991) Wing dimorphisms and the evolution of migratory polymorphisms among the insecta. Am Zool 31: 243–251

18 Spence JR, Andersen NM (1994) Biology of water striders: interactions between systematics and ecology. Ann Rev Entomol 39: (in press)

19 Tauber MJ, Tauber CA, Masaki S (1986) Seasonal adaptations of Insects, Oxford Univ. Press, New York, 411 pp

20 Wilcox RS, Maier HA (1991) Facultative estivation in the water strider *Gerris remigis*. Can J Zool 69: 1412–1413

ZOOLOGICAL SCIENCE 11: 859–863 (1994)

Bioconversion of 17α-Hydroxyprogesterone into 17α,20α-Dihydroxy-4-pregnen-3-one and 17α,20β-Dihydroxy-4-pregnen-3-one by Flounder (*Platichthys flesus*) Spermatozoa

KIYOSHI ASAHINA*, JAN G. D. LAMBERT, and HENK J. TH. GOOS

Department of Experimental Zoology, Research Group Comparative Endocrinology, University of Utrecht, Padualaan 8, 3584 CH Utrecht, The Netherlands

ABSTRACT—Flounder (*Platichthys flesus*) spermatozoa were incubated with 17α-hydroxyprogesterone at 20°C for 18 hr. After extraction of the steroids from the incubation medium, steroid metabolites were analyzed by gas chromatography-mass spectrometry (GC-MS). Selected ion monitoring with 25 possible steroid metabolites as standards represented that main metabolites were 17α,20α-dihydroxy-4-pregnen-3-one (17α,20α-P) and 17α,20β-dihydroxy-4-pregnen-3-one (17α,20β-P). In addition small amounts of androstenedione and 17α-hydroxy-5β-pregnane-3,20-dione were detected. Major two metabolites were further identified using full mass spectrograms to be 17α,20α-P and 17α,20β-P, respectively. These results indicate that flounder sperm cells show both 20α- and 20β-hydroxysteroid dehydrogenase activities.

INTRODUCTION

Mature sperm cells of salmonid fishes show very high 20β-hydroxysteroid dehydrogenase (20β-HSD) activity *in vitro*, which enzyme converts 17α-hydroxyprogesterone (17α-P) into 17α,20β-dihydroxy-4-pregnen-3-one (17α,20β-P) [13, 19]. However, common carp (*Cyprinus carpio*) [2] and goldfish (*Carassius auratus*) [1] spermatozoa mainly produce 17α,20α-dihydroxy-4-pregnen-3-one (17α,20α-P), the isomer of 17α,20α-P, when incubated with 17α-P. 20α-Hydroxysteroid dehydrogenase (20α-HSD) activity also appears to be present in sperm cells of marine flatfish, the dab (*Limanda limanda*) and plaice (*Pleuronectes platessa*) [7]. In *Platichthys flesus*, another marine flatfish, however, both enzymes seem to be active in sperm cells; in a preliminary experiment using sperm incubation with tritiated steroid precursor followed by thin-layer chromatography (TLC), we got a strong indication that both progestogens 17α,20α-P and 17α,20β-P could be formed from 17α-P. To identify these steroids a gas chromatographic-mass spectrometric study was carried out.

MATERIALS AND METHODS

Chemicals

All organic solvents (Baker) were of analytical grade and were distilled twice before use. Leibovitz-15 (L-15) medium were purchased from Serva. Reference steroids were obtained from Steraloids, Sigma, and Merk; Sep Pak C18 mini columns from Waters Associates, and the derivatization reagents *O*-methylhydroxylamine-hydrochloride and *N*-trimethylsilylimidazol from Supelco and Fluka, respectively.

Accepted October 24, 1994
Received September 19, 1994

* Correspondence and present address: Department of Fisheries, College of Agriculture and Veterinary Medicine, Nihon University, 1866 Kameino, Fujisawa-shi, Kanagawa 252, Japan

Fish

Male flounder (*P. flesus*) were kept with females in a large outdoor tank (40×40×2 m) under natural temperature and photoperiod conditions at the Netherlands Institute for Sea Research, Texel. In February 1993, three spermiating males were selected from the tank and transported to University of Utrecht. Milt samples were collected with glass pipettes from their genital pores by applying gentle pressure to the abdomen. Sperm motility was checked microscopically after diluting an aliquot of the milt sample with sea water.

Incubation

Sperm cells were carefully washed twice with culture medium (L-15) and collected by centrifugation at 2000 rpm for 15 min. A preliminary TLC analysis represented that sperm cells from one male represented rather high conversion and that the metabolic activity was weak in those of other two individuals. Since the metabolic pattern was almost the same, the former specimen was used for further analysis.

The incubation was carried out in 5 ml L-15 medium containing 240 μM NADPH, 25 μg 17α-P dissolved in 25 μl ethanol, and approximately 400 mg wet weight of washed spermatozoa. They were incubated in a 50 ml round-bottomed flasks for 18 hr at 20°C. After the incubation, the medium was centrifuged at 2000 rpm for 15 min, and the supernatant was stored at −20°C until analysis.

Extraction

Before extraction of the supernatant fluid with diethyl ether (10 ml×2), 50 ng of an internal standard (5β-androstane-3α,11β-diol-17-one) was added. After evaporation, the extract was reconstituted with 5 ml distilled water in succession. Sep Pak C_{18} columns were activated and equilibrated with methanol (5 ml), methanol-distilled water (1:1, 5 ml), and distilled water (5 ml). The aqueous sample was applied to the activated column. The column was rinsed with 10 ml distilled water and 5ml methanol-distilled water (1:1), and finally the steroids were eluted with methanol (5 ml).

Derivatization

For GC-MS analysis methoxime-trimethylsilyl derivatives were prepared according to Vermeulen *et al* [22]. Derivatized steroids

were dissolved in 2 ml hexane and polar compounds (nonsteroidal derivatives) were removed by extraction with acetonitrile (3×200 μl). Finally, the steroid derivative fraction was dissolved in 5 μl of hexane and an aliquot of 1 μl was subjected to GC-MS.

Gas chromatography-mass spectrometry

GC-MS analysis was carried out as described by Vermeulen *et al* [22]. A Hewlett-Packard (HP) 5970B mass-selective detector linked to a HP 5890 gas chromatograph with a HP fused silica capillary column (ultra 1, cross linked methyl silicone; film thickness, 0.52 μm, 25 m×0.31 mm I.D.) was used with helium as carrier gas at a flow rate of 2 ml/min.

Identification and quantification

Identification of the metabolites was based on the comparison of full mass spectra and/or three characteristic mass fragments in relation to their retention times of each metabolite to those of 25 standard steroids [22]. To compare the full mass spectra obtained from sperm preparation with the standards, similarity indices [14] were calculated. Steroids were quantified by comparing ion current abundance between the metabolites and an internal standard steroid of a known concentration, based on calibration curve of each steroid, as described by Schoonen *et al.* [15].

RESULTS

GC-MS analysis using selected ion monitoring (SIM) with 25 standard steroids on the incubation medium extract showed the presence of at least six metabolites (Table 1). Two major metabolites were, as expected after TLC analysis (results not shown), 17α,20α-P (71.3 ng/ml) and 17α,20β-P (49.8 ng/ml); SIM analysis of these metabolites using some of the characteristic fragments (m/z 388.4, m/z 298.3, and m/z 268.2) showed that these ions were present at the expected retention times with abundance ratios comparable with the *cis* and *trans* configuration of both the steroid drivatives (Table 1, Fig 1).

Two minor metabolites were tentatively identified as androstenedione (1.0 ng/ml) and 17α-hydroxy-5β-pregnane-3,20-dione (0.5 ng/ml) (Table 1). There were also two unidentified metabolites which were closely related to authentic 3α,17α,20α-trihydroxy-5β-pregnane and 3α,17α,20β-trihy-

TABLE 1. Calculated concentrations and relative abundances of specific ion fragments of steroid metabolites detected with selected ion monitoring in the incubation medium of sperm cells of *P. flesus*

Steroid derivatives	Conc. in medium (ng/ml)	Config.	Rt. (min)		Relative abundances (%) of specific ion fragments		
4-Androstene-3,17-dione	1.0			ionfragments	313.2	344.2	345.2
(Androstenedione)		cis	18.6	standard	63	100	27
(dimethoxime)				sample	60	100	25
		trans	18.8	standard	64	100	26
				sample	65	100	32
5β-pregnane-3α,17α,20β-triol				ionfragments	255.3	345.3	435.4
(tri-TMS)			23.5	standard	100	29	60
Unidentified metabolite I			24.0	sample	100	15	68
5β-Pregnane-3α,17α,20α-triol				ionfragments	255.3	345.3	435.4
(tri-TMS)			24.7	standard	100	18	55
Unidentified metabolite II			25.2	sample	100	18	59
17α-Hydroxy-5β-pregnan-3,20-dione	0.5			ionfragments	319.3	431.5	462.4
(dimethoxime-TMS)		cis	24.5	standard	37	100	26
				sample	38	100	39
		trans	24.9	standard	31	100	22
				sample	20	100	21
17α,20β-Dihydroxy-4-pregnen-3-one	49.8			ionfragments	267.2	298.3	388.4
(17α,20β-P)		cis	31.6	standard	49	26	100
(methoxime-diTMS)				sample	52	30	100
		trans	32.5	standard	13	41	100
				sample	16	44	100
17α,20α-Dihydroxy-4-pregnen-3-one	71.3			ionfragments	267.2	298.3	388.4
(17α,20α-P)		cis	33.2	standard	52	27	100
(methoxime-diTMS)				sample	58	32	100
		trans	33.6	standard	14	43	100
				sample	16	44	100

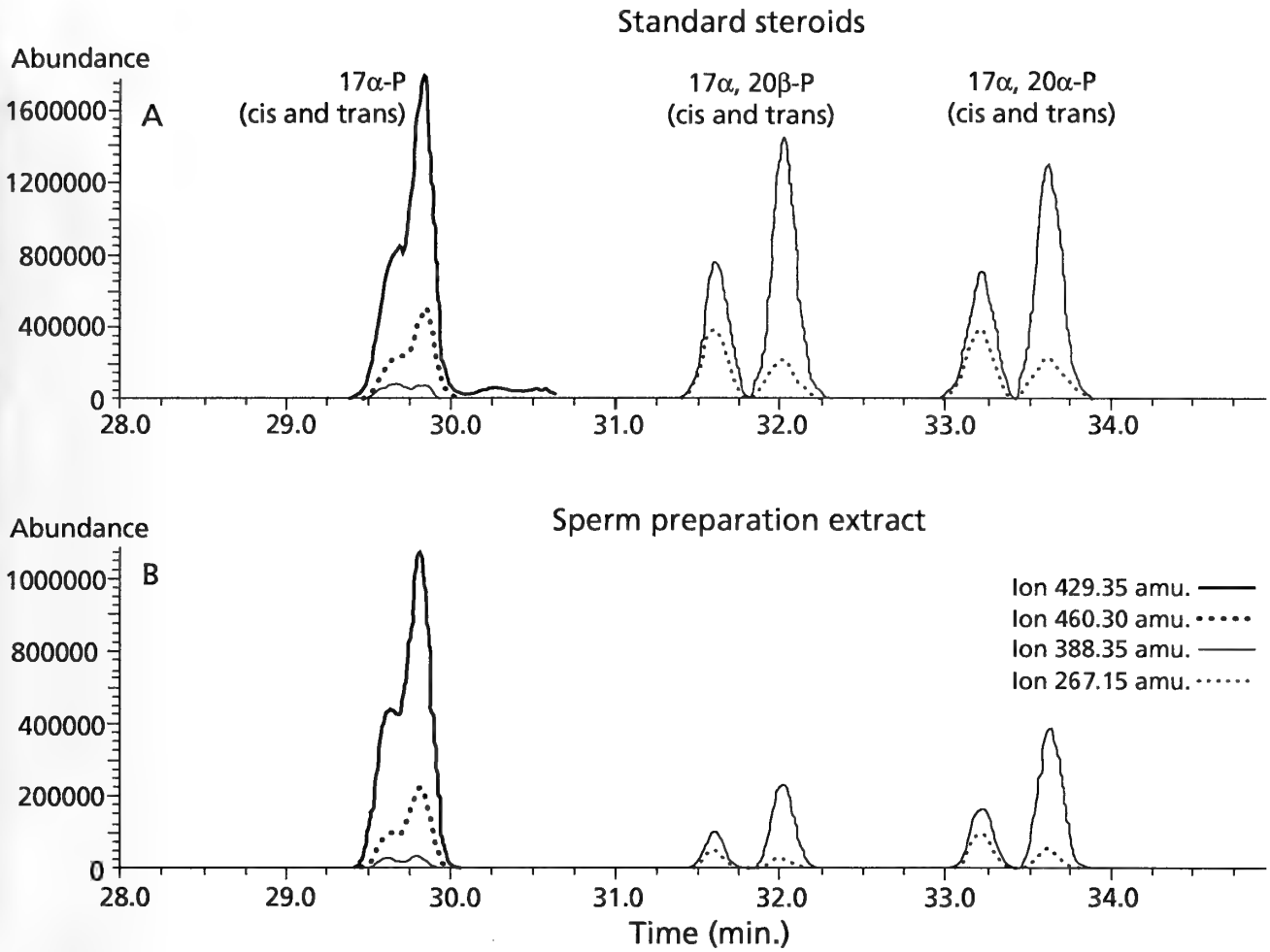

FIG. 1. SIM analysis of standards (A) and flounder sperm incubation medium extract (B) between 28 and 35 min GC-run. The characteristic ions of 17α-P, 17α,20α-P, and 17α,20β-P were present at the correct retention times.

droxy-5β-pregnane, respectively, in retention times and characteristic mass fragments (Table 1).

For the major metabolites, 17α,20α-P and 17α,20β-P, full mass spectrograms were taken and were compared with those of authentic preparations. Although these two steroids manifest themselves in a so-called *cis* and *trans* configuration when derivatized, only the *trans* configuration with retention times of 32.0 min and 33.6 min, respectively, were used for identification by total ion monitoring (TIM). TIM for the steroid fraction of the sperm preparation resulted in full spectra at 32.1 min and 33.7 min which demonstrated the presence of the methoxime-diTMS derivatives of 17α,20α-P and 17α,20β-P, since the mass spectra correlated very well (Similarity index>0.9 for both steroids) with those of standards (Fig. 2).

DISCUSSION

This is the first clear demonstration of both 20α- and 20β-hydroxysteroid dehydrogenase (20α- and 20β-HSD) activities in mature teleost sperm cells. Only 20β-HSD activity has been reported in the spermatozoa of salmonid species [13, 19]. On the other hand, 20α-HSD activity was dominant in the sperm cells of two cyprinid [1, 2], and of two pleuronectid species [7].

In addition to the main products 17α,20α-P and 17α,20β-P, selected ion monitoring showed the presence of small amounts of androstenedione and 17α-hydroxy-5β-pregnane-3,20-dione (Table 1), which is indicative of C17-C20 lyase and 5β-reductase activity in flounder sperm cells. The activity of 5β-reductase was the main steroid metabolic enzyme of Japanese flounder and bluefin tuna spermatozoa (K. Asahina, unpublished results).

Two unidentified metabolites were closely related to authentic 3α,17α,20α-trihydroxy-5β-pregnan and 3α,17α,20β-trihydroxy-5β-pregnan, respectively, in retention times and characteristic mass fragments (Table 1). Since 5β-reductase activity appears to exist in the flounder spermatozoa, we suspect that these metabolites are 3β-isomers; 3β,17α,20α-trihydroxy-5β-pregnan and 3β,17α,20β-trihydroxy-5β-pregnan, respectively. The plasma level of the former steroid is reported to increase following hCG administration

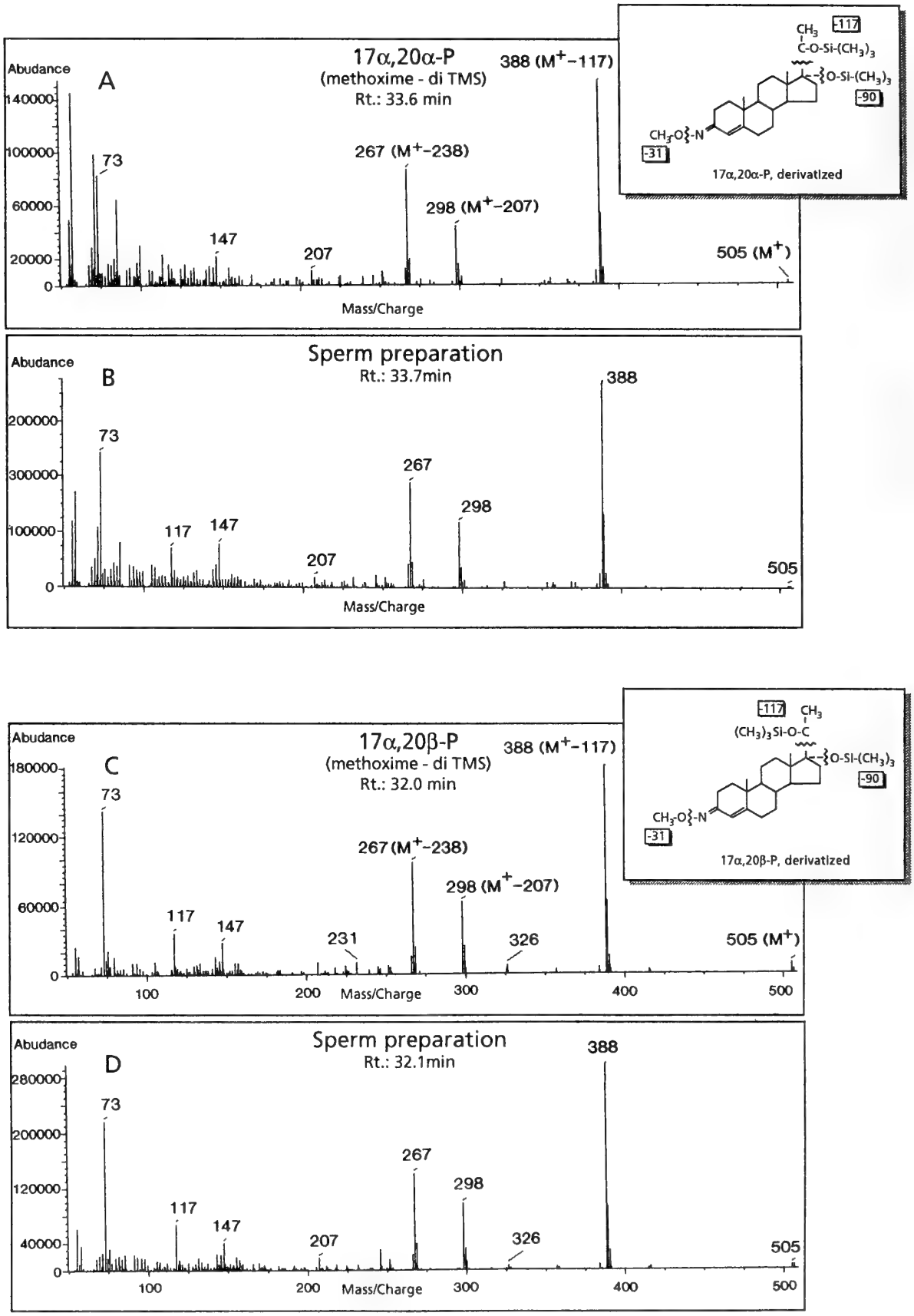

FIG. 2. Full mass spectra of derivatized authentic 17α,20α-P (A), 17α,20β-P (C), and the corresponding spectra (B, D) from the derivatized medium extract of flounder spermatozoa incubated with 17α-hydroxyprogesterone.

in male dab [6].

High concentrations of serum or plasma 17α,20β-P during the spawning season have been reported in some salmonids [16, 18, 21] and cyprinid species [4, 10, 17]. The steroid induces spermiation in amago-salmon and goldfish [20], and it inhibits androgen production in common carp [3]. Recently, Miura *et al.* [11] demonstrated that 17α,20β-P induce the acquisition of sperm motility in salmonids; the steroid acts to increase sperm duct pH, which in turn increases cAMP in sperm to allow the acquisition of sperm motility. From our results, however, it is reasonable to hypothesize that both 17α,20α-P and 17α,20β-P have a role in regulating spermiation in the flounder. Profiles of plasma steroids, including 17α,20α-P, 17α,20β-P, and 5β-reduced progestogens of both male and female flounder during the annual reproductive cycle are currently under investigation.

As for the steroid metabolic enzyme activity in sperm preparation, Barry *et al.* [5] suggested the contamination of Sertoli cytoplasts which are pinched off during spermiation in elasmobranchs [12]. In teleosts, however, the principal cellular source of steroids seems to be the interstitial Leydig cells [8]. Furthermore, several HSDs have been demonstrated in mature sperm cells of mammals [9]. Therefore, we conclude that 20α- and 20β-HSD are localized in flounder sperm cells. Further studies are required to determine, however, whether another metabolic enzymes, such as C17-C20 lyase and 5β-reductase, are also localized in flounder sperm cells.

ACKNOWLEDGMENTS

We gratefully acknowledge Dr. R. Schulz for critical reading of the manuscript, and Dr. G.J. Vermeulen for helpful advice in GC-MS analysis. This work was partly supported by Overseas Researcher Fellowship of Nihon University given to K.A.

REFERENCES

1 Asahina K, Aida K, Higashi T (1993) Biosynthesis of 17α,20α-dihydroxy-4-pregnen-3-one from 17α-hydroxyprogesterone by the spermatozoa of the goldfish, *Carassius auratus*. Zool Sci 10: 381–383

2 Asahina K, Barry TP, Aida K, Fusetani N, Hanyu I (1990) Biosynthesis of 17α,20α-dihydroxy-4-pregnen-3-one from 17α-hydroxyprogesterone by spermatozoa of the common carp, *Cyprinus carpio*. J Exp Zool 255: 244–249

3 Barry TP, Aida K, Hanyu I (1989) Effects of 17α,20β-dihydroxy-4-pregnen-3-one on the in vitro production of 11-ketotestosterone by testicular fragments of the common carp, *Cyprinus carpio*. J Exp Zool 251: 117–120

4 Barry TP, Santos AJG, Furukawa K, Aida K, Hanyu I (1990) Steroid profiles during spawning in male common carp. Gen Comp Endocrinol 80: 223–231

5 Barry TP, Thomas P, Callard GV (1993) Stage-related production of 21-hydroxylated progestins by the dogfish (*Squalus acanthias*) testis. J Exp Zool 256: 522–532

6 Canario AVM, Scott AP (1991) Levels of 17α,20α-dihydroxy-4-pregnen-3-one, 3β,17α,20α-trihydroxy-5β-pregnane, and other sex steroids, in blood plasma of male dab, *Limanda limanda* (marine flatfish) injected with human chorionic gonadotrophin. Gen Comp Endocrinol 83: 258–264

7 Canario AVM, Scott AP (1989) Synthesis of 20α-hydroxylated steroids by ovaries of the dab (*Limanda limanda*). Gen Comp Endocrinol 76: 147–158

8 Fostier A, Le Gac F, Loir M (1987) Steroids in male reproduction. In "Reproductive Physiology of Fish 1987" Ed by DR Idler, LW Crim, JM Walsh, Memorial University of Newfoundland, St. John's, Newfoundland, pp 239–245

9 Guraya SS (1987) Biology of spermatogenesis and spermatozoa in mammals. Springer Verlag, Berlin, pp 294–301

10 Kobayashi M, Aida K, Hanyu I (1986) Gonadotropin surge during spawning in male goldfish. Gen Comp Endocrinol 62: 70–79

11 Miura T, Yamauchi K, Takahashi H, Nagahama Y (1992) The role of hormones in the acquisition of sperm motility in salmonid fish. J Exp Zool 261: 359–363

12 Pudney J, Callard GV (1986) Sertoli cell cytoplasts in the semen of the spiny dogfish (*Squalus acanthias*). Tissue 18: 375–382

13 Sakai N, Ueda H, Suzuki N, Nagahama Y (1989) Involvement of sperm in the production of 17α,20β-dihydroxy-4-pregnen-3-one in the testis of spermiating rainbow trout, *Salmo gairdneri*. Biochem Res 10: 131–138

14 Schoonen WGEJ, Lambert JGD (1987) Gas chromatographic-mass spectorometric analysis of steroids and steroid glucuronides in the seminal vesicle fluid of the African catfish, *Clarias gariepinus*. Gen Comp Endocrinol 68: 375–386

15 Schoonen WGEJ, Lambert JGD, Van Oordt PGWJ (1988) Quantitative analysis of steroids and steroid glucuronides in the seminal vesicle fluid of feral spawning and feral and cultivated nonspawning African catfish, *Clarias gariepinus*. Gen Comp Endocrinol 70: 91–100

16 Scott AP, Baynes SM (1982) Plasma levels of sex steroids in relation to ovulation and spermiation in rainbow trout (*Salmo gairdneri*). In "Reproductive Physiology of Fish 1982" Ed by CJJ Richter and HJT Goos, Center for Agricultural Publishing and Documentation, Wageningen, pp 103–106

17 Scott AP, MacKenzie DS, Stacey NE (1984) Endocrine changes during natural spawning in the white sucker, *Catostomus commersoni*. II. Steroid hormones. Gen Comp Endocrinol 56: 349–559

18 Ueda H, Hiroi O, Hara A, Yamauchi K, Nagahama Y (1984) Changes in serum concentrations of steroid hormones, thyroxine, and vitellogenin during spawning migration of the chum salmon, *Oncorhynchus keta*. Gen Comp Endocrinol 53: 203–211

19 Ueda H, Kambegawa A, Nagahama Y (1984) In vitro 11-ketotestosterone and 17α,20β-dihydroxy-4-pregnen-3-one production by testicular fragments and isolated sperm of rainbow trout, *Salmo gairdneri*. J Exp Zool 231: 435–439

20 Ueda H, Kambegawa A, Nagahama Y (1985) Involvement of gonadotrophin and steroid hormones in spermiation in the amago salmon, *Oncorhynchus rhodurus*, and goldfish, *Carassius auratus*. Gen Comp Endocrinol 59: 24–30

21 Ueda H, Young G, Crim LW, Kambegawa A, Nagahama Y (1983) 17α,20β-Dihydroxy-4-pregnen-3-one: plasma levels during sexual maturation and in vitro production by the testes of amago salmon (*Oncorhynchus rhodurus*) and rainbow trout (*Salmo gairdneri*). Gen Comp Endocrinol 51: 106–112

22 Vermeulen GJ, Lambert JGD, Lenczowski MJP, Goos HJT (1993) Steroid hormone secretion by testicular tissue from African catfish, *Clarias gariepinus*, in primary culture: identification and quantification by gas chromatography-mass spectrometry. Fish Physiol Biochem 12: 21–30

ZOOLOGICAL SCIENCE 11: 865–870 (1994)

Calcitonin Induces Hypertrophy and Proliferation of Pars Intermedia Cells of the Rat Pituitary Gland

Toshi Horiuchi, Mitsui Isobe, Minoru Suzuki and Yasuo Kobayashi[1]

Safety Research Department, Teikoku Hormone Mfg. Co., Ltd., Shimosakunobe, Kawasaki 213 and [1]Department of Biology, Faculty of Science, Okayama University, Okayama, Japan

ABSTRACT—The effects of subcutaneous administration of synthetic salmon calcitonin (sCT) on the pars intermedia (PI) cells of the pituitary gland in the rat were investigated histologically, immunohistochemically, and electron microscopically. Chronic administration of sCT at 0.75, 7.5, 30 or 120 IU/kg/day for 4 or 52 weeks to male and female rats induced hypertrophy of PI cells and thickening of the PI without any sign of toxicity. The mean size of PI cells was significantly increased in sCT-treated rats compared to vehicle treated rats, and the magnitude of increase was dose-dependent. sCT treatment of male rats at 120 IU/kg for 3, 7 and 14 days induced 2.8-, 2.6-, and 2.3-fold increase, respectively, in the rate of cell proliferation in the PI estimated by labeling of the nuclei with bromodeoxyuridine. Electron microscopic examination in male rats after sCT treatment at 120 IU/kg for 4 weeks disclosed Golgi complex hypertrophy with electron-dense secretory granules and expansion of rough endoplasmic reticulum. Immunohistochemical staining of the PI for α-melanocyte stimulating hormone and β-endorphin disclosed no marked differences between the control and sCT-treated rats. These results suggest that sCT at pharmacological doses stimulates and increases the thickness of the PI of the rat pituitary gland by increasing the rate of cell proliferation and by inducing hypertrophy of individual cells.

INTRODUCTION

The pars intermedia (PI) of the murine pituitary gland contains several peptides cosynthesized in a common precursor, proopiomelanocortin (POMC). These include α-melanocyte stimulating hormone (αMSH), βMSH, γMSH, corticotropin-like intermediate peptide, γ-lipotropin, met-enkephalin and β-endorphin [8, 24]. In mammals, αMSH and β-endorphin play a role in the control of pigmentation and are thought to be involved in the regulation of the endocrine and cardiovascular systems and in central processes such as analgesia, attention, and arousal [13, 25]. The PI is known to be regulated primarily by dopaminergic neurons emanating from the arcuate nucleus of the hypothalamus and terminating directly on PI cells [3, 31]. Thus, pharmacological manipulation with dopaminergic drugs has been shown to elicit changes in the rat PI morphology, secretion of POMC-derived peptides, POMC mRNA content, and rate of cell proliferation [4, 6, 7, 9, 14].

Recently, we observed non-functional tumors in the pars distalis of the rat pituitary gland [26] following the administration for one year of synthetic salmon calcitonin (sCT), which lowers the serum calcium level by inhibiting bone resorption [28]. In these experiments, we also noted hypertrophy of the PI in the sCT-treated rats. To elucidate the effects of sCT on the cells in the rat PI, we histologically and immunohistochemically examined the cell size and the cell proliferation rate after subchronic and chronic treatment with sCT, using monoclonal antibody against bromodeoxyuridine (BrdU), together with ultrastructural observation.

Accepted September 26, 1994
Received March 16, 1994

MATERIALS AND METHODS

Six-week-old male and female Sprague-Dawley rats (Charles River Japan Inc., Atsugi) were used in the experiments. The rats were housed individually in plastic cages and given standard laboratory feed (CE-2, Clea Japan Inc., Tokyo) and tap water ad libitum. The rats were kept under room temperature and relative humidity conditions of $22\pm2^{\circ}$C and $60\pm10\%$, respectively, on a 12–12 hr light-dark cycle.

The sCT (Teikoku Hormone Co. Ltd., Kawasaki) is the type-I form of naturally produced salmon calcitonins [11], and has a potency of about 5000 IU/mg. The sCT was dissolved in an acetic buffer (pH 4.0). Haloperidol (Wako Pure Chemical, Tokyo) was suspended in saline solution containing 1% Tween-80, and BrdU (Sigma, St. Louis, USA) was dissolved in 50% dimethylsulfoxide solution.

In the first experiment, the effects of long-term administration of sCT at various doses on the size and morphology of PI cells were examined. This experiment was carried out as a part of a one-year chronic toxicity study of sCT. Groups of 10 rats of each sex were injected subcutaneously with vehicle or with sCT at 0.75, 7.5, 30 or 120 IU/kg once daily for 4 or 52 weeks. The rats were killed on the day after the last injection under ether anesthesia. The pituitary glands were removed, fixed in 10% buffered formalin, and embedded in paraffin. Sections 4 μm thick were cut in the frontal plane and stained with hematoxylin and eosin. In the measurement of the size of PI cells, 3 sections were obtained from the mid-portion of each PI. On the light micrographs of these sections, the number of nuclei of PI cells was counted, and the area occupied by these cells was measured. Finally, for each PI, the size of a single cell was calculated by dividing

the total area by the number of nuclei. Immunohistochemical staining for αMSH and β-endorphin was carried out on sections of the pituitary from 5 male rats in each group treated with vehicle or sCT (120 IU/kg) for 4 or 52 weeks by the avidin-biotin-peroxidase complex (ABC) method [15], using a Nichirei ABC Kit (Nichirei, Tokyo). The antibodies against αMSH (dilution, 1:2000) and β-endorphin (1:4000) were obtained from UCB-Bioproducts, Belgium. For the ultrastructural observation, the pituitary glands of 5 male rats treated with vehicle or sCT (120 IU/kg) for 4 weeks were fixed in 2.5% glutaraldehyde for 3 hr at 4°C, followed by 1% OsO_4 for 1 hr, and then embedded in Quetol 812. Ultrathin sections were stained with uranyl acetate and lead citrate, and examined with a JEOL-1200EX electron microscope.

In the second experiment, the effect of sCT on the PI cell proliferation was estimated by the BrdU immunohistochemical technique described by Tatematsu *et al.* [30]. In this study, before the rat was killed, continuous administration of BrdU (120 μg/hr) into the peritoneal cavity was carried out for 72 hr through Alzet osmotic minipumps (Model 2001, Alza Corp.,Palo Alto, Calif., USA). The superior sensitivity of continuous labeling in comparison with pulse labeling for assessment of DNA replication in rodent tissues has been well documented [10]. Groups of 15 male rats each received daily administration of vehicle or sCT (120 IU/kg) by subcutaneous injection or haloperidol (10 mg/kg) orally once daily for 3, 7 or 14 days. Five rats in each group were sacrificed on days 3, 7 and 14. The pituitary glands were fixed in Bouin's solution for 4 hr, embedded in paraffin, and sectioned in the frontal plane. Sections 4 μm thick were hydrolyzed with 2N HCl for 20 min at 25°C and neutralized with 0.1 M boric acid-borate buffer (pH 7.6) for 10 min at 25°C, and then digested for 3 min at 37°C with 0.04% actinase (Kaken Kagaku, Tokyo) in 0.01 M phosphate-buffered saline. The monoclonal antibody of BrdU (Becton-Dickinson, Mountain View, CA, USA; dilution, 1:100) was used for immunohistochemical staining using the Nichirei ABC-Kit. After immunostaining, the sections were counterstained with hematoxylin. The BrdU labeling index was defined as the percentage of BrdU-labeled cells per total cells (more than 1000 PI cells) in 2 sections of each PI.

Data are expressed as mean±SD. Statistical analyses were conducted with multiple comparison test after one-way analysis of variance (ANOVA) of the data for the PI cell area and Student's t-test for the BrdU labeling index.

RESULTS

PI histology and mean cell size

In the vehicle-treated rats, the PI was composed of 10 or more layers of closely packed cells divided into lobules by strands of connective tissue. The principal type of PI cells was a polyhedral cell with an ovoid smooth nucleus (Fig. 1a). A small number of interstitial cells were also distributed throughout the parenchyma of the PI.

Chronic sCT treatment for 4 or 52 weeks induced hypertrophy of the PI cells in both male and female rats (Fig. 1b). sCT treatment also increased the thickness of the PI without inducing any disorder of the lobular structure or degeneration of PI cells. Compared with that in the vehicle-treated rats, the mean cell size was significantly increased in the male rats treated with sCT at the doses of 7.5 IU/kg or more and in the female rats treated with sCT at the doses of 30 and 120 IU/kg (Table 1). The magnitude of this increase was dose-dependent.

TABLE 1. The mean PI cell area in male and female rats treated subcutaneously with sCT for 4 or 52 weeks

sCT (IU/kg/day)	Mean PI cell area±SD (μm^2)	
	4 weeks	52 weeks
Male		
0	(10)[a] 131.3±14.3	(10) 116.3± 9.9
0.75	(10) 141.5±18.0	(10) 124.7±11.9
7.5	(10) 155.2±18.6*	(8) 136.2±23.8
30	(10) 178.8±17.6**	(5) 160.2±26.2
120	(10) 187.5±18.0**	(6) 200.7±21.5**
Female		
0	(10) 110.0± 6.0	(10) 105.4±10.3
0.75	(10) 107.7± 8.6	(10) 105.6± 7.0
7.5	(10) 113.7± 8.6	(10) 109.4±11.1
30	(10) 126.0±11.5**	(10) 156.1± 9.7**
120	(10) 151.0±14.1**	(10) 186.4±12.3**

[a] No. of rats.
* $p<0.05$.
** $p<0.01$ vs. vehicle control.

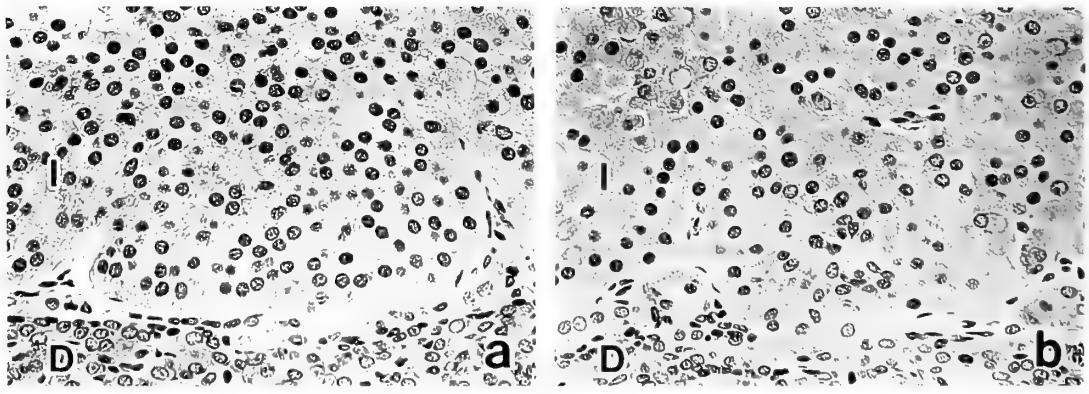

FIG. 1. Light micrographs of the PI of the pituitary gland in male rats treated subcutaneously with vehicle (a) or 120 IU/kg of sCT (b) for 4 weeks. The PI cells in the rat given sCT demonstrate diffuse hypertrophy. I, pars intermedia; D, pars distalis. Hematoxylin-eosin, × 150.

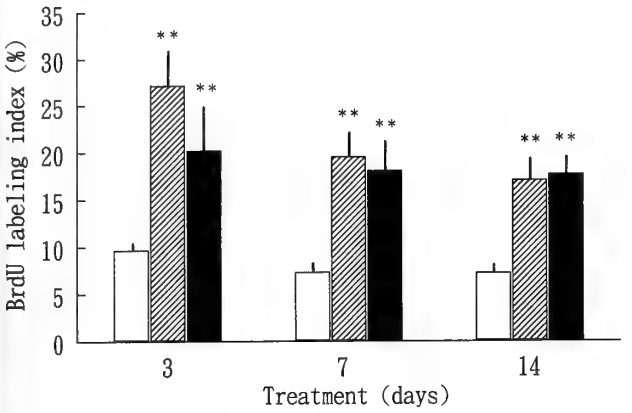

FIG. 2. Effect of repeated sCT or haloperidol treatment on BrdU labeling index in the PI of the rat pituitary gland. Groups of five rats each were treated with vehicle (s.c.), 120 IU/kg of sCT (s.c.), or 10 mg/kg of haloperidol (p.o.) for 3, 7 and 14 days. BrdU (120 μg/hr) was injected continuously through an osmotic minipump for 72 hr prior to sacrifice. Data are expressed as mean$\pm$SD. Open columns, vehicle-treated; hatched columns, sCT-treated; closed columns, haloperidol-treated. **, $p<0.01$ vs. vehicle controls.

Cell proliferation in PI

After the treatment for 3, 7, and 14 days, the mean BrdU labeling indices in the sCT-treated rats were significantly higher (2.8-, 2.6-, and 2.3-fold, respectively) than those in the rats given vehicle only (Figs. 2 and 3). Haloperidol also significantly increased the number of cells labeled by BrdU (more than 2-fold) after all 3 treatment periods.

Ultrastructural findings of PI

In the vehicle-treated rats, the glandular cells of the PI contained numerous secretory granules of variable density (Fig. 4). Secretory granules were distributed randomly throughout the cytoplasm. The Golgi complexes, with a small number of electron-dense granules, were rather inconspicuous (Fig. 4). The rough endoplasmic reticulum was scarce.

The PI cells in the sCT-treated rats were highly enlarged, and the secretory glanules were located at the periphery of the cells. The Golgi complexes showed marked hypertrophy associated with an increase in the number of electron-dense

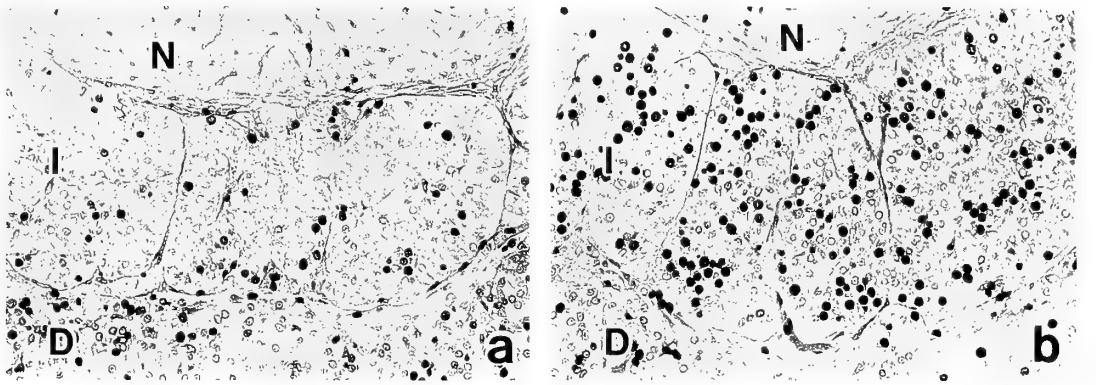

FIG. 3. Immunohistochemistry of BrdU in the pituitary PI of male rats treated with vehicle (a) or 120 IU/kg of sCT (b) for 3 days. The dark nuclei are BrdU-labeled nuclei. The sCT treatment markedly increased the number of BrdU- positive cells. I, pars intermedia; D, pars distalis; N, pars nervosa. $\times$130.

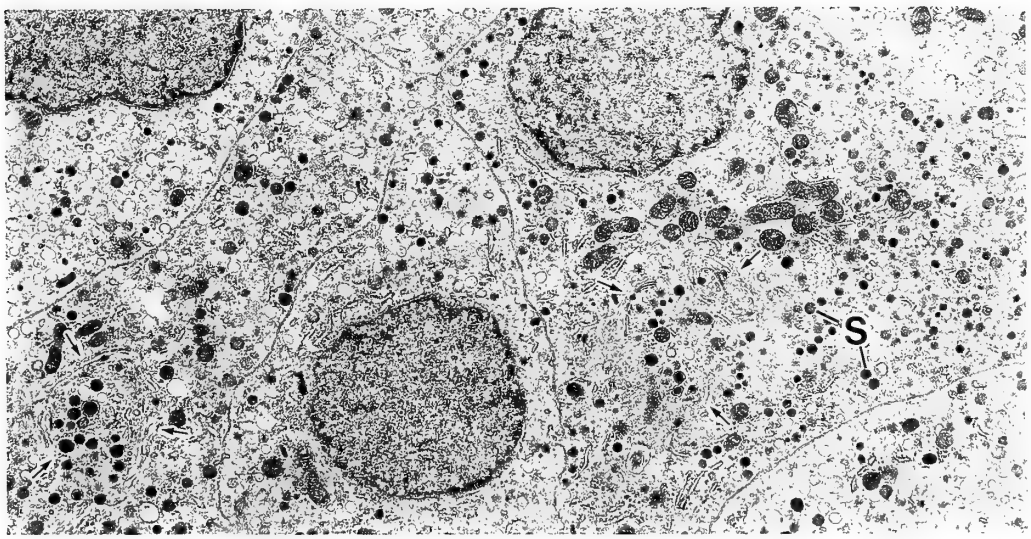

FIG. 4. Electron micrograph of the PI cells in a male rat treated with vehicle for 4 weeks. The cytoplasm contains numerous secretory granules (S) and Golgi complexes (arrows) with a small number of electron dense granules. $\times$6500.

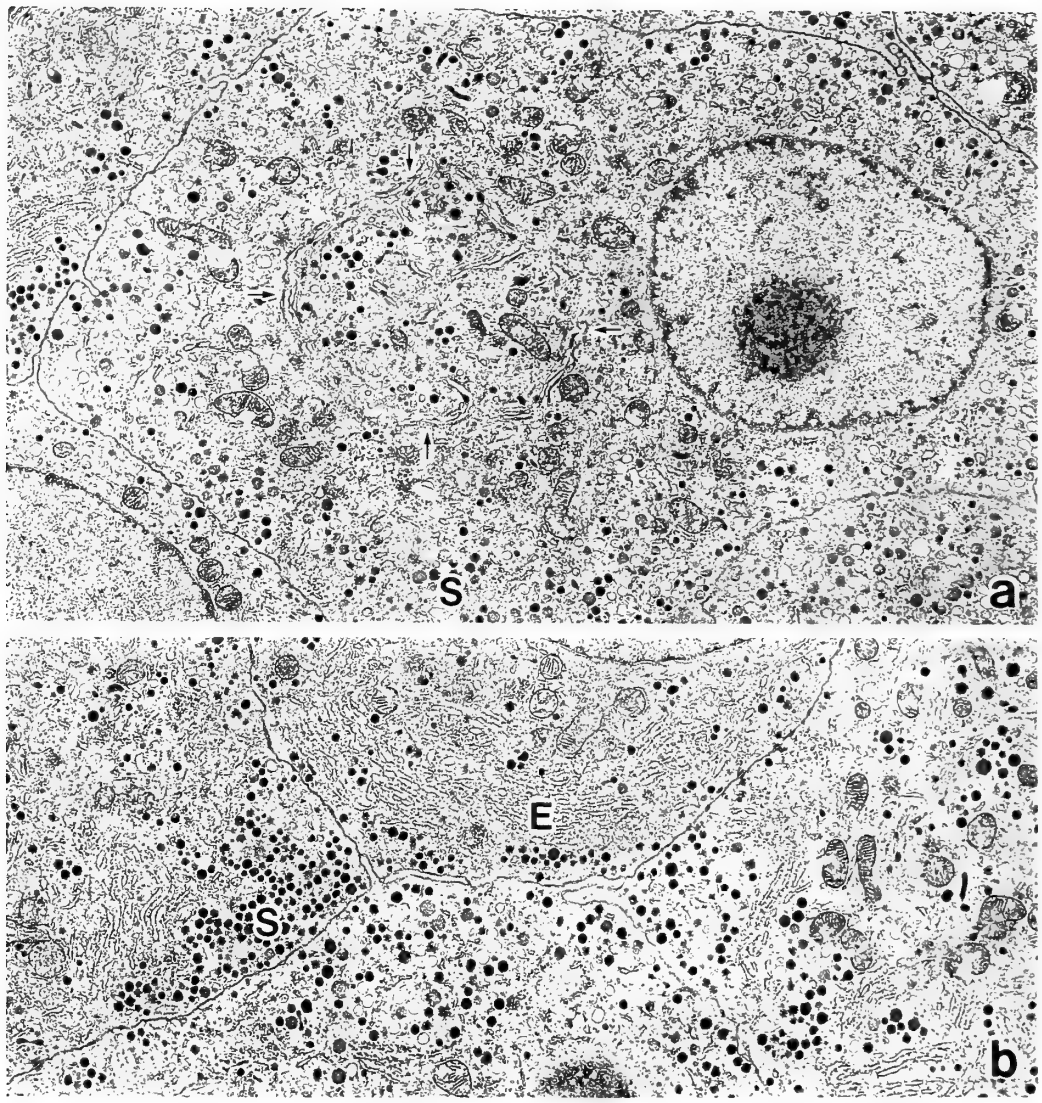

FIG. 5. Electron micrographs of the PI cells in a male rat treated with 120 IU/kg of sCT for 4 weeks. Note the activated Golgi complex (arrows), accumulation of secretory granules (S) in the cell periphery (a), and well-developed rough endoplasmic reticulum (b). E, rough endoplasmic reticulum. ×6500.

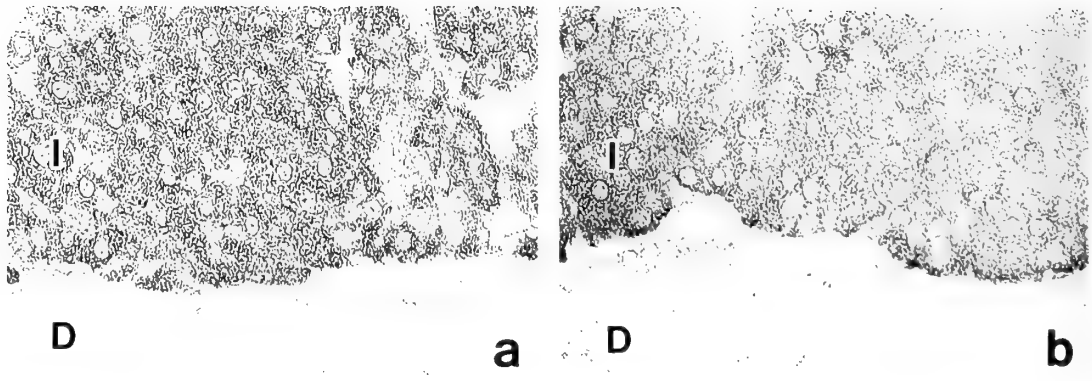

FIG. 6. Immunohistochemistry for αMSH (a) or β-endorphin (b) in the pituitary PI of male rats treated with 120 IU/kg of sCT for 4 weeks. Except for interstitial cells and cleft cells, all PI cells are equally stained by antibodies against αMSH and β-endorphin. I, pars intermedia; D, pars distalis. ×165.

secretory granules (Fig. 5a). The rough endoplasmic reticulum was conspicuous and well developed, and many of the PI cells showed parallel arrays of rough endoplasmic reticulum (Fig. 5b).

Immunohistochemistry for α-MSH and β-endorphin

All PI cells were equally stained by antibodies against αMSH and β-endorphin in both vehicle- and sCT-treated rats excepting the cells of the interlobular connective tissue, interstitial cells, and marginal cells lining Rathke's cleft (Figs. 6a and b). A small number of cells in the pars distalis were also stained by antibodies against αMSH and β-endorphin. These immunohistochemical staining features were identical to those described by Kurosumi *et al.* [22]. No difference was seen between the control and sCT-treated rats in the immunostaining for αMSH and β-endorphin.

DISCUSSION

Chronic treatment of rats with sCT was shown to induce hypertrophy of PI cells and increased thickness of the PI without any sign of toxicity or alteration of immunostaining for αMSH and β-endorphin. The size of PI cells showed dose-dependent increase in the sCT-treated rats. Electron microscopic examination revealed that sCT treatment caused hypertrophy of Golgi complexes associated with an increase of electron-dense secretory granules and expansion of rough endoplasmic reticulum. Such cytological changes have been observed in dark-adapted amphibians [27], which are known to release MSH under that condition [12]. In mammals, the PI cells also exhibit changes similar to those described herein under a variety of conditions or during drug treatment which enhance the activity of the PI, such as exposure to bright light and loud noises [23], variation in hydromineral intake [17–21], and reserpine, metapirone and haloperidol injection [7, 29, 32]. Thus, the morphological changes after sCT treatment strongly suggest that sCT enhances the activity of the PI of the rat pituitary gland.

The increase in the rate of cell proliferation of the PI is further evidence that the PI is stimulated by sCT treatment. The daily administration of sCT for 3, 7 and 14 days produced 2.8-, 2.6-, and 2.3-fold increase, respectively, in the rate of cell proliferation estimated by BrdU labeling. This increase after sCT treatment is indicative of hyperfunction of the PI, since haloperidol, a D-2 dopamine receptor antagonist which enhances PI function, increases and bromocriptin, a D-2 agonist which inhibits the PI, decreases the rates of cell proliferation as determined by the uptake of [^{3}H]thymidine or by the mitotic index [7]. In the present experiment, haloperidol also produced more than a 2-fold increase in the rate of cell proliferation in our model.

It has been shown that sCT administration to rats markedly increases the urine water and sodium excretion and causes hyponatremia [1, 16]. The diuretic and natriuretic activities of sCT were confirmed in the present studies (data not shown), and the sCT-treated rats developed pronounced polyuria within a few days. Although the mechanism is poorly understood, there is considerable evidence for the involvement of the PI in hydromineral regulation through the control of aldosterone secretion by the adrenal cortex [5, 17, 20]. Therefore, variation in salt intake alters the function and morphology of the PI. Dehydration selectively activates the tuberohypophyseal dopaminergic neuronal system and inhibits the PI in rats [2]. On the other hand, hyponatremia induced by dietary sodium deprivation [17, 18, 21] as well as excessive water intake induced by food deprivation and concurrent free access to glucose solution [19], conditions exactly the opposite to dehydration, enhance the activity of PI cells. The physiological state induced by sCT treatment is similar to a condition opposite to dehydration. Thus, there is a posibility that alteration of hydromineral metabolism by sCT attenuates the dopaminergic inhibitory control and stimulates the PI cells. Further biochemical studies and urinalyses in relation to the function of the adrenal zona glomerulosa are in progress to examine the mechanism of activation of the PI in rats after sCT treatment.

ACKNOWLEDGMENTS

The authors thank K. Ito, K. Iizuka, A. Sato and K. Takahashi for their expert technical assistance.

REFERENCES

1 Aldred JP, Kleszynski RR, Bastion JW (1970) Effects of acute administration of porcine and salmon calcitonin on urine electrolyte excretion in rats. Proc Soc Exp Biol Med 134: 1175–1180

2 Alper RH, Demarest KT, Moore KE (1980) Dehydration selectively increases dopamine synthesis in tuberohypophyseal dopaminergic neurons. Neuroendocrinology 31: 112–115

3 Baumgarten HG, Björklund A, Holstein AF, Nobin A (1972) Organization and ultrastructural identification of catecholamine nerve terminals in the neural lobe and pars intermedia of the rat pituitary. Z Zellforsch 126: 483–517

4 Beaulieu M, Goldman ME, Miyazaki K, Frey EA, Eskay RL, Kebabian JW, Cote TE (1984) Bromocriptine-induced changes in the biochemistry, physiology, and histology of the intermediate lobe of the rat pituitary gland. Endocrinology 114: 1871–1884

5 Brownie AC, Pedersen RC (1986) Control of aldosterone secretion by pituitary hormones. J Hypertention 4 (Suppl 5): s72-s75

6 Chen CLC, Dionne FT, Roberts JL (1983) Regulation of the pro-opiomelanocortin mRNA levels in rat pituitary by dopaminergic compounds. Proc Natl Acad Sci USA 80: 2211–2215

7 Chronwall BM, Millington WR, Griffin WST, Unnerstall JR, O'Donohue TL (1987) Histological evaluation of the dopaminergic regulation of proopiomelanocortin gene expression in the intermediate lobe of the rat pituitary, involving *in situ* hybrization and [^{3}H]thymidine uptake measurement. Endocrinology 120: 1201–1211

8 Eiper BA, Mains RE (1980) Structure and biosythesis of pro-adrenocorticotropin/endorphin and related peptides. Endocr Rev 1: 1–27

9 Farah JM, Malcolm DS, Mueller GP (1982) Dopaminergic inhibition of pituitary β-endorphin-like immunoreactivity secretion in the rat. Endocrinology 110: 657–659

10 Goldsworthy TL, Morgan KT, Popp JA, Butterworth BE (1991) Guidelines for measuring chemically induced cell proliferation in specific rodent target organs. In "Chemically Induced Cell Proliferation: Implication for Risk Assessment Vol 369" Ed by BE Butterworth, TJ Staga, W Farland, M McClain, Wiley-Liss Inc, New York, pp 253–284

11 Guttmann S (1981) Chemistry and structure-activity relationship of natural and synthetic calcitonins. In "Calcitonin-Chemistry, Physiology, Pharmacology and Clinical Aspects" Ed by A Pecile, Excerpta Medica, Amsterdam, pp 11–24

12 Hadley ME, Bagnara JT (1975) Regulation of release and mechanism of action of MSH. Am Zool 15 (Suppl 1): 81–104

13 Hirsch MD, O'Donohue TL (1986) Structural Modifications of proopiomelanocortin-derived peptides markedly alter their behavioral effects. J Pharmacol Exp Ther 237: 378–385

14 Höllt V, Bergmann M (1982) Effects of acute and chronic haloperidol treatment on the concentrations of immunoreactive β-endorphin in plasma, pituitary and brain of rats. Neuropharmacology 21: 147–154

15 Hsu SM, Raine L, Fanger H (1981) Use of avidine-biotin-peroxidase complex (ABC) in immunoperoxidase techniques: A comparsion between ABC and unlabeled antibody (PAP) procedures. J Histochem Cytochem 29: 577–580

16 Keeler R, Walker V, Copp DH (1970) Natriuretic and diuretic effects of salmon calcitonin in rats. Can J Physiol Pharmacol 48: 838–841

17 Kobayashi Y (1974) Quantitative and electron microscopic studies on the pars intermedia of the hypophysis. Alterations of the pars intermedia and the adrenal zona glomerulosa of albino mice following sodium restriction. Annot Zool Jap 47: 221–231

18 Kobayashi Y (1974) Quantitative and electron microscopic studies on the pars intermedia of the hypophysis. Effect of short-term administration of a sodium deficient diet on the pars intermedia of mice. Cell Tissue Res 154: 321–327

19 Kobayashi Y, Kumazawa T, Takeuchi M (1984) A new method for inducing copious drinking and the accompanying stimulation on the pars intermedia of the mouse pituitary gland. Arch Histol Jap 47: 71–77

20 Kobayashi Y, Okada M (1990) Urea stimulation of pituitary pars intermedia cells of suckling under copious drinking. Zool Sci 7: 281–286

21 Kobayashi Y, Takema M (1976) A morphometric study on the pars intermedia of the hypophysis during impairment of the renin-angiotensin-aldosterone system in sodium depleted mice. Cell Tissue Res 168: 153–159

22 Kurosumi K, Tanaka S, Taniguchi Y, Tokuyasu K (1986) Differential subcellular localization of ACTH and related peptides in rat anterior pituitary corticotrophs. In "Pars Distalis of the Pituitary Gland-Structure, Function and Regulation" Ed by F Yoshimura, A Gorbman, Excerpta Medica, Amsterdam, pp 163–169

23 Moriarty GC, Halmi NS, Moriarty CM (1975) The effect of stress on the cytology and immunohistochemistry of pars intermedia cells in the rat pituitary. Endocrinology 96: 1426–1436

24 Nakanishi S, Inoue A, Kita T, Nakamura M, Chang AC, Cohen SN, Numa S (1979) Nucleotide sequence of cloned cDNA for bovine corticotropin-beta-lipotropin precursor. Nature 278: 423–427

25 O'Donohue TL, Dorsa DM (1982) The opiomelanotropinergic neuronal and endocrine systems. Peptides 3: 353–395

26 Osamura RY, Murakoshi M, Inada R, Horiuchi T, Watanabe K (1992) Biological aspects of pituitary turmors induced by synthetic salmon calcitonin (TZ-CT) in Sprague-Dawley rats. Acta Pathol Jpn 42: 401–407

27 Perryman EK (1974) Fine structure of the secretory activity of the pars intermedia of Rana pipiens. Gen Comp Endocrinol 23: 94–110

28 Raisz LG, Au WYW, Friedman J, Niemann I (1967) Thyrocalcitonin and bone resorption. Studies employing a tissue culture bioassay. Am J Med 43: 684–690

29 Saland LC (1978) Effects of reserpine administration on the fine structure of the rat pars intermedia. Cell Tissue Res 194: 115–123

30 Tatematsu M, Fukushima S, Aoki T, Mera Y, Inoue T, Ito N (1987) Patterns of epithelial proliferation revealed by continuous administration of bromodeoxyuridine during urinary bladder carcinogenesis in rats. Jpn J Cancer Res 78: 879–882

31 Tilders FJH, Smelic PG (1977) Direct neural control of MSH secretion in mammals: The involvement of dopaminergic tuberohypophysial neurons. Front Hormone Res 4: 80–93

32 Weman B, Nobin A (1973) The pars intermedia of the mink, Mustela vison. Fluorescence, light and electron microscopical studies. Z Zellforsh 143: 313–327

ZOOLOGICAL SCIENCE 11: 871–878 (1994)

Variation in the Composition of the Ruminal Bacterial Microflora during the Adaptation Phase in an Artificial Fermentor (Rusitec)

SYLVIE PREVOT[1], JEAN SENAUD[1], JACQUES BOHATIER[1,2] and GÉRARD PRENSIER[1]

[1]*UA CNRS 138 "Biologie Comparée des Protistes", Université Blaise Pascal (Clermont-Ferrand II), Complexe Scientifique des Cézeaux, 63 177 AUBIERE Cedex, and* [2]*Laboratoire de Biologie cellulaire, Faculté de Pharmacie, Université d'Auvergne (Clermont-Ferrand I), 28 place Henri Dunant, 63 001 CLERMONT-FERRAND Cedex, France*

ABSTRACT—The RUSITEC system, in its present design, could not maintain microbial populations in conditions comparable to those encountered "*in vivo*". During the adaptatin period, the microfauna and microflora underwent quantitative and qualitative variations (decrease by almost 99% of the ciliate population). Ten bacterial species, which were specifically identified and counted by immunofluorescence, increased during the first two days after the inoculation of the fermentation units. This loss of balance in the indigenous rumen microbial populations suggested that essential interactions occurred between bacteria and between ciliates and bacteria. In RUSITEC at the end of the adaptation phase, as in defaunated animals, propionate productions increased (while acetate productions were reduced) and there were qualitative in the bacterial populations. However, there were differences in the nature of these populations, since in RUSITEC methanogenesis was not inhibited and total VFA production remained stable.

INTRODUCTION

RUSITEC (rumen simulation technique) [6], is a semi-continuous device designed to simulate the functions of the rumen, which is a natural fermentor in the digestive tract of ruminants. *In vivo*, this gastric compartment harbours a large number of anaerobic microorganisms (protozoa, bacteria and fungi) which act in the degradation of the feed ration ingested by the animal. Our understanding of how the fermentative processes become established "*in vitro*" in this kind of fermentor is still incomplete because not enough is known about the behaviour of the different bacterial species. One of the main difficulties in making population counts is a great specific diversity of the groups of bacteria.

So, in this work, we have studies 10 bacterial species with enzymatic abilities representative of the ruminal microflora, and we have followed their evolution by indirect immunofluorescence during the crucial period of stabilization of the fermentative processes, which corresponds to the adaptation phase of the artificial system.

MATERIALS AND METHODS

We have used the RUSITEC fermentation system as previously described by Czerkawski and Breckenridge [6]. Ground lucern hay (15g dry matter) was placed in 8×13 cm nylon bags having a 250 μm porosity. The characteristics of the substrate have been detailed elsewhere [13]. The two fermentation units used, fermentor I and II, were perfused with a solution of artificial saliva, prepared according to Mc Dougall's formula [19] with a delivery rate of 0.03 h-1. The experiment was made during the adaptation phase of the fermentors, the first week after the initial inoculation (days 1 to 5). Microbial counts and analysis of the fermentative parameters were made in the "*sensu stricto*" liquid phase of the reactors [21] at different times before (T0) and after introduction of the lucern hay (T1.5h, T3h, T5h, T7h, T10h, T14h, T19h and T24h=T0 of the following day). In this work, we have chosen to analyse only the liquid phase, because the sampling times were too close to allow a good regeneration of the fermentative conditions if we had taken samples on the solid and the liquid-associated-to-the-substrate phases (these samplings need an opening of the fermentation units). A further publication will compare the microbial populations and the fermentative parameters between the three phases.

Inoculation and running of the system

The two fermentors were intially inoculated with both a liquid and a solid fraction sampled from fasted sheep fitted with rumen canula [6]. The animals were fed with lucern and had conventional flora and fauna harbouring the 4, 5 or more common genera of protozoa (*Isotricha, Dasytricha, Epidinium, Eudiplodinium* and *Entodinium*). The rumen fluid was filtered at 39°C first on a metal grid (mesh 1.5 mm) and then on 2 layers of gauze. Five hundred ml of this homogenised filtrate were poured into each reactor followed by the same volume of a mixture of artificial saliva (300 ml) and distilled water (200 ml), adjusted to pH 7. The solid phase, which was picked up on the grid after filtration, was used to fill the bags called "initial inoculation bags" (one bag of about 50 g by reactor), providing half-digested matter and a good variety of microorganisms, attached to the plant particles. A single bag of 15 g of lucern hay was also placed in each fermentor. Throughout the experimental period, the RUSITEC was run according to the protocol of Czerkawski and Breckenridge [6].

Microbial counts

At each sampling, the ciliate protozoa were fixed by a lugol

Accepted November 14, 1994
Received April 5, 1994

solution, in Dolfuss jars and counts were made immediately afterwards [22]. The bacterial samples (1 ml of "fermentor fluid" fixed with 1 ml of neutralized formalin at 4% in PBS buffer) were kept at 4°C. Indirect fluorescence counts of total bacteria were made after staining with acridine orange (AO), which is a commonly used method [2, 7, 9] and which has been adapted to the rumen ecosystem [21]. The staining of bacteria was made by mixing 1 volume of the diluate sample with 1 volume of an acridine orange solution at 2% (w/v); after 10 min, this solution was filtrated on a polycarbonate filter (Irgalan blue Nuclépore DMF 25 mm, porosity 0.2 μm) using a vacuum system. Some drops of Triton X-100 were put before filtration on the filter, to minimize the ground fluorescence and to obtain a more homogeneous distribution of the bacteria. The filters were then put on a slide and were observed under an epifluorescence microscope (×575).

For immunofluorescence counts, specific antibodies were raised against the 10 species having fermentative, hydrolytic and/or methanogenic activities representative of rumen bacteria (see Table 1). All strains were obtained from INRA collection (Zootechnical Center of Clermont-Theix, France). The antibodies (A.B.) were prepared in our laboratory with pure strains injected in white New Zealand rabbits, according to the technique of Conway de Macario et al. [4]. A first series of experiments showed that no cross-reactions could be detected between the different species of bacteria with our A.B., and that their S titre varied between 1/400 and 1/800 and their T titre between 1/32 000 and 1/64 000. The primary A.B. were used at a 1/100 concentration with an incubation of 30 min in a damp chamber at 39°C. They were then visualized by binding with a goat-anti-rabbit IgG conjugate (FITC) with a concentration of 1/100 in the same conditions as for primary A.B. Bacterial counts were made on slides and were observed under an epifluorescence microscope (×575).

We have based our counting technique on that of Ogimoto [20], i.e. we have counted only some fields of a known area and then we have estimated the total bacterial concentration. For that, we have also determined the surface of each "dried drop" of bacterial deposit, which was an ellipse; the two diameters were measured under microscope (×575) with a squared reticle (10×10), which was also used as counting field. To minimize the heterogeneity of bacterial distribution of the deposit, we have used a low dilution rate for samples ($2.5\ 10^{-2}$), with a drop volume of 2 μl. As we have considered that the average concentration of total bacteria in the rumen fluid was 10^{10} cells/ml (see results), the deposit volume was equivalent to 5.10^5 bacteria/drop.

Microscopic examination has confirmed the low heterogeneity in cell distribution. We have counted x fields having an area of s μm^2 (the fields were selected both at the periphery of the drop and near the center), and so we have obtained ($m \pm \sigma$) bacteria counted in a single field. Using the formula for total bacterial counts after AO staining [21], we have obtained:

$$\frac{mS\ 10^6}{sv} \pm \frac{\sigma S\ 10^6}{sv} \text{ cells/ml}$$

where $S = \pi\ DI/4$ (D and I being the 2 diameters of the elliptic drop) and v the volume of the sample including the dilution rate ($v = 5.10^{-5}$ ml). Generally, and because of the quick fading of fluorescence, we used to count $x = 5$ fields.

To calculate the percentage of the 10 bacterial species counted by immunofluorescence in relation to the total population (stained by AO), we have determined the cell concentration of some pure cultures with both methods and we have compared the results to determine a corresponding factor. The Table 2 gives example of some results obtained with two pure cultures of bacteria. We have checked that the difference between the two methods was almost constant whatever can be the strain, but depended of the worker. Here, the same experimenter had counted the bacteria.

Fermentative parameters

At each sampling, the pH and the redox potential were measured with a Schott-Gerate CG 817-T apparatus equipped with a 1042 A (pH) or a Pt 42A (mV) electrode. Ammonia nitrogen ($N\text{-}NH_3$) content was measured according to the method of Weaterburn [23]. The analysis of short-chain organic acids (volatile fatty acids = VFA) was made in a gaseous phase chromatograph fitted with a flame ionization detector [15]. The gas mixture produced was also analy-

TABLE 1. Morphological and metabolic specifications of the 10 bacterial species belonging to the AB flora (see text)

Bacteria	Strains	Form	Gram	Ferm. subst.	Gas	Products
S. bov	FD10	C	+	S, Ce, P, SS		L (A, F)
R. fla	007	C	+	C, Ce	CO_2, H_2	A, Sc (F, L)
R. alb	7	C	+	C, Ce	CO_2, H_2	A, E (F, L)
E. cel	C	R	+	C, Ce		A, B, F, L, Sc (Pr)
E. lim	20543	R	+	Ce	CO_2, H_2	
M. rum	Mr	R	+	H	CH_4	
F. suc	S 85	R	−	S, C, Ce		A, Sc
S. rum	W	R	−	S, GI, L, P, SS	H_2S	A, L, Pr (Sc)
L. mul	LM	R	V	S, Ce, P, Pe	CO_2, H_2	A, E, F, L, Sc
B. fib	D1	R	V	S, C, P, SS	CO_2, H_2, H_2S	F (A, B)

S. bov: Streptococcus bovis
R. alb.: Ruminococcus albus
E. lim: Eubacterium limosum
F suc: Fibrobacter succinogenes
L. mul: Lachnospira multiparus
R. fla: Ruminococcus flavefasciens
E. cel: Eubacterium cellulosolvens
M. rum: Methanobrevibacter ruminantium
S. rum: Selenomonas ruminantium
B. fib: Butyrivibrio fibrisolvens

C: cocci; R: rod; +, − and V: positive, negative and variable Gram staining; Ferm. subst.: fermented substrates; Ce: cellobiose; C: cellulose; Gl: glucose; H: hydrogen; L: lactate; P: proteins; Pe: pectines; S: starch; SS: soluble sugars; Products: A: acetate; B: butyrate; E: ethanol; F: formate; L: lactate; Pr: propionate; Sc: succinate.

TABLE 2. Comparison between the 2 numbering methods ($\times 10^9$ cells/ml)

Bacteria	S	AB	AO
R. flavefasciens	1	4.27	7.12
	2	3.55	6.46
	m	3.91±0.55	6.79±0.47
	D	−42.4%	100%
F. succinogenes	1	3.12	5.30
	2	2.86	4.44
	m	2.99±0.18	4.87±0.61
	D	−38.6%	100%
	M	−40.5%	100%

AB: immunological counts (antibodies): AO: counts by Acridine Orange; D: difference in % between the 2 methods for a specific bacterial strain; m: average value for 2 samples (S1 and S2) by a given method; M: total average percentage of dissapearance.

sed by gas-chromatography at 80°C (Girdel 30 apparatus) [15].

RESULTS

Ciliates

During the adaptation phase, the ciliates population decreased by almost 99% falling from 10^5 cells/ml after inoculation (D1, T0) to 10^3 cells/ml at D5 T24h (Figure 1A). Slight variations in the total number of ciliates were observed in the liquid phase, but there was no regular daily fluctuation. This overall pattern involved all the present ciliates: *Entodinium, Isotricha, Dasytricha, Epidinium* and *Eudiplodinium*. This last genus disappeared entirely from the liquid phase after 4 days of running (Figure 1B). The decrease in numbers was observed in both fermentation units and was greatest during the first 48 hours: the total ciliate density was 93% lower than the start density by the beginning of the third day (D3, T0) (Figure 1A). At the end of the experimental period, only the ciliates belonging to the genus *Entodinium* were present in large numbers.

Bacteria

Bacterial counts on pure culture obtained with the immunofluorescence method which used specific antibodies were 40% lower than those yielded by epifluorescence after AO staining (see Table 2). This lower result of AB staining, compared with the AO one, probably came from the washings made to eliminate the AB-FITC solution. In all the following results, the values concerning the 10 bacterial species have been corrected by the corresponding factor. Although less marked than in the ciliates, the decrease in the total number of bacteria reached an average of 70% during

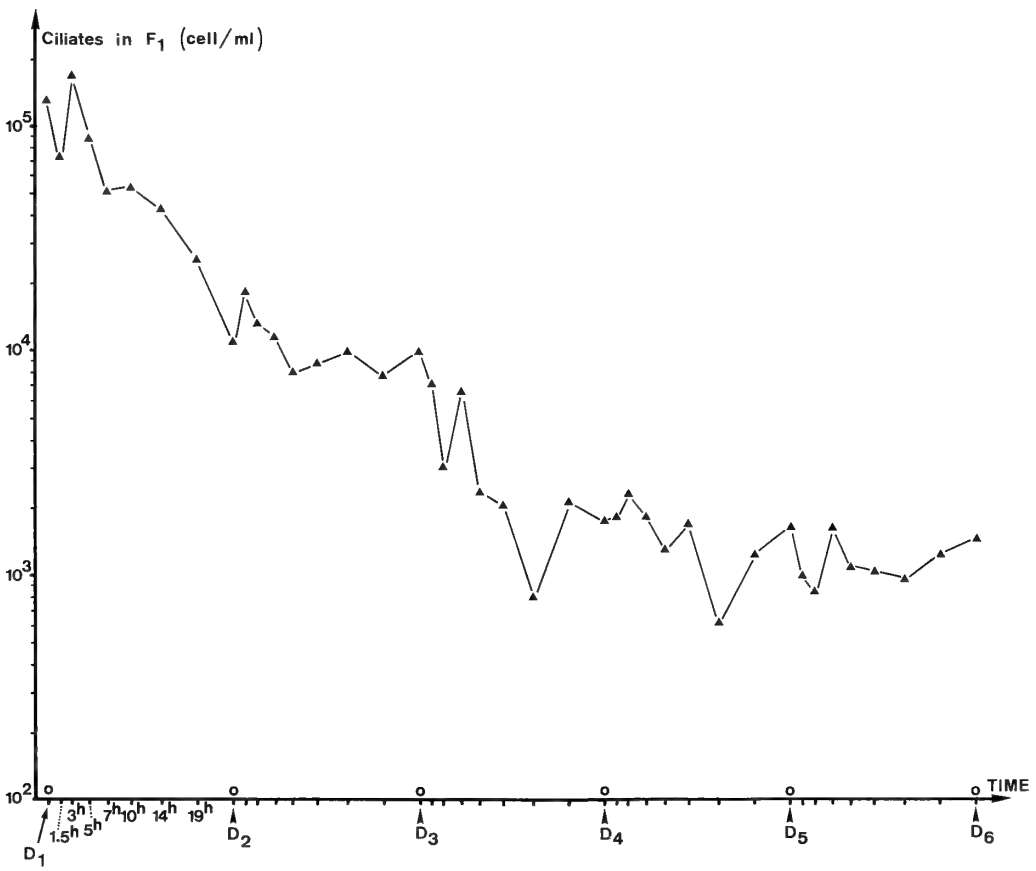

FIG. 1A. Evolution of the total ciliate population during the adaptation period (D1 to D6: example, fermentation unit 1).

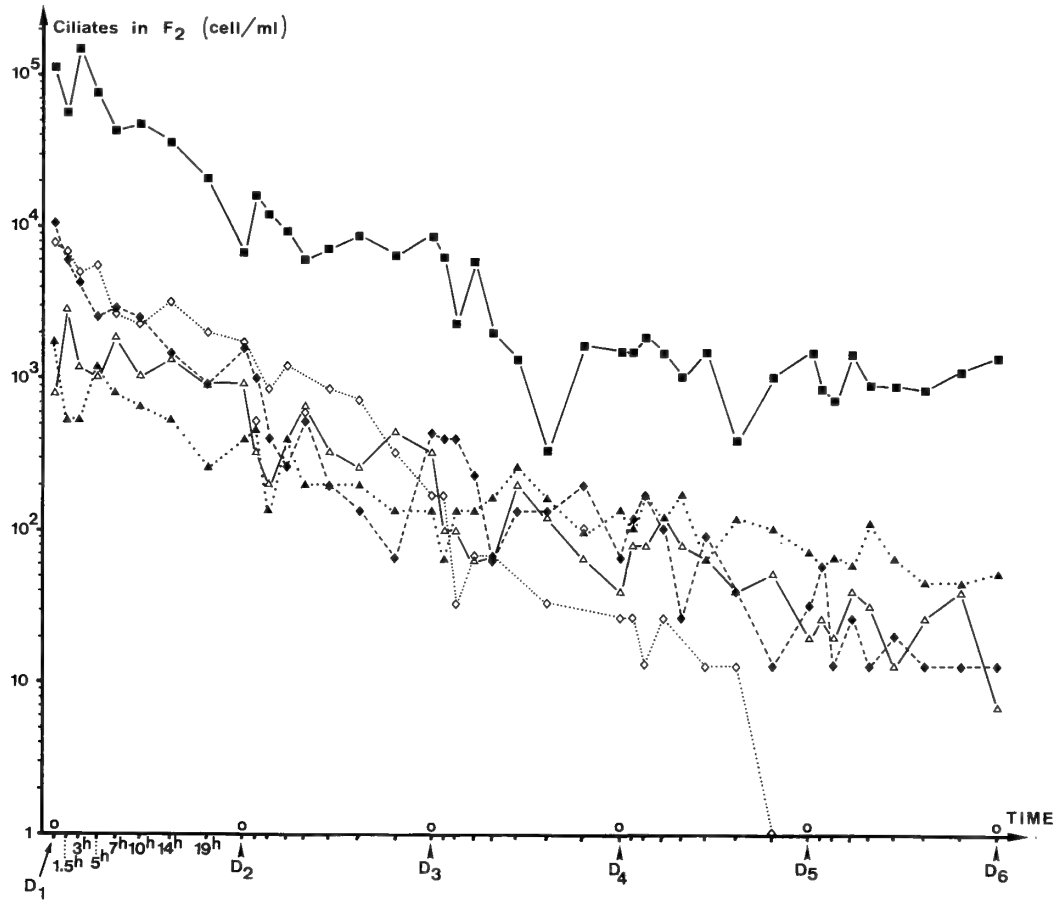

FIG. 1B. Evolution of the different ciliate populations during the adaptation period (D1 to D6: example, fermentation unit 2). △: *Isotricha*; ▲: *Dasytricha*; ◆: *Epidinium*; ◇: *Eudiplodinium*; ■: *Entodinium*.

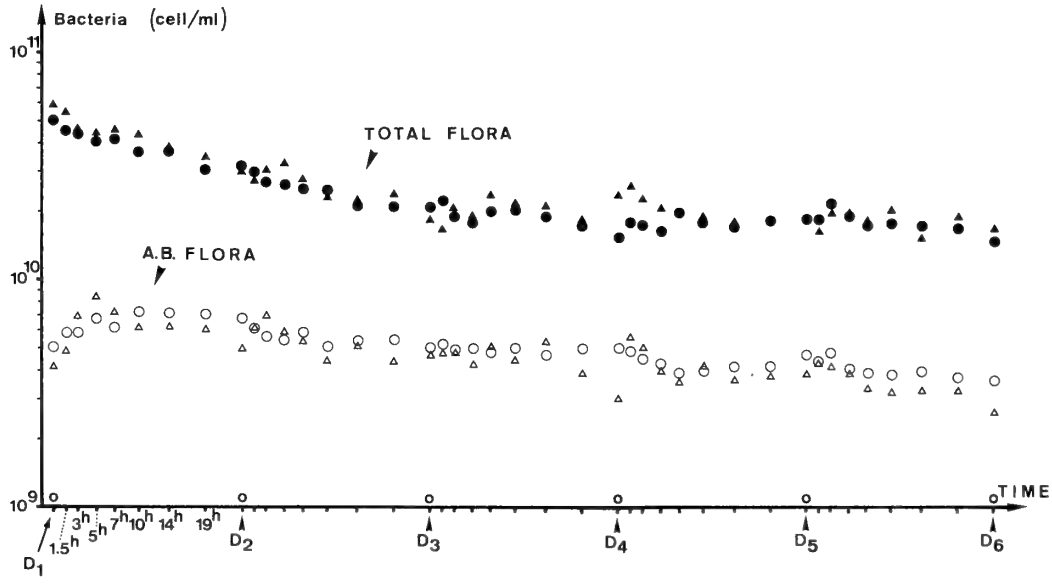

FIG. 2. Evolution of the total bacterial population (black symbols) and of the AB flora (see text) (while symbols) in the 2 fermentors. F1: triangles; F2: circles.

the adaptation phase of RUSITEC (Figure 2), and, as in the former population, the decrease was greatest during the 2 first days (−58% in one fermentation unit and −69% in the other).

The predominant type of bacteria was cocci, which were observed throughout the experimental period at an almost constant level of 86% (Table 3). Bacteria staining by AO appear red or green, depending on the cellular concentration

TABLE 3. Average percentage of cocci during the different experimental days (D) in the 2 fermentation units

Day	F1	F2
1	86.2±0.9	86.1±1.1
2	86.8±1.5	86.0±1.7
3	86.4±1.9	86.3±3.2
4	85.6±2.1	84.9±3.3
5	86.5±1.6	86.0±2.3

of nucleic acids (DNA and RNA): the red bacteria (full of RNA) are considered as the most physiologically active cells, and the green ones (where the RNA concentration is too low to hide the green fluorescence of DNA) are considered as the less active cells [21]. These results are related to the ATP, ADP and AMP levels [21].

In our experiment, the percentage of red bacteria varied 72 to 66% in one fermentor and from 73 to 66% in the other, during the adaptation period, and in particular during the first 2 days after inoculation (Table 4). The total bacterial concentration was equivalent to the sum of red and green bacteria. The 10 bacterial species selected for counts represented 7 to 10% of the initial inoculum (=total inoculum) (Table 5). Unlike in the overall population (total flora), the numbers of bacteria recognised by their specific antibodies (AB flora) increased during the first 2 days (Figure 2), by 40 to 42% depending of the fermentation unit (Table 6). Of the 10 species which were immunologically recognised, the most abundant were *Ruminococcus albus, R. flavefasciens, Methanobrevibacter ruminantium* and *Fibrobacter succinogenes*, and the less abundant *Butyrivibrio fibrisolvens* and *Lachnospira multiparus* (Table 5). The statistical comparisons (Student's test) made between the daily average percentages of each of the 10 species showed that their distribution range was not modified during the adaptation period (Table 6).

TABLE 4. Daily average values (%) of red bacteria (after AO staining) in the 2 fermentors

Day	F1	test	F2	test
1	73.4±2.7	1–2	71.7±1.3	1–2#
2	70.5±2.4	2–3#	69.2±1.4	2–3
3	65.4±2.6	3–4	66.9±2.8	3–4
4	67.2±3.1	4–5	65.3±2.2	4–5
5	67.6±3.6	1–5#	65.8±1.8	1–5#
		2–5		2–5#

#: significant difference (Student test, α=5%). We have: 100% of bacteria=red bacteria+green bacteria.

TABLE 5. Density of specifically labelled bacterial populations ($\times 10^8$ cells/ml) and percentages in comparison with the total bacterial population (AO counts) (day 1, T0)

Bacteria	F1		F2	
	numbers	%	numbers	%
R. alb	6.05±0.91	1.03±0.16	7.74±0.92	1.54±0.18
R. fla	5.91±1.29	1.01±0.22	7.59±0.41	1.51±0.08
F. suc	3.68±0.77	0.63±0.13	4.91±1.12	0.98±0.22
S. bov	3.74±0.84	0.64±0.14	3.98±0.39	0.79±0.08
M. rum	2.81±0.29	0.48±0.05	6.26±0.43	1.25±0.09
S. rum	5.10±0.85	0.87±0.14	4.48±0.74	0.89±0.15
E. cel	3.61±1.08	0.61±0.18	6.43±0.42	1.28±0.08
E. lim	5.04±1.20	0.86±0.20	3.64±0.25	0.73±0.05
B. fib	3.82±0.83	0.65±0.14	3.44±0.22	0.69±0.04
L. mul	2.17±0.63	0.37±0.11	2.69±0.24	0.54±0.05
Total	41.93±8.69	7.15±1.47	51.16±5.14	10.20±1.02

TABLE 6. Statistical comparisons (Student test: α=5%) of the daily average concentrations of the 10 specifically labelled bacteria (AB flora): days 1 to 5 (D1 to D5)

Bacteria	D1-D2	D2-D3	D3-D4	D4-D5	D1-D5	D2-D5
R. alb	*+		°−		°+	°+
R. fla	*+		*−		*+	°+
F. suc	°+	°+	°−		*+	
S. bov	*+	°+	°−		*+	
M. rum	*+	°+			*+	
S. rum	°+	°+			°+	
E. cel	°+	°+			°+	
E. lim	°+	*+			*+	°+
B. fib		°+			*+	
L. mul	*+	°+	°−		*+	°+

*: significant difference in the 2 fermentation units; °: significant difference in a single fermentation unit; + and −: general evolution.

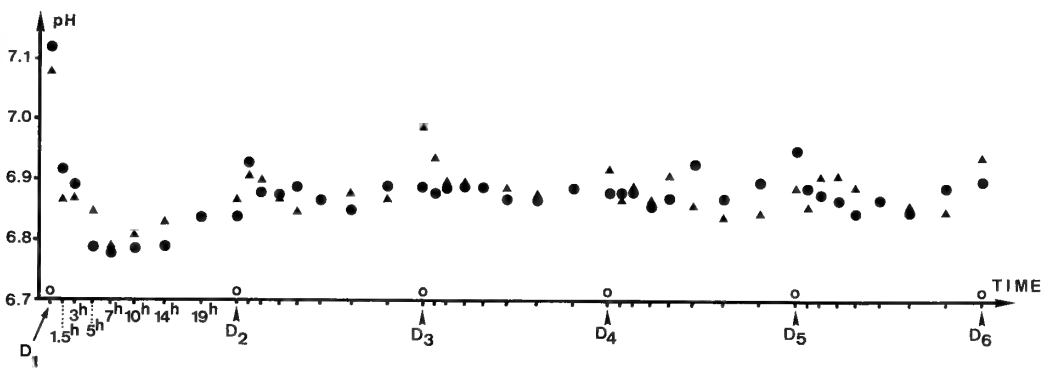

FIG. 3. pH evolution in the 2 fermentation units. F1: triangles; F2: circles.

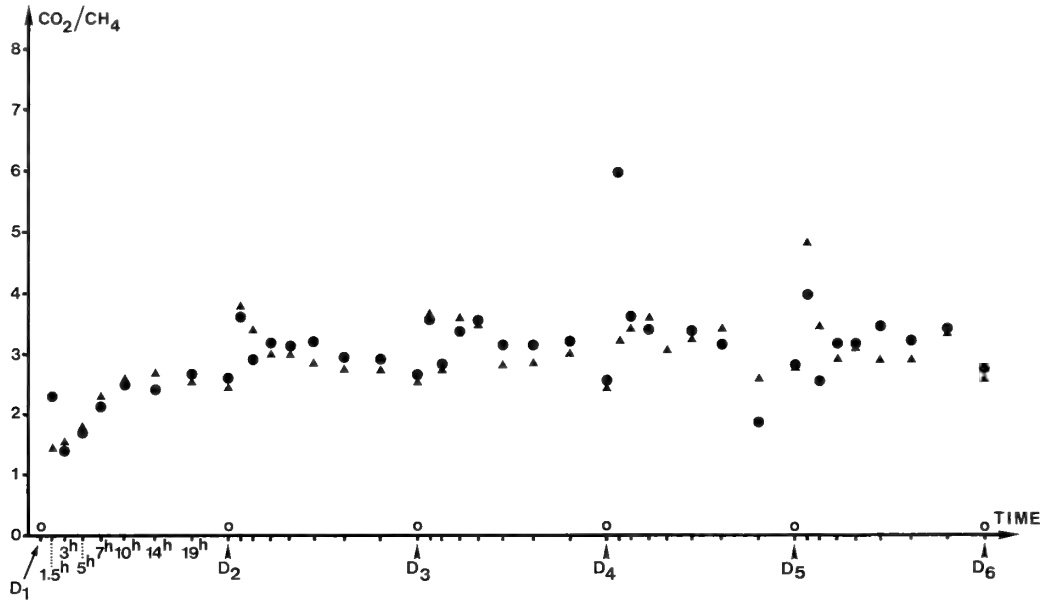

FIG. 4. Evolution of the CO_2/CH_4 ratio in the 2 fermentation units. F1: triangles; F2: circles.

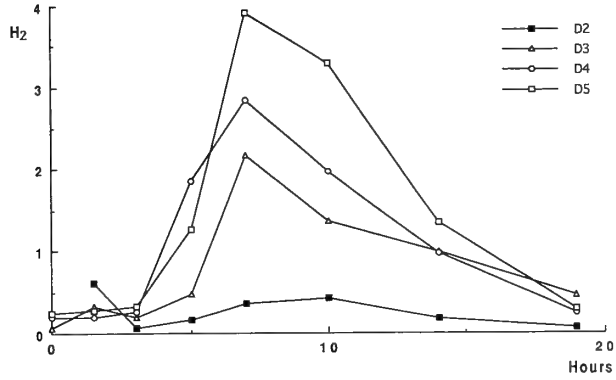

FIG. 5. Evolution of hydrogen concentration (% in the gas mixture) during the adaptation period: days 2 to 5 (D2 to D5) (example: fermentation unit 1).

Fermentative parameters

The fermentative profile obtained during the adaptation period was satisfactory in spite of the decrease in the microbial populations since, at the end, the remaining bacteria were able to maintain the fermentation process. The redox potential varied between −320 and −360 mV and the pH between 6.8 and 7.0 (Figure 3), values which were compatible with the survival of the microorganisms. Gas production showed very little variations during the experimental period. The high proportion of CO_2 in the gas mixture produced (73–78%) shows that anaerobic conditions in the fermentors were well sustained. The proportion of methane ranged from 20 to 30%: it was greatest at T0, decreased at T1.5h and rose again sharply at T3h. The CO_2/CH_4 ratios varied between 2 and 4, and were highest at T1.5h (Figure 4). Hydrogen production followed a regular daily pattern: peak concentrations occurred between T7h and T10h, and were higher at the end of the experimental period (D4, D5) (Figure 5).

Apart from the fluctuations observed on D1, there was a gradual decrease in N-NH3 production (Table 7) during the adaptation phase, while that of the volatile fatty acids remained fairly stable at around 72–76 mM/l (Table 7). Analysis of the percentage of each VFA produced in the mixture showed a change in the fermentation profile during the adaptation period in both fermentors (Tables 8 and 9). The proportion of acetic and butyric acids decreased, from 70 to 65.5% and 1.2 to 0.7% respectively, while that of propionic, butyric valeric and caproic acids increased, from 18 to 20%, 7.3 to 9.4%, 1.5 to 2.0% and 0.15 to 0.40% respective-

TABLE 7. Daily average values of ammonia (mg/l) and VFA (mM/l) productions in the 2 fermentation units (F1 and F2)

Day	NH^3				VFA			
	F1	test	F2	test	F1	test	F2	test
1	106.3	1–2#	110.9	1–2#	52.33	1–2#	58.84	1–2#
2	150.6	2–3#	140.3	2–3	74.19	2–3	72.25	2–3
3	115.4	3–4#	143.1	3–4#	75.79	3–4	73.66	3–4
4	90.0	4–5	109.7	4–5	76.22	4–5	71.24	4–5
5	83.8	1–5	90.3	1–5	77.41	1–5#	74.36	1–5#
		2–5#		2–5#		2–5		2–5

Statistical comparisons (Student test: α=5%). #: significant difference.

TABLE 8. Daily average percentages of the different VFAs produced (example: fermentation unit 1)

Day	C2	C3	IC4	C4	C5	C6
1	69.60±0.80	18.56±0.16	1.17±0.07	7.28±0.44	1.45±0.16	0.15±0.01
2	68.54±0.71	19.11±0.32	1.08±0.08	7.66±0.47	1.57±0.05	0.17±0.02
3	68.17±0.39	19.62±0.25	0.85±0.09	7.96±0.41	1.59±0.05	0.21±0.01
4	66.69±0.86	19.94±0.49	0.71±0.09	8.86±0.42	1.82±0.11	0.30±0.03
5	65.56±0.93	20.03±0.28	0.72±0.05	9.38±0.67	1.98±0.06	0.41±0.03

C2: acetic acid; C3: propionic acid; IC4: isobutyric acid; C4: butyric acid; IC5: isovaleric acid; C5: valeric acid; C6: caproic acid.

TABLE 9. Statistical comparisons (Student test: $\alpha=5\%$) of the daily percentages of each VFA produced in the mixture: days 1 to 5 (*D1 to D5*)

VFA	D1-D2	D2-D3	D3-D4	D4-D5	D1-D5	D2-D5
C2	*−	°−	*−	°−	*−	*−
C3	*+	*+			*+	*+
IC4	*−	*−	°−		*−	*−
C4	°+		*+		*+	*+
IC5			*−		*+	
C5		°+	*+	*+	*+	*+
C6	*+	*+	*+	*+	*+	*+

*: significant difference in the 2 fermentation units; °: significant difference in a single fermentation unit; + and −: general evolution.

ly. The proportion of isovaleric acid was at a stable level of 1.7% on average (Table 8).

DISCUSSION

Microorganisms

The considerable decrease in the ciliate and bacterial populations (−99% and −70% respectively) did not result in correspondingly adverse effects on the overall fermentation profile: VFA production during the adaptation phase remained high (72–76 mM/l), as did the production of methane (25–30%) and ammonia (higher than 50 mg/l), in spite of the fact that dilution rate of the liquid phase was 0.03h-1. At the end of the experimental period (from D3 to D5, T24H), The remaining bacterial species-like those of the AB flora-seemed to possess the multienzymatic abilities to achieve successfully the fermentation. There are various possible reasons for the decrease in the ciliate and bacterial populations, related to both the design and the running of RUSITEC: presentation of the substrate, mixing system, delivery and chemical composition of the artificial saliva, outflow of the liquid phase and microorganisms.

In contrast, pH values did not seem to affect the microbial populations and, like the values of the redox potential, were always compatible with the survival of the cells. It is also possible than the decrease in cell number of Protozoa was due partly to modification of essential interactions between ciliates and bacteria. Various authors have shown that ciliates can be selective predators for bacteria [1, 3, 8, 24]. The absence of certain bacterial species, as the result of the *in vivo-in vitro* transition, could therefore have a direct effect on one or several ciliate genera. Likewise, in the symbiotic-type relations between bacteria [5] or between ciliates and bacteria, the cell deficit in some bacterial populations, or a metabolic deficiency in the fermentor, could affect the development and the maintenance of the other populations [11, 12].

The evolution of the AB flora showed that during the adaptation period of RUSITEC there was a qualitative change in the bacterial populations, since the total and relative percentages of the bacterial species which were specifically recognized increased during the first 2 days of the experimental period. There are two possible explanations for this change: 1) there was a selection in the AB flora of populations that were better adapted to the culture conditions of RUSITEC; 2) there was a decrease in the number of other bacteria (that were not counted by AB but only by AO), because they were more "sensitive" to the same conditions. These two possibilities should be taken into account since it is likely that the strains of the AB flora are among the most easily isolated bacteria and therefore the less sensitive to the changes in physiological conditions.

The increase in the number of bacteria in the AB flora was accompanied by a decrease in that of the ciliates populations, and these two facts may be correlated. However, the decrease in ciliate numbers cannot be positively attributed to some variation in the AB flora. It would be of interest to do further studies using other immunological markers. The decrease in the percentage of red bacteria (which are the most physiologically active cells) was observed mainly during the first two days, which lends weight to the hypothesis that a certain microbial "stress" occurred when the fermentors were inoculated. This fact was correlated to the increase of the percentage of green bacteria, less active than the red ones (as we have total bacteria=red+green bacteria).

Fermentative parameters

In the RUSITEC content at the end of the experimental period, there was a variation in the composition of the VFA produced, similar to that observed in comparisons of the faunated and unfaunated states *in vivo* [16]. In particular there is a reduction of acetate production which could be due in part to the fact that ciliates producing acetic acid during carbohydrate fermentation [10] were only present in very small numbers at the end of the experimental period. This

reduction leads to an increase of the relative percentage of propionate which could also be the reflect of non optimal conditions for methanogenesis. Hence, since propionic acid has an inhibitory effect on protozoa [18], a rise in its proportion could increase the extent of disappearance of the ciliates.

The metabolic pattern of VFA formation in RUSITEC could also come from a shift in production from acetyl-coA to butyrate, which would decrease the production of acetate, as observed in the rumen of defaunated animals receiving a diet rich in carbohydrates [16]. Because the ciliates populations were smaller during the second half of the experimental period, they had less effect on proteolysis, and this may have contributed to the decrease in total ammonia production observed in the contents of fermentors. As the amount of amino-acids produced by the degradation of proteins and alimentary peptides decreased, the production of ammonia from these metabolites was also lower.

Fermentation in the RUSITEC system at the end of the adaptation period is similar to that in defaunated animals, and in both cases there are qualitative variations in the composition of the bacterial populations [13, 15]. However the composition of the bacterial populations is not probably the same since, unlike in defaunated animals [12], the total VFA production in RUSITEC did not decrease during the experimental period and the methanogenesis was not inhibited.

CONCLUSION

The RUSITEC system, as designed by Czerkawski and Breckenridge in 1977, is an interesting technique fot studying fermentation "*in vitro*", but can only simulate "*in vivo*" defaunated states. In its present form, the RUSITEC system cannot reproduce the "*in vivo*" state of conventionally reared animals: ciliate populations are eliminated in the fermentor and probably many bacterial species too, and so certain parameters need to be studied and perhaps modified.

Modifications could be made on the physical parameters (such as variations in the rate of artificial saliva, changes in the form of substrate, addition of a solid matrix to increase the retention of the ciliates) on the chemical parameters (such as a second inoculation with new microorganisms at the end of the adaptation period).

The desappearance of ciliates in RUSITEC is due to a loss of balance in the bacterial populations. Recognizing one bacterial species amongst all the others in the rumen is still a difficult problem to surmount. However, techniques using immunological markers to recognize bacteria may lead to a better understanding of the intricate microbial interactions that occur between ciliates and bacteria in the rumen ecosystem.

REFERENCES

1 Abe M, Kandatsu M (1969) Utilization of non-protein nitrogenous compounds in ruminants. III. Ingestion of Bacteria by Protozoa in the rumen. Jap J Zootech Sc 40: 313–319

2 Bergstrom I, Heinanen A, Salonen K (1986) Comparison of acridine orange, acriflavine and bisbenzimide stains for enumeration of bacteria in clear and humic waters. Appl Env Microbiol 51(3): 664–667

3 Coleman GS, Sandford DL (1979) The engulfment and digestion of mixed rumen bacteria and individual species of rumen ciliates protozoa grown *in vivo*. Agr Sc 92: 729–742

4 Conway de Macario E, Macario AJL, Wollin MJ (1982) Specific antisera and immunological procedures for characterization of methanogenic bacteria. J Bact 149: 320–328

5 Costerton JN, Geesey GG, Cheng KJ (1978) How bacteria stick. Sci Ann 238: 86–95

6 Czerkawski JW, Breckenridge G (1977) Design and Development of a long term rumen simulation technique (RUSITEC). Br J Nut 38: 371–384

7 Delattre JM (1986) Le contrôle bactérien rapide des eaux par épifluorescence. J Fr Hydrobiol 17(1): 59–70

8 Denholm AM, Ling JR (1984) *In vitro* metabolism of bacterial cell wall by rumen protozoa. Can J anim Sc 64: 18–19

9 Dutton RJ, Bitton G, Koopman B (1986) Application of a direct microscopic method of the determination of active bacteria in lakes. Wat Res 20(11): 1461–1464

10 Howard BH (1959) The biochemistry of rumen protozoa. I. Carbohydrate fermentation by *Dasytricha* and *Isotricha*. Bioch J 71: 671–675

11 Imai S, Tsunoka K (1972) Scanning electron microscopic observations on the surface structures of ciliated protozoa in sheep rumen. Nat. Inst. Am Hlta Quart 12: 74–88

12 Imai S, Ogimoto K (1978) Scanning electron and fluorescent microscopic studies on the attachment of spherical bacteria to ciliate protozoa in the ovine rumen. Jap J Vet Sc 40(1): 9–19

13 Itabashi H, Kadata A (1976) Studies on nutritional significance of rumen ciliate protozoa in cattle. 2. Influence of protozoa on amino-acids concentrations in some rumen fractions and blood plasma. Bull Tohoku Nat Agr Exp Stat 52: 169–176

14 Jarrige R (1978) Alimentation des ruminants. Act Sci Agr (INRA Pub. Ed.) pp 597

15 Jouany JP (1978) Contribution à l'étude des protozoaires ciliés du rumen: leur dynamique, leur rôle dans la digestion et leur intérêt pour le ruminant. Thèse n°256, Université de Clermont-Ferrand II pp 195

16 Jouany JP, Demeyer DI, Grain J (1988) Effect of defaunating the rumen. Ann Feed Sc Tech 21: 229–265

17 Jouany JP, Zainab B, Senaud J, Groliere CA, Grain J, Thivend P (1981) Role of rumen ciliate protozoa *Polyplastron multivesiculatum, Entodinium* sp. and *Isotricha prostoma* in the digestion of a mixed diet in sheep. Rep Nut Dev 21: 871–884

18 Kobayashi T, Itabashi H (1986) Effect of intra-ruminal VFA infusion on the protozoal population of the rumen. Bull Nat Inst An Ind 44: 47–54

19 Mc Dougall EI (1948) Studies on ruminant saliva. I. The composition and output of sheep's saliva. Bioch J 43: 99–109

20 Ogimoto K, Imai S (1981) Atlas of Rumen Microbiology. Jap Sc Soc Press pp 231

21 Prevot S, Senhaji M, Bohatier J, Senaud J (1988) Comptage par épiflurescence des bactérie du rumen, cultivées *in vitro*. Estimation de leur état physiologique. Rep Nut Dev 281(1): 137–138

22 Senaud J, Jouany JP, Grain J (1979) Influence de la fréquence des repas sur le comportement alimentaire des moutons et sur les variations de densité des populations de ciliés au cours du nycthémère. Ann Biol Bioch 17(4): 567–572

23 Weaterburn MW (1967) Phenol-hypochlorite reaction for determination of ammonia. Anat Chem 39: 871–974

24 Williams AG (1986) Rumen holotrich ciliate protozoa. Microbiol Rev 50(1): 25–49

ZOOLOGICAL SCIENCE 11: 879–882 (1994)

Is the Coelomic Plasma of *Phascolosoma arcuatum* (Sipuncula) Hyperosmotic and Hypoionic in Chloride to the External Environment?

KAH W. PENG AND YUEN K. IP

Department of Zoology, National University of Singapore, 10 Kent Ridge Crescent, Kent Ridge, Singapore 0511, Republic of Singapore

ABSTRACT—Since *Phascolosoma arcuatum* lives in the mud of the mangrove swamp, which is subjected to extremely variable salinities, the present studies were undertaken to examine if this sipunculid could, to a certain extent, regulate ions and/or volume. When acclimated to 30% or 100% seawater (SW), *P. arcuatum* maintained its coelomic plasma (CP) slightly, but significantly, hyperosmotic to the external medium. Maintenance of a slightly hyperosmotic coelomic fluid would favor a constant, yet small, osmotic water influx which would compensate for urine production and any other process by which water is lost. The Cl^- concentration in the CP of this sipunculid was always lower than that of the external medium. The difference in the Cl^- concentration between the CP and the external medium in specimens acclimated to 100% SW was greater than that in specimens acclimated to 30% SW. Specimens acclimated to 100% SW also contained significantly greater concentrations of inorganic phosphate, organic phosphates and water-soluble proteins in the CP than those acclimated to 30% SW. The hypoionic Cl^- condition in the CP of this worm might be essential for the accommodation of negatively charged organic osmolytes in the CP without violating electroneutrality. Hence, it was concluded that *P. arcuatum* could regulate to a certain extent its ionic compositions in the CP and maintain the CP hyperosmotic to the external medium.

INTRODUCTION

The question of whether sipunculids possess the ability to regulate body volume, especially in an environment of changed salinities, has been a matter of some controversy [12]. There have been studies on perhaps ten species but most of these reports are inconclusive. Some of these reports provide no data but just state that the worms do (or do not) regulate volume after a salinity transfer [13]. No species is known from areas with markedly low salinities. The only possible exception is the species *Phascolosoma arcuatum*, which was referred to as *Physcosoma lucro* by Harms and Dragendorff [6] or *Phascolosoma lucro* by Oglesby [13, 14] as reviewed by Rice and Stephens [21] and Stephens and Edmonds [24]. The high mangrove swamp habitat of this species, subjected to extremely variable salinities which is an atypical situation for a sipunculid, suggests that it may be able to regulate ions and/or volume.

The consistently hyperosmotic coelomic fluid of *P. arcuatum* [6] has been regarded as the result of active osmoregulation [5, 8]. However, Oglesby [12] suggested that such observations might have been caused by progressive desiccation in its semi-terrestrial habitat. On the other hand, Green and Dunn [4] claimed that the CP of this sipunculid kept for up to 64 hr in the laboratory in 40–100% artificial SW were uniformly isosmotic to the external media. They further reported that *P. arcuatum* showed no indication of volume recovery after a hypoosmotic or hyperosmotic salinity transfer. To date, whether *P. arcuatum* can maintain a hyperosmotic coelomic fluid to its external environment is still disputable, though it is apparent that few, if any, invertebrates are isosmotic with their environment [19]. Furthermore, although reports on the sipunculids, *Themiste dyscritum* [7], *T. signifer* [9] and *Phascolopsis gouldi* [23], confirm the Cl^- concentration of the CP to be hypoionic to that of the external medium, Green and Dunn [4] concluded that *P. arcuatum* was uniformly isoionic in terms of Cl^- to the external artificial SW. Hence, the present studies were undertaken to determine if the CP of *P. arcuatum* was hyperosmotic and hypoionic in Cl^- to its external medium. In addition, the concentrations of Na^+, HCO_3^-, inorganic phosphate (P_i), organic phosphate (P_o) and water-soluble proteins in the CP were also determined to reveal the possible contribution of organic molecules to the maintenance of electroneutrality in, and to the total osmotic concentration of, the coelomic fluid of *P. arcuatum*.

Accepted November 14, 1994
Received June 13, 1994

MATERIALS AND METHODS

Collection and maintenance of specimens

P. arcuatum were collected from the mud-flats of the mangrove swamp at Mandai, Singapore, and maintained at 25°C in the laboratory in aquaria with aerated 50% (15‰ salinity) SW. The worms were not fed. Experiments were performed after 10 days of acclimatization of the worms to laboratory conditions.

Determination of weight after transfer from 50% SW to 30% or to 100% SW

Individual worms (2.5–3.5 g) were gently blotted dry with moist filter paper, weighed and put in plastic cups containing 500 ml of 30% (9‰ salinity) or 100% (30‰ salinity) SW. Weight was measured to the nearest milligram with a Shimadzu Libror EB-280M balance.

Half of the water in the plastic cup was changed daily. At time intervals of 6 hr, 12 hr, 24 hr, 36 hr, 48 hr, 60 hr and 72 hr, the worm was carefully removed from the cup, blotted dry with moist filter paper and weighed.

Determination of water content in the tissues

In a separate experiment, worms were acclimated to either 30% or 100% SW for 48 hr. After 48 hr, the worm was sampled individually and an incision was made on the body wall to drain the coelomic fluid. The worm body was dissected open, gently blotted dry with moist filter paper, weighed and dried in the oven at 95°C to constant weight. The water content was calculated as the difference between wet weight and dry weight of the sample.

Analyses of CP and the external medium

The worms in groups of 15 were acclimated to 10 l of aerated 30% or 100% SW for 48 hr. After acclimation, a sample of the external medium to which the worms were acclimated were collected in ice-cold test-tubes and various assays were performed on them within 3 hr. The worms were quickly blotted dry. A small incision was made on the body wall, from which the coelomic fluid was drained into ice-cold test-tubes. Coelomic fluid was centrifuged at $1,000 \times g$ at 4°C for 10 min to obtain the CP. The osmolalities ($mosmol \cdot kg^{-1}$) of the CP and SW samples were determined by a Wescor 5500 Vapour Pressure Osmometer (Wescor, UT, USA). Na^+ and Cl^- concentrations were determined using a Corning 410C Flame Photometer and Corning 925 Chloride Analyzer, respectively. HCO_3^- concentration was determined by a Corning 965 Carbon Dioxide Analyzer. P_i was analyzed using a Tecator Aquatec System equipped with a Phosphate Cassette according to the Tecator Application Note ASN 146-05/90. Total phosphate (P_T) and protein analyses were performed on the CP of *P. arcuatum* only. P_T was assayed by the Tecator Aquatec System following the Application Note ASN 147–05/90. P_o concentration was calculated as the difference between the concentrations of P_T and P_i. Water-soluble protein present in the CP was determined by the method of Bradford [2]. Bovine gamma globulin dissolved in 25% glycerol was used as a standard for comparison.

Statistics

Results were presented as means ± standard error (SE). Student's *t* test was used to compare differences between means. Differences with $P<0.05$ were regarded as statistically significant.

RESULTS

After being transferred from 50% SW to 30% SW, *P. arcuatum* rapidly gained weight (14% after the first 6 hr of exposure), presumably due to an osmotic influx of water (Fig. 1). Conversely, specimens transferred from 50% SW to 100% SW for 6 hr lost 31% of their initial body weight (Fig. 1). This sipunculid was able to recover its volume partially from the water gained and lost in 30% SW and 100% SW, respectively, and reached a steady state after 48 hr. The water content in the body tissues increased from 72.7±1.1% in 50% SW to 77.4±0.4% after 48 hr in 30% SW. The water content in the body tissues of worms acclimated to 100% SW for 48 hr was 68.0±0.3%, a loss of 4.7% compared to that of the worms kept in 50% SW. Since *P. arcuatum* appeared to reach a steady state with its environment after 48 hr, all subsequent experiments were performed with worms acclimated to 30% or 100% SW for this period of time unless

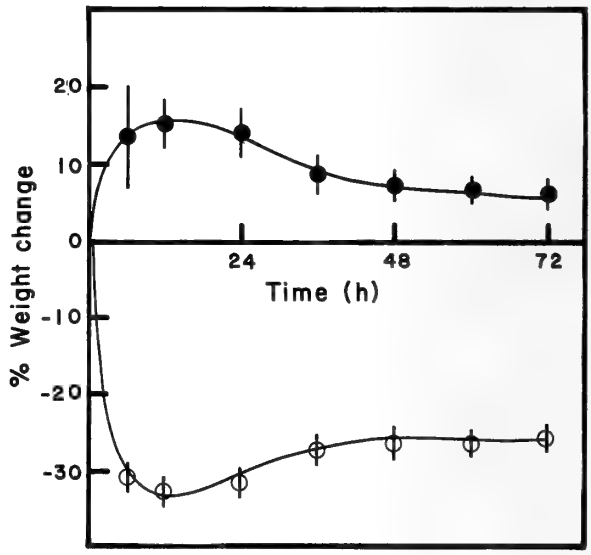

FIG. 1. A time course study on the percentage of weight change in *P. arcuatum* after it has been transferred from 50% SW to 30% SW (●) or 100% SW (○) for three days. Each point represents the average weight of 7 individuals. Verticle bars show standard errors.

TABLE 1. Osmolality ($mosmol \cdot kg^{-1}$) of and Na^+, Cl^-, HCO_3^- and P_i (inorganic phosphate) concentrations (mM) in the external medium (EM) in which specimens had been kept for 48 hr and the coelomic plasma (CP) of *P. arcuatum* exposed for 48 hr to 30% or 100% SW

SW	Sample	Osmolality	Na^+	Cl^-	HCO_3^-	P_i
30%	EM	310.9±2.0 (7)	136.5±0.6 (6)	180.3±1.3 (7)	1.46±0.06 (7)	0.0029±0.0001 (7)
	CP	316.9±1.3 (7)[1]	136.0±0.5 (6)	174.1±0.9 (7)[1]	4.22±0.22 (7)[1]	0.055 ±0.007 (7)[1]
100%	EM	1022.3±1.9 (7)	470.6±3.9 (7)	567.1±1.1 (7)	1.51±0.03 (7)	0.0097±0.0010 (7)
	CP	1034.1±2.0 (7)[1]	479.6±2.7 (7)	552.6±1.6 (7)[1]	3.23±0.16 (7)[1]	0.69 ±0.34 (7)[1]

Data represent means±SE with the number of determinations in parenthesis
[1] significantly different from the corresponding EM value ($P<0.05$).

stated otherwise. No significant change in weight was observed for specimens transferred from 50% SW to 50% SW for 48 hr.

The osmolalities of the CP of worms acclimated to 30% or 100% SW were slightly, but significantly, higher than those of the respective external media (Table 1). Similar results were obtained when the worms were acclimated to 30% or 100% SW for seven days. The concentration of Na^+ in the CP of these specimens was not significantly different from that of the respective external media, but the Cl^- concentration in the CP was always significantly lower than that of the external medium (Table 1). In contrast, the HCO_3^- and P_i concentrations in the CP of specimens acclimated to 30% or 100% SW were significantly higher than the respective values in the external media.

The P_T (1.19 ± 0.22 mM, n=7) and P_o (0.50 ± 0.09 mM, n=7) concentrations in the CP of *P. arcuatum* acclimated to 100% SW were significantly greater than those (0.109 ± 0.016 mM, n=7 and 0.055 ± 0.007 mM, n=7, respectively) of the specimens acclimated to 30% SW. The water-soluble protein concentration in the CP of the former (2.37 ± 0.24 $mg \cdot ml^{-1}$, n=5) was also significantly greater than that of the latter (0.86 ± 0.18 $mg \cdot ml^{-1}$, n=5). Such differences in the P_T, P_o and water-soluble protein concentrations could not be explained by the increase and decrease in water content of the CP in 30% and 100% SW, respectively. After recalculation to eliminate the respective dilution and concentration effects, the water-soluble protein concentrations of worms in 30% (0.93 ± 0.19 $mg \cdot ml^{-1}$) and 100% SW (1.71 ± 0.18 $mg \cdot ml^{-1}$) were still significantly different from each other.

DISCUSSION

Contrary to the report of Green and Dunn [4], *P. arcuatum* lost some of the water gained initially in 30% SW and reached a steady state of 6.8% greater than the initial weight by the 48th hr. Similarly, specimens were able to regain some of the water lost initially after being transferred from 50% SW to 100% SW. Our results also contradict those of Green and Dunn [4] by confirming *P. arcuatum* to be capable of maintaining its CP slightly, but significantly, hyperosmotic to its external medium. Maintenance of a slightly hyperosmotic coelomic fluid would favor a constant, yet small, osmotic water influx which could compensate for urine production and any other processes by which water is lost [16]. Thus, the majority of invertebrates [15, 18, 20] and some vertebrates (hagfish, shark and rays, the coelacanth, and the crab eating frog) [10] are always slightly hyperosmotic although they are osmoconformers.

In addition, contrary to Green and Dunn's [4] claim, our results verify that the Cl^- concentration in the CP of *P. arcuatum* was always significantly lower than that of the external medium, be it 30% or 100% SW. In this regard, it is important to notice that no standard deviation or SE was presented for the data on the external media in the report of Green and Dunn [4], and the comparison of the Cl^- concentration in the CP to that in the external medium in their studies was apparently subjective.

The cause of the hypoionic Cl^- condition in the CP of sipunculids is still uncertain [13]. One hypothesis is that concentrations of inorganic anions, such as HCO_3^- or SO_4^{2-}, may be considerably higher in the coelomic fluid than in the external medium. However, measured SO_4^{2-} concentrations in sipunculid coelomic fluids are lower than those in the external SW [1, 22]. Our results indicate that HCO_3^- and Pi, though present in significantly greater concentrations in the CP than in the external media, could only partially account for the difference in Cl^- concentration between these two samples.

Gross [5] suggested that osmotically active particles, of an unspecified chemical nature, could be exchanged between the coelomic fluid and the tissues of sipunculids, altering the osmotic concentration and, therefore, composition of the coelomic fluid during certain condition of osmotic stress. If the particles involved were negatively charged at physiological pH, regulating the Cl^- concentration in the CP of *P. arcuatum* to be consistently lower than that of the ambient water would be essential to maintaining electroneutrality of the ions present. Indeed, *P. arcuatum* is capable of using free amino acids (FAAs) to regulate cell volume [17]. After a downward transfer from 50% to 30% SW, there is a release of FAAs from the body tissues into the CP. When being confronted with an upward transfer from 50% to 100% SW, *P. arcuatum* exhibits a small uptake of FAAs from the CP by the body tissues during the initial phase of the transfer [17]. However, most FAAs, being zwitterions, do not carry any net charge at physiological pH. Hence, some other organic osmolytes must be involved in maintaining electroneutrality in the CP of this sipunculid.

P_o and water-soluble proteins are normally negatively charged at pH 7.42 of the coelomic fluid of *P. arcuatum* [11]. Our results indicate that the CP of specimens acclimated to 100% SW had significantly greater concentrations of P_o and water-soluble proteins than that of specimens acclimated to 30% SW. In aggreement with such an observation, the difference in Cl^- concentration between the CP and the ambient medium in specimens acclimated to 100% SW was greater than that in worms acclimated to 30% SW. Since worms fasted for 10 days were used through out the experiment, it is reasonable to assume that this increase in protein concentration reflects the degradation of some proteins in the tissues and the release of smaller water-soluble units into the CP. Indeed, Peng *et al.* [17] reported that the significant increase in the total FAA content in the tissues of the worms acclimated to 100% SW was mainly due to an increase in protein catabolism. Chew *et al.* [3] further demonstrated that increased protein catabolism occurred in the internal organs, but not in the body wall of *P. arcuatum* in such a condition. Some of the water-soluble proteins could have been released from the internal organs to the CP to be transported to the tissues of the body wall. In addition, the release of proteins into the CP of worms acclimated to 100%

SW might be essential to the maintenance of hyperosmoticity, since some of the FAAs in the CP were absorbed by the body tissues [17].

Hence, we concluded that *P. arcuatum* could regulate to some extent its volume and ionic composition as for its CP. This is in agreement with the results of Harms and Dragendorff [6] and Gross [5].

REFERENCES

1 Bialaszewicz K (1933) Contribution a l'etude de la composition minerale des liquides nourriciers chez les animaux marins. Archs Int Physiol 36: 41–53

2 Bradford MM (1976) A rapid and sensitive method for the quantitation of microgram quantities of protein utilizing the principle of protein binding. Anal Biochem 72: 248–259

3 Chew SF, Peng KW, Low WP, Ip YK (1994) Differences in the responses between tissues of the body wall and the internal organs of *Phascolosoma arcuatum* (Sipuncula) to changes in salinity. Comp Biochem Physiol 107A: 141–147

4 Green JP, Dunn DF (1976) Chloride and osmotic balance in the euryhaline sipunculid *Phascolosoma arcuatum* from a Malaysian mangrove swamp. Biol Bull 150: 211–221

5 Gross WJ (1954) Osmotic responses in the sipunculid *Dendrostomum zostericola*. J Exp Biol 31: 402–423

6 Harms JW, Dragendorff O (1933) Die Realisation von Genen und die konsekutive Adaptation-3. Mitteilung: Osmotische Untersuchungen an *Physcosoma lucro* Sel. und de Man aus den Mangrove-Vorlandern der Sunda-Inseln. Z wiss Zool 143: 263–322

7 Hogue EW, Oglesby LC (1972) Further observation on salt balance in the sipunculid worm *Themiste dyscritum*. Comp Biochem Physiol 42A: 915–926

8 Hyman LH (1959) The invertebrates: Smaller coelomate groups. In "The Coelomata Bilateria, Vol. 5" Ed by LH Hyman, MacGraw-Hill, New York, pp 610–696

9 Kamemoto FI, Larson EJ (1964) Chloride concentrations in the coelomic and nephridial fluids of the sipunculid *Dendrostomum signifer*. Comp Biochem Physiol 13: 477–480

10 Kirschner LB (1979) Control mechanisms in crustaceans and fishes. In "Mechanisms of Osmoregulation in Animals. Maintenance of cell volume" Ed by R Gilles, John Wiley, New York, pp 157–222

11 Lim RWL, Ip YK (1991) The involvement of phosphoenolpyruvate carboxykinase in succinate formation in *Phascolosoma arcuatum* (Sipuncula) exposed to environmental anoxia. Zool Sci 8: 673–679

12 Oglesby LC (1968) Responses of an estuarine population of the polychaete *Nereis limnicola* to osmotic stress. Biol Bull 134: 118–138

13 Oglesby LC (1968) Some osmotic responses of the sipunculid worms *Themiste dyscritum*. Comp Biochem Physiol 26: 155–177

14 Oglesby LC (1969) Inorganic components and metabolism; ionic and osmotic regulation: Annelida, Sipuncula, and Echiura. In "Chemical Zoology, Vol IV" Ed by M Florkin, BT Sheer, Academic Press, New York, pp 211–310

15 Oglesby LC (1978) Salt and water balance. In "Physiology of Annelids" Ed by PJ Mill, Academic Press, New York, pp 555–658

16 Oglesby LC (1981) Volume regulation in aquatic invertebrates. J Exp Zool 215: 289–301

17 Peng KW, Chew SF, Ip YK (1994) Free amino acids and cell volume regulation in the sipunculid *Phascolosoma arcuatum*. Physiol Zool 67: 580–597

18 Pierce SK Jr (1970) The water balance of *Modiolus* (Mollusca: Bivalvia: Mytilidae): Osmotic concentrations in changing salinities. Comp Biochem Physiol 36: 521–533

19 Pierce SK Jr (1982) Invertebrate cell volume control mechanisms: A co-ordinated use of intracellular amino acids and inorganic ions as osmotic solute. Biol Bull 163: 405–419

20 Remmert H (1969) Über Poikilosmotic und Isoosmotic. Z Vergl Physiol 65: 424–427

21 Rice ME, Stephen AC (1970) The type specimens of Sipuncula and Echiura described by JE Gary and W Baird in the collection of British Museum (Natural History). Bull Brit Mus (Nat Hist) Zool 20: 49–72

22 Robertson JD (1953) Further studies on ionic regulation in marine invertebrates. J Exp Biol 30: 277–296

23 Steinbach HB (1940) The distribution of electrolytes in *Phascolosoma* muscle. Biol Bull 78: 477–480

24 Stephen AC, Edmonds SJ (1972) The phyla Sipuncula and Echiura. British Museum Natural History Publ No 117, British Museum (Natural History), London, 528 pp

ZOOLOGICAL SCIENCE 11: 883–887 (1994)

Control of Seasonal Development by Photoperiod and Temperature in the Linden Bug, *Pyrrhocoris apterus* in Belgorod, Russia

AIDA H. SAULICH[1], TATYANA A. VOLKOVICH[1] and HIDEHARU NUMATA[2]*

[1]*Laboratory of Entomology, Biological Research Institute, St. Petersburg University, St. Petersburg 198904, Russia* [2]*Department of Biology, Faculty of Science, Osaka City University, Sumiyoshi, Osaka 558, Japan*

ABSTRACT—The life cycle of the Belgorod population of the linden bug, *Pyrrhocoris apterus* (L.) (Heteroptera, Pyrrhocoridae) was observed in the field, and under quasi-natural rearing conditions. There were univoltine and bivoltine pathways in the life cycle. The emergence of diapause adults under quasi-natural conditions was consistent with the parameters of photoperiodic response obtained by experiments at constant photoperiod and temperatures. The temperature dependence of the photoperiodic induction of diapause plays a significant role in life cycle adaptation in this species.

INTRODUCTION

It is accepted that photoperiodic responses play a major role in the control of seasonal life cycles in insects [2–4, 14]. However, it is often difficult to apply laboratory results obtained under constant photoperiods and temperatures to predict seasonal development in the field. Therefore, phenological observation in the field and experiments under natural conditions are better ways to discuss life cycle adaptation in an insect.

The linden bug, *Pyrrhocoris apterus*, has an adult diapause controlled by a long-day photoperiodic response [5, 9, 12, 16]. In a previous paper, we showed the photoperiodic response of *P. apterus* in Belgorod Region, Russia, under conditions of constant temperature and under thermoperiodic conditions in the laboratory. Although thermoperiod had a slight effect on the induction of diapause, the critical day-length essentially depended on the mean temperature [9]. However, the adaptive significance of this temperature dependence remained unclear.

In all populations of *P. apterus* examined until the present, the diapause is facultative [5, 9, 12, 16], and therefore they all have the possibility to produce two or more generations a year. However, a univoltine life cycle has been observed in the population in Paris, France [10], and in that in central Bohemia [5, 6]. In Kazakhstan and Ukraine, the possibility of a partially bivoltine life cycle was reported [1, 15]. Until recently, however, no reliable evidence has been shown of the voltinism in *P. apterus*, because adults of this species have a long life-span and oviposition period and therefore it is difficult to discriminate the generation of adults. Recently, Socha and Šula [13] showed the occurrence of two generations of *P. apterus* in one year in southern Bohemia.

In the present study, we first observed the life cycle of the Belgorod population of *P. apterus*, and then reared the insects under quasi-natural conditions. We discuss a likely role for temperature dependency of the photoperiodic response in the life cycle adaptation of *P. apterus* based on a comparison of the laboratory findings [9] with those under quasi-natural conditions.

MATERIALS AND METHODS

Observations and experiments were carried out in the reservation, "Forest on the River Vorskla" (50°N, 36°E), in Belgorod Region, Russia, on the local population of *P. apterus* in 1990 and 1991.

Nymphs of *P. apterus* were reared from the first instar in a meteorological booth placed in the open, by the methods previously described [9]. The shelf where insects were reared was about 130 cm high from the ground. Only the north side of the booth opened and the insects inside were protected from direct sunlight. The temperature in the booth was recorded. After adult emergence, the insects were reared as male and female pairs in Petri dishes (9 cm diameter). Oviposition was recorded daily, and if a female did not lay eggs for 30 days from emergence we judged it to be in diapause.

Fifth- (final-) instar nymphs were collected from the field and raised to adults in cages (45 cm diameter, 80 cm height) on the soil surface. The cage was made of a wire-frame with a gauze net covering the top and sides, and the frame was buried into the soil at a depth of 10 cm. Thick branches and pieces of bark were placed in the cage to protect the insects from rain and direct sunlight. The temperature on the soil surface in the cage was recorded. The incidence of diapause was examined as for the insects in the booth.

Some insects were reared from the first instar in the laboratory under 18L-6D at 25±1°C, and transferred to 16L-8D or 12L-12D during the fifth instar. Their diapause status was examined as stated above.

Received June 24, 1994
Accepted November 14, 1994
* To whom all correspondence should be addressed.

RESULTS

Phenological observation

Adults after overwintering appeared on the ground in late April both in 1990 and in 1991. On warm sunny days from early May, we observed mating and oviposition. Thereafter we found both nymphs and adults until late autumn. Because adults lived and continued to lay eggs for a long period, it was difficult to divide generations only by field observations. We could only determine the beginning of emergence of new adults, because they had a richer red color and softer integument than older adults. These differences disappeared a few days after adult emergence. In 1990, we observed new adults at the beginning of July, although we did not record the date of their earliest emergence. In 1991, new adults emerged from mid-June.

Rearing from the first instar

To define the number of generations in a year, we reared *P. apterus* from the first instar in a meteorological booth under quasi-natural conditions in 1990 and 1991. We used eggs laid by adults after overwintering. In 1990, we placed first-instar nymphs just after hatching in the booth on 3, 13 and 20 June. In this year, it was cool in June; the mean temperature for ten days was 13.6–15.5°C. Therefore, the nymphs developed slowly and new adults first emerged as late as 7 August. All adults entered diapause except for only one that emerged on 10 August (Fig. 1).

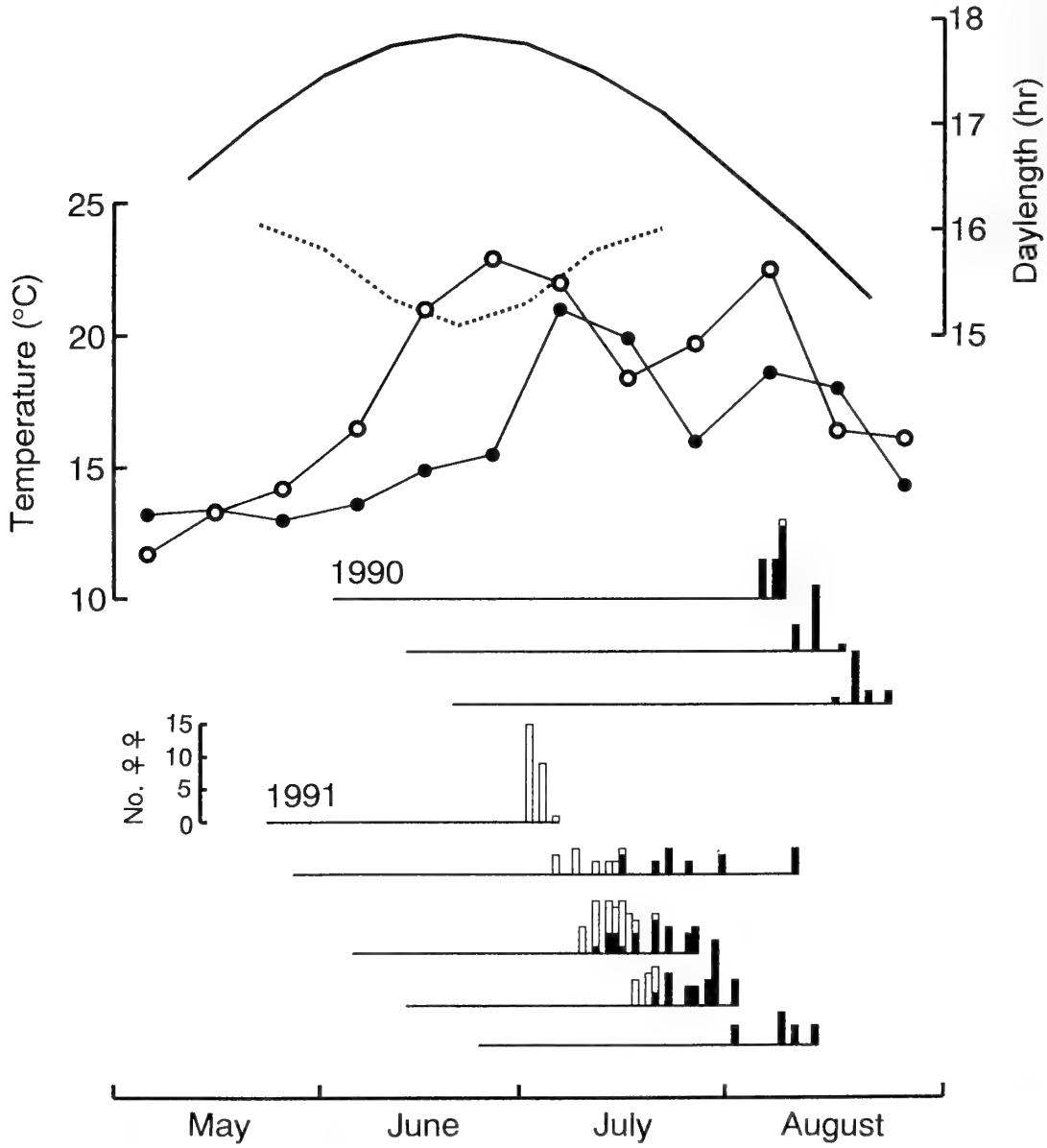

FIG. 1. Induction of adult diapause in *Pyrrhocoris apterus* under quasi-natural conditions in 1990 and 1991. Each horizontal line shows an experimental series. The outset corresponds to the hatching of the nymphs. Date of adult emergence in females is shown at the end of line as histograms. Black, diapause; white, reproductive. Circles show the mean temperatures for ten days in the meteorological booth used for the experiments in 1990 (closed) and in 1991 (open). Solid line, natural daylength including civil twilight at 50°N (after Beck [2]). Dotted line, critical temperature for the induction of diapause in *P. apterus* (after Numata *et al.* [9]) (see Fig. 2).

In 1991, we placed first-instar nymphs in the booth on 23 and 27 May, 6, 13 and 25 June. In this year, the mean temperature for ten days in June was 16.5–22.9°C, and therefore nymphs developed much faster than in 1990. New adults first emerged on 2 July. All females emerging before 10 July laid eggs. From 12 to 21 July, both reproductive and diapause female adults emerged, and all females emerging after 22 July entered diapause (Fig. 1).

Rearing of the field-collected nymphs

Thus, we knew when diapause adults emerged in the booth under quasi-natural conditions. However, the temperature in the booth used in this experiment differed from that on the soil surface where the insects develop in nature. Furthermore, the nymphs of this species behaviorally select microhabitat [8]. Therefore, to determine the actual time of emergence of diapause adults, we collected fifth-instar nymphs from the field and kept them in cages on the soil surface in 1991. After adult emergence, we examined their diapause status (Table 1). From the samples collected on 7 June, adults emerged on 9–14 June, which corresponded to the first emergence of new adults in nature. They were all nondiapause adults and began to lay eggs in late June. On 21 July, the first diapause adults emerged, and thereafter diapause adults prevailed in the samples. In some periods there was only a little difference between the temperature on the soil surface and that in the meteorological booth, although in other periods the former was much higher than the latter. For example, in late April the mean temperature of the soil surface was 23.3°C and that in the booth was 10.3°C, while in mid- and late July, the difference was 3.6–3.8°C.

TABLE 1. Incidence of adult diapause in *Pyrrhocoris apterus* collected as fifth-instar nymphs from the field in 1991

Date of collection	No. of nymphs collected	Date of adult emergence	No. of adult pairs	% diapause
7 June	46	9–14 June	20	0
2 July	35	4–6 July	22	0
12 July	32	14–18 July	18	0
		21 July	6	33
22 July	70	30 July-2 August	19	84
		6 August	15	75

Photoperiodic sensitivity

In *P. apterus*, the photoperiodic sensitivity commences in the fourth or fifth instar and continues throughout the adult life [5]. Five or six short-day cycles experienced before adult emergence were enough to induce diapause in the population from central Bohemia [7]. We examined the photoperiodic sensitivity in the Belgorod population at 25°C. We used 18L-6D as long-day conditions, and 16L-8D or 12L-12D as short-day conditions, because the critical daylength was about 17 hr at 25°C [9].

Nine short-day cycles experienced before adult emergence were enough to induce adult diapause in all individuals, and four cycles were critical, irrespective of the short-day conditions used (Table 2).

TABLE 2. Effect of photoperiodic transfer from long-day to short-day conditions before adult emergence on the induction of adult diapause in *Pyrrhocoris apterus* at 25°C

Photoperiodic conditions	Photoperiodic transfer, −days before adult emergence	No. of pairs used	% diapause
18L-6D→16L-8D	12	25	100
	9	26	100
	8	20	80
	4	24	50
	0	25	8
18L-6D→12L-12D	9–11	26	100
	4	17	35
	0	26	0

DISCUSSION

Interaction between photoperiod and temperature

In the Belgorod population of *P. apterus*, the photoperiodic induction of adult diapause depends on temperature, and the critical daylength is longer at lower temperatures [9], as in many other insects with long-day photoperiodic responses [2–4, 14]. Moreover, the critical daylength under thermoperiodic conditions is close to that at the constant temperature equivalent to the mean temperature of the thermoperiod [9]. This species is slightly sensitive to a gradual increase of the photophase only in the threshold range [17]. Therefore, we examined whether we could apply the photoperiodic response obtained experimentally at constant photoperiods and temperatures to the natural induction of diapause. First, we determined the critical temperature for a given daylength, as we had ascertained the critical daylengths at each temperature (Fig. 2). Then, we showed

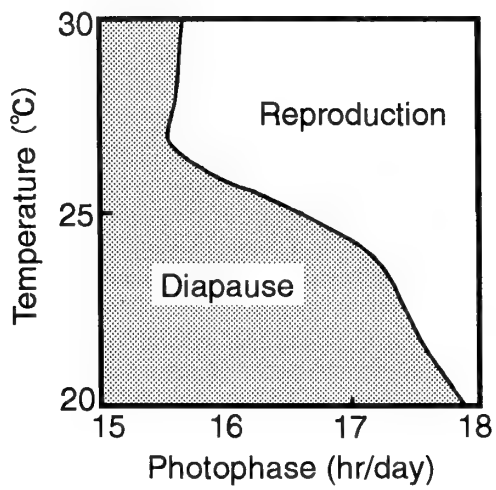

FIG. 2. Effect of photoperiod and temperature on the induction of adult diapause in *Pyrrhocoris apterus* (after Numata *et al.* [9])

the critical temperature for the natural daylength as a dotted line in Figure 1. During periods when the environmental temperature is lower than this value, diapause might be induced.

Voltinism of the Belgorod population

In the Belgorod population of *P. apterus*, there were two alternative pathways in the life cycle, i.e., univoltine and bivoltine. In 1990 (cool weather), new adults emerged from early August, and most of these entered diapause. The mean temperature for ten days never exceeded the critical value for the induction of diapause. Low temperature contributed to the induction of diapause in two ways: First, it lengthened the critical daylength for the induction of diapause. Second, it delayed nymphal development, and therefore the sensitive stage was postponed to the period when the daylength was short enough to induce diapause.

In 1991 (warm weather), however, new adults emerged from early July, and early emerging adults of the first generation reproduced. Their progeny, i.e., the second generation, developing in August and September should enter diapause. Furthermore, late emerging adults of the first generation also entered diapause. The mean temperatures for mid- and late June and early July were higher than the critical value for the induction of diapause. All adults emerging on and after 22 July entered diapause. When insects were transferred from long-day to short-day conditions nine days before adult emergence in the laboratory, all of them entered diapause. Therefore, the emergence of diapause adults under quasi-natural conditions is consistent with the parameters of photoperiodic response obtained by the experiments at constant photoperiods and temperatures.

In the regions where the duration of the growing season in individual years is nearly constant, photoperiod is an effective cue for the prediction of the coming season. Sauer *et al.* [11] regarded the temperature dependence of the critical daylength in *Pieris brassicae* both as an adaptation to the low predictability of the end of the growing season, and as an adaptation related to migration. *P. apterus* does not migrate and therefore the temperature dependence of the photoperiodic response has adaptive significance where the temperature varies much between years as in Belgorod Region.

Although Honěk and Šrámková [8] pointed out that the production of the second generation as an unfavorable modification of the life cycle in *P. apterus* in central Bohemia, there is no doubt that the Belgorod population of *P. apterus* partially produces two generations in warmer years. However, it seems that even in cooler years the Belgorod population is not homogeneously univoltine, because we found some new adults laying eggs in early July even in 1990, when it was cool (unpublished). Furthermore, the proportion of diapause adults emerging from the fifth-instar nymphs collected from the field was lower than that in insects reared from the first instar under quasi-natural conditions in 1991. We attribute these differences in part to the differences in temperature between the meteorological booth and the soil surface where *P. apterus* lives in nature, because the temperature on the soil surface was sometimes much higher than that in the meteorological booth. Furthermore, we observed in spring that nymphs and adults aggregated in warm places on the soil surface where the temperature was much higher than in the meteorological booth because of radiant heat. Therefore the behavioral regulation of body temperature may also contribute the difference between the quasi-natural and the real natural conditions. However, we cannot predict the seasonal development of *P. apterus* with the temperature on the soil surface, because during the warm seasons the nymphs of *P. apterus* select microhabitat where the temperature is much cooler than on the soil surface [8].

Retardation of nymphal development

The nymphal development of *P. apterus* is retarded at the critical daylength for the induction of adult diapause or a little shorter [9, 12]. The combination of photoperiod and temperature in early July in 1990 was in the range where nymphal development is retarded in the laboratory [9], although it is unclear whether the slow development of nymphs under quasi-natural conditions in 1990 resulted from retardation due to the threshold range or only from the normal effect of temperature. The combination of photoperiod and temperature in both mid-June and early July in 1991 was also in the range where nymphal development is retarded in the laboratory [9]. Thus, in warmer years nymphs possibly meet with threshold conditions twice throughout the season.

We assume that at threshold conditions before summer solstice, nymphs had not reached the sensitive stage for the retardation of development because no nondiapause adults had an extremely long nymphal period in the present study. Under threshold conditions after the summer solstice, prolongation of the nymphal period will delay the emergence of diapause adults, as Saunders [12] suggested in the univoltine life cycle in the population of this species in central Bohemia. In the second series in 1991 under quasi-natural conditions, some adults emerged much later than the others and entered diapause. It has been generally accepted that the range of temperature and photoperiod for the induction of winter diapause is adequate to reach the diapause stage before winter (e.g., [11]). The diapause adults developing in earlier seasons have enough time before winter and prolongation of the nymphal period is less harmful for them than for those developing in later seasons. If the diapause adults emerging after an extended nymphal period have a larger body size, higher fecundity or lower mortality in winter, the retardation of nymphal development would have adaptive significance. Further studies are needed to clarify these.

ACKNOWLEDGMENTS

We thank Dr. Ivo Hodek, Institute of Entomology, Czech Academy of Sciences, for critical reading of the manuscript.

REFERENCES

1 Asanova RB, Iskakov BV (1977) Harmful and Useful Heteroptera of Kazakhstan. Alma Ata, Kainar, pp 124–126 (in Russian)

2 Beck SD (1980) Insect Photoperiodism. Academic Press, New York, 2nd ed

3 Danks HV (1987) Insect Dormancy: An Ecological Perspective. Biological Survey of Canada, Ottawa

4 Danilevskii AS (1961) Photoperiodism and Seasonal Development of Insects. Leningrad University Press, Leningrad (in Russian)

5 Hodek I (1968) Diapause in females of *Pyrrhocoris apterus* L. (Heteroptera). Acta Entomol Bohemoslov 65: 422–435

6 Hodek I (1971a) Termination of adult diapause in *Pyrrhocoris apterus* (Heteroptera: Pyrrhocoridae) in the field. Entomol Exp Appl 14: 212–222

7 Hodek I (1971b) Sensitivity of larvae to photoperiods controlling the adult diapause of two insects. J Insect Physiol 17: 205–216

8 Honěk A, Šrámková K (1976) Behavioral regulation of developmental cycle in *Pyrrhocoris apterus* L. (Heteroptera: Pyrrhocoridae). Oecologia 24: 277–281

9 Numata H, Saulich AH, Volkovich TA (1993) Photoperiodic responses of the linden bug, *Pyrrhocoris apterus* under conditions of constant temperature and under thermoperiodic conditions. Zool Sci 10: 521–527

10 Pouvreau A (1963) Cycle biologique et interprétation de l'arrêt de dévelopment chez *Pyrrhocoris apterus* L. (Heteroptera, Gymnocerate, Pyrrhocoridae). Bull Soc Zool France 88: 180–196

11 Sauer KP, Spieth H, Grüner C (1986) Adaptive significance of genetic variability of photoperiodism in Mecoptera and Lepidoptera. In "The Evolution of Insect Life Cycles" Ed by F Taylor, R Karban, Springer Verlag, New York, pp 153–172

12 Saunders DS (1983) A diapause induction termination asymmetry in the photoperiodic responses of the linden bug, *Pyrrhocoris apterus* and an effect of near-critical photoperiods on development. J Insect Physiol 29: 399–405

13 Socha R, Šula J (1992) Voltinism and seasonal changes in haemolymph protein pattern of *Pyrrhocoris apterus* (Heteroptera: Pyrrhocoridae) in relation to diapause. Physiol Entomol 17: 370–376

14 Tauber MJ, Tauber CA, Masaki S (1986) Seasonal Adaptations of Insects Oxford Univ Press, New York

15 Vasyliev VP (1973) Pests in agriculture, stock farming and forest plantation. Urodjai, Kiev 1: 340–341 (in Russian)

16 Volkovich TA, Goryshin NI (1978) Evaluation and accumulation of photoperiodic information in *Pyrrhocoris apterus* L. (Hemiptera, Pyrrhocoridae) during the induction of oviposition. Zool Zh 57: 46–55 (in Russian)

17 Volkovich TA, Goryshin NI (1979) Influence of constant and gradually increasing photoperiods on induction of reproductive activity in *Pyrrhocoris apterus* (Hemiptera, Pyrrhocoridae). Zool Zh 58: 1327–1333 (in Russian)

ZOOLOGICAL SCIENCE 11: 889–894 (1994)

Multivariate Analyses of Elytral Spot Patterns in the Phytophagous Ladybird Beetle *Epilachna vigintioctopunctata* (Coleoptera, Coccinellidae) in the Province of Sumatera Barat, Indonesia

HARUO KATAKURA[1], SATORU SAITOH[1], KOJI NAKAMURA[2] and IDRUS ABBAS[3]

[1]*Division of Biological Sciences, Graduate School of Science, Hokkaido University, Sapporo, 060,* [2]*Ecological Laboratory, Faculty of Science, Kanazawa University, Kakuma, Kanazawa, 920-11, Japan, and* [3]*Department of Biology, Faculty of Science, Andalas University, Padang, Sumatera Barat, Indonesia*

ABSTRACT—We analyzed geographic trends of elytral spot variations in the phytophagous ladybird beetle *Epilachna vigintioctopunctata* in the Province of Sumatera Barat, Indonesia. An UPGMA analysis revealed two distinct clusters of populations, one of which was further subdivided into two minor clusters. A principal component analysis also indicated the presence of the two major clusters. However, a closer analysis of the data suggested that the two clusters represented a complicated intraspecific variation rather than two distinct taxa. The dichotomy of the populations seemed to be caused by the pausity of samples at particular altitudes, which makes a continuous series of variation as if they are composed of two distinct subsets. The first two principal components accounted for approximately 90% of the variance. The first component mainly expressed the number of elytral spots, and the scores increased with an increase of altitude. The second component expressed the frequencies of particular types of spot confluences.

INTRODUCTION

The phytophagous ladybird beetle *Epilachna vigintioctopunctata* (Fabricius), which is a serious pest of solanaceous crops and is widespread from southeast Asia through Australia, exhibits a wide range of infra- and interpopulational variation in their elytral spot pattern [1–4]. Katakura *et al.* [3] mentioned that individual beetles of *E. vigintioctopunctata* in the Province of Sumatera Barat, Indonesia, possessed 6 to 14 spots on each elytron, and some of these spots were often coalesced. They recognized two forms, formae A and B, in the Sumatran *E. vigintioctopunctata* that were identical in structural character but were different in body coloration, pronotal and elytral spot variations and vertical distribution. Later, Abbas *et al.* [1] divided populations of *E. vigintioctopunctata* in the same area into four groups based on their spot pattern variations. Group I, occurring in the coastal plains and inland lowlands, and Group IV, confined to the highlands, were two extremes of the spot pattern variations, the latter having many more non-persistent spots and confluences, larger body size and more advanced melanism than the former. Group I consisted of forma A individuals while Group IV was made up of forma B individuals, but the two groups were connected with each other via the intermediate groups II and III. On the basis of these findings, Abbas *et al.* [1] considered that the two forms of Katakura *et al.* [3] represent a largely altitude-linked intraspecific variation rather than two distinct but closely related species.

Accepted October 17, 1994
Received August 19, 1994

The present paper aims to confirm these previous results and conclusions through multivariate analyses of the data provided by Abbas *et al.* [1]. It also aims to elucidate major components involved in the geographic variation of elytral spot patterns in west Sumatran *E. vigintioctopunctata*.

MATERIALS AND METHODS

Area surveyed (Fig. 1)

The Province of Sumatera Barat occupies the western part of Central Sumatra, ranging from 0°54'N to 3°30'S, and 98°36'E to 101°53'E. The coastal plain is very narrow, only a few to 25 km in width, and soon gives way to the steep western slope of the Barisan Mountains, which run parallel to the coast with numerous peaks higher than 2,000 m. The eastern slope of the mountains is far less steep, forming a plateau 200 to 1,000 m high [3].

Specimens

Abbas *et al.* [1] reported that, although individuals of both sexes showed a similar pattern of geographic variation, females had a slightly but significantly larger number of spots than males from the same locality. For the sake of brevity, then, we used only male specimens in the present analyses. From the materials used by Abbas *et al.* [1], we chose 53 population samples (Fig. 1), each of which contained more than 20 males. The number of specimens examined and the elevation of the collected site of each population are listed in Appendix.

Spot patterns

The standard elytral spot patterns of *E. vigintioctopunctata* are given in Figure 2. The basic pattern consists of six black "persistent" spots (*1–6*) on each elytron. This pattern may be modified by the addition of one to eight "non-persistent" spots (*a-h*) on each

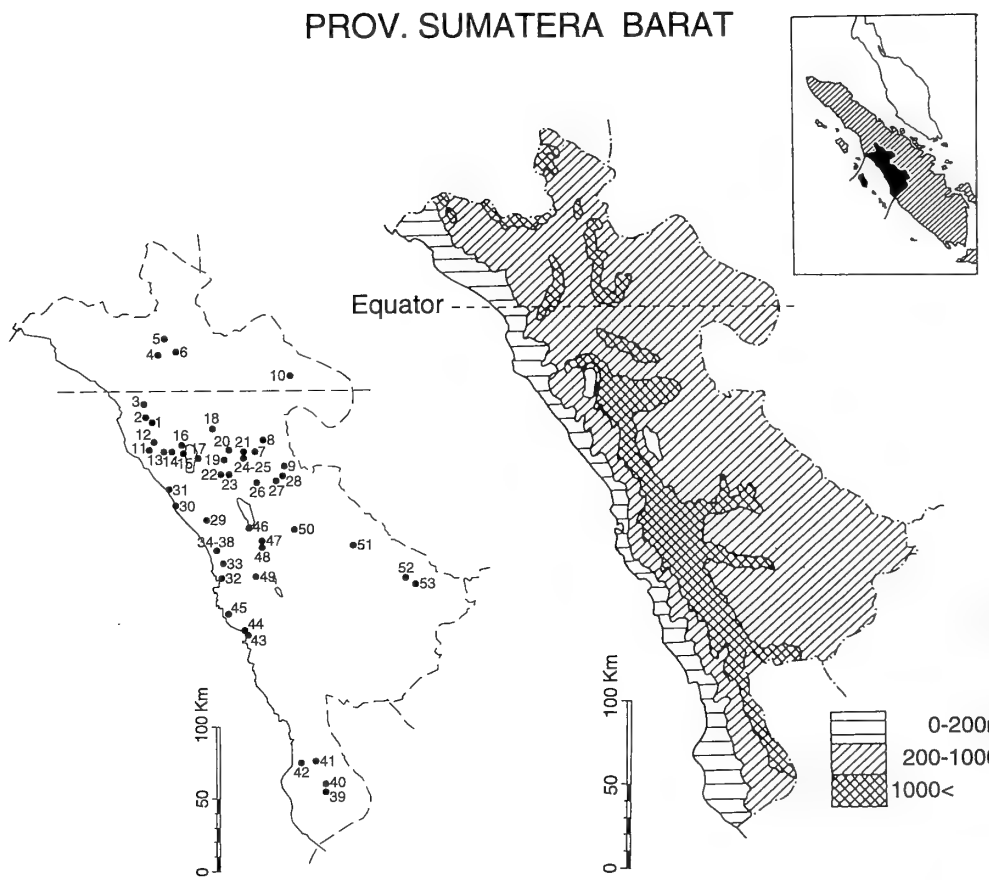

FIG. 1. Relief map of Sumatera Barat (modified from Katakura *et al.* [3]) and provenance of the studied populations. Populations were shown with the code numbers given in Appendix.

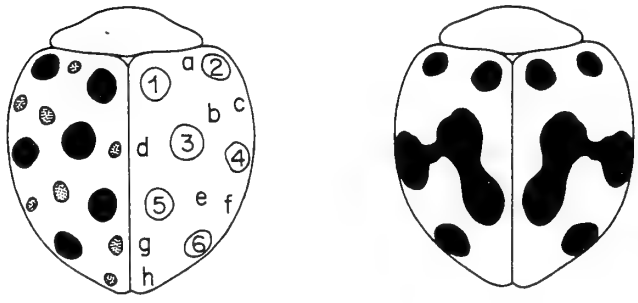

FIG. 2. Left: Standard elytral spot patterns of *E. vigintioctopunctata*, showing codes for persistent spots (*1–6*) and non-persistent spots (*a-h*). Right: The confluence of spots exemplified by *4+3+5*. (From Katakura *et al.* [3])

elytron, or by the enlargement and confluence of several spots [2]. Spot *a* is very rare and did not appear in the present materials [3]. All other non-persistent spots appeared with various frequencies according to populations. In addition, the following seven types of confluences, all between persistent spots, and combinations of some of these confluences were recognized: *1-2, 1-3, 2-4, 3-4, 3-5, 4-6,* and *5-6*.

Data analyses

We treated each non-persistent spot (except *a*) and each type of confluence as a character in the following analyses. We recorded the presence or absence of each non-persistent spot and each confluence type for each specimen. If an individual had a joint confluence consisting of more than two spots (as shown in Figure 2 right where spots *4-3-5* fused), the individual was regarded to have two or more confluences (e.g., *3–4* and *3–5*). We then calculated percentage ratios of respective non-persistent spots and confluence types for each population. As the raw data set, we used arcsine transformed values [9] of these percentage ratios.

As a measure of the dissimilarity of elytral spot pattern variations, we calculated the Euclidean distances between populations from the raw data. Then a dendrogram using UPGMA (unweighted pair group method using arithmetic means [8]) was depicted. Next, we carried out a principal component analysis based on the covariance matrix of the fourteen characters (seven non-persistent spots plus seven confluence types) for all the 53 populations to extract the major components of interpopulational variations. Finally, to visualize the geographic pattern of variations, contour lines of the principal component scores standardized between 1 (the maximum score) and 0 (the minimun score) [8] were drawn on the map at an interval of 0.1, using Delaunay triangulation [5] and linear interpolation techniques. Delaunay triangulation and the drawing of the contour lines were performed on a SAS graph program package (Proc G3D, Proc Gcontour [6]).

RESULTS

Figure 3 is a UPGMA dendrogram based on the dissimi-

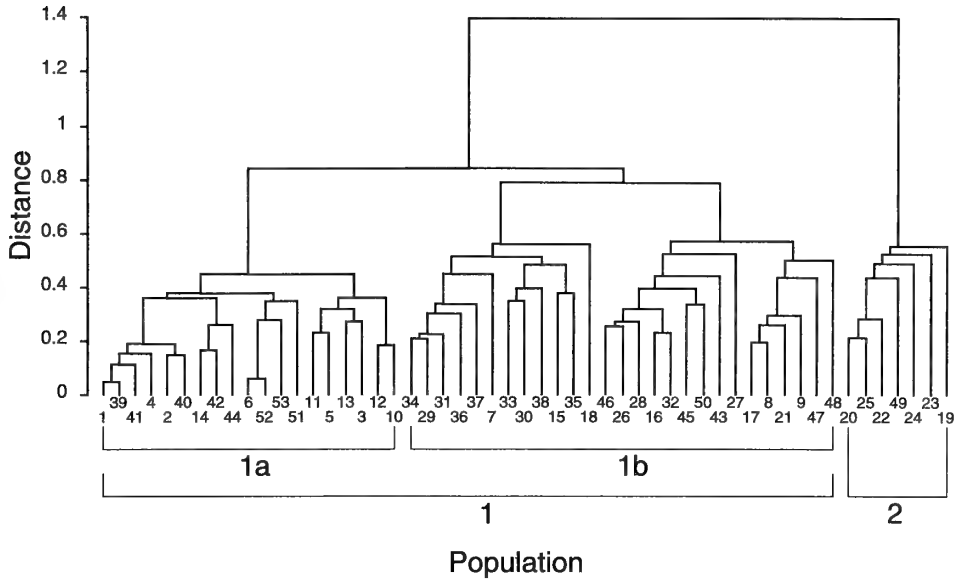

FIG. 3. A dendrogram resulting from UPGMA cluster analysis of elytral spots of 53 populations of *E. vigintioctopunctata* in Sumatera Barat. Populations were shown with the code numbers given in Appendix.

larity of the elytral pattern variation between populations. There are two major population clusters. One of the two clusters is further subdivided into two minor clusters. We hereafter call these three clusters 1a, 1b and 2 as indicated in Figure 3. Figure 5a shows the distribution of these three clusters. Cluster 2 (denoted by rectangles) occupies the mountain area whereas the population clusters 1a (circles) and 1b (triangles) are distributed in lower altitudes.

The results of the principal component analysis are summarized in Table 1. The first two components account for approximately 90% of the variance. The first component (explaining 72% of the variance) has positive and comparatively high loadings for all non-persistent spots and confluences *3–4* and *3–5*. On the other hand, the second component (17% of the variance) has high positive loadings for confluences *3–4*, *3–5*, and weak negative loadings for all non-persistent spots. In other words, the first component mainly expresses the frequencies of non-persistent spots, whereas the second component mainly expresses the frequencies of particular types of spot confluences.

TABLE 1. Loadings of the 14 characters (seven non-persistent spots and seven types of confluences) on the first two principal components (PCs)

Character	PC1	PC2
b	0.277	−0.254
C	0.313	−0.156
d	0.310	−0.173
e	0.251	−0.121
f	0.256	−0.136
g	0.375	−0.180
h	0.466	−0.212
1–2	0.131	0.051
1–3	0.017	0.003
2–4	0.012	−0.002
3–4	0.382	0.531
3–5	0.251	0.587
4–6	0.019	0.060
5–6	0.125	0.372
Explained variance (%)	71.5	16.7

Population projections on the first two axes (Fig. 4) show that the two major clusters recognized by UPGMA (1a+b, 2) are also clearly separated by the scores of the first principal component. On the other hand, the two minor clusters 1a and 1b are contiguous along the first axis. The three clusters are not separable along the second axis, and there was a very large variation in the minor cluster 1b.

Geographical variations of the first two principal components are shown in Figure 5b and 5c. The score of the first

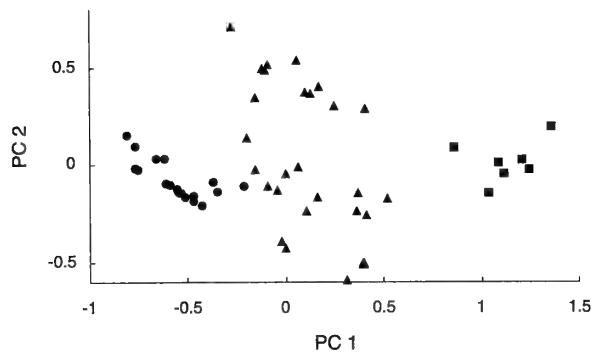

FIG. 4. Projections of principal component scores of 53 populations onto the first two axes. Symbols denote the clusters recognized by UPGMA cluster analysis: circles, cluster 1a; triangles, cluster 1b; rectangles, cluster 2.

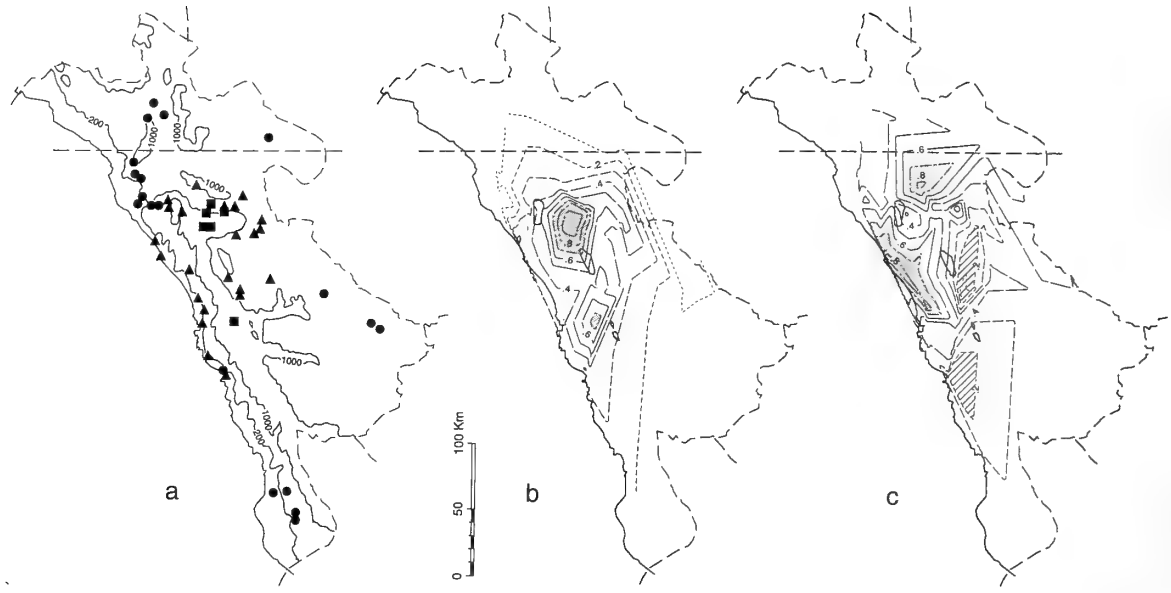

FIG. 5. a: Distribution of the three clusters recognized by UPGMA analysis; symbols are the same with those of Fig. 4. Contour lines are for 200 m and 1,000 m above sea level. b and c: Geographic variations of the first (b) and the second (c) principal component scores, expressed by contour lines; areas with scores higher than 0.8 are shaded, and in c, those lower than 0.2 hatched.

component (Fig. 5b) tends to become large at higher altitudes, with two conspicuous peaks of scores amid the Barisan mountains. On the other hand, the scores of the second component vary geographically in a complicated manner (Fig. 5c). The areas with large second component scores occupy the middle part of the west coast of Sumatera Barat, and a mountainous area just south of the equator. The lowest scores are found near a crater lake and on the western slope of the southern part of the mountain regions. Consequently, a steep east-west cline of the second component scores runs near the central part of Sumatera Barat across the mountains.

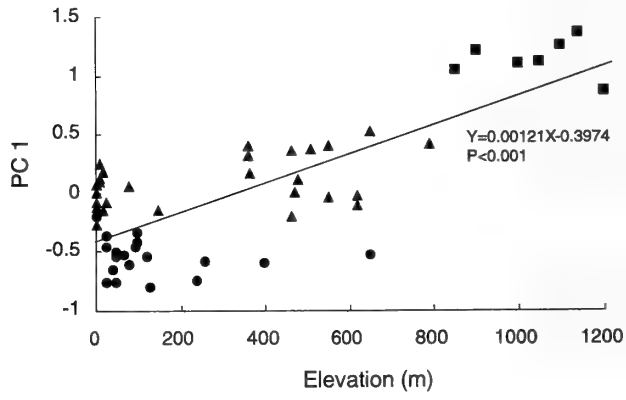

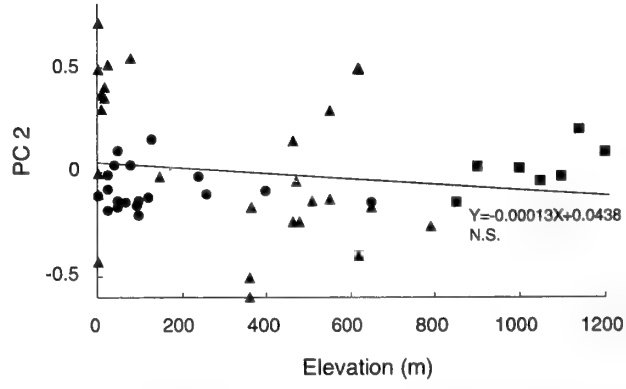

FIG. 6. Relationships between elevations of collected sites and the first two principal component scores of populations.

DISCUSSION

Abbas *et al.* [1] considered that the two forms of *E. vigintioctopunctata* reported by Katakura *et al.* [3] were a largely altitude-linked infraspecific variations. The results of the present analyses support their view. The UPGMA analysis showed that *E. vigintioctopunctata* populations in the studied area were divided into three clusters by the dissimilarity of elytral spot variations (Fig. 3), and moreover, two of them were still distinct by the principal component analysis based on 14 elytral spot characters (Fig. 4). Geographic mapping of populations showed that cluster 2 occupied the mountainous areas (Fig. 5a). However, these clusters may be artifacts. As shown in Figure 6, two minor clusters (1a and 1b) are contiguous when the principal component scores are plotted against the elevations of the sites where collected, and the distinction of the two major clusters (1 and 2) seems to be largely dependent on the pausity of population samples around 800 m altitude. It is likely that if an adequate number of populations are sampled around this altitude, the two major clusters will be united and form a continuous array of variation. The regression coefficient of the first component to elevations is highly significant ($P<0.001$). Thus, we regarded clusters 1 and 2, or forma A and B to be infraspecific

variations rather than two closely related species, although the possibility of the latter situation cannot be completely ruled out at the present.

The present study elucidated two major principal components that were involved in the interpopulational variations of elytral spot patterns. The first component mainly concerned the incidence of non-persistent spots, and the second component concerned the confluences of persistent spots *3–4* and *3–5*. The second component scores showed a complicated geographic variation not correlated with altitudes (Fig. 6b), for which we cannot present any appropriate explanation. On the other hand, we consider that the first component may be either directly or indirectly related to thermal conditions. Abbas *et al.* [1] mentioned that the beetles collected at higher elevations tended to have more non-persistent spots than those from lower elevations. In the present study, this relationship was more precisely defined as the significant positive regression of the first principal component scores to elevation (Fig. 6a). It is also known that the temperate conspecific populations of *E. vigintioctopunctata* in Japan usually have a full number of 14 spots on each elytron [2, 7]. These facts suggest that the number of elytral spots, or degree of melanization in *E. vigintioctopunctata*, increases with the decrease of ambient temperatures. Both environmental and genetic factors seem to be responsible for the determination of elytral spot patterns in *E. vigintioctopunctata* [1]. Yet, it is still unknown whether the increase of melanization *per se* is adaptive in cooler conditions or it is a byproduct of other adaptive characters that change with the change of thermal conditions.

ACKNOWLEDGMENTS

We wish to express our thanks to Prof. Emerit. S. Kawamura, Kyoto University, and all other members of the Sumatra Nature Study for their support and encouragement in the course of the present study. We also thank Prof. H. Sasaji, Fukui University, for his expert advice on coccinellid taxonomy. This study was partly supported by the Grant in Aid (No. 05041086) for the Overseas Scientific Survey from the Ministry of Education, Science and Culture of Japan.

REFERENCES

1 Abbas I, Nakamura K, Katakura H, Sasaji H (1988) Geographical variation of elytral spot patterns in the phytophagous ladybird, *Epilachna vigintioctopunctata* (Coleoptera: Coccinellidae) in the Province of Sumatera Barat, Indonesia. Res Popul Ecol 30:43–56

2 Dieke G H (1947) Ladybeetles of the genus *Epilachna* (sens. lat.) in Asia, Europe, and Australia. Smithsonian Misc Collect 106: 1–183

3 Katakura H, Abbas I, Nakamura K, Sasaji H (1988) Records of epilachnine crop pests (Coleoptera, Coccinellidae) in Sumatera Barat, Sumatra, Indonesia. Kontyû (Tokyo) 56: 281–297

4 Richards A M (1983) The *Epilachna vigintioctopunctata* complex (Coleoptera: Coccinellidae). Intl J Entomol 25: 11–41

5 Ripley B D (1981) Spatial Statistics. John Wiley & Sons, New York

6 SAS Institute Inc (1985) SAS/GRAPH® User's Guide, Version 5 Edition. SAS Institute Inc, Cary, North Carolina

7 Sasaji, H. (1971) Fauna Japonica, Coccinellidae (Insecta: Coleoptera). Keigaku Publ Co, Tokyo

8 Sneath P H A, Sokal R R (1973) Numerical Taxonomy. W H Freeman & Co, San Francisco

9 Sokal R R, Rohlf F J (1981) Biometry (2nd ed.). W H Freeman & Co, San Francisco

APPENDIX

The following is a list of populations studied in the present study. For each population the following information is given: Code number in parentheses, locality name, altitude, number of specimens examined, forma (A or B, Katakura *et al.* [3])-group (I to IV, Abbas *et al.* [1]; ?, not specified)-cluster (1a, 1b or 2, the present study) to which the population was assigned.

(1) Padang Kotomarapak, 70m, 45 males, A-I-1a; (2) Kapundung, 100m, 22 males, A-I-1a; (3) Kinali, 25m, 42 males, A-I-1a; (4) Tinggam Sinurut, 650m, 35 males, A-I-1a; (5) Panti, 240m, 20 males, A-I-1a; (6) Ampang Gadang, 260m, 22 males, A-I-1a; (7) Piladang, 550m, 29 males; B-III/IV-1b; (8) Napar-Tarok (Payakumbuh), 510m, 60 males, AB-III/IV-1b; (9) Halaban, 790m, 24 males, A-III-1b; (10) Koto Ameh-Koto Masjid-Koto Ateh, Pangkalan, 130m, 25 males, A-?-1a; (11) Manggopoh, 40m, 82 males, A-I/II-1a; (12) Sungai Jaring, 50m, 31 males, A-I/II-1a; (13) Kampung Tangah-Desa Sikabu, 80m, 37 males, A-I/II-1a; (14) Batukarak, 100m, 49 males, A-I/II-1a; (15) Muko-muko, 465m, 46 males, A-I/II-1b; (16) Batu Anjing-Sawar Panjang, 470m, 52 males, A-I/II-1b; (17) Kakuban-Sungai Batang, 465m, 50 males, AB-III-1b; (18) Palupuh-Panorama Baru-Bukittingi, 620m, 25 males, AB-?-1b; (19) Ladang Cakiah, 900m, 30 males, B-IV-2; (20) Biaro, 850m, 122 males, B-IV-2; (21) Padang Tarab, 650m, 51 males, B-IV-1b; (22) Pandai Sikek, 1100m, 39 males, B-IV-2; (23) Gunung Merapi, 1140m, 53 males, B-IV-2; (24) Pincuran Puti, 1050m, 30 males, B-IV-2; (25) Tanjung Alam, 1000m, 65 males, B-IV-2; (26) Koto Panjang, 480m, 35 males, B-III-1b; (27) Batu Bulat, 620m, 31males, A III-1b; (28) Balai Tangah, 550m, 43 males, A-III-1b; (29) Kasiak (Lubuk Alang), 20m, 39 males, A-II-1b; (30) Pauh (Pariaman), 5m, 27 males, A-II-1b; (31) Simpang Ampar, 10m, 40 males, A-II-1b; (32) Bungus, 2m, 51 males, A-II-1b; (33) Pasar Baru, 25m, 32 males, A-II-1b; (34) Ikur Koto, 10m, 66 males, A-II-1b; (35) Koto Panjang, 20m, 27 males, A-II-1b; (36) Lubuk Minturum, 80m, 58 males, A-II-1b; (37) Lolo Gunungsarik, 10m, 94 males, A-II-1b; (38) Gunung Sarik, 5m, 30 males, A-II-1b; (39) Dusun Baru, 50m, 90 males, A-I-1a; (40) Tanjung Pondok, 50m, 20 males, A-I-1a; (41) Sungai Gemuruh, 25m, 28 males, A-I-1a; (42) Indrapula, 25m, 32 males, A-I-1a; (43) Painan, 2m, 22 males, A-I/II-1b; (44) Salido, 5m, 64 males, A-I/

II-1a; (45) Api-api, 2m, 37 males, A-I/II-1b.(46) Kasiak (Sumani)-Sikumbang-Padang Belimbing, 365m, 69 males, A-III-1b; (47) Solok, 360m, 23 males, A-III-1b; (48) Koto-baru, 360m, 28 males, A-III-1b; (49) Batang Barus, 1200m, 21 males, B-III/IV-2; (50) Padang Sibusuk, 150m, 40 males, A-I/II-1b; (51) Rasam Tapanggang, 350m, 22 males, A-I/II-1a; (52) Suigai Kambuik-Sungai Daleh, 120m, 29 males, A-I-1a; (53) Gunung Medan, 95m, 44 males, A-I-1a.

AUTHOR INDEX

P

R

S

T

ACKNOWLEDGMENTS

The editors express their gratitude to the following reviewers, who evaluated papers for ZOOLOGICAL SCIENCE Volume 11. Without their assistance the journal could not function.

Abe, Hisashi
Abe, Shin-ichi
Agui, Noriaki
Aida, Katsumi
Akimoto, Shinichi
Amemiya, Syonan
Ando, Masaaki
Aoki, Junichi
Aoki, Kiyoshi
Aotsuka, Tadashi
Azumi, Kaoru

Benno, Yoshimi

Eguchi, Eisuke
Ehara, Shozo
Endo, Takeshi

Fujisawa, Hajime
Fujishima, Masahiro
Fukuda, Hiroyuki
Fukushi, Tsukasa

Hamaguchi, Satoshi
Hayashi, Shinji
Higashinakagawa, Toru
Hikida, Tsutomu
Hirano, Tetsuya
Hisada, Mitsuhiko
Horiuchi, Shiro
Hoshi, Motonori

Ichikawa, Toshio
Ide, Hiroyuki
Iga, Tetsuro
Igarashi, Yoshihiko
Iguchi, Taisen
Imajima, Minoru
Inaba, Kazuo
Inoue, Kinji
Inui, Yasuo
Ip, Yuen K.
Ishihara, Katsutoshi
Ishikawa, Hajime
Ishikawa, Kazuo
Ishizaki, Hironori
Itakura, Teruyoshi
Iwamatsu, Takashi
Iwao, Yasuhiro
Iwasawa, Hisaaki
Izawa, Masako

Kagawa, Hirohiko
Kageyama, Tetsuo
Kamata, Takashi
Kamishima, Yoshihisa
Kaneko, Toyoji
Kanou, Masamichi
Kanzaki, Ryohei
Katagiri, Chiaki
Katagiri, Chihiro
Katagiri, Yasuo
Katakura, Haruo
Katayama, Heizaburo
Kato, Yoshiomi
Katoh, Setsuko
Kawahara, Akira
Kawamura, Kazuo
Kawamura, Satoru
Kawashima, Seiichiro
Kayano, Haruo
Kiguchi, Kenji
Kikuyama, Sakae
Kitada, Yasuuki
Kobayashi, Makoto
Kobayashi, Tetsuya
Kobayashi, Tohru
Kobayashi, Yuta
Kohno, Sei-ichi
Koizumi, Osamu
Kojima, Shigeaki
Komatsu, Mieko
Kominami, Tetsuya
Kuramoto, Mitsuru
Kurita, Shirou
Kuroda, Masaaki

Machida, Takeo
Mashiko, Kazuo
Matsuda, Ryoichi
Matsui, Masafumi
Matsumoto, Akira
Matsushima, Osamu
Matuno, Akira
Mineta, Amao
Miura, Ikuo
Miura, Takeshi
Miyatake, Mutsuo
Mizunami, Makoto
Mori, Takao
Morisawa, Masaaki
Moriya, Tsuneo
Motokawa, Tatsuo
Mugiya, Yasuo
Mukai, Hiroshi
Muramoto, Atsuko

Nagahama, Yoshitaka
Nagao, Tadayasu
Nagasawa, Hiromichi
Naito, Nobuko
Neya, Toshiaki
Ninomiya, Yuzou
Nishida, Takao
Nozaki, Masumi
Numata, Hideharu

Obika, Masataka
Obinata, Takashi
Ohmuro, Hiromi
Ohta, Suguru
Ohta, Yasuhiko
Ohtaki, Tetsuya
Oishi, Tadashi
Oka, Yoshitaka
Okada, Mitsumasa
Ozaki, Koichi
Ozaki, Mamiko
Ozato, Kenjiro

Sakai, Masaki
Saotome, Kyoko
Sasaki, Masami
Sasayama. Yuichi
Sata, Masanori
Satoh, Noriyuki
Sawada, Tomoo
Sawara, Yuji
Sekiya, Kunio
Seto, Takeshi
Shibuya, Tatsuaki
Shigei, Michio
Shigenaka, Yoshinobu
Shikama, Keiji
Shimada, Hiraku
Shimada, Ichiro
Shimizu, Isamu
Shimozawa, Tateo
Shiokawa, Koichiro
Shirai, Hiroko
Shiraishi, Akio
Shirayama, Yoshihisa
Shirotani, Youko
Shiroyama, Yoshihisa
Suemitsu, Takashi
Sugahara, Takashi
Suhama, Mikio
Suzuki, Emiko
Suzuki, Norio

Tabata, Mitsuo
Taguchi, Yasuko
Takagi, Takashi
Takagi, Yoshiomi
Takahashi, Akiyoshi
Takahashi, Sumio
Takei, Yoshio
Takeichi, Masatoshi
Takeuchi, Shigeo
Tanaka, Kunio
Tanaka, Shigeyasu
Tasaka, Masao
Tazaki, Kenro
Terakado, Kiyoshi
Tokunaga, Fumio
Tomioka, Kenji
Tomiya, Masako
Tomonaga, Susumu
Tsuchiya, Teizo
Tsujimura, Hidenobu
Tsukahara, Junzo
Tsukahara, Yasuo
Tsukamoto, Risa
Tsuneki, Kazuhiko
Tsurusaki, Nobuo
Tsutsui, Kazuyoshi

Uchiyama, Minoru
Ueda, Hiroaki
Ueda, Hiroshi
Ueno, Shun-ichi
Ueshima, Tsutomu
Urano, Akihisa

Watanabe, Tsuyoshi
Watanabe, Yuichi

POWERFUL PARTNERS FOR LONG-TERM PATCH CLAMPING

The MHW-3 water hydraulic micromanipulator features a refined slide mechanism and a 5:1 hydro/mechanical ratio to keep drift to an absolute minimum — just 1/17.5th of earlier, oil-based hydraulic units. Consequently, patch recording is accurate and reliable over extended periods. The MHW-3 has a full, pipette movement range of 2mm in ultra-fine 0.2μm graduations to allow fine remote control movement in all three axes, thereby providing exceptionally precise specimen pinpointing.

The MHW-30 features a movement range of 10mm, minimum graduations down to 1μm, and a 1:1 hydraulic system.

Three-Dimensional Water Hydraulic Micromanipulators

with coarse and fine manipulation

MHW-3 and MHW-30

For further information and maintenance service:

NARISHIGE JAPAN

NARISHIGE SCIENTIFIC INSTRUMENT LAB.
9-28, Kasuya 4-chome, Setagaya-ku, Tokyo 157, Japan
Phone: (INT-L) 81-3-3308-8233 Fax: (INT-L) 81-3-3308-2005 Telex: NARISHIGE J27781

U.S. NARISHIGE INTERNATIONAL INC.
404 Glen Cove Avenue, Sea Cliff, New York 11579, U.S.A.
Telephone: +1 (516) 759-6167 Telefax: +1 (516) 759-6138

NARISHIGE INTERNATIONAL LTD.
Unit 7, Willow Business Park, Willow Way, London SE26 4QP, UK
Telephone: +44 (0) 81-699-9696 Telefax: +44 (0) 81-291-9678

ZOOLOGICAL SCIENCE

VOLUME 11 NUMBER 6 DECEMBER 1994

CONTENTS

INDEXED IN:
Current Contents/LS and AB & ES,
Science Citation Index,
ISI Online Database,
CABS Database, INFOBIB

Issued on December 15
Front cover designed by Saori Yasutomi
Printed by Daigaku Letterpress Co., Ltd., Hiroshima, Japan

ISSN 0289-0003

64
4

An International Journal

ZOOLOGICAL SCIENCE

Vol. 11 Supplement

December 1994

SUPPLEMENT

Proceedings of the Sixty-Fifth Annual Meeting of the Zoological Society of Japan

October 5–8, 1994
Nagoya

published by Zoological Society of Japan
distributed by Business Center for Academic Societies Japan
VSP, Zeist, The Netherlands

ZOOLOGICAL SCIENCE

The Official Journal of the Zoological Society of Japan

The Zoological Society of Japan:
Toshin-building, Hongo 2–27–2, Bunkyo-ku,
Tokyo 113, Japan. Phone 03-3814–5461
Fax 03-3814-5352

Officers:
President: Hideo Mohri (Chiba)
Secretary: Takao Mori (Tokyo)
Treasurer: Makoto Okuno (Tokyo)
News Editor: Akira Matsumoto (Tokyo)
Librarian: Masatsune Takeda (Tokyo)
Auditors: Hideshi Kobayashi (Tokyo)
Hiromichi Morita (Fukuoka)

ZOOLOGICAL SCIENCE is devoted to publication of original articles, reviews and rapid communications in the broad field of Zoology. The journal was founded in 1984 as a result of unification of Zoological Magazine (1888–1983) and Annotationes Zoologicae Japonenses (1897–1983), the former official journals of the Zoological Soceity of Japan. An annual volume consists of six regular numbers and one supplement (abstracts of papers presented at the annual meeting of the Zoological Society of Japan) of more than 850 pages. The regular numbers appear bimonthly.

MANUSCRIPTS OFFERED FOR CONSIDERATION AND CORRESPONDENCE CONCERNING EDITORIAL MATTERS should be sent to:

Dr. Tsuneo Yamaguchi, Editor-in-Chief, Zoological Science, Department of Biology, Faculty of Science, Okayama University, Okayama 700, Japan, in accordance with the instructions to authors which appear in the first issue of each volume. Copies of instructions to authors will be sent upon request.

SUBSCRIPTIONS. ZOOLOGICAL SCIENCE is distributed free of charge to the members, both domestic and foreign, of the Zoological Society of Japan.To non-member subscribers within Japan, it is distributed by Business Center for Academic Societies Japan, 5–16–9 Honkomagome, Bunkyo-ku, Tokyo 113. Subscriptions outside Japan should be ordered from the sole agent, VSP, Godfried van Seystlaan 47, 3703 BR Zeist (postal address: P. O. Box 346, 3700 AH Zeist), The Netherlands. Subscription rates will be provided on request to these agents. New subscriptions and renewals begin with the first issue of the current volume.

[Publication of Zoological Science has been supported in part by a Grant-in-Aid for Publication of Scientific Research Results from the Ministry of Education, Science and Culture, Japan.]

Proceedings of the
Sixty-Fifth Annual Meeting of the
Zoological Society of Japan

October 5–8, 1994
Nagoya

ZOOLOGICAL SCIENCE 11: Supplement: 3 (1994)

[THE ZOOLOGICAL SOCIETY PRIZE]

STUDIES ON THE MECHANISMS OF PIGMENT PATTERN FORMATION AND LIMB PATTERN FORMATION

HIROYUKI IDE

Biological Institute, Tohoku University, Aoba, Sendai 980-77, Japan

To analyze cellylar mechanisms of pattern formation, we have studied amphibian pigment pattern and avian limb cartilage pattern, especially in cell culture. The pigment pattern of the amphibian body surface is specified by the distribution of three types of chromatophores. These chromatophores are of neural crest origin and differentiate depending on the environmental prepattern of the skin. The cartilage pattern of avian limb is specified in the distal of the limb bud, progress zone (PZ) under the control of the AER and ZPA.

We have succeeded in the clonal culture of three types of chromatophores isolated from bullfrog tadpoles. The proliferating melanophores retained the activity of melanin synthesis and melanin dispersion in clonal culture. However, iridophores and xanthophores transdifferentiated into melanophores in clonal culture, although *in vivo,* these chromatophores proliferated without the transdifferentiation. Thus, some factors must be operating to stabilize the differentiated states of these chromatophores involved in pigment pattern formation. We have cultured the iridophores in the medium containing the serum of bullfrog tadpoles. In this medium, iridophores proliferated without the conversion. One of such factors, melanization inhibiting factor (MIF), has been isolated later from the skin of *Xenopus laevis*. The MIF inhibited the differentiation of the melanophores and was rich in the ventral skin, suggesting some roles in the dorsoventral pigment pattern formation.

The cartilage pattern of chick limb bud is specified in the PZ, where the cells are maintained in an undifferentiated state by factors from the AER. We have found that FGF-2 (basic fibroblast growth factor) is one of the factors and induces the expression of MSX-1 and AV-1, which are markers of the progress zone, in the cultured PZ cells. The proliferation and chondrogenesis of the PZ cells were stimulated by retinoic acid (RA) in culture as in the case of RA-induced duplicate formation *in vivo*.

A positional heterogeneity of interaction was found in cultured limb bud fragments and mesenchymal cells. The cells of anterior margin responded to the signal from the posterior margin (ZPA) and proliferated. This type of interaction seems to be involved in the regulation of pattern in limb development.

The positional values along the anteroposterior and proximodistal axes of the limb bud are allotted to the PZ cells isolated from different parts of the limb bud must have different characteristics which are specified by the positional values. We have segregate from each other. This difference in cell affinity reflected the positional values specified in the PZ and was retained in the proximal tissues. Further, the cell affinity changed by the RA-treatment; posteriorization and proximalization on the cell surface characteristics occurred as *in vivo*.

ZOOLOGICAL SCIENCE 11: Supplement: 4 (1994)

[THE ZOOLOGICAL SOCIETY PRIZE]

SPERM-ACTIVATING PEPTIDES IN THE EGG JELLY OF SEA URCHINS

NORIO SUZUKI

Division of Biological Sciences, Graduate School of Science, Hokkaido University, Sapporo 060, Japan

In 1981, we first isolated a decapeptide (GFDLNGGGVG) from the solubilized jelly layer of the sea urchin *Hemicentrotus pulcherrimus* and demonstrated that this peptide stimulated the respiration and motility of *H. pulcherrimus* spermatozoa. Subsequently, the peptide has been shown to produce a number of biological effects on *H. pulcherrimus* spermatozoa including increases in cAMP and cGMP levels, activation of an Na^+/H^+ exchange system, and increases in intracellular pH (pH_i)and $[Ca^{2+}]$ ($[Ca^{2+}]_i$). The peptide activates the metabolism of endogenous phosphatidylcholine and promotes the acrosome reaction as a specific co-factor of a major acrosome reaction-inducing substance, fucose sulfate glycoconjugate (FSG). The peptide also induces an electrophoretic mobility change in the guanylate cyclase of the sperm plasma membrane with concomitant dephosphorylation and inactivation of the enzyme.

In the past decade, we have purified and determined the structures of seventy-four peptides from the solubilized jelly layer of seventeen species of sea urchins distributed over five taxonomic orders. These peptides show essentially the same biological effects on sea urchin spermatozoa although these effects and the structures of the peptides are specific at the ordinal level. Therefore, I proposed to call these peptides sperm-activating peptide (SAP) as the general name. SAPs can be classified into five groups, i.e. SAP-I (GFDLNGGGVG) from species in the order Echinoida, SAP-II (SAP-IIA: CVTGAPGCVGGGRL and SAP-IIB: KLCPGGNCV) from species in the order Arbacioida, SAP-III (DSDSAQNLIG) from species in the order Clypeasteroida, SAP-IV (GCPWGGAVC) from species in the order Diadematoida, and SAP-V (GCEGLFHGMGNC) from species in the order Spatangoida.

Prior to the induction of these physiological and biochemical events, SAPs bind to specific receptors on the sperm plasma membrane. Analysis of the data obtained from the equilibrium binding of a radioiodinated SAP-I analogue [GGGY(^{125}I)GFDLNGGGVG] to *H. pulcherrimus* spermatozoa suggests the presence of two classes of receptors (high affinity and low affinity) specific for SAP-I binding. Considering the Kd values of these receptors and EC_{50} values for SAP-I's biological activity, we presume that the high affinity receptor is associated with respiration-stimulating activity and elevations in intracellular pH, while the low affinity receptor is coupled to elevations in cGMP and $[Ca^{2+}]_i$. The radioiodinated SAP-I analogue crosslinks to a 71 kDa protein which appears to be associated with a 220 kDa WGA-binding protein on *H. pulcherrimus* sperm plasma membrane. A cDNA encoding the 71 kDa protein was isolated and an open reading frame predicted a protein of 532 amino acids containing a 30-residue amino terminal signal peptide, followed by a large N-terminal extracellular domain and a single transmembrane region at the almost C-terminal end of the protein.

A cDNA clone encoding SAP-I was isolated and an open reading frame predicted a protein of 334 amino acids containing five SAP-I and seven SAP-I-like decapeptides, each separated by a single lysine residue. *In situ* hybridization with an RNA probe synthesized using the cDNA demonstrated that abundant SAP-I precursor transcripts were expressed in the accessory cells, but not in the growing oocyte. A similar pattern was also seen for FSG.

ZOOLOGICAL SCIENCE 11: Supplement: 5–6 (1994)

[THE ZOOLOGICAL SOCIETY PRIZE]

MECHANISM OF CONTROL OF CELL DEATH AND HISTOLYSIS ASSOCIATED WITH REMODELING OF ANIMAL TISSUES

KATSUTOSHI YOSHIZATO

Laboratory of Developmental Cell Biology, Hiroshima University, Higashihiroshima, Hiroshima 724, Japan

Anura are one of unique and useful experimental animals for the study which aims at revealing the mechanism of formation of animal's body shape, because their life cycle contains the period of larva that drastically changes its body shape into adult form (metamorphosis, transformation of body morphology). At the metamorphosis, larva-specific tissues stop functioning and fall into histolysis and likewise larval cells fall into cell death (apoptosis), which occurs in a regionally and temporally regulated manner, suggesting that some specific program ("death program") governs these processes. Our study has been developed to know the entity of the death program at the cellular and molecular levels. For this aim, a special interest has been paid to the mechanism of action of thyroid hormone (TH) because the expression of death program is strictly controlled by TH.

Prolaction (PRL) has been known as an endocrine factor that stimulates the growth and development of anuran larvae. We showed that PRL is especially effective in developing connective tissues of the tadpole tail and stimulates the collagen synthesis more than 20 times. Northern blot analysis showed that PRL enhances the expression of collagen genes but suppresses that of collagenase genes. Our study supports the idea that PRL plays some role for the normal larva to adult transition by constantly activating larval cells that are engaged in "the last day job" in the regressing tail tissues.

TH triggers the death of larval cells such as tail skin cells. Therefore, it had been considered that the initial event of very complex cascades of biochemical reactions involved in the cell death is the formation of a complex of TH and thyroid hormone receptor (TR). We characterized nuclear TR of tail cells by the Scatchard analysis and demonstrated the presence of the high affinity and low capacity receptor for the first time in the amphibian. The capacity but not the affinity of TR increases at the climax stage of metamorphosis. Recently, as described below we showed the presence of cis-acting element for TR in tadpole collagenase gene.

The skin of tadpole does not show regional specificities in the morphology at the beginning of its development, but acquires the regionality during larval development: the body skin becomes different from the tail skin in their structure and metamorphic changes. We described the process of this region-specific change histologically and immunologically. Tail epidermal cells remain as larval cells and keep to express larval antigens, while the body epidermis produces epidermal pregerminative cells of adult-type and adult antigens. Larval epidermal cells and adult pre-germinative cells show quite different responses to TH: the former falls into apoptosis and the latter is stimulated to proliferate and differentiate.

The subepidermal mesenchyme was shown to induce the regional specificity of epidermis described above: the tail mesenchyme has the potency to change the back epidermis to the tail epidermis when the former is artificially combined with the latter, and *vice versa*. This mesenchymal inducing activity is lost at the early stage of premetamorphosis when TH-dependent remodeling of the mesenchyme occurs. The concentration of TH required at this stage is much lower than that required to initiate the climax change of metamorphosis.

Larva-specific tissues are subject to histolysis when plasma level of TH increases to around 10^{-9} M as of triiodothyronine. To know biochemical and molecular biological mechanism of the TH-induced histolysis, we have placed a target of the study on collagenase which is responsible for the breakdown of collagens. We purified tadpole collagenase, produced polyclonal antibodies against it and cloned cDNA and genes of the enzyme. Western and northern blot analyses showed that the expression of collagenase genes is up-regulated by TH. Immunohistology identified cells producing the enzyme as epidermal cells and mesenchymal cells in the collagen layer. The gene of anuran collagenase has a quite unique structure consisting of 4 exons as compared to the mammalian gene that contains 10 exons. Most interestingly, the tadpole gene has the thyroid hormone responsive element (TRE) in the transcription regulatory region, while the mammalian gene dose not as far as we have checked. We speculate that TH-dependent regulation of expression of collagenase is unique in amphibian. We succeeded in discovering a unique and new thiol endoprotease (ProteaseT_1) that degrades effectively and preferentially actin and characterized it biochemically. This enzyme is also TH-responsive and functions in the breakdown of muscle tissues by attacking the I band.

There still remain questions unanswered whose resolutions much contribute to the understanding of molecular and cellular mechanism of amphibian metamorphosis such as: the

origin of adult-type pre-germinative epidermal cells; the entity of mesenchymal factor which donates the regional specificity to the larval skin; transcription factors that regulate the TH-responsive and metamorphosis-associated proteins. We plan to develop studies to solve these questions.

IDENTIFICATION AND CHARACTERIZATION OF ESTROGEN RECEPTOR IN THE STINGRAY ULTIMOBRANCHIAL GLANDS

Kazutoshi Yamamoto[1], Nobuo Suzuki[2], Noriyuki Takahashi[1], Tsuyoshi Kojima[2], Yuichi Sasayama[3], and Sakae Kikuyama[1]
[1]Dept of Biol, Sch of Educ, Waseda Univ, Shinjuku, Tokyo 169-50, [2]Dept of Biol, Fac of Sci, Toyama Univ, Toyama 930, [3]Noto Marine Lab, Fac of Sci, Kanazawa Univ, Ishikawa 927-05, Japan

On the basis of our previous observation that estrogen may stimulate calcitonin secretion by the ultimobranchial glands in the stingray, Dasyatis akajei, experiments were conducted to examine the presence of estrogen receptor (ER) and its mRNA in the gland, employing the techniques of exchange assay and northern blot analysis. The optimal incubation condition of exchange assay for cytosolic ER was found to be at 25°C for 2 hr. Scatchard analysis for cytosolic ER yielded a straight line with a dissociation constant of 0.29 nM and the maximum number of binding sites of 187.2 fmol/mg protein. Total RNA extracted from the ultimobranchial glands was subjected to northern blot analysis using a rat uterus ER cDNA as a probe, which encodes the B- through F-domains of the full length of the rat ER protein. A positive signal was detected at 2 kb. The results suggest that the stingray ultimobranchial glands express the ER gene.

WHY CHICKEN LUTEINIZING HORMONE (LH) IS RECOGNIZED AS FOLLICLE-STIMULATING HORMONE (FSH) BY MAMMALIAN GONADAL RECEPTORS : A MOLECULAR APPROACH

S. Ishii[1], Y. Miya[1] and H. Wako[2]. [1]Department of Biology, School of Education and [2]School of Social Sciences, Waseda University, Tokyo 169-50.

We found that specific binding of radiolabeled rat FSH to testicular receptors of the rat was competitively inhibited by both chicken LH and FSH. Furthermore, the inhibition by chicken LH was stronger than that by chicken FSH and as strong as that by rat FSH. To explain this discrepancy, we compared the primary structure between beta subunits of LH and FSH of various vertebrates. Two different sequences, one Position 40–48 and another Position 101–106 in the primary structure of the chicken LH beta subunit differed largely from corresponding sequences in mammalian LH beta subunits but almost identical to those in mammalian FSH beta subunits. We estimated the secondary structure common through all the beta subunits of the gonadotropin/thyrotropin family members, and constructed a three dimensional model of them using our data on the estimated secondary structure and other data. Regions containing both of the above mentioned sequences were estimated as loops of the secondary structure and to be exposed to the surface of the globular molecule. The sequence of 40–48 is included partely in "the large loop" that was reported by Keutmann et al. (1987) as the sequence necessary for binding to LH receptor, and the sequence of 101–106 locates just next to "the determinant loop" recognized of its importance to biological activity by Ward and Moore (1979). Presence of such FSH–unique sequences in and near the biologically important domains in the chicken LH beta subunit molecule is considered to be the cause of the strong affinity of chicken LH to mammalian FSH receptors. The two sequences may be important for recognition of hormone species. Biological effects of chicken LH on mammalian FSH target cells are now being studied to know whether binding of chicken LH to mammalian FSH receptors can evoke subsequent biological actions or not, or chicken LH can be an agonist or antagonist of mammalian FSH.

EXOGENOUS ESTROGEN ACTS DIFFERENTLY ON PRODUCTION OF ESTROGEN RECEPTOR IN THE PREOPTIC NUCLEUS (PON) AND THE MEDIOBASAL HYPOTHALUMUS (MBH)

C.Orikasa, K.*Mizuno, H.Okamura and S.Hayashi. Dept. of Anat. & Embryol, * Dept of Microbiol. & Immunol., Tokyo Metropolitan Inst. for Neurosci., Tokyo.

Estrogen receptor (ER) mediates action of estrogen as a transcription factor, which initiates *de novo* protein synthesis and eventually regulates neuronal function. Being related to the control of reproductive function, hypothalamic nuclei in the MBH and the PON, contain numerous ER. We investigated influence of exogenous estrogen on ER-mRNA and ER protein molecules in these nuclei in the newborn female rats. Pups have recieved daily injections of 10μg estradiol benzoate (EB) for 5 or 10 consecutive days from the day of birth and killed on days 6 and 11. ER was investigated at the gene level by *in situ* hybridization histochemistry (ISHH) and by RT-PCR/Southern analysis, while at protein level by immunohistochemistry (IHC). At first, the expression of ER gene and protein was examined by ISHH and IHC, respectively. Both ER mRNA and ER protein were suppressed by EB in MBH. In PON, on the contrary, EB suppressed ER protein, but not ER-mRNA. The results obtained by RT-PCR were in good agreement with those by ISHH. One possible explanation of these observations is that the ER mRNA expressed in the PON is aberrant even if it was still detectable, so that the mature protein can not be translated. This mRNA, however, might still maintain base sequences detectable by the cRNA probes we used. In MBH, in contrast, ER-mRNA seemed to be suppressed directly, and then ER protein synthesis eventually decreased. Thus, EB seemed to act on the different steps of gene expression between PON and MBH. All these mechanisms may contribute to irreversible changes in the specific sets of genes involved in neuronal function.

IN SITU DETECTION OF GONADOTROPIN-RELEASING HORMONE RECEPTOR mRNA EXPRESSION DURING THE DEVELOPMENT OF RAT OVARIAN FOLLICLES.

H. Kogo[1]. A. Kudo[2], M. K. Park[1], T. Mori[1] and S. Kawashima[1], [1]Zool. Inst., Grad. Sch. of Sci., Univ. of Tokyo, Tokyo, [2]Dept. of Anat., Kyorin Univ. Sch. of Med., Tokyo

The expression of ovarian GnRH receptor mRNA was examined histologically by in situ hybridization in immature rats treated with PMSG only or in combination with hCG. ^{35}S-labeled sense and antisense strand RNA probes of GnRH receptor were used for in situ hybridization, and only antisense probe exhibited specific hybridization signals. Strong hybridization signals were observed in the granulosa cells of atretic follicles. However, no significant signals were found in the granulosa cells of healthy small, preantral or early antral follicles. Healthy Graafian and preovulatory follicles showed intense signals in their mural granulosa cells, but no signals were detected in the cumulus oophorus cells of these mature follicles. Corpora lutea showed only weak signals, but luteinizing follicles probably after atresia exhibited signals of moderate intensity in their luteinized and remaining granulosa cells. No signals were detected in the theca cells and oocytes in all the follicles. Interstitial cells sometimes exhibited some hybridization signals when the cells were eosinophilic. Pretreatment with different combinations of gonadotropins yielded different ovarian histological state, but this had no influence on the localization of hybridization signals. The present results showing that the expression of authentic GnRH receptor mRNA was limited in a certain ovarian cell population, suggest the ovarian GnRH is playing a role in various ovarian functions including follicular development, atresia, ovulation and luteinization.

EXPRESSION OF BIOLOGICALLY ACTIVE RECOMBINANT PORCINE FSH

Y. Kato[1], I. Sato[2], T. Ihara[2], K. Tomizawa[1], K. Gen[1], T. Kato[1], J. Mori[3], T. Nagai[4], M. Geshi[4], K. Okuda[5], T. Inaba[3], S. Ueda[2]. [1]Inst. of Endocrinol., Gunma Univ., [2]Nippon Inst. for Biol. Sci., [3]Coll. of Agric., Univ. of Osaka Pref., [4]Tohoku Natl. Agric. Exp. Stn., [5]Coll. of Agric., Okayama Univ.

This study aimed to produce a biologically active porcine follicle-stimulating hormone (pFSH). The expression vector was constructed by ligation of porcine α[1] and FSHβ[2] cDNAs, separately, into a single baculovirus vector pAcUW3 which contains two promoters, P10 and polyhedrin promoters. The vector was expressed in Tn5 cells. The culture media were collected and the viruses were inactivated. Glycosylation of recombinant porcine FSH (r-pFSH) was observed. Purification of r-pFSH was performed on a S-Sepharose column following by a ConA affinity chromatography. Purified r-pFSH was recovered in six fractions. Heterogeneity of the carbohydrate moiety might cause the separation. Biological activity of the r-pFSH *in vitro* was assayed by the activities for the secretion of progesterone from the porcine granulosa cells, for the germinal vesicle break down of the porcine oocytes and the estrogen production in rat sertoli cells. All results showed that r-pFSH has similar activities to that of pituitary derived porcine FSH (w-pFSH), though some fraction showed slightly low activity. When the testosterone production using mouse lydig cells was examined, the testosterone production was not observed for r-pFSH, whereas the w-pFSH showed 0.1% activity of the same amount of pLH. Thus, the r-pFSH produced in this study is biologically active and is free from LH activity. 1) Hirai *et al.*, Mol. Cell. Endocrinol. **62**, 135-139 (1989). 2) Kato *et al.*, Mol. Cell. Endocrinol. **62**, 47-53 (1989).

DETERMINATION OF TARGET ORGANS FOR SALMON AND CHICKEN II GNRHS IN SALMONID BY MEANS OF THE EXPRESSION EXPERIMENT USING *XENOPUS* OOCYTES.

K.Kubokawa[1], H.Nagasawa[1] and Y.Kubo[2], [1] Dept. of Mol. Biol., Ocean Res. Inst., Univ. of Tokyo, Nakano, Tokyo, [2] Dept. of Neurophysiol., Tokyo Metropolitan Inst. for Neurosci., Fuchu, Tokyo.

Salmons have two types of GnRH, salmon (sGnRH) and chicken II (cGnRH-II) GnRHs. Salmon GnRH fibers are distributed in various brain regions and innervate the pituitary. Chicken GnRH-II fibers show similar distributions with sGnRH fibers except that they do not innervate the pituitary. However, characterization and localization of their receptors have not yet been studied in salmonids. To find target organs of GnRHs in the salmonids, we employed the *Xenopus* oocyte expression system. We can detect binding of GnRHs to their receptors by measuring the chloride current, since the GnRH receptors are known to belong to members of the G-protein coupled receptor superfamily. Messenger RNA was extracted from the brain, pituitary and ovary of masu salmons, and injected into Xenopus oocytes. Then, injected oocytes were exposed to each GnRH. Oocytes injected with brain or ovary mRNA responded to both sGnRH and cGnRH-II. Oocytes injected with pituitary mRNA responded to sGnRH. Mammalian GnRH elicited little response. These results suggest that functional GnRH receptors of the masu salmon can be expressed in the *Xenopus* oocyte, and that not only the brain but also the ovary has receptors for both sGnRH and cGnRH-II in the masu salmon.

CLONING AND SEQUENCING OF MOUSE MSH-R GENES.

M. Yabuuchi[1], H. Suzuki[1], S. Takeuchi[1] and C. Sato [2]
[1]Dept. of Biol., Fac. of Sci., Okayama, [2]Super Molecular DIV., Electrotechnical Lab.

The stimulation of melanogenesis in melanocytes is the most clearly established function for MSH .A number of additional functions has been proposed over the years, such as a variety of biological activities in the brane, the pituitary, immune system, and in other areas, however, it has not yet been established. To understand the bases of these variety functions , it is necessary to clone and characterize the MSH receptor genes.

In this study, we obtained 400bp of PCR products using mouse genomic DNA as a substrate. Using it as a probe , we screened a cDNA library derived from cultured melanocyte cell line, TM10 and obtained MSH-R cDNA with the length of 1.8kb . Some genomic clones were also isolated by screening genomic library by the means of plaque hybridization with the cDNA.

Cloning of a bullfrog proopiomelancortin cDNA

T.Aida , S.Iwamuro , S.Kikuyama and S. Miura.[1] Dept. of Biol., Sch. of Educ., Waseda Univ., Tokyo and [1]Yokohama City Univ. Sch. of Med., Yokohama.

A cDNA library was constructed from total RNA of bullfrog (Rana catesbeiana) neurointermediate lobes and a full-length cDNA for bullfrog proopiomelanocortin(POMC) was isolated. The cDNA clone contained an open-reading frame of 783bp that predicted a 261 amino acid POMC protein. The deduced amino acid sequence contained exact sequences of POMC peptides that were determined by direct sequensing of purified peptides. However, it disaccorded by six amino acid residues with the sequence of POMC of the same species reported previously by other investigators. The reason for this discrepancy is not clear.

CLONING AND SEQUENCING OF MSH RECEPTOR GENE IN THE CHICKEN.

H. Suzuki, S. Hirose, M. Yabuuchi and S. Takeuchi
Fac. of sci., Okayama University, Okayama

A chick genomic clone designated gCMR1 has been isolated by homology screening with a cDNA probe representing mouse MSH receptor (MC1). It was found to encode a 314 amino acid protein, which shared 64% identity with mammalian MSH receptors. Several motifs possibly involved in the regulation of the gene expression were recognized in both 5' and 3' non-coding flanking regions of the gene. Interestingly identical amino acid substitution, as observed in mutant mice with a dominant extension allele, was found in the deduced amino acid sequence. These results suggest that gCMR1 encodes a chick MSH receptor which may be active constitutively .

This is the first report of the cloning of a receptor gene which belongs to the melanocortin receptor family in non-mammalian species.

ISOLATION OF PARTIAL cDNA CLONES AND EXPRESSION OF BULLFROG THYROGLOBULIN.

Shintaro Suzuki and Masayuki Suda
Inst. for Molecular & Cellular Regulation.
Gunma Univ., Maebashi, Japan

Thyroglobulin, prothyroid hormone is a large glycoprotein with a molecular weight of 660,000. Thyroid hormones, thyroxine and triiodothyronine are produced in the moiety of this molecule. In amphibians, thyroid hormones are indispensable and play an important role in metamorphosis. In order to clarify the hormonogenic sites and gene structure of this glycoprotein, we isolated and analyzed thyroglobulin cDNA clones of the bullfrog, Rana catesbeiana. By screening a tadpole thyroid cDNA library with a mixed sequence oligonucleotide probe based on a partial amino acid sequence of bullfrog thyroglobulin, we obtained partial cDNA clones. Three of them we characterized covered in total ca. 1.6kb region of the thyroglobulin. We determined the 5' and 3' terminal parts of the region. The amino acid sequences deduced from the 5' and 3' terminal parts could be aligned successfully with the amino acid sequence of mammalian thyroglobulin, and contained a type 1 repeating unit characteristic of thyroglobulin primary structure. By using one of these clones as a probe it was shown that thyroglobulin mRNA greatly increased after administration of bovine TSH even in adult frogs.

TRANSCRIPTION FACTORS IN THE PORCINE ANTERIOR PITUITARY

K. Gen, T. Kato and Y. Kato. Hormone Assay Center, Inst. of Endocrinol. Gunma Univ. Gunma

We have observed previously that the binding factors to the cAMP-responsive element (CRE) and the AP1 factor binding site (AP1) in the porcine anterior pituitary might alter the dimer form by changing each respective partner to bind CRE and/or AP1 (1, 2). This heterodimerization of pituitary factors would provide varied specificity to recognize given specific gene. This study focused to investigate transcription factors binding to CRE and AP1 using human CREB, cFos and cJun cDNAs. Screening of porcine anterior pituitary cDNA library constructed in λgt 11 at low stringent conditions gave positive clones by respective probes, except for CREB. Analyses of nucleotide sequences for purified clones showed that they are porcine cJun and cFos with more than 90% homology to human cDNAs. Other clones belong to their family were not obtained. Even if the anterior pituitary contains family of transcirtion factors as well as cJun and cFos to form alternative heterodimer to recognize CRE and/or AP1, they may have distinct nucleotide sequences from CREB, cJun and cFos.

(1) Ezashi,T., Kato, T., Wakabayashi, K. and Kato,Y. *Biochem. Biophys. Res. Commun.* **188**, 170-176 (1992). (2) Kato,Y., Kato, T., Ezashi,T. and Inoue, K. *ibid.* **195**, 963-968 (1993).

CLONING AND EXPRESSION OF SEMINAL VESICLE SPECIFIC PEPTIDE OF TERRESTRIAL ISOPOD, ARMADILLIDIUM VULGARE.

H.Nagasawa[1], H.Hatayama[1,5], Y. Hasegawa[2], K.Haino[3], Y.Katakura[4] and T.Yanagisawa[5]. [1]Ocean Res. Inst., Tokyo Univ., Tokyo, [2]Dept. Biol., Keio Univ., Yokohama, [3]Dept. of Biol., Tokyo Metropolitan Univ., Tokyo, [4]Dept. of Bioengineering, Soka Univ. Tokyo and [5]Fac. of Agr., Utsunomiya Univ., Tochigi.

During the course of purifying androgenic gland hormone from male reproductive organs of the terrestrial isopod, Armadillidium vulgare, a novel peptide was isolated and characterized. The peptide was found to have 59 amino acid residues with two intramolecular disulfide bonds, and had no sequence homology with other known peptides. By using RT-PCR with two mixed oligonucleotide primers corresponding to the amino acid sequences from Asn(19) to Cys(25) and from Glu(45) to Ala(51), a part (98 bp) of cDNA for this peptide could be amplified from single strand cDNA prepared from mRNA of male reproductive organs. The amino acid sequence deduced from the nucleotide sequence was identical with that of the natural peptide. Northern hybridization using this cDNA as a probe revealed that the gene encoding the peptide was expressed only in seminal vesicle and vas deferens but not in androgenic gland, testis or ovary and that the size of the transcript was about 0.95 kb. The expression site was consistent with the results from Western blot analysis.

TROUT VENTRICULAR NATRIURETIC PEPTIDE: PRIMARY STRUCTURE AND BIOLOGICAL ACTIVITY

Y. Takei[1], M. Takano[2], T. X. Watanabe[3] and K. R. Olson[4] [1]Ocean Res. Inst., Univ. Tokyo, Tokyo, [2]Res. Inst., Zenyaku Kogyo Co. Ltd., Tokyo, [3]Peptide Inst. Inc., Minoh and [4]Indiana Univ. Sch. Med., U.S.A.

We have isolated a new ventricular natriuretic peptide (VNP) from cardiac ventricles of the rainbow trout, Oncorhynchus mykiss, and determined its amino acid sequence. The trout VNP consists of 35 amino acid residues with a C-terminal sequence of 14 amino acid residues that extend from a intramolecular ring. Thus, characteristic structure of VNP is also conserved in the trout VNP. A C-terminally truncated form with 31 amino acid residues was also isolated.

Trout VNP induced hypertension in intact trout and hypotension in phenoxybenzamine-treated trout. The former was observed only in the trout and caused by sympathetic activation. The trout VNP was no more potent than human ANP in the homologous trout in both effects. It has been shown that eel VNP is 100-fold more potent than human ANP in the homologous eel for vasodepressor effect. However, trout VNP was more potent than eel VNP, and equipotent to human ANP for either vasodepressor or natriuretic effect in the rat. The potent effects of trout VNP in the rat may be due in part to its long-lasting effect.

EFFECTS OF ENVIRONMENTAL SALINITY ON PLASMA ATRIAL NATRIURETIC PEPTIDE (ANP) LEVELS IN EELS

H. Kai-ya and Y. Takei Ocean Res. Inst., Univ. of Tokyo, Tokyo,

Although ANP is known to regulate water and electrolyte balance in mammals, little is known about its function in fish. In this study, we have examined changes in plasma ANP levels after transfer of eels from fresh water (FW) to seawater (SW) or vice versa using homologous radioimmunoassay, to know whether ANP is involved in the osmoregulation of the eel. First, we found that ANP levels in plasma taken from the ventral aorta was higher than that from dorsal aorta of FW eels. Thus, ANP released from the heart seems to be extracted by the gill. Second, we did not detect any difference in ANP levels in conscious and anesthetized eels, but the level increased when pericardium was opened. It seems that distension of the atrium may stimulate ANP release. Based on these results, we did transfer experiments and found that plasma ANP level increased for 3 hours after exposure of eels from FW to SW. Furthermore, clearance rate of ANP was greater in SW eels than in FW eels. Since plasma ANP levels were not different between both groups of eels, secretion rate of ANP may be higher in SW eels than in FW eels. These data suggest that ANP may play important roles in SW adaptation in the eel.

EFFECT OF SALMON PROLACTIN ON PLASMA OSMOLALITY IN THE SAFFRON COD DURING THE WINTER

M.Ogawa[1], R.Masui, A.Shimizu[2] and M.Fukuchi[3]

1 Grad.Sch.Policy Sci., 2 Dept.Reg.Biol., Fac.Sci., Saitama Univ., Urawa and 3 Natl.Inst.Polar Res.,Tokyo.

Saffron cod, Eleginus gracilis, survives the ice-laden coastal water during the winter possessing a high concentration of antifreeze glycoprotein(AFGP). In contrast to the well-vascularized glomeruli seen in the fish collected during the summer, the shrunk glomeruli were observed during the winter. This may be related to the conservation of AFGP for cold water.

Plasma osmolality was increased during the winter than during the summer. The decreased osmolality was obtained by salmon prolactin(PRL) injection(20 μg/Kg/D X 3). In this treatment, the size of glomeruli increased significantly. The same dose of salmon growth hormone(GH) had no effect for both of osmolality and glomerulus.

It is recently evident that GH inhibits the anti-freeze protein synthesis in the liver of the winter flounder(Idler et al., '89). The results obtained here reconfirmed the previous consideration(Ogawa et al., '93) in which PRL may act on the kidney and possibly on clearing of AFGP by increasing glomerular filtration.

ELEVATION OF PLASMA SOMATOLACTIN LEVELS DURING ACIDOSIS IN RAINBOW TROUT.

S. Kakizawa, T. Kaneko, S. Hasegawa and T. Hirano.
Ocean Res. Inst., Univ. of Tokyo, Tokyo

Somatolactin (SL) is a putative pituitary hormone structurally related to both growth hormone and prolactin. To clarify the possible involvement of SL in acid-base regulation, the relation between blood pH and plasma SL concentration was examined in rainbow trout.

The fish were exposed to acidic water, adjusted at pH 5.0 with sulfuric acid, for 7 days. In the acid-exposed trout, plasma SL increased and reached a peak on day 1, the level being significantly higher than those in the initial or the control (pH 7.2) fish. Blood pH in acid-exposed fish was significantly lower than those in the initial or the control fish on day 1. Throughout the experiment, plasma SL levels in acid-exposed fish were kept higher than those in the control fish. Exhaustive exercise by chasing the fish in shallow water for 8 min also resulted in an increase in plasma SL and a decrease in blood pH. Within 3 h after the exhaustive exercise, blood pH was restored to the initial levels. In both experiments, elevation of plasma SL was always accompanied with blood acidosis, whether environmental water is acidic or not. These results strongly suggest that SL restores the blood pH during acidosis in rainbow trout.

EXPRESSION OF VASOTOCIN GENE DURING METAMORPHOSIS IN THE BULLFROG HYPOTHALAMUS.

Susumu Hyodo
Graduate School of Arts and Sciences, University of Tokyo, Tokyo.

Most of anurans change their ecological situation from an aquatic to a semi-terrestrial habitat during metamorphosis. Thus, physiological roles of vasotocin (VT), an anti-diuretic hormone in non-mammalian tetrapods, are of interest in metamorphosing anuran tadpoles. In the present study, expression of VT gene was studied by Northern blot analysis in metamorphosing bullfrogs to assess the activity of VT producing neurons. Effects of osmotic stimulation on the VT mRNA levels were also studied. The signal for VT mRNA could be detected from limb bud stage (stage V). Intensity of signal for VT mRNA was gradually and consistently increased during prometamorphic development. Then, the VT mRNA level was markedly increased at the metamorphic climax (from stage XX). Plasma osmolality was unchanged before metamorphosis, and was increased after stage XX. Effects of osmotic stimulation were examined by immersion in 30% seawater (SW) for 3 days. At all stages examined, SW treatment increased plasma osmolality. After stage XV (prometamorphic stage), the VT mRNA levels were significantly increased by SW treatment. These results suggest that VT has important roles in hypo-osmoregulatory mechanisms of metamorphosing bullfrog, including the change of habitat to a semi-terrestrial area following metamorphosis.

CLONING AND SEQUENCE ANALYSIS OF VASOTOCIN-I GENE OF CHUM SALMON

Y. Satomi[1], K. Kubokawa[2], H. Ando[1], M. Ono[3] and A. Urano[1]
Div. of Biol. Sci., Grad. Sch. of Sci., Hokkaido Univ., Sapporo[1], Ocean Res. Inst., Univ. of Tokyo, Tokyo[2], Dept. of Mol. Biol., Kitasato Univ. Sch. Med., Sagamihara[3].

The nucleotide sequence of chum salmon (*Oncorhynchus keta*) vasotosin-I (VT-I) gene was analyzed to investigate mechanisms of regulation of VT-I gene expression. VT-I gene was isolated from a genomic library using chum salmon VT-I cDNA as a probe. VT-I gene is constructed from three exons divided by two introns in positions corresponding to those found in the gene of their mammalian counterpart, vasopressin. The nucleotide sequence of its 5'flanking region up to about 1kb from the putative TATA box shows that this region lacks AP-2 consensus sequences and has several putative CAT boxes which have not been found in mammals. Furthermore, a half-ERE-palindrome motif TGACC, which can be a binding site of receptors for estrogen, retinoic acid, or thyroxine, was located in this region. The TGACC was not found in the genes of tetrapod vasopressin family, however presents in oxytocin genes. These differences in response elements for transcriptional factors may reflect different regulatory mechanisms of chum salmon VT-I gene expression from other neurohypophysial hormone genes.

EFFECTS OF ENDOTHELIN-1 ON VASOPRESSIN RELEASE IN RATS.
S. Nakamura[1], T. Yamamoto[1], T. Hirohama[1], K. Aoki[2], and H. Uemura[1]. [1]Biol. Lab., Kanagawa Dent. Coll., Yokosuka, [2]Div. of Biol., Natl. Inst. Radial. Sci., Chiba.

Effects of endothelin-1 (ET-1) on release of vasopressin (VP) from the rat neural lobe was investigated ultrastructurally. Rats were sacrificed by decapitation 5 min after intra-atrial infusion of ET-1 (50, 500 ng/1 ml isotonic saline), and the neural lobe was fixed with the ordinary fixative using microwave irradiation. Control animals were infused with the same volume of vechicle. In the neural lobe of the rat infused with ET-1, the number of secretory granules in the VP axons was considerably decreased and the features suggesting exocytosis were often observed. In rats infused with hypertonic saline (3.5% NaCl) instead of ET-1, the number of secretory granules in the VP axons decreased conspicuously over a course of time observed at 5, 10, and 20 min intervals, but the exocytotic figurations were not seen. In electron-microscopic autoradiography using ^{125}I-endothelin, silver grains were deposited in the VP axons and the capillary walls. These results suggest that ET-1 may act on the VP axon to accelerate the VP release.

ULTRASTRUCTURAL PLASTICITY OF THE SUPRAOPTIC NUCLEUS DURING LACTATION.
S-H. LIN, S.MIYATA, T.NAKASHIMA, and T.KIYOHARA. Dept. of Appl. Biol., Kyoto Inst. of Tech., Matsugasaki, Sakyo-ku, Kyoto 606

It has been so far known that magnocellular neuroendocrine cells (MNCs) of the supraoptic nucleus (SON) and paraventricular nucleus (PVN) reveal drastic morphological plasticity during parturition and lactation. First, we examined changes in cell size of the oxytocinergic and vasopressinergic MNCs, and expression of *c-fos* immunoreactivity in MNCs during gestation and lactation. The hypertrophy of oxytocinergic MNCs was greater than that of vasopressinergic. C-FOS immunoreactivity was detected only at parturition. Second, we investigated the effect of ovariectomy on the milk let-down and the structural plasticity in the supraoptic nucleus (SON) of rat hypothalamus during lactation. There was no significant difference in the increase of litter weight between the ovariectomized and normally lactating rats. The percentage of the juxtapositions and the number of multiple synapses in the ovariectomized females were not significantly different from those of control. Thus, we concluded that maintenance of ultrastructural changes in the SON during lactation is depend on the suckling stimulation by litters.

AUTORADIOGRAPHIC STUDIES OF THE DISTRIBUTION OF ENDOTHELIN-1 BINDING SITES IN THE BULLFROG HYPOPHYSIS
T. Yamamoto[1], S. Nakamura[1], T. Hirohama[1], K. Aoki[2], and H. Uemura[1]. [1]Biol. Lab., Kanagawa Dent. Coll., Yokosuka, [2]Div. of Biol., Natl. Inst. Radiol. Sci., Chiba

The distribution of [^{125}I]endothelin-1 (ET-1) binding sites was examined in the hypophysis of the bullfrog, *Rana catesbeiana*, both at the light- and electron-microscopic levels. At the light-microscopic level, silver grains were dense in the pars nervosa and pars distalis, and moderate in the pars intermedia. At the electron-microscopic level, silver grains were seen in the terminals of the pars nervosa, which contain many electron-dense secretory granules (200-270 nm). Sometimes, these terminals also contained several large (320-380 nm) secretory granules. In the terminals grains were located on the plasma membrane as well as within the terminals. On the other hand, only a few silver grains were observed in the terminals containing 150-250 nm moderately electron-dense secretory granules. In the pars distalis, certain cell types contained many silver grains. Preferential binding of [^{125}I]ET-1 suggests that ET-1 regulates hypophysial functions in the specific terminals and adenocytes.

EFFECTS OF OXYTOCIN ON K^+ CURRENTS OF THE SUPRAOPTIC NEURONS IN VIRGIN FEMALE RATS.
T. Nakashima, Y. Sato and T. Kiyohara. Dept. Appl. Biol., Kyoto Inst. Tech., Kyoto.

It has been reported that firing activity of oxytocin (OXT) neurons in the supraoptic nucleus is facilitated by OXT in male animals. In contrast to males, we found an inhibitory response of the OXT neurons to OXT application in virgin female rats. To investigate the mechanism of this inhibition, we studied the action potentials during OXT superfusion of supraoptic neurons in the adult (7-10 weeks old) virgin female rats using slice whole-cell patch-clamp methods. OXT prolonged the duration of action potentials. OXT decreased the current through the delayed rectifier K^+ channels but the early transient K^+ (A) current was not affected. These results indicate that the decrease of the current through the delayed rectifier K^+ channels broadens the action potentials, and inhibits the activity of OXT neurons in virgin female rats.

STRUCTURAL PLASTICITY OF THE HYPOTHALAMIC SUPRAOPTIC NUCLEUS DURING CHRONIC DEHYDRATION.
S.MIYATA, T.ITOH, T.NAKASHIMA, and T.KIYOHARA. Dept. of Appl. Biol., Kyoto Inst. of Tech., Matsugasaki, Sakyo-ku, Kyoto 606

In chronic dehydration induced by drinking of hyperosmotic NaCl solution, both the percentages of membrane contacts (juxtaposition) and the soma sizes of the magnocellular neuroendocrine cells (MNCs) in the supraoptic nucleus (SON) increased in response to the rise of plasma osmolarity and decreased to control levels on the 7th day of rehydration. During dehydration the numbers of multiple synapses per 100 μm soma membrane were significantly higher than those of controls. Furthermore, most of the multiple synapses were observed to contact soma and dendrites preferentially, indicating the special interaction of multiple synapses to soma by acting on adjacent dendrites. C-FOS positive cells were observed continually in the SON and paraventricular nucleus (PVN) in rats given hyperosmotic solution for 10 days or deprived of water for 5 days. The immunoreactivity of the growth-associated protein GAP-43 was observed to correspond well with MNCs of the SON and PVN with chronic dehydration. The results suggest that neuronal sprouting and/or elongation is closely associated with structural plasticity in the hypothalamic MNCs.

SCATTERED NEUROSECRETORY CELLS IN DORSAL CORD OF ASCIDIANS : ACTH-LIKE IMMUNOREACTIVE CELLS
K.Terakado[1], T.Yamazaki[1] and M.Ogawa[2]

1,Dept. of Regul.Biol., Fac. of Sci., and 2, Grad.Sch. Policy Sci., Saitama Univ., Urawa.

Last year, we reported the presence of numerous neurosecretory cells scattered in the dorsal cord of the ascidian, Halocynthia roretzi. Similar neurosecretory cells were also found in the dorsal cord of the closely related species, Halocynthia aurantium. By means of the immunocytochemical method, ACTH-like immunoreactivity was demonstrated in some of these scattered neurosecretory cells and in some peripheral cells of the cerebral ganglion. In the former, it was found that the ACTH-like immunoreactive cells were widely distributed throughout the length of the dorsal cord along it. No positive reaction was obtained in the neural gland cells, which differs from the previous work (Pestarino,1985).

The results reported here suggest that some cells of the scattered neurosecretory cells in the dorsal cord and the cerebral ganglion of the ascidian possess vertebrate ACTH-like molecule(s), and these cells may be homologous with the ACTH-cells of vertebrate pituitary, though the function of the ACTH-like immunoreactive cells is still unknown.

CHARACTERISTICS OF PROLACTIN SECRETION IN NORMAL AND ESTROGEN-TREATED PITUITARIES OF RATS AT A SINGLE CELL LEVEL.

K. Kawamoto[1], M.Yoshikawa[2], A. Ito[3] , S. Takahashi[4].
[1]Dept. of Biol., Fac. of Sci., Toyama Univ., Toyama, [2]Dept. of Neurosurg., School of Med., [3]Dept. of Cancer Res., Res. Inst. for Nuclear Med. and Biol., Hiroshima Univ., Hiroshima, [4]Dept. of Biol., Fac. of Sci., Okayama Univ., Okayama.

We studied prolactin (PRL) secretion from individual pituitary cells in normal and estrogen (E2)-treated female F344 rats using a reverse hemolytic plaque assay. A multimodal distribution of plaque area was observed in normal pituitary cells (NPC), whereas, a bimodal distribution was found in E2-treated pituitary cells (EPC). The mean plaque area for EPC was smaller than that for NPC. Thyrotropin-releasing hormone (TRH) promoted PRL secretion in both NPC and EPC, and responsiveness to TRH was higher in EPC than in NPC. Dopamine (DA) suppressed PRL secretion from NPC. In contrast, DA promoted PRL secretion from EPC. These findings suggest that E2 treatment diminishes functional heterogeneity of PRL cells and changes the responsiveness to hypothalamic hormones.

CHANGES IN THE EXPRESSION OF GLYCOPROTEIN HORMONE α AND GTH IIβ SUBUNIT mRNA DURING OVARIAN DEVELOPMENT IN JAPANESE EEL, *ANGUILLA JAPONICA*

*M. Nagae[1], K. Gen[2], Y. Kato[2], S. Adachi[1] and K. Yamauchi[1]. [1] Dept. of Biol., Fac. of Fish., Hokkaido Univ., Hakodate, [2] Hormone assay center, Inst. of Endocrinol., Gunma Univ., Maebashi.

Under conditions of cultivation, female Japanese eel has immature ovary, which never develop without injections of exogenous pituitary homogenates. This treatment affects not only ovary but also pituitary to increase endogenous gonadotropin (GTH) content. In the present study, the changes in the expression of Japanese eel glycoprotein hormone α and GTH IIβ subunit mRNA were examined by northern blot hybridization using previously cloned their cDNAs as the probe.

The expression of glycoprotein hormone α subunit mRNA was observed at all stages of oocyte and its amount increased during ovarian development. Especially, its expression increased markedly at late vitellogenic and migratory nucleous stage. In contrast, the expression of GTH IIβ subunit mRNA was detected only at late vitellogenic and migratory nucleous stage. These results suggest that GTH II synthesis is accelerated at the stage after late vitellogenesis and further indicate that the expression of each subunit is under the different regulations

RADIOIMMUNOASSAY OF XENOPUS PROLACTIN

K. Yamashita, K. Yamamoto, Y. Hayakawa, Y. Hanaoka[1] and S. Kikuyama
Dept. of Biol., Sch. of Educ., Waseda Univ., Shinjuku-ku, Tokyo 169-50, [1]Inst. of Endocrinol., Gunma Univ., Maebashi, 371, Japan.

Antiserum against Xenopus prolactin was produced by immunizing rabbits with a mixture of two molecular forms of prolactin (xPRL-I and xPRL-II)purified from adenohypophyses of Xenopus laevis. Histological studies on the Xenopus adenohypophysis revealed that the cells that were immunologically reacted with this antiserum corresponded with those that were immunoreactive with an antiserum against bullfrog prolactin. The Xenopus prolactin antiserum was used to develop a radioimmunoassay (RIA) in which the mixture of xPRL-I and xPRL-II were used as the standard and the radioligand. In this system, both xPRL-I and xPRL-II exhibited similar inhibition curves. RIA for plasma prolactin levels revealed that in both sexes plasma concentrations showed a moderate elevation as their body weight increased (from 3.3 g to 38.5 g). Pituitary prolactin concentrations also increased as they gained their body weght. Differences in plasma and pituitary prolactin levels between males and females with similar body weight were not noted.

cDNA CLONING OF RIBOSOMAL PROTEIN S2 IN SOCKEYE SALMON, ONCORHYNCHUS NERKA

S. Hiraoka[1], M. Iwata[2], T. Yanagisawa[2] and A. Urano[1]. [1]Div. of Biol. Sci. Hokkaido Univ, Sapporo, [2]Natl. Inst. of Aquaculture Nikko-Branch, Nikko, and [3]Dept. of Agri. Chem. Utsunomiya Univ. Utsunomiya.

We obtained cDNA encoding ribosomal protein S2 in sockeye salmon, Oncorhynchus nerka, during cloning process using a PCR method for hypothalamic neurohormone, TRH. Ribosomal protein S2 was amplified since it has the similar sequence to the PCR primer for TRH. Ribosomal protein S2 cDNA was composed of 882 nucleotides; it has a 5'-noncoding sequence of 141 bases, 702 base open reading frame coding a 233 amino acid polypeptide and 39 base 3'-noncoding sequence. The nucleotide sequence of the ribosomal protein S2 cDNA from sockeye salmon is highly homologous to that from rat (80.1 %) and Drosophila melanogaster (70.7 %).

Southern blot analysis showed that there may be single copy of the S2 gene, although it has been previously reported that there are 23-28 copies in rat genome. Northern blot analysis in sockeye salmon showed that S2 probe was hybridized with RNA isolated from brain, pituitary, liver, kidney, heart, muscle, ovary and testis.

EFFECT OF PROLACTIN ON THE LHRH-INDUCED RELEASE OF LH FROM DISPERSED PARS DISTALIS CELLS OF THE BULLFROG.

A. Oguchi, S. Tanaka[1], K. Yamamoto, S. Kikuyama. Dept. of Biol., Sch. of Educ., Waseda Univ., Tokyo and [1]Inst. of Endocrinol., Gunma Univ., Maebashi.

LH cells are frequently surrounded by prolactin (PRL) cells in the anterior pituitary lobe of the bullfrog (*Rana catesbeiana*). This lead us to study the effect of PRL on the release of LH *in vitro*. Experiments were conducted to see whether the addition of PRL into the culture medium affects the LHRH-induced release of LH. Enzymatically dispersed cells were preincubated for 24 hours. Subsequently, they were subjected to LHRH and/or PRL. The release of LH was enhanced during a 3 hour-culture by LHRH and PRL as compared with LHRH alone. PRL alone did not affect the release of LH. Possible paracrine effect of PRL on the LH cells were suggested.

DEVELOPMENT OF NPY-IMMUNOREACTIVE CELLS IN THE GEP SYSTEM OF THE CLOUDY DOGFISH.

A. Chiba[1], S. Oka[1]and Y. Honma[2]. [1]Dept. of Biol., Sch. of Dent. at Niigata, Nippon Dental Univ., Niigata and [2]Sado Mar. Biol. Stat., Fac. of Sci., Niigata Univ., Niigata.

We analyzed ontogeny of neuropeptide Y-immunoreactive (NPY-ir) cells in the gastroenteropancreatic (GEP) system of the dogfish, *Scyliorhinus torazame*, using a streptavidin-biotin method. Embryos (15-80mm in total length), juveniles (95-125 mm) and adults (370-400mm) were examined. NPY-ir cells first appeared in the pancreatic rudiment of an embryo, 15mm in total length. Subsequently, the cells of the pancreas increased in number and labeled cells occurred also in the vitellointestinal duct and proximal region of the spiral intestine. In a 40mm-long embryo, NPY-ir cells were further demonstrated in the internal yolk sac, but no labeled cells were seen in the esophagus, stomach or colon/rectum regions. Embryos of 54 and 74mm long showed increased density of the cells in the pancreas and duodeno-spiral region of the intestine, and displayed NPY-ir fibers in the muscle layer of esophagus. In the stages just before and after hatching, NPY-ir cells extended into the stomach epithelium, whereas the cells of the internal yolk sac decreased in density. In a 125 mm-long juvenile, the NPY-ir cells of the GEP system were developed and comparable with those of adult fish, though there were still fewer labeled cells in the pyloric region.

ONTOGENETIC DEVELOPMENT OF NPY- AND GnRH-IMMUNOREACTIVITIES IN THE BRAIN OF THE CHUM SALMON, ONCORHYNCHUS KETA

S.Oka[1] ,A.Chiba[1] ,Y.Honma[2]. [1]Dept.of Biol.,Nippon Dent.Univ., Niigata, [2]Sado Mar.Biol.Stat.,Fac.of Sci.Niigata Univ.,Niigata

Using specific antisera raised against neuropeptide Y (NPY) and gonadotropin-releasing hormone (GnRH), we examined development of NPY- and GnRH-immunoreactive cells and fibers in the olfactory and brain areas of the chum salmon, Oncorhynchus keta.

Our main interest was focussed on a possible relationship between the NPY and GnRH and on ontogenetic changes in the immunolabelings for these peptides. Specimens at stages from 16 days after fertilization through 1 year after hatching were studied by use of a streptavidin-biotin technique. NPY-immunoreactive cells first appeared in the olfactory placode (OP) and in the midventral areas of the midbrain of a 16-day-old embryo. In this specimen, NPY-positive cells of the OP were identified as the cells stained also with GnRH antiserum, showing coexistence of both peptides. Thereafter, these NPY/GnRH cells developed into the terminal nerve along the olfactory nerve. On the other hand, NPY-positive cells demonstrated in non-olfactory areas were not stained with GnRH antiserum.

These data suggest that the NPY neurons in the salmon brain have multiple origins.

IDENTIFICATION OF THE LATENT FORM OF NOVEL SERINE PROTEASE IN PORCINE OVARIAN FOLLICULAR FLUIDS

J. Ohnishi, and T. Takahasi

Division of Biological Sciences, Graduate School of Science, Hokkaido University, Sapporo

The porcine ovarian follicular fluids (FFs) was shown to contain the latent form of a novel trypsin-like protease and to exist from the early stage of the developing follicles. No activity was detected in untreated FFs, while exposing to exogenous trypsin resulted in marked elevation of the activity. The activated form of this enzyme preferebly hydrolysed Arg-MCA bond of the peptide 4-methylcoumaryl-7-amide (MCA) substrates. The enzyme responsible for these activities was thought to be a serine protease as judged from its strong inhibition by aprotinin. The molecular mass of this enzyme was evaluated as ~200 KDa from gel-filteration analysis. The novel enzyme described here may play a role in regulating the complex mechanism during folliclar maturation and ovulation.

PURIFICATION, CHARACTERIZATION, AND LOCALIZATION OF FOLLIPSIN, A NOVEL SERINE PROTEINASE FROM THE FLUID OF PORCINE OVARIAN FOLLICLES.

T. Hamabata, H. Okimura and T. Takahashi. Dev. of Biol. Sci., Graduate School of Sci., Hokkaido Univ., Sapporo.

Follipsin, an enzyme which accumulates in the follicular fluid of porcine ovary during follicular maturation, was purified to apparent homogeneity. The purified enzyme consists of two different polypeptide chains having M_r =45,000 and 32,000 each, associated covalently. The enzyme activity was strongly inhibited by diisopropylfluorophosphate, benzamidine, leupeptin and antipain, indicating that follipsin is a serine proteinase. Using synthetic peptide substrates containing 4-methylcoumaryl-7-amide, follipsin was shown to hydrolyze preferentially Arg-X bonds but not Lys-X bonds. The NH_2 -terminal amino acid sequences of the 45kDa and 32kDa polypeptides were highly homologous with those of the heavy and light chains, respectively, of human plasma kallikrein and human factor XI_a. Immunological analyses and substrate specificity studies, together with other existing evidence, indicated that follipsin is distict from the kallikrein and factor XI_a, thus being a novel type of serine proteinase. Follipsin is immunohistochemically localized in follicular fluid as well as in stroma cells of porcine ovary. The results strongly suggest that follipsin originates from interstitial cells of ovarian stroma.

PREGNENOLONE BIOSYNTHESIS IN THE AVIAN BRAIN.

K. Tsutsui and T. Yamazaki

Fac. Integrated Arts and Sci., Hiroshima Univ., Higashi- Hiroshima

Steroid hormones are supplied to the brain by peripheral steroidogenic glands. Therefore, the brain is considered to be a target site of steroid hormones. The brain is also a site of steroid metabolism. For example, gonadal androgens act on brain to influence neuroendocrine function and reproductive behavior in birds. These actions are often mediated by the enzymatic activity that catalyzes the conversion of androgen to estrogen. However, little is known regarding the formation of pregnenolone, the main precursor of steroid hormones, in the brain of birds. The present study was conducted to determine pregnenolone biosynthesis in adult males of the Japanese quail. Using specific antibodies against the bovine adrenal cytochrome P450scc, Western immunoblot analysis was performed after SDS-gel electrophoresis of the whole brain. A protein recognized the antibody as a band of electrophoretic mobility similar to P450scc. When the mitochondrial fraction was incubated with cholesterol, pregnenolone production was detected in mitochondria as a function of incubation time. On the other hand, the pregnenolone concentration in brain was much larger than that in plasma. Hypophysectomy led to decreases in the plasma and brain pregnenolone levels, but the change in brain was less pronounced. These results unanimously suggest *de novo* pregnenolone biosynthesis in the avian brain. Most pregnenolone accumulation in the brain may be independent of the peripheral endocrine gland system.

STRUCTURAL COMPARISON OF FOLLIPSIN WITH PLASMA KALLIKREIN AND FACTOR XIa.

H. Okimura, T. Hamabata, J. Ohnishi, and T. Takahashi, Division of Biological Sciences, Graduate School of Science, Hokkaido University, Sapporo.

Follipsin, a serine endopeptidase recently discovered from the fluid of porcine ovarian follicles, was shown to have enzymatic properties similar to those of two blood clotting proteinases, plasma kallikrein and factor XIa. In order to compare further follipsin with these enzymes structurally, seven tryptic peptides were isolated from purified follipsin, and subjected to amino acid sequence analysis. The peptides showed the homology with the corresponding regions of both human plasma kallikrein and factor XIa. The extent of homology was greater with the kallikrein than with factor XIa.

IMMUNOHISTOCHEMICAL STUDY WITH CYTOCHROME P450scc IN THE AVIAN BRAIN.

M. Usui, S. Kominami and K. Tsutsui

Fac. Integrated Arts and Sci., Hiroshima Univ., Higashi- Hiroshima

We have demonstrated that the avian brain as well as peripheral steroidogenic glands can produce pregnenolone, the main precursor of steroid hormones, on the basis of biochemical studies (Tsutsui and Yamazaki, this meeting). Therefore, the immunohistochemical study with cytochrome P450scc, which is involved in pregnenolone formation, was undertaken to determine the distribution of this enzyme in the brain of adult male Japanese quails. Specific antibodies against the bovine adrenal cytochrome P450scc were used in this study. Cytochrome P450scc-immunoreactive cells were found within the cerebellum, between-brain, midbrain and optic lobe. In the cerebellum, abundant immunoreactive cells, which were large with a spherical nucleus, exhibited an intense reaction and delineated between the granular and molecular layers in the cortex. Immunoreactive fibers were also evident in the molecular layer. In the between-brain, midbrain and optic lobe, immunoreactivity was relatively weak, but clusters of positively stained cells were observed in several regions. These results show the immunohistochemical localization of cytochrome P450scc in the avian brain and strongly support our previous biochemical results indicating *de novo* pregnenolone biosynthesis.

ISOLATION OF A NOVEL PEPTIDE UNDERLYING OVIPOSITION IN THE JAPANESE QUAIL.

D. Li[1], T. Uesaka[1], K. Tsutsui[1], Y. Muneoka[1], T. Ikeda[2], H. Minakata[2] and K. Nomoto[2]
[1] Fac. Integrated Arts and Sci., Hiroshima Univ., Higashi-Hiroshima;
[2] Suntory Inst., Bioorganic Res., Osaka.

Oviposition, expulsion of the egg from the oviduct, is a unique phenomenon in vertebrates other than eutherian mammals. In birds, oviposition is conducted by vigorous movements of the uterine muscle and the vaginal sphincter. It is well established that avian oviposition is regulated, at least partly, by a neurohypophysial hormone (arginine vasotocin) and ovarian hormones (prostaglandin E_2 and $F_{2\alpha}$) through the induction of uterine contractions. However, the production of the bioactive substance that contributes to the regulation of oviposition has not yet been defined in the oviduct. We now describe the isolation of a novel peptide underlying oviposition from oviduct extracts of the Japanese quail. The extracts from 200 quail oviducts were forced through C-18 reverse-phase column. The retained material was subjected to cation- and anion-exchange and reverse phase HPLC purifications. An isolated substance from the oviduct potentiated spontaneous contractions of the vaginal sphincter. Amino acid sequence analysis characterized the substance to be a novel peptide and 26 amino acid residues long. These results suggest that the oviduct synthesizes a peptide that is involved in the regulation of oviposition in the bird.

THYROID HORMONE-BINDING PROTEIN IN BULLFROG TADPOLE PLASMA IS TRANSTHYRETIN.

K. Yamauchi, N. Minamihara[1], H. Hayashi[2] and R. Horiuchi[3]. [1]Dept. of Biol., Fac. of Sci., Shizuoka Univ., Shizuoka, [2]Gunma Pref. Coll. Health Sci., Maebashi, [3]Dept. of Pharm., Gunma Uwiv. School of Med., Maebashi

We purified major thyroid hormone-binding protein, which consists of four identical subunits with a molecular weight of 16 kDa, from tadpole plasma of Rana catesbeiana, in order to characterize the molecular and hormone binding properties. The amino acid composition of the protein and the amino acid sequence of its N-terminal portion were highly homologous with those of mammalian transthyretins (TTRs). This is the first case that TTR was found in amphibian. In contrast to mammalian TTRs, the affinity of the bullfrog TTR for T_3 was 360 times higher than that for T_4. Scatchard analysis revealed that the bullfrog TTR possessed a single class of T_3-binding site, with a K_d of 0.67 nM at 0 C. This high affinity of is comparable to those of T_3 receptors. These results suggest that the bullfrog TTR may play an important role in transporting T_3 in the blood during metamorphosis.

SEXUAL DIFFERENTIATION IN THE ISOPOD, ARMADILLIDIUM VULGARE : ANDROGENIC GLAND AND COPULATORY ORGAN.

S. Suzuki[1] and K. Yamasaki[2]. [1]Biol.Lab.,Kanagawa Pref.Col. Yokohama. [2]Dept.of Biol., Tokyo Metropol.Univ., Tokyo.

The androgenic gland hormones (AGH) have been thought to control the differentiation of male in crustaceans. This hypothesis is acceptable in hormonal control of sexual differentiation of A. vulgare, because sexual reversal was observed in experimental animals bearing or not bearing the androgenic glands (AGs). However, it is not clear whether AGs are responsible or not for the determination of all male sexual characters.

In young male of A. vulgare, the endopods of the first abdominal appendages develop at each molting and grow completely in mature male as the copulatory organs. The elongation of the endopods, one of the secondary male characters, was often observed in the females whose gonads had been removed in juvenile life. It is suggested that AGs did not exist or were not functional in these gonadectomized females at least, for vitellogenin could be detected in their hemolymph.

AGs may not always necessary for the differentiation of male secondary characters. Morphological observation on sexual differentiation of male gonads is under investigation for analyzing the relationship between the formation of male copulatory organs and the roles of AGs.

MORPHOLOGICAL METAMORPHOSIS AND "BIOCHEMICAL METAMORPHOSIS" IN HYNOBIUS RETARDATUS

M.Wakahara[1], N.Miyashita[1], A.Sakamoto[1] and T.Arai[2]. [1]Biol.Sci., Grad. Sch. Sci., Hokkaido Univ., Sapporo and [2]Mitsubishi Material, Sapporo.

Several biochemical transitions from larval to adult types were studied during ontogeny of a salamander, Hynobius retardatus, which had been reported to show neotenic reproduction. A transition of hemoglobins in normally metamorphosing and T_4-induced precociously metamorphosed animals was analysed using SDS-PAGE. The transiton of hemoglobins from larval to adult types occurred on the same time schedule in both normally metamorphosing and precociously metamorphosed animals. A changeover from ammonotelism to ureotelism was analyzed by determining amounts of ammonia and urea excreted from normal and metamorphosis-arrested animals. A basic changeover from ammonotelism to ureotelism also occurred even in metamorphosis-arrested, aquatic larvae on the similar time schedule in normally metamorphosing and metamorphosed animals. It is, thus, concluded that either transition of hemoglobins from larval to adult types or pattern of nitrogen excretion from ammonotelism to ureotelism are independent on the morphological metamorphosis in H. retardatus.

EFFECT OF THYROID HORMONE ON THE FIRST SKIN-SHEDDING IN PIPPING AND HATCHLING SNAKES.

M.Yoshihara[1], T.Murakami[1] and C.Oguro[2]. [1]Dept. of Oral Physiol., The Nippon Dental Univ., Niigata, [2]Toyama Univ., Toyama.

It is well known that thyroid hormone stimulates molting in urodele amphibians, birds, and generally in skinks. On the contrary, it has been reported that thyroid hormone inhibits skin-shedding in snakes.

In the present study, embryos (just after pipping) and hatchlings of the snakes, Elaphe quadrivirgata and E. climacophora were used. In these species, the first skin-shedding takes place 1 week after hatching. They were injected with large dose of thyroxin (8 µg/100g bw/day) or control saline. In the control snakes, the first skin-shedding took place normally. However, in thyroxin administered embryos no skin-shedding occurred until 1 month after hatching. On the other hand, in hatchlings with thyroxin injection skin-shedding occurred more than 1 day earlier than in control snakes. These results indicate that thyroid hormone inhibits to the initiation of new skin preparation of pipping snakes. After the initiation of the new skin preparation, however, thyroid hormone accelerates the progress of entire process of skin-shedding in hatchling snakes.

A POSSIBLE INVOLVEMENT OF ANNETOCIN, AN ANNELID OXYTOCIN-RELATED PEPTIDE, IN EGG-LAYING BEHAVIOR OF ANNELIDS

T.Oumi[1], K.Ukena[1], O.Matsushima[1], T.Ikeda[2], T.Fujita[2], H.Minakata[2] and K,Nomoto[2]. [1]Biol. Sci., Fac. of Sci., Hiroshima Univ., Higashi-Hiroshima, [2]Suntory Inst., Bioorganic Res., Osaka.

We purified an oxytocin-related peptide from the earthworm, Eisenia foetida, and termed it annetocin. Annetocin elicited pulsative contraction of the nephridia of E. foetida and was suggested to participate in the regulation of water balance. Recently, however, we found that a hypodermic injection of annetocin induced a series of egg-laying-like behaviors in E. foetida and the leech, Whitmania pigra, which include mucus secretion from the clitellum and conspicuous constriction of both ends of the clitellum. Oxytocin-related peptides such as annetocin seem to be involved in reproductive events of annelids, which is of special interest in relation to the role of oxytocin in mammals.

GROWTH-BLOCKING PEPTIDE cDNA AMPLIFIED BY PCR TECHNIQUE.
Y. Hayakawa. Biochem. Lab., Inst. of Low Temp. Sci., Hokkaido Univ., Sapporo.

GBP has initially been purified from last instar larval hemolymph of the armyworm parasitized by parasitoid wasps. (J. B. C., 265, 10813-10816 (1990)). The detailed structure and physiological fractions has been already reported (J. B. C., 266, 7982-7984 (1991)). In the present study, I prepared oligonucleotide primers based upon the peptide sequence information and a parasitized whole larval cDNA library for PCR. Using PCR technique, a cDNA fragment with approximately 100bp was amplified. The cDNA fragment was demonstrated to be the DNA encoding GBP by sequencing it. Furthermore, hybridization of the GBP cDNA fragment with RNAs from the parasitized host larvae was demonstrated to be higher than those from the unparasitized host. This observation supported the previous observation that GBP is naturally occurring in the host insect larvae but its hemolymph level is enhanced by parasitization.

QUANTIFICATION OF A GROWTH-BLOCKING PEPTIDE (GBP) IN LARVAL HEMOLYMPH OF ARMYWORM USING ANTI-GBP MONOCLONAL ANTIBODY.
A. Ohnishi and Y. Hayakawa Biochemical Laboratory, Institute of Low Temperature Science, Hokkaido University, Sapporo, Japan.

In order to quantify GBP, anti-GBP monoclonal antibody was prepared. Three kinds of the specific monoclonal antibodies were obtained and one of them was used for analyzing quantitative changes of hemolymph GBP. The preliminary experiments showed that two plasma proteins other than GBP were cross-reacted with the monoclonal antibody. Therefore, the peptide fraction containing GBP was purified from the crude plasma preparation using a reversed phase C_8 HPLC column and applied to the analysis by ELISA technique. The quantitative analysis demonstrated that the plasma GBP levels in penultimate instar larvae were much higher than those in last larval instar but parasitization by parasitoid wasp in early stages of last larval instar elevated the GBP level in plasma.

ELEVATION OF DOPAMINE LEVELS IN PARASITIZED INSECT LARVAE.
H. Noguchi and Y. Hayakawa Biochemical Laboratory, Institute of Low temperature Science, Hokkaido University, Sapporo, Japan.

Last instar larvae of the armyworm, *Pseudaletia separata*, parasitized with the parasitoid wasp, *Cotesia kariyai*, suffer from retarded growth and do not initiate metamorphosis. Dopamine levels in hemolymph and nerve cord of host last instar larvae were increased by parasitization with parasitoid wasp. The elevation of dopamine levels was reproduced by injection with polydnavirus or growth-blocking peptide (GBP). Injection of dopamine or the dopamine agonist, (-)-Quinpirole, disturbs normal development of the armyworm larvae. These results suggest that the GBP level elevated by polydnavirus infection causes an increase of dopamine in hemolymph and nervous system, which is closely related to a disturbance of normal larval development.

SEXUAL ACTIVITY-DEPENDENT CHANGES IN MAUTHNER CELL MORPHOLOGY IN RED-BELLIED NEWTS.
A. Matsumoto (1), Y. Arai (1), T. Kouki (2) and S. Kikuyama (2). (1) Dept. Anat., Juntendo Univ. Sch. Med., (2) Dept. Biol., Sch. Edu., Waseda Univ., Tokyo

Mauthner cells (M cells) in newts are located at the level of the VIIIth cranial nerve root in the medulla oblongata. The M cells are involved in tail movement. Tail movement has been considered to play a crucial role in courtship behavior of sexually mature male newts. As one step to clarify neuronal functions of the newt M cells, we examined sexual activity-dependent changes in M cell morphology in male red-bellied newts, *Cynops pyrrhogaster*. Sexually active or inert male newts were perfused with a mixture of 1% paraformaldehyde and 1% glutaraldehyde in 0.1 M phosphate buffer. The medulla oblongata containing M cells was sectioned and stained with toluidine blue. The mean areas of neuronal nuclei and cell bodies of M cells and mean maximum and minimum diameters of the cell bodies in the sexually active males were significantly larger than those in the sexually inert ones ($p<0.05$). In the hypophysectomized male newts, all these parameters were not significantly different from those in the sexually inert ones. These values were significantly increased by treatment with both ovine prolactin and human chorionic gonadotropin every other day for 2 weeks after hypophysectomy ($p<0.05$), and these measures were comparable to those in the sexually active males. These findings suggest that sexual activity-dependent changes in M cell morphology in male newts are due to alteration in hormonal milieu. (Supported by grants from the Ministry of Education, Culture and Science of Japan).

EFFECTS OF VASOTOCIN AND FEMALE SEX STEROID HORMONES ON THE RELEASE VIBRATION IN THE FEMALE JAPANESE TOAD (*Bufo japonicus*)
M. Kikuchi and S. Ishii. Dept. Biol., Sch. Edu., Waseda Univ., Tokyo.

Female Japanese toads show "the release vibration" when clasped by a male during a period soon after oviposition. Migrating female toads for breeding were collected in Tochigi-ken on May 4, and transported to the laboratory. When 0.5 mg of vasotocin was injected into each of 16 females intraperitonealy prior to oviposition, frequency of the release vibration induced by a manual stimulus increased 3 hr after the injection in 10 females. The mean frequencies of the vibration of the 16 females before and 3 hr after the injection were 6.0 and 12.2 per minute, respectively. The mean frequency returned to initial level by 10 hr after the injection. The mean frequency in control females injected saline did not change significantly during this period. Intraperitoneal injections of 0.4 mg of estradiol-17 β or progesterone did not affect the frequency of the release vibration. From these results the following possibility was suggested: a promotive mechanism by vasotocin exists in the neuronal control system of the release vibration in females of the toad during the breeding season, although a conflicting result was reported by Diakow (1978) in *Rana pipiens* females.

EFFECTS OF STRESS, FEMALE SEX STEROID STEROID HORMONES ON THE RELEASE VIBRATION OF JAPANESE TOADS, *Bufo japonicus*
Susumu Ishii and Yuriko Ooka. Department of Biology, School of Education, Waseda University, Tokyo 169-50

We confirmed reported facts that most females of the Japanese toad show no release vibration during the migration toward the pond for breeding in the spring, they start to show the release vibration while they are breeding in the pond, and then most post-breeding females soon after landing exhibit the release vibration. We found that the frequency of the release vibration decreased after the breeding season, but did not diminish completely in the non-breeding season. In contrast, most males of this species showed the release vibration through out the year. Capture and subsequent confinement of migrating females (showing no release vibration) induced the release vibration with a high frequency (c.a. 40/min) The frequency decreased gradually to about 10/min three days after capture. Injection of 0.4 mg estradiol 17- β or progesterone did not influence the frequency of the release vibration of females confined in plastic containers. The same dose of estradiol 17- β did not change the frequency of the release vibration in males confined in containers. Female sex steroids may not control the release vibration in female toads, although their secretions show drastic changes before and after ovulation.

CHANGES IN THE ELECTROOLFACTOGRAM WITH SEASON AND STAGES OF THE BREEDING MIGRATION IN THE JAPANESE TOAD, *Bufo japonicus*

H. Nakazawa[1], K. Koh[1], W. Takahashi[1], S. Ishii[1] and S. Kaji[2]. [1]Department of Biology, Waseda University, Tokyo 169-50 and [2]Shizuoka Institute of Science and Technology, Fukuroi, Shizuoka-ken

We recorded a slow extracellular voltage changes (electro-olfactogram or EOG) evoked on the ventral surface of the olfactory mucosa by applying an olfactory stimulus with an air stream. In September toads, only a simple typical EOG known in various amphibian species was observed. When studied monthly between January and June, oscillatory potential changes superimposed on the typical EOG were observed. In this species, the oscillations (OSC) were observed only in the breeding season (personal communication with Dr. N. Ai). During the breeding migration, the mean maximal amplitude of OSC increased as toads approached to the breeding pond and was highest (c.a. 5mV) in landed toads studied soon after the breeding. It decreased to the initial level (c.a. 0.5mV), when they arrived at areas more than 50 m from the pond. There were no sexual differences in the occurrence and amplitude of OSC. Changes in the amplitude of the typical OEG were not so conspicuous as OSC. Our results as well as that of Ai suggest a physiological correlation between OSC and the breeding migration.

EFFECTS OF GLUCOCORTICOIDS ON HIPPOCAMPAL NEURONS IN MALE MICE.

H.Matsumoto[1], T.Shinkai [2], S.Kobayashi[2] and T.Machida[1] [1]Dept. of Regul, Biol., Fac. of Sci., Saitama Univ., Urawa 338 and [2]Tokyo Metropol. Inst. of Gerontol., Itabashi, Tokyo 173.

The hippocampus of the rodent loses neurons with age. Neuronal loss of the hippocampus is thought to be accelerated by glucocorticoid exposures. To clarify morphological features of glucocorticoid-induced changes of hippocampal neurons, single sc injection of corticosterone (CORT) was given to male mice and discrete regions of the hippocampus were examined. Three days after CORT treatment, a decrease of intact neurons and concomitant increment of affected neurons were found in regions CA2 and CA3. Electron microscopy further revealed an increase of pyramidal neurons with electron-dense cell bodies in these regions. Within a week of CORT administration, affected neurons disappeared and populations of intact neurons recovered their number. On the other hand, chronic exposure to CORT first caused a decrease in intact neurons and an increase of affected neurons although intact neurons recovered their number in two weeks. These results indicate that glucocorticoid effect on hippocampal neurons may be temporal.

HIGH PLASMA LEVEL OF ESTRADIOL IS A NECESSARY FACTOR FOR COPULATORY SOLICITATION DISPLAY IN THE FEMALE ZEBRA FINCH.

T.Yasugi, T.Matsushima and K.Aoki. Life Sci. Inst., Sophia Univ., Tokyo.

In the process of courtship, just prior to copulation, a receptive female shows solicitation display (SD) in response to courtship behavior (song and dance) of male. We analyzed how important the plasma level of estradiol (E_2) is for controlling SD. Total cumulative duration of SD was scored during behavioral tests (twice for 3 min each, once every week). On the next day after the test, E_2 level in blood sample was measured by means of time-resolved fluoroimmunoassay (Delfia System, Pharmacia Co.).

High E_2 level proved to be necessary, but not sufficient for SD. Females with low E_2 level showed shorter SDs. On the other hand, those females supplemented with exogenous E_2, so had high E_2 level, showed longer SDs. However, these females did not always show long SDs, and often failed to respond to male. Further, the E_2 levels fluctuated synchronously among intact females in the same room under a condition of regular photoperiod and constant room temperature.

These results suggest that high E_2 level just makes females ready to court physiologically, while some other unknown factors could gate the expression of SD, then courtship behavior of male finally release SD.

IMPAIRMENTS OF RADIAL MAZE PERFORMANCE FOLLOWING PROLONGED EXPOSURE TO GLUCOCORTICOIDS IN MALE MICE.

H.Tanaka[1], K.Ogaki [1], S.Kobayashi[2] and T.Machida[1] [1]Dept. Regul. Biol., Fac. Sci., Saitama Univ., Urawa 338 and [2]Tokyo Metropol. Inst. Gerontol., Itabashi, Tokyo 173.

Learning performance in an eight-arm radial maze was examined in C57BL/6 male mice of 6 to 26 months of age. Performance was found impaired in aged mice in their results of initial correct responses (ICRs) and of distance value (DV). Since it has been known that hippocampal pyramidal neurons are involved in spatial learning and that adrenal glucocorticoids exert accelerating influences on age-related neuronal loss of the hippocampus, radial maze learning performance was examined in male mice following prolonged exposure to corticosterone (CORT). Both ICRs and DV were found impaired in CORT-treated animals. The results indicate that glucocorticoids cause impairment in learning performance through their damaging effects on hippocampal neurons in mice.

TESTOSTERONE MODULATES THE DISTRESS CALL TO FORM THE CROWING PATTERN IN THE JAPANESE QUAIL CHICK.

Y.Yazaki, T.Matushima and K.Aoki, Life Sci. Inst., Sophia Univ., Tokyo

Through the course of ontogeny, quails develop a wide variety of call patterns. Distress call (d.c.) is raised by chicks (before 3 weeks) of both sexes, while crowing appears only in sexually matured males (at 5 weeks and afterward) after the plasma testosterone (T) level starts to increase. It has also been reported that crowing disappears after castration, and T therapy restores it.

Here, we hypothesized that the crowing in adult males is derived from distress call in chicks, and that T modulates motor pattern generating mechanism in the brain. To examine this hypothesis, we implanted Silastic tube (containing either T, 5 α-DHT, 5 β-DHT, E2 or cholesterol) subcutaneously in chicks, and analyzed the frequency of d.c. and crow-like vocalization (c.l.).

The following 3 lines of evidence were obtained supporting this idea. (1) C.l. was induced with only T and 5 α-DHT within a few days, indicating a distinct mechanism from those for the sexual behavior. (2) C.l. was induced in both of sexes and disappeared after removal of Silastic tube, indicating that the activational effects of androgen does not depend on the genetic gender. (3) Similarly to d.c., c.l. was suppressed when paired with another chick, suggesting that both of c.l. and d.c. share a behavioral context. Furthermore, implantation of paraffin pellets containing a small amount of T into midbrain was also successful in inducing c.l. within a few hours. A search for the precise site of the action is now underway.

SEASONAL CHANGES IN GONADAL FUNCTIONS AND INCIDENCE OF SEXUAL BEHAVIOR IN AN ENCLOSED GROUP OF JAPANESE MONKEYS

M. Nozaki[1], F. Mitsunaga[1], M. Inoue[1], A. Takenaka[1], O. Takenaka[1], Y. Sugiyama[1], H. Osawa[1], K. Shimizu[1], K. Taya[2], and G. Watanabe[2], [1]Primate Research Institute, Kyoto University, Inuyama and [2]Tokyo University of Agriculture and Technology, Fuchu.

Seasonal changes in gonadal functions and incidence of sexual behavior were studied in an enclosed group (n=55) of Japanese monkeys (*Macaca fuscata fuscata*). Blood samples were collected from all individuals once a week and sexual behavior was observed daily throughout the breeding season. Plasma concentrations of testosterone and inhibin of adult male monkeys (n=10) increased during the transition into the breeding season, reached peak levels during early breeding season, and then decreased gradually. Ovarian functions of nonlactating adult females (n=12) increased during early breeding season, and most of them conceived after their first ovulations during the first half of the breeding season. Most impregnated females exhibited continuous estrus during early pregnancy up to 7 to 9 weeks, so that high incidence in sexual behavior was observed throughout the mid-breeding season.

Reflexive and psychogenic erections in male rats: Opposite effect of serotonin synthesis inhibitor, P-chlorophenylalanine (PCPA).

Y. Kondo[1], T. Matsumoto[2], B.D. Sachs[3] and K. Yamanouchi[2] [1]Dept. Physiol, Nippon Med Sch, Tokyo, [2]Dept Basic Human Sci, Waseda Univ, Saitama and [3]Dept Psychol, Univ Conn, CT, USA.

Occurrences of both reflexive and psychogenic erections (RE and PGE, respectively) are dependent on androgen and regulated by the spinal cord and the brain. Serotonergic neural system is thought to be involved in the regulation of male sexual behavior. In this study, to clarify the role of the serotonergic neurons in regulating erection, PCPA was injected and two types of erection tests were performed in rats.

Male rats were castrated and implanted with 2 Silastic tubes (5cm length, No.602-285, Dow-Corning) containing testosterone (T). The RE test and the PGE test were carried out on the 14th day and the 21th day of T-implantation, respectively. The males were injected with 100 mg/Kg PCPA or saline daily for 4 days from the 11th to 14th day and from the 18th day to 21th day.

In the RE test, the number of erections in the PCPA group was lower than that of the saline group. In contrast, the incidence of PGE in PCPA-males was higher than that in saline-males. These results suggest that the serotonergic neural system exerts facilitatory influence for reflexive erection and inhibitory influence for psychogenic erection in male rats.

MALE SEXUAL BEHAVIOR IN FEMALE RATS : EFFECTS OF MESENCEPHALIC RAPHE NUCLEI LESIONS.

T.Matsumoto and K.Yamanouchi
Neuroendocrinology, Dept. of Basic Human Science, Sch. of Human Sciences, Waseda University, Tokorozawa.

In female rats, even when ovariectmized and treated with a large amount of androgen, the capacity to display male sexual behavior is very low. The serotonin is known to play an inhibitory role in regulating male sexual behavior in male rats. In the present experiment, to clarify the role of the mesencephalic raphe nuclei which contain a large number of serotonergic neurons in females, the nuclei were lesioned in ovariectmized rats and male sexual behavior was observed after implantation of two Silastic tubes containing testosterone. The females with the lesions displayed high levels of mounting behavior, compared to ovariectmized control rats. This result suggests that the mesencephalic raphe nuclei exert inhibitory influence in regulating male sexual behavior in female rats.

EFFECT OF GABAERGIC AGONIST ON MALE RAT LORDOSIS FACILITATED BY DORSAL RAPHE NUCLEUS LESIONS OR SEPTAL CUT.

M. Kakeyama and K. Yamanouchi.
Neuroendocrinology, Dept. of Basic Human Sciences, Sch. of Human Sciences, Waseda University, Tokorozawa.

The role of GABA neurons in regulating lordosis was investigated in male rats with the dorsal raphe nucleus lesion or the septal cut (ARD). Castrated male rats with DRL or ARD were implanted with Silastic tubes containing estradiol and injected with $GABA_B$ receptor agonist, baclofen (10 mg/kg) or vehicle. In the behavioral test, DRL or ARD males showed higher levels of lordosis quotient (LQ) than non-brain surgery control males. Baclofen-treated ARD males showed no lordosis. In contrast, baclofen-treated DRL males showed high LQ value, comparable to that of vehicle-treated DRL males. Thus, baclofen suppressed lordosis in ARD males, but had no effect in DRL males. The results suggest that the GABAergic system operate dependently on lordosis inhibiting system of the dorsal raphe nucleus in male rats.

INHIBITORY EFFECT OF PROGESTERONE ON LORDOSIS BEHAVIOR FACILITATED BY ESTROGEN IN MALE AND FEMALE RATS WITH SEPTAL LESIONS

M. Satou and K. Yamanouchi
Neuroendocrinorogy, Dept. of Basic Human Sciences, Sch. of Human Sciences, Waseda University, Saitama.

Progesterone(P) plays not only facilitatory, but also inhibitory roles in regulating lordosis in female rodents. In this study, the inhibitory effect of P on lordosis in male and female rats with septal lesions (SL) was examined.

In castrated rats with the SL, 1hr prior to injection of 5 μg/kg estradiol benzoate(EB), 5 mg P or oil was given. Forty hours after EB, all animals were treated with 0.5 mg P and behavioral test was carried out 8 hrs after P. Male rats with SL showed low score of lordosis quotient(LQ) being comparable to that of females with SL. These results suggest that the septum can be excluded to be a candidate of acting site of P in lordosis-inhibition. Furthermore lordosis-inhibiting mechanisms of progesterone exist in the male central nervous system, as well as females.

MALE-ATTRACTANT IN OVIDUCT OF THE FEMALE NEWTS, *CYNOPS PYRRHOGASTER*

K. Matsuda[1], F. Toyoda[2], H. Hayashi[3] and S. Kikuyama[4]
[1]Dept. Pharmacol., Nippon Medical Sch., Tokyo, [2]Dept. Physiol., Nara Medical Sch., Kashihara, [3]Gumna Pref. Coll. Health Sci., Maebashi and [4]Sch. Educ., Waseda Univ., Tokyo.

Our previous experiment revealed that sexually inert female newts treated with prolactin and gonadotropin released male-attracting substance(s) into the water in which they had been kept. The water in which oviduct-ablated females receiving similar hormonal treatment had been kept did not attract males of the same species. Attempts were made to isolate and characterize the male-attracting substance(s). The active substance(s) in the oviduct was water-soluble rather than organic solvent-soluble. Sephadex G-100 chromatography revealed that the molecular mass of the active substance(s) is less than 5,000 dalton. The activity was abolished by pronase-digestion. When the Sephadex fraction retaining the attracting activity was subjected to reverse-phase HPLC equipped with Puresil C18 column, the active substance(s) was eluted with acetonitrile with gradient concentration of 5 %.

FEMALE NEWT-ATTRACTING PEPTIDE, SODEFRIN AND ITS LOCALIZATION.

S. Tanaka[1], F. Toyoda[2], H. Hayashi[3], H. Mochida[1] and S. Kikuyama[4]. [1]Inst. Endocrinol., Gunma Univ., Maebashi. [2]Dept. Physiol., Nara Medical Sch., Kashihara. [3]Gunma Pref. Coll. Health Sci., Maebashi. [4]Dept. Biol. Sch. Educ. Waseda Univ., Tokyo.

We have purified a female-attracting peptide, sodéfrin from the abdominal glands of male newts (*Cynops pyrrhogaster*). According to the aminoacid sequence, synthetic sodéfrin was prepared by solid phase chemistry. The synthetic sodéfrin exhibited female-attracting activity similarly to the native one. The minimum effective concentration lay within the range of 0.1-1.0 pM. Antiserum against the synthetic sodéfrin C-terminally extended with Cys that was coupled with hemocyanin, was generated in a rabbit. The antiserum intensely stained the apical region of the epithelial cells of the abdominal gland of the cloaca, indicating sodéfrin is secreted by these cells.

OLFACTORY SENSITIVITY TO A FEMALE-ATTRACTING PEPTIDE, SODEFRIN IN THE NEWT, CYNOPS PYRRHOGASTER.

F.Toyoda and S.Kikuyama
Dept. of Physiol., Nara Med. Univ., Kashihara and Dept. of Biol., Sch. of Educ., Waseda Univ., Tokyo.

The preference of the female newts for a female-attracting peptide, sodéfrin purified from cloacal glands of male newts, was found to be completely abolished in the female by the nostril plugging. To determine the sensitivity of the olfactory receptor cells to the synthetic sodéfrin, electro-olfactograms (EOGs) were recorded from the ventral olfactory epithelium exposed to the peptide solution. The peptide elicited a dose-dependent EOG response in the sexually inert females treated with prolactin (PRL) and gonadotropin (GTH). The EOG responses in the PRL and GTH-treated females to the peptide were considerably greater than those in either the PRL and GTH-treated males or untreated females.

EFFECT OF MESENCEPHALIC TEGMENTAL LESIONS ON INDUCTION OF PSEUDOPREGNANCY BY RESERPINE IN FEMALE RATS

F.Maekawa, K.Yamanouchi
Neuroendocrinology, Dept. of Basic Human Sciences, Sch. of Human Sciences, Waseda University, Saitama

The role of the midbrain tegmentum in induction of pseudopregnancy(PSP) was examined in female rats. The females with regular 4 day-estrous cycle were subjected to dorsomedial tegmental lesion(DML) or ventromedial tegmental lesion(VML). Reserpine (1 mg/kg) was injected to female rats with or without lesions on the next day of ovulation to induce PSP. Three days after the injection, silk thread was passed through and placed in the left uterine horn to induce the deciduma. Then 4 days after the traumatization, all rats were sacrificed and decidual response was investigated. In most females with no lesions or VML, PSP ensued. In contrast, the DML disrupted to induce PSP. This result suggests that the dorsomedial tegmental area of midbrain play an important role in induction of PSP.

EFFECTS OF STRESS ON NORADRENALINE AND SEROTONIN CONCENTRATIONS IN RAT STOMACH

Y. Kobayashi[1] and K. Matsubara[2]. [1]Depts of Pharmacol. and[2]Legal Med., Shimane Medical University, Izumo.

Effects of water immersing stress (14 hours) on the sympathetic nerve and peripheral serotonin (5HT) concentration of rats were studied. Catecholamines and 5HT concentrations were measured by high performance liquid chromatography. Hormones were measured by radioimmunoassay. Corticosterone, rat ACTH, adrenaline (Ad) and noradrenaline (NA) concentrations in serum enhanced significantly in stress group. Simultaneously, concentrations of Ad in the adrenal gland, NA in the atrium and the mesenteric artery reduced significantly. On the other hand, NA concentration in the stomach did not change and significant enhancement of 5HT concentration in the stomach was observed. Stress-induced gastric mucosal damage was apparently observed. The present experiments indicated different response to stress in sympathetic system between stomach and cardiovascular tissues or adrenal gland. The different response in sympathetic system and enhancement of serotonin concentration may correlate to mucosal damage in the stomach.

ESTROGEN RECEPTOR mRNA EXPRESSION IN THE GENITAL TRACT OF FEMALE MICE BY ESTROGEN (DES) AND ANTI-ESTROGEN (TAMOXIFEN).

T. Sato, [1]Y. Ohta, [2]H. Okamura, [2]S. Hayashi and T. Iguchi
Grad. Sch. Integrated Sci., Yokohama City Univ., Yokohama; [1]Dept. Biol., Fac. General Education, Tottori Univ., Tottori; [2]Dept. Anat. Embryol., Tokyo Metropol. Inst. Neurosci., Tokyo.

A synthetic estrogen, diethylstilbestrol (DES), stimulates cell proliferation in the female genital tract. Tamoxifen (Tx), a nonsteroidal anti-estrogen, has also an estrogenic effects in mice. In adult ovariectomized mice, a single injection of 3 μg DES and 100 μg Tx increased estrogen receptor (ER) mRNA of uterine and vaginal epithelial cells 12 h later; cell division of these epithelial cells occurred 24 h later. By contrast, in newborn mice given a single injection of 3 μg DES, ER mRNA expression in the uterus and vagina was increased 4 h later; similar injection of 100 μg Tx significantly increased ER mRNA expression in the uterine and vaginal stromal cells 4 h later. In the newborn mouse uterine epithelial cells showing no ER, ER mRNA slightly increased 8 h after the Tx treatment. Cell division, however, was not altered in neonatal vaginal and uterine epithelial cells. These results suggest that Tx acts as estrogen in the uterus and vagina of female mice, but the tissue response to Tx is different between adult and newborn mice.

EFFECTS OF PHOTOPERIODS AND LOW TEMPERATURE ON TERMINATION OF REPRODUCTIVE ACTIVITY IN WHITE-CROWNED SPARROWS.

M. Wada, T. P. Hahn*, S. Schoech*, and J. C. Wingfield*. Depr. Gen. Educ., Tokyo Med. Dent. Univ., Ichikawa, Chiba JAPAN and *Dept. Zool., Univ. Washington, Seattle, Washigton 98195 U. S. A.

Male and female photosensitive mountane white-crowned sparrows (*Zonotrichia leucophrys oriantha*) were photostimulated on 16L:8D for 40 days at 20 C and then received different treatments; the first group 16L:8D at 5 C (LD), the second group 8L:16D at 20 C (SD), and the third group 8L:16D at 5 C (SDLT). Photostimulation induced a rapid increase in plasma levels of LH and a delayed increase of prolactin. The body mass decreased gradually as well as the fat scores. The cloacal protuberance in the male developed steadily until Day 40. Short day treatment decreased plasma levels of LH and prolactin regardless of the temperature (SD and SDLT). The gonads and the cloacal protuberance reflected the decrease in gonadotropin. In LD group, plasma levels of these hormones did not change at all even though the ambient temperature was reduced. The testes and ovaries of the LD group maintained their activity until Day 66. The body mass and fat score increased in SD and SDLT birds while remained the preceding levels in LD birds. These results indicate that in white-crowned sparrows photoperiod is dominant and low temperature has no modifying effects to short day treatment, which is very different from the results obtained in Japanese quail.

EFFECTS OF SEX HORMONES AND ANTI-ESTROGEN ON BONE FORMATION IN MOUSE FETUS.

M. Ohta, *Y. Uesugi and T. Iguchi
Dept. Biol., *Grad. Sch. Integrated Sci., Yokohama City Univ., Yokohama

Bone formation in fetus begins from day 11 of gestation, and the ossification starts from day 15 of gestation. Pregnant ICR mice were subcutaneously given 9 daily injections of 2-2000 μg diethylstilbestrol (DES), tamoxifen or 5α-dihydrotestosterone (DHT) from days 11 to 18 of gestation. Fetuses were removed by cesarean section on day 19 of gestation. The fetal mice treated prenatally with DES or tamoxifen in daily doses of 100 μg or more died on days 16-19 of gestation. However, pregnant mice treated with 2-2000 μg DHT maintained normally their pregnancy. Skeletons of all fetuses were stained by a modified differential method (alcian blue for cartilage, alizarine red for ossified bone). All control male and female mice had 13 pairs of ribs. In contrast, prenatally tamoxifen-treated mice (male, 2/11; female, 1/9) and DHT-treated male mice (2 μg, 1/10; 20 μg, 3/8; 200 μg, 2/13; 2000 μg, 2/3) had 14 pairs of ribs. Furthermore, in tail bones, rate of the number of ossified bones were significantly lower in tamoxifen-treated mice than controls. These results suggest that in mouse fetuses prenatally administered that DHT and tamoxifen increase the number of rib, and that tamoxifen retards the ossification of the tail bone.

EFFECT OF A SINGLE INJECTION OF ESTROGEN IN COMBINATION WITH PROGESTERONE TREATMENT ON RAT UTERINE EPITHELIAL CELLS

Y. Ohta[1] and T. Iguchi[2]. [1]Dept. of Biol., Fac. of Gen. Edu., Tottori Univ. Tottori. [2]Dept. of Biol., Yokohama City Univ. Yokohama.

Involvement of an brief surge of estrogen(E) during early pregnancy in implantation is well documented in rats and mice. However, the role of the surge on the endometrium remains undefined. We have already reported that in ovariectomized rats, a single injection of E associated with progesterone(P) treatment induced morphological changes in the luminal surface structure of the epithelium similar to those associated with implantation(1992). Surface structures of the uterine epithelium in response to ovarian steroids were investigated with electron microscope in persistent estrous(PE) rats treated neonatally with 100 or 1250μg testosterone propionate(TP). A single injection of E in combination with the P treatment failed to induced the morphological changes in surface structures of the epithelial cells in PE rats, regardless of the dose of TP. These cells showed neither E-dependent increase in number of cytoplasmic protrusion nor the increase in ratio of carboxylic mucopolysaccharide, e.g., sailic acid, contents in the surface coat of the cells demonstrated by colloidal iron reaction. Since neonatal androgenization induces a permanent reduction in the uterine response to deciduogenic stimulus, it is evident that the morphological changes in surface structures of the epithelial cells at the preimplantation stage play an important role in implantation, which may be induced by the brief surge of E.

CELL PROLIFERATION OF MOUSE UTERINE EPITHELIAL CELLS IN VITRO.

S.Takahashi[1], M.Shiraga[1], A.Okada[1], T.Iguchi[2], and H.Fukamachi[3]. [1]Dep. of Biol., Fac. of Sci., Okayama Univ., Okayama, [2]Dept. of Biol., Yokohama City Univ., Yokohama, [3]Zool. Inst., Fac. of Sci., Univ. of Tokyo, Tokyo.

We had previously reported that insulin stimulated the proliferation of the luminal uterine epithelial cells in the mouse. To clarify the mechanism of insulin actions, we studied the proliferation of cultured uterine epithelial cells in the mouse. Female mice of ICR strain (21-25-day old) were used. Uterine epithelial cells were dissociated by trypsin, and were cultured in a serum-free DME/F12(1:1) medium in the collagen gel-coated plate. The cell number was determined by the MTT method. The number of bromodeoxyuridine-uptake epithelial cells was increased by insulin. Insulin and insulin-like growth factor I (IGF-I) increased the number of epithelial cells in a dose-dependent manner. IGF-I was more effective (10-100 fold) than insulin. This suggests that insulin exerts actions through type I IGF receptors. EGF increased the number of epithelial cells as had been previously reported. These results indicate that IGF-I (or insulin) is involved in the proliferation of uterine epithelial cells.

UTERINE RESPONSE TO OVARIAN STEROIDS IN NEONATALLY ANDROGENIZED RATS.

A. Suzuki[1], Y. Fukazawa[1], N. Nishimura[1], T. Iguchi[1], and Y. Ohta[2]. [1]Dept. of Biol., Yokohama City Univ. Yokohama, [2]Dept. of Biol., Fac. of Gen. Edu., Tottori Univ. Tottori.

Neonatal treatment of female rats with androgen results in a permanent reduction of the uterine responsiveness to deciduogenic stimulus. Uterine response to progesterone(P) and estrogen(E) injections supportive of the development of deciduomata was investigated in ovariectomized rats sterilized by 100 or 1250μg testosterone propionate given neonatally to define the effect of androgen on the uterus. A single injection of E in association with 3 daily injections of P increased uterine weights in both the control(NR) and androgenized rats(AR). In NR, the E treatment had no effects on mitotic activity of the uterine epithelial cells; the activity of the stromal cells was increased by the treatment with E. In the AR, however, the E treatment stimulated the mitosis in both the epithelial and stromal cells. In NR, E injection lessened the P-induced reduction in P receptor(PR) immunostaining of the epithelial and stromal cells. By contrast, in AR, the E treatment surpressed the appearance of PR in the epithelial cells. In association with the P treatment in the NR, 13 proteins were separated by two-dimensional gel electrophoresis; only 4 proteins of them were synthesized, if E injection was given together with the P treatment. The number of protein spots was decreased in AR receiving the treatment with P alone(5 spots) or that with P plus E(1 spot). From these results, it is concluded that uterine response to the steroids is markedly affected in AR, which is responsible for the lowered decidual response.

ULTRASTRUCTURE OF APOPTOSIS IN THE GRANULOSA LAYERS OF RAT ATRETIC OVARIAN FOLLICLES.

Y. Takeo. Department of Anatomy, Tokyo Medical College, Tokyo.

The polycystic ovarian syndrome was induced in adult rats by treatment with continuous illumination to study follicular atresia. The atretic granulosa zone of mature ovarian follicles showed the characteristic features of apoptosis ultrastructurally, including several condensed nulcei and many apoptotic bodies, in addition to phagocytosis of the dead cells and their fragments by neighboring cells. This study, moreover, suggested that a special phenomenon of cell to cell phagocytosis , namely, a granulosa cell ingesting a cell of the same type with a normal appearance could occur at the earliest stage of follicular atresia. The phagocytic cell possessed abundant free ribosomes , well-developed rough endoplasmic reticulum and mitochondria, but few lysosomes. The ingested cell was similar in appearance to phagocytic cell. In addition, granulosa cells were also observed ingesting the cells with pyknotic nuclei and regressing cellular organelles, and possessing a large vacuole filled with nuclear fragments and degenerative cellular organells. These findings suggested a process of apoptosis in the granulosa cells during follicular atresia.

TISSUE INTERACTIONS IN THE REGRESSION OF THE QUAIL MULLERIAN DUCT BY EMBRYONIC TESTIS IN ORGAN CULTURE.

Y. Hirota and T. Noumura. Dept. of Regulat. Biol., Fac. of Sci., Saitama Univ., Urawa.

Quail Müllerian duct(Md) are induced to regress in response to Müllerian inhibiting substance(MIS) from the embryonic testis only during a defined period from 6.5 to 9 days of embryonic age. The role of tissue interactions in this process was studied in various epithelial-mesenchymal recombinations in organ curture.

Md epithelium and its surrounding mesenchyme were isolated following enzymatic digestion of 7-day (MIS-responsive) and 12-day(MIS-inresponsive) Mds of female quail embryos and cultured separately or as recombinants for 3 days, with or without embryonic testis.

Isolated epithelia did not form ductal structures in the absence of homotypic mesenchyme and failed to regress in response to co-cultured embryonic testis. In homochronic recombinants, young-young pairs were induced regressive changes in the presence of testis, but not old-old pairs. In heterochronic recombinants, the old epithelium-young mesenchyme pairs failed to regress by MIS from testis, while the young epithelium -old mesenchyme pairs were induced to regress.

The results suggest that both mesenchyme specificity and epithelial responsiveness are essential for MIS-induced Müllerian duct regression.

MOLECULAR MECHANISM OF APOPTOSIS IN PREGNANCY-DEPENDENT MAMMARY TUMOR OF GR/A MICE.

H. Kojima[1], A. Suzuki[1], Y. Hayashi[2], A. Matsuzawa[3], Y. Tsujimoto[4] and T. Iguchi[1]
[1] Grad. Sch. Integ. Sci., Yokohama City Univ., Yokohama;
[2] Biochem. Res. Inst., Morinaga Milk Ind. Co., Zama;
[3] Lab. Animal Res. Cent. Inst., Univ. Tokyo. Med. Sci., Tokyo.
[4] Biomed. Res. Cent., Osaka Univ. Med. Sch., Osaka

Pregnancy-dependent mammary tumors (PDMT) appear at the middle of pregnancy and continue to grow until parturition, but rapidly regress after parturition. Following this regression, DNA fragmentation, a marker of apoptosis, was observed from the 20th day (Day 20) of pregnancy to parturition. In the present study, we examined the molecular mechanism of apoptosis in PDMT. Fas-antigen mRNA, the receptor of apoptotic signal transduction, was expressed from days 17-20 of pregnancy to parturition. However, its translation occurred on days 19 and 20 of pregnancy. In PDMT, Fas-ligand was not expressed, while TNF-alpha was expressed. Bcl-2, a suppressor of apoptosis, also showed a drastic change: Bcl-2 mRNA was decreased on day 17; Bcl-2 protein was also decreased on day 19. On the other hand, in malignant mammary tumors, Bcl-2 was over expressed, whereas Fas-antigen and TNF-alpha were not expressed. These data suggest that TNF-alpha causes apoptosis by binding to Fas-antigen in PDMT.

METABOLISM OF ECDYSONE IN DIAPAUSE EGGS AND NON-DIAPAUSE EGGS OF THE SILKWORM, BOMBYX MORI.

H. Tokushige and H. Sonobe. Dept. of Biol., Konan Univ., Kobe.

The silkworm eggs contain large amounts of ecdysteroids. Using the RIA method we had shown that ecdysteroid titers in diapause eggs and non-diapause eggs changed dramatically during early embryonic development.

In the present study, in order to compare the metabolism of ecdysone between the diapause eggs and non-diapause eggs, [^{3}H]ecdysone was injected into two types of eggs. The resultant radioactive metabolites were analyzed by a reverse-phase HPLC.

In the diapause eggs, most of the radioactivity was detected in the conjugated ecdysteroid fraction (mainly, 3-epiecdysone 22-phosphate). On the other hand, in the non-diapause eggs, the radioactivity was scarcely detected in the conjugated ecdysteroid fraction, alternatively most of [^{3}H]ecdysone was efficiently converted to 3-epi-20,26-dihydroxyecdysone. These results suggest that epimerization followed by phosphate-conjugate formation is the major pathway in the diapause eggs, however, in the non-diapause eggs hydroxylation at C-20 and C-26 followed by epimerization is the dominant metabolic pathway.

NEW ECDYSTEROIDS FROM OVARIES AND EGGS OF THE SILKWORM, *BOMBYX MORI*.

M. Kamba[1], H. Sonobe[1], K. Yoshida[1], N. Hara[2] and Y. Fujimoto[2]. [1]Dept. of Biol., Fac. of Sci., Konan Univ., Kobe and [2]Dept. of Chem., Tokyo Inst. of Tech., Tokyo.

In ovaries and eggs of the silkworm, *Bombyx mori*, ten free ecdysteroids and their phosphoric esters have already been identified. We recently demonstrated that various unidentified ecdysteroids are still present in mature ovaries and developing eggs of *B. mori*.

In the present study, six unidentified ecdysteroids were isolated from about 6 kg of ovaries and about 9 kg of eggs of *B. mori* by several chromatographic techniques, e.g. liquid chromatography on silicic acid column, and HPLC on reverse-phase and anion-exchange columns. Their structures were analyzed by means of FAB-mass spectrometry, EI-mass spectrometry and ^{1}H-NMR spectroscopy. The structures of their ecdysteroids were determined as 2,22-dideoxy-23(S)-hydroxy-ecdysone and its 3-phosphate, and 3-epi-22-deoxy-20,26-dihydroxyecdysone and its 2-phosphate. The remainder of the compounds were estimated to be 3-epi-22-deoxy-17(β),20-dihydroxyecdysone and its 2-phosphate. These six 22-deoxy-ecdysteroids were newly isolated in the present study.

ISOLATION OF THE PUTATIVE ECDYSONE RECEPTOR SEQUENCE OF THE SILKWORM, BOMBYX MORI

M. Kamimura[1], S. Tomita[1] and H. Fujiwara[2]. [1]Natl. Inst. of Ser. Ent. Sci. Tsukuba, [2]Zool. Inst., Graduate School of Sci., Univ. of Tokyo, Tokyo.

In insects, the larval molts and metamorphosis are triggered by the steroid hormone, 20-hydroxy-ecdysone. The action of 20-hydroxyecdysone is mediated by the ecdysone receptor (EcR) to control the gene expression. EcR has been shown to be a member of the steroid hormone receptor superfamily, which commonly has well conservative DNA binding domain (C region) and ligand binding domain (E region). To identify the ecdysone receptor of B. mori, we conducted RT-PCR by using the conserved sequences between Drosophila melanogaster EcR (DEcR) and Manduca sexta EcR (MEcR) as primers and obtained a 620 bp DNA fragment. The sequence of the putative C region included in this fragment showed 100 % and 96 % amino acid identity with MEcR and DEcR, respectively. And the partially sequenced putative E region of this fragment was approximately 80 % and 65 % homologous to that of MEcR and DEcR, respectively. D region, which is generally not conserved, also shared approximately 70 % homology with that of MEcR. These results indicated that the DNA fragment obtained here was a part of the EcR gene of B. mori.

GENOMIC STRUCTURE AND EXPRESSION OF THE ECDYSONE RECEPTOR GENES OF LEPIDOPTERAN INSECTS

H. Fujiwara[1], M. Kamimura[2] and S. Tomita[2]. [1]Zool. Inst., Graduate School of Sci., Univ. of Tokyo, Tokyo, [2]Natl. Inst. of Ser. Ent. Sci. Tsukuba

An ecdysone receptor (EcR) plays the important roles in the tissue differentiation during metamorpohosis of insects. In Drosophila, three different EcR isoforms are produced by alternative promoting or alternative splicing from one EcR gene and expressed in a tissue specific manner (Koelle et al., 1993). This observation indicates that different isoforms are important in the regulation of different metamorphic responses. In lepidopteran order of insect, the EcR gene has been indentified firstly in the tobacco hornworm, Manduca sexta (Fujiwara et al., 1993). In Manduca, only one mRNA of about 6kb in size has been observed in various tissues of this insect. However, based on the sequence comparison of one RT-PCR product and a cDNA clone for MEcR, we found different structure between them, suggesting that there seems at least two different EcR transcripts. Further, we also isolated two genomic MEcR clones which have different structure mainly in the intron region. We report here, the genomic structure and thier expression of the MEcR, and compare it to the Bombyx putative EcR.

PURIFICATION AND CHARACTERIZATION OF 3-DEHYDROECDYSONE REDUCTASE FROM BOMBYX LARVAL HAEMOLYMPH

M. Komatsuzaki, Y. Nomura, M. Iwami and S. Sakurai
Department of Biology, Faculty of Science, Kanazawa University, Kanazawa 920-11

Prothoracic gland (PG) secretes 3-dehydroecdysone (3DE) in addition to ecdysone (E). 3DE does not show any biological activity and expresses its activity after conversion to E by reductase. 3DE was first identified in gut and peripheral tissues as an inactive metabolite of ecdysone and the reductase has been studied on those tissues so far. We found strong activity of the enzyme in Bombyx larval haemolymph and thus haemolymph of gut purged larvae was used for enzyme purification. After 6 step purification, the enzyme was purified by about one million fold. The optimal pH of the purified enzyme was 6.6, which is very similar to that of larval haemolymph. The enzyme showed its activity under presence of a co-enzyme, NADH or NADPH but the Km values for NADH and NADPH were 5.4 and 0.9 uM, respectively, indicating that the natural co-enzyme may be NADPH though we have not succeeded to find NADPH in haemolymph yet. Western blot analysis of various tissues of larvae by using antiserum against the purified enzyme showed that a strong signal band was found for haemocytes, ovary, testis and fat body in addition to haemolymph, but not for epidermis, mid gut, ganglia and malpighian tubules. These results indicate that the reductase may be supplied from haemocytes and/or fat body though the generating system of NADPH remains to be determined.

ECDYSTEROID IN THE BEAN BUG, *RIPTORTUS CLAVATUS*: IDENTIFICATION AND THE TITER IN THE HEMOLYMPH DURING DEVELOPMENT

J. Matsuo[1], H. Numata[1], Y. Tanaka[2] and S. Takeda[2]. [1]Dept. of Biol., Fac. of Sci., Osaka City Univ., Osaka, [2]Natl. Inst. of Seric. Entomol. Sci., Tsukuba.

We identified the major ecdysteroid in the hemolymph of the fifth (final) instar nymphs of the bean bug *Riptortus clavatus* (Turnberg) (Heteroptera: Alydidae) as makisterone A or a closely related steroid by high performance liquid chromatography and radioimmunoassay. This species shows a facultative adult diapause controlled by photoperiod. We determined the ecdysteroid titer in the hemolymph during the 5th instar and the first 7 days in the adult by radioimmunoassay under diapause-averting long-day (16L-8D) and diapause-inducing short-day (12L-12D) conditions at 25 °C. The titer increased gradually after the 4th nymphal ecdysis, reached a peak at day 4 of the 5th instar. Then the titer decreased promptly and was constantly low in the early adult period. There was no marked difference in the titer between long-day and short-day conditions, or between males and females. We conclude that in *Riptortus clavatus* ecdysteroid does not control the reproduction and adult diapause as suggested in some other insects.

THE EFFECT OF ADMINISTRATION OF SUSTAINED LOW CONCENTRATION OF ECDYSONE ON THE DEVELOPMENT OF NON-MOLTING MUTANT LARVAE OF THE SILKWORM, *BOMBYX MORI*.

Y. Tanaka and M. Yonemura. Natl. Inst. Seric. Entomol. Sci., Tsukuba.

The non-molting mutant strain of *Bombyx* (*nm-g*) remained in the first instar and finally died without undergoing ecdysis due to the low level of ecdysone synthesis by prothoracic gland, but administration of high concentration of ecdysone can induce the nm-g larvae to molt to the next instar. However, when they grew to as large as the normal third instar larvae, the larvae fed normal diet early in the instar began to spinning by administration of high concentration of ecdysone whereas the larvae of *nm-g* fed 10 ppm ecdysone molted to the fourth instar. These result suggest that the sustained low level of ecdysteroids play significant role on the maintenance of larval character.

WHAT IS THE ROLE OF BOMBYXIN? REAPPRAISAL OF HEMOLYMPH SUGARS OF *BOMBYX* LARVAE

Y. Oda, M. Iwami and S. Sakurai (Dep. of Biol., Fac. of Sci., Kanazawa Univ., Kanazawa 920-11)

Bombyxin is an insulin-related peptide hormone purified from *Bombyx* brains. Though its physiological role remains to be determined yet, bombyxin has been estimated to be involved in hemolymph sugar homeostasis because of its amino acid sequence and three dimensional structure analogous to insulin. Trehalose is thought to be a major hemolymph sugar in *Bombyx* larvae, but the effect of bombyxin on trehalose metabolism is obscure (Satake *et al.*, 1993). On the other hand, concentration of sorbitol-6-phosphate (S-6-P) in larval hemolymph is higher than that of trehalose, which led us to reexamine the hemolymph sugars by a convenient and accurate method for quantitative analysis using gas-liquid chromatography. Results showed that concentration of S-6-P in larval hemolymph before gut purge was twice as much as that of trehalose and decreased at the onset of wandaring stage. Hemolymph bombyxin titer is reported to increase at the onset of wandering stage (Saegusa *et al.*, 1992), suggesting that S-6-P could be the sugar whose concentration is under the control of bombyxin though details should be examined for conclusion.

DEVELOPMENTAL CHANGES IN THE TITER OF PROTHORACICOTROPIC HORMONE(PTTH) IN *BOMBYX* HEMOLYMPH

A. Mizoguchi[1], Y. O'hashi[1], S. Satake[1], J. Ishibashi[2], H. Kataoka[2] and A. Suzuki[2]. [1]Dep. of Biol., Sch. of Sci., Nagoya Univ., Nagoya and [2]Dep. of Agri. Chem., Fac. of Agri., Univ. of Tokyo, Tokyo.

Time-resolved fluoroimmunoassay for *Bombyx* PTTH was developed. Since some substance(s) that interferes the assay existed in the *Bombyx* hemolymph, hemolymph samples were processed by acetone precipitation, washing with acetone and heating. The interfering substance was removed from the sample by this course of treatment with a good recovery of PTTH. The PTTH titer in the hemolymph was examined at a 12-hr interval in the fifth larval stadium. Simultaneously, ecdysteroid titer was measured by radioimmunoassay for the same samples. A small rise and a large increase in ecdysteroid titer were observed on day-6 and day-8, respectively, of the instar. PTTH was present almost all the time, but its titer fluctuated to make five peaks. The last two peaks occurred 12 hr prior to each of the two ecdysteroid increments. One day before pupation, the PTTH titer decreased to a very low level. The PTTH contents in the brain also changed sharply and a mirror image relationship in the amount of PTTH was observed between the hemolymph and the brain.

IDENTIFICATION OF THE BOMBYXIN A AND C FAMILY GENES THAT ARE TRANSCRIPTIONALLY ACTIVE IN THE BRAIN.

M. Ino[1], M. Furuno[2], S. Sakurai[1], and M. Iwami[1] ([1]Fac. of Sci, Kanazawa Univ., Kanazawa, 920-11, [2]Sch. of Sci., Nagoya Univ., Nagoya, 464-01)

Bombyxin, a brain neurosecretory peptide of *Bombyx mori*, is structurally related to the insulin and functionally to the prothoracicotropic hormone. The bombyxin family consists of highly heterogeneous molecular species. Thirty-eight bombyxin genes have been isolated so far and classified into A, B, C, and D families. Among these genes, 20 form pairs, 12 form triplets, while 6 lie singly. In the pairs, two genes that belong to the different family are apposed closely at opposite orientation. In the triplets, the A and B family genes lie at opposite orientation, and C family genes lying between them are pseudogenes. Identification of the genes that are actually expressed should bring about important clues for understanding the transcriptional regulation. In the present study, we have sequenced more than 50 cDNA copies of the bombyxin A and C family mRNAs from *Bombyx* pupal brains and demonstrated that most of the mRNAs are transcribed from the genes belonging to the pairs. Results indicated that the genes in the triplets are mostly silent and bombixin A and C family genes in the pairs could be under a spesific transcriptional regulation.

BOMBYXIN INDUCES A GLYCOGEN REDUCTION IN THE FAT BODY.

S.Satake, A.Mizoguchi, K.Nagata*, H.Kataoka* and A.Suzuki*. Dept. of Biol., Sch. of Sci., Nagoya Univ., Nagoya and *Dept. of Agr. Chem., Fac. of Agr., Univ. of Tokyo, Tokyo.

When neck-ligated larvae of Bombyx mori were injected with bombyxin, an insulin-related peptide produced in the Bombyx brain, the hemolymph trehalose concentration of the larvae was significantly reduced. Moreover, the bombyxin injection increased the trehalase activity of the midgut. Therefore, the bombyxin-induced hypotrehalosemia is likely to result from the increase in the trehalase activity. Trehalase hydrolyzes trehalose into two glucose moieties and plays an important role in the energetics to produce a glycolytic flux. Since no increase in hemolymph glucose was observed after bombyxin injection, the glucose generated by the hydrolysis of trehalose should be transported into the peripheral tissues. Insulin induces hypoglycemia by increasing the rate of glucose uptake and promoting the glycogen production from the glucose in the insulin-sensitive tissues. So it was examined whether bombyxin stimulates the accumulation of glycogen in the tissues of Bombyx larvae. The bombyxin-II injection, surprisingly, induced the decrease, but not the increase, in the amount of fat body glycogen. The effect of bombyxin was dose-dependent. However, this bombyxin effect was not observed in the midgut. These results suggest that the mechanisms by which the hormone decreases the blood sugar is quite different between bombyxin and insulin.

EXTRACTION AND PARTIAL PURIFICATION OF PUPAL CUTICLE BROWNISH FACTOR IN PAPILIO XUTHUS.

K.Endo, F.Nishida and N.Kawamura. Biol. Inst., Fac. of Sci., Yamaguchi Univ., Yamaguchi.

Papilio xuthus has green-colored and brwnish-colored pupae in addition to the intermediates under long day conditions. The color of pupal cuticle was shown to be determined by environmental factors, i.e. characteristics of pupation site and smells through a factor secreted from brain-suboesophageal ganglion-prothoracic ganglion complex (Br-SG-PG complex).

We tried to extract a factor(s) changing the pupal cuticle to be brownish from Br-SG-PG comples of P. xuthus and P. machaon mature larvae and the activity was assayed using isolated abdomens of P. xuthus pharate pupae.

The factors changing the pupal cuticle to be brownish in P. xuthus pupae could be extracted from Br-SG-PG complexes of mature larvae of P. xuthus and P. machaon. The activity colud be detected by a biological assay mentioned as above.

In addition, a factor showing the same activity as the P. xuthus ones was found in Br-SG extracts of B. adults. It may be a peptide of M.W. about 2,000.

STRUCTURE OF PUTATIVE DIAPAUSE HORMONE PRODUCING CELLS IN THE SILKWORM *Bombyx mori*

T. Ichikawa[1] and I. Shimizu[2]. [1]Dept of Biol., Fac. of Sci., Kyushu Univ., Fukuoka. [2]Ecological Research Center, Kyoto University, Kyoto.

The suboesophageal ganglion of the silkworm has twelve cells that are immunoreactive to an antiserum against diapause hormone (DH). Somata of these cells are located at the ventral side of the ganglion and form three clusters: anterior, medial and posterior. Structure of these putative DH producing cells has been visualized by means of intracellular injection of Lucifer Yellow.

A pair of cells in the posterior cluster has a soma beside the ventral midline of the suboesophageal ganglion (SG) and project bilaterally symmetric dendritic branches to the anterior half of the SG at the larval stage or to the anterior edge of the SG around the oesophageal foramen after metamorphic fusion of the brain and the SG at the pupal stage. Axons of the cells, passing through the brain, enter the NCC 3 to spread varicose terminal branches in the corpus cardiacum (CC) and associated nerves of the CC. The cells in the anterior and medial clusters have a dendrite in the same region as the posterior cells' dendritic field. Their axons enter the maxillary nerve innervating the musculature of the maxilla. Most axons appeared to terminate at the surface of muscles. Some axons of medial cells travel between muscle bundles, extending short branches to the muscle, and reach the CC.

When all putative DH cells except for one or two posterior cells were surgically removed at the pupation, female moths laid diapause eggs. When a pair of posterior cells were removed from a pupa of diapausing-egg producer, the moth laid non-diapause eggs. Results of the structural and surgical experiments suggest that DH is largely released from axon terminals of the posterior cells into the haemolymph.

IDENTIFICATION OF MELATONIN IN DIFFERENT ORGANS OF THE CRICKET, GRYLLUS BIMACULATUS

M.T.Itoh[1], Y.Sumi[1], A.Hattori[2], T.Suzuki[2]. Department of Chemistry and Anatomy, St. Marianna University School of Medicine[1], Kawasaki[2].

The possible presence of melatonin was investigated in different organs of adult female crickets. The organs were homogenized in 0.1 M perchloric acid. After centrifugation, the supernatant was extracted with chloroform. The chloroform phase was washed with distilled water and evaporated. The extracts were dissolved in 30% methanol in 50 mM ammonium acetate (pH 4.2) and analyzed by reversed-phase high performance liquid chromatography (RP-HPLC) with fluorometric detection. Aliquots of RP-HPLC fraction were evaporated and dissolved in 10 mM phosphate buffered saline (pH 7.4). The melatonin content of each fraction was determined by radioimmunoassay. Melatonin was detected in the compound eye, antenna, ovipositor, palp, cercus, leg, wing, brain, ovary, digestive tube and Malpighian tube, indicating that melatonin was very widely distributed in the crickets. The results suggest that melatonin in these organs might be involved in the local control of various aspects of rhythmic activity as reported in vertebrates.

CHROMOSOMAL EVOLUTION OF POMACENTRID FISHES. III.

A.Takai
Osaka Shin-Ai College, Osaka

Karyotypes and distribution of nucleolus organizer regions (NORs) of eight species of Pomacentridae (Perciformes) were investigated. Chromosome numbers were 2n=48 in *Pomacentrus nagasakiensis*, *Abudefduf septemfasciatus*, *A. bengalensis*, *Paraglyphidodon melas*, *Chrysiptera leucopoma*, 2n=42 in *C. cyanea*, and 2n=36 in *C. rex*. *Amblyglyphidodon curacao* had two different karyotypes, 2n=48 and 2n=44. Fundamental numbers varied between 50 and 80. NORs were found on a single specific chromosome pair in all the species, but the positions of NORs and the sizes and morphologies of NOR-bearing chromosomes showed variations among the species.

The karyotypes of *Chrysiptera cyanea* and *Chrysiptera rex* had large bi-armed chromosomes that may have been formed by Robertsonian fusions. *Amblyglyphidodon curacao* with 2n=44 had also such large chromosomes. The present result demonstrated that the karyotypes of this family have been differentiated by Robertsonian fusions as well as by pericentric inversions. It seems that the diversified karyotypic features of this family derive from the results of active occurrences of chromosomal rearrangements, which could have also brought about diversified distribution of NORs. Generally, the karyotypic evolution of this family is characterized by increase of fundamental number and decrease of chromosome number.

THE EFFECTS OF MICROWAVE IRRADIATION ON DROSOPHILA MELANOGASTER IN VIVO AND HUMAN SPERMATOZOA IN VITRO

Y.Tonomura[1], Y.Kamiguchi[1], S.Watanabe[2] and H.Tateno[2].
[1]Tokyo Woman's Christ. Univ., Tokyo, [2]Asahikawa Med. Col., Asahikawa.

These studies were undertaken to examine cytogenetic effects of microwave (MW) on D. melanogaster in vivo and human sperm in vitro, using household electronic range (2.45 GHz, 200 or 500W). (1) By exposing larvae of flies to MW and a heat shock (40 min, 37℃), Tonomura studied their cytogenetic effects on germ cells, ganglion cells and salivary gland cells, and found that there was a great discrepancy between her results and Ashburner's results (1976). The effect of simple heat stress was quite different from that of MW accompanied by corresponding strength of heat stress, suggesting that MW itself has mutagenic effects. (2) Kamiguchi et al. studied the effects of MW on human sperm chromosomes, using an in vitro fertilization system between human sperm and zona-free hamster oocytes. Sperm were exposed to MW for 5 (Group Ⅰ) and 10 seconds (Group Ⅱ). Sperm motility in Group Ⅰ (80-90%) did not differ from that in the control, whereas the motility decreased remarkably in Group Ⅱ (40%) due to the heat shock. The incidence of sperm with structural chromosome aberrations was 10.4%, 12.6% and 8.3% in the control and Groups Ⅰ and Ⅱ, showing no significant difference between them.

SEX DIFFERENCES IN RECOMBINATION FREQUENCY BETWEEN SEX CHROMOSOMES IN THE MEDAKA

H. Wada, K. Naruse, A. Shimada and A. Shima, Zoological Institute, School of Science, University of Tokyo, Tokyo.

In the Medaka (*Oryzias latipes*), the stable sex determination with male-heterogamety (XY/XX type) was demonstrated through the inheritance of a sex-linked color locus *r* (colorless xanthophore). The sex chromosomes of the Medaka are morphologically indistinguishable and this undifferentiated state represents a primitive stage in evolution of sex chromosomes in vertebrates.

We used three inbred strains for genetic mapping and found that the *lf* (leucophore-free) locus, which was previously known to be autosomal, was strictly linked to the sex determining locus. We have also detected 7 RAPDs (Random Amplified Polymorphic DNAs) markers on sex chromosomes, and generated the linkage maps both in males (XY) and females (XX). The map distances (i.e. recombination frequencies) near the sex determining locus were remarkably reduced in males (XY). The restriction of recombination between sex chromosomes in heterogametic sex has been found in various species, and our results on the Medaka suggest that this restriction may precede the sex chromosome differentiation.

DIFFERENT STATES OF THE P-M SYSTEM IN TWO NATURAL POPULATIONS ARE STABLE OVER 10 YEARS RESPECTIVELY.

T.Shobu, E.T.Matsuura, S.I.Chigusa, Dept. Biol. Ochanomizu Univ., Tokyo

In our previous studies, a large number of isofemale lines of *Drosophila melanogaster* derived from 28 localities in Japan between 1982 and 1984 were tested for their characteristics in the P-M system by scoring GD sterility. The results showed an extinsive geographic variation in P-M characteristics. Among them, the two island populations, Chichi-jima and Iriomote-jima exhibited a striking contrast, that is, Q to M' population from Chichi-jima and P to Q from Iriomote-jima. However, *sn*^{w} hypermutability test in Chichi-jima population showed a few *sn*^{e} mutants, which may indicate that P elements carried by these strains include a small number of autonomous elements. In the last two years we collected flies again in these islands and tested them in the same way as before. The analysis revealed that the two island populations have kept their own equilibrium states of P element dynamics over a period of 10 years. Based on recent genetic analyses as well as molecular data about P elements cloned from these two populations, maintenance mechanisms will be discussed.

RESTRICTION ENZYME BANDING IN THE APODEMUS ARGENTEUS CHROMOSOMES —— PAYING SPECIAL ATTENTION TO THE C-BLOCK OF THE X CHROMOSOME.

K. Saigusa and Y. Obara. Dept. of Biol., Fac. of Sci., Hirosaki Univ., Hirosaki.

The chromosomes of the small Japanese field mouse Apodemus argenteus carry rather large centromeric C-heterochromatin in most elements. Especially, the X chromosome carries an unusually large block of C-heterochromatin (C-block), which forms almost two-fifth of its entire length and shows a delayed response of fluorescence to the QM and DA/DAPI stainings (Obara 1993). In order to assess the mechanisms of this unique cytologic phenomenon, we investigated the in situ digestion effect of the restriction endonuclease AluI on the C-block. The AluI bands basically corresponded to the C-bands in their distribution pattern. The C-block showed strong resistance to the AluI treatment. However, this nature of resistance was drastically gone by applying the acid and/or alkaline pretreatment, as shown by the marked decline of Giemsa stainability. Thus, it may be reasonable to consider that the AluI bands in the C-block of A. argenteus reflect the specificity in its chromatin organization rather than that in its base composition. This view may be compatible with our previous finding that the delayed QM-fluorescence in the C-block of A. argenteus could change to the ordinary pattern of fluorescence by the acid and alkaline pretreatments.

INTERPOPULATIONAL GENETIC DIFFERENTIATION OF FOUR CLOSELY RELATED GOBIID FISHES.

T.Mukai[1], T.Sato[1], K.Naruse[2], K.Inaba[1], A.Shima[2], and M.Morisawa[1].
[1]Misaki Marine Biological Station, School of Sci., Univ. of Tokyo, Kanagawa. [2]Zool. Inst., School of Sci., Univ. of Tokyo, Tokyo.

The gobiid fishes of the genus *Tridentiger* live around brackish waters and show habitat segregation among closely related species from littoral areas to lower rivers. In this study, we investigated the interpopulational genetic differentiation among four such segregated species (*T. trigonocephalus* in littoral areas, *T. bifasciatus* and *T. obscurus* in estuaries, and the amphidromous *T. brevispinis* usually seen in lower rivers) by analyzing their allozymic variations.

The degree of differentiation was higher in *T. obscurus* than in the other three species. Kishi(1977) reported the larger size of eggs and newly hatched larvae of the *T. obscurus* compared to the other species. These results suggest that the settling ability determined by the size of the newly hatched larvae affects the geographical differentiation of the brackish water fishes.

GENETICS AND EXPRESSION OF FUSED TARSI, A QUANTITATIVE TRAIT OF THE GERMAN COCKROACH.
A. Tanaka[1] and M. H. Ross[2]. [1]Dept. of Biol., Nara Women's Univ., Nara and [2]Dept. of Entomol., VPI & SU, Virginia, USA.

The fused tarsi trait of the German cockroach, Blattella germanica (L.), is characterized by fusion of the second and third tarsomeres. A stock was developed by selection in which the trait was strongly expressed on most legs of all individuals. Expression of the trait in the selected stock and in standard genetic crosses was estimated using three methods: (1) individuals with at least one fusion between adjacent tarsomeres, (2) the number of legs with fused tarsomeres, and (3) the number of tarsomeres. In the last method, which gives the most reliable analysis of the trait, the degree of fusion was classified into five grades by the number of tarsomeres: [5] wild type, [4 3/4] slightly fused, [4 1/2] half fused, [4 1/4] almost fused, and [4] completely fused. Expression did not differ significantly between sexes, right and left legs, and fore-, mid- and hindlegs. The F_1 was closer to wild type than to individuals in the selected stock (ft). Analysis of the F_2 suggested that ft is a quantitative trait controlled by more than one gene. Expression was suppressed in individuals heterozygous for T(9;10)/9;10Pw in the F_1 and backcrosses to ft.

DELETERIOUS EFFECT OF THE MELANOTIC TUMOURS ON THE VIABILITY OF THEIR CARRIERS IN DROSOPHILA MELANOGASTER.
K. Kosuda. Biol. Lab., Fac. of Sci., Josai Univ, Saitamama.

A large number of melanotic tumourous strains have been reported since Bridges(1916). Kosuda (1989) found a new tumourous strain, C-104, in which melanotic tumours develop only in the adult stage, exclusively in the vicinity of female spermathecae. They very often envelope either or both spermathecae. It is generally accepted that the melanotoic tumour is the aggregation of blood cells accompanied by melanization. The aggregation of haemocytes, melanization and the subsequent encapsulation are considered to be a common non-self recognition or self defence reaction in insects. In the present experiment, the incidence of melanotic tumour development was disclosed to be higher in the dead flies than in the live ones. The result explicitly shows the deleterious effect of the melanotic tumours on the adult viability. This fact may imply that non-self recognition or sef defense reaction is accomplished by paying some costs.

GENETIC FACTOR FOR DETERMINATION OF JAPANESE QUAIL BODY WEIGHT
A.Nakamura. Dept.of Biol.,Univ. of Shizuoka, Hamamatsu College, Hamamatsu.

Mammalian body weight is determined by a polygene, while a chicken's body size is reported to be controlled by a dwarf gene(as one gene), and this is used for producing broilers.

Genetic factors for weight control are also found in quail. These genes independently influence a quail's weight. General determination of body size is controlled by the growth rate and termination of the growth period, but the basic growth rate is uniform for several quail body weight types. We have concluded that the difference in body weight types is caused by the suppression or termination of the growth period.

RECOVERY OF ABNORMAL VISUAL PATHWAYS IN ALBINO MICE BY INTRODUCING TYROSINASE TRANSGENE.
T.Takeuchi[1,2], Y. Ohfuji[1], T.Sasamura[1], S.Tanaka[1], M.Tanaka[1], H.Yamamoto[1] and S.Yokoya[3]. [1]Biol. Inst., Tohoku Univ., Aoba-ku, Sendai, [2]Nihon Gene Research Lab.,Inc., Miyagino-ku, Sendai, [3]Cell Science Lab., Fukushima Medical College, Fukushima.

Abnormality of optic neuronal pathways is found in association with the albino mutation in various mammals. In order to elucidate the role of melanogenesis in the formation of normal optic pathway, we produced transgenic mice by microinjecting a tyrosinase minigene into fertilized eggs of BALB/c albino mice. Animals of the transgenic lines exhibited pigmentation in eyes and hair follicles. We examined retinogeniculate pathways on the pigmented, albino and transgenic mice by staining optic nerves with a fluoresent dye, DiI. Considerable recovery of the ipsilateral retinogeniculate projection in the transgenic mice that expressed pigmentation in the retina was observed.

CHARACTERIZATION OF JAPANESE SIKA DEER POPULATIONS BY RANDOM AMPLIFIED POLYMORPHIC DNAs.
H. Tamate[1] and T. Tsuchiya[2]. [1]Dept. Biotech., and [2]Dept. Basic Sciences, Ishinomaki Senshu Univ. Ishinomaki.

Sika deer (Cervus nippon) that once distributed throughout Japan have been confined to restricted areas as their habitat been fragmented. To assess an extent of their genetic diversity, we have surveyed randomly amplified polymorphic DNA (RAPD) markers in deer DNA. Samples were collected from four independent populations in Ashoro (Hokkaido), Goyosan (Iwate), Kinkasan (Miyagi) and Wadayama (Hyogo). Among 65 primers tested, several primers generate polymorphic DNAs with an average number of 8. Genetic traits of those markers were analyzed in known pedigrees of the Kinkasan herd.

Bandsharing and mean average percentage difference between populations indicated that genetic heterogeneiety of Kinkasan population was greately reduced while that of Goyosan population remained at higher degree. Pedigree analysis also revealed that those RAPDs markers are useful in discriminating individual and/or family group.

DETECTION OF CYST SPECIFIC PROTEIN IN *ACANTHAMOEBA CASTELLANII*.

Y. Hirukawa[1], S.Izumi[1], T. Tsuruhara[2], and S. Tomino[1].
[1]Dept. Biol.,Tokyo Metropol. Univ., Tokyo.
[2]Dept. Biol., Tokyo Gakugei Univ., Tokyo.

Starvation induces cell differentiation in vegatative trophozoite of a small soil amoeba, *Acanthamoeba*, to form dormant double walled cyst. *Acanthamoeba* are classified into three groups based on morphological features of the cyst. To analyze molecular mechanism of encystment, we attempted to detect the cyst specific proteins in *Acanthamoeba castellanii* Neff strain (group II).

SDS-PAGE analysis of cellular proteins revealed the appearance of several cyst specific proteins during encystment. We purified one of these proteins (21K protein) from the cyst extract by preparative gel electrophoresis, and raised polyclonal antibody against this protein. Immunoblot analysis demonstrated that this 21K protein is not detectable in trophozoites at logarithmic growth phase nor those at stationary phase, and first appears in the cells at late phase of encystment. Immunoblot also revealed that this antibody reacts with cystic protein of *A. polyphaga*, belonging to same group as *A. castellanii*, while the antibody failed to react with cysts of *A. astronyxis* (group I) and *A. culbertsoni* (group III).

We isolated mRNA from trophozoites and encysting cells, and translated in a reticulocyte lysate system, which showed the presence of mRNAs coding for cyst specific proteins in the cell during encystment. The result conforms to that of the cellular protein analysis by SDS-PAGE. In addition, immunoprecipitation analysis confirmed that translation products of mRNA from encysting cells but not from trophozoites contain the protein which reacts with the antibody against 21K cyst specific protein.

LIFE CYCLE AND THE LENGTH OF LIFE OF PARAMECIUM BURSARIA.

T. kosaka. Dept. of Biol. Sci., Fac. of Sci., Hiroshima Univ., Higashihiroshima.

Studies were made on the life cycle stages and the life span of Paramecium bursaria syngen 1. Sixteen exconjugant clones from a cross between stock OK-312 (mating type I) and stock OK-223 (IV), collected from a natural pond in Hiroshima Prefecture, were used in this study. The lengths of immaturity and adolescence were 35 to 57 and 0 to 17 fissions, respectively. A transition stage from maturity to senility was unclear. However, the clones showed a depression of fission rates from 2 or more to 0.5 or less, and produced various types of cells with abnormality in shape and lost of endosymbiotic algae in senility. The total life spans which were studied in 5 clones were 151 to 281 fissions (171 to 260 days).

PHOTORECEPTOR OF UNICELLULAR ORGANISM, *BLEPHARISMA*

T. Matsuoka. Dept. of Biol., Fac. Sci., Kochi Univ., Kochi

The cells of *Blepharisma* which possess pink pigment called blepharismin show photoresponse (temporal ciliary reversal caused by sudden increase in light intensity). We conclude that the blepharismin pigment mediates the photoresponse based on following evidences.

(1) Bleaching of the cells by cold shock raised a threshold light intensity for the photoresponse.

(2) The absorption spectrum of the pigment coincided with the action spectrum for photoresponse.

(3) The pigment localizes in pigment granules distributed over the cortical region of a cell. Freeze-fracture and thin section electron microscopy revealed that the pigment granules contained honeycomb-like structure presumably constructed of folded membrane, the structure that aids absorbing light effectively.

Furthermore, the pigment granules were isolated, detergent-solubilized and analyzed on SDS-PAGE. SDS-PAGE showed that the pigment granules exclusively contained a 200-kDa membrane protein. In gel filtration chromatography of detergent-solubilized components obtained from whole cells, a fraction containing proteins bound with pigment was obtained. SDS-PAGE of the fraction showed that the fraction contained 200-kDa protein.

TRICHOCYSTS IN *PARAMECIUM* AS DEFENSIVE ORGANELLES AGAINST THE PREDATORY CILIATE *MONODINIUM*.

A. Miyake[1] and T. Harumoto[2]. [1]Dept. Cell Biol., Univ. Camerino, Camerino, Italy, [2]Dept. Biol., Nara Women's Univ., Nara.

Trichocysts are, like other extrusomes, organelles that can discharge their content responding to stimuli. We recently verified a putative defensive function of trichocysts by showing that their discharge can defend *Paramecium* against the predatory ciliate *Dileptus*. Previously, however, their defensive function was repeatedly questioned based on the observation that trichocysts are of little use against *Didinium*.

In this work, we tested the defensive function of trichocysts against *Monodinium*, which is closely related to *Didinium*. In both *P. caudatum* and *P. tetraurelia*, trichocyst-non-discharge mutants were much more vulnerable to *M. balbiani* (killed 20 times more often by the predator under certain conditions) than wild-type cells. Trichocyst-deficient cells, obtained by treating wild-type cells with lysozyme, were similarly vulnerable. We conclude that trichocysts can defend *Paramecium* against *Monodinium*.

We assume that trichocysts can defend *Paramecium* against many predators and that *Didinium* has overcome the defense mechanism of *Paramecium* by acquiring pexicysts, unique offensive organelles.

ISOLATION OF BLEPHARISMIN-BINDING PROTEINS RESPONSIBLE FOR PHOTORESPONSES IN BLUE FORM OF *BLEPHARISMA*

A. Fuke, T. Tsuda, K. Taneda and T. Matsuoka. Dept. of Biol., Fac. of Sci., Kochi Univ., Kochi

The pink-colored pigment (blepharismin) responsible for the step-up photophobic response of *Blepharisma* cells might be weakly bound to 200-kDa protein. The 200-kDa protein is eluted in one (fraction I) of the pink-colored fractions (monitored by absorbance at 580 nm) when the detergent-solubilized sample obtained from the normal (pink-colored) cells is gel-filtered. In this case, a large amount of free pigment possibly dissociated from the protein is eluted in the other fractions.

Pink-colored pigment changed its color to blue on exposure of the living cells to white light in the presence of excess oxygen. In the gel filtration chromatography of the detergent-solubilized sample obtained from blue form of *Blepharisma*, peak value of the fraction I was enhanced. When TLC-purified free pigment was gel-filtered, a peak corresponding to the fraction I was not detected. The results suggest that the blue form of blepharismin may be strongly bound to the protein. SDS-PAGE of the fraction I showed that not only 200-kDa protein but 230-kDa protein were contained in this fraction.

DEFENSIVE FUNCTION OF PIGMENT GRANULES IN *STENTOR*.

T. Harumoto[1] and A. Miyake[2]. [1]Dept. Biol., Nara Women's Univ., Nara, [2]Dept. Cell Biol., Univ. Camerino, Camerino, Italy.

Colored heterotrichous ciliates, such as *Stentor coeruleus* (blue) and *Blepharisma japonicum* (red), have pigmented extrusomes (extrusive organelles) called pigment granules (PGs). We recently showed that PGs in *B. japonicum* are defensive organelles.

In this work, we tested PGs in *S. coeruleus* for defensive function against the predatory ciliate *Dileptus margaritifer*. Normal blue cells of *Stentor* were often observed to ward off the attacking predator by discharging a cloud of blue pigment. Pale-blue or nearly colorless cells obtained by changing culture conditions or by treating blue cells with lysozyme (e.g., 50-100 μg/ml, 10 min), were much more vulnerable (killed 10 times more often by the predator under certain conditions) than blue cells. If a blue cell (but not a pale-blue cell) and a single *Dileptus* cell were kept together in a small space (e.g., 100 μl), the predator was often killed.

These results are consistent with the assumption that PGs in *S. coeruleus* are defensive organelles and support our working hypothesis that extrusomes are organelles for predator-prey interaction in unicellular organisms.

TIME KEEPING ON THE MATING TYPE REVERSAL RHYTHMS IN *PARAMECIUM MULTIMICRONUCLEATU*

I. Miwa and S. Kamiya. Biol. Lab., Coll. of Gen. Educ., Ibaraki Univ., Mito.

Cells of *Paramecium* show many kind of circadian rhythms of the physiology and behavior activity. In *Paramecium multimicronucleatum*, cycler stocks express the rhythms involving a sequential alternation of the two complementary mating type (III and IV). We examined the characters of the mating type reversal rhythms of stock 110B.

The transition III to IV occurred 11 hours after onset of darkness in the various LD cycles. Cells also showed free running rhythms of mating type reversal in the DD and the time of period of rhythm was about 25 hours. Mating type reversal rhythms of this stock have been gone ahead with two type clocks of hour-glass and circadian. The transition time of III to IV was delayed by a light pulse at 3 hours after onset of darkness. The term of expression of type IV was shortened by a light pulse at 6 hours after onset of darkness. In action spectrum of light pulse for 3 hours, the lights of long wave length were effective to delay the time of transition III to IV. Temperature cycle (25°C and 15°C) was effective to entrain the mating type reversals rhythm as same as LD cycle.

On the other hand, the proteins of detached cilia from the cells of mating type III and IV phase were compared with SDS-PAGE. A few bands of protein were different in the cells of type III and IV.

NUCLEAR DIFFERENTIATION AFTER CONJUGATION IN *PARAMECIUM BURSARIA*.

T. Watanabe and H. Tanaka. Biological Institute, Fac. Science, Tohoku University, Sendai.

Macro- and micronuclei of *Parameciucm* are differentiated from synkaryon. The vegetative micronucleus of *P. bursaria* is a *chromosomal micronucleus*. The microlamella partially separated chromosomes at one end of ellipsoidal micronucleus. The synkaryon subsequently divides twice, producing four nuclei. All four nuclei look identical under electron microscopy. At 26 hours after beginning of the conjugation, two of the four become swelling. In the swelling nuclei, the chromatin and the microlamella become to disperse, whereas remaining two still contain condensed chromosomes. At 40 hours, two macronuclear anlagen show several dense bodies and also more electron opaque bodies which consist of granular materials. These two bodies might be the nucleoli. The chromatin of the anlage looks amorphous and electron opaque filamentous structure.

CONJUGATION OF HOMOPOLAR DOUBLET IN *TETRAHYMENA THERMOPHILA*.

T.Sugai and M.Okazaki. Dept. of Biol., Fac. of Sci., Ibaraki Univ., Mito.

Homoplar doublet(HD) cell of *Tetrahymena* has two sets of cortical structure, but has a macronucleus and a micronucleus. HD conjugate with two other cells as it has two oral apparatus. HD conjugation which has not been studied so far will provide new conjugation pathway. When HD cells were mixed with normal cells of different mating type, triplet which consists of 1 HD and 2 normal cells was formed. It's nuclear process was observed using alkaline-Giemsa method which stain both nuclei and cortical structure. HD cells underwent normal meiosis. Three patterns of behavior of meiotic products was observed. Gametic nuclei formation, nuclear exchange and fertiliaztion pattern was also differerent from normal pattern. After fertilization, HD cell contained 2n or 3n or 4n micronuclei. Implication of the results was discussed.

MATING TYPE -RECOGNITION AFTER PAIRING IN *TETRAHYMENA*.

J.Harada and T.Sugai. Dept. of Biol., Fac. of Sci., Ibaraki Univ., Mito.

During conjugation of *Tetrahymena thermophila*, mating type recognition occurs in two steps. First step is "co-stimulation" which is a period of pairing readiness. Pairing is mating-type-nonspe-cific, but homotypic pairs are soon detached, only heterotypic pairs persist and go into next stage. This is the second mating type recognition step. Using detaching and re-pairing method, we examined whether re-pairing of cells which completed the second recognition step is mating-type-specific or not. We found that, before the onset of meiosis, cells re-paired mating-type-nonspecifically, but cells at stage I of meiotic prophase re-paired mating-type-specifically. The finding of decline of mating-type-nonspecificity and concomitant increase of mating-type-specificity was unexpected, and will shed light on the role of mating substance during conjugation of this species.

MONOCLONAL ANTIBODY SPECIFIC FOR 67K PROTEIN OF ENDONUCLEAR SYMBIONT HOLOSPORA OF CILIATE PARAMECIUM CROSS-REACTS WITH MITOCHONDORIA OF VARIOUS ORGANISMS.

M. Fujishima, H. Dohra and I. Miyakawa. Biological Institute, Faculty of Science, Yamaguchi University, Yamaguchi.

Monoclonal antibody (mAb) IR-2-1 was originally developed against a purified 67K protein of endonuclear symbiont Holospora obtusa of the ciliate Paramecium caudatum. Previously, we reported that this mAb also cross-reacted with decorated spongiomes of radial canals of contractile vacuole complex of various Paramecium species, and contractile vacuole membranes of Tetrahymena pyriformis, and fibrous structures in the macronucleus of T. thermophila (J. Euk. Microbiol., in press; Europ. J. Protistol., in press).

In the present study, we found that mAb IR-2-1 cross-reacts with mitochondoria of P. caudatum, T. thermophila, Saccharomyces cerevisiae and Dictyosterium discoideum, too. We show that localities and molecular weights of the mitochondorial antigens by indirect immunofluorescence microscopy and immunoblots.

ACTIVATED FORM SPECIFIC ANTIGENS OF MACRONUCLEAR ENDOSYMBIONT HOLOSPORA OBTUSA OF CILIATE PARAMECIUM CAUDATUM.

M. Kawai and M. Fujishima. Biological Institute, Faculty of Science, Yamaguchi University, Yamaguchi.

The Gram-negative bacterium H. obtusa is a macronucleus specific symbiont of the ciliate P. caudatum. When the infectious forms of this bacterium are mixed with paramecia, they are soon engulfed into the host digestive vacuoles, appear in the host cytoplasm and then penetrate the host macronuclear envelope with their special tip first. Prior to infection into the macronucleus, the infectious forms changed their morphology, buoyant density, and differentiate into the activated forms.

To detect the activated form specific substances, in the present study, we isolated the activated forms of H. obtusa from host homogenates by Percoll density gradient centrifugation. The bacteria were then injected into mice to get monoclonal antibodies. We got several monoclonal antibodies including the activated form specific ones. We show intra-cellular localities and molecular weights of the antigens, and timings of the appearance and disappearance of the antigens in infection process.

MONOCLONAL ANTIBODIES INHIBITING MATING REACTIVITY OF MATING TYPE O^3 IN *PARAMECIUM CAUDATUM*.

Y. Azuma, E. Kaku, F. Maruo and M. Takahashi Inst. Biol. Sci., Univ. of Tsukuba, Ibaraki

A specific cell-to-cell recognition between complementary mating type takes place under the interaction between mating type substances located on cilia of complementary mating types in *Paramecium*. Though indirect evidences suggested the substances to be protein, no one has so far succeeded to isolate the substances from the cilia nor mating type specific antibodies.

Detached cilia from highly reactive mating type O^3 belonging to syngen 3 were injected to mice and 5 monoclonal antibodies (OmA, OmB, OmC, OmD and OmE) were obtained after screening. All of them were identified as IgG class antibodies and inhibit mating reactivity of all O^3 strains examined, but of no E^3 strains. Among 6 other syngens, strong cross reaction in syngen 1 was observed and weak in syngen 5 but no in syngen 4, 6, 12, 13. Localization of antigen(s) recognized by these antibodies was examined under a laser scanning confocal microscopy. When three antibodies, OmA-3, OmD-7 and OmE-1, were used immunofluorescence was observed on ventral surface cilia, mostly of anterior top that looked like beads in a line. These results suggest that the antibodies recognize the O^3 mating type substances.

PRODUCTION OF MONOCLONAL ANTIBODIES SPECIFIC TO THE CYST WALL OF THE STICHOTRICH CILIATE, *HISTRICULUS CAVICOLA*.

T. Matsusaka and M. Himura, Dept. of Biol. Sci., Fac. of Sci., Kumamoto Univ., Kumamoto

In order to trace the genesis of cyst wall of the stichotrich ciliate, *Histriculus cavicola*, we have attempted to raise polyclonal antisera against cyst wall polypeptides as the reliable probes. We have obtained several antisera but most of them are not so specific, except for an antiserum, whose titer was very high and monospecifically recognizes the 180kD polypeptide. Its antigen located in the endocyst, the innermost layer of the cyst wall. In order to obtain more specific probes for the cyst wall, we tried to produce monoclonal antibodies (mAbs) against each layer of the cyst wall. Five mAbs were obtained and localization and molecular weight of their antigens and their immunoglobulin subtypes were determined. Four mAbs detected endocyst and one of them monospecifically recognized 180kD polypeptide and were IgG1. The other 3 mAbs recognized 180, 120, and 110kD polypeptides and were IgM. Another mAb was also IgM and decorated ectocyst but very weakly. About 54kD polypeptide band was weakly stained by this mAb.

NUCLEAR BEHAVIOR OF THE TRANSPLANTED MICRONUCLEI BETWEEN THE DIFFERENT SPECIES OF EUPLOTES.

K.Sato. Dept. of Biol., Naruto University of Education, Naruto, Tokushima.

The micronuclei from the two different species of Euplotes (E. octocarinatus and E. patella syngen 2) were reciprocally transplanted between them. In both cases, about 10 % of the operated cells grew into clones. When their progeny were induced into homotypic conjugation, the transplanted micronuclei (of different species) underwent meiosis and oval macronuclear anlagen were observed. But these anlagen could not elongate. In this study, the micronuclei were transplanted between E. aediculatus and E. octocarinatus in the same way. When the micronuclei of E. octocarinatus were transplanted into E. aediculatus cell, all of the operated cells died out. In other hand, 4 clones are alive, if E. aediculatus micronuclei were into E. octocarinatus. Two of the four clones were induced into homotypic conjugation by gamones (pheromones) of E. octocarinatus. All of the exconjugants died out, although the transplanted micronuclei underwent meiosis and the other nuclear changes. Oval macronuclear anlagen appeared, but they did not elongate into rod-like form. Thus, some species-specific interactions may be necessary at the time when oval macronuclear anlagen elongate in these Euplotes.

MORPHOLOGICAL PROFILES OF THE FATE OF MACROPINOSOME IN *ACANTHAMOEBA*.

S. Kurota[1], A. Kihara[2] & T. Tsuruhara[1].
[1]Dept. of Biol., Tokyo Gakugei Univ., Tokyo,
[2]Lab. of Biol., Hosei Univ., Tokyo.

Acanthamoeba ingests solute substances via a macropinosome by phagocytosis-like engulfment. Based on the experiments with a DIC and a confocal microscope, we have found that the invagination of macropinosome was occurred and it fragmented into smaller vacuoles. In this paper we report electron microscopic observations on the fate of macropinosome with horseradish peroxidase as a tracer. Horseradish peroxidase-positive tiny vesicles (about 150nm in diameter) were observed around these smaller vacuoles. The number of the vesicles increased depending on time. These observations suggest that the tiny vesicles-pinched off from the smaller vacuoles are responsible for recycling of the endocytic pathway in addition to the ingestion of solute molecules via pinosomes.

ENVIRONMENTAL FACTORS AND ENCYSTMENT IN EUPROTES SP. (CILLOPHORA: NASSOPHORA: EUPROTIDA)

A. Tomaru and A. Shimizu. ,Dept. Biol., Fac. Sci., Nara Women's Univ., Nara.

The encysted state is of common in Protozoa, but internal and external factors which control encystment are not well understood.

In this study, we examined the effect of food deficiency on the encystment in the hypotrichous ciliate, Euplotes sp. isolated in Nara. This species was grown on the Chalkely's medium inoculated with Klebsiella pneumoniae. We counted bacteria and vegetative cells and cysts of Euplotes sp. every 12 or 24 hr for 5 or 10 days. Under these conditions, the number of cysts increased as the bacteria density decreased. Encystment started earlier in cultures initiated with more ciliates than in cultures initiated with fewer ciliates. Euplotes sp. placed in the Chalkely's medium without bacteria encysted earlier (about 1 day after transfer) than those placed in the medium inoculated with bacteria (a few days after transfer). These results support the idea that deficiency of food is one of the important factors for inducing encystment.

ON THE BIREFRINGENT NATURE OF CHROSOMES IN DINOFLAGELLATES IN BOTH INTERPHASE AND MITOSIS.

H. Sato[1] and K. Kato[2]. Nagano Univ., Ueda, Nagano and Biol. Lab., Nagoya City Univ., Nagoya.

Based on the nature of the chromosomal birefringence (BR), dinoflagellates can be classified into three groups (Sato et. al., '89).
A type, characterized by a strong positive and intrinsic BR, condensed state and lack of basic protein which was observed in Gyrodinium sp.: B type, a mixture of positively and negatively birefringent chromosomes and appeared as a rosary shape possessed a few basic proteins but not histone. Ceratium represent B type. C type, which showed a weak negative form BR such as Oxyrrhis sp., apparently possed basic nuclear protein but again, not histone. BR pattern and the appearance of chromosomes are not well matched with the current pglogenetic tree, however, further analysis going on.

It is ionteresting to know that histone is not detected in all three groups. Histone, an important nuclear protein and thought to be acquired in an early stage of evolution of eukaryotes, is erased and substituted another type of basic protein(s) in dinoflagellates. Why and when are quite important questions because the ocean blooms are caused by the over populated dinoflagellates. Further study to isolate and identify this nuclear protein is in progress.

16S RIBOSOMAL RNA SEQUENCES OF METHANOGENIC SYMBIONT IN A TERMITE.

[1]SHINZATO,N., [2]A.YAMAGISHI, [2]T.OSHIMA, and [1]I.YAMAOKA,
[1]Dept.of Biol.,Yamaguchi Univ., [2]Dept. of Life Science, Tokyo Inst. of Tech.

In the hindgut ecosystems of termites, hydrogen and bicarbonate are produced from cellulose by anaerobic fermentation of microbial symbionts. They are converted to methane by methanogenic bacteria.

A part of the 16S ribosomal RNA gene of methanogenic bacteria present in the gut of a termite, *Reticulitermes speratus* were amplified by polymerase chain reaction using *Methanobacteriales* specific primers.The amplified DNA fragments were cloned into *E.coli*, and the sequence was analyzed. All the analyzed clones showed the identical sequence with minor differences about 0.2% from each other. The sequences were most homologous to the corresponding ribosomal RNA sequence of *Methanobacterium formicicum* reported so far. We are on our way to analyze the microbiol population in the gut by *in situ* hybridization analysis with the probes specific to the sequence.

COMPARISON OF THE FEMALE GENITAL ORGANS IN SEVERAL LAND PLANARIANS.

Y. Shirasawa and N. Makino. Dept.of Biol., Tokyo Med.Coll.,Tokyo.

The structures of the female genital organs, germaria, yolk glands and oviducts, in the land planarian, genus Bipalium were investigated by light microscopy. Materials are the different types of reproduction way B. fuscatum, B. fuscolineatum, and B. pennsylvanicum are the types of only sexual reproduction, and B. multilineatum is the only asexual reproduction(fission) and B. nobile is the type of both ways. In the large, only fission type specimen, the female genital organs, especially yolk glands and oviducts were observed slightly, and the static germaria which contained yolk granules sparsely, also observed. Moreover, no typical testes but rudimentary ones were seen in the region near the organs. On the other hand, the sexual types showed that many active testes were observed in well-developed female genital organs near by.
These observations indicated that the functions of the female genital organs were influenced by testes.

ULTRASTRUCTURAL AND IMMUNOHISTOCHEMICAL IDENTIFICATION OF GUT ENDOCRINE CELLS IN THE FRESHWATER OLIGOCHAETE, TUBIFEX HATTAI.

H. Jaana. Biol. Lab., Asahikawa campus, Hokkaido Univ. of Education, Asahikawa.

In order to obtain knowledge about a gut endocrine system of the freshwater oligochaete, Tubifex hattai, the epithelia of the pharynx, the esophagus and the intestine were examined by electron microscopical and histochemical techniques.

The epithelium of the esophagus contained basal-granulated cells with vasoactive intestinal peptide (VIP)-like immunoreactivity. These cells were decanter-shaped, and contained a number of granules which were usually round with a moderate electron density and homogeneous texture. Although no exocytotic granule release in the basal-granulated cells were observed, these cells seems to function morphologically as endocrine cells.

The epithelium of the pharynx contained another type of granulated cells; these granules were round with a high electron density. Careful observations revealed that the granulated cells were in fact the parts of pharyngeal gland cells which enclosed the pharynx. Thus, the granulated cells of the pharynx were not endocrine cells.

TWO TYPES OF PIGMENT GRANULES IN THE OMMATIDIA CELLS OF *D. MELANOGASTER*.

Shingo Ohkubo, Hiroshi Sawada and Motoo Tsusué
Biological laboratory, School of Liberal Arts, Kitasato University

Many eye color mutant has been reported in *D. melanogaster*. The pigments are divided into two groups, one is tryptophan metabolite and the other is pteridines.

Early work of Shoup (1966) observed compound eyes of of wild type flies and *bw* ones from late pupa to the adult fly by electron microscope and found that there were two types of granules, one was electron dense and another was not. He discussed that electron dense granules contained ommochrom and another type granules were carrying pteridines.

In the present work, we used *sepia* mutant flies as a material. By use of light microscope we also observed two types of granules, first type was red and another was yellow. Successive operation of cell fractionation and sucrose density gradient centyrifugation, two types of the granules could be separated. By high performance liquid chromatography, we proved that pigment contained in red granules and yellow granules were identical with xanthommatin and sepiapterin respectively.

THE FINE STRUCTURE ON THE STARVATION IN BOTRYOIDAL TISSUE OF LAND LEECHES,HAEMADIPSA ZEYLANICA VAR. JAPANICA

H.Inamura
Dept.of Biol.,Tokyo Med.Coll.,Tokyo

Under starvation the botryoidal tissue gradually showed black color and shrinkage was studied by light and electron microscopy in mature stage land leeches, Haemadipsa zeylanica var. Japanica.The starved leeches lost weight at the rate of 50-60% for 8 months and at the rate of 60-70% for 12 months.The botryoidal tissue that consists of a network of capillary are lined by swollen globular cells which are laden with three different kinds of granules;(1)oil droplets:L1,(2)including lots of particles :L2,(3)lysosome-like:L3.After 12 months starved,the cells became including L2 granules and L3 granules.On the base of the cells,rER which surrounded nucleus disappeared and then a lots of L3 granules surrounding nucleus accumulated.On the apex of the cells,L2 granules acumulated,and a lots of vesicles disappeared,and microvilli became degenarate. Glycogen particles disappeared.Golgi apparatus formed a few secretory vesicles in low density.L2 granules accumulated a dense body.
We concluded that the metabolism took a control of degenaration of L2 granules and vesicles.

STRUCTURE OF THE OVARY IN A MYODOCOPID, *VARGULA HILGENDORFII* (CRUSTACEA: OSTRACODA).

K. Ikuta and T. Makioka. Inst. of Biol. Sci., Univ. of Tsukuba, Tsukuba.

An adult female *Vargula hilgendorfii* has a pair of sac-like ovaries, which are flattened laterally on both sides of the alimentary canal in the posterior region of the thorax. Two oviducts open separately to the gonopores just behind the seventh limbs. The ovarian wall of each ovary consists of a monolayered ovarian epithelium and encloses a narrow ovarian lumen. Germaria or young germ cell-zones are found in the ovarian wall faced the alimentary canal. Synchronously growing oocytes are protruded outward from the germaria of paired ovaries into the hemocoel, connected with the ovarian walls by short stalks consisting of some epithelial cells. Mature eggs should be ovulated into the ovarian lumen through the stalks and transported to the oviducts.

The ovarian structure in *V. hilgendorfii* seems to have some similarities to those in many chelicerates rather than those in many other crustaceans.

SEROTONINLIKE IMMUNOREACTIVE CELLS IN THE CENTRAL NERVOUS SYSTEM OF THE SLUG, LIMAX MARGINATUS.

N. Seo and N. Makino, Dept. of Biol., Tokyo Med. Coll., Tokyo

We studied the endocrine control system of the sexual growth of the slug Limax marginatus. We reported that neurosecretory cells in the central nervous ganglion produced a few stimulation ovotestis hormones by the in vitro culture of the ovotestis and the developmental change of neurosecretory cells. As a part of those studies, the central nervous system is experimented with the immunohistochemical staining method used an antiserotonin antibody.

The cerebral, pedal, right parietal and visceral ganglia in the central nervous system have some clusters of serotoninlike immunoreactive (SLIR) cells and SLIR neuropile. The cluster of neurosecretory cells contains SLIR fibers. The SLIR cells cluster is composed a few large and many small SLIR cells. The number of small SLIR cells increases along with the growth of the slug, reaching a peak in the mature stage and decreases rapidly in the post-reproductive stage. The slugs kept in the dark and light for 10 days, their SLIR neuropiles in both of surroundings stain deeply. These morophological observations provide the possibility that the neurosecretory cells is controled SLIR cells in the central nervous system of the slug.

STUDIES ON THE PIGMENTS OF THE COMPOUND ASCIDIAN, *POLYANDROCARPA MISAKIENSIS.*

Teruhisa Ishii and Yasunori Saito. Shimoda Marine Research Center, University of Tsukuba, Shimoda, Shizuoka.

The compound ascidian, *Polyandrocarpa misakiensis* shows red color. In this species, red pigments mainly distribute in the epidermal layer. However, the area between the branchial and the atrial siphons lacks red pigments, and then the white blood cells distributed in the mesenchymal space can be seen through the epidermal layer. In this study, the solubility of the pigments was examined. The pigments were dissolved in ethyl ether, methanol, ethanol and ammonia water, especially dissolved strongly in acetone and acetic acid, slightly in formalin. According to these results, both lipid-soluble and water-soluble pigments are involved in the pigments of *P. misakiensis.*

We also observed the pigmented cells by TEM. We detected some particular granules that existed more in the red pigmented epidermal layer than in the nonpigmented one. Hence those granules may express red color in the animal. On the contrary, the white blood cells were filled with some vacuoles. With the observation at the LM level, we conclude that the white blood cells are "nephrocytes."

CYTOPLASMIC DISTRIBUTION OF HETEROTRIMERIC G PROTEINS.

K. Chiba, [1]S. Takaoka, and M. Hoshi. Department of Life Science, Tokyo Institute of Technology, Yokohama. [1]Utsunomiya-higashi Hospital, Uthunomiya.

Heterotrimeric G proteins mediate signal transduction from receptor to effector enzymes. Although it is generally accepted that G proteins are plasma membrane-bound, cytoplasmic or nuclear distribution of G protein has recently been suggested. In order to localize the G protein in cells, we raised a specific monoclonal antibody against mammalian G protein β subunit. In indirect immunofluorescence microscopy of several mammalian cell lines, staining of cytoplasm and/or plasma membrane is seen with the antibody. Immunoblotting analysis revealed that this antibody is reactive with starfish G protein β subunit. When starfish oocytes are stained with the antibody, a network of fibers are detected in cytoplasm. These results indicate that G proteins exist in cytoplasm as well as plasma membrane.

SPHEROIDAL CELLS BREAKING OUT ON THE GILL AND ATRIAL EPITHELIA IN THE ASCIDIAN, CIONA SAVIGNYI.

Z.Hoshino[1] and A.Ueyama[2]. [1]Dept. of Biol., Fac. of Educ. and [2]Research Center for Electron Microscopy, Iwate Univ., Morioka.

The gill and atrial epithelia of the ascidian, Ciona savignyi, were investigated by scanning and transmission electron microscopies.

The branchial sac is surrounded by the atrial cavity in ascidian.

The walls of the branchial and atrial cavities consist of flat non-ciliated epithelia, although the walls of branchial sac are perforated by very large numbers of stigmata, the margins of which are lined by ciliated cells.

In scanning electron micrograghs the many spheroidal cells are found on the surface of the gill and atrial epithelia.

In transmission electron micrographs, besides the cells being shed from the gill epithelium, the cells migrating from the vascular cavity into the gill epithelial cells are found.

These results suggest that the breaking out of the spheroidal cells is caused by whether exfoliation of epithelial cells or excretion of blood cells.

MESENCHYMAL PIGMENT CELLS EXPRESSING THE COLONY COLOR IN THE TWO COLONIAL ASCIDIANS.

E. Hirose[1], T. Yoshida[2], T. Akiyama[3], and Y. Iwanami[4]. [1]Col. Ag./Vet. Med., Nihon Univ., Fujisawa, [2]Col. Human./Sci., Nihon Univ., Tokyo, [3]Dept. Biol. Keio Univ., Yokohama, and [4]Dept. Chem. Keio Univ., Yokohama.

Pigmentation in ascidians were investigated on histological and biochemical in the two colonial species, *Botrylloides simodensis* (Botryllidae, Stolidobranchia) and *Leptoclinides echinatus* (Didemnidae, Aplousobranchia). The pigments of *B. simodensis* were localized in the blood cells classified as "pigment cells" or "nephrocytes", These pigment cells adhere to the epidermis. Four color types of cells were recognized in *B. simodensis*; white , red-yellow, violet, and black. On the other hand, some tunic cells of botryoidal shape in *L. echinatus* were loading black-violet or orange-yellow pigments. The results exhibit that these ascidians contain the analogous pigments to those of vertebrates but the quite different pigment cells from vertebrates' chromatophores in morphology.

ULTRASTRUCTURAL RESPONSES OF THE GILL CHLORIDE CELLS ASSOCIATED WITH THE ACCLIMATION TO THE SEAWATER IN AN EURIHALINE STURGEON, *ACIPENSER TRANSMONTANUS*

S. Kikuchi[1], Y. Takagi[2], Y. Nakagawa[3], T. Yamanome[4], and K. Yoshida[4] [1]Dept. Biol., Sch. Lib. Arts and Sci., Iwate Med. Univ., Morioka, [2]Otsuchi Marine Res. Ctr., Ocean Res. Inst., Univ. Tokyo, Otsuchi, [3]Lab. Molec. Endocrinol., Sch. Fish., Kitasato Univ., Sanrikucho, [4]Sunrock Ltd., Kamaishi

The gill chloride cells (CCs) were studied by TEM and SEM in the fish reared in fresh water (FW), and 70% and 100% seawater (SW) for three months. In the FW fish, solitary CCs were scattered throughout the lamellar and interlamellar epithelia and were characterized by deep infoldings of the apical cell membranes and abundant tubular invaginations of the baso-lateral cell membranes associated with numerous mitochondria. The SW-acclimated CCs, on the contrary, mostly accumulated in the basal and interlamellar area, interdigitated with neighboring cells, and were connected by 'leaky junctions' to form multicellular complexes. They had a higher density of mitochondria and a more extensive tubular system than those of the FW-CCs. In the fish acclimated to 70% SW, the distribution and characteristics of CCs resembled those in 100% SW. No apical pit was found even in the SW-CCs. These facts are compatible with the results of our previous physiological study, i.e., an increase in Na^+-K^+-ATPase activity and the successful regulation of the plasma Na level during SW acclimation, indicating a high adaptability of this fish to the SW.

ULTRASTRUCTURAL STUDY ON THE DIGESTIVE TRACT OF THE LOACH (MISGURNUS ANGUILLICAUDATUS).

Y.Sasaki and N.Makino. Dept. of Biology.,Tokyo Med.Coll., Tokyo.

Intestinal epithelial cells of the loach,that have the intestinal respiration were observed by electron microscopy. On the anterior part and transitional part of the intestine, epithelial cells were constituted by the simple columnar cells. These columnar cells have long microvilli facing the intestinal lumen. The lateral surfaces of the cells make smooth contact with neighboring cells. And desmosomes can be seen between the epithelial cells of the under microvilli. Large oval nuclei of the epithelial cells locate below the middle of the cell. Numerous mitochondria are observed bacilliform in shape below the nucleus but also they are scattered above the nucleus. Golgi apparatus is mainly composed of lamellae and vesicles. In the cytoplasm of the columnar cell,many vesicles,vacuoles,rough surfaced endoplasmic reticulum and multivesicular body are observed. Small vessels and capillaries can be seen under the basement membrane but can't find out the epithelium. On the posterior part of intestine, epithelial cells change the shape and these cells have much idented lateral surface.The epithelial cells facing the lumen have a few microvilli and the desmosome are seen under the microvilli. Capillaries belong the basement membrane are observed between the columnar cells and also the apical portion of these cells. But capillaries don't contact with the lumen. Between the capillaries and the lumen, there are the narrow cytoplasm of the epithelial cells, the basement membrane and the endthelial cells of the capillary. Cytoplasmic organelles are the same as the columner epithelial cells. Many goblet cells are found among the epithelial cells at the three portions of intestine.

LOCAL DIFFERENCES IN A PROCESS OF THE TESTICULAR DEVELOPMENT OF RANA RUGOSA.

M. Takase. Lab. Amphibian Biol., Fac. Sci., Hiroshima Univ., Hiroshima.

It has been reported that a constitution of the sex chromosome pairs in Rana rugosa was different among local races (Nishioka et al., 1993). In the present study, I used this species collected from Hamakita, Shizuoka Pref. (XY type in which X and Y chromosomes can be distinguished morphologically from each other), Saijo, Hiroshima Pref. (XY type in which X and Y chromosomes are not distinguished morphologically from each other) and Kanazawa, Ishikawa Pref. (ZW type in which Z and W chromosomes are distinguished morphologically from each other). The development of their gonads were observed at the stages from the 10th day after hatching to metamorphosis, in order to know the differences in sex differentiation among the three populations. It was found that the sex was differentiated at stage I in the Hamakita popuoation, that is, there was no secondary genital cavities in the testes. In the Saijo population, the anterior portion of the testis had no genital cavities, while the posterior portion had distinct secondary genital cavities at st. I. In the Kanazawa population, most of the tadpoles at st. I had large secondary genital cavities and showed that the sex differentiation was remarkably delayed in this population.

CEREBROVASCULA AMINERGIC AND ACETYLCHOLINESTERASE-POSITIVE INNERVATION IN THE NEWT, WITH SPECIAL ATTENTION TO THE CHOROID PLEXUS.

K.Andō. Biological Lab., Dept.of Regional Culture, Fac.of International Studies of Culture, Kyushu Sangyo Univ., Fukuoka.

The distribution and origin of cerebrovascular adrenergic and acetylcholinesterase positive (AChE) nerves were investigated in the newt. Adrenergic nerves supplying the cerebral arterial tree and choroid plexus usually come from extracranial side, but sometimes originated from noradrenaline or adrenaline-containing nerve cells intrinsic to the walls of the major cerebral arteries. On the other hand, AChE nerves innervating these two cerebral vasculatures, which showed high level of AChE activity, were all of extracranial side (probably parasympathetic in nature). Adrenergic and AChE nerves in the newt major cerebral arteries are characterized by an unbalanced distribution with a lesser density of the latter type. The most characteristic feature of cerebrovascular adrenergic and AChE innervation in this urodelan species was that a large number of these two types of nerves were concentrated in the microvascular-epithelial regions of the choroid plexus, despite a poor nerve supply of adrenergic and AChE nerves to the major cerebral arteries. This, in conjunction with other findings, suggests that adrenergic and cholinergic neuronal mechanisms might deeply participate in the critical role of the choroid plexus for the brain nutrition and metabolism via the cerebrospinal fluid.

RELATIONSHIP BETWEEN MULTIPOLAR AND UNIPOLAR NEURONS.

N. IWAHORI, Dept. of Anat., Fac. of Med., Nagasaki Univ., Nagasaki.

The central nervous system of the urodela contains unipolar (UN) as well as multipolar neurons (MN), for which reason it is usefull for elucidating relationship between these two types of neurons. In the present study, the intrinsic organization of the spinal cord in the salamander was studied using the rapid Golgi method, with special reference to relationship between the UN and MN.

The UN are the main constituents of the spinal cord and are distributed throughout the gray matter. A single process extends superficially from the outer pole of the somata and divides into the axon and the dendrites. The dendrites travel superficially terminating within the white matter. The MN are few in number and are located mainly in the superficial region of the gray matter. The dendrites of the MN are superficially distributed into the white matter. As seen in the spinal cord at early developmental stages, the MN are transformed from the UN by the migration of the cell bodies superficially toward the periphery of the process.

Thus, the MN are a modified form of the UN and are transformed by the migration of the cell bodies of some UN superficially toward the periphery of the process.

CONCENTRIC LAMELLAR BODIES IN AXON TERMINALS OF PURKINJE CELLS IN GROGGY MUTANT RATS.

I.K. Takeuchi[1], E. Aoki[1], and Y.K. Takeuchi[2].
[1]Inst. Dev. Res., Aichi Prefec. Colony, Kasugai,
[2]Gifu Coll. Med. Technol., Seki.

More than twenty years ago, Sotelo and Palay (1972) suggested that the concentric lamellar bodies (CLBs) in axon terminals may represent a degenerative phase of cellular organelles in the axonal remodeling process contributing to neuronal plasticity. However, their precise nature and function still remain unsolved, probably because only a few number of these bodies have been observed in the nervous tissues hitherto examined. In the groggy rat, numerous CLBs appeared in the axon terminals of the cerebellar and vestibular nuclei from 40 days of age onward. They were measured about 1-5 μm in diameter and classified into four types, which apparently represented the process of formation and degradation of one and the same CLB. They were positive to acid phosphatase cytochemistry and also to ubiquitin immunocytochemistry. Since a number of degenerative nerve fibers appear in many regions of the groggy rat brain at 20 to 60 days of age, the abrupt increase of CLBs in the groggy rat from 40 days of age may represent an active axonal remodeling function of Purkinje cell nerve fibers saved from fiber degeneration.

THE DISTRIBUTION OF SEROTONIN AND NEUROPEPTIDES IN DEVELOPING TASTE BUDS OF MOUSE VALLATE PAPILLAE, AS REVEALED WITH A CONFOCAL LASER SCANNING MICROSCOPE.

M. Kudoh. Dept. of Biology, Fukushima Medical College, Fukushima.

Immunohistochemical localization of serotonin, neuron specific enolase (NSE) and protein gene product 9.5 (PGP 9.5) was examined in taste buds of mouse vallate papillae with a laser scanning microscope. Immunoreactivity to serotonin was localized mainly in several cells of a taste bud from a mouse treated with 5-hydroxytryptophan. These reactive cells, presumably type III cells, were slender, extending apically from the base to the taste pore, and such profiles were quite similar to those of monoamine-containing fluorescent cells detected by the Falck-Hillarp method. This finding may indicate the availability of serotonin as a marker substance for the type III cell. Immunoreactivity to PGP 9.5 and NSE was found in many intragemmal nerve fibers and also in some of taste bud cells, the profiles of which resembled serotonin-immunoreactive cells very closely.

In infant mice, immunoreactivity to PGP 9.5 and NSE occurred in some of epithelial cells of the undifferentiated papillae at 1 to 2 days after birth, while immunoreactivity to serotonin appeared in taste bud cells at 4 to 5 days when taste perception was supposed to be functional by completion of taste pores.

ESTROGEN EFFECT ON THE DECREASE OF INTRACELLULAR LAMININ IN THE ANTERIOR PITUITARY OF FEMALE RATS

T. Kikuta and H. Namiki
Dept. Biol., Sch. Educ., Waseda Univ., Tokyo

We (1988) have demonstrated the quantitative sexual difference of laminin positive LH cells in the rat anterior pituitary at puberty. In the case of the female, the number of laminin positive cells decreased at sexual maturation. And we (1991, 1992) reported the instant decrease of laminin positive cells of prepubertal ovariectomized (OVX) and non-OVX female rats provided estrogen.

In the present study, we immunohistochemically examined changes in number of the positive cells and estrogen receptor (ER)-immunoreactive LH cells of 25 day-old non-OVX female rats given estradiol (1 μg/g weight). Laminin-positive cells decreased in number at day 3 and minimized at day 5. And ER level in the laminin-positive cells were decreased simultaneously. Further more, the immunoreactivity of anti-LH-β in the majority of gonadotrophs declined. To quantify the alteration of immunoreactivity, microscopical images of LH-β-immunoreactive cells were printed through a digital output device and measured the spectroreflection (480 nm) of individual cells. A high reflex, indicating low immunoreactivity of LH-β, in the laminin- and ER-negative gonadotrophs was observed at day 5. On the contrary, the immunoreactivity in the laminin-positive gonadotrophs still remained high, despite the decrease of the number of the cells.

The decline of immunoreactivity of LH-β was considered as a result of gonadotropin surge. And these results suggest that intracellular existence of laminin in LH cells is restrainable for release of gonadotropin.

A NEW PATHWAY OF FAS-MEDIATED APOPTOSIS IN MOUSE REPRODUCTIVE ORGANS.

A. Suzuki[1], H. Kojima[1], Y. Hayashi[2], A. Matsuzawa[3], Y. Tsujimoto[4], Y. Ohta[5] and T. Iguchi[1]
[1] Grad. Sch. Integ. Sci., Yokohama City Univ., Yokohama; [2] Biochem. Res. Inst., Morinaga Milk Ind. Co. LTD., Zama; [3] Lab. Animal Res. Cent. Inst., Univ. Tokyo Med. Sci., Tokyo; [4] Biomed. Res. Cent., Osaka Univ. Med. Sch., Osaka; Dept. Biol., Fac. General Education, Tottori Univ., Tottori.

Fas-antigen, a cell surface protein belonging to the NGF/TNFR family, mediates apoptotic signal transduction induced by Fas-ligand protein, a novel member of TNF family. Fas-ligand/Fas-antigen system causes apoptosis in immunocytes. Gonadectomy induces apoptosis in mouse vagina, prostate and epididymis. In this apoptosis, TNF-alpha was expressed instead of Fas-ligand. Fas-mRNA was always expressed, but it was translated only when apoptosis occurred. Far-Western blotting revealed that TNF bound to Fas-antigen. Anti Fas antibody and TNF induced apoptosis in those tracts after 6 h culture. In *lpr* mice lacking Fas-antigen, apoptosis was not induced by gonadectomy, indicating that Fas-antigen plays an important role in apoptosis of these tracts. A decrease in Bcl-2, suppresor of apoptosis, occurred before the translation of Fas mRNA, suggesting that Bcl-2 directly or indirectly participates in a translation of Fas mRNA. Here, we propose that TNF-alpha/Fas-antigen system shows as a new apoptotic signal transduction pathway.

MOTOR UNIT SIZE OF THE VENTER CAUDALIS OF M. DIGASTRICUS IN THE MOUSE.

M. Aikawa and A. Shimozawa
Dept. of Anat., Dokkyo Univ. Sch. of Med., Tochigi.

To elucidate the relation between the caliber of myelinated nerve fibers (MNFs) and motor unit size, mean motor unit size was measured for the venter caudalis of m. digastricus (VCMD) in the mouse. All muscle fibers and MNFs were counted morphologically, and mean motor unit size was calculated for each muscle under the assumption that almost all of the total MNFs in r. digastricus are efferent (Semba and Egger, 1986), so the mean motor unit size was about the same as the innervation ratio (total muscle fiber number / total MNF number) for VCMD. The result showed that the total muscle fiber number in VCMD was 1975.6±148.4 (average±S.D., n=12), and the total MNF number in r. digastricus was 45.5±6.0 (n=12), resulting in an innervation ratio for VCMD of 44.1±6.1 (n=12). The average of 12 mean motor unit sizes for the mouse VCMD (44.1 ±6.1), innervated by extra-large MNFs, was greater than that for the mouse m. stapedius (6.5±1.3) (Aikawa and Shimozawa, 1994), innervated by large MNFs; and those for the mouse VCMD and m. stylohyoideus (35.8±8.2) (Aikawa and Shimozawa, 1994), innervated by extra-large MNFs, roughly resembled each other.

MELANOSOME FORMATION IN AMELANOTIC MELANOPHORES OF RANA BREVIPODA BY GENE TRANSFECTION.

H. Okumoto[1], M. Nishioka[1], I. Miura[1] and M. Obika[1,2]. [1] Laboratory for Amphibian Biology, Fac. of Sci., Hiroshima Univ., Hiroshima and [2] Department of Biology, Keio Univ., Yokohama.

cDNA(Tyr-N) encoding tyrosinase(TYN) of Rana nigromaculata was introduced into cultured amelanotic melanophores of R. brevipoda by means of calcium phosphate coprecipitation. The established cell line of amelanotic melanophores employed here has an origin in the dermal cells of an albino frog and has been maintained for more than 9 years with high proliferative activity. The cells are colorless but contain typical premelanosomes with fibrillar internal structure. Tyrosinase activity was not detected throughout the cytoplasm by a DOPA reaction at EM level. Transfection assay was carried out using the cells in two dishes, to which calcium phosphate-cDNA was added and incubated for 24 h at 25°C. On the 4th or 6th day following transfection, a small number of pigmented, stellate or dendritic cells were detected in each dish by light microscopy. Numerous melanosomes at various stages of maturation were observed by EM in these transformants. The profiles of these melanosomes were comparable with those found in wild type melanophores.

MORPHOLOGICAL STUDIES ON THE ONTOGENY OF THE RAT LUNG. (VI) DIRECTIONS & ANGLES OF THE PULMONARY AIR-WAY SYSTEM.

A. Kimura[1], T. Gomi[1], Y. Kikuchi[1], K. Kishi[1], Y. Kitazawa[2]
[1]Dept. of Anat., [2]Dept. of Pathol., Sch. of Med. Toho Univ., Tokyo

We analyzed the formation of the fetal and neonatal pulmonary air-way system of the rat. Secondary bronchi were devided into the following four groups, 1) lateral bronchial group (L), 2) medial bronchial group (M), 3) dorsal bronchial group (D) and 4) ventral bronchial group (V). Each bronchial group consisted of 1 to 6 bronchi. Secondary bronchi began after the 11th day of observation in the following patterns. The 12th day fetus: (Right: D1, L1; Left: L1). The 13th day fetus: (Right: D1, L1-2; Left: L1-L2). The 14th day fetus: (Right: D1-4, L1-4, M3, V1, V6; Left: D2-5, L1-4, M3). The 15th and 16th day fetus: (Right: D1-5, L1-5, M2-5, V1, V6; Left: D2-5, L1-5, M2-5). 17th day fetus: (Right: D1-5, L1-6, M2-5, V1, V6; Left: D2-5, L1-5, M2-4). The completion of the divergence was seen by the 17th day in the fetus lung. The directions of the secondary bronchi from the primary bronchi were constant in spite of the changing stages of the fetus. However, the angels of the secondary bronchi were changed at the opposite side of the growth of the pulmonary lobes, according to the aging of fetus. This change suggests that the development of the peripheral area of the bronchi, that is the appearance of tertiary bronchi and the extension of bronchus, may change the angles of the secondary bronchi.

CELL ADHESION RECEPTORS FOR EXTRACELLULAR MATRIX COMPONENTS IN RABBIT ARTERIAL SMOOTH MUSCLE CELLS IN CULTURE

K. Yamamoto and M. Yamamoto. Dept. Cell Biol., Tokyo Metropol. Inst. Gerontol., Tokyo.

We examined the cell adhesion receptors and binding sites on type I collagen, heat-denatured type I collagen, and fibronectin in rabbit arterial smooth muscle cells (SMC) in culture. The results suggest that rabbit SMC in synthetic state have one or more specific surface receptors recognizing each substrate. On fibronectin, the attachment and spreading of rabbit SMC after 1 and 24 h of culture are mediated by α3β1 and α5β1 integrins, which recognize the RGD adhesion sequence. In contrast, rabbit SMC adhere to native type I collagen through collagen fibril-binding receptor (α1β1 integrin) which recognize a sequence in triple helical structure. On the other hand, they adhere to denatured type I collagen through collagen peptide-binding receptors (α2β1 and α3β1 integrins) for the sequences DGEA and RGD in the α1(I) chain. Moreover, α1β1 integrin may be involved in the initial adherence to each substrate and relocated at the pre-proliferative adherence.

REGULATION OF THE MIGRATION OF HUMAN FETAL SKIN FIBROBLASTS: EFFECTS OF INTERFERON.

H. Kondo and Y. Yonezawa. Dept. Exp. Biol., Tokyo Metropol. Inst. of Gerontol., Tokyo.

We previously reported that the migration of human fetal skin fibroblasts into a denuded area of a cell monolayer was stimulated by growth factors (bFGF and PDGF) and the extracellular matrix (collagen). Since human fetal skin fibroblast migration decreased with in vitro aging, a study was done to determine factors inhibiting cell migration. In the present study, we examined the effects of interferon (IFN) on the migration of human fetal skin fibroblasts since it has been reported that IFN α and γ suppressed the chemotactic activity of human skin fibroblasts and IFN β was produced by them. Cell migration was determined by the method of Stenn (1980). Among IFN α, β and γ examined, IFN β caused the largest inhibition of fibroblast migration. Next, an experiment was performed to determine whether growth factors and the extracellular matrix reverse IFN-induced inhibition of cell migration. Collagen and fibronectin did not reverse the inhibition, but bFGF partially reversed.

CHARACTERISTICS OF FLUORESCENT MATERIALS ACCUMULATED IN CULTURED NEUROBLASTOMA CELLS AND EFFECT OF REACTIVE OXYGEN SPECIES ON ITS ACCUMULATION

Y. Mochizuki, M.K. Park, T. Mori, and S. Kawashima
Zoological Institute, Graduate School of Science, University of Tokyo, Tokyo

The N2a cells, a clonal cell line of C1300 mouse neuroblastoma, gradually accumulate lipofuscin-like fluorescent materials, when they are maintained at a high density in culture. The fluorescence characteristics of the organic solvent soluble and insoluble fractions derived from the neuroblastoma cells at 15 days after plating were analyzed without any special correction in measurement.

The fluorescent materials in the organic solvent soluble fraction had an excitation maximum of 350-360nm and an emission maximum of 432-435nm. The inorganic solvent insoluble fraction solubilized in Tris-HCl buffer (10mM, pH7.4) containing 15% SDS and 0.15M NaCl exhibited fluorescence with an excitation maximum of 350-360nm and an emission maximum of 440-455nm. These fluorescent characteristics were identical to those for lipofuscin so far reported. Both fluorescent intensities were enhanced by treatment with 10-15mU/ml glucose oxidase for 5 days.

The present results suggest that the fluorescent materials in the neuroblastoma cells are lipofuscin and its accumulation is enhanced by reactive oxygen species.

PREVENTION OF SERUM-INDUCED CELL DEATH BY HEAT SHOCK

T.Kurita, S.Tokoro and H.Namiki
Department of Biology, School of Education,
Waseda University, Tokyo

We have already reported about serum-induced apoptosis and its prevention by thiols. In the present study we found that process of serum-induced apoptosis was interfered by heat shock treatment. 43℃ heat treatment prevented serum-induced cell death of TIG-1 human fibroblasts *in vitro*. When temperature of culture was lowered to ordinary used 37℃, the interfered cell death process started to progress. We already demonstrated that both decline of intracellular thiol content and protein synthesis were necessary for the apoptosis, and reagents affecting intracellular thiol-content or protein synthesis prevented cell-death. But the heat shock treatment prevented apoptosis without affecting quantitatively those metabolisms.

SERUM ALBUMIN INDUCED CELL DEATH

T.Sakiguchi, T.Kurita and H.Namiki
Department of Biology, School of Education,
Waseda University, Tokyo

We have previously reported that cell-death was induced when serum or plasma was highly concentrated in medium, and this cytotoxicity exists in a low molecular weight fraction of serum (M.W.<1,000) by ultrafiltration. The low molecular weight fraction was found to be contaminated with macro molecular protein. The most of contaminating protein was serum albumin and the cell-death inducing toxicity was due to serum albumin with several kinds of amino acids. The serum toxicity was reconstructed with serum albumin and the low molecular weight fraction, as well as cyst(e)ine-free basal medium.

MORPHOLOGY AND CULTURE OF THE INFUSORIFORM EMBRYO OF DICYEMIDS (MESOZOA).

H. Furuya[1], K. Tsuneki[1] and Y. Koshida[2]
[1]Dept. of Biol., Fac. of Sci., Osaka Univ., Toyonaka.
[2]Natl. Cent. for Univ. Ent. Exam., Tokyo.

Infusoriform embryos of several species of dicyemids belonging to the genera Dicyema, Pseudicyema, and Dicyemennea, were studied morphologically. These infusoriforms were different in cell numbers, nuclear numbers of urn cells, numbers of anterior ventral cells, and the presence or absence of anterior lateral cells. However, the genera were not recognized by these differences.

In order to study the developmental process from an infusoriform embryo to the vermiform stage, culture medium was prepared by modifying the method of Japan and Morowitz(1975). In the medium, infusoriform embryos became immobile only within two to three days. Then, their four urn cells were expelled and were frequently observed on the bottom of the culture well. Even after the infusoriform body was lysed, the urn cells have remained intact about for two days. This event may be a step for further development.

EXAMINATION OF THE JAPANESE BRYOZOAN SPECIMENS DESCRIBED BY ORTMAN IN 1889

S. F. Mawatari and T. Suwa. Div. of Biol. Sci., Grad. Sch. Sci., Hokkaido Univ., Sapporo

The German naturalist L. H. P. Doderlein stayed in Japan from 1879 to 1881 as a professor at Tokyo Imperial University. During his stay, he collected many specimens of marine invertebrates, mainly from Sagami Bay, and shipped them to Germany. A. Ortmann is one of the taxonomists who examined the Doderlein collection. In 1889, he published a monograph on Japanese bryozoans based on the specimens from this collection. Although his work is still a usefull resource for Japanese bryozoan research, his style of describing species is now out of date and does not fit into modern taxonomic practices. Redescription of those specimens originally described by Ortmann was needed. Consequently, we examined those deposited in the Musee Zoologique in Strasbourg, France. Specimens of 136 taxa out of the original 159 Ortmann described are found there. Among them, samples of *Diachoseris dischoderminae* and *Chorizopora discreta* were broken specimens and useless for redescription. The others were well kept, but some lost the cuticle covering of zooids. As a result of our study, twenty-four misidentified species are now redescribed.

KARYOLOGICAL AND TAXONOMIC STUDIES OF THE DUGESIA SPECIES IN SOUTHEAST ASIA. XIX. CHROMOSOMES OF 3 SPECIES COLLECTED AT NAGASAKI AND THE RESULTS OF WATER ANALYSIS OF THEIR HABITATS IN THE URAKAMI RIVER.

S.Tamura[1], K.Yamamoto[2], M.Takai[3], I.Oki[4] and M.Kawakatsu[5]. [1]Ôsaka Pref.Inst.Publ.Health, Ôsaka, [2]Junshin High School, Nagasaki, [3]Saga Med.School, Saga, [4]OEPA, Ôsaka, [5]Fuji Women's College, Sapporo.

The distribution of 3 Dugesia species is now known in the Urakami River running through the City of Nagasaki, Kyûshû, in South Japan (cf. Kawakatsu, Tamura, Takai, Yamamoto, Ueno & Oki, 1993). These species are: Dugesia japonica Ichikawa et Kawakatsu, 1964 (a common species in the Far East); Dugesia ryukyuensis Kawakatsu, 1976 (a species distributed in the Southwest Islands of Japan); Dugesia tigrina (Girard, 1850)(originally the North American species). D.tigrina was sometimes found in tanks and ponds of tropical fishes in Japan; the first naturalized population in Japan was found in the Urakami River.

Up to the present, the following karyological data were obtained. 1) D.japonica: diploid (2x=16), triploid (3x+SB=24+SB) and mixoploid (2x & 3x=16 & 24). 2) D.ryukyuensis: diploid (2x=14). 3) D.tigrina: diploid (2x=16).

According to the result of water analysis, D.tigrina is found in polluted waters showing a high BOD value than those of the other 2 species occurred.

CORRELATION BETWEEN PATTERNS OF METAMORPHOSES AND TYPES OF ANCESTRULAE IN ASCOPHORAN BRYOZOANS.

S. F. Mawatari[1], H. Ikezawa[1], T. Suwa[1], and R. M. Woollacott[2]. [1]Zool. Inst., Fac. of Sci., University of Hokkaido, Sapporo, [2]Museum of Comparative Zoology, Harvard University, Cambridge

In bryozoans, metamorphosis produces an ancestrula, the founding individual of a colony. Ancestrulae vary in complexity and are important in phylogenetic analyses at the species and higher levels. Ancestrulae also dictate initial budding patterns and, as such, are ecologically significant in determining both colony form and growth rate. Two sources of ancestrular body wall tissues can be identified within larvae. The aborally-situated pallial epithelium forms the body wall in ctenotomes and the orally-situated metasomal (internal) sac does so in anascan cheilostomes. Both the pallial epithelium and metasomal sac reportedly participate in body wall histogenesis, however, in the only case known from ascophoran cheilostomes. To more fully understand ancestrular development in ascophorans, we examined body wall derivation in ancestrulae of 6 species in 3 genera of the Ascophora. Two species of *Microporella* possess a tata-type ancestrula in which the frontal membrane is uncalified. The body wall has a dual origin in both: metasomal sac for uncalcified basal and calcified lateral walls; and pallial epithelium for the frontal. *Pseudocelleporina triplex* and 3 species of *Celleporina* possess a schizoporelloid-type ancestrula in which the entire body wall is heavily calcified. In these species, the body wall arises exclusively from the metasomal sac. In conclusion, we found that larval anatomy and ancestrular type were correlated which enabled us to accurately predict the derivation of the ancestrular body wall in all species.

THE ROTIFERA FROM PULAU PINANG,MALAYSIA IN FEBRUARY.

M.Sudzuki.Biol.Lab,Nihon Daigaku Univ.Omiya,

Five taxa,new to science,have been encountered;1) *Lepadella* sp.resembling *triba* but with much longer & square lorica(65-70x32-35mμ).Foot:18-23,Toes:20-28,2) *Trichocerca* sp.with tapering head consisting of 2-4 long,6-8 short plates.Body:95-110x48-52.Toe:68-72,3) *Monostyla quadridentata* ssp.whose occipital edge with extremely long median spines,4) *Polyarthra minor* ssp. mostly *aptera* in form,small(60-70x40-50),with 4-6 nucl eated vitellarium,5) *Anuraeopsis fissa* ssp.whose caudal extremity with pointed projection.New record for Malaysia: *Brach. calycif. dorcas*(Fp), *Anura. f. haueri*(Fp), *A. n.navicula*(F,D♀), *Colur. obtusa*(Gp), *C. uncinata deflexa*(Gp), *Mono. bul. constricta*(Gp). *Taphro. selenura*(Gp), *Cephal. mucronata*(Gp), *Diur. weberi*(Gp), *Asco. salt. indica*(B), *Test. patina intermedia*(Gp).-- All these were collected from diches & ponds of Taman Rimba(R),Taman Belia(B),Batu Ferringgi(F) & Botanic Gardens(Gp) during 13-14/II.'93.

TERRESTRIAL TARDIGRADES FROM HOKKAIDO.

M.Imai, Systematics and Evolution, Div. of Biol. Sci., Grad. Sch. of Sci., Hokkaido Univ., Sapporo.

A survey of terrestrial tardigrades was initiated by obtaining samples of mosses, lichens, and litter from a number of regions throughout Hokkaido. Tardigrades were isolated by Baermann extraction. Fourteen species representing seven genera were found.

Attempts were made to obtain eggs from isolated ovigerous females of species collected at the same locality. Females of four species laid eggs. The structural features of eggs are important taxonomic traits in many species, especially in the genus *Macrobiotus*. Utilization of ovulated eggs rather than examining eggs while in the ovary provides more reliable characters as such eggs are of known developmental age.

Echiniscus sp 1 collected at Kussharo (710 m altitude) resembles *E. laterosetosus* Ito, 1993. *Echiniscus*. sp 1 can be distinguished from the latter, however, by its possession of longer E1 appendages near E appendages. Also, minute twig-like articles occur on lateral filamentous appendages C and D or on C, D and E. This latter character is previously known from marine tardigrades, but its occurrence in terrestrial tardigrades is reported here for the first time.

AN UNDESCRIBED *ANISONYCHES* SP. (TARDIGRADA) WITH A LARGE BASAL SPUR ON THE EXTERNAL CLAW FROM RYUKYU ISLANDS.

H. Noda. Dep. Biol., Tokyo Women's Med. Col., Tokyo.

An undescribed *Anisonyches* (Echiniscoididae) was collected from Ishigaki-jima Island, Ryukyu Islands, Aug. 1993 and Nov. 1993. Outer basal spur of external claw in adult is extremely large, and is seen as a secondary hook. First instar has two claws of the same type as the external claw in adult in each leg. Eye pigment spots are present or absent and if present they are black in color in formalin preserved specimens. Median cirrus is always present. Presence of eyes and median cirrus sugests the present species is related to *A. mauritianus*. Claw structure in this genus resembles that of the *Carphania* rather than that of the *Milnesium*.

ZOEA OF A NEW DEEP-SEA PAGURID SPECIES WITH NOTES ON LARVAL MORPHOLOGY OF THE FAMILY PAGURIDAE (CRUSTACEA, DECAPODA, ANOMURA).

K. Konishi [1] and P.A. McLaughlin [2]. [1] Natl. Res. Inst. of Aquaculture, Mie, Japan, and [2] Shannon Point Mar. Center, Western Washington Univ., U.S.A.

Despite abundant fauna of hermit crabs of the family Paguridae in Japan, life histories of this group has been poorly documented: i.e., larvae of these hermit crabs have been described in only 20% of the species in this family. In this study, we obtained first zoeae by laboratory-hatching from a new deep-sea species of hermit crab. The present zoea is different from that of other *Pagurus* species in having two distal plumose setae on antennal endopod. In Japan, this morphological feature is only known in *Pagurus similis* (Ortmann, 1892). The zoea of the present species belongs to the Group B according to Roberts' (1970) classification for pagurid larvae. In Japanese species, most previously known larvae of this family are included in the Group A. The main larval character of *P. similis* and the present species seems to be a plesiomorphic character of antennal setation, in contrast to that of the remainder of Japanese *Pagurus* species. We also suggest, from the zoeae, that Group A contains most of the species that are distributing along the coast of the cold current in northern Indo-Pacific region.

KARYOTYPIC DIFFERENTIATION AND HYBRID ZONES OF *NELIMA NIGRICOXA* SATO AND SUZUKI (ARACHNIDA, OPILIONES) IN THE CHUGOKU DISTRICT, HONSHU, JAPAN.

N. Tsurusaki, N. Aoki, and M. Irie. Dept. of Biol., Fac. of Educ., Tottori Univ., Tottori.

We found that *Nelima nigricoxa* Sato and Suzuki is geographically differentiated in chromosome number in the Chugoku district, western Honshu, Japan. Four karyotypes recognized are allopatric or parapatric in distribution: 2n=16 (1st/7th & 8th/9th fusions of chromosomes in the karyotype with 2n=20: from the east of the Asahi River to Hyogo Pref.), 18a (8th/9th fusion: from the eastern half of Mt. Daisen to Mts. Hiruzen), 18b (1st/7th fusion: southern part of Okayama Pref.), and 20 (the rest of Chugoku district westward from the line connecting Mt. Daisen to the Asahi R.). They form two hybrid zones between two contiguous populations in the northern mountainous area extending from Mt. Daisen to the Hirusen Highland. Width of the hybrid zone between 2n=20 and 18a is 1-2 km in the south (western part of Hiruzen area), and ca. 500 m in the north (northern slope of Mt. Daisen); whereas that formed by 2n=18a and 16 is ca. 4 km wide. Frequency of individuals with 2n=19 in a hybridized population (2n=20/19/18a: Kawadoko on the northern slope of Mt. Daisen) was significantly lower than the expected value from Hardy-Weinberg's theorem ($p<0.02$). This indicates decrease of fitness in hybrids between 2n=20 and 18a and in turn it may partly account for the narrowness of the hybrid zone. Individuals with 2n=22, which are suspected to have arisen by the addition of two large iso-chromosomes, were also found in considerable frequencies among populations with 2n=20.

LARVAE OF TWO *CALAPPA* SPECIES WITH SPECIAL REFERENCE TO LARVAL CHARACTERS OF THE FAMILY CALAPPIDAE (CRUSTACEA: DECAPODA)

H. Taishaku [1] and K. Konishi [2]. [1] Toba Aquarium, Mie, Japan, and [2] Natl. Res. Inst. of Aquaculture, Mie, Japan

The knowledge of larvae of the family Calappidae is fragmentary, because of difficulty in rearing. Among 22 species of this family, only three species have been described its larvae. We described first zoeas of two calappid crabs, *Calappa japonica* Ortmann, 1892 and *Calappa gallus* (Herbst, 1803), based on laboratory-hatched materials. The main morphological characters of the present two *Calappa* zoeas are compared with those of previously described species within the family. The zoeas of the present two species are almost identical each other except for its size and the number of spinules on rostral spine. We can also hardly recognize remarkable morphological difference among *Calappa* zoeas within the subfamily, while the zoeas are conspicuously distinguished from each other among three subfamilies: i.e., Calappinae, Matutinae and Orithyinae. The zoeas of three calappid subfamilies are different in the morphology of carapace, abdominal somite, and the setation of maxillar and 1st maxillipedal endopods.

PHYLOGENETIC RELATIONSHIPS AND EVOLUTIONARY HISTORIES OF FOUR GENERA IN THE SUBFAMILY RHOMBOGNATHINAE (ACARI, HALACARIDAE).

H. Abé. Dept. of Mar. Sci. and Technol., Sch. of Engineer. Hokkaido Tokai Univ., Sapporo.

The phylogenetic relationships of four genera: *Rhombognathus, Isobactrus, Rhombognathides,* and *Metarhombognathus* in the subfamily Rhombognathinae were elucidated on the basis of the 46 morphological characters by using cladistic approach. The polarity of each transformation series was determined mainly by using the out-group comparison, and the branching pattern was reconstructed according to the principles of synapomorphy and parsimony.

Monophyly of Rhombognathinae was corroborated by the green body color, double row of minute apodemes on pharyngeal plate, the presence of carpite on tarsi, and para-laterodorsal protuberances on the rostrum. The most parsimonious cladogram implied that *Rhombognathus* was the earliest derivative genus, thereafter *Isobactrus, Rhombognathides* and *Metarhombognathus* were derived from their common ancestors successively.

In addition to the geological evidence, the area cladogram for five continents was reconstructed on the basis of the inferred phylogenetic relationships of four genera in Rhombognathinae by using the brooks parsimony method.

The basal polytomy of the area cladogram, and the cosmopolitan distribution of *Rhombognathus* and *Isobactrus* illustrated that these two genera were derived from their most recent common ancestor on the coastal zones of the supercontinent Pangaea before its broken-up in the late Palaeozoic era. The dichotomy of Eurasia and North America in the area cladogram, and the limited trans-Atlantic distribution of *Rhombognathides* and *Metarhombognathus* indicated that these two genera were derived from their most recent common ancestor occurred on the coast of Laurasia with the origination of the Atlantic Ocean and the separation of North America and Eurasia in Palaeocene or Eocene.

PHYLOGENY OF THE SUBTRIBE LIMONARIA (INSECTA: DIPTERA: TIPULIDAE: LIMONIINAE).

T. Torii. Dept. Nat. Hist., Fac. Sci., Tokyo Met. Univ., Hachioji.

The subtribe Limonaria contains about 2,300 species. Typical members have the following morphological features: antenna with 12 or 14 flagellomeres; wing vein Rs not long, concave in outline or oblique; only two branches of Rs reach the wing margin; vein M_{1+2} unbranched; mesothoracic merons strongly reduced; tibial spurs lacking. The intergeneric and intersubgeneric relationships within the subtribe have been scarcely discussed.

In this study, a phylogenetic relationship of the subtribe Limonaria is discussed on the basis of cladistic analysis of imaginal morphological characters of the Recent species. In total 50 imaginal characters are evaluated; the computer software PAUP 3.0s is partially applied to cladistic analysis.

As a result of the above analysis, the phylogeny of the Limonaria is obtained, and an annotated Linnaean classification (Wiley, 1981) is presented for the subtribe, i.e.:

1) The following five genera are formed into a monophyletic group with the phylogeny indicated by the formula: *Protohelius* (*Dicranoptycha* (*Limnorimarga* (*Helius, Orimarga*)));

2) *Limonia*, s. lat.—consisting of ten monophyletic subgroups—is a sister group of the group 1).

RELATIONSHIP OF THE SHAPE AND SURFACE STRUCTURE TO THE COLOR OF THE SCALE IN THE *PAPILIO* BUTTERFLIES.

T.INOUE. Depertment of Insect Physiology and Behavior,National Institute of Sericultural and Entomological Science, Tsukuba.

From the schanning electron microscope research, relationships were found among the shape, surface structure and color of the hind-wing scales in *Papilio* butterflies. These relationships were recoginized among the species of this Genus. The black scale seemed to have a most basic surface structure, whereas the scales colored by papiliochrome-pigments (yellow, red, green, etc.) were somewhat modified. Contrary to this result, the shape seemed to be most basic in Papiliochrome-colored scales. High ultraviolet-reflecting white scale was similar to these, but the modification was extreme in both shape and surface. In almost *Papilio* species, the blue-spangle scale was thought to be formed from the black scale, but in the species belonging to the subgen. *Achillides*, this scale was very different from that of any other species. The type of blue-spangle scales seem to be limited in the subgen. *Achillides* at present.

DISTRIBUTION AND CHARACTERISTICS OF INDONESIAN FOUR SPECIES SEA URCHINS, GENUS *ECHINOMETRA*.

Y. Arakaki, Faculty of International Studies, Dept. of Tourism, Meio Univ. Nago, Okinawa, Japan

Four types of the sea urchin *Echinometra mathaei* (Blainville) are seen on the coast of Okinawan islands and they are distinguishable by color patterns and other characteristcs. Recently, these four types have been treated as four different species. In this course of study, these species' distribution in Indonesia was researched and the characteristics (appearances, spicules in gonads and tubefeet, and the ratio of four pore pairs) of these species which live in different islands of Indonesia were compared with Okinawan species. As to the distribution, it was not necessarily occurred four species in every island which were investigated. As to the characteristics, the Indonesian species were not completely equal to the Okinawan species. Even within the Indonesian species, especially species D, the characteristics were not completely equal within each species which live in different islands. As far as species D, the population of Biak Island is very different from the other islands' population. The implication of these results is (1) these species are not high-dispersal marine organisms and (2) species D can be grouped into two subgroups, namely Pacific Ocean group and Indian Ocean group.

EFFECTS OF TEMPERATURE AND SALINITY ON FERTILIZATION AND EARLY CLEVAGE OF THE FOUR SIBLING SPECIES OF ECHINOMETRA (ECHINODERMATA:ECHINOIDEA) FOUND IN OKINAWA.

D.Sumilat and T.Uehara, Department of Biology, University of the Ryukyus, Nishihara, Okinawa 903-01, Japan

Recent studies of the four species of Echinometra have shown that they are in fact separate species (designated tentatively as A, B, C and D). These four species occur in different micro-habitats showing partial overlapping and exhibit distinctly different degree of reproductive synchrony. Little is known about the responce of the unfertilized eggs and cleaving embryos to various temperatures and salinities. The data indicate that cleavage is more sensitive to increased temperature(36 °C) and reduced salinity (25 ‰) than is fertilization. It was also shown that Fertilization rates of the species C and D at 25 ‰S and 36 °C are hihger than those of the species A and B. Unfertilized eggs were still viable, dividing when fertilized after 1 h exposure at 36 °C. However, significant effect were noted for exposure treatments of 2 h and above, showing that unfertilized eggs of species C and D are more tolerant to high temperature than those of species A and B. These results show that the physiological differences among the four species are reflection of their habitat and reproductive periods

MORPHOLOGY OF TUBE FEET OF ASTEROIDS AND ITS SYSTEMATIC SIGNIFICANCE.

M. Komatsu[1], M. Sugiyama[1] and C. Oguro[2].[1]Dept. of Biol., Fac. Sci., Toyama Univ., and [2]Toyama Univ., Toyama.

Sea stars generally have suckered tube feet, but species belonging to only Luidiidae and Astropectinidae have pointed tube feet which lack suckers at their tips. The presence or absence of suckered tube feet has been an important character in sea star taxonomy (Blake 1987). In the present study, external and internal morphology of tube feet in adults and juveniles of about 10 species was observed by SEM and light microscopy of 1 μm sections. This analysis demonstrated some species lack suckers although they had been believed to have suckered tube feet. No differences between suckered and pointed tube feet of juveniles exist in external morphology while they are difference in internal morphology. These results indicate necessity for a more detailed analysis of the structure of the asteroid tube foot.

ON THE NATURAL HYBRIDS BETWEEN SPECIES OF SEA URCHINS, TOXOPNEUSTES ELEGANS AND TOXOPNEUSTES PILEOLUS.

K.Fukuchi and T.Uehara, Department of Biology, University of the Ryukyus, Nishihara, Okinawa 903-01, Japan

Toxopneustes elegans and Toxopneustes pileolus co-occur and have the same spwaning season in winter in Okinawa. T. elegans, which can be identified by its medium size and the purplish-black stripe on its spine, was recorded for the first time in Okinawa in 1992. The external appearance is uniform in T. elegans, but varies considerably in T. pileolus. In same locality, a few individuals (natural hybrid ?) were found with purplish-black stripe (characteristic of T. elegans) and a large test (characteristic of T. pileolus).

Crossing experiments resulted in a high fertilization rate when eggs of T. pileolus were inseminated with a low concent ration of sperm from T. elegans, but a low fertilization rate in reverse cross. This shows that cross-fertilization in the field should be possible only between eggs of T. pileolus and sperm of T. elegans. On the basis of comparative morphologies between individuals produced experimentally and found in nature, both individuals appeared same color on its spine and the central part of grobiferous pedicellaria. Thus, intermediate individuals collected from field should be hybrids between T. elegans and T. pileolus. These findings will be a great help in attacking the problem of "speciation" for sea urchins.

MOLECULAR PHYLOGENY OF ASTEROIDEA WITH SPECIAL REFERENCE TO THE EVOLUTION OF THE LARVAL FORMS.

H.Wada[1], M.Komatsu[2], N.Satoh[1]. [1]Dept. of Zool., Fac. of Sci., Kyoto Univ., Kyoto. [2]Dept. of Biol., Fac. of Sci., Toyama Univ.,Toyama.

In Asteroidea, there are four types of embryonic development. In the indirect type of development, two distinct stages of larval form can be seen; bipinnaria and brachiolaria. However, the direct type and the nonbrachiolarian type pass through only one stage; bipinnaria for the nonbrachiolarian type, and brachiolaria for the direct type. Another type is the barrel-shaped larva which has neither a digestive system nor brachiolar arms. It is almost accepted that the direct type and barrel-shaped larva are evolved secondarily from the indirect and the nonbrachiolarian type, respectively, accompanied by the evolution from planktotrophy to lecithotrophy. However it yet remains to be determined which is the primitive type of development in Asteroidea, the indirect or the nonbrachiolarian type. In this study, we reexamined the phylogenetic relationships among Asteroidea from a standpoint of molecular phylogeny based on the nucleotide sequences of mitochondrial rDNAs. The molecular phylogenetic trees obtained prefer the idea that the nonbrachiolarian type is the primitive form in Asteroidea.

GENETIC VARIABILITY OF MITOCHODRIAL DNA *Halocynthia rotetzi.*

F. Takizawa, T. Kakuda & A. Hino
Dept. of Biological Sciences, Fuc. of Sci. Kanagawa Univ. Hiratuka.

Halocynthia roretzi distributes all around Honsyu island and also Hokkaido. To analyze the relationship between geographic isolation and genetic variability the restriction fragment polymorphism of mitochondrial DNA of *H.r.* was studied. The analysis of mtDNA restriction fragments by enzymes was done as the previous report and also the southern blotting was also tried in this study. We have been analyzed over 150 individuals which classified into tree types according to the difference of breeding seasons, and we found out 9 genotypes in 7 populations. 11.1% of total individual showed polymorphism of mtDNA restriction profile. Then we compared our data with the sequence analysis of *H.r.* mtDNA (Yokobori, personal communication). These restriction sites of polymorphism were evenly distributed in about 16kbps of mtDNA. And we conformed the restriction maps of 10 enzymes which we analyzed for this study.

PHYLOGENETIC RELATIONSHIPS OF THE GENERA *ORYZIAS* AND *XENOPOECILUS*.

K. Naruse[1], A. Shima[1], M. Matsuda[2], M. Sakaizumi[2], T. Iwamatsu[3], B. Soeroto[4] and H. Uwa[5]
[1]Zool. Inst., School of Sci., Univ. of Tokyo, Tokyo, [2]Dep. of Biol.,Coll. of General Edu., Niigata Univ., Niigata, [3]Dept. of Biol., Aichi Univ. of Edu., Kariya, [4]Dept. of Fisheries. Sam Ratulangi Univ., Manado, Indonesia. [5]Dept. of Biol., Fac. of Sci., Shinshu Univ., Matsumoto

Phylogenetic relationships of 12 species of the genus *Oryzias* and one species of the genus *Xenopoecilus* were analyzed using the mitochondria 12s ribosomal gene. The result of the maximum persimony analysis suggests that 3 groups (the monoarmed, the biarmed and the fused chromosome groups) which were classified by karyotype analysis by Uwa, were monophyletic. But *O. minutillus* which was categorized as the monoarmed group, did not belong to any groups.

Fish of the genus *Oryzias* which was collected from Tammanroya river system in Sulawesi was closely related to *O. javanicus*. This result suggests that two phylogenetically different species were distributed in Sulawesi. Karyological and morphological analyses are needed to determine the classification of this species.

Genetic distance between *Oryzias* and *X. oophorus* was smaller than those within the genus *Oryzias*. There are two explanations for this result. One is acceleration of morphological change of *X. oophorus*. Another is introgression of mitochondria DNA of the genus *Oryzias* to the genus *Xenopoecilus*. It is necessary to investigate the phylogenetic relationships using the nuclear genome to clarify this hypothesis.

PHYLOGENETIC STUDY OF *CHAENOGOBIUS* SP. (GOBIIDAE) BY ISOZYME POLYMORPHISMS.

K. Itogawa[1], T. Shinozaki[1], M. Hayashi[2], A. Iwata[3] and M. Hatsumi[1].
[1] Dept. Biol. Shimane Univ. Matsue, [2] Yokosuka City Museum, Yokosuka, [3] Lab. Biol. Imperial Household, Tokyo.

Chaenogobius sp. (Japanese tentative name; Shinjikohaze) is discriminated from its relatives, *C. castaneus* or *C. laevis*, by two pairs of pit organs on its head. Previous study showed *C.* sp. from Lake Shinji is closely related to *C. laevis* from Lake Hachirou-gata and Nei's genetic distance between them was 0.114. Recently the distribution of *C.* sp. was reported in several places near the Sea of Japan, that makes us to analyze isozyme polymorphisms of four populations of *C.* sp. and *C. laevis* to clarify the phylogenetic position of *C.* sp. Genetic distances were calculated by allelic frequencies of nineteen loci estimated from electromorphs of thirteen enzymes and a phylogenetic tree was constructed from genetic distances. Four populations of *C.* sp. formed one branch in the tree, suggesting *C.* sp. is not only different in its morph but also different species from *C. laevis*.

MATING CALLS OF AUTO- AND ALLOPOLYPLOID MALES IN POND FROG SPECIES DISTRIBUTED IN THE FAR EAST.

H. Ueda. Lab. for Amphibian Biol., Fac. of Sci., Hiroshima Univ., Higashihiroshima.

Mating calls of artificial auto- and allopolyploid males were recorded at 24 ± 1℃ in the laboratory and their structure was sonagraphically analyzed.

In the mating calls of autotriploid and autotetraploid males as well as diploid males of *Rana nigromaculata*, call duration, note duration and pulse rate tended to decrease with increasing ploidy, though the latter two parameters varied with a wide range which overlapped to a large extent with those of other ploidies.

Mating calls of three kinds of amphidiploid males consisting of two *R. nigromaculata* genomes and two *R. b. brevipoda* genomes, two *R. b. brevipoda* genomes and two *R. plancyi chosenica* genomes, and two *R. b. brevipoda* genomes and two *R. plancyi fukienensis* genomes showed intermediate parameters between those of the two original diploid species, though the influence of tetraploidy on some parameters was observed.

Reciprocal triploid hybrid males between *R. nigromaculata* and *R. b. brevipoda*, and those between *R. b. brevipoda* and *R. plancyi chosenica* had intermediate calls between the species offering two genomes and the respective diploid hybrids.

MITOCHONDRIAL DNA SEQUENCE VARIATION AMONG JAPANESE WILD POPULATIONS OF THE MEDAKA, *ORIZYAS LATIPES*

M. Matsuda[1], H. Yonekawa[2] and M. Sakaizumi[3]. [1]Grad. Sch. of Sci. & Tech., Niigata Univ., Niigata, [2]The Tokyo Metropol. Inst. Med. Sci., Tokyo and [3]Dept. of Environ. Sci., Fac. of Sci., Niigata Univ., Niigata

By allozymic analysis, Japanese wild populations of the medaka (*Oryzias latipes*) were divided into two major populations, the Northern population and the Southern population (Sakaizumi et al. 1983). Restriction-fragment length polymorphism (RFLP) analysis using eight enzymes of mitochondrial DNA revealed 97 haplotypes, which could be divided into 23 haplotype groups.

In order to clarify the relationship among RFLP haplotype groups, we amplified the cytochrome b genes of 20 representative haplotypes (18 from Japan, one Korea and one China) by the PCR and directly sequenced. We compared the sequences of 500 bp segment, and constructed a phylogenetic tree. *O. mekongensis* was used as an outgroup. The tree generated by neighbour-joining method as implemented by PHYLIP. No additions or deletions were detected, hence the alignment was unambiguous. The Kimura's two-parameter method for genetic distance was used with a transition:transversion ratio of 2.0.

Each RFLP haplotype analyzed gave different sequence haplotype (genotype). Eighteen genotypes derived from Japan were monophyletic and were splited into two major clusters. The first cluster included three genotypes from the Northern population and their pairwise sequence divergence values ranged from 0.4% to 1.6%. The second included 15 genotypes from the Southern population. The sequence divergence values among them were 0.1%-5.4%. The monophyly of southern and northern cluster was strongly supported by bootstrap replications (100%). The sequence divergences between northern and southern genotypes ranged from 9.8% to 13.0%. This grouping agreed well with the result of allozymic analysis.

GENETIC DIFFERENTIATION IN THE MOUNTAIN BROWN FROG RANA ORNATIVENTRIS.

M. Sumida and M. Nishioka. Lab. for Amphibian Biol., Fac. of Sci., Hiroshima Univ., Higashihiroshima.

This study was carried out to investigate the degree of geographic differentiation in the mountain brown frog Rana ornativentris which is distributed in mountain regions of Honshu, Shikoku and Kyushu in Japan. Fifteen enzymes and two blood proteins were analyzed using starch gel electrophoresis in 136 individuals of 16 populations of R. ornativentris collected from a wide range of Honshu. These enzymes and blood proteins were encoded by 24 presumptive loci, each of which had 4.3 phenotypes produced by 2.7 alleles on the average. A relatively high level of genetic differentiation was demonstrated between the western and eastern populations at seven loci, IDH-B, MPI, Pep-A, SOD-A, SOD-B, Ab and Hb-II, being 0.313-0.876, 0.568 on the average, in Fst. Nei's genetic distances among 16 populations ranged from 0.011-0.313, 0.127 on the average, whereas those between the western four and eastern 12 populations were 0.128-0.313, 0.225 on the average. The UPGMA dendrogram constructed from Nei's genetic distances shows that R. ornativentris was first divided into the western and eastern groups and then the latter branched out into the southern, central and northern subgroups.

ESTIMATION OF PHYLOGENETIC RELATIONSHIPS AMONG JAPANESE BROWN FROGS FROM DNA SEQUENCES.

T. Tanaka[1], M. Matsui[1] and O. Takenaka[2]. [1]Grad. Sch. Hum. Env. Stud., Kyoto Univ., Kyoto and [2]Primate Res. Inst., Kyoto Univ., Inuyama.

We determined the nucleotide sequence of cytochrome b gene in mtDNA among 6 species of Japanese brown frogs (*Rana pirica*, *R. ornativentris*, *R. japonica*, *R. tagoi tagoi*, *R. sakuraii*, *R. okinavana*) using PCR-direct sequencing method, and attempted to elucidate phylogenetic relationships among them by UPGMA method and neighbor-joining method. 1)The sequences only slightly varied within one deme of *R. ornativentris*, *R. japonica* and *R. tagoi tagoi*, 2)The pattern of variation among demes in *R. tagoi tagoi* was very complex, and a simple geographic cline was not observed. *R. ornativentris* could be roughly divided into northeastern (Aomori and Toyama) and southwestern (Hyogo, Kochi and Oita) groups. 3) *R. okinavana*, having 2n=26 chromosomes, phylogenetically more closely related to *R. tagoi tagoi*, *R. sakuraii* and *R. japonica* with same number of chromosomes than to *R. pirica* and *R. ornativentris* with 2n=24 chromosomes. This result conformed to the idea proposed chiefly on the bases of morphological and ecological evidences.

PHYLOGENETIC POSITION OF DIPLOBLASTS INFERRED FROM AMINO ACID SEQUENCES OF ELONGATION FACTOR 1-α.

M.Kobayashi, H.Wada and N.Satoh. Dept. of Zool., Fac. of Sci., Kyoto Univ., Kyoto.

Recent studies of molecular phylogeny including our own analysis, based upon almost the complete sequences of small subunit ribosomal DNA, support the monophyly of the metazoa. However, it's still uncertain from those investigations whether the diploblasts (porifera, ctenophora and cnidaria) form a monophyletic unit which is a sister group of triploblasts, or those are paraphyletic. In order to reexamine this issue, we determined almost the complete sequences of elongation factor 1-α for diploblasts using RT-PCR and the direct-sequencing method. We discuss the phylogenetic position and evolutionary relationships of diploblasts based on results of the present and preceding molecular phylogenetic studies.

INTRA- AND INTER-SPECIES PHYLOGENETIC DIVERGENCE IN THE JAPANESE DORMOUSE, *Glirurus japonicus*.

H. Suzuki[1], S. Sakurai[1], S. Minato[2], K. Tsuchiya[3].
[1]Div. of Molecular Genet., Jikei Univ. Sch. Med., Tokyo,
[2]Kumanogawa Element. Sch., Kumanogawa-cho, [3]Miyazaki Med. College, Miyazaki.

The Japanese dormouse,*Glirurus japonicus*, has been classified as a single species. However, in the case of individuals collected from Wakayama prefecture, the nuclear ribosomal DNA (rDNA) spacer yielded restriction fragment patterns that were distinct from those collected from the Kanto district (Yamanashi and Nagano). The estimated sequence divergence (SD) was 2.2%, corresponding to divergence of these populations 1-2 million years ago. Mitochondrial DNA (mtDNA) sequences, namely, 402 bp of the gene for cytochrome b, were examined by a direct sequencing method. The value of the SD between the two populations was estimated to be 7% on average. We examined two continental species of dormice, the European dormouse and the common dormouse, and found that, on average, the SDs between the continental species and the Japanese species for the rDNA and mtDNA were 15% and 22%, respectively.

PHYLOGENETIC POSITION OF THE CATENULID FLATWORM (PLATHYHELMINTHES, CATENULIDA) INFERRED FROM THE 18S RIBOSOMAL DNA SEQUENCE

Tomoe Katayama and Masamichi Yamamoto
Ushimado Marine Laboratory, Okayama University

Catenulid flatworms are regarded as the most primitive turbellarians by some authors (Ehlers, 1985; Ax,1989). They have a simple pharynx and a sac-like gut, and their messenchyme are sometimes reduced to a fluid matrix. We determined nucleotide sequences of 18S rDNA in a catenulid, Stenostomum sp.and inferred its phylogenetic position based upon comparisons of the sequence with those of various metazoans. We constructed phylogenetic trees together with various metazoans by the neighbor-joining method. In these trees, Stenostomum always occupied a position in the triploblastic category. In the phylogenetic tree including some diploblastic animals, a dicyemid mesozoan, an acoel flatworm and some other higher triploblastic animals, Stenostomum was the sister taxon to all other triploblastic animals included + the dicyemid mesozoan. These results seem to support the idea that the catenulid flatworm is the earliest diverged turbellarian in the triploblastic lineage.

MOLECULAR PHYLOGENY OF THE FAMILY MUSTELIDAE, INFERRED FROM MITOCHONDRIAL CYTOCHROME B NUCLEOTIDE SEQUENCES

R. Masuda[1,2] and M.C. Yoshida[1,2]
([1]Chromosome Res. Unit, Fac. of Sci., and [2]Grad. Sch. of Environ. Earth Sci., Hokkaido Univ., Sapporo)

To study the phylogenetic relationships between the Japanese species of the family Mustelidae, by using the improved PCR product-direct sequencing method, the mitochondrial cytochrome b nucleotide sequences (375 bases) were determined on ten species from five genera. The molecular phylogenetic tree indicated a clear separation of the five genera: Mustela, Martes, Meles, Lutra, and Enhydra. Although, in the previous classification, Mustela itatsi and M. sibirica were included in one species or different subspecies, the present results suggested that it is reasonable for the two animals to be divided into distinct species. M. vison was distantly related to the other Mustela species. The molecular phylogeny of the Mustelidae were discussed in detail, as compared with the previous morphological and karyological taxonomy.

EVOLUTIONARY DIVERGENCE IN GENOMIC STRUCTURES OF GASTROPODAN MITOCHONDRIAL DNA

R. Ueshima and N. Nishizaki. Inst. of Biol. Sci., Univ. of Tsukuba, Tsukuba

Genomic strucutures of mitochondrial DNAs are relatively conserved among eucoelomate metazoan phyla. In contrast, recently published data on blue mussel and stylommatophoran land snail mtDNAs showed unusual genomic structures that are highly divergent from those of other metazoan phyla. In order to understand the diversity and molecular evolution of molluscan mtDNAs, we have determined the complete nucleotide sequence of a Japanese abalone, *Nordotis gigantea*, mtDNA. mtDNAs of the abalone and pulmonate land snails were highly divergent in (1) total genome size, (2) structures of mitochondrial tRNAs, (3) gene order on the genomes, and (4) amino acid sequences of the proteins encoded by the genome. Such a high level of divergence has not been found in any other phyla and suggests that mtDNA structures evolved much faster in mollusca, especially in gastropoda, than in other phyla. Changes in mtDNA structures would be an useful marker for reconstructing the gastropodan phylogeny.

PHYLOGENETIC POSITION OF VESTIMENTIFERA REVEALED BY MOLECULAR INFORMATION.

S. Kojima[1], R. Segawa[2], T. Hashimoto[3] and S. Ohta[1]. [1]Ocean Res. Inst., Univ. Tokyo, [2]Dept. Biol., Tokyo Metropolitan Univ., [3]Inst. Statistical Mathematics.

Vestimentifera, a novel gutless animal, is one of the most dominant members of unique communities in the deep-sea reducing environments. On the basis of amino acid sequence of extracellular hemoglobins and the early development, Vestimentifera is thought to be closely related to Annelida. The maximum likelihood analysis of amono acid sequence of elongation factor-1alpha suggested the probability that Vesimentifera is one group of Polychaete. In order to assess the validity of this hypothesis, we sequenced a part of the COI region of mitochondrial DNA from two species of vestimentiferans and some polychaetes, and analyzed the phylogenetic relationship among them.

ROOTS OF INTRACELLULAR SYMBIONT OF APHID

H. Harada, T. Fukatsu and H. Ishikawa
Zoological Institute, Graduate School of Science, University of Tokyo, Hongo, Bunkyo-ku, Tokyo 113, Japan

Judging from the location of the intracellular symbionts in insects, it is generally believed that they originated from gut microbes, which are descendants of free-living bacteria taken in together with diet by the insects in the evolutionary past.

Pea aphid, *Acyrthosiphon pisum* harbors prokaryotic intracellular symbionts and at least, two species of gut microbes. It has been shown that the aphid symbiont is more closely related to *Escherichia coli* than to any other free-living bacterium. Analysis of RFLP of their 16S rDNA and *groE* homologues suggested that one of the gut microbes is a close relative of *E. coli*.

To understand better the evolutionary relationships of these bacteria, we sequenced almost the entire regions of 16S rDNA and *groE* homologue of this gut microbe using PCR direct sequencing method, and carried out molecular phylogenetic analysis. It turned out that this microbe is the closest relative of E. coli based on 16S rDNA, and its GroE homologue has the highest known identity to that of aphid intracellular symbionts.

THE PHYLOGENETIC RELATIONSHIPS AMONG PLATYHELMINTHES, MOLLUSCA, ARTHROPODA, ECHINODERMATA, AND VERTEBRATES INFERRED FROM MULTIPLE PROTEIN DATA

Nikoh, N[1]., Iwabe, N.[1], Kuma, K.[1], Ueshima R.[2], Miyata, T.[1] [1]Dept. of Biophys., Faculty of Sci., Kyoto Univ., Kyoto and [2]Inst. of Biol. Sci., Univ. of Tsukuba, Ibaraki.

The phylogenetic relationships among major groups of animal are still controversial issue both on molphological and molecular level; In spite of many morphological and embryological studies, these relationships still remain poorly understood. Also in molecular approach, the proposed phylogenetic relationships differ for different authors, depending on molecules and methods. These results suggest close divergence times between ancestors leading to the animal phyla. To infer a reliable phylogenetic relationship among Platyhelminthes, Mollusca, Arthropoda, Echinodermata, and Vertebrates, we have carried out a molecular phylogenetic analysis using 2 sets of multiple protein data based on maximum likelihood method. 1) From an analysis of 15 protein data, Mollusca is more closely related to Arthropoda than Vertebrates, and Echinodermata is more closely related to Vertebrates than Arthropoda. 2) From an analysis of other 15 protein data, Platyhelminthes has branched off first among Platyhelminthes, Arthropoda, and Vertebrates. These results are consistent with the phylogeny of Margulis and Schwartz (Five kingdoms 1988).

MOLECULAR PHYLOGENETIC ANALYSES OF EVOLUTION OF ENDOSYMBIOTIC MICROORGANISMS IN CERATAPHIDINI APHIDS

Fukatsu T. and Ishikawa H.
Zool. Inst., Fac. Sci., Univ. of Tokyo, Tokyo.

The tribe Cerataphidini is a relatively small aphid group found in south-eastern Asia. More than 60 species of 10 genera have been described. Although almost all aphids harbor prokaryotic intracellular symbionts in the mycetocytes, huge cells in the abdomen specialized for this purpose, we discovered that some Cerataphidini species do not have them but possess yeast-like extracellular symbionts in the hemocoel. This finding suggested that in a lineage of Cerataphidini a yeast-like microbe had displaced the original intracellular symbiont.

In order to understand the process of the replacement of symbiont and to know the origin of the yeast-like symbiont, we performed molecular phylogenetic analyses of Cerataphidini aphids and their endosymbionts. Gene fragments of mitochondrial cytochrome oxidase I and II (aphids), SymSL (intracellular symbionts) and 18SrRNA (yeast-like symbionts) were amplified by PCR and directly sequenced. Analysis of 18SrRNA genes showed that yeast-like symbionts of Cerataphidini belong to Ascomycota, Pyrenomycetes. Molecular phylogeny of cytochrome oxidase genes confirmed that the tribe Cerataphidini is constituted by two major monophyletic groups, one with multiple cavity galls and the other with yeast-like symbionts. Cytochrome oxidase phylogeny and SymSL phylogeny showed highly identical tree topology, suggesting that the intracellular symbionts of Cerataphidini are of a single origin, and no horizontal transfer and replacement by foreign bacteria of the symbionts have occurred.

A SPICULE MATRIX PROTEIN GENE OF THE CRINOIDEA *METACRINUS ROTUNDUS*

*K.Kajihara[1], S.Amemiya[2], H.Fujisawa[1] and T.Higashinakagawa[3]
[1]Department of Biology, Fac. of Education, Saitama University, Saitama, [2]Misaki Marine Biological Station, Fac. of Sci., Tokyo University, Kanagawa, [3]Mitsubishi Kasei Institute of Life Sciences ,Tokyo.

Within the phylum Echinodermata, the class Crinoidea, commonly known as the sea lilies, flourished about 500 million years ago. Although it is only one of living subphylum Pelmatozoa, it appears to be the most primitive group in Echinodermata. For analyzing phylogenetic relationship in Echinodermash, it is very important to compare Crinoidea with other classes in the phylum. In the present study we isolated genomic DNA from the sperm of the Crinoidea, *Metacrinus rotundus*, and tried to identify a gene encoding its spicule matrix protein. Southern hybridization was performed using a biotin-labeled cDNA clone representing the spicule matrix protein pHS72 from the sea urchin, *Strongylocentrotus purpuratus*, as a probe. In the first experiment, hybridization was performed under conditions of high stringency (68°C). Hybridization signals were observed at positions expected for *S. purpuratus* and *Hemicentrotus pulcherrimus* DNA, respectively. In a second experiment, hybridization was done at intermediate stringency (60°C). In this case, bands were detected in *Lytechinus pictus* DNA. Finally, when hybridization was done at low stringency (55°C), the discrete bands were observed also in the lane of *M. rotundus* DNA, suggesting the existence of spicule matrix protein gene homologues in this organism. Base upon these observations, a *M. rotundus* genomic library was constructed for the purpose isolating these homologues.

PURIFICARION AND CHARACTERIZATION OF SOLUBLE VITELLIN BINDING PROTEIN FROM OVARY OF *LOCUSTA MIGRATORIA*.

N.Shinya and K.Yamasaki.
Dept. Biol. Tokyo Metropol. Univ. Tokyo.

Soluble vitellin binding protein(s-VBP) that formed complex with vitellin and is supposed to be responsible for highly condensation of the protein in yolk. F_B,the active protion of s-VBP was prepared by purification including proteolysis. The preparation,F_B was suggested to be lipid contaning substance because of the behavier for organic solvent systems and chemical analysis. The insoluble portion of F_B released by methanolysis that held 30 % of the preparation was shown to contain mainly C23 to C33 strait saturated chain hydrocarbones by GC-MS analysis. So,s-VBP was highly suppoused to be hydrocarbon bearing molecule.

In order to ascertain the hypothesis, s-VBP was purified by ultra centrifugation on sucrose density gradient and the hydrocarbon contents in s-VBP was determined in relation to the binding activity during the process. VBP acitivity was found in very high density fractions. And the hydrocarbon contents in the fractions were highly corelated with the activities.

ESCHERICHIA COLI INJECTION RESULTS IN SELECTIVE INDUCTION OF NOVEL GENES IN *RIPTORTUS CLAVATUS*

K. Miura[1], S. Ueno[1]1, K. Katsumi[2] and Y. Chinzei[1].
[1]Dept. Med. Zool., Mie Univ., Tus and [2]Dept. Biol., Osaka City Univ., Osaka.

E. coli injection into *Riptortus clavatus* induced rapidly bactericidal activity in the hemolymph. This activity reached its maximum at 9 h after the injection and thereafter declined slowly. This indicates the *E. coli* injection can elicit an acute phase response in this species. By differential screening, two sort of acute phase related cDNA clones designated as λdiff2 and λdiff16 were isolated. Northern blot analyses revealed rapid (within 1 h) induction of mRNAs corresponding to these clones after the injection. λdiff16 encoded for 151 amino acid residues, which showed, in some regions, similarity to *cecropia* attacin E. λdiff2 had 2242 bps encoding an open reading frame of 678 amino acids, which consisted of fourteen tandem repeats. Each repeat was rich in charged residues and had a proline-rich region which had similarities to bactericidal peptides from other insects. An proline-rich motif, RPTPPRP, was fond to be very similar to binding motif for SH-3 domain of phosphatidylinositol 3-kinase.

PURIFICATION AND CHARACTERIZATION OF A STORAGE PROTEIN OF THE SWEET POTATO HORNWORM, *AGRIUS CONVOLVULI*.

M.Shimoda, H.Saito, M.Nakamura and M.Kiuchi.
National Institute of Sericultural and Entomological Science, Tsukuba.

A storage protein of the sweet potato hornworm, *Agrius convolvuli*, was purified from larval hemolymph using hydrophobic interaction chromatography and ion exchange chromatography. It was a heterohexamer with subunits of Mr approximately 76,000 and 73,000. The N-terminal amino acid sequences showed homology to the arylphorin-type storage proteins of *Bombyx mori* and *Manduca sexta*.

PROPERTIES OF PHENOLOXIDASE FROM SILKWORM EGGS AND ITS ACTIVATION AT THE DIAPAUSE INITIATION.

A. Horii, N. Kakumu and T. Ohoka, Department of Biol., Fac. of Sci., Tokyo Metropol. Univ., Tokyo)

It is well known that in Diapause egg of silkwom, *Bombyx mori*, accunulated 3-hydroxykynurenine is turned to xanthommatine, and deposit on to serosal membrane of the egg. Although it was established that the pigment formation and the diapause initiation have no direct relation, these two phenomena occurs at the same developmental period.
The enzyme responsible for the oxidation of 3-hydroxykynurenine was investigated and no other enzyme was found than phenoloxidase. The enzymatic properties, substrate and inhibitor specificities and enzyme localization were investigated by an oxygen consumption method and also by Dopa-chrome absorption method, and it was revealed that silkworm egg phenoloxidase is one of laccase type enzyme. The activity significantly increases from 0-day to 1-day, suggesting some activation mechanisms are working at the diapause initiation.

MOLECULAR CLONING AND SEQUENCE ANALYSIS OF STORAGE HEXMAER OF *HALYOMORPHA MISTA*

K. Kamiya[1], K. Miura[2], Y. Chinzei[2] and H. Numata[1].
[1]Dept. Biol., Osaka City Univ., Osaka and Dept. Med. Zool., Mie Univ., Tsu.

Purification, molecular cloning and sequence analysis of the storage protein from the hemipteran insect, *Halyomorpha mista* (HmSP) were done. HmSP, which is a major component of the hemolymph of this species through the nymphal and adult stages were purified to homogeneity by using gel filteration and anion exchange chromatography. Chemical cross-linking analysis revealed that the HmSP had a hexamric structure constructed by the assembly of identical 76 kD subunits. The λgt11 cDNA library constructed from the polyA(+) RNA of the nymphal fat body were screened with a specific antiserum, and several clones encoding HmSP isolated. The clone bearing the longest cDNA insert of 2154 pbs and an open reading frame of 686 amino acid residues were deduced. The predicted amino acid composition was relatively high in aromatic amino acids. Sequence analysis of the entire insert eslablished the homologies to other insect storage proteins so far sequenced.

ACTIVATION OF LACCASE-TYPE PROPHENOLOXIDASE IN THE CUTICLE OF INSECT. XI. PROPERTIES OF PROLACCASE IN OOCYTE CUTICLE OF SILKWORM, *BOMBYX MORI*.

H.I.Yamazaki.,Biol.,Lab.,Atomi Gakuen Women's Univ.,Saitama.

Laccase-type phenoloxidase is found in cuticular matrix and supposed that the enzyme mediates the hardening and darkening process. The hardening and darkening process of cuticle has been studied on larval-larval, larval-pupal, and pupal-adult ecdysis. In all cases described above, the laccase itself is involved in the newly tanned cuticular matrix. The inactive prolaccse is found in newly formed larval, pupal, and adult cuticle bound tightly with it. And active portion of the laccase can be released by proteolytic digestion and analyzed biochemically.

The involvement of laccase has also been suggested in the tanning process during embryonic development. The cuticle of egg shell is formed at the period of egg maturation in ovary in *Bombyx mori*, so, the oocytes were collected from ovaries and analyzed by the methods described previously. The molecules of prolaccase were detected by electrophoresis and the mass of each proenzyme was 55 and 57 KDa, respectively. The two forms of embryonic prolaccase were recognized by antiserum raised from pupal laccase.

PURIFICATION OF THE PRECURSOR FORM OF PRO-PHENOLOXIDASE ACTIVATING ENZYME FROM CUTICLE OF THE SILKWORM , *Bombyx mori*.

D. Sato, M. Ochiai and M. Ashida.
Biochem. Lab., Inst. of Low Temp. Sci., Hokkaido Univ. Sapporo.

The precursor form of prophenoloxidase activating enzyme (proPPAE) and proPPAE activating factor (proPPAE-AF) were extracted from larval cuticle of silkworm, *Bombyx mori*, by using an acidic extraction medium containing EDTA and *p*-amidinophenylmethyl-sulfonylfluoride. ProPPAE in the cuticle was purified by column chromatography on CM-Toyopearl, phenyl-Toyopearl, TSK-gel CM-5PW, and hydroxylapatite. ProPPAE was detected by both proPPAE-AF and anti-PPAE antibody during the purification. The final preparation of proPPAE was judged to be homogeneous by SDS-PAGE. The molecular weight was estimated to be 45,000 by SDS-PAGE under the reducing conditions. Some other properties of the purified proPPAE were also reported.

SYMBIONIN IS A NOVEL TYPE OF HISTIDINE PROTEIN KINASE.

M. Morioka[1], K. Yamamoto[2] and H. Ishikawa[1]. [1]Zool. Inst., Grad. School of Sci., [2]Fac. of Pharm. Sci., Univ. of Tokyo, Tokyo.

Symbionin, a GroEL homologous molecular chaperone produced by an intracellular symbiont of the pea aphid, is autocatalytically phosphorylated *in vitro* to produce the protein with a high-energy phosphate bond. A part of the free energy in the phosphorylated symbionin is available for the production of ATP from ADP. These characteristics of symbionin are reminiscent of the bacterial histidine protein kinase (HPK), or a sensor molecule, of the two-component pathway.

In an effort to identify symbionin as a HPK, we determined the phosphorylation site of symbionin and searched for possible response regulator, an partner protein of the two-component pathway. As a result, peptide sequence analysis and TLC analysis of ^{32}P-labeled tryptic fragment of symbionin demonstrated that the site of phosphorylation of symbionin is His-133. Also, when symbiotic proteins were electrophoretically separated, blotted onto a PVDF-membrane and incubated with ^{32}P-labeled symbionin, radioactivity was found on several kinds of polypeptides, indicating that the phosphoryl-group transfer from symbionin to other symbiotic proteins, which correspond to response molecules, took place. These results suggested that symbionin has a possible role in the signal transduction, as a HPK, in the endosymbiont. However, symbionin is not similar in amino acid sequence to any other of the HPK's so far known.

PRIMARY STRUCTURE OF THE PEPTIDES RELEASED FROM PROPHENOLOXIDASE DURING THE ACTIVATION BY ACTIVATING ENZYME

Y.Yasuhara[1], M.Ochiai[1], T.Kawabata[2] and M.Ashida[1].
[1]The Institute of Low Temperature Science , Hokkaido University, Sapporo and [2] Wako Pure Chemicals inc., Osaka.

The prophenoloxidase (proPO) of the silkworm, Bombyx mori is proposed to be a hetero dimer and peptides containing N-termini of the proPO subunits have been shown to be released during the activation by proPO activating enzyme. In the present study, we investigated the primary structure of these peptides by the techniques of cDNA sequencing, amino acid sequencing and matrix-assisted laser-desorption ionaization (MALDI) mass spectroscopy. The results indicated that the structures of the released peptides are as follows:

Peptide-I :
Ac-SDAKNNLLLFFDRPSEPCFMQKGEENAVFEIPDNYYPEKYQRV SNAIGNR-OH

Peptide-II :
Ac-ADVFESLELLFDRPNEPLITPKGENNSVFQLTEQFLTEDYANN GIELNNR-OH

AUTOPHOSPHORYLATION ACTIVITY OF GROEL *IN VITRO*.

K. Sadakane[1], M. Morioka[1], K. Yamamoto[2], H. Ishikawa[1]. [1]Zool. Inst., Grad. Sch. of Sci., [2]Fac. of Pharm. Sci., Univ. of Tokyo, Tokyo.

GroEL protein, a major heat shock protein of *Eschelichia coli*, is structurally homologous to symbionin. The two proteins share functionally common activities; ATPase and chaperonin activity. Symbionin has been reported to have the autokinase activity[*1] and phosphotransferase activity[*2]. We examined the properties of GroEL using the same procedure used for symbionin. As a result, GroEL, like symbionin , was autocatalytically phosphorylated in the presence of Zn-ATP *in vitro* in response to the temperature shift-up. However, no phosphotransferase activity was observed. Peptide sequence analysis of ^{32}P-labeled GroEL fragment showed that the phosphorylation site of GroEL was different from that of symbionin.

[*1] M. Morioka & H. Ishikawa J. Biochem. *111*, 431-435 (1992)
[*2] M. Morioka et al. J. Biochem. *114*, 246-250 (1993)

FRACTIONATION OF THE COMPONENTS OF THE PROPHENOLOXIDASE CASCADE IN PLASMA OF THE SILKWORM, *Bombyx mori*.

M. Ochiai and M. Ashida
Biochem. Lab., Inst. of Low temp. Sci., Hokkaido Univ., Sapporo.

The prophenoloxidase cascade of insect hemolymph is considered to play some important roles in the defense reaction. The cascade is triggered by microbial cell wall components such as ß-1,3-glucan and peptidoglycan. Although the cascade is presumed to be composed of the recognition proteins, some zymogens of serine protease, prophenoloxidase and other unknown factors, the activating mechanism of the cascade has not been worked out yet.

We tried to fractionate the essential components of the cascade in the plasma of silkworm, *Bombyx mori*, using a chain of columns of SP-Sepharose, Q-Sepharose and sulfate-cellulofine. The fraction eluted from Q-Sepharose was then further fractionated on a chain of columns of heparin-Toyopearl and DEAE-Toyopearl. Each fraction eluted from the columns was shown to contain at least one essential component as inactive form. We could reconstruct a prophenoloxidase cascade using these fractions. The reconstructed cascade was triggered by ß-1,3-glucan but not by peptidoglycan, suggesting that peptidoglycan recognition protein was removed in this fractionation method.

PRODUCTION OF ESSENTIAL AMINO ACIDS BY THE INTRA-CELLULAR SYMBIONTS OF PEA APHIDS.

T. Sasaki and H. Ishikawa. Zool. Inst., Grad. School of Sci., Univ. of Tokyo, Tokyo

Evidence has accumulated that glutamine is a key compound in the symbiosis of aphids. Glutamine is one of the major amino acid constituents in the phloem sap on which the aphids feed, and deprivation of symbionts results in striking elevation of glutamine in tissues and honeydew of the aphid. In the present study, we investigated uptake and metabolism of glutamine by the mycetocyte isolated from the aphids. While mycetocytes isolated from the aphids took up glutamine actively, the intracellular symbionts isolated from the mycetocytes scarcely took up the amino acid, and instead took up glutamic acid actively. [^{14}C]Glutamine incorporated by mycetocytes was converted into glutamate. When [ε-^{15}N]glutamine was introduced into mycetocytes, [^{15}N]glutamate was found in the cytosol. These results suggested that glutamine taken up by mycetocytes was hydrolyzed into glutamic acid and ammonia, and at least a portion of ammonia was assimilated into glutamate in the cytosol, probably through reaction with α-ketoglutarate. When isolated symbionts were incubated with [^{15}N]glutamic acid, the following amino acids were found highly labeled: alanine, aspartic acid, glutamine, isoleucine, leucine, phenylalanine, proline and valine.

CATHEPSIN E: TISSUE DISTRIBUTION AND HYDROLYTIC SPECIFICITY FOR BIOLOGICALLY ACTIVE PEPTIDES

T. Kageyama[1], M. Ichinose[2], K. Miki[2], M. Tatematsu[3], and S. Yonezawa[4]. [1]Primate Res. Inst., Kyoto Univ., [2]Fac. Med., The Univ. Tokyo, [3]Aichi Cancer Res. Ctr. Inst., [4]Aichi Pref. Colony

Cathepsin E was distributed in various types of tissues; contractile tissues, such as stomach, colon, and urinary bladder; immune-associated tissues, such as thymus and spleen; malignant tissues, such as gastric carcinoma and ovarian mucinous tumors; and some fetal tissues such as liver. Cathepsin E hydrolyzed various biologically active peptides maximally at around pH 5. Cathepsin E was active in the generation of functional peptides, such as angiotensin I, endothelin, and neurotensin, from their respective precursors. The enzyme hydrolyzed tachykinins, such as substance P and neurokinin A, very rapidly, with specific cleavage of sequences essential for their activity. Cathepsin E may regulate the physiological activities of certain types of cells or tissues which are mediated by angiotensin I, substance P, and other biologically active peptides.

REFERENCES
T. Kageyama et al. J. Biol. Chem. 267, 16450 (1992).
T. Kageyama Eur. J. Biochem. 216, 717 (1993).
T. Kageyama Methods Enzymol. (1994) in press.

MULTIPLE OCCURRENCE OF *BOMBYX* CYSTEINE PROTEINASE (BCP).

Y. Yamamoto[1], S. Y. Takahashi[1], K. Takimoto[2], K. Kato[3] and Y. Yokota[4]. [1]Dept. of Biol., Fac. of Liberal Arts and [2]RI Laboratory, Yamaguchi Univ., Yamaguchi, [3]Dept. of Biol., Fac. of Liberal Arts, Nagoya City Univ., Nagoya, [4]Biol. Lab., Aichi Pref. Univ., Nagoya.

We have isolated and sequenced a 1486-base-pair near full-length cDNA coding for *Bombyx* egg cystine proteinase (BCP). The cDNA encodes 344 amino acid residues containing a typical signal peptide sequence (16 residues), pro-peptide (104 residues), and the sequence for mature BCP (224 residues). Sequence alignments show that the BCP is similar to lobster cysteine proteinase (61 % identity), Aleurain (52 %), Oryzain (54 %), and cathepsin L (59 %). The amino-terminal sequencing of the BCP indicates that the BCP purified as an inactive form from eggs is a pro-enzyme. This may be the first demonstration of physiological pro-cysteine proteinase. By SDS-PAGE and immuno-staining, occurrence of these molecular forms was studied in other tissues of the silkmoth. In fat bodies, both the pro-enzyme and mature enzyme were found, whereas mature enzyme were detected predominantly in testes. These results suggest that the BCP functions in different ways in those tissues. The data obtained by immuno-electron microscopy gave an additional information about the distribution of the enzyme.

CHARACTERIZATION OF CATHEPSIN E TYPE ACID PROTEINASE FROM BULLFROG, *RANA CATESBEIANA*

T. Mineta[1], T. Inokuchi[2], K. Kobayashi[1] and S. Horiuchi[1]. [1]Life Sci. Inst., Sophia Univ., Tokyo, [2]Dep. of Biol., Fac. of Educat., Utsunomiya Univ., Utsunomiya.

Acid proteinase which is similar to mammalian cathepsin E exists in larval fore-gut and adult stomach of bullfrog. This enzyme purified from mucosal extract of adult stomach consists of two identical subunits of 45kDa. We examined some properties of this enzyme: it was activated from proenzyme to mature enzyme at the pH of five and under, and it localized in larval hind-gut as well as in fore-gut. PAGE, SDS-PAGE and two dimensional PAGE techniques were mainly used for those analyses. In addition to the dimeric form of enzyme, a monomeric enzyme is probably present in fore-gut and stomach. Now we are preparing anti-cathepsin E type enzyme antibody for immunohistochemical studies.

PHYSIOLOGICAL FUNCTIONS OF μ-CALPAIN IN EPIDERMOID CARCINOMA KB CELLS.

W.Harigaya[1], T.C.Saido[1], K.Suzuki[1,2], S.Kawashima[1],. [1]Dept. of Mol. Biol., Tokyo Metro. Inst. of Med. Sci., [2]Inst. of Mol. and Cell Biosci., Univ. of Tokyo

μ-Calpain, an isozyme of calcium-activated neutral protease ubiquitously present in animal cells, plays a unique intracellular role as a calcium receptor by mediating limited proteolysis. Based on our previous reports that calpain is involved in cytoskeletal regulation and that it undergoes two step autolysis upon activation, we examined its behavior in KB cells stimulated by epidermal growth factor (EGF). Immunofluorescence microscopy using antibodies that distinguish among preautolytic, intermediate, and postautolytic forms of μ-calpain large subunit revealed that EGF treatment induces dynamic changes in intracellular localization of these forms of μ-calpain. Because these changes paralleled morphological responses of KB cells that were suppressed by a calpastatin peptide, μ-calpain activation plays an important role in cellular morphogenesis.

AUTOLYTIC ACTIVATION MECHANISM OF *BOMBYX* CYSTEINE PROTEINASE (BCP).

S.Y. Takahashi[1], Y. Yamamoto[1] and S. Watabe[2]. [1]Dept of Biol., Fac. of Liberal Arts, and [2]RI Laboratory, Yamaguchi Univ., Yamaguchi.

Acid cysteine proteinase in the eggs of the silkmoth, Bombyx mori (BCP), exists as an inactive proenzyme and is activated at acidic pH. Upon the activation, pro-form (47 kDa) was converted to a smaller molecular form (39 kDa). The rate of conversion was not affected by increasing concentrations of the enzyme and BCP immobilized to AH-Sepharose was autolyzed, indicating that the reaction might be an intramolecular reaction. Taken together these data and kinetic experiments suggest that the mechanism is likely a stepwise reaction, in which procysteine proteinase is activated to mature enzyme through intermediate forms releasing small peptides stepwisely. These intermediate forms were isolated and characterized. The results suggest that the intramolecular reaction is a major processing in the activation of the cysteine proteinase from the eggs of the silkmoth, *Bombyx mori*. This is the first report to demonstrate directly the cleavage sites of pro region of cysteine proteinase directly during activation.

BIOCHEMICAL ACTIVITY OF SP-22, A SUBSTRATE PROTEIN FOR MITOCHONDRIAL ATP-DEPENDENT PROTEASE IN BOVINE ADREAL CORTEX.

S. WATABE[1], H. HASEGAWA[2], S. Y. TAKAHASHI[3], T. HIROI[4], H. KOHNO[4] and N. YAGO[4]. [1]Radioisotope Lab., Yamaguchi Univ., Yamaguchi, [2]Dept. of Bioscience, Nishi-Tokyo Univ., Yamanashi, [3]Dept. of Biol,. Faculty of Liberal Arts, Yamaguchi Univ., Yamaguchi, and [4]Radioisotope Res. Inst., St. Marianna Univ., Kawasaki.

Amino acid sequence of SP-22, a substrate protein for mitochondrial ATP-dependent protease with unknown function (Watabe *et al.* (1994), J. Biochem., **115**, 648-654), is homologous to a thiol-specific antioxidant (thiol radical scavenger) in yeast. Therefore, we measured radical scavenging activity of SP-22. The activity was measured as protection of tryptophan hydroxylase against radicals Radicals were generated by adding Fe^{2+} ion (50 μM) to 15 mM dithiothreitol solution. Using this method we detected radical scavenging activity peak in DEAE-Biogel fractions which was completely coincided with SP-22 peak. We also found that horse serum potentiated the radical scavenging ativity of SP-22 fractions. The potentiating factor was macromolecular. Since purified SP-22 had no activity, SP-22 might have been inactivated by the purification procedures as suggested by the presence of cysteine-sulfinic acid (Cys-SO_2H) in the purified protein which was probably an oxidized product of cysteine-sulfenic acid (Cys-SOH). Alternatively, some unkown component(s) might be necessary to exert the scavenging activity

CLONING OF cDNA OF VETEBRATE TYPE COLLAGENASE FROM INVERTEBRATES

○T. Sawada , K. Oofusa and K. Yoshizato. Dev. Biol. Lab., Dept. of Biol. Sci., Fac. of Sci., Hiroshima Univ., Higashihiroshima

Vertebrate type collagenase is a metalloproteinase that binds zinc at the putative active site, and cuts peptide bond between first Gly and Leu(Ile) of X-Gly-Leu(Ile)-Y-Gly-Z (neither Pro nor Lys at X, Y, Z residues) at a physiological condition. This type collagenase has not been found in invertebrates. The deduced amino acids sequence of sea urchin Hemicentrotus pulcherrimus collagen contains a site that might be sensitive to vertebrate type collagenase. Planaria Dugesia japonica dissolved collagen gels, which was inhibited by both TIMP and EDTA. These results strongry suggest that vertebrate type collagenase exists also in invertebrates. In this study, we tried to isolated cDNA clones from these invertebrate animals by using PCR cloning methods.

THE DISTRIBUTION OF CELLULASES IN THE ALIMENTARY CANAL OF HIGHER TERMITES.

G. Tokuda[1] , H. Watanabe [2] , H. Noda [2] , I. Yamaoka[3] and T. Matsumoto [1] .
[1] Dept. of Biol., Coll. of Arts and Sci., Univ. of Tokyo., Tokyo. [2]Natl. Inst. of Seric. and Entomol Sci., Tsukuba, Ibaraki. [3]Biol. Inst., Fac. of Sci. Yamaguchi Univ., Yamaguchi.

We have reported on the fine structure of the alimentary canal in higher termites and we have discussed about functions of the midgut including the mixed segment, and the hindgut.

In this report, two kinds of cellulase activity and their distributions were examined to know where is the site of cellulose breakdown and the origin of cellulase in higher termites.

In lower termites, it is well-known that the endo-β1,4-glucanase is produced in the salivary glands. But in a higher termite, *Nasutitermes takasagoensis*, the β-glucosidase activity was detected at the salivary glands. On the other hand, in *Odontotemes formosanus*, the endo-β1,4-glucanase activity was detected at the salivary glands.

PREVENTION BY TYPE III COLLAGEN OF CELL DAMAGE FROM ACTIVE OXYGEN

M.Kashiwagi, H,Namiki
Dept.,of Biol.,Sch,of Educ.,Waseda Univ.,Tokyo

The role of active oxygen and its metabolites in the regulation of collagen changes have not been widely studied.

Type III collagen localize only in flexible parts of the embryo skin and its content decreases during aging.

The role of type III collagen in vivo is not well understood.

In the present study,when mouse fibroblasts were treated with hydroxyl radical,cell damage was prevented by type III collagen but not by type I collagen. Denatured type III collagen did not prevent the damage.

Another finding was that collagen extracted from aged mouse might have an ability to catabolize active oxygen through an oxidation-reduction exchange.

EFFECTS OF EDTA AND BIVALENT METAL IONS ON THE ACTIVITY OF ARTEMIA TREHALASE

Z. Nambu and F. Nambu. Dep. of Biol., Univ. of Occupational and Environm. Health, Japan, Sch. of Nursing and Med. Technol. Kitakyushu.

In order to characterize Artemia trehalase, effects of EDTA and bivalent metal ions were investigated on it, because it has been reported that a neutral trehalase derived from baker's yeast was absolutely dependent on Ca^{++} or Mn^{++} ions and strongly inhibited by EDTA. Artemia trehalase was partially purified from 40 hr-cultured nauplii by acetone treatment, DEAE-Sepharose FF chromatography, Con A-Sepharose chromatography and TSKgel TOYOPEARL HW-55F chromatography. In a phosphate buffer, the activity was 43 % inhibited by 5 mM EDTA, on the other hand, no such inhibition was observed in a HEPES buffer. The inhibition in the phosphate buffer was recovered by addition of Mn^{++}, Mg^{++} or Ca^{++}. In the HEPES buffer, 1 mM Hg^{++}, Cd^{++}, Cu^{++} or Zn^{++} strongly inhibited the activity, Ni^{++}, Co^{++} or Fe^{++} considerably affected it, Mn^{++}, Ca^{++} or Mg^{++} slightly hindered it. 100 mM phosphate buffer reduced the activity to 40%.

THE PARTIAL AMINO ACID SEQUENCE OF A PLASMA SERINE PROTEASE INHIBITOR (SERPIN) FROM THE HEMOLYMPH PLASMA OF *HALOCYNTHIA RORETZI*

F. Shishikura, T. Abe, S. Ohtake, and K. Tanaka
Department of Biology, Nihon University School of Medicine, Tokyo

A plasma protease inhibitor of *Halocynthia roretzi* (HRPI) has been previously purified to be a single-chain glycoprotein with an apparent molecular weight of 58 kDa. It is thought to be a member of the serpin superfamily in terms of its inhibitory activity towards a cognate protease as well as other proteases (thrombin, trypsin), a covalent-bonded complex formation with these enzymes, and glycosaminoglycan-dependent acceleration on the inhibitory activity.

The partial amino acid sequence of HRPI was analyzed by a gas-phase sequencer, Shimadzu PPSQ-10, and compared with known amino acid sequences of the members of serpin superfamily. The first 30 N-terminal sequence is NH_2-Thr-Lys-Lys-Asp-Gly-Glu-Glu-Lys-Val-Ala-Leu-Asn-Asp-Phe-Arg-Met-Ser-Leu-Arg-Glu-Phe-Ser-Gly-Asn-Leu-Leu-Tyr-Tyr-Ile-Ser- and shows less homology towards those of the other members of the serpin superfamily. However, amino acid sequences of lysyl endopeptidase-digested peptides derived from the inner part of HRPI show significant sequence identities to several members of the serpin superfamily.

ROLE OF ATP IN MEMBRANE-BOUND GUANYLYL CYCLASE ACTIVATION BY CRUSTACEAN HYPERGLYCEMIC HORMONE (CHH)

S. Aizawa, T. Ohoka. Department of Biol., Fac. of Sci., Tokyo Metropol. Univ. Tokyo

Membrane-bound guanylyl cyclae, prepared from Procambarus heart was significantly stimulated by crustacean hyperglcemic hormone. The condition were precisely examined by utilizing membrane preparation from several tissues and purified crustacean hyperglycemichormone (CHH) from sinus glands of the same species. The result showed that CHH-stimulated guanylyl cyclase activity was more enhanced in the presence of ATP.

The activation depended entirely to concentration of CHH and divalent cations, Mg^{2+} or Mn^{2+}, but the stimulation degree by hormone was rather prominent in presence of Mg^{2+}. Examining the conditions of the hormonal stimulation, ATP was newly found to have an additional stimulating effect in presence of hormone and divalentcation. The presence of CHH decrese Km values and Vmax for GTP of guanylyl cycase activity. Furthermore, addition of ATP changed Km values and Vmax. ATP analogues, Adenosine 5'-thitriophosphate (ATPγS) also showed similar stimulatory effect. From these results, a signal transduction mechanism was suggested that the ATP was not used for protein phospholylation, but the binding of thenucleotide resulted stimulatory effect.

ISOFORMS OF SEPIAPTERIN REDUCTASE IN VERTEBRATES MODIFIED BY PHOSPHORYLATION.

S.Katoh[1], T.Sueoka[1], Y.Yamamoto[2] and S.Y.Takahashi[2].
[1]Dept. of Biochem., Meikai Univ. Sch.of Dent., Sakado, [2]Dept. of Biol., Fac. of Lib. Arts, Yamaguchi Univ., Yamaguchi.

We found that tetrahydrobiopterin generating enzymes of sepiapterin reductase (SPR) and dihydropteridine reductase are phosphorylated by Ca^{2+}-dependent protein kinases when these were incubated with [γ-^{32}P]ATP in the system of Ca^{2+}/calmodulin-dependent protein kinase II (CaM-KII) and PKC. pI of the purified SPR of rats was 4.9, while that of SPR in the tissue homogenate was mainly 4.4. SPR in the pI 4.4-fraction showed a more alkaline pI after treatment with alkaline phosphatase or calcinulin in somewhat. The purified SPR phosphorylated by CaM-KII was completely dephosphorylated by the extract from rat brain and this dephosphorylation was not inhibited by okadeic acid. Thus, phosphorylated SPR may be regulated by phosphatases of types 2B and 2C. SPR was separated from its phosphorylated form(s) by CaM-KII by isoelectlic focusing (IEF) or HPLC on a hydroxyapatite column. Plural forms of SPR were also observed by IEF or HPLC of the liver extracts of human, chiken, fish, and frog, and of the extract from the fat body of silkworms as well. These suggest that the native SPR is mostly modified by phosphorylation.

PHOSPHORYLATION OF THE ROUGH ENDOPLASMIC RETICULUM RIBOSOME-ACCEPTOR PROTEIN p34

J. Uchiyama, N. Ikuta, T. Ichimura and S. Omata. Dept. of Biochem., Fac. of Sci., Univ. of Niigata, Niigata.

We previously isolated from rat liver rough microsomes (RM) an integral membrane protein with a relative molecular weight of 34 kDa (which we termed p34), and showed that it plays an important role in the ribosome-membrane association. Primary sequence analysis suggested that p34 contains several consensus sequences for phosphorylation that could be phosphorylated by four types of protein kinases. Here we investigate the effects of the four protein kinases on the phosphorylation and functional modification of p34. The purified p34 was found to be phosphorylated by two out of the four protein kinases, i.e., Ca^{2+}-, calmodulin-dependent protein kinase II (CaM-kinase II) and casein kinase II. On the other hand, when analyzed using intact RM, only CaM-kinase II phosphorylated p34. In addition, the ability of p34 to bind ribosomes decreased through the phosphorylation of p34 by CaM-kinase II. The studies including the detailed characterization of the phosphorylation site(s) are now in progress.

COMPARATIVE BIOCHEMICAL STUDY OF PYRUVATE KINASE : PYRUVATE KINASE ISOZYMES OF BLACK BASS (MICROPTERUS SALMOIDES)

T. Fukui, Y. Urata and K. Imamura. Dept. of Biochem., Fac. of Sci., Okayama Univ. of Science, Okayama.

A zymogram of pyruvate kinase isozymes of various tissues of a fish, black bass (Microputerus salmoides) was compared with that of mammalian rat. Isozyme patterns and their tissue distribution of black bass were similar to those of rats. Although the anatomical form of the black bass heart is quite different from that of the mammalian rat, the isozyme pattern showed presence of M1(skeletal muscle type) −M2 (prototype) hybrid form . This is particulary interesting as the phenomena was observed in tissues during early development of rat , while in those tissues of the adult animal, only the M1 type isozyme was expressed. Currently, black bass isozymes are being kinetically characterized.

PROTEIN DEGRADATION OF TRYPTOPHAN HYDROXYLASE AND A CELLULAR DETERMINANT OF THE ENZYME LEVEL.

H. Hasegawa, K. Oguro, and M. Kojima
Dept. of Bioscience, Nishi-Tokyo Univ., Yamanashi

A rapid turnover of tryptophan hydroxylase, a key enzyme in serotonin biosynthesis, was described with RBL2H3 cells, a rat basophilic leukemia cell line. The cells in monolayer culture were given cycloheximide (1 μg/ml) and the effect on the amount of tryptophan hydroxylase was analyzed: a half life of tryptophan hydroxylase was estimated to be about 20 min or less. Pulse-labeling with use of [^{35}S]-methionine and chase experiment revealed that the observed disappearance was driven with proteolytic fragmentation of the enzyme protein. Another culture of a murine mastocytoma cell line contains a large amount of tryptophan hydroxylase, but the turnover of the enzyme was found to be much slower. The cellular amount of this enzyme seems to be primarily determined by the rapid degradation of the enzyme protein.

STUDIES ON CEMENT PROTEINS OF THE CYPRID LARVA OF THE BARNACLE *Megabalanus rosa*.

Katsuhiko Shimizu, C. Glenn Satuito, Wakana Saikawa and Nobuhiro Fusetani. FUSETANI Biofouling Project, ERATO, JRDC, Yokohama.

Cyprid larvae of barnacles permanently attach themselves to substrates by secreting proteinaceous cement from the cement glands after free-swimming planktonic stages. Cement proteins are stored in eosinophilic granules of the cement glands. In order to elucidate properties of cement proteins, the cement glands were isolated from the cyprid larva of the barnacle *Megabalanus rosa* and contents of cement glands were examined. Eosinophilic granules in the cement glands were soluble in 62.5 mM Tris-HCl buffer, pH 6.8 containing 2% sodium dodecylsulfate (SDS), 8M urea and 5% 2-mercaptoethanol (SB), but not in the same buffer containing 2% NP-40 instead of SDS (NB). Polyacrylamide gel electrophoresis analysis of NB- and SB-soluble fractions revealed that 110K and 36K proteins were only found in SB-soluble fraction. These results suggest that 110K and/or 36K protein are main components of the cement substance.

A PROTEIN COMPLEX, INDUCING LARVAL SETTLEMENT, FROM THE BARNACLE, *Balanus amphitrite*.

K.Matsumura, S.Mori, M.Nagano and N.Fusetani
FUSETANI Biofouling Project, ERATO, JRDC, Yokohama.

Barnacles live gregariously, and chemical cues from conspecies are believed to induce settlement of cyprid larvae. We attempted to purify the settlement inducing proteins from the adult barnacle, *Balanus amphitrite*. The new settlement assay system using nitrocellulose membrane was developed, which was useful for research of active proteins adsorbed on a surface. By using this assay method, we isolated active protein complex with a high molecular weight, which bind to lectins, LCA and ConA, respectively. Moreover, we found that the adult extract-induced settlement was inhibited either by LCA or ConA, but neither by WGA nor PNA. LCA and ConA did not affect the motility of the cyprids. These results suggest that a sugar chain of the settlement inducing protein plays an important role in larval settlement.

PURIFICATION AND CHARACTERIZATION OF INSECTICYANIN FROM THE HEMOLYMPH OF THE SWEET POTATO HORNWORM, *AGRIUS CONVOLVULI*

H. Saito, M. Shimoda and M. Kiuchi. Dept. of Insect Genetics and Breeding, National Institute of Sericultural and Entomological Science, Tsukuba.

The biliverdin-binding protein (Insecticyanin:INS) was found in the hemolymph of the fifth instar larvae of the sweet potato hornworm, *Agrius convolvuli*. It was purified from the hemolymph using hydrophobic interaction chromatography, ion exchange chromatography and gel-filtration. The highly purified INS showed a Mr of approximately 56,000 by gel permeation analysis using a Superdex 200 pg column. SDS-PAGE showed a single band of Mr approximately 27,000. These results indicate that the native INS is dimer. The blue coloration of INS was due to the presence of biliverdin type pigments, as judged from its absorption spectra.

PURIFICATION AND CHARACTERIZATION OF PLASMA LECTINS FROM SEA CUCUMBER, *STICHOPUS JAPONICUS*.

T. Matsui[1], Y. Ozeki[1], M. Suzuki[1], A. Hino[2] and K. Titani[1]. [1]Div. of Biomed. Polymer Sci., Inst. for Comprehensive Med. Sci. Fujita Health Univ., Toyoake, [2]Dept. of Biol. Sci., Fac. of Sci., Kanagawa Univ., Hiratsuka.

Two Ca^{2+}-dependent lectins (SPL-1 and -2) were purified from coelomic plasma of sea cucumber *S. japonicus* by affinity chromatography on a porcine stomach mucin-agarose column followed by FPLC on Superose 6 and HiTrap Q columns. SPL-1 and -2 showed different spectra in the sugar binding specificity, Ca^{2+}-sensitivity and native molecular mass. Amino-terminal sequences of both SPLs showed a significant degree of similarities to C-type animal lectins, especially to echinoidin, a sea urchin coelomic fluid lectin. SPLs were adsorbed to coelomocyte-clot in a Ca^{2+}- and sugar-dependent manner. However, the clotting of coelomocytes was not influenced by SPL-specific sugars, but inhibited by EGTA or RGD peptide. These results may suggest that integrin, but not the SPL-sugar recognition, plays a role in the clotting events.

MULTIDOMAIN STRUCTURE OF THE EXTRACELLULAR HEMOGLOBIN OF *INDOPLANORBIS EXUSTUS*.

T. Ochiai[1] and M. Hiura[2]. [1]Dept. of Biol.,Fukushima Med. Coll., Fukushima and [2]Ojiyanishi High Sch., Niigata.

The structural units of *Indoplanorbis* hemoglobin are equivalent polypeptide chains with a molecular weight of $17x10^4$. Each chain has a multidomain structure of a linear sequence of domains with a MW of about $2x10^4$ containing one heme. The native hemoglobin was cleaved with subtilisin at protein /protease ratios from 2000 to 50 and gel filtrated on Sephacryl S-200. Several heme-containing fractions were obtained, and MW of the fractions which appeared in any of the protein/protease ratios examined were $30x10^4$ (IV), $12.2x10^4$(III), $5.06x10^4$ (II) and $2.23x10^4$(I). These are considered to be octa-, tetra-, di-, and mono-domain units, respectively. Each fraction showed a heterogeneous pattern by PAGE, containing at least 4, 6, 10 and 13 components, respectively. Relative amount of the 13 components of fraction I depends on the proteolysis condition. Several of the components were isolated by Mono Q chromatography.

THE pH-DEPENDENT INTRAMOLECULAR TRANSFORMATION IN FERRIC HEMOGLOBIN FROM A MIDGE LARVA (*TOKUNAGAYUSURIKA AKAMUSI*).

K. Akiyama, A. Matsuoka and K. Shikama.
Biol. Inst., Fac. Sci., Tohoku Univ., Sendai

The hemoglobin from the 4th-instar larva of *Tokunagayusurika akamusi*, a common midge (*Diptera*) found in eutrophic lakes in Japan, is composed of as many as eleven separable components (IA, IB, II, III, IV, V, VIA, VIB, VII, VIII, IX) on a DEAE-cellulose column, and these can be divided into two groups on the basis of their presence or absence of the distal (E7) histidine residue. For instance, hemoglobin VII consists of 150 amino acid residues and contains the usual distal histidine at position 64, whereas component V replaces it by a leucine at position 65 (1).

When the aquomet-form of *T. akamusi* hemoglobin VII, a major component in the larval hemolymph, was placed in acidic pH range, its Soret peak was considerably blue shifted and accompanied by a marked decrease in intensity, indicative of the protein being converted into a structure quite similar to that of *Aplysia* myoglobin lacking the distal histidine residue.

(1) Fukuda, M., Takagi, T., and Shikama, K. (1993) *Biochim. Biophys. Acta* **1157**, 185-191.

A METMYOGLOBIN REDUCING FACTOR: ISOLATION AND KINETICS

Kariya,M., Sado,K., Namiki,H..
Dept.of Biol.,Sch.of Educ.,Waseda Univ.,Tokyo

We previously reported beef heart muscle was found to contain an NADPH-dependent metmyoglobin reducing factor different from known reductases and reducing reagents. In the present study, we report an improved method for isolation and purification, characterization and identification, and kinetics of this reducing factor. The water-soluble and low molecular weight (m.w.500-1000) fraction was separated from vobine cardiac muscle. The crude sample was washed with ethanol, and applied on several kinds of HPLC columns (anion exchanger, cation exchanger, size exclusion, and ODS). Through these processes a thoroughly purified sample was obtained. Biochemical and spectrum analyses revealed that it was a pyrimidine nucleotide analogue of m.w. about 600. We tentatively propose that this factor may be a kind of oxidation-reduction ribozyme.

SULCULUS HEMOGLOBIN EVOLVED FROM INDOLEAMINE 2,3-DIOXYGENASE IV. The complete structure of *Sulculus* hemoglobin gene.

T. SUZUKI, H. J. YUASA
Dep.Biol., Fac.Sci., Kochi Univ.

Sulculus diversicolor and *Nordotis madaka* contains an unusual tissue hemoglobin (myoglobin) in radular muscle. The hemoglobin consists of about 40kDa polypeptide chain, contains one heme per molecule and forms homodimer in physiological conditions (1). *Sulculus* hemoglobin can bind oxygen reversibly. The cDNA-derived amino acid sequence of *Sulculus* and *Nordotis* hemoglobins showed high homology (35%) with human indoleamine 2,3-dioxygenase (IDO), a tryptophan degrading enzyme containing heme, and suggests that these hemoglobins evolved from IDO gene, but not from hemoglobin gene (2,3). As a first step to make clear the evolutionary origin, we have determined the complete structure of 15,329bp of *Sulculus* hemoglobin gene. The gene consisted of 12 introns and 13 exons. The splice junctions of the eight introns were conserved exactly in the genes of *Sulculus* hemoglobin and human IDO, suggesting that they were conserved for at least 600 million years. The 5' flanking region contained the interferon-stimulable response element (ISRE)-like sequence, just like human IDO gene. (1) Suzuki & Furukohri (1989) *Experientia* **45**, 998-1002. (2) Suzuki & Takagi (1992) *J. Mol. Biol.* **228**, 698-700. (3) Suzuki (1994) *J. Protein Chem.* **14**, 9-13.

ON THE HETEROGENEITY OF LOUCST TROPOMYOSIN.
T. Ishimoda-Takagi and K. Yagi. Dept. of Biol., Tokyo Gakugei Univ., Tokyo.

Loucst tropomyosin has been investigated using cloned cDNA of loucst tropomyosin (Krieger *et al.*, 1990) . However, molecular feature of loucst tropomyosin is still remained to be examined. Thus, we investigated molecular heterogeneity and tissue specificity of tropomyosin from the locust, *Loucsta migratoria*. Three main isoforms of tropomyosin were detected in two-dimensional SDS gel electrophoresis, and these tropomyosin isoforms showed tissue-specific distribution. All of three tropomyosin isoforms were detected in the extracts obtained from head and abdominal regions of an adult loucst. However, one of three isoforms of tropomyosin was not recognized in the flight and leg muscles, although this isoform was detected in the extracts from the wholes of thorax and femurs. It is known that flight activity of gregarious-phase loucst is higher than that of solitary-phase loucst. Therefore, we compared tropomyosin isoforms from the gregarious-phase loucst with those from the solitary-phase loucst. Three kinds of tropomyosin isoforms were also detected in the gregarious-phase loucst. However, there was no difference between solitary- and gregarious-phase loucsts not only in the tissue specificity of tropomyosin but also in the tropomyosin content involved in the flight muscle.

CHANGES IN TROPOMYOSIN DURING POSTEMBRYONIC DEVELOPMENT OF LOCUST.
K. Yagi and T. Ishimoda-Takagi. Dept. of Biol., Tokyo Gakugei Univ., Tokyo

Three main isoforms of tropomyosin are involved in the adult of the locust, *Locusta migratoria*. Locust undergoes incomplete morphogenesis, and morphology of each instar larva resembles that of the adult. Thus, we investigated changes in tropomyosin during postembryonic development of locust. All of three adult-type tropomyosin isoforms were detected in the larvae during postembryonic development, and tissue specificity of these isoforms in the postembryonic larvae was similar to that of the adult. In addition, three or four larva-specific tropomyosin isoforms, of which pI values were slightly higher than those of the adult-type isoforms, were detected in all instar larvae. Periodic appearance or disappearance of these isoforms associated with molt cycle was observed in each of larval instar. The larva-specific isoforms of tropomyosin could not be detected in early stages of each instar. In middle stages, however, these isoforms were recognized clearly in all tissues examined and abundantly in abdominal region. In the latest stages of each instar, these isoforms might decrease rapidly. Furthermore, the larva-specific tropomyosin isoforms seemed to locate near the epidermal structures.

SOME PROPERTIES OF SEA ANEMONE TROPOMYOSIN.
M. Fujinoki and T. Ishimoda-Takagi. Dept. of Biol., Tokyo Gakugei Univ., Tokyo.

There is no report on the cnidarian tropomyosin except that a tropomyosin cDNA clone was isolated from the hydrozoan, *Podocoryne carnea* (Baader *et al.*, 1993). Therefore, we tried to detect and identify tropomyosin involved in the anthozoan, one of classes of Cnidaria, using a species of the sea anemone, *Anthopleura japonica*. When sea anemone tropomyosin extract was subjected to two-dimensional urea-shift gel electrophoresis, four or five components revealed retarded mobilities on SDS gel in the presence of urea. Apparent molecular weights and pI values of these components were approximately 30,000 to 35,000 and around 4.6, respectively. All of these components were heat stable and possessed the ability to form paracrystals. Three of them were obtained at both 30-50% saturated ammonium sulfate (SAS) and 50-70% SAS fractionations, and the remaining components predominantly at 50-70% SAS fractionation. From these results, we concluded that all or most of these components were sea anemone tropomyosin isoforms. Distribution of these components was tissue-specific. Two of these components lacked in the oral disc and pedal disc, and were predominant in the tentacles. Furthermore, similar results were obtained from another species of the sea anemone, *Actinia equina*.

CROSS-REACTION OF MONOCLONAL ANTIBODIES RECOGNIZING FLAGELLAR MOVEMENT-INITIATING PHOSPHOPROTEIN COMPLEX IN SALMONID SPERMATOZOA WITH PROTEINS OF SEA URCHIN SPERMATOZOA.
T.Matsumura., Z.Jin. and H.Hayashi. Sugashima Marine Biological Laboratory, Nagoya University, Toba.

cAMP dependent phosphorylation is important for the initiation of the flagellar movement in Salmonid spermatozoa. Recently, we purified and characterized flagellar movement initiating phosphoprotein(MIPP) complex. Two of these mAbs,FMI7 and FMI27 recognized 38kDa protein located at basal position of axoneme, blocked the movement as well as the cAMP dependent phosphorylation of MIPP. Involvement of cAMP dependent phosphorylation is also argued for flagellar oscillation of sea urchin sperm. Therefore we tried possible cross reaction with these proteins of sea urchin sperm.
Immunoblotting and immunostaining of sea urchin Hemicentrotus pulcherrimus spermatozoa showed that the protein recognized by FMI7 was 53kDa and located at the proximal portion of axoneme. Although molecular weight and localization are different from 38kDa protein of salmonid fish, FMI27 also blocked the cAMP dependent phosphorylation of many proteins. These results suggest that 53kDa protein has a similar role as 38kDa protein of salmonid fish.

IDENTIFICATIONS OF α AND β TUBULIN IN SPERM 950-KDA PROTEASE COMPLEX.
K. Inaba, K. Ohkawa and M. Morisawa. Misaki Marine Biological Station, Faculty of Science, University of Tokyo, Miura, Kanagawa 238-02.

We have previously shown that sea urchin and chum salmon sperm contain a 950-kDa multisubunit protease that contains some of the proteasome subunit. The 53-kDa components (doublet) in the complex had the same electrophoretic mobilities as those of α and β tubulins of sperm flagella. Peptide mapping of 53-kDa bands with V8 protease also showed the identities of 53-kDa subunits to that of sperm tubulins. In order to confirm that the 53-kDa components are the integral components of 950-kDa protease complex, we prepared affinity-purified antibody against some of the proteasome subunit to isolate the 950-kDa protease complex without any contaminations. The 950-kDa protease obtained also contained the 53-kDa polypeptides which reacted with anti-tubulin antibody. These results indicate that tubulins are the integral components of 950-kDa protease and suggest that this protease is involved in the regulation of microtubule-mediated cell motility.

EXTRACELLULAR PROTEASE ACTIVITY THAT INCREASES DURING THE GROWTH OF *TETRAHYMENA*
K. Suzuki[1], N. Hosoya[2], H. Mohri[3], T. Takahashi[1], and H. Hosoya[1].
[1]Dept. of Biol. Sci.; Fac. of Sci., Hiroshima Univ., Higashi-Hiroshima, [2]Otsuma Women's Univ., Tokyo, and [3]Univ. of the Air, Chiba.

The population density of *Tetrahymena* is kept constant in the stationary phase. We sought to investigate this mechanism by using the ciliate, *T. pyriformis* . Here, we found that protease activity in the culture medium markedly increased during the growth of the ciliate. We tried to purify this protease activity from the culture medium in the stationary phase of *Tetrahymena* in combination with DEAE cellulose, hydroxylapatite, and gel-filtration column chromatographies. This protease activity was eluted as a single peak by gel filtration using HPLC. SDS-PAGE showed that this peak contained 2 components of 26kD and 28kD, respectively. This protease activity showed pH optima at 7.5-8.0. TPCK or TLCK but not leupeptin, trypsin inhibitor, PMSF, pepstatin, or EDTA effectively inhibited the protease activity. Amino acid sequence analysis showed that the N-terminal sequence of the 28kD component was similar with that of chymopapain and stem bromelain. Further works are in progress to elucidate whether this protease have an activity to regulate cell proliferation.

DYNAMICS OF β-ALANINE ASSOCIATED TO DEGRADATION OF mRNA AND SCLEROTIZTION OF THE CUTICLE OF THE SILKWORM.

M. Osanai, N. Kurata and Y. Umebachi. Dept. of Biol., Fac. of Sci., Kanazawa Univ., 920-11 Kanazawa, Japan.

At metamorphosis of the silkworm, Bombyx mori, not only various proteins but also mRNAs corresponding to their active syntheses are much synthesized. After utilized, mRNAs are degrated to purine and pyrimidine bases. Purine is converted to pigments such as uric acid, guanine and pterins to accumulate in the scales of the body surface and wing as endproducts of nitrogen compounds. Pyrimidine is catabolized to uracil and then to β-alanine, which forms β-alanyldopamine with dopamine derived from tyrosine, a degradation product of proteins at metamorphosis. Cuticle proteins produced at metamorphosis are closs-linked by β-alanyl-dopamine, resulting in sclerotization of the cuticle. The concentration of free β-alanine in the hemolymph showed the two peaks at pupation and just before emergence. The concentration of total β-alanine contained in the whole body showed the similar changes during pupal period. It was also found that β-alanine is reserved as a conjugated form(s) in the hemolymph of the mid pupa and accumulated in the cuticle of adults. Radioactivity of [5,6-^{3}H]uracil injected to pharate pupa or early pupa was incorporated into β-alanine in the hemolymph and cuticle.

MOTILITY OF SINGLE-HEADED KINESIN.

Y. Y. Toyoshima, M. Edamatsu and H. Fukazawa. Dept. of Pure and Applied Sciences, College of Arts and Sciences, Univ. of Tokyo, Tokyo.

Single kinesin molecule can move microtubule continuously. Whether two heads of a kinesin molecule is necessary for movement or single head is enough is yet to be established. To approach this problem, we have prepared single-headed kinesin and developed a new motility assay system.

Kinesin motor domain of 5 different lengths were expressed in *E. coli*: they consist of N-terminal 340 to 410 amino acids and were supplemented by a cystein residue at the C terminus ends. Whether they exist as monomers was examined by several methods. The cystein residue was labeled with maleimide-biotin and tethered to glass surface *via* avidin and biotinylated BSA. All of 5 expressed kinesin heads moved microtubules. The velocity was lower for smaller heads.

BIOCHEMICAL CHARACTERIZATIONS OF SPERM FLAGELLAR SKY CAHINS

K.Kasahara[1],K.Inaba[1],T.Yonaha[2],S.Morisawa[2],E.Yokota[3],I .Mabuchi[4], and M. Morisawa[1],[1]Misaki Marine Biological Station, School of Sci. Univ.of Tokyo, Miura,[2]EM.Lab. and Biol.Lab.,St.Marianna Univ.,Kawasaki, [3]Dep.Life Sci,Faculity of Sci.,Himeji Institute of Technology, Hyogo,[4]Dep.Biol.,College of.Art.and Sci.Univ.of Tokyo,Tokyo

Sky chain 1,2,3 are high molecular weight polypeptides (MW>500K) which were first found in the axonemes of sea urchin sperm flagella.In contrast to a lot of studies on dynein ATPases, little is known about structure and functions of sky chains.In the prezent study, extracted sky chains were clearly separated from dyneins by sucrose density gradient centri-fugation. Further purification of the sky chain 1 revealed that it had no ATPase activity, but could bind to purified brain microtubules. Negative staining revealed that the sky chain 1 was a fibrous molecule with no large globular domain. Furthermore,the sky chains were not cleaved by the 365 nm irradiation in the presence of ATP and vanadate. These results suggest that the sky chains are not dyneins and construct structures other than dynein arms. We also found out sky-chain-like polypeptides in sperm axonemes of starfish and chum salmon, suggesting that sky chains are ubiquitous compornents of sperm flagella.

EXPRESSION OF *TETRAHYMENA* CALCIUM-BINDING 25kDa PROTEIN IN *ESCHERICHIA COLI* AND ITS IMMUNOLOCALIZATION IN *TETRAHYMENA* CELLS

K.Hanyu1, T.Takemasa2, O.Numata1, M.Takahashi1 and Y. Watanabe3. [1]Inst. of Biol. Sci., Univ. of Tsukuba, Tsukuba, [2]Dep. of Anatomy I, Nippon Med. Sch., Tokyo and [3]Jyobu Univ., Gunma.

Tetrahymena calcium-binding 25kDa protein (TCBP-25) contains four EF-hand-type Ca^{2+}-binding domains and is a member of the calmodulin family. To examine the biolog-ical functions of the TCBP-25, we analyzed immnofluores-cence localization of TCBP-25 in *Tetrahymena* cells.

The TCBP-25 gene was expressed in *Escherichia coli* as glutathion-S-transferase fusion protein, using the expression vector pGEX-2T. The four TAA and one TGA codons in this gene, which are used as glutamine codons in *Tetrahymena*, were changed to CAAs by site-directed mutagenesis. Recombinant TCBP-25 showed a Ca^{2+}-depen-dent shift in electrophoretic mobility, reflecting a conformational change by Ca^{2+}-binding.

A polyclonal antibody against a recombinant TCBP-25 was used to examine the localization of the TCBP-25 in *Tetrahymena* cells. Strong immunofluorescence was observed in cell cortex.

EF-1-LIKE PROTEINS ARE CONSTITUENTS OF THE ISOLATED CLEAVAGE FURROW FROM THE SEA URCHIN EGGS.

Hirotaka Fujimoto and Issei Mabuchi. Department of Biology, College of Arts and Sciences, University of Tokyo, Tokyo, 153.

It should be a good project to directly isolate the cleavage furrows from dividing cells in order to study the mechanisms of cytokinesis. Recently, the isolation of the cleavage furrows from dividing sand dollar eggs (*Clypeaster japonicus*) has been successful in our laboratory (S.Yonemura *et al.*, 1991). Furthermore, we have isolated the cleavage furrows from several other sea urchin species. On two-dimensional gel electrophoresis, a number of protein spots were found specifically and commonly in the cleavage furrow fractions from eggs of several sea urchin species examined so far. These proteins were also found in Calyculin-A-induced cleavage furrow-like apparatus from unfertilized eggs. Examples are an acidic 32kD protein, acidic 35-37kD proteins and a basic 51kD protein. Anti-MTOG 51kD protein antibody (HP-2) (K.Ohta *et al.*, 1988) specifically recognized this basic 51kD protein. This protein was also recognized by anti-silk grand EF-1α antibody. These results suggest that the 51kD protein is sea urchin EF-1α or a highly related protein. The acidic 32kD protein and acidic 35-37kD proteins were recognized by anti-silk grand EF-1ββ' antibody. From the N-terminal amino acid sequence, the acidic 32kD protein was found to be homologous to EF-1β.

PURIFICATION AND IMMUNOELECTRON MICROSCOPICAL LOCALIZATION OF THE MUTANT GENE PRODUCT (P85) OF A *TETRAHYMENA CDAA1* MUTANT.

K.Nishibori[1], H.Suzuki[1], O.Numata[1]and Y.Watanabe[2] [1]Institute of Biological Sciences, University of Tsukuba, Tsukuba, Ibaraki 305, [2]Joubu University, Isesaki, Gumma 372

Previously, we have identified a possible gene product (p85) of *cdaA1* mutant which has a ts-defect in the determination of division plane. The p85 was localized on the equatorial basal bodies before the formation of the fission zone. We suggested the hypothesis that the polymerization of contractile ring microfilament was nucleated at the zone of p85 deposits. To examine this hypothesis, we purified native p85 from *Tetrahymena* cell extract and determined its amino-terminal amino acid sequence. Moreover, by immunoelectron microscopy, we demonstrated that during cell division, immuno-gold for p85 appeared in the accessory portion of basal body on the fission zone using an antiserum against p85.

CLONING AND CHARACTERIZATION OF *CHLAMYDOMONAS* ACTIN GENE

Y. Sugase, M. Hirono and R. Kamiya.
Zool. Inst., Sch. of Sci. , Univ. of Tokyo, Tokyo.

In the motile unicelluler green alga *Chlamydomonas reinhardtii,* actin is a major constituent of the fertilization tubule in mating cells and the contractile ring at cytokinesis, and associated with flagellar inner dynein arms. As a first step to study these actin functions, we have determined the nucleotide sequences of cDNA and genomic clones of the *Chlamydomonas* actin gene. Only one actin gene was detected in the genome by Southern blot analysis. The sequence of the deduced 377 amino acids is highly homologous to actins from other eukaryotes (e. g., 98%, 89% and 85% identical to *Volvox* , rabbit skeletal and soybean actins, respectively). The intron structure of the gene is the same as that of *Volvox carteri* actin gene: it has eight introns in coding region and one in the 5' untranslated region. The present study thus suggests that only one conserved actin serves many functions in the cytoplasm and flagella of this organism.

SEA URCHIN OUTER-ARM DYNEIN INTERMEDIATE CHAIN 3 CORRESPONDS TO ODA6 OF *CHLAMYDOMONAS*.

K. Ogawa. Natl. Inst. for Basic Biol., Okazaki.

Microtubule motor dyneins are very large and complex molecules that consist of heavy, intermediate, and light chains. Antibodies directed against sea urchin intermediate chains also bound separately to two intermediate chains from *Chlamydomonas*. A cDNA encoding intermediate chains 3 of sea urchin ciliary dynein was cloned and sequenced. The predicted amino-acid sequence shows a high degree of sequence homology with that of the 70-kDa intermediate chain (ODA6) of *Chlamydomonas*, which is essential for assembly of a stable outer arm.

IDENTIFICATION OF *TETRAHYMENA* 14NM FILAMENT PROTEIN AS CITRATE SYNTHASE

H.Kojima and O.Numata. Inst.of.Biol.Sci., Univ.of Tsukuba, Tsukuba, Ibaraki, Japan

Recent cloning of a cDNA encoding *Tetrahymena* 14nm filament protein, indicated that its primary structure exhibits a high sequence identity with porcine citrate synthase. This led to the hypothesis that 14nm filament protein has dual functions as a citrate synthase in mitochondria and as the cytoskeleton in the cytoplasm. To examine this hypothesis, we established a modified method for isolating the citrate synthase from *Tetrahymena* mitochondria, being purified to 95% purity, and compared antigenesity and properties of enzyme activity between purified citrate synthase and 14nm filament protein. Anti-14nm filament protein antibody cross-reacted with citrate synthase and inhibited its enzyme activity. The enzyme properties of these proteins were identical. Thus, we concluded that 14nm filament protein and mitochondrial citrate synthase are identical. Moreover, to study compertmentarization of these proteins, By two-dimensional gel elctrophoresis, we examined the possibility of the post-translational modification of 14nm filament protein and citrate synthase.

CLONING OF ENDOSYMBIOTIC ALGAE IN *PARAMECIUM BURSARIA*.

○N.Nishihara , T.Takahashi , T.Kosaka and H.Hosoya.
Department of Biological Science , Faculty of Science , Hiroshima University , Hiroshima , 724 , Japan.

The green paramecium has many symbiotic algae (SA) (400 to 700 algae per paramecium). It has been reported that the host and the symbiont can be cultivated independently under laboratory conditions. The SA are morphologically very similar to free-living *Chlorella*, but not yet identified as *Chlorella*. When the aposymbiotic paramecium was re-infected with the SA, these SA began to proliferate in the host cell and apparently stopped their proliferation. To make clear the mechanisms of algal cell division, we tried cloning of these SA. Here we are going to discuss the conditions of cloning of these SA.

ncd MOTOR DOMAIN ATPase.

Takashi Shimizu[1], Elena Sablin[2], Ron Vale[2], and Edwin Taylor[3]
[1]Natl. Inst. Biosci. Human-Tech. & Natl. Inst. Adv. Interdiscipl. Res., Tsukuba, Ibaraki 305 Japan, and [2]Univ. Calif. San Francisco, CA 94143, U.S.A., and [3]Univ. Chicago, IL 60637, IL, U.S.A.

ncd is a protein having a domain homologous to the kinesin motor domain and has been shown to have motor activity by in vitro motility assay. While kinesin's motor domain is on the N-terminus of the 120 kDa heavy chain, ncd's motor domain is on the C-terminus of its 80 kDa polypeptide. More surprisingly, ncd was found to move towards the microtubule minus end, which is opposite to the polarity of kinesin, although their motor domains are homologous.

In the present study, we investigated the properties of ncd motor domain ATPase. ncd motor domain was expressed in *E. coli*, and purified by S-Sepharose chromatography. ncd motor domain thus obtained contained tightly bound adenine nucleotide that was exchanged with added ATP, and ADP, but not ATP, was found to be bound to ncd motor domain. This indicates that although the binding of ADP is tight, ADP and ncd motor domain polypeptide are in an equilibrium of associated state and dissociated state. Dissociation of ADP from ncd motor domain was very slow, but was accelerated by microtubules to a large extent. These properties are very similar to those of kinesin motor domain.

CO-POLYMERIZATION OF TUBULIN AND DYNEIN -γ-complex formation-

N.Ishikawa and T.Miki-Noumura
Department of Biology,Ochanomizu Univ.,Otsuka,Tokyo.

It has already been reported that dynein from *Tetrahymena* ciliary axonemes and DEAE-column purified tubulin from porcine brain co-polymerize into tubulin-dynein complex.

We studied the effect of dynein on the co-polymerization of the complex. Various concentration of dynein was added to tubulin at 0℃ and incubated at 37℃ for co-polymerization.The co-polymerized complex(γ-complex)was applied to SDS-polyacrylamide gradient gel electrophoresis to measure band density of the polymerized tubulin.At the concentration used (3mg/ml tubulin,>0.8mg/ml dynein), dynein seemed to have a little effect on the amounts of tubulin in the γ-complex.The complex formation and structure was further confirmed under a dark field microscope and an electron microscope.

THE EFFECTS OF ADP AND RIBOSE-MODIFIED ATP ON SLIDING DISINTEGRATION OF *TETRAHYMENA* CILIARY AXONEMES.

S.Kinoshita[1], T.Miki-Noumura[1], C.K.Omoto[2]. [1]Dept. of Biol., Ochanomizu Univ., Tokyo, [2]Dept. of Genetics & Cell Biol., Washington State Univ., Pullman, USA.

Previously we reported the stepwise sliding disintegration, measured by turbidimetric assay at 350nm, of *Tetrahymena* ciliary axonemes at high concentrations of ATP (Tanaka & Miki-Noumura, 1988).

To analyze the effect of high concentrations of ATP, we examined the effect of ADP and ATP analogs on sliding disintegration. High ATP concentration inhibited the extent of sliding disintegration. The inhibitory effect was eliminated by the addition of ADP in combination with low concentrations of ATP. The additions of higher ATP concentration in the presence of ADP inhibited sliding disintegration. The turbidimetric response was proportional to increasing concentrations of mantATP. Thus in contrast to the observation with ATP, higher concentrations of mantATP was not inhibitory.

These results show that ATP acts as an inhibitor to sliding disintegration and that ADP relieves this inhibition. The ATP inhibition is observed at concentrations above that necessary to cause sliding disintegration and suggests the affinity for ATP at the inhibitory site is lower than that at a catalytic site.

INTERACTION OF DOUBLET MICROTUBULES WITH 22S DYNEIN -THE EFFECTS OF CALCIUM-

A.Ishihara and T.Miki-Noumura.
Department of Biology,Ochanomizu Univ.,Otsuka,Tokyo.

Using *in vitro* motility assay, we found that movement of doublet microtubules on 22S dynein of *Tetrahymena* ciliary axonemes was strongly inhibited above 0.5mM ATP without Ca ions and 0.05 to 1mM ATP in the presence of 1mM Ca ions (Mori & Miki-Noumura, 1992).

To analyse how Ca ions regulate the motility *in vitro* of doublet microtubules on 22S dynein, we examined here the effect of Ca ions on association and dissociation of 22S dynein to doublet microtubules, based on the turbidimetric assay previously reported by Mitchell and Warner(1980). Furthermore, the effect of Ca ions on ATPase activity of 22S dynein was surveyed.

INTERACTION MECHANISM BETWEEN MICROTUBULES AND ACTIVE FRAGMENT OF A MICROTUBULE-ASSOCIATED PROTEIN.

K. Hayashi[1] K. Tokuraku[1], H. Murofushi[2], and S. kotani[1]. [1] Dept. of Biochem. Eng. Sci., Kyushu Inst. Tech., Iizuka, Fukuoka, and [2]Dept. of Biophys and Biochem., Fac of Sci., Univ. of Tokyo, Tokyo.

Microtubule-associated proteins (MAPs) consist of an amino-terminal projection domain and a carboxyl-terminal microtubule-binding domain. A MAP truncated fragment (A_4 fragment), which contains four repetitive microtubule binding sequence, was reported to be essential for microtubule formation (Aizawa *et al.*, *J. Biol. Chem.* **266**, 9481-9846 (1991)).

In this study, we furthered the analysis on the assembly-promoting mechanism of A_4 fragment. A_4 fragment binded to microtubules at a constant ratio. Equilibrium binding study indicated that the binding was a coorperative reaction. We also prepared a new truncated fragment, A_4-t fragment, excluding hydrophobic tail region from A_4 fragment. A_4-t fragment retained a high activity for the promotion of tubulin assembly. The assembled microtubules were morphologically normal, suggesting that the tail region is not important for assembly promoting activity.

CHARACTERIZATION OF MYOSIN LIGHT CHAIN KINASE FROM SEA URCHIN EGGS.

Go Totsukawa , Tadao Takahashi , Toshikazu Kosaka , and Hiroshi Hosoya.
Dept. of Biol. Sci., Fac. of Sci., Hiroshima Univ., Higashi-Hiroshima.

Myosin light chain kinase (MLCK) is thought to play important roles in regulation of the contractility of the actomyosin system during mitosis. To make clear the roles of MLCK during mitosis, we investigated the activity of MLCK in eggs of the sea urchin, *Hemicentrotus pulcherrimus*. Here, we detected the MLCK activity in the soluble cytoplasmic fraction of unfertilized sea urchin eggs. We fractionated unfertilized egg extract by using a gel filtration column (Sephacryl S-300) and its fraction had two peaks of MLCK activities (peak 1 and peak 2). Peak 1 was eluted at higher molecular weight and had MLCK activity either in the presence of EGTA or Ca^{2+}- calmodulin. Peak 2 was eluted at lower molecular weight and its MLCK activity was inhibited in the presence of Ca^{2+}-calmodulin. Two dimensional phosphopeptide mapping analysis showed that phosphorylation sites of myosin light chain (MLC) by peak 1 were similar to those by chicken gizzard MLCK. Phosphorylation sites of MLC by peak 2 differed from those by peak 1. These results suggest that Peak 1 kinase is different from peak 2 kinase.

MITOSIS SPECIFIC PHOSPHORYLATION OF MYOSIN LIGHT CHAIN KINASE (MLCK) IN SEA URCHIN EGGS.

Eiko Nakamura[1], Hikoichi Sakai[2], and Hiroshi Hosoya[1]. Faculty of Science, Hiroshima University, Hiroshima .[1] Faculty of Science, Japan Women's University, Tokyo .[2]

Myosin light chain kinase (MLCK) is known to direct contraction of the contractile ring. To understand how MLCK are controled during mitosis, we investigated roles of MLCK during mitosis in sea urchin eggs. Here we have detected an activity of MLCK Kinase (MLCKK) in soluble cytoplasmic fraction from both unfertilized and fertilized eggs of sea urchin, *Hemicentrotus pulcherrimus*. The MLCKK activity did not change during fertilization and showed temporary increase before cell division (metaphase). Two dimensional phosphopeptide mapping analysis showed that this mitosis - specific phosphorylation site of MLCK was different from phosphorylation sites of MLCK by cdc2 kinase.

ANALYSIS FOR PHOSPHORYLATION SITES OF DYNAMIN BY CDC2-KINASE

S.Komatsu[1], T.Shimizu[2], N.Hosoya[3], H.Mohri[4], M.Kunimoto[5], E.Nakamura[1], H.Hosoya[1] ([1]Department of Biological Science, Hiroshima University, Higashi-Hiroshima, [2]National Institute of Bioscience and Human-Technology, Tsukuba, [3]Otsuma Women's University,Tokyo, [4]University of the Air, Chiba, [5]The National Institute for Environmental studies)

Reorganization of the microtubule cytoskeleton is a typical mitotic phase-specific event. It is believed that cdc2 kinase plays an important role in the destruction of the interphase network of microtubules and the formation of the mitotic spindle at the G2 to M phase transition.

We have reported that a 100kD nucleotide-sensitive microtubule-bundling protein dynamin was mitotic-specifically phosphorylated by cdc2 kinase, and that microtubule-binding and GTPase activities of phosphorylated dynamin were reduced. Here we show that the phosphorylation sites of dynamin by cdc2 kinase are located within COOH-terminal domain which seems to be the microtubule-binding domain. Moreover, we found that dynamin has the sequence similar to that of an actin-binding protein α-actinin.

CHANGES IN CYTOSKELETAL AND REGULATORY PROTEINS DURING THE PROCESS OF ENUCLEATION IN EMBRYONIC ERYTHROID CELLS OF SYRIAN HAMSTER

H. Takano-Ohmuro and K. Morioka*, Dept. of Pharmacol., Fac. of Med., Univ. of Tokyo, Tokyo, *Div., of Tumor Biochem., The Tokyo Metropol., Inst. of Med. Sci., Tokyo

The process of enucleation in mammalian red blood cells appears to be analogous to cytokinesis. First, nuclear condensation occurs followed by nuclear peripherization (access of nucleus to the cell membrane) and subsequent enucleation.

We analyzed cytoskeletal proteins during this process in embryonic yolk-sac derived erythroid cells from Syrian hamster embryos from days 10, 11, 12 and 13. The localization of actin filaments around the nucleus was observed after nuclear condensation by TRITC-labeled phalloidin staining. With immunoblotting using antibodies against regulatory proteins, the existence of cofilin and profilin were detected for the first time in embryonic erythroid cells. In addition, caldesmon, tropomyosin and gelsolin which were also detected consistent with previous reports. The localization of these proteins is under investigation.

FOOT PROTEIN IN THE OBLIQUELY-STRIATED MUSCLE OF A MOLLUSCAS

T. ABE and A. MATSUNO. Dept. Biol., Fac. Sci., Shimane Univ.

The obliquely striated muscle has no T-systems, but has SR attached directly with cell membrane. Foot proteins (ryanodine receptors) were observed ultrastructurally at the space between the SR and cell membrane. We tried to prepare the SR-fraction including cell membranes and foot proteins from these cells, and tried to characterize the foot protein. The SDS-PAGE of the SR-fraction showed a thick band of foot proteins at 285.2KD, which is slightly smaller than ones of a rabbit (330.8KD) and a frog (330.8KD). The calsequestrine which was a Ca-binding protein in a rabbit (55KD) was not recognized, but another Ca-binding protein of highter molecular weight was appeared at 299KD.

INDUCTION OF MEMBRANE RUFFLING BY GROWTH FACTORS IN MORPHOLOGICALLY TPA-RESISTANT BALB/C3T3 TR4 CELLS

T.Enomoto [1,2] and Y.Asano[2]. [1]Dept of Rad. Biophys. and gen., Kobe Univ. Sch. of Med.,Kobe 650,Japan. [2]Dept of Oncogene Res.Inst.for Mic.Diseases, Osaka Univ., Osaka 565, Japan

To investigate the biological characteristics of a Balb/c 3T3 variant TR4 clone which is morphologically resistant to TPA and hyper-sensitive to v-src induced metastasis,we compared the responsiveness of the variant and its parent cells to growth factor-induced membrane ruffling. When the confluent cells were stimulated with PDGF, membrane ruffling was rapidly induced in TR4 but not in the parent cell cultures. There were no apparent differences in ^{125}I-PDGF binding kinetics between TR4 and parent cells. Similar membrne ruffling was induced by other growth factors such as insulin, IGF-I, acidic or basic FGF only in TR4 cells. Five out of 6 clones of stable fusion cells between TR4 and parent cells showed the parental type of responses to TPA and growth factors, indicating that the TR4 phenotype is recessive. These results suggest that the variant TR4 cells may acquire the genetic and recessive alterlation of a cellular factor which is responsible for the regulation of growth factor-mediated membrane ruffling and that this genetic alteration occurs at a common step downstream of growth factor-mediated cascades, rather than at their receptor level.

A 260-kDa PEPTIDE IN THE SMOOTH MUSCLE CELLS OF CHICKEN GIZZARD.

M.Tachikawa and K. Ohashi. Dept. of Biol., Fac. of Sci., Chiba Univ., Chiba.

Several cytoskeleton-associated components such as filamin, talin, vinculin, α-actinin and zyxin have been isolated from the low salt alkaline extract of chicken gizzard smooth muscle. In the extract, we found a 260-kDa peptide which was distinguishable from filamin on an SDS-PAGE gel. The extract was applied to a DEAE-Cellulofine column in the presence of 50 mM NaCl and eluted with 0.6 M NaCl. This fraction was then applied to a hydroxylapatite column and eluted with a solution containing 50 mM sodium phosphate buffer (pH 7.6). At this step, the 260-kDa peptide fraction was contamininted with actin and other minor proteins. Therefore, the band of the 260-kDa peptide was cut out from an SDS gel and injected into a rabbit. The antiserum reacted exclusively with the 260-kDa peptide among the whole peptides of the gizzard smooth muscle. The membrane affinity-purified anti-260-kDa peptide antibody was used for immunofluorescence microscopy. Mechanically isolated smooth muscle cells from a chicken was reacted with this antibody. Ovoid structures, which seemed to be dense plaques of the plasma membrane, were strongly fluorescent.

PURIFICATION OF *TETRAHYMENA* GROWTH PROMOTING FACTOR IN FETAL BOVINE SERUM

T. Matsuoka, T. Takahashi, T. Kosaka, and H. Hosoya.
Dept. of Biol.Sci., Fac. of Sci., Hiroshima Univ., Higashi-Hiroshima, Hiroshima, 724,

The growth and differentiation of cells are regulated to a large extent by extracellular signals. Many kinds of growth factors play important roles in mammals as such signals. As for other vertebrats and invertebrats, several reports have suggested the existence of proteins homologous to mammalian growth factors. To date, however, direct proof for such growth factors produced in lower vertebrats and invertebrats has not been reported.

Here we examined the effect of fetal bovine serum (FBS), which has growth promoting activities for mammalian cells, on the growth of *Tetrahymena pyriformis*. Our experiments showed the FBS has a marked activity to promote *Tetrahymena* growth. This growth promoting activity was purified from FBS by fractionating on several chromatographies using DEAE cellulose, hydroxylapatite, and phosphocellulose columns. The promoting activity was finally purified by a gel filtration column using Sephacryl S-300 and eluted at a molecular weight of 60kD to 100kD. The activity was heat stable, and not inactivated by dialysis.

KETTIN-LIKE 500 KDA PROTEIN FROM CRAYFISH CLAW CLOSER MUSCLE.

S. Maki, Y.Ohtani, S. Kimura and K. Maruyama.
Dept. Biol., Chiba Univ., Chiba.

Bullard and coworkers (1993) reported a new protein, kettin, localized in the periphery of the Z line in waterbug striated muscle (500 kDa in flight and 700 kDa in leg muscle). In the present work, kettin-like 500 kDa protein was isolated from crayfish claw closer muscle using a modified procedure to isolate connectin from crayfish closer muscle (Manabe *et al.*,1993).

Kettin-like protein, 500 kDa, was a filament of approximately 300 nm under an electron microscope. This length was significantly longer than that of projectin, 1200 kDa (240-280 nm). Polyclonal antibodies to the 1200 kDa fragment of α-connectin from rabbit skeletal muscle (Pc1200) crossreacted with the crayfish 500 kDa protein. Immunofluorescence with Pc1200 revealed that kettin-like protein was localized in the periphery of the Z line in the I band as in insect striated muscle. Immunoelectron microscopy confirmed this result. Thus the present work strongly suggests that the 500 kDa protein of crayfish clow muscle is closely related to insect muscle kettin. Furthermore, it appers that kettin is widely distributed in arthropod striated muscle.

DIFFERENCES IN LOCALIZATION OF CONNECTIN-LIKE PROTEINS BETWEEN LEG AND FLIGHT MUSCLE OF A BEETLE

Y. Ohtani, S. Maki, S. Kimura and K. Maruyama. Dept. Biol. , Chiba Univ., Chiba.

Indirect flight muscle of some insects has a sarcomere consisting of short I band and regular size of A band, with a sarcomere length of about 3 μm at rest. On the other hand, leg muscle sarcomere is long (about 7 μm at rest). The present immunofluorescence and immunoelectron microscopic study was carried out to reveal localizations of connectin-like proteins in flight and leg muscle of a horned beetle, Allomyrina dichotomus.

Projectin, 1200 kDa, were present in both types of muscles. Projectin was localized in the I band in flight muscle, but was localized in the A bane in leg muscle. These different localizations are the same as in crayfish claw opener and tail stretcher muscles (Manabe et al., 1993).

In the beetle leg muscle, connectin-like 3000 kDa protein appeared to be localized in the I band, as in crayfish claw giant sarcomeres. To detect the localization, SM1, monoclonal antibody to chicken breast muscle connectin and polyclonal antibodies to crayfish claw muscle 3000 kDa protein were used. The two kinds of the antibodies reacted with the beetle leg muscle protein.

Thus it is concluded that in arthropod giant sarcomeres connectin-like 3000 kDa protein behaves as vertebrate skeletal muscle connectin.

LOCALIZATION OF DESMIN IN SKELETAL MUSCLE : EFFECT OF SARCOMERE LENGTH.

[1]M. Kuroda, Y.[2]Jinguuji, [3]Y. Kawamura, and [3]K. Maruyama.
[1] Dept. of Biol., Fac. of Sci. Shimane Univ. Matsue, [2] Gunma Prefectural College of Health Sciences, Maebashi, and [3] Dept. of Biol. Fac. of Sci. Chiba Univ. Chiba.

As have shown previously, desmin filaments form loose 3D-network around myofibrils of skeletal muscle. In this paper, we will report the distribution of desmin filament network at various sarcomere lengths. Immunofluorescence microscopy of glycerinated chicken breast muscle indicated that anti-desmin fluorescence patterns did not change upon contraction of myofibrils. Major staining was observed at Z-disks. Immuno-electron microscopy of chemically skinned myofibers prepared at different sarcomere lengths gave similar results. The protein-A conjugated gold labels for desmin were detected mainly around the Z-disk regions and along inter-myofibrillar spaces irrespective to the sarcomere length. These results also suggested that the spatial arrangement of desmin filaments did not change significantly during contraction-relaxation.

EMBRYONIC TYPE OF α-CONNECTIN IN CHICKEN SKELETAL MUSCLE.

H. Ohtsuka, H. Kume, S. Kimura and K. Maruyama. Dept. Biol., Chiba Univ., Chiba.

α-Connectin is approximately 3000 kDa in chicken skeletal muscle and it links the Z line to the myosin filament in a sarcomere. Yoshidomi and coworkers (1985) reported that embryonic α-connectin was larger in molecular mass than adult one. The present study confirmed this conclusion but could not find any intermediate-sized α-connectin (neonatal type).

SDS gel electrophoresis was performed according to the Laemmli's procedure using 2-2.5 % polyacrylamide gels. α-Connectin was detected in 12 day embryonic muscle and its mobility was slightly but significantly slower than that of adult skeletal muscle α-connectin. There was only this band for α-connectin in embryonic muscle. The mobility did not change during embryonic development and during hatch. One day after hatch a new band appeared below the embryonic band and the mobility was the same as that of adult breast muscle α-connectin. The relative amount of adult type α-connectin gradually increased accompanied by decrease in the amount of embryonic type until 10 day after hatch. At 12 day after hatch the embryonic type completely disappeared.

CONTRACTION OF THE MECHANICALLY ISOLATED SMOOTH MUSCLE CELLS.

H.Nakagawa, A.Kumagai and K. Ohashi, Dept. of Biol., Fac. of Sci., Chiba Univ., Chiba.

Single smooth muscle cells from gizzard were isolated without using protease. Fresh chicken gizzaed smooth muscle was sliced into small pieces, dipped in a solution containing 75 mM NaCl, 10 mM Na-PO_4 buffer (pH 7.2), 10 mM EDTA, 0.5 mM PMSF, and 50% glycerol, and stored for more than one week at -20°C. A piece of the tissue was then homogenized gently in a solution containing 10 mM EGTA. Spindle-shaped smooth muscle cells were isolted from the tissue. In the presence of calcium ions, the isolated cells as a whole contracted into ovoid structures with several stripes. In the pH 6.8 solution, the ATP dependent contraction of single cells occurred at KCl concentrations from 20 mM to 150 mM. As the concentration of KCl became higher, several cytoskeletal/ contractile components such as filamin, myosin, caldesmon, actin, tropomyosin, and calponin were released easily from the cells during isolation and contraction. When the KCl concentration was 50 mM, the isolated cells were able to contract in the pH range of 6.0 to 7.5.

CHANGE OF RHODAMINE-PHALLOIDIN STAINING PATTERNS DURING STRIATED MUSCLE MYOFIBRILLOGENESIS.

M. Sasaki and M. Kuroda. Dept. of Biol., Fac. of Sci., Univ. of Shimane, Matue.

It is known that rh-PHD, a specific fluorescence probe for F-actin, does not stain I-filaments of myofibrils uniformly. When glycerinated myofibrils was used, rh-PHD stained Z-line and 30~50% of pointed end regions of I-filaments. In this paper we show that rh-PHD staining pattern on I-filaments changes during muscle development: from the nonmuscle type to muscle specific type. We classified the fluorescence staining patterns during myofibrillogenesis of striated muscle as following; (1) uniform staining along stress fiber-like structures, (2) periodic dot-like staining on I-bands, (3) staining on Z-line and entire I-filament but not H-zone, and finally (4) the same pattern detected in matured glycerinated myofibrils. These patterns were observed both in skeletal and cardiac muscles in culture. Relation of rh-PHD staining patterns to myofibrillogenesis is discussed in conjunction with the corresponding localization of scaffolding proteins.

ACTIN-LINKED REGULATION IN SCALLOP STRIATED MUSCLE. 1. TEMPERATURE DEPENDENCE

Y. Yazawa[1] and M. watanabe[2].
[1]Dept. of Nutritional physiol., Hokkaido Univ. of Education at Asahikawa, Asahikawa
[2]Medical coll. of Kitazato, Kanagawa.

In many invertebrates, notably mollusca, the regulation is associated with myosin. In scallop myosin molecule, EDTA light chain has been shown to be directly involved in the regulation mechanism. Goldberg and Lehman reported that an actin-linked troponin-like system might be present in scallop striated muscle. We isolated thin filaments and actin from acetone dried powder of scallop striated muscle. When scallop thin filaments were added to scallop myosin, the Ca^{2+} sensitivity became much higher than that of actomyosin reconstituted of scallop myosin and actin. Tempereture dependences of Mg^{2+}-ATPase activities were investigated in scallop natural actomyosin and reconstituted actomyosin at 15℃ or 25℃. The Ca^{2+} sensitivities of Mg^{2+}-ATPase activity were a little higher at 15 ℃ than that at 25℃.

ACTIN-LINKED REGULATION IN SCALLOP STRIATED MUSCLE. 2. THE Ca^{2+} SENSITIVITIES OF DESENSITIZED AND RECONSTITUTED SCALLOP ACOMYOSIN Mg^{2+}-ATPase ACTIVITIES

Y. Yazawa & M. Kamidochi
Dept. of Nutritional Physiol., Hokkaido Univ. of Education at Asahikawa, Asahikawa

The Ca^{+} sensitivities of natural, desensitized, and reconstituted actomyosin (NAM, DAM, RAM) Mg^{2+}-ATPase activities were investigated. DAM was prepared with the EDTA treatment of NAM. NAM treated with EDTA was centrifuged after dilution and the precipitates was obtained as DAM and the supernatant was composed of thin filaments and EDTA-LC of myosin (thin+EDTA−LC). Mg^{2+}-ATPase activities of DAM were 0.27 μmol Pi/mg. min (U) irrespective of Ca^{2+} concentrations, when EDTA-LC was added to DAM, the Ca^{2+} sensitivity was restored to 50%. The Ca^{2+} sensitivity of Mg^{2+}-ATPase activity of actomyosin reconstituted from DAM and (thin+EDTA−LC) was 83.3%.

Our results have shown the existence in scallop striated muscle of a new actin-linked system different from the TN-TM system, in addition to the myosin-linked system.

EXPRESSION OF COFILIN ISOFORMS IN DYSTROPHIC MOUSE AND OTHER MAMMALS.

K. Okada, M.Takano,K. Mohri, T. Totsuka*, S.Ono, H. Abe, and T. Obinata. Department of Biology, Chiba University, Chiba263,and *Inst. of Dev. Res., Aichi Pref. Colony,Aichi

Cofilin, a low Mr actin- regulatory protein, is widely distributed in eukaryotes.We have previously demonstrated that two isoforms of cofilin are present in mouse tissues; one is predominantly expressed in muscle tissues (M-type cofilin) and the other exist in nonmuscle tissues (NM-type cofilin) . In addition,we have reported that the a mount of cofilin in skeletal muscle is significantly increased in dystrophic dy mouse. In this study, the diversity of cofilin isoforms among other mammals was examined by a combination of two-dimentional gel electrophoresis and immunoblotting and by Northern blotting. Interestingly, in rabbit, a single cofilin isoform,the mobility of which is the same as M-type cofilin, was detected in both muscle and nonmuscle tissues.The cDNA probe for the mouse M-type cofilin hybridized more strongly with rabbit brain RNA. These results suggest that a single cofilin, which is structurally similar to M-type cofilin, is expressed in rabbit. On the other hand, we confirmed by Northern blotting that the expression of M-type cofilin is predominantly increased in dystrophic skeletal muscle.

DETERMINATION OF THE DOMAIN STRUCTURE OF TWO ACTING BINDING PROTEINS, COFILIN AND DESTRIN, USING LIMITED PROTEOLYSIS AND SECONDARY STRUCTURE PREDICTION.

M. Imanaka, J. Yasuda, T. Oonuma, K. Arima, and S. Kotani. Dept. of Biochem. Eng. Sci., Kyusyu Inst. Tech., Iizuka, Fukuoka.

Cofilin and destrin are two related mammalian actin-binding protein. They both have the conserved actin binding sequence, and their entire primary structures show 84% homology. However, the two proteins possess distinct properties in some points.

In order to understand more clearly the actions of cofilin and destrin on actin, it is necessary to determine their complete tertiary structure. For this purpose, we are analysing the two proteins by nuclear magnetic resonance spectroscopy (Oonuma *et al, Zool. Sci.* 10, 6s). In this report, domain structures of cofilin and destrin were studied by limited proteolysis, circular dichroism spectroscopy, and secondary structure prediction. Among several types of protease, Chymotrypsin most effectively digested destrin, giving a stable fragment with an apparent molecular mass of 8kDa. Our preliminary sequence analysis indicated that the fragment contains the actin binding dodecapeptide sequence.

PRIMARY STRUCTURE AND TISSUE DISTRIBUTION OF COFILIN/ADF HOMOLOGUES IN XENOPUS.

H.Abe, T. Obinata, M. Zuber *, and J. R. Bumburg *. Department of Biology, Chiba University, Chiba 263 and * Department of Biochemistry, Colorado State University, CO 80523, USA.

Cofilin, a pH-dependent actin-regulatory protein, is widely distributed in eukaryotes. In this study, we screened cDNA library constructed from srage 30 Xenopus embryos with chiken cofilin and ADF cDNA as probes. Two types of cofilin/ADF homologues, designated as A9 and A11, were obtained with the respective probes. Both cDNAs encoded entire coding sequences of 168 amino acids and their primary structures were 92.9% identical with each other. Since *Xenopus laevis* is of pseudotetraploid origin, these two homologues may be derived from duplicated genes. Northern blot analyses revealed that both homologues are expressed in brain, heart, and stomach of adult frog, but scarcely in adult skeletal muscle. Strong signals were also detected in RNA extracted from oocytes with the respective probes, while their sizes were different from those in the other tissues. *In situ* hybridization studies demonstrated that both homologues were abundantly expressed in the neural tissues and the somites of stage 22 to 35 embryos.

PROTEINS FORMING Ca^{2+} DEPENDENT DNA-PROTEIN COMPLEX FROM VARIOUS ORGANS OF THE RAT

T. Kido and H. Namiki
Department of Biology, School of Education,
Waseda University, Tokyo

When extract of nuclear with Tris-HCl buffer was mixed with DNA in the presence of 5mM Ca^{2+}, several types of proteins were coprecipitated along with DNA, some of which could be dissolved in a buffer containing EGTA. The result of electrophoretic analysis of these proteins coprecipitated with various DNA, suggests that they form Ca^{2+} dependent DNA-protein complex (CaDPC). CaDPC-proteins have no or very low binding capacity for Mg^{2+}. Comparative studies of CaDPC-proteins among organs (liver, kidney, brain and testis) showed molecular diversity on SDS PAGE. They may play important roles in differentiated cellular functions.

OCCURRENCE OF RETINAL AND ITS ISOMER COMPOSITION IN THE EGGS OF THE ASCIDIAN, *HALOCYNTHIA RORETZI*.

S. KAJIWARA[1], T. IRIE[2] and T. SEKI[3]. [1]Dept. of Biol., Fac. of Edu., Iwate Univ, Morioka, [2]Osaka Meijo Women's Coll., Osaka, [3]Dept. of Health Sci., Osaka Kyoiku Univ., Osaka.

The retinoids in the eggs of the solitary ascidian, *Halocynthia roretzi*, were analyzed by high-performance liquid chromatography. Most retinoids contained were retinal (>>99%). The four isomers of retinal were present in the eggs; all-trans (50%), 9-cis (8%), 11-cis (21%) and 13-cis (21%), although most retinal in vertebrate eggs is all-trans form. This isomer composition of the ascidian eggs is similar to that of light equilibrated retinal solubilized in ethanol. Retinol or retinyl ester was hardly detected. Most retinal was present in the supernatant of the egg homogenate, showing that the retinals are bound to a water soluble protein.

These results suggest that retinal is the most important retinoid in the ascidian eggs, similarly to the eggs of amphibians and teleosts. However, the molecular environment around the retinal is different from that in the vertebrate eggs. It should be considered that the presence of retinal(s) in the eggs of vertebrates is inherited from those of protochordates through the evolutional process.

PTERIDINE BIOSYNTHESIS IN THE THREE PHENOTYPES OF A TERRESTRIAL ISOPOD ARMADILLIDIUM VULGARE

S.Negishi[1], Y.Hasegawa[1], T.Sueoka[2] and S.Katoh[2]. [1]Dept. of Biol., Keio Univ., Yokohama and [2]Dept. of Biochem., School of Dentistry, Meikai Univ., Sakado, Saitama.

A terrestrial isopod, Armadillidium vulgare (wild type) displays a black or grey body color due to ommochrome pigment granules in chromatophores of the integument. The red and white phenotypes of A. vulgare are thought to be deficient in the pigment genesis by the observation of a fine structure of the integument. Ommochrome contents of the red phenotype are different in males and females as well as those of the wild type, while pteridine contents in the integument of the red phenotypes have not yet determined. The white phenotype has few ommochrome pigment granules in the integument, however, it exhibits yellow markings under a light microscope. The determination of pteridine contents by HPLC and fluorescent and/or ultraviolet spectro-photometry revealed that the white phenotype has the same kinds of pteridines as those of the wild type and red phenotype. Electron micrographs of the white phenotype integument depict a number of electron-lucent granules to be located in a cell beneath the epidermal cells. These facts suggest that pteridine-containing yellow chromatophores are involved in the expression of the white body color.

COMPARATIVE STUDIES ON PHOSPHOLIPIDS OF DEEP-SEA AND SHALLOW -SEA BIVALVES

K. Nishimura[1], A.C. Suzuki[1], M. Nakazawa[2], E. Eguchi[2]. [1]Dept. Biol., Keio Univ. Sch. Med., Yokohama, [2]Dept. Biol. ,Yokohama City Univ., Yokohama

Phospholipids and their fatty acid compositions of deep-sea bivalve mollusca *Calyptogena soyoae* and shallow-sea bivalve mollusca *Meretrix lusoria* were comparatively studied by thin-layer chromatography and gas-liquid chromatography. In their gill, foot and adductor, relative amounts of the major phospholipids, phosphatidylethanolamine and phosphatidylcholine were different by species. The predominant part of polyunsaturated fatty acids in *Calyptogena* was 20:2, while in *Meretrix* 20:5 and 22:6 were abundant. The ratio of unsaturated acids / saturated acids of *Calyptogena* was significantly higher than that of *Meretrix.* In *Calyptogena* gill carrying endosymbiotic bacteria, lyso-PE and lyso-PC were markedly abundant.

PROPERTIES OF OMMOCHROME-BINDING PROTEIN FROM THE PIGMENT GRANULES OF THE SILKWORM, *BOMBYX MORI*.

H. Sawada[1], M. Tsusué[1] , T. Iino[2]
[1]Biological Lab. School of Liberal Arts, Kitasato Univ., Sagamihara [2]Dept. of General Education, Nihon Univ., Tokyo

We have already reported that the pigment protein separated by SDS-PAGE had an activity binding with xanthommatin. Furthermore, we reported an occurrence of ommin in larval integument of the insect for the first time. In the present study, we report that the pigment protein separated by 2-dimentional-PAGE has also an activity binding with not only xanthommatin but also with cinnabarinic acid and ommin. The protein has an affinity for phenoxazinone ring of ommochrome. These data indicate that xanthommatin and ommin were localized with the same binding protein in the pigment granules of epidermal cells. This fact suggests an important function in localization and accumulation of ommochrome. The protein was found to be glycosylated. Lectin analysis suggested that mannose, fucose and sialic acid were present. N-terminal sequence of the protein can not be determined because N-terminal blockage. We tried to release of N-terminal blockage. However, it was not successful by deacetylation, depyroglutamation and deformylation. The amino acid composition of the protein was determined. Ommochrome granules are synthesized through rough-surfaced endoplasmic reticulum via Golgi complex, because fucosyltransferase and sialyltransferase were localized in Golgi complex. The present data give us a part of a whole image of ommochrome synthesis and accumulation of the pigment in insects.

COLD ADAPTATIONS IN *DROSOPHILA*. I. EVIDENCE FOR SUBSTRATE SPECIFICITY DURING FATTY ACID INCORPORATION INTO TRIACYLGLYCEROLS.

T. Ohtsu*[1], M. T. Kimura+ and C. Katagiri‡, *Dept. Biol., Fac. Sci., +Grad. Sch. Envi. Earth Sci., and ‡Biochem. Lab., Inst. of Low Temp. Sci., Hokkaido Univ., Sapporo.
[1]Present address; Hibernation control Project, Kanagawa Academy of Science and Technology Foundation.

Some cool-temperate species belonging to the *Drosophila melanogaster* species group avoid to solidify triacylglycerols (TAGs), a major energy reservoir, during overwintering by increasing of unsaturated fatty acid synthesis and decreasing of saturated TAG synthesis. In order to clarify the latter phenomena, the compositions of fatty acids at the secondary position of TAGs were analyzed by lipase digestion. The compositions of TAG molecular species were further simulated on the basis of thir unsaturation index and the compositions of fatty acids constituents. In consideration of TAG synthesis, the results support that 1-acyl 3-phosphoglycerol acyltransferease plays a key role in the low percentages of saturated TAGs in cool-temperate species.

COLD ADAPTATION IN *DROSOPHILA*
II. PHYSIOLOGICAL ROLES OF CUTICULAR HYDROCARBONS

C. Katagiri[1], M.T. Kimura[2] and T. Ohtsu[3,4].
[1]Biochem. Lab., Inst. of Low Temp. Sci., [2]Grad. Sch. Envi. Earth Sci. and [3]Dept. Zool., Fac. Sci., Hokkaido Univ. Sapporo.
[4]Present address; Kanagawa Acad. Sci. Technol. Found.

We have studied roles of lipids in cold adaptation of insects. In the present paper, we examined cuticular hydrocarbons of diapausing and non-diapausing adults of a cool-temperate species, *Drosophila triauraria.* Cuticular hydrocarbons have long been recognized to be important regulators of cuticular permeability, but their exact roles have remained unresolved. GLC and GC-MS studies revealed that the cuticular hydrocarbon compositions are completely different between the diapausing and non-diapausing adults. TLC-FID measurements also showed that the hydrocarbons of the diapausing are highly unsaturated compared with those of the non-diapausing. Taking account of the thermal behaviour of the hydrocarbons, the cuticular hydrocarbons were demonstrated to contribute to the cuticular permeability even when insects overwinter.

IDENTIFICATION OF FURIN mRNA OF *BOMBYX MORI*

K. Yano, S. Izumi and S. Tomino
Dept. Biol., Tokyo Metropol. Univ., Tokyo

Many of secretory proteins are synthesized as high molecular weight precursors which are then cleaved to produce mature proteins. Previously, we have shown that two subunits of vitellogenin of *Bombyx mori* are derived from a primary translation product by proteolytic cleavage. R-S-R-R sequence just upstream of the cleavage site of *B. mori* previtellogenin is consistent with the consensus sequence for recognition site of mammalian proprotein converting enzyme, furin. To examine whether proteolytic processing system analogous to those of mammals exists in insect, we attempted to detect mRNA for furin homologue in *B. mori*.

A 335 bp DNA fragment was amplified from the fat body poly(A)$^+$ RNA by RT-PCR method. Deduced amino acid sequence of this fragment was highly homologous to those of furin members. RNA blotting with the PCR product as a probe indicated that a 4.2 kb-RNA exists in the fat body cells through the larval to pupal stages and in the gut of the fifth instar larvae.

PURIFICATION OF SP1 RECEPTOR FROM SILKWORM, *BOMBYX MORI*

J. Wang, S. Izumi and S. Tomino
Dept. Biol., Tokyo Metropol. Univ., Tokyo

In the silkworm, *Bombyx mori*, storage proteins occur in two forms termed SP1 and SP2, respectively. Specific sequestration of storage proteins by the fat body cells takes place at about the stages of silk-spinning to larval-pupal ecdysis. To study the mechanism of storage protein uptake in *B. mori*, we have purified the SP1 receptor from the fat body plasma membrane.

Plasma membrane of the fat body cells from female larvae at about the silk-spinning stage specifically interacted with the ^{125}I-labeled SP1. When the Triton-X extract of plasma membrane was incubated with an anti-SP1 antibody in the presence of Ca^{++}, a 120 kDa protein was found in the immunoprecipitate in addition to the subunits of SP1 and immunoglobulin. Ligand-blotting of the membrane proteins with the ^{125}I-labeled SP1 probe together with the competition experiments strongly suggested that 120 kDa protein is SP1-receptor. Purification of 120 kDa protein was achieved from the membrane extract by means of preparative gel electrophoresis, and an antibody was SP1 prepared against purified protein. By use of the antibody, interaction of SP1 with the fat body plasma membrane was studied.

DEVELOPMENT OF CELL-FREE TRANSCRIPTION SYSTEM AND ANALYSES OF TRANSCRIPTION FACTORS FROM FAT BODY OF THE SILKWORM, *BOMBYX MORI*

E. Mine, S. Izumi and S. Tomino. Dept., Biol., Tokyo Metropol., Univ., Tokyo.

A nuclear extract was prepared from the larval fat body of *Bombyx mori*, and a homologous *in vitro* system was developed for the transcription of major plasma protein genes of *B. mori*. The gene for SP1 and adenovirus 2 major late (AdML) gene were faithfully transcribed in the nuclear extract prepared from the fat body of female fifth instar larvae. To identify and characterize candidates for transcription factors which regulate the tissue-specific expression of SP1 gene, gel-retardation assay and footprinting analysis of the fat body nuclear extracts were performed. The upstream regions of SP1 and SP2 genes share a stretch of nucleotide sequence in common. This sequence interacted with fat body nuclear factors to form specific complex whose electrophoretic mobility is distinct from those with the nuclear extracts of posterior silk glands and cultured BmN cells. Based on the result of DNase I footprinting analysis together with the computer search for promoter regions of other insect genes transcribed in the fat body cells, a consensus sequence "TGAA(T/A)TT(T/A)(T/A)" is proposed for a sequence element which may participates in the fat body specific expression of insect genes.

A INITIATOR PROTEIN FOR THE INITIATION OF DNA REPLICATION IN *XENOPUS* EGGS

K. Okuhara[1], M. Shioda[2], K. Murakami-Murofushi[3], H. Murofushi[1]
[1]Dept. of Biophys. and Biochem., Fac. of Sci., [2]Dept. of Physiol. Chem. and Nutri., Fac. of Med., Univ. of Tokyo, Tokyo, [3]Dept. of Biol., Fac. of Sci., Ochanomizu Univ., Tokyo.

Local opening of duplex DNA is the first step in DNA replication. This process would be catalyzed by a protein factor (initiator protein), however, no such factor has been identified in eukaryotic cells. Here, we purified a protein with a molecular mass of about 300 kDa from *Xenopus* eggs, based on the ability to introduce a negative twist to double-stranded DNA. This protein catalyzed unwinding of duplex DNA and could induce *de novo* DNA synthesis on the duplex DNA templates together with DNA polymerase α-primase. Therefore, this protein is suggested to be a initiator protein of eukaryotes.

UP-REGULATION OF CATHEPSIN D EXPRESSION BY THYROID HORMONE IN METAMORPHOSING TADPOLE OF *XENOPUS LAEVIS*.

M. Mukai and K. Yoshizato. Dept. Biol. Sci., Hiroshima Univ., Higashihiroshima, Hiroshima 724.

In amphibian metamorphosis thyroid hormone (TH) triggers the transition from larva to adult. Recent studies on mammalian TH - thyroid hormone receptors (THRs) reveals that TH interacts nuclear THRs or RXR/THR complexes which directly regulates gene expression through the thyroid hormone responsive element (TRE) located in the up-stream of target genes. In this context, amphibian metamorphosis may be considered as a transcriptional shift from larval state to adult one which driven directly by TH on each genes. However, little is known about gene regulation by TH in amphibian metamorphosis. We aims at understanding how TH changes larval system to adult one at the gene expression level.

In this study we analyze transcriptional regulation of cathepsin D which is involved in the process of removal of larval tissues. We found that TH enhances cathepsin D expression in premetamorphic larvae and the cathepsin D gene is categorized as a late responsive gene for the TH stimulation.

AGE-RELATED CHANGES OF MITOCHONDRIAL TRANSLATION CAPACITIES OF MOUSE.

D. Takai and J.-I. Hayashi. Inst. of Biol. Sci., Univ. of Tsukuba, Tsukuba, Japan.

Reduction of mitochondrial respiratory functions, particularly of COX activities, and accumulation of various somatic mutations in mtDNA have been proposed to be involved in human aging. However, there is no convincing evidence that the mtDNA mutations are responsible for the age-related mitochondrial dysfunction. In this study, we developed the procedure to analyze mtDNA translation capacities in isolated mitochondria. Using this procedure, we found that the capacities in isolated mitochondria from brain, liver, and skeletal muscle of mice declined with aging. Therefore, our systems are very useful to study the age-related dysfunction of the mitochondrial proteins coded in mtDNA.

GENETIC POLYMORPHISM OF THE INTRON IN NA+/K+-ATPASE ALPHA-SUBUNIT GENE OF THE SEA URCHIN, *HEMICENTROTUS PULCHERRIMUS*.

K. Yamazaki, M. Asami, T. Maruyama, T. Ihara, K. Mitsunaga-Nakatsubo* and I. Yasumasu. Dept. of Biol., Sch. of Educ., Waseda Univ., Tokyo and *Dept. of Gene Sci., Fac. of Sci., Hiroshima Univ., Hiroshima.

One of the introns in Na+/K+-ATPase α–subunit gene of the sea urchin, *H. pulcherrimus*, varies in sequence and length as a genetic polymorphism.

Genomic PCR, with two primers that lie on the exons and can amplify the intron sequence, generates two kinds of the PCR products from genomic DNA of a sea urchin embryo although only one product from that of a parthenogenesis-embryo. These results suggest that this gene exists as a single copy gene in haploid genome.

Now we are studying a whole sequence of the intron and a polymorphism in length on another intron.

5'-END CLONING OF NA+/K+-ATPASE α SUBUNIT cDNA OF THE SEA URCHIN, *HEMICENTROTUS PULCHERRIMUS*.

C. Okamura, K.Yamazaki and I. Yasumasu. Dept. of Biol., Sch. of Educ., Waseda Univ., Tokyo.

Primer extension reaction, using a specific primer to Na+/K+-ATPase α subunit cDNA, indicated 3 bands in sea urchin embryos development, 2 among which were found in mesenchyme blastulae, gastrulae and prisms. These 2 bands were larger about 50 - 65 bp than a known clone and another band, found at all examined stages, was almost the same length to a known clone. Three different clones were also obtained, using a total RNA at the late gastrula stage as a template and specific primers to a known clone as a primer by 5' RACE(5' Rapid amplification of cDNA ends) method. Probably, 2 of 3 clones were transcribed in embryos development between the mesenchyme blastula and prism stage.

AN ANALYSIS OF THE DISTRIBUTION PATTERN OF POLYPS OF AURELIA AURITA

K. Iwao, H. Miyake and Y. Kakinuma
Dept. of Biol., Fac. of Sci., Kagoshima Univ., kagoshima

There found a variety of invertebrate species which adhere to the bottom of the floating bridges around the Kagoshima Bay area. Furthermore, the formation of the colony of Aurelia aurita polyps is observed on the surface of these invertebrates; in particular, many polyps were found on the shell of Mytilus edulis and on the bodies of Styela plicata. The distribution shows a random one through a year. Moreover, the population formation of the asexual reproduction of transplanted polyps were observed and analyzed in our laboratory. At the early stage, all four modes of the asexual reproduction of polyp show a concentrated pattern and the pattern was independent of inhabited circumstances, an amount of food, and temperature changes. The distribution pattern becomes random as the colony grows. From this fact it can be inferred that there exist some recognition and identification between polyps.

NEMATODE ASSEMBLAGE IN A SMALL COVE POLLUTED BY FISH FARMING.

K. Kito[1] and T. Kikuchi[2]. [1]Dept. of Biol., Sch. of Med., Sapporo Medical Univ., Sapporo, [2]Amakusa Mar. Biol. Lab., Fac. of Sci., Kyushu Univ., Amakusa.

Fauna and population dynamics of the nematode assemblage was studied in the Tomoe Cove, Amakusa, where bottom water and sediment were polluted by the organic input from fish farming. Periodic sampling was carried out from June 1993 to June 1994, to investigate the seasonal change of the assemblage in response to the fluctuations of physico-chemical conditions of the bottom environment. The present report has dealt with a part of the results concerning species composition, abundance and distribution of the nematodes in the cove.

Diversity of the nematode fauna was low and 14 species have been distinguished for the present. Individual number of the nematodes was abundant at the station located near the floating cages for fish farming and facing on the mouth of the cove, more than 2800 ind./10 cm^2 throughout the year. Nematode density decreased in September when the total sulfide content increased and the RPD layer rose up to near or on the surface of the bottom sediment. Significant decrease of their number occurred at the station surrounded by the cages, 4 ind./10 cm^2 at lowest. Nematode species respectively showed a specific vertical distribution in the sediment.

AGE, GROWTH, MATURATION, AND PHENOMENON OF THE UPS-AND-DOWNS OF AURELIA AURITA.

H. Miyake, K. Iwao and Y. Kakinuma.
Dept. of Biol., Fac. of Sci., Kagoshima Univ., Kagoshima

In Kagoshima Bay, ephyra emerges during January and March, metephyra emerges during February and April, and medusa does from late in February. By determining the age from the number of water vascular canal branches, it was found that the population consists of the biennial (1993) and new (1994) individuals. The population of these individuals' growth rapidly in the period of a rising water temperature-during March and June; the new individual becomes the same size mode as the biennial one after June. The degree of maturation by age indicates that the sixth-branched biennial reached its maturation in March, the fifth- branched biennial reached the maturation in April, and after May the fourth branched new individual reached the maturation and ejected planulae.

The ups-and-downs of Aurelia aurita disappears from the surface and moves in the bottom where the change of the salt concentration is less affected. The same result was also obtained by our Laboratory experiment. Thus it can be said that the main cause of the ups-and-downs in the salt content of sea water.

THE NUDIBRANCH, *GYMNODORIS NIGRICOLOR* BABA, PARASITIC WITH MARINE GOBIES.

D. Osumi[1] and T.Yamasu[2]. [1]Dept. Biol. Fac.Sci. and [2]Dept. Biol. Div. Gen. Edu., Univ. Ryukyus.

A short report on symbiosis between a nudibranch and a goby has been described (Williams Jr and Williams, 1986) from Okinawan water. Similar associations between the same nudibranch species and the same and other two species of gobies were confirmed in Oujima and Sesokojima islands, both off shore the Okinawajima island in 1993 and 1994. The adult nudibranchs, *Gymnodoris nigricolor* Baba were found abundant on the fins of the three species of gobies, *Amblyeleotris ogasawarensis*, *Ctenogobiops pomastictus* and *C. feroculus* simbiotic all with snapping shrimps.

Population densities were 1.8 nudibranchs / 15.4 gobies (per every $25m^2$) and 1 / 50 in Oujima and Sesokojima respectively. The nudibranchs attached to all kinds of fins of fishes. They fed on fin membranes usually and even on fin rays rarely in the laboratory. Under a laboratoey condition in a small container they attached even to the free living goby, *Fusigobius neophytus* ?. Glass tubes used as habitats for the fishes attracted the nudibranchs (5 / 7 and 4 / 5) suggesting the nudibranchs may be attracted to mucus secreted by fishes.

Spawnings by adult were observed in the laboratory. An egg mass consisted of about 700 single eggs (ca 150 μm in diameter) contained in an egg capsule (ca 180 μm). Hatching occured at about ten days from oviposition. Hatched veliger larvae bore a brown shell and paired eyes.

Feeding behavior of the nudibranch shown above revealed that this type of association seems to be parasitic rather than symbiotic.

RELATIONS BETWEEN THE PHASE MODALITY OF TIDAL RHYTHMS AND THE HABITAT IN INTERTIDAL AND ESTUARINE CRABS

M. Saigusa. College of Liberal Arts & Sciences, Okayama University, Okayama.

The larval release activity of intertidal and estuarine crabs is synchronized with the times of high tide. This study focussed on how the phase modality of these tidal rhythms is determined. Experimental animals were Hemigrapsus sanguineus inhabiting intertidal shores, Macrophthalmus japonicus, an inhabitant of the lower part of estuary, and Sesarma erythrodactylum inhabiting the upper part of estuary. The tidal rhythm of H. sanguineus coincided with the semidiurnal unequality of tides, showing a UNIMODAL phase IN APPEARANCE. The pattern of the tidal rhythm of M. japonicus showed a BIMODAL phase, but that of S. erythrodactylum was a UNIMODAL phase, and larval release occurred only at night. Comparison of these activity patterns with the habitat of each species suggested that the phase modality of tidal rhythms is strongly correlated to tidal conditions in each habitat.

BEHAVIORAL ANALYSIS ON TRACKS OF CELL LOCOMOTION OF THE HELIOZOAN Actinophrys sol

M. Sakaguchi, T. Suzaki, Y. Shigenaka.
Laboratory of Cell Physiology, Faculty of Integrated Arts and Sciences, Hiroshima University, Higashi-Hiroshima.

Motile behavior of heliozoan cells is in most cases mediated by shortening and re-elongation of axopodia which carry out various kinds of activities such as locomotion, food capture and cytokinesis.

In this study, we made an analysis of tracks of the heliozoan Actinophrys sol to clarify the mechanism of mutual recognition among cells during the locomotory behavior. The tracks of organisms were monitored by a video camera interfaced to a personal computer. A software was made to detect positions of the cells, to follow their tracks for a predefined period of time, and to calculate direction and speed of movement for further mathematical analysis.

PHOTOTAXIS IN FUNGIID CORALS

H.Yamashiro and M.Nishihira.
Radioisotope Lab., Univ. of the Ryukyus and Laboratory of Animal Ecology, Faculty of Science, Tohoku University, Japan

This is the first demonstration that some fungiid corals (Scleractinia, Fungiidae) perform phototaxis. Positive phototaxis was observed in free-living fungiid corals, such as discs of Fungia that had detached from the stalks via asexual reproduction and Diaseris. Many species with different sizes moved toward a light. On the sand substrate, small and active coral D. distorta moved faster (max. speed of 1cm h^{-1}) than other species tested. Soft tissues in a shaded portion of a coral swell during movement. The mechanism of movement, however, was not elucidated. These corals have symbiotic unicellular alga, but their behavior was not affected by the treatment of DCMU (5μM), a specific inhibitor of photosynthesis. Corals moved even on a glass plate and climbed up a gentle slope. It is suggested that phototaxis in fungiid corals must be an important talent to escape from unfavorable shaded sites such as under rocks.

RELATION OF EMERGENCE OF THE MUDSKIPPER ON THE MUDFLAT TO TIDAL CYCLE AND TEMPERATURE.

Y.Ikebe, and T.Oishi, Dept. of Biology, Nara Women's Univ., Nara

The mudskipper, *Periophthalmus modestus* is amphibious fish and inhabits tideland. In summer, this fish feed and court on the mud flat at ebb tides.

We investigated the influences of tidal cycles and temperature on the number of emergence and the number of crawling fish onto the tidal flat at ebb tides in two different populations of the mudskipper at Kasaoka and Wakayama.

In both populations, the number of emergence and the number of crawling fish onto the tidal flat in the mudskipper decreased in association with the duration of emersion of the mudflat. This tendency was clear in summer, especially at Kasaoka. Temperature does not seem to be a direct factor to induce these behaviors, but dryness of mudflat due to high temperature is the important factor. The dryness of mudflat becomes greater in association with the duration of emersion of mudflat. To avoid desiccation of the epidermis even though the mudskipper needs skin respiration. They seem to retreat into the mud in a hole full of sea water. Thus, population at Kasaoka, where desiccation of the mudflat is severer seems to have shown a more distinct pattern in retreating into the mud.

THE EFFECTS OF FOOD DEPRIVATION, FOOD AND WATER DEPRIVATION AND NON-STARVATION ON THE FRACTAL FEEDING BEHAVIOR IN Drosophila

Y. Shiraiwa and I. Shimada. Biol. Inst., Fac. of Sci., TohokuUniv., Sendai.

The difference in the effects of non-starvation, food andwater deprivation, food deprivation on the feeding behavior was clearly observed in the dwelling time distribution on food. The order of effects generally increases in the same manner, but fractal dimensions were almost unchanged. Autocorrelation in the dwelling time under the food and water deprivation condition was higher than those under the other two conditions. Locomotor velocity, cumulative dwelling time and displacement were analyzed quantitatively and compared each other under the above three conditions.

CIRCADIAN LOCOMOTOR ACTIVITY RHYTHMS IN THE AFRICAN CLAWED FROGS: INFLUENCE OF AGING AND BLINDING.

Y. Harada[1], H. Fujisawa[2], K. Kegasawa[2] and T. Oishi[2].
[1]Dept.of Environ. Biol. Resources, Fac. of Agr., Univ. of Nagoya, Nagoya, [2]Dept. of Biol., Fac. of Sci., Nara Women's Univ., Nara.

We recorded locomotor activity rhythms in the African clawed frog (*Xenopus laevis*) under light-dark cycles (LD 12:12) and in constant darkness (DD) and constant light (LL).

Under LD12:12, tadpoles, youngs just after metamorphosis and adults showed nocturnal behavior. The L/D ratio in the amount of activity for adults was significantly higher than those for tadpoles and youngs.In adults, locomotor activity rhythms in both intact and blinded frogs were entrained to LD cycles. Direct response to light onset was observed at high intensity of light in blinded frogs. Under DD, free-running periods of locomotor activity rhythms in blinded frogs were significantly shorter than those in intact frogs. Under LL, however, the free-running periods between intact and blinded frogs were not significantly different.

In conclusion, (1) the L/D ratio in the amount of activity increases during the course of aging, (2) there is a circadian oscillator somewhere outside the eye, and (3) the eyes are involved in the circadian oscillator system of frogs.

SOCIAL BEHAVIOR AND SEMIOCHEMICALS IN THE JAPANESE, *Apis cerana japonica* Rad. AND EUROPEAN HONEYBEE, *Apis mellifera* L.

H. Sasagawa[1], S. Matsuyama[2], R. Yamaoka[3], M. Sasaki[4], T. Suzuki[2], and Y. Hirai[1].
[1] Dept. of Insec. Physiol. and Behav., Natl. Inst. Seric. and Entomol. Sci., Tsukuba, [2] Inst. of Appl. Biochem., Univ. of Tsukuba, Tsukuba, [3] Dept. of of Appl. Biol., Kyoto Inst. of Technol., Kyoto, and [4] Fac. of Agri., Tamagawa Univ, Tokyo (Japan).

In 1877, the European honeybee (*Am*) was introduced into Japan. Since then, the Japanese honeybee (*Acj*) has been obliged to share the same habitat. Scientific studies of *Am* have been conducted worldwide and the resulting literature is extensive. On the other hand, little is known about the chemical ecology of *Acj*. In this paper, the role played by semiochemicals in *Acj* social behavior was investigated, and the results were compared with *Am*.

Social behavior such as alarm behavior, aggregation behavior, and recognition are controlled by semiochemicals from the sting apparatus, Nasonov gland, feet, and cuticles. Extracts from the sting apparatus, Nasonov gland, tarsi, and body surface of both species were analyzed by GLC and GC/MS. Nasonov gland extracts induced aggregation behavior in both species, but the GLC profiles of the extracts from *Am* and *Acj* were quite different. Similar GLC profiles were obtained with sting apparatus extracts, but alarm behavior was different between the two species. *Am* hydrocarbon profiles were more complicated than *Acj* profiles. Differences between the species might be due to differences in semiochemicals, sensitivity, and signal processing in the CNS.

LOCOMOTOR ACTIVITY RHYTHMS IN WHITE AND EYELESS STRAINS OF THE AXOLOTL

Y. Yamaga[1], T. Oishi[1] and H. Takeuchi[2]. [1]Dept. of Biol., Fac. of Sci., Nara Women's Univ., Nara, [2]Dept. of Biol., Fac. of Sci., Shizuoka Univ., Shizuoka

We recorded locomotor activity rhythms in white and eyeless strains of the axolotl (*Ambystoma mexicanum*) and blinded animals in the white strain under light-dark cycles (LD 12:12) of different light intensities (10 and 500 lux) and constant dim light (1 lux).

All males in the white strain were entrained to L-D cycles and showed nocturnal activity. Females in the white strain showed a similar tendency with a few non-entrained animals. Locomotor activity rhythms in the eyeless strain were less clear than those in the white strain. Entrained animals in the eyeless strain were diurnal under L-D cycles of 10 lux and nocturnal under L-D cycles of 500 lux. Blinded animals were entrained to L-D cycles of 10 lux but could not be entrained to L-D cycles of 500 lux. Thus, the axolotl has an extra-ocular photoreceptor(s), but the extra-ocular photo-receptor seems to less functional than the eyes. Free-running rhythms were observed in the eyeless strain and in the blinded animals of the white strain and there were no differences in the free-running periods among groups. This indicates that the circadian oscillator is somewhere outside the eye.

INDISTINGUISHABLE ACOUSTICAL PROPERTIES OF TWO SONG BEHAVIORS DIFFERING IN CONTEXTS.

M. Ikeda and K. Aoki Life Sci. Inst., Sophia Univ., Tokyo

Song behaviors in the male Bengalese finch *Lonchura striata* can be classified into two types, depending on the behavioral contexts. One is undirected song behavior (US) addressing no particular objects, and the other is directed song behavior (DS) produced during courtship. Although the US and DS sound similar to human ears, they differ in testosterone-dependency (Ikeda *et al.* 1993). We analyzed and compared acoustical properties of US and DS in order to examine whether they are acoustically distinguishable.

Analysis using a sound spectrograph indicated that US and DS had a basic structure of phrase (song unit) in common, but US was significantly more rigid than DS with respect to stereotypy of temporal pattern, stability of sequence and so on. ***Sound pressure level*** that was measured at 10 m away from a singing subject did not significantly differ between US and DS.

To test whether conspecific birds can discriminate between US and DS, we observed ***female solicitation displays*** in response to playback of US and DS. There was no significant difference in the females' responses to US and DS.

These results suggest that US and DS are acoustically indistinguishable. Although US and DS differ in the behavioral context and the hormonal regulation, they may share a common song production mechanism.

LATITUDINAL COMPARATIVE STUDY OF SEXUAL REPRODUCTION OF *Oulastrea crispata* IN JAPAN.

Y. Nakano[1] and K. Yamazato[2] [1]Sesoko Station, Tropical Biosphere Research Center, Univ. of the Ryukyus, Okinawa, and [2]Dept. of Biology, Col. of Sci., Univ. of the Ryukyus, Okinawa.

We compared the development of gonads in *O. crispata* from Sesoko, Okinawa (26°38'N), Aitsu, Kyushu, Shirahama, Kii peninsula, Ushimado, Seto inland sea, Shimoda, Izu peninsula and Uchiura, Noto peninsula (37°18'N) within use hystlogical samples collected in each month from March in 1993 to February in 1994. We could identify mature gonads from July to September from Sesoko. However, mature gonads were observed only in July and/or August in other northern places. Living colonies were transplanted from Shirahama and Uchiura to Sesoko on the fall of 1992 and 1993. We observed spawning behavior of these specimens in the following summer. The specimens collected at Sesoko continually spawned eggs at an interval of several days, from July to October, regardless of the lunar phase. In July, the spawning was firstly observed after attaining 29 ℃ in sea water temperature. The corals from Shirahama and Uchiura have started spawning of eggs and sperm in middle May when the sea water temperature was about 23 ℃ at Sesoko.

ENTRAINMENT PATTERN OF LOCOMOTOR ACTIVITY RHYTHMS TO LIGHT-DARK CYCLES IN THE JAPANESE WOOD MOUSE

A. Masuda and T. Oishi. Dep. of Biol., Fac. of Sci., Nara Women's Univ., Nara.

In the activity rhythms of Japanese wood mice, we found much difference in the phase angle difference for activity onset between animals under a long photoperiod and under a short photoperiod. In order to investigate the relation between the duration of dark phase and phase angle difference, we lengthened the dark phase by advancing light-off in the long photoperiod group and shortened the dark phase by delaying ligt-off in the short photoperiod group. In both cases, activity onset and offset did not change much, so that the phase angle difference for activity onset depended on the duration of dark phase. But when we lengthened the dark phase by delaying light-on by 2 hours, the onset of activity scarcely changed, although the offset of activity somewhat delayed. So, the phase angle difference for activity onset seems to be influenced not only by the duration of dark phase, but also by the direction of change of dark phase. When we delayed the whole dark phase, the activity phase shifted according to the shift of dark phase. Therefore, the timing of activity onset appears to be determined by both signals of light-on and light-off in the Japanese wood mouse.

ABSENCES OF WATER SURFACE AND FOOD AFFECT LONGEVITY AND REPRODUCTION IN WATER STRIDERS, AQUARIUS PALUDUM AND GERRIS LATIABDOMINIS.

T. Harada. Biol. Lab., Fac. of Educ., Kochi Univ., Kochi.

Overwintered adults collected in spring were transferred under one of the following three conditions after reared for 13-20 days on water surface with sufficient food: (A) on water surface and supplied with sufficient food; (B) on water surface and with no food; (C) on wet paper and with no food. Adults in the three groups were reared under 15.5L-8.5D and at 20±2°C. In the both species, females of B- and C-groups survived for 7.1-10.7 days on the average after the reproductive period of 4.4-6.1 days, while females of A-group continued to lay eggs for 9.7 (A. paludum) or 14.1 days (G. latiabdominis) and died. There were no significant differences in the longevity of females and males among the three groups in G. latiabdominis. In A. paludum, both sexes of B- or C-group survived longer than those of A-group. There were no significant differences in the fecundity between B- (16.4 eggs per 1 female: mean) and C- (20.9) groups in G. latiabdominis. Females in B-group (59.3) tended to be more fecund than those in C-group (42.1) in A. paludum. Even overwintered adults, which reproduce actively seem to have some tolerance to absence of water surface and accompanying starvation.

THE CHANGE OF THE HABITAT WATER QUALITY AND INHABITATION OF FRESHWATER SPONGES IN THE RIVER YOKOTONE.

Y. Suzuki and Y. Watanabe. Dept. of Biol., Ochanomizu Univ., Tokyo.

The distribution of freshwater sponge species can be correlated with physicochemical properties of the habitat water and the individual tolerance of the species to those factors. The River Yokotone that connect the Lake Kasumigaura to the River Tone was the water area abundant in freshwater sponge species. Till the middle of 1980's seven species of fresh water sponges distributed there, and number of individuals and size were large. Recently, the number of species and individuals in this area has rapidly decreased, and large size sponges could not find. The reason is considered that the water pollution of this area has affected sexual and/or asexual reproduction.
Compared with the water area of the River Shintone that is inlet of the Lake Kasumigaura, both number and species were much abundant. Compared with the water quality on pH, COD, DO, turbidity, silicon, nitrogen and phosphoric acid of both water bodies, special differences not distinguished. The River Yokotone is a fishing place of Carassius, and there had lived many Macrobrachium and Gipangopaludina till 1980's. Recently the fauna component has extremely changed. The larva of Chironomus and Pectinatella have replaced Gipangopaludina and Macrobranchiuum.
When gemmules cultured in filtrate habitat water of Yokotone they could hatch 100%, and developed normally. It is considered that the change of water condition in freshwater sponges is more affected by the pollution of delicate eutrophication than changes of physicochemical component of habitat water.

LIFE CYCLE ADAPTATION IN *AELIA FIEBERI* IN RELATION TO HOST PLANTS

H. Numata and K. Nakamura, Dept. Biol., Fac. Sci., Osaka City Univ., Osaka.

Many true bugs (Insecta, Heteroptera) reproduce under long-day conditions whereas enter adult diapause under short-day conditions. The critical daylength for these photoperiodic responses is between 13 and 14 hr in many species in Japan. However, *Aelia fieberi* Scott, which feeds on seeds of gramineous grasses, has a longer critical daylength of about 14.5 hr for the induction of adult diapause. Seeds of gramineous grasses exist in the field from spring to autumn, although some of them were suitable and the others were unsuitable as food for the development of *Aelia fieberi*. The suitable food disappears in August, and therefore *Aelia fieberi* has a longer critical daylength and enters adult diapause as early as in August.

DOWNSTREAM DIFFERENCES IN LIFE CYCLES OF *MICRASEMA QUADRILOBA*.

Y. Isobe and T. Oishi. Dept. of Biol., Nara Women's Univ., Nara.

A species of stream-living caddisflies, *Micrasema quadriloba*, have a one-year life cycle, and the timing of life cycle events is highly synchronous with emergence occurring in spring at Takami River, Nara Pref.

We studied the differences in development and growth of this species on five successive downstream stations and a tributary station of the Takami-River to investigate the influence of water temperature on the life history. Samples were taken once a month from May 1993 to June 1994.

First instar larvae appeared in early June, and third instar larvae in late July. The development from the first to the third instar at higher stations was slower than that at lower stations. In contrast to the preceding instars, the occurrence of the fourth instar larvae (mostly in October) was earlier at higher stations. But, after the molting, the development accelerated more at lower stations. Most of the larvae overwintered in the state of fifth instar, and grew constantly during winter at all stations except the highest one. The size of full-grown larvae based on their cases in March was larger in relation to the downward length of the river.

These results suggest that high water temperature over some critical point in summer inhibits the development of larvae, but higher temperature in the other seasons accelerates the development and growth of this species.

CLONING OF THE CHICKEN SKELETAL MUSCLE TROPONIN T GENE

I. Yonemura, T. Watanabe and T. Hirabayashi
Inst. of Biol. Sci., Univ. of Tsukuba, Tsukuba, Ibaraki 305, Japan

Troponin T is a member of muscle contraction regulating proteins, and has many isoforms expressed during myogenesis. Several variants of chicken cDNA encoding skeletal muscle troponin T were already isolated, suggesting the existence of the chicken breast muscle-specific exon. However, the genomic gene encoding the protein was not cloned yet. We could isolate and partially sequence it. The sequence included it's promoter/upstream region, which had several sequence motifs expected for eukaryotic promoters, including putative TATA, SP-1, and CCAAT homologies. Therefore, one MEF-2 like and two E-box like motifs resided within this region, just as in other contractile protein gene promoters.

IDENTIFICATION OF A PHOSPHORYLATION SITE RESPONSIBLE FOR STRUCTURAL CHANGES IN MYOGENIN

N.Hashimoto[1], M.Ogashiwa[1], T.Endo[2], E.Okumura[3] and T.Kishimoto[3]. [1]Mitsubishi Kasei Inst. Life Sci., Machida, [2]Chiba Univ., Chiba, [3]Tokyo Inst. Tech., Yokohama.

Myogenin, a member of the MyoD family which governs skeletal muscle differentiation, was identified as a pair of phosphorylated bands on SDS-PAGE during myogenesis. The slow migrating form was found to be hyperphosphorylated myogenin. *In vitro* phosphorylation by CDC2 kinase caused a prominent reduction in the electrophoretic mobility of myogenin. Furthermore, we demonstrated that phosphorylation of the threonine residue contributes to the modification of myogenin *in vivo* and *in vitro* resulting in the reduction in electrophoretic mobility. We propose here that a CDC2-like proline-directed kinase regulates myogenin activity through phosphorylation.

ANALYSIS OF QUAIL SKELETAL MUSCLE TROPONIN T EXPRESSION

N. Nakatani, M. Kudo, Y. Yao and T. Hirabayashi
Inst. of Biol. Sci., Univ. of Tsukuba, Japan

Yao et al. (1992) grafted 2-day old chick pectoralis muscle in leg muscle, and detected the breast type isoforms in the regenerated donor muscle tissue. They suggested that the expression of troponin T isoforms was fixed in the cell lineage. However, since the operation was autotransplantaion, this study could not remove the possibility that the breast type isoforms were expressed in the host leg muscle cells. Then, we thought that the possibility could be removed by using quail tissue as the donor tissue which can be distinguished histologically by nuclear morphology from the host chick tissue.

We report that there are several individual variations in the quail troponin T isoform expression, and that chick and quail breast type troponin T isoforms can be distinguished each other by using 2-D gel electrophoresis. Then, we grafted the quail pectoralis muscle in the chick leg muscle, and analyzed the isoform composition in the regenerated quail muscle in order to conclude finally that the troponin T isoform expression was fixed cell lineage.

SPATIO-TEMPORAL PATTERN OF VASCULAR SMOOTH MUSCLE CELL DIFFERENTIATION DURING DEVELOPMENT OF MOUSE EMBRYO.

Y. Takahashi and T. Takano. Dept. of Microbiol. & Molec. Pathol., Fac. of Pharm. Sci., Teikyo Univ., Kanagawa and Vessel Research Laboratory Co., Tokyo.

In order to investigate spatial pattern of smooth muscle cell differentiation, distribution of cells expressing α-smooth muscle actin, a molecular marker for smooth muscle, was analyzed immunohistochemically in developing vascular system of mouse embryo at 9, 10 and 11 gestation days. In 9 day embryo, α-smooth muscle actin-positive cells were localized only in dorsal aortas and allantoic mesoderm close to umbilical artery. The cells were distributed sparsely along dorsal aortas, whereas they formed a monolayer in the allantoic mesoderm. In 10 day embryo, layer of α-actin-positive cells appeared in most part of dorsal aortas and in extraembryonic part of umbilical artery, right umbilical vein and omphalomesenteric artery. Alpha-actin positive smooth muscle cells were also observed in 3rd and 4th aortic arches and omphalomesenteric vein. At 11 day, α-actin-positive cells appeared in intersomitic arteries, while they were never detected in venal system of embryo proper.

IMPROVEMENT OF CHEMICALLY DEFINED MEDIUM FOR PRIMARY MYOGENIC CELLS FROM CHICK EMBRYOS

○M.SHIOZUKA, T.HIRAISHI and I.KIMURA.
Dept. of Basic Human Sci., Sch. of Human Sci., Waseda Univ., Tokorozawa

The development of the chemically defined media is increasing the importance in the invitro research of the cells. This research is aiming at the improvement of a chemically defined medium suitable for primary culture of chick myogenic cells from embryonic pectoral muscle.

It was found that the medium composed of transferrin, insulin, fibroblast growth factor, serum albumin, and Dulbecco's modified Eagle minimum essential medium showed the effectiveness comparable to that of a standard serum-containing medium. It was also found that the medium suppressed the proliferation of contaminated fibroblasts. Moreover, was suggested a possibility that the availability of this medium might be more improved by paying attention to the extracellular matrix substances.

Subcellular localization of actin isoforms in cultured chicken skeletal muscle cells.

K .Hayakawa, R .Nagaoka, and T .Obinata. Dept. of Biol., Fac. of Sci., Univ. of Chiba, Chiba.

Actin is a major cytoskeletal component in variety of eukaryotic cells. In higher vertebrates, several actin isoforms are distributed in a tissue specific manner. In developing skeletal muscle cells, however, the actin isoforms of cytoplasmic β, γ- type and striated muscle α-type are co-expressed. It is, then, matter of interest how the actin isoforms localize in developing muscle cells during myofibrillogenesis. In this study, we prepared a monoclonal antibody (SKA-06) specific for skeletal and cardiac α-actin. Using SKA-06 and a polyclonal antibody (PcAb) against chicken gizzard actin which recognizes both non-muscle and smooth muscle β and γ-actins, we compared subcellular localization of α-actin with that of cytoplasmic β and γ-actins by immunocytochemical methods. Cultured chicken skeletal myotubes were stained dually by SKA-06 and the affinity purified PcAb. While in developing myotubes, α, β and γ-actins were mostly co-localized in the cytoplasm, α-actin predominated in striated myofibrils. When FITC-labeled β and γ-actins from chicken gizzard were introduced in young myotubes by a microinjection method, the β and γ-actins were incorporated into myofibrils to co-localize with endogenous α-actin. These results suggest that α-actin as well as β and γ-actins can be assembled into myofibrils, but that there may be some mechanism that enables the former to be incorporated preferentially into myofibrils.

TRANSPLANTATION OF CHICKEN EMBRYONIC TISSUES INTO YOUNG CHICKEN SKELETAL MUSCLE

Y. Yao and T. Hirabayashi, Inst. of Biol. Sci., Univ. of Tsukuba, Tsukuba

Skeletal muscle of vertebrates is a relatively simple and large tissue attached to bone, the contraction of which is regulated by neural influences. On the way of investigating troponin T isoform expression, we transplanted chicken embryonic tissues into 2-day-old chicken leg muscle. The histological observation of the transplants on the 58th day after the operation revealed that various non-muscle tissues could differentiate in the skeletal muscle tissue. Therefore, we considered that the skeletal muscle was one of favourable culture media for the differentiation of the transplanted tissues.

CULTURE OF CHICKEN SKELETAL MUSCLE TISSUE ON CHORIO-ALLANTOIC MEMBRANE

K. Nakada, Y. Yao and T. Hirabayashi, Inst. of Biol. Sci., Univ. of Tsukuba, Tsukuba

We examined whether chicken skeletal muscle tissue could be cultured on the chorio-allantoic membrane (CAM) of chicken embryos. Pieces of breast muscle tissue (pectoralis major, 5mm x 5mm) from 1 day old chickens were grafted onto the CAM of 9 day old embryos. The muscle tissues grafted on CAM started to degenerate with pyknosis in the tissue area near CAM after 5 hour grafting. Hematoxylin positive cells appeared among the degenerating fibers near CAM after 25 hour grafting. These cells proliferated rapidly and fused to form myotubes. At later stages, regenerating muscle tissue which had central nuclei and striation was engulfed in the mesodermal layer of CAM. Based on these observations, we consider that the skeletal muscle tissue can be cultured on the CAM and the culture system using chorio-allantoic membrane is very useful in understanding the mechanism of muscle degeneration and regeneration without innervation.

DISTRIBUTION OF FIBROBLASTS POSITIVE FOR STROMELYSIN-3 mRNA DURING INTESTINAL REMODELING OF THE METAMORPHOSING XENOPUS TADPOLES

A.Ishizuya-Oka[1], A.Shimozawa[1] and Y.-B.Shi[2].
[1]Dept. of Anat., Dokkyo Univ. Sch. of Med.,Tochigi and [2]Lab. of Mol. Embryol., NIH, Bethesda, USA.

Gene of stromelysin-3 (ST3), one of matrix metalloproteinases, is known as a thyroid hormone response gene in the small intestine of Xenopus tadpoles. To obtain basic information on roles of ST3 in intestinal remodeling during metamorphosis, we examined developmental changes in expression pattern of ST3 gene by in situ hybridization. Cells positive for ST3 mRNA were morphologically fibroblasts. They were first detected at stage 58 and then increased in number in the entire region of larval intestinal connective tissue. After stage 60, when the basal lamina suddenly became thick, the positive cells were restricted to the region near the basal lamina. The epithelium lined by the thick basal lamina most rapidly transformed by larval cell death and adult cell proliferation. Thereafter, with thinning of the basal lamina, the positive cells decreased in number. These results indicate the close relationship between ST3 gene expression and thickening of the basal lamina in the small intestine, suggesting that ST3 produced by fibroblasts may influence epithelial cell death and/or proliferation by changing basal lamina components.

ANALYSIS OF THE *aproctous*, A *Drosophila* MUTANT THAT LACKS PROCTODEUM-DERIVED TISSUES

R.Murakami[1], A.Shigenaga[1,4], M.Kawakita[1], I.Yamaoka[1], K.Takimoto[2], K.Akasaka[3], and H.Shimada[3]. [1]Dept. of Biol., Fac. of Sci. and [2]Dept. of Biol. Chem., Fac. of Agric., Yamaguchi Univ., Yamaguchi, Japan., [3]Graduated Dept. of Gene Sci., Hiroshima Univ., Higashi-Hiroshima, Japan, [4]Biol. Lab., Kyushu Univ. Ropponmatsu, Fukuoka, Japan.

aproctous (*apro*) is a *Drosophila* mutant isolated by P-*lacZ* insertion mutagenesis (formerly called *proc*). In homozygous apro embryos, tissues derived from proctodeum, i. e., hindgut, Malpighian tubules, and anal pads, degenerated during embryonic stage 12-14. Expression of *apro*, as deduced by the expression of the *lacZ* reporter gene, began at a cellular blastoderm stage (st. 6) in a posterior region extending from 10 to 15 % egg length (EL), which corresponded to future proctodeum and a posterior-most part of visceral mesoderm. Expression domain of *apro* is controlled largely by two gap genes, *tll* and *hkb*. *tll* activates the *apro* expression, and *hkb* suppresses the *apro* expression in the region posterior to 10 % EL, thus restricting the expression domain of *apro*. *fkh*, *sal*, and *hb* did not affect the expression of *apro*. *apro* was mapped to 68DE on the 3rd chromosome. *apro* is thought to have a key role in the development of procdodeum-derived tissues.

SIZE REGULATION OF REGENERATED ORGANS DURING MORPHALLACTIC REGENERATION IN THE COMPOUND ASCIDIAN, *POLY-ANDROCARPA MISAKIENSIS*.

A. Nagao and Y. Taneda. Dep. of Biol.,Fac. of Educat., Yokohama Natl. Univ.,Yokohama.

Fragments of the zooid of the compound ascidian, *Polyandrocarpa misakiensis* can produce entire miniature animals by morphallactic regeneration. Small anterior fragments without guts regenerate small guts and large ones do large guts. How does the fragment know its own size, and how does it regulate the size of regenerated gut? In order to answer the question how the fragment know its own size, we made two modes of half zooid, anterior half and left half, which had similar volume and different anteroposterior axial length. The sizes of regenerated guts were proportional to anteroposterior axial length. Therefore, it is concluded that the fragment knew its own size not by the volume of the fragment, but by anteroposterior axial length. However, when the anterior part was removed from regenerating anterior half or both anterior and posterior parts were removed at the same time, the regenerated guts were larger than control. Therefore, posterior cut position plays an important role as the information of fragment size. Comparing to regeneration kinetics between large and small fragments, it was revealed that the size of regenerating guts were determined by the size of gut rudiments.

ISOLATION AND ANALYSIS OF THE *Drosophila* MUTANTS, *arim* AND *aric*, WHICH HAVE DEFECTS IN GUT MORPHOGENESIS.

T.Arima, I.Yamaoka, and R.Murakami. Dept. of Biol., Fac. of Sci., Yamaguchi Univ., Yamaguchi 753, Japan.

P-*lacW* insertion mutagenesis was performed to find new genes that regulate morphogenesis of the gut of *Drosophila*. 137 lethal strains were established and screened by detection of the pattern of *lacZ* expression in the embryos. Two strains were isolated that had defects in midgut morphogenesis and ectodermal parts of the gut, with corresponding *lacZ* expression patterns. They were named *arrested invagination of midgut* (*arim*) and *arrested invagination of ectoderm* (*aric*), respectively.

Expression of the *arim*, as deduced by the expression of *lacZ* reporter gene, started at stage 8 in both anterior and posterior midgut primordia, and continued throughout embryogenesis. In homozygous *arim* embryos, invagination of endoderm was incomprete, resulting in a failure of midgut formation. *aric* was expressed at invaginating ectodermal tissues: stomodeum, proctodeum, salivary glands etc. In homozygous *aric* embryos, invagination of these tissues stopped on the way. Both mutations were rescued by removing the P-*lacW* vector from the genome, indicating that the mutations were caused by the P-*lacW* insertion.

MECHANISM OF EPITHELIAL-MESENCHYMAL INTERACTION IN DIFFERENTIATION OF GLANDULAR STOMACH EPITHELIAL CELLS OF RAT FETUSES

H. Fukamachi[1], M. Ichinose[2], S. Tsukada[2] and K. Miki[2]. [1]Zool. Inst., Fac. of Sci., [2]First Dept. of Int. Med., Fac. of Med., Univ. of Tokyo, Tokyo

We have shown that fetal rat glandular stomach epithelial cells express just cathepsin E but not pepsinogens in primary culture in the absence of mesenchymes, but that they express pepsinogens when cultured with mesenchymes in organ culture, suggesting that mesenchymes play important role(s) in inducing pepsinogen expression in the glandular stomach epithelial cells. Here we examined the mechanism of the epithelial-mesenchymal interaction in the glandular stomach.

Gastro-intestinal mesenchymes were put on membrane filters, covered with collagen gels, and glandular stomach epithelial cells were cultured on them. Pepsinogens were immunohistochemically detected in the cells cultured on collagen gels and mesenchymes. The cells on collagen gels only never expressed pepsinogens. Pepsinogens were expressed in the cells even when the cells were separated from the mesenchymes by collagen gels. We concluded that mesenchymes secrete humoral factor(s) which induce pepsinogen expression in the glandular stomach epithelial cells.

THE DIFFERENTIATION POTENCY OF CULTURED PROVENTRICULAR EPITHELIAL CELLS FROM CHICKEN EMBRYOS.

H. Tabata and S. Yasugi. Dep. Biol., Fac. Sci., Tokyo Metropol. Univ., Tokyo.

To establish the *in vitro* system for analyzing the mesenchymal influences on the differentiation of the epithelial cells of the chicken embryonic digestive tract, we examined the conditions of primary culture and differentiation potency of proventricular (PV) epithelial cells. The expression of pepsinogen (Pg) in cultured epithelial cells was analyzed by RT-PCR method. Epithelial cells of 6-day PV cultured for 7 days and of 11-day PV cultured for 2 days expressed much reduced amounts of Pg mRNA compared to that of 13-day PV epithelial cells. Moreover, PV epithelial cells cultivated for 2 days differentiated when they were cultivated with PV mesenchyme. These results suggest the importance of mesenchymal factor(s) for maintaining the differentiated state of PV epithelial cells.

DEVELOPMENTAL CHANGES IN THE MESENCHYMAL ABILITY TO INDUCE THE DIFFERENTIATION OF INTESTINAL EPITHELIUM AND THE ENDODERMAL COMPETENCE IN THE DIGESTIVE TRACT OF THE CHICK EMBRYO.

S. Matsushita. Dept. of Biol., Tokyo Women's Medical College, Tokyo.

Dissociation and reassociation experiments were carried out in vitro using the endodermal epithelia and mesenchymes of the digestive organs in the chick embryos of various developmental stages, and the inductive ability of the mesenchyme to elicit the differentiation of intestinal epithelium and the competence of the endoderm were analyzed.

The endoderms of oesophago-tracheal and stomach regions of 3-day-old embryos were highly competent to respond to the inductive effect of the mesenchyme. The responsiveness in the endoderms of oesophagus and proventriculus declined in 5-day embryos and was almost lost in 6-day embryos, while that of the gizzard endoderm remained to be high in 5-day embryos but was lost in 7-day embryos. The inductive ability in the mesenchyme was found to be high in the small intestine of 3- to 8-day embryos, which got lower in 10-day embryos and was negligible in 14-day embryos. It was also suspected that the presumptive small-intestinal mesoderm of 1.5-day embryos had the intestinal identity but not the inductive ability.

CHICKEN HOMEOBOX GENE *Cdx-A*: ITS EXPRESSION AND ROLE FOR INTESTINAL EPITHELIAL DIFFERENTIATION.

Y. Ishii[1], K. Fukuda[2] and S. Yasugi[1].
[1]Dept. of Biol., Fac. Sci., Tokyo Metropolitan Univ., Tokyo, [2]Hirohashi Cell Config. Project, ERRTO, JRDC, Tsukuba.

Developmental fate of presumptive intestinal endoderm is determined at very early developmental stage. We showed by *in situ* hybridization and Northern hybridization that *Cdx-A* expression is restricted to the intestinal epithelium from 3-day embryo to adult. Tissue recombination experiments using epithelia and mesenchymes isolated from digestive organs of 6-day embryo revealed that expression of *Cdx-A* and sucrase in the intestinal epithelium is not affected by the influence of mesenchyme. These results suggest that *Cdx-A* expression is involved in the commitment and maintenance of differentiated state of the intestinal epithelium.

AN ANTIGEN LOCALIZING IN THE EPITHELIA OF ANTERIOR DIGESTIVE TRACT IN THE CHICKEN EMBRYO

N. Yoshida, K. Urase and S. Yasugi. Dept. Biol., Fac. of Sci., Tokyo Metropolitan Univ., Tokyo

We obtained a monoclonal antibody which recognized the luminal epithelia of esophagus, proventriculus and gizzard of embryos from 6-day on but not the intestinal epithelium throughout development. This antibody did not react to the glandular epithelium of the proventriculus which synthesizes embryonic chick pepsinogen (ECPg). This suggests that the antigen is involved in ECPg expression and/or gland formation. The expression of antigen in the gizzard epithelium was not affected by the influence of the intestinal mesenchyme, indicating that the antigen may serve as specific maker of epithelia of anterior digestive tract.

BRANCHING MORPHOGENESIS OF EMBRYONIC MOUSE LUNG EPITHELIUM IN THE ABSENCE OF MESENCHYME.

H.Nogawa[1] and T.Ito[2].
[1]Dept. Biol., Fac. Sci., Chiba Univ., Chiba and [2]Dept. Pathol., Yokohama City Univ. Sch. Med., Yokohama.

Branching morphogenesis of lung epithelium proceeds through interactions with a mesenchymal tissue, but the nature of mesenchymal influences has been unclear. We developed the culture system in which lung epithelium underwent branching morphogenesis in the absence of mesenchymal cells in the present study. Lung epithelium was isolated from 11-day mouse embryos and cultured, covered with Matrigel (basement membrane-like substratum), in the medium containing EGF, basic FGF or acidic FGF for 2 days. EGF stimulated neither epithelial cell growth nor specific morphogenesis. Basic FGF stimulated epithelial cell growth but resulted in abnormal morphogenesis of epithelium different from branching. Acidic FGF (500 ng/ml) stimulated epithelial cell growth and induced epithelial branching, and the epithelium constructed a simple columnar cell layer with a lumen. These results showed that embryonic lung epithelium was able to branch in the mesenchyme-free culture condition in which basement membrane matrices and acidic FGF were substituted for the mesenchyme.

EXPRESSION OF β-ACTIN mRNA AND FORMATION OF F-ACTIN AT THE EDGE OF CLOSING WOUND IN FETAL RAT SKIN.

S. Ihara and Y. Motobayashi[1]. Dev. Biol. Lab., Dept. of Plast. Surg., and [1]Dept. of Biochem., Kitasato Univ. Sch. of Medicine, Sagamihara.

As an initial step for elucidation of the mechanisms of wound closure, we have localized F-actins and β-actin mRNA in wounded skin of the fetal rat (Sprague-Dawley). Open wounds (1 mm in diameter) were made in the dorsal skin of day-16 fetuses and allowed to heal either in utero or in an organ culture system. In both healing systems, a rapid wound closure was observed as we reported previously. In the present study, we employed FITC-labeled phalloidin staining for detection of F-actins and in situ hybridization for β-actin mRNA in the 24h-postoperative skin. The results were essentially the same, irrespective of healing system. Fluorescence staining showed that F-actins were enriched in cells located around the closing wounds. Particularly strong fluorescence detected within a few epidermal cells close to the wound edge may be comparable to "actin cable" formed around chick embryonic wounds as reported by Martin and Lewis (1992). More interestingly, in situ hybridization revealed that the signals for β-actin mRNA were intensified in the epidermis at the wound edge, suggesting transcriptional activation of β-actin gene by wounding.

RECONSIDERATION OF "PRIMITIVE" TYPE AND "DEFINITIVE" TYPE IN ERYTHROPOIESIS

K. Morioka[1], R. Minamikawa-Tachino[2], H. Takano-Ohmuro[3]. [1]Div Tumor Biochem, [2]Computer Centr, The Tokyo Metropol Inst Med Sci, Tokyo, [3]Dept Pharmacol, Fac of Med, Univ of Tokyo, Tokyo

According to the classical point of view, "primitive" erythroid cells are produced in the yolk-sac, are nucleated, are megaloblastic, produce embryonic hemoglobins, and are unable to evolve into more mature forms. However, observations suggesting that such concepts are not correct have been accumulated. We herein present several pieces of evidence, obtained from the morphological and the biochemical study, that the boundary between "primitive" and "definitive" erythropoiesis is vague. Based on those experimental results, we propose that the consecutively changing yolk sac → fetal liver erythropoiesis should be included in the category of "primitive" type, comparing with the stable bone marrow "definitive" type erythropoiesis.

ABNORMAL DEVELOPMENT OF THE BLOOD VESSELS IN THE EMBRYONIC SKIN AND FEATHER GERMS OF THE JAPANESE QUAIL MUTANT (*Bh*, BALCK AT HATCH)

N. Shiojiri[1], H. Satoh[1], T. Shinkai[2] and A. Nakamura[3]. [1]Dept. of Biol., Fac. of Science, Shizuoka Univ., Shizuoka, [2]Dept. of Cell Biol., Tokyo Metropol. Inst. of Gerontol., Tokyo, and [3]Dept. of Biol., Univ. of Shizuoka, Hamamatsu College, Hamamatsu.

We have shown that *Bh* homozygotes die during early development due to subcutaneous hemorrhage and liver degeneration. However, it still remains to be revealed which tissues express the *Bh* gene in this mutant. In the present study, we examined the abnormal development of the homozygotes with histological technique and transmission electron microscopy.

Bh embryos at 5 to 10 days of incubation were used. Paraffin sections were stained with hematoxylin-eosin-Alcian blue or azan. Tissues for electron microscopy were processed with standard methods.

In the skin and feather germs of 10-day homozygotes, the blood vessels were dilated and blood capillaries were poorly developed, comparing to those of wild-type and heterozygotes. These abnormalities may cause subcutaneous hemorrhage in homozygotes, and may be related to the change of the pigmentation in feather germs of both heterozygotes and homozygotes.

Inductive ability of long term cultured dermal papilla cells to form hair follicles from epidermal cells.

T. Matsuzaki, M. Inamatsu and K. Yoshizato. Yoshizato MorphoMatrix Project, Erato, JRDC, Higashi-Hiroshima.

It have been thought that dermal papillae (DP) have the ability to induce a hair follicle from skin epidermis. However, the cell division of the DP cells is limited *in vitro* and lose thire inductive ability during early passages of cell culture. We previously established the culture method for DP cells utilizing conditioned medium of keratinocytes, which allows them to proliferate rapidly and without limitation. In the present work, we examined whether the DP cells cultured in many passages still retain their inductive ability. The DP cells or Swiss 3T3 cells were stuffed between dermis and epidermis of footpad skin about 3 mm square (sandwich culture). Then the skin sandwiches were implanted under kidney capsules for 8 weeks. Frozen sections of the implants were prepared and treated with several monoclonal antibodies specific to different follicular tissues. Although we could not find out any hair follicle structure in the skin stuffed with Swiss 3T3 cells, thin hair shafts and follicular bulbs were observed in the skin combined with the DP cells which had been cultivated for 36 passages. Therefore, we conclude that the DP cells cultured by our method retain the ability to induce a hair follicle.

IDENTIFICATION AND CHARACTERIZATIN OF M1-8 POSITIVE CELLS IN PERIPHERAL BLOOD AND BONE MARROW.

S. Tanaka and H. Uda. 2nd Dept. of Pathology, Kagawa Med. School, Kagawa.

Dendritic cells (DC) in T-dependent area of several lymphatic organs have been specialized as antigen presenting cells. Although, it has been reported that DC in the skin or lymphoid organs arise from bone marrow (Steinman *et al.*, 1993), the precursor of these cells remain to be determined. It has been shown that monoclonal antibody (mAb) M1-8 (Maruyama *et al.*, 1989) could be used to recognize DC including Langerhans cells (LC) and interdigitating reticulum cells (IDC). We observed that this mAb binds to some cells of peripheral blood (PB) and bone marrow (BM) of BALB/c mice. Analysis by flowcytemeter of surface markers of these cells were undertaken. Results of the experiment showed that 1-4% of mononuclear cells in PB and 20-30% of those in BM were M1-8 positive. With two-color immunofluorescence and flowcytometry, more M1-8 positive cells were found to express Thy 1.2 and Ia antigen in PB than those in BM in ratio. Some M1-8 positive cells in BM were shown to be bound by ER-MP 20, an anti-macrophage precursor antibody. The monocytes in PB did not show positive reaction with M1-8. Electron microscopic observation showed that M1-8 positive mononuclear cells were lymphocyte like small cells and M1-8 bound to the cytoplasm. The ultrastructural localization of endogenous peroxidase was in the nuclear envelope, but not in endoplasmic reticulum. These data indicate a possibility that M1-8 positive cells in PB and BM are immature cells in granulocyte-macrophage or macrophage lineage, and can be precursor cells of DC population.

VIDEO MICROSCOPY OF EPITHELIAL SHAPE CHANGE AND MESENCHYMAL FLOW DURING MORPHOGENESIS OF THE MOUSE EMBRYONIC SUBMANDIBULAR GLAND.

Y.Hieda, T.Morita, Y.Nakanishi. Department of Biology, Faculty of Science, Osaka University, Osaka.

Shape change of the epithelium of the mouse embryonic submandibular gland mainly derives from repetitive lobular formation and requires interactions with the surrounding mesenchyme. The lobular formation, which takes 8 to 10 hours, starts with cleft formation in the epithelium and ends in the stabilization of the new lobules.

Nakanishi et al. have previously reported that clefts in the epithelium could be formed by constriction of collagen fibers, that formation of many tiny clefts precedes the occurrence of two deep clefts on the average and that the flow activity of mesenchyme correlates with the ability to support the epithelial branching. It is likely that there is an interplay between the form fluctuation, that is, tiny clefts of the epithelium, the stabilization of a few tiny clefts leading to deep clefts and the mesenchymal flow.

We made video microscopy of cultured mouse embryonic submandibular gland to get some insights about the relationships between the form fluctuation of the epithelial surface, the cleft formation and the mesenchymal flow during the lobular formation.

EXPRESSION OF HEPATOCYTE GROWTH FACTOR GENE DURING MOUSE CEPHALOGENESIS.

T.Yamaai, T.Takebayashi, F.Myoukai, E.Koyama, T.Nohno[1], K.Matsumoto[2], T.Nakamura[2] and S.Noji[3]. Okayama Univ.Dent.Sch., Okayama, [1]Kawasaki Med.Sch., Kurashiki, [2]Osaka Univ.Med.Sch., Osaka, [3]Tokushima Univ.Fac.Engin., Tokushima.

Expression of hepatocyte growth factor(HGF) gene during cephalogenesis was found by in situ hybridization. From 10-day to 17-day fetal C3H mice were fixed by microwave oven(BioRad, H2500, 300W, 37°C, 3min) with 4% Paraform-aldehyde buffered with 0.15M Na-cacodylate, pH7.3. In situ hybridization with ^{35}S labeled rat HGF riboprobes were performed on 5mm serial paraffin sections. Signals were detected by autoradiographically.

A recurring pattern of HGF gene expression was observed from 13-day fetal mesenchymal tissues. In the tooth germ, HGF gene expression was observed on ectomesenchymal cells of the dental follicle as well as mesenchymal cells of the eye lids, mesenchymal cells among the follicles of the whiskers, the ethmoid and the sphenoid bone anlarge. No significant signal was observed on the epithelial tissues and the tissues belong to the intramembraneous ossification.

ANALYSIS OF MITOTIC APPARATUS IN TETRAPLOID NEUROBLASTS.

M. Sato. Lab. of Biol., Rakunou-Gakuen Univ., Ebetsu, Hokkaido.

Binucleate neuroblasts were induced by preventing cytokinesis with Cytochalasin treatments. After removing the effect of Cytochalasin, the mitotic phase of two nuclei in the binucleate neuroblasts was strictly synchronized. In the early stage of mitotic division, two distinct mitotic apparatus (MA) was formed, and then the two MAs were fused till metaphase. The binucleate cell divided unequally along the dorso-ventral axis, forming two types of daughter cells, a large neuroblast type, and a small ganglion cell type. Each daughter cell contained one tetraploid nucleus. The subsequent division of tetraploid neuroblasts were traced in the living state and by electron microscopic observation. Four centrosomes, which are twice as many as those in the normal daughter neuroblasts, were observed at interphase, as duplication of centrosomes had been completed by that stage. In the successive mitotic stages, the four centrosomes remained distinctly, and a spindle formed was characterized by its having two separate poles on both sides. The result showed that normal unequal cell division as well as polarity in the grasshopper neuroblast is not influenced by doubling of genomes or centrosomes.

DIFFERENTIATION OF HEPATOCYTES IN THE MOUSE LIVER PRIMORDIUM CULTURED *IN VITRO*

T. Koike and N. Shiojiri. Dept. of Biology, Fac. of Science, Shizuoka University, Oya 836, Shizuoka.

During an early liver development in birds and mammals, the presumptive hepatic endoderm interacts with the adjacent mesenchyme. However, the mechanisms of the interactions are still unknown, and an *in vitro* culture system of the liver primordial cells has not been established yet, which might allow us to reveal the molecular nature of these interactions. In the present study, we cultured immature liver primordia from mouse embryos *in vitro*.

C3H/HeSlc strain mice were used. The liver primordia at 9.5 days of gestation were cultured in a Trowell-type organ culture system. DMEM supplemented with 10% fetal bovine serum, EGF, insulin were used as a culture medium. Dexamethasone was added in some experiments. Expressions of alpha-fetoprotein (AFP), albumin (ALB), calbamoylphosphate synthethase I (CPSI), and storage of glycogen were analysed histochemically.

After 5 days of culture, endodermal cells in the explants differentiated into large hepatocytes which expressed AFP, ALB, CPSI, and stored glycogen. Their differentiation state corresponds to that of neonatal hepatocytes. Dexamethasone stimulated hepatocyte differentiation prominently.

PURIFICATION AND IDENTIFICATION OF A SECRETED FACTOR REQUIRED FOR THE INITIATION OF DEVELOPMENT IN *Dictyostelium discoideum*.

N.Iijima, T.Takagi, Y.Maeda. Biol. Inst., Fac. of Sci, Tohoku Univ., Sendai.

Transition of *Dictyostelium* cells from growth to differentiation is believed to be trigered by a secreted factor(s) in addition to nutritional deprivation; intercellular communication as well as starvation are essential for the initiation of development. Using an unique assay system of cellular development, we tried to purify and identify a factor(s) capable of inducing the initiation of development. Under low nutrient (1/20 concentration of normal nutrients) and low cell density (8×10^5 cells/cm^2) conditions, cells could not progress their development. Macromolecules that had been secreted by *Dictyostelium* cells into culture medium were biochemically fractionated, and active components were searched by adding then into the above assay system. As a result, the addition of a 450 kDa protein was found to induce cellular development, thus indicating the presence of intercelluar communication mediated by this diffusible macromolecule.

CORTICAL BEHAVIOR IN DIVIDING NEUROBLASTS TREATED WITH LOW CONCENTRATION COLCEMID.

K.Kawamura, Biol. Lab., Rakuno Gakuen Univ., Ebetsu, Hokkaido.

Grasshopper neuroblasts always divide unequally to produce a large daughter neuroblast to the ventral side (cap cell (CC) side) of the embryo, and a small daughter ganglion cell (GC) to the dorsal side. In normal cell division, a contraction wave (CW), which appeared on the CC pole at the beginning of middle anaphase, traveled toward the GC pole at late anaphase. As reported previously, only one transition of the CW was observed in normal neuroblasts, whereas the CWs in Cytochalasin B-treated cells repeatedly appeared at regular intervals. In this study, cortical movements throughout the mitotic cycle were analyzed by means of cinematography and photokymography in low concentration Colcemid-treated neuroblasts. The development of mitotic apparatus (MA) was suppressed, the time required for mitosis was somewhat prolonged, and GC-side pole of MA failed to anchor on the polar cortex. In such cells, shifting of MA during anaphase was less active, and the repeats of CWs continued in the daughter neuroblasts at short interval. These results suggest that squeezing action of CW pushes the MA towards the GC-side, and anchoring of spindle pole on the GC-side cortex may be the essential factor to stop the reappearance of CW on the CC pole of the cell.

CELL-TYPE PROPORTIONING AND ITS RELATION TO RESPIRATORY ACTIVITY OF MITOCHONDRIA IN *Dictyostelium* CELLS.

S. Matsuyama, Y. Maeda. Biol. Inst., Fac. of Sci., Tohoku Univ., Sendai.

Along a long axis of migrating *Dictyostelium discoideum* slugs, clear regional differentiation is noticed : the anterior prestalk cells (pst) and posterior prespore cells (psp). The number ratio of pst/psp is usually constant. In differentiating prespore cells, an unique organella (PSV; prespore-specific vacuole) is formed, possibly from vesicles and/or mitochondria. In this connection, rhodamine123, the fluorescent dye, which is known to accumulate only in actively respirating mitochondria, was found to stain more strongly prespore cells than prestalk cells. This raised a possibility that artificial modifications of mitochondrial respiratory activities may affect the pst/psp ratio. To test this possibility, we examined effects of several respiration inhibitors on cell-type proportioning. Interestingly, benzohydroxamic acid, a specific inhibitor of cyanide-resistant respiration, blocked prespore differentiation in a concentration dependent manner, thus suggesting a close relationship between cell differentiation and mitochondrial respiratory activity.

LOCALIZATION OF THE ANTIGEN FOR THE MONOCLONAL ANTIBODY ③ 11A7-C.

S. Ishida and S. Kinoshita.
Dept. of Biol., Fac. of Sci., Hirosaki Univ., Hirosaki.

Monoclonal antibody (mAb) ③ 11A7-C specific to the nerve cells of Phagocata vivida has been produced (Shirakawa et al. 1991), but localization of the specific antigen has not been clarified yet. We identified the localization of this antigen by immuno-electron microscopy. Synapses, neurosecretory granules, neurotubules and mitochondria showed no reaction. But fine filaments distributed as a network in the nerve cells showed a positive reaction. In the photoreceptor cells of the eyes, rhabdome showed no reaction. The base of conical body showed a positive reaction. In the base, few mitochondria distributed and the network of fine filaments was observed.

DISTRIBUTION OF MYOPLASMIC CYTOSKELETAL DOMAINS AMONG EGG FRAGMENTS OF THE ASCIDIAN *CIONA SAVIGNYI*

Y.Marikawa. Dept. of Zool., Fac. of Sci., Kyoto Univ., Kyoto.

The myoplasm of the ascidian egg contains muscle determinants and is composed of myoplasmic cytoskeletal domain (MCD). MCD consists of two interacting parts, a plasma membrane lamina (PML) and a deep filamentous lattice (DFL). We showed that , among the four types of egg fragments that are produced by centrifugation of unfertilized *Ciona savignyi* eggs, muscle determinants are concentrated in only one type (black fragment) and are virtually absent in the others (clear, brown and red fragments). In this study, we compared the distribution of PML and DFL among the egg fragments. Actin filament, which is a component of PML, was found in all fragments. In contrast, the NN18 antigen, which is a component of DFL , was highly concentrated in black fragments and excluded from the others. Thus, the distribution of muscle determinants among the egg fragments coincided with that of DFL, suggesting that muscle determinants are associated with DFL rather than with PML.

SCREENING FOR GENES EXPRESSING IN CNS DURING METAMORPHOSIS IN DROSOPHILA.

H.Tsujimura, E.Kohda, I.Kashihara. Lab. of Biol., Tokyo Univ. Agri. Tech., Fuchu, Tokyo 183, Japan.

For the study of molecular and cellular mechanisms of the alteration of the CNS during metamorphosis, we are screening from about 100 enhancer trap lines for genes expressing in CNS in that time.

In most of the lines, the CNS of late 3rd instar larvae was stained. Some imaginal discs were stained simultaneously with the CNS. In many flies, the CNS and leg imaginal discs were stained. In other many lines, the CNS and all imaginal discs were stained. In few lines, only the CNS, the CNS and wing discs, or the CNS and eye discs were stained. In the CNS, many cells in certain regions are stained in some lines. In some other lines, small number of cells in the CNS were stained in certain patterns. In another small number of lines, cells scattering in some or whole region of the CNS were stained. This result suggests that many genes expressing in the CNS in this time are not specific for the CNS and may work for specification of small groups of cells in the CNS.

A MEMBRANE PROTEIN RELATING TO OOGENESIS AND DEVELOPMENT OF NERVOUS SYSTEM IN CIONA INTESTINALIS.

K.Takamura, Y.Nakazawa and Y.Yamaguchi. Div. of Biotech., Fac. of Engineering, Fukuyama Univ., Fukuyama.

We prepared several monoclonal antibodies against ovary homogenate of Ciona intestinalis. One of them, UA301 antibody, reacted with the boundary between oocyte and test cells during oogenesis, since test cells entered into the surface of oocyte and until they migrated out into the previtelline space. Extraction of this antigen from ovary required detergents, such as Triton X-100 or Lubrol PX. Western blot analysis showed the molecular weight of this antigen was 200Kd. These results suggest it is the membrane protein, which is concerned with test cell-oocyte interaction. During embryogenesis, this antibody did not react with any part of embryos. However, in larva and juvenile, its central and peripheral nervous systems were strongly reacted with this antibody. We have not determined whether the antigen in ovary and in nervous systems was same or not. Now, we are attempting to isolate and identify this antigen by affinity chromatography.

DISTRIBUTION OF THE CYTOPLASMIC DETERMINANTS IN UNFERTILIZED EGGS OF THE ASCIDIAN *Halocynthia roretzi*

A. Yamada and H. Nishida.
Department of Life Science, Tokyo Institute of Technology, Yokohama.

To investigate the localization of cytoplasmic determinants in unfertilized eggs of the ascidian *Halocynthia roretzi*, we carried out cytoplasmic-transfer experiments by fusing blastmeres and egg fragments from various regions of unfertilized eggs. The results are as follows.

· Endoderm and Muscle determinants

In unfertilized eggs, it was suggested that both determinants are widely distributed in the area except for the animal pole region, and that they are more abundant in the vegetal pole region than in the equatorial region.

· Epidermis determinants

It was suggested that epidermis determinants are widely distributed all over the unfertilized egg, with the highest abundance in the animal pole region.

MONOCLONAL ANTIBODY(4E9R) SPECIFIC FOR MOUSE NEURAL CREST CELLS RECOGNIZES A VIMENTIN-RELATED ANTIGEN.

Y.Kubota, T.Morita and K.Ito
Dept. of Biol., Fac. of Sci., Osaka Univ., Osaka.

We isolated a rat anti-mouse monoclonal antibody 4E9R which recognized mouse neural crest cells. We showed that the antigen recognized by 4E9R was present on intermediate filaments or components associated with them.

In this study, we have attempted to analyze in detail the intracellular localization of this antigen using a confocal laser scanning microscope and characterize biochemically it by dot blotting analysis. Data indicate that the antigen recognized by 4E9R is related with vimentin. 4E9R may recognize the vimentin-related epitope modified specifically in some embryonic cell-types including mouse neural crest cells.

TRANSIENT ACCUMULATION OF LECTIN BINDING GLYCANS ON PURKINJE, GRANULE AND BERGMANN GLIA CELLS IN THE CEREBELLUM OF THE RATS

H. Keino, and J. Suzuki, Dep. Perinatology, Inst. for Dev. Res., Kasugai.

Cerebella from suckling rats were examined histochemically with biotin-labelled DSL, PNA, and UEA-I. Purkinje cells from postnatal day 7 rats may be rich in sugars with terminal sugar structures that resemble blood group-related antigens (Type H), because they showed a remarkable ability to bind UEA-I. The sugars were observed on Purkinje cells in granule cell-free cerebellum. Granule cells in the stage of migration or post migration reacted with PNA. Granule cells of which migration were inhibited never showed an ability to bind PNA. Bergmann glial fibers binded to DSL, indicating an accumulation of complex type glycans. The ability was not shown on Bergmann fibers which had been inhibitted from contact with migrating granule cells.

BDNF PREVENTS NEURONAL DEATH OF CEREBELLAR GRANULE CELLS *IN VITRO*

K. Suzuki and T. Koike. Lab. of Neurobiol., Graduate Program in Biological Sciences, Hokkaido Univ., Sapporo.

Cerebellar granule neurons isolated from 7-day-old postnatal rats undergo massive degeneration around DIV 5-6, which appears to mimic neuronal death due to unavailable trophic factor that occurs during development. In support of this notion, this neuronal death was prevented by treating the cells with cycloheximide (0.1-1 μM) or cordycepin (1-3 μM), suggesting that it is an active process requiring protein and mRNA synthesis. It was previously shown that both chronic depolarization with high potassium and NMDA prevent this cell death in a dose-dependent manner. By measuring intracellular Ca2+ levels, we generated a correlation curve between [Ca2+]i and neuronal survival similar to that for sympathetic neurons. Besides sustained levels of [Ca2+]i , various drugs including TPA, cAMP, cGMP or others so far tested failed to support the survival. In constrast, BDNF (50ng/ml) completely prevented this neuronal death. Moreover, semi-qantitative PCR measuremets revealed that *trk B*, the proto-oncogene encoding a signal-transducing subunit for the BDNF receptor, was up-regulated during DIV 5-6, just before neuronal death occurred. However, up-regulation did not occur for the message of the truncated form of *trk B* lacking tyrosine kinase domain. These results suggest a pivotal role of BDNF in regulating neuronal death/survival of cerebellar granule cells *in vivo*.

BC3H1 MOUSE MUSCLE CELLS EXPRESS BOTH SKELETAL MUSCLE AND NEURON SPECIFIC MARKERS

M. Abe and R. Matsuda. Dept. of Biol., Univ. of Tokyo, Komaba, Tokyo

Mouse muscle cell line BC3H1 is an established cell line derived from murine brain tumor. BC3H1 cells express myogenin in low serum medium and differentiate to skeletal muscle cells. We have recloned this cell line and isolated a subline, BC3H1-18, with neuron-like morphology. By using immunoblotting and immunofluorescence, this subline was found to express neuron specific markers such as ß-tubulin isotype III and neurofilament 68. In low serum medium, BC3H1-18 also expressed skeletal muscle cell markers such as myogenin and sarcomeric myosin heavy chain. The result indicates that a single cell line, BC3H1-18, can express both neuron and skeletal muscle cell markers. Buckingham (1994) reported the existence of myogenin-positive neuron-like cells in developing mouse brain. These myogenin-positive brain cells and our BC3H1-18 may share a regulatory mechanism to express both neuron and skeletal muscle cell specific phenotypes.

THE DEVELOPMENTAL EXPRESSION OF CLATHRIN ASSEMBLY PROTEIN AP-3 IN RAT BRAIN.

M. Sugano and H. Nakae

Advanced Research Laboratory, Research and Development Center, Toshiba Corporation., Kawasaki.

Clathrin assembly protein AP-3 is a component of clathrin-coated vesicles. It binds to clathrin and promotes the assembly of uniform clathrin cages. Because it is localized in synapse specifically, it is thought to may play a significant role in synaptic functions. The developmental expression of AP-3 in rat brain was previously reported. Its first appearance was observed on postnatal day 7 when synapses has been matured.

We prepared a monoclonal antibody Mab R-18 by immunizing Balb/c mice with membrane fraction of rat brain. Mab R-18 has been considered as an original antibody against AP-3, based on the results mentioned as follows. (1) The estimated molecular weight of the Mab R-18 antigen was about 180kDa, (2) the isoelectric point of the antigen was acidic, (3) the antigen exhibited brain specific expression, (4) the antigen is localized in synapse rich region of rat cerebellum, and (5) the nucleotide sequences of cDNA clones isolated with Mab R-18 immunochemically were almost identical with the AP-3 cDNA sequence.

We have then investigated the developmental expression of AP-3 by Western blot analysis using Mab R-18. Consequentially, the Mab R-18 antigen was detected even in rat embryo during synaptogenesis. It implicated that the novel AP-3 isoform expressed from the early stage.

EFFECTS OF INSULIN AND INSULIN-LIKE GROWTH FACTOR-1 ON PROLIFERATION AND MORPHOGENESIS OF THE CENTRAL NERVOUS SYSTEM IN VITRO

M.Hiratochi[1], T.Iguchi[1], Y.Tomooka[2]. [1]Grad. Sch. of Integrated Sci.,Yokohama city Univ.,Yokohama, [2]Dep. of Biol. and Tech.,Science Univ. of Tokyo, Noda.

Dissociated neural precursor cells (NPCs) isolated from mouse embryonic brains (E9-10) were cultured in 3-dimensionally in collagen gel matrix. NPCs embedded in collagen gel extended neurites by the 9th day in culture and constructed ball like structures (neural balls, NBs). Majority of NBs developed lumen structures in NBs and immunocytochemical studies of NBs revealed that layers of NPCs were located near the lumen and differentiated neurons were toward in the outer layer of NBs. This is exactly the neural tube-like structure. Cell number and the number of NBs were drastically enhanced by addition of insulin to culture medium. Furthermore, IGF-1 which had high homology structure to proinsulin enhanced NB formation and cell growth. Considering immunocytochemical localization of IGF-1 in the central nervous system at E10 in vivo, the results indicate that IGF-1 is one of the possible factors in morphogenesis of the central nervous system.

EFFECTS OF HYDROCORTISONE ON THE PROLIFERATION AND DIFFERENTIATION OF MOUSE EPIDERMAL MELANOCYTES IN SERUM-FREE CULTURE.

T. Hirobe. Div. of Biol., Natl. Inst. Radiol. Sci., Chiba.

Disaggregated epidermal cell suspensions derived from newborn mouse skin were cultured in a serum-free medium supplemented with dibutyryl cyclic adenosine 3',5'-monophosphate and basic fibroblast growth factor. Melanoblasts proliferated dramatically around keratinocyte colonies and after 12-14 days pure and enriched cultures of melanoblasts (ca. 75%) and melanocytes (ca. 25%) were obtained. However, when epidermal cell suspensions were cultured with the serum-free medium supplemented with various concentrations of hydrocortisone, the number of melanoblasts gradually decreased and by contrast the number of melanocytes increased in a dose-dependent manner. Over 95% of melanogenic cells were differentiated melanocytes in the dishes cultured with serum-free medium supplemented with 10 nM hydrocortisone. These effects of hydrocortisone were observed only in the presence of keratinocytes. These results suggest that hydrocortisone inhibits the proliferation of mouse epidermal melanoblasts and stimulates the differentiation of melanocytes in culture in the presence of keratinocytes.

A STUDY OF 3D BIOIMAGES-2: ANALYSIS OF CELL PROLIFERATION KINETICS IN DEVELOPING NEURAL PLATE OF A CHICK EMBRYO.

S. Tanaka[1], Y. Yamazaki[1], T. Tsuji[1], Y. Kawasaki[1], T. Saitoh[1], A. Nomura[2], [1] Lab of BioImages, Mitsubishi Kasei Institute of Life Sciences, Tokyo, [2] Dept. of Zoology, Fac. of Science, Kyoto University, Kyoto.

Quantitative studies on cell proliferation kinetics in 3 dimension were conducted on neuroepithelial cells of the neural plate of a chick embryo. Following labeling with BrdU and immunohistochemical detection of S cells with FITC conjugated 2nd antibody, embryos were stained with propidium iodide (PI). Images of optical sections with dual parameters of FITC and PI were simultaneously collected along z-axis by a confocal laser scanning microscope. Images were processed to discriminate respective nuclei and S cells and 3D images were reconstructed by a software of Voxel View. Amount of DNA, volume, and center of gravity of individual nuclei were also computed by a personally developed software of 3D labeling.

EFFECTS OF ECTODERM ON PROGRAMMED CELL DEATH OF CHICK LIMB BUDS.

Minoru Omi and Hiroyuki Ide
Biol. Inst., Fac. of Sci., Tohoku Univ., Sendai

In the chick limb bud, a massive mesenchymal cell death occurs between the developing digits, and thus, they completely separate into individual digits. Hurle and Ganan (1986, 1987) reported that extra digit was formed when the ectoderm of interdigital tissue was surgically removed. However, little is known about the cell death in interdigital area.

To study the effects of ectoderm on the interdigital cell death, we cultured the interdigital mesenchymal tissue with or without ectoderm for 24 hours in the organ culture system established by Tone et al.. Nile Blue staining and TUNEL method (Gavrieli et al., 1992) were used for the detection of cell death. Positive region was limited at the proximal area when the mesenchyme was cultured without ectoderm, however cell death occurred widely from proximal to distal in the mesenchymal tissue with ectoderm. These results suggest that limb bud ectoderm is involved in the progress of interdigital cell death.

APOPTOSIS IN NEURAL RETINA OF DEVELOPING CHICK EMBRYOS.

Y.Yokoyama[1,2], H.Namiki[1], K.Kano[2], J.Arai[2], Y.Seyama[2], K.Shirama[3], Y.Hayashi[4] (1.Dept. of Biology, Faculty of Education, Waseda Univ. Tokyo, 2. Dept of Physiological Chemistry and Nutrition, Faculty of Medicine, Univ. of Tokyo, Tokyo, 3. Dept. of Anatomy, Tokyo Medical College, Tokyo, 4. Res. Institute, Morinaga Milk Ind.)

In the developing nervous systems, neurons that fail to make correct connection or to locate their exact positions in certain circumstance die. Apoptotic cell death of the neural retina of chicken embryos has been characterized by the typical morphological changes. One of the most characteristic indices of the apoptosis is the interchromosomal fragmentation of DNA. Recently, it was reported that the DNA fragmentation occurred in the neural retina cells of chicken embryos on day 10. The maximal amount of fragmentation was reached around day 11 and 12. To examine exact nature of the apoptosis of developing neural retina of chicken embryo, the culture methods and the effects of cell adhesion molecules were determined. DNA fragmentation in the dispersed cell and minced tissue culture systems occurred in a different manner. The effect of various growth factors on the neural retina was also examined.

HEDGEHOG HOMOLOG OF NEWT

T.Takabatake [1], K.Takeshima [1], K.Inoue [2], T.Kobayashi [3], [1] Radioisotope Research Center, Nagoya Univ., Nagoya, [2] Dept. of Biophys., Fac. of Sci., Kyoto Univ., Kyoto, and [3] Graduate School of Human Informatics, Nagoya Univ., Nagoya

Sonic hedgehog, a homolog of the Drosophila segment polarity gene, has been recently reported to be cloned from the embryos of several vertebrate including mouse, chick and zebrafish. The putative signal proteins encoded by these genes are believed to play a key role in inductive interaction that regulates polarity of the central nervous system and limbs. We have isolated an amphibian homolog expressed in newt(*Cynops pyrrhogaster*) neurula embryo. The 1.8kb cDNA contains a single long open reading frame.

Comparison of the predicted newt homologous protein to those of other species revealed the following features; 1, The protein contains a hydrophobic region homologous to chicken Sonic hedgehog in the amino terminal. 2, It also contains the conserved 6 amino acids stretch, CGPGRG, just downstream the predicted signal peptide cleavage site. 3, The alignment is highly conserved in the amino terminal region, but not in the carboxyl terminal stretch. These features were commonly observed in cross-species comparison of hedgehog proteins. A slight difference was observed in the newt untranslated region upstream the initiation codon, in which two AUG codons sifted from the open reading frame existed.

NCAM(Neural Cell Adhesion Molecule)GENES OF NEWT

Y.Nagai [1], K.Itoh [2], H.Y.Kubota [2], T.C.Takahashi [3], T.Takabatake [4], K.Takeshima [4], [1] Graduate School of Human Informatics, Nagoya Univ., Nagoya, [2] Dept. of Zool., Fac. of Sci., Kyoto Univ., Kyoto, [3] Biohistory Research Hall, Takatsuki, and [4] Radioisotope Research Center, Nagoya Univ., Nagoya

A *Xenopus* monoclonal antibody(NEU-1; specific for neural tissue, DGD,31, 563-571,1989) was used to probe a λ gt11 cDNA library constructed from newt swimming larva(St.34-36). Sequencing of the largest clone (named CPN104) revealed extensive homology to the published sequence of NCAM. It corresponded to the carboxyl terminal(55%) of the large cytoplasmic domain(ld) form of NCAM including the 3' untranslated region. The library was screened further with the oligonucleotides probe deduced from the 5' end of CPN104. The clone CPN20D positive to the probe coded for 90% amino acids of the predicted carboxyl terminal sequence of the small cytoplasmic domain(sd) form of NCAM. Finally, the clone CPN315, which was isolated with the probe designed from the 5' end of CPN20D, extended the DNA sequence encoding the amino terminus of the polypeptides and a 5' non-coding region. These results provides the complete amino acid sequences of the two major(ld and sd) polypeptides of newt(*Cynops pyrrhogaster*)NCAM, and most of the nucleotide sequences of their mRNAs.

ANALYSIS OF NEWT EPIDERMIS SPECIFIC GENE

M.Ogawa [1], T.C.Takahashi [2], T.Takabatake [3], K.Takeshima [3]
[1] Graduate School of Human Informatics, Nagoya Univ., Nagoya.
[2] Biohistory Research Hall, Takatsuki, [3] Radioisotope Research Center, Nagoya Univ., Nagoya.

An epidermis specific gene, originally isolated from *Cynops pyrrhogaster* neurula cDNA library(DGD, 34, 277-283, 1992), appeared to have 4 homologous transcripts of different sizes. Their expression changed at metamorphosis; i.e. 1.9 kb and 2.3 kb for embryonic type to 2.9 kb and 4.0 kb for adult type. It is interesting to analyze the relationship between the change(s) in the function of skin and the regulation of the gene expression at metamorphosis. We constructed new cDNA libraries from swimming larva(St.48) and from adult skin, and screened them by the originally isolated cDNA as a probe. The isolated clones were classified into four groups corresponding to the transcripts mentioned above. Sequence analysis revealed that the size of open reading frames(ORFs) were almost same, although the size of non-coding regions varied significantly. The differences in sequences among the ORFs of the four groups seemed to be beyond the changes introduced by alternative splicing of minor exsons. It seemed that their transcription might be regulated by the homologous but independent genes.

FUNCTIONAL ANALYSIS OF A CADHERIN IN EARLY EMBRYOGENESIS OF *Xenopus laevis*.

K. Iwami[1], T. Tajima[1], and A. S. Suzuki[2].
[1]Dept. of Biol. Sci., Fac. of Sci., Kumamoto univ., Kumamoto.
[2]Dept. of Biol., Fac. of Gen Edu., Kumamoto univ., Kumamoto.

A cDNA clone encoding an entire sequence of cadherin was isolated from a *Xenopus* A6 cell cDNA library. Tke deduced amino acid sequence was supposed that the cadherin is an isoform of XB-cadherin. Northern and western analysis revealed that the cadherin was already detected in cleavage stage and the amount increased from gastrula stage to neurula stage, then decreased after neurula stage.

To determine the function of the cadherin in early development, the mutant mRNA, which lacked a part of the extracellular domein that was necessary for normal adhesion, was injected into dorsal side of blastomeres at eight cell stage embryo. The outer layer of the animal hemisphere of the embryos changed to rough at late-blastula stage and developed rips around there with gastrulation. The unpigmented inner cells went out from the rips. In the most striking case, the embryos were failed to complete gastrulation. These morphogenetic disorder suggests that the cadherin is closely related to cell migration and movement in gastrulation.

GERMINATION INHIBITTING SUBSTANCE ON GEMMULES IN *EPHYDATIA FLUVIATILIS*.

Y. Nakamura, T. Iwasaru and Y. Watanabe. Dept. of Biol., Ochanomizu Univ., Tokyo.

Gemmules of freshwater sponges show two dormant forms: quiescence and/or diapause. The gemmules of *Ephydatia fluviatilis* are known as non-diapausing type. Although the gemmules of *E. fluviatilis* are prevented from hatching as far as they lie within living sponge tissue, they are able to hatch as soon as they are removed form the parental tissue. It has been assumed that the living sponge may secret some diffusible substance that inhibits gemmule germination. Rasmont named this inhibiting substance gemmulostasin (GS) whose chemical nature was not still clarified.
We tried to examine its nature and effects of this inhibiting factor on gemmule germination. Conditioned medium was prepared as GS containing medium from 10ml culture medium in which 100gemmules were cultured for 10 days.
The gemmules that were incubated in the GS medium at 24° C, perfectly inhibited hatching, and this activity were reversible. When gemmules were incubated in diluted medium, the effect of inhibition showed concentration dependent. We tried to concentrate GS medium *in vacuo* and filtrate through Millipore filter. The molecular weight of GS estimated less than 5000. The activity of inhibition of gemmule germination was not lost by heating at 100° C for 30 minutes. We performed histologically to examine what stage of germination suppressed by GS.

Structure and expression pattern of the ascidian Hox gene *HrHox-1*

Y. Katsuyama, S. Wada and H. Saiga
Dept. of Biol. , Fac. Sci., Tokyo Metropolitan Univ. Tokyo

To understand the characteristic morphogenesis of an ascidian with the molecular evolution of the genes essential for animal development, we study the structure and expression of ascidian HOM/Hox type genes. In this report we isolated a cDNA clone of one of the ascidian Hox genes, *HrHox-1*. Conceptual translation of *HrHox-1* cDNA shows that the homeodomain is highly homologous to those of vertebrate Hox genes of paralogue 1. Northern analysis shows that the expression of *HrHox-1* begins at the gastrula stage, increases at the larva stage, reaching maximum at the swimming-larva stage and then it is maintained at lower level through the metamorphosis process. Whole mount in situ hybridization shows that the expression is first detected in epidermis of the junction of head and tail at the early tailbud stage and thereafter the signal in dorsal region becomes remarkable. At the late tailbud stage the expression extends anteriorly and posteriorly both in dorsal and ventral epidermal regions and in the spinal cord. These results suggest that *HrHox-1* may be involved in the pattering of a neural tissue and epidermis along the anteroposterior axis.

CELL DEATH DURING DEVELOPMENT OF PALLEAL BUDS IN THE POLYSTYELID ASCIDIAN, *Polyandrocarpa misakiensis*.

S. Hirata, Y. Kawatsu, S. Fujiwara and K. Kawamura. Dept. of Biol., Fac. of Sci., Kochi Univ., Kochi.

During the early phase of bud development of the ascidian *Polyandrocarpa misakiensis*, mesenchymal cells decrease highly in number at the morphogenesis region. The same phenomenon was observed at the ectopic field of morphogenesis induced by retinoic acid(RA). We examined whether this cell loss accompanied cell death, by the methods of terminal deoxynucleotidyl transferase-mediated dUTP-biotin nick end labeling(TUNEL) and amido black staining. During bud development, only vacuolated cells, named morula cells, became TUNEL-positive. The result suggested that they underwent DNA fragmentation, characteristic of apoptotic cell death. But, morula cell was inconsistent with cell type(leucocyte) that decreased significantly in number during bud development. In contrast, leucocytes were heavily stained with amido black at the morphogenesis area immediately after bud development, suggesting that necrotic cell death took place. RA promoted amido black staining of leucocyte. These results suggest that during bud development of *P. misakiensis* the loss of mesenchymal cell may be caused by necrotic cell death rather than apoptotic cell death.

EFFECT OF TEST CELL REMOVAL ON THE DEVELOPMENT OF *CIONA INTESTINALIS*.

Y. Sato , M. Morisawa
Misaki Marine Biological Station, Sch. of Sci., Univ. of Tokyo, Kanagawa.

Test cell has been supposed to play some roles in the development of ascidian larva, e.g. provision of nutritional material to oocyte during vitellogenesis, production of hatching enzymes and formation of fin of larval tunic at the neural stage. However, no attention has been paid on the test cell in the swimming period and metamorphosis.

We removed the test cells from fertilized eggs with steel needles and each egg was developed in artificial sea water containing antibiotics in an agar coated multiwell at 18°C. Progress of metamorphosis of the test cell - free larva (naked larva) was slow as compared with that of normally developed larva. A part of tail of naked larva was not resorbed and remained even after cerebral organs rotated through about 90 degrees an arc. The tail was finally resorbed after expansion of branchial basket.

We found newly produced cells on the surface of naked larva. When we developed eggs without test cells, the embryo has become got new cells on the surface of the body in the tail bud stage. Morphological features of the new cells were similar to the test cells and its number increased until the beginning of metamorphosis.

DEVELOPMENTAL EXPRESSION OF PROTEASES INDUCED BY RETINOIC ACID IN BUDDING TUNICATES.

K. Kawamura and S. Fujiwara Dept. of Biol., Fac. of Sci., Kochi Univ. Kochi.

In the budding tunicate, *Polyandrocarpa misakiensis*, mesenchymal cells that have incorporated retinoic acid (RA) can induce an ectopic bud axis. This study was designed to examine what signal(s) were emitted by RA-incorporated mesenchymal cells and could cause transdifferentiation of the multipotent atrial epithelium. Protease activities such as trypsin, collagenase, aminopeptidase and cathepsin were enhanced in the sera of developing buds. The serum also contained an activity of trypsin inhibitor. The inhibitor activity was elevated significantly during budding, whereas it became low at the morphogenetic area of the developing bud. The proteases mentioned above were also induced *in vitro* by RA. Cathepsin was secreted into the culture medium of mesenchymal cells within 24 hours after RA treatment. The enzyme activity was 4-5 times higher than that of the control without RA treatment. Explants of the atrial epithelium have lost the differentiation antigen, when they were soaked with the conditioned medium of RA-treated cells. These results suggest that in *P. misakiensis* several kinds of proteases are up-regulated by RA and that they play roles in dedifferentiation of the atrial epithelium.

EXTERNAL AND INTERNAL FACTORS INFLUENCING LARVAL SETTLEMENT IN THE HYDROID *Tubularia mesembryanthemum*

K. Yamashita, S. Kawaii, M. Nakai and N. Fusetani
FUSETANI Biofouling Project, ERATO, JRDC. Yokohama

Upon settling and metamorphosing actinula larvae of *Tubularia mesembryanthemum* show the "nematocyst-printing" behavior, discharging from their tentacle chips numbers of atricous isorhiza nematocysts as means of temporary attachment.

In our studies on mechanism of larval settlement and metamorphosis, we examined external and internal factors influencing the nematocyst-printing behavior and settlement of actinula larvae.

As the results, the nematocyst-printing behavior and settlement were induced by the mechanical stimulus from contact-collision as water movement and by increasing K+ concectrations in sea water.

The amounts of printed nematocysts were also important for the larval settlement, inducing larva-larva communication for gregarious settlement mediated by the printed nematocysts. Moreover, the aged actinula-larvae were more sensitive to these inducers.

A VITELLOGENIN-LIKE PROTEIN IN THE COELOMIC FLUID OF *ARAEOSOMA OWSTONI*.

Y. Yokota[1] and S. Amemiya[2]. [1]Biol. Lab., Aichi Pref. Univ., Nagoya and [2]Misaki Marine Biol. Station, Fac. of Sci., Univ. of Tokyo, Miura.

Occurence of a vitellogenin-like protein in coelomic fluid of *A. owstoni* was confirmed and immunological relationships between *A. owstoni* vitellogenin-like protein and vitellogenin of *Hemicentrotus pulcherrimus, Anthocidaris crassispina, Temnopleurus hardwicki* and *Scaphechinus mirabilis* was investigated using antibodies raised against *A. owstoni* vitellogenin-like protein and *H. pulcherrimus* vitellogen. SDS-polyacrylamide gel electrophoresis and immunoblot analyses indicated that the coelomic fluid of *A. owstoni* contains a protein with the characteristics of sea urchin vitellogenin, which has been reported so far. The relative amount of vitellogenin to total proteins in coelomic fluid was estimated to be 20.3% based on the band intensity in *A. owstoni*, whereas the protein band of vitellogenin accounted for more than 60% in other 4 species.

ORIGIN OF MESODERMAL TISSUES OF ASCIDIAN JUVENILE.

T.Hirano, H.Nisida. Department of Life Science, Tokyo Institute of Technology, Yokohama

Cell linages during larval development of the ascidian, *Halocynthia roretzi*, have been described in detail, but origin of adult tissues is less understood. To study the origin of mesodermal tissues of juvenile, which has metamorphosed into adult body plan, we traced the cell fates by intracellular injection of horseradish peroxidase (HRP) into identified blastomeres at 110-cell stage. Descendants of the injected cells were histochemically detected at juvenile stage. It was shown that tunic cells and blood cells originate from larval mesenchym cells. Blood cells are also derived from trunk lateral cells of the larvae. Body wall muscle cells are derived from trunk ventral cells of the larvae.

EXPRESSION OF TYROSINASE GENE FAMILY IN ASCIDIAN EMBRYO

S. Sato, K. Tamura, H. Ide, T. Takeuchi and H. Yamamoto
Biol. Inst., Facl. Sci., Tohoku Univ., Sendai

Ascidian embryos develop two different types of pigment cells in the brain. The pigment cell precursors express an activity of tyrosinase, the key enzyme for melanin biosynthesis, around the time when the neural tube closes. We examined the expression of tyrosinase mRNA by *in situ* hybridization. Tyrosinase mRNA was first detected in two precursor cells at neural plate stage, soon after the determination of pigment lineage cells. We also cloned cDNAs for tyrosinase-related-proteins, TRP-1 and TRP-2, which were suggested to be involved in the formation of melanin pigment. Surprisingly the expressions of their mRNAs were detected in blastomeres that do not give rise to pigment cells in normal embryogenesis. This difference in the expression may presage the expression patterns of vertebrate tyrosinase gene family.

NOTOCHORD INDUCTION AND THE EXPRESSION OF A HOMOLOGUE (*AS-T*) OF *BRACHYURY* GENE DURING ASCIDIAN EMBRYOGENESIS

Y. Nakatani[1], H. Yasuo[2], N. Satoh[2], and H. Nishida[1]
[1]Department of Life Science, Tokyo Institute of Technology, Yokohama,
[2]Department of Zoology, Faculty of Science, Kyoto University, Kyoto

In the ascidian embryo, inductive interactions are involved in the formation of notochord. Notochord induction starts at the 32-cell stage and is completed by the 64-cell stage. A homologue of the mouse *Brachyury (T)* gene has been isolated from ascidian, *Halocynthia roretzi*, termed *As-T*. The expression is first detected at the 64-cell stage, exclusively in the presumptive-notochord blastomeres.

Presumptive-notochord blastomeres isolated at the 32-cell stage neither developed into notochord nor expressed *As-T* gene. However, when the presumptive-notochord blastomeres at the 32-cell stage were recombined with the inducer blastomeres, which are the presumptive-endoderm blastomeres and the presumptive-notochord blastomeres themselves, the expression of *As-T* was observed.

These results indicated that the expression of *As-T* is closely correlated with the determined state of the notochord precursor cells.

TIMING OF THE EXPRESSION OF MUSCLE-SPECIFIC GENES IN THE ASCIDIAN EMBRYO PRECEDES THAT OF DEVELOPMENTAL FATE RESTRICTION IN THE PRIMARY LINEAGE CELLS.

Y.Satoh, T.Kusakabe and N.Satoh
Dept. of Zool., Fac. of Sci., Kyoto Univ., Kyoto

Muscle cells of the primary lineage (B4.1-line) in ascidian embryos differentiate autonomously, depending on cytoplasmic determinants invested in the myoplasm. In this study, we re-examined by in situ hybridization of whole-mount specimens exact timing of expression of muscle actin genes in the primary lineage.

B6.2 in the 32-cell embryo contains developmental potential to give rise to muscle, mesenchyme and notochord. B7.4 in the 44-cell embryo, one daughter cell of B6.2, gives rise to only muscle (fate restriction), while another daughter cell B7.3 gives rise to mesenchyme and notochord. Transcripts of muscle actin gene are evident in B6.2 as well as B7.4 and absent in B7.3.

B6.4 in the 32-cell embryo gives rise to muscle and mesenchyme. B6.4 divides to B7.7 and B7.8 of the 64-cell embryo. Developmental fate of B7.8 is restricted to give rise to muscle, whereas that of B7.7 to mesenchyme. Transcripts of muscle actin gene are found in B6.4 and B7.8 but not in B7.7.

These results indicate that the expression of the muscle-specific gene precedes timing of developmental fate restriction in the lineage.

EXPRESSION ANALYSIS OF *NOTCH* HOMOLOGUE DURING ASCIDIAN EMBRYOGENESIS.

S.Hori[1], K.W.Makabe[2], H.Nishida[1] ([1]Department of Life Science, Tokyo Institute of Technology, Yokohama. [2]Division of biology, California Institute of Technology, Pasadena, U.S.A.)

An ascidian larva has two sensory pigment cells termed ocellus and otolith within the brain vesicle. The precursors of these pigment cells constiute an "equivalence group", in which the ocellus pathway is dominant(primary) fate. To investigate the molecular basis of cellular interactions in the equivalence group, we have used the PCR-based strategy to isolate the ascidian homologue of *Drosophila Notch*, which acts as a receptor for lateral inhibition signal during neurogenesis. The cDNA fragment which has both *lin/Notch* repeats and EGF repeats was amplified from the neurla mRNA by RT-PCR method. Expression analysis using this clone showed that the maternal mRNA exists in unfertelized eggs, and that its zygotic expression is restricted to the cranial region including the pigment cell precursors, in neurla and tailbud embryos.

Amyloid protein precursor-like gene in *Drosophila melanogaster*.

T. Aigaki[1], A. Nishimura[1], and K. White[2]. [1]Dept. of Biology, Tokyo Metropol. Univ., Tokyo, [2]Dept. of Biology, Brandeis Univ., Waltham, USA.

Drosophila amyloid protein precursor-like gene (*Appl*) is a homologue of human APP which is implicated in Alzheimer's disease. *Appl* is located on the X chromosome and expressed exclusively in the central nervous system and the peripheral nervous system neurons. Flies deleted for *Appl* gene has subtle defects in behavior (Liqun et al, 1992).

We examined the viability of *Appl*$^-$ flies during development. We set up crosses between *Appl*$^-$/*Appl*$^-$ females and *Appl*$^+$/Y males, and the number of progeny which developed to adult were compared between the sexes. The number of F_1 males (*Appl*$^-$/Y) were slightly less (about 10 %) than that of females which were *Appl*$^-$/*Appl*$^+$. Reduced viability of males were rescued by a transgene in which Appl cDNA was fused to 5' regulatory sequence of *Appl* gene, demonstrating that it has a developmental function.

IN VITRO DIFFERENTIATION AND DEDIFFERENTIATION OF CLONAL CELL LINES OF THE ASCIDIAN, *POLYANDROCARPA MISAKIENSIS*

N. Shibata, S. Fujiwara and K. Kawamura. Dept. of Biol., Fac. of Sci., Kochi Univ., Kochi

Recently, we have succeeded in the establishment of clonal cell lines of the ascidian, *Polyandrocarpa misakiensis*. The cell was derived from the explant of the atrial epithelium. When it was cultured in the growth medium consisting of modified milipore-filtered seawater (MMS), DMEM and FBS, it proliferated at the doubling time of about 14hours. MMS (pH6.8, 700~780mOsM) was prepared by adding HEPES and H_2O to seawater. The cell did not proliferate without this modification of seawater. Ultrastructural studies showed that, when low in density, clonal cells contained several granules in the cytoplasm, like the atrial epithelial cells. When the cells became confluent, they often gathered to form aggregates of variable size. The aggregates contained a few new types of cell. The smaller cells showed no specialized feature, like undifferentiated stem cell. The larger cells had several vacuoles in the cytoplasm, like vacuolated cells in the blood. These results suggest that cell lines we established have bipotential to the atrial epithelium and blood cells, and that stem cell described previously might arise as dedifferentiation of differentiated cell.

METAMORPHOSIS OF A DEMOSPONGE: CELLS AND STRUCTURE OF PARENCHYMELLA LARVA

S. Amano[1] and I. Hori[2]

[1]Cancer Res. Inst., Kanazawa Univ., Kanazawa, [2]Dept. of Biol., Kanazawa Medical Univ., Uchinada.

Sponge development is unique among metazoans, and many controversies are left surrounding the cells' fates and lineages in this process. We show the fine structure of the parenchymella larva in Haliclona sp. The flagellated columnar cells cover the larva except at the posterior pole which is covered with a layer of archeocytes instead. A few number of vesicular cells are scattered in the flagellated epithelium. In the intermediate layer, collencytes with many small vesicles predominate. In the central cell mass, there are archeocytes with a conspicuous nucleolus, scleroblasts with a monaxon spicule, gray cells loaded with yolk-like granules, and granulous cells with a peculiar morphology.

PROLIFERATION- AND DIFFERENTIATION-INDUCING ACTIVITIES OF TUNICATE CYTOKINES ON CLONAL CELL LINE ESTABLISHED FROM *POLYANDROCARPA MISAKIENSIS*.

M.Nakatani, S.Fujiwara, and K,Kawamura. Dept. of Biol., Fac. of Sci., Kochi Univ., Kochi.

This study was designed to elucidate endogenous cytokines that would regulate the proliferation and differentiation of multipotent cells of the budding tunicate, *Polyandrocarpa misakiensis*. Clonal cell lines have been established from an explant of the atrial epithelium. They hardly proliferated in the incomplete cell culture medium that lacked FBS. They did not show an antigen of atrial epithelium-specific ALPase, while not a few cells expressed the peroxydase activity, a differentiation marker of a certain type of blood cells. The pellet of *Polyandrocarpa* homogenates was digested and extracted with trypsin. The extract enhanced significantly the proliferation of clonal cells in the serum-free medium. It also induced the cells to develop an atrial epithelium-specific ALPase. After gel filtration chromatography, the activities were recovered from the void volume. The results suggest that in *P.misakiensis* trypsin-extractable cytokine(s) play roles in both proliferation and differentiation of *in vitro* multipotent cells.

Atrichous isorhiza, a kind of nematocysts, formation in *Hydra magnipapillata*

H. Amano[1], O. Koizumi[2] and Y. Kobayakawa[3]. [1]Social & Cultural Studies, Kyushu Univ., [2]Phisiol. Lab., Dept. Sci., Fukuoka Women's Univ., [3]Dept. of Biol., Fac. of Sci., Kyushu Univ.

Nematocytes in *Hydra* differentiate from interstitial stem cells. Nematocyte morphogenesis involves complex processes of nematocysts' capsule formation; establishment of nematocyst thread regions within the external tube and invagination.

A monoclonal antibody AE03, specifically recognized atrichous isorhiza, one of four kinds of nematocysts in tentacles and some nematoblast nests in body column region. We distinguished a series of morphogenetic stages of the AE03-positive nematoblasts of the nests. The stages showed successive transformation of capsule and nematocyst thread. Nematoblasts in one nest showed same stage. AE03-positive nematocysts at the last stage and atrichous isorhizas were alike. The number of atrichous isorhizas and the AE03-positive nematoblasts in the body column were same order. These results suggest that AE03-positive nests were made of atrichous isorhizas' nematoblasts. Therefore, using AE03, we were able to investigate the process of atrichous isorhiza formation in *Hydra* in detail from beginning of the nematocysts' capsule formation, for the first time.

LOCALIZATION OF MITOCHONDORIAL LARGE RIBOSOMAL RNA IN THE EGG CHAMBER OF *Dorosophila melanogaster*

H.Saito, S.Kobayasi, M.Okada, Inst. of Biol. Sci.,Univ. of Tsukuba, Tsukuba.

In *Dorosophila*, mitochondrial large ribosomal RNA (mtlrRNA) is localized in polar granules of cleavage embryos, and plays a role in the mechanism underlying pole cell formation (Kobayashi et al. 1993). However, it remains to be revealed how and when mtlrRNA is transported out of mitochondria to polar granules. In early embryos, the mtlrRNA has already been localized in polar plasm. Thus we decided to see distribution of mtlrRNA outside mitochondoria during oogenesis by the *in situ* hybridization method. In this study, we found that mtlrRNA was localized to the perinuclear regions of the nurse cells and the oocyte. Localized mtlrRNA to the posterior region of oocytes was detected in a small fraction of the latest stage (st. 14) oocytes. These results suggest two possible routes for mtlrRNA to reach polar plasm. It is transported out of mitochondoria in nurse cells, then it is carried to the posterior region of oocytes from the nurse cells. Alternatively, extramitochondorial mtlrRNA stays in the perinuclear cytoplasm in nurse cells, and transfer of mtlrRNA out of mitochondria occurs again in the polar plasm. It is also possible that both of two processes take place. Similar observations are in progress in ovaries of flies with mutations in posterior group genes.

A NOVEL ORGAN-CULTURE METHOD FOR ANALYSIS OF THE *ter* GENE FUNCTION IN MOUSE FETAL GONADS.

M. Noguchi and N. Yamada, Dept. of Biol., Fac. of Sci., Shizuoka Univ., Shizuoka.

Embryonic germ cell deficiency occurs in *ter/ter* male and female mice of 129/Sv-*ter* strain. To analyze the function of the *ter* gene in germ cell deficiency, we investigated whether the *ter* gene causes germ cell deficiency in fetal gonads *in vitro*. We studied, first, the rolling tube method for organ culture of fetal gonads, and using it cultured during 9 days the testes and ovaries of 13.5-Day fetuses obtained from matings between +/*ter* animals of 129/Sv-*ter* strain. The results showed that numerous spermatogonia or oocytes surrounded with follicles differentiated in nomally appearing testes or ovaries cultured, respectively. However, germ cell deficiency occurred in about 29 % of gonads cultured. They were considered to be *ter/ter*. Thus, a novel method suitable for analysis of the *ter* gene function in fetal gonads *in vitro* was established.

MALE ACCESSORY GLAND PROTEINS ARE INCORPORATED BOTH INTO THE CYTOPLASM OF THE OOCYTE AND THE THORACIC GANGLIONIC CELLS IN MATED *DROSOPHILA MELANOGASTER* FEMALE.

F. Hihara Lab. of Biology, Fac. of General Education, Ehime Univ., Matsuyama.

In *Drosophila*, the proteins or peptides of the male accessory gland (AgPs) affect the behavior and physiology of the female after mating, including a stimulation of oviposition and a decrease in female receptivity to courtship. The fate of AgPs in the female after their transfer during mating, however, has not been ascertained. Using the method of autoradiography, I chased fates of AgPs labelled with ^{35}S - methionine which was fed just after eclosion of the male flies. In mated females, the labelled AgPs were detected in the following organs ; the inner reproductive system, circulatory system, the muscle and the nervous system. In the nervous system, AgPs were incorporated into the external cortex of the pro-, meso- and metathoracic neuromeres. AgPs were not detected in the brain. In the reproductive system, AgPs were found in the follicle cells of the egg chambers of the previtellogenic stages. Later, in the vitellogenic stages, AgPs were distributed uniformly in the cytoplasm both of the oocyte and the nurse cells. AgPs were found neither in the nucleus nor in the yolk particles of the egg cytoplasm. Structure of the eggs oviposited by the virgin females was compared with those of mated females to know if or not AgPs incorporated in the oocyte cytoplasm would have some role on the entry into meiosis or on the cleavage occurring in the syncytium embryo.

THE *ter* GENE CAUSES GERM CELL DEFICIENCY BY ITS EXPRESSION IN SOMATIC CELLS OF MOUSE FETAL TESTES.

M. Noguchi and K. Niwa, Dept. of Biol., Fac. of Sci., Shizuoka Univ., Shizuoka.

The *ter* gene causes primordial germ cell deficiency in *ter/ter* mice. In order to analyze whether the *ter* gene is expressed in germ cells or environmental somatic cells of fetal testes in LTXBJ-*ter* strain, we examined germ cell proliferation and differentiation in the testes reconstituted from germ cells and somatic cells with different *ter* genotypes. The 13.5-day fetal testes were dissociated, and germ cells were separated from somatic cells. Then, +/+ and +/*ter* germ cells were reaggregated with +/+ and +/*ter* or *ter/ter* somatic cells by hanging drop-gyratory culture, respectively. The resultant reaggregates were grafted to the adult testes. It was found that the seminiferous tubules were reconstituted in both combinations, and that germ cells proliferated and differentiated in the former combination, but became deficient in the latter.

It is concluded that the *ter* gene induces germ cell deficiency by its expression, at least, in gonadal somatic cells.

DEVELOPMENT OF THE GONADS WITH REDUCED NUMBER OF GERM CELLS IN THE MEDAKA, *ORYZIAS LATIPES*.

A. Shinomiya and N. Shibata. Dept. of Biol., Fac. of Sci., Shinshu Univ., Matsumoto.

It is generally accepted that the gonad formation in embryos proceeds under interactions between germ cells and somatic cells. To see the role of germ cells in gonadal sex differentiation in lower vertebrates, we observed the gonadal development of the medaka, *Oryzias latipes* with experimentally reduced number of germ cells.

Busulfan, a drug which selectively eliminates primordial germ cells in rat embryos, was used to reduce number of germ cells. Embryos were incubated in 25 mg/l of busulfan solution from st. 17 to st. 31. The germ cell number was counted at st. 31, 0 day, 10 days, and 20 days after hatching. A marked reduction of the germ cell number were observed in about half of the specimens at the day 10 and the day 20. In addition, some fry at 9-15 mm in standard length had few germ cells; germ cells were absent for the most region of the gonads.

In males, the globular structure was observed in the gonadal regions where the germ cells were absent. These structure were constructed with single layer of somatic cells and placed regularly along anterior-posterior axis around the efferent duct. We concluded that the globular structure was equal to the seminiferous tubule. These results indicate that the seminiferous tubule is developed regardless of the contact with germ cells in male gonad of *O. latipes*.

ESTABLISHMENT OF THE MOUSE CONGENIC STRAINS LTXBJ-*CSA* AND *CSA* EXPRESSION

M. Noguchi[1], M. Tsunesada[1], T. Harumi[1], K. Toyooka[1], and M. Kusakabe[2].
[1]Dept. of Biol., Fac. of Sci., Shizuoka Univ., Shizuoka,
[2]Lab. of Cell Biol., Inst. of Phys. and Chem. Res., RIKEN, Tsukuba.

Anti-*CSA*-antibody recognizes almost all cells in C3H strain of the mouse. In order to analyze ovarian teratocarcinogenesis by using chimeric mice between LTXBJ strain which is highly susceptible to spontaneous ovarian teratomas and other strains, the *CSA* gene was introduced from C3H strain to LTXBJ strain by repeated backcrosses, and *CSA* congenic strains, LTXBJ-*CSA*/*CSA* and -+/+ (N12+F3) were established. The former cells were *CSA* positive and the latter were negative immunohistochemically, and their *CSA* genotypes were detected by PCR-RFLP for *CSA* primer. The incidence of ovarian teratomas in both strains were similar to that of LTXBJ. It is concluded that in the newly established LTXBJ-*CSA* /*CSA* strain the *CSA* gene is expressed in LTXBJ genetic background.

REPEATING GUERRIER AND NEANT'S OBSERVATION (1986) ON OOCYTE/EGG HYBRID OF STARFISH.

M. Yoneda, Takiyama 5-7-7, Higashikurume, Tokyo 203

Guerrier and Néant (1986) fused an immature oocyte (with the GV) and a mature egg (with the pronucleus) of starfish and observed that both GV and pronucleus in the oocyte-egg hybrid broke down. They interpreted this as due to an MPF activity formed de novo by "metabolic cooperation" between cytoplasms of oocyte and egg. To repeat their observation here I used the hybrid of GV-oocyte and mature egg of Asterina pectinifera. Both GV and pronucleus in the hybrid simultaneously broke down some 1-2hr, confirming Guerrier-Néant's observation. Whether this breakdown of nuclei is ascribed to the "cooperation" to form MPF activity is however not certain, since I found also that homologous egg/egg fusion still sometimes induces a similar breakdown of pronuclei.

Solubilization and partial characterization of the protein subunits of the medaka egg envelope (chorion).

H. Sugiyama, K. Murata, I. Iuchi and K. Yamagami
Life Sci. Inst., Sophia Univ., Tokyo.

The inner layer of oocyte envelope of medaka, solubilized by 6.5% SDS or 8M guanidium chloride, consists of three glycoprotein subunits, ZI-1,2(74-76K) and ZI-3(49K) on SDS-PAGE. However, when the oocyte envelope was solubilized in 8M urea previously, the molecular weights of ZI-1,2 and ZI-3 became seemingly higher, being about 95-110K and 65K, respectively, on SDS-PAGE. The relative mobilities of these subunits were found to decrease in parallel with the increased length of time of previous treatment of the oocyte envelope with 8M urea at 60°C. Despite the change in the apparent molecular weights, there was only a little difference in amino acid compositions, i.e., in the relative contents of Cys and Lys, between the corresponding subunits obtained from the SDS-solubilized and urea-solubilized materials. This result suggest that medaka oocyte envelope subunits are not significantly changed by solubilization with 8M urea. Therefore, subunit proteins solubilized and isolated in the presence of 8M urea can be used for characterization of chorion proteins such as determination of the primary structure.

EFFECT OF DOUBLE-STRANDED RNA INJECTION ON MORPHOLOGICAL CAHNGES OF STARFISH OOCYTES AND ACTIVATION OF A PROTEIN KINASE ACTIVITY.

T. Kasahara, M. Matsunaga, N. Itoh and S. Ikegami.
Dept. Applied Biochem., Hiroshima Univ., Higashi-hiroshima, Hiroshima.

Microinjection of cytoplasmic polyhedrosis virus or its double-stranded RNA genome into the cytoplasm of an oocyte of the starfish, Asterina pectinifera, induces malformation of the cell with concomitant activation of a protein kinase that phosphorylates proteins with the molecular masses of 24,000, 35,000 and 36,500 Daltons. The oocyte eventually disintegrates due to a force prooduced by actin polymerization in the regeion near the vegetable pole. Addition of 1-methyladenine to an oocyte that received injection of double-stranded RNA prevents these morphological changes. These results show that an starfish oocyte aquires a defense mechanism to fight against invading double-stranded RNA molecules during meiotic maturation.

ON THE ROLE OF CATHEPSIN D IN XENOPUS VITELLOGENESIS.

N. Yoshizaki and K. Nakamura. Dept. of Biol., Fac. of Gen. Educ., Gifu Univ., Gifu.

Ovarian cathepsin Ds of 43 kDa and 36 kDa were purified by both QAE-cellulose and pepstatin-sepharose chromatography. The cathepsin Ds exhibited in SDS-PAGE analyses an activity cleaving vitellogenin into lipovitellins under mildly acidic conditions. This activity was pepstatin-sensitive and inhibited by monospecific anti-rat liver cathepsin D antibody. The amount of cathepsin D per oocyte increased from stage I to V during oocyte development and reached a plateau, whereas the total amount of yolk proteins increased steadily from stage III to VI. In the homogenate of stage VI oocytes, 75% of the enzyme proteins resided in the supernatant fraction and 25% in the yolk fraction.

Immunocytochemical staining revealed that the enzyme was located within dense lamellar bodies in the cortical cytoplasm of stage I and II oocytes and in primordial yolk platelets and small yolk platelets of stage III oocytes. In stage IV and V oocytes, small yolk platelets had retained the immuno-staining but that of the large yolk platelets had decreased. No immuno-positive signals were observed in oocytes at stage VI. These results indicate that the cathepsin Ds cleave endocytosed vitellogenin into yolk proteins in developing oocytes, and that they decompose in large yolk platelets.

The analysis of expression of mRNA encoding L-SF, a precursor protein of the egg envelope, induced by estradiol-17β (E_2) in the liver of male fish, Oryzias latipes.

K. Murata[1], S. Yasumasu[1], I. Iuchi[1], I. Yasumasu[2] and K. Yamagami[1].
1: Life Sci. Inst., Sophia Univ., Tokyo. 2: Dept. of Biol., Sch. of Educ., Waseda Univ., Tokyo.

Precursor proteins of the egg envelope, H-SF and L-SF, are produced in the liver of spawning female fish, Oryzias latipes during the breeding season. They are found to be produced in the liver of also male fish, when the fish were administered estrogen (estradiol-17 β , E_2). Thus, the synthesis of these proteins in the liver is considered to be regulated by estrogen. In the present experiment, we found that mRNA encoding L-SF was synthesized in the liver incubated in vitro in the medium containing E_2. Moreover, the gene expression-inducing activity of some other oogenesis-related hormones was examined by Northern blot analysis and RT-PCR. The localization of the mRNA encoding this protein synthesized by E_2 administration in vivo, was examined according to the method of in situ hybridization to the liver sections.

MATURATION AND EXPANSION OF THE PERI-VITELLINE SPACE OF DEFOLLICULATED OOCYTES OF THE ASCIDIAN, *HALOCYNTHIA RORETZI*, BY TREATMENT WITH OVARY EXTRACTS.

[1]T. Numakunai, and [2]H.Yokosawa, [1]Mar. Biol. Stat., Fac. of Sci., Tohoku Univ., Asamushi, [2]Dept. of Biochem., Fac.of Pharmaceutical Sci. Hokkaido Univ., Sapporo.

When the ovary extract, which is prepared from spawning animals of the ascidian, *Halocynthia roretzi*, was subjected to gel filtration on a Sephadex G-75 column, we found two peaks showing activities to induce the oocyte maturation and the expansion of the peri-vitelline space (self-sterility). The first peak fraction and bovine pancreas trypsin (Sigma Type III) induced the expansion of the peri-vitelline space of defulliculated oocytes, whereas the second peak fraction of low molecular weigh had little inducing activity to expand the peri-vitelline space. These results suggest that follicle cells play a role in the expansion of the peri-vitelline space, leading to establishment of the self-sterility.

EFFECT OF CA^{2+}-FREE SEAWATER TREATMENT ON 1-METHYLADENINE PRODUCTION IN STARFISH OVARIAN FOLLICLE CELLS.

M. MITA. Dept. of Biol., Sch. of Educ., Waseda Univ., Tokyo, Teikyo Junior Coll., Tokyo.

Resumption of meiosis in starfish oocytes is induced by 1-methyladenine (1-MA) secreated by ovarian follicle cells following stimulation by a gonad-stimulating substance (GSS) released from nervous system. When follicle cells from ovaries of the starfish *Asterina pectinifera* were washed with Ca^{2+}-free seawater (CaFSW), the production of 1-MA and cyclic AMP in the presence of GSS was dependent on extracellular Ca^{2+} concentration, and was considerably reduced at a Ca^{2+} concentration below 1 mM. Thus, the decrease of 1-MA production by follicle cells after treatment with CaFSW is due to the low levels of cAMP. Furthermore, and ADP-ribosylation experiment using [α - ^{32}P]NAD^{+} in the presence of cholera toxin and pertussis toxin with membrane preparations of follicle cells treated with CaFSW revealed the presence of two types (stimulatory and inhibitory) of G-proteins. However, activity of adenylyl cyclase was not influenced by GSS regardless of the presence or absence of GTP. These findings may suggest that GSS is unable to bind to its receptor in follicle cells after washing with CaFSW.

CHARACTERIZATION OF KINASES RESPONSIBLE FOR INDUCING OOCYTE MATURATION IN GOLDFISH AND *XENOPUS*.

N. Yoshida, T. Tanaka and M. Yamashita.
Div. of Biol. Sci., Graduate School of Sci., Hokkaido Univ., Sapporo.

Oocyte maturation is presumably induced by the sequential actions of several kinases, of which MPF, a histone H1 kinase, and MAP kinase, a myelin basic protein (MBP) kinase, are known to play pivotal roles. However, additional kinases responsible for inducing oocyte maturation have not yet been characterized. To identify these other kinases, we examined kinase activities toward 47 exogeneous substrate proteins during oocyte maturation in goldfish and *Xenopus*. We found that 8 substrates were phosphorylated in goldfish oocyte extracts, and 6 in *Xenopus* extracts. Among them, 3 substrates (histone H1, MBP and pepsin) were phosphorylated in both extracts. Changes in the activity toward histone H1 and MBP during oocyte maturation were similar in both species, but those seen for pepsin were quite different. These results suggest that different kinase cascades are involved in goldfish and *Xenopus* oocyte maturation, although MPF and MAP kinase are common to both species.

DITHIOTHREITOL-INDUCED ACTIVATION OF CDC2 KINASE IN A CELL-FREE SUPERNATANT OF STARFISH OOCYTES: POSSIBLE INVOLVEMENT OF A CHYMOSTATIN-SENSITIVE PROTEASE.

K. Sano. Marine Biol. Station, Hokkaido Univ., Akkeshi.

Meiotic maturation of starfish oocytes is resumed by the formation of maturation-promoting factor after 1-methyladenine action on the cell surface. Maturation-promoting factor is shown to be cdc2 kinase, but the reaction chains resulting the formation of active cdc2 kinase is still obscure. Previously we reported that adding dithiothreitol initiates spontaneous activation of histone H1 kinase from a diluted supernatant of G2 stage starfish oocytes (1987). We have examined whether the histone H1 kinase activated is cdc2 kinase or not, and also examined factors involved in the activation process of cdc2 kinase. To assay cdc2 kinase activity, we measured histone H1 kinase activity precipitated specifically with p13suc1-Sepharose 4B. As a results, the kinase activated by adding dithiothreitol was confirmed as cdc2 kinase. Moreover, this activation was suppressed by adding a protease inhibiotor, chymostatin. These results suggest that in the cell-free activating system triggered by dithiothreitol, a chymostatin-sensitive protease activity participates in the activation process of cdc2 kinase.

ROLE OF GOLDFISH MO15 KINASE AS A CDC2 KINASE ACTIVATION FACTOR

S.ONOE[1,3], M.YAMASHITA[2], Y.NAGAHAMA[3]
[1]Dept. of Mol. Biomechanics, School of Life Science, Grad. Univ. for Advanced Studies, Okazaki, [2]Graduate School of Sci., Hokkaido Univ., Sapporo.,[3]Lab. of Reprod. Biol., Natl. Inst. for Basic Biol., Okazaki.

The activity of cdc2 kinase, a catalytic component of maturation-promoting factor (MPF), is controlled by its phosphorylation and dephosphorylation. MPF activation in goldfish oocytes is induced by cdc2 activation through its Thr161 phosphorylation. We have previously isolated a cDNA clone encoding MO15 kinase (GF-MO15), a kinase which is thought to phosphorylate Thr161 on cdc2 kinase, from a goldfish oocyte cDNA library. In this study, we examined if goldfish MO15 acts as a cdc2 activating enzyme. In immature goldfish oocyte extracts from which GF-MO15 was immunodepleted by anti-MO15 polyclonal antibodies, cdc2 kinase was not activated by cyclin B. Cyclin B-induced cdc2 activation was restored when GF-MO15 produced in rabbit reticulocyte lysate was added to the immunodepleted extracts. These results indicate that GF-MO15 play an important role in the activation of cdc2 kinase during oocyte maturation.

CDC2 EXISTS IN MONOMERIC FORM IN IMMATURE OOCYTES OF FISHES AND AMPHIBIANS EXCEPT *XENOPUS*.

T. Tanaka and M. Yamashita. Div. of Biol. Sci., Graduate School of Sci., Hokkaido Univ., Sapporo.

Maturation-promoting factor (MPF), a key regulator of oocyte maturation, consists of cdc2 and cyclin B. We investigated the state of cdc2 during oocyte maturation in fishes (goldfish, carp, loach, catfish and lamprey) and amphibians (*Xenopus*, frog (*Rana*) and toad (*Bufo*)). Anti-cdc2 immunoblotting of the consecutive fractions of oocyte extracts eluted from a Superose 12 gel filtration column showed that immature oocytes of all of these species with the exception of *Xenopus* contained only monomeric cdc2 (ca. 35 kDa). Cyclin B-bound cdc2 (ca. 100 kDa) was present only in immature *Xenopus* oocytes. Cdc2-cyclin B complex was, however, found in mature oocytes of all the species examined in this study. Cdc2 should therefore bind to cyclin B during oocytes maturation in all of these species, except *Xenopus*. These results suggest that the binding of cdc2 to cyclin B is a critical step for MPF activation during oocyte maturation in fishes and many amphibians. This is in striking contrast to the situation in *Xenopus* and starfish, where cdc2-cyclin B complex pre-exists in immature oocytes as pre-MPF, and its chemical modifications are required for MPF activation.

TRANSLATIONAL CONTROL OF CYCLIN B mRNA DURING GOLDFISH OOCYTE MATURATION.

Y. Katsu[1,3], M. Yamashita[2] and Y. Nagahama[3]. [1]Dept. of Mol. Biomechanics, School of Life Science, Grad. Univ. for Advanced Studies, Okazaki, [2]Div. of Biol. Sci., Graduate School of Sci., Hokkaido Univ., Sapporo and [3]Lab. of Reprod. Biol., Natl. Inst. for Basic Biol., Okazaki.

De novo synthesis of cyclin B protein is required for the activation of maturation-promoting factor during goldfish oocyte maturation. 17α,20β-Dihydroxy-4-pregnen-3-one (17α,20β-DP) - induced oocyte maturation was inhibited by a protein synthesis inhibitor (cycloheximide), but not by an RNA synthesis inhibitor (actinomycin D). Northern blot analysis showed that cyclin B mRNA is present in both immature and mature oocytes. These results suggest that the synthesis of cyclin B protein is under the translational control. It is known that changes in the translational activity of specific mRNAs is correlated with changes in the length of their poly(A) tails. In general, mRNAs that receive poly(A) become translationally active. To examine the polyadenylation state of cyclin B mRNA during goldfish oocyte maturation, we used a PCR poly(A) test, and found that cyclin B mRNA is polyadenylated during oocyte maturation. These results suggest that 17α,20β-DP stimulates cyclin B synthesis *via* poly(A) elongation of cyclin B mRNA.

PROTEASOME-MEDIATED DEGRADATION MECHANISM OF CYCLINB UPON EGG ACTIVATION

T.Tokumoto[1], M.Yamashita[2] and Y.Nagahama[1], [1]Lab. of Reprod. Biol., Natl. Inst. for Basic Biol., Okazaki. [2]Grad. School of Sci., Hokkaido Univ., Sapporo.

The role of active proteasome in the regulation of cyclin B degradation was investigated for the first time, using *E. coli* produced goldfish cyclin B and purified goldfish active proteasome. It was found that active proteasome can digest the wild type cyclin B, yielding 42 kDa intermediate cyclin. In contrast, cyclin B mutants lacking the first 41,68, and 96 amino acids were not digested by active proteasome, suggesting that the N-terminal amino acids are necessary for cyclin B digestion. Amino acid sequence analysis of the 42kDa intermediate cyclin revealed that active proteasome cuts the C-terminal peptide bond of lysine 57. Full-length goldfish cyclin B was also degraded in *Xenopus* egg extracts after activation by the addition of Ca^{2+}, but mutant cyclin Bs were not. Furthermore, a point mutant of cyclin B (Cyc K57R) was not digested by purified active proteasome and not degraded in *Xenopus* extract. Taken together, these results provide the first evidence to indicate that cyclin B is degraded through the first cutting on N-terminal by active proteasome.

ACTIVATION OF PROTEASOME IN RESPONSE TO CALCIUM ADDITION IN ASCIDIAN EGG CELL-FREE EXTRACT.

H. Kawahara and H. Yokosawa. Dept. of Biochem., Fac. of Pharmaceutical Sci., Hokkaido Univ., Sapporo.

The Proteasome is a high molecular weight protease complex, functioning in intracellular selective proteolysis of poly-ubiquitinated proteins.

We have previously reported that the proteasome is activated in response to intracellular calcium mobilization during ascidian egg activation.

To define calcium-regulated factors functioning in the activation of the proteasome triggered by intracellular calcium transit, we developed an ascidian egg cell-free system, in which the increase of chymotrypsin-like activity in response to calcium addition is detectable. In the cell-free system, the activity was increased by addition of calcium only when both ATP and 2-glycerophosphate were included. AMP-PCP, a nonhydrolyzable ATP analog, was ineffective. The increase was blocked by EGTA or W-7, a calmoduin antagonist. The activated activity was not inhibited by calpain inhibitors, and it was immunoprecipitable by anti-proteasome antibody. Thus a calcium-regulated mechanism leading to the activation of the proteasome works in asidian egg cell-free system, developed in this study.

CHANGES IN ACTIVITIES AND MOLECULAR SPECIES OF PROTEASOME DURING STARFISH OOCYTE MATURATION

M. Takagi Sawada[1], K. Izumi[1], M. Hanai[2], H. Yokosawa[2] and H. Sawada[2] [1]Biosci. Chem. Div., Hokkaido Natl. Indust. Res. Inst. and [2]Dept. of Biochem., Fac. of Pharm. Sci., Hokkaido Univ., Sapporo.

We have previously reported that a chymotrypsin-like activity of the proteasome may play a key role in activation of a pre-MPF during oocyte maturation of the starfish, *Asterina pectinifera*. Here, we examined whether a ubiquitin (Ub)/ATP-dependent proteolytic complex (26S proteasome) undergoes a change in activity during the oocyte maturation. Superose 6 gel filtration of the oocyte extracts indicated that the 26S proteasome activities toward Suc-Leu-Leu-Val-Tyr-MCA and Ub-[^{125}I]-lysozyme increased prior to GVBD in response to 1-MeAde. The oocytes preincubated in [^{32}P]-phosphate were treated with 1-MeAde and the aliquots were frozen and immunoprecipitated with anti-proteasome antibody. The precipitates were subjected to SDS-PAGE and autoradiography. It was found that the proteasome subunit was phosphorylated prior to GVBD, suggesting that the changes in proteasome activity may be regulated by phosphorylation of the proteasome subunit(s). Immunocytochemical analysis suggested that the proteasome is localized in the nuclear membrane as well as in the cytoplasm before GVBD.

MEIOTIC CELL CYCLE EXTRACTS FROM XENOPUS OOCYTES.

K.Ohsumi, W.Sawada, E.Kurosaki and T.Kishimoto. Fac. of Biosci., Tokyo Inst. of Technol., Yokohama 227.

Meiotic cell cycles differs from mitotic cycles in that the former lacks S-phase between meiosis I and meiosis II. To study the regulatory mechanism of the cell cycle unique to meiosis, we prepared a cell-free extracts from maturing *Xenopus* oocytes which had undergone germinal vesicle breakdown. When mitotic chromosomes attached to spindles were incubated with the extracts, they entered anaphase and subsequently reformed condensed metaphase chromosomes without passing through interphase. The lack of DNA replication during the period intervening the two metaphase was confirmed. We then examined changes in H1 kinase activity of cdc2/cyclin B complex immunoprecipitated with anti-cyclin B antibodies. The kinase activity was as high as that of metaphase II-arrested eggs at the beginning of the incubation, declined to a minimum level at the anaphase transition, and then re-increased to a high level in accordance with the re-formation of metaphase chromosomes. We also found that the tyrosine-phosphorylated form of cdc2 protein did not occur during the period intervening the two metaphase. All these changes in chromosomal morphology and cdc2 kinase are essentially same as those in maturing oocytes, demonstrating the progression of the meiotic cycle from metaphase I to metaphase II in the extracts.

CHANGES IN PROTEASOME ACTIVITY DURING ACTIVATION OF XENOPUS EGGS INDUCED BY CALCIUM IONOPHORE.

H. Aizawa, H. Kawahara, and H. Yokosawa. Dept. of Biochem., Fac. of Pharmaceutical Sci., Hokkaido Univ., Sapporo.

We have previously reported that the proteasome (a high molecular weight protease complex) undergoes cell cycle-dependent changes in activity and distribution during meiotic and mitotic cell division cycles of the ascidian Halocynthia roretzi.

To investigate whether such a change of the proteasome activity in the cell cycle progression is also found in other animal eggs, we measured proteasome activity during Xenopus egg activation induced by treatment with calcium ionophore. We found that a chymotrypsin-like activity of the 26 S proteasome is transiently activated and then inactivated in this process, that is, during the meiotic metaphase-anaphase transition. The activated activity was completely immunoprecipitable by treatment with anti-proteasome antibody. The fact that the pretreatment of eggs with BAPTA-AM, a cell-permeable calcium chelating agent, blocked the change in the proteasome activity strongly suggests that the proteasome activity is regulated by intracellular calcium mobilization during Xenopus egg activation.

OBSERVATION ON CHROMOSOME BEHAVIOR DURING MEIOSIS IN INTERSPECIFIC HYBRIDS BETWEEN *Oryzias latipes* AND *O. curvinotus*

Y Shimizu and N. Shibata

Dept of Biol., Fac of Sci., Shinshu Univ., Matsumoto.

Homologous chromosome pairing and segregation during meiosis are important processes in gametogenesis. Previous observations on interspecific hybrids between *Oryzias latipes* and *O. curvinotus*, it was indicated that: 1) in ovaries of hybrid females, some oocytes grow and mature as seen in normal ovaries, but they have both paternal and maternal chromosome sets. 2) in hybrid males, although they were sterile, sperm with larger head diameter were produced. In the present study, we examined chromosomal behavior during meiosis in those hybrid karyologically and histologically. Chromosome number of testicular is expected as 24 and 48, since both parental species have 2n=48 chromosomes. However, observed number of chromosome in hybrids varied between 24 and 48. In histological observations, although we could not find any unusual structure m mitosis, some chromosomes were found as a group beside metaphase plate during meiosis. These results suggest that, in interspecific hybrids between *O. latipes* and *O. curvinotus*, abnormal sperm were produced due to the lack of homologous chromosome pairing and segregation.

TEGULA'S VITELLINE COAT LYSIN cDNA: PCR CLONING AND SEQUENCE ANALYSIS

K.Haino-Fukushima[1], K.Tsuda[1], S.Yasumasu[2] and K.Yamagami[2]. [1]Dept. of Biol., Tokyo Metropolitan Univ. and [2]Life Sci. Inst., Sophia Univ., Tokyo.

The vitelline coat(VC) lysins of three species in the genus Tegula, T. pfeifferi, T. rustica(Ise) and T. lischkei, are each a single polypeptide consisting of 140 amino acid residues and the sequences of these lysins are the same in the N-terminal 76 residues and C-terminal 48 residues among three species.

We tried to get the cDNAs encording the VC lysins in two species of the genus Tegula, T. rustica(Yamaguchi) and T. nigerrima by polymerase chain reaction (PCR). Oligonucleotide primers were designed from the N-terminal (YGPGVRV-) and the C-terminal (-RTPGRFA) amino acid sequences of T. pfeifferi. Complimentary DNAs of about 420 base pairs (418 base pairs in T. pfeifferi) were produced by reverse transcription of two species' testicular RNAs as tempeletes, and by PCR amplification of first strand cDNAs with two oligonucleotide primers. The sequences of PCR amplification products were directly analyzed by the dideoxy chain termination method. This result showed the sequences of two species resembled closely to that of T. pfeifferi's VC lysin. The full-length cDNAs including 5'- and 3'-noncording regions will be cloned by rapid amplification of cDNA end (RACE) method.

THE AMINO ACID SEQUENCES OF VITELLINE COAT LYSINS OF JAPANESE ABALONES.

Y. Yamakami, A. Ito and K. Haino-Fukushima. Dept. of Biol., Fac. of Sci., Tokyo Metropol. Univ., Tokyo.

The vitelline coat(VC) lysin of Californian red abalone(*Haliotis rufescens*) has species-specificity on the vitelline coats lysis. It was found that the Japanese abalones, which are composed of the subgenus *Nordotis* and *Sulculs*, do not have species-specificity on the lytic action with the same subgenus but have it with the other subgenus. It seemes that the species-specificity on the lysis of vitelline coats of abalones has relation to the amino acid sequences of their lysins.

In the last study, we reported the amino acid sequence of VC lysin(15.5K) of *Haliotis discus*, one of the subgenus *Nordotis*. In this study, the VC lysin of *Haliotis gigantea*, which belong to the same subgenus, was purified and the amino acid sequence was determined, by the same method as *Haliotis discus*. The determined sequence showed high homology to that of *Haliotis discus* lysin. But the VC lysin of *Haliotis gigantea* lacked the 7 amino acid residues in the N-terminus, and the sequence showed microheterogeneities at the several positions.

MECHANISM OF INITIATION OF EMBRYONIC DEVELOPMENT IN THE CHUM SALMON (*ONCORHYNCHUS KETA*).

W. Kobayashi
Division of Biological Sciences, Graduate School of Science, Hokkaido University, Sapporo.

The native inducer of activation of salmon eggs is not a fertilizing sperm but the immersion of eggs in fresh water. Upon immersion of the unactivated eggs in Na^+ free salmon Ringer (SR), they showed exocytosis of cortical vesicles (CV). However, neither polar body extrusion nor blastodisc formation was observed. When unactivated eggs were immersed in Cl^- free SR, they showed polar body extrusion and blastodisc formation, but CV exocytosis was incomplete. Membrane potential of unactivated eggs was -31 mV in normal SR. When normal SR was perfused with 3.5% normal SR, the potential sifted to -20 mV. This depolarization was transient and followed by a hyperpolarization (to -56 mV) and returned to -33 mV. When normal SR was perfused with Na^+ free SR, unactivated eggs showed a depolarization (12 mV amplitude). The potential returned to the initial level upon reintroduction of normal SR. A longer immersion (10-50 min) in Na^+ free SR caused a large hyperpolarization. A similar hyperpolarization was precociously induced by A23187. Incubation of unactivated eggs in Cl^- free SR resulted in a large depolarization (31 mV amplitude). The potential did not return to the initial level upon reintroduction of normal SR. A23187 did not induce a hyperpolarization in Cl^- free SR, suggesting that the hyperpolarization is correlated with CV exocytosis and is caused by efflux of cations. These results suggest that decrease in external Cl^- is essential to egg activation in the chum salmon.

DOES FERTILIZATION ENVELOPE FORMATION INDUCED IN BUTYLIC ACID TREATED EGGS FOLLOWING WASHING WITH ARTIFICIAL SEA WATER DEPEND ON Ca^{2+} RELEASE FROM MITOCHONDRIA ?

K. Asai, Y. Kamata, A. Fujiwara and I. Yasumasu. Dept. of Biol., Sch. of Educ., Waseda Univ., Tokyo.

In sea urchin eggs, $[Ca^{2+}]_i$ and pHi decreased markedly during treatment with butylic acid and increased following washing eggs with ASW, which resulted in fertilization envelope formation. In eggs to which EGTA was injected, pH_i changed during butylic acid treatment and washing with ASW in the same manner as in eggs without EGTA-injection though $[Ca^{2+}]_i$ was maintained quite low and fertilization envelope hardly found. When eggs treated with butylic acid in the presence of DNP and FCCP was washed with ASW, they exhibited an increase in pH_i without evident increase in $[Ca^{2+}]_i$ and failed to undergo fertilization envelope formation. At low pH, Ca^{2+} uptake in mitochondria was augmented and Ca^{2+} in mitochondria was released when pH was made high.

TWO CALCIUM SOURCES CONTRIBUTE TO AN INTRACELLULAR CALCIUM INCREASE AT FERTILIZATION IN *MYTILUS EDULIS* OOCYTES.

R. Deguchi and K. Osanai. Mar. Biol. Stn., Asamushi, Tohoku Univ., Aomori.

Spawned oocytes of the marine bivalve *Mytilus edulis* are arrested at the first metaphase until fertilization. Using the fluorescent Ca^{2+} indicators fura-2 and calcium green, we have detected an increase in intracellular Ca^{2+} ($[Ca^{2+}]_i$) at fertilization in single oocytes. Normally fertilized oocytes initially showed a transient $[Ca^{2+}]_i$ increase which was followed by a period of sustained elevation. The first transient was a uniform $[Ca^{2+}]_i$ increase over the whole oocyte rather than a wave-like increase. Even if external Ca^{2+} was removed shortly after fertilization, $[Ca^{2+}]_i$ changes at fertilization still lasted. Injection of heparin, an inositol 1,4,5 trisphosphate (IP_3) receptor antagonist, also failed to abolish the sperm-induced $[Ca^{2+}]_i$ increase. In the heparin-injected oocytes, however, elevated $[Ca^{2+}]_i$ immediately returned to the resting level following external Ca^{2+} removal. The oocytes injected with "caged IP_3" and then exposed to UV light showed a $[Ca^{2+}]_i$ increase, indicating that an IP_3-induced Ca^{2+} release actually exists in *Mytilus* oocytes. These results suggest that both external Ca^{2+} influx and Ca^{2+} release from internal stores, which may be sensitive to IP_3, are responsible for a $[Ca^{2+}]_i$ increase at fertilization in *Mytilus* oocytes.

CALCIUM TRANSIENTS CAUSED IN FERTILIZED EGGS BY SPERM EXTRACT ARE MEDIATED BY IP_3.

M. Osawa[1], N. Kaneko[2], A. Terakawa[2], T. Kitani[2], R. Kuroda[2] and H. Kuroda[3]. [1]Ntl. Cardiovascul. Ctr. Res. Inst., [2]Dept. Biol. and [3]Dept. Environ. Biol./Chem., Fac. Sci., Toyama Univ., Toyama

Fertilization is known to initiate a transient increase of $[Ca^{2+}]_i$ (Ca-transient) in sea urchin eggs. Ca^{2+} are released from at least two independent, IP_3-dependent and IP_3-independent, stores. We have found that sperm and its soluble extract (spex) repeatedly cause a similar Ca-transient in fertilized eggs (Dev. Biol., *in press*).

Here we report the effects of heparin, an inhibitor of IP_3-mediated Ca^{2+}-release, and a G-protein inhibitor GDP-βS on Ca-transients in fertilized eggs by sperm (refertilization) and spex and on the Ca-transient during fertilization of *Hemicentrotus pulcherrimus*. Microinjection of heparin did not diminish Ca-transients during fertilization and refertilization but inhibited the transient by spex. Heparin had no effects on the peak values of transients during fertilization and refertilization, but prolonged their latent periods. Also in GDP-βS-loaded eggs, sperm elicited the Ca-transients during fertilization and refertilization but sperm extract could not cause Ca-transient. We measured the mass change of IP_3 by the isotope dilution methods. The IP_3 contents in the fertilized eggs were transiently increased by spex. These results show that sperm release Ca^{2+} from IP_3-dependent and IP_3-independent stores both in unfertilized and fertilized eggs but spex worked only on IP_3-dependent store via G-protein.

CHANGES OF cGMP AND IP_3 CONTENTS IN SEA URCHIN EGGS UPON FERTILIZATION

T. Kitani[1], R. Kuroda[1], Y. Tanaka[1] and H. Kuroda[2]. [1]Dept. of Biol. and [2]Dept. of Environ. Biol. / Chem., Fac. of Sci., Toyama Univ., Toyama.

Transient increase of the intracellular calcium ion concentration ($[Ca^{2+}]_i$) in the early stage of fertilization of sea urchin eggs is considered to be due to the calcium release from intracellular stores, which is mediated by inositol-1,4,5-trisphosphate (IP_3) and its receptor and by Ca^{2+} and ryanodine receptor. The latter mechanism is characteristic of sea urchin, and cyclic ADP-ribose (cADPr) is considered to be its modulator. Galione et. al. (1993) have reported cGMP to stimulate cADPr synthesis. Then, we measured mass changes of IP_3 and cGMP by the isotope dilution method and the $[Ca^{2+}]_i$ change by a Ca^{2+}-sensitive fluorescent dye, indo-I, in the early stage of fertilization. An egg contained a few ten attomoles IP_3 and a little less cGMP, and $[Ca^{2+}]_i$ was about 100 nM before fertilization. Cyclic GMP began to increase immediately after the insemination, reaching the first peak before the $[Ca^{2+}]_i$ increase did not yet start, and formed the second peak after $[Ca^{2+}]_i$ attained the peak of 1-2 μM. The first increase was not due to the acrosomal reaction. IP_3 began to increase slightly later than cGMP but earlier than $[Ca^{2+}]_i$, and reached a maximal level of about 200 attomoles/egg behind the $[Ca^{2+}]_i$ peak. Two pathways might have different roles in the Ca^{2+} transient.

DISTRIBUTION OF CORTICAL GRANULES AND THE FORMATION OF THE FERTILIZATION ENVELOPE IN IMMATURE AND MATURING STARFISH OOCYTES.

S. Nemoto[1], S. Nakajima[2], K.H. Kato[2] and S. Washitani-Nemoto[3]. [1]Tateyama Marine Lab., Ochanomizu Univ., Chiba, [2]Dept. of Biol., Fac. of Gen. Edu., Nagoya City Univ., Nagoya, [3]Biol. Lab., Hitotsubashi Univ., Tokyo.

When activated by sperm or artificial activators such as A23187, maturing oocytes undergo cortical granule (CG) exocytosis causing fertilization envelope elevation, while immature oocytes form only a weak envelope and no elevation is observed, suggesting the oocytes undergo little CG exocytosis. We observed the distribution of CGs and their breakdown on fertilization and A23187 activation in both immature and maturing oocytes of the starfish, Asterina pectinifera.

In immature oocytes, a significant number of CGs were observed apart from the cell surface, while most of CGs were located along the cell surface. The animal pole region was rich in CGs compared with the vegetal pole region. On fertilization, most of CGs underwent exocytosis in maturing oocytes, while a significant number of CGs remained unbroken in immature oocytes. This was the same in A23187 activation. In normal fertilization of maturing oocytes, CG exocytosis was lasting at least for 10 min., fertilization-envelope elevation took place slowly taking more than an hour, and the formed fertilization envelope consisted of three layers.

ASTER FORMATION NUCLEATED BY SPERM HEAD-MIDPIECE FRACTION IN SEA URCHIN EGG EXTRACTS.

K.Kuroishi, M.Hattanda, T.Murakami and M.Toriyama. Dept. of Biology, Fac. of Liberal Arts, Shizuoka University, Shizuoka.

In the fertilization of sea urchin eggs, sperm centrioles turn into the centrosome by gathering the maternal pericentriolar material around them. This procedure is necessary for the normal mitosis and normal development. For the construction of the model to analyze the mechanizms of the centrosome formation in fertilized eggs, we prepared the sperm head-midpiece fraction and egg extracts from unfertilized and fertilized eggs. Incubated with phosphocellulose purified tubulin, the sperm head-medpiece fraction nucleated microtubules in a template manner. In the fertilized egg extracts, it also nucleated microtubules and formed an aster-like structure. In the mitotic extract, more microtubules were nucleated than in the interphase extract. The sperm head-midpiece fraction nucleated no microtubule in the unfertilized egg extract, although enough tubulin was existed in the extract. These results indicate that the in vitro model we constructed in this experiment reflect the condition of the equivalent stage of the egg cytoplasm.

POLYSPERMY PREVENTING-MECHANISM IN THE OOCYTE OF THE MUSSEL, *MYTILUS EDULIS*.

T. Togo[1,2], K. Osanai[1], and M. Morisawa[2]. [1]Asamushi Mar. Biol. Stn., Tohoku Univ., Aomori and [2]Misaki Mar. Biol. Stn., Univ. of Tokyo, Kanagawa.

Apparent physical barrier against sperm such as a fertilization envelope in sea urchin is not formed in bivalve oocytes. Dufresne-Dubé *et al.* (1983) suggested that no complete block to polyspermy is established in *Mytilus galloprovincialis*.

We show here that the fertilized oocyte of *Mytilus edulis* is normally monospermic, and that the plasma membrane of the oocyte depolarized temporarily soon after insemination. The reduction of external Na^+ concentration decreased the amplitude of depolarization and induced polyspermy. When sperm were added to fertilized oocyte, almost sperm could not undergo acrosome reaction. Furthermore, the acrosomal process of remaining sperm, which underwent the acrosome reaction, reached to the plasma membrane of the oocyte, but sperm could not fuse with it. These results suggest the existence of polyspermy-preventing mechanisms in the oocyte of *M. edulis*; fast electrical block and prevention of the fusion of membranes of spermatozoon and oocyte, and the inhibition of acrosome reaction at the oocyte surface.

FERTILIZATION ENVELOPE FORMATION IN SEA URCHIN EGGS FOLLOWING TREATMENT WITH SDS.

Y. Kamata, T. Tojo, A. Fujiwara and I. Yasumasu. Dept. of Biol., Sch. of Educ., Waseda Univ., Tokyo.

$[Ca^{2+}]_i$ increase followed by fertilization envelope formation in sea urchin eggs was induced by SDS (sodium dodecyl sulfate) but was not found following SDS-treatment performed on eggs in the absence of external Ca^{2+} and on eggs to which EGTA had been injected. In nicotinamide injected eggs, SDS enhanced $[Ca^{2+}]_i$ but did not induce fertilization envelope formation. Injection of SDS hardly induced the envelope formation and caused cytolysis in many eggs. SDS resulted in breakdown of cortical vesicles in isolated egg cortices in the presence and absence of EGTA or nicotinamide. SDS probably cause breakdown of plasma membrane and cortical vesicle membrane but SDS-induced fertilization envelope formation does not seem SDS-caused direct breakdown of cortical vesicles.

CHANGES OF MICROTUBULE POLYMERIZATION IN THE POLY-SPERMIC NEWT EGGS.

Y.Iwao, M.Narihira, J.Q. Jiang* and Y.Nagahama* . Dept.of Biol., Fac. of Sci., Yamaguchi University, Yamaguchi. *Div. of Reprod. Biol., Natl. Inst. for Basic Biol., Okazaki.

In the physiologically polyspermic newt, *Cynops pyrrhogaster* eggs, only a principal sperm pronucleus can approach to an egg pronucleus. In this study, changes in microtubule polymerization during zygote formation by confocal fluorescece microscopy. There were many cytoasters in the cortex of unfertilized eggs, which formed arrays of cortical microtubules after fertilization. The principal sperm nucleus with a large aster approached to the egg nucleus to form a zygote nucleus. Asters of the sperm nuclei in the vegetal hemisphere remained until M phase. Together with our finding that microtubule-depolymerizing agents inhibits movement of sperm nuclei, these results suggest that the sperm asters play an important role in the selection of sperm nuclei in the polyspermic newt eggs.

Analysis of Chorion Hardening of Rainbow Trout Egg

Iuchi, I., H. Sugiyama, C.R. Ha and K. Nomura*
Life Science Institute, Sophia Univ. and
* Tokyo Met. Inst. of Gerontology, Tokyo, Japan.

Chorions of unfertilized eggs of rainbow trout, Oncorhynchus mykiss, become hardened after water activation. We estimated the chorion hardening by increase in resistance of an egg to rupture by extraneously added pressure and by decrease of the solubility of chorion in 8M urea. During the hardening process, some high molecular weight protein components were detected by SDS-PAGE and the contents of γ Glu-ε Lys increased. The chorion hardening was inhibited by the incorporation of monodansyl cadaverine into the chorions. These observations imply that the crosslink formation between constituent proteins of the chorion by transglutaminase is mainly responsible for the chorion hardening.

We examined the activity and some properties of transglutaminase (TGase) in unfertilized eggs. TGase activity was inhibited by EDTA and iodoacetamide. It was localized mainly in the chorions of unfertilized eggs, interpreting "chorion hardening of eggs without perivitelline space formation (Iuchi et al, 1993)" and "in vitro hardening of chorions isolated from unfertilized egg (Iuchi et al, 1991)".

TRANSFER OF ENDOSYMBIOTIC BACTERIA IN THE OVARY OF THE GIANT CLAM, *CALYPTOGENA SOYOAE*

J.Tsukahara. Dept. of Biol., Fac. of Sci., Kagoshima Univ., Kagoshima

Around deep hydrothermal vents certain invertebrate species maintain intracellular chemoautotrophic bacteria which aid in oxidation of reduced-sulfur compounds and provide energy to the host animals(Cavanaugh et al. 1981). *Calyptogena* harbors symbiotic bacteria in branchial epithelia (Fiala-Medioni and Metivier 1986, Endow 1988). Endo and Ohta (1990) described that intracellular bacteria were found in primary oocytes and follicle cells of the *Calyptogena soyoae*. However they could not find how the symbionts enter into the oocyte. The present study provides observations concerning the mechanism by which endosymbionts are tansmitted to host offspring during oogenesis of *C. soyoae*.

Samples of *C. soyoae* were collected by the unmanned submersible "Dorphin 3K" from Sagami Bay (1160m depth) off Hatsushima Island on 2 August 1991 and 18 November 1991.

There were scarcely differences in the stage of oogenesis among animals collected on August and November.

Many endosymbiotic bacteria were found in the cytoplasm of epithelial cells and nutritive phagocytes of the ovary. However, the symbionts are not found in the vitellogenic oocyte cytoplasm but only contacted with the oocyte surface and partially buried into the oocyte cortex. Phagocytotic vesicles formed frequently on the surface of the oocyte had no bacteria. On the surface of fully grown oocytes many bacteria stuck firmly. The present result is evidently different from that of Endo and Ohta(1990).

HORMONAL REGULATION OF ACTIVIN B PRODUCTION IN THE JAPANESE EEL TESTIS

T. Miura[1], C. Miura[1], K. Yamauchi[1] and Y. Nagahama[2]
[1]Fac. of Fisheries, Hokkaido Univ., Hakodate, and [2]Lab. of Reprod. Biol., Natl. Inst. for Basic Biol., Okazaki

In the Japanese eel testis human chorionic gonadotropin (HCG) induces activin B mRNA expression. To determine whether HCG action on activin B production is direct or mediated through other hormones such as 11-ketotestosterone (11-KT, an androgen which is shown to induce all stages of spermatogenesis in eel *in vitro*), we investigated the effect of HCG and 11-KT on activin B mRNA expression and protein secretion using an organ culture system for eel testis. Both HCG and 11-KT induced activin B mRNA expression and protein secretion. Furthermore, eel activin B extracted from cultured medium induced spermatogonial proliferation *in vitro*. These results suggest that in eel testis HCG stimulates Leydig cells to produce 11-KT, which, in turn, induces activin B production leading to the initiation of spermatogenesis.

ACTIVIN PRODUCTION BY SERTOLI CELLS IN THE JAPANESE EEL TESTIS

C. Miura[1], T. Miura[1], K. Yamauchi[1] and Y. Nagahama[2]
[1]Fac. of Fisheries, Hokkaido Univ., Hakodate
[2]Lab. of Reprod. Biol., Natl. Inst. for Basic Biol., Okazaki

We have previously shown that activin β-B mRNA expression in Sertoli cells mediates human chorionic gonadotropin (HCG)-induced spermatogenesis in the Japanese eel testis. In this study a newly developed Sertoli cell culture system was used to determine whether Sertoli cells can produce activin A, B and AB. Sertoli cells were cultured for a period of 6 days with or without 11-KT (100 ng/ml) or HCG (1 IU/ml). Even without hormonal stimulation, Sertoli cells produced a significant amount of activin A, B, and AB. However, there was no significant increase in the production of the activins in response to either hormone, except for a slight increase in activin A production by 11-KT. These results indicate that Sertoli cells in culture can produce activins. This cell culture system will provide useful models on hormonal regulation of testicular production of activins.

CLONING OF GENES DIFFERENTIALLY EXPRESSED AT MEIOSIS BY RT-PCR

T.Yamamoto and S. -I. Abe
Dept. of Biol. Sci., and Fac. of. Sci., Kumamoto Univ.

To elucidate the molecular mechanism whereby meiosis commences during newt spermatogenesis we have analyzed some genes differentially expressed at meiosis and isolated cDNA clones for calcium dependent phospholipid binding protein, annexin.

In this study, using mRNA differential display by RT-PCR (Liang and Pardee, Science 1992), we tried to isolate another differentially expressed genes in the secondary spermatogonia and primary spermatocytes. As a results several primary spermatocytes-specific genes (clone 5, 25, 35) were isolated. Northern blot analysis and in situ hybridization revealed that clone 25 was expressed scarcely in the secondary spermatogonia and t hen markedly in the germ cells from primary spermatocytes. These results suggested that clone 25 play an important role in the spermatogenesis.

SPERMATOGENESIS IN THE BENTHIC ARROW WORM *PARASPADELLA GOTOI* (CHAETOGNATHA).

T. Goto and Y. Hayashi. Dept. Biol., Fac. Educ., Mie University, Mie.

All chaetognaths are hermaphroditic and the male reproductive organ is located in the anterior end of the tail coelom. Spermatogonia released from the testes develop through circulating in the tail coelom. Various developmental stages were detected in the isolated male germ cells. The cells formed a cluster, the so-called "polyplast", which was found to be syncytium under electron microscopical observation. From the profiles of the polyplast stained with Hoechst 33342 or acetic orcein, it was revealed that the spermatogonia resulted in 64 spermatocytes, then underwent meiosis and spermiogenesis, and finally formed thin filiform mature spermatozoa. Moreover, it was evident that a pair of chromosomes, the so-called "X" chromosome, migrated to the opposite poles of the spindle earlier than the other chromosomes at the metaphase I and II of meiosis. The spermatids with elongated nuclei formed a few masses in which they were regularly arranged like a brush facing their nuclei within each mass. The elapsed time from spermatogonium release to mature sperm was estimated to be about 20 days.

FERTILIZATION OF *SYCON CALCARAVIS*, CALCAREOUS SPONGE
II. THE STRUCTURE OF SPERMATOZOON IN THE MATERNAL CHOANOCYTE

K. Okada and Y. Watanabe. Dept. of Biol., Ochanomizu Univ., Tokyo.

In the fertilization of *Sycon calcaravis*, we had observed the spermiocyst directly attached to the oocyte with two accessory cells. At this stage, spermiosyst did not enter any cells such as carrier cells. Therefore we supposed that the spermatozoon of this species might not enter into the choanocyte, but pass through between the two choanocytes. These choanocytes may change to accessory cells and carry the spermiocyst to the oocytes. However, recently we observed several choanocytes, ligned choanoderm, enguifed a spermatozoon. It is sure that at first spermatozoon enter into the choanocyte like as the other calcareous sponges.

In the choanocyte, the spermatozoon had long cylindrical nucleus with anterior concavity and several mitochondria at the end of the nucleus aligned in the ring. No flagellum was found. We recognized that some of the spermatozoa in the choanocytes had been changing its appearance. The ultrastructure of the spermatozoon in the choanocyte was greatly different from that of the spermiocyst between two cells near the oocyte. It indicated that the spermatozoon might be transformed after entrance into the choanocyte, which would ultimately later change into the carrier cell during transport to the oocyte.

At the final stage of sperm transportation, the spermiocyst may exclude from the carrier cell and directly attached to the oocyte. We discuss how the spermatozoon is carried to the oocyte, and which of the two accessory cells is really carrier cell, and how the spermatozoon is transformed in the carrier cell.

DECREASE IN THE RESPIRATORY RATE OF SEA URCHIN SPERMATOZOA DURING INCUBATION IN SEAWATER

T.Ohtake, M.Mita, *E.Tazawa, Y.Kamata, A.Fujiwara, I. Yasumasu Dept. of Biol. , School of Education, Waseda Univ. and *Biol. Inst., Yokohama City Univ.

Dry sperm of sea urchin (*Hemicentrotus pulcherrimus*) were diluted by 100-times with artificial sea water (ASW) (pH 8.2) at 20℃, and the respiratory rate was measured polarografically. During incubation in ASW, the respiratory rate and motility of sperm decreased almost linearly. At 4 hr of incubation, the respiratory rate became about 60% of the initial level. Activity of NADH-cytochrome *c* reductase decreased during incubation in ASW, although cytochrome *c* oxidase activity was hardly changed at least up to 8 hr of incubation. In these aged sperm, photoactivation of respiration occured at 430, 530, and 570nm. However, aged sperm were able to fertilize eggs until 10hr of incubation. It seems that mitochondrial respiratory system in sea urchin sperm is gradually degenerated after initiation of swimming, even when they have the ability to fertilize eggs.

MORPHOLOGICAL CHANGES IN MARINE INVERTEBRATE SPERM AT FERTILIZATION.

R. SATOH, N. SAKAKIBARA & A. HINO
Department of Biological Sciences, Kanagawa Univ. Hiratsuka

It is already reported that the sea urchin sperm changed its shape of mitochondria when they interacted with glutaraldehyde-fixed unfertilized eggs. In this situation, sperm became immotile and then finally their rate of respiration became almost to zero level (Hino et al, DGD. Vol. 22). In this year, Ohtake *et. al.* reported that the same morphological changes in sperm were also induced by Mg-free artificial sea water not by Ca-free seawater (Annual meeting of Japanese Society of Developmental Biologists). In *Halocynthia roretzi* they also changed their shape of sperm mitochondria in Mg-free sea water but their mitochondria did not separate from nucleus. In *Urechis unicinctus*, the sperm mitochondria became spherical not only by the fixed egg also by the Mg-free sea water. In *Asteria pectinifera*, their sperm did not show morphological change by the treatment of Mg-free sea water nor fixed eggs but when they acrosome-reacted, the sperm mitochondria always became spherical. Such morphological changes in sperm mitochondria seem ubiquitous phenomena at fertilization in these marine invertebrates.

BIOTINYLATED SEA URCHIN SPERM SURFACE PROTEINS.

Y. Satoh, T. Shimizu and N. Suzuki. Division of Biological Science, Graduate School of Science, Hokkaido University

In order to identify receptor proteins on sperm membranes which mediate the effect of the acrosome reaction inducing substance fucose sulfate glycoconjugate (FSG), membrane fractions were prepared from biotinylated sea urchin spermatozoa. Biotinylated proteins were separated using SDS-PAGE and characterized by comparison with known sperm membrane proteins from the sea urchin (*H. pulcherrimus*). Gel filtration chromatography of purified FSG combined with solubilized biotinylated sperm membranes indicated two proteins (63kDa, 50kDa) which coeluted with FSG. The interaction between FSG and these biotinylated proteins was shown to be species specific.

PHOTO-ACTIVATION OF NADH·CYTOCHROME c REDUCTASE IN SPERM OF ECHIUROID, OYSTER AND SEA URCHIN

E.Tazawa, A.Fujiwara and I.Yasumasu (Biol. Institute, Yokohama City Univ., Yokohama and Dept of Biol., Waseda Univ.,Tokyo)

Photo-activation of NADH·cytochrome c reductase occurred in sperm homogenates of echiuroid, oyster and sea urchin with peaks of activation at 430, 530 and 570nm, corresponding to the absorption peaks of reduced cytochrome b. During rearing animals for a long time in aquarium, the activity of cytochrome c oxidase was maintained but the activity of NADH·cytochrome c reductase evidently decrease in their sperm. In these aged sperm, photo-activation of respiration occurred with peaks of activation at 430, 530, 570nm. Photo-activation of cytochrome b reaction probably becomes apparent as an increase in the respiratory rate in sperm, when this reaction is rate-limiting in mitochondrial respiratory chain.

LOCALIZATION OF ARIS-BINDING SITES ON SPERM OF THE STARFISH, *Asterias amurensis*

A. Ushiyama[1], F. J. Longo[2], K. Chiba[1], M. Hoshi[1]. [1]Dept. of Life Sci., Tokyo Institute of Technology, Yokohama, Japan. [2] Dept. of Anatomy, Univ. of Iowa, Iowa, USA.

In starfish, *Asterias amurensis*, the acrosome reaction is induced by three components present in egg jelly coat; ARIS (acrosome reaction-inducing substance), Co-ARIS (cofactor for ARIS) and SAP (sperm activating peptides). ARIS is a very large and highly sulphated glycoprotein and is capable of inducing acrosome reaction in alkaline or high calcium sea water. Thus, ARIS is thought to be an essential molecule for inducing acrosome reaction. Our recent data suggest that species specific ARIS receptor exists on the plasma membrane of sperm head.

We have electromicroscopically localized the sites of ARIS binding on sperm using colloidal gold conjugated ARIS (gold-ARIS). In intact sperm, gold-ARIS specifically bound to anterior-lateral aspect of sperm. The binding remained on the plasma membrane even after the acrosome reaction.

STRUCTURE-ACTIVITY RELATIONSHIP OF STARFISH SPERM-ACTIVATING PEPTIDES

T. Nishigaki[1], K. Chiba[1], M. Yoshida[2], M. Morisawa[2], M. Hoshi[1] [1]Department of Life Science, Tokyo Institute of Technology, Yokohama and [2]Misaki Marine Biological Station, Univ. Tokyo, Misaki.

Sperm-activating peptide (SAP) is one of the bioactive components of the jelly coat of echinoderm eggs. It stimulates sperm respiration and motility, increase of intracellular pH, [Ca2+], [cGMP] and [cAMP]. SAPs purified from the starfish, *Asterias amurensis*, are glutamine-rich peptides consisted of 34 amino acid residues and have an intramolecular disulfide linkage at position 8 and 32. Although the ring region is not variable, the amino-terminal region is quite variable.

The activity is resistant to the deletion of amino-terminal pentapeptide, but it is susceptible to the cleavage of disulfide linkage by S-pyridylethylation. Thus, the disulfide linkage is essential for the activity of SAPs.

Starfish SAP changes sperm swimming patterns going from a circular swimming pattern to one with a straighter trajectory in normal sea water. It also induces the acrosome reaction in cooperation with ARIS, the major component of the acrosome reaction inducers. They suggest that SAP affects spermatozoa in various ways to cause efficient fertilization in echinoderm.

STRUCTURE AND IMMUNO-LOCALIZATION OF THE VITELLINE COAT GLYCOPROTEIN HRVC-70 IN THE ASCIDIAN, *HALOCYNTHIA RORETZI*

°S. Takizawa, M. Matsumoto, M. Hoshi (Dept. of Life Sci, Tokyo Inst. of Tech., Yokohama)

The vitelline coat is an extracellular layer of glycoproteins. It is suggested that the vitelline coat is the site of self-nonself recognition in ascidian fertilization. In the ascidian, *Halocynthia roretzi*, we have studied the structure of vitelline coat 70kD glycoprotein(HRVC-70).The N-terminal eicosapeptide and four other fragments(60 residues in total) of HRVC-70 have been sequenced. Immunohistochemical studies, using anti HRVC-70 IgG, demonstrated that HRVC-70 is localized at the reticulation of the vitelline coat. Since acrosome-intact spermatozoa bind to the vitelline coat in the close vicinity of the reticulation, it is suggested that HRVC-70 is involved in sperm-egg interaction. Cloning of cDNA of HRVC-70 is under progress.

CHARACTERIZATION OF CYCLIC NUCLEOTIDE-DEPENDENT HISTONE KINASE IN SPERMATOZOA OF THE SEA URCHIN HEMICENTROTUS PULCHERRIMUS.

K.Hoshino[1],T.Harumi[2] and N.Suzuki[1]. [1]Div. of Biol. Sci., Graduate School of Science, Hokkaido Univ., Sapporo and [2]Dept. of Anatomy, Asahikawa Med. College, Asahikawa.

We have identified a 48kDa protein which is rapidly phosphorylated in sperm homogenates of the sea urchin, Hemicentrotus pulcherrimus and is dephosphorylated in a cyclic nucleotide-dependent manner. The 48kDa protein is associated with a 39 kDa protein to form a larger oligomer of about 400kDa. The 400kDa protein showed cyclic nucleotide-dependent histone kinase activity in a concentration dependent manner. cAMP was a more potent activator of the enzyme than cGMP. The cAMP-dependent protein kinase inhibitor peptide (TTYADFIASGRTGRRNAIHD) inhibited these activities. The kinase phosphorylated histone H1 and H2B from calf thymus as well as sea urchin sperm head histones. The histone kinase was incubated with 1μM cAMP and subjected to gel filtration on a Superose 6 culumn equilibrated 5μM cAMP containing buffer. Fractions containing 39kDa subunit had histone kinase activities. Several peptide fragments obtained from purified 39kDa or 48kDa protein were micro-sequenced (peptide39-1;GPGDASQFDEYEEEALK,39-3;AGVADIKLHKWFQSTD WIAIYGGRVD.48-1;VAIYNQGQYFGE,48-2;YDPEADNDTDTQK, 48-4;RGVTFTAPEDAESDIDDEPPELPK).

ACIDIC N-LINKED OLIGOSACCHARIDES OF VITELLINE COAT ARE ESSENTIAL FOR SPERM BINDING IN ASCIDIAN HALOCYNTHIA RORETZI.

N. Hirohashi and M. Hoshi

Dept. of Life Sci., Tokyo Inst. of Tech., Yokohama.

Spices specific sperm binding to the vitelline coat(VC) of eggs is an important steps for fertilization in various animals. We have suggested that the binding is mediated by sperm fucosidase and N-linked oligosaccharides(N-glycans) of vitelline coat(VC) glycoproteins. Acidic chains, presumably due to sulfation constituted about 60 % of VC N-glycan. Acidic N-glycans, but not neutral ones, competitively inhibited both sperm binding to the VC and fertilization. The inhibitory activity against fertilization of acidic N-glycans, was lost completely by mild-methanolysis, and partially by fucosidase or hexsosaminidase treatment. Similarly mild-methanolysis and fucosidase treatment rendered acidic N-glycans unable to inhibit sperm binding. From these data, it was suggested that terminal fucose and sulfate groups are essential for sperm binding ligand.

IDENTIFICATION AND CHARACTERIZATION OF SPERM-ACTIVATING PEPTIDE I (SAP-I) RECEPTORS IN THE SEA URCHIN *HEMICENTROTUS PULCHERRIMUS*

T.Shimizu[1], K. Yoshino[2], N. Suzuki[1]. [1]Div. of Biological Science, Graduate School of Science, Hokkaido University, Sapporo, [2]Institute for Protein Research, Osaka University, Osaka.

We characterized putative receptors specific for sperm-activating peptide I (SAP-I: GFDLNGGGVG) in spermatozoa of the sea urchin *Hemicentrotus pulcherrimus*. Analysis of the data obtained from binding assay showed the presence of two classes of receptors specific for SAP-I in spermatoza. The incubation of intact spermatozoa as well as sperm tail or sperm membranes prepared from *H.pulcherrimus* spermatozoa with GGGY(^{125}I)SAP-I and a chemical crosslinking reagent resulted in the radiolaleling of the a 71 kDa protein. We isolated a cDNA encoding 71 kDa protein from a *H.pulcherrimus* testis cDNA library. The amino acid sequence of 71kDa protein has homology with cysteine rich domain of a human macrophage scavenger receptor.

SOYBEAN AGGLUTININ BINDING TO TESTIS OF CRICKET *GRYLLUS BIMACULATUS*.

A.C.Suzuki, K.Nishimura. Dept. of Biol., Keio Univ., Yokohama.

Sugar chain expression in germ cells of cricket *Gryllus bimaculatus* during the spermatogenesis was cytochemically detected using soybean agglutinin (SBA) as a probe. Testes were fixed in Bouin's solution, embedded in paraffin, and their affinities to SBA were tested with biotinylated SBA and streptavidin-peroxidase. Electron microscopic analysis was also done to specify the labelled organelle.

SBA showed spermatogenesis stage-specific binding to germ cells: it intensely bound to cell surface and some granular structure in early spermatocytes; but the reactivity on cell surface disappeared at later spermatocytes; in early spermatids, SBA bound exclusively to Golgi apparatus.

The binding activity was readily removed by a treatment with α-*N*-acetylgalactosaminidase before cytochemistry. These results suggest that some glycoconjugates with terminal α-*N*-acetylgalactosamine, especially those of cell surface, change their structure according to the process of meiosis.

Expression of protamine gene during the spermatogenesis in the medaka, *Oryzias latipes*.

M. Tamura[1], A. Watanabe[1], H. Yamamoto[2] and K. Onitake[1].
[1]Dept. of Biol., Fac. of Sci., Yamagata Univ., Yamagata,
[2]Biol. Inst., Fac. of Sci., Tohoku Univ., Sendai.

Protamines or sperm specific basic proteins are small highly basic proteins that substitute for histones in the chromatin of sperm during the spermatogenesis. They compact sperm DNA into highly condensed, stable and inactive complex. We cloned cDNA of medaka protamine in order to examine the molecular mechanisms in spermatogenesis of the medaka (*Oryzias latipes*). A medaka testis cDNA library constructed in lambda *gt*11 contained 2.78 x 10^6 independent recombinants. Many positive clones were obtained immunoscreening with polyclonal antibody against the medaka protamine. A positive clone, named MP-1, encoded arginine clusters, characteristic of protamine. The putative amino acid sequence of MP-1 revealed a remarkable extent of homology with other fish protamines.

Northern hybridization using a MP-1 cDNA probe showed that MP-1 mRNA was present exclusively in the testes and that it gave three detectable bands: a major band of 280 b, and two others of 400 b and 500 b.

In situ hybridization with a complementary RNA probe (digoxigenine-UTP-labeled MP-1 RNA) revealed that MP-1 mRNA was localized in a part of secondary spermatocytes and spermatids, but not in primary spermatocytes nor spermatogonia.

IMMUNOHISTOCHEMICAL LOCALIZATION OF CALCIUM/CALMODULIN DEPENDENT PROTEINPHOSPHATASE, CALCINEURIN, IN THE MOUSE TESTIS.

M. Moriya[1], K. Fujinaga[2], M. Yazawa[2] and Ch. Katagiri[1].
[1]Zool. Inst. and [2]Dept. Chem., Fac. Sci., Hokkaido Univ., Sapporo.

Previous studies showed that calmodulin is unusually rich in spermatogenic cells at stages from mid-pachytene spermatocytes to elongating spermatids. The antibodies raised against the scallop testis calcineurin reacted with both brain and testis calcineurin of the mouse. Using this antibodies, the mouse testis tissues embedded in LR-Gold resin were subjected to indirect immunofluorescence. Positive reaction was observed only in nuclei of round and elongating spermatids: calcineurin started to accumulate in nuclei from the acrosomal cap phase and peaked at the initial stage of nuclear elongation and decreased thereafter. There was almost no signal in the cytoplasm. Spermatogenic cells in other stages including spermatogonia, spermatocyte, mature sperm, and other somatic cells in the seminiferous tubules were totally negative. Immunoelectron microscopy gave the same result, on the basis of the changes in the density of immuno-gold particles. These results suggest the role of calcineurin in remodeling the nuclear states in metamorphosing spermatids.

IMMUNOHISTOCHEMICAL LOCALIZATION OF FGF IN TESTES OF *Salvelinus leucomaenis* AND *Oryzias latipes*.

A. Watanabe and K. Onitake. Dept. of Biol., Fac. of Sci., Yamagata Univ. Yamagata.

In teleost, spermatogenesis proceeds in the cyst formed by germ cells and Sertoli cells around them. It is known that testicular somatic cells including Sertoli cells interact with germ cells and control the proceeding of spermatogenesis. 11-keto - testosterone and activin B are thought as factors concerning those interaction.

Fibroblast growth factor (FGF) deeply concerns germ cell development. It is known in mammal that FGF is important as a maintenance factor for primodial germ cells, and that it can control granulosa cell proliferation and differentiation in ovarian morphogenesis.

In this study, to estimate the role of FGF on germ cell development in teleostean testis, we investigated the localization of FGF proteins in the testis of *Salvelinus leucomaenis* and *Oryzias latipes* by immunofluoresence staining using anti-basic FGF antibody .

In *Salvelinus*, most of the germ cells were spermatogonia in winter testis, and they were stained by this antibody. When human chorionic gonadotropin was injected, signals were clearly observed at the margin of cysts including Sertoli cells. Little were observed in spermatogonia.

In *Oryzias*, every differentiating stages of the germ cells always existed in a testis. Strong signals were observed at the margin of cysts including Sertoli cells. This localization is very similar to that of hormone treated*Salvelinus* testis. These results suggest that FGF may play some roles on spermatogenesis in the teleostean testis.

NOVEL GENES THAT EXPRESS AFTER MEIOSIS

M. Jinbo, M. Matsumoto, M. Hoshi
Department of Life Science, Tokyo Institute of Technology, Yokohama

Sperm have a very specified role to transport one's genes to an oocyte. To achieve this role, the spermatids after meiosis drastically change their form; the condensation of the nucleus, the development of the flagellum, the removal of cytoplasm, etc. Therefore, when spermatids differentiate to the capacitated sperm, it seems that the genes that they express are regulated the temporal and spatial expression. In short, spermatid specific genes must involve the spermatogenesis.

Therefore we tried to find the genes specifically expressed in haploid spermatids. From mouse testis cDNA library, we identified the 4 independent clones with the differential screening. It was also found that haploid spermatids only expressed these isolated 4 independent clones.

STABILITY OF MANCHETTE (MICROTUBULE BUNDLES) IN NEWT ELONGATE SPERMATIDS.V: PHOSPHORYLATION OF MAPS AND THEIR ACTIVITY.

M. Hama[1], K. Takamune[1], T. Kishimoto[2] and S.-I. Abe[1]. [1]Dept. of Biol. Sci., Fac. of Sci., Kumamoto Univ., Kumamoto and [2]Lab. Cell and Develop. Biol., Tokyo Inst. Technol., Yokohama.

We previously showed that manchette structure in newt elongate spermatids was resistant to the treatment with Ca^{2+} and low temp, that 1M NaCl sup from the testes contained MAPs which promoted tubulin polymerization and low temp-resistance of the microtubules, and that MAPs were present from spermatogonial to elongate spermatids stage (1991, 1992, Annual Meeting of the Zoological Society).

In this study, we examined the effect of phosphorylation and dephosphorylation of newt testes MAPs on their activity. Treatment with cdc2 kinase or A kinase reduced the activity of MAPs, while the treatment with alkaline phosphatase enhanced the activity of MAPs. These results indicated that the activity of MAPs in situ were regulated by their phosphorylation and dephosphorylation.

HERRING SPERM-ACTIVATING PROTEINS ARE HOMOLOGOUS TO KAZAL-TYPE TRYPSIN INHIBITORS.

S.Oda[1], H.Ohtake[2], Y.Igarashi[3], K.Manaka[4], K.Sakai[5], N.Shimizu[5], and M.Morisawa[6]. [1]Dept. Physiol. TWMC., Tokyo. [2]Dept. Physiol., [3]Dept. Biochem. and [4]Lab. of Tissue Culture, Dokkyo Univ. Sch. Med., Tochigi. [5]Dept. Mol. Biol., Keio Univ. Sch. Med., Tokyo. [6]MMBS., Fac. Sci., Univ. of Tokyo, Kanagawa.

Unfertilized eggs of the pacific herring, Clupea pallasii, release the sperm-activating proteins (HSAPs) into seawater at the time of fertilization. A cDNA clone encoding 73 amino acids of the HSAP was isolated from the ovarian cDNA library. The amino acid sequence of the HSAP shows a striking similarity to those of Kazal-type trypsin inhibitors, such as acrosin inhibitor. Actually, some trypsin inhibitors could activate the herring sperm. These suggest that the herring eggs release the HSAPs (trypsin-inhibitor-like proteins) to activate the motility of sperm and facilitate the fertilization.

INITIATION MECHANISMS OF SPERM MOTILITY IN THE NEWT, *CYNOPS PYRRHOGASTER* (2) Partial characterization of sperm motility–initiating substances reside in egg jelly

M.Ukita and K.Onitake. Dept. of Biol., Fac. of Sci., Yamagata Univ., Yamagata.

Our previous study showed that, in *Cynops pyrrhogaster* (Amphibia Urodele), the sperm motility–initiating substance (SMIS) derived from the egg jelly initiated the movement of sperm in the normal fertilization process. This observation was the first report that the amphibian egg jelly had a function of initiaing the sperm motility.

In the present study, we tried to isolate and characterize SMIS. When sperm was suspended in a jelly extract (JE), sperm began to move. These results indicate that water–soluble substance can initiate the sperm motility, and that a three–dimentional jelly matrix is not required to the initiation of sperm motility. The characterization of SMIS was pursued as followed. (1) JE was subjected to size exclusion fractionation using molecular weight of 10 kDa cutoff membrane. (2) JE was boiled for 30 minutes at 100 °C. (3) Isolated jelly layers were ashed for 10 hours at 700 °C.

When JE was filtrated by 10 kDa cutoff membrane, sperm motility–initiating activity remained in the non–filtrated fraction. Furthermore, it was revealed that sperm motility–initiaing activity was not inactivated after boiling of JE or ashing of isolated jelly layers.

From above results, it is suggested that SMIS is water–soluble, heat stable and non–organic substance which may closely bind to high molecular components in the newt egg jelly, but its activity does not depend on the existence of high molecular components of the egg jelly.

ROLES OF EGG JELLY LAYERS ON FERTILIZATION IN THE NEWT, *CYNOPS PYRRHOGASTER*

S. Kamimura and K. Onitake. Dept. of Biol., Fac. of Sci., Yamagata Univ., Yamagata

We have reported that jelly layers (JLs: composed of J1, J2, J3, J4, from the innermost to the outermost) and sticky layer (SL) investing JLs had a high inducing activitiy of acrosome reaction (AR) and also might have a function of limiting the number of sperm passing through JLs in the newt which is physiologically polyspermy. In this study, using JLs model systems composed of JLs fragments, we attempted to make clear the role of each jelly layer on ferilization, specially focusing on the gentle mechanism of polyspermy block and the AR–inducing activity. When J1 alone model system was inseminated, the number of sperm passing through it was decreased as well as that of normal full jelly layers. The histological analysis showed that the outside of J1 was covered with SL–like layer, when J1 was separated only from other JLs and fixed. The SL–like layer (outer layer of J1) trapped a large number of sperm as like as SL of control egg, and the number of sperm penetrated into inner layer of J1 was limited strongly by it. After insemination, J2 alone model system had sperm four to five times as many as other layers in it and more than 90% of inseminated sperm seemed to be trapped in J2 layer, because all of heads and tails of sperm showed the zigzag shape.

On the other hand, it was showed that each of four layers had AR inducing activity equally and the specific layer to AR induction might not exist.

From these results, it was suggested that JLs, especially SL, J2, and the outer layer of J1 had a gentle function of polyspermy block by trapping a large number of sperm in them, and that the efficient AR was induced by the cooporation of AR–inducing factor involved in all four jelly layers.

CHARACTERIZATION OF AN EGG-ACTIVATION FACTOR IN THE NEWT SPERM.

A.Miki, M.Kobayashi, and Y.Iwao. Biol. Inst., Fac. of Sci., Yamaguchi Univ., Yamaguchi.

We have reported that not only *Cynops pyrrhogaster* sperm, but their extracts activate *Xenopus leavis* eggs, accompanied with hyperpolarization and a positive-going fertilization potential. In this report, we have tried to characterize an egg-activation factor in the newt sperm. The sperm extract precipitated by SBA induced egg activation, and it had a heavy proteolytic activity against Arg-MCA substrates. This protease was partially purified with an SBA-agarose affinity chromatography, an ion-exchange chromatography, and gel filtration. The molecular weight of this protease was about 100 kDa, and its activity was inhibited by aprotinin and leupeptin. The egg activation by the sperm extract was inhibited by Arg-MCA substrates and these inhibitors. The protolytic activity was localized in the acrosomal region. These results indicate that the egg-activation factor is an acrosomal protease .

MECHANISM OF ACTIVATION IN *XENOPUS* EGGS BY THE NEWT SPERM EXTRACT.

M.Kobayashi, A.Miki, and Y.Iwao. Biol. Inst., Fac. of Sci., Yamaguchi Univ., Yamaguchi.

Unfertilized *Xenopus laevis* eggs were activated by the extract of the newt, *Cynops pyrrhogaster* sperm. In this report, we have studied a role of Ca^{2+} ions in the activation of *Xenopus* eggs. When $[Ca^{2+}]_o$ was less than 1.5 μM or when the eggs were treated with Ca-channel blockers: amiloride, $NiCl_2$, $CoCl_2$, or $CdCl_2$, the egg activation was completely inhibited. The egg activation was not, however, affected when $[Ca^{2+}]_o$ was more than 34 μM. The egg activation was blocked by injection of BAPTA which chelates intracellular free Ca^{2+} or heparin which inhibits IP_3 receptor. The egg activation was not affected by injection of thapisigargin which inhibits CICR.These results indicated that a factor in the newt sperm binds to an egg surface receptor to open the Ca channels on egg's plasma membrane. Once $[Ca^{2+}]_i$ increases in a part of the egg, it would trigger Ca^{2+} wave via IP_3 receptor of endoplasmic reticulum.

GLYCOPROTEIN CONSTITUENTS OF THE VITELLINE COAT RESPONSIBLE FOR SPERM BINDING IN FERTILIZATION OF BUFO

S.Omata [1] and Ch.Katagiri[2], [1]Dept. Immunol., Univ. Occup. Environ. Health, [2]Div. Biol. Sci., Hokkaido Univ.

The rates of binding of sperm to the unit area of vitelline coat (VC) in Bufo japonicus correlate well with the fertilizability of eggs, and thus the binding constitutes an essential step of fertilization process. The rates of sperm binding to the VC were lowered in the presence of SDS-solubilized VC. Molecular entities involved in this binding were analyzed, with the results that the rates of binding are (1) completely lost after oxidation of VC by periodate, and (b) significantly decreased by pretreatment with monovalent antibodies which are reactive to carbohydrate moieties of VC. Determination of the rates of inhibition of the binding in the presence of VC materials after gel-filtration indicated that 36-39kD but not 67kD or 112kD components of VC are responsible for the binding. On Western blotting, 36-39kD components reacted specifically with DBA and anti-GM2 antibodies, weakly with WGA, but not at all with ConA. These results suggest that the carbohydrate-containing moieties in the VC play an important role in the initial binding process of sperm to the VC, although the involvement of protein moieties cannot be excluded.

THE PRESENCE OF FIBRONECTIN IN THE VITELLINE ENVELOPE OF FISH EGGS

S. Kudo[1] and S. Yazawa[2]. Depts. of [1]Anat. and [2]Legal Med. Gunma Univ. Sch. of Med., Maebashi

It is well known that the vitelline envelope of fish eggs is formed between the oocyte and follicular epithelial cells during the process of oocyte development. The histological location of the envelope in developing oocytes corresponds to that of the basement membrane, which forms between two different kinds of cells, for example between endothelial cells and podocytes in the renal corpuscles of vertebrates. Therefore, using immunohistochemistry and immunoblot analysis, an attempt was made to clarify whether the vitelline envelope (VE) of fish eggs contains fibronectin as components. Purified and unfixed VEs were subjected to immunohistochemistry using anti-fibronectin antibody. The immunoreactivity was found to be localized in the interior of the VE. For immunoblot analysis, purified VEs were finally pulverized after lyophilization, and the pulverized material was solubilized in 70% formic acid containing cyanogen bromide, or by pepsin digestion. Precipitates obtained from the solution by addition of NaCl were used for immunoblot analysis. Immunoreactive bands were revealed upon application of anti-fibronectin antibody, suggesting that the components of fish egg VE may contain fibronectin.

QANTIFICATION OF MOTILITY OF BOVINE SPERMATOZOA COCULTURED WITH BOVINE OVIDUCTAL EPITHELIAL CELLS BY COMPUTER ASSISTED SEMEN ANALYSER SYSTEM.

H. Abe, S. Yamashita, S. Konno, T. Satoh, Y. Araki* and H. Hoshi. Res. Inst. for the Funct. Peptides, Yamagata and *Dir. Inst. Adv. Med. Tech., Tochigi.

In mammals, the interaction between oviductal epithelial cells and sperm play important roles for maintenance of sperm functions. In this study, Computer Assisted Semen Analyser (CASA) was used to measure curvilinear velocity (*CV*), average linearity of progression (*Lin*), and amplitude of lateral head displacement (*ALH*) of bovine spermatozoa incubated with bovine oviductal epithelial cells (BOEC), in conditioned medium (CM) from BOEC, or in medium alone. Fertilizing capacity of their spermatozoa was evaluated by *in vitro* fertilization (IVF) system. Significant maintenance of both *CV* and mean *ALH* was observed in the cocultured spermatozoa for 60 h, but in spermatozoa incubated in CM and medium alone. Coculture with BOEC significantly elevated *Lin*, in comparison with all other culture conditions assesed. Fertilizing capacity was extended for 12 h in spermatozoa incubated with BOEC, but not in spermatozoa incubated medium alone. Normal fertilization also takes place in IVF medium without heparin.

A STUDY OF 3D BIOIMAGES-1: DISTRIBUTION PATTERN OF CHROMATIN PARTICLES IN GERMINAL VESICLE OF STARFISH OOCYTES.

A. Nomura[1], S. Tanaka[2], Y. Yamazaki[2], T. Tsuji[2], Y. Kawasaki[2], T. Saitoh[2], [1]Dept. of Zoology, Fac of Science, Kyoto University, Kyoto, [2] Lab. of Bioimages, Mitsubishi Kasei Institute of Life Sciences, Tokyo.

We developed a practical application software on Macintosh computer that automatically find three-dimensional particles from serial two-dimensional images obtained from optical sections of confocal laser scanning microscope (CLSM). Three-dimensional information about each particles (coordinate of the centroid, volume, DNA contents, and so on) was then calculated. We applied this software on the chromatin of the starfish, Asterina Pectinifera.

We first stained Germinal vesicle (GV) in the oocytes with propidium iodide. We observed some chromatin particles with the CLSM. We then execute the software and obtained the coordinates and the volume of each chromatin. Results plotted in a three-dimensional space were rotated on a computer display. We will numerically examine if the distribution of the chromatin particle shows a specific pattern in the GV of starfish oocytes.

ANALYSIS OF MOTILITY AND FERTILIZATION PROCESS IN HAMSTER SPERMATOZOA CULTURED IN TWO KINDS OF MEDIA

N.Uto & Y.Yamahama.
Dept.of Biol. Hamamatsu Univ. Sch. of Med., Hamamatsu.

In mammalian spermatozoa, capacitation and hyperactivation must be caused before fertilization can occur. Hamster spermatozoa were incubated in a modified tyrode's solution containing polyvinylalcohol (TL-PVA) or bovine serum albumin (TL-BSA) for 6 hr at 37.5 °C in 10% CO_2. Sperm motility bioassay evalution was based on the method of Bavister and Andrews ('88). At 4 hr of incubation, most of motile spermatozoa in TL-BSA medium showed vigorous swimming scoring maximum index and those motilities diminished during next 2 hr. In this batch, clumping groups of spermatozoa were observed. On the other hand, spermatozoa in TL-PVA scarcely formed clumping group and continued vigorous swimming even during next 2 hr. The spermatozoa cultured for 3 hr in two kinds of media were inseminated respectively, and the process of penetration into egg were observed. There were variations between batches of sperm with respect to the motility and penetration into egg.

ROUNDS OF DNA SYNTHESIS AND THE CLONAL AGE REQUIRED FOR MATING TYPE EXPRESSION AFTER CONJUGATION OF *PARAMECIUM*

Y. Itoh and K. Mikami, Res. Inst. for Sci. Educ., Miyagi Univ. of Educ.

Paramecium caudatum has a period of sexual immaturity that immediately follows conjugation. After the immaturity period, cells are ready to mate between complementary mating types O and E. Further dozens of fissions after immaturity period, mating pairs (selfing) appear in a culture of originally pure E type cells, because the phenotipic expression of E type cell becomes unstable and some cells show O type. The clonal ages required for these phenomena are measured by the number of cell cycles.

In stock 16BKC, the maturity sets in at about 50 fissions and the selfing occurs 70-80 fissions after conjugation. The clonal age required for maturity was found to be shortened by repetitive removal (about 10 times) of a part (ca. 3/4 of the mac. volume) of the macronucleus. However, the age required for selfing was not shortened by the repetive removal. The results shows that the clonal age for maturity is measured in rounds of chromosome replication or DNA synthesis rather cell divisions and that the clonal age required for selfing seems to be counted by other system.

PRODUCTION OF NEW HISTONE COMPLEXES AND THEIR SIGNIFICANCE IN EMBRYOGENESIS OF THE STARFISH EMBRYO

T.Shimizu, K.Hozumi, S.Ikegami. Dept. of Applied Biochem., Hiroshima Univ., Higashi-hiroshima, Hiroshima.

We have reported that there are new covalent complexes of histones H2B and H2B (designated p29), and of histones H2B and H4 (designated p28) in the blastula of the starfish, *Asterina pectinifera*. They appear in the blastulating embryo at the 256-cell stage, at which G1 phase first appears. Their contents increase through the blastula stage and they are abundant in many adult tissues. We found that they also exist in sperm but the sequence of histone H2B composed of sperm p29 and p28 differs from that composed of embryonic p29 and p28.

Hyperacetylation of core histones by the treatment of the embryo with trichostatin A, a selective inhibitor of histone deacetylase and a blocker of starfish embryogenesis, suppresses the formation of p28 but not that of p29. This suppression may be the cause of the development arrest of the embryo at the early gastrula stage.

NON-LOCALIZATION OF CYTOPLASMIC DETERMINANT INDISPENSABLE FOR DEVELOPMENT IN STARFISH

Yutaka Kuroiwa and Hiroko Shirai
Ushimado Marine Laboratory, Okayama University, 130-17, Kashino, Ushimado, Oku, Okayama 701-43.

In starfish animal egg fragments alone develop into so-called permanent blastulae, and the determinant of archenteron is localized at the vegetal pole (about 10% of a whole egg volume). Since progress of the development takes place only through the archenteron formation, the determinant is indispensable for the development.

The roles of animal cytoplasm was examined as for developmental ability. Fertilized eggs which had been severed from various animal cytoplasm developed into juveniles through metamorphosis.

It is clearly concluded that any cytoplasmic determinants indispensable for the complete development are not localized at the animal hemisphere.

INHIBITION OF PROTEIN SYNTHESIS CAUSES INAPPROPRIATE DNA SYNTHESIS IN SEA URCHIN UNFERTILIZED EGGS

T. Machida, K. Tachibana, and T. Kishimoto, Fac.of Bioscience and Biotechnology, Tokyo Institute of Technology, Nagatsuta, Yokohama, Kanagawa.

Little is known about the processes that regulate the activation of DNA synthesis and the subsequent onset of the mitotic cycle in fertilized eggs. Although extensive study has demonstrated the important factors controlling cell cycle such as MPF, the molecular basis for this major developmental switch is still unclear. The early stages of embryogenesis are easily observed in sea urchin eggs, and it is easy to prepare large amount of synchronized eggs. These make sea urchin a useful organism to study cell cycle after fertilization.

Here, we report the observation that inhibition of protein synthesis causes DNA synthesis in unfertilized eggs of sea urchin, *Hemicentrotus pulcherrimus*. DNA synthesis is induced with protein synthesis inhibitors, emethin and puromycin, and inhibited with aphidicolin which inhibits specifically DNA polymerase a. Similar results were observed in starfish, *Asterina pectinifera*, eggs.

On the basis of these results, we propose that labile protein(s) plays a role in the mechanism that normally represses DNA synthesis in the unfertilized eggs.

DEVELOPMENT AND CHROMOSOME IN HYBRIDS OF THE SEA URCHINS, HEMICENTROTUS PULCHERRIMUS AND GLYPTOCIDARIS CRENULARIS

K. Saotome, Yokohama City Institute of Health, Yokohama.

Chromosomes of sea urchin hybrids were actively studied in the early 20th century in foreign species. However, chromosomes of the two parental species in the hybrids could not be clearly identified because of sectioning method.

Since Hemicentrotus pulcherrimus and Glyptocidaris crenularis differed much in chromosome number, karyotype, taxonomic situation and skeleton structure in larvae, hybrids were produced between them. Their development and chromosomes prepared by air-drying method were examined.

When H. pulcherrimus eggs after treatment with trypsin of low concentration were inseminated with G. crenularis sperm, the cross-fertilization rate was high and their hybrids developed to the normal plutei. The skeleton structure and chromosomes of hybrid larvae showed basically intermediate characters of both parental species.

PROTEIN PHOSPHORYLATION BY PROTEIN KINASES IN SEA URCHIN EMBRYOS DURING ERALY DEVELOPMENT.

M. Okuyama, Y. Kamata, and I. Yasumasu. Dept. of Biol., Sch. of Educ., Waseda Univ., Tokyo.

After whole homogenates of sea urchin embryos were incubated with (γ-^{32}P)-ATP in the presence of protein kinase activators or inhibitors, proteins were separated by SDS-PAGE and proteins phosphorylated by protein kinases were detected by autoradiography.

The results showed that protein with apparent molecular weight of about 63kD on SDS-PAGE was strongly labeled on autoradiograph in the presence of Ca^{2+} and calmodulin, and when W-7 was supplemented, this protein was scarcely labeled. Thus this protein seemed to be specifically phosphorylated by Ca^{2+}-calmodulin dependent protein kinase.

We investigated phosphorylation of this protein by Ca^{2+}-calmodulin dependent protein kinase in the presence of inhibitors (W-5, W-7, KN-04, KN-62, ML-7) and the phosphorylation rate of this protein was found to change.

NUCLEAR INVOLVEMENT IN ESTABLISHMENT OF CLEAVAGE PERIODICITY IN *XENOPUS* EGGS.

T. Gotoh and A. Shinagawa. Dept. of Biol., Fac. of Sci., Yamagata Univ., Yamagata.

Shinagawa (1992) found that the nucleus is involved in accelerating the periodicity of cyclic stiffening of cleavage-arrested *Xenopus* eggs and egg fragments 10-15%. The present study examines whether the nucleus is also involved in the normal process of establishment of cleavage periodicity. Eggs prevented from DNA-duplication show about 10% longer periodic times of cleavage, after first or second cleavage, than intact eggs; though they show the first cleavage, and often the second as well, with the same periodicity as intact eggs. Eggs fertilized with u.v.-irradiated sperm and deprived of the female pronucleus, which contain no nucleus but centriols, show more than 30% longer periodic times. Eggs that contain the male or the female nucleus show nearly the same periodic times of cleavages as those that contain the zygote nucleus. We presume from these results that the presence of the nucleus itself shortens the periodic times for cleavage in *Xenopus* eggs.

CHANGE IN THE CAPACITIES OF BINDING BETWEEN 5' UPSTREAM OF EARLY EMBRYONIC HISTONE H3 GENE AND PROTEINS DUE TO PROTEIN PHOSPHORYLATION.

M. Sato, S. Katori, M. Kettoku and I. Yasumasu. Dept of Biol., Sch. of Educ., Waseda Univ., Tokyo.

In sea urchin embryoes, expressin of early embryonic H3 gene formed at the stages in pre-hatching period was augmented by Ca^{2+} ionophore, A23187, and was blocked by ruthenium red and tetracaine as well as by W7. Proteins obtained from isolated nuclei, which had been treated with Okadaic acid, an inhibitor of protein phospatase, as well as by W7, a potent calmodulin antagonist, hardly bind with 5' upstream of early embryonic H3 gene. Phosphorylation of proteins isolated from nuclei by exogeneous protein kinases resulted in alterations of their binding to 5' upstream of early embryonic 3H gene. Probably binding of nuclear proteins to 5' upstream is affected by modification of these proteins.

CHANGES IN CORTICAL "ACIDIC VESICLES" WERE VISUALIZED IN SEVERAL SPECIES OF SEA URCHIN EMBRYOS BY REAL TIME CONFOCAL MICROSCOPY.

Michio Abe. Dept. of Biology, Fac. of Sci., Tokyo Metropolitan Univ., Tokyo.

Acidic vesicle is one of the remarkable structure in the fertilization process of sea urchin eggs. Lee and Epel reported the movement of acidic vesicles while fertilization and egg activation in *Lytechinus pictus* and *Strongylocentrotus purpuratus* (Dev.Biol. 98:446-454, 1983) and recently, Mizuno *et.al.* reported the distribution of acidic vesicles in *Anthocidaris crassipina.* (Develop. Growth & Differ., 35(5), 539-549, 1993). The vital staining of acidic vesicles with acridine orange is an useful method, but it is difficult to visualize inner area of whole mounted embryos because of the size of eggs and out-of-focus blur. To avoid this disadvantage, I observed acidic vesicles in an optical section with real-time confocal microscopy (INSIGHT-plus IQ, Meridian Instruments Inc.). In optical slice, acidic vesicles were rare in unfertilized eggs, and after fertilization, accumulated at the cortical area. At the mitotic stage, acidic vesicles also localized in the periphery of mitotic apparatus and outer-membrane at the late telophase. I also checked the existence and change of acidic vesicles in several species of sea urchins as *Hemicentrotus pulcherrimus, Anthocidaris crassipina, Strongylocentrotus nudus* and *Clypeaster japonics.* The possible role of acidic vesicles as dynamic and generic phenomena in the early development of sea urchin was discussed.

THE ROLE OF INTRACELLULAR TRANSPORT IN SEA URCHIN SPICULOGENESIS.

Masato Kiyomoto and Taiko Miki-Noumura
Dept. of Biol.,Ochanomizu Univ., Tokyo.

Spicules of sea urchin embryo are produced by the primary mesenchyme cells derived from micromeres. Main inorganic component of the spicules is the calcite, $CaCO^3$. During the spiculogenesis Ca^{2+} are incorporated and deposited to form spicules in the syncytia of primary mesenchyme cells. The measurement of $[Ca^{2+}]$ (intracellular concentration of free calcium ion) of these cells showed lower level. The active transport of the spicule components, such as Ca^{2+}, may keep lower level of $[Ca^{2+}]$ in these cells.

To confirm this hypothesis we examined the effect of some inhibitors of intracellular transport for the spiculogenesis and for the $[Ca^{2+}]$. The formation and the elongation of spicules suppressed by inhibiters and the $[Ca^{2+}]$ increased. These results show that the intracellular transport may play an important role for spiculogenesis, regulatory of the $[Ca^{2+}]$.

CELL PROLIFERATION DURING ARCHENTERON ELONGATION OF SEA URCHIN EMBRYO.

H.Mizoguchi. Lab. of Biol., Jr. Col. of Rissho Univ., Saitama.

During archenteron elongation of sea urchin embryo, cell proliferation was estimated to clarify the cellular mechanism of archenteron formation.

Eggs of the sea urchin, *Hemicentrotus pulcherrimus*, were used throughout the study. Quantitative measurements of cell proliferation were done following 5-bromodeoxyuridine (BrdU) labeling, assayed by immunocytochemistry using monoclonal antibody against BrdU and streptavidin-biotin-peroxidase system. Detection of S phase cells was possible by this method. S phase cells were localized at vegetal hemisphere at the mesenchyme blastula stage. During elongation of archenteron, the number of S cells was decreased at the vegetal hemisphere of blastula-wall. At the early gastrula and mid-gastrula stage, percentage of S phase cells number to total cell number was almost the same with that of early gastrula.

It seems that S phase cells in vegetal hemisphere of blastula-wall at the mesenchyme blastula were participated to archenteron elongation.

Purification of EGIP-D binding protein in the sea urchin *Anthocidaris crassispina*

Y. Fujita, K. Yamasu, T. Suyemitsu and K. Ishihara.
Dept. of Reg. Bio., Fac. of Sci., Saitama Univ., Urawa .

Exogastrula-inducing peptide D (EGIP-D) binds to the protein in the extracellular matrix of sea urchin embryos (Fujita et al., 1994). For characterization of this protein, we purified an EGIP-D binding protein from homogenates of mesenchyme blastulae by a conventional procedures such as ion exchange chromatography and gel filtration. The purified EGIP-D-binding protein was demonstrated to be a protein with an apparent molecular weight of 33,000 and be able to form dimer with a molecular weight of 67,000 under non-reducing condition. The amino acid composition and the N-terminal sequences of the purified 33-kDa protein were determined. Comparison of the N-terminal sequence of this protein showed no homology with known protein sequences. In addition to the ability to bind EGIP-D, it had ability to reduce the rate of exogastrulation by EGIP-D in coexistence. These results suggest that 33-kDa protein may act as modulator of EGIP-D.

A CHANGE OF THE CYTOSKELETAL LOCALIZATION DURING SEA URCHIN GASTRULATION VISUALIZED WITH CONFOCAL LASER SCANNING MICROSCOPY.

Isao Uemura. Dept. of Biology, Tokyo Metropolitan Univ. Tokyo.

Whole mount cytoskeletal specimens of sea urchin embryos were viewed with confocal laser scanning microsopes (CLSM) to see the change in localization of the cytoskeleton and its role in sea urchin gastrulation, in particular, the primary invagination. Treatment of whole mount specimens with a protein-conjugating reagent, m-Maleimido-benzoyl-N-hydroxysuccinimide ester (MBS), resulted in remarkable preservation of actin filament networks. At blastula stage rhodamine-phalloidin treated embryos showed even localization of actin filaments both in the apical and the basal cortex among the ectoderm cells viewd with CLSMs (Zeiss LSM 410). At the onset of the vegetal plate thickening actin filaments began concentrating in the basal cortex of the vegetal plate ectoderm. Using anti-tubulin antibody (Amersham) as the first probe and FITC-anti-Ig as the second, microtubules are scarcely visible inside the protruding cytoplasm of these cells contrary to dense localization of actin filaments. These results suggest a possible role of actin filaments in pulsatory activity of the protruding cytoplasm during primary invagination.

INFLUENCE OF Li^+ ON VEGETAL-POLE-DELETED EMBRYOS AND ANIMAL-HALF BLASTOMERES OF STARFISH

R. Kuraishi and K. Osanai. Asamushi Mar. Biol. Stn., Tohoku Univ., Aomori.

In order to gain information concerning the distribution of the factor(s) responsible for archenteron formation in starfish embryos, we treated partial embryos and blastomeres which do not have capacity to form archenteron with LiCl, a known vegetalizing reagent.

We have reported that the cytoplasmic factor(s) only participates in determination of the anterior part of the archenteron (Areal) and the rest part of the archenteron is induced by Areal. Deletion of a vegetal oocyte fragment including all the presumptive area of Areal strongly suppressed both archenteron formation and expression of alkaline phosphatase (AP). However, when these embryos had been incubated in seawater containing 10-30 mM LiCl, some of them expressed AP. When a blastomere in the animal half of eight-cell stage embryos had been injected with 100-500 mM LiCl, the descendants of the injected blastomeres sometimes formed the secondary archenteron in the equatorial zone, expressed AP and gave rise to organs which are normally derived from Areal.

These results suggest that the factor(s) distribute not only in Areal but also in the rest part of the embryo and that Li^+ increase the effect of the factor.

ISOLATION OF A RGDS-PEPTIDE BINDING PROTEIN FROM SEA URCHIN EMBRYO AND ITS HISTOLOGICAL DISTRIBUTION DURING EARLY DEVELOPMENT

H. Katow[1], Y. Yamamoto[2] and S. Sofuku[2]. [1]Biol. Lab., Rikkyo Univ., and [2]Dep. of Chem., Col. of Sci., Rikkyo Univ., Tokyo

It has been suggested that RGDS-peptide receptor is present, and plays basic roles in sea urchin embryogenesis based upon our previous studies that RGDS-peptides perturb primary mesenchyme cell (PMC) migration in sea urchin embryos.

In the present study we have attempted to isolate a RGDS-peptide receptor using a synthetic cyclic RGDS-peptide (FR-1) from *Clypeaster japonicus* embryos. We have found (1) that FR-1-binding sites are restricted to particular embryonic areas according to histochemistry using a dansyl-conjugated FR-1, (2) that the histochemical localization of FR-1-binding sites well explains presumed perturbed sites by FR-1 introduction during embryogenesis, such as inhibition of PMC migration and gastrulation, and (3) that a FR-1 binding protein was able to be isolated using FR-1-CH Sepharose 4B column. *Mr* of the FR-1 binding protein was 57 kDa, and it was not affected by the presence or absence of 2-mercaptoethnol, suggesting that the receptor is a monomeric protein.

ORIGIN OF BOTTLE CELLS AND THEIR ROLE IN ANTERIOR-POSTERIOR AXIS FORMATION IN *CYNOPS* EMBRYO.

M.Katagiri, M.Ueki, Y.Yamamoto, and A.S.Suzuki.
Dep. of Biol.,Fac. of Gen Edu.,Kumamoto Univ.,Kumamoto.

It is suggested that, for determination of axial-mesoderm differentiation, the morphogenetic movement accompanied with invagination of blastopore is essential. It is well-known fact that the bottle cells of the blastopore play an important role also in initiation of the invagination process. In this study, mechanisms in determination of axial-mesoderm differentiation were investigated during early gastulation of *Cynops* embryo.

At first, to confirm the origin of bottle cell, fluorescein dextran amine (FDA) was injected into the dorsal blastomere of 32-cell embryo and the descendant cells of each labelled blastomere were traced until early gastrula and neural stages.

It was indicated that the bottle cells of the blastomere originated from descendant cells of the blastomere of the dorsal third or fourth tier.
In addition, we will report the results of three experiments ; removal of dorsal third blastomere of 32-cell embryo, culture of isolated blastomere, and UV-irradiated embryos.

BODY AXIS AND CELL POLARITY IN HYDRA DETECTED BY MOLECULAR MARKERS.

°M.Hatta[1], M.Sakaguchi[2], Y.Kobayakawa[3], T.Sugiyama[1]
[1]Natl.Inst.Genet., Mishima, [2]Dept.Biol., Fac.Ped., Shinshu Univ.,Nagano, [3]Dept.Biol., Fac.Sci.,Kyushu Univ., Fukuoka, [4]Dept.Genet., Adv.Grad.School, Mishima.

We isolated 5 cDNA clones from Hydra and also mono-specific antibodies against products of the cDNAs by epitope selection method. One of the clones showed similarity to Myosin Heavy Chain and its native product was detected in muscle processes of ectodermal epitheio-muscular cells by antibody staining. The processes extend along the apico-basal body axis, suggesting to reflect polarity of the cells along the axis. When new axes arose during budding or regeneration, rapid reorganization of muscle patterns was observed even before morphological changes were detected. Rearrangement of the muscle processes, and maybe cell polarity, were thought to be an important early event in Hydra morphogenesis.

MECHANISMS OF DETERMINATION OF AXIAL-MESODERM DIFFERENTIATION AT THE Cynops GASTRULA STAGE. I. In vitro EXPERIMENT.

K. Naraki[1], Y. Yamamoto[2], S. A. Suzuki[3]. [1]Int. Biol. Sci., Fac. Sci., Kumamoto Univ., [2]Nat. Envi. Sci. Grad. School Sci. Tech., Kumamoto Univ. [3]Dept. Biol., Fac. Gen. Educat., Kumamoto Uni.

Lower dorsal lip (endodermal epitherium) of early Cynops gastrula has axial mesoderm-inducing activity. This activity disappears immediately after beginning of gastrulation. The fact suggests that axial mesoderm induction may occur planarly before gastrulation. Dorsal marginal zone with lower dorsal lip was separated and cultured under several conditions. Explants which were kept to be in single layer or folded along the animal-vegetal direction (Keller sandwich) showed poor axial mesoderm differentiation. While, when explants were divided into two pieces at the median line and the pieces were conversely recombined, well-differentiated axial mesoderms were observed.
The present study suggests that determination of axial mesoderm differentiation depends on interactions with other germ layers.

ULTRAVIOLET LIGHT INHIBITS BODY AXIS FORMATION IN ORYZIAS LATIPES EGG (II)

Y. Ebina and S. Yokoya. Inst. Biomed. Sci., Fukushima Med.Coll., Fukushima

Ultraviolet light irradiation of the vegetal halves of fertilized Oryzias latipes eggs produces embryos that are deficient in or lack body axial structures. In order to find the critical time and the target substance for this effect, the vegetal half of the fertilized egg was irradiated with UV at different times and detection of tublin in the vegetal surface was accomplished immunocytochemically.
We found that the critical time for this effect is 15 min after fertilization at 25°C. After this critical time, microtubules were detected in the vegetal surface. UV irradiation at the critical time prevented the formation of the microtubules. These results suggest that the microtubules may play a role in body axis formation.

MECHANISMS OF DETERMINATION OF AXIAL-MESODERM DIFFERENTIATION AT THE Cynops GASTRULA STAGE. II. In vivo EXPERIMENT.

Y.Yamamoto[1], and A.S.Suzuki[2]. [1]Nat. Envi. Sci. Grad. School Sci. Tech., Kumamoto Univ. [2]Dept. Biol., Fac. Gen. Educat., Kumamoto Univ

The dorsal marginal zone plays an important role in the formation of the body axis in amphibian embryo. To examine the role of dorsal marginal zone for the axial formation, the dorsal marginal zone of early gastrula embryos in Cynopus was removed. These embryos lacked anterior head structure, but formed trunk tail structure with notochords and neural tubes. While, the isolated ventral marginal zone was transplanted into same region of the removed gastrula, the lateral marginal zone cells of the embryos couldn't invaginate, and these couldn't form dorsal mesoderm and neural. These results suggest that the lateral marginal zone cells are not determined yet to form axial mesoderm. These cells may be determined to form axial mesoderm after the invagination. In addition, there were a correlation between amount of the removed dorsal marginal zone and development of the anterior head structures. Therefore, we can discuss the relationship between the morphological movement and the differentiation of the anteroposterior axis specification with axial mesoderm.

THE MIGRATION PATHWAY OF PRIMORDIAL GERM CELLS IN TELEOSTS, *ORYZIAS* SPECIES.

H.Ninomiya[1,2] and N.Shibata[2]
[1]Dept. of Biol., Univ. of Tokyo, Komaba, Meguro-ku, Tokyo 153.
[2]Dept. of Biol., Univ. of Shinsyu, Asahi, Matsumoto 390.

In teleosts, there are some reports that primordial germ cells (PGCs), the former of gamete, emerge at lateral-ventral side of the embryonic body, and migrate to the gonadal anlage. However, the migration pathway of PGCs is not well known, since the observations were only carried out in terms of dorsal-ventral axis. We also analyzed the migration pathway of PGCs on anterior-posterior axis in teleost, *Oryzias latipes* to clarify the migration pathway of the PGCs to whole embryo. In *O. latipes*, PGCs first moved to posterior on lateral-ventral side of embryonic body together with extension of embryonic body. During these movement, PGCs formed aggregates and gathered just beneath the presumptive gonadal anlage. We also attempted the same analysis on *O. minutillus* to see inter specific differences on migration of PGCs. In *O. minutillus*, gonadal anlage was formed more anterior than that of *O. latipes*, and it leaned to right accompany to the position of dorsal mesentry. These results indicate that migration of PGCs in *Orizyas* species is well coordinated to the morphogenesis and is probably passive process.

EFFECT OF CALCIUM IONOPHORE ON THE AXIS FORMATION OF *XENOPUS LAEVIS* EMBRYOS

T. Gotou[1], K. Kinoshita[2], T. Kinoshita[1] [1]Dev. Biol. Fac. of Sci., Kwansei Gakuin University, Nishinomiya, [2]Biol. Lab., Nippon Medical School, Kawasaki.

Calcium ion plays an important role in the fertilization of *Xenopus* eggs. It is also known that calcium ion works as a regulator or mediator of the various physiological function within the cell. However, effect of calcium ionophore on the early embryogenesis has not been reported.

In order to study the role of calcium ion during early embryogenesis, *Xenopus* embryos were reared in 10^{-6} M calcium ionophore solution. The embryos which were soaked in calcium ionophore solution soon after fertilization could not proceed to develop. The embryos treated after 2-cell stage showed interesting alteration in the formation of the anterior-posterior axis. The embryos treated at the early cleavage stages showed deletion of the trunk and the tail, whereas the embryos treated at morula and blastula stages formed dwarf head or developed into headless embryos. These results suggest that calcium ion plays an important role in the axis formation of the embryos during the early developmental stages prior to gastrulation.

LOCALIZATION AND BEHAVIOR OF DORSAL DETERMINANTS IN UNCLEAVED *XENOPUS* EGGS.

M. Kikkawa and A. Shinagawa.
Dept. of Biol., Fac. of Sci., Yamagata Univ., Yamagata.

This study follows localization and behavior of dorsal determinants in *Xenopus* eggs during the first cell cycle. Eggs deprived, at about 30% time of the first cell cycle, of the vegetal pole cortex along with 2-10% relative volume of nearby cytoplasm lose the ability to form dorso-anterior structures. Eggs gradually gain the ability as the timing of removal of cytoplasm is delayed even though they are deprived of the same parts after that. Eggs do not lose the ability when they are deprived of the cortex of future dorsal, ventral or lateral subequatorial region along with 2-10% relative volume of nearby cytoplasm. Eggs do not lose the ability when they are deprived of only 2-15% relative volume of cytoplasm from either the vegetal pole, dorsal subequatorial or ventral subequatorial region. These results suggest that although the dorsal determinants are localized to a rather confined region around the vegetal pole during very early stages of first cell cycle they are gradually dispersed after that; probably, mainly toward the future dorsal regions.

DEVELOPMENT OF *XENOPUS* EGGS EXPOSED TO CENTRIFUGAL FORCE IN THE ANTI GRAVITY DIRECTION DURING THE FIRST CELL CYCLE.

Y. Hatakenaka and A. Shinagawa. Dept. of Biol., Fac. of Sci., Yamagata Univ., Yamagata.

Neff and coworkers reported that amphibian eggs kept in the anti-gravity direction throughtout development failed gastrulation as well as pattern formation. The present study examines how resistant to centrifugal force the factors necessary for gastrulation and pattern formation are. *Xenopus* eggs are exposed to 1-200g of centrifugal force in the vegetal pole to animal pole direction at various times of first cell cycle. Eggs centrifuged at 40g at around 40% time of the first cell cycle undergo gastrulation successfully and develop to perfect embryos. All components required for gastrulation and pattern formation thus can be dispaced by 40g or stronger centrifugal force. Their development is quite normal in every view of critria except the position of blastopore formation and the pattern of pigmentation. In those eggs, although the reason is unknown, the blastopore is usually formed in an oblique position with respect to the direction of centrifugal force.

CENTRIFUGATION OF UNCLEAVED *XENOPUS* EGGS IN THE ANIMAL POLE TO VEGETAL POLE DIRECTION RESULTS IN HYPERDORSO-ANTERIORIZATION OF THEIR DEVELOPMENT.

K.Takano and A.Shinagawa.
Dept. Biol., Fac. Sci., Yamagata Univ., Yamagata.

We have occasionally found that centrifugation at 71-160g of Xenopus eggs in the animalpole to vegitalpole (A →V) direction at 20-30% time of the first cell cycle result in hyperdorso-anteriorization of their development as seen in the development of D2O-treated eggs. We assume that centrifugation in that manner may cause distribution of dorsal determinants to broader regions than the normal Niuekoop center and cause formation of larger Spemann's organizer and thereby larger dorsoanterior structures. Interestingly, eggs irradiated slightly with u.v. light, which can develop to almost normal embryos, often develop to extremely ventroposteriorised embryos when they are centrifuged in the same manner as above. We interpret this that distribution of the determinants reduced by u.v.-irradiation to broader regions results in shortage of their concentration for inducing Spemann's organizer.

CHEMOTAXIS OF THE CHICK PRESTREAK AND INITIAL STREAK CELLS TO THE PEPTIDE GROWTH FACTORS

R. Toyoizumi and S. Takeuchi.
Dept. Biol. Sci., Kanagawa Univ., Hiratsuka.

In avian embryo, a cellular aggregation is formed at the most posterior part of the *area pellucida*, the central embryonic region of the blastoderm. This is the first axial structure along the embryonic axis, and this aggregation grows up to be primitive streak (PS aggregation). Eyal-Giladi and her colleagues revealed that neighboring posterior marginal zone induces the PS aggregation aside. Last year, we reported the evidence suggesting that posterior marginal zone secretes diffusive chemoattractants which cause the chemotactic migration of the prestreak epiblast cells to the posterior part of the blastoderm.

To advance this work, we tried to find the candidates for the chemotactic factors. We investigated the chemotaxis of cell clusters of the PS aggregation or those of prestreak epiblast toward the ion exchange beads soaked various kinds of peptide growth factors under the serum-free condition. These cells showed chemotactic response to the beads soaked FGF-2 or FGF-4. They will be possible candidates for chemotactic migration involved in the PS aggregation formation *in vivo*.

QUANTITATIVE ANALYSES OF EXPRESSION OF GENES INTRODUCED IN SEA URCHIN EMBRYO BY PARTICLE GUN

K. Akasaka, A. Nishimura & H. Shimada
Graduate Dept. of Gene Science, Faculty of Science, Hiroshima Univ. Higashi-Hiroshima.

We reported that the expression of fusion-genes introduced in sea urchin embryos by particle gun were controlled as that of endogenous genes in the previous meeting of this society.

In this meeting, we will report the normalization method of gene expression of introduced reporter-fusion constructs.

The experimental constructs which contain luciferase gene as a reporter and reference constructs which contain CAT gene were co-introduced into sea urchin embryos. We have demonstrated that the constructs do not interfere with gene expression and that the expression level of experimental construct varies in proportion to the amount of the construct, if they are linearized with different restriction enzymes.
It is suggested that this method provides reliable quantitative experiments of gene expression in sea urchin embryos.

cis-REGULATORY ELEMENTS IN THE 5'-FLANKING REGION OF THE SEA URCHIN, *Hemicentrotus pulcherrimus* ARYLSULFATASE GENE.

J. Morokuma, A. Nishimura, K. Akasaka and H. Shimada.
Dept. of Gene Sci., Fac. of Sci., Hiroshima Univ., Higashi-Hiroshima 724.

Previously, we have reported the nucleotide sequence of the sea urchin arylsulfatase (Ars) gene and the presence of *cis*-acting elements in its 5'-upstream region. Recently, we have found many errors in the nucleotide sequence of the Ars gene.

The present study describes the results of the re-examination of *cis*-acting elements in the 5'-flanking region of the Ars gene based on the corrected nucleotide sequence. Ars-luciferase fusion gene constructs were introduced into sea urchin eggs by a particle gun mediated gene transfer system. The sea urchin early type Histone H1-CAT (chloramphenicol-acetyl-transferase) fusion construct that shows a constant level of expression during early development was co-transferred with the Ars-Luciferase constructs to normalize the luciferase activity. Results show that an Ars sequence from +38 to-700bp retains all necessary elements for proper temporal expression of the Ars gene. By deleting the Ars sequence of the luciferase constructs in various ways, it was found that the elements related to the temporally restricted expression are present between -250 and -700bp.

EMBRYONIC TEMPERATURE TOLERANCE OF SEA URCHINS AND THE MEMBRANE FLUIDITY OF THE EMBRYONIC CELLS.

H. Fujisawa and S. Oshida, Fac. of Educ., Saitama Univ., Urawa.

Various species of sea urchin show different biogeographical distributions and seasonalities of breeding. The thermotolerance of the embryos is generally correlated with species distribution and spawning season. I have confirmed that this thermotolerance is maternally determined.

The aim of the present study was to investigate the correlation between embryonic thermotolerance and membrane fluidity of sea urchin embryonic cells. Three species, *Echinometra mathaei*, *Anthocidaris crassispina* and *Strongylocentrotus intermedius* were used. Swimming blastulae of these sea urchins were dissociated into single cells in 0.44 M sucrose - 0.1 mM EDTA, and the membrane fluidity of the cells was measured by the fluorescence depolarization method using diphenylhexatriene as a fluorescence probe. Although the optimal temperature ranges for the embryos of these three species are different, the range of membrane fluidity within these optimal temperature ranges was found to be almost constant.

POSITIVE CIS-ELEMENTS IN THE INTRON OF THE ARYLSULFATASE(Ars) GENE OF THE SEA URCHIN EMBRYO

Y.Iuchi, K.Akasaka, H.shimada. Graduate Dept. of Gene Sci., Fac. of Sci., Hiroshima Univ., Higashi-Hiroshima

Recently we reported that the region within the first and the third introns($I_1$and I_3) of the Ars gene also retain ability to enhance the expression of the Ars gene. To investigate how these two regions are related to transcription of the Ars gene, we constructed the ars 5'flanking region-luciferase fusion genes and inserted I_1 and I_3 into the upstream of the Ars sequence of the constructs. The gene constructs were introduced into sea urchin eggs by a particle gun mediated gene transfer system. The results suggest that I_1 strongly enhances the Ars gene expression while I_3 has little effect. Deletion of the Ars upstream sequence showed that the 450bp fragments from -250 to -700bp diminishes the enhancing activity of I_1.

SEA URCHIN HATCHING ENZYME (ENVELYSIN): cDNA CLONING AND SPECIFIC DEGRADATION OF THE FERTILIZATION ENVELOPE PROTEINS

K. Nomura [1], T. Shimizu [2], H. Kinoh [3], and N. Suzuki [2].
[1]Dept. of Biochem., Tokyo Metropol. Inst. Gerontol., Tokyo, [2] Dept. of Biol. Sci., Grad. Sch. of Sci., Hokkaido Univ., Sapporo, and [3] Cancer Res. Inst., Kanazawa Univ., Kanazawa.

The hatching enzyme (HEz) of the sea urchin *Hemicentrotus pulcherrimus* was purified as a 37 kDa protein that is prone to autolytic degradation into 32 kDa molecular mass. Both types of enzyme were inhibited by the synthetic cysteine-switch peptides and rTIMP-1. We next synthesized the probes for the cDNA cloning, based on the N-terminal amino acid sequence of the mature enzyme, YVTGGIAWPR-NVAVTYSFGT-LSNDLNQNAI-KNEIRRAFQV and the partial sequence of the C-terminal domain derived by autolysis, QRRTRIRRYF-GNILYALIDR-VEAVR. We will report about the structure of the cDNA of the *H. pulcherrimus* HEz as compared with that of *P. lividus* and the MMPs.

We also investigated the action of HEz on the homologous sea urchin fertilization envelope (FE). When the soft FE, prepared by fertilizing the eggs in the presence of 2 mM aminotriazole, was incubated with HEz, the high Mr fraction containing the 230 kDa proteoliaisin was rapidly degraded into low Mr fragments. The isolated 70 kDa ovoperoxidase was also rapidly degraded, but due to the limited action, reached to the stable 47 kDa fragment via 50 kDa intermediate. In contrast, the 100 kDa and 50 kDa component proteins were scarcely degraded. These results lead to the speculation that the attacks of HEz is directed only to the proteins with essential roles to maintain the integrity of the FE structure.

G STRING BINDING PROTEINS IN SEA URCHIN EARLY EMBRYO

S.Tanaka, K.Akasaka, H.Shimada. Dept. of Biol.,Fac. of Sci.,Hiroshima Univ.,Higashi-Hiroshima.

Poly G sequences, called G strings, frequently exist in the upstream resion of eukaryotic genes and have been implicated in gene regulation in several studies. Previously we reported that the sea urchin arylsulfatase(Ars) gene also contains G strings, and partially purified G string binding proteins from sea urchin embryos (S.Tanaka et al ,64nd annual meeting of Zoological society of Japan).Based on these data,we purified the G string binding protein from the sea urchin embryo in a large quantity, monitoring its activity by gel shift assay . The target sequence of this protein was determined by footprinting. In this meeting we will report the result of these analyses.

TWO KINDS OF ACTIVE SUBSTANCE IN THE HATCH WATER OF ESTUARINE CRABS.

T. Akiyama[1] and M. Saigusa[2], [1]Ushimado Marine Laboratory, Okayama University, Okayama and [2]College of Liberal Arts & Sci., Okayama Univ., Okayama.

Two kinds of active substance have been found in the hatch water of estuarine crabs. One of these substance, named ovigerous hair stripping substance (OHSS), causes detachment of ovigerous hairs from the coat wrapping them. This substance was partially purified by gel filtration and ion-exchange chromatography. Its molecular weight was estimated around 35kDa on SDS-PAGE. Another active substance shows a caseinolytic activity, and also digested debris of isolated egg membranes. This enzyme is eluted near the void volume on Sephacryl S-200 column chromatography. Screening of the fractions from the column previously equilibrated with the buffer containing 1M NaCl shows two or three peaks of caseinolytic activity, which may suggest some heterogeneity in nature. Neither OHSS nor caseinolytic enzyme have hatching activity. So it is not known yet whether these substances are really the hatching enzyme of crustaceans.

The differentiation of the hatching gland cells in early medaka embryos

K.Inohaya[1], S.Yasumasu[1], M.Ishimaru[2], A.Ohyama[3], I.Iuchi[1] and K.Yamagami[1]
1:Life Sci. Inst.,Sophia Univ.,Tokyo.
2:School of Health Sciences,Okayama Univ.
3:ALOKA Co.,Tokyo.

The whole-mount in situ hybridization analysis on early medaka embryos was carried out to identify the earliest developmental stage on which the expression of the hatching enzyme genes started. The experiment using the hatching enzyme cDNAs as probes revealed that the hatching enzyme mRNAs were first expressed in a few cells in the anterior end of the hypoblast layer at late gastrula stage, indicating that the hatching gland cells originated from these cells. This result also shows apparently that the haching gland cells of medaka originate from organizer and the differentiation mechanism of the hatching gland cells is inputted to the programs for morphogenesis in the early embryo.

In addition, we found that treatment of the early stage embryos with retinoic acid caused a significant effect on the development of the hatching gland cells.

DIFFERENTIATION OF NEUROBLASTS FROM ECTODERMAL CELLS IN GRASSHOPPER EMBRYOS.

E. Nagao and K. Kawamura. Biol. Lab., Rakuno Gakuen Univ., Ebetsu, Hokkaido.

The ectodermal cells become partitioned into non-neuronal ectodermal cells (non-nEC) and neuronal ectodermal cells (nEC). The latter give rise to many types of cells, such as neuroblasts, cap cells, ganglion cells, dermatoblasts and so on. In the present study, the embryos at the early stages were cultured in the medium containing dibromodeoxyuridine (BrdU). The embryos were sectioned by the routine paraffin method and stained by using the BrdU-specific antibody. BrdU was incorporated into the ectodermal cells uniformly in 6 days old embryo. In 7 days old embryo, almost no nECs incorporated BrdU, while constant incorporation of BrdU was revealed in the non-nECs. The previous study confirmed that the first appearance of neuroblasts occurred in 8 days old embryo. In the embryos of this age, the neuroblasts and ectodermal cells in a specific region of nEC began the synthesis of DNA again. It seems that the differentiation of neuroblasts in the nEC region may be closely correlated with the temporal pause of DNA synthesis.

CHARACTERIZATION OF THE PROMOTER REGION OF THE GENES OF HCE AND LCE, THE HATCHING ENZYME OF MEDAKA.

S. Yasumasu, K. Inohaya, K. Yamazaki*, I. Iuchi and K. Yamagami. Life Sci. Inst., Sophia Univ., Tokyo. *Dept. of Biol., Sch. of Edu., Waseda Univ., Tokyo.

The hatching enzyme of medaka is composed of two types of zinc-proteases, HCE and LCE. HCE and LCE have similarity in amino acid sequence (55%) and belong to astacin family. However, their gene structures are quite different. LCE gene is a single copy gene consisting of eight exons and seven introns, while the genes of HCE are intron-less and multicopy gene. In the present study, the promoter regions of both genes were characterized. The primer extension analysis of the LCE gene showed three different transcription start sites, which were sequentially located at 30-28 bp upstream from TATAA sequence. On the other hand, from the results of primer extension analysis using a sequence which is found in common in all HCE genes as the primer, a cluster of six start sites and two separate minor start sites were detected, which located at 15-32 bp upstream from TATA box consensus sequences. S1 nuclease mapping using specific probes to several HCE genes also suggested that there were multiple start sites. These results suggested that the multiple transcription start sites were present in every HCE gene. Neither CAAT nor GC box consensus sequence was found in the upstream regions of both genes.

FORMATION OF THE PRIMARY PHARYNX IN THE EARLY EMBRYONIC DEVELOPMENT OF FRESHWATER PLANARIAN.

T. Sakurai. Div. Cell Sci., Fukushima Med. Col., Fukushima.

The ultrastructural features of the primary pharynx have previously been reported. In the present study, I ultrastructurally examined its formation from 64 to 74 hours after egg laying. Precursor cells of the primary pharynx moved peripherally as a group close behind the primordium of the primary epidermis. During the moving, individual cells adhere to one another and give rise to a pharyngeal rudiment inside the primary epidermis after 70-72 hours. It is the characteristic feature of the rudiment that muscle-typed cells and vacuole-containing cells appear among the cells. When the pharynx suck the extra-embryonic yolk cells (73-74 hours after), muscular filaments develop and the vacuoles enormously increase in size. As a result, the sponge-like tissue occurs and constructs the most part of the pharynx. In addition, a common ultrastructural feature is recognized in both types of cells: rough ER of sac-like profile containing fibrous material of low electron density. These data suggest that the primary pharynx is the organ of mesodermal nature.

MECHANISM OF NEUROBLAST SEGREGATION FROM THE ECTODERM IN GRASSHOPPER EMBRYOS.

N. Yamashiki. Biology, Rakuno Gakuen Univ., Ebetsu, Hokkaido.

Differentiation of neuroblasts in grasshopper embryos involves rearrangement of the ectodermal cells. The first sign of neuroblast differentiation is formation of a bottle cell (BC) which extends a cytoplasmic process toward the ventral surface. With the recession of the process, the BC is segregated from the ectoderm, a young neuroblast being formed. EM observations revealed that the adhering junctions which were lined with microfilaments were present between the tip of the cytoplasmic process and the adjacent cells. The cytoplasm in the BC was rich with microtubules arranged parallel to the long axis of the process. The incision of the process near the tip occurred by a constriction across the microtubules. The loss of the junction induced the recession of the process. The treatment of early embryos with Cytochalasin D interfered with the formation of the constriction on the process. Though the junction among the ectodermal cells were maintained, the recession of the cytoplasmic process was progressed. These results suggest that the recession of the cytoplasmic process is induced not only by a microfilament-dependent factor, but by another factor which the BC possesses intrinsically.

CHANGE OF THE 1ST ABDOMINAL SEGMENT OF HORSESHOE CRAB INTO THE 2ND SEGMENT BY TRICHOSTATIN A.

T. Itow, Y. Kato, S. Mochizuki, Y. Shiozawa, M. Okamura. Dept.of Biol., Fac.of Edu., Shizuoka Univ., Shizuoka.

When histones of chromatins are deacethylated, genes can not express. It means that RNA are not synthesised under this condition. On the other hand when histones are acethylated, genes are released and RNA are synthesised. Trichostatin A specially inhibited the enzyme which induces the deacethylation of histones. Therefore under the treatment of trichostatin A, histones are not deacethylated and gene expressions continue.

For the purpose of making clear the relationship of the gene expression and morphogeneses, we treated horseshoe crab embryos with trichostatin A. As the result, special malformations were induced. The 1st abdominal appendages of this malformation became the 2nd appendages-like ones. In normal embryos and adults, the 1st appendages (chilaria) are very small and the 2nd ones (operculum) are large. We will try the analysis of morphogenesis especially segmentations of horseshoe crabs in use of this malformation.

PARTICIPATION OF THE MICROFILAMENTS IN THE MYOPLASMIN-C1 LOCALIZATION IN THE ASCIDIAN EGGS.

S. Chiba and T. Nishikata. Fac. of Sci., Konan Univ., Kobe.

The myoplasm of the ascidian egg is the specific sector of the egg cytoplasm which believed to contain muscle determinants. The myoplasm also contains various kinds of cytoskeletal filaments which act on the ooplasmic segregation and are very important for the precise localization of muscle determinants. The segregation consists of two phases, each mediated by different systems, the first by microfilaments and the second by microtubles (Sawada & Schatten, 1989).

Myoplasmin-C1 is one of the myoplasmic components which are thought to play an important role in the muscle cell differentiation. In order to examine the interaction of myoplasmin-C1 and microfilaments, the microfilament and myoplasmin-C1 were double stained on the same sections or in the same whole mount specimens, using molecular and/or immunological probes. The relationship between myoplasmin-C1 and microfilament was examined in normal embryos and in experimental embryos treated with cytochalasin B or griseofulvin, which inhibit the polymerization of actin and tubulin, respectively. The confocal microscopic observation revealed the distribution patterns of both molecules in detail.

During the first phase of the segregation, the distribution of myoplasmin-C1 was closely related to that of the actin, and the segregation of myoplasmin-C1 inhibited by cytochalasin B. Then, myoplasmin-C1 migrated posteriorly together with the sperm aster. As far as we examined, the microfilament was not obvious during second phase. These results implicate the participation of the microfilament in the myoplasmin-C1 localization and shed light on the role of the myoplasmin-C1.

DEVELOPMENT OF MESENCHYME CELLS IN STARFISH EMBRYOS

N.Kômoto, Y.K.Maruyama Dept. of Zool., Fac. of Sci., Kyoto Univ., Kyoto

Mesenchyme cells of starfish (*Asterina pectinifera*) are released into the blastocoel from the tip of the archenteron at the gastrulae stage. To investigate the development of these cells, I transplanted single mesenchyme cells from RITC-stained gastrulae into the blastocoel of non-stained gastrulae. Three days later, these embryos had become bipinnaria larvae. I examined them with fluorescent microscopy. Almost all of transplanted cells became in contact with epidermis or digestive tract. Most larvae contained single stained cells, but some larvae contained two or more, suggesting that some transplanted cells divided.

IMMUNOELECTRON MICROSCOPIC STUDY OF A SECRETORY FUNCTION IN THE TEST CELL IN THE ASCIDIAN, CIONA INTESTINALIS

T.Okada[1], K. Takamura[2], Y.Yamaguchi[2] and M.Yamamoto[1]. [1] Ushimado Marine Lab., Okayama Univ. [2] Dept. of Biotech., Fac. of Tech., Fukuyama Univ.

We have obtained a monoclonal antibody UA165, which specifically recognizes the test cells in the ovary of Ciona intestinalis. Immunoelectron microscopic study using UA165 as a probe revealed that the antibody specifically recognized the content of oval vacuoles ca. 1 μm in diameter in the test cell cytoplasm. The vacuoles were formed during oogenesis, keeping a constant number through early developmental stages. At the tailbud stage, the vacuoles decreased in number and the antigen of UA165 was released from the test cells into the perivitelline space. Exocytosing oval vacuoles were sometimes observed. The antigen gradually diffused from the test cells toward the tunic, a thin covering of the embryoic surface, and finally became distributed around the test cell and near the outer surface of the tunic. Simultaneously with the arrival of the antigen at the tunic, an electron-dense layer of a fluffy appearance was added outside the smooth surface of the tunic. These results clearly show that the test cells participate in the formation of the larval tunic.

PROGRAMMED CELL DEATH AT THE PERIPHERY OF THE PUPAL WING OF PIERIS RAPAE.

A. Yoshida[1], R. Kodama[2], M. Motoyama[1], T. Mitsui[3] and G. Eguchi[2]. [1]Biohistory Res. Hall, Takatsuki, [2]Div. of Morph., Natl. Inst. Basic Biol., Okazaki and [3]Lab. of Insect Toxicol. and Phsiol., Inst. of Phys. and Chem. Res. (Riken), Wako.

Wing morphogenesis of the lepidopteran insect involves cell death at the peripheral region of the pupal wing. This "programmed cell death" was studied with Pieris rapae by following methods; 1) morphological observations by light and electron microscopy, 2) detection of DNA fragmentation by TUNEL method (Gavrieli et al., 1992). 3) administration of cycloheximide (protein synthesis inhibitor). The results are as follows. 1) Dying cells and their organelles were contracted and fragmented. 2) DNA's of dying cells were fragmented. 3) Dying cells were engulfed by phagocytes. 4) The number of dying cells decreased by the administration of cycloheximide. These coincides with the features of apoptotic cell death described in other organisms.

MORHOLOGICAL CHANGES OF ECHINODERM EMBRYOS PRODUCED BY JASPISIN, A SELECTIVE INHIBITOR OF MATRIX METALLO-ENDOPROTEINASES.

S. Ikegami[1], H. Kobayashi[1], N. Yamafuku[1], N. Kitai[1], Y. Myotoishi[1] and K. H. Kato[2]. [1]Dept. Applied Biochem. Univ. Hiroshima, Higashi-hiroshima, Hiroshima and [2]Col. Gen. Educ., Nagoya City Univ., Mizuho-ku, Nagoya.

A specific inhibitor of the activity of hatching enzyme of the sea urchin Hemicentrotus pulcherrimus was isolated from the extract of the marine sponge, Jaspis species. Chemical and spectral data of the purified substance, which was designated jaspisin, showed that it is a novel substance with the structure of (E)-5,6-dihydroxystyryl sulfate. Jaspisin inhibited the activity of collagenase-type metallo-endoproteinases but did not affect other types of metallo-endoproteinases such as hatching enzymes of medaka and thermolysin. Trypsin, chymotrypsin, and papain were immune to jaspisin. When a fertilized egg was cultured in jaspisin, the embryo developed through the mesenchymal blastula stage. However, it was unable to hatch from the fertilization envelope, and spiculogenesis was prevented. Jaspisin also inhibited sperm-egg fusion without affecting the sperm acrosome reaction or the egg cortical reaction. Because metallo-endoproteinases are suggested to be involved in both sperm-egg fusion and fusion of primary mesenchyme cells, it may inhibit fusion of gametes and spicule-forming cells through blockage of metallo-endoproteinases that are involved in membrane fusion processes.

Cartilage formation at the pharyngeal arch of flounder embryos and localization of a 22.5 kD fibroblast growth factor.

T. Suzuki and T. Kurokawa. Metabolism Sec. Natl. Res. Inst. of Aquaculture, Mie.

Cartilage formation and cell growth at the pharyngeal arch of flounder, *Paralichthys olivaceus*, embryos were observed. At hatching (2.5 days post-fertilization), primordia of mandibular and hyoid arches had not yet been formed. Deposition of cartilage matrices first started from the mandibular arch at 4 days post-fertilization. During the next 2.5 days, cartilages were formed in the order mandibular, hyoid and gill bars. Proliferation of chondroblasts were active around oral/gill cavity under the otic vesicles.

Using antiserum to a 22.5 kD fibroblast growth factor (FGF) isolated from swim-bladder of porgy, homologous FGF was immunocytochemically localized in flounder embryos. Signals were detected from epithelium of oral and gill cavity, and optic vesicles. Thus, 22.5 kD FGF was localized in the vicinity of the region where chondroblasts rapidly proliferate.

EXPRESSION OF ISL-1 HOMOLOGUES (ZISH-1,2,3) DURING EMBRYOGENESIS IN ZEBRAFISH

M. Takahashi[1], Y. Hotta[1,2], K. Uemura[3] and H. Okamoto[1,3] ([1]Dev. of Cellular Communication., Natl. Inst. for Basic Biol., Okazaki, [2]Tokyo Univ., Tokyo, [3]Keio Univ., Tokyo.)

Isl-1 is a LIM domain/homeodomain-type transcription regulator that has been originally identified as an insulin gene enhancer binding protein. Isl-1 is considered to be involved in the differentiation of the neuronal cells. We have cloned the Isl-1 homologues from zebrafish cDNA library and named them ZISH-1,2 and 3.

We examined the mRNA expression pattern of each homologue using *in situ* hybridization to whole-mount embryos. All three homologues were expressed in Rohon-Beard neurons. However the expression in primary motoneurons diverged. ZISH-1 mRNA was expressed in the RoP (Rostral Primary motoneuron) or MiP (Middle Primary motoneuron). ZISH-2 mRNA was expressed in the CaP (Caudal Primary motoneuron). ZISH-3 mRNA was expressed in the ventral region of the somites but not in the primary motoneurons. These results raise possibilities that the Isl-1 homologues may be involved in the specification and/or target recognition by the primary motoneurons.

RETINOIC ACID POSSIBLY AFFECTS LATENTLY THE TAIL FIN OF GOLD FISH(*Carassius carassius*), CAUSING DEGENERATION OF IT.

H. Ohkawa, S.Takeuchi, Dept.Biol.Sci.,Fac.Sci.,Kanagawa Univ.,Hiratsuka.

Gold fishes(body length, ca.,50-60mm), left pelvic fin of which were dissected at the level just distal to pelvis, were treated with five kinds of chemicals as follows: **1**. 0.3nM Retinoic acid(RA, in a diluted fish saline solution, x40, DFSS) for 10 days, **2**. 0.3nM RA for 5 days, **3**. 0.03nM RA for 10 days, **4**. 0.3mM Retinol for 10 days, and **5**. 5mM dimethylsulfoxide for 10 days(20-25 fishes for each) . Beside, as control, some fishes were treated only with DFSS for 10 days. After reared for 2 month or more in pond water(water temperature, 20-25°C), each fish was examined macroscopically, photographed, and fixed with Bouin's fluid.

The regeneration of pelvis fin was inhibited with RA in various degree according to the density and the period of treatment. All of regenerated fins were normaly shaped. It should be noted, in group **1**, the tail fin reduced remarkably in size during a latter half of rearing period.The ratio of area of tail fin mapped on a plane to that of body surface deccreased significantly in comparison with those of the other group. Histological observation revealed the collagenous fin rays were resorbed at the distal end, and thus, became shortened. The other organs as far as surveyed(gill, intestine, liver, kidney) showed no histological change. RA possibly affected the tail fin, as well as the blastema of pectoral fin, during 10 days of treatment to inhibit the formation of new fin rays at the blastema and to cause latently the resorption of old ones in the tail fin.

A BLOOD-VESSEL-LESS MUTANT, nc, FROM THE X-IRRADIATED GERNLINE OF AN INBRED STRAIN OF THE MEDAKA.

Y. Ishikawa[1], Y. Hyodo-Taguchi[1] and H. Tsuji[2]
[1]Div. of Biol. and [2]Div. of Genetics, Natl. Inst. of Radiol. Sci., Chiba.

In the course of a study on the transmission of radiation-induced malformations in the medaka (Oryzias latipes) to the subsequent generations, we found a recessive embryonic lethal mutant, nc (non-circulation), by three-generation crosses. Males of an inbred strain, HO4C, were irradiated with 5 Gy of X-rays and pair-crossed with nonirradiated females to generate F_1 founders. Each F_1 fish was pair-crossed with non-irradiated fish to generate F_2 lines. For each F_2 line , several single pair crosses between siblings were performed. The eggs were examined with a stereomicroscope during whole period of embryonic development. We found putative recessive mutations in three F_2 lines. Complementation tests showed that all the mutants belonged to the same complementation group. The blood circulation was not established in the nc/nc embryo at stage 26, although the heart had begun to pulsate at stage 24. No blood vessels were formed on the york sphere. The heart continued to pulsate for several days, but finally the embryo died. The nc mutant was autosomal, and the chromosome number of the nc/nc embryo was identical to that of wild-type embryo.

THE EFFECTS OF RETINOIC ACID (RA) AND DETECTION OF RA BINDING PROTEINS DURING EMBRYOGENESIS OF *XENOPUS LAEVIS*

Y.Miyanaga[1], H.Uchiyama[2], T.Momoi[3] and M.Asashima[4]. [1]Zool. Inst., Univ. of Tokyo, Tokyo, [2]Dept. of Biol., Yokohama Citry Univ., Yokohama, [3]Laboratories of Differentiation and Development, National Institute of Neuroscience, NCNP, Tokyo. [4]DEPT. OF BIOL., Univ. of Tokyo, Tokyo

Retinoic acid exhibits diverse effects on pattern formation, both in vivo and in vitro. RA presents in *Xenopus* embryos and has been implicated as an endogenous developmental signalling molecule in vertebrate embryos. Blastulae of *X. laevis* were treated with increasing concentrations of all-trans RA and allowed to develop to tadpole stage. The RA-treated embryos were examined microscopically and histologically. Moreover, we studied the distribution of cellular RA binding protein (CRABP) in normal development embryos. Anti-CRABP antibody recognized different tissues or organs in different stages of development. CRABP and RARα were studied by RT-PCR analyses. These mRNAs were transcribed from the blastula stages. The results are discussed the possible endogenous role of RA and CRABP.

CLONING OF A GUANYLATE CYCLASE GENE FROM AN *ORYZIAS LATIPES* GENOMIC LIBRARY.

K.Takeda, T.Shimizu and N.Suzuki. Div. of Biol Sci., Graduate School of Science , Hokkaido Univ., Sapporo.

Many soluble and membrane forms of guanylate cyclase have been identified in several species. It is known that the intracellular domains (kinase-like, cyclase catalytic) are highly conserved among the various types. We screened a genomic library for *Oryzias latipes* using cDNA containing the catalytic domain of the membrane form of guanylate cyclase from *Hemicentrotus pulcherrimus* testis as a probe and isolated eight positive clones. By sequence comparison one of the clones isolated included sequences showing a high similarity to the exons of rat guanylate cyclase A (GC-A).

EFFECTS OF CITRAL, AN INHIBITOR OF RETINOIC ACID FORMATION, ON CARTILAGE PATTERN FORMATION IN CHICK LIMB BUD.

Mikiko Tanaka, Koji Tamura, Hiroyuki Ide. Biol. Inst., Tohoku Univ.

Exogenously applied retinoic acid (RA) is known to affect cartilage pattern in developing and regenerating limbs. There are, however, little reports which directly demonstrate the participation of endogenous RA in the limb pattern formation.

In an organ culture system, we attempted to reduce the concentration of endogenous RA in the limb buds by treatment with citral (3,7-dimetyl-2,6-octadienal), an inhibitor of retinoic acid formation. After this treatment, the cultured limb buds were grafted to the stumps of host embryos. These citral-treated limb buds frequently formed abnormal cartilage pattern and the defect was rescued by simultaneous treatment with a certain amount of RA.

These results suggest that endogenous RA plays a role in the cartilage pattern formation of chick limb bud.

EFFECT OF REGIONAL DIFFERENCES IN THE SURAFCE PROPERTIES OF MESENCHYMAL CELLS ON THE PATTERN FORMATION OF CHICK LIMB BUD.

N.Wada[1], H.Ide[2] and I.Kimura[1].([1]Sch. of Human Sci. Waseda Univ., Tokorozawa, [2]Biol. Inst., Tohoku Univ., Sendai.)

We have previously reported the sorting out *in vitro* between chick limb bud mesenchymal cells prepared from different region along the proximo-distal and anterior-posterior axes or progress zones at different developmental stages. These results suggest that regional differences of limb bud mesenchymal cells shown by the expression patterns of Hox genes may be reflected in cell surface differences, e.g. cell affinities, and these surface differences may affect to the cell-to-cell interaction and final cartilage pattern.

In this study, we investigated the relation of cell adhesion properties to such regional differences in cell affinities. Dissociated progress zone cells prepared from stage 20 and stage 25 limb buds were placed on agar and incubated for 24-36hr. The cells at stage 25 formed larger cell aggregation compared to those at stage 20. This suggests that cell surface differences shown by sorting out experiment may reflected cell adhesiveness. So, some cell adhesion molecules may influence the sorting out *in vitro*.

IN VITRO DEGENERATION OF LARVAL TAIL TISSUES INDUCED BY SYNGENEIC ADULT SPLENOCYTES IN *XENOPUS*

Y. Izutsu & S. Tochinai
Div. Biol. Sci., Grad. Sch. Sci., Hokkaido Univ., Sapporo.

We have previously shown that the adult splenocytes of the MHC homozygous J strain *Xenopus laevis* proliferate in response to larval tail tissues *in vitro* (Izutsu *et al.*, `93, Zool. Sci., 10; 82). It was suggested that adult lymphocytes recognize larval tissues as non-self. To examine whether the splenocytes could exert cytotoxicity to the syngeneic larval tissues, we have cultured larval tissues with adult splenocytes in 70% L-15 medium supplemented with 10% heat-inactivated adult *Xenopus* serum. The tail tissues were excised from tail fin of stage 53/54 larvae as a square piece about 2x1 mm^2 of full thickness block, and co-cultured with $7x10^5$ leukocytes obtained from adult and/or metamorphic climax spleen. The degeneration of larval tissues were observed macroscopically and electromicroscopically. Cell death was also evidenced by the demonstration of the DNA ladder on electrophoresis of gemomic DNA obtained from larval tissues. We assume that the adult-type splenocytes might be involved in elimination of the larval cells from tail tissues during metamorphosis.

IDENTIFICATION OF PROTEIN C IN SERUM OF THE FROG, Rana nigromaculata.

M.Nakamura, M.Sumida and M.Nishioka. Lab. for Amphibian Biol., Fac. of Sci., Hiroshima Univ., Higashi-Hiroshima.

When serum from the frog, Rana (R.) nigromaculata, was run on starch-gel electrophoresis (SGE), several bands were seen in an electrophoretic pattern of proteins. This pattern appeared th same at the stages XIV, XV and XXI, and in the adult frog. However, the pattern at satge X was different. A protein, designated "protein C", did not appear clearly at this stage, but afterwards. This protein was the second richest among serum proteins of mature frogs. Protein C (Mr= 180 kD, when estimated by SDS-PAGE) was obtained after SGE and then subjected to an NH_2-terminal sequence analysis. Sequence of protein C from R. nigromacula was NH_2-TDPMYVIFIPQTLXE for the first 15 amino acids. Homology search of GenBank sequences indicated no significant similarity with any known proteins. The results suggest that protein C is a new protein, and that it may play an important role(s) in the serum after stage X in this species.

PEROXISOMAL ENZYME ACTIVITY CHANGES IN THE TAIL OF ANURAN TADPOLES DURING SPONTANEOUS AND THYROXINE-INDUCED METAMORPHOSIS.

A.Kashiwagi. Laboratory for Amphibian Biology, Faculty of Science, Hiroshima University, Higashihiroshima.

This study attempts to clarify peroxisomal enzyme activity changes associated with tail growth and regression in anurans. Changes in catalase, D-amino acid oxidase and urate oxidase activity were spectrophotometrically investigated using tadpole tails of Rana japonica and Rana nigromaculata. In Rana japonica, total catalase activity decreased in tails undergoing regression during spontaneous metamorphosis, whereas total D-amino acid oxidase and urate oxidase activity increased. Specific activity of these three peroxisomal enzymes decreased. In Rana nigromaculata, total and specific activity of catalase decreased in tails regressing spontaneously. Total D-amino acid activity increased during advanced stages of tail regression, but total urate oxidase activity decreased. Specific activity of D-amino acid oxidase remained high at later stages of tail regression, while that of urate oxidase did not. DL-thyroxine (T_4) treatment was also found to be effective on peroxisomal enzyme activity in the tail of Rana japonica tadpoles.

THE LOCALIZATION AND CHARACTERIZATION OF TROPOMYOSIN PROTEINS IN EARLY *XENOPUS* EMBRYOS

T. S. Tanaka and K. Ikenishi. Dept. of Biol., Fac. of Sci., Osaka City Univ., Osaka, Japan.

In the process of monoclonal antibody (Mab) production against the 38-kDa protein which is lacking in the gastrula-arrested mutant embryos from *Xenopus* female No. 65 (Ikenishi & Tsuzaki, 1988), we incidentally obtained two kinds of Mabs recognizing tropomyosin (TM) proteins in *Xenopus* embryos. As the first step toward the understanding the role of TM proteins in the early development, we performed the characterization of the corresponding antigens to those Mabs by immunoblotting and silver staining for two-dimensional (2-D) gels. The localization of the antigens was also investigated in *Xenopus* embryos by fluorescent microscopy.

Judging from the results by 2-D immunoblotting and fluorescent microscopy, it is likely that the two 30-kDa protein spots with a pI of ca. 4.9-5.0 which were detected in embryos at stages extending from the fertilized to the neurula are non-muscle TM isoforms, and that the 38-kDa spot with a pI of ca. 4.9 detected from the tailbud to the tadpole is a striated muscle TM isoform.

ANALYSIS OF SPOT PATTERN FORMATION IN THE DORSAL SKIN OF METAMORPHOSING *XENOPUS LAEVIS*

S.Tochinai and M.Hanazato
Div.Biol.Sci., Grad.Sch.Sci., Hokkaido Univ., Sapporo

Many frog species exhibits a varied spectrum of dorsal skin patterns, depending on their genetic background. The J-strain South African clawed frog, ***Xenopus laevis***, has a small number of sparsely scattered large spots, and another species of the same genus, ***X. borealis***, has many tightly packed smaller spots. Hybrid frog made between the two exhibits an intermediate pattern. Darker areas of the skin are characterized by the more extensive expansion of dermal melanophores distributed almost equally in the whole dorsal area, and less abundant dermal iridophores. The epidermal malanophores and the dermal xanthophores do not have specific correlation with the macroscopic pattern in either size, shape or number.

When the J strain animals were developmentally arrested before metamorphosis for several months, the dorsal pattern changed so as to have many but smaller spots. Conversely, when the tadpoles metamorphosed more quickly than usual, frogs had fewer but larger spots than normal ones. Although the pattern develops during the late metamorphic period, it was suggested from larval skin graft experiments that the pattern is created under the control of `prepattern' that is laid down much earlier during premetamorphic stages.

CHANGES IN PROTEIN PATTERNS OF *XENOPUS* SKIN DURING METAMORPHOSIS.

H.Kobayashi and K.Yoshizato. Yoshizato Project, ERATO, JRDC, Tsukuba.

Two-dimensional gel electrophoresis has been used to examine changes in the protein patterns of skins from back and tail during *Xenopus* metamorphosis. We have previously shown by silver staining method the appearance of several new proteins in back skin and the little change in protein patterns of tail fin. In the present study, we identified some spots on 2-D gels (keratins, collagenase, etc.). In addition we analyzed the rate of protein synthesis by labeling skins with [^{35}S]methionine. We detected in premetamorphic tail fin the synthesis of keratin II, a major component of adult back skin, which however does not accumulate. At metamorphic climax the syntheses of several proteins are reduced in tail fin.

COMPARATIVE STUDY OF CYTOPLASMIC PROTEINS OF NEWT EMBRYOS DURING EARLY DEVELOPMENT

T. Asao, Dept. of Biol., Sch. Med., St.Marianna Univ., Kawasaki

Some cytoplasmic moieties distributed in fertilized eggs or early cleavage embryos are believed to determine the course of differentiation of the embryonic cells. We studied the differences of the cytoplasmic proteins from newt embryos by the developmental stages and by the embryonic regions, by using of SDS-PAGE or electrofocusing chromatography. Several proteins below 25 kD present in the early cleavage embryos decreased or were not detected at early gastrula, while many other proteins above 30 kD seemed to be not changed throughout cleavage. Our experimental results obtained in the past have shown that several kinds of proteins in uncloven egg cytoplasm were found in the nuclear extract of tail bud embryos. These two results suggest that some kinds of cytoplasmic proteins probably move into the nuclei in the course of cell- proliferating phase. On the other hand, the regional difference of proteins in the early cleavage and early gastrula was hardly appreciated. The electrofocusing chromatography showed that the proteins of isoelectric point from 4 to 7 at least were commonly present between dorsal and ventral regions of 2 cell embryos.

REGULATION OF PROLIFERATION AND DEATH OF EPIDERMAL CELLS OF ANURAN TADPOLES BY THYROID HORMONE.

○M. Chono, K. Oofusa & K. Yoshizato, Dev. Biol. Lab., Dept. of Biol. Sci., Fac. of Sci., Hiroshima Univ., Higashihiroshima.

The epidermis of anuran tadpole contains two types of cells: larva-specific cells and precursor cells of adult-type epidermis. The former cells (skein cells) is subject to apoptosis and the latter (basal cells) is activated to proliferate upon thyroid hormone (TH) stimuli. The present study aimed at visualizing in vivo responses of these cells under the influence of TH. DNA synthesis and cell death were visualized in situ on the histological section prepared from BrdU-incorporated animals and on the section subjected to TUNEL method, respectively. The body and tail epidermal cells were surveyed for DNA synthesis and cell death during the course of TH treatment. The tail epidermis in which skein cells dominate showed a low DNA synthesis and a high TUNEL reactivity. In contrast the back epidermis that contain basal cells showed a high DNA synthesis.

EXPRESSION OF AXOLOTL MSX1 AND MSX2 GENES IN LIMB REGENERATION BLASTEMA

K. Koshiba[1], A. Kuroiwa[2], H. Yamamoto[1] and H. Ide[1]. [1]Biol. Inst., Tohoku Univ., Sendai and [2] Dept. Mol. Biol., Nagoya Univ., Nagoya

Msx genes, msh-like homeobox genes, express in the distal marginal zone of chick and mouse limb buds where cells are maintained at undifferentiated state. We amplified axolotl Msx genes (Amsx genes) by using PCR from cDNA of blastema at medium bud stage and screened the cDNA library of axolotl blastema. We isolated two axolotl Msx genes, Amsx1 and Amsx2. The expression of Amsx1 and Amsx2 during limb regeneration was examined by Northern blot analysis using poly(A)$^+$ RNA from 0, 6, 12, 18 and 24 days postamputated limb. The expression of Amsx2 seemed to reach the peak at 12 days postamputation when the blastemas were obtained at early and medium bud stages. At 24 days postamputation, when redifferentiation started, the signals became weak again. The signal of Amsx1 was much weaker than Amsx2 even at 12 days post-amputation, because the number of transcripts of Amsx1 might be fewer than that of Amsx2. The expression of Amsx1 was maintained even at 24 days postamputation.

These results suggest that Amsx genes relate the blastema formation and the maintenance of blastema at dedifferentiated state and that Amsx1 and Amsx2 play different roles in the maintenance of blastema.

REGION-SPECIFIC REGULATION OF BULLFROG COLLAGEN GENE EXPRESSION BY THYROID HORMONE

○ K.Asahina, S.Yomori, K.Oofusa and K.Yoshizato. Dev. Biol. Lab., Dept. of Biol. Sci., Fac. of Sci., Hiroshima Univ., Higashihiroshima

Anuran metamorphosis is induced by thyroid hormone (TH). Anuran metamorphosis contains resorption of larval tissues and formation of adult tissues. We studied these two phenomena at a molecular level forcussing collagen genes as a thyroid hormone responsive gene. RNA blot analyses with the cDNA of human α_1(I) collagen revealed that the bullfrog collagen mRNA was up-regulated in body, while down-regulated in the tail by TH. Thus, collagen genes are regulated by TH in a region specific manner. We isolated two bullfrog collagen cDNA clones (1A and 6A-1). We characterized in detail these clones and the mechanism of region dependent regulation of collagen gene expression by TH was studied using these clones as a probe.

THE EXPRESSION PATTERN OF BONE MORPHOGENIC PROTEIN RECEPTOR mRNA IN LIMB BUD AND BLASTEMA OF *XENOPUS LAEVIS*.

T. Endo, K. Tamura, N. Ueno* and H. Ide.
Biol. Inst., Tohoku Univ., Sendai. *Fac. of Pherma. Sci., Hokkaido Univ., Sapporo.

Limb buds of *Xenopus laevis* are interesting because they gradually lose a regeneration capacity during development and because the relationship between limb development and limb regeneration can be analyzed at the same time. We, however, have little knowledge about the cause of this decrease in the regeneration capacity.

As a first step to approach this phenomenon from molecular aspects, we have focused on Bone Morphogenic Protein (BMP). BMP is suggested to participate in some morphogenetic processes such as body axis formation and limb pattern formation. *In situ* hybridization revealed that mRNA of BMP receptor (XBMPRa) expressed in the limb bud and regenerating blastema of *Xenopus laevis*. This result suggests that BMP-2 or (and) BMP-4, ligands of XBMPRa, play a role in the process of limb development and regeneration in *Xenopus laevis*.

HYPERPOLARIZATION OF MEMBRANE POTENTIAL DURING CELL CYCLE.

S.Enoki[1], E. Sato[2] and T.Matsusaka[3]
1 Dept. of Biol.,Fac. of Sci.,Kumamoto Univ.,Kumamoto
2 Dept. of Biol.,Fac. of Gen. Edu., Kumamoto Univ., Kumamoto
3 Dept. of Biol. Sci., Fac. of Sci., Kumamoto Univ. ,Kumamoto

The electrical changes of the membrane potential (Em) and the membrane resistance (Rm) were investigated during cell division cycle. As described previously, Em and Rm oscillated during cell cycle.

In this experiment, using macromeres of the newt (*Cynops pyrrhogaster*) embryos at morula stage, the effects of potassium and chloride ions on the oscillations of Em and Rm were examined with inhibitors of the channels. Remarkable differences of the effects between TEA and 4-AP, which are the inhibitors of the potassium channel, were observed. In the case of 4-AP, Em was hyperpolarized to -120 mV after perfusion. Similarly , in the case of 4-AP added with DIDS, which is the inhibitor of the chloride channel, Em was hyperpolarized immediately. These results suggest that the hyperpolarization of Em bofore the cleavage is due to the closing of the 4-AP dependent K^+ channel, not due to that of the Cl^- channel in normally dividing cell.

MOLECULAR CLONING OF PLANARIAN SEROTONIN RECEPTORS

O.Saitoh[1], H.Orii[2], K.Agata[2], K.Watanabe[2] and H.Nakata[1].
[1]Dept. of Mol. and Cell. Neurobiol., Tokyo Metropolitan Inst. for Neuroscience, Tokyo and [2]Dept. of Life Science, Fac. of Science, Himeji Inst. Tech., Hyougo.

Planarians are well known for their ability of regeneration. Although previous studies suggest a significant role of serotonin for the planarian regeneration, the molecular and cellular mechanism underlining the phenomenon are not well understood. We therefore explored the possibility that the planarians express novel serotonin receptors which are critical for the early stage of regeneration. By PCR technology using degenerate primers, we could amplify four clones which contained consensus sequences of the G-protein coupled receptors from planarian cDNA. Judging from the homology comparison, all the four clones appeared clearly related to serotonin receptors. A cDNA clone of the major receptor (PLAR4) was then isolated from a planarian cDNA library. Its open reading frame encoded 478 amino acid residues and the hydropathy analysis showed seven putative transmembrane domains which are characteristic for G-protein coupled receptors. The amino acid sequence exhibited a significant similarity with 5-HT1A type serotonin receptor, especially when compared within transmembrane domains. Its tissue distribution and physiological functions were also investigated.

EYE OR EPIDERMAL MUTATION IN PLANARIAN

K.Watanabe[1], K.Agata[1], H.Orii[1] and T.Sakurai[2].
[1]Lab. of Regeneration, Fac. of Sci., Himeji Inst. of Tech., Hyougo. [2]Div. Cell Sci., Cent. Res. Lab., Fukushima Med. Col., Fukushima.

By mating the clonal population (GI line) of planarian, Dugesia japonica, we have obtained two types of abnormal offspring. A worm with small black eyes (Sbe) repeated degeneration and regeneration of the pigment eye cup, and sometimes form a new eye. Regenerants formed by fission delayed in eye regeneration and showed the similar phenotype of Sbe. Another worm with black epidermis (Bs) was different from GI line with brown one. Sbe or Bs phenotype may come from single dominant mutation.

ULTRASTRUCTURE OF THE RECONSTITUTION BODIES FROM DISSOCIATED PLANARIAN CELLS.

K. Kobayashi, A. Yoshida and S. Ishida.
Dept. of Biol., Fac. of Sci., Hirosaki Univ., Hirosaki.

It is known that planarians have the vast capacities for regeneration, but it is difficult to reconstitute a complete worm from dissociated planarian cells. Spherical cell aggregates covered with an epithelial layer were obtained but these were less than 500μm in diameter. Previous reconstitution experiments have been performed only for fresh-water triclads, and whether reconstitution occur or not has yet to be confirmed by means of ultrastructural study. In this study, fresh-water triclads and marine polyclad were used and the ultrastructure of these cell aggregates were studied, which suggested that reconstitution actually occurred.

Induction of Heat Shock Gene (HSP90) Expression After Decapitation of Planarian *Dugesia japonica japonica*

T.Saheki[1], H.Tsukagoshi[1], H.Hamana[1], K.Yamaura[1], S.Matsumoto[2], I.Yahara[2], and T.Shinozawa[1]
[1]Dept. of Biol. and Chem. Engineering, Fac. of Engineering, Gunma Univ., Gunma.
[2]The Tokyo Metropolitan Institute of Medical Science, Tokyo.

Planarian is known for their high ability in regeneration. To study the mechanism of regeneration, it is important to investigate what kind of proteins express during regeneration. We have isolated planarian HSP90 cDNA and analyzed the mRNA expression after decapitation by RT-PCR.

In this study, Northern analysis was performed to investigate the time and the place of the HSP90 mRNA expression. Furthermore a cDNA of another heat shock protein, HSP70, was isolated, sequenced, and analyzed the mRNA expression after decapitation. The transient expressions of these mRNAs, HSP70 and HSP90, during 14-20 h after decapitation were observed.

EFFECT OF NEUROPEPTIDES ON THE BLASTEMA FORMATION IN REGENERATING PLANARIAN DUGESIA.

I. Hori. Dept. of Biol., Kanazawa Med. Univ., Ishikawa.

Immediately after dissection of the planarian body part, undifferentiated cells (so-called neoblasts) start migration from the stump region to the wound surface. These cells are derived from the parenchyma near the wound region. During the cell migration, they change not only their external shape but also their cytoplasmic profile; a polarized form and a cytoplasm developing RER. These cells are termed regenerative cells since they are a predominant type among the blastema-forming cells. Such regenerative cells seem to be not enough for a complete formation of the blastema. Thus it is reasonable to consider that the blastema formation needs cell proliferation at least in later stages. In the present report, the effect of neuropeptides (a possible mitogen of planarian cells) on the blastema formation has been examined light and electron microscopically. Treatment of the reagent showed a remarkable effect on the blastema formation. Mitotic figures of the undifferentiated cells could be observed throughout the wound region in earlier stages. This result induced a rapid development of the blastema. Possible relationship between enhancement of the regeneration and cell proliferation is discussed.

A NOVEL OPTICAL MICROSCOPE FOR NANOMETER-PRECISION MEASUREMENT AND MICROMANIPULATION.

T. Tani and S. Kamimura. Dept. of Biol., Coll. of Arts and Sci., Univ. of Tokyo, Komaba, Meguro, Tokyo 153.

The resolution of images obtained with optical microscopes is limited to about 0.2 μm. Nevertheless, nanometer or subnanometer precision to measure the displacement of a specimen under the optical microscope can be achieved using sensitive position detecting devices. The technique we have developed has been applied to analyze the active nanometer-scale vibrating motion of microtubules in the flagellar axonemes of sea-urchin spermatozoa (Kamimura & Kamiya, 1989, 1992) and Chlamydomonas (Yagi *et al.*, 1994). To obtain more detailed information about the molecular mechanism of microtubule sliding, further improvement of measuring precision is indispensable. However, it is hampered by the insufficient mechanical stability of conventional microscopes of usual upright type. The problem is crucial when we are going to combine the nanometer-precision technique with the micromanipulation method with glass microneedles, which we are going to use for exact measurement of the active forces of microtubule sliding.

In order to improve the mechanical stability of apparatus we have designed and developed a new optical microscope with horizontal optical axis. Further efforts have been done to improve the mechanical stability of specimen holders of the microscope. We succeeded to develop a microscope almost free from any mechanical disturbance. We could measure displacements under the microscope with sub-nanometer scale precision. A noise-free nanometer-precision micromanipulating technique with glass microneedles has been achieved as well.

FORCE GENERATED BY CILIA AND FLAGELLA AS ESTIMATED FROM MOTILITY OF SINGLE CELLULAR ORGANISMS IN VISCOUS SOLUTIONS

I. Minoura and R. Kamiya. Zool. Inst., Fac. of Sci., Univ. of Tokyo, Tokyo.

To investigate the properties of force generation by cilia and flagella, we measured the swimming velocities of *Chlamydomonas*, *Paramecium* and sea urchin sperm in solutions of 0–13% (w/v) Ficoll (viscosity: 0.9–11 cP) and estimated the force working on the cell body from (viscosity) × (velocity) × (body size). The force generated by *Chlamydomonas* was found to increase from about 21 pN at 1 cP to up to about 28 pN at viscosities raised to 2–6 cP. This increase in force at high viscosity was observed also in sea urchin sperm, but not in *Paramecium*. Next, to assess the contribution of different species of dyneins, we used *Chlamydomonas* mutants lacking either entire outer-arm dynein (*oda*1), the α outer-arm heavy chain (*oda*11) or different parts of the inner-arm dynein (*ida*1 and *ida*4). The viscosity-dependence of *ida*4 differed greatly from wild type and all other mutants in that it alone displayed a marked decrease in swimming velocity at high viscosity. This indicates that the inner-arm heavy chains missing in *ida*4 are important in generating force in viscous environments.

BEHAVIOURAL RESPONSE OF *CHLAMYDOMONAS* TO POLARIZED LIGHT BASED ON GLIDING MOVEMENT.

K. Yoshimura and R. Kamiya. Zool. Inst., Grad. School of Sci., Univ. of Tokyo, Tokyo.

The photoreceptor of *Chlamydomonas* is localized at the eyespot, which is an orange inclusion at the equator of the cell body. We have reported that the amplitude of the photoreceptor current changes with the change in the direction of the e-vector of polarized light incident parallel to the membrane overlying the eyespot. This result not only reveales the direction of the chromophore but also demonstrates that the *Chlamydomonas* can sense the direction of the e-vector of the polarized light. However, no behavioural responses to polarized light have been reported in *Chlamydomonas*. Here we report a behavioural response of cells that are attached to the glass surface by the flagella. Such cells show a gliding movement based on the surface motility of the flagellar membrane. When the cells were illuminated with polarized light incident perpendicular to the glass surface, i.e. parallel to the eyespot membrane, they tended to orient their flagella obliquely to the direction of the e-vector. The direction of the orientation was independent of light intensity. This result suggests that the cells tend to orient themselves to a fixed direction with respect to the direction of the e-vector of the polarized light.

ACTIVATION OF PROTEIN PHOSPHORYLATION BY GLYCEROL IN CILIARY AXONEMES FROM *PARAMECIUM*.

M. Noguchi[1], T. Kitani[2], M. Sawada[2], M. Saitoh[2] and T. Ogawa[2]. [1]Dept. of Environ. Biol. and Chem., [2]Dept. of Biol., Fac. of Sci., Toyama Univ., Toyama.

Cilia on the cortical sheets from Triton-extracted *Paramecium* (0.01% Triton) never beat and never cause water flows toward posterior of the cell even in the reactivation solution containing EGTA to make Ca^{2+} concentration low enough to produce forward swimming. Micromolar cyclic nucleotides or above 20% glycerol is necessary for inducing ciliary beat toward posterior direction. To determine whether the effect of glycerol on the ciliary response is produced via protein phosphorylation, we examined the effect of glycerol on protein phosphorylations in ciliary axonemes. In the presence of minute amount of cAMP, phosphorylations of 29kDa and 65kDa polypeptides were markedly stimulated by glycerol in a concentration dependent manner. However, glycerol did not stimulate any phosphorylation without cyclic nucleotides. This indicates that glycerol induces ciliary beat toward posterior of the cell, through stimulation of cAMP dependent phosphorylations of the axonemal peptides, presumably because of an activation of axonemal cAMP dependent protein kinase.

EFFECTS OF CYCLIC NUCLEOTIDES ON BEAT FREQUENCY OF CILIA IN INTACT CORTICAL SHEETS FROM *PARAMECIUM*.

K. Fujita[1] and M. Noguchi[2]. [1]Dept. of Biol., [2]Dept. of Environ. Biol. and Chem., Fac. of Sci., Toyama Univ., Toyama.

Cilia in intact cortical sheets from *Paramecium caudatum* were reactivated and beat toward reversed direction, when the sheets were perfused with reactivation solutions containing Ca^{2+} and Mg-ATP. Beat frequency of the reactivated cilia was measured using handmade detector equipped with phototransistor. The beat frequency of cilia decreased with increasing cAMP concentration to 10 μM cAMP in the presence of Ca^{2+}. The beat frequency, however, increased with increasing cAMP concentration when the cAMP concentration was above 10 μM. This suggests that the action of cAMP on beat frequency , as well as on beat direction, competes with Ca^{2+}.

We also examined the effect of electric field on beat frequency of cilia in the intact sheets whether the electric stimulation elevates intraciliary cAMP concentration by an activation of adenylate cyclase which is thought to be activated by hyperpolarization of the cell membrane.

THE ROLE OF CALCIUM IONS ON THIGMOTAXIS IN PARAMECIUM CAUDATUM.

T.Hirano and K.Iwatsuki. Dept. of Biology, Fac. of Education, Kagawa Univ. Takamatsu, Kagawa.

We reported that we succeeded in the induction of thigmotaxis of Paramecium caudatum by means of changing ionic condition (Sixty-fourth Annual Meeting of the Zoological Society of Japan). To know the mechanism of the thigmotaxis , CNR (Ca-channel mutant) were used. The effect of caffeine, Ruthenium red and $LaCl_3$ on the thigmotaxis were also studied.

We found that Rutenium red and $LaCl_3$ suppressed the thigmotaxis of the organisms, and the caffeine enhanced. CNR hardly showed the thigmotaxis. We conclude that Ca^{2+} is tightly related to the thigmotaxis.

CHARACTERISTICS OF THE DEPOLARIZING AND HYPERPOLARIZING QUININE RECEPTOR POTENTIALS IN *PARAMECIUM CAUDATUM*

K. Oami Inst. Biol. Sci. Univ. of Tsukuba, Tsukuba.

Characteristics of the quinine receptor potentials in the ciliate *Paramecium caudatum* were examined using conventional electrophysiological techniques. A Ni-paralyzed CNR specimen produced a depolarizing receptor potential in response to a local application of quinine-containing solution to its anterior region, but a hyperpolarizing receptor potential in response to an application to its posterior region. Peak level of the depolarizing receptor potential shifted toward the depolarizing direction when the external Ca^{2+} concentration was raised, while the peak hyperpolarizing receptor potential shifted toward the depolarizing direction when the external K^+ concentration was raised. Membrane conductance increased during the activation of both the anterior and posterior receptors. The inward receptor current induced by a stimulation to the anterior region reversed its polarity at around +15 mV, while the outward receptor current produced by a posterior stimulation reversed its polarity at around -40 mV. It is concluded that the depolarizing quinine receptor potential in *Paramecium* is produced by an activation of Ca^{2+} channel located in the anterior region of the cell, while the hyperpolarizing quinine receptor potential is produced by an activation of the K^+ channel located in the posterior region of the cell.

CHAOTIC VARIATION IN CILIARY BEAT PERIOD

M.Okano, Y.Mogami, and S.A.Baba.
Dept. Biol., Ochanomizu Univ., Tokyo.

We used the large abfrontal cilium of *Mytilus edulis*, and measured period lengths of beating precisely and continuously with a FIFO trend counter (Model UCM-4398BPC, Micro Science Co., Tokyo). The period lengths apparently varied randomly. So we attempted to determine whether the variation is derived from a Marcov process or from deterministic chaos underlying the beating mechanism. In a pseudo-phase space plot of n+1_th period vs n_th period which is known useful for analyzing time series of events, trajectories form a strange attractor. Many of them entered into the attractor at the lower edge from distant points and left it at the upper edge. Most of these attractors had an elliptical shape rather than a circle, which indicates that the underlying mechanism of beating is not just a Marcov process. Further, the Lyapunov exponent, which shows chaotic property of the system, turned out to be positive and hence indicates the system is chaotic.

EFFECTS OF ETHANOL IN CILIATES.

T. Tsuda, T. Matsuoka, K. Taneda.
Dept. of Biol., Fac. of Sci.,
Kochi Univ., Kochi.

It is suggested that anesthetics are nonspecifically bound to lipid bilayer, and cause anesthesia by modifying membrane. Alcohol causes anesthesia. In order to elucidate mechanism of anesthesia in unicellular organisms, we examined effects of ethanol on behavioral responses in two kinds of ciliates. The cells of *Blepharisma japonicum* responded to application of ethanol by striking ciliary reversal and increase in percentage of swimming cells. In *Paramecium multimicronucleatum*, ethanol had no effect on ciliary reversal response, and caused decrease in percentage of swimming cells. Effective concentration resembled each other.

ULTRASTRUCTURAL STUDIES ON OUTER ARM DYNEIN IN CILIA AND FLAGELLA IN THE ANIMAL KINGDOM.

M. Kubo-Irie and H. Mohri, The Univ. of the Air, Chiba

Based on biochemical data and ultrastructural observations, the outer arm dynein of the axoneme in Protozoa has a three-headed structure, whereas that in fish, sea urchin and mouse sperm has a two-headed structure. We examined whether the outer arm dynein of flagella and cilia in other animals, especially Coelenterata, Porifera, etc., is two-headed or three headed.

When it is hard to get sufficient amount of material for biochemical analysis, electron microscopical observation is effective in revealing the number of heads of the outer arm dynein (Zool. Sci., 10, Suppl., 99, 1993). The obtained results indicated that the outer arm dynein of flagella and cilia in the sea anemone and sponge as well as the crustacean, annelid and flatworm are also two-headed. The reduction in the number of heads would have occurred during the evolution from Protozoa to Metazoa. Alternatively, the outer arm dynein molecule in Protozoa seems to be specialized to facilitate their complicated behavior.

VERIFICATION OF THE MODEL OF GRAVITY SENSING OF PARAMECIUM: AN APPROACH FROM THE THREE DIMENSIONAL ANALYSIS OF SWIMMING TRAJECTORIES.

Y.Mogami[1], Y.Shinohara[2], and S.A.Baba[1].
[1]Dept. Biol., Ochanomizu Univ., Tokyo, [2]Zool. Inst., Fac. Sci., Univ. of Tokyo, Tokyo

We proposed a model mechanism of physiological gravity sensing of Paramecium, in which gravity dependent deformation of cell membrane is transmitted by the unique antero-posterior distribution of mechanosensitive channels, and the resultant minor shift of membrane potential (depolarization in upward orienting cells and hyperpolarization in downward orienting cells) is reflected to the changes in membrane potential-coupled propulsive parameters, leading to the changes in the direction of the helical swimming trajectories (Ooya, et al, 1992, J. Exp. Biol., 163). According to the numerical simulations, the model predicts the upward swimming of paramecia along a super-helical trajectory, a higher order helix composed of the 'conventional' helices of individual cells (Mogami, et al, 1992, Zool. Sci. 9-6). In order to confirm the theoretical prediction of super-helical swimming, we analyzed the swimming trajectories of individual cells in three dimensions. Free swimming of the cells under quasi-unbound and low thermal-convection conditions were recorded by two synchronized TV-cameras (Baba et al, 1991, Rev. Sci. Instrum., 62). Analyses of the reconstructed three-dimensional trajectories revealed that about 25% of the cells swam upward along the super-helical trajectory.

EFFECTS OF CALCIUM ON FORWARD MOTILITY OF FOWL SPERMATOZOA

Y. OZEKI[1], R. KODAIRA[2] & K. KIMURA[2].
[1]Grad. Sch. of Sci. & Techn. and [2] Dept. of Appl. Biol. Sci. Shinshu Univ., Ueda, Nagano, 386

Ejaculated and washed spermatozoa of fowl become immobile in most simple salt-based media at the normal body temperature of 40-41°C, and that motility can be restored quickly by lowering incubation temperature again (Takeda, 1982). It is reported that this reversible immobilization involves either a loss of intracellular Ca^{2+} to the suspending medium (Wishart & Thomson, 1989) or a reversible temperature-dependent immobilization of the axonemes (Ashizawa *et al.*, 1989).

To examine the forward motility in fowl sperm, the reactivation of demembranated model was investigated at 40°C. The reactivation of demenbranated sperm was need calcium but not cAMP. Concentration of Ca^{2+} in a reactivation mixture affected the forward motility of the model and the models were most reactivated in the presence of 5×10^{-7}M Ca^{2+} in the reactivation mixture. These results suggest that a change in intracellular Ca^{2+} concentration is a candidate for the trigger for the temperature-dependent immobilization of fowl spermatozoa.

EFFECTS OF EXTERNAL PH ON THE VOLTAGE DEPENDENT ION CHANNELS IN THE MARINE DINOFLAGELLATE *NOCTILUCA MILIARIS*

M. Koike and K. Oami
Institute of Biological Sciences, University of Tsukuba, Tsukuba 305

In order to investigate characteristics of voltage dependent ion channels, we examined the effects of external pH on the ionic currents exhibited by the specimen of *Noctiluca miliaris* under voltage clamp conditions. A specimen of *Noctiluca* produced a transient inward current when the membrane was depolarized from a holding potential of -80mV to potential levels more positive than -50 mV. The inward current came to be followed by a transient and a steady outward current with depolarizations more positive than 0 mV. These membrane current responses correspond to the positive spike of the tentacle regulating potentials in *Noctiluca*. When the external pH was lowered below 5,the peak value of the inward current became smaller and the increasing phase of the current became slower. Threshold potential for activation of the current shifted toward the depolarizing direction and the reversal potential of the current shifted toward hyperpolarizing direction. When the external pH was raised above 9, the transient outward current following the initial inward current became smaller. Other current components were unaffected by changes in the external pH range 4 -10. The present results indicate that the external pH modulates the characteristics of the specific voltage-gated ion channels in *Noctiluca*.

IMMUNOHISTOCHEMICAL LOCALIZAITON OF P70-LIKE SUBSTANCE IN GERBIL BRAIN.

A. Seto-Ohshima[1], K. Uchida[2], T. Isobe[2] and M. Onozuka[3], [1]Div. Morph., Inst. for Develop. Res., Aichi, [2]Fac. of Sci., Tokyo Metropolitan Univ., Tokyo, [3]Gifu Univ. Sch. Med., Gifu.

Recently, we have found a specific protein of 70K (P70) in the cobalt-induced epileptic focus of rat cerebral cortex which is capable of inducing epileptiform seizure activities. In order to genetically evaluate a P70-associated mechanism of epileptogenesis, we immunohistochemically examined the localization of P70 in the brain of seizure-prone strain gerbils (MGS/Idr) of Mongolian gerbil (*Meriones unguiculatus*), a genetical animal model of epilepsy. When brain sections of adult gerbils were stained with the antiserum against P70, immunoreactivity was, in disagreement with the previous finding with rats, found in nuclei of cells, mostly of the neuron type in the superior colliculus and some other regions. A similar observation was also obtained in young animals without any behavioral seizure activity. The location of these immunopositive cells in the superior colliculus corresponded to the area which has been proposed to be involved in the rapid movement in other animal species. These results suggest that P70 and/or P70-like protein may be related to the inherent instability of some sensory system of this model of epilepsy.

MEPP FREQUENCY AFTER A TETANIC NERVE STIMULATION IN THE PERFUSION SOLUTION WITHOUT DIVALENT CATION

N.Tanabe, Daiichi Hoiku Junior College, Dazaifu

After a repetitive nerve stimulation, the transmitter release from frog neuromuscular junction increases. We can know it by measuring EPP amplitude or MEPP frequency. In the perfusion solution with Mg ion and without Ca ion, MEPP frequency during a tetanic stimulation increases and after the stimulation, MEPP frequency decreases. This decay is composed of two components of augmentation and potentiation. It became clear that the rate of increase of MEPP frequency changes with Mg ion concentration. The magnitude of augmentation decreased with the increase of Mg ion concentration. When there were not divalent cations in the perfusion solution, I studied how was the frequency of MEPP after a tetanic nerve stimulation. Even if an experiment carried out in such solution, MEPP frequency increased with a repetitive stimulation. In spite of no divalent cation, the increase speed of augmentation tended to be faster than the speed of the control experiment.

EFFECT OF CALMODULIN INHIBITOR 'W-7' ON CALCIFICATION AND OXGEN PRODUCTION IN SCLERACTINIAN CORALS.

Y.Isa. Dept. of Biol., Fac. of Sci., Univ. of Ryukyus, Okinawa.

In corals, symbiotic associations between a unicellular algae, zooxanthellae, and its host tissue still remain metabolically uncertain. An involvement of metabolic modulator 'calumodulin' to the association was investigated by the measurement of the effects of W-7 to the rate of calcification and of oxgen production in three species of the scleractinians.

The inhibitor W-7 reduced the calcium carbonate deposition under light irradiance of 600 umoles/m^2·s in a microcolony of Stylophora pistillata (Observatoire Océanologique Européen,Centre Scientifique de Monaco), as well as the oxgen production in pieces of colonies of S. pistillata, Pocillopora damicornis and Galaxea fascicularis. These results were discussed in association with the inhibitory effects of DCMU and DIAMOX, the inhibitors of photosynthesis and carbonic anhydrase, respectively.

CHANGES IN C-FOS IMMUNOREACTIVITY IN THE RAT BRAINS DURING COLD ACCLIMATION.

M.ISHIYAMA, S.MIYATA, T.NAKASHIMA, T.KIYOHARA. Dept. of Appl. Biol., Kyoto Inst. of Tech., Matsugasaki, Sakyo-ku, Kyoto 606

Changes in the immunoreactivity for C-FOS in the rat brains were investigated during cold acclimation. The sites of C-FOS immunoresponded cells were classified into three types on the basis of time course of the C-FOS expression. First, C-FOS immunoreactivity was seen in the animals exposed to the cooling enviroment for 3 h and 24 h, but not found in the cold adapted (14 days); in the lateral ventral septum nucleus, parvocellular parts of paraventricular nucleus, posterior hypothalamus, supramammiliary nucleus, and substantia nigra. Second, C-FOS-positive cells were persistently found in the rats exposed to cold from 3h to 14 days; in the preoptic/anterior hypothalamus, paraventricular nucleus thalamus, medial forebrain bundle, zona incerta, subparafascicular nucleus thalamus , central grey, lateral reticular formation, and spinal cord (layer 1, 2). Third, C-FOS immunoreactivity were not observed in the animals exposed to the cooling for 3 h and 24 h, but it appeared in the cold adapted; in the ventromedial portion of ventromedial nucleus hypothalamus. These data reveal that changes in the sites of C-FOS immunoreactive cells are correlated with the alternation of thermogenic mechanism in the rat brains with cold acclimation.

CENTRAL PATHWAYS FOR EXCITATION AND INHIBITION OF NEURONS INNERVATING THE CARDIOARTERIAL VALVES IN THE ISOPOD CRUSTACEAN, *BATHYNOMUS DOEDERLEINI*.

J. Okada and K. Kuwasawa. Dept. of Biol., Tokyo Metropolitan Univ., Tokyo.

The cardioarterial valves are located at the junctions between the heart and the arteries. The valve of the 5th lateral artery which supplies haemolymph to the swimmerets is innervated by inhibitory axons from the 5th lateral cardiac nerve (LCN5). Excitation and inhibition of LCN5 resulted in, respectively, an increase and a decrease of the haemolymph flow to the swimmerets. We previously showed that the impulse rate of LCN5 increased during augmented movements of the swimmerets, and that there are reflex pathways from mechanoproprioceptors in the swimmerets to LCN5. Central input to the LCN5 neuron was recorded intracellularly from its cell body. Excitation or inhibition of the LCN5 neuron was elicited by stimuli applied to axons of the ventral nerve cord at the thorax or the abdomen. Oscillatory potentials of motorneurons for swimmeret muscles showed correspondence to oscillatory potentials of the LCN5 neuron. Injection of hyperpolarizing current into an identified stretch receptor neuron generated impulses or increased of impulse rate in the LCN5 neuron.

IDENTIFICATION OF CARDIOINHIBITORY AND CARDIO-ACCELERATORY NEURONS IN THE CNS OF THE STOMATOPOD CRUSTACEAN *SQUILLA ORATORIA*.

H. Ando and K. Kuwasawa.
Dept. of Biol., Tokyo Metropolitan Univ., Tokyo.

The *Squilla* heart has the intrinsic cardiac ganglion and receives extrinsic cardio-regulatory nerves from the CNS. The nerves consist of one pair of cardioinhibitory nerves (CIs) and two pairs of cardioacceleratory nerves (CA1s and CA2s). CI arises from the 10th nerve root of the subesophageal ganglion (SEG). CA1 and CA2 originate from, respectively, the 16th and 19th nerve roots of SEG.

Candidates for the CI and CA2 cell bodies were stained in the CNS by means of back-filling with Co^{++} and Ni^{++} at cut-stumps of CI and CA2 axons. SEG is divided into six segments with five septa. A candidate for the CI cell body (about 30μm in diameter) was located near the midline at the posterior half in the 1st segment of SEG. A candidate for the CA2 cell body (about 30μm in diameter) was located near the midline at the posterior half in the 4th segment of SEG.

A HPLC ANALYSIS OF DOPAMINE IN THE CARDIAC GANGLION OF THE DECAPOD CRUSTACEAN ANICULUS ANICULUS.

T.Yazawa[1], M.Yasumatsu[1], K.Kuwasawa[1] and M.Otokawa[2].
[1]Dept. of Biol., Tokyo Metropolitan Univ., Tokyo,
[2]Dept. of Biol., Fac. of Sociology, Hosei Univ.,Tokyo.

We suppose that dopamine may be a candidate for the neurotransmitter of cardiac ganglionic neurons in the hermit crab, Aniculus aniculus, based on histochemical and pharmacological experiments. We analyzed the ganglion by means of HPLC with electrochemical detection. One to sixteen ganglia were homogenized in 200 μl 0.1 M perchloric acid. Each extract was centrifuged and 10 μl of the resulting supernatant analyzed directly onto the HPLC column.Separations were achieved on a C-18 column (100 x 1.0 mm I.D., 3 μm spherical particle; 30°C,700 mV,40 μl/min flow rate). The mobile phase contained 0.1 M tartaric acid, 0.1 M sodium acetate pH 3.2, 0.5 mM EDTA-2Na, 0.2% THF, 4% acetonitrile and 550 μM sodium 1-octane sulfonate (MW, 216.28). Solutions of DOPA, DOPAC, nor-adrenaline, adrenaline, dopamine and serotonin were used as standards. Analyzing chromatograms of the standards and the ganglion extracts we obtained the dopamine contents, 350.6 ± 39.8 fmol./mg wet weight (15 ganglia). Results may support that it is likely that dopamine is the neurotransmitter of cardiac ganglionic neurons.

EFFECTS OF COOLING ON THE LOBSTER CARDIAC NEURONS.

T. Kuramoto and M. Tani. Physiol. Lab., Shimoda Mar. Res. Ctr., Tsukuba Univ., Shizuoka

Membrane potentials and impulses of cardiac neurons were recorded in isolated and opened hearts of the lobster Panulirus japonicus while the perfusion saline (20± 2°C) was switched to cold one (10-15°C). The rate, magnitude and duration of cooling were a range of 0.5-3°C/min, 1-5°C and 2-6 min, respectively.

With the cooling, frequency of impulse bursts of the large and small cardiac neurons decreased with a slight decrease in firing rate in the burst. Whereas, the burst duration increased or decreased due to a change in bursting pattern. Moreover, a new type of impulses was observed to start in response to cooling. These impulses could be often recorded from a trunk portion of the ganglion. The firing rate of cooling-induced impulses was lower than that driving the heartbeat.

Resting membrane potentials of the large neuron somata increased more or less by cooling though frequency of burst discharges decreased significantly. In contrast, the burst amplitude did not change with cooling but increased markedly just after rewarming. In a few instances, resting potentials, being probably of their dendrites or axons, clearly decreased with falling temperature. Therefore, the cardiac neurons may have a sensory portion which is receptive to cold stimuli and may compensate the reduced membrane excitability with falling temperature.

HEART FORMATION AND CHANGES IN HEART RATE DURING EMBRYONIC DEVELOPMENT OF LIGIA EXOTICA.

A. Mori. and H. Yamagishi. , Inst. of Biol. Sci., Univ. of Tsukuba , Tsukuba.

We studied the embryonic development of the isopod crustacean Ligia exotica to determine developmental stages with special reference to the heart formation and to examine changes in the heart rate during development. After copulation, a female breeds about 100 eggs into the brood chamber formed on her ventral thorax. The eggs in the brood chamber took about 20 days to hatch as a juvenile when the mother was reared at 25°C. The juveniles were kept in the brood chamber for 5 to 7 days after hatching, and then released. We referred to the day when the eggs were laid as the 1st day (1d) of the development, and examined the embryos by taking eggs from the brood chamber day by day. The results obtained were as follows: 1) At 1d, the nuclear division took place in the yolk and superficial cleavage began. At 6d, the limb buds became visible. The outer egg membrane, chorion, split at 11d. At 14d, the embryo reversed its position. 2) At 12d, the cardioblasts of both sides met along the dorsal midline and the heart was formed progressively from the posterior end. At 13d, the heart began to beat irregularly and its rate became stable at 14d. The heart rate increased during embryonic development.

DEVELOPMENTAL CHANGES IN ACCELERATORY REGULATION OF THE HEART IN AN ISOPOD CRUSTACEAN, *LIGIA EXOTICA*.

A.Sakurai and H.Yamagishi
Inst.of Biol.Sci.,Univ.of Tsukuba,Tsukuba.

Each of the anterior cardiac nerves (ACNs) of *Ligia exotica* contains two cardio-acceleratory fibers (CA1, CA2). We identified their routes from the CNS to the heart by anatomical and electrophysiological methods. Then we examined changes in acceleratory regulation of the heart associated with the transfer of the pacemaking site from the heart muscle to the cardiac ganglion during the juvenile development. The results obtained were as follows: 1) CA1 and CA2 originate from paired lateral nerves of the 1st and the 2nd thoracic ganglia, respectively. 2) In adult neurogenic hearts, stimulation of either CA1 or CA2 increased both frequency and contractile force of the heart beat by affecting the activities of both the cardiac ganglion and the heart muscle. 3) The stimulation of CA1 caused a significantly greater chronotropic effect than that of CA2. 4) In early juvenile hearts, stimulation of either CA1 or CA2 accelerated the myogenic heart beat, and CA1 had a significantly greater chronotropic action than CA2.

EFFECTS OF ACETYLCHOLINE, OCTOPAMINE, DOPAMINE, AND ELECTRICAL STIMULATION ON THE CONTRACTION OF SPINE MUSCLE OF THE SEA URCHIN, *ANTHOCIDARIS CRASSISPINA*.

M. Yamaguchi and C. Shingyoji. Zool. Inst., Fac. of Sci., Univ. of Tokyo, Tokyo.

The basal region of each sea urchin spine is surrounded by spine muscle and a "mutable" connective tissue known as the catch apparatus. Since spines can move in any direction, muscle contraction on one side of the spine must be accompanied by relaxation of both the muscle and the catch apparatus on the opposite side. To elucidate the mechanism of such coordination, we studied the effects of several drugs that have been reported to affect the stiffness of the catch apparatus, and of electrical stimulation on the contraction of the spine muscle. Acetylcholine (ACh) induced three types of contraction: a rapid phasic, a slow tonic, and a rapid tonic contraction. Both octopamine and ATP induced a slow tonic contraction. Dopamine and noradrenaline did not induce contraction, but relaxed the contraction and inhibited the slow tonic contraction caused by ACh, octopamine, or ATP. Electrical stimulation of the test surface near the muscle induced a rapid phasic and a rapid tonic contraction similar to the one induced by ACh. Its tonic component was also inhibited by dopamine. The results suggest a possible mechanism controlling the spine movement.

EFFECT OF SINUSOIDAL VIBRATIONS ON THE ACETYLCHOLINE-INDUCED CONTRACTURE TENSION IN THE LONGITUDINAL BODY WALL MUSCLE OF A SEA CUCUMBER *STICHOPUS JAPONICUS*.

T. Kobayashi, H. Sugi, H. U shitani, H. Wada, J. Inoue and T. Kawakami. Department of Physiology, School of Medicine, Teikyo University, Itabashi-ku Tokyo.

Mechanical vibrations are known to reduce contractile tension in mammalian smooth muscles. We have examined the effect of sinusoidal mechanical vibrations (0.5-2.5%, 5-100 Hz) on the acetylcholie (ACh)-induced contracture tension in an invertebrate somatic smooth muscle, using the longitudinal body wall muscle of a sea cucumber *Stichopus japoicus*. The steady contracture tension induced with a supramaximal concentration of ACh (10^{-3} M) was reduced by 20-50% by applying vibrations (2.5%, 5-100 Hz), while the steady contracture tension induced with a submaximal concentration of ACh (10^{-5} M) was reduced by 70-80%, suggesting that actin-myosin linkages can be detached with vibrations more readily in submaximally activated fibers than in maximally activated fibers. When temperature of the experimental solution was lowered to 0°C, the magnitude of maximal contracture tension increased by about 50%, and the vibrations became ineffective in reducing the contracture tension suggesting that vibrations are no longer effective in detaching actin-myosin linkages if their turnover rate is sufficiently reduced.

CHARACTERISTICS OF UNLOADED CONTRACTION OF SINGLE MYOCYTE ISOLATED FROM RAT HEART.

T.Tameyasu, Dept. of Physiol., St.Marianna Univ., Sch. of Med., Kawasaki.

Some characteristics of unloaded contraction were examined at a cellular and a sarcomere level in isolated single rat ventricular myocytes. Both velocity and extent of an electrically-triggered contraction were independent of the size of myocyte. Among myocytes isolated separately from the right ventricle and inner and outer layers of the left ventricle, no differences were observed in any of their size, the velocity and extent of the contraction. Both the velocity and extent of contraction of an individual sarcomere varied to some extent during a low frequency stimulation. The variation occurred independently each other among several consecutive sarcomeres in a myocyte, suggesting a labile nature of Ca^{2+} release from the sarcoplasmic reticulum (SR). The contraction velocity of the individual sarcomere decreased with a decrease of the resting sarcomere length (SL) in the range of 1.6-2.1 μm. Such a dependence was not observed in a spontaneous contraction. Though a similar Ca^{2+} induced Ca^{2+} release mechanism of the SR has been thought to underly both the electrically-triggered and the spontaneous contractions, the detailed mechanism may be different between the two.

LOW-FORCE CROSSBRIDGES PRESENT DURING MUSCLE CONTRACTION.

H. Iwamoto and H. Sugi. Dept. Physiol., Sch. Med., Teikyo Univ, Tokyo.

It is known that a fraction of the attached myosin crossbridges exist in low-force forms during contraction. Such low-force crossbridges are populated during the rise of tension, during isotonic shortening and in the presence of inorganic phosphate. To test whether the low-force crossbridges found under these experimental conditions represent a single reaction intermediate of the actomyosin ATPase cycle, the mechanical responses to ramp stretches were compared in skinned rabbit or living frog skeletal muscle fibers. The responses had several characteristics in common: 1) The magnitudes of the responses were larger than expected for isometrically contracting fibers in a steady state, 2) the responses were accompanied by a decrease of the viscous component of tension, and 3) the responses showed nonlinear dependence on the amplitude of the stretch. These results suggest that the low-force crossbridges found under those conditions represent a single intermediate, presumably one of the A•M•ADP•Pi states.

CHANGES IN THE LEVELS OF ANSERINE AND CARNOSINE AND THEIR RATIO IN SKELETAL MUSCLES OF RAT AND MDX MOUSE.

M.Tanaka.Dept.of physiol.,St.Marianna Univ.Sch.Med., Kawasaki.

The present study was undertaken to elucidate the mechanism of changes of anserine and carnosine level and their ratio in the skeletal muscles. Changes in the levels of both peptides and their ratio in the fast and slow twitch muscles from Wistar rat and mdx mouse were examined. The ratio of anserine to carnosine level increased with age in both EDL and SOL muscles of rat from 5 to 46 weeks. During endurance training, a significant decrease in both peptides levels and their ratio,especially in EDL were observed .On the other hand, in muscle from mdx mouse carnosine level was significantly decreased in comparison with normal ones bringing about an increase of the ratio in both muscles from 7 to 40 weeks of age. (Age 20 weeks; $p < 0.001$). Moreover, carnosine level in EDL from mdx mouse was close to the value in SOL from normal mouse of the same age. These observations reflect a shift of dystrophic skeletal muscle towards oxidative metabolism and suggest the fibre type conversion of fast to slow-twitch muscle. These findings, including the transformation of muscle fibre are discussed.

ELECTRON MICROSCOPIC STUDIES ON THE MYOSIN HEAD MOVEMENT IN LIVING THICK FILAMENTS WITH A GAS ENVIRONMENTAL CHAMBER.

H. Sugi, T. Akimoto, S. Chaen, S. Shibayama, I. Shirakawa, and N. Oishi. Department of Physiology, School of Medicine, Teikyo University, Itabashi-ku, Tokyo.

We have succeeded in recording the myosin head movement in living thick filaments using a gas environmental chamber, with which the filaments can be kept in wet state under electron microscopic observation. The position of individual myosin heads is marked by attaching gold particles of 15 nm diameter using antibodies against the junction between 50 K and 23 K segments of myosin heavy chain. The filament images are recorded with image plates (exposure time, 0.1 s). The results obtained up to the present time are as follows: (1) the position of the myosin heads does not change significantly with time in the absence of ATP; (2) on iontophoretic application of ATP, the myosin heads move for a distance of 10-30 nm parallel to the filament long axis: (3) the heads move towards the center (bare region) of the filaments; and (4) iontophoretic application of ADP produces no significant myosin head movements.

We are currently planning to examine the ATP-induced myosin head movement in the presence of thin filaments.

VERTICAL MIGRATION OF THE FIREFLY SQUID IN THE SPAWNING SEASON.

Y.Kito[1], H.Uragami[2], K.Narita[1], O.Inamura[3], M. Michinomae[4] and M. Seidou[5, 1] Dept. Biol., Osaka Univ., Toyonaka, [2]Yokata Fish. Coop.,[3]Uozu Aquerium, Toyama,[4]Dept. Biol. Konan Univ., Kobe, and [5]Aichi Pref. Art Univ. Aichi.

Large shoal of firefly squid, Watasenia scintillans, come to coast of Toyama of the Japan Sea for spawning in spring. This squids live at the 200 m depth in the day. They move up near the coast at night. We found around the sunset an intense scattering layer at 10 m depth near Yokata port of Toyama on the fish school finder, which was specially designed for searching squid by Furuno Elec. Comp (Nishinomiya). The squid population in the layer was estimated more than 5 individuals per 1 m. This dense layering of the squid appears to be the specific behavior characteristic of the firefly squid in spawning season. Daily vertical migration of deep-sea animals may depend mostly on the underwater light intensity and its spectrum. We measured spectral intensities of 10 m depth around the set-net and of 200 m depth at the mid-day and estimated the critical intensity for their vertical movement.

STRAIGHT HOMING OF KOKANEE SALMON BY VISUAL CUE FROM OPEN WATER TO NATAL AREA

H.Ueda[1], M.Kaeriyama[2], A.Urano[3], K.Yamauchi[1] and K.Kurihara[4]. [1]Fac.of Fish., [3]Grad.School of Sci., [4]Fac.of Pharm.Sci., Hokkaido Univ., [2]Hokkaido Salmon Hatchery, Hokkaido.

Mechanisms of an amazing ability of salmon to migrate a long distance from open water to natal streams for spawning are still unknown. Kokanee salmon (*Oncorhynchus nerka*) in Lake Toya offers an excellent model system for studying the orientation mechanism in open water, because matured fish return to the natal area with a high accuracy. We telemetrically tracked matured male kokanee salmon in Lake Toya, and found that the fish released at a long distance from the natal area retured directly to the vicinity of the natal area. Interference of the magnetic cue by the attachment of NdFe magnet ring on the lateral head did not affect their direct return. Blockage of the visual cue by the injection of a mixture of carbon toner and corn oil into eyeball to cause detached retinas made them move randomly. But a blinded fish happened to find the natal area probably using his olfactory cue. These findings suggest that the fish return directly to the vicinity of the natal area mainly using their visual cue.

ACQUIREMENT OF TRICHROMAT IN PRIMATES

Y. Yashiro[1], O. Hisatomi[2], H. Tokunaga[3], T. Oishi[1]. [1]Dept. of Biology, Fac. of Sci., Nara Women's Univ. Nara, Depts. of [2]Biology and [3]Earth and Space Sci., Fac. of Sci., Osaka Univ. Toyonaka.

Most mammals except some primates, studied so far, are dichromats. Most prosimians and New World monkey are also dichromats, whereas Old World monkeys (including humans) are trichromats. It is thought that the LW (long wave length sensitive) and MW (middle wavelength sensitive) pigments were separated by a gene duplication after the separation between New and Old World monkeys about 36 million years ago. However a male spider monkey (a New World monkey) was classified as a trichromate by a psychological study, so the duplication may have occurred earlier than the separation. We examined the partial sequence of the MW or LW pigment genes and investigated the phylogenetic relationships of the opsin genes of some prosimians (Lemur, Galago), New World monkeys (Ateles, Aotus) and other mammals (Tupaia). We prepared genomic DNA from the blood of 5 male animals, and amplify the region of exon 5 by using polymerase chain reaction. It is suggested that the polymorphic LW and MW pigment genes of New World monkeys separated into MW pigment gene group, and that the duplication of these genes has occurred earlier than the divergence of the Old world monkeys from New World one.

QUANTITATIVE IMMUNOCYTOCHEMICAL STUDIES ON THE RETINAL PHOTORECEPTOR CELLS OF DIURNAL LIZARDS.

Y. Taniguchi[1], and M. Yoshida[2]. [1]Dept. Biol. Oita Univ., Oita and [2]Oita Univ., Oita.

Retinal photoreceptors of diurnal lizards, *Japalura polygonata polygonata*, were studied immunocytochemically using the anti-gecko opsin mAb G6 (Yoshida and Mifune, 1992) and the anti-rhodopsin mAb Rh29 (Tokunaga et al., 1989). The number of photoreceptors labelled with immunocytochemical SAB reaction was counted to evaluate the range of wavelength suitable for cone-type vision in diurnal lizards. Outer segments of double cones were recognized with mAb G6. Nearly 70 % of single cones with yellow oil droplets were bound to mAb G6, whereas the rest of them were labelled with Rh29. Unlike the feature of other diurnal lizards, single cones with clear oil droplets were labelled with Rh29. The single cones with blue oil droplets did not react to both mAbs. Three-dimensional submicroscopic architecture of retinal photoreceptors exposed after removal of cytosol from the cracking plane of frozen specimens was presented.

LOCALIZATION OF PHOTORECEPTOR PROTEINS IN RETINAL AND EXTRA-RETINAL PHOTORECEPTORS OF JAPANESE GRASS LIZARDS. *Takydromus tchydromoides*

T. Yoshikawa[1], T. Oishi[1], K. Kokame[2] and Y. Fukada[2] [1]Dept. of Biol, Fac. of Sci, Nara Women's Univ. and [2]Dept. of Pure and Appl. Sci., College of Arts and Sci., Univ.of Tokyo

Birds and lower vertebrates are known to have extra-retinal photoreceptors, such as pineal complex and deep brain. Although the photoreceptive function of the pineal has been investigated well, the exact location and the nature of the deep brain photoreceptor are not known. We have previously reported the exact location of deep brain photoreceptors in bullfrogs immunohistochemically (Yoshikawa et al. 1993). In this study, we try to localize visual pigments and signal transduction proteins immunohistochemically in the Japanese grass lizard. Three antisera are used, anti-bovine rhodopsin (Rh-As), anti-rod and cone transducin α-subunit (anti-pTrα and anti-pTcα, respectively). The frontal organ of frogs and parietal eye of lizards have similar location in the head, and both are a part of the pineal complex. The parietal eyes are immunonegative to Rh-As, while the frontal organs are immunopositive to Rh-As. Some cells in the hypothalamus are immunopositive to Rh-As. Many cells near the third ventricle in the hypothalamus were stained by anti-pTcα. These cells stand in a line along the third ventricular surface and have immunoreactive nerve processes. Anti-pTrα stained the fibrous structures in the third ventricle. In the pineal, there are no immunoreactivities to any of the three antisera. These results indicate that each extra-retinal photorecceptor has different photopigments and transduction proteins.

MORPHOGENETIC CHANGES OF THE OUTER SEGMENTS OF RODS AND CONES IN *Xenopus* RETINA DURING DEVELOPMENT: IMMUNOGOLD LABELING - SEM.

H. Takahama, Ins. of Biol., Fac. of Edu., Oita Univ., Oita

In larval retinas of amphibians, all photoreceptors possess a poined outer segment while rods with a long cylindrical outer segment (ROS) is distinguished from cones with a short conical outer segment (COS) in adult retinas. In the present study, morphogeneic changes of the rod outer segment and cone outer segment were examined by scanning electron microscopy immunogold-labeling with a rhodopsin-specific antibody during early photoreceptor development of *Xenopus* retina. At stage 31/32, a photoreceptor cell possessed a short cilium. At stage 33/34, the cilia of the photoreceptor cells were dilated and swelled at the apical region, and a part of them were labeled by gold particles. At stage 37/38, the morphogenesis of the ROS and COS was more developed as compared to the previous stage. Many calycal processes contacted radially around the COS, whereas there were a few calycal processes around ROS. The ROSs varied in morphology, and a part of them was revealed a transitional form from conical shape to cylindrical shape. At stage 41/42, many ROSs contacted many calycal processes and are cylindrical. These results show that the ROS and COS appear simultaneously but an accomplishment in shape to the adult-type is earlier in COS than in the ROS. Appearance of the calycal processes may be related to the morphogenesis of the outer segments of the photoreceptor cells.

Ca^{2+}-BINDING PROTEINS IN FROG RETINA

O. Hisatomi[1], T. Ishino[2], S. Matsuda[1], S. Kawamura[3], and F. Tokunaga[4].
[1]Dept. of Biol., and [4]Dept. of Earth and Space Sci., Fac. of Sci., [2]Dept. of Pharmacol., Fac. of Pharmacol., Osaka Univ., Osaka. [3]Dept. of Physiol., Keio Univ. Sch. of Med., Tokyo.

S-modulin is a Ca^{2+}-binding protein, and acts as a sensitivity modulator in the light adaptation process of frog rods. We cloned cDNAs encoding S-modulin and s26 which was a S-modulin-like Ca^{2+}-binding protein existed in frog retina. We tried to express these Ca^{2+}-binding proteins in *E-coli*, and to investigate the molecular mechanism of light-dark adaptation.

First, the S-modulin cDNA was inserted into an expression vector (pKK233-2) and introduced into *E-coli*, MV1184. S-modulin was expressed with the amount more than 1% of the total protein. Like S-modulin isolated from frog retinas, the expressed S-modulin inhibits rhodopsin phosphorylation in a Ca^{2+}-dependent manner.

Next we used a pET vector which could express the inserted genes under the control of the T7 promoter. The constructs were introduced into *E-coli* (B21 cells), and these Ca^{2+}-binding proteins were expressed and purified. Judging from CBB staining patterns of SDS polyacrylamide gel electrophoresis, S-modulin and s26 were expressed with the amount more than 50% of the total protein.

VISUAL PIGMENTS OF FROG

S.Kayada[1], O.Hisatomi[1], and F.Tokunaga[2]
[1]Dept. of Biol., [2]Dept. of Earth and Space Sci., Fac. of Sci., Osaka Univ., Osaka

Vision of frog is well studied biochemically and electrophysiologically. Frog has two types of rod (red and green) and two arrangements of cone (single and double). There are rhodopsin and a visual pigment which has wavelength maximum at 432 nm in the red and the green rod, respectively. In addition to these pigments, frog has at least two kinds of cone pigments.

We carried out polymerase chain reaction (PCR) using frog (*Rana catesbeiana*) retinal cDNA as a template. A cDNA fragment which has more than 60% identities with vertebrate violet-sensitive pigments was cloned in addition to two kinds of cDNA fragments which have more than 75% identities with vertebrate rhodopsins and red-sensitive pigments, respectively*1. The complete coding region of the gene was then obtained by the separate amplification of both cDNA ends. Deduced amino acid sequence showed more than 60% identities to those of vertebrate violet-sensitive pigments. It was suggested that the cloned cDNA encodes the visual pigment which is expressed in green rod of frog.

*1: S.Kayada, O.Hisatomi, and F.Tokunaga, Zool. Sci. (1993) 10 suppl., p118

MOLECULAR EVOLUTION OF LIGHT-DARK ADAPTATION SYSTEM IN PHOTORECEPTOR CELLS

S. Matsuda[1], O. Hisatomi[1], and F. Tokunaga[2]
[1]Dept. of Biol., and [2]Dept. of Earth and Space Sci., Fac. of Sci., Osaka Univ., Osaka

S-modulin and rhodopsin kinase act as sensitivity modulators regulating rhodopsin phosphorylation in a Ca^{2+}-dependent manner. We suggested that there are at least two groups among S-modulin like proteins in retina (Matsuda *et al.*, (1993) Zool. Sci. Suppl. 10. 118.). It seems that there are also several kinds of visual pigment-kinases in retina.

We made oligonucleotide primers corresponding to amino acid sequences highly conserved among G-protein-coupled receptor kinases, and carried out the amplification using retinal cDNAs of frog, goldfish, danion, and newt as templates. We isolated seven kinds of cDNA fragments encoding putative receptor kinase-like proteins, and made phylogenetic tree from the deduced amino acid sequences. The tree suggests that there are at least three groups in G-protein coupled receptor kinase-like proteins in retina. Two of them are very similar to GPRK6 and rhodopsin kinase, respectively, and the other may encode novel G-protein coupled receptor kinases.

PHOTOREACTION OF RETRO-γ-RETINOCHROME

N.Kajimura[1],K.Ozaki[1],F.Tokunaga[2],Y.Katsuta[3]and M.Ito[3]
[1]Dept.Biol.and [2]Dept.Space and Earth Sci.,Osaka Univ.,Toyonaka.[3]Kobe Pharm.Univ.,Kobe.

Retinochrome is a photosensitive protein in the visual cell of mollusca. This protein has an all-*trans*-retinal as the chromophore. Retinochrome is converted by light into meta-retinochrome which contains 11-*cis* retinal as the chromophore.

In the present report, in order to clarify whether or not the whole conjugated double bond system of retinal is essential for the *cis-trans* isomerization process, we synthesized an artifitial pigment of retinochrome with the retinal analog retro-γ-retinal which has two dissected chromophoric system. The absorbtion spectrum of pigment formed with retro-γ-retinal showed its absorbsion maximum at 415nm and the "opsin shift" of the analog pigment was smaller than that of retinochrome. This pigment was converted into meta-form by yellow light (>430nm). In the dark,meta-retinochrome thermally converted into retinochrome,but bleached meta-retro-γ-retinochrome did not. HPLC analysis showed that meta-retro-γ-retinochrome had pigment 11-*cis* retinal as the chromophore. This indicates that photoisomerization of the chromophore in retinochrome does not require the whole conjugated double bond system.

STUDY ON SIGNAL COUPLING PROTEINS OF ASCIDIAN LARVA, *Halocynthia roretzi*.

T.Iwasa, T.Azuma, T.Yanai and M.Tsuda. Dept. of Life Science, Fac. of Sci., Himeji Institute of Technology, Harima Science Garden City, Hyogo

We have investigated the phototransduction mechanism in octopus photoreceptors. The proteins involved in octopus phototransduction system are different from that of vertebrate; final photoprocess are different between vertebrate and invertebrate visual pigment, and transducin, vertebrate photoreceptor G-protein, is not expressed in invertebrate photoreceptor. Instead Gi/Go and Gq class are major G-protein coupled with light-activated rhodopsin. Ascidian larva is speculated to be an ancestral form of the vertebrate and represents negative phototaxis. Therefore it is interesting to elucidate what kind of signal coupling proteins are involved in the phototransduction system of ascidian. We tried to amplify the signal coupling protein cDNA by polymerase chain reaction with primers for rhodopsins, G-protein alpha-, and beta-subunit using cDNA library of ascidian larva. In the case of rhodopsin, the primer for invertebrate rhodopsin gave about 200 bp band and the primer for vertebrate rhodopsin gave the 500 bp band. The primers for G-protein alpha-subunits, constructed according to the amino acid sequence of three conserved domains, gave 200, 500 and 700 bp fragments, respectively. We also obtained about 90 bp fragment with primers for G-protein beta-subunit. The nucleotide sequence of them are now under investigation.

KILLIFISH VISUAL PIGMENTS EXPRESSED IN THE RETINA

T.SATOH[1],O.HISATOMI[1],F.TOKUNAGA[2]
[1]Dept. of Biol., [2]Dept. of Earth and Space Sci, Fac. Sci. Osaka Univ., Osaka

The killifish (*Orizias Laptis*) retina possesses a typical square-mozaic-like arrangement of cone photoreceptors, and continues to expand outward with cell proliferation after hatching. We are interested in the mechanism of this phenomenon, but we had no means to detect cone photoreceptor differentiation, except for the morphology. We tried to distinguish cone photoreceptors each other, using moleculer biological techniques.

We isolated four opsin cDNA clones from a killfish retina cDNA library, and sequenced. All of them contains the entire coding region of putative visual pigments. On the basis of homology to previously characterized visual pigments, the cloned cDNAs were classified into red-, blue-, and violet-sensitive cone pigment groups, and rhodopsin group respectively. Each of the killifish visual pigments shows striking similarity to that of other fishes like the goldfish.

We also studied about expression of these visual pigments in the retina by *in situ* hybridization, and showed the relationships between visual pigments and photoreceptor morphology.

INTERACTION BETWEEN SQUID RHODOPSIN AND CYTOSKELETAL ELEMENTS.

A.Kishigami, K.Sakata-Sogawa, Y.Tsukahara and H.Tashiro.
Photodynamics Res. Cent., The Institute of Physical and Chemical Research (RIKEN)., Sendai.

The photsensitive apparatus of squid visual cells is contained in the microvilli. Cytoskeletal structures in the microvilli are known from freeze-fracture electron microscopy to be disorganized following irradiation. The filamental structure at the center of each microvillus appears to be an actin filament, so we are studying the relationship between rhodopsin and actin and actin-binding proteins in the visual cell of the squid (Todarodes pacificus). A preparation of microvilli was made by sucrose flotation and solubilization in sucrose monolaurate detergent. When the actin contained in the solution was polymerized by phalloidin, the filamentary actin could be precipitated by ultracentrifugation. At this time, rhodopsin was also precipitated in proportion to a rise in the quantity of the sedimentary actin. Following irradiation and incubation in a buffer containing 1mM ATP and 100mM sodium chloride, there was increased sedimentation of a 42Kd-protein. These results are further evidence supporting the presence of an interaction between rhodopsin and actin.

EXPRESSION OF *DROSOPHILA* OPSIN IN CULTURED INSECT CELLS

K.Katanosaka[1], K.Ozaki[1], F.Tokunaga[1] and K.Arikawa.[2]
[1]Fac.of Sci., Osaka Univ., Toyonaka. [2]Dept. of Biol., Yokohama City Univ., Yokohama.

In the visual cell of *Drosophila melanogaster*, a visual pigment, rhodopsin, localizes at rhabdomal plasma membrane. Before reaching rhabdomere in its mature form, rhodopsin is subjected to some posttranslational modifications, i.e., chromophore binding, transient glycosylation and unknown modification causing a decrease in molecular weight of about 1K.

Using a gene expression system of a recombinant baculovirus and an insect cell line (Sf9), we synthesized the *Drosophila* opsin (apoprotein of rhodopsin). The transfer vector pVL1392 containing opsin cDNA was co-transfected with linear wild type virus into cultured cells, so as to transplant the cDNA to the viral polyhedrin gene locus by homologous recombination. The recombinant viruses were infected into cultured cells. Immunoblotting analysis showed that opsin peptide was expressed from 2days post-infection and mainly found in the membrane fraction of the cell. However, it was not subjected to either glycosylation or the unknown 1kDa-modification. According to the immunoelectronmicroscopy, opsin was located in the cytoplasm but little in the plasma membrane. Thus, the *Drosophila* opsin synthesized in this cell is likely to remain in cytoplasmic membranes without posttranslational modifications.

A METABOLIC PATHWAY TO FORM (3S)-3-HYDROXYRETINAL IN THE COMPOUND EYE OF DROSOPHILA MELANOGASTER.

T. Seki[1] and K. Isono[2].
[1]Dept. of Health Sci., Osaka Kyoiku Univ., Osaka
[2]Graduate School of Information Sci., Tohoku Univ., Sendai.

In Insecta, retinal (RAL_1) and two enantiomers of 3-hydroxyretinal (RAL_3), (3R)- and (3S)-RAL_3, are used as visual pigment chromophores. In the insect groups using RAL_3, (3S)-RAL_3 is found only in the group Cyclorrhapha of Diptera, and other insect groups so far examined use only (3R)-RAL_3. (3R)-RAL_3 is expected to be produced directly from 3-hydroxy-xanthophills such as zeaxanthin [(3R,3'R)-β,β-carotene-3,3'-diol] and lutein A [(3R,3'R,6'R)-β,ε-carotene-3,3'-diol] synthesized by plants. However, the metabolic pathway to form (3S)-RAL_3 by the species in the group Cyclorrhapha is yet to be clarified.

To investigate the metabolic pathway, adults D. melanogaster grown on carotenoid-free medium were supplied with all-trans RAL_1 or β-carotene, and the chirality of RAL_3 isomers was analyzed by using chiral column HPLC. The ratio of (3R)-enantiomer to sum of the two enantiomers was < 0.1 for both all-trans and 11-cis RAL_3 isomers extracted from flies supplied with β-carotene, and the ratio was 0 for both isomers extracted from flies supplied with all-trans RAL_1. These results suggest that the D. melanogaster has product specificity, on hydroxylation of carbon 3 in the β-end group, to produce (3S)-enantiomer.

THE EXPRESSION OF *DROSOPHILA* RAB PROTEINS IN THE CAROTENOID-DEPRIVED FLY.

A. Kohno[1], K. Ozaki[1] and F. Tokunaga[2]. [1]Dept. Biol. and [2]Dept. Space and Earth Sci., Fac. Sci., Osaka Univ., Toyonaka.

Rab protein family is a group of the small molecullar G-proteins (SMGs), and plays important roles in the vesicle transport. We reported last year that 23kDa SMG was a major component of retinal SMGs, and increased by carotenoid-deprivation.

In the present study, we cloned the retinal cDNA fragments of 13 different rab or its relative proteins : 9 homologues of mammalian rabs (DRAB1,2,3,4,7,8, 10,11,14) and 4 novel members of rab (DRAB related protein (DRABR)1,2,3,4). By the use of these cDNA fragments as probes, we carried out screening of the *Drosophila* head cDNA library, and determined the complete sequence of DRAB1,2 and DRABR4. DRAB1 and DRAB2 consist of 205 and 214 amino acid residues, respectively, having 84 and 90% identities with mammalian rab1 and rab2. DRABR4 encodes a protein containing 197 amino acids.

By northern hybridization, we quantitatively measured the expression of each DRAB and DRABR mRNA in the carotenoid-deprived flies, and compared it with that in the normal flies. In the retina, the amount of DRABR4 mRNA increased when flies were raised in the carotenoid-deprived medium. In contrast, the expression of DRAB3 and 14 was suppressed in the same condition. No remarkable changes in mRNA expression were observed in DRAB1,2,10 and DRABR2. The similar effects of carotenoid-deprivation were also observed in the brain, while any detectable changes were not seen in other parts of the fly.

LIGHT-ACTIVATED PHOSPHOLIPASE C IN SQUID RHABDOMAL MEMBRANES

T.Suzuki[1], K.Nagai[1], K.Narita[2], K.Yoshihara[3] and Y.Kito[2]. [1]Dept. of Pharmacol., Hyogo Coll. of Med., Nishinomiya, [2]Dept. of Biol., Osaka Univ., Toyanaka, [3]Suntory Inst. for Bioorg. Res., Mishima.

The phototransduction mechanism in invertebrate photoreceptors is still obscure. The major G-protein in cephalopod photoreceptors is Gq-class which is thought to activate phosphatidylinositol-specific phospholipase C (PI-PLC). We studied the activation of PI-PLC by light and tried to purify the enzyme.

Rhabdomal membranes of squid photoreceptors were isolated under low ionic strength, and PI-PLC activities were determined using [^{3}H]-PIP2 as substrate. The PI-PLC was activated about three fold by light in the presence of GTP but only slightly in the absence of GTP. GDP, ATP and ADP had no effect. The activation by light was observed when the irradiated membrane was incubated at 10°C in dark and then mixed with GTP. The PI-PLC was found in soluble fraction after treatment with 500mM KCl and partially purified with a heparin-agarose column. A 130 kD protein was recognized by anti-PLCβ4/norpA antibody, which was co-purified with PI-PLC activity.

These results suggest that stable metarhodopsin activates PLCβ4 /norpA-like enzyme via Gq.

INHIBITION OF RHODOPSIN SYNTHESIS AND VESICLE TRANSPORT IN THE *DROSOPHILA* PHOTORECEPTOR CELLS.

K. Ozaki[1], K. Arikawa[2], K. Katanosaka[1], A. Kohno[1] and F. Tokunaga[3]. [1]Dept. Biol. and [3]Dept. Space and Earth Sci., Fac. Sci., Osaka Univ., Toyonaka and [2]Dept. Biol., Yokohama City Univ., Yokohama.

In the *Drosophila* photoreceptor cells, maturation of major rhodopsin (NINAE) is inhibited by the irradiation with blue light. This irradiation also causes the remarkable changes in the ultrastructure of photoreceptor cells : the large invadination of rhabdomal membranes into cytoplasm and the accumulation of rough endoplasmic reticulum (rER) just beneath the rhabdomal microvilli. Although the invadination of rhabdomal membrane occured within several minutes after blue-irradiation, the accumulation of rER was first found when flies were kept in the dark for 7 h after the irradiation. *norpA* is a mutant in the gene encoding a phospholipase C, which functions in the phototransduction cascade in the cells. We had reported that rhodopsin maturation is not inhibited by blue-irradiation in this mutant. We thus carried out the electronmicroscopic observations of the retinas of *norpA* flies. The results showed that the accumulation of rER was not found in *norpA* mutant, while the invadination of microvillar membrane occured. Based on above results, we assumed that activation of phototransduction cascade induced by blue-irradiation blocks the vesicle transport in the photoreceptor cells, which subsequently causes the abnormal accumulation of rER. Since the vesicle transport is essential for correct processing of protein, the inhibition of rhodopsin maturation would be associated with the blockage of vesicle transport caused by blue-irradiation.

LIGHT-MODULATED LOCALIZATION OF ALPHA-SUBUNIT OF GTP-BINDING PROTEIN Gq IN THE CRAYFISH PHOTORECEPTOR.

A.Terakita[1], H. Takahama[1], S. Tamotsu[2], T.Hariyama[3] and Y.Tsukahara[3]. [1]Inst. of Biol., Fac. of Educ., Oita Univ., Oita, [2]Dept. of Physiol., Hamamatsu Univ. School of Med., Hamamatsu, and [3]Graduate School of Inform. Sci., Tohoku Univ., Sendai.

Subcellular localization of Gq (CGqα) in the crayfish photoreceptor was investigated to know the details of interaction between CGqα and activated rhodopsin (Rh*) in relation to phototransduction.

Dark-adapted crayfish were kept in the light for 4 hr and then in the dark for 4 hr. The retinas from them were analyzed immunocytochemically (1) and biochemically (2) by using an anti-CGqα antibody. (1)The slices of those retinas were stained with the antibody. In the darkness, CGqα was found abundantly in the rhabdom. In the light, however, it was distributed in the cytoplasm of all over the photoreceptor cell as well as the rhabdom. In the case of dark-adaptation following the light-adaptation, CGqα was localized in the rhabdom again. (2)The membrane and soluble fractions were obtained from the retinas and analyzed with immunoblotting. CGqα was abundantly detected in the membrane fraction in the dark. In the light, CGqα was found in the soluble fraction as well as membrane fraction.

These results suggest that light modulates the subcellular localization of CGqα and controls the amount of CGqα which can interact with Rh* in the rhabdomeric membranes.

RHODOPSIN AND G-PROTEIN IN THE DOUBLE-LAYERED RETINA OF THE SCALLOP, *CHLAMYS* (*MIACHLAMYS*) *NOBILIS*: AN IMMUNOHISTOCHEMICAL STUDY.

H. Ohtsuki, N. Ono and A. Terakita. Inst. of Biol., Fac. of Educ., Oita Univ., Oita.

An eye of some scallops has a double-layered retina, distal and proximal retinae, which respectively contain ciliary-type (Ci) and microvili-bearing (Mv) photoreceptors. It has been reported that light induces hyperpolarizing responce in Ci photoreceptor and depolarizing one in Mv photoreceptor. We investigated immunohistochemical reactions of anti-rhodopsin and anti-G-protein antibodies to the retina slices of the scallop, *Chlamys* (*Miachlamys*) *nobilis*, in order to know differences of phototransduction cascades in each photoreceptor.

Polyclonal antibody against Gβ (specific to the C-terminus of common β) heavily stained outer segments of both types of photoreceptors. Polyclonal antibodies against squid rhodopsin and against crayfish Gqα, however, specifically reacted with outer segments of the Mv photoreceptors in the proximal retina.

Our findings suggested that Ci photoreceptor contained different structural rhodopsin(s) and α subunit(s) of G-proteins from those in Mv photoreceptors.

COLOR INFORMATION PROCESSING IN ONCHIDIUM EXTRA-OCULAR PHOTORECEPTOR CELLS.

T. Gotow and T. Nishi. Dept. of Physiol., Sch. of Med., Kagoshima Univ., Kagoshima.

Both two extra-ocular photoreceptor cells, A-P-1 and Es-1, in the Onchidium ganglion respond to light with a depolarization. However, the spectral sensitivity peaks at 490 nm (blue-green) in A-P-1 and at 580 nm (yellow) in Es-1. Furthermore, Es-1 receives an inhibitory input from A-P-1. This inhibitory input causes Es-1 to produce photoresponses of opposite polarity in response to light of different colors, indicating that this color-opponent response of Es-1 function as color discrimination. To test the possibility that such A-P-1 and Es-1 could discriminate between differences in the color of natural incident light, we measured the amount of 490 and 580 nm light transmitted by the animal's body wall and compared it with the amount required for the photoresponse. The transmittance of 490 and 580 nm light was 1-0.1 % through the dorsal side and 10-30 % through the ventral side. However, 580 nm light transmitted 3-5 times more than 490 nm light through both the body wall. On the other hand, the threshold response of Es-1 required light intensity 10-100 times higher than that of A-P-1.

These results suggest that the body wall of Onchidium transmits enough 490 or 580 nm light to depo- or hyperpolaeize Es-1, under ambient conditions.

Localization of spectral receptors in the proximal half of the ommatidium of a butterfly *Papilio xuthus*.

Kentaro Arikawa, Hiroyuki Uchiyama, and Eisuke Eguchi.
Department of Biology, Yokohama City University, Yokohama 236.

The compound eye of a butterfly, *Papilio xuthus*, contains five types of spectral receptors: peak at uv, violet, blue, green, and red. We previously studied the localization of the receptors in the distal half of the tiered ommatidium by recording spectral and polarization sensitivies (SS and PS) from single photoreceptors. Here we applied the same method for the proximal and basal regions.

We recorded the SS and PS from over 100 photoreceptors in proximal tier of the ommatidia in the lateral-looking eye region. All recorded cells were either red or green receptors. Distribution of the peak angle of PS indicated that there were three groups of cells: PS peaks at ca. 35° (R6 or R8), 145° (R5 or R7), and 180°=0° (R9), respectively. About 80% of R5-8 and 50% of R9 were red type, whereas the rest were green type: the proximal tier of the ommatidium is dominated by red receptors.

In flies the long visual fibers serve inputs to the visual pathway for color vision. The long visual fibers are R1, 2, and 9 in *Papilio*. Our results indicate that R1 and 2 are either uv, violet, or blue and R9 are green and red. Thus, all the five spectral receptors are most likely involved in the butterfly color vision.

EFFECT OF pH ON THE PHOTOBLEACHING PROCESS OF CHICKEN GREEN.

H. Imai,[1] Y. Imamoto,[2] and Y. Shichida[1].
[1]Dept. of Biophys., Fac. of Sci., Kyoto Univ., Kyoto, [2]Dept. of Earth and Space Sci., Fac. of Sci., Osaka Univ., Toyonaka.

In spite of the similarty in amino acid sequence and absorption spectrum to rod visual pigment rhodopsin, chicken green, a green-sensitive cone visual pigment present in chicken retinas, displays molecular properties required for a cone visual pigment that are clearly different from rhodopsin. Here, we have investigated why chicken green displays faster formation and faster decay of physiologically active intermediate, meta II-intermediate than rhodopsin. The most prominent difference between chicken green and rhodopsin is the isoelectric points (pI) calculated from their deduced amino acid sequences. Namely, chicken green as well as the other cone pigments are basic, while rhodopsins are acidic. Therefore, we have changed the pH of chicken green sample to make the net charge of chicken green to be similar to that of rhodopsin and investigated its effect on the thermal behavior of meta II-intermediate. The results showed that formation and decay of meta II-intermediate were greatly suppressed in alkaline condition, suggesting that thermal behavior of meta II-intermediate is regulated by the charged properties of the protein moiety.

THE LOCATION OF THE PHOTOPERIODIC RECEPTORS IN *RIPTORTUS CLAVATUS*

A. Morita and H. Numata. Dept. of Biol., Fac. of Sci., Osaka City Univ., Osaka.

The bean bug, *Riptortus clavatus* (Insecta, Heteroptera) has a long-day photoperiodic response. In this study, we examined the effect of complete or partial removal of the compound eyes or complete removal of the ocelli on the photoperiodic response.

1) The adults with the compound eyes completely removed lost the photoperiodic sensitivity; they became reproductive irrespective of the photoperiod. In contrast, the adults with the ocelli removed maintained the sensitivity.

2) After removal of 50% ommatidia of one compound eye and the whole contralateral one, the adults lost the photoperiodic sensitivity, whether the anterior, posterior, dorsal, or ventral region was removed.

3) When the central region of one compound eye and the whole contralateral one were removed, the adults lost the photoperiodic sensitivity, even though more than 50% ommatidia remained. However, the adults with the peripheral region removed maintained the sensitivity, even though they had less than 50% ommatidia.

Thus, the central region of the compound eye plays a major role as the photoperiodic receptors.

EXPRESSION OF MUTANT OF GECKO VISUAL PIGMENT

T. Oura[1], D. Kojima[1], Y. Shichida[1], O. Hisatomi[2], F. Tokunaga[2], T. Okano[3], Y. Fukada[3], T. Yoshizawa[4]. [1]Fac. Sci., Kyoto Univ., [2]Fac. Sci., Osaka Univ., [3]College Arts & Sci., Univ. Tokyo, [5]Fac. Engineering, Osaka Sangyo Univ.

In the retinas of Tokay Gecko (*Gekko gekko*), there are two types of visual pigments, P521 and P467, the latter of which has an amino acid sequence quite similar to rod visual pigments rhodopsins. However, absorption spectrum and photobleaching process of P467 are quite different from those of rhodopsin. To examine which part of the protein moiety in P467 is the origin of these differences, we constructed two chimeric mutants termed P467(3/4)Rh and P467(4/5)Rh, which contain N-terminus to helix III of P467 and helix IV to C-terminus of rhodopsin, and N-terminus to helix IV of P467 and helix V to C-terminus of rhodopsin, respectively, and made them expressed in 293S cells. The absorption maxima of P467(3/4)Rh and P467(4/5) Rh are 473 nm and 478 nm, respectively, suggesting that helix IV as well as the other helixes region might contribute the spectral tuning of P467. The thermal stability of meta II-intermediates increased as the mutant contains more sequence of rhodopsin. Since overall homology in amino acid sequence between P467 and rhodopsin is quite high, these results enable us to speculate distinctive amino acid resides which determine the properties of P467.

LOCALIZATION OF HETEROGENEOUSLY FATTY-ACYLATED TRANSDUCIN α-SUBUNIT IN BOVINE RETINA.

K. Kokame[1], O. Shono[1], M. Watanabe[1], Y. Fukada[1], M. Araki[2], T. Takao[3], Y. Shimonishi[3] & T. Yoshizawa[4]. [1]Dept. Pure and Appl. Sci., College of Arts and Sci., Univ. Tokyo, Tokyo, [2]Dept. Biol., Kyoto Pref. Med. College, Kyoto, [3]Inst. Protein Res., Osaka Univ., Osaka, [4]Fac. Engineering, Osaka Sangyo Univ., Osaka.

Photoreceptor G protein, transducin (Tα/Tβγ), plays a central role in visual transduction of vertebrate rod cells. Recently, we have found that the N-terminus of bovine rod Tα is modified with four distinct fatty acids: C12:0, C14:0, C14:1 (5-*cis*) and C14:2 (5-*cis*, 8-*cis*). We also showed that the coupling efficiency between Tα and Tβγ is altered by the heterogeneous fatty acids [Nature, **359**, 749-752 (1992)]. However, the localization of the four isoforms of Tα has not been investigated yet. In the present study, we prepared monoclonal antibodies recognizing the N-terminal fatty acyl chains of Tα by immunizing mice with synthetic fatty-acylated peptides corresponding to the N-terminal region of Tα. In immunohistochemical analyses of bovine retinal sections, almost all of the rod outer segments were stained by the antibody which recognizes only C12:0-Tα, indicating the presence of C12:0-Tα in all rod cells. This observation strongly suggests that the photon-signal captured by one rod cell is transduced by the four isoforms of Tα modified with heterogeneous fatty acids.

INTERACTION AMONG FOUR LARGE STEMMATA FOR SWITCHING OF VISUAL BEHAVIORS IN THE TIGER BEETLE (CICINDELA CHINENSIS) LARVA.

A. Mizutani and Y. Toh. Dept. of Biol., Fac. of Sci., Kyushu Univ., Fukuoka.

The tiger beetle larva shows the predatory or escape response to a target moving above the head. These two behaviors switch to each other depending upon size and distance of moving targets. The switching has been considered to be caused by the interaction among two pairs of large stemmata, because the four stemmata co-operate to see a whole celestial hemisphere. In the present study, such co-operation has been behaviorally examined by partial occlusion of the four large stemmata.

Occlusion of three of the four stemmata resulted in decrease in probability of the escape response, but it scarcely affected the predatory response. Moreover, such larvae with a single intact stemma often showed the predatory response even to the visual stimuli that always triggered the escape response in the intact larva. These results suggest that more than two stemmata must co-operate to cause the escape response.

MECHANOSENSORY CELLS LABELED WITH CARBOCYANINE DYE IN THE LINGUAL EPITHELIUM OF THE AXOLOTL.

T. Nagai [1] and H. Koyama[2] [1] Dept. Physiol., Teikyo Univ. Sch. Med., Tokyo and [2] Dept. Anat., Sch. Med., Yokohama City Univ., Yokohama

The glossopharyngeal (IX) nerve of the salamanders responds to chemical and mechanical stimuli applied to the lingual epithelium. Chemical stimuli are transduced by taste receptor cells in the taste bud, whereas transduction elements for mechanical stimuli remain unclear. Fluorescent carbocyanine dye (dil), applied to the IX nerve of axololts (*Ambystoma mexicanum*), transneuronally labeled not only cells in the taste buds but also solitary cells in the non-taste lingual epithelium. With diaminobenzidine (DAB), the dil was photoconverted to a dark, electron-dense product for subsequent electron microscopic observations. The solitary cells labeled with the dil had a large nucleus with invaginations, dense-cored vesicles in the cytoplasm, and finger-like processes. These are reminiscent of morphological features of cutaneous Merkel cells, which is thought to be a tactile receptor in mammals. The results suggest that solitary cells innervated by the IX nerve are associated with mechanosensory function of the IX nerve system.

CYTOSKELETONS OF INSECT MECHANORECEPTORS.

Y. Toh and A. Mizutani. Dept of Biol., Fac. of Sci,, Kyushu Univ., Fukuoka.

There are three types of mechanoreceptors in insects: campaniform sensilla, chordotonal sensilla and stretch receptors. They are characterized by specific arrangement of cytoskeletons. Receptor cells of these three mechanoreceptors have been observed by electron microscopy of rapid frozen methods. Campaniform sensilla and chordotonal sensilla of the cockroach antenna, campaniform sensilla and chordotonal sensilla of the Drosophila halter, and wing stretch receptors of the locust were examined in the present study. A sensory cilium of the campaniform sensillum contained closely packed microtubules and other unidentified filaments in the distal region. A sensory cilium of the chordotonal sensillum appeared as a slender flagellar form, and it contained an axoneme of 9+0 pattern throughout its length. A stretch receptor of the locust wing was a large non-ciliated cell, which possessed many slender dendritic processes. The dendrites, which projected deep in the surrounding connective tissues, possessed many actin-like filaments. Cytoskeletons of these mechanoreceptive cells are thought to contribute to stiffness and elasticity of the receptor region and to the primary process of the mechanoreception.

Fine structure of the extraocular dermal photoreceptor cell of juvenile *Onchidium* (Marine gastropod).

N. Katagiri[1], Y. Katagiri[2], Y. Shimatani[2], Y. Hashimoto[2] and E. Aikawa[3] ([1] Med. Res. Inst., [2]Dept. of Physiol., [3]Dept. of Anat. & Develop. Biol., Tokyo Women's Med. Coll., Tokyo)

Two weeks after hatching, the stalk as well as dorsal eyes can be discernible as dark spots, whereas the extraocular dermal photoreceptor cell (DPC) is only detected with light microscope. In contrast to clustering of adult's, juvenile DPCs are singly located in the subepidermal connective tissue, near the dorsal eye and giant gland cells, and along the thick nerve bundles. DPC is oval in shape and smaller than a half of adult's DPCs in size. A large nucleus is located in the proximal cytoplasm and its envelope is smooth in contour, meanwhile an elaborately maze-like incision characterizes the adult DPC nucleus. Distal one third of the cell is occupied by massive microvilli. Supranuclear cytoplasm contains Golgi apparatus, mitochondria and a few lysosomal dense bodies. It is notable that the photic vesicles are distributed in peri- and infranuclear cytoplasm in cluster. Flattened supportive cells surround the DP cell surface. Presumably, juvenile DPCs we examined had reached the functional phase to get organized in the multiple photoreceptive system peculiar to this species, although only in a miniature scale, consisting of by far less numerous component cells as compared with the adult.

THE EFFECTS OF GTPγS, A G-PROTEIN ACTIVATOR, ON THE LABELLAR TASTE RECEPTORS IN THE FLESHFLY.

M. Koganezawa and I. Shimada
Dept. Biol. Inst., Fac. Sci., Tohoku Univ, Sendai.

To reveal the taste transduction mechanisms, we tested the effects of GTPγS, an activator of G-protein, on the labellar taste receptor cell in the fleshfly. After treatment with GTPγS in 0.03% DOC solution of the tip of a chemosensory hair, the response of sugar receptor cell to Glucose, Fructose, L-Phe, L-Val and the reponse of salt receptor cell to cAMP, were enhanced maximally about two times before the treatment. These results suggested that resposes to these taste stimulants were mediated by G-protein coupled pathway. On the other hands, the response of salt receptor cell to NaCl did not show such enhancing effects. The response to NaCl, therefore, may be mediated by other transduction mechanisms.

SUGAR STIMULATION-DEPENDENT PROTEIN PHOSPHORYLATION IN THE LABELLAR TASTE ORGAN OF THE FLY.

M. Ozaki[1], W. Idei, T. Amakawa[2] and F. Tokunaga[3].
[1]Dept. of Biol., Fac. of Sci., Osaka Univ., [2]Dept. of Natural Environment, Fac. of Human Development, Kobe Univ., [3]Dept. of Earth and Space Sci., Fac. of Sci., Osaka Univ.

Using the blowfly taste sensilla, we observed that protein kinase inhibitors and activators affect the response of the sugar receptor cell. Thus, the target molecules of the protein kinases may be key proteins contributing to the sugar taste response.

With the 32P-autoradiogram of the SDS-PAGE pattern of labellar extract, we found two protein components of 31 and 32kDa being phosphorylated in a sucrose stimulation-dependent manner.

On the other hand, we have detected two types of sugar receptor candidate protein showing different sugar binding specificities from each other in the labellum and tarsus extracts. One of them having sucrose-binding ability was divides into two components of 31 and 32kDa by SDS-PAGE. These components appeared to have the same molecular weights of the sucrose stimulation-dependent phosphorylated protein components mentioned above.

This study was supported by Hayashi Memorial Foundation for Female Natural Scientists to M. O.

TWO TYPES OF SUGAR RECEPTOR CANDIDATE PROTEIN IN TARSUS OF THE BLOWFLY, PHORMIA REGINA.

W.Idei[1], M.Ozaki[1], F.tokunaga[2].
[1]Dept. of Biol., Fac. of Sci., Osaka Univ. , [2]Dept. of Earth and Space Sci., Fac. of Sci., Osaka Univ.

Taste organs of the fly mainly exist in labellum and tarsus in the shape of sensory hair. In labellum of Phormia regina, two types of sugar receptor candidate protein had been isolated, by using the receptor site specific inhibitory polysaccharides. This time, as we detected the putative sugar receptor proteins in tarsus, we report on them, comparing the labellar putatives.

Proboscis extension behavior experiment and electrophysiological experiment with inhibitory polysaccharides suggested that there were two types of sugar receptor site also in tarsus. These sites were inhibited by starch and levan, respectively. Thus, by affinity electrophoresis using starch or levan as an affinity ligand, we detected two types of sugar receptor candidate protein from the tarsal extract. The molecular weight of one type of the protein is 27,000, while that of the other is 31,000 or 32,000. these values are quite similar to those of labellar sugar receptor candidate proteins.

DIFFERENT SPECTRUM IN RESPONSES OF DETERRENT RECEPTOR CELLS IN *SAWA-J*, A STRAIN OF THE SILKWORM, *BOMBYX MORI*, WITH ABNORMAL FEEDING HABIT

K. Asaoka, Natl. Inst. Sericul. & Entomol. Sci., Tsukuba

Sawa-J is a strain of the silkworm which is feed on various kinds of plant leaves in addition to mulberry leaves. It was reported that the abnormal feeding habit of *Sawa-J* was determined mainly by a recessive gene and by some modified genes. To know the possibility whether the genes have any effect on the gustation, gustatory spike responses were recorded and compared between *Sawa-J* and normal strains, using standard tip-recording method. Responses in a strain which was bred by crossing *Sawa-J* to introduce genes were also recorded. Sucrose, inositol, and various deterrent substances were used as stimuli.

There were little differences between the strains in their responses to sucrose and inositol from sugar receptor cells and inositol receptor cells, respectively. Response thresholds to O-glycosides in deterrent receptor cells were much higher in both *Sawa-J* and its related strains than normal ones. Deterrent receptor cells of all strains responded to alkaloids, and the cell of *Sawa-J* responded with more frequent spikes than the normal strain to some alkaloids and 20-hydroxyecdysone at certain concentrations. It is supposed that the different spectrum of the deterrent cell of *Sawa-J*, lack in response to O-glycosides, is functioned by the genes and have an effect on the feeding habit.

IDENTIFICATION OF HYGRO- AND THERMORECEPTIVE SENSILLA ON FIREFLY ANTENNAE.

M. Iwasaki, T. Itoh, F. Yokohari and Y. Tominaga.
Dept. of Biol., Fac. of Sci., Fukuoka Univ., Fukuoka.

Antennal sensilla of male fireflies, *Luciola cruciata*, were examined seeking for hygro- and thermoreceptive sensilla. Several types of sensilla have been observed with a field emission scanning electron microscope (FESEM); chaetic, trichoid, basiconic, capitular, campaniform and marginal sensilla. Extracellular recordings from single sensilla revealed three types of cells: moist, dry and cold receptors. These recorded sensilla were afterward examined with a FESEM, which demonstrated that capitular sensilla were the hygro- and thermoreceptive sensilla. About 30 capitular sensilla per an antenna distributed only on the ventral surface of flagellar segments. This sensillum had a conical cuticular apparatus (ca. 3 µm in base diameter, ca. 1.5 µm in tip diameter) without taste and olfactory pores. These morphological and electrophysiological characteristics were quite similar to those of well investigated hygro- and thermoreceptive sensilla, such as those of the cockroach and cricket.

RESPONSE CHARACTERISTICS OF HYGRORECEPTORS OF THE TICK, *Amblyomma variegatum*

K. Mori[1], F. Yokohari[2], Y. Toh[1] ([1]Dept. of Biol., Fac. of Sci., Kyushu Univ., Fukuoka. ; [2]Dept. of Biol., Fac. of Sci., Fukuoka Univ., Fukuoka.)

The tick has no antennae but instead the first legs fill such roles as those of the antennae of insects. Behavioral studies have suggested that the tick has hygroreceptors on the legs, but there have been no direct evidence supporting the suggestion. There is the Haller's organ on the dorsal surface of tarsus of first leg. The organ is a cavity with a slit-shaped opening where there are many morphological types of sensilla. We have succeeded to record the impulse responses to humidity stimuli from the organ of adult of the tropical bont tick, *Amblyomma variegatum*.. Two types of hygroreceptors were physiologically found. One was a moist receptor which was excited by increases in humidity and the other was a dry receptor which was excited antagonistically by decreases in humidity. The responses of both types of hygroreceptors were of a phasic-tonic response manner like those of the hygroreceptors of insects. As these responses were recorded simultaneously by an electrode inserted into the cavity, these receptors may be in a single sensillum.

Effect of temperature on vibratory communication of wandering spider Cupiennius salei.

I. Shimizu[1] and F. G. Barth[2]. [1]Center for Ecological Research, Kyoto University, Kyoto, Japan. [2]Institut für Zoologie der Universität Wien, Wien, Austria

C. salei is a typical wandering spider having a habitat associated with a particular type of monocotyledonous plants in the rain forest of Central America. Both male and female of the spider show nocturnal locomotive activities. The male and female use the vibratory signals for communicating each other during their courtship. The male of C. salei starts to emit vibrations by the arousal contact with a pheromone of the dragline deposited by female onto the plant. The male signals reach the female through the plant and female responds to the male signals with her own vibrations. Then the male orients himself and moves to the female. Thus the vibratory courtship of C. salei is characterized by reciprocal signalling of the male and female partners. The male signals have a particular temporal pattern. They are constructed by a train of syllables produced by opithosomal oscillations and by pedipalpal dramming against the substraum. The female response which occurs typically within a narrow time frame after the end of one male series have a simple temporal structure compared to the male signals. Effect of temperature on the temporal pattern of the vibratory signals of the spider was investigated to reveal the production and reception mechanism of the signals.

THE EFFECTS OF TEMPERATURE AND LIGHT ILLUMINATION ON FATTY ACID COMPOSITIONS AND RHABDOM STRUCTURE OF ARTHROPOD COMPOUND EYES.

T.Kashiwagi, Y.Ogawa, K.Okamoto, E.Eguchi. Dept.Biol., Yokohama City Univ. Yokohama.

Fatty acid compositions of the compound eyes of 3 insect and 3 crustacean species were comparatively analyzed by gas-chromatography. In insects, 16:0 and 18:0 were the main saturated fatty acids, and 18:1 was the dominant unsaturated fatty acid. In crustaceans, the main saturated fatty acids were 16:0 and 18:0, and the main unsaturated fatty acids were 20:4, 20:5 and 22:6. Fatty acid analysis of compound eyes of grapsid crabs for the seasonal changes of temperature revealed that the ratios of unsaturated fatty acids / saturated fatty acid (U/S ratio) varied from 1.0 in summer to 2.5 in winter. Fatty acids such as 18:0 and 20:1 showed the significant correlation with the change of seasonal temperature. Fatty acid analysis of the developing compound eyes of silk moths during pupal stage revealed that eicosapentaenoic acid(20:5) showed a remarkable increase in parallel with the development of rhabdom. The fine structure of rhabdom microvilli of crayfish compound eyes was severely disorganized by a sudden change of temperature with a strong illumination. The result was discussed in relation to the fatty acid composition of crayfish rhabdom.

MORPHOLOGICAL CHANGES OF THE INTRAORAL TASTE ORGANS DURING T4-INDUCED METAMORPHOSIS IN THE NEOTENIC AXOLOTL, *AMBYSTOMA MEXICANUM.*

S.Ido[1], H.-A.Takeuchi[1,2] and T.Nagai[3]. [1]Dept. of Biol., Fac. of Sci., Shizuoka Univ., Shizuoka, [2]Life Sci. Inst., Sophia Univ., Tokyo and [3]Dept. of Physiol., Teikyo Univ. Sch. of Med., Tokyo.

Metamorphosis of the neotenic axolotls was induced by thyroxine (T4) treatment (Zool.Sci.9:1244, 1992) and morphological changes of their intraoral taste organs were studied. In the metamorphosing axolotls, the oral floor between the rostral end of the tongue and the lower jaw protruded to form a tongue-like structure, while the tongue regressed caudally with decrease of its volume. The axolotl had many taste buds on the tongue, gill arch and palatal mucosa, but metamorphosis decreased dramatically the number of taste buds on the tongue (pre: ca.10/mm^2; post: <2/mm^2). The tongue-like structure had many foldings which were reminiscent of mammalian foliate papillae. A cell mass like a taste bud was often seen on the top of foldings. These intraoral taste organs of metamorphosed axolotls were basically similar to those of naturally metamorphosed Ezo salamanders (*Hynobius retardatus*), but were different from those of adult bullfrogs (*Rana catesbeiana*).

ADULT DIAPAUSE IN THE BLOWFLY *PROTOPHORMIA TERRAENOVAE*: PHOTOPERIODIC INDUCTION AND EFFECTS OF OPTIC LOBE AND RETINA REMOVAL.

S. Shiga and H. Numata, Dept. Biol., Fac. Sci., Osaka City Univ., Osaka.

Photoperiodic control of adult diapause and effects of surgical operation in the visual system on ovarian development were investigated in the blowfly *Protophormia terraenovae*. The flies raised under a long-day photoperiod (18L-6D) and transferred to a short-day photoperiod (12L-12D) on adult emergence at 25 °C entered a reproductive diapause in which yolk deposition is suspended. The adults kept constantly under 18L-6D became reproductive. Under the diapause-inducing condition, removal of the compound eyes, optic lobes or ocelli were carried out on first day adults. Both bi- and unilateral removals of the compound eye or optic lobe caused significant decrease in the diapause incidence compared with sham-operated groups. However, removal of ocelli had no effects. These results suggest that this fly employs long-day photoperiodic response for winter diapause and visual elements may play some role in the regulation of reproduction.

THE MARINE DINOFLAGELLATE *Alexandrium tamarense* HAS A LARGE AMOUNT OF GABA.

Y. Muneoka[1], T. Takahashi[1], B.M. Twarog[2], R. R. L. Guillard[2], T. Ikeda[3] and K. Nomoto[3]. [1]Fac. of Integrated Arts and Sci ., Hiroshima Univ., Higashi-Hiroshima, [2]Bigelow Lab. for Ocean Sci., Maine, U.S.A. and [3]Suntory Inst. for Bioorganic Res., Osaka.

An attempt was made to isolate bioactive substances from the two cultured strains (GT 429 and PLY 173) of *A. tamarense*. The amounts of the strains subjected to the experiments were 1,800 mg and 880 mg in dry weight, respectively. The extract of each strain was forced through C18 cartridges, and thus two materials, flowthrough and retained materials were obtained. We tested the materials on several kinds of muscles and found that they have an excitatory activity or an inhibitory activity on all the muscles used. The materials were then subjected to HPLC purification. However, most of the activities were disappeared during the purification. Only two active substances, one showed an inhibitory activity on the crop of the cricket *Gryllus bimaculatus* and the other showed an excitatory activity on the rectum of the quail *Coturnix japonica*, were isolated from the flowthrough of GT 429, and only one active substance which showed an inhibitory activity on the crop was isolated from the flowthrough of PLY 173. The inhibitory substance of PLY 173 was determined to be GABA by chemical and pharmacological analyses. From the pharmacological effectiveness of the purified inhibitory substance, the amount of GABA in PLY 173 was estimated to be at least 20 mg/1000 mg dry weight.

FINE STRUCTURE OF CHEMOSENSORY HAIRS OF *PAPILIO XUTHUS*.

J. Karasawa[1], K. Arikawa[2] and K. Maruyama[1] Dept. Biol., Chiba Univ., Chiba[1] and Dept. Biol., Yokohama City Univ., Yokohama[2]

The swallowtail butterfly, *Papilio xuthus*, lay eggs onto the undersurface of a leaf of the plants belonging to the family *Rutacea*. Alighting on the plants, the butterfly females vigorously drum upon the leaf surface with their forelegs. After detecting, through their tarsal chemosensory hairs, some specific oviposition stimulants contained in their host plants, the females then lay eggs.

In the present study, the fine structure of the chemosensory hairs of the 5th tarsus of the female foreleg was observed under an electron microscope. The hair was 50-60 μm long and 5-10 μm wide. There was a small hole at the hair tip. At the basal region there were five sensory cells extending one dendrite toward the tip and one axon toward the central nerve system. One dendrite ended on the half way to the tip and it appeared that the dendrite came from a mechanosensory cell. There were a number of microtubules running toward the tip of the hair. At the base of a dendrite, a ciliary structure (9+ 0) was always present. Observations on a series of thin sections have elucidated the fine structure of a *Papilio xuthus* chemosensory hair.

PLANATENSIN: A NEUROTENSIN-LIKE PEPTIDE ISOLATED FROM THE PLANARIAN, *Dugesia japonica*.

S. Kinjo[1], T. Takahashi[1], M. Ohtani[1], Y. Muneoka[1], K. Watanabe[2], Y. Umezono[2], T. Takao[3] and Y. Shimonishi[3]. [1]Fac. of Integrated Arts and Sci., Hiroshima Univ., Higashi-Hiroshima, [2]Dept. of Life Sci., Fac. of Sci., Himeji Inst. of Technol., Himeji and [3]Inst. for Protein Res., Osaka Univ., Suita.

Specimens (50g) of the cultured freshwater planarians, *Dugesia japonica*, were frozen in liquid nitrogen, steeped in cooled acetone and homogenated with a Polytron. The homogenate was centrifuged. The precipitate was again homogenized in water and centrifuged. Two supernatants were pooled and concentrated. The concentrated material was forced through C18 cartridges. The retained material was eluted with 10% methanol and then with 60 % methanol. The bioactive substances in the 60%-methanol eluate were purified with an HPLC system. The rectum of the quail, *Coturnix japonica*, was used as the bioassay system. Thus, a substance with a strong contractile activity on the rectum was isolated. The substance was subjected to amino acid sequence analysis and FAB-MS measurement, and its structures was determined to be as follows: H-Thr-Ser-Lys-Gly-Lys-Arg-Lys-Pro-Tyr-Val-Phe-OH. The sequence of C-terminal penta-peptide fragment of the peptide is significantly homologous with that of neurotensin. Further, the planarian peptide was found to show neurotensin-like action on some vertebrate intestines. Therefore, we designated the peptide planatensin.

NOVEL BIOACTIVE PEPTIDES ISOLATED FROM TWO SPECIES OF OLIGOCHAETE ANNELIDS.

O. Matsushima[1], K. Ukena[1], T. Oumi[1], T. Ikeda[2], T. Fujita[2], H. Minakata[2] and K. Nomoto[2].
[1]Biol. Sci., Fac. of Sci., Hiroshima Univ., Higashi-Hiroshima and [2]Suntory Inst., Bioorganic Res., Osaka.

The isolated gut (crop-gizzard) preparation was used as a bioassay system to isolate bioactive peptides that influence the spontaneous contractile activity of the gut. Several bioactive peptides were purified from the extracts of the gut or whole body of the two species of earthworm (Eisenia foetida and Pheretima vittata) through reversed-phase, cation-exchange and anion-exchange HPLC. Among them, three peptides, which potently augmented spontaneous contractions of the isolated gut preparation of E. foetida, were found to be structurally related to each other by amino acid sequence analysis. These peptides did not appear to belong to any peptide family reported so far and may be distributed solely among annelids.

AN ALLATOTROPIN-MATPS-LIKE PEPTIDE ISOLATED FROM THE GUT OF THE EARTHWORM, EISENIA FOETIDA.

K. Ukena[1], T. Oumi[1], O. Matsushima[1], T. Ikeda[2], T. Fujita[2], H. Minakata[2] and K. Nomoto[2]. [1]Biol. Sci., Fac. of Sci., Hiroshima Univ., Higashi-Hiroshima and [2]Suntory Inst. Bioorganic Res., Osaka.

We purified a bioactive substance from the gut of the earthworm, Eisenia foetida (about 3,000 animals) by using the isolated anterior gut (crop-gizzard) as the bioassay system. Its structure was determined by amino acid sequence analysis, amino acid analysis and FAB-MS analysis. The sequence of the peptide was somewhat related to that of allatotropin isolated from an insect, Manduca sexta, which stimulates the secretion of juvenile hormone from corpora allata. Further, this peptide was homologous to myoactive tetradecapeptides (MATPs) purified from the two species of molluscs, Fusinus ferrugineus and Achatina fulica, and to a peptide isolated from Lymnaea stagnalis. This peptide showed a potent excitatory action on spontaneous contractions of the anterior gut of the earthworm. It appears to be involved in the regulation of gut motility of the animal.

STRUCTURE AND ACTION OF NOVEL BIOACTIVE PEPTIDES (PY PEPTIDES) ISOLATED FROM MOLLUSCS.

M. Fujiwara-Sakata[1], K. Fujita[1], T. Ikeda[2], H. Minakata[2], K. Nomoto[2] & M. Kobayashi[1]
[1]Physiol. Lab., Fac. of Integrated Arts & Sci., Hiroshima Univ., Higashi-Hiroshima & [2]Suntory Inst. for Bioorganic Res., Osaka.

Three novel bioactive peptides having closely related structures were isolated from the buccal ganglia of pulmonate *Achatina fulica* and the buccal muscles of prosobranch *Rapana thomasiana*, and they were termed PY peptides. Their structures were determined to be as follows:

Achatina Pro-Tyr-Leu-Glu-Tyr-OH
Rapana Pro-Tyr-Met(O)-Gln-Tyr-OH
Pro-Tyr-Met-Glu-Tyr-OH

Modulatory action of these peptides and an analog on the contraction of the radula retractor from the two species were observed. On the muscle of *A. fulica*, *Achatina* PY peptide showed the most potent modulatory effect among these peptides. *Rapana* Met(O)^3- PY peptide had no significant effect. In *R. thomasiana*, on the contrary, one of *Rapana* peptide (PYMEY) showed the most significant effect. *Rapana* Met(O)^3-PY peptide and a synthetic analog, in which Met(O)^3 was replaced by Met, had similar modulatory action.

SIMILARITY OF NEUROPEPTIDE STRUCTURES BETWEEN MOLLUSCS AND ANNELIDS.

T. Takahashi[1], Y. Muneoka[1], O. Matsushima[2], T. Ikeda[3], H. Minakata[3] and K. Nomoto[3]. [1]Fac. of Integrated Arts and Sci., Hiroshima Univ., Higashi-Hiroshima, [2]Biol. Sci., Fac. of Sci., Hiroshima Univ., Higashi-Hiroshima and [3] Suntory Inst. for Bioorganic Res., Osaka.

FMRFamide and FLRFamide are the representative molluscan neuropeptides. These two peptides have been shown to be also present in annelids. Recently, we isolated a bioactive peptide, AMGMLRMamide, from a polychaete annelid. This peptide is apparently a member of myomodulin-CARP family, one of the well-known molluscan neuropeptide family. Furthermore, we found AKSGFVRIamide and VSSFVRIamide in the polychaete. They are members of S-Iamide family, which is also one of the molluscan neuropeptide family. Two molluscan peptides, GFRMNSSNRVAHGFamide and MRYFVamide, have been found to show a strong contractile activity and a strong inhibitory activity on the esophaguses of annelids, respectively. Therefore, peptides closely related to these substances have been believed to be also present in annelids (Muneoka et al., 1994). In fact, such peptides were found in an annelid (Matsushima, unpublished). Quite recently, Oumi et al. (1994) isolated a member of the oxytocin-vasopressin superfamily from an annelid. The sequence of the peptide is more homologous with that of a member found in a mollusca than those of the other members found in other phyla. The overall structural property of annelidian neuropeptides seems to be very similar to that of molluscan neuropeptides.

A NEUROTENSIN-FAMILY PEPTIDE ISOLATED FROM A NEWT, *Cynops pyrrhogaster*.

H. Teranishi[1], M. Ando[1], T. Uesaka[1], Y. Muneoka[1], C. Chiba[2], T. Saito[2], T. Takao[3] and Y. Shimonishi[3]. [1]Fac. of Integrated Arts and Sci., Hiroshima Univ., Higashi-Hiroshima, [2]Inst. of Biol. Sci., Univ. of Tsukuba, Tukuba and [3]Inst. for Protein Res., Osaka Univ., Suita.

After the heads and the visceral organs had been removed from the specimens (300) of the newt, *Cynops pyrrhogaster*, the bodies were frozen in liquid nitrogen and pulverized. The pulverized material was homogenized in acetone and centrifuged. The precipitate was then homogenized in water and centrifuged. Two supernatants were pooled and concentrated. The concentrated material was forced through C18 cartridges. The retained material was eluted with 10% methanol and then with 60% methanol. The peptidic substances in the 60%-methanol eluate were purified with an HPLC system. The rectum of the quail, *Coturnix japonica*, was used as the bioassay system. Thus, a substance which showed a strong contractile activity on the rectum of the quail was isolated. The substance was subjected to amino acid sequence analysis and FAB-MS measurement, and its structure was determined to be as follows: H-Val-Lys-Lys-Pro-Arg-Arg-Pro-Tyr-Ile-Leu-OH. That is, the substance is a decapeptide of the neurotensin family. The sequence of the C-terminal octapeptide fragment of the newt neurotensin is the same as that of the bovine neurotensin.

ISOLATION OF BIOACTIVE SUBSTANCES FROM A LIBRARY OF PENTAPEPTIDES SYNTHESIZED WITH A MULTIPLE PEPTIDE SYNTHESIZER.

M.Ohtani[1], Y.Muneoka[1], N.Kanemoto[2], K.Ogino[2], Y.Masui[2] and S.Aimoto[3]. [1]Fac.of Integrated Arts and Sci., Hiroshima Univ., Higashi-Hiroshima, [2]Inst. for Cellular Technol., Otsuka Pharmaceutical Co., Ltd., Tokushima and [3]Inst. for Protein Res., Osaka Univ., Suita.

Using the rectum of the quail, *Coturnix japonica*, as the bioassay system, an attempt was made to isolate bioactive substances from a peptide library consisting of approximately 2.5-million species of C-terminus-free pentapeptides synthesized with a multiple peptide synthesizer.

It was shown in the preliminaly experiments that the C-terminal pentapeptide fragments of neurotensin and xenopsin had a strong excitatory effect on the rectum of the quail. The threshold concentrations of the fragments for the effect were found to be between 10^{-10} M and 10^{-9} M. Therefore, it was expected that the same substances as these peptide fragments could be obtained from the library.

As expected, two strong excitatory substances, whose structures were determined to be H-Arg-Pro-Tyr-Ile-Leu-OH and H-Arg-Pro-Trp-Ile-Leu-OH by chemical analyses, were isolated from the library. The sequences of these peptides are the same as those of the C-terminal pentapeptide fragments of neurotensin and xenopsin, respectively. In addistion to these peptides, several analogues of them were also isolated.

The synthesizing and isolation methods mentioned above are considered to be avairable for finding agonists and antagonists of oligo-neuropeptides.

FUNCTIONS OF NEUROPEPTIDE Y-RELATED PEPTIDE ISOLATED FROM EEL GUTS.

T. Uesaka[1], K. Yano[2], M. Yamasaki[2] and M. Ando[1]. [1]Lab. of Physiol., Fac. of Integrated Arts and Sci., Hiroshima Univ., Hiroshima and [2]Tokyo Res. Lab., Kyowa Hakko Co., Ltd., Tokyo.

Neuropeptide Y-related peptide was isolated from the gut of the eel, *Anguilla japonica*, and the primary structure was established as; YPPKPENPGEDASPEEQAKYYTALRHYINLITRQRY-NH_2. This sequence was identical to the eel neuropeptide Y-related peptide from the American eel pancreas by Conlon *et al.* (1991). To determine physiological role of the eel neuropeptide Y-related peptide (eNPY), we synthesized it by a FMOC solid phase method. The retention time of the synthesized peptide was coincident with that of the native peptide both on reverse-phase and on cation-exchange HPLC, indicating that eNPY is successfully synthesized. When eNPY was applied to the eel atrium, the contractility was enhanced in a dose-dependent manner. On the other hand, the same peptide also increased the short-circuit current, due to active Cl^- absorption across the seawater eel intestine. Since it is already known that water follows the Cl^- transport across the intestine, this means that eNPY enhances water absorption across the intestine. Combining these effects of eNPY on heart and intestine, this peptide may act as a hypertensor in the eel.

COMPARISON OF SEAWATER AND FRESHWATER EELS FOR THE EFFECTS OF VARIOUS REGULATORS ON ION TRANSPORT ACROSS THE INTESTINE

M. Ando and I. Hara. Lab. of Physiol., Fac. of Integrated Arts & Sci., Hiroshima Univ., Hiroshima.

Effects of serotonin (5HT), methacholine (MCh; a muscarinic acetylcholine receptor agonist), eel atrial natriuretic peptide (eANP) and adrenaline (AD) on the transepithelial potential difference (PD), short-circuit current (Isc) and tissue resistance (Rt) across the intestine were compared between sewater (SW) and freshwater (FW) eels. The dose-response curves and the medial effective concentrations (EC_{50}) of 5-HT, MCh and eANP on the Isc were not significantly different between SW and FW eels. However, the SW eel intestine was three times more sensitive to AD than FW eels. When cortisol (0.5 mg/100g) was injected intraperitoneally into FW eels, the AD-sesitivity was enhanced to the SW level. The Isc in SW and FW eels were diminished almost completely after addition of 10^{-5} M bumetanide, a specific inhibitor of Na^+-K^+-Cl^- cotransport, into the mucosal fluid, indicating that the Isc in both SW and FW eels are due to Na^+-K^+-Cl^- cotransport. The bumetanide-sesitive Isc in the cortisol-treated FW eels was almost the same as that in SW eels. These results suggest that cortisol may systhesize AD receptors and Na^+-K^+-Cl^- cotransport system in the intestine following sea water acclimation of eels.

CALCIUM-DEPENDENT INHIBITORY FACTOR (CIF) FROM CHO-K1 CELL

Akio Nakamura, Tuyoshi Okagaki, Takashi Takagi[1], Takeshi Tanaka[2] and Kazuhiro Kohama. (Dept. Pharmacol., Gunma Univ., School of medicine, Maebashi, [1] Biol, Inst., Fac, Sci., Tohoku Univ., Sendai, [2] Res. Division, Saitama Red Cross Blood Center, Saitama, Japan.)

We have previously reported that Ca^{2+} exerts "Calcium inhibition" to *Physarum* actomyosin system, which involves phosphorylation of myosin by myosin light chain kinase (MLCK). The regulation of MLCK activity by Ca^{2+} is quite distinct from that of vertebrate MLCK by Ca^{2+}; *Physarum* MLCK is active without requiring calmodulin. Further, Ca^{2+} exerts an inhibitory effect to the activity. The calcium-binding protein responsible for the inhibition was purified from *Physarum* as a Calcium-dependent inhibitory factor (CIF).

We cloned cDNA encoding CIF and expressed it in *E. coli*. The polyclonal antibody was raised from this the recombinant CIF. Using this antibody, we localized of CIF in *Physarum* plasmodia . The results indicate that CIF are located in not only cytoplasm but also nucleolus.

In an attempt to extend the observation into vertebrate cells, we carried out an indirect immunofluorescence study with CIF antibody. We found that the antibody stained the nucleolus of CHO-K1 cell. The Western blot analysis of nucleus fraction indicated that the antibody recognized a protein of 40 kDa, that is similar to the mass of CIF of *Physarum*. Discussion would be mode about the role of this protein in nucleolus with special reference to cell cycle.

EFFECT OF BAFILOMYCIN, A SPECIFIC INHIBITOR OF H^+-ATPASE, ON CONTENTS OF INTRACELLULAR VANADIUM IN VANADOCYTES

T. Uyama and H. Michibata, Mukaishima Marine Biol. Lab., Hiroshima Univ., Hiroshima.

Ascidians, belonging family Ascidiidae, are known to accumulate high levels of vanadium from sea water in their blood cells, concentrating vanadium by a factor of 10^7. Among several different types of blood cells, the vanadocytes have both high levels of vanadium and a low pH values.

We have previously demonstrated that existence of vacuolar type H^+-ATPase in vanadocytes. These observations suggest the possibility that the activity of the enzyme is linked to the accumulation of vanadium.

We intend to make clear that the gradient of protons energetically conjugates with the accumulation of vanadium. We, therefore, examined whether addition of bafilomycin, a specific inhibitor of vacuolar type H^+-ATPase, to vanadocytes results in decrement of contents of vanadium. As the results, the efflux of vanadium corresponding to about 30% of total intracellular vanadium was observed.

LOCALIZATION OF TWO TYPES OF VACUOLAR BLOOD CELLS IN THE ASCIDIAN, *ASCIDIA SYDNEIENSIS SAMEA*

A. Kaneko, T. Uyama and H. Michibata, Mukaishima Marine Biol. Lab., Hiroshima Univ., Hiroshima.

Ascidians belonging to Ascidiidae have more than 10 types of blood cells. However, little is known how stem cells of ascidian blood cells differentiate through the progenitor cells to become vanadocytes, with their unusual ability to accumulate high levels of vanadium and have low pH values.

We raised monoclonal antibodies against several types of blood cells both to identify each types of blood cells and to determine the localization of blood cells in adult tissues. We reported that a monoclonal antibody C2A4, specific to compartment cell, recognized 200kDa protein. The result obtained by immunohistochemistory, using S4D5 (monoclonal antibody specific to vanadocyte) and C2A4, showed that vanadocytes localized in connective tissue around intestine. While, compartment cells mainly located in branchial blood vessels not in connective tissue around intestine.

EXTRACTION OF VANADIUM-BINDING SUBSTANCE FROM PLASMA OF THE ASCIDIAN, *ASCIDIA SYDNEIENSIS SAMEA*

Y. Nosé and H. Michibata, Mukaishima Marine Biol. Lab., Hiroshima Univ., Hiroshima.

The unusual ability of ascidians to accumulate vanadium in excess of 10 million times its level in seawater has attracted much interest. However, the pathway of vanadium following the uptake from seawater to the so-called vanadocytes of ascidians is unknown. We tried to extract a vanadium-binding substance from the plasma of ascidians in order to clarify the first step of accumulation of vanadium in ascidians.

Ascidia sydneiensis samea were used as materials. Plasma collected was purified by ion-exchange and/or gel chromatography. Content of vanadium in each fraction was measured by flameless atomic absorption spectrophotometry. As a result, an approximate 10 kDa vanadium-binding protein was obtained. This protein associates with vanadium at pH 7 but dissociates with it at pH 2.

VANADIUM-BINDING PROTEIN EXTRACTED FROM BLOOD CELL MEMBRANE OF THE ASCIDIAN, *ASCIDIA AHODORI*

Junko Wuchiyama and Hitoshi Michibata . Mukaishima Marine Biol. Lab., Hiroshima Univ.. Hiroshima

Ascidians are known to accumulate vanadium in their vanadocytes at high levels. We have attempted to extract vanadium-binding proteins from the membrane of blood cells to reveal the mechanisms of vanadium accumulation in ascidians. We have already obtained some vanadium-binding proteins with SDS-PAGE. Then, further purification of them was performed.

Blood cells of *Ascidia ahodori* were suspended into 50mM Tris-HCl buffer (pH 8.5), containing 400mM NaCl. The suspension was homogenized and centrifuged at 500 x g for 1 min. Cell membranes collected from the supernatant were solubilized with 50mM Tris-HCl buffer (pH 8.5) containing 2% Triton X-100. After desalting, proteins were applied to DEAE-Sephacel ion exchanger. Vanadium contents of each of fractions were measured with a flameless atomic absorption spectrophotometry. Proteins were determined by the dye-binding method. As a result, vanadium-binding protein eluted with a step-wise at 0.2M NaCl in 50mM Tris-HCl buffer (pH 8.5) containing 0.2% Triton X-100. Raising antibodies against the purified proteins is in progress.

SYNAPTIC AND EXTRASYNAPTIC JUNCTIONS IN THE COCKROACH DUM NEURONS.

H. Washio. Dept. Biotech. Ishinomaki Senshu Univ. Miyagi, Mitsubishi Kasei Inst. Life Sci. Tokyo.

Both L-glutamate and GABA produced a depolarization or a hyperpolarization at resting membrane potential of the dorsal unpaired median (DUM) neurons in the thoracic ganglia of the cockroach, *Periplaneta americana*. The reversal potential (about -40 mV) was always the same for L-glutamate and GABA. The responses to the amino acids were completely blocked by picrotoxin and sensitive to a low chloride saline. On the other hand, very small spontaneous depolarizing and hyperpolarizing potentials were recorded from the soma membrane of the DUM neurons in the saline containing TTX. These potentials were completely abolished when Ca^{2+} was omitted from the external saline. Also the frequency was increased with increasing an external k^{+} concentration. The results suggested that these potentials were miniature junctional potentials derived from remote synaptic sites and the synaptic junctions are distinguished from the extrasynaptic ones.

ISOLATION OF cDNA CLONES FOR BLOOD CELL SPECIFIC GENES OF THE VANADIUM-RICH ASCIDIAN *Ascidia sydneiensis samea*.

T.Wakabayashi[1], T.Ueki[2], N.Satoh[2], and H.Michibata[1],[1]Mukaishima Marine Biol. Lab., Hiroshima Univ., Hiroshima. [2]Dept. of Zoology, Fac. of Sci., Kyoto Univ., Kyoto.

Ascidians, belonging family Ascidiidae, are known to accumulate high levels of vanadium in their blood cells. However little is known about the mechanism of accumulation and the function of this metal. To explore the molecular mechanisms involved in the accumulation, we attempt to isolate cDNA clones expressed specifically in blood cells. A cDNA library was constructed from mRNAs of blood cells of the ascidian *A. sydneiensis samea*. Differential screening of the library with a total cDNA probe from blood cells and similar probe from body wall yielded several cDNA clones positive for blood cells. We are now trying to ascertain whether they are specific for blood cells.

LOCALIZATION OF CHOLINE ACETYLTRANSFERASE EXPRESSING NEURONS IN THE LARVAL VISUAL SYSTEM OF *DROSOPHILA*.

K.Yasuyama[1,2],T.Kitamoto[2] and P.M.Salvaterra[2]. [1]Department of Biology, Kawasaki Medical School, Okayama, [2]Division of Neurosciences, Beckman Research Institute of the City of Hope, California, USA.

The previously identified neural components of the larval visual system in *Drosophila* include the photoreceptor organ known as Bolwig's organ(Bolwig, 1946), and the first order interneurons described as optic lobe pioneers (OLPs; Tix et al., 1989). The neurotransmitters used by these neurons have not been identified. In this study, we provide evidence for the involvement of acetylcholine in these two components by using *in situ* hybridization with a cRNA probe to *Drosophila* choline acetyltransferase (ChAT) mRNA and by immunocytochemistry using a monoclonal antibody against *Drosophila* ChAT. In stage 15 embryos, a digoxigenin labeled cRNA probe revealed a large number of cells expressing ChAT transcript in both the CNS and PNS. In the PNS, three pairs of sensory organs of the gnathocephalon, including Bolwig's organ, showed strong hybridization signals. The brain of the late third instar larva displayed strong ChAT-like immunoreactivity in the neuropil region and in a few cell bodies, such as a cell located near the insertion site of the optic stalk. The axon of this neuron fasciculates with Bolwig's nerve and projects to the larval optic neuropil in the region of the presumptive medulla neuropil. Bolwig's nerve also shows strong ChAT-like immunoreactivity. The morphology of the identified ChAT expressing neurons in the larval optic lobe is very similar to that of the OLPs. These observations suggest that acetylcholine may be a neurotransmitter of the larval photoreceptor organ and the visual first order interneuron.

EFFERENT SYSTEM OF THE EYES IN ORB WEAVING SPIDERS

S. Yamashita and F. Arita. Biol. Lab., Kyushu Inst. of Design, Fukuoka.

Efferent fibers in the optic nerve control the photoreceptor cells in the orb weaving spiders Argiope amoena and A. bruennichii (Yamashita and Tateda, 1981). In the present study, we recorded ERGs elicited by a flash of 2.5 msec duration presented every 10 seconds given to the anterior median eye under a constant darkness and leg extensions which are due to the increase in internal hydrostatic pressure. During the "night state", the ERG amplitude decreased following the leg extension. In contrast, during the late "night state" and the "day state", the ERG amplitude little decreased following the leg extension. Since the efferent impulses increase during the night state, it is suggested that the efferent neurons receive inhibitory input from some neurons which are related to the hydrostatic system.

The anatomy of the efferent system was examined by cobalt fillings from the eyes or the cut optic nerves.

HYSTERESIS OF SPIKE INITIATION IN CRICKET CERCAL SENSORY NEURON.

Y.Baba, T.Shimizu, T.Akazawa and T.Shimozawa.

Lab.of Neuro-Cybern.,Res.Inst.for Electronic Sci.,Hokkaido Univ.,Sapporo

Spike initiation properties of the wind sensitive cercal mechanoreceptor of cricket were studied by using Gaussian white noise stimuli. Signal transduction from the stimulus to spike train of the neuron was modeled to be equivalent to a cascade of a linear filter followed by a static nonlinear pulse density encoder. However, a comparison of the peri-stimulus-time histogram to a repetition of the same stimulus with the model output suggested that the spike firing probability of the neuron depends not only on instantaneous value of the encoder input, but also on its time derivative.

Response dynamics of horizontal system (HS) cells in the lobula plate of the fly.

J. Okuma, Y Hasegawa, Y Kondoh. Honda R&D Co. Ltd., Wako Research Center, Saitama.

One group of giant interneurons in the lobula plate of the fly, horizontal system (HS) cells, respond to large field motion in the horizontal axis. We have analyzed quantitatively response dynamics of the HS cells by means of Wiener kernel method and compared these results with computer simulation implemented in the correlation type motion detector to understand computational mechanisms underlying motion detection of the fly visual system.

Responses to motion in the HS cells were characterized by biphasic 1st-order kernels, indicating that they are velocity-sensitive. When picrotoxin was applied to the animal to prevent inhibitory interactions, the response could be decomposed into the sum of the linear and 2nd-order nonlinear components. The 2nd-order kernel that characterizes the nonlinear component was also differentiating, having two depolarizing peaks on the diagonal with two off-diagonal hyperpolarizing valleys. Thus, the linear component codes the velocity and direction of motion, whereas the 2nd-order component codes the power of motion. Computer simulation showed that the nonlinear response represents the output of the multiplication (correlation) process in which the motion vector and power are produced. These results suggest that the HS cells extract the motion vector as a final output by eliminating the power component which is inevitably produced at the multiplication process.

COMPARISON OF AXOTOMY- AND DEPOLARIZATION- INDUCED LONG-LASTING FIRINGS IN AN IDENTIFIED CRAYFISH MOTONEURON.

A. Muramoto, Fukushima Biomed. Inst. of Environm. & Neopl. Dis., Futaba-gun.

I have reported previously that axotomy of an identifiable anal motoneuron of the crayfish, Procambarus clarkii induces a long-lasting firing that persists for more than an hour and shows a characteristic discharge pattern. Moreover a prolonged depolarizing current to the cut end of this motoneuron was also capable of inducing a similar response.

In this study, I compared firing pattern (plots of sequential spike intervals against interval number during a firing) of axotomy- and depolarization-induced firings by changing position of axotomy and strength of stimulation. Similar characteristics in firing patterns were observed in these two cases. Even though a hyperpolarizing current to the cut end could block the response of a firing during this stimulation, it could not alter the time course of pattern of a firing induced by axotomy.

These results support my previous idea that the axotomy-induced long-lasting firings must be based on a prolonged depolarization occurring locally at the cut site.

VOLTAGE AND CALCIUM RESPONSES OF THE EARTHWORM GIANT AXON FOR BATH-APPLIED GLUTAMATE AGONISTS.

H. Ogawa, K. Oka and S. Fujita.
FUJITSU LABORATORIES LTD.

In CNS of an earthworm, giant fibers (MGF and LGFs) are the most famous and important interneurons associating various behavior, e.g. contract reflex and escape response. We have reported the electrical tetanic stimulation could induce calcium wave propagation in the giant axon. This wave was triggered by the Ca^{2+} influx through voltage dependent channels localized on the plasma membrane and propagated by the calcium induced calcium release (CICR) mechanism. On the other hand, it is well-known that invertebrates including the earthworm have the glutamate receptors at neuromuscular junction, but there are few studies on their function in CNS.

We examined neuronal activity of the giant fiber during bath-application of the glutamate and four kinds of agonists (NMDA, kainate, quisqualate, trans-ACPD) using fluorescent imaging techniques. CCD imaging of the ventral ganglia stained by potentiometric dye, RH414 showed that ionotropic typed agonists induced larger depolarization of the giant fiber than matabotropic typed one. Combination study of confocal laser-scanning microscopy and calcium indicator, Indo 1 indicated that bath-application of 1 mM glutamic acid transitorily increased the intracellular free calcium concentration, $[Ca^{2+}]_i$ in the giant axon. These observations suggest that the earthworm giant fiber have glutamate receptors modulating membrane potential and $[Ca^{2+}]_i$. In CNS of the earthworm, these receptors may have an important role in control of their behavior.

DEVELOPMENT OF HISTAMINE-LIKE IMMUNOREACTIVE NEURONS IN THE OPISTHOBRANCH MOLLUSC *PLEUROBRANCHAEA JAPONICA*.

K.Ohsuga and K.Kuwasawa. Dept. of Biol., Tokyo Metropolitan Univ., Tokyo.

In *Pleurobranchaea* trochophores are transferred to veligers in egg capsules and then the veligers hatch as free-swimming pelagic larvae 7 days after fertilization. Veligers metamorphose into benthic juveniles 20 days after hatching. A pair of the velar lobes functioning as feeding and swimming organs disappears during a period of metamorphosis. The young juveniles grow into mature animals in about 3 months after metamorphosis.

We studied cellular organization of histamine-like immunoreactive (HIR) neurons on developmental stages from embryo to adult. We examined HIR neurons with paraffin sections and whole mount preparations by means of peroxidase-antiperoxidase and fluorescein isothiocyanate methods. In veligers just after hatching HIR neurons were observed in the cerebral ganglion and the statocysts. Before metamorphosis HIR neurons appeared in the pedal ganglion. Just after metamorphosis HIR neurons appeared in the rhinophore and oral-veil ganglia. In adult HIR neurons were found all central ganglia except for the visceral ganglion. Many HIR cells were observed in epithelial tissues surrounding the rhinophore and oral-veil ganglia.

POSTEMBRYONIC DEVELOPMENT OF SPINAL MOTONEURONS IN ANGELFISH, *PTEROPHYLLUM SCALARE*.

M. Fudoji, M. Yoshida, K. Uematsu and K. Namba. Lab. of Fish Physiol., Fac. of Applied Biol. Sci., Hiroshima Univ., Higashi-Hiroshima.

To reveal the postembryonic development of the spinal motoneurons in angelfish, spinal neurons of larval angelfish were retrogradely labeled by applying HRP to the trunk muscles. Three types of spinal neurons were identified: (1) primary motoneurons, (2) secondary motoneurons and (3) mechanosensory Rohon-Beard neurons. Primary motoneurons, having relatively large spindle-shaped cell body and thick axon, were located in dorsal part of the spinal motor column. At the day of hatching (day 1), 7-10 primary motoneurons per spinal hemisegment were retrogradely labeled and the number of labeled neurons did not changed throughout the experimental period (day 1-day 12). Secondary motoneurons, having small spherical cell body and thinner axon, were labeled in ventral part of the spinal motor column after day 2. The labeled secondary motoneurons were markedly increased in number by day 3 and did not show obvious increase thereafter. As the larva developed, both types of motoneurons extended their dendritic arborization dorsally and laterally to the cell bodies.

CENTRAL PROJECTIONS OF THE PINEAL ORGAN IN LARVAL ANGELFISH, *PTEROPHYLLUM SCALARE*.

M. Yoshida, K. Uematsu and K. Namba. Laboratory of Fish Physiology, Faculty of Applied Biological Science, Hiroshima University, Higashi-Hiroshima.

For several days after hatching, angelfish larva respond to abrupt dimming of illumination with tail beats. This response has been suggested to be mediated by photoreception in the pineal organ. As a first step to reveal the central pathway eliciting the dimming-induced tail beat, central neural projections from the pineal organ in larval angelfish were investigated by injecting a fluorescent tracer DiI into the pineal organ.

DiI-labeled neural tracts, after entering the brain, ran bilaterally along the fasciculus retroflexus. Each tract branched out two major bundles: one to the diencephalon and the other toward the caudal part of the brainstem. Bundles in the diencephalon supplied axons abundantly in this region. Fibers that emerged from the caudal bundles and terminated in the mesencephalic tegmentum were observed. In young larva, at least until the fifth day after hatching, axonal projections in the medulla terminated as varicose fibers near the ventral margin of this region were labeled.

GABA-INDUCED CURRENTS IN CONE-DRIVEN HORIZONTAL CELLS OF CATFISH RETINA.

K.-I. Takahashi[1], S. Miyoshi[2] and A. Kaneko[1]. [1]Dept. Physiol. and [2] Dept. Int. Med., Keio Univ. Sch. Med., Tokyo.

To learn about the role of GABA in horizontal cells, the GABA-induced current (I_{GABA}) was studied in cone-driven horizontal cells dissociated from the retina of the catfish (*Ictarulus punctatus*) under whole-cell voltage-clamp conditions with almost symmetrical Cl^- on each side of the membrane. At a holding potential of -50 mV, 100 μM-GABA induced a sustained inward current, which consisted of 2 components; a picrotoxin (PTX)-sensitive main (75 - 95 %) component, and a Na^+-dependent minor (5 - 25 %) component.

PTX-sensitive current: The reversal potential of the PTX-sensitive I_{GABA} agreed well with the equilibrium potential for Cl^-, indicating that the receptor gates Cl^- channels. The current was not influenced by bicuculline (500 μM), pentobarbital (100 μM) and diazepam (100 μM). Baclofen (500 μM), a $GABA_B$ agonist, had no effect. *Cis*- and *trans*-4-aminocrotonic acid (CACA and TACA), GABAc receptor agonists, were effective. These results suggest that the PTX-sensitive I_{GABA} flows through a GABAc receptor channel. The reversal potential of GABA-induced voltage-responses recorded with a conventional intracellular technique was measured at approximately -30 mV. It is likely that GABA released from horizontal cells depolarizes *per se* through activating GABAc-gated Cl^- channels thereby facilitating the GABA release.

Na^+-dependent current: This current component was abolished by substituting LiCl for NaCl. The Na^+-dependent I_{GABA} was also dependent on the extracellular Cl^- concentration. The current was suppressed by nipecotic acid (100 μM) or SKF89976A (100 μM), neuronal-type GABA transporter inhibitors, while β-alanine, a glial-type GABA transporter inhibitor, at mM concentrations blocked the Na^+-dependent I_{GABA} to some extent. These results suggest that horizontal cells express a neuronal type of GABA transporter which takes up GABA from the synaptic cleft.

INHIBITORY ACTIONS OF ENDOGENOUS OPIOID PEPTIDES ON THE HYPOTHALAMIC AND PREOPTIC NEURONS IN THE JAPANESE QUAIL.

Y.Furukawa and K.Tsutsui. Physiol. Lab., Fac. Integrated Arts & Sci., Hiroshima Univ., Higashi-hiroshima.

For the expression of instinct behaviors, such as the aggressive behavior, the function of the hypothalamus and the preoptic area is considered to be essential. However, little information is available on cellular basis of such behaviors. To understand cellular mechanisms of the aggressive behavior, we started cellular analysis of the hypothalamic and preoptic areas in the adult male Japanese quail. In the present study, effects of three endogenous opioid peptides (Met-enkephalin, Met-enkephalin-RF and Leu-enkephalin, which were actually purified from avian brains; Kotegawa et al., Zool Sci 10:126, 1993) on the electrical activities of hypothalamic and preoptic neurons were examined in brain slices of the quail. All of the three opioid peptides inhibited the spontaneous firing activities of subsets of neurons. In a few cells, Leu-enkephalin rather potentiated the spontaneous activities, resulting in the increase of firing rates or the decrease of inter-burst intervals. These results together with the previous reports by others showing the existence of binding sites for opiates in avian hypothalamic regions suggest that there are opiate receptors in the subsets of hypothalamic and preoptic neurons, and that the depressant actions of endogenous opiates may regulate the aggressive behavior of the Japanese quail.

SYNAPTIC CONNECTION PATTERNS BETWEEN FROG RETINAL GANGLION CELLS AND TECTAL NEURONS

H. Nakagawa and N. Matsumoto Fac. of Computer Science and Systems Engineering, Kyushu Inst. of Technology, Iizuka

In frog, *Rana catesbeiana*, the synaptic connections between retinal ganglion cells and tectal neurons were examined by pulse-triggered averaging analysis. Activities of retinal ganglion cells (R1/2, R3, R4) were recorded extracellularly, while intracellular activities were recorded from tectal neurons using whole-cell recording technique *in vivo*.

In five tectal neurons, monosynaptic EPSPs from R3 retinal ganglion cells were observed. The mean latency was 0.7± 0.3 (mean ± SD) ms (n=7). The mean amplitude and 10-90% rise time were, respectively, 0.81 ± 0.33 mV and 2.2 ± 0.3 ms (n=7). One tectal neuron was found to receive EPSPs from both an R1/2 and R3 retinal ganglion cell simultaneously. The latency of the averaged EPSPs from the R1/2 and R3 retinal ganglion cells were 2.0 and 0.9 ms respectively. Their 10-90% rise time were 6.2 and 2.1 ms respectively. The long latency showed a possible disynaptic pathway from the R1/2 retinal ganglion cell. The long rise time suggests that the former makes synaptic contact far from the cell body of the tectal neuron, while the latter makes it close to the cell body.

AUTOXIDATION OF HUMAN HEMOGLOBIN

M. Tsuruga, A. Matsuoka and K. Shikama.
Biol. Inst., Fac. of Sci., Tohoku Univ., Sendai

The oxygenated form of HbA is known to be converted easily to the ferric met-form with generation of the superoxide anion. The met-species thus formed cannot be oxygenated and is therefore physiologically inactive. In comparison with myoglobin molecule as a monomer form, we have studied the autoxidation rate of HbA as a function of its concentration in 0.1 M buffer at 35 °C and in the presence of 1 mM EDTA.

At pH 6.5, HbA showed a biphasic autoxidation curve followed by first-order kinetics with the two independent rate-constants, k_f for the α-chain and k_s for the β-chain in the molecule. Under HbO_2 concentration of 1×10^{-3} M in heme, for instance, we obtained the values of $k_f = 0.052\ h^{-1}$ and $k_s = 0.0102\ h^{-1}$, indicative of the α-chain being much more susceptible to autoxidation than the β-chain by a factor of five.

In addition, we have found that the autoxidation rate of the α-chain was markedly enhanced by the dissociation of $\alpha_2\beta_2$ into $\alpha\beta$ dimers. The rate of the β-chain, on the other hand, was almost constant over a wide range of HbO_2 concentration of 1×10^{-3} M to 3×10^{-6} M in terms of the heme basis.

A PHOTOTRANSDUCTION MECHANISM IN CHICKEN PINEAL: CHARACTERIZATION OF PINEAL PHOTOSENSITIVE PIGMENT, PINOPSIN.

T. Okano[1], K. Yamazaki[1], Y. Fukada[1] and T. Yoshizawa[2]. [1]Dept. of Pure and Appl. Sci., College of Arts and Sci., Univ. of Tokyo, Tokyo and [2]Dept. of Information Systems Engineering, Fac. of Engineering, Osaka Sangyo Univ., Osaka.

A chicken pineal cell has a photon-signal transduction system which may be closely related to a circadian pacemaker regulating the rhythmic production of melatonin. Therefore, investigations of the pineal phototransduction pathway would be a fruitful approach to the molecular mechanism of the biological clock.

Recently, we have isolated a cDNA clone encoding a putative photoreceptive pigment in chicken pineal. The coded protein was named 'pinopsin' (opsin in pinealocyte). The RNA blot analysis revealed that the mRNA of pinopsin is transcribed only in the pineal among chicken tissues examined. Like rhodopsins and other cone visual pigments, pinopsin had a lysine residue in the seventh membrane-spanning helix, suggesting that pinopsin is a pineal photoreceptor molecule. To confirm this, the cDNA encoding pinopsin was subcloned into a eucaryotic expression vector (pREP4), and transfected into 293EBNA cells for production of pinopsin. After mixing with 11-cis-retinal, the expressed protein in the membrane fraction of the transfected cells was extracted with a buffer containing CHAPS and egg yolk phosphatidylcholine. The difference absorption spectrum of the extract before and after the irradiation with an orange light (>520nm) showed the λ_{max} at ~470nm in the presence of 10mM NH_2OH. We concluded that pinopsin is a photosensitive pigment in chicken pinealocytes.

THE ROLE OF CALCIUM AND CYCLIC AMP ON SPERM ACTIVATION AND CHEMOTAXIS IN THE ASCIDIAN, *CIONA SAVIGNYI*.

*M.Yoshida, *K.Inaba, **K. Ishida, and *M. Morisawa.
*Misaki Mar. Biol. Stn., School of Sci., Univ. of Tokyo, Kanagawa., and **Dep. of Urology, School of Med., Teikyo Univ., Tokyo.

The factor released from the egg of *Ciona savignyi* activates and attracts sperm (Yoshida *et al.*, 1993). Here, we partially purified the sperm-activating and -attracting factor (SAAF) from the egg seawater by ethanol extraction and subsequent separation with two-phase system of chloroform and water. The SAAF did not cause the activation of sperm motility and increase of cAMP in the sperm in CaFSW, but both motility activation and cAMP increase were induced when Ca^{2+} was added. T-type Ca^{2+} channel antagonist, flunarizine, inhibited the sperm activation by the SAAF.

Theophylline, a phosphodiesterase inhibitor, elevated cAMP concentrations of sperm and activated sperm motility in CaFSW. The theophylline-activated sperm were not attracted toward the glass capllary containing the SAAF in the tip of it in CaFSW, but attracted in the presence of Ca^{2+}. These results suggest that the SAAF induces the sperm activation by Ca^{2+} influx through T-type Ca^{2+} channel and increases in intracellular cAMP. Only Ca^{2+} regulates the chemotactic behavior of sperm in *Ciona*.

ROLES OF EXTERNAL OSMOLALITY AND INTRACELLULAR SALT CONCENTRATION ON THE INITIATION OF SPERM MOTILITY IN MARINE AND FRESH-WATER TELEOSTS

H. Takai and M. Morisawa
Misaki Marine Biological Station, School of Sci., Univ. of Tokyo. Kanagawa.

Spermatozoa of marine fishes and freshwater cyprinid fishes are immotile in the male reproductive tract, suppressed by the osmolality isotonic to the seminal plasma. Initiation of sperm motility is induced by exposure to hypertonic osmolality of seawater in marine fishes and hypotonic osmolality of fresh water in fresh-water fishes. (Morisawa and Suzuki, 1980). In the present study, when sperm motility of marine fish, puffer, was initiated in hypertonic solution, volume of sperm decreased, and intracellular salt concentration increased. Sperm of which the plasma membrane was removed with NP-40, were quiescent in the reactivation medium which contained salt concentration equivalent to the seminal plasma. Reactivation occurred when salt concentration of reactivation medium increased. In freshwater fish, zebrafish, initiation of sperm motility was induced in hypotonic solution and reactivation of the demembranated sperm occurred as the decrease in salt concentration of reactivation medium. These results suggest that changes in external osmolality are converted into a signal, increase or decrease in intracellular salt concentration, and that the signal affects flagellar axoneme, resulted in the initiation of axonemal motility.

Increase in intracellular pH (pH_i) has been considered to be a factor for the initiation of motility in marine teleosts (Oda and Morisawa, 1993). We show here that motility of puffer sperm was induced in isotonic medium when intracellular pH increased by the treatment with ionophore. Elevation of pH in reactivation medium caused the initiation of axonemal movement. However, increase in intracellular pH was not observed when sperm motility was induced in the hypertonic solution, suggesting that pH_i affects axonemal movement but may be not a physiological factor for the initiation of sperm motility in marine teleosts.

EFFECT OF SALT CONCENTRATION AND OSMOTIC PRESSURE TO THE NEUROMUSCULAR TRANSMISSION IN THE RED MUSCLE OF PECTORAL FIN OF FISH.

S. Shinogi[1], T. Hidaka[2]. Dept. of Biol., [1]Fac. of Sci. and [2]Fac. of Gen. Edu., Kumamoto Univ., Kumamoto.

The pectoral fin muscle of fish consists of red muscle fibers. By stimulating the spinal nerve innervating this muscle, three types of junction potential —excitatory junction potential (ejp), inhibitory junction potential (ijp) and diphasic junction potential (diphasic jp)— have been obtained intracellularly from the neuromusclular junction.

We studied the effect of external Na^+ concentration to the junction potentials in carp living in freshwater, in order to explain the differences among three ion characteristics of junction potential. We studied the change of salt concentration to the neuromuscular transmission in mutsugoro living in seawater of a half salt concentration, in order to explain the reciprocal relations between their habitats and the response by the salt concentration changes in physiological saline.

The result of the experiments was that the amplitude of three junction potentials decreased in every case of Na^+ concentration in both carp and mutsugoro. Na^+ concentration change decreased occurring frequency of miniature excitatory junction potential (mejp) in carp.

MORPHOLOGY OF NEURONS DISSOCIATED FROM THE PUPAL BLOWFLY ANTENNA IN CELL CULTURE

A.Nakagawa, A.Iwama, and A.Mizukami.
Tsukuba Research Center, SANYO Electric Co., Ltd., Ibaraki.

We have produced a primary culture of cells dissociated from pupal antennae of the blowfly, *Phormia regina*. Within 24 hr after plating, some cultured cells were found to regenerate new neurites. Then, vigorous outgrowth of neurites was observed. These cells exhibited more than one processes, sometimes with extensive branching. Cultured cells survived for more than two weeks. Antibodies against horseradish peroxidase (anti-HRP) has been described to label neuron-specific molecules over the entire neuronal surface in insects. We employed the anti-HRP antibodies to the cell cultures in order to recognize neuron-like cells and to visualize fine neuritic extensions. At least 3 types of cells were identified in the cultures based on the morphology, such as the growth pattern of neurites. The survival and growth of these cells were likely to be influenced by the presence of 20-hydroxyecdysone in the culture medium.

THE ACTION OF DUM NEURONS CONCERNING CHARACTERISTIC CHANGE OF MUSCLE CONTRACTION IN FEMALE CRICKET, *TELEOGRYLLUS COMMUDUS*.

M.Ueda and N.Ai. Dep.of Biol.,
Tokyo Gakugei Univ., Koganei,Tokyo

In adult female cricket, five clusters of DUM neuron are oriented on the dorsal surface of the last abdorminal ganglion (AG-V). We have already presented that these neurons innevate respectively to the tergal muscle(M4), the intervalvular muscle (M5,6) and the tergosternal muscle(M7) by back-filling staining. These neurons is examined by intracellular staining with Lucifer Yellow respectively. They have symmetrically branching inside of AG-V, and innevation to the target musclatuer with blanching along the seventh lateral root (N7). By using sulphide silver staining method, we observed that DUM neuron in AG-V, octopamine is clearly presented as neuromodulater. And so, as pharmacological observation, we examined with these monoamine treatments(proctolin, serotonin, epinephrine) on the effect of substances of secretion from DUM neurons for variation of neuromuscular activities.

NERVE NET FORMATION AFTER NERVE PRECURSOR CELLS ARE REINTRODUCED INTO NERVE-FREE HYDRA.

O.Koizumi, A.Sasaki and S.Minobe.
Physiol.Lab., Fukuoka Women's Univ., Fukuoka

Hydra has a simple nervous system consisting of a nerve net that extends through the body. We studied the nerve net formation in the regenerating head and budding head of hydra in the previous studies.

In this study, we have examined the nerve net formation in the repopulation system. Epithelial hydra that contains no nerve cells was produced. Hydra (*Hydra oligactis*) was treated with colchicine to eliminate all nerve precursor cells, interstitial cells. The resultant hydra could be maintained by force-feeding, eventually nerve free hydra, called epithelial hydra was obtained. After the interstitial cells were reintroduced into the epithelial hydra, we could see nerve net formation.

The nerve net formation in the hypostome was examined using RFamide antiserum and a monoclonal antibody RC9 specific to interstitial cells and ganglion cells. The nerve net formation started at the base of the hypostome, and later expanded to the apex in the repopulation system, while it occurred at the apex at first, and expanded to the base in the regenerating head.

GROWTH AND DIFFERENTIATION OF THE OPENER MUSCLE OF OVIPOSITOR IN FEMALE CRICKET, *TELEOGRYLLUS COMMODUS*.

T. Ai[1], M. Ogawa[2] and N. Ai[3]
1 Grad. Sch. Sci. Eng., 2 Grad. Sch. Poli. Sci., Saitama Univ., Urawa, Saitama., and 3 Dept. Biol., Tokyo Gakugei Univ., Koganei, Tokyo.

We have already reported that the opener muscle of ovipositor in female cricket is innervated by both motoneurons and DUM neurons of the terminal ganglion. During the last larval instar stage (LLI), the opener muscle and DUM neurons have well developed. Thus, these DUM neurons have been stained specifically by neutral red, and rER and Golgi apparatus have highly developed in the somata of DUM neurons. The other side the opener muscle starts to form the striation and evoke contraction yield by electrical stimulation after the last molt.

In this experiment, we examined the developmental process of the opener muscle by the tissue culture method. At first, we tried to determine the proper composition of tissue culture medium for the opener muscle. In such a culture medium, the opener muscle of 10 days after LLI (LLI-10) has not developed yet for 4 days culture. Being added to this medium with octopamine, however, the opener muscle of LLI-10 has developed and formed the striation.

These results suggest that octopamine secreted from DUM neurons may be deeply concerned in the growth and differentiation of opener muscles of ovipositor.

Distribution of SQSCI mRNA in tissues of squid *Loligo bleekeri*.
C. Sato, K. Hirota, T. Kimura, O, Shouno and Gen Matsumoto
Electrotechnical Laboratory, Supermolecular Science Division, Tsukuba, Ibaraki 305,

The sodium channel is a voltage-gated ionic channel essential for the generation of action potentials. In the previous papers, we reported the cloning of the cDNA, SQSCI, which encoded complete coding region of the putative sodium channel from squid optic lobe. The cDNA clone was characteristic of its shortest amino acid sequence among other sodium channels so far cloned and sequenced. Its length is almost 3/4 of those of rat sodium channels.

The transcriptional products were detected in all the nervous systems examined; optic lobes, cerebral ganglia and giant stellate ganglia. However, it was not detected in the muscle, suggesting the SQSCI gene is specific for sodium channels of squid nerve cells. SQSCI is more widely distributed in the nervous system than the GFLN1 which was known as specifically expressed in stellate ganglion of the squid (Rosenthal and Gilly, P. N. A. S. USA 90, 10026-10030, 1993).

CHARACTERIZATION OF THE *UNC-18* GENE PRODUCT IN THE NEMADODE *C. ELEGANS*.
H.Ogawa[1], T.Sassa[2], I.Hori[3], T.Kobayashi[1] and R.Hosono[4]. [1]Fujita Health Univ., [2]Tokushima Univ., [3]Kanazawa Med. Univ., [4]Kanazawa Univ.

It is suggested that the *unc-18* gene product (UNC-18) plays an important role in the synaptic transmission of *C. elegans*. To clarify its function, the coding region of *unc-18* cDNA was introduced into *Spodoptera frugiperda 21* cells with baculovirus and UNC-18 was over-expressed. The expressed UNC-18 occupied about 40% of the total proteins in the insect cells infected with the recombinant virus. Most of UNC-18 was collected in the soluble fraction of the cells by ultracentrifugation. The immuno-electron microscopic observation revealed that this protein widely distributed in cytosol. This results are coincident with the observation that the protein is hydrophilic and therefore may be localized in the cytoplasm as soluble form. UNC-18 was purified to be almost homogenous by the following purification steps: 100k x g centrifugation, DEAE- and CM-Sepharose tandem column, PEG_{4000} precipitation, and Sephacryl S-200 column. This protein was a monomer of 67kD and its isoelectric pH was 7.0. It was assumed from the amino acid sequence of UNC-18 that the protein could be phosphorylated by protein kinase A, casein kinase II and protein kinase C, but the purified protein was phosphorylated only by protein kinase C. Phosphorylation occurs with the exclusive phosphoamino acid being threonine and serine at least four distinct sites on UNC-18. The role of the phosphorylation in the synaptic transmission is now in progress.

SEROTONIN PHASE-SHIFTS THE CRICKET OPTIC LOBE CIRCADIAN PACEMAKER *IN VITRO*
K. Tomioka. Dept. Biol., Fac. Sci., Yamaguchi Univ., Yamaguchi.

Serotonin is one of the major putative neurotransmitters active in insect optic lobes. We have so far shown that serotonin content in the optic lobe, the circadian pacemaker tissue, of the cricket *Gryllus bimaculatus* fluctuates in a circadian manner and regulates the responsiveness of the visual interneurons in the tissue. To examine whether the serotoninergic system involved in the circadian pacemaker system, we have examined the effect of exogenous serotonin application on the phase of the optic lobe pacemaker. We continuously recorded neural activity from the optic stalk of an isolated optic lobe-compound eye system kept *in vitro* using an oil gap chamber. Under constant darkness the neural activity showed a clear circadian rhythm, peaking at the beginning of the subjective night. When exogenous serotonin was applied for 6 hrs in the incubation medium, a phase-shift of the pacemaker as well as a reduced neural activity were induced. The phase shift occurred not only in a dose-dependent manner but also in a phase dependent manner: delay shifts were induced by the treatment during the subjective night, while advance shifts occurred during the subjective day. The phase response curve is similar to that induced by a mutual interaction between pacemakers. These data suggest that serotonin is a potent regulator of the pacemaker system and may be involved in the mutual entrainment pathway.

LOCALIZATION OF CIRCADIAN PACEMAKER WITHIN THE OPTIC LOBE AND ITS OUTPUT PATHWAY IN THE CRICKET.
H. Mori, K. Tomioka. Dept. Biol., Fac. Sci., Yamaguchi Univ., Yamaguchi.

Although the circadian pacemaker driving the locomotor rhythm resides in the optic lobe in the cricket *Gryllus bimaculatus*, its location within the optic lobe is still unknown. The optic lobe consists of three neuropiles, i.e. lamina, medulla and lobula, from distal to proximal. In the present experiment, we examined the effects of partial destruction of one optic lobe following removal of the contralateral one on the locomotor rhythm to localize the pacemaker within the optic lobe. Assay of the locomotor rhythm was performed under constant darkness at a constant temperature of 26°C. Removal of outer two neuropiles, lamina and medulla, resulted in a loss of rhythmicity in all the operated animals. When lamina was removed, more than 70% of the operated animals were rhythmic. However, after partial removal of the medulla, ratio of rhythmic animals significantly decreased. These results suggest that the medulla region is the likely locus of the pacemaker. We then attempted partial destruction of the optic stalk near the medulla to reveal the output pathway for driving the locomotor rhythm. The rhythm immediately disappeared in a majority of the animals, receiving the destruction of dorsal half of the stalk while it survived the lesion of ventral half of the optic stalk. These results suggest that the output pathway of the pacemaker runs dorsal side of the stalk near the medulla.

ANALYSIS OF NEURONS INVOLVED IN MUTUAL INTERACTIONS BETWEEN CRICKET OPTIC LOBE CIRCADIAN PACEMAKERS
M. Yukizane, K. Tomioka. Dept. Biol., Fac. Sci., Yamaguchi Univ., Yamaguchi.

In the cricket *Gryllus bimaculatus*, the circadian locomotor rhythm is driven by two, bilaterally paired optic lobe circadian pacemakers. The pacemakers interact one another to keep their synchronous movement and a stable temporal structure in animal's behavioral rhythm. The mutual interaction includes mutual entrainment and mutual activity suppression during the subjective day phase. Both are mediated by the neurons running the ventral side of the optic stalk. Most of them are large bilateral neurons with their somata near proximal region of the medulla and their axons project to the contralateral medulla. Single unit analysis with intracellular recording and staining with Lucifer yellow CH injection revealed that those neurons are light-sensitive neurons. They have a particular receptive fields in the ipsilateral compound eye which is roughly corresponds to their dendritic field. To examine their role in mutual interaction, we examined the effects of partial destruction of the compound eye on the mutual interaction appearing in the locomotor rhythm. The results obtained suggest that the neurons with receptive field in the dorsal posterior region are involved in the mutual entrainment, but the phase dependent suppression of activity is mediated by a mechanism irrespective of the visual field.

PHARMACOLOGICAL ANALYSIS OF THE MONOSYNAPTIC SENSORY INPUT TO A NONSPIKING NEURON OF CRAYFISH
A. Takashima and M. Takahata. Div. Biol. Sci., Grad. Sch. Sci., Hokkaido Univ., Sapporo

We studied pharmacological properties of the monosynaptic input to LDS interneuron, an identified sensory nonspiking cell in the terminal abdominal ganglion of the crayfish *Procambarus clarkii* Girard by perfusing acetylcholine (ACh) agonists. LDS interneuron receives direct mechanosensory input from the cuticular surface of the tailfan. The synaptic response to electrical stimulation of the third sensory bundle was recorded by a microelectrode which impaled the cell at its thick transverse neurite near the midline. The abdominal nerve cord was isolated from the rest of the body to be used as the preparation.

Perfusion of 0.1mM oxotremorine or 0.1mM pilocarpine, ACh agonists in the vertebrate muscarinic synapse, caused a reduction in the peak amplitude of the synaptic response. They had no effect on the membrane potential. Perfusion of 1mM carbachol, an ACh agonist in the nicotinic synapse, also caused a reduction in the amplitude of the synaptic response and a sustained depolarization of the cell. The suppressive effect of carbachol on the synaptic response of LDS interneuron therefore seemed to be based on a decrease in the sensitivity of ACh receptors due to their prolonged exposure to the ACh agonist. The absence of membrane potential change during the perfusion of muscarinic agonists suggests that they do not act directly on the interneuron membrane. Perfusion of carbachol after the synaptic input to LDS interneuron was suppressed under the low-Ca^{2+}, high-Mg^{2+} condition caused the similar depolarization. This finding further confirms that the interneuron membrane has ACh receptors which resemble the nicotinic receptor of vertebrates in the sensitivity to ACh agonists.

PHARMACOLOGICAL STUDY ON THE SYNAPTIC TRANSMISSION BETWEEN MECHANOSENSORY AFFERENTS AND ASCENDING INTERNEURONS OF THE CRAYFISH

T. Ushizawa, T. Nagayama and M. Takahata
Div. Biol. Sci., Grad. Sch. Sci., Hokkaido Univ., Sapporo

In the crayfish, twenty-four in about 60 ascending interneurons which originate in the terminal abdominal (6th) ganglion have been identified. A constant short central delay of 0.7-1.5ms indicates that they receive direct excitatory inputs from mechanosensory afferents originating from the cuticular hairs on the uropod surface. The amplitude of excitatory postsynaptic potential (EPSP) evoked by a single hair movement was increased by hyperpolarization. The input resistance during the EPSP was decreased. These findings indicate that the connection between the afferents and the interneuron is chemically mediated. We studied the pharmacological properties of this synapse.

One of the candidate substances is acetylcholine (ACh). Pharmacological experiments were performed by bath application of drugs. By perfusing the isolated 6th abdominal ganglion with cholinergic antagonists, curare (1mM) and atropine (1mM), the peak amplitude of the EPSPs generated by electrical stimulation of 2nd sensory bundle was reduced. Perfusion of cholinergic agonists, nicotine (10μM) and carbachol (100μM), also caused a reduction in the EPSP amplitude. Since nicotinic agonists caused a sustained depolarization of interneurons, the suppressive effect of these drugs on the synaptic response seemed to be based on the desensitization of receptors on the interneurons. Each single drug affected several kinds of interneurons in the same way. These results suggest that the mechanosensory afferents release ACh as the neurotransmitter to activate the nicotinic receptors on the ascending interneurons. The muscarinic agents presumably acted on the presynaptic sensory terminal to suppress indirectly the synaptic response of interneurons.

IMMUNOCYTOCHEMICAL EVIDENCE FOR THE GABAERGIC INNERVATION OF THE STRETCH RECEPTOR NEURONS IN *LIGIA EXOTICA*.

A. Niida, M. Nakakubo, and T. Yamaguchi. Dept.of Biol., Fac. of Sci., Okayama Univ., Okayama.

GABAergic innervation of the stretch receptor neurons of the Isopoda *Ligia exotica* has been investigated by means of light microscope immunocytochemistry using an antibody to GABA. The stretch receptor is supplied by one principal GABA-immunoreactive axon, which gives off several branches that innervate two types of stretch receptor neurons as well as a receptor muscle. Whole-mount preparation revealed a massive GABAergic innervation of fast adapting stretch receptor neurons. The stout dendritic region of the fast adapting stretch receptor neuron was profusely covered by GABA-immunoreactive varicose fibers but there was no such immunoreactive fibers in the cell body and in the initial axon segment. Likewise, GABAergic innervation of the slowly adapting stretch receptor neuron was found throughout its branching dendrites which run in both directions along total length of the receptor muscle.

CRAYFISH SPIKING LOCAL INTERNEURONES: MORPHOLOGY AND FUNCTIONAL PROPERTIES

T. Nagayama and H. Namba. Anim. Behav. & Intel., Div. of Biol. Sci., Grad. Sch. of Sci., Hokkaido Univ., 060 Sapporo.

Twenty spiking local interneurones are identified by their gross morphology and physiological properties, including sensory inputs from the uropod and their outputs onto the uropod motor neurones. Morphologically, the spiking local interneurones can be divided into three groups based on the position of their cell bodies: anterior (sp-ant), medial (sp-med), and posterior(sp-pos). All interneurones of the medial group have profuse bilateral branches. The main branches of interneurones of the other groups usually extend on the side contralateral to the cell body. Physiologically, all receive excitatory exteroceptive inputs directly from the afferents innervating the exopodite on the side ipsilateral to their main branches. Some interneurones also receive direct excitatory proprioceptive inputs from afferents innervating a chordotonal organ in the tailfan. They are usually silent, and spike only in response to sensory stimulation. Trains of spikes induced by current injection tend to increase the activity of the closer motor neurones and decrease that of the opener motor neurones. Simultaneous intracellular recordings show that spikes of certain spiking local interneurones elicit a short and constant latency (less than 1 msec) IPSPs in the nonspiking local interneurones. The connection is direct and chemically-mediated.

ACTIVITY OF MUSHROOM BODY NEURONS OF FREELY WALKING COCKROACHES.

M. Mizunami[1], J. IKEDA[1] and N. J. STRAUSFELD[2]. [1]Lab. of Neuro-Cybernetics, Res. Inst. for Electronic Sci., Hokkaido Univ., Sapporo and [2]Arizona Res. labs., Div. of Neurobiol., Univ. of Arizona, Tucson, USA.

Enamel-coated copper wires were implanted chronically into the mushroom body of the cockroach, *Periplaneta americana*, and unit activity was recorded while the cockroach walked freely in an arena. After the experiment, copper ions were impregnated by passing a positive current to reveal profiles of neurons in the vicinity of the electrode tip. Units recorded in the MB's input area (the calyces) were exclusively sensory, responding to visual, olfactory or mechanical stimulations. Motor-associated units, which were active during locomotion, and motor preparatory units, whose activity was preceded the initiation of a specific locomotory action, were recorded from output neuropils (the pedunculi and lobes). The results suggest that mushroom bodies participate in the control, and possibly planning, of locomotory behaviors.

THE CONTROL OF COMPENSATORY EYESTALK MOVEMENTS OF THE CRAYFISH PROCAMBARUS CLARKII, DURING WALKING.

Hiroyuki FURUDATE, Yoshinori OKADA and Tsuneo YAMAGUCHI
Department of Biology, Faculty of Science, Okayama University, Okayama, Japan.

In either of intact and statolith-ectomized crayfishes, freely walking was found to be accompanied by eyestalk movements as well as by rolling, yawing, and pitching of the body itself. That is, the eyestalks showed the compensatory movements toward the directions opposite to those of body tilts in roll, yaw, and pitch. The amplitude of compensatory eyestalk movements in roll during freely walking was larger in intact animals than in statolith-ectomized animals. In tethered intact animals the eyestalks responded to sinusoidal body tilts under the dark or bright condition, and the amplitude of responses was larger during freely walking than during standstill. In statolith-ectomized animals the eyestalks responded both to sinusoidal body tilts in roll under dorsal illumination and to tilts of a substrate under the walking legs. In intact and statocyst-ectomized animals the amplitude of responses was larger during tetherd walking than during standstill. These results suggest that the compensatory eyestalk movements during walking are not only under the influence of orientation cues, such as gravitational, visual, and substrate inputs, but also under the influence of outputs from the walking motor center.

ASSOCIATIVE LEARNINGS OF *LYMNAEA STAGNALIS*.

S. Kojima and E. Ito.
Lab. Animal Behav. Intel., Div. Biol. Sci., Grad. Sch. Sci., Hokkaido Univ., Sapporo.

Pond snail (*Lymnaea stagnalis*) can show some associative learnings with trainings by combination(s) of physical and chemical stimulation. Physical stimulation, such as a light irradiation and a mild spit stroke upon the shell or the head, induce a change in the behavioral pattern. Chemical stimulation like sucrose (a sweet taste for man), 10mM NaCl (salty) and 10mM sodium glutamate (*umami*) increase a taste-attraction behavior. This behavior was defined as continuous feeding responses (bites). On the other hand, quinidine sulfate (bitter), acetate (sour) and KCl (salty and bitter) evoke a taste-aversion behavior, which is a withdrawal of its body into the shell. The quinidine and the acetate can be received by the body surface of *Lymnaea* as well as by its lip, with being affected by pH change of its circumstance.

The procedures of the associative learnings with above stimulation are as follows. (1) Classical conditioning: Light irradiation (conditioning stimulus, CS) and sucrose to a lip (unconditioning stimulus, UCS) are simultaneously applied. Mild spit stroke (CS) and sucrose (UCS) can also be used for this conditioning. (2) Taste-aversion conditioning: KCl (UCS) was applied following sucrose (CS). (3) Sensory preconditioning: Two CS's and one UCS used in (1) are associated. (4) Operant conditioning: Sucrose was rewarded, whenever *Lymnaea* put its head out of water.

MORPHOLOGICAL FEATURES OF PROCEREBRAL LOBE OF THE SLUG, *LIMAX MARGINATUS*.

H. Suzuki, T. Kimura, T. Sekiguchi, A. Yamada, E. Kono, Tsukuba Research Center, SANYO Electric Co. Ltd., Tsukuba.

The terrestrial slug, *Limax marginatus*, possesses a pair of procerebral (PC) lobes which locate on both lateral sides of the cerebral ganglia. We have reported previously that the PC network plays important roles in their olfactory behavior and recognition, whereas the detail structure of PC lobe is still unclear, besides the PC lobe consisted of cell layer, medial mass and inner mass. In this study, we investigated the structure of PC lobe using various morphological techniques.

Three types of input fibers were observed in the PC lobe. The one type of fibers was arising from neurons in the tentacle tip and terminated in the medial mass. The others were 5-HT and FMRFamide like immunoreactive fibers. From the results of GOLGI staining, it was revealed that a large amount of monopolar interneurons in the cell layer, which were the PC intrinsic neurons, projected their processes into the inner mass through the medial mass.

MOTOR OUTPUT DURING THANATOSIS IN THE CRICKET *Gryllus bimaculatus*.

H. Nishino and M. Sakai, Dept. of Biol., Fac. of Sci., Okayama Univ.,Okayama.

The cricket *Gryllus bimaculatus* shows an immobile posture with all the legs flexed in response to a light pressure on the prothorax (Zool. Sci. 1987, 1991). This posture is maintained for 3-4min without respiration. To examine which muscles are concerned and in what manner they contract, electromyographic recording was made from the femoral muscles in the hindleg under different conditions, free-moving, rest, and thanatosis. The results showed that the phasic component recorded from the proximal region was inactive during thanatosis, while the tonic component kept active as during the rest. These results reveal that the flexed posture during thanatosis in the cricket is maintained by the mechanism different from that of the weta by which the defense posture is maintained.

OLFACTORY REPRESENTATION IN THE OUTPUT REGION (INNER MASS) OF PROCEREBRAL LOBE IN THE SLUG BRAIN.

T. Kimura, H. Suzuki, E. Kouno, A. Yamada and T. Sekiguchi, Tsukuba Research Center, SANYO Elect. Co. Ltd., Tsukuba.

It has been considered that the procerebral (PC) lobe in the brain plays important roles in olfactory recognition and learning in the slug. Many of the PC interneurons of which cell body located in the PC cell-layer project a fine process into the inner mass (IM) which is a PC neuropile connecting with mesocerebral neuropile. To reveal how mesocerebral interneurons interpret the odor information represented on the PC lobe, we investigated the olfactory responses of the PC inner mass.

When local field potential (LFP) was recorded from the whole IM by a suction electrode, a spontaneous oscillatory activity was observed. The LFP oscillation recorded from IM always synchronized to that from the cell layer. Thus, it is considered that the IM oscillation is originated from that occurred in the PC interneurons. In addition, stimulation using an aversive conditioned odor decreased the frequency of IM oscillation, and induced a stabilization of the wave form which had usually fractured spontaneously. This fact suggests that odor information within the IM also represented on the oscillatory activity as same as that within the cell-layer.

WING FLUTTERING DURING THE ORIENTATION WALKING TOWARD THE ODOR SOURCE IN A SILKWORM MOTH, *BOMBYX MORI*.

R.Kanzaki, T.Ariyoshi and M.Ueno
Inst. of Biol. Sci., Univ. of Tsukuba, Tsukuba, Ibaraki

Male moths *Bombyx mori* shows a characteristic zigzagging walking with wing fluttering in response to the pheromones. We suggest that the walking is controlled by a self-generated turning programs (Zool.Sci.9:515). Although their body is too heavy to fly, the moths could show similar zigzagging movements on the ground only by their wing vibration when all the legs were dissected.

High-speed video analysis revealed that wings on the outside of the turn were remoted at the bottom of the stroke and wings on the inside of the turn were remoted at the top. Thus, changes in phase of wing remotion to wing depression were related to the zigzagging turning.

Motor activity patterns of wing depressor muscles (DLMs) and steering muscles, i.e. 3rd axillary muscles (3AXMs), which remote the wings, were electrophysiologically recorded simultaneously during the tethered flight. 3AXMs were activated at the same phase with DLMs during the inside turn, while out of phase relationship was elicited during the outside turn. It seems that the *Bombyx* uses a wing system similar to flying moths. Results of air stream analysis using a smoke jet during the zigzagging movements also support the idea.

Intermittent pheromonal stimulation elicited regular changes in the phase relationship between these muscles. We predict that the self-generated turning programs also affect the wing system of *Bombyx* males.

PIT-CONSTRUCTION BEHAVIOR BY ANTLION LARVAE

S. Miyagawa and K. Taneda. Dept. of Biol. Fac. Sci. Kochi Univ., Kochi

Pit-construction behavior by antlion larvae was observed. The behavior consists three stages. (1)The specimen moves backwards under the surface of the sand in what appear to be random directions . (2)It then moves in a circular path during which it flicks sand to the outside of the circle. (3)It deepens and expands the furrow it creates, until a conical pit is formed. At 2nd stage, the specimen flicks sand to the outside of the circle. However, when it moved along the circular wall, it flicks sand to the inside of the circle. A posture of the specimen under the sand is not visible, so its behavior on the substratum without sand was recorded on VTR. The bending angle of the head was measured using a video projector and a digitizer in both cases when the specimen moved in a circular path and when it moved along the circular wall. The result suggests that the difference in both behaviors described above is due to the difference in the bending angles of the head. Moreover, the bending angle was closely correlasted with the radius of the circular path. The flicking angle of the sand was measured using the sand-filled container. The angle was also correlated with the radius of the circular path. Consequently, the flicking angle of the sand by antlion larvae seems to be due to the bending angle of the head. Removal of the sensory hairs at some portions of the body surface altered the flicking angle of the sand.

The genital photoreceptor of the male butterfly is necessary for establishment of the copulation.

Daisuke Suyama, Kentaro Arikawa, and Eisuke Eguchi
Department of Biology, Yokohama City University, Yokohama 236.

The mating behavior of a swallowtail, *Papilio xuthus*, can be divided into eight steps: the male 1. finds a female, 2. touches the female with the legs, 3. curls the abdomen and opens the valva, 4. get the position 'face to face' with the female; 5. seeks the female's genitalia with the own genitalia, 6. grasps the female's genitalia with the valva, holding the female between the wings, 7. copulates, and 8. the mates separate after about 1 h of copulation time.

We have found in the male that the light stimulation of the genitalia induces valva-opening response, which appears e.g. at step 3 of the mating behavior, suggesting that the genital photoreceptors (GPs) are somehow involved in controlling the mating behavior.

In this study we video-taped and closely observed the mating behavior of males with the fixed females in the cage. The GP input of the males was ablated by heating the photoreceptive sites with the fine soldering iron or by covering the site with opaque material. Despite the methods of operation, the mating behavior of the operated males stopped before the step 6, although they could normally copulate if hand-paired with virgin females. The results indicate that the GP is required for stabilizing the copulation posture.

PHENOLOXIDASE-LIKE ACTIVITY IN ASCIDIAN HEMOCYTES.

K. Azumi, S. Hata, and H. Yokosawa. Dept. of Biochem., Fac. of Pharmaceutical Sci., Hokkaido Univ., Sapporo.

We have previously reported that hemocytes of the solitary ascidian, *Halocynthia roretzi*, have several DOPA-containing peptides including antimicrobial substances, halocyamine A and B. We also found in *H. roretzi* hemocytes a phenoloxidase-like activity toward 4-methylcatechol, a substrate for insect phenoloxidase.

To define whether a prophenoloxidase-like enzyme exists in hemocytes or plasma of *H. roretzi*, we measured its activity in hemocyte extracts prepared with 10 mM EDTA and with 2 mM DFP. Both the extracts showed almost the same phenoloxidase-like activity as that in the extract prepared without inhibitors. It was also found that a phenoloxidase-like activity was undetectable in plasma treated with LPS, β1-3 glucan, or zymosan (100 μg/ml), and also in intact plasma. Halocyamines exist in only one type of hemocytes named vacuolated cells. Phenoloxidase-like activity was found to be detected only in the extract of the vacuolated cells which were separated by percoll gradient centrifugation. Thus, we conclude that a phenoloxidase-like enzyme exists in hemocytes but not in plasma of *H. roretzi* .

ALLO-RECOGNITION IN THE ASCIDIAN, H. RORETZI: HEMOCYTES RELEASE PHENOLOXIDASE IN RESPONSE TO NON-SELF EGGS

N. AKITA & M. HOSHI

Dept. of Life Sci., Tokyo Inst. of Tech., Yokohama

Two types of allo-recognition are known in the ascidian, H. roretzi; self-sterility in gametes and contact reaction in hemocytes. We have reported that 'contact reaction" is accompanied by a respiratory burst due to phenoloxidase released from hemocytes. We found that the hemocytes similarly release phenoloxidase when they are mixed with non-self, but not with self, oocytes. This result suggests a common mechanism underlying allo-recognition of the ascidian, both in gametes and in somatic cells.

TISSUE DISTRIBUTION AND BIOLOGICAL FUNCTIONS OF THE ANTIGEN RECOGNIZED WITH THE ANTIBODY THAT INHIBITS ASCIDIAN CELLULAR DEFENSE REACTIONS.

H. Takahashi, K. Azumi, and H. Yokosawa. Dept. of Biochem., Fac. of Pharmaceutical Sci., Hokkaido Univ., Sapporo.

We have previously reported the production of a monoclonal antibody (A74) that inhibits hemocyte aggregation in the ascidian *Halocynthia roretzi*, and characterized the antigen recognized with the A74 antibody. The A74 antigen was found to be a glycoprotein with the molecular mass of 160 kDa.

In this study, we analyzed the localization of the A74 antigen in various tissues of *H. roretzi*, and also the inhibitory effects of the A74 antibody on phagocytosis and fertilization in *H. roretzi*. Immunocytochemical and western blot analyses indicate that the A74 antigen is widely distributed in various tissues of *H. roretzi* such as ganglia and muscles, and also in *H. roretzi* eggs and embryos at various developmental stages. It was also found that the A74 antibody strongly inhibited the phagocytosis of sheep erythrocytes by the hemocytes and also the fertilization of the eggs. Thus the A74 antigen, which is widely distributed, may play basic and important roles in various biological systems.

THE FINE STRUCTURE AND PHAGOCYTIC ABILITY OF HEMOCYTES OF *HALOCYNTHIA HISPIDA*

S. Ohtake[1], T. Abe[1], F. Shishikura[1], K. Tanaka[1] and M. Arai[2]. [1]Dept. of Biol., Nihon Univ. Sch. of Med., Tokyo and [2]Dept. of Biol. Sci. Tech., Sci. Univ. of Tokyo, Chiba

The hemocytes of *H. hispida* were classified by light and electron microscopy and the phagocytic ability of these hemocytes was studied *in vitro*. Three types of granular amebocytes, five types of vacuolated or vesicular cells and lymphoid cells were usually observed in the hemolymph. The granular amebocytes, SG1, SG2 and LG, were distinguished from each other by the size, stainability and electron density of the granules in their cytoplasm. The vacuolated or vesicular cells were distinguished from each other by the size of vacuole and the nature of inclusion. SG1 and SG2 ultrastructurally resembled the small granular amebocyte and LG resembled large granular amebocyte of *Halocynthia roretzi*. Other types of hemocytes also ultrastructurally resembled the hemocyte of *H. roretzi*. Freshly collected hemolymph was incubated at 23 °C for 30 min with glutaraldehyde treated SRBC, Latex beads (φ1, φ5 μm) suspended in Pantin's artificial sea water (HEPES, pH 7.2) and examined by light and electron microscopy. SG1 actively phagocytosed all kinds of the particles. Small parts of SG2, LG and V1 ingested small Latex beads and their activities were weaker than SG1. We found no particles in other types of hemoyctes.

THE QUANTITATIVE ASSAY OF ALLOGENEIC REACTION OF *HALOCYNTHIA RORETZI*

M.Arai[1],Y.Ohga[1],S.I.Ohtake[2],K.Tanaka[2] and J.Chiba[1]
[1]Dept. of Biol. Sci. Tech., Sci. Univ. of Tokyo, Chiba 278,
[2]Dept. of Biol., Nihon Univ. Sch. of Med., Tokyo 173

Coelomic cells (CC) of a solitary ascidian, *Halocynthia roretzi*, exhibit an allogeneic cell reaction (ACR) /contact reaction. Contact of isolated CC from different individuals *in vitro* results in their reciprocal lysis. We developed a novel method for quantitative assay of ACR using a fluorescent viability stain, calcein AM (CAM). CC from different individuals were incubated for 30 min in the dye-containing medium and then washed. After mixing of CAM-labeled CC, intensity of fluorescence was measured with a fluorescence multiple plate scanner, Fluoroscan II (Flow Lab.). Significant decrease of intensity of fluorescence (IF) was observed at 5 min after mixing of $2x10^6$ cells from allogeneic two individuals and maximum decrease of IF was observed by about 150 min after mixing. No significant decrease of IF was observed when autologous or non-allogeneic CC were reacted. This fast, sensitive and quantitative method would be useful for analysis of ACR *in vitro*.

THE RELATIONSHIP BETWEEN HEMOCYTE LYSIS AND PLASMA GELATION IN HEMOLYMPH COAGULATION OF THE SPINY LOBSTER, *PANULIRUS JAPONICUS*.

H. Aono National Research Institute of Aquaculture, Mie

In hemolymph coagulation of crustaceans, cytolysis of hemocytes occurs followed by gelation of hemolymph. The relationship between these two steps was examined in *Panulirus japonicus* by *in vitro* experimental systems utilizing hemocytes, plasma and serum. The liquid fraction of hemolymph drawn with anticoagulant was used as plasma, while supernatant from centrifuged coagulated hemolymph was used as serum. To examine the effect of Ca^{2+}, plasma and serum were dialyzed against buffer with Ca^{2+} (plasma$^+$, serum$^+$) or without Ca^{2+} (plasma$^-$, serum$^-$). The cytolytic activity was assessed microscopically by adding plasma or serum to hemocytes in a microwell plate. Gelation was tested by mixing plasma or serum with hemocytes in a test tube. Plasma$^+$ was cytolytic to hemocytes, and the plasma$^+$ gelled rapidly after mixed with hemocytes. Plasma$^-$ showed neither cytolytic activity nor gelation. However, the plasma$^-$ with hemocytes gelled after hemocytes were ruptured manually and Ca^{2+} was added. Serum$^+$ had cytolytic activity, but gelation did not occur. Serum$^-$ did not show cytolytic activity, and no gelation was detected. These results indicate that cytolytic activity of plasma and serum is Ca^{2+}-dependent, and plasma gelation requires both Ca^{2+} and factor(s) released from lysed hemocytes. In addition, an essential coagulogen present in plasma is required as shown by the lack of gelation in serum$^+$. Therefore, hemolymph coagulation is a cooperative two step process requiring hemocyte lysis which releases an essential factor activating the coagulogen found only in plasma followed by gelation.

ALLOGENEIC RECOGNITON BY MACROPHAGE-LIKE CELLS OF THE LAND SLUG, INCILARIA FRUHSTORFERI

K. Yamaguchi, E. Furuta and A. Shimozawa
The Lab. of Med. Sci. and Dept. of Anat., Dokkyo Univ. Sch. of Med., Tochigi

There have been only two reports on allo-recognition immunity in molluscs. The snail could not reject allografts (digestive glands) while the land slug could reject allografts (gonads) although the reaction might be depending on the site of transplantation. It is practically difficult to perform transplantation experiments in molluscs especially in the land slug. So, in this study, we examined the presence or absence of allo-recognition ability in hemocytes of the land slug, Incilaria fruhstorferi, using in vitro co-cultivation of hemocytes that were collected from two other individuals. Before collection of hemocytes, yellow-green latex beads were injected into the hemocoel of slug A and red beads into slug B. Hemocytes of slug A which spread over the surface of the dish changed their shape into round by the addition of hemolymph of slug B. When the hemocytes were mixed, hemocytes of slug A did not contact strongly with those of slug B. These results suggest that the hemolymph of land slug makes the hemocytes of other individuals lose the phagocytic function.

Presence of cytokine-like molecules in the land slug.

E. Furuta[1], K. Yamaguchi[2], and A. Shimozawa[1]
[1]Dept. of Anat. and [2]Lab. of Med. Sci., Dokkyo Univ. Sch. of Med.

The major system of host defense in the land slug is a cellular response. The hemolymph of the slug includes macrophage-like(Mϕ), lymphocyte-like(Ly) and fibroblast-like cells(Fb). Of these three cells Mϕ and Fb are involved in phagocytic reaction. The number of blood cells rapidly increases after injection of foreign materials. The cells were phagocytic and they detached from the linning cells of hemocoel wall which consists mainly of fibroblasts. Little is known about their regulation or control. IL-1α and TNF-α are major immunoregulatory molecules produced by macrophages and other related cells. They are act as the molecular constituents of non-specific host defense mechanisms against multiforious insults. When the blood cells from normal or from yeast-injected slug were treated with anti-human IL-1α and TNF-α monoclonal antibody, these molecules were present in blood cells with phagocytic activity. These data show the presence of cytokine-like molecules in the land slug and suggest that cytokines are important, ancient, and functionally conserved molecules.

TRANS-EPITHELIAL ELIMINATION OF INTRAPERITONEALLY INJECTED FOREIGN MATERIALS BY PHAGOCYTES IN CYPRINID FISH, CARASSIUS AURATUS and PUNTIS TETRAZONA

H.Nakamura and A.Shimozawa. Dept. of Anat.,Dokkyo Univ. Sch. of Med.,Mibu,Tochigi

In our previous studies of the medaka skin, intracutaneously injected carbon particles and sheep red blood cells were phagocytosed by macrophages and eventually eliminated from fish skin's surface by cellular transport. In this study, a possible role of trans-epithelial elimination of intraperitoneally injected foreign materials was examined in cyprinid fishes Carassius auratus and Puntis tetrazona. Five to 6 days after carbon injection, the abdominal part of the fish skin became blackish. Histologically, injected carbon particles were first taken up by macrophages, and within 5 days of injection, some of them were translocated in the epithelium of the abdominal part of the skin and freed from the skin's surface. The skin of the abdominal wall may play some part in trans-epithelial elimination of intraperitoneally injected foreign materials in cyprinid fish.

MORPHOLOGICAL ASPECTS OF THE INITIAL PHASE OF CELLULAR ENCAPSULATION IN SAMIA CYNTHIA RICINI

Sohji Takahashi, Department of Biology, Nara Women's University.

The globule of silicon oil is encapsaulated by hemocytes, when a small quantity (10ul) of it is injected into the larva of Samia cynthia ricini. The initial phase of the encapsulation was examined by SEM. Within 2-3 min after injection, the oil globule was coated with gelatinous clot, to which granulocytes attached. These cells disintegrated and released granules. Within several hours, network structure appeared around the oil surface, resulting in the formation of the innermost layer of the capsule. Melanization did not occur. This type of encapsulation seems to be elicited by activation of humoral components, to which granulocytes attached. Hemolymph coagulation will constitutethe first phase of the encapsulation.

EFFECTS OF GASTRIC DISTENTION ON APOMORPHINE-INDUCED EMESIS IN FROGS

C.Suzuki and T.Naitoh. Dept. of Biol.,Fac. of Sci., Shimane Univ., Matsue.

It has been reported that the frog vomits in response to the same emetic agents that cause vomiting in mammals. In those studies on emesis with frogs, subjects were usually fed before the injection of an emetic, and the ejection of stomach contents was the criterion for vomiting. However, little attention has been paid to the volume and kind of food given to the frogs. In the present study, we examined whether or not such gastric contents have some effects on frogs' responses to emetic challenges. We used Japanese pond frog Rana nigromaculata and the centrally acting emetic apomorphine.

The following results were obtained: (1) The number of frogs that vomited in response to apomorphine injected into the dorsal lymph sacs increased with an increase in gastric volume. (2) This relationship between the emetic propensity and stomach contents appeared regardless of the type of food. (3) Latency seems short in case where the degree of the distention of the stomach was considered large. These results show that the distention of the stomach augments responsiveness to emetic challenges, such as apomorphine, in frogs.

EMETIC RESPONSES OF AMPHIBIANS TO NEUROACTIVE PEPTIDES

S.Yokota and T.Naitoh. Dept.of Biol.,Shimane Univ.,Matsue

We studied the emetic effects of the peptides, angiotensin II and arginine-vasotocin on the newt Cynops pyrrhogaster and angiotensin I, angiotensin II, neurotensin, arginine-vasotocin, peptide YY, and leucine-enkephalin on the frogs Xenopus laevis and Rana ruqosa.

One, two and three out of five newts vomited after injection of angiotensin II at the dosage of 0.2μg/g, 10μg/g and 20μg/g body weight, respectively. Two out of eight X. laevis and two out of six R. ruqosa vomited after the injection of angiotensin II at dosage of 0.2μg/g and 10μg/g, respectively. Arginine-vasotocin at a dosage of 0.1μg /g weakly induced emesis in one out of ten R. ruqosa. The newt twisted and bent its trunk vigorously after injection of angiotensin II ; but this behavior was inhibited by the anti-emetics metoclopramide and chlorpromazine. R. ruqosa showed bending of the torso backward after the injection of arginine-vasotocin, but, again, this behavior was inhibited by the anti-emetics. Except for angiotensin II and arginine-vasotocin, the other peptides were ineffective in inducing emesis.

The two peptides that induced emesis indicate that the some endogenously produced peptides can cause emesis in amphibians, as they evidently do in mammals.

CLONAL DELETION BY B CELLS AND CLONAL ANERGY BY DENDRITIC CELLS IN THE DEVELOPING THYMUS

M. Hosono[1], M. Inaba[2], K. Inaba[3], S. Muramatsu[3], S. Ideyama[1] and Y. Katsura[1]. [1]Dept. of Immunol., Chest Dis. Res. Inst., [3]Fac. of Sci., Kyoto Univ. & [2]Dept. of Pathol., Kansai Med. Univ., Osaka

Vβ6 T cell receptor-bearing autoreactive T cells developed in the newborn thymus of *Mls*a-antigen-bearing mice and deleted within a week after birth. The role of different types of non-T cells in the induction of tolerance in the thymus was assessed. B cells, dendritic cells and macrophages isolated from thymi of *Mls*a mice were injected into the thymus of newborn *Mls*b mice. One week later, the number of *Mls*a-reactive, Vβ6$^+$ T cells in the thymus and the capacity of thymocytes to induce a graft-vs-host reaction in popliteal lymph nodes of *Mls*a mice were measured. Injection of B cells deleted Vβ6$^+$ T cells in the thymus and induced tolerance to the *Mls*a determinant. Injection of dendritic cells also induced tolerance, but the Vβ6$^+$ cells were anergized rather than deleted. Macrophages did not induce tolerance. Therefore, different types of bone marrow-derived non-T cells have different capacities for inducing tolerance by distinct mechanisms. Thus, B cells in the developing thymus, though small in number, are important in deletion of autoreactive T cells in the thymus.

ESTABLISHMENT AND CHARACTERIZATION OF RAT TUMOR CELL LINE RT130 WHICH PRODUCTS HAEMOPOIETIC FACTOR.

K.Hatakeyama, H.Kasai, and K.Sugiyama.
Dept.of Biol., Fac.of Sci., Hirosaki Univ., Aomori.

A new cell line RT130 was established from spontaneously occurring rat tumor. The tumor, found incidentally in the old female(130 weekes old) inbred Wistar strain rat were enzyme(Dispase)-digested, and were cultivated in α MEM supplemented with 5% FCS(fetal calf serum) in a plastic culture flask at 37°C, 5% CO_2 in air. Part of the tumor was fixed in Bouin's solution and embedded in paraffin for the histological inspection. The cultured cells have been maintained for 12 months with more than 100 passages. The RT130 cells showed fibroblast-like or polygonal morphology under the phase-contrast microscopy.

We also detected haemopoietic activity in the culture fluid of RT130 by clonal assay. Bone marrow cells were derived from femurs of female BDF1 mice, and cultivated in semi-solid culture system using methyl cellulose with RT130 culture fluid or rIL-3(200U/ml). Colony types were determined on day 7 of incubation by *in situ* observation on an inverted microscope. The colonies found in the rIL-3 containing cultures were granulocyte-macrophage type. The RT130 culture fluid effectively supported only macrophage colonies from normal mice bone marrow cells. Culture fluid of RT130 cells stimulated with TPA(0.5ng/ml) were enhanced this activity. IL-3 or SCF-like activity were not detected.

FINE STRUCTURE OF MELANOPHORES OF JAPANESE HAGFISH, *EPTATRETUS BURGERI.*

E. Nakata and N. Oshima. Dept. of Biomolecul. Sci., Fac. of Sci., Toho Univ., Funabashi.

We have shown that melanophores in the skin of the hagfish, *Eptatretus burgeri*, do not respond to hormones and a neurotransmitter (Nakata *et al.*, 1994). In the present study, we examined the morphology of hagfish skin. Light microscopy of 8-10 μm sections revealed that melanophores were not present in the epidermis where many mucous cells were seen, and that dermal melanophores were distributed just beneath the basement membrane, under which the very thick layer of collagenous fibers stained with eosin was observed. By electron microscopy, each melanophore was found to be undulated in the layer of collagenous fibers. In Japanese sculpin (*Cottus pollux*; a teleost fish capable of changing body color), that we used as control material, there were epidermal and dermal melanophores that contained many pigment granules having diameter of 500-600 nm. In contrast, the number and size of pigment granules (200-300 nm in diameter) within hagfish melanophores were very small, and only a few microtubules and microfilaments were observed. The relationship between a lack of cell motility and a scarcity of cytoskeletal elements was discussed.

INTEGUMENTARY PATTERN FORMATION IN THE FLATFISH DURING ADAPTATION TO BACKGROUND PATTERNS.

S. Ohsumi And T. Naitoh, Dept. of Biol., Fac. of Sci., Shimane Univ., Matsue

Variagated integumentary patterning of the flatfish *Pararichthys olivaceus* was studied. There are two types of small spots in the skin ; dark spots and white spots. The dark spots consist of densely gathered melanophores. They are distributed in several places, which correspond to the large dark patches. White spots consist of small number of melanophores and densely developed iridophores. They are in the majority in places other than the dark patch areas. Dark spots are surrounded by fewer melanophores than those of dark spots, while white spots are surrounded by both melanophores and iridophores. When melanophores located between the dark spots bridge them by dispersion, large dark patches appear in the skin. At the same time, the iridophores that come up due to the aggregation of the melanophores located between the white spots bridge them, large pale areas appear. When, in contrast, dark spots as well as white spots are separated from each other by the regionally differential responses of melanophores located between the dark/white spots, dark and white spotted-pattern appears in the skin.

ADENOSINE RECEPTORS AND ADRENERGIC RECEPTORS IN THE ERYTHROPHORE OF THE GOBY *Tridentiger obscurus.*

H. Katayama[1] and Y. Omura[2]. [1] Mukaishima Mar. Biol. Lab., Hiroshima Univ., Mitugi-gun, Hiroshima-ken and [2] Biol. Sci., Fac. of Sci., Hiroshima Univ., Higashi-hiroshima.

Subtypes of adenosine receptors and adrenergic receptors of the erythrophore in the caudal fin of the goby were investigated. Pigment within erythrophores maintained the aggregated condition in physiological saline. Adenosine and adenosine analogs evoked the dispersion of pigment within the cells. The order of potency of the agents used was as follows: 5'-N-ethylcarboxamido-adenosine > 2-chloroadenosine(2Cl-Ads) > adenosine > ATP > N^6-cyclohexyladenosine. The pigment-dispersing effect of these agents was inhibited by caffeine. Adenosine receptors of the erythrophore are considered to be A_2-type. In the presence of propranolol, both adrenaline and noradrenaline(NA) induced the aggregation of erythrophore pigment which had been made to disperse by 2Cl-Ads. The effect of the catecholamines was inhibited by phentolamine. Dobutamine, NA and salbutamol caused the dispersion of pigment in the presence of phentolamine. Metoprolol(beta-1 antagonist) inhibited the pigment-dispersing effect of dobutamine and that of NA, while it failed to inhibit the effect of salbutamol. It is probable that the erythrophore possesses alpha-, beta-1 and beta-2 adrenergic receptors.

THE EFFECT OF OKADAIC ACID ON THE PIGMENT AGGREGATION IN THE CULTURED MELANOPHORE OF THE BLACK-MOOR GOLDFISH, CARASSIUS AURATUS.

F. Morishita[1], H. Nakayama[1] and H. Katayama[2]
[1]Dept. Biol. Sci., Fac. Sci., Hiroshima Univ., Higashi-Hiroshima, [2]Marine Biol. Lab., Fac. Sci., Hiroshima Univ., Mukaishima

To study the involvement of protein phosphatase (PP) in the pigment aggregation in the melanophore of the black-moor goldfish, Carassius auratus, the effects of a PP inhibitor, okadaic acid (OA), on the cells was examined. OA reduced the pigment-aggregating action of α-agonists depending on the concentration and duration of OA-treatment. For example, pretreatment with OA (10 μM) for 10 min reduced the action of α-agosnists to 30% of control. The effective concentration of OA to reduce the cell response was within the range reported to inhibit the Ca^{2+}-calmodurin dependent phosphatase, PP 2B. Then, we measured the phosphatase activity in the crude-enzyme preparation of the melanophores using the *p*-nitrophenylphosphate as substrate. The activity was elevated to 2-folds in the presence of Ca^{2+}. Mg^{2+} also potentiated the activity to 3-folds, which is characteristic for PP 2C. At present, we assume that the PP 2B is important for the aggregation of pigments in the goldfish melanophores, although the cell also possesses the PP 2C.

COLOR PATTERN FORMATION ON THE SKIN OF JAPANESE TREEFROG, *Hyla arborea japonica*.

Y. Shirakata and Y. Kamishima
Department of Biology, Faculty of Education, Okayama University, Okayama 700

Japanese treefrogs show various patterns on their skin coloration. We have previously shown that each of the three types of pigment cells that form dermal chromatophore unit shows two different states, that is, expanded or contracted one in the xanthophores and melanophores, and blue or pale one in the iridophores. The colorations of the treefrogs are basically produced by combination of the three types of chromatophores in either state, that naturally makes eight different fundamental colorations on the skin.

In this study, we have tried to clarify the mechanism of dark patterns of stripes or patches appeared against the fundamental skin colorations. It is shown that melanophores distributed in the stripes or patches showed stronger responses to the MSH stimulation than those distributed in the background portions. Xanthophores also showed the same diverse sensitivity to the noradrenaline, a potent stimulant.

CHANGES IN PATTERNS OF ADRENERGIC INNERVATION TO CHROMATOPHORES DURING PROLONGED BACKGROUND ADAPTATION IN THE MEDAKA, *ORYZIAS LATIPES*.

M. Sugimoto and N. Oshima. Dept. of Biomolecul. Sci., Fac. of Sci., Toho Univ., Funabashi.

Prolonged adaptation of the medaka to a white or black background induces the changes in the density and pattern of adrenergic innervation to melanophores in scales along with the change in the number of melanophores. The reversibilities of these phenomena were examined when the background colors exchanged mutually, and the changes in the innervation to amelanotic melanophores and leucophores were compared by autoradiography with ^{3}H-norepinephrine. The change in the number of melanophores preceded the change in the pattern of nerve distribution, although the cell number and the innervation pattern in scales were well recovered to adapt to new background colors 30 days later. As to the changes in the innervation pattern to amelanotic melanophores of the medaka, orange-red variety, a similar result was obtained. However, no exact plexuses of labeled fibers were confirmed around leucophores of which the number increased in the fish adapted to a white background.

CIRCADIAN COLOR CHANGES OF THE BROWN-TAILED PENCILFISH, *NANNOBRYCON EQUES*.

H. Hayashi, A. Masagaki and R. Fujii. Dept. of Biomolecul. Sci., Fac. of Sci., Toho Univ., Funabashi.

We found that the characteristic pigmentary pattern of the skin of the brown-tailed pencilfish, *Nannobrycon eques*, varied largely during the night. Namely, the dark longitudinal stripe seen in the daytime changed to two large dark spots at night. Microscopic observations revealed that in the dark area melanosomes in the melanophores were dispersed, while they were aggregated in the blanched area. When the fish were immersed in solutions of melatonin, the night pattern could be induced even in the daytime. Melanophores in pieces of skin from most parts of the trunk responded to melatonin by the aggregation of melanosomes as usual. Closer observations, however, indicated that, in the areas within the spots but outside the longitudinal daytime stripe, melanosomes in the melanophores dispersed in response to melatonin. These melanophores are supposed to possess beta-melatonin receptors, which we have lately described in some melanophores of *Nannostomus* pencilfish. The areas where the darkening in response to melatonin take place were larger than those observed in *Nannostomus*. Thus, the species may be of use for the analyses of beta melatonin action of melatonin and its analogues on melanophores.

RESPONSIVENESS OF MELANOPHORES AFTER PROLONGED BACKGROUND ADAPTATION IN THE MEDAKA, *ORYZIAS LATIPES*--CHANGE IN THE SENSITIVITY TO CAMP.

H. Nagamori, M. Sugimoto and N. Oshima. Dept. of Biomolecul. Sci., Fac. of Sci., Toho Univ., Funabashi.

We previously reported that 10-days adaptation of the medaka to a black (*B* fish) or white background (*W* fish) induced the morphological color change and the change in the responsiveness of melanophores to hormones and neurotransmitter. In the present study, therefore, we investigated whether the prolonged background adaptation also affected the intracellular signal transduction. We made use of a permeabilized melanophore model which reacted to exogenous ATP and cAMP by melanosome dispersion, and compared the extent of the melanosome dispersion in melanophores from *B* fish to that from *W* fish, changing the concentration of cAMP in the bathing solution. The minimum effective concentration of cAMP for pigment dispersion in *B* fish (10 μM) was larger than that in *W* fish (1 μM). These results suggest that the change in the melanophore responsiveness caused by prolonged background adaptation may result, at least partially, from the change in the intracellular signaling system.

EFFECTS OF ENDOTHELINS ON LEUCOPHORES OF THE MEDAKA, *ORYZIAS LATIPES*.

T. Fujita and R. Fujii. Dept. of Biomolecul. Sci., Fac. of Sci., Toho Univ., Funabashi.

Endothelin-1 (ET-1) aggregated pigmentary organelles, the melanosomes, in melanophores of teleosts [Fujii *et al.*, 1993]. There exist, in addition to the light-absorbing chromatophores, leucophores in some teleosts. Having different optical properties, the leucophores take different parts in the coloration of the skin. Thus, their motility is differently regulated from the light-absorbing cells. We have therefore tried to examine the effects of mammalian ETs (ET-1, -2, -3) on the leucophores. All ETs did not aggregate the pigment within the leucophores of the medaka, *Oryzias latipes*, but they equally dispersed the pigment effectively and dose-dependently. They seemed to act directly on the leucophores, because denervated cells responded quite similarly. A beta-adrenergic blocker, propranolol, an alpha blocker, phentolamine, and BQ-123, an inhibitor of mammalian ET-1 receptors (ET_A receptors), did not interfere with the action of ETs. Their action may be mediated by their specific receptors existing in the leucophores. Along with the action on light-absorbing chromatophores, ETs may take part in the delicate control of the integumentary hues and patterns, especially by making the pattern more conspicuous.

EFFECTS OF MELANIN CONCENTRATING HORMONE AND MELANOPHORE STIMULATING HORMONE ON *CORYDORAS* MELANOPHORES.

N. Nakamaru and N. Oshima. Dept. of Biomolecul. Sci., Fac. of Sci., Toho Univ., Funabashi.

Using skin preparations of the peppered corydoras, *Corydoras paleatus*, we examined the action of melanin concentrating hormone (MCH) and several fragment analogs (MCH_{1-14}, MCH_{5-15}, MCH_{5-17}) on melanophores. MCH and the analogs caused pigment aggregation, and the potency ranking was determined to be: MCH > MCH_{5-17} > MCH_{5-15} > MCH_{1-14}. When melanophores were exposed to MCH at doses more than 1 μM, almost complete aggregation of pigment, which was accomplished within several min after the application of the peptide, was followed by gradual dispersion of pigment in the continued presence of MCH. Fragment analog MCH_{5-17} did not have such effect. Thus, the MSH-like activity of MCH seems to relate to N-terminus of the hormone. In addition, it was shown that the N-terminus also participate in pigment-aggregating activity of MCH, because MCH_{5-17} was less active (about 1/10th) than the native hormone. Furthermore, to investigate the receptor mechanism, the action of α-MSH on *Corydoras* melanophores was comparatively studied.

DIRECT EFFECT OF K^+ ON THE MEDAKA XANTHOPHORES IN PRIMARY CULTURE.

H. Sekine and N. Oshima. Dept. of Biomolecul. Sci., Fac. of Sci., Toho Univ., Funabashi.

Generally, potassium ions cause the release of neurotransmittes from sympathetic nerve fibers by stimulating the nerve endings, which, in turn, causes pigment aggregation within pigment cells (Fujii, 1959). However, Iga (1969) and Iwakiri *et al.* (1988) reported that the ions stimulated directly xanthophores in scales of the medaka, *Oryzias latipes*. In the present study, we examined the responses to potassium ions of cultured xanthophores of the medaka (orange-red variety). In physiological saline, some of cultured xanthophores retained their pigment in the dispersed state, and other cells assumed aggregated state. We used the latter cells, because they surpassed in motile activity. After pigment granules were dispersed by application of α-MSH, reaggregation of pigment induced by potassium ions was quantitatively analyzed by video image analyzer system (LUZEX-F). The rinse with K^+-rich solution of medaka xanthophores surely accelerated the aggregation of pigment. The time required for 50% aggregation was about 3.8 min: about 57% of the control. To study the mechanism of the direct action of potassium ions, we also examined the effects of calcium-channel blockers.

A ROLE OF PROLACTIN IN COLOR CHANGE OF FISHES.

N. Oshima and M. Makino. Dept. of Biomolecul. Sci., Fac. of Sci., Toho Univ., Funabashi.

We have reported the pigment-dispersing effects of smaller prolactin of the tilapia *Oreochromis mossambicus* ($tPRL_{177}$) and ovine prolactin (oPRL) in tilapia (*Oreochromis niloticus*) xanthophores (1993). In the present study, the responses to these prolactins of cultured xanthophores and erythrophores isolated from some fish species were examined. Xanthophores of the tilapia, medaka and paradise goby responded by pigment dispersion in a dose-dependent manner, and the minimum effective concentration was 100 pM or 1 nM. Those of the dark chub and rose bitterling did not respond to the peptides. In winter, prolactins did not affect cultured erythrophores from the tilapia and paradise goby, although they caused pigment dispersion in platy erythrophores. In spring, however, erythrophores isolated from the rose bitterling and tilapia assuming nuptial coloration (♂) responded to prolactins by pigment dispersion. Therefore, it is likely that prolactin might be involved in the morphological color change and play a part in the manifestation of yellow or red color of fishes. On the other hand, prolactins did not affect melanophores, and α-MSH was always effective in inducing pigment dispersion in xanthophores, erythrophores and melanophores.

A NOVEL TYPE OF CHROMATOPHORES FOUND IN THE REDFIN VELVETFISH, HYPODYTES RUBRIPINNIS.

T. Iga and A. Matsuno. Dept. Biol., Fac. Sci., Shimane Univ., Matsue.

In the integument of the redfin velvetfish, Hypodytes rubripinnis, there exist five types of chromatophores; melanophores, xanthophores, iridophores(non-motile type) and unusual chromatophores, which appear dull brown in transmitted light, but yellowish in reflected light. These novel chromatophores are relatively flattened cells with radially directed processes and are motile cells that respond to external stimulation with the intracellular migration of pigment. Nervous and norepinephrine stimulation induced aggregation of the pigment granules. The effects were effectively inhibited by an alpha adrenergic antagonist, yohimbine. Melatonin and MCH also induced the pigment aggregation response. On the other hand, isoproterenol induced pigment dispersion and the response was blocked by a beta adrenergic antagonist, propranolol. Forskolin was effective for inducing pigment dispersion. The movements of these chromatophores were characteristically slow as compared with those of erythrophores and xanthophores. The present experiments suggested that the unusual chromatophores are pigment cells of a new type.

RESPONSES TO NOREPINEPHRINE OF MELANOPHORES FROM THE FLATFISH, *PARALICHTHYS OLIVACEUS*, SUBJECTED TO BACKGROUND CHANGES.

U. Kikutani and C. Shingyoji. Zool. Inst., Fac. of Sci., Univ. of Tokyo, Tokyo.

Flatfish change their colour according to the background (bg). We have reported that plain bg's induce uniform coloration, while check bg's induce spotted patterns with both dispersed and aggregated melanophores. The dispersed cells occur only in round spots: there are three large (LBS) and many small black spots (SBS). We aimed to determine whether the melanophores in these spots and other regions (i.e., general bg, GBG) respond differentially to norepinephrine (nEp). Young flatfish, *Paralichthys olivaceus*, were either adapted to a black, check, or white bg for >7 days, or subjected to cyclic (daily) changes of the three bg's for several months. Scale slips were then obtained from LBS, SBS, and GBG of each fish. Although 10^{-5} M nEp induced aggregation of all melanophores, 5×10^{-6} M nEp induced varied responses in melanophores from different regions and after various adaptation protocols, except those from the peripheral regions of LBS, which were always dispersed. The period of bg adaptation significantly affected the response. The results suggest a possible mechanism controlling the colour change.

COMPARATIVE STUDIES ON THE IRIDOPHORES OF SOME CORAL-REEF TELEOST FISHES.

M. Goda and R. Fujii. Dept. of Biomolecul. Sci., Fac. of Sci., Toho Univ., Funabashi.

Among iridophores, those which are involved in the revelation of silvery glitters and whiteness of belly skin have long been known. Recently, the iridophores which function to generate fluorescent-like hues through the multilayered thin-film interference phenomenon of the non-ideal type, have been found in some teleost species. In the present study, electron microscopic observations of the skin were made on a few species of coral-reef fishes, which constitute most beautiful group of animals. The materials were the blue damselfish, *Chrysiptera cyanea* (Pomacentridae), the dusky cherub, *Centropyge bispinosus* (Pomacanthidae), the blue-blotched butterfly-fish, *Chaetodon plebeius* (Chaetodontidae), the common surgeonfish, *Paracanthurus hepatus* (Acanthuridae), the three-spot humbug, *Dascyllus trimaculatus* (Pomacentridae), the clown fish, *Amphiprion clarkii* (Pomacentridae), the black-bar triggerfish, *Rhinecanthus aculeatus* (Balistidae), and some others. In the former three species, iridophores were present in a single layer. In the dermis of the surgeonfish, they were found in a double layer. In the white parts of the latter three speies, iridophores were accumulated in a multilayer, in each of which platelets were rather randomly oriented.

A POSSIBLE RETINAL INFORMATION ROUTE TO THE CIRCADIAN PACEMAKER THROUGH THE PRETECTAL AREA IN THE HAGFISH.

S. Ooka-Souda[1], H. Kabasawa[2], T. Kadota[3] and H. -A. Takeuchi[4]. [1]Atomigakuen Jr. Colle., Tokyo, [2]Aburatsubo Mar. Par. Aqu., Miura, [3]Dept.of Anat., Yokohama City Univ. Sch. of Med., Yokohama, [4]Dept. of Biol., Fac. of Sci., Shizuoka Univ., Shizuoka.

We have shown that the circadian pacemaker of the hagfish may be located in the preoptic nucleus in the hypothalamus, and that the circadian rhythms are entrained by light information from the eyes. In the present study, we examined the possibility that light information from the eyes may reach the circadian pacemaker by way of the pretectal area where most of the retinal fibers project. Partial removal and cutting of brain structures were done with scissors. The locomotor activity of operated animals was measured by means of an infrared photocell system connected to a computerized recording system. After recording locomotor activity, the surgical lesions in the brains of all operated animals were examined histologically. After ablation of only the mesencephalic tectum, the animals showed normal nocturnal activity. But after ablation of both the mesencephalic tectum and the pretectal area, the animals showed free-running rhythm under 12L:12D. These results show that one of the most important routes of retinal information to the circadian pacemaker may be through the pretectal area.

A WHOLE-CELL PATCH-CLAMP ANALYSIS OF TTX-RESISTANT PERSISTENT SODIUM CURRENT UNDERLYING PACEMAKER POTENTIALS OF TERMINAL NERVE-GNRH CELLS.

Y. Oka, Zool. Inst., Sch. of Sci., Univ. of Tokyo, Tokyo

Endogenous pacemaker activities are important for the putative neuromodulator functions of the gonadotropin-releasing hormone (GnRH)-immunoreactive terminal nerve (TN) cells. By using the whole-cell patch-clamp technique in *in vitro* whole-brain preparation of a small fish brain, I analyzed pharmacological and kinetic characteristics of a TTX-resistant persistent Na current, $I_{Na(slow)}$, which I have shown to play an important role in the generation of pacemaker potentials (PPs) of TN-GnRH cells. $I_{Na(slow)}$ could be isolated pharmacologically by blocking K^+ currents (internal Cs^+ and external TEA and 4AP), Ca^{2+} currents (internal EGTA, external Mn^{2+} or La^{3+} or Cd^{+2}, and low concentration of external Ca^{2+} and high concentration of Mg^{2+}) and conventional fast Na^+ current (TTX). It was characterized by 1) reversible block by Na^+-free solutions and resistance to block by ouabaine of electrogenic Na^+ pumps, 2) overlap of activation and inactivation curves near the resting potential, 3) very slow inactivation and deinactivation kinetics. On the other hand, current clamp experiments showed that PPs are inhibited by noradrenaline (NA), while they are facilitated by salmon GnRH (sGnRH). Voltage clamp experiments showed that NA inhibits PPs by blocking $I_{Na(slow)}$.

EFFECT OF INHIBITION BY THE FM COMPONENTS IN ECHO ON DELAY-TUNED FM-FM NEURONS IN THE AUDITORY CORTEX OF THE MUSTACHED BAT.

M. Kanou[1] and N. Suga[2]. [1]Biological Institute, Faculty of General Education, Ehime Univ., Matuyama and [2]Department of Biology, Washington Univ, St. Louis, U.S.A.

In the auditory cortex of the mustached bats, *Pteronotus parnellii*, FM-FM neurons show strong facilitative response to a pair of FM components in the pulse(P)-echo(E) pair. They are tuned to particular echo delays and form an echo delay axis in the FM-FM area (Suga et al. 1978, O'Neill and Suga 1979, Suga and O'Neill 1979). Their facilitative response is, however, partially inhibited by the FM sound overlapped with echo.

The inhibitory frequency-tuning curves were measured to investigate the inhibitory area of FM-FM neurons in the FM-FM area by delivering test FM sounds together with echo. Inhibitory frequency-tuning curves suggested that echo harmonics which were not essential for facilitation inhibited the facilitative response effectively. The inhibition evoked by nonessential harmonics in EFM sharpened delay-tuning curves of FM-FM neurons, i.e. the resolution of target range was improved by the inhibition. Furthermore, the inhibition occured in larger number of FM-FM neurons when the target was in short distance. Finer target range resolution of FM-FM neurons must be required in the terminal phase of target-directed flight for accurate prey catching or safety landing to a roosting place.

LOCAL CIRCUITS AND SYNAPTIC LONG-TERM POTENTIATION IN THE HYPERSTRIATUM VENTRALE OF THE QUAIL CHICK: NEURONAL MECHANISM OF IMPRINTING.

T.Matsushima and K.Aoki, Life Sci. Inst., Sophia Univ., Tokyo.

In domestic chicks, the intermediate and medial part of the telencephalic hyperstriatum ventrale (HV) has been shown to be involved in a variety of learning processes, such as filial imprinting and one-trial passive avoidance learning task. However, to date, the synaptic organization of the HV remains unknown, thus leaving the cellular understanding of the imprinting process largely speculative. In this study, acute slices (0.5mm thick) were prepared from quail chicks (1-12day of age), and whole-cell patch electrode recording was applied to the HV neurons *in vitro*. Analysis of post-synaptic current responses to local electrical stimulations revealed plasticity in the local circuit of the HV.

Single electrical pulses (up to 0.3mA x 0.5ms at 10 sec intervals) elicited EPSC-IPSC complex in nearby neurons (located <0.5mm from the stimulating electrode), and only IPSC in further neurons, respectively. The early phase of the EPSC was sensitive to 10^{-5}M DNQX, but not to 10^{-4}M DL-AP5, thus proved to be mediated by glutamate receptors of the non-NMDA type. On the other hand, the IPSC was suppressed by 10^{-5} M bicuculline methiodide, and its polarity was reversed above -55mV, thus proved to be due to the $GABA_A$-ergic transmission. Furthermore, blockade of the $GABA_A$-ergic inhibition unmasked spontaneous slow waves, which was suppressed by 10^{-4}M DL-AP5. And finally, tetanic stimulation (5-10Hz x 30-60sec) combined with post-synaptic membrane depolarization induced long-term potentiation of the EPSC responses.

Effect of vasoactive intestinal peptide and ginsenosides on spatial memory deficits in the rat

Y. Yamaguchi, K. Haruta and H. Kobayashi
Research laboratory, Zenyaku Kogyo Co., Ltd., Tokyo.

Effects of vasoactive intestinal peptide (VIP) and ginsenosides Rg1, Rb1 and Rd on spatial cognitive deficits induced in the rat by scopolamine were examined in a radial-arm maze. A single intraperitoneal (i.p.), subcutaneous or intracerebroventricular injection of VIP and a single i.p. injection of Rg1 inhibited the reduction in the number of initial correct responses in rats with scopolamine-induced amnesia, but neither Rb1 nor Rd was effective. The inhibition of the reduction in initial correct responses was associated with a bell-shaped dose-response curve for VIP and Rg1. However, Rg1 did not improve spatial cognitive deficits induced in the rat by a lesion in the medial septum. It is suggested that cholinergic neurons in the medial septum are involved in the ameliorative effect of Rg1 on spatial cognitive deficits induced by scopolamine.

DIFFERENT ROLES OF FOREBRAIN NUCLEI HVc AND RA IN THE SONG PATHWAY OF THE BENGALESE FINCH.

J. Miki, T. Matsushima and K. Aoki. Life Sci. Inst., Sophia Univ. Tokyo

In song birds, repertoire of characteristic song elements (syllables) and their rigid sequences constitute the song pattern. Where are these syllables and sequences stored in the bird brain? To answer this question, unilateral forebrain nuclei (HVc and RA) were chemically lesioned by microinfusion of kainate (an excitatory neurotoxic agent), and the effects on the song patterns were examined in sexually matured male adults of the Bengalese finch (*Lonchura striata*).

Corresponding to the extent of the lesion , the following three types of effects were obtained. **(1) Selective HVc lesion distorted the sequences (n=2).** HVc was unilaterally lesioned, and the syllables in the pre-lesion songs were completely lost during the initial days after the lesioning. The birds gradually recovered from the temporal "aphasia", and all of the pre-lesion syllables reappeared until the post-lesion day 12, but their sequences remained distorted. **(2) Partial RA lesion resulted in a partial loss of syllable repertoire (n=1).** HVc and a part of RA were unilaterally lesioned, and one of the pre-lesion syllables never re-appeared and their sequences were distorted. **(3) Whole RA lesion resulted in a total loss of the syllable repertoire (n=5).** Both HVc and RA were unilaterally lesioned, and all of the pre-lesion syllables were lost and never reappeared.

These results suggest that HVc may encode temporal structure such as the sequence of syllables, while RA may encode acoustic structure such as the form of each syllable.

FEMALE ODOUR INDUCES STRUCTURAL CHANGES OF SYNAPSES IN ACCESSORY OLFACTORY BULB OF MALE RAT.

M. Ichikawa Dept. of Anat. & Embryol., Tokyo Metropolitan Inst. for Neurosci., Tokyo

The effects of soiled bedding on synaptic morphology in the accessory olfactory bulb (AOB) were examined in adult male rats. Forty-day-old male rats were isolated. First group was exposed to bedding soiled by male and female rats (MF). Second one was only to male soiled bedding (M). Third one was only to female soiled bedding (F). Forth one was exposed to clean bedding (N). After 2 months, the animals were sacrificed for electron microscopy. The size and the numerical density of synapses were measured in the glomerulus and the granule cell layer. In the glomerulus, the length of the synaptic active zone was significantly greater in the MFC and FC than in the MC and the IC, while there was no statistically significant difference in the density of synapses among the four groups. Two types of synapses were classified in the granule cell layer: (1) perforated synapses, which are characterized by discontinuities in their active zone and (2) nonperforated synapses. For perforated synapses, the length of the synaptic active zone was significantly greater in the MF and F than in the M and the N. For nonperforated synapses, there was no statistically significant difference in the length of the synaptic contact zone among the three groups. In the density of both perforated and nonperforated synapses, there was no statistically significant difference among the four groups. These results demonstrated that exposure to bedding soiled by female rats, which contains female odour substances (pheromones) can induce structural changes of the synapses in the AOB of male adult rats.

PHOTOPERIODIC RESPONSES OF PHOTOTAXIS AND REPRODUCTION BY THE OVERWINTERING ADULTS OF A WATER STRIDER, AQUARIUS PALUDUM.

I. Ono and T. Harada. Biol. Lab., Fac. of Educ., Kochi Univ., Kochi.

Overwintering adults of Aquarius paludum were collected and kept under quasi-natural conditions for 18 or 28 days. After that, they were reared under 14.75L-9.25D, 12L-12D or 10L-14D, and at 20±2°C. High degree (about 60 %) of positive phototaxis shown under the quasi-natural conditions decreased to less than 30 % on the 18th day after the transferrence to the 12L-12D or 10L-14D. The decreasing under 10L-14D occurred earlier than that under 12L-12D: the degree was 30 % in the former and 50% in the latter on the 11th day. However, the high degree was kept under 14.75L-9.25D. The females under the quasi-natural conditions continued to lay eggs and they did not enter diapause after the transferrence to each of the three photoperiodic conditions. Oviposition processes of the three conditions were similar and there were no significant differences in the fecundity for 1 week after the 16th day among the three conditions. The photoperiodic response of reproduction does not remain but that of phototaxis is kept even after the overwintering in A. paludum.

PHOTOSENSITIVE STAGES IN PHOTOPERIODISM FOR WING FORM IN A WATER STRIDER, AQUARIUS PALUDUM II

T. Inoue and T. Harada, Biol. Lab., Fac. of Educ., Kochi Univ., Kochi.

Aquarius paludum were transferred once from 15.5h light-8.5h dark (15.5:8.5) to 12:12 or vice versa on the first day of a particular instar (second through fifth instars), or they were raised exclusively under the long-day (15.5:8.5) or short-day (12:12) photoperiod. Individuals transferred from 15.5:8.5 to 12:12 on the first day of the fifth instar exhibited a significant increase in the frequency of brachypterous form relative to those transferred on the first day of the fourth instar or earlier. Transferring A. paludum from 12:12 to 15.5:8.5 on the first day of the third instar or earlier resulted in higher frequency of brachypterous form than transferring at the beginning of the fourth instar or later. When individuals were transferred from 12:12 to 15.5:8.5 on the first day of the second or third instar, part of macropterous adults showed a little shorter wing lengths than macropterous adults grown exclusively under the short-day photoperiod.

The third and fourth instars seem to be important stages for the determination of wing form of A. paludum.

AGE-DEPENDENT CHANGES IN BODY TEMPERATURE AND AMOUNT OF SEVERAL SERUM COMPONENTS WITH STARVATION IN THE MOLOSSINUS MOUSE.

T.A.Nomaguchi. Dept. of Cell Biol., Tokyo Metropolitan Institute of Gerontology, Tokyo.

Energy consumption is closely related to maintain a constant level of body temperature for the mammals in smaller size. In the mouse fasting on water for 15 hours in 18-09 o'clock and feeding, body weight, body temperature and several serum components were determined. Examined animal is a very small strain in body weight throughout life derived from the house mouse, Mus musculus molossinus. The body weight decreased about 11% from start level of starvation in all ages and the recovery was still low level for 9 hours after feeding. The body temperature markedly declined with starvation, but rapidly recovered a constant level with feeding. Decreased blood sugar also rapidly increased in all ages and kept higher level in younger animals. Other hand, recovery to a constant level of extremely decreased serum triglyceride after feeding required for 2 hours in 3 months, 5 hours in 6 and 12 months, 9 hours in 18 and 24 months. Serum urea content increased with starvation except 24 months, further increased until 2 hours after feeding in all ages and recovery to a constant level required for 9 hours in all ages. Serum albumin and creatinine levels also were determined.

MECHANISM OF SETTLEMENT AND MATAMORPHOSIS OF CYPRID LARVAE OF BARNACLE, BALANUS AMPHITRITE ••• I.

--- METAMORPHOSIS WITHOUT ATTACHMENT ---

H.Yamamoto, A.Tachibana, K.Matsumura and N.Fusetani. Fusetani Biofouling Project., ERATO., Research Development Corporation of Japan., Yokohama

In our studies on mechanism of larval settlement and metamorphosis of marine organisms such as barnacles, musseles and hydroids, we examined effects of various agents involved in signal transduction on cyprid larvae of the barnacle, Balanus amphitrite.

Calmodulin inhibitors, amitriptyline and imipramine, PKC activators, phorbol esters, and juvenile hormone-I induced metamorphosed larvae that did not attach to the substrates. In addition, most of these larvae grew up to adult barnacles without abnormal appearance.

In conclusion, this suggests that signals for larval settlement and metamorphosis might flow different pathways.

CHANGE OF MECHANICAL PROPERTIES IN THE CIRRI OF *METACRINUS ROTUNDUS* (CRINOIDA, ECHINODERMATA)

R. Birenheide, T. Motokawa (Tokyo Institute of Technology, Biological Laboratory, Tokyo, Japan)

Cirri of *Metacrinus rotundus* anchor the animal by clinging to hard surfaces. The cirri do not contain any muscles so that the grasp has to rely on ligament properties. In the present study we investigated for the first time stiffness changes of cirri after stimulation of the animal in vivo using video observations. We tested the influence of electric stimulation on the ligament stiffness of isolated cirri using a mechanical bending test. The effect of putative neurotransmitters was also tested. The results show that the cirri of *Metacrinus rotundus* undergo rapid and dramatic changes in their mechanical properties after electrical stimulation and under the influence of neurotransmitters.

MORPHOLOGICAL AND MECHANICAL ASPECTS OF THE PERIODONTAL LIGAMENT IN ECHINOIDS

A. Tsuchi, R. Birenheide and T. Motokawa
Biological Laboratory, Faculty of Science, Tokyo Institute of Technology, Tokyo

Sea urchins feed on algae by scraping with their teeth on hard surfaces of rocks. During feeding each tooth is fixed to the jaw firmly by periodontal ligaments. The ligaments are, however, supposed to be soft so that the tooth slides along the jaw in order to compensate abrasion, because new hard materials are added to the tooth only at its proximal end. Electron microscopical studies on the periodontal ligaments in echinoids, *Diadema setosum*, showed that the ligament contains no muscle cells and is similar to echinoderm catch connective tissue that can change its stiffness reversibly under nervous control. In mechanical tests on the ligaments, we found that acetylcholine or artificial sea water with high potassium concentration cause reversible changes of their stiffness. We concluded that the periodontal ligament in echinoids consists of catch connective tissue: in its stiff state it fixes the tooth to the jaw firmly during feeding and in its soft state it allows sliding of the tooth during tooth growth.

ANNOUNCEMENTS

THE 66TH ANNUAL MEETING OF THE ZOOLOGICAL SOCIETY OF JAPAN

The 66th Annual Meeting of the Zoological Society of Japan will be held at Tokyo from September 15 to 17, 1995. Further information and application forms will be sent to the domestic members in the 'Biological Science News' (1995 February issue). The deadline for application is July 8, 1995.

For application from abroad, please contact:

Professor K. Kuwasawa
Department of Biology
Tokyo Metropolitan University
Minamiosawa 1-1, Hachioji-shi
Tokyo 192-03, Japan
Fax : 81-(0)426-77-2559
Phone: 81-(0)426-77-2578

ZOOLOGICAL SCIENCE AWARD

The Zoological Society of Japan will present the Zoological Science Award for the best original papers published in ZOOLOGICAL SCIENCE during the preceding calendar year. Every original paper published in this journal will automatically be candidates for the award. The aim of the award is to encourage contributions to this journal. Selection Committee for the award will be organized every year.

ZOOLOGICAL SCIENCE AWARD 1994 was given to the following three papers.

Singtripop, T., T. Mori, M. N. Park, K. Shiraishi, T. Harigaya and S. Kawashima: Prolactin binding sites in normal uterus and the uterus with adenomytosis in mice. Vol. 10, No. 2: 353–360 (1993)

Nakagawa, S., R. Adachi, M. Miyake, T. Hama, K. Tanaka and T. Mayumi: Production of normal↔macular mouse chimeras: the presence of critical tissue in the macular mutant mouse, a model of Menkes' Kinky hair disease. Vol. 10, No. 4: 653–660 (1993)

Tsurusaki, N., S. Nakano and H. Katakura: Karyotypic differentiation in the phytophagous ladybird beetles *Epilachna vigintioctomaculata* complex and its possible relevance to the reproductive isolation, with a note on supernumerary Y chromosomes found in *E. pustulosa*. Vol. 10, No. 6: 997–1015 (1993)

AUTHOR INDEX
(Abstracts)

I

J

K

L

M

N

O

T

U

V

W

Y

Z

ZOOLOGICAL SCIENCE

VOLUME 11 SUPPLEMENT DECEMBER 1994

CONTENTS

PROCEEDINGS OF THE 65TH ANNUAL MEETING OF THE ZOOLOGICAL SOCIETY OF JAPAN

INDEXED IN:
Current Contents/LS and AB & ES,
Science Citation Index,
ISI Online Database,
CABS Database, INFOBIB

Issued on December 15
Printed by Daigaku Letterpress Co., Ltd.,
Hiroshima, Japan